Tritium Manual

R.-D. Penzhorn



Tritium Laboratory Karlsruhe

Institute for Astroparticle Physics (IAP)

Karlsruhe Institute of Technology

Preface

The idea of publishing a Tritium Manual was first promoted by M. Glugla, formerly Scientific Leader of the Tritium Laboratory Karlsruhe at Karlsruhe Institute of Technology. His perception was a manual not only focused on the chemical and physical properties of tritium but also emphasizing design peculiarities, technological requirements, and safety demands imposed on tritium systems serving and supporting fusion devices. After he became 2006 Head of the Fuel Cycle Engineering Division of the ITER Team the manual was further fostered by L. Doerr and B. Bornschein, the following leaders of TLK. Their sustained support, patience, and most valuable encouragement is acknowledged in deep gratitude. The continued generous sponsorship by Karlsruhe Institute of Technology is also greatly appreciated.

Karlsruhe, in May 2025 *R.-D. Penzhorn*



Except where otherwise noted, content in this work is licensed under a Creative Commons Attribution 4.0 International license

Acknowledgement

Careful reviewing of an early version of the manuscript together with plentiful constructive comments and numerous contributions mostly concerning components, procedures, and materials were provided by A.S. Poore, SRNL, Defense Program Technology; R.L. Rabun, SRS Defense Program; and Bernice C. Rogers, Savannah River National Laboratories. Their contributions are gratefully acknowledged. The author is very much indebted to B. Krasch, S. Niemes and I. Müller for their efficient, competent and diligent assistance in revising the manuscript, structuring and cataloging the literature and converting the original Tritium Manual text into the LaTeX format. S. Baygin, A. Böhmländer, J. Braun, K. Raczka and P. Strack also helped greatly by carefully adapting various sections of the Manual into the LaTeX format. Thanks, in measure beyond words go to my wife Youko for her constant and persistent endorsement during the come into being of the manuscript.

Karlsruhe, in May 2025 *R.-D. Penzhorn*

Contents

1 Preamble: Purpose and Scope **1**

2 Tritium Properties **7**

2.1 Chemical properties 8

2.2 Physical and nuclear properties 8

2.3 Radioactive decay heat 12

2.4 Annual Limit for Intake and Derived Air Concentration values for tritium 13

2.5 Physical and physicochemical properties of molecular tritium and tritium oxide . 13

2.5.1 Molecular tritium 13

2.5.1.1 Molar volume of hydrogen and deuterium 13

2.5.1.2 Dissociation energies ($\boldsymbol{D}$), zero-point energies ($\boldsymbol{E_0}$), and ionization energies ($\boldsymbol{I}$) of hydrogen isotopes 14

2.5.1.3 Rotational states of hydrogen 15

2.5.1.4 Boiling points, triple points and critical points 20

2.5.1.5 Vapour pressures 21

2.5.1.6 Viscosity 23

2.5.1.7 Volumetric calculation of tritium inventories at elevated pressures 25

2.5.1.8 Isotopic scrambling 26

2.5.1.9 Infrared and Raman absorption 27

2.5.1.10 Heat capacity 29

2.5.2 Physical constants of water isotopologues 29

2.5.2.1 Density 30

2.5.2.2 Relative vapour pressures 30

2.5.2.3 Ionisation constants of water isotopologues 31

2.5.2.4 Luminescence 31
2.6 Penetration of tritium beta particles into matter 32
2.6.1 Range of beta particles in hydrogen 32
2.6.2 Range of beta particles in dense matter 36
2.6.3 More on beta energy absorption by gases 37
2.6.4 Secondary radiation generated by tritium beta particles 39
2.7 Isotope effects 40
2.7.1 Elemental hydrogen isotopologues 40
2.7.2 Isotope effects of water isotopologues 43
2.8 Natural and man-made sources of tritium; needs of ITER and IFMIF 44
2.8.1 Natural sources 44
2.8.2 Man-made sources 45
2.8.3 Tritium needs of ITER and IFMIF 48
2.9 Applications of tritium other than for fusion 52
2.10 Radiochemical and chemical properties of elemental tritium and tritiated water . 53
2.10.1 Self-radiolysis of T_2 53
2.10.2 Helium hydride, helium tritide 56
2.10.3 Synthesis and self-radiolysis of T_2O 57
2.10.3.1 Synthesis of T_2O 57
2.10.3.2 Self-radiolysis of T_2O 57
2.10.4 Self-radiolysis of tritiated water immobilized in solid absorbers 64
2.10.5 Reaction of T_2 with oxygen. Inflammability, explosion, and detonation . . 67
2.10.6 More reactions leading to the formation of tritiated water 74
2.10.7 Reaction of T_2 with nitrogen 76
2.10.8 Exchange reaction between T_2 and H_2 or D_2 78
2.10.9 Isotopic exchange between molecular tritiated hydrogen and water 79
2.10.10 Kinetics of the exchange reaction between molecular tritium and methane 81
2.10.11 Reaction of molecular tritium with carbon monoxide 85
2.10.12 Reaction of molecular tritium with carbon dioxide 87
2.10.13 Reaction of per tritiated water with carbon dioxide 89

2.10.14 Erosion of carbon from the first wall of fusion machines: hydrogen isotope effect . . . 89
2.10.14.1 Hot atom chemistry of tritium . . . 90
2.11 Interaction of hydrogen isotopes with metals and alloys from the perspective of tritium storage . . . 92
2.11.1 Uranium . . . 95
2.11.1.1 Selected physical properties of uranium and uranium hydride . . . 95
2.11.1.2 Properties of uranium in view of tritium storage . . . 95
2.11.2 Palladium . . . 108
2.11.3 Titanium . . . 112
2.11.4 Zirconium . . . 116
2.11.5 Zirconium cobalt . . . 116
2.11.6 Lanthanum nickel and its alloys . . . 127
2.11.7 Zirconium nickel . . . 131
2.11.8 Getters contemplated for the Storage and Delivery System of ITER . . . 132
2.11.9 Encapsulation of hydrogen in molecular sieves . . . 134
2.12 Interaction of tritium with selected organic and inorganic materials commonly used in tritium handling facilities . . . 135
2.12.1 Interaction of molecular tritium or tritiated water with polymers . . . 135
2.12.1.1 General remarks . . . 135
2.12.1.2 Properties of single polymers and their potential for application in tritium systems . . . 137
2.12.1.2.1 General remarks . . . 137
2.12.1.2.2 Assessment of single elastomers . . . 138
2.12.1.3 More results on the resistance of polymeric elastomer materials towards tritium . . . 146
2.12.1.4 Effect of fillers on the radiation resistance of polymers . . . 148
2.12.1.5 Glove materials . . . 149
2.12.2 Interaction of tritiated water with organic construction materials employed in areas of restricted access . . . 152
2.12.2.1 Interaction of tritiated water with paints . . . 154

2.12.2.2 Interaction of tritium with concrete 158
2.12.2.3 Cladding of concrete with a tritium impermeable barrier 165
2.13 Interaction of hydrogen isotopes or helium with glass 167
2.14 Interaction of tritium with steel, welds and several pure metals that find application in tritium handling facilities 169
2.14.1 Interaction of molecular hydrogen isotopologues with stainless-steel 171
2.14.1.1 Hydrogen content of as-received stainless-steel 171
2.14.1.2 Factors influencing uptake and release of tritium from stainless-steel 172
2.14.1.3 Annealing 180
2.14.1.4 Mechanism of hydrogen/water conversion on the surface of metals 180
2.14.1.5 Transport of tritium across stainless-steel's commonly employed in tritium handling systems 186
2.14.1.6 Pre-treatment of stainless-steel specimens for experimental studies 198
2.14.1.7 Transport of hydrogen isotopologues across a lengthy stainless-steel (or copper) pipe 199
2.14.1.8 Tritium in-growth into stainless-steel containments 200
2.14.1.9 Heterogenous oxidation of tritium permeated up to the backside of stainless-steel 202
2.14.1.10 Rudiments on corrosion of iron or stainless-steel in absence of hydrogen isotopologues 203
2.14.1.11 Changes of mechanical and surface properties of stainless-steel induced by hydrogen isotopologues and or helium 204
2.14.1.12 Hydrogen-assisted embrittlement of stainless-steel and other metals 209
2.14.1.13 Neutron activation of stainless-steel 213
2.14.1.14 Tritium permeation into blanket cooling water 214
2.14.1.15 Trapping of hydrogen in stainless-steel 216
2.14.1.16 Permeation parameters of tritium through some heat resistant alloys, ferritic, and austenitic construction materials, pure stainless-steel base metals, and low permeability materials 216
2.14.1.17 Interaction of tritium with advanced low activation materials and iron 220

2.14.1.18 Interaction of tritium with welds . . . 230
2.14.1.19 Corrosion of steel induced by tritiated water . . . 230
2.14.2 Interaction of hydrogen isotopologues with copper and copper-based alloys 233
2.14.2.1 Physical-chemical properties . . . 233
2.14.2.2 Application of copper in fusion machines . . . 239
2.14.3 Interaction of hydrogen isotopes with copper alloys and copper-gold brazing alloys . . . 241
2.14.4 Interaction of hydrogen isotopologues with silver and gold . . . 242
2.14.5 Interaction of hydrogen isotopologues with nickel . . . 245
2.14.6 Interaction of hydrogen isotopes with beryllium . . . 253
2.14.6.1 Physical and physicochemical properties . . . 253
2.14.6.2 Chemical properties . . . 258
2.14.6.3 Analysis of beryllium . . . 262
2.14.6.4 Working with and handling of beryllium . . . 263
2.14.6.5 Application of beryllium in fusion devices as plasma facing material or neutron multiplier in blankets . . . 263
2.14.7 Interaction of hydrogen isotopologues with tungsten . . . 271
2.14.7.1 Physical-chemical properties . . . 271
2.14.7.2 Chemical properties . . . 277
2.14.7.3 Application of tungsten as plasma facing material in fusion devices 278
2.14.7.4 Consequences of high heat fluxes . . . 279
2.14.7.5 Erosion by plasma . . . 281
2.14.7.6 Formation of traps and blisters in plasma exposed first wall materials 282
2.14.7.7 Recovery of tritium from plasma facing tungsten . . . 289
2.14.7.8 Formation of tungsten fuzz . . . 290
2.14.7.9 Fine spray/droplet ejection from a tungsten melt layer . . . 290
2.14.7.10 Heat sink for high heat flux components . . . 290
2.14.7.11 Tungsten waste . . . 291
2.14.8 Interaction of hydrogen isotopologues with palladium and alloys of palladium 292
2.14.8.1 Physical-chemical properties . . . 293
2.14.8.2 Applications of palladium in tritium technology . . . 299

2.14.9 Interaction of hydrogen isotopologues with metals and materials of less common application in tritium facilities . . . 300
2.14.10 Candidate plasma facing first wall materials for fusion machines . . . 302
2.14.11 Interaction of tritium with alumina . . . 314
2.14.12 Some fundamental aspects on the interaction of atomic hydrogen, molecular hydrogen or water with metals and oxide surfaces . . . 316

3 Basic design principles for the installation of tritium systems, typical small and large components, and key processes employed in tritium handling facilities 317

3.1 Materials and chemicals . . . 322
3.1.1 Stainless-steel . . . 322
3.1.2 Passivation of stainless-steel . . . 325
3.1.3 Copper . . . 329
3.1.4 Aluminium . . . 329
3.1.5 Glass, ceramics, and other non-metallic solids . . . 330
3.1.6 Chemicals to be avoided in primary systems . . . 331
3.2 Typical small auxiliary components used in tritium handling facilities . . . 331
3.2.1 Pipes . . . 331
3.2.1.1 Pipe materials . . . 331
3.2.1.2 Pipe specifications . . . 332
3.2.1.3 Precautions during pipe installation . . . 332
3.2.2 Vessels . . . 334
3.2.2.1 Surface treatments . . . 334
3.2.3 Valves . . . 335
3.2.3.1 Design guidelines . . . 335
3.2.3.2 Design requirement . . . 335
3.2.3.3 Stem and gasket materials . . . 337
3.2.3.4 Quality assurance . . . 338
3.2.3.5 Worldwide experience with commercial valves tested in tritium service . . . 339
3.2.3.5.1 Manual and automatic valves . . . 340

3.2.3.5.2 Variable leak and modulating valves 343
3.2.4 Fittings, flanges, gaskets, and sinter filters 344
3.2.4.1 Fittings 344
3.2.4.2 Flanges 345
3.2.4.3 Gaskets 345
3.2.4.4 Sinter filters 346
3.2.5 Electrical feed-trough 347
3.2.6 connection options for components 347
3.2.6.1 Joining by welding, brazing, or soldering 347
3.2.6.2 Mechanical joints 349
3.2.7 Bellows and membranes 349
3.2.8 Rupture discs 350
3.2.9 Filters 350
3.3 Oils and lubricants 350
3.4 Design of heated components 351
3.5 Thermal insulation of heated components 352
3.6 Active cooling of tritium processing components 353
3.6.1 Active cooling with chilled water 353
3.6.2 Active cooling with gas 355
3.7 Soldering 356
3.8 Welding 356
3.8.1 Welding procedures 357
3.8.2 Welding requirements 358
3.8.3 Welding inspection 359
3.8.4 Welding acceptance criteria 361
3.8.5 Welding of tritium-contaminated stainless-steel 362
3.8.6 Remote welding 364
3.9 Remote/automated operation of tritium handling systems 364
3.10 Radiation protection of workers 367
3.11 Handling of contaminated materials or equipment 368

3.12 Cleaning stainless-steel surfaces to minimize formation of tritiated hydrocarbons 369
3.12.1 Cleaning austenitic steel surfaces . . . 370
3.12.2 Cleanliness verification . . . 372
3.12.3 Cleaning of ferritic steel . . . 372
3.13 Leak rates . . . 373
3.14 Typical components used in tritium systems . . . 376
3.14.1 Pumps . . . 376
3.14.1.1 Magnetically suspended turbo molecular pumps . . . 377
3.14.1.1.1 Long-term endurance tests of turbo molecular pumps with tritium . . . 379
3.14.1.2 Turbo molecular drag pumps . . . 383
3.14.1.3 Multistage positive displacement rotary pumps . . . 385
3.14.1.4 Moving spiral (scroll) pumps . . . 385
3.14.1.5 Metal bellows pumps . . . 394
3.14.1.6 Vane pumps . . . 396
3.14.1.7 Cryogenic pumps . . . 397
3.14.1.8 Pumps based on cryo-trapping in frost layers . . . 406
3.14.1.9 Roots pumps . . . 409
3.14.1.10 SRTI pumps . . . 412
3.14.1.11 Sputter ion pumps . . . 413
3.14.1.12 Titanium sublimation pumps . . . 414
3.14.1.13 Reciprocating compressor . . . 415
3.14.1.14 Permeation pumps . . . 416
3.14.1.14.1 Palladium alloy membrane pump . . . 417
3.14.1.14.2 Bilayer metal membrane pump . . . 417
3.14.1.15 Mercury linear diffusion pump and mercury ring pump (KALPUREX process) . . . 418
3.14.1.16 Installation of pumps in glove boxes . . . 420
3.14.2 Tritium storage . . . 421
3.14.2.1 Gaseous storage of tritium . . . 421

3.14.2.2 Storage in getter beds 422
3.14.2.2.1 Getters 422
3.14.2.2.2 Design and safety aspects of getter beds employed for tritium handling 423
3.14.2.2.3 Technical storage bed 434
3.14.2.2.4 Further applications of getter beds 442
3.14.2.3 Metal hydrides as compressors 443
3.14.2.4 “In-bed” calorimetry 444
3.14.2.4.1 Static gas method 445
3.14.2.4.2 Adiabatic/isothermal calorimetry with vacuum insulation 445
3.14.2.4.3 Flowing gas procedure 446
3.14.2.4.4 Isothermal calorimetry 452
3.14.3 Permeator as purifier 456
3.14.4 Catalysts and catalyst beds 466
3.14.5 Molecular sieve beds 473
3.14.6 Electrolyzer 474
3.14.7 Cryogenic traps for the retention of water 476
3.14.8 Retention of hydrogen isotopes by cryo-adsorption trapping 480
3.14.8.1 Basic aspects 480
3.14.8.2 Experience with technical scale cryogenic adsorber traps 491
3.14.8.3 Targets for cryogenic inertial fusion 492
3.14.9 Tritium purification utilizing hot metal getter beds 493
3.14.10 Organic getters for hydrogen 496
3.14.11 Molecular sieve ”membrane” 496
3.15 Measurement of process parameters 497
3.15.1 Pressure and vacuum gauges 498
3.15.1.1 Pressure gauges 498
3.15.1.2 Vacuum gauges 500
3.15.2 Temperature sensors 501
3.15.2.1 Thermocouples 501
3.15.2.2 Pyrometers 501

3.15.3 Hygrometers . . . 502
3.15.3.1 Electrolytic hygrometer . . . 503
3.15.3.2 Condensation hygrometer (mirror dew point) . . . 503
3.15.3.3 Capacity humidity sensor . . . 504
3.15.3.4 Vibrating quartz crystal hygrometer . . . 504
3.15.3.5 Moisture meter calibration . . . 505
3.15.4 Oxygen monitor . . . 506
3.15.5 Gas flow meters . . . 506
3.16 Analysis of gases in tritium-handling facilities . . . 508
3.16.1 Determination of volumes . . . 508
3.16.2 Preparation of gas mixtures for calibrations . . . 512
3.16.3 Grab sampling or in-line . . . 515
3.16.3.1 Grab sampling . . . 516
3.16.3.2 In-line analysis . . . 516
3.16.4 Infrared analysis . . . 518
3.16.5 Laser Raman spectroscopy . . . 522
3.16.5.1 Calibration of laser Raman systems . . . 531
3.16.6 Mass spectrometry . . . 537
3.16.6.1 Sector field mass spectrometer . . . 538
3.16.6.2 Quadrupole mass spectrometer . . . 542
3.16.6.3 Omegatron . . . 543
3.16.6.4 Special mass spectrometers . . . 545
3.16.6.5 Calibration of mass spectrometers . . . 545
3.16.6.6 Sampling for mass spectrometry . . . 546
3.16.7 Gas chromatography . . . 548
3.16.7.1 Conventional gas chromatography . . . 548
3.16.7.1.1 Analysis of hydrogen isotopes . . . 549
3.16.7.1.2 Analysis of mixtures of hydrogen isotopes together with other species . . . 552
3.16.7.2 Micro gas chromatography . . . 557
3.16.7.3 Calibration of gas chromatographs . . . 559

3.17 Determination of tritium radioactivity in gases, liquids and solids 561
3.17.1 Ionisation chamber 561
3.17.2 Proportional counter 567
3.17.3 Liquid scintillation counting 568
3.17.4 Smear technique 570
3.17.5 Tritiated water vapour determination in a gaseous stream 571
3.17.6 Continuous aqueous tritium monitoring 571
3.17.7 Beta scintillator 573
3.17.8 Accelerator mass spectrometry 574
3.17.9 Elastic recoil detection analysis (ERDA) 576
3.17.10 Nuclear reaction analysis (NRA) 577
3.17.11 Calorimetry 579
3.17.12 Bremsstrahlung counting of tritium 590
3.17.13 Beta-induced X-ray spectroscopy (BIXS) 591
3.17.14 Autoradiography and tritium imaging plate technique 595
3.17.15 PIN diode 598
3.17.16 Catalytic oxidation of gaseous tritium 598
3.17.17 Chemical or electrochemical etching 599
3.17.18 Thermal de-sorption 602
3.17.19 Full combustion 604
3.17.20 Indirect determination of tritium via mass spectrometric measurement of decay ^{3}He 607
3.17.21 Routine calibrations 607
3.18 Basic processes in small and large tritium-handling installations 608
3.18.1 Evacuation 610
3.18.2 Gas re-circulation 611
3.18.3 Tritium transfer procedures 611
3.18.4 Processes for chemical purification and recycling of tritium from fusion devices 614
3.18.4.1 Loop combining a nickel catalyst with a palladium/silver permeator (CAPRICE) 615

3.18.4.2 Isotopic swamping device PERMCAT 620
3.18.4.3 Loop combining a nickel catalyst/permeator system CAPRICE with a PERMCAT unit (CAPER) 622
3.18.4.4 Combination of catalyst/permeator into a single unit (PMR) . . 627
3.18.4.5 Plasma exhaust clean-up at TFTR 634
3.18.4.6 Other plasma exhaust clean-up process concepts 636
3.18.4.7 Processes proposed for the recovery of tritium from highly tritiated water 638
3.18.4.7.1 Reduction on hot metals 638
3.18.4.7.2 Electrolysis 642
3.18.4.7.3 PERMCAT and two stage PERMCAT 642
3.18.4.7.4 Catalyzed isotopic exchange 645
3.18.5 Extraction of tritium from the blanket purge gas of a Helium Cooled Ceramic Breeder Test Blanket Module 647
3.18.6 Tritium extraction from a lead lithium breeding blanket 652
3.18.6.1 Helium-Cooled Lithium Lead Test Blanket Module 652
3.18.6.2 Dual Cooled Lead Lithium breeding blanket: tritium extraction by vacuum-enhanced permeation 653
3.18.7 Isotope separation of molecular hydrogen isotopes 653
3.18.7.1 Cryogenic isotope separation 654
3.18.7.2 Displacement gas chromatography (DGC) 658
3.18.7.3 Thermal diffusion 663
3.18.7.4 Thermal cycling absorption process (TCAP) 666
3.18.8 Water de-tritiation 667
3.18.9 Modelling of fuel cycle subsystems and their interdependence 683
3.18.10 Decontamination of air from tritium employing wet scrubbers 684
3.18.11 Tritium storage and delivery 685
3.18.12 Tritium accountancy 688
3.18.12.1 Accountancy of gaseous tritium 689
3.18.12.2 Accountancy of tritium retained by adsorbents, catalysts, or storage beds 690

3.18.12.3 Empirical estimation of the contamination of stainless-steel by tritium . . . 695

4 Containment and confinement principles 697

4.1 Primary containment systems . . . 701

4.1.1 Integral leak rates of primary containment . . . 701

4.1.2 Transfer of hydrogen isotopologues or other gases within primary systems inside of a glove box . . . 701

4.1.3 Supply of gases to primary systems . . . 702

4.1.3.1 Inert and reagent gases . . . 702

4.1.3.2 Supply of gaseous tritium . . . 704

4.1.3.2.1 Supply of small inventories . . . 704

4.1.3.2.2 Supply of intermediate inventories on mostly national routes . . . 707

4.1.4 Pumping systems . . . 709

4.1.4.1 Vacuum pumping systems . . . 709

4.1.4.2 Pumps for gas re-circulation . . . 713

4.1.4.3 Pressurization of tritium . . . 714

4.1.5 Alarms . . . 715

4.1.6 Primary containment interlocks . . . 717

4.1.7 Protective measures against over-pressure . . . 719

4.1.7.1 Design guidelines . . . 719

4.1.7.2 Design measures against over-pressure . . . 721

4.1.8 Protective measures against over-temperature . . . 722

4.1.9 Protective measures against tritium release from primary containments . 723

4.1.10 Component failure data analysis . . . 728

4.1.11 Planing of tritium systems incorporating maintenance . . . 733

4.2 Primary and secondary confinement options . . . 736

4.2.1 Confinement options . . . 736

4.2.1.1 Tent . . . 738

4.2.1.2 Hood . . . 739

4.2.1.3 Glove box . . . 740
4.2.1.4 Caisson . . . 743
4.2.1.5 Dedicated large stainless-steel vessels . . . 744
4.3 Design of glove boxes and peripheral auxiliary equipment . . . 746
4.3.1 Gases for the operation of glove boxes . . . 746
4.3.1.1 Gases for the operation of glove boxes . . . 746
4.3.1.2 Gas for the operation of pneumatic valves . . . 746
4.3.1.3 Gas supply to primary systems . . . 747
4.3.2 Tritium removal systems for glove boxes . . . 748
4.3.2.1 Air atmosphere . . . 749
4.3.2.2 Chemically inert gas atmosphere . . . 761
4.3.2.2.1 Nitrogen or noble gas atmosphere containing a small fraction of oxygen . . . 762
4.3.2.2.2 Pure inert gas . . . 770
4.3.2.3 Oxygen/air supply and oxygen monitoring in glove boxes . . . 774
4.3.2.3.1 Oxygen/air supply . . . 774
4.3.2.3.2 Oxygen monitoring . . . 774
4.3.2.4 Catalytic exchange . . . 774
4.3.3 Regeneration of molecular sieves . . . 775
4.3.3.1 In line regeneration . . . 775
4.3.3.1.1 Replacement Tritium Facility at SRS . . . 775
4.3.3.1.2 Molecular Sieve Regeneration System at TSTA . . . 776
4.3.3.1.3 Combined Effluent Tritium Removal Facility, Glove Box Gas Purification System, and Air Clean-up System at TPL . . . 777
4.3.3.2 Off-line regeneration of molecular sieve beds . . . 779
4.3.3.2.1 AMOR facility at TLK . . . 780
4.3.3.2.2 Two stage PMR . . . 782
4.3.3.2.3 Molecular sieve regeneration at TFTR . . . 785
4.3.4 Tritium monitoring . . . 785
4.3.4.1 Ionisation chamber . . . 786

4.3.4.2 Continuous monitoring of radioactive or chemically contaminated particles in air . . . 789
4.3.4.3 Air sampling techniques for monitoring . . . 789
4.3.4.4 Smear technique . . . 790
4.3.5 Sensing primary instrumentation inside of glove boxes . . . 792
4.3.6 Tritium-compatible materials utilized for the manufacture of confinements 792
4.3.6.1 Glove box windows . . . 792
4.3.6.2 Electrical cables inside of glove boxes . . . 793
4.3.7 Integral leak rates of confinements . . . 793
4.3.8 Cleaning and protection of glove box surfaces . . . 794
4.3.9 Assembly . . . 794
4.3.10 Weldings . . . 794
4.3.11 Drainage . . . 795
4.3.12 Airlock . . . 795
4.3.13 Glove box feedtrough . . . 795
4.3.14 Glove box pressure control . . . 799
4.3.15 Glove box pressure relief bubblers . . . 799
4.3.16 Glove box blowers . . . 799
4.3.17 Glove box gloves . . . 800
4.3.18 Fabrics and insulation materials in glove boxes . . . 801
4.3.19 Solvents and detergents . . . 802
4.3.20 Materials to be avoided in a primary tritium **containment** . . . 802
4.3.21 Items to be avoided in **confinements** . . . 803
4.3.22 Glove box atmosphere cooling . . . 804
4.3.23 Moisture control in glove boxes . . . 805
4.3.24 Fire and explosion hazards . . . 805
4.3.25 Handling of liquid cryo-coolants in glove boxes . . . 806
4.3.26 Liquid nitrogen supply . . . 806

5 Safety philosophy in tritium handling facilities 809

5.1 General design recommendations and advice for safe operation of tritium handling facilities . . . 810

5.2 Confinement interlocks . . . 812

5.3 Fire and explosion protection . . . 813

5.4 Basic way of conduct in Tritium Control Areas in view of radiological protective safety and safeguards . . . 818

5.5 Some typical rules regulating work in Tritium Controlled Areas . . . 821

5.6 Technical Delivery and Acceptance Terms as well as Applicable Manufacturing Codes . . . 823

5.7 Automated Control Systems in tritium handling facilities . . . 824

6 Remote handling 837

7 Occupational hygiene 839

8 Wastes 841

8.1 Gaseous tritiated waste . . . 846

8.1.1 Inorganic gaseous tritiated waste . . . 846

8.1.2 Organic gaseous tritiated waste . . . 853

8.2 Liquid waste . . . 855

8.2.1 Non-burnable liquid waste . . . 855

8.2.1.1 Low contamination level . . . 855

8.2.1.2 Intermediate and high contamination level . . . 857

8.2.2 Interim storage of highly tritiated water . . . 859

8.2.2.1 Storage as liquid water . . . 859

8.2.2.2 Storage adsorbed on molecular sieves or silica gel: . . . 861

8.2.3 Burnable liquid wastes . . . 864

8.3 Solid waste . . . 865

8.3.1 Non-burnable solid waste . . . 866

8.3.2 Burnable solid waste . . . 872

8.3.3 Operational waste from ITER . . . 874
8.3.3.1 In-vessel radioactive operational waste . . . 875
8.3.3.2 Plasma-exposed non-steel metals . . . 879
8.3.3.3 Plasma-facing carbon waste . . . 885
8.3.3.4 Ex-vessel solid operational waste . . . 885
8.3.4 Environmental waste . . . 887
8.4 Decontamination procedures . . . 888
8.4.1 Decontamination of stainless-steel . . . 888
8.4.2 Decontamination of liquid organic wastes . . . 898
8.4.2.1 Decontamination of tritiated solvents, pharmaceuticals, and liquid scintillation cocktail . . . 898
8.4.2.2 Decontamination of tritiated oil . . . 900
8.4.3 Decontamination of adsorber beds with concomitant tritium recovery . . 901
8.4.4 Decontamination of getter beds . . . 901
8.4.5 Decontamination of service waste . . . 904
8.4.6 Decontamination of the inner surfaces of glove boxes and equipment inside 906
8.4.7 Decontamination of materials constituting the first wall of a tokamak . . 908
8.4.7.1 In situ decontamination . . . 908
8.4.7.2 Ex situ decontamination . . . 914
8.4.7.3 First wall protective layers: boronization, molybdenumisation or siliconisation , molybdenumisation, siliconisation . . . 917
8.4.8 Decontamination of walls and floors of buildings . . . 918
8.4.9 Sentencing of waste . . . 919
8.4.10 Packaging of waste . . . 929
8.4.10.1 Packaging of liquid tritium-contaminated waste . . . 929
8.4.10.2 Packaging of solid tritium-contaminated waste . . . 932
8.5 Central Decontamination and Storage Facility . . . 934
8.6 National/international transport of tritium and tritium-contaminated materials . 934
8.6.1 International transport of tritium . . . 934
8.6.2 National transport of tritium (USA) . . . 937

8.6.3 Transport of tritium-contaminated material/waste (housekeeping waste, CFC tiles, carbon flakes, etc.) . . . 937
8.7 Beryllium facility . . . 941

9 Building for tritium handling **945**
9.1 Basic design requirements of tritium buildings . . . 947
9.2 Building design guidelines . . . 949
9.2.1 Environmental protection concepts in representative tritium-handling facilities . . . 951

10 Compact fusion reactor **959**

11 Concluding remarks **963**

Appendices **969**

A Miscellaneous acronyms . . . 973

B Constants and conversions . . . 977

C Tritium compressibility factors at 295 K in the low-pressure range . . . 979

D Van't Hoff plots of metal hydrides with potential for application in tritium handling systems . . . 981

E Radiation resistance of polymers (information supplied by CEA) . . . 983

F Diffusivities and solubilities of tritium in fusion relevant metals . . . 985

G Optical microscopy of flakes from JET after DTE1 . . . 987

H Tritium profiles of the plasma-exposed and plasma-shadowed sides of JET tile 004/1-44 after the DTE1 campaign . . . 989

I Chemical composition of austenitic stainless-steels habitually used in tritium handling systems . . . 991

J Designations of some common standardized steels used in tritium handling facilities 993

K Chemical composition of structural stainless-steel specified for ITER, i.e. SS316L (N) . . . 995

L Tolerable pressure and temperature ranges of Swagelok valves with VCR® connections (for not radiographed valves the pressure ratings should be reduced by 15 %) . . . 997

M Nupro® shut-off SS316 valves (B series valves feature demontable bonnets for cleaning or replacement purposes) . . . 999

N Selected list of US specifications, regulations, guidelines, rules, standards, handbooks, and manuals . . . 1001

O Selected list of design and manufacture specifications, regulations, guidelines, rules, standards, handbooks, and manuals applied at Tritium Laboratory Karlsruhe 1005

P Cryo-adsorption of hydrogen on active charcoal as function of temperature and pressure . . . 1009

Q Dew point conversions . . . 1011

R Mass spectrometric resolutions required for the separation of the isotopes of hydrogen and helium . . . 1013

S Calorimetric measurements of the tritium inventory in a transportable uranium tritide vessel performed with four different calorimeters 1015

T Vacuum technology relevant data of selected gases 1017

U Temperature profile along a saturated and a non-saturated molecular sieve adsorber bed during regeneration 1019

V Licenses, Radiation Protection Instructions, Working Instructions, Working Procedures, Working Permits, Inspection Handbook, etc. regulating the operation of Tritium Laboratory Karlsruhe (TLK) 1021

W Exemption values, clearance levels, allowed activity concentration, and dosis coefficients for tritium 1025

X Some codes and standards applicable to the design and manufacture of the ITER fuel cycle 1029

Y Main isotopes in structural stainless-steel 56 mm inside of the plasma front side of the outboard shielding blanket of ITER 100 years after final shutdown of ITER . 1031

Bibliography **1033**

Index **1269**

List of Figures

2.1 Decay of tritium and concomitant pressure build up 9

2.2 Dependence of the specific tritium fraction from radioactive decay time 12

2.3 Potential energy as function of the inter-atomic separation of molecule HB 15

2.4 Viscosities of fluid D-T as function of temperature (and therefore of pressure) at several densities 25

2.5 Linear energy transfer function $L(E)$ for the deposition of tritium beta particle energies in hydrogen 34

2.6 Transmission curve for initially mono-energetic electrons 37

2.7 Comparison between the radiation chemistry of T_2O in the presence of 386 mbar T_2 as suppressor and without 61

2.8 Hydrogen production as function of storage time at three specific concentrations of tritium in water 62

2.9 Comparison of the rates of formation of tritiated hydrogen and oxygen from water containing 74 $TBq\,l^{-1}$ of tritium between experiment and theory 63

2.10 Initial reaction rates of formation of HTO as function of the initial concentration of tritium under a broad variety of experimental conditions 68

2.11 Sequential production routes of T_2O as function of time 70

2.12 Explosion limits of a stoichiometric hydrogen-oxygen mixture taking place in a spherical vessel of 7.4 cm diameter 74

2.13 Detonation velocities of hydrogen – oxygen mixtures 75

2.14 Reaction rate constant for the reaction of T_2 with D_2 as function of initial concentration of tritium 80

2.15 Evolution of tritium-substituted methane isotopologues as function of time in a 2.8 % CH_4 – 95.5 % T_2 mixture at ambient temperature 83

2.16 Evolution of the partial pressures of T_2, HT and H_2 as function of time in a T_2 : CH_4 = 2:1 mixture at ambient temperature determined in situ by laser Raman spectroscopy 84
2.17 Reaction of molecular tritium with carbon dioxide 87
2.18 Comparison of the rate of hydrogen pressure change in two different small storage getter beds containing uranium powder as function of overpressure 99
2.19 Dissociation pressures of uranium hydride, uranium deuteride and uranium tritide as function of inverse temperature 100
2.20 Pressure-composition isotherms of the hydrogen-uranium system (only the highest H/U atom ratios are displayed) 102
2.21 Cooling of a primary vessel holding 3 kg of uranium in a double-contained storage bed either under vacuum or with the annulus backfilled with argon or helium (broken line = theory and solid line = experiment) 103
2.22 Plot of data and illustration of an idealized spherical particle on the decomposition of uranium hydride 105
2.23 Release rate of decay helium from uranium as function of ageing time 107
2.24 Desorption isotherms of protium, deuterium and tritium at 343 K, 353 K and 363 K from the respective palladium hydrides 109
2.25 Desorption plateau pressures of protium, deuterium and tritium in the α+β two-phase region of palladium as function of inverse temperature 111
2.26 PCT data of the hydrogen-titanium system showing boundary locations 113
2.27 Uptake and release of hydrogen isotopologues from ZrCo at several temperatures 119
2.28 Desorption of a nearly equimolar hydrogen-deuterium mixture from a ZrCo bed . 125
2.29 Hydrogen isotopologue release from a ZrCo bed initially loaded with a D:H = 1:1 mixture 126
2.30 Monomer of Vespel® 139
2.31 Effect of dose on storage modulus of Nafion® films at 333 K after exposure to either gamma radiation from a ^{60}Co source or beta radiation emitted by tritium 143
2.32 Leak rate across valves furnished with O-rings of either Buna N, Viton A, or EDPM exposed to 53.3 mbar tritium as function of time 148

2.33 Evolution of the glass transition temperature, T_g, of elastomers expressed in Kelvin with time of exposure to 10^5 Pa gaseous tritium 149
2.34 Absorption of HTO (650-700 Bq cm^{-3}) by cement paste, cement paste coated with epoxy paint and cement paste coated with urethane paint 156
2.35 Calculated depth profiles of tritiated water in concrete exposed to air containing 2.1×10^5 Bq m^{-3} of tritium as function of exposure time 160
2.36 Modelling of the tritium concentration profile in concrete after exposure to air contaminated by tritiated moisture 164
2.37 Tritium distribution between surface and bulk of stainless-steel SS316 and corresponding BIXS results 178
2.38 Outgassing of differently pre-treated SS316 specimens in consecutive 100-degree steps: (a) mass spectrometrically determined total outgassing and (b) outgassing of water 183
2.39 Comparison of Sieverts constants determined for hydrogen and tritium in type SS316 and SS316L stainless-steel as function of inverse temperature by several investigators 187
2.40 Comparison of hydrogen and tritium diffusivities across stainless-steel type 316 and SS31L as function of inverse temperature determined by different research teams 188
2.41 Comparison between experimentally determined total long-term loss at ambient temperature from stainless-steel type 316 specimens 196
2.42 Depth profiles of tritium in non-homogeneously loaded type 316 stainless-steel specimens of 6 mm width supplied to HRC by JET 197
2.43 Calculated tritium depth profiles in initially non-homogeneously loaded stainless-steel 316L material 198
2.44 Calculated semi logarithmic plot of deuterium depth in a stainless-steel tube as function of tube length and time between injection and measurement at ambient temperature 200
2.45 Guideline for the prevention and control of damage by hydrogen 210
2.46 Number of bubbles in % as function of bubble diameter in nm at two helium concentrations in stainless-steel 316L 211
2.47 Tritium release at 323 K from two equally loaded GAS type specimens 224

2.48 Comparison of the average solubility values of hydrogen in low-activation materials with the solubility in iron as function of inverse temperature 228
2.49 Equilibrium concentrations of tritium in a Reduced Activation Ferritic/Martensitic (RAFM) membrane as function of hydrogen partial pressure in helium 230
2.50 Semi logarithmic plot of the solubility of hydrogen in copper as function of inverse temperature 235
2.51 Lennard-Jones potential diagram of the deuterium/copper system 238
2.52 Calculated specific activities and total activity (shown in fat black) in copper after irradiation with 4.15 MW m^{-2} for 2.5 years as function of time 242
2.53 Hydrogen and tritium solubility in gold 244
2.54 Diffusivities of tritium in nickel as function of inverse temperature 248
2.55 Calculated and experimental diffusion coefficients of H, D and T through Ni as function of inverse temperature 251
2.56 Diffusivities of hydrogen across beryllium 254
2.57 Permeation coefficients of hydrogen across beryllium as function of inverse temperature 257
2.58 Oxidation of beryllium (weight gain) under a stream of helium containing 1 % water vapour at temperatures up to 1023 K 260
2.59 Diffusion coefficients of hydrogen isotopes in tungsten as function of inverse temperature 275
2.60 Brittle to ductile transformation as function of temperature and comparison between typical brittle and ductile strain stress diagrams 279
2.61 Small model of the vertical divertor target from ITER and emerging macro cracks 280
2.62 Depth profile of deuterium in differnet locations in a tungsten crystal 288
2.63 Diffusion coefficients of hydrogen through palladium as function of inverse temperature 294
2.64 Melting thickness of Be and W calculated for vertical displacement events 303
2.65 Vaporization thickness of Be, W, or C calculated as function of time for a VDE event 304
2.66 Temperature rise of a copper substrate protected by either thick layers of C, Be, or W 304

2.67 Primary mechanisms describing the interaction of energetic hydrogen particles generated in a plasma with carbon-based materials 307
2.68 Toroidal distribution of tritium (in mg) in the divertor of JET 310
2.69 Tritium inventory increase as function of operation time calculated for ITER assuming several plasma-facing component combinations 314

3.1 Nupro SS316 stainless-steel valves with VCR® fittings, welded fittings, or Swagelok fittings 340
3.2 Nupro bellows valve 341
3.3 Typical UHV-tight gate valves 343
3.4 VCR® ultra-high vacuum tight assembly 345
3.5 Different types of Helicoflex gaskets 346
3.6 Flange to pipe welding 348
3.7 Examples of butt welding between the welded piping 348
3.8 Radiographic examination techniques of butt welds 361
3.9 Redundant alarms from tritium monitoring at TLK 368
3.10 Pressure rise in an evacuated chamber caused by a leak, and due to outgassing from a chamber wall 374
3.11 Simplified cross section drawing of Leybold turbomolecular pump examined at TLK for tritium contamination 381
3.12 Novel Turbo-V 750/850 TwisTorr turbo drag pump from Agilent Technologies featuring high compression ratio, high pumping speed and compact design 384
3.13 Hydrogen throughput of a $60\,m^3\,hour^{-1}$ pump determined as function of increasing constant exhaust pressures 386
3.14 Pumping throughput of a $18\,m^3\,hour^{-1}$ NORMETEX scroll pump as function of suction pressure for several gases 388
3.15 Pumping speeds for nitrogen and helium with a NORMETEX 15 scroll pump backed by a MB601 HP pump as function of suction pressure 391
3.16 Experimental arrangement for the investigation of the influence of water vapour on the performance of a NORMETEX pump 392

3.17 Scheme of a cryo-pump assembly showing the adsorber zone and the array of condensing Chevrons 398
3.18 Cryo-adsorption isotheres for helium and hydrogen on charcoal 401
3.19 Sequential desorption of some typical plasma exhaust components as function of temperature 403
3.20 Detailed drawing of an ITER prototype cryo-pump and of the integrated concentric array of 28 cryo-adsorption panel´s 406
3.21 Cryogenic pumping section (CPS) of KATRIN 408
3.22 Pumping speed as function of inlet pressure of Edwards EH1200 and EH250 multistage roughing pumps 411
3.23 Schematic view of the oil-free TOYO/JAERI reciprocating pump with four compression stages 416
3.24 Simplified KALPUREX process proposed for the inner fuel cycle of DEMO (DIR = direct internal recycling) 419
3.25 Isotherms showing the dependence of pressure in the U - H_2 system from composition expressed in H/U atom ratio 424
3.26 Effect of isothermal, adiabatic, or non-coooled/non-evacuated operation of a getter bed on the pumping efficiency of hydrogen 428
3.27 Fast delivery storage bed fabricated at KIT 435
3.28 Comparison between the release rate of deuterium expressed as loading fraction at time t 438
3.29 Schematic drawing of the SRS hydride storage bed 440
3.30 Temperature evolution as function of time in a JET uranium tritium storage bed and empirical calibration results with one of JET storage beds 447
3.31 Simplified diagram of a tritium storage bed designed for “in bed” calorimetry and typical temperature evolution during an inventory measurement 454
3.32 Metal hydride flowing gas calorimeter 455
3.33 Cross section of a tritium storage bed with “in-bed” calorimetry 455
3.34 Diffuser from Resource Services Incorporated 459
3.35 Model of a permeator cascade 460
3.36 Calculated permeation of a D:T = 1:1 mixture across a Pd/Ag membrane maintained 462

3.37 Influence of increasing partial pressures of CO in hydrogen on the specific permeation rate of hydrogen and permeation rate of pure hydrogen and hydrogen in the presence of various substances through a palladium / silver membrane 463
3.38 Novel platinum TKK-KNOITS catalyst applied either on a stainless-steel honeycomb carrier or a silicon carbide carrier 469
3.39 Turnover rate for the methanation of CO over diverse nickel catalysts as function of inverse temperature 472
3.40 Cryogenic trap concepts for the retention of water from a helium stream tested at Fontenay-aux-Roses and at TLK 479
3.41 Cubic array of 8 truncated octahedrons in the corners of the zeolite type A framework 488
3.42 Model to explain molecular sieving of hydrogen isotopologue molecules by zeolite 3A at cryogenic temperatures 490
3.43 Functional diagram of a differential Baratron® capacitance manometer (MKS) . 499
3.44 Schematic diagram of a humidifier 506
3.45 Operation principle of a mass controller 508
3.46 Determination of small volumes by the Variable Volume method showing scheme of principle and commercial device 511
3.47 Experimental arrangement for the determination of small volumes according to the Discontinuous Variable Volume method 512
3.48 Relative Raman intensities of H_2, HD, and D_2 as function of the initial fraction of H2 515
3.49 Infrared absorption bands of gases observed in the plasma exhaust of fusion machines 519
3.50 First and second vibration bands in the FTIR transmission spectra of liquid hydrogen and liquid deuterium and equilibrium concentrations of hydrogen and deuterium in the gas phase 522
3.51 Laser Raman cell and adjacent optics housed in a black box 524
3.52 Raman spectra of equilibrated hydrogen isotopologue mixtures 527
3.53 Raman spectroscopy employing a long hollow silver-lined glass fibre capillary . . 529
3.54 Raman spectrum of a hydrogen isotopologue mixture together with the radio luminescence lines of helium 530

3.55 Closed loop with integrated Raman cell for the preparation of calibrated $H_2/HD/D_2$ gas mixtures 532
3.56 Scheme of the A-loop of TRIHYDE 535
3.57 Calibration factor ratios 537
3.58 Mass spectrum of six hydrogen isotopes and ^3He 539
3.59 Mass spectrum of the products of the reaction of carbon monoxide with tritium obtained with an omegatron 544
3.60 Gas chromatographic separation of a D_2, DT, and T_2 mixture 550
3.61 Comparison of the eluate when a mixture of six hydrogen isotopologues is injected into an iron-doped alumina column held at cryogenic temperature 554
3.62 Exploded view of a TLK ionisation chamber 564
3.63 Calibration plots of current vs. specific activity of a small ionisation chamber at several total pressures 566
3.64 Combination of water purification and tritium monitoring of effluent water at Savannah River Site 573
3.65 The principle of operation of the accelerator mass spectrometer in Rossendorf and the depth profile of tritium and deuterium in specimen supplied by ASDEX after exposure to D-D-plasmas 575
3.66 Simplified schematic drawing of a twin cell inertial temperature control (ITC) calorimeter with integrated inertial feedback control 584
3.67 Schematic illustration of the TLK vacuum calorimeter type IGC-V05 586
3.68 BIXS set up and plot of the integral counting rate as function of the Q_2 (Q = H, T) 593
3.69 Tritium-compatible BIXS detector showing the beryllium window and the silicon drift detector utilized for the determination of HTO 594
3.70 Tungsten plate cut into several smaller fragments after retrieval from the TEXTOR limiter where the plate was subjected to numerous plasmas 597
3.71 Experimental set up to investigate the chemical form of tritium released during etching of stainless-steel 601
3.72 Quartz device for full combustion 606
3.73 Equilibrium decomposition of ethylene on a nickel catalyst in closed loop operation mode first without and then with integrated permeator 617

3.74 Original PERMCAT device options 621
3.75 Much simplified diagram illustrating the process principle of CAPER 623
3.76 Prototype plasma exhaust cleaning facility CAPER showing the PERMCAT device and the CAPRICE facility 624
3.77 Comparison between the old and the new layout of the PERMCAT used at TLK 625
3.78 Cross section of a first stage PMR permeator and schematic drawing of a second stage PMR permeator 628
3.79 Integrated Fuel Clean-up System and Isotope Separation System at TSTA for testing first and second stage PMR reactors 629
3.80 Block diagram of the basic process steps of the GE Healthcare Waste Treatment and Enrichment plant in Cardiff, UK (Q = H, D, T) 634
3.81 Operation principle of the zirconia electrolysis cell 637
3.82 Process concept for the detritiation of highly tritiated water displaying a double stage PERMCAT 644
3.83 Flow diagram of the tritium extraction system of a HCCB Test Blanket Module 650
3.84 Block diagram of the cryogenic hydrogen isotope distillation system installed at JET 656
3.85 Configuration of the cryogenic isotope separation process of ITER 658
3.86 Simplified scheme of the displacement gas chromatography isotope separation system of TLK 662
3.87 Simplified block diagram of the CECE process for recycling of tritium-contaminated heavy water operated at Chalk River Laboratories 671
3.88 Block diagram of the facility TRENTA encompassing a Water Detritiation System and an Isotope Separation System 673
3.89 Layout of the TRENTA permeator 675
3.90 Schemes of the solid polymer electrode and of a single unit of the water – hydrogen isotopic exchange column 678
3.91 Block diagram of the water detritiation system of JET 680
3.92 Wet scrubber for the decontamination of air from tritium 685
3.93 Uranium bed bake-off profile taken in 30 min intervals 693

4.1 GE Healthcare tritium transport concept 706

4.2 Configuration of the multi-purpose central pumping system of TPL 710
4.3 Configuration of a cryo-pump of ITER 712
4.4 Upgraded recombiner design and updated adsorber bed design 725
4.5 Simplified scheme of the TLK tritium removal concept from primary systems, glove boxes, and laboratory air 727
4.6 Commercial impermeable air supplied plastic suit for protection against open contamination 737
4.7 Safety cabinet for pressurized cylinders used at TLK 747
4.8 Unreacted fraction of hydrogen as function of catalyst temperature at several residence times and superficial velocities 753
4.9 Tritium removal from a glove box with an adjacent Tritium Removal System . . 756
4.10 Oxidation efficiency of diverse hydrocarbons on Hopcalite as function of temperature 763
4.11 Distribution of the tritium activity between a Pd or Pt catalyst and the cold trap at several catalyst temperatures after completion of the tests 765
4.12 Block diagram of the two stripper systems of the Replacement Tritium Facility each servicing 15 glove boxes 766
4.13 Flow diagram of the primary and secondary stripper systems of Replacement Tritium Facility at Savannah River Site 767
4.14 Flow diagram of the glove box stripper system at RTF 769
4.15 Schematic layout of a standalone inert gas glove box equipped with a getter clean-up system 773
4.16 Molecular sieve regeneration process developed at SRS 777
4.17 Dryer regeneration system of TPL 779
4.18 Simplified sketch of the AMOR system at TLK 781
4.19 Working principle of two different palladium/silver membrane reactors (PMR) employed to demonstrate the recovery of tritium from tritiated water thermally released from molecular sieve beds 784
4.20 Standard commercial feedthroughs supplied by GS Glove Box System Technik . . 796
4.21 Glove-box penetrating cable 797
4.22 Glove box penetration for tritium pipe including confinement jacket 798

5.1 Simplified scheme of the TLK ventilation system 814
5.2 Configuration of a flame arrester 816
5.3 Effect of pressure on the maximum experimental safe arrester gap 817
5.4 Schematic diagram of the modernized Instrumentation and Control (I&C) System of TLK 827
5.5 Simplified block diagram of the ITER inner deuterium/tritium fusion fuel cycle . 832

8.1 Tritium released via stack as HT and HTO from TPL during the fiscal years . . 848
8.2 Stack discharges of HTO through the Active Gas Handling System of JET in comparison to stack releases from the site as a whole 852
8.3 Storage tank for high level tritiated water displaying loop for the oxidation of hydrogen and a depression flow of rate F 859
8.4 Total activity and specific activities of the principal transmutation products expected in ITER structural steel SS316L(N) 878
8.5 Total radioactivity and radioactivity of tritium in potential pure first wall materials after one full power year (FPY) of operation 884
8.6 Thermal release of tritium from eight SS316 equally charged specimens under an argon stream 892
8.7 Thermal release of HTO and of HT from stainless-steel in two consecutive thermal steps 895
8.8 Thermal release of HTO and HT from stainless-steel SS316 during prolonged heating in two consecutive steps at constant temperatures 897
8.9 Schematic drawing of a reactor for the oxidation of tritiated solvents and reagents 899
8.10 Direct decontamination of a JET tile employing an oxygen – methane burner . . 916
8.11 Tritium outgassing from a waste bag into a bubbler as function of time 925
8.12 Schematic diagram of the arrangement employed for the indirect determination of the tritium inventory 926
8.13 Detailed drawing of the TPL-92-Y-450K transport vessel and a design for future transport vessel 935
8.14 KAERI concept of BU type vessel for the international transport of tritium . . . 936
8.15 Drawing of the JET vacuum cleaner 940

9.1 Interlinked Tritium Removal Systems at TPL 955

9.2 Tritium confinement and detritiation concept for the ITER tritium and tokamak buildings 957

10.1 Two diverse compact fusion reactor configurations 960

D.1 Van't Hoff plots of metal hydrides with potential for application in tritium handling systems 981

F.1 Diffusivities and solubilities of tritium in fusion reactor relevant metals 985

G.1 Optical microscopy of flakes from JET after DTE1 987

H.1 Tritium distribution on the plasma-exposed and plasma-shadowed sides of JET tile 004/1-44 after the DTE1 campaign 989

U.1 Temperature profile along a saturated and a non-saturated molecular sieve adsorber bed during regeneration 1019

List of Tables

2.1 Nuclear properties of tritium 11
2.2 Radioactive decay heat of elemental tritium 12
2.3 Molar volume of molecular hydrogen and deuterium in $cm^3\,mol^{-1}$ 14
2.4 Zero point energies (E_0), dissociation energies (D_0, D_{298}) and ionization energies (I) of all hydrogen isotopologues 16
2.5 Rotational states of hydrogen 16
2.6 Equilibrium population of the odd J-levels of elemental protium, deuterium and tritium 18
2.7 Fraction of hydrogen isotopologue molecules in the $J = 1$ state at cryogenic temperatures 19
2.8 Boiling points, triple points and critical point constants of molecular hydrogen isotopologues 21
2.9 Vapour pressures of tritium-containing elemental hydrogen isotopes at cryogenic temperatures 22
2.10 Saturation vapour pressures of all six isotopologues of molecular hydrogen 23
2.11 Coefficients for the calculation of the pressure dependence of viscosity for hydrogen 24
2.12 Equilibrium constants for hydrogen isotope mixtures at several temperatures . . 27
2.13 Gas phase transitions of isotopic hydrogen molecules in cm 28
2.14 Selected physical constants of liquid isotopic water 30
2.15 Ionisation constants of protium oxide and deuterium oxide at several temperatures 31
2.16 Assumed average energy losses per beta particle - molecule collision 33
2.17 Penetration depths of tritium β-particles into different materials at two $E(\beta)$ energies 35
2.18 Linear energy absorption coefficients of tritium beta particles by gases 39

2.19 Solubility decrease (in %) when H_2O is replaced by D_2O 43
2.20 Calculated steady state concentrations of products (in $\mathrm{mol\,cm^{-3}}$) from the self-radiolysis of T_2 at 298 K 54
2.21 Limits of inflamability of hydrogen – oxygen mixtures diluted in chemically inert gases 73
2.22 Kinetics of the reaction $H_2 + T_2 \longleftrightarrow 2\,HT$ 79
2.23 Equilibrium constant for the exchange reaction between water and tritiated hydrogen 81
2.24 First order exchange rates 85
2.25 Properties of the most promising getters for storage, handling and pressurizing tritium 94
2.26 Effective thermal conductivity of solid uranium, non-oxidized uranium metal powder and uranium hydride partly measured in the presence of inert gases . . . 95
2.27 Thermodynamic properties of uranium hydrides 100
2.28 A and B parameters and enthalpy of solution of hydrogen isotopes in pure Ti and Ti containing oxygen 115
2.29 Van´t Hoff parameters of the $ZrCoQ_x$ (Q=H, D, T) system 118
2.30 Sieverts´ constants (K_S) for the solubility of hydrogen (H) and deuterium (D) in zirconium cobalt (ZrCo) 120
2.31 Arrhenius parameters for disproportionation and reproportionation of ZrCo induced by hydrogen isotopes 122
2.32 Tritium tests of elastomers exposed to 93 % tritium (balance deuterium and helium) for more than 4 month at ambient temperature 147
2.33 Diffusivity, solubility and permeability of water vapour across glove materials at (312 ± 1) K 150
2.34 Permeability constants of HT and HTO through rubbers 152
2.35 Comparison of sorption coefficients of water on organic construction materials, common paints and cement 154
2.36 Diffusivities, solubilities and permeabilities of tritiated water of various paints at ambient temperature 155
2.37 Water released thermally from hardened cement paste 159
2.38 Tritium sorption on concrete or cement after exposure to HTO 163

2.39 Tritium sorption by glass exposed to humid air containing HTO and HT 168
2.40 Fraction of tritium leaching into water from stainless-steel exposed to gaseous tritium at ambient or elevated temperature 177
2.41 Sieverts constants for hydrogen isotopes in several austenitic stainless-steels and nickel alloys 189
2.42 Diffusion coefficients of hydrogen isotopes through ITER-relevant austenitic stainless-steels and nickel alloys 190
2.43 Pre-exponential factors and activation energies for solubility, diffusivity and permeability of hydrogen isotopologues across SS316L 193
2.44 Sieverts constants of hydrogen in austenitic stainless-steels 207
2.45 Tritium, deuterium and hydrogen permeation parameters through pure stainless steel base metals (Fe, Ni), as well as several ferritic and austenitic heat-resistant construction materials 219
2.46 Material properties of type F82H as function of temperature 223
2.47 Arrhenius constants for the diffusivity and solubility of hydrogen isotopes in "virgin" α-iron, MANET, F82H and BATMAN 226
2.48 Molar enthalpies and relative partial molar excess entropies for hydrogen in copper 234
2.49 Diffusion coefficients of hydrogen isotopes in copper 236
2.50 Arrhenius constants for the permeability of hydrogen across copper 237
2.51 Molar enthalpies and relative partial molar excess entropies for the solubility of hydrogen in silver and gold 243
2.52 Permeability of hydrogen across gold and silver 246
2.53 Arrhenius constants for diffusivity and solubility of hydrogen isotopes in nickel . 247
2.54 Diffusion, solubility and permeation data of hydrogen isotopes in beryllium . . . 255
2.55 Evolution as function of decay times of the specific activity of activation products generated in beryllium 267
2.56 Sieverts' constants and diffusivities for hydrogen isotopes in different types of tungsten materials 273
2.57 Calculated evolution at three decay periods of the specific activity of the activation products generated in tungsten exposed in the divertor to an average fluency of 0.091 MW year m^{-2} 292

2.58 Diffusion parameters of hydrogen in palladium and palladium/silver alloys at 533-913 K and low hydrogen concentrations 295
2.59 Two phase transition entropies and enthalpies of the Pd-X and $Pd_{0.90}Al_{0.1}$–X systems (X = H, D, T) 296
2.60 Long-term permeator durability tests under tritium at 623 K 298
2.61 Compilation of Arrhenius parameters used for the calculation of diffusivities and solubilities of tritium in metals and alloys of minor relevance to fusion 301
2.62 Comparison of relevant properties of potential armour materials 305

3.1 Leak test of Swagelok valves 338
3.2 Hydrostatic pressure test of Swagelok valves 339
3.3 Maximum helium leak rates of ultra-high vacuum equipment 376
3.4 Vacua attainable with relevant plasma exhaust gases employing three different scroll pumps 387
3.5 Pumping data of several dry mechanical NORMETEX pumps 389
3.6 Pump characteristics of scroll pumps in series or scroll pumps operated in series also in combination with a Metal Bellows pump 390
3.7 Edwards pump with suction blanked off and utilizing a metal bellows backing pump 393
3.8 Vacua achievable with hydrogen isotopologues employing a single pump or a pump combimation 396
3.9 Cryo-sorption of hydrogen and deuterium on different adsorbers at 1000 mbar equilibrium pressure (in cm^3 (STP) /g) 482
3.10 Langmuir constants of hydrogen isotopes (Q_i) on molecular sieves 4A and 5A, and active carbon at 77 K 486
3.11 Separation factors of HD/H_2 and D_2/H_2 by molecular sieving adsorption using zeolite 3A 491
3.12 Gas chromatographic columns and detectors used to identify the gaseous species observed at CAPER 557
3.13 Ionization induced by tritium in several gases 563
3.14 Determined water quality parameters at SRS 572

3.15 Comparison of several calorimeters used in laboratories worldwide for the determination of tritium inventories in solid and liquid materials 589
3.16 Chemical form of tritium released from stainless-steel SS316 into an etching solution at ambient temperature 602

4.1 Failure frequency of components in tritium service at TPL during the period April 1988 – March 1999 735
4.2 Regeneration of molecular sieve beds with the AMOR facility 782

8.1 Stack concentrations of tritium-bearing species measured at JET during PTE in 1991 $kBq\,m^{-3}$ 850
8.2 Effective G_{H_2} values for the self-radiolysis of tritiated water at 293 K 861
8.3 Chemical composition of JET flakes determined by two independent research teams 870
8.4 Characterization of carbon dust from TFTR and JET 871
8.5 High temperature outgassing of stainless-steel at temperatures in the range 873-1873 K for a period of 10 min at each temperature 893

C.1 Tritium compressibility factors at 295 K in the low-pressure range 979

E.1 Radiation resistance of polymers (information supplied by CEA) 983

I.1 Chemical composition of austenitic stainless-steels habitually used in tritium handling systems 991

J.1 Designations of some common standardized steels used in tritium handling facilities 993

K.1 Chemical composition of the structural stainless-steel specified for ITER, i.e. SS316L (N) 995

L.1 Tolerable pressure and temperature ranges of Swagelok valves with VCR® connections (for not radiographed valves the pressure ratings should be reduced by 15 %) 998

M.1 Nupro® shut-off SS316 valves (B series valves feature demontable bonnets for cleaning or replacement purposes) 999

P.1 Cryo-adsorption of hydrogen on active charcoal as function of temperature and pressure 1009

Q.1 Dew point conversions 1011

R.1 Mass spectrometric resolutions required for the separation of the isotopes of hydrogen and helium 1013

S.1 Calorimetric measurements of the tritium inventory in a transportable uranium tritide vessel performed with four different calorimeters 1015

T.1 Vacuum technology relevant data of selected gases 1017

W.1 Exemption values, clearance levels, allowed activity concentration, and dosis coefficients for tritium 1025

Y.1 Main isotopes in structural stainless-steel 56 mm inside of the plasma front side of the outboard shielding blanket of ITER 100 years after final shutdown of ITER . 1031

1 Preamble: Purpose and Scope

The worldwide population increase and the need to raise standards of living in developing and transition countries has generated enormous energy demands that can only be contented by new energy technologies. Along this line, fusion offers the expectation of a nearly limitless, safe, economically competitive, and environmentally acceptable source of energy [Tos97; ITE99; Lac00; Tos01; War05; Chu12a, and others]. Advantageously, fusion energy raises no concerns about fuel availability, nuclear proliferation, long-lived radioactive waste, the possibility of meltdown (intrinsic safety), or the emission of greenhouse gases. The scientific base for a fusion powered electricity generating plant of the future is currently being laid by research activities taking place worldwide in large experimental fusion devices such as JET[1] in Abingdon, Great Britain (now under decommissioning) [Haa89; Pam01; Roo13]; JT-60SA (since 2023 the largest experimental fusion machine worldwide) in Naka, Japan [Nin90; Oik02; Mat04]; Tore Supra in Cadarache, France [Sao09]; ASDEX Upgrade in Garching, Germany [Sip02; Kal11]; General Atomics DIII-D at the National Fusion Facility in San Diego, USA [Sch10]; Wendelstein 7X in Greifswald, Germany [Wob97; Weg09; Rum13][2]; ALCATOR C-Mod, MIT, Cambridge [Gre14]; or the Large Helical Device at National Institute for Fusion Science in Nagoya, Japan [Fuj00]. Significant contributions have furthermore been acquired from numerous research activities carried out while dismantling machines like TEXTOR in Jülich (dismantled 2016), Germany [Sam99; Tan00a; Tan00b; Phi07] or TFTR in Princeton, USA [And95c; Mue97; Wil97] or the tritium facility TSTA in Los Alamos [Wil02; Tes05]. The operation of the available fusion machines and construction of major new fusion-relevant experiments like the facility IFMIF, Japan [Moe06; Moe07], lead to activities and campaigns planned and performed by closely collaborating, frequently fluctuating, multinational research teams. Publications like [Hug92b], [Sip02], or [Kal11] illustrate by way

[1] For acronyms refer to Appendix A.

[2] The Wendelstein stellarator fusion device achieved 2018 a record 30 s plasma at 6 MW with an input heating of 200 MJ and a 100 s plasma at 2 MW at reduced power.

of example the magnitude of these collaborations and the tremendous international joint effort required from scientists, engineers, support personnel, and project managements. Important complementary contributions mostly in form of fundamental scientific research comes from several large, medium, and small sized tritium-handling laboratories like TLK, Karlsruhe, Germany [Ach90; Sch91a; Vol95; Bes97; Pen00b; Bah02]; TPL, Tokai mura, Japan [Nar90; Oku97; Yam11a; Oya14]; Valduc, Is-sur-Tile, France [Gir92]; SRS, Aiken, USA [Ort90; Poo05]; STAR, Idaho Falls, USA [And02; And05]; the now disassembled facility TSTA, Los Alamos, USA [And77; And88]; and a large number of institutions like for example Ontario Hydro, Canada [Shm92; Hei88a]; HRC in Toyama, Japan; or KAERI at Yuseong, Korea [Chu08b; Chu08a; Chu11; Chu12b]; etc. similarly dedicated to fusion-relevant activities with tritium. Additional input has been provided by numerous studies mostly within international cooperations like STARFIRE [Bak81]; "Assessment of Technical Risks and R&D Requirements for a Magnetic Confinement Fusion Fuel System" prepared by the Electric Power Research Institute in California, USA [DeF83]; the European Programme on Safety and Environmental Assessment of Fusion Power (SEAFP) [Mit93; Coo00; Tay00a]; the High Average Power Laser (HAPL) Inertial Fusion Energy Reactor [Raf06; Sha07]; or ARIES ACT advanced tokamak fusion reactor study [Naj91; Naj06]; to name just a few. The latter report describes a conceptually planned fusion power plant featuring advanced technologies comprising SiC/SiC composite structures of low activation, high temperature resilient materials, and molten eutectic lead-lithium (PbLi) alloy fluid that acts both as coolant and breeder.

For decades now most of the multinational activities have been coordinated by well-established international organizations like for example the Next European Torus Team (NET-Team) [Cha88c] or the Fusion4Energy Team [Par97; Par98; Mur00; Glu06c; Ski08]. The transnational decision taken June 2005 to erect and operate the International Thermonuclear Experimental Reactor (ITER) [Aym97; Aym01; How04; Jan07; Hol07] in Cadarache, France, constitutes a further crucial step towards the joint creation of prototype fusion reactors. Main objectives of the basic science and technology program of ITER are i) achievement of self-sustained thermonuclear burns, ii) demonstration of extended burn times, and iii) testing of several diverse tritium breeder blankets. The long-term goals of the activities are demonstration of i) the technological feasibility, ii) operational safety, iii) environmental compatibility, iv) economic viability, and last not least v) the capability to meet the energy needs of society.

A first conceptual design of ITER was completed 1991 in a collaborative effort between the EU, Japan, Russia, and USA; a detailed engineering design was completed 2001. China and Korea joined the ITER project 2003; USA re-joined the project the same year. The last to join was India in 2005. Non-member technical cooperation agreements have been signed by the ITER Organisation with Australia and Kazakhstan in 2017. Within the frame of the Fusion4Energy Program established 2007, whose objective is to coordinate Europe's contribution to ITER, a large number of sizeable tritium-relevant research programs are currently ongoing in Europe. For example, as part of the development of a vacuum pumping system, a program on procurement of pre-production components whose parametric testing may contribute effectively to reduce programmatic, technological, and cost risks for ITER, is presently under way [Pap11]. Another important contribution was provided by the JET machine, where all plasma facing carbon-based components installed in the vacuum vessel - already contaminated with tritium - have been replaced by beryllium tiles and a full tungsten divertor in order to investigate ITER-plasmas under simulation of a typical ITER first wall arrangement [Pia07; Rom09; Phi10; Mat11; Hor12]. Under these conditions, temeratures of about 150 million degrees were attained at JET for the duration of five seconds releasing an energy of about $11\,\mathrm{MW\,s^{-1}}$. With full metal plasma facing components (PFC's), i.e. Be and W for main wall and divertor, tests were peformed to obtain pertinent information on tritium retention in the first wall[Rom09]. This topic is of high priority to establish a database on fuel retention of mobilizable tritium (the limit by nuclear license is 700 g in ITER). The properties of tungsten as plasma-facing component havealso been evaluated experimentally from the perspective of ITER needs by diverse scientist teams at ASDEX Upgrade, at JET, Culham [Roo13] and in smaller laboratories within the frame of an ITER-like Wall (ILW) program [Bre15; Hat19; Ash20]. Further JET enhancements have included a new pellet injection system, an upgrade of the vertical stability, and improved diagnostics. The broader aim of the program was to demonstrate integrated operational scenarios with ITER-relevant fuel in time before completion of the construction phase of the ITER machine. To ensure efficient tritium breeding with DEMO, nearly all ITER member countries are contributing to a Test Blanket Module programme comparing two solid breeders and five liquid breeder concepts to be evaluated with six different mock ups [Gia06; Gia07; Gia12]. In support of the ITER licensing process a revised set of documents encompassing a preliminary safety report and an environmental impact study has been submitted March 2010 by the ITER Organisation to

the French Nuclear Safety Authorities [Tay12]. Substantial progress has likewise been achieved with the inner fuel cycle of the ITER machine, which has been designed for flexible and reliable processing of considerable amounts of deuterium and tritium at unprecedented flow rates as well as unprecedented decontamination factors both with respect to effluents as well as release streams [Yos02; Glu06c; Glu07]. Because constant supply and self-sufficiency of tritium are critical to the implementation of fusion energy, the availability of a safe and absolutely dependable **fusion fuel cycle** is of paramount importance to the achievement of sustained ignition and burns of long duration in deuterium/tritium plasmas [Lae99b; Yos01; Yos02; Glu06c].

According to present planning, the construction of ITER, which is already under way, will be completed not earlier than 2034. The magnitude of the task is visualized by the volume of ITER, which is about eight times larger than JET. A prolonged commissioning phase beginning with hydrogen and continuing with deuterium containing traces of tritium is aimed at testing promising physic regimes and demonstrating the operation of all systems collectively. First plasmas with a 1:1 mixture of deuterium and tritium are expected in 2039 or later.

Another rather substantial complementary effort known as **Broader Approach (BA)** comprises activities running in parallel to those for ITER. They are mostly carried out in Japan within the frame of international collaborations with other ITER partners. The BA activities, which encompass the International Fusion Materials Irradiation Facility (IFMIF) [Mar96; Moe06; Moe07]; the International Fusion Energy Research Centre; and a Satellite Tokamak [Nis12]; are progressing well. As part of the Engineering Validation and Engineering Design Activities for IFMIF, the construction and installation of a lithium test loop containing approximately 2.5 t of lithium has been finalized at the O-arai site of Japan Atomic Energy Association (JAEA) [Kon12]. Moreover, a deuteron injector is being completed and the installation of a RF quadrupole accelerator as well as of a RF power generator are well in progress.

The next step following ITER is **DEMO**, for which the development of an overall design concept has been ongoing for many years [Tob06; Jan07]. Principal aim of the controlled thermonuclear reactor DEMO is demonstration of large-scale production of electrical power while achieving and maintaining fuel self-sufficiency [Saw06]. Of overriding importance for this goal is the development and demonstration under realistic conditions of a reliable **blanket concept**. Currently, efforts have been focussed on only two diverse reference concepts: a **helium cooled lithium lead** (HCLL) blanket and a **helium cooled pebble bed** (HCPB) blanket

employing EUROFER as structural material [Boc04; Gia05; Gia07; Gia12]. In spite of substantial progress of the DEMO project, there are still important unresolved tritium technology issues. For example, Nakamura et al. [Nak06] concluded in a paper on prognosticated tritium inventory and permeation issues of DEMO, that unless additional permeation barriers are installed, the tritium losses into the coolant systems of the presently selected plasma facing component combination would by far exceed the agreed upon guidelines.

Remarkably, tritium technology developed at TLK for fusion has been the main justification for choosing this laboratory to host the technical-sized Karlsruhe Tritium Neutrino (KATRIN) Experiment whose objective is the direct measurement of the absolute mass of the electron antineutrino by precise monitoring of the tritium β-spectrum near its end point [Wei99; Ase01; Wei05; Bor11; Bor15]. The expected results could be of consequence to particle physics, astrophysics, and cosmology. Conversely, numerous research outcomes pertaining for instance qualitative and quantitative analytics of hydrogen isotopologues or pumping of tritium by the so-called argon frost technique, presently under development at TLK to satisfy unique and stringent requirements of the KATRIN experiment, are not only indispensable for the success of KATRIN [Eic08; Stu10; Stu21] but may also be of benefit to tritium technology needed for the fusion program.

The present Tritium Manual introduces the main physical, chemical, and physicochemical properties of tritium and reviews compactly major technologies developed, demonstrated, and upgraded over past decades to handle and process fusion relevant tritium-bearing chemical species. The manual goes over working principles and construction characteristics of selected small and large tritium-compatible components, and discusses and evaluates processes emphasizing those recognized as having high probability for implementation in tritium systems for ITER. Whenever deemed appropriate, a comparison of alternative process options has been presented. Abundant information's are provided on the chemical and physicochemical interactions of tritium with relevant pure metals and alloys as well as organic and inorganic materials. Design measures and working practices for safe handling of tritium emerged from a vast body of experience accumulated worldwide are dealt with in some depth. Several important topics like breeder blankets and breeder materials, radiological hazards and dosimetry, environmental monitoring of tritium, or its fate in the environment have been left out to avoid excessive extension of the manual. Conversely, much attention has been focused on basic design principles and technologies

such as needed for i) the containment and confinement of tritium, ii) processes destined to remove tritium from effluent gases, iii) the immobilization and storage of tritium, iv) concepts for the recovery of tritium from process streams, v) processes for the recovery of tritium from highly tritiated water, vi) technologies for isotope separation, vii) component failure analysis, viii) criteria for waste sentencing, and ix) procedures for waste conditioning. Recommendations are given for the conception and construction of tritium-compatible equipment while complying with high safety standards of the kind needed for the conduction of experimental programs or routinely operated systems. Whilst understandably the manual relies heavily on experience accumulated during design, construction, and various operation phases of the Tritium Laboratory in Karlsruhe (TLK) it also considers to a very large extent operational and research results gained in other tritium installations worldwide. The Manual provides easy access to tritium-related literature not only pertaining ITER but also - and to a significant extent - to work beyond the scope of this project.

2 Tritium Properties

2.1 Chemical properties

Tritium is a colourless, odourless, and tasteless radioactive isotope of hydrogen. All hydrogen isotopologues have essentially the same chemical properties. However, self-radiolysis processes induced by decay via generation of radicals and ionizing beta-particles emitted by tritium can influence significantly mechanisms and rates of chemical reactions. Accordingly, tritium can undergo reactions with a wide variety of compounds and materials either directly or via isotopic exchange. Direct reactions are possible because the relatively weak energy of the beta particles emitted by tritium is still sufficiently high to break organic and other bonds. Many reactions of tritium are therefore of radiolytic nature. When tritium replaces hydrogen atoms of a hydrogenous material and subsequently decays into inert helium the material becomes damaged and susceptible to molecular rearrangement. Tritium constitutes about 10^{-18} % of hydrogen in nature[1].

All molecular isotopologues of hydrogen are flammable and can undergo detonations if the right conditions prevail.

2.2 Physical and nuclear properties

Tritium is the only isotope of hydrogen that is radioactive. It decays by emission of a weak beta particle (electron) into ^{3}He and an antineutrino ($\bar{\nu}$) from one of the tritium neutrons according to the reaction

$$^3_1\mathrm{H} \longrightarrow {}^3_2\mathrm{He} + \beta^- + \bar{\nu} \ .$$

The released decay energy is constant; it is shared between the beta particle and the antineutrino. Thus, all beta particles emitted by tritium will not all have the same energy. Their energy will vary from zero up to 18.6 keV and have an average value of 5.69 keV. Tritium does not emit γ-radiation.

The occurrence of a transmutation reaction with formation of helium has implications on numerous technical issues such as for example tritium analytics, tritium storage in getter materials, tritium material balance, mechanical and welding properties of structural materials, permeability

[1] The natural abundances of hydrogen and deuterium are 99.985 % and 0.015 %, respectively.

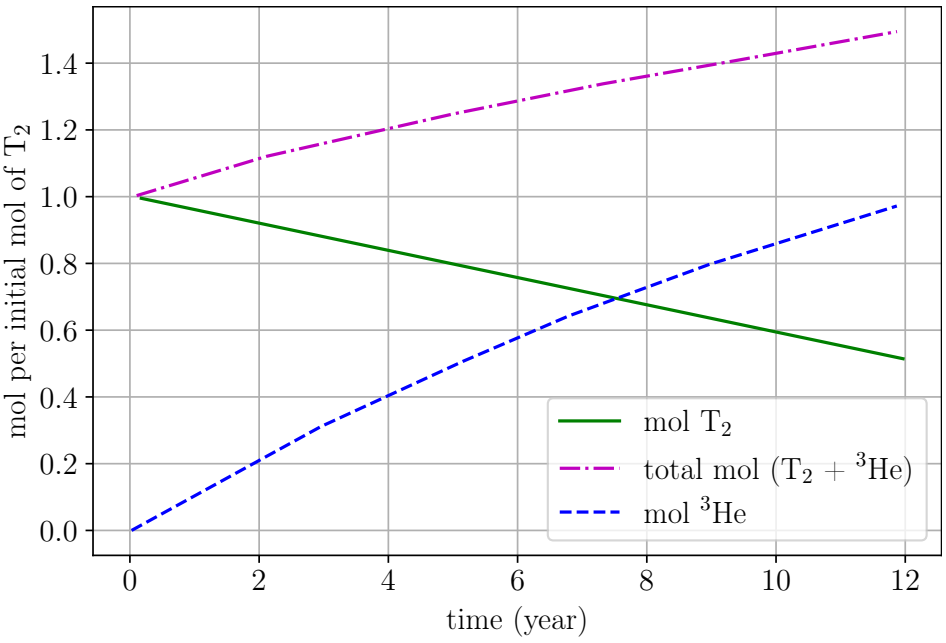


Figure 2.1: Decay of tritium and concomitant pressure build up.

across tritium purification membranes, storage of tritium in closed vessels, the mechanism and kinetics of chemical reactions, etc.

Numerical values of a number of well-known and frequently utilized basic nuclear and physical properties of tritium are compiled in Table 2.1. Because of the rather different masses of molecular protium, deuterium, and tritium, their physicochemical properties show substantial isotope effects.

As is the case with all radioactive nuclei, the decay of tritium follows first order kinetics. When pure tritium decays isochorically at constant temperature, the tritium partial pressure will decrease and that of helium increase with progressing time (the full decay of one mol T_2 will yield two mol ^{3}He). Hence, at infinite time, the total pressure in the container will double. The moles of molecular tritium (T_2), of the helium isotope ^{3}He, and the total number of moles (T_2 + ^{3}He) establishing after a period of time of t years can be calculated from the following three equations (see also fig. 2.1):

$$n_{T_2} = n^0_{T_2} \exp\left(\frac{t \ln 0.5}{12.32}\right)$$
$$n_{^3He} = 2n^0_{T_2}\left(2 - \exp\left(\frac{t \ln 0.5}{12.32}\right)\right)$$
$$n_{T_2} + n_{^3He} = n^0_{T_2}\left(2 - \exp\left(\frac{t \ln 0.5}{12.32}\right)\right) \ .$$

The increase in total pressure, p_{tot}, which establishes in a closed vessel when pure molecular tritium decays for a period of t years can be calculated from expression

$$p_{tot} = p^0_{T_2}\left(2 - \exp\left(\frac{t \ln 0.5}{12.32}\right)\right) \ .$$

To visualize the impact of radioactive decay on the fraction of individual nuclides in waste containing radioactive isotopes of different half-life's the decay of single nuclides is frequently plotted as displayed in Fig. 2.2.

The half-life of tritium has been determined by a number of researchers using diverse techniques such as beta counting, helium-3 collection, calorimetry, and Bremsstrahlung counting. A comprehensive review and critical evaluation of these measurements was performed by Lucas and Unterweger [Luc00]. For the half-life of tritium, they recommended a value of (4500 ± 8) d where 8 d denotes standard uncertainty. In another more recent evaluation, a value of (4497 ± 4) d was calculated [Mac06].

Experimental evidence provided by Akulov and Mamyrin [Aku04; Aku05] revealed that the triton beta decay constant has slightly different values, i.e. (12.296 ± 0.017) year and (12.264 ± 0.018) year depending on whether the measurement relies on atomic or molecular tritium, respectively. These values were obtained when comparing the helium-3 generated by radioactive decay in samples containing either atomic (ground atomic state) or molecular tritium together with a known amount of helium-4 used as reference. Atomic tritium was generated with a RF discharge across molecular tritium under conditions that allowed achievement of a plateau corresponding to nearly 100 % dissociation. The value of the dissociation degree was determined mass spectrometrically as well as spectroscopically employing Balmer series spectral lines.

Table 2.1: Nuclear properties of tritium [Eva75; Mac73; Sou86].*

Half-life	(4500 ± 8) d or 12.323 year [Luc00], (4497 ± 4) d [Mac06]
Decay constant	$1.782 \times 10^{-9}\,\mathrm{s}^{-1}$
Specific activity	$3.559 \times 10^{14}\,\mathrm{Bq\,g}^{-1}$ of T_2 gas at STP
	$1.184 \times 10^{14}\,\mathrm{Bq\,ml}^{-1}$ of T_2O (l)
	$9.75 \times 10^{3}\,\mathrm{Ci\,g}^{-1}$ or $361\,\mathrm{Bq\,g}^{-1}$
	$5.61 \times 10^{8}\,\mathrm{atoms_T\ Bq}^{-1}$
Mean β energy	5.685 keV
Derived air concentration (DAC)	$8 \times 10^{5}\,\mathrm{Bq\,m}^{-3}$ (HTO) and $2 \times 10^{10}\,\mathrm{Bq\,m}^{-3}$
Maximum β energy	18.6 keV
Decay energy density	$0.3240\,\mathrm{W\,g}^{-1}$ or $1.944\,\mathrm{W\,mol}^{-1}$
Tritium decay factor	$0.999\,846\,0\,\mathrm{d}^{-1}$
Specific ^{3}He generation rate	$1.3205 \times 10^{-5}\,\mathrm{cm^3\ STP\ s^{-1}\ g_{T_2}^{-1}}$
Atomic weight	3.016 05
Melting point	20.62 K
Heat of sublimation	$1.645\,\mathrm{kJ\,mol}^{-1}$ at triple point
Boiling point	25.04 K
Heat of vaporization	$1.394\,\mathrm{kJ\,mol}^{-1}$
Molecular weight	6.032 10
Dissociation energy ($T_2 \longrightarrow 2\,T$)	4.59 eV
Ionisation energy ($T \longrightarrow T^+ + e$)	13.55 eV
Max. range of β (18.6 keV) in air	4.5 - 6 mm
Max. range of β (18.6 keV) in H_2O	0.005 - 0.007 mm
Max. range of β (18.6 keV) in SS	0.0008 mm
Approx. diameter of a T atom	1.1 Å
Monomolecular layer of T on SS	$8.5 \times 10^{14}\,\mathrm{molecules\,cm}^{-2}$
Monomolecular layer of HTO on SS	$6.8 \times 10^{14}\,\mathrm{molecules\,cm}^{-2}$ [Dic92]
Nuclear spin	½
T-T bond energy	447.15 kJ at 298 K

STP = standard temperature 273.15 K and pressure 101.325 kPa

SS = stainless-steel

For constants and conversions consult Appendix B

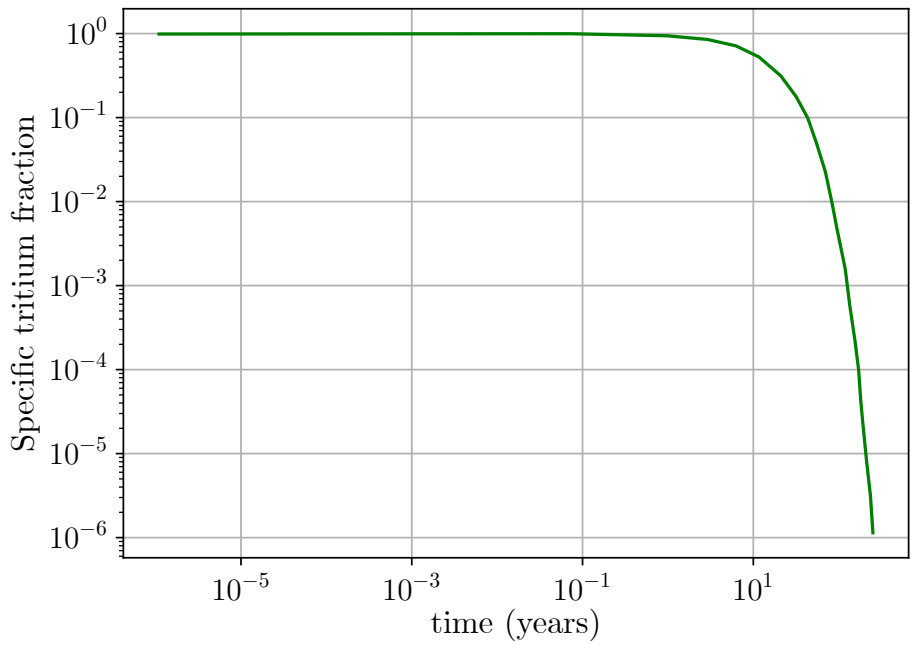


Figure 2.2: Dependence of the specific tritium fraction from radioactive decay time.

2.3 Radioactive decay heat

Gaseous, liquid, and solid tritiated species are self-heating due to self-absorption of the emitted β-particles. Table 2.2 lists the decay heat of pure elemental tritium in two states of aggregation, i.e. gas at STP and solid. Owing to the difference in density, the specific radioactive decay heat of solid tritium is substantially higher than that of gaseous tritium.

Table 2.2: Radioactive decay heat of elemental tritium.

T_2	$W\,cm^{-3}$
Gas at STP	0.000 087 1
Solid at 4 K	0.104

2.4 Annual Limit for Intake and Derived Air Concentration values for tritium

The permissible Annual Limit for Intake (ALI) for the inhalation of tritium is 7.4×10^8 Bq. It is customary to give the ALI in units of radioactivity because this value is easier to determine and control than the intake by a worker.

The Derived Air Concentration (DAC) is the concentration of tritium in air expressed in ($\mathrm{Bq\,m^{-3}}$), which yields the permissible level after one year of inhalation. Since the breathing rate at work of a „reference person“ is on the average $2400\,\mathrm{m^3}$ per year a DAC value of $3.1 \times 10^5\,\mathrm{Bq\,m^{-3}}$ can be estimated from the ALI if it is assumed that the person spends about $2000\,\mathrm{hour\,year^{-1}}$ at work (see also table 2.1).

2.5 Physical and physicochemical properties of molecular tritium and tritium oxide

Selected physical and chemical properties of molecular tritium and tritiated water, particularly when of possible relevance to tritium-handling systems of the fusion fuel cycle, are reviewed and discussed in this chapter.

2.5.1 Molecular tritium

This section focuses on some basic physical and physico chemical properties of elemental tritium, i.e. density, dissociation energies, zero-point energies, ionization energies, rotational states of hydrogen, triple and critical points, vapour pressures, viscosities, isotopic scrambling, infrared and Raman absorption, etc.

2.5.1.1 Molar volume of hydrogen and deuterium

A selection of hydrogen and deuterium molar volumes (also called inverse molar density) at liquid nitrogen and ambient temperature are listed in Table 2.3 within the broad pressure range 3.2×10^3 - 3.2×10^9 Pa [Sou86].

Table 2.3: Molar volume of molecular hydrogen and deuterium in $cm^3\,mol^{-1}$ (after [Sou86]).

Pressure	77.36 K		300 K	
Pa	H_2	D_2	H_2	D_2
3.16×10^9	**9.25***	**9.00***	10.00	9.82
1.00×10^8	22.3	22.1	40.9	40.6
1.00×10^6	633	631	2.51×10^3	2.51×10^3
3.16×10^4	2.03×10^4	2.03×10^4	7.89×10^4	7.89×10^4
3.16×10^3	2.03×10^5	2.03×10^5	7.89×10^5	7.89×10^5

* Solid phase

2.5.1.2 Dissociation energies (D), zero-point energies (E_0), and ionization energies (I) of hydrogen isotopes

The potential energy function describing a bond between atom H and atom B (or several atoms) other than hydrogen is plotted in Fig. 2.3 The distance between the atoms at equilibrium is given by r_0 and the energy at which dissociation takes place by D_0. The energy of dissociation, D_e, of a diatomic molecule is actually given by the difference between the potential energy of the atoms when infinitely separated and their energy when the atoms are at rest at the equilibrium separation. As apparent, the dissociation energy difference of bonds between hydrogen isotopologues and B is considerable.

Since the vibrationally unexcited molecule retains a residual energy, i.e. zero-point energy $E_0 = 1/2h\nu QB$ (Q = H, D, T), the expression of vibrationally not exited molecules and the dissociation energy D_0 at 0 K of the H-B, D-B or T-B bonds of vibrationally not exited molecules becomes

$$D_e = D_o(\mathrm{HB}) + \frac{1}{2}h\nu_{\mathrm{HB}} = D_0(\mathrm{DB}) + \frac{1}{2}h\nu_{\mathrm{DB}} = D_0(\mathrm{TB}) + \frac{1}{2}h\nu_{\mathrm{TB}}$$

respectively. As evident from Fig. 2.3, the smaller the zero-point energy the higher the dissociation energy D_0. Therefore, the smaller the zero-point energy the shorter the distance between the atoms. Zero-point energies and dissociation energies of all six molecular hydrogen isotopologues are listed in Table 2.4. The Table also lists the respective molecular ionisation energies, I,

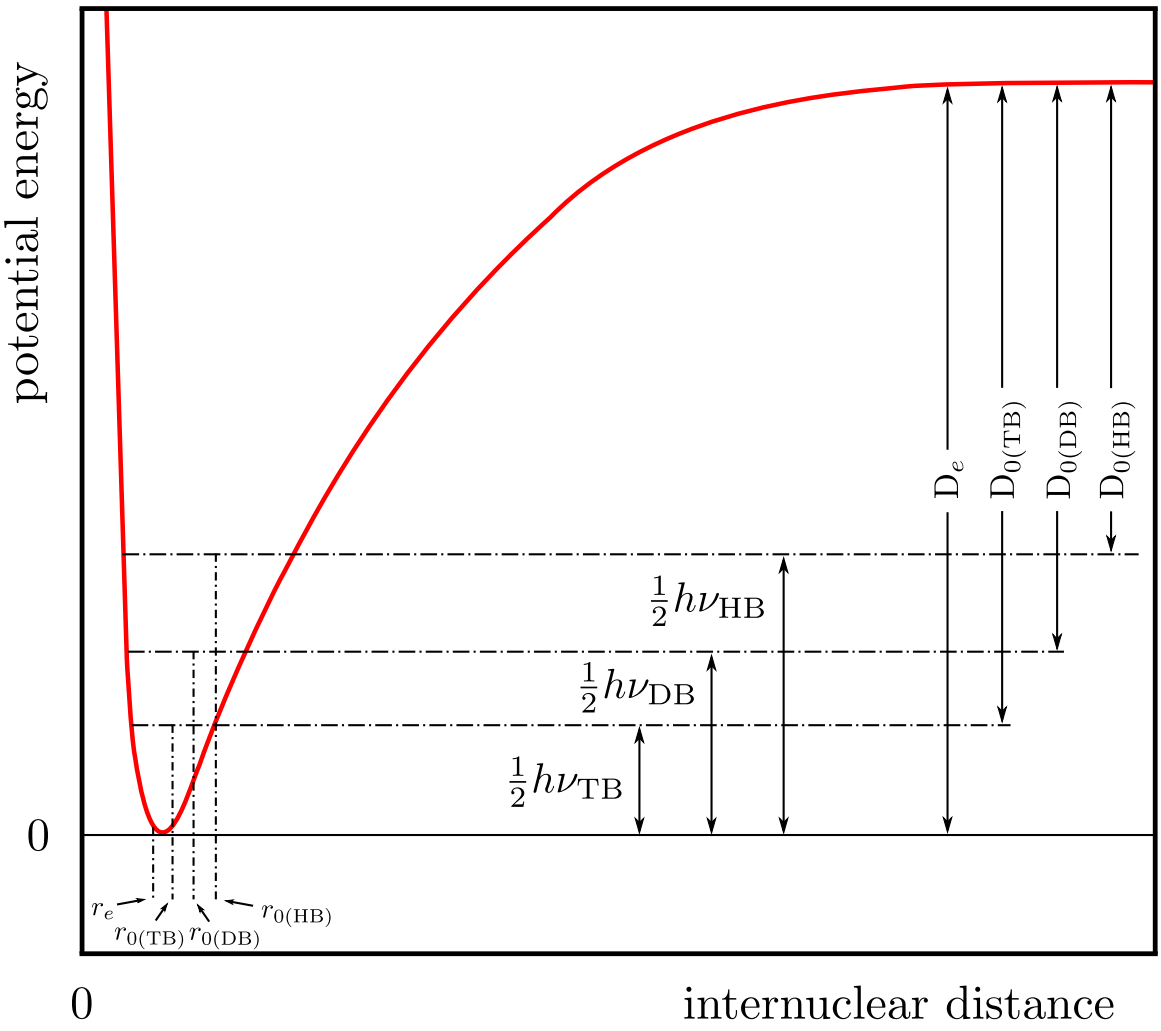


Figure 2.3: Potential energy as function of the inter-nuclear separation of molecule HQ (Q = M, D, T).

required to generate Q_2^+ ions (Q = H, D or T). The data in Fig. 2.3 and Table 2.4 also document that elemental tritium (T_2) is the most stable molecular hydrogen isotopologue.

2.5.1.3 Rotational states of hydrogen

Depending on whether the nuclear spins of two hydrogen, deuterium or tritium atoms constituting a homo-molecular hydrogen molecules are aligned parallel or anti parallel they are called ortho or para states, respectively. Another nomenclature, proposed by Souers [Sou86], relies on whether the hydrogen atoms have even or odd rotational numbers. This more generally valid nomenclature

Table 2.4: Zero point energies (E_0), dissociation energies (D_0, D_{298}) and ionization energies (I) of all hydrogen isotopologues [Mac73; Sou86].

Hydrogen isotope	H_2	HD	D_2	HT	DT	T_2
E_0 / kJ mol^{-1}	25.96	22.53	18.44	21.26	16.85	15.10
D_0 / kJ mol^{-1}	431.94	435.37	439.46	436.63	441.03	442.83
D_{298} / kJ mol^{-1}	436.26	439.61	443.80	440.87	445.48	447.15
I / kJ mol^{-1}	1488.14	1489.95	1491.76	1490.55	1491.36	1493.56

Table 2.5: Rotational states of hydrogen [Sou86].

At high temperature	At low temperature	Old nomenclature
even-J H_2	$J = 0$ H_2	para H_2
even-J D_2	$J = 0$ D_2	ortho D_2
even-J T_2	$J = 0$ T_2	para T_2
odd-J H_2	$J = 1$ H_2	ortho H_2
odd-J D_2	$J = 1$ D_2	para D_2
odd-J T_2	$J = 1$ T_2	ortho T_2

for the designation of ortho and para species is compared with the former nomenclature in Table 2.5.

Elemental ortho or para hydrogen molecules cannot convert from one to another except in the presence of a catalyst or an adsorber [Bon29]. It follows that any bond breaking process that yields atomic hydrogen can cause interconversion between the ortho – para modifications, e.g.

$$\mathrm{Q} + \mathrm{oQ_2} \longrightarrow \mathrm{pQ_2} + \mathrm{Q} \quad (\mathrm{Q} = \mathrm{H},\ \mathrm{D},\ \mathrm{T})\ .$$

The rate of this exchange reaction is accelerated considerably with increasing temperatures. Equilibrium compositions are provided in Table 2.6 for the population of the odd-J levels of H_2, D_2 and T_2 at several temperatures. Equilibrium values are denoted in the table by the letter "e". The data refer to molecules being in the vibrational ground state. Therefore, at ambient temperature only the rotational states of the $\nu = 0$ level, i.e. even J states with $J = 0, 2, 4$ ...

and odd J states with $J = 1, 3, 5$ … need to be considered. At very low temperature all even J states fall to $J = 0$ and all odd states to $J = 1$. At 300 K the equilibrium odd J fraction for nH_2 as well as for nT_2, which have both a nuclear spin of 1/2, is 0.75[2]. At the same temperature, the equilibrium odd J fraction of D_2 is 0.333. Diatomic isotopologues of hydrogen, i.e. HT, DT or HD, on the other hand, are self-catalysed and characterized by an instantaneous thermal energy flow, the most common transitions taking place according to selection rule $\Delta J = \pm 1$. From this it follows, that the rotational energies of the diatomic isotopologues of hydrogen are always in equilibrium with the ambient. They adjust immediately to temperature changes. In case of hydrogen molecules consisting of two identical nuclei, e.g. H_2, D_2 or T_2, the situation is more complex because de-excitations are governed by a $\Delta J = \pm 2$ selection rule, which causes them to proceed at a much slower rate. In other words, even-J and odd-J homonuclear hydrogens will not equilibrate rapidly. Table 2.7 lists the fraction of hydrogen isotopologues $f(1)$ that are in the $J = 1$ state at cryogenic temperatures within the temperature range 4.2 - 40 K. Therefore, the relationship

$$f(1) + f(0) = 1$$

holds and hence $f(1)$ is nearly equal to f(odd-J). This is so, because under the prevailing conditions all other J states are not or almost not occupied. Noticeably, when normal homonuclear hydrogen at 293 - 300 K is cooled down to 4.2 K the even J levels fall in $\Delta J = -2$ increments to the $J = 0$ state and the odd J levels drop in $\Delta J = -2$ increments to the $J = 1$ state. Conversely, the $(J = 1)/(J = 0)$ ratio at 4.2 K remains unchanged in comparison to the $(J = 1)/(J = 0)$ ratio at 300 K (unless an equilibration by a catalyst has taken place or the β-radiation of tritium has induced reactions). At low temperatures the $J = 1$ of H_2 and the $J = 1$ state of T_2 comprise 75 % of the population; the $J = 1$ state of D_2 encompasses 33 % of the population. Because para hydrogen is marginally more stable than ortho hydrogen, para hydrogen becomes the dominant isomer when hydrogen gas is cooled. The percentage of para-hydrogen depends on temperature. At 20 K or less it is present in a concentration of almost 100 %.

[2] The equilibrium composition at ambient temperature is denoted by the letter n ("normal"). Normal only refers to the fraction of rotational states that are odd or even. No information is provided on the J levels they occupy.

Table 2.6: Equilibrium population of the odd *J*-levels of elemental protium, deuterium and tritium [Mac73; Sou86].

Temperature Kelvin	e-H_2	e-D_2	e-T_2
0	-	0.000	0.000
10	-	0.030	0.028
20	-	0.020	0.338
30	-	0.079	0.567
40	0.113	0.148	0.666
50	0.229	0.207	0.712
60	0.344	0.251	0.732
77.4	0.500	0.297	0.745
100	0.614	0.322	0.749
150	0.714	0.332	0.750
200	0.740	0.333	0.750
250	0.747	0.333	0.750
300	0.749	0.333	0.750

Table 2.7: Fraction of hydrogen isotopologue molecules in the $J = 1$ state at cryogenic temperatures* [Sou86].

Temperature K	e-H_2	HD	HT	e-D_2	DT	e-T_2
Triple point	4.5×10^{-5}	1.3×10^{-3}	4.5×10^{-3}	1.5×10^{-2}	7.38×10^{-2}	6.48×10^{-1}
4.2	2.1×10^{-17}	1.6×10^{-13}	3.7×10^{-12}	1.9×10^{-9}	1.1×10^{-7}	9.9×10^{-6}
6	4.1×10^{-12}	1.5×10^{-9}	1.4×10^{-8}	8.9×10^{-7}	1.9×10^{-5}	6.1×10^{-4}
8	5.0×10^{-9}	3.2×10^{-7}	1.7×10^{-6}	3.2×10^{-5}	3.8×10^{-4}	6.7×10^{-3}
10	3.6×10^{-7}	8.0×10^{-6}	3.0×10^{-5}	2.8×10^{-4}	2.3×10^{-3}	2.69×10^{-2}
12	6.1×10^{-6}	6.8×10^{-5}	2.0×10^{-4}	1.1×10^{-3}	7.5×10^{-3}	6.77×10^{-2}
14	4.6×10^{-5}	3.1×10^{-4}	8.0×10^{-4}	3.2×10^{-3}	1.74×10^{-2}	1.26×10^{-1}
16	2.1×10^{-4}	9.8×10^{-4}	2.2×10^{-3}	6.9×10^{-3}	3.26×10^{-2}	1.95×10^{-1}
18	6.9×10^{-4}	2.4×10^{-3}	5.0×10^{-3}	1.25×10^{-2}	5.26×10^{-2}	2.66×10^{-1}
20	1.8×10^{-3}	4.9×10^{-3}	9.4×10^{-3}	1.99×10^{-2}	7.62×10^{-2}	3.33×10^{-1}
22	3.9×10^{-3}	8.7×10^{-3}	1.57×10^{-2}	2.92×10^{-2}	1.03×10^{-1}	3.93×10^{-1}
24	7.3×10^{-3}	1.41×10^{-2}	2.41×10^{-2}	4.00×10^{-2}	1.31×10^{-1}	4.46×10^{-1}
26	1.26×10^{-2}	2.10×10^{-2}	3.45×10^{-2}	5.20×10^{-2}	1.59×10^{-1}	4.92×10^{-1}
28	2.00×10^{-2}	2.97×10^{-2}	4.68×10^{-2}	6.49×10^{-2}	1.86×10^{-1}	5.30×10^{-1}
30	2.97×10^{-2}	3.99×10^{-2}	6.06×10^{-2}	7.85×10^{-2}	2.14×10^{-1}	5.63×10^{-1}
32	4.19×10^{-2}	5.15×10^{-2}	7.58×10^{-2}	9.24×10^{-2}	2.40×10^{-1}	5.91×10^{-1}
34	5.64×10^{-2}	6.43×10^{-2}	9.20×10^{-2}	1.06×10^{-1}	2.65×10^{-1}	6.14×10^{-1}
36	7.32×10^{-2}	7.81×10^{-2}	1.09×10^{-1}	1.20×10^{-1}	2.87×10^{-1}	6.34×10^{-1}
38	9.21×10^{-2}	9.28×10^{-2}	1.26×10^{-1}	1.34×10^{-1}	3.08×10^{-1}	6.51×10^{-1}
40	1.13×10^{-1}	1.08×10^{-1}	1.44×10^{-1}	1.48×10^{-1}	3.27×10^{-1}	6.65×10^{-1}

* The remaining molecules are in the $J = 0$ level, with the exception of T_2 at about 40 K, where approximately 0.15 % are in the $J = 2$ level.

2.5.1.4 Boiling points, triple points and critical points

At the triple point, the solid, liquid and vapour phases of a species are in equilibrium at fixed pressure and temperature. Because three phases co-exist, the system has no degree of freedom and is therefore invariant. This manifests experimentally when a solid at a temperature below the triple point is heated up to the triple point. While at temperatures below the triple point pressure and temperature increase, at the triple point they stay constant until the solid turns into liquid. Once all solid becomes liquid temperatures and pressures begin to rise again.

Boiling points, triple points and critical points of all tritiated molecular hydrogens are displayed in Table 2.8. The characteristic temperature above which a gas cannot be liquefied is called critical temperature, T_c and the pressure that just suffices to liquefy a gas at T_c is called critical pressure, p_c.

Table 2.8: Boiling points, triple points and critical point constants of molecular hydrogen isotopologues [Gri51; Mac73; Sou86].

Species	Boiling point at 1 bar	Triple point		Critical point	
		Temperature	Pressure	Temperature	Pressure
	K	K	Pa	K	MPa
H_2	20.4	14.0	6 965	33.2	1.256
HD	22.4	16.8	12 753	36.4	1.481
D_2	23.6	18.5	16 088	38.3	1.609
HT	23.6	17.7	14 580	37.1	1.571
DT	24.3	19.8	20 080	39.4	1.773
T_2	24.9	20.6	21 600	40.4	1.850

2.5.1.5 Vapour pressures

Saturated vapour pressures of all tritiated hydrogen molecules at cryogenic temperatures are summarized in table 2.9 [Sou86]. Values given for HT and DT are estimated. Liquid - vapour saturation pressures from the triple point (2.16 K) up to 29 K of molecular tritium can be calculated from equation

$$\ln p = 18.7852 - \frac{181.732}{T} + 4.605 \times 10^{-4}(T - 25)^2$$

where p is given in Pa and T in K [Gri51].

Saturation vapour pressures of all six isotopic hydrogen can be calculated from relationship

$$\ln p = a - \frac{b}{T} + c \ln T$$

where p is given in Pa and T in K.

Numerical values of constants a, b and c have been tabulated in Table 2.10. The Table also lists sublimation and vaporization enthalpies at the corresponding triple points.

Table 2.9: Vapour pressures of tritium-containing elemental hydrogen isotopes at cryogenic temperatures*.

Temperature	HT	DT	T_2
K	Pa	Pa	Pa
4.2	$5 \times 10^{\mathbf{-8}}$	$4 \times 10^{\mathbf{-10}}$	$2 \times 10^{\mathbf{-11}}$
6	$1 \times 10^{\mathbf{-3}}$	$4 \times 10^{\mathbf{-5}}$	$6 \times 10^{\mathbf{-6}}$
8	$3.9 \times 10^{\mathbf{-1}}$	$4 \times 10^{\mathbf{-2}}$	$1 \times 10^{\mathbf{-2}}$
10	$1.5 \times 10^{\mathbf{1}}$	2.6	1.0
12	$2.0 \times 10^{\mathbf{2}}$	$4.7 \times 10^{\mathbf{1}}$	$2.2 \times 10^{\mathbf{1}}$
14	$1.27 \times 10^{\mathbf{3}}$	$4.0 \times 10^{\mathbf{2}}$	$2.2 \times 10^{\mathbf{2}}$
16	$5.37 \times 10^{\mathbf{3}}$	$2.06 \times 10^{\mathbf{3}}$	$1.26 \times 10^{\mathbf{3}}$
18	$1.68 \times 10^{\mathbf{4}}$	$7.63 \times 10^{\mathbf{3}}$	$5.06 \times 10^{\mathbf{3}}$
20	3.84×10^{4}	$2.20 \times 10^{\mathbf{4}}$	$1.58 \times 10^{\mathbf{4}}$
22	7.68×10^{4}	4.74×10^{4}	$3.74 \times 10^{\mathbf{4}}$
24	1.38×10^{5}	9.08×10^{4}	7.41×10^{4}
26	2.29×10^{5}	1.58×10^{5}	1.33×10^{5}
28	3.55×10^{5}	2.56×10^{5}	2.20×10^{5}
30	5.24×10^{5}	3.92×10^{5}	3.41×10^{5}
32	7.43×10^{5}	5.76×10^{5}	5.06×10^{5}
34	1.02×10^{6}	8.13×10^{5}	7.21×10^{5}
35	1.18×10^{6}	9.54×10^{5}	8.50×10^{5}
36	-	1.10×10^{6}	9.94×10^{5}
37	-	1.28×10^{6}	1.16×10^{6}
38	-	-	1.33×10^{6}

* Bold values are over the solid and the others over the liquid.

2.5.1.6 Viscosity

According to the kinetic theory of gases the viscosity of a gas, η, is described by equation

$$\eta = \frac{1}{\pi\sigma^2}\sqrt{\frac{kTM}{\pi}}$$

where σ, T and M stand for molecular diameter, temperature and molecular weight, respectively. The direct dependence of η from $\sqrt{TM}$ is only approximately true for temperatures exceeding 230 K [Sou86]. For hydrogen the increase of η with pressure can be estimated from relationship

$$\frac{\eta}{\eta_0} = 1 + AP + BP^2$$

in which A and B are constants and the subscript referring to zero pressure. Table 2.11 [Sou86] lists constants A and B for hydrogen at several temperatures.

Table 2.10: Saturation vapour pressures of all six isotopologues of molecular hydrogen [Gri51; Mac73].

Phase	species	a	b	c	$\Delta H^0_{\mathrm{sub\,TP}}$ / J mol^{-1}
solid	n-H_2	9.2458	92.610	2.3794	1028
	HD	9.7731	116.66	2.3769	1270
	HT	9.8954	126.29	2.3758	1370
	n-D_2	10.427	138.31	2.2891	1470
	DT	10.821	150.34	2.2389	1580
	T_2	11.559	164.77	2.1189	1690
					$\Delta H^0_{\mathrm{vap\,TP}}$ / J mol^{-1}
liquid	n-H_2	9.64596	83.5177	1.98042	911
	HD	11.5827	109.419	1.57756	1110
	HT	12.7295	123.995	1.3444	1190
	n-D_2	12.6317	130.249	1.38962	1270
	DT	14.2203	147.349	1.04950	1360
	T_2	15.8148	164.486	0.707997	1460

Table 2.11: Coefficients for the calculation of the pressure dependence of viscosity for hydrogen (after [Sou86]).

Temperature	A	B
K	MPa^{-1}	MPa^{-2}
30	0.0	2.71×10^{-1}
40	3.80×10^{-1}	-6.74×10^{-4}
60	9.98×10^{-2}	-1.24×10^{-4}
100	2.25×10^{-2}	7.34×10^{-5}
300	1.13×10^{-3}	2.53×10^{-5}

Viscosities at constant volume paths on the vapour side of the phase boundary of fluid DT are shown at four densities as function of temperature in Fig. 2.4.

Viscosities of hydrogen and helium at 273 K and 1 bar are 84.2×10^{-6} and 187×10^{-6} poise, respectively (poise = $\mathrm{g\,cm^{-1}\,s^{-1}}$). Numerical calculations of the viscosity of molecular tritium at 30 K performed by Sharipov [Sha03b] yielded a value of $24.25 \times 10^{-6}\,\mathrm{g\,cm^{-1}\,s^{-1}}$.

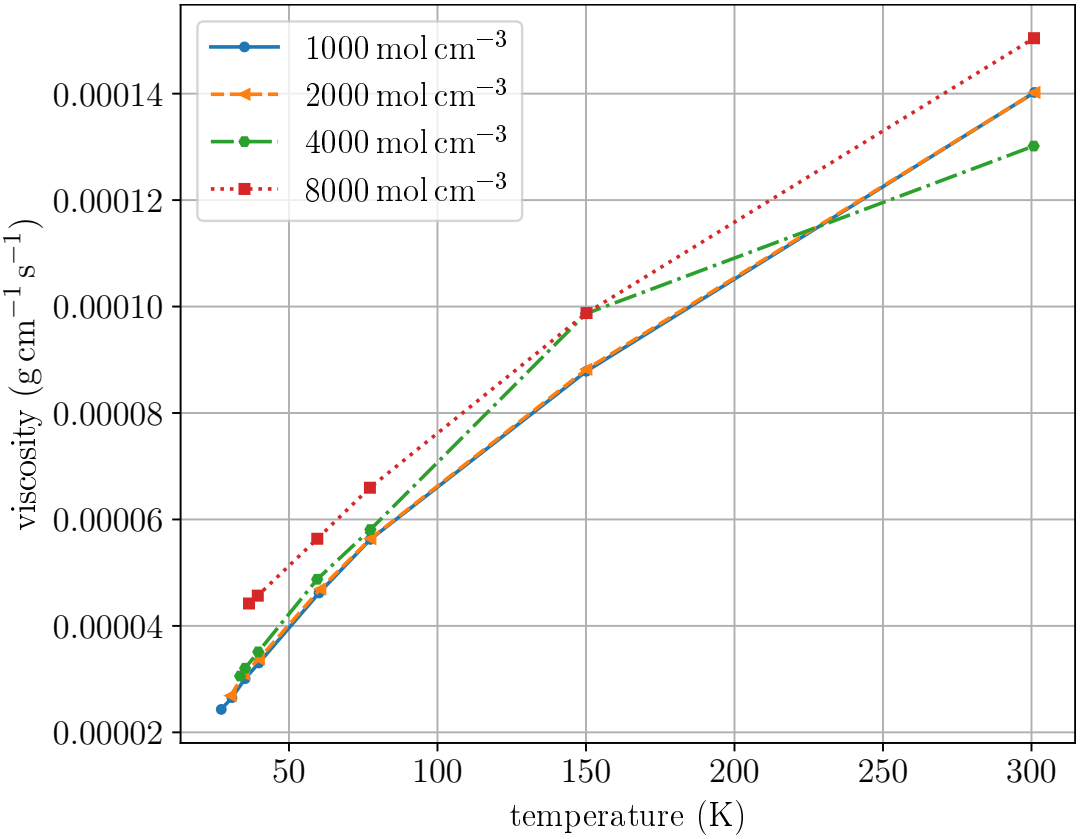


Figure 2.4: Viscosities of fluid D-T as function of temperature (and therefore of pressure) at several densities (after [Sou86]).

2.5.1.7 Volumetric calculation of tritium inventories at elevated pressures

The total number of gaseous moles, n, in a given container can be calculated from the well-known equation

$$n = \frac{PV}{zRT}$$

where P is the pressure in mbar, V the volume of the container in l, z the compressibility factor, R the gas constant and T the temperature in K.

Some compressibility values for gaseous tritium are listed in Appendix C. They can also be estimated from relationship

$$z(T_2) = 1 + \left[\frac{p \cdot 0.001107}{1000}\right]$$

where p stands for the pressure of T_2 in mbar. This equation applies for a temperature of 295 K.

2.5.1.8 Isotopic scrambling

When all molecular hydrogen isotopologues, i.e. H_2, HD, HT, D_2, DT and T_2, are in equilibrium it is possible to calculate from known two all the other [Gen70]. For this purpose, reactions

$$H_2 + D_2 \longrightarrow 2\,HD$$

$$D_2 + T_2 \longrightarrow 2\,DT$$

$$H_2 + T_2 \longrightarrow 2\,HT$$

and their corresponding equilibrium constants at 298 K

$$K_1 = \frac{[HD]^2}{[H_2][D_2]} = 3.26$$
$$K_2 = \frac{[DT]^2}{[D_2][T_2]} = 3.82$$
$$K_3 = \frac{[HT]^2}{[H_2][T_2]} = 2.57$$

are needed.

The time required for the attainment of full equilibrium in a mixture of isotopic hydrogen is dependent among other factors from the specific activity of tritium and the prevailing temperature. For example, equilibrium induced by β-rays emitted during the decay of 6 % tritium in hydrogen will be reached at ambient temperature after about one month [Sch71].

Equilibrium constants for hydrogen isotope mixtures are compiled within the temperature range 0 - 500 K in Table 2.12.

Table 2.12: Equilibrium constants for hydrogen isotope mixtures at several temperatures [Mac73; Sou86].

Temperature K	K_2	K_3	K_1
0	0	0	0
4.2	4.8×10^{-2}	2×10^{-17}	4.9×10^{-8}
6	2.0×10^{-1}	4×10^{-12}	1.4×10^{-5}
8	4.7×10^{-1}	5×10^{-9}	3.6×10^{-4}
10	7.8×10^{-1}	3.8×10^{-7}	2.6×10^{-3}
12	1.10	6.5×10^{-6}	9.6×10^{-3}
15	1.46	1.1×10^{-4}	3.6×10^{-2}
20	1.74	2.0×10^{-3}	1.3×10^{-1}
25	1.94	1.1×10^{-2}	2.9×10^{-1}
30	2.09	3.4×10^{-2}	4.9×10^{-1}
50	2.57	3.3×10^{-1}	1.41
77.4	3.06	6.4×10^{-1}	1.94
100	3.29	9.5×10^{-1}	2.26
200	3.69	1.94	2.9
300	3.82	2.58	3.26
500	3.99	3.81	3.97
∞	4.00	4.00	4.00

2.5.1.9 Infrared and Raman absorption

Infrared and Raman spectroscopy are valuable analytic tools for the qualitative and quantitative determination of isotopically substituted elemental hydrogen. A number of transitions of all six isotopic substituted molecular hydrogen are compiled in Table 2.13. It should be remarked that the elementary hydrogen molecule displays Raman lines even though it shows no infrared spectrum.

Detailed rotation-vibration infrared spectra of the isotopologue water molecules D_2O and HDO were published by Benedict et al. [Ben56]. Staats et al. [Sta56] and Carpenter et al.[Car72] investigated the vapour phase infrared spectra of T_2O, THO, and TDO in the spectral region

Table 2.13: Gas phase transitions of isotopic hydrogen molecules in cm [Her50; Vei85; Sou86; Uda91].

Hydrogen isotope	$\nu(\nu = 0 \rightarrow 1)$	$\nu(\nu = 0 \rightarrow 2)$
H_2	4161	8087
HD	3632	7088
HT	3435	6713
D_2	2994	5872
DT	2745	5394
T_2	2468	4862

700 - 7000 cm^{-1}. The experimentally observed frequencies were found to be in satisfactory agreement with calculated values. Kobayashi et al. [Kob11] reported recently, some near-infrared spectroscopical measurements of tritiated water in the 7220 cm^{-1} region.

Infrared absorption bands at frequencies of 1024, 1388, 1645, 1130 and 1460 cm^{-1} have been used for the quantitative analysis of isotopic-substituted water molecules like T_2O, HTO, H_2O, DTO, and D_2O, respectively [Cec56] [Rev73]. A detailed description of the procedure used to determine the composition of isotopic substituted water is given in ref. [Rev73]. The procedure is based on the well-known Lambert-Beer law. At equilibrium the molecular isotopic composition can be obtained from the T/D ratio using the following relationships:

$$\frac{[T_2O]}{[DTO]} = \frac{[T]}{2[D]}$$
$$\frac{[DTO]}{[D_2O]} = 2\frac{[T]}{[D]}$$
$$\frac{[T_2O]}{[D_2O]} = \left(\frac{[T]}{[D]}\right)^2$$

The apparent molar absorption coefficient of T_2O at 981.5 cm^{-1} was found to be 3.8×10^{-3} $cm^2\,mol^{-1}$ [Ich85]. At this wave length it is possible to determine T_2O quantitatively even at very low partial pressures.

Kanesaka et al. [Kan84] compared the infrared spectra of $T_2{}^{18}O$ and $T_2{}^{16}O$.

Raman spectroscopy of molecular hydrogen has also been proposed for the accurate determination of high temperatures taking advantage of characteristic rotational and vibrational

Raman intensities [Vei85]. The technique has the distinct benefit that for pure rotational spectra of hydrogen isotopes the absolute intensity of the scattered light can be determined from first principles.

Crane and Gush [Cra66] published infrared spectra of solid deuterium and solid hydrogen deuteride.

2.5.1.10 Heat capacity

Herzberg [Her50] discussed comprehensively the dependence of the rotational heat capacity, C_p of hydrogen from temperature within the temperature range 50 - 300 K. The rotational heat capacity was obtained from the total heat capacity after subtraction of the translational contribution, i.e. 5/2 R. It was shown that the heat capacity of ordinary hydrogen consisting of a 3 : 1 mixture of ortho and para hydrogen results from the contribution of the single heat capacities according to the expression

$$C_p^0 = \frac{3}{4} C_p^0 \text{ (ortho)} + \frac{1}{4} C_p^0 \text{ (para)}$$

provided no ortho/para interconversion has taken place. This was actually the case for ordinary hydrogen in the 50 - 300 K temperature range, within the time in which the measurements were carried out.

2.5.2 Physical constants of water isotopologues

A number of physical constants of liquid water isotopologues are compared in Table 2.14. As evident, some constants, like density or ionisation constants, show more pronounced differences than others. The highest triple point pressure and critical pressure are the ones of D_2O.

Table 2.14: Selected physical constants of liquid isotopic water.

Property	T_2O	D_2O	H_2O	Ref.
Triple point temperature K	277,49	276,82	273.010	[Jon68]
Triple point pressure mbar	6.5595	6.6928	6.1062	[Jon68]
Normal boiling point K	374.51	374.42	373.00	[Jon68]
Critical temperature K	643	644.5	647.2	[Pey78]
Critical pressure bar	207.90	214.37	214.28	[Kir51]
Density at 298 K $\mathrm{g\,cm^{-3}}$	1.2137	1.1077	1.00	[Gol64] [Kir51]
Ionisation constant at 298 K	6.1×10^{-16}	1.43×10^{-15}	0.99×10^{-14}	[Gol69]
Molecular weight	22.032	20.028	18.015	-

2.5.2.1 Density

The density of T_2O (l) at 298 K is $1.2137\,\mathrm{g\,cm^{-3}}$. Densities at other temperatures can be calculated from expression

$$D = 1.213124 + 2.9129 \times 10^{-4}t - 1.1954 \times 10^{-5}t^2 + 5.301 \times 10^{-8}t^3\,\mathrm{g\,cm^{-3}}\ ,$$

where t stands for the temperature in °C [Gol64]. At 13.4 °C the density goes through a maximum of $1.215\,02\,\mathrm{g\,cm^{-3}}$.

2.5.2.2 Relative vapour pressures

The relative vapour pressures of the pure liquids H_2O and T_2O or H_2O and D_2O as function of temperature can be calculated from equations

$$\ln\left(\frac{p_{H_2O}}{p_{T_2O}}\right) = \frac{-103.87 \pm 0.57}{T} + \frac{48\,480 \pm 210}{T^2}$$
$$\ln\left(\frac{p_{H_2O}}{p_{D_2O}}\right) = \frac{-70.87 \pm 0.43}{T} + \frac{33\,630 \pm 160}{T^2}$$

Table 2.15: Ionisation constants of protium oxide and deuterium oxide at several temperatures [Wea70].

Temperature K	H_2O	D_2O
273	1.39×10^{-15}	
283	2.92×10^{-15}	2.98×10^{-16}
293	6.81×10^{-15}	7.31×10^{-16}
303	1.47×10^{-14}	1.64×10^{-15}
313	2.92×10^{-14}	3.40×10^{-15}
323	5.47×10^{-14}	6.58×10^{-15}

where T is given in K. The vapour pressure crossover temperatures for three different water isotopologue pairs are (389.4 ± 0.5) K, (363.2 ± 10.0) K and (493.9 ± 0.1) K for the D_2O-T_2O, H_2O-D_2O and H_2O-T_2O system, respectively [Jon68].

2.5.2.3 Ionisation constants of water isotopologues

The ionisation constants of T_2O, D_2O and H_2O were determined by the electromotive force method without using a liquid junction. They were found to be 6.1×10^{-16}, 1.43×10^{-15} and 0.988×10^{-14} at 298 K for T_2O, D_2O and H_2O, respectively [Rob30; Gol69]. The marked effect of temperature on the ionisation constant of H_2O and D_2O is illustrated in Table 2.15.

2.5.2.4 Luminescence

Solid T_2O(s) displays a characteristic luminescence at cryogenic temperatures, which is induced by the radioactivity of tritium. The emission of this luminescence has a maximum at approx. 550 nm [Jon52; Pey78].

2.6 Penetration of tritium beta particles into matter

The penetration of beta particles emitted by tritium (0 - 18.6 keV) into gases, metals or other materials will be discussed in this section. Rudiments on secondary radiation generated by beta particles will also be provided.

2.6.1 Range of beta particles in hydrogen

When beta particles emitted by tritium interact with the electron cloud of molecular hydrogen a fraction of their energy is transferred by each collision until eventually the electrons become thermal[3] and combine with a positive charge. During collisions the mechanism of energy transfer changes because the energy carried by the particles decreases.

To a first approximation the absorption of beta particles [Sou86] by a gaseous, liquid or solid medium can be calculated from equation

$$E_{\mathrm{t}} = 5.69\, e^{4.425\,\rho\,x}$$

where E_t is the transmitted energy in keV, ρ the density of the medium in $\mathrm{mol\,m^{-3}}$ and x the thickness in m. The term 5.69 keV denotes the mean energy of the incident beta particles. The impact of isotopic differences is only minor.

A more realistic approach is based on the assumption that energy transfer takes place in bundles. The assumed magnitudes of energy lost by a beta particle during a collision with diverse molecules are listed in Table 2.16. From the provided values it can be estimated that approximately 15 eV are lost via ionisation and molecular excitation during each collision with a tritium beta particle.

The linear energy transfer function $L(E)$ that includes all mechanisms of energy loss is described by expression

$$L(E) = \frac{\mathrm{d}E}{\rho\,\mathrm{d}x}\ ,$$

[3] This is the case when the kinetic energy of the beta particles is determined by ambient temperature.

Table 2.16: Assumed average energy losses per beta particle - molecule collision [Sou86].

Electron energy eV	Average energy loss per collision eV	Type of interaction
20 - 18 500	15	Ionisation and molecular excitation
10 - 20	5	Molecular dissociation
1 - 10	0.5	Vibrational excitation

which upon rearrangement yields

$$\rho\Delta x = \frac{\Delta E}{L(E)} \ .$$

where ρ is the density, Δx the distance travelled by the beta particle between collisions, E the actual energy of the beta particle and ΔE the amount of energy lost in a collision.

For energies in the range 70 - 10 000 eV the transfer function $L(E)$ can be calculated from relationship

$$L(E) = 4.2 \times 10^{-14} \exp\left(-0.085 \cdot (\ln(E) - 1.15)^2\right)$$

where $L(E)$ has units of $\mathrm{J\,m^2}$ and E of aJ (a = atto = 1×10^{-18}). At energies below 70 eV this equation is no longer valid, because the energy of the beta particles has become insufficient for dissociation transfers. This change in mechanism becomes apparent by the discontinuity at energies below 70 eV of the $L(E)$ vs energy plot displayed in Fig. 2.5.

If by way of example the energy loss of electrons having an energy of 3 keV is followed mathematically step by step until the energy drops to a value of 45 eV it is seen that this is the case after about 198 collisions. When the total distance travelled by the particle after these collisions is added up, a value for ρx of $5.57 \times 10^{-2}\,\mathrm{mol\,m^{-2}}$ is obtained [Sou86]. This value can be used for all hydrogen densities, i.e. gas, liquid and solid. The value is not sensitive to the type of molecular isotope.

Recapitulating, at kinetic energies below the electron rest mass, i.e. < 0.5 MeV, the beta particles emitted by tritium lose their energy principally through atomic or molecular ionization and excitation. A small fraction of energy is also lost by the emission of radiation via

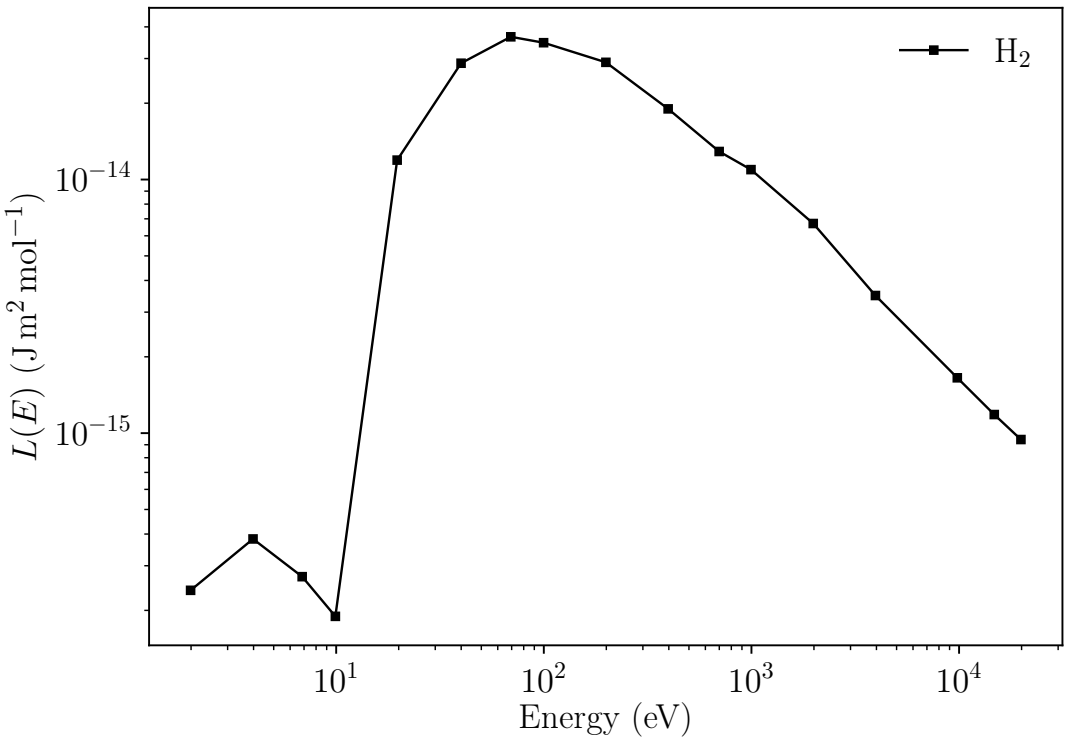


Figure 2.5: Linear energy transfer function $L(E)$ for the deposition of tritium beta particle energies in hydrogen (see also [Sou86]).

bremsstrahlung and fluorescence. At very low energies, i.e. about 10 eV, the electrons lose their energy to molecular dissociation or vibrational and rotational excitations. Because of the large deflections suffered by the electrons during these collisions, their path through matter becomes highly tortuous and the mean path length significantly longer than the mean path range (average distance travelled in a given direction).

The mean range of the electrons in a medium is approximately given by the product of the material properties and an energy dependent function, i.e.

$$R = \frac{A}{\rho Z} 0.20 E^{(1.265 - 0.0954 \ln E)}$$

where R is the range in cm, A the atomic weight of the medium, ρ the density of the medium, Z the atomic number of the medium and E stands for the kinetic energy of the electron.

The maximum range of β-particles emitted by tritium has been estimated to be in the range 4.5 - 7 mm in air and 5 - 7 µm in water or solids. Given that the penetration depth is a function

Table 2.17: Penetration depths of tritium β-particles into different materials at two *E*(β) energies (after [US 94]).

Material	E (β) eV	Mean range cm
T_2 gas, STP*	5.7	0.26
T_2 gas, STP	18.6	3.2
Air, STP	5.7	0.036
Air, STP	18.6	0.45
Water, soft tissue (and oils/polymers of density $1\,g\,cm^{-3}$)	5.7	0.4 µm
Water, soft tissue (and oils/polymers of density $1\,g\,cm^{-3}$)	18.6	5.0 µm
Stainless-steel	5.7	0.06 µm
Stainless-steel	18.6	0.8 µm

* STP = Standard temperature (273.15 K) and pressure (1 bar)

of energy and the beta rays emitted by tritium have not all the same energy, it is customary to list the penetration for the highest energy (18.6 keV) as well as that for the average most representative energy, i.e. 5.7 keV. Several values calculated for these two energies using the equation for R given above are listed in Table 2.17. These results are comparable to maximum penetrations observed in experiments. The reason for this is that most experimentalists rely on the last half of the absorption curve for their measurements. At this point scattering has reached equilibrium and the angular distribution of electrons has become isotropic [Eva55].

From the above it can be inferred, that tritium does not constitute an external hazard to people because the emitted radiation cannot penetrate through a layer of skin or clothing. For the same reason, tritium contained in glass, ceramic or metallic equipment/containments is sufficiently shielded from the emitted β-radiation. On the other hand, tritium does constitute a radiation hazard when inside of the human body. In the body, it distributes uniformly in all liquids, to a large extent bound organically.

It should be kept in mind that tritium beta rays can generate low energy X-rays (see below), but these are not exceedingly penetrating and normally not considered to constitute a hazard.

While virtually all inhaled tritiated water is absorbed within the body, only 0.004 % of inhaled molecular tritium-bearing hydrogen is converted into the oxide form and retained. The average **biological half-life** of tritiated water is of the order of 10 d. This half-life can be reduced significantly by increased consumption of liquids [Llo86].

2.6.2 Range of beta particles in dense matter

Beta particles exhibit no defined range displaying considerable scattering in dense matter with frequent changes in direction because of electrostatic interactions with atomic nuclei and electrons. They may therefore come out in widely different directions and have traversed paths of different lengths in the material. In absorption measurements, thicknesses are frequently expressed in $\mathrm{g\,cm^{-2}}$, i.e. superficial density (see Fig. 2.6). The point where the linear extrapolation of the curve intercepts the background is designated with "practical range", R_P, and the maximum range, R_0, is defined as the point where the absorption curve runs into the background. The range of a given beta particle depends not only on its initial energy but also on the number of electrons with which the particle collides in passing through the absorber. The latter number will depend on the density of electrons in the absorber, i.e. number of electrons per unit mass.

The ability of an element to stop β-particles will depend on the ratio of the atomic number (Z) to the mass number (A), i.e. Z/A. Although this ratio decreases from the light to heavy elements, the effect of this variation on the thickness needed to stop β-particles is not very pronounced.

Katz and Penfold [Kat52] proposed an empirical equation to describe the range of beta particles as function of beta ray energy for the absorption of mono-energetic electrons by aluminium. The equation

$$R = 412\,E_0^{(1.255-0.0954\ln(E_0))} \quad \mathrm{mg\,cm^{-2}}$$

in which R is the range and E_0 the energy in MeV of beta rays is valid within the range $0.01 < E_0 < 2.5\,\mathrm{MeV}$. The equation was shown to describe correctly the results from the most

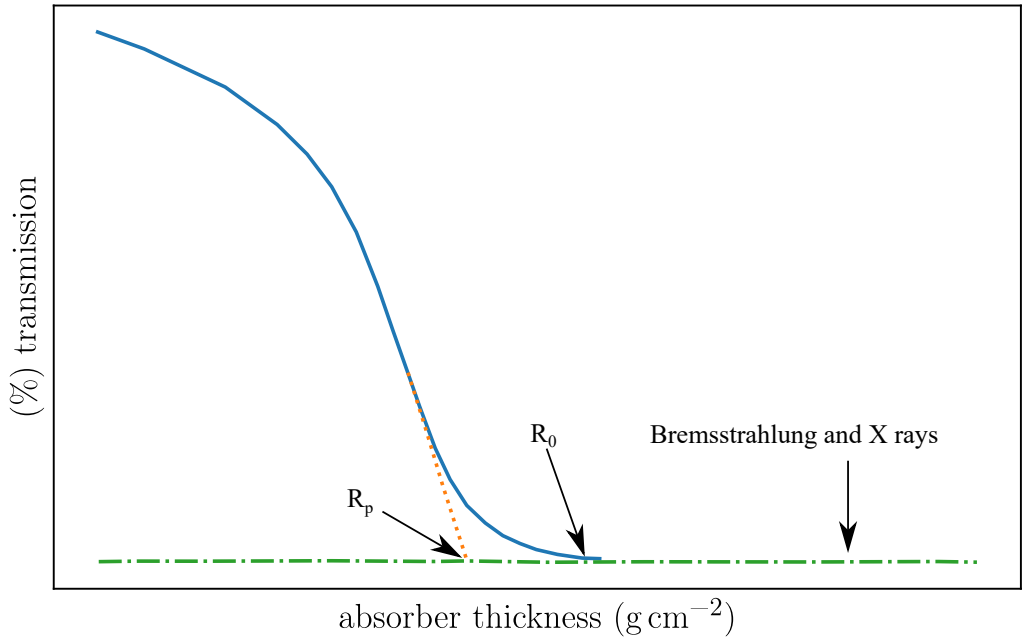


Figure 2.6: Transmission curve for initially mono-energetic electrons. R_{P} is defined as the "practical range" and R_0 as maximum range.

reliable investigations published prior to 1952. For beta particles having higher energies, i.e. $\leq 25\,\mathrm{MeV}$, the range can be obtained from the relationship

$$R = 530\,E_0 - 10^6\,\mathrm{mg\,cm^{-2}}$$

2.6.3 More on beta energy absorption by gases

Dorfman [Dor54a] investigated experimentally the absorption of beta particles emitted by tritium in hydrogen, helium, and other gases. He used a small spherical ionisation chamber of 57 mm diameter, in which the gas served both as absorber as well as ionisation medium. From absorption curves, he obtained half thickness[4] values of 0.03, 0.06 and 0.08 $\mathrm{mg\,cm^{-2}}$ for hydrogen, helium and oxygen, respectively.

Mueller [Mue61] calculated the fraction of beta energy emitted by tritium, which is absorbed by a gas or a mixture of gases in a spherical vessel. The proposed model is based on the

[4] Half thickness = thickness of absorbing material necessary to reduce the intensity of radiation which passes through it by one half.

empirically validated assumption that the absorbed energy per spherical shell surrounding a point tritium source can be represented by an exponential function. Equations were developed for gases of low atomic number. They were found to be applicable to all states of aggregation of these gases.

In a first approximation the total dose rate E in a spherical volume gas was estimated without inclusion of backscattering. Energy absorption from a point source of tritium was assumed to be given by a function decreasing exponentially with distance from the source

$$D(r) = A \exp(-\mu r)$$

where $D(r)$ is the dose rate for a spherical shell of radius r concentrically surrounding the point source and μ the linear energy absorption coefficient of the absorbing gas (see Table 2.18). The total dose rate was calculated from the expression

$$E = 4\pi a^3 \epsilon_0 \sum_{n=0}^{\infty} \frac{(-1)^n (n+3)}{(n+4)!} (2\mu a)^{(n+1)}$$

where a is the radius of the sphere and ϵ_0 the beta energy emitted per second and unit volume of gas.

Taking G to be the fraction of emitted beta energy absorbed by a sphere of gas and replacing by α it was shown that

$$G = 1 - \frac{3}{2\alpha} + \frac{3}{\alpha^3}[1 - (\alpha + 1)\exp(-\alpha)]$$

for α greater than unity.

In this equation the term α depends on density, the composition of the gas, and the diameter of the emitting volume. As already indicated, the absorption energy calculated by this equation neglects contributions from backscattering. In a next step therefore, the contribution of backscattered beta particles to the absorption of energy was included in the calculation. It was assumed that an appreciable fraction of the beam is scattered back when an electron beam is incident on a somewhat dense medium. This fraction, which is called the 2π back scattering coefficient, increases distinctly with the atomic number of the back-scattering medium and depends on the angle of incidence of the electrons. For high atomic numbers back-scattering

Table 2.18: Linear energy absorption coefficients of tritium beta particles by gases [Mue61].

Substance	Density at 298 K and 1 bar	μ at 298 K and 1 bar
	$g\,l^{-1}$	cm^{-1}
H_2	0.0824	1.81
He	0.1635	1.68
N_2	1.146	11.0
O_2	1.309	12.4
Ne	0.8249	7.59
Ar	1.634	12.9
Kr	3.397	23.4
Xe	5.360	33.4
CH_4	0.6567	8.40
CO_2	1.811	17.3
Air	1.185	11.3
H_2S	1.410	13.5

can be considerable, e.g. 0.7 for lead. The effect of electron energy on the back-scattering coefficient is comparatively small. Primary and successive back scattering at the wall of the vessel were estimated using a rather approximate calculation. In spite of this, the agreement between experiment and calculation was surprisingly good over a wide range of gas pressures.

2.6.4 Secondary radiation generated by tritium beta particles

X-ray radiation generated when beta particles emitted by tritium decelerate near a molecule constitute bremsstrahlung. Both, the spectrum of the beta particle that generates bremsstrahlung and that of the generated bremsstrahlung are continuous. The bremsstrahlung radiation yield depends on the atomic number of the constituents of the material contaminated with tritium and from the kinetic energy of the electrons. The maximum energy of the generated bremsstrahlung X-rays will not exceed that of the β–rays but the escape depths of bremsstrahlung X-rays are significantly higher than of the tritium β–rays. During passage of beta particles of certain energy through matter, the amount of generated bremsstrahlung will be most pronounced for elements

of high atomic number. Bremsstrahlung will eventually be fully absorbed after passing through a considerable thickness of material.

2.7 Isotope effects

Because of the large difference in mass between the hydrogen isotopes protium, deuterium and tritium, these species display large isotope effects.

2.7.1 Elemental hydrogen isotopologues

The small size of hydrogen isotopologues and the weak interaction of hydrogen with metal lattices explains the high mobility of hydrogen isotopes through metals [Hau79]. Within restricted temperature ranges plots of D(T) vs 1/T yield good straight lines from which well-defined activation energies can be obtained.

According to classical theory, the diffusivities of hydrogen isotopologues are related in first approximation to the masses of the corresponding isotopes by the expressions (holds strictly only for the diffusivity of gaseous hydrogen)

$$D_T = \frac{\sqrt{2}}{\sqrt{3}} D_D = \frac{1}{\sqrt{3}} D_P$$

where the subscripts T,D,P denote tritium, deuterium, and protium, respectively. The implication is that only the pre-exponential factors of the respective diffusivities should depend on the inverse square root of mass, the classical activation energies remaining isotope-independent. Therefore, the isotope effect should be independent from temperature [Rie86]. In real life, however, this assertion is often not obeyed. This is on one hand attributed to crystallographic and quantum mechanical effects and on the other to deformations of the lattice during interstitial jumps. Hence, isotope effects frequently exhibit structure and temperature dependences. The solubility of hydrogen isotopes in metals is considered to be isotope-independent because it is a static non-kinematic process.

Isotope effects can be calculated employing a harmonic oscillator model. However, this model is not much better than the simple classical approximation. Therefore, in first approach there is no compelling reason to prefer the oscillator approach.

The following isotope effects of diffusion coefficients of hydrogen isotopologues across metals have been described:

- Metals with a body centred cubic (BCC) lattice like Fe, V, Nb, or Ta display approximately equal pre-exponential factors at all temperatures, i.e. D1 ≈ D2 ≈ D3, and activation energies exhibiting moderate dependency from the hydrogen isotope mass, i.e. $E_1 < E_2 < E_3$. In view of this E_i (i = H, D, T) sequence, the elements V, Nb, and Ta can be considered representative for a "normal" isotope effect.

- Metals of face centred cubic (FCC) lattice, e.g. Ni, Cu, or Pd, show an inverse isotope effect. They exhibit activation energies strongly dependend upon the hydrogen atom mass and, at least at temperatures above 400 K, a reverse sequence of activation energies, i.e. $E_3 < E_2 < E_1$, to that characteristic of metals of BCC lattice [Kat71; Hoh82; Rie86; Bai99b; Wim08]. Because at low temperatures the activation energies for nickel and copper follow the order $E_1 < E_2 < E_3$, tritium will diffuse faster through these metals than deuterium and deuterium faster than hydrogen, which is in line with classical theory [Yam79]. At intermediate temperatures two cross-over regions in which either $E_3 < E_1 < E_2$ or $E_1 < E_3 < E_2$ prevail, become apparent. In view of the above, the elements Pd, Cu, and Ni are considered typical for a reverse isotope effect. An inverse isotope effect in terms of solubility, diffusivity, and permeability of hydrogen isotopes is also followed by palladium-silver membranes. In practice, protium is found to be more soluble in palladium-silver than deuterium or tritium, and the diffusion coefficients of hydrogen through this alloy to increase with increasing isotopic hydrogen mass, i.e. $D_1 < D_2 < D_3$. When diffusion is rate determining, elemental tritium is the least permeating hydrogen isotope. In case of palladium, hydrogen and deuterium behave as they do in nickel or copper but tritium in palladium displays higher activation energy than deuterium. The pre-exponential factor, on the other hand, roughly follows classical square root behaviour. Isotope effects are explained by the different crystal field stabilization of the three hydrogen isotopes.

- For metals like hafnium (Hf) of hexagonal close packed (HCP) lattice, the activation energy appears to be independent from the hydrogen isotopic mass. Notably, when D(T) is plotted against 1/T over a sufficiently wide range of temperatures an upward curvature is observed

instead of a straight line. This behaviour cannot be explained by a single activation energy [Bai99b].

Baird and Schwartz [Bai99b] employed a quantum barrier crossing model to calculate the jumping frequency governing the transfer of hydrogen isotopologue atoms between interstitial sites of the metals. The jump frequency, $\nu_i(T)$, is governed by equation

$$D_i(T) = 0,1666 f d^2 \nu_i(T)$$

in which D_i is the diffusion coefficient characteristic for each atomic mass number of the hydrogen isotope (with $i = P, D, T$), d stands for the jump distance, and f is a factor that accounts for the correlation between successive jumps. For their calculations they used parameters such as i) the Debye temperature of the metal lattice, ii) the H atom local mode vibrational temperature, iii) the electronic energy binding the H atom to an interstitial site in the lattice, and iv) a constant related to the high temperature limiting pre-exponential value D(∞). By proper selection of the parameters, they were able to fit the experimental mass-dependences of the diffusion coefficients of hydrogens reported by different researchers for metals like Fe, V, Nb, Hf, Ni, Cu and Pd at all temperatures and for Ta at high temperatures. At sufficiently low temperature, the isotope effect for Fe, V, Nb and Ta was found to be "normal", i.e. $E_1 < E_2 < E_3$, and at appropriately high temperatures inverse, i.e. $E_3 < E_2 < E_1$. This finding agrees with evaluations of diffusion coefficients across Ni, Cu and Pd performed by Katz et al. [Kat71]. The dependency of the activation energies of diffusion coefficients Ni, Cu and Pd from the hydrogen atom mass for was only weak and the determined sequence of isotopic activation energies inverse, i.e. $E_3 < E_2 < E_1$.

A general conclusion valid for all metals considered is that the high temperature limiting diffusion coefficients decrease with increasing isotopic mass of hydrogen. When chemical reactions between chlorine atoms and molecular hydrogens are contemplated in which hydrogen is involved in a rate determining step, i.e.

$$H_2 + Cl \longrightarrow HCl + H$$
$$T_2 + Cl \longrightarrow TCl + T$$

the ratio of rate constants at 298 K can be as high as $k_H/k_T \approx 25$ [Per66].

Table 2.19: Solubility decrease (in %) when H_2O is replaced by D_2O (after [Kru70]).

Compound	Temperature in K	%
KCl	273	16.4
	453	1.7
NaCl	298	14.9
NaBr	278	11.9
Benzene	298	36
Nitrobenzol	298	21

2.7.2 Isotope effects of water isotopologues

Water displays rather noteworthy isotope effects . For instance, several inorganic and organic compounds are up to 36 % less soluble in deuterated water (D_2O) than in water (H_2O). A few examples are presented in Table 2.19.

When refraction indices are considered, the isotope effect is no longer dependant on differences in mass or on volume but rather on the different speed of light propagation in the isotopic media. This effect is rather small in gases but considerable in liquids. For example, the refraction index of H_2O is 1.3325 and that of D_2O is 1.3278.

2.8 Natural and man-made sources of tritium; needs of ITER and IFMIF

Sources of tritium may be classified into natural and man-made, the latter surpassing the natural sources by many orders of magnitude [Pen08].

2.8.1 Natural sources

Natural production of tritium takes place mostly in the upper troposphere and lower stratosphere where tritium is generated by reactions of cosmic ray neutrons with nitrogen according to

$$
\begin{aligned}
{}^{14}_{7}\mathrm{N} + {}^{1}_{0}\mathrm{n} &\longrightarrow {}^{12}_{6}\mathrm{C} + {}^{3}_{1}\mathrm{H} - 4.3\,\mathrm{MeV} \\
{}^{14}_{7}\mathrm{N} + {}^{1}_{0}\mathrm{n} &\longrightarrow {}^{4}_{2}\mathrm{He} + {}^{3}_{1}\mathrm{H} - 11.5\,\mathrm{MeV}\ .
\end{aligned}
$$

Since both reactions are endothermic, energetic neutrons are required for these reactions to take place. The average cross section for neutrons with sufficient energy to make the reaction proceed, i.e. 4.4 MeV, was determined to be (11 ± 2) mb [Fir53]. Additionally, there is a nucleonic contribution by protons having energies of more than 100 MeV. Cross sections for the production of tritium by 2.2 GeV protons with nitrogen and oxygen were found to be (28 ± 4) mb and (33 ± 4) mb[5], respectively; and cross sections for the production of neutrons by 2.2 GeV protons were determined to be (1000 ± 400) mb for nitrogen and (650 ± 250) mb for oxygen, respectively [Fir55].

Tritium may also reach the atmosphere via direct extraterrestrial accretion into the stratosphere from solar wind [Cra57]. This conclusion is based on a mismatch observed between production rate calculations and actual tritium content measurements, which were found to be considerably higher than expected. Tritium from cosmic ray and extraterrestrial sources reach the earth surface mainly as HT via convection streams. Transport from the stratosphere into the atmosphere occurs predominantly during spring (so called spring leak of the tropopause). In the atmosphere tritium is slowly oxidized into tritiated water and then incorporated into the hydrologic cycle. In consequence, tritium is present predominantly as HTO on the earth surface. It was estimated that a steady state concentration of several kilogram establishes on the

[5] $1\,\mathrm{cm}^2 = 10^{24}$ b, b = barn

earth surface, resulting from natural production on one hand and losses by radioactive decay and transport of tritium into the oceans by rain, snow and rivers carrying continental water on the other. The natural inventory of tritium during the Seventies was estimated by several investigators to be in the range 3.5 - 11 kg [Mic76; Bur79; Eis79]. Of this tritium nearly 90 % was thought to be in the oceans and land water in form of HTO. A typical T/H ratio determined 1949 in atmospheric hydrogen using a mass spectrometric technique was $(16.7 \pm 1.2) \times 10^{-15}$ [Fir61]. The global mean production rate was assessed to be $(0.5 \pm 0.3)\,\mathrm{atoms\,cm^{-2}\,s^{-1}}$ [Cra61].

An increase of the atmospheric tritium inventory at the end of the Seventies by a factor of almost 30 in comparison to that of the Fifties was rationalized by nuclear weapon testing during the years 1952 – 1962 [Gro54; Gon59; Fir61]. It has been calculated that about 197 kg of tritium were released into the atmosphere by atomic bombs which resulted in an atmospheric inventory of approximately 176 kg (7×10^{19} Bq) in 1965 [Eri65]. Another estimate of the amount of tritium introduced into the atmosphere by weapon tests up to 1963 was reported by Fontes[Fon86]. According to this researcher the amount was nearly double as high, i.e. 323 kg (1.2×10^{20} Bq). An even larger value of 550 kg (10^{20} Bq) for the global tritium inventory arising from weapon tests performed within the period 1945 – 1975 was calculated by Michel [Mic76]. Fortunately, during the past decades this rather large inventory has decayed to values approaching the activity prior to nuclear weapon tests.

2.8.2 Man-made sources

CANadian Deuterium Uranium (CANDU) reactors use natural uranium (composition 99.28 % ^{238}U and 0.72 % ^{235}U) as fuel[6,7]. Of the two uranium isotopes only ^{235}U is *fissionable* by neutrons of all energies, i.e. from thermal to millions of electron volts. For fission of ^{238}U to occur fast neutrons with energies in excess of 1 MeV are necessary. With neutrons displaying less than 1 MeV threshold energy the only possible reaction with ^{238}U is radiative capture. Thereby ^{238}U is converted into the fissile plutonium species ^{239}Pu (*fertile* nuclide), which requires slow neutrons to undergo fission. Therefore, to achieve criticality with natural uranium perdeuterated water is utilized as moderator. D_2O moderator is rather effective because in each collision it decreases

[6] The production of tritium in a heavy water reactor by fission alone has been estimated to be in the range 7.4×10^{14} - 8.9×10^{14} Bq/GW_e/year [Bau92].

[7] By comparison, while 200 MeV are released from fission of a single ^{235}U atom only 4 MeV are liberated during the combustion of a single atom of ^{12}C.

the energy of fission neutrons considerably without absorbing neutrons as readily as water. By slowing down some of the neutrons to the point at which they can cause fission of ^{239}Pu, a self-sustained reaction with natural uranium can be maintained. An additional very important function of heavy water is to cool the fuel rods. When CANDU fission reactors are operated, tritium is generated by several nuclear reactions taking place in the uranium fuel elements. It is also produced in comparatively large amounts as sort of by-product in the heavy water moderator. In this case, tritium is generated via the absorption of neutrons by the deuterium constituent of heavy water according to reaction

$$\mathrm{D(n,\gamma)T}\ .$$

Conversion of deuterium into tritium causes slow but progressive radioactive contamination of the moderator. It should be noted that in spite of the rather small cross section of the neutron capture reaction, the total amount of tritium produced is still significant because of the fairly large mass of water necessary for the efficient and safe operation of the reactor. Heavy water used as moderator must be free from impurities because they may capture neutrons and concomitantly generate radioactive species which may convert the cooling system into a hazardous one. A further incentive for high purity water is minimization of corrosion and avoidance of scale formation [Gla94].

In view that tritium accumulating in heavy water constitutes a major contributor to the internal dose for plant workers and in order to minimize tritium releases into the environment, it is necessary to extract periodically this nuclide from the moderator. The extraction of tritium (as well as of protium) from deuterated water is currently carried out at acceptable costs at the Replacement Tritium Facility (RTF) of Ontario Power Generation in Darlington, Canada. TRF is probably the worldwide largest facility of this kind. The two stage process comprises a vapour phase catalytic extraction step, which extracts tritium in vapour form and a second stage consisting of a cryogenic distillation process which delivers tritium of purity better than 98 % at the bottom of the second of two columns. This tritium is stored for further utilization in suitable storage beds containing titanium as getter material. The extraction facility, which is in operation since 1990, can process up to 2500 t of heavy water per year and produce a few ml of liquified tritium gas each week or about 2.5 kg tritium per year.

Ontario Power Generation is one of two major civilian producers of tritium in the world (about $1\,\mathrm{kg\,year^{-1}}$). Other producers are Reviss Services (UK) Ltd (formerly Amersham) in Chesham, UK and Korean Electric Power Co. The tritium production facility for weapons in UK (Chapelcross Processing Plant in south west Scotland) which was operated from 1980 until 2005 is now closed. The same holds for the weapons tritium production reactor in the US, which was shut down 1988 (produced since 1955 more than 200 kg). Tritium recycling for the military is carried out in Savannah River, South Carolina. Warheads are shipped to the facility, emptied from tritium and recharged with recycled tritium.

Another efficient man-made production procedure consists in the irradiation of lithium targets using thermal neutrons generated in a nuclear reactor. The pertinent nuclear reaction is

$$^6\mathrm{Li(n,\alpha)T}.$$

In practice, chemical compounds containing natural lithium (7.5 % ^{6}Li and 92.5 % ^{7}Li) or lithium enriched in the lighter lithium isotope can be used as targets. Preferred targets are ceramics like **lithium meta aluminate** ($LiAlO_2$, MP = 2173 K) or **lithium aluminum alloys** [Kis66; Abe81; Tan87]. Aiming at the production of 3.7×10^{13} Bq of tritium, a tritium extraction experiment utilizing **lithium aluminum alloy** (1 % of 95.5 % enriched ^{6}Li) was conceived and the generation of tritium demonstrated experimentally in Tokai, JAERI [Abe81]. Irradiation over 11 d was performed in the JRR-2 reactor at JAERI (thermal flux $3 \times 10^{13}\,\mathrm{neutrons\,cm^{-2}\,s^{-1}}$). The ^{6}Li Al target was rolled to a plate, clad with Al plates and then submerged into 7 l of water in order to be in a position of detecting possible leakage out of the target. Irradiation for up to 70 d was carried out with a neutron flux of $2 \times 10^{14}\,\mathrm{neutrons\,cm^{-2}\,s^{-1}}$. More than 95 % of the generated tritium could be extracted thermally within 1 hour at 773 K. At this temperature the equilibrium pressure of tritium over lithium aluminum alloy is more than 300 times higher than over pure LiT [Owe76]. Hence, significantly milder extraction conditions suffice for the release of tritium from lithium – aluminum alloy, e.g. 673 K. The release mechanism is described by reaction

$$\mathrm{LiT + Al \longrightarrow LiAl + \frac{1}{2}\,T_2}\ .$$

A further advantage of Li – Al alloy is a product of rather high purity.

Almost 100 % of the tritium generated in **lithium meta aluminate** can be extracted at 1173 - 1273 K when performed under evacuation.

Regardless of the selected ceramic, a subsequent chemical purification of the liberated tritium from ^{3}He, carbon oxides and other impurities is necessary. Usually a Hopcalite bed, which acts as a catalytic oxidizer of molecular hydrogens, is used for this purpose. The resulting water species are collected downstream on an adsorber bed designed to retain water selectively at 323 K. Other gases like helium-3 or carbon oxides which pass through the adsorber bed are discarded. Highly enriched tritium is obtained either with a gas chromatographic or a cryogenic isotope separation system.

Tritium can also be generated in **boron carbide** pellets such as used in commercial light water reactors for the absorption of neutrons

$$^{10}\mathrm{B} + {}^{1}\mathrm{n} \longrightarrow {}^{7}\mathrm{Li} + {}^{4}\mathrm{He}$$

$$^{10}\mathrm{B} + {}^{1}\mathrm{n} \longrightarrow 2\,{}^{4}\mathrm{He} + {}^{3}\mathrm{T}$$

$$^{7}\mathrm{Li} + {}^{1}\mathrm{n} \longrightarrow {}^{4}\mathrm{He} + {}^{3}\mathrm{T} + {}^{1}\mathrm{n}\ .$$

Most of the produced helium will diffuse out of the pellets. Tritium generated in absorber rods is recovered and purified in the USA at the Tritium Extraction Facility operated at Savannah River Site.

One more man-made source of tritium are the blankets of fusion machines containing lithium ceramics like lithium ortho silicate (Li_4SiO_4) or lithium titanate (Li_2TiO_3). Purpose of these blankets is the achievement of tritium self-sufficiency of the fusion machine onto which they are integrated [Boc04]. Excessive generated tritium may serve to supply other fusion machines. Within this frame, much research is currently under way to improve understanding of the release mechanism of tritium from diverse ceramics and on the technical design of test blanket modules (see for example [Pen94; Mun01; Kak02; Mun03; Oka04; Fur05; Kaw05; Kin05; Mun05b; Ver05; Cho08; Sal08; Zha10b; Kul11; Ric11; Vit11; Yam11b]).

2.8.3 Tritium needs of ITER and IFMIF

For the operation of ITER most tritium and all deuterium will have to be supplied by external sources. At least during the initial phases, the contribution from breeding in Test Blanket

Modules will be comparatively small. For each GW d of generated thermal power approx. 150 g of tritium are consumed. Therefore, DT fusion systems will consum tritium (burn up) at a rate of 55.6 kg per full power year (FPY) of operation at 1 GW fusion power [Saw06; Tan11]. Consumption of external tritium will be reduced significantly once breeding of tritium at high breeding ratios is incorporated into the fusion fuel cycle. The necessary start up inventory of tritium is estimated to be 3 kg [Wil03]. This large and unprecedent amount of tritium will have to be introduced progressively into the Inner Fuel Cycle, the Long Term Storage Subsystem, the Vacuum Vessel, the Hot Cells and the Blanket until steady state conditions are established [Glu05]. The routine operation of ITER with deuterium/tritium plasmas will necessitate of the order of 2 - 3 kg of tritium. Prognostications of the amount needed during the whole basic physics phase are in the range 15 - 30 kg [Gie96]. The amount required for the extended physics phase is expected to be even higher.

Tritium, for the initial operation of ITER, will most probably be that extracted from the heavy water moderator of CANDU fission reactors. It is regularly being extracted using highly developed and efficient tritium handling technology [Lae08]. Main incentive for tritium extraction is not the commercial exploitation but rather compliance with radiation protection demands. Because the moderator volume in CANDU reactors is fairly large, sufficient tritium is obtainable from this source to fully meet the needs of ITER. To initiate the operation of ITER approximately 20 to 25 kg of tritium are presently on hand worldwide (mostly in Canada). This tritium inventory decreases on one hand by that sold on the world market for diverse applications and on the other by radioactive decay at a rate of $5.47\,\%\,\mathrm{year}^{-1}$.

A vessel containing titanium getter, has been designed and manufactured for the long-term storage of up to 1.9×10^{16} Bq of tritium generated in CANDU reactors. The vessel has been subjected to an extensive testing program to demontrate its storage capacity[Pae05]. Vessels of this kind serve for the long-term storage of tritium arising at the Wolsong Tritium Removal Facility operated by the Wolsong Nuclear Generation Station of South Korea. Titanium storage vessels heated for tritium retrieval are subsequently given to waste.

The ITER machine has been designed for 0.5 GW fusion power, $72\,\mathrm{g\,d}^{-1}$ burnup, and 3.5 $\mathrm{kg\,d}^{-1}$ tritium throughput. During the later stages of the operation of ITER the amount of tritium obtainable from ITER blanket modules is estimated to be approximately[8] $25\,\mathrm{mg\,d}^{-1}$.

[8] Lässer, R. 2012. Personal communication.

In comparison, DEMO is being designed for 3.7 GW fusion power, $0.5\,\mathrm{kg\,d^{-1}}$ tritium burnup, of the order of $35\,\mathrm{kg\,d^{-1}}$ tritium throughput, and approximately $550\,\mathrm{g\,d^{-1}}$ of tritium generated via breeding [Lae08]. It should be noted that, for DEMO only about double as high deuterium tritide feed flow rates (DT feed flow $\simeq 300\,\mathrm{Pa\,m^3\,s^{-1}}$) than for ITER (feed flow $\simeq$ $120\,\mathrm{Pa\,m^3\,s^{-1}}$ are expected because of the significantly higher burnup efficiency of DEMO (burn-up efficiencies of ITER and DEMO are 0.5 % and 1.5 %, respectively).

The current program schedule for ITER contemplates first plasmas in 2025, commissioning of tritium systems beginning 2027, and full power DT operation commencing 2035 (first introduction of tritium into the ITER torus). Accordingly, a first delivery of 100 g tritium is planned for 2027 followed by a 200 g delivery in 2030 for the commissioning of the tritium systems. In a next step, tritium is to be supplied at a rate of 800 g per year beginning 2031 in order to build up the necessary operation inventory ahead of full DT operation of 1.1 kg in 2035 [Glu07; Pea18].

The amount of tritium available 2003 for fusion research purposes was estimated at the time to be 18.5 kg or 6.68×10^{18} Bq [Wil03]. A more precise estimation for the same year yielded 21.1 kg [Fon12]. According to a more recent estimate, the inventory of tritium in Darlington was of the order of several dozen kilograms[9].

Several investigators [Wan13; Kov16; Pea18] have recently estimated the availability of tritium in the near future. These estimations have taken into account the uncertainties over the life extension of the global CANDU reactors and the potential impact on tritium demands by other DEMO-independent, non-collaborative fusion projects of nations like China or Korea, as well as possible worldwide demands by any other major research efforts. These projections lead to the conclusion that tritium from CANDU reactors remain sufficient to support the full operation of ITER. The support with tritium of DEMO and all other projects currently under development are, however, much more uncertain. In case these additional needs develop and corresponding international agreements can be reached, countries like South Korea, Romania, India and China have the potential of closing the gap by boosting the global production of tritium. With this in mind and in view that full breeding capability of DEMO is not expected to be demonstrated before 2050, Pearson et al. [Pea18] encouraged fast-tracked development of several concurrent compact fusion programs. Incorporation of tritium breeding technology into these nearer-term

[9] Canadian Coalition for Nuclear Responsibility, www.ccnr.org. Last visited on 16.09.2020.

devices requiring smaller quantities of tritium and operating at much smaller fusion power, would permit valuable tests under realistic conditions.

The International **Fusion Materials Irradiation Facility** (IFMIF) is of paramount importance to the ITER fusion programme. Only with this machine will it become possible to evaluate under truly realistic conditions the applicability of structural and fuctional materials of the kind needed for ITER and more advanced fusion machines like DEMO [Lae08]. This research facility will produce an intense high-energy neutron beam with sufficient irradiation volume to allow relevant and reliable testing of candidate materials and components. Neutrons will be generated at IFMIF by shooting deuterons into a target system consisting of a stable fast moving lithium jet. Duties of this jet are not only to produce neutrons by deuteron - lithium reactions such as

$$^{7}\mathrm{Li}(\mathrm{d}, 2\,\mathrm{n})^{7}\mathrm{Be}$$

$$^{6}\mathrm{Li}(\mathrm{d}, \mathrm{n})^{7}\mathrm{Be}$$

$$^{6}\mathrm{Li}(\mathrm{n}, \mathrm{T})^{4}\mathrm{He}$$

but also to remove the heat generated by the beam. According to the design, highly available, stable and continuous irradiation will be achieved at IFMIF with two continuous-wave linear accelerators generating 40 MeV deuterons each with a beam current of 125 mA. The accelerator modules will operate in parallel. Radiation will strike a single thick flowing lithium target under a 20-degree impinging angle. Under these conditions an intense neutron flux of about $10 \times 10^{18}\,\mathrm{neutrons\,m^{-2}\,s^{-1}}$ with a broad peak near 14 MeV will be delivered. Ultra-high heat resulting from stopping radiation produced by the 10 MW deuteron beam load is predicted to be in the $\mathrm{GW\,m^{-2}}$ region. According to expectations, an irradiation volume of about 0.5 l at a neutron wall loading of the order of $10 \times 10^{18}\,\mathrm{neutrons\,m^{-2}\,s^{-1}}$ will be possible [Moe07]. The IFMIF machine should be capable of an irradiation rate of up to 50 dpa / full power year (dpa = displacement per atom). The concentration of tritium in the recirculating lithium jet will be about 6 g per full power year [Sim04]. Generated tritium will be removed continuously from the liquid metal with getters in order to avoid releases of radioactivity during a conceivable lithium spill. Precautions required for safe handling of tritium are described in the comprehensive design concept edited by Martone [Mar96].

The EVEDA[10] Engineering Lithium Test Loop (ELTL) constitutes an important component of IFMIF. This facility was i) designed, ii) constructed, iii) approved by the local fire protection authorities and iv) comissioned at the O-arai site of JAEA beginning 2011 [Kon12]. A total of 1600 lithium ingots (each 240 mm long and 124 mm in diameter) weighting almost exactly 2.5 t have been introduced into the test loop utilizing a glove box built exclusively for this purpose. The ELTL comprises two lithium loops, i.e. a main loop and a purification loop. The main loop with a maximal flow rate of $3000\,\mathrm{l\,min^{-1}}$, encompasses as main components a quench tank, an electromagnetic pump, an electromagnetic flow meter, a lithium cooler and a dump tank. The purification loop essentially consists of a nitrogen hot trap, a cold trap and a hydrogen hot trap.

2.9 Applications of tritium other than for fusion

Tritium finds application in devices that glow in the dark. They are employed for instance as landing signs at remote airports, or exit signs of airplanes [Des73; Jen84; Jen85; Mul92; Ren94]. For their manufacture, tritium is fed into slim glass tubes, which are thereafter closed by melting. Inside of the tubes, beta particles emitted by tritium strike a phosphorescent coating applied throughout the inner wall which causes the coating to glow. One exit sign requires about 12 tubes containing in total approx. 2.5 mg tritium.

In another application, tritium is used extensively as an injected tracer in meteorology, cosmology, geohydrology [Mos76], biology, medical sciences, and agriculture [Mur90b].

Elemental tritium is also employed in some nuclear weapons. The amount required is within the range 2 - 4 g per weapon. Tritium reservoirs in warheads must be replenished about every eight years to compensate for radioactive decay.

[10] Engineering Validation and Engineering Design Activities (EVEDA) expenditures are estimated to be 81 MICF (MICF = Million IFMIF Conversion Factor with 1 ICF = 1 US dollar).

2.10 Radiochemical and chemical properties of elemental tritium and tritiated water

Whilst the chemical properties of hydrogen, deuterium, and tritium are essentially the same, in case of tritium the emitted β-radiation can have strong influence on the mechanism of reactions, particularly when the activity level is high. In the following a number of fusion fuel cycle relevant reactions of tritium with selected gases, liquids and solids are briefly discussed.

2.10.1 Self-radiolysis of T_2

Foremost ionic self-radiolysis product of T_2 is ${T_3}^+$. This species is formed via reactions such as

$$T_2\,(\text{radiolysis}) \longrightarrow {T_2}^+ + \text{other products}$$
$${T_2}^+ + T_2 \longrightarrow {T_3}^+ + T$$

and depleted by electron-ion recombination according to

$${T_3}^+ + e^- \longrightarrow 3\,T\ .$$

In view that the concentration of ${T_3}^+$ quickly reaches steady state, the formation rate of ${T_3}^+$ will become equal to that of ${T_2}^+$ which in turn is proportional to the concentration of T_2. Taken that the concentration of electrons and ${T_3}^+$ ions are approximately equal, it is easy to show that the steady state concentration of ${T_3}^+$ is obtainable from relationships

$$\frac{\mathrm{d}[{T_3}^+]}{\mathrm{d}t} \cong k_0[T_2]_0 - k_1[{T_3}^+]^2$$
$$[{T_3}^+] \cong [e^-] \cong \sqrt{\frac{(k_0[T_2]_0)}{k_1}}\ .$$

Here k_0 is the rate constant for ${T_2}^+$ formation and k_1 the rate constant for the recombination of ${T_3}^+$ ions with electrons.

Failor et al. [Fai88] calculated the steady state concentrations of all self-radiolysis products generated in pure T_2 at two pressures using a germane set of rate constants. The results are compiled in Table 2.20. As can be seen, only at very low pressures, e.g. 10^{-1} Pa, is there a

Table 2.20: Calculated steady state concentrations of products (in mol cm^{-3}) from the self-radiolysis of T_2 at 298 K.

Species	At a pressure of 10^5 Pa	At a pressure of 10^{-1} Pa
T_2	4.1×10^{-5}	2.9 x 10^{-11}
T_3^+	1.5×10^{-14}	1.2 x 10^{-17}
e^-	1.5×10^{-14}	1.3 x 10^{-17}
T	3.5×10^{-11}	2.5 x 10^{-11}
T^+	1.1×10^{-18}	6.4 x 10^{-19}
T_2^+	7.6×10^{-22}	7.2 x 10^{-22}

noteworthy percentage of T_2 converted into radiolysis products (note that T_3^+ is the major ionic radiolysis product). As likewise apparent, the steady state concentrations of T, T^+ and T_2^+ are essentially independent of the tritium pressure, which is consistent with the fact that their formation and depletion reactions are both first order in tritium. The time to reach approximately 90 % of the steady state concentrations of the T_2 self-radiolysis products at 298 K and 10^{-1} Pa is about 2 s for T_3^+, e^+, T_2^+ and T^+ and 6.5 s for T. Hence, steady state concentrations are established fairly rapidly.

The above discussion reveals that molecular tritium is effectively comparable to a plasma having a low steady state concentration of ions. These ions will basically control all chemical reactions taking place in the gas phase [McC83a; McC88]. Both ion density and relative ion distribution in molecular tritium are pressure dependent. The dominant ionic species at very low pressures is T_2^+. As the pressure is raised up to 100 Pa T_3^+ becomes the prevailing ion. As already indicated before, this ion is formed by reaction of T_2^+ with T_2.

When the pressure is increased up to $> 10^3$ Pa, a third-order reaction

$$T_3^+ + T_2 + T_2 \longrightarrow T_5^+ + T_2$$

becomes dominating. The concentration of T_5^+ that establishes under these conditions can be estimated from the expression [Sou81]

$$[T_5^+] = [T_3^+]\, p\, (3.7 \times 10^{-11}\,\mathrm{Pa}^{-1}) \exp\left(\frac{4804\,\mathrm{K}}{T}\right) .$$

where p is given in (Pa) and the equilibrium constant is valid for the temperature range 240 - 435 K. Accordingly, at 300 K and 10^5 Pa of tritium the ratio T_5^+/T_3^+ has a value of 37.6 indicating that T_5^+ is the prevailing ion. To calculate the ratio T_{11}^+/T_9^+ within the temperature range 100 - 120 K, an equilibrium constant of $6 \times 10^{-10}\,\mathrm{Pa}^{-1}$ and an exponent of 1200 K was experimentally determined. At even lower temperature, e.g. 20 K, the major cluster ions over pure tritium are rather heavy, i.e. T_{31}^+ and T_{33}^+.

Positively charged heavy hydrogen ion clusters generated in reactions such as

$$H_3^+ (H_2)_{n-1} + H_2 = H_3^+ (H_2)_n$$

were likewise observed in hydrogen at temperatures in the range 100 - 300 K employing a pulsed electron beam high ion source pressure mass spectrometer [Hir75; Hir87]. The equilibrium rate constant shown above displayed proportionality to inverse temperature by $T^{-2.3}$. The forward reaction was found to be given by

$$k_1 = 9 \times 10^{-30}\,\mathrm{cm}^6\,\mathrm{molecules}^{-2}\,\mathrm{s}^{-1}$$

and the inverse reaction by

$$k_{-1} = 8.7 \times 10^{-6} \exp\left(\frac{-8.4}{R\,T}\right) \mathrm{cm}^3$$

where the activation energy is in $\mathrm{kcal\,mol}^{-1}$.

Excited molecules and ions as well as impurities like CT_4, N_2T^+ and T_3O^+, whose presence cannot be fully excluded in a stainless-steel vessel even when using meticulously purified molecular

tritium[11], reduce the total ion density in molecular tritium. For instance, the reaction of pertritiated methane with T_3^+ proceeds according to

$$CT_4 + T_3^+ \longrightarrow CT_5^+ + T_2$$

yielding the ionic species CT_5^+. The increase in relative concentration of this species with increasing concentration of CT_4 is documented by the CT_5^+/T_3^+ ratio, which takes values of 0.0103, 11.11 and 11160 at CT_4 concentrations of 0.001, 1.0 and 1000 ppm, respectively.

2.10.2 Helium hydride, helium tritide

The main ions generated by radioactive decay of HT, i.e. $(He^3H)^+$, or of T_2, i.e. $(He^3T)^+$, display strong tendency to remain bound [Sne57; Wex59; Wol65]. The relative probabilities of formation of the principal ions resulting from beta decay of HT are estimated to be $((93.2 \pm 1.9)\,\%)$, $((5.1 \pm 0.3)\,\%)$, $((1.55 \pm 0.16)\,\%)$, and $((0.14 \pm 0.01)\,\%)$, for $(He^3H)^+$, $(He^3)^+$, H^+, and $(He^3)^{++}$, respectively [Sne57]. When in case of T_2 a beta particle is emitted, the remaining species is a stable $(He^3T)^+$ helium tritide ion. According to Souers [Sou86], the "best guess" as to the relative probability of formation of ions generated during beta decay of $(He^3T)^+$ are 58 %, 32 %, 9.2 %, and 0.8 %, for $(He^3T)^+$, $(He^3)^+ + T$, $He + T^+$, and $(He^3)^{++} + T + e$, respectively. Calculations by Ikuta et al. [Iku77] support these values. The product distribution favoured by Souers is, however, significantly different from that obtained experimentally for $(He^3H)^+$ by Snell et al. [Sne57]. The most probable fate of $(HeT)^+$ is

$$HeT^+ + T_2 \longrightarrow T_3^+ + He + 3.0\,eV\,.$$

Very limited information is available on ion-molecule reactions of $(HHe)^+$ (or $(THe)^+$) ions with molecules such as O_2, N_2, CO, or CO_2.

[11] CT_4 is characteristically generated in steel vessels containing molecular tritium. N_2T^+ and T_3O^+ are formed when traces of air are present in molecular tritium by reactions such as

$$T_3^+ + N_2 \longrightarrow N_2T^+ + T_2$$
$$2\,T_3^+ + O_2 \longrightarrow 2\,T_3O^+\,.$$

2.10.3 Synthesis and self-radiolysis of T_2O

2.10.3.1 Synthesis of T_2O

A straightforward procedure for the preparation of T_2O consists in exposing dry platinic oxide to pure molecular tritium [Swa58]. For high conversion platinic oxide was used in excess of that required for the oxidation of all added gaseous tritium.

Ghormley and Allen [Gho48] obtained T_2O by passing pure oxygen generated by thermal decomposition of potassium permanganate alongside of a heated palladium thimble. When gaseous tritium was passed through the inside of the thimble permeating highly pure molecular tritium gas was immediately oxidized into water by catalysis on the hot palladium surface.

Other investigators [Gol64; Pey78; Gil84] synthesized T_2O by passing T_2 over heated copper oxide at temperatures within the range 573 - 673 K. Gill [Gil84] synthesized a known amount of tritiated water by re-circulating a precalculated amount of gaseous T_2 through a CuO column maintained at (623 ± 50) K. In his experiments the conversion into water was completed in less than 10 min. Generated water was trapped in a cooled quartz cuvette. Unreacted gas and impurities were removed by pumping. Resulting water was frozen out in a thin tube, e.g. capillary, using liquid nitrogen.

Another approach has been the oxidation of tritium-labelled hydrogen with Hopcalite, an "oxidising catalyst", at 773 K [Ito07]. In this case, several millilitres of tritiated water could be collected in a trap maintained at low temperature by cooling with dry ice.

2.10.3.2 Self-radiolysis of T_2O

The radioactive decay of tritiated water is described by reactions

$$\mathrm{HTO} \longrightarrow {}^3\mathrm{He}^+ + \beta^- + \bar{\nu} + \mathrm{OH}^*$$
$$\mathrm{T_2O} \longrightarrow {}^3\mathrm{He}^+ + \beta^- + \bar{\nu} + \mathrm{OT}^* \ ,$$

where OH^* and OT^* are excited radicals. In a closed system, helium will progressively manifest as "overpressure". In addition, tritiated water will decompose by self-radiolysis induced by the beta-radiation emitted by tritium. The energy transferred by beta-radiation to T_2O molecules conducts to the formation of i) T_2O^+ ions, ii) excited T_2O^* molecules, iii) aqueous or hydrated

electrons e^- (aq)[12], iv) T_3O^+ ions, v) $T\cdot$ radicals and vi) $OT\cdot$ radicals. These species, which are not produced homogeneously in space but rather along the short track of beta-particles, will undergo further reactions either to regenerate the starting reagents, i.e.

$$T_3O^+ + e^- (aq) \longrightarrow T\cdot + T_2O$$

$$T\cdot + OT\cdot \longrightarrow T_2O$$

$$e^- (aq) + T\cdot \longrightarrow OT^-$$

$$OT\cdot + T_3O \longrightarrow 2\,T_2O$$

or other products like

$$T\cdot + T\cdot \longrightarrow T_2$$

$$e^- (aq) + e^- (aq) \longrightarrow T_2 + 2\,OT^-$$

$$e^- (aq) + T\cdot \longrightarrow T_2 + OT$$

$$OT\cdot + OT\cdot \longrightarrow T_2O_2\ .$$

Hence, the principal primary products of the radiolysis of tritiated water are T_2 and T_2O_2. As the reaction progresses, these species undergo further reactions with radicals and aqueous electrons eventually leading to the formation of O_2. In summary, the initial radiochemical reaction gives rise to radical products (G_R) and to molecular products (G_M), where G is defined as the number

[12] Aqueous electrons are hydrated thermalized electrons.

of species formed per 100 eV of absorbed energy. G-values determined by Collinson et al. [Col62] are

$$G_{(\mathrm{T^+e^{-(aq)}})} = 2.9$$
$$G_{\mathrm{TO_2}} = 0$$
$$G_{\mathrm{OT}} = 2.0$$
$$G_{\mathrm{T_2}} = 0.55$$
$$G_{\mathrm{T_2O_2}} = 0.97$$
$$G_{-\mathrm{T_2O}} = 3.97$$
$$\frac{G_{\mathrm{R}}}{G_{\mathrm{M}}} = 3.2\ .$$

Within the concentration range of tritium of 2×10^{16} - $1.6 \times 10^{18}\,\mathrm{Bq\,m^{-3}}$ the effective G-value for the formation of hydrogen was found to increase with decreasing concentration of tritium [Hay06]. The effect of temperature on the primary radiochemical reactions was only minor. However, increasing the temperature of water was found to decrease the solubility of gases which modified the overall reaction mechanism.

In an early and rather comprehensive investigation, Peyrat [Pey78] studied the effect of temperature, volume, isotopic purity and presence of inorganic as well as organic impurities on the radiation chemistry of tritiated water. According to his observations, the pressure in a vessel containing T_2O increases regularly due to tritium transmutation and radiochemical reactions which leads to the formation of helium-3 and oxygen in the proportion 4 : 1 = He : O_2. Additionally, radiolysis reactions initiated by the beta rays emitted by tritium cause formation of molecular hydrogen isotopologues and oxygen in stoichiometric proportions. When these reactions reach equilibrium the final pressure that establishes will dependent on the purity of T_2O and on the prevailing temperature. Pressures as high as 70 bar may develop if the vessel containing T_2O is filled up to 50 % of its capacity [Pey78]. The continuing pressurization demands adequate preventive measures, like i) sufficient free volume above the water, ii) storing in a pressure-resistant vessel or iii) regular and frequent depressurizations in order to prevent leaks or even vessel rupture. Since the radiolysis gases constitute an explosive mixture, there is an added safety relevant incentive for recurrent removal of gases.

During storage of T_2O tritium peroxide progressively accumulates in the liquid phase at concentrations that will not surpass $0.001\,\mathrm{mol\,l^{-1}}$. In the presence of nitrogen, species such as NO_3^-, NO_2^- and H_3O^- will additionally build up. These ions can react with stainless-steel constituents like iron, nickel or chromium and cause corrosion [Pey78].

With the aim of researching factors causing corrosion and influencing material balance calculations Gill [Gil84] measured quantitatively the amount of tritium peroxide (T_2O_2) that builds up in the T_2O liquid phase as function of elapsing time. In addition, he examined the effect of gaseous T_2 as suppressor of the radiolytic decomposition of T_2O and hence formation of tritium peroxide. Radiolytic equilibration was found to be attained at an overpressure of 1.59 bar. At this point, the rate of gas production is balanced by the rate of recombination. The experiments were performed in a quartz cell attached to a pressure transducer. This arrangement permitted determination of the pressure increase over pure pertritiated water while at the same time assaying the formation of tritium peroxide via UV absorption spectroscopy at a wave length of 227 nm. Gill carried out two consecutive experiments: one in the presence of T_2, which acts as a **suppressor** because it reacts with oxygen and another without T_2 (after cooling the water and evacuating the gas phase). The pertinent reactions were:

$$\begin{aligned} T_2O &\longrightarrow {}^3He + OT^{\cdot} + \beta \\ 2\,OT^{\cdot} &\longrightarrow T_2O + \frac{1}{2}\,O_2 \\ &\longrightarrow T_2O_2 \\ T_2\,(\text{suppressor}) + \frac{1}{2}\,O_2 &\longrightarrow T_2O. \end{aligned}$$

As apparent from Fig. 2.7 (left), in the presence of a suppressor the pressure initially increases linearly with time simply because for every tritium atom that decays one ^3He atom and one fourth O_2 molecule is generated. At the same time $(1/2)\,T_2$ molecule disappears yielding in total 3/4 generated gas molecules. After elapsing of 14 d of storage a large fraction of the suppressor has been consumed and the overpressure begins to increase much faster. At this point in time, the increase is governed by the formation of decay helium as well as by the generated radiolysis gases T_2 and O_2. At the same time, because at day fourteen most of the suppressor has been consumed, the concentration of T_2O_2 experiences a sudden and pronounced drop to almost the

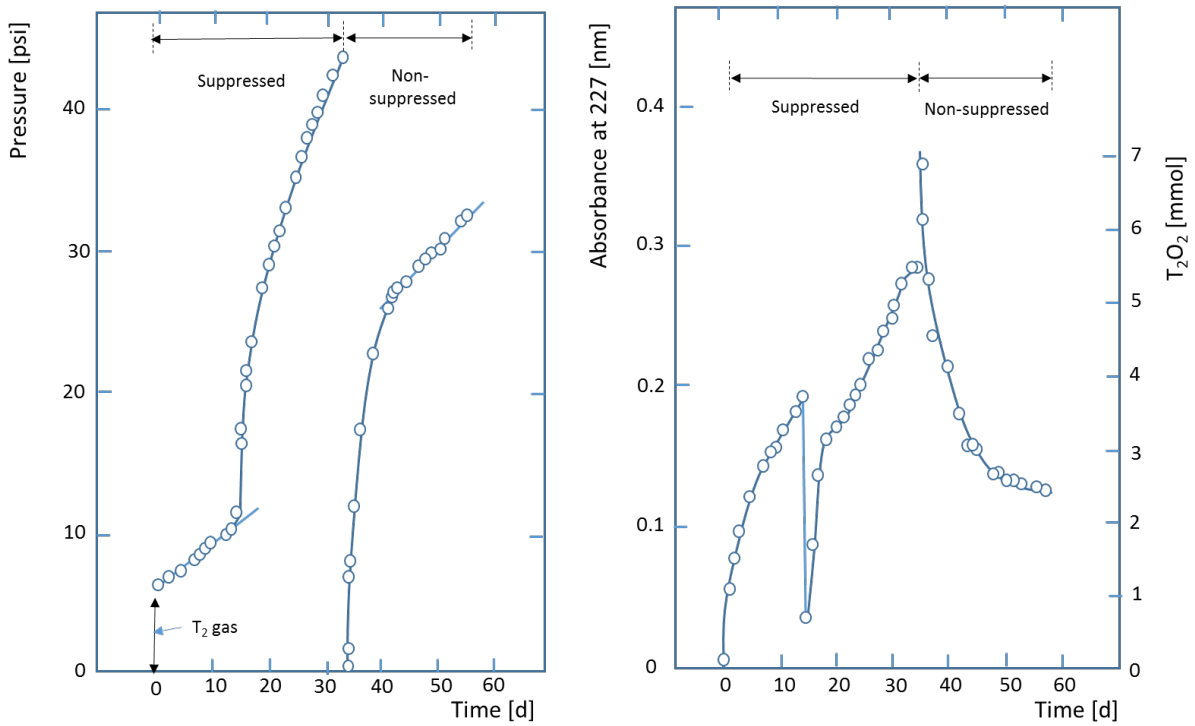


Figure 2.7: Comparison between the radiation chemistry of T_2O in the presence of 386 mbar T_2 as suppressor and without. The figure on the left shows the pressure buildup in the gas phase above T_2O and the one on the right the absorbance by T_2O_2 as function of time in the liquid phase (after [Gil84]).

detection limit (see Fig. 2.7, right). Subsequently, the concentration of T_2O_2 commences again to raise, but in a somewhat erratic fashion. Repeating the experiment without suppressor (see Fig. 2.7, left) yields first radiolysis and transmutation products and, once equilibrium has been attained, only the latter. The liquid phase, on the other hand, displays only a decrease in T_2O_2 concentration from that initially remaining after completion of the previous experiment. With progressing ageing, the data exhibit a tendency towards establishment of equilibrium.

Whereas tritiated water of low specific tritium concentrations, e.g. 0.01 - 0.01 PTBq/m^3 displays nearly neutral pH values, in case of high specific concentrations, e.g. 1 - 1000 PTBq/m^3 acidic values, i.e. $3 < \mathrm{pH} < 5$, prevail, regardless of the duration of storage. Low pH values will contribute significantly to enhance corrosion by tritiated water [Hay06].

As put on view in Fig. 2.8, Itoh et al. [Ito07] observed that the rates of formation of tritiated hydrogen (and of tritiated hydrogen peroxide, not shown in the figure) depend strongly on the specific concentration of tritium in the water. The rate of formation of hydrogen peroxide was

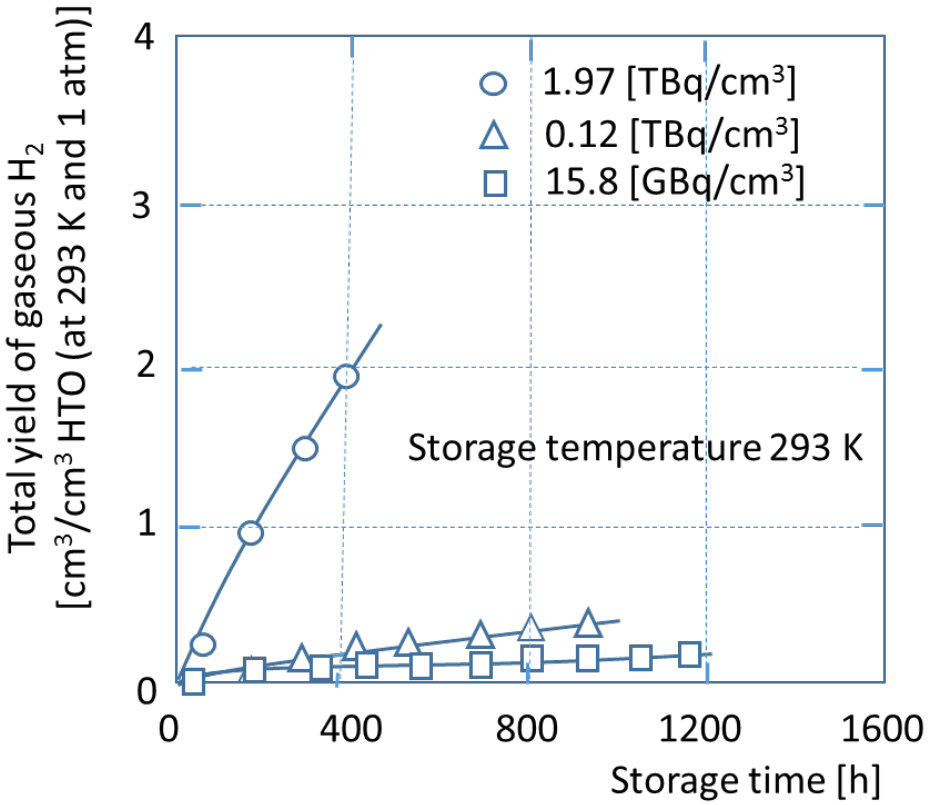


Figure 2.8: Hydrogen production as function of storage time at three specific concentrations of tritium in water (after [Ito07]).

followed by UV spectroscopy at wavelengths of 215 nm and 230 nm. For the interpretation of the results it was assumed that i) all involved gases have a singular solubility in tritiated water and ii) the formation of peroxides requires the presence of molecular oxygen in water. While the G-values of hydrogen and oxygen increased with temperature those of hydrogen peroxide remained essentially constant. Interestingly, metals dipped into water containing 0.12 TBq cm^{-3} of tritium and maintained at 293.15 K influenced the G-values, i.e. SS316L slightly enhanced and SS304 considerably retarded the yield of radiolysis gases per 100 eV absorbed energy. Under the prevailing conditions no signs of corrosion of the immersed metals were detected.

The isochoric self-radiolysis of low activity tritiated water was recently modelled by Heinze et al. [Hei05] utilizing a code developed by Kirkegaard and Bjergbakke [Kir01]. It was postulated that tritiated water vapour in equilibrium with the liquid phase constitutes the main source of beta particles in the gas phase. A typical comparison between experiment and calculations

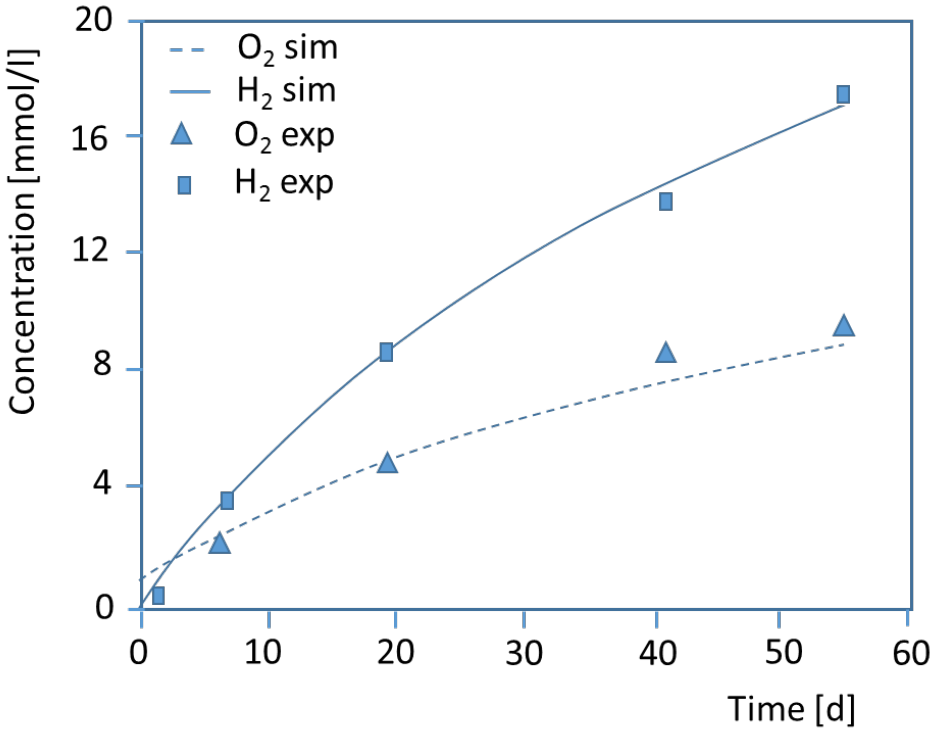


Figure 2.9: Comparison of the rates of formation of tritiated hydrogen and oxygen from water containing 74 TBq l^{-1} of tritium between experiment and theory (sim = simulation and exp. = experiment) (after [Hei05]).

illustrating the build-up of hydrogen and oxygen as function of time is plotted in Fig. 2.9. The simulation takes into account radiochemical and chemical processes in the liquid phase as well as back reactions in the gas phase leading to the formation of water. As apparent, experimental results and simulation reveal satisfactory agreement.

In earlier work carried out by Ghormley and Allen [Gho48] under challenging experimental conditions, the self-decomposition of HTO (T ranging from 2 % to 19 % of total hydrogens) was investigated at temperatures ranging from liquid nitrogen up to 418 K. HTO was synthesized by oxidation of tritiated hydrogen and condensed into small silica ampoules. Subsequently, the ampoules were evacuated, sealed, and placed inside of an evacuated vessel made of soft glass. Because helium readily diffuses across silica but not through fused glass the activity in the ampoules could be determined by measuring periodically the pressure rise (due exclusively to decay helium) in the soft glass vessel. After a few weeks, the rate of helium accumulation in the vessel becomes independent of time, i.e. the rate of formation of decay helium is equal to that of

helium diffusion out of the ampoule. Activities determined by this procedure were occasionally verified by calorimetry. Several experiments were carried out submerging small sealed silica ampoules containing HTO ice (with 15 % T) into liquid nitrogen for extended periods of time. Under these conditions, the G-values of radiolysis products decreased progressively from 0.27 to 0.04 over a period totaling 92 hours. The decrease in G-values was attributed to possible back reactions.

Itoh et al. [Ito07] essentially confirmed the effect of temperature on G-values reported in [Gho48] (see also Fig. 62) . They noted that HTO (1.97 TBq cm^{-3}) maintained at (303, 293, 288, 283, or 278) K displays G-values for the gases generated by self-radiolysis of 1.16, 0.39, 0.28, 0.2, or 0.16, respectively. Hence, only about $1/10^{\text{th}}$ of the gases are liberated when the temperature is reduced from 303 down to 278 K.

Along the same line, Peyrat [Pey78] had previously pointed out that already at temperatures of 278 K or below the pressure evolution from T_2O is substantially reduced (essentially only transmutation gases) in comparison to that at ambient temperature. Experimental evidence indicates that trapping of electrons and of free radicals in the solid matrix cause the yield of molecular products to become much smaller because recombination reactions practically cease to occur.

At Centre d´Etudes de Bruyères-le-Châtel, France, 5 cm^3 of tritiated water were stored in a 100 cm^3 glass vessel at 252 K for a period of 47 d.

2.10.4 Self-radiolysis of tritiated water immobilized in solid absorbers

Pure per-tritiated water is difficult to store over prolonged periods of time at ambient temperature because of the constant generation of radioactive radiolysis gases and transmutation gases. The resulting reaction products lead not only to pressurization but are also very corrosive even when highly diluted. Corrosive properties are primarily attributed to radiolytic free radicals. To minimize the danger of spilling and preclude corrosion, it is generally recommended to transport and store tritiated water in absorbed form. Good results have been obtained with absorbers such as **clay** (absorption capacity approx. 60 % by volume) or **molecular sieves** (absorption capacity approx. 20 % by weight). It should be noted that the absorption of water does **not prevent pressurization**!

One more widely used absorber for the immobilization of hazardous liquids or storage of explosive materials is **Vermiculite**. This natural mineral exfoliates when heated, expands considerably at temperatures of 673 K or above and melts at 1623 K. Vermiculite consists of magnesium aluminum silicate with an absorption capacity for water of about 20 % by weight. Because of the latter property and its non-hydrogenous composition, it has been successfully employed for the transport of tritiated water, tritiated octane, as well as contaminated pump oil [Bib77].

As already pointed out, substantial self-radiolysis takes place during storage of pure liquid tritiated water. Interestingly, the formation of gaseous tritiated hydrogen by self-radiolysis of adsorbed tritiated water is significantly dependent on the nature of the matrix in which the tritiated water is immobilized, e.g. cement plaster [Tad80], silica gel [Nak86], or molecular sieve [Nak87].

In some cases, like silica gel, the self-radiolysis of adsorbed tritiated water is much larger than that of liquid water [Tad80; Nak86]. The effect was explained by energy transfer phenomena similar to those observed during the gamma radiolysis of water on silica gel. There is some evidence indicating that the predominant mechanisms of hydrogen formation in gamma and beta irradiations are similar. Factors influencing the yield of hydrogen formation from adsorbed water are surface coverage and the concentration of hydroxyl groups on the adsorber surface. Radiolysis-enhancing effects were attributed to fundamental harmonic oscillator relationships involving excitation of the substrate. Silica gel appears to act as kind of energy sink for the decomposition of adsorbed water.

Notably, opposed to the radiolysis of pure tritiated water, practically no oxygen was detected among the products. The reactions explaining the radiolysis of adsorbed tritiated water were postulated to be

$$\beta + H_2O \longrightarrow H + OH$$

$$H + H \longrightarrow H_2$$

$$OH + H_2 \longrightarrow H_2O + H \ .$$

In case of isochoric storage, the rates of the last two reactions will eventually become equal and the pressure of hydrogen reach a steady state value. This condition is attained when

the radiation-induced rate of water decomposition becomes equal to that of hydrogen atom recombination and scavenging of molecular hydrogen by OH radicals. Remarkably, the enhancing effect of the absorber was found to depend on the nature of the substrate. This was explained by absence of hydroxyl fragments in some substrates. Analysis of the isotopic composition of gaseous hydrogen liberated by radiolysis of adsorbed tritiated water was found to be different from that generated during self-radiolysis of pure liquid tritiated water. This suggests different reaction mechanisms [Wal97].

Walters [Wal97] proposed the following rate law to calculate the pressure rise in a closed container until equilibrium is established

$$\mathrm{H_2} = 2.4 \times 10^6 [\mathrm{H_2O}] \frac{A_0}{\lambda} (1 - \exp(-\lambda t)) \quad \text{molecules}\,\mathrm{Bq}^{-1}\,\mathrm{d}^{-1}$$

Here, A_0 is the initial activity in the molecular sieve, λ the decay constant of tritium in days and $\mathrm{H_2O}$ the fraction of water remaining at time t. With the above rate law, a satisfactory modelling of the experimentally obtained data was possible.

In more recent work, Walters et al. [Wal02] noticed, in contrast to the results of Nakashima and Tachikawa [Nak86; Nak87] or Tadlock et al. [Tad80], that several disposable molecular sieve beds (DMSB) from PPL containing tritiated water failed to generate hydrogen gas by self-radiolysis of tritiated water at the expected rate. Evidently, scavenging of the radical fragments generated by interaction of beta radiation with OH groups in the molecular sieve cavities by **residual molecular oxygen** present in the DMSB suppresses markedly the formation of molecular hydrogen. It was conjectured that the gas phase rate constant for the production of hydrogen gas is probably orders of magnitude smaller than the third order rate constant for scavenging of radical fragments by oxygen. Under oxygen scavenging conditions, the rate constant for the production of hydrogen gas was calculated to be $k = (19.6 \pm 4.5)\,\mathrm{s}^{-1}$. The effect of oxygen was corroborated in a parametric study using 10 g samples of molecular sieve loaded with water and placed in several $15\,\mathrm{cm}^3$ vessels filled with various pressures of oxygen but exposed to nearly equal γ–ray doses. Under these conditions, the production of hydrogen decreased with increasing partial pressures of oxygen in the supernatant gas.

The **resistance** of molecular sieves **towards radiation** has been discussed by Breck [Bre74]. Molecular sieve 13X showed first damage when exposed to a fast neutron dose of 6.2×10^{17}

neutrons/cm^2. Only when the dose was increased up to 7×10^{19} neutrons/cm^2 was a complete collapse of the crystal structure observed [Ree65]. Radiation caused contraction of the crystal structure which manifested by increased density, i.e. from 2 to 2.4 g cm^{-3}. Zeolites used in clean-up operations in nuclear power stations have been found to function at doses of up to 2×10^{19} Gy for a 10-year period of time [Qur91]. Because of their radiation resistance, inorganic ion exchangers like zeolites have also been used to remove fission products, activation products, and artificial heavy atoms from liquid wastes [Rod81]. It should be noted that during uninterrupted irradiation of the crystalline matrix a fraction of tritiated water persistently remains sequestred in the adsorber.

Exposure to lower doses, as is the case with molecular sieve used as desiccants for the retention of tritiated water released after processing of plasma exhaust gases, has not led to a worsening of the adsorption properties even after numerous adsorption/desorption cycles. With respect to this application, there is a vast body of experience documenting reliable and stable performance of molecular sieves during prolonged utilization in Tritium Removal Systems.

2.10.5 Reaction of T_2 with oxygen. Inflammability, explosion, and detonation

According to the early work of Dorfman et al. [Dor54b; Dor54a], the initial rate, R_i, of molecular tritium with oxygen is directly proportional to the partial pressure of tritium. The reaction was investigated in a spherical cell of 73 mm diameter with a total reaction volume of 248 cm^3. In such a vessel practically all the β-particle energy is absorbed by the gas phase provided the gas density is sufficiently high. The measured rate followed the relationship

$$R_i = k c_{\mathrm{T_2}} (1 + 0.3\, m_{\mathrm{H}})$$

where k is the rate constant 1.2×10^{-4} min^{-1}, $c_{\mathrm{T_2}}$ the concentration of tritium in mol l^{-1} and m_{H} stands for the mol fraction of protium in the reactant hydrogen. As evident from the equation, the influence of small partial pressures of protium on the reaction rate is only minor.

Robins et al. [Rob84] evaluated fourteen publications (see references [Dor54b; Cas62; Yan64; Gev64; Eak71; Bel75; She80; Eas83] and others) relying on different experimental techniques and conditions but all devoted to the investigation of the conversion of elemental tritium into tritiated water (see Fig. 2.10). The evaluated experimental results included i) homogeneous

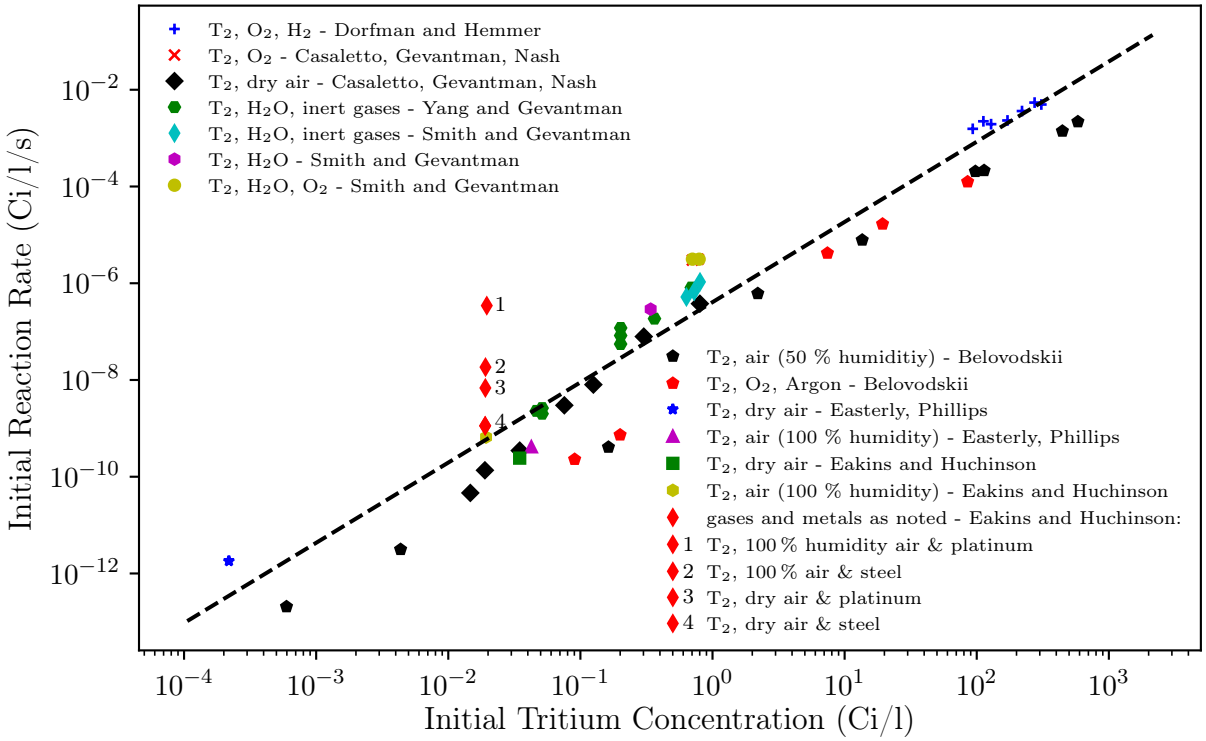


Figure 2.10: Initial reaction rates of formation of HTO as function of the initial concentration of tritium under a broad variety of experimental conditions [Rob84].

gas phase oxidation reactions, ii) isotopic exchange reactions with atmospheric moisture and iii) heterogeneous surface catalytic reactions influencing the homogeneous or isotopic exchange reactions. From a plot of the initial reaction rates vs the initial concentration of tritium used in these experiments the following empirical rate equation was obtained

$$R = 1 \times 10^{-7} \cdot c_{\mathrm{T}}^{1.5}$$

in which R is the rate of the reaction in Ci/l/s and c_{T} is given in Ci/l. The constant 10^{-7} was estimated from a least square fit of all results.

From the data it was inferred that while the production of tritiated water in air undergoes significant enhancement by i) the presence of water vapour, ii) increasing temperatures or iii) catalytically active metal surfaces, it is essentially independent from the partial concentration of oxygen. Rates calculated from the equation proposed by Dorfman and Hemmer [Dor54b] agreed well with the best-fit straight line of Robins. The evaluation of literature data [Rob84]

furthermore revealed that whereas at high concentrations of tritium the rate is first order in tritium, it becomes second order in tritium at moderate concentrations and turns again into first order when the concentrations of tritium becomes very low.

The principal reactions describing the oxidation of molecular tritium with oxygen to yield tritiated water are:

$$2\,T_2 + O_2 \longrightarrow 2\,T_2O$$

$$(2\,HT + O_2 \longrightarrow 2\,HTO, \text{etc.})$$

$$O_2 \text{ radiolysis} \longrightarrow O^+ \text{ and } O\,(^1D)$$

$$O^+ + T_2 \longrightarrow OT^+ + T$$

$$OT^+ + O_2 \longrightarrow OT + {O_2}^+$$

$$O\,(^1D) + T_2 \longrightarrow OT + T$$

$$OT + T_2 \longrightarrow T_2O + T\ .$$

Major reactions conducing to the formation of T_2O are:

$$OT + TO_2 \longrightarrow T_2O + O_2$$

$$OT + T_2O_2 \longrightarrow T_2O + TO_2$$

$$OT + T_2 \longrightarrow T_2O + T\ .$$

Failor et al. [Fai88; Fai89] modelled on the basis of reactions such as illustrated above the oxidation reaction of T_2 in the presence of O_2 at tritium concentrations within the range 0.0001 - 1.0 mol %, a constant pressure of 100 kPa, and ambient temperature. They also investigated the effect of self-radiolysis products from the reaction of T_2 with O_2 on the reaction mechanism. This was accomplished by comparing the reaction rate of pure T_2 with oxygen with that of T_2 already containing steady state concentrations of the major T_2 radiolysis products from the reaction with molecular oxygen. The results indicate that inclusion of self-radiolysis products is only important during the initial stage of the T_2/O_2 reaction (see Fig. 2.11). To interpret the overall kinetics and perform model calculations no less than 40 sequential and parallel elementary reactions involving ions, radicals, and electrons were considered.

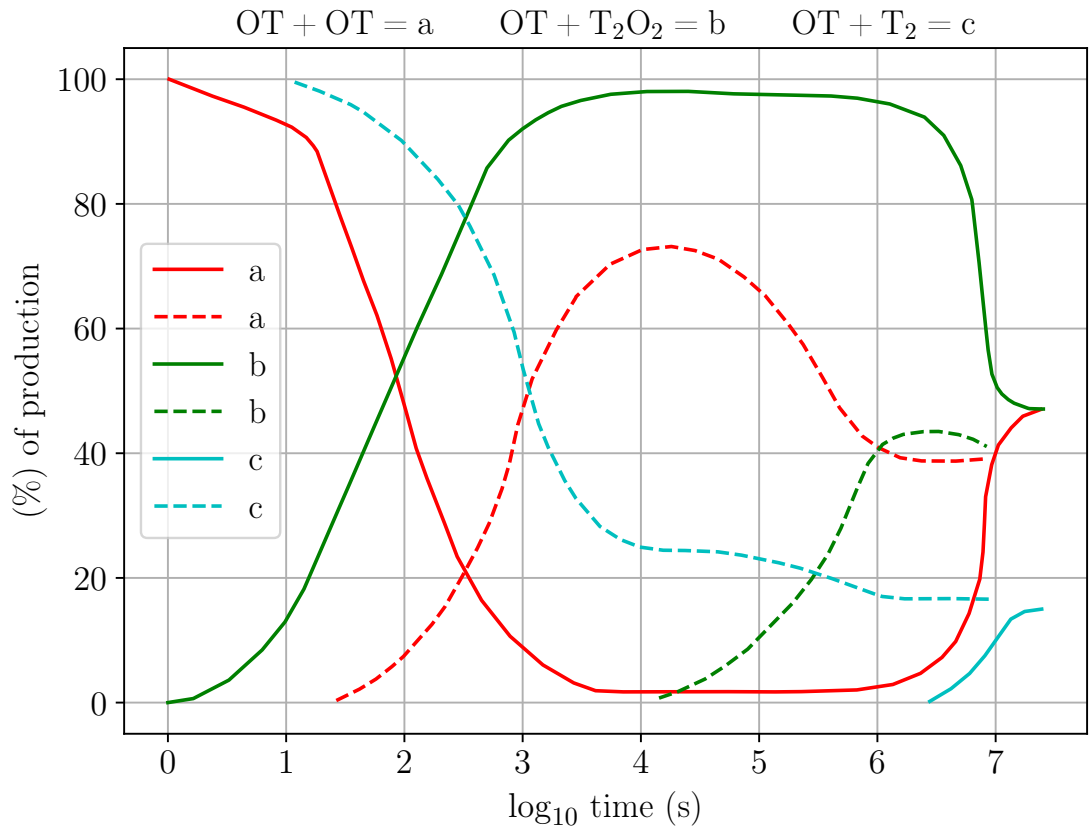


Figure 2.11: Sequential production routes of T_2O as function of time. The solid lines depict the production rate for a mixture of tritium initially containing radiolysis products and to which oxygen was added and the broken lines that from pure tritium without initial radiolysis products to which oxygen was rapidly added. Both experiments were performed under constant volume conditions and the same initial concentration of tritium in oxygen, i.e. 10^{-4} mol % (after [Fai88]).

Three major mechanisms, each characterized by a singular order with respect to the concentration of molecular tritium and a different overall rate expression, were identified at ambient temperature: i) first order regime within the range 3×10^7 - 3.7×10^{11}, ii) approx. second order within the range 3.7×10^{11} - 3.7×10^{14} and iii) again first order at concentrations exceeding 3.7×10^{14} Bq m^{-3} [Eas85; Fai89]. Experimental and theoretical evidence obtained within the examined concentration ranges showed ozone and tritium peroxide to constitute important intermediate products. Even though qualitative agreement between model and experiment was achieved, for a better agreement it appeared important to consider contributions from surface effects [Bal74]. With pure tritium reagent, i.e. initially not contaminated by extraneous radiolysis products, the reaction between OT and T_2O_2 is predicted to become important only after a

reaction time of approximately three hours. When on the other hand, radiolysis products are present, the reaction between OT and T_2O_2 becomes significant already 10 s after T_2 has been added to oxygen. Calculations brought to light the importance of the initial concentration of tritium in a mixture with oxygen for the OT - T_2O_2 reaction as source of T_2O, e.g. the reaction sets in at 0.1, 100 or 1000 s when the initial concentrations of tritium are 1.0, 0.01 or 0.0001 %, respectively. Another conclusion from the work of Failore [Fai88] was that the total T_2O concentration reached within reaction times of less than 10^6 s – time at which most T_2O is formed - is essentially unaffected by the presence of early radiolysis products in molecular tritium.

In a Raman spectroscopic study of the reaction of gaseous T_2 with humid air which contained twice as much tritium than oxygen, the quantities of pertritiated water were found to be much lower than expected from the stoichiometric ratio [She98]. T_2O was identified unequivocally by Raman spectroscopy utilizing the weak vibrational band at 2241 cm^{-1}. According to the results molecular oxygen disappeared completely after only about 50 % of T_2 was consumed. Thereafter, i.e. in the absence of O_2, T_2 continued to vanish but at a much slower rate. A conceivable explanation proposed for these observations was the reaction sequence

$$T_2 + O_2 \longrightarrow T_2O_2$$
$$T_2O_2 + T_2 \longrightarrow 2\,T_2O\ .$$

The fact that ammonia was not detected among the products was attributed to the formation of either tritium peroxide or nitrogen oxides.

Easterly and Benett [Eas83] researched the concurrent effect of tritium concentration (self-catalysis) and external radiation on tritium - air mixtures within the range of tritium concentrations 3.7×10^8 - 3.7×10^{10} Bq m^{-3}. Studies of the self-catalysed reaction at $< 3.7 \times 10^{10}$ Bq m^{-3} indicated that within the first 24 - 48 hours (crucial time for a tritium spill) less than 0.1 % of possible HTO formation had taken place. Even though on the basis of the generated data no unambiguous answer to the question of whether the reaction is first or second order was possible, it was at first assumed that the reaction proceeded with first order kinetics with a rate constant of 2×10^{-9} s^{-1}. Results with tritium in air mixtures under static conditions in Pyrex glass flasks of approx. 350 cm^3 at 293.15 K provided additional evidence that the self-catalysed

reaction is first order in tritium concentration. In a further investigation, flasks were exposed to an external radiation field (either a ^{60}Co source or a bare unshielded reactor) which promoted the establishment of a virtual steady state concentration of HTO. Mechanistic results were based on determinations of reacted (HTO) and unreacted (T_2) tritium. Under conditions of low tritium concentration, i.e. $< 3.7 \times 10^{10}\,\mathrm{Bq\,m^{-2}}$ and a dose of $6.4 \times 10^{3}\,\mathrm{rad\,hour^{-1}}$, the establishing equilibrium concentration of HTO appeared to depend on the concentration of tritium. The practical consequence of this is that upon termination of the external irradiation by the reactor consisting of 88 % neutrons and 12 % gamma the production of tritiated water by self-radiolysis did no longer play a role.

Combustion, deflagration and detonation: Within a certain set of pressure, temperature and composition values of a gas mixture, on which also the vessel configuration plays a role, chain branching reactions like

$$H + O_2 \longrightarrow OH + O$$

become sufficiently frequent compared to reactions that cause removal of hydrogen atoms. When this is the case the mixture is explosive. On the other hand, below critical pressures the reaction rate becomes unmeasurably slow. This is illustrated in the pressure vs. temperature diagram of a stoichiometric hydrogen – oxygen mixture displayed in Fig. 2.12. As the pressure is raised above the first critical pressure (explosion limit) the mixture becomes explosive until a second critical pressure is attained.

As the pressure is gradually raised a second explosion limit appears which is explained by the progressively increasing frequency of the three-body collision reaction

$$H + O_2 + M \longrightarrow HO_2 + M$$

in which M denotes any molecule that enhances the combination reaction of H radicals with O_2. Because this reaction competes with the branching reaction

$$H + O_2 \longrightarrow OH + O$$

shown above, it has a chain-breaking effect. Under the assumption that free HO_2 radicals are less reactive than the reactant radicals, they may diffuse up to the wall of the vessel and get over there

Table 2.21: Limits of inflamability of hydrogen – oxygen mixtures diluted in chemically inert gases (after [Lew61]).

Hydrogen %	Oxygen %	Nitrogen %	Carbon dioxide %
5.0	5.0	90.0	-
7.5	7.5	28.0	57.0

deactivated by collision. Therefore, once the pressure reaches a given value and the frequency of ternary chain-breaking collisions surpasses that of binary branching collisions explosions will no longer take place. Above the second limit, the reaction rate again becomes very slow until a third pressure limit is reached. At temperatures exceeding 873 K a stoichiometric mixture of hydrogen and oxygen explodes spontaneously at any pressure and below about 673 K there is no explosion at any pressure unless the mixture is exposed to a spark or a flame.

Combustions that propagate at velocities below the speed of sound are defined as **deflagrations**. They are associated with a significant and rapid increase in pressure, which, may cause equipment damage. Combustions that propagate at speeds higher than that of sound are defined as **detonations**. Detonations can be fuelled by solids, liquids or pressurized/oxygen-rich gases. In gases, they take place with a very fast reaction rate, which is self-accelerating when unburned gases ahead of the flame are pre-compressed and preheated. The high-pressure shock wave generated by a detonation may cause severe damage at large distances from the blast origin.

Some limits of **inflamability** of hydrogen – oxygen mixtures diluted in chemically inert gases are compiled in Table 2.21; limits for detonability are provided in Fig. 2.13. As can be seen, the lower limit of detonability is observed at 15 % and the upper one at 90 % hydrogen, respectively. It is evident that the velocity of the detonation wave is essentially proportional to the hydrogen content in the gaseous mixture.

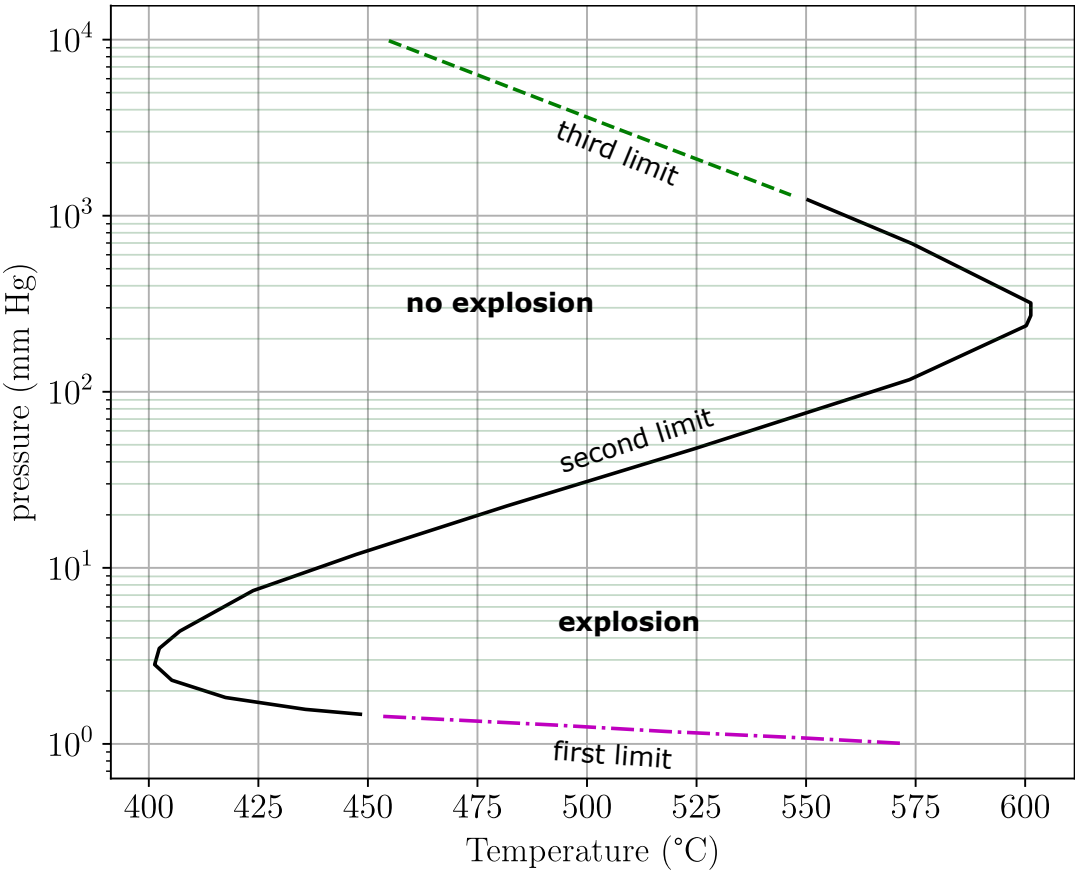


Figure 2.12: Explosion limits of a stoichiometric hydrogen- oxygen mixture taking place in a spherical vessel of 7.4 cm diameter (after [Lew61]).

2.10.6 More reactions leading to the formation of tritiated water

Tritiated water is generated when tritiated hydrogen interacts with materials such as stainless-steel, mineral oxides or certain organic substances. The reaction is usually enhanced by the presence of air, particularly when humid.

Finn and van Deventer [Fin88] investigated the heterogeneous reaction taking place between permeated tritium and helium containing oxygen on the backside of a stainless-steel tube held at 823 K. In some experiments, protium was added to the helium stream. According to their observation's oxygen concentrations in excess of 2000 ppm are necessary to achieve a high conversion into water, i.e. 98 %. The presence of protium in the backside sweep gas was found to have an inhibiting effect on the conversion. This was attributed either to a reduction of iron oxide present on the surface of stainless-steel or to the occupancy of active sites on the metal oxide surface.

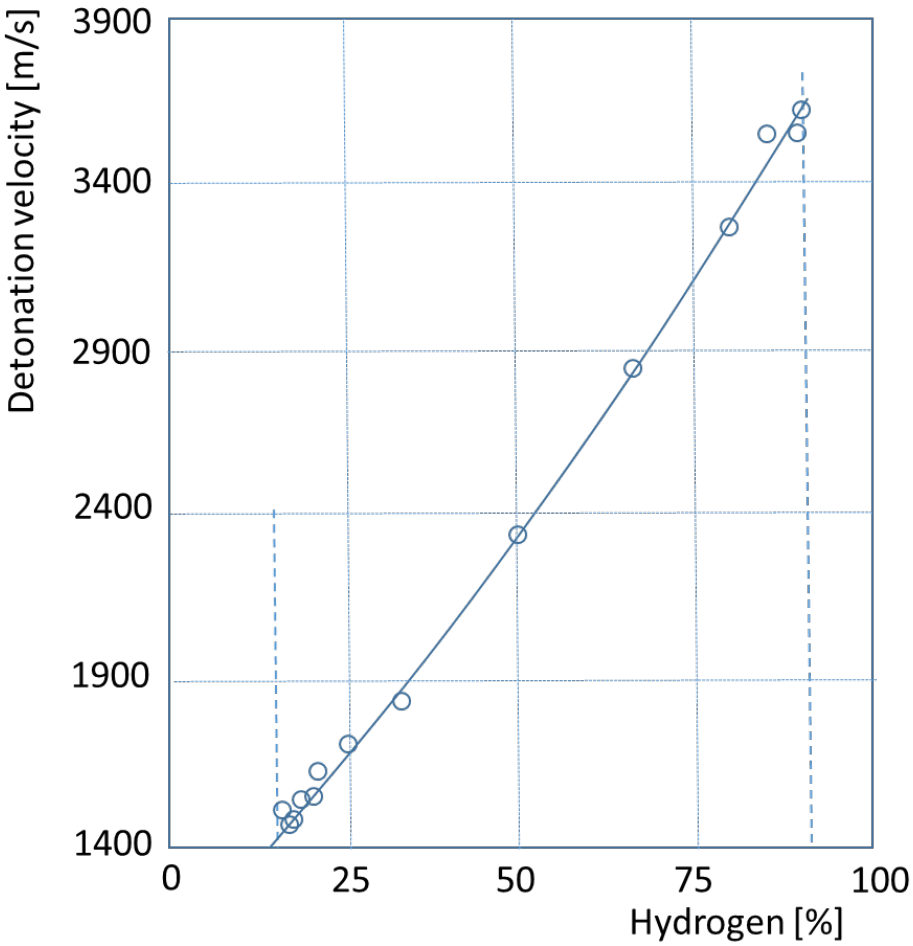


Figure 2.13: Detonation velocities of hydrogen – oxygen mixtures (after [Lew61]).

Molecular tritiated hydrogen incorporated thermally into stainless-steel via an adsorption - dissociation - atomic chemisorption sequence is mostly released as tritiated water [Hir84a; Sur88b; Pen06]. The transport mechanism of atomic tritium from the bulk into the gas phase with formation of tritiated water involves an exchange reaction with ambient moisture on the surface [Aka08] (for more information see section 2.14.1.2).

Tritiated water is also generated by isotopic exchange of molecular tritiated hydrogen or molecular tritium with gaseous, liquid or adsorbed water, i.e.

$$HT + H_2O \longrightarrow H_2 + HTO$$

$$T_2 + H_2O \longrightarrow HT + HTO\ .$$

The rate between tritium gas (1.85×10^9 - $2.6 \times 10^{10}\,\mathrm{Bq\,l^{-1}}$) and water vapour at 295 K was found to be independent of water provided $[H_2O] \gg [T_2]$ and second order in tritium concentration according to expression [Yan64].

$$\frac{\mathrm{d[HTO]}}{\mathrm{d}t} = 1.14 \times 10^{-17}[T_2]^2\,\mathrm{l\,Bq^{-1}\,s^{-1}}$$

Factors enhancing the reaction rate comprise i) radiation emitted by tritium, ii) increasing temperature, or iii) the presence of metal catalysts, especially precious metals such as platinum or palladium. On the other hand, the reaction is strongly inhibited by the presence of nitric oxide, hydrogen, or ammonia in the reaction mixture.

2.10.7 Reaction of T_2 with nitrogen

The interaction of molecular tritium with gaseous nitrogen requires attention not only from a mechanistic and kinetic point of view but also from the perspective of tritium material balance and glove box inertization [Gil88a]. The radiation-induced reaction describing the formation of ammonia is

$$N_2 + 3\,T_2 = 2\,NT_3\ .$$

A pressure drop accompanies the conversion of nitrogen into ammonia because it takes place with a net decrease of two molecules. G values for the production of NT_3 fluctuate within the range 1 - 2 molecules (NH_3)/100eV; the self-decomposition of NT_3 proceeds exponentially with G values of 15 - 30 [Gil88a]. The maximal auto-radiolysis rate of tritiated ammonia (specific activity $3.7 \times 10^{11}\,\mathrm{Bq\,g^{-1}}$) just above the melting point was reported to be 186 ppm/d. When stored at ambient temperature at a pressure of 3×10^4 Pa the rate was even smaller, i.e. 37 ppm/d [Blo69]. These values are in agreement with the rate of 111 ppm/d determined for NT_3 of 98.8 % isotopic purity in tritium reported in reference [Zel66]. The apparent auto-radiolysis half-life of gaseous $NH_{1.5}T_{1.5}$ which was determined to be 550 hours at ambient temperature by Glugla et al. [Glu88], is in good agreement with previous studies. Consequently, from the perspective of the plasma exhaust clean-up for ITER, this species is considered to be rather stable.

Because in early days only the rate of formation of ammonia was considered and the back reaction, i.e. the decomposition of NT_3 into the elements, neglected, neither formation rates nor

the finally establishing equilibrium concentrations could be predicted accurately [Mai84; Wal91a]. In view of this, Heung [Heu95d] proposed a rate law that included the reverse reaction, i.e.

$$\frac{\mathrm{d}[\mathrm{NT_3}]}{\mathrm{d}t} = k_\mathrm{f}[\mathrm{N_2}][\mathrm{T_2}]^3 - k_\mathrm{d}[\mathrm{NT_3}]^2 \ .$$

where k_f and k_d are the rate constants of formation and decomposition of tritiated ammonia, respectively. According to this equation, the rate of ammonia formation is first order in nitrogen and third order in tritium and the reverse reaction second order in ammonia. With this improved mechanism, rates and equilibrium concentrations for various nitrogen/tritium mixtures could be predicted correctly.

In **glove boxes** with nitrogen atmosphere the formation of tritiated ammonia takes place rather slowly [Mai84; Gil88a; Wal91a; Heu95d]. Depending on the specific concentration of tritium, the attainment of full equilibrium may require weeks or even months. The rate of formation of ammonia in a glove box of nitrogen atmosphere can be calculated from the following relationship [Heu95d]

$$\frac{\mathrm{d}[\mathrm{NT_3}]}{\mathrm{d}t} = 1.46[\mathrm{T_2}]^3[\mathrm{N_2}] - 0.09[\mathrm{NT_3}]^2$$

in which reactants and products are given in $\mathrm{mol\,l^{-1}}$ and the rate of formation of product ammonia in $\mathrm{mol_{NT_3}l^{-1}\,hour^{-1}}$. Because at equilibrium

$$\frac{\mathrm{d}[\mathrm{NT_3}]}{\mathrm{d}t} = 0$$

the equilibrium constant, K_e, becomes

$$K_\mathrm{e} = \frac{k_1}{k_2} = \frac{[\mathrm{NT_3}]^2}{[\mathrm{T_2}]^3[\mathrm{N_2}]} = 16.2\,\mathrm{l^2\,mol^{-2}} \ .$$

Assuming a leak of 10 g tritium into a glove box of $17\,\mathrm{m^3}$ volume whose atmosphere is pure nitrogen and assuming further that chemical equilibrium has established, it can be calculated that only approx. 1.2 % of the tritium will be converted into $\mathrm{NT_3}$. This corresponds to a concentration of pertritiated ammonia in the glove box of approx. $8 \times 10^{-7}\,\mathrm{mol\,l^{-1}}$. When the initial rate is taken to be $5.7 \times 10^{-14}\,\mathrm{mol\,l^{-1}\,hour^{-1}}$, full equilibrium will only be established after 107 hours.

Hence, the fraction of tritium converted into ammonia after 100 hours is 4×10^{-8}. What is more, rate and equilibrium concentration strongly depend upon the initial partial pressure of tritium in nitrogen: when the T_2 concentration in a N_2/T_2 mixture is varied from 0 to 100 % keeping the total pressure constant at 1 bar the rate of NT_3 formation goes from zero up to a maximum of $4 \times 10^{-7}\,\mathrm{mol\,l^{-1}\,hour^{-1}}$ at about 70 % tritium and then again back to zero. In summary, the reaction between tritium and nitrogen is extremely slow particularly at small partial pressures of tritium. The rate of ammonia formation is considerably accelerated by the presence of metals like palladium or palladium-silver.

When dealing with ammonia it should be kept in mind, that in this molecule one nitrogen atom binds three atoms of tritium and that ammonia may condensate, particularly in the presence of moisture. This may cause the inventory of tritium in tanks containing nitrogen contaminated by tritium to apparently decrease with progressing time.

2.10.8 Exchange reaction between T_2 and H_2 or D_2

Mixtures of H_2 and T_2 or D_2 and T_2 will not remain pure for long because of β–ray catalysed disproportionation exchange reactions such as

$$H_2 + T_2 \longrightarrow 2\,HT$$
$$D_2 + T_2 \longrightarrow 2\,DT\ .$$

Therefore, the kinetics of these reactions must be kept in mind when dealing with cryogenic distillation or the supply of a mixture of tritium-bearing molecular isotopologues to a fusion machine.

As Dorfman and Mattraw [Dor53] showed, the same equations describing the homogeneous equilibration between H_2 and D_2 can be applied to the H_2 - T_2 system. Pyper and Briggs [Pyp78] not only further developed the model, but also predicted correctly the half-life of the $H_2 + T_2 = 2\,HT$ exchange reaction. Table 2.22 compares estimated and measured half-times for several T_2/H_2 mixtures to an accuracy of 10 %. Half-times were obtained from equation

$$t_{(1/2)} = \frac{\ln 2}{k}\ .$$

Table 2.22: Kinetics of the reaction $H_2 + T_2 \longleftrightarrow 2\,HT$ (after [Pyp78]).

Tritium pressure mbar	Total pressure mbar	k estimated $10^4 \cdot \text{min}^{-1*}$	Half time estimated min	Half time measured min
61.5	78.7	9.8 (8.47)	707	818
86.1	159.1	11.9 (12.6)	582	550
108.8	164.9	12.4 (13.3)	558	522
44.3	284.3	12.9 (13.7)	537	504
196.9	393.9	21.6 (19.5)	321	355
178.1	533.2	22.2 (26.7)	286	260

*In parenthesis: k experimental

The half-time values are fairly large unless the partial pressure of T_2 becomes very high.

McConville [McC83b; McC85] reported much shorter reaction times. His results were explained by the presence of impurities, the effect of surface reactions and/or the influence of the reaction cell configuration on the range of beta particles. When the experimental results were analysed by a plot of $\ln Q$ vs. t using equation

$$\ln Q = \ln 1 - \frac{(DT(t) - DT(0))}{(DT(\infty) - DT(0))} = kt$$

the obtained straight line went through the origin at $t = 0$. The dependence of the reaction rate constant from the initial concentration of tritium is displayed in Fig. 2.14. As evident, the reaction between molecular tritium and deuterium is strongly inhibited by the presence of per-tritiated methane [McC85]. Even at very low concentrations of CT_4 the reaction rate increases nearly exponentially with raising initial concentration of molecular tritium.

2.10.9 Isotopic exchange between molecular tritiated hydrogen and water

Equilibrium constants for the exchange reaction between molecular tritiated hydrogen and water according to

$$HT + H_2O = H_2 + HTO$$

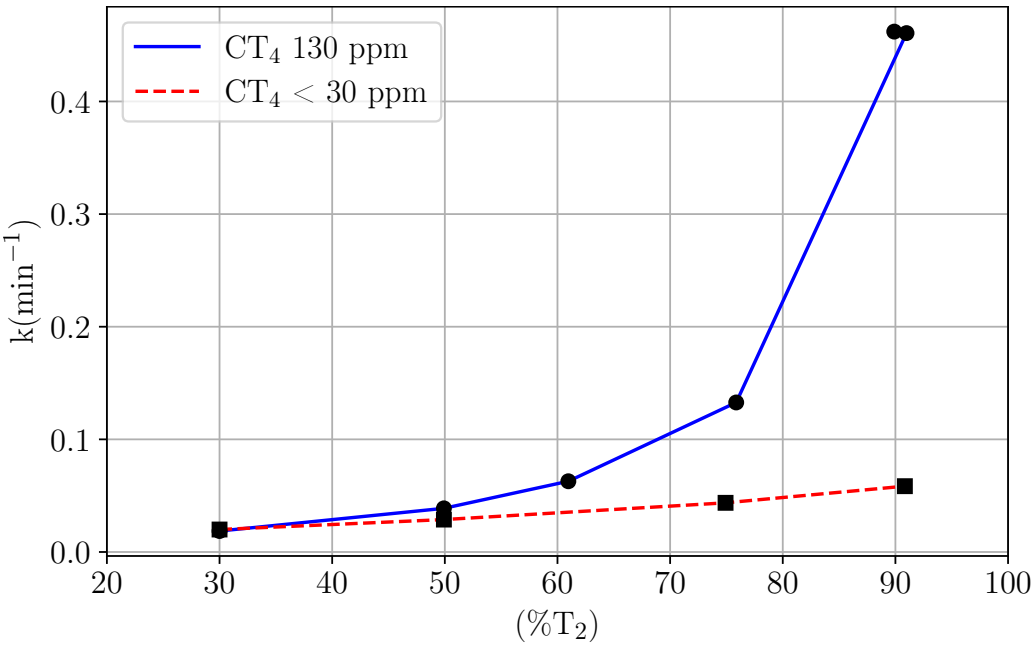


Figure 2.14: Reaction rate constant for the reaction of T_2 with D_2 as function of initial concentration of tritium (■ with no detectable CT_4 and • with 130 ppm CT_4 (after [McC85])).

were determined by Black and Taylor [Bla43] at temperatures in the range 289 - 576 K (see Table 2.23. As evident, the equilibrium constants, which agreed well with theoretically derived values, decrease significantly with increasing temperature.

Equilibrium constants can also be calculated from the relationship

$$\log K = 0.292 \log T + \frac{336.5}{T} - 1.055$$

where T is given in K. The reaction proceeds very slowly when no active catalyst is present (see also section 2.10.6).

Table 2.23: Equilibrium constant for the exchange reaction between water and tritiated hydrogen [Bla43].

Temperature K	K_e
289.0	6.75 ± 0.04
293.2	6.47 ± 0.02
298.0	6.25 ± 0.05
329.2	5.05 ± 0.05
352.6	4.37 ± 0.05
384.2	3.76 ± 0.04
431.4	3.10 ± 0.06
490.1	2.64 ± 0.04
575.9	2.17 ± 0.02

2.10.10 Kinetics of the exchange reaction between molecular tritium and methane

CH_4/T_2 mixtures at ratios of 1:1 or 1:9 were used to investigate the isotopic exchange reaction between molecular tritium and methane. Products of the reaction were tritium-enriched methane´s, tritium-substituted ethane´s, and other higher gaseous and liquid hydrocarbons [Pra61; Kan63; Kan64; Oku93; Uda92c; Uda92a]. When the methane/hydrogen ratio was lower than 0.06 only exchange takes place without formation of higher hydrocarbons, irrespective of the prevailing H/T ratio or the presence of inert gases. Tritium exchange reactions are induced by ions, hot atoms and radicals. Equilibrium constants calculated from steady state concentrations were found to be close to extrapolated high temperature classical values [Kan64]. The rates of the reactions were neither affected by temperature changes (within the range 300 - 573 K) nor by the presence of a palladium membrane [She92]. The T_2 - CH_4 exchange reaction was found to proceed up to equilibrium within days.

Meticulous work of McConville and Menke [McC93] on the progressive incorporation of tritium into methane at methane concentrations of less than 3 mol % provided evidence for an exchange

reaction initiated by T_5^+ ions, the main ionic species in T_2 at ambient temperature and a pressure of $>10^3$ Pa (see section 2.10.1)

$$T_5^+ + CH_4 \longrightarrow CH_4\,T^+ + T_2 + T_2\ .$$

Subsequently, the most probable reactions are

$$CH_4\,T^+ + CH_3\,T \longrightarrow CH_3\,T_2^+ + CH_4$$
$$CH_4\,T^+ + e^- \longrightarrow CH_3\,T + H$$
$$CH_3\,T_2^+ + e^- \longrightarrow CH_2\,T_2 + H\ .$$

followed by more isotopologue methane-methane collisions and ion-electron recombination up to the formation of CT_4. Gas analysis was mainly carried out by mass spectrometry and when needed by gas chromatography. Fig. 2.15 depicts the successive buildup of CH_3T, CH_2T_2, CHT_3 and CT_4. As apparent, it constitutes a relatively slow process. When the reaction is allowed to proceed over an extended period of time carbon will progressively segregate from the gas phase and plate out on the vessel surface as graphite. After 18 months only 0.2 % CT_4 remained in the 3 % CH_4 experiment. When sufficient carbon is formed back reactions will take place and a dynamic steady state will be established. A detailed reaction mechanism is provided in reference [McC93].

Uda et al. [Uda92c] studied the reaction of molecular tritium with methane utilizing a Raman cell manufactured from Pyrex glass. This material was selected to preclude catalytic effects. To investigate the kinetics of the reaction they first introduced 40 kPa of T_2 (purity 99 %) and thereafter 20 kPa of methane into the cell and determined by laser Raman spectroscopy the rate of formation of hydrogen, tritiated hydrogen and the rate of disappearance of molecular tritium (see Fig. 2.16). For the quantitative analysis of H_2, HT and T_2 at ambient temperature Raman peaks at 587 cm^{-1}, 395 cm^{-1} and 200 cm^{-1}, respectively, were selected. As evident from Fig. 2.16, isotopic exchange reactions are slow, the establishment of equilibrium requiring much more than 1100 hours. Values of estimated exchange reaction rate constants are tabulated in Table 2.24. The quantitative evolution of progressively substituted methane´s could likewise be followed by laser Raman spectroscopy when the same partial pressures of methane and tritium

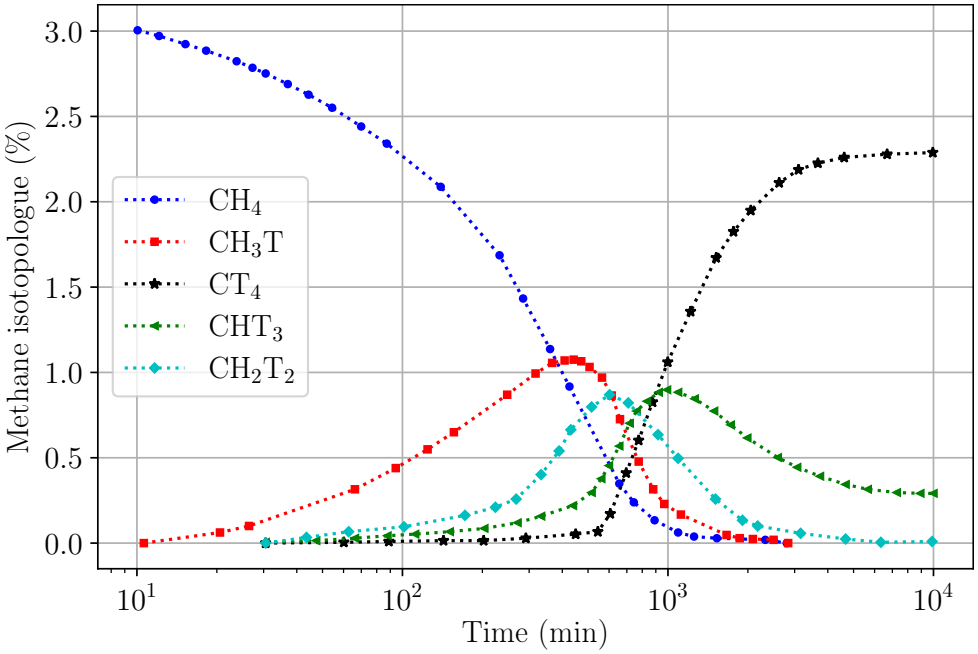


Figure 2.15: Evolution of tritium-substituted methane isotopologues as function of time in a 2.8 % CH_4 – 95.5 % T_2 mixture at ambient temperature (after [McC93]).

as above ($CH_4 : T_2 = 1 : 2$) were mixed at ambient temperature. The gradual conversion of methane into tritiated methane´s is induced by the beta-rays emitted by tritium. As apparent from Fig. 2.16 the results on the evolution of tritiated hydrogen isotopologues are well in line with observations by McConville et al. [McC93] (see Fig. 2.15).

The overall reaction mechanism was described by reactions such as [Uda92c]

$$CH_4 + n\,T_2 = CH_{4-n}\,T_n + n\,HT$$

$$2\,HT = H_2 + T_2\ .$$

The time required for 50 % conversion of methane into tritiated methane´s was found to lie within the range 150 - 220 hours [Uda92b; Uda92c]. A similar half-life of 250 hours was found by Glugla et al. [Glu88] for the disappearance of CH_2T_2 by self-radiolysis. In this case, the only additional product was HT. When comparing the results of both investigations it must be taken into account that the experimental conditions differed considerably.

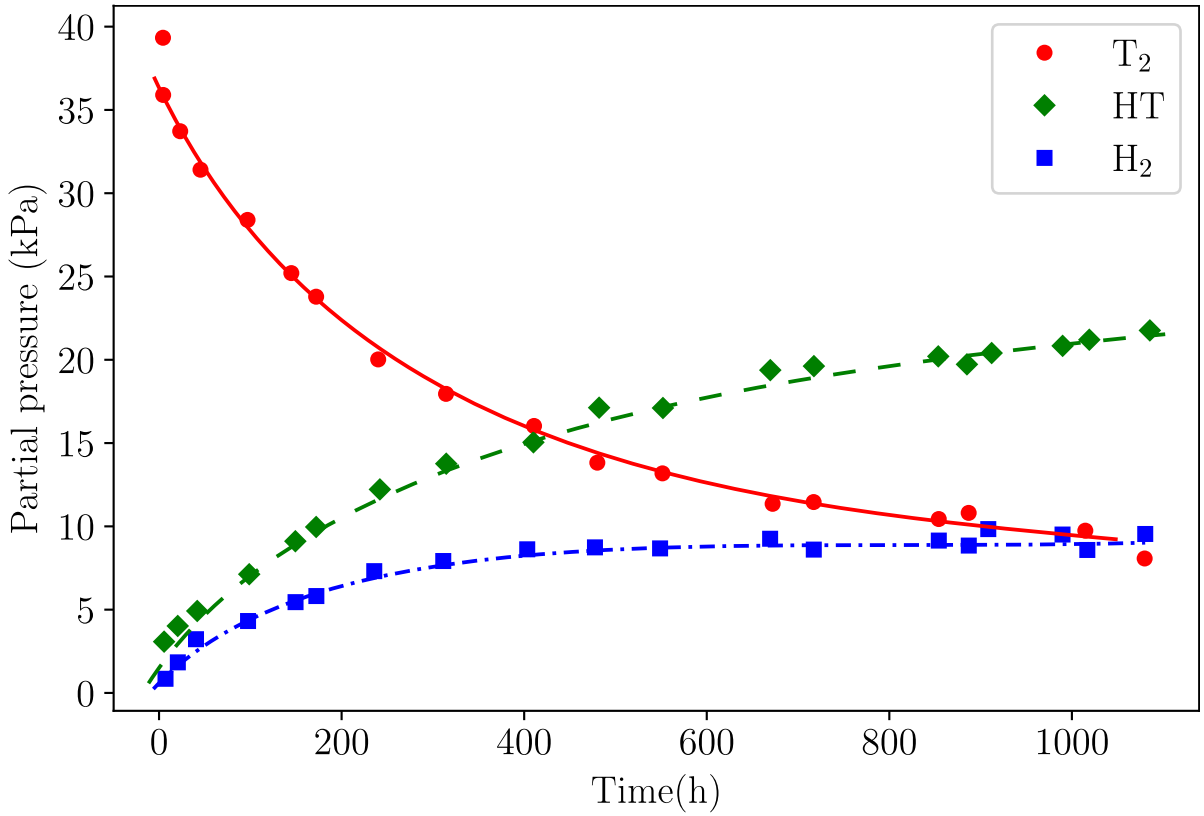


Figure 2.16: Evolution of the partial pressures of T_2, HT and H_2 as function of time in a T_2:CH_4 = 2:1 mixture at ambient temperature determined in situ by laser Raman spectroscopy (after [Uda92c]).

Shimizu et al. [Shi83] investigated the radiation-induced reaction of methane in the presence of molecular sieves like 3A, 4A, 5A and 13 X. According to their results, the irradiation of methane over 4A selectively generates - at least initially - C_2 hydrocarbons and over 5A C2 and C_3 hydrocarbons. With progressing irradiation time, a carbonaceous solid deposit's on the molecular sieve surface. Irradiation of this deposit in the presence of a hydrogen atmosphere yields low molecular weight hydrocarbons.

Table 2.24: First order exchange rates [Uda92c].

Gas mixture	Mixing ratio	Initial pressure of T2 kPa	Product species	Rate constant $hour^{-1}$
$H_2 : T_2$	1 : 1	40.5	HT	5.5×10^{-2}
$CH_4 : T_2$	1 : 2	39.8	H_2	4.8×10^{-3}
			HT	2.9×10^{-3}
			T_2	3.2×10^{-3}
			$CH_{4-x}T_x$	3.9×10^{-3}

2.10.11 Reaction of molecular tritium with carbon monoxide

During the radiation-induced reaction of molecular tritium with carbon monoxide a slow pressure drop was observed which was attributed to the formation of a white solid identified as being predominantly paraformaldehyde [Dou55]. Methane was not found among the products. Beattie [Bea73a] revisited the self-radiolysis of T_2 - CO mixtures at temperatures in the range 75 - 373 K. He identified CT_4, T_2O and a white solid polymer as main products. The polymer was tentatively assumed to be paraformaldehyde. In addition, smaller amounts of CO_2, C_2T_4 and traces of CT_2O were detected. The rates of formation of CO_2 and CT_4 were found to be nearly independent from the prevailing temperature.

O´Hira et al. [Ohi95] observed in experiments carried out with a stoichiometric mixture of molecular tritium and carbon monoxide only the products CO_2 and a residual solid having approximately the composition $C_{1.4}T_{3.0}O_{1.0}$. Species such as T_2O, CT_2O or CT_4 were not detected. In an analogous study performed at ambient temperature under partial simulation of the composition of the plasma-exhaust gas of a fusion machine, i.e. DT or T_2 containing 1 - 6 % CO and 0 - 3 % He, the reaction was found to be directly proportional to the initial partial pressure of tritium. The identified products were tritiated methane, tritiated higher hydrocarbons and carbon dioxide [Pen00a]. Evidently, more experiments are needed to fully understand the underlying reaction mechanism.

O´hira et al. [Ohi00b] subsequently studied the reaction of molecular tritium with carbon monoxide at a reactant concentration ratio of 1:1 employing two Fourier Transform infrared

(FT-IR) spectrometers and a quadrupole mass spectrometer. For safety purposes they contained the gas cell equipped with sapphire windows in a second containment provided with KRS-5 windows (see Fig. 2.17, upper figure and section 3.16.4)[13]. Peaks in the infrared spectra could be assigned to solid products such as aldehydes (R-CTO), alcohols (R-OT) and carboxylic acids (R-COOT) and to gaseous products such as tritiated water, tritiated methane and carbon dioxide (see Fig. 2.17, lower figure). The analysis of solids was mostly carried out after evacuation of the gases. An unexpected result was the incorporation of tritium present in the gas phase into the solid products at a rate of approx. $5\,\%\,\mathrm{d}^{-1}$. The solids, which had deposited all over the cell, were found to consist principally of carboxylic acids and be of rather persistent nature. Important advantage of Fourier Transform-IR spectroscopy over previously employed laser Raman spectroscopy [Ohi95] was that during gas analysis the deposited solids were not subjected to heating by the laser beam.

Recapitulating, in practically all CO/T_2 studies, methane, water, and carbon dioxide have been identified as main gaseous products and their evolution in time been determined. Additionally, a white radioactive solid polymer of not jet unambiguously identified composition was observed. With the advent of more sophisticated analytical techniques some further products such as alcohols, aldehydes and carboxylic acids - all generated in small concentrations - can expected to be singled out.

[13] A conceptually similar safety cell to investigate the reaction of molecular tritium with carbon oxides by infra red spectroscopy was implemented successfully at TLK [Pen95c].

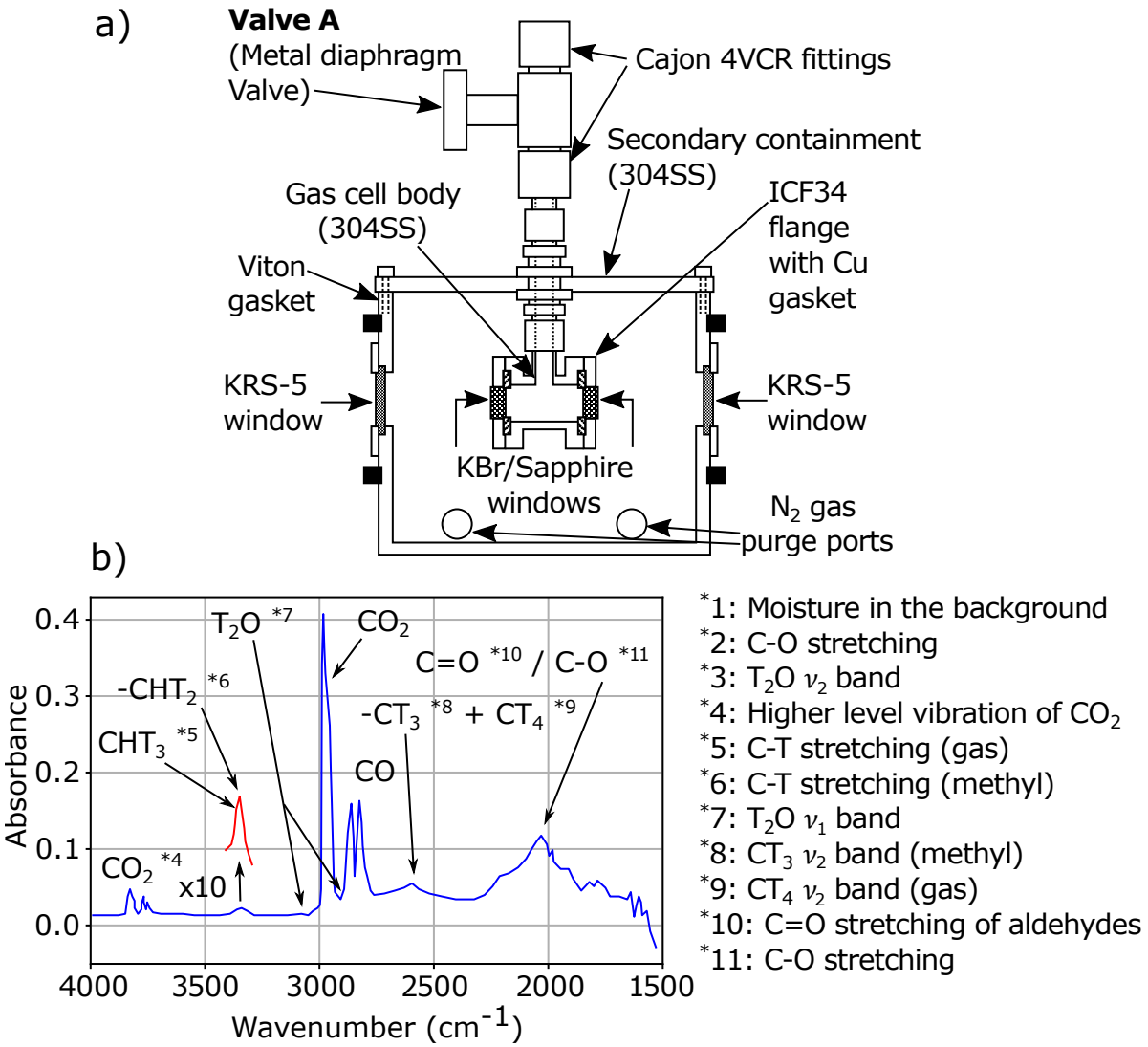


Figure 2.17: Reaction of molecular tritium with carbon dioxide. The safety gas cell employed in the investigation by Fourier Transform infra-red spectroscopy is depicted in the upper figure. The lower figure displays peaks at wave numbers in the range 1500 - 4000 cm^{-1} observed 265 hours after mixing the reactants. Species assigned to the absorbance peaks are given in figure (b) (after [Ohi00b]).

2.10.12 Reaction of molecular tritium with carbon dioxide

Beattie [Bea72] researched the self-radiolysis of tritium in the presence of carbon dioxide at temperatures in the range 193 - 373 K, pressures within the range 10^4 - 10^5 Pa and the presence of water vapour or a noble gas. Main observed reaction products were CO, CT_4, C_2T_4, T_2O and a white polymer of undefined composition. The initial rates of carbon dioxide disappearance

did not show dependency from temperature. The rates were, however, proportional to the partial pressures of CO_2 and T_2. Whereas the addition of noble gases stimulated the reaction, water vapour had an inhibiting effect on the rate. Similar observations were reported by Tingey [Tin66] who irradiated a mixture of carbon dioxide and hydrogen with an external γ-ray source. Condensation of the generated water by freezing brought about a change in reaction mechanism.

Shu et al. [Shu05] reported in another recent experimental study on the gaseous reaction between T_2 and carbon dioxide. They detected CO and T_2O as principal reaction products. In view of this, they proposed the reaction

$$CO_2 + T_2 \longrightarrow T_2O + CO$$

to describe the overall reaction mechanism. In addition, the formation of a solid decomposing thermally into CO, CO_2, T_2 and T_2O when heated up to 523 K was described.

Isobe et al. [Iso11] also carried out an investigation on the reaction between molecular tritium and carbon dioxide ($T_2 : CO_2 = 1 : 1$) over periods of up to 4 weeks at comparatively elevated temperatures, i.e. 373 - 573 K. Main reaction products detected by mass spectrometry were tritiated water, tritiated methane and carbon monoxide. Whereas the partial pressure of carbon monoxide and of tritiated methane continued to increase during a period of up to 4 weeks, that of tritiated water already levelled off after only two weeks. Within the broad range of investigated temperatures, its influence was relatively minor.

In general, solid deposits on inner walls of tritium handling systems are of concern not only because they may constitute a significant tritium sink but also because they may behave as an unpredictable source of tritium influencing the composition of gaseous mixtures [Wag15]. What is more, they may be the cause for clogging of capillary tubing or small apertures from equipment that, once contaminated, cannot be cleaned physically or be heated to remove the polymer by thermal vaporization. This pertains especially flow meters, needle valves, or gas chromatographic equipment. Possible corrosion induced by tritium-bearing polymers has neither been reported nor investigated.

2.10.13 Reaction of per tritiated water with carbon dioxide

The reaction of T_2O with carbon dioxide appears to be very slow. Gaseous products or condensed phases have not been observed [Oya02].

2.10.14 Erosion of carbon from the first wall of fusion machines: hydrogen isotope effect

Another type of interaction between hydrogen and solids pertains sputtering of the first wall of fusion machines during operation with plasmas. Physical sputtering affects all elements of the first wall and occurs with incident particles of energies above a certain threshold value. In fusion machines having a first wall protected by a carbon fibre composite (CFC) armour, significant chemical erosion takes place by sputtering with hydrogen ions. The interaction of plasma particles with the first wall leads not only to material release into the gas phase eventually contaminating the confined plasma, but also to deposits on more distant wall zones or even to zones shadowed from the plasma. The threshold energy for the impact of protium, deuterium and tritium on carbon lies within the range 22 - 28 eV. Chemical erosion of graphite by deuterium appears to be larger than by protium in line with the expected square root mass dependency. While at higher energies, i.e. 100 - 3000 eV, physical sputtering brought about by impinging deuterium and tritium atoms was found to be similar, that by protium atoms was consistently lower by a factor of 2 to 3 [Haa06]. When the first wall of the machine is made up of several constituent materials like carbon, tungsten, beryllium and others, combinations of these materials containing trapped tritium may re-deposit. Because information on this type of polyelement deposition is rather scarce, more relevant experimental studies are needed.

Processes like implantation of ions escaping the plasma, co-deposition of tritium with other elements or tritium generation by transmutation may cause significant build-up of tritium in diverse regions of the first wall, also remote ones.

2.10.14.1 Hot atom chemistry of tritium

Energetic tritium atoms are generated in nuclear recoil reactions like

$$^{3}\mathrm{He(n,p)}^{3}\mathrm{H}^{\star}$$

$$^{6}\mathrm{Li(n,}\alpha)^{3}\mathrm{H}^{\star}$$

which take place with neutron capture cross sections and recoil energy releases of 5400 b and 1.9×10^5 eV and 945 b and 2.7×10^6 eV, respectively. When these hot atoms undergo reactions, the energy needed for reactions to proceed is almost exclusively provided by translationally excited tritium atoms. Because these energetic atoms are at no time in thermal equilibrium with their surroundings the reactions of hot atoms are in first approximation independent of temperature. A requirement for the formation of stable reaction products is that the initial energy of the hot tritium atoms be cooled down to less than about 1000 eV. Cooling takes place by electronic interactions, emission of radiation and elastic as well as inelastic collisions.

Thermal[14] and hot hydrogen atoms yield different products when reacting with organic compounds like methane, higher alkanes, cycloalkanes or other substituted organic molecules.

Principal reactions of hot tritium atoms with organic molecules are:

- abstraction of hydrogen [Roo65]

$$\mathrm{T}^{\star} + \mathrm{RH} \longrightarrow \mathrm{HT} + \mathrm{R}$$

- displacement of hydrogen, alkyl groups, halogens or other groups

$$\mathrm{T}^{*} + \mathrm{R{-}R}^{'} \longrightarrow \mathrm{RT} + \mathrm{R}^{'}$$

$$\mathrm{T}^{*} + \mathrm{RH} \longrightarrow \mathrm{RT} + \mathrm{H}$$

$$\mathrm{T}^{*} + \mathrm{RX} \longrightarrow \mathrm{RT} + \mathrm{X}$$

$$\mathrm{X} = \text{halogen, hydroxyl, nitro, carboxylic acid, amino group}$$

More on the substitution of $-\mathrm{NH_2}$, $-\mathrm{NO_2}$, $-\mathrm{OH}$, $-\mathrm{COOH}$, $-\mathrm{F}$, $-\mathrm{Cl}$, $-\mathrm{Br}$ or $-\mathrm{J}$ species by partially "cooled" recoil tritium is discussed in reference [Sch64].

[14] In so called "thermal reactions" reactants and products are always at the same temperature.

- fragmentation (at very high collisional energies)

$$T^* + RH \longrightarrow T + R + H$$

(here T^* = energetic ^3H) [Sch64; Tan65; Kun70].

Because the above described abstraction, displacement and fragmentation reactions are not observed when thermal deuterium atoms react with organic molecules, they can be ascribed exclusively to reactions involving hot tritium atoms. The yields of HT from hot abstraction reactions by energetic tritium atoms from hydrocarbons is remarkably sensitive to the strength of the R-H bond being broken displaying excellent correlation with the bond dissociation energies of the involved C-H bonds [El-58; Roo65; Bak68]. Inert gases influence the yield of hot reaction products because they modify the energy spectrum of the energetic atoms.

When hot tritium atoms react with substituted cyclopropanes at least 20 significant products were generated which is explained by the occurrence of ring opening steps [Lee60; Tan65]. Additional details on reaction mechanisms and isotope effects as well as model calculations when hot tritium atoms react with different organic molecules are discussed in an overview paper by Schmidt-Bleek and Rowland [Sch64].

A study on the reaction of hot tritium atoms with ammonia provided evidence that the product yield from abstraction, i.e. HT, was about four times lower than that of displacement, i.e. NH_2T [Cas75]. The surprisingly high displacement yield was explained by unimolecular decomposition of an energized intermediate complex that is formed when tritium interacts with the electron pair of the ammonia molecule.

Experiments on the reaction of recoil tritium with H_2/D_2 mixtures enriched in para-hydrogen revealed that the HT/DT ratio in the high energy "hot" region is almost independent of the spin state of H_2 [Haw86]. Conversely, highly moderated tritium atoms react preferentially with the ortho-spin isomer of hydrogen. This surprising sensitivity to the nuclear spin of H_2 was attributed to the ability of ortho-hydrogen to polarize the tritium atom in such a way that its nuclear spin is aligned parallel to that of the ortho-hydrogen molecule.

In early work, Boothe and Ache [Boo78] investigated the reaction of recoil tritium with graphite from the perspective of the operation of a thermonuclear reactor. Ionic recoil tritium

was mostly generated by the nuclear reaction ^{3}He(n,p)T. The average kinetic energy of the generated tritium was estimated to be 0.195 MeV. These highly energetic ions were observed to penetrate deeply into the graphite matrix. They became strongly bound and were therefore highly resistant to thermal release. This was considered detrimental to the implementation of measures such as needed to keep the tritium inventory in the vacuum vessel of a thermonuclear device within tolerable levels.

In summary, hot atom reactions have been demonstrated in the gas [Sch64; Haw86], liquid [Tan65], and solid phase [Boo78; Ara82]. Their occurrence and significance in fusion devices requires more attention.

2.11 Interaction of hydrogen isotopes with metals and alloys from the perspective of tritium storage

Rudman [Rud83] resolved the kinetics of hydriding and dehydriding of metals into three interacting processes, i.e. intrinsic kinetics, heat flow, and mass flow. Of these three, the intrinsic kinetic process was further classified into three simultaneous processes taking place in series, i.e. surface process, diffusion and phase transformation. In a theoretical approach, the viewpoint was adopted that a **nucleation and growth theory** is applicable to treat the interplay between the three simultaneous intrinsic processes [Avr39; Avr40]. Knize and Cecchi [Kni83] developed at about the same time a similar theoretical approach on the bulk gettering of diatomic gases, which includes the effects of surface reactions and bulk diffusion and is applicable to both pumping and desorption. These investigators assumed pumping to proceed by dissociative adsorption with a time-independent sticking coefficient followed by bulk diffusion. The process, which depends upon the getter material, temperature and type of gas, can be described employing a sticking coefficient and solubility as well as diffusivity of tritium in the bulk. For the case of pumping at constant pressure, the theory predicts that the pumping speed is independent of pressure provided the surface-limited absorbed flux is lower than the diffusion-limited flux. In the opposite regime, the pumping speed varies as $p^{-0.5}$. Desorption exhibits initially a diffusion-limited behaviour, which subsequently becomes surface-limited, the concentration in the alloy decreasing as $1/t$. Predictions of the theory, were found to be in excellent agreement with the experimentally researched performance of the ZrAl – hydrogen system.

Watanabe et al. [Wat89] examined critically and compiled heats of hydride formation of numerous getter materials potentially suitable for handling and storage of tritium. The list comprises experimentally obtained values as well as theoretically predicted ones.

Van´t Hoff plots of a number of metal hydrides of high potential for application in tritium handling systems have been compared in Appendix D.

Metals like uranium, palladium or titanium, as well as certain inter-metallic compounds like zirconium/cobalt, zirconium/nickel and lanthanum/nickel alloys, are known to react with hydrogen to generate solid hydrides [Dev90; Dev93; Pen90; Pen91b; Wer94] (see Table 2.25). Because of several advantageous properties of these materials, they have been employed for safe handling, interim storage, long-term storage and compression of tritium-bearing hydrogen isotopes.

Another storage option for hydrogen is based on thermal **encapsulation** in the cavity system of molecular sieves [Fra77] (see also section 2.11.9 below). This route, which so far has only been explored for the purpose of supplying hydrogen as fuel for transportation, may also be applicable in certain cases of tritium handling.

Because the physical, chemical and thermodynamic properties of the candidate getter materials differ greatly, they are discussed below singly.

Table 2.25: Properties of the most promising getters for storage, handling and pressurizing tritium.

Property	**U**	**ZrCo**	**Ti**	**Pd**	**$LaNi_{4.25}Al_{0.75}$**
Molecular weight	238	150.1	47.9	106.4	408.7
Solid metal hydride	UQ_3	$ZrCoQ_3$	TiQ_2	PdQ	$LaNi_{4.25}Al_{0.75}Q_7$
Volume expansion after hydrogen uptake %*	75	20	19	11.2	35
Hydride dissociation pressure mbar**					
at 298 K	1.2×10^{-6}	1.0×10^{-4}	1.1×10^{-13}	8.6×10^{-3}	~200 at 303 K
at 673 K	469	1590	0.35	65.6	~600 at 353 K
					[Men79; Wer94]
Disproportionation	none	full reproportionation at 723 K possible	none	none	none
		[Dev92; Kon95a; Bek00]			[Goo84]
H/M vs p plateau	flat	slightly sloping	flat	flat at < 636 K	slightly sloping
Restricted handling	yes	no	no	no	no
Compatibility with stainless-steel	Good below 973 K	No data available	No data available	No data available	Good[Wer93]
Release of decay He	After ~3 year release rate equals production rate	Very low up to 2 year even at 773 K. Release after [He/metal] > 0.35	Release after [He/metal] > 0.3		Nearly full ^{3}He trapping over 5.4 year
	[Mal76]	[Hay94; May95]	[Bow78; Sch89a]	[Cor88; Abe90b; Emi92]	[Wer93; Sta15]
Pyrophoricity	high	low	ignites at 713 K	none	none
Poisoning by carbon oxides	high	small		none	small [Han89b]
Poisoning by O_2, H_2O	high	low		none	small and recoverable [Lon88]
Max. weight % of hydrogen in getter	1.25	1.97	4.04	0.93	1.7

Q = H, D, T; * Volume expansion on hydrogenation $= \left[\frac{V_{\text{hydride}} - V_{\text{metal}}}{V_{\text{metal}}}\right] \cdot 100$; **Only approximate values

2.11.1 Uranium

2.11.1.1 Selected physical properties of uranium and uranium hydride

As well known, uranium may exist in one of three phases: orthorhombic (α-uranium at $< 961\,\mathrm{K}$), tetragonal (β-uranium at 961 K and 1049 K) or body centred cubic (γ-uranium at $> 1049\,\mathrm{K}$) [Bee13]. Density (and crystal structure) of uranium and uranium hydride are $19.05\,\mathrm{g\,cm^{-3}}$ (orthorhombic) and $10.92\,\mathrm{g\,cm^{-3}}$ (cubic), respectively[15]. The lattice constants of i) uranium are $a = 0.2854\,\mathrm{nm}$, $b = 0.5870\,\mathrm{nm}$, $c = 0.4955\,\mathrm{nm}$ with $\alpha = \beta = \gamma = 90°$ and of ii) uranium hydride are $a = 0.6625$ nm with $\alpha = \beta = \gamma = 90°$ (as determined for UT_3 [Joh76]), respectively.

A number of physical properties of uranium and uranium hydride with implications to handling and storage of tritium have recently been compiled and discussed by Kolasinski et al. [Kol10]. They also tabulated the effective thermal conductivities, K, of solid uranium, uranium powder, and uranium hydride (see Table 2.26).

Table 2.26: Effective thermal conductivity of solid uranium, non-oxidized uranium metal powder and uranium hydride partly measured in the presence of inert gases [Swi66; Eri83; Kol10].

Material	Gas	K $\mathrm{W\,m^{-3}\,K^{-1}}$
Solid uranium	N/A	24.7
Uranium powder	Ar	0.255
	N_2	0.343
	He	1.34
Uranium hydride	N/A	1 - 2

N/A=no information available

2.11.1.2 Properties of uranium in view of tritium storage

Uranium powder reacts fast and reversibly with hydrogen isotopes at ambient or higher temperatures to yield uranium hydride, deuteride or tritide. After repeated cycling the grain size of the powder becomes smaller than 1 µm. For this reason, its tendency to spread into components adjacent to the storage getter bed is large and its isolation in the storage bed challenging. Mea-

[15] Monolithic uranium hydride and deuteride can be obtained by growing UH_x crystals from the melt at temperatures $> 1348\,\mathrm{K}$ under H_2 (or D_2) at a pressure of 125 MPa followed by quenching to ambient temperature at high pressure [Cos90]. Synthesized species were verified by X-ray and Auger spectroscopy.

surements have demonstrated that at 300 K the dissociation pressure over the hydride powder is very low, i.e. approx. 0.3×10^{-3} Pa and at 700 K very high, i.e. approx. 10^5 Pa. Because of this property, uranium is widely used for i) tritium handling, ii) interim pressure-less storage as UT_3 or iii) tritium pumping by thermal cycling.

At constant hydrogen pressure and raising temperature the rate of the reaction

$$U + \frac{3}{2} H_2 \longrightarrow UH_3$$

goes through a maximum because at temperatures exceeding 373 K the contribution of the reverse reaction, i.e. decomposition of the hydride into the elements, becomes increasingly important. The observed hysteresis, i.e. dependence of the $p - c$ curve on whether uranium hydride is being formed or decomposed, was attributed by Wicke and Otto [Wic62] to mechanical tensions arising from considerable volume expansion taking place during uptake and release of hydrogen (see Table 2.25). According to Mallet [Mal58] and Kolasinski et al. [Kol10] the hysteresis pressure of hydrogen absorbed or desorbed from uranium can be calculated from expressions

$$\log P = -\frac{4701}{T} + 11.81 \quad \text{(absorption)}$$
$$\log P = -\frac{4216}{T} + 11.08 \quad \text{(desorption)}$$

where P is given in Pa and T in K.

Considerable effort has been invested into the investigation of the kinetics of the reaction of hydrogen with uranium [Alb56; Alb58; Wic62; Ami66; Ali70; Has73; Con73; Nor75; Con75; Sta79; Con80; Blo81; Blo90; Pow91]. Early work by Albrecht and Mallett [Alb56; Alb58] on the reaction of hydrogen with a rod of uranium was performed at temperatures within the range 373 - 672 K. Two different initial reactions were observed: one in the temperature range 373 - 523 K initially characterized by a gradual increase in rate that progressively becomes linear and another in the range 523 - 673 K, which follows a parabolic law. Amilihat-Caralp et al. [Ami66] investigated the reaction of hydrogen with massive metal and reported occurrence of an initial induction period whose duration decreased with increasing temperature. Their observations were corroborated by Bloch and Mintz [Blo90]. Alire et al. [Ali70], on the other hand, showed that the induction period could be eliminated by using high purity gases and preparing the metallic

specimens under high vacuum in order to completely exclude oxygen. When the deuterium - uranium reaction was carried out at temperatures within the range 460 - 623 K, they noticed initially formation of a uniform adherent layer of UD_3 on the metal surface. With progressing conversion, the reaction was governed by diffusion of molecular (or perhaps atomic) deuterium across this layer. The effect of thermal annealing on the hydriding kinetics of uranium was researched more closely several years later by Bloch and Mintz [Blo81]. Hashino and Okajima [Has73] developed a treatment to calculate the reaction rate utilizing a statistical mechanical approach. Condon et al. [Con73; Con75; Con80] reported good agreement between experimental rates of hydriding and dehydriding of uranium with values calculated using a model based on the rate of formation of nuclei and a growth function for each hydride crystallite employing a mechanism proposed back in 1939 by Avrami [Avr39; Avr40].

A further kinetic study of the reaction of gaseous hydrogen with massive uranium metal (sheet or rod) at several temperatures was performed by Powell et al. [Pow91]. The reaction was observed to be initiated by pitting of the uranium surface. According to the observations of these investigators, the rate shows a half power pressure dependence, which, provided some adaptations of the theory are carried out, follows rather well an earlier model developed by Wicke and Otto [Wic62]. Teter et al. [Tet01] provided evidence that the time to nucleate increased and the maximum rate of hydriding decreased with increasing thickness of the oxide layer on the uranium surface. Conversely, performing vacuum outgassing of specimens in order to remove oxygen impurities, dramatically decreased the nucleation time and increased the maximum hydriding rate.

Pressure-composition isotherms at very high temperatures ($873 < T < 1119$ K) and pressures ($p \leq 700$ bar) were determined by Northrup [Nor75].

The rate of the reaction of hydrogen with uranium powder was examined among others by Stakebake [Sta79] and Kherani et al. [Khe89]. According to Stakebake, the reaction order is independent of temperature and varies from 2/3 at 13.3 kPa to first order at 26.6 kPa. Kherani et al. proposed the following overall hydrogen rate equation for the reaction of hydrogen with uranium powder placed inside of a small getter bed

$$-\frac{\mathrm{d}H_2}{\mathrm{d}t} = k(\omega, T, U, A)(p - p_\mathrm{e})$$

where $k(\omega, T, U, A)$ stands for a first order pressure independent reaction rate constant, $(p - p_e)$ denotes the hydrogen overpressure, and p_e is the equilibrium pressure. The parameter ω is dependent from the design of the bed, T is the temperature, U the remaining active uranium powder and A the surface area per gram of uranium. If isothermal conditions prevail, e.g. $T \sim 298\,\mathrm{K}$, then p_e is approximately zero and the above equation turns into

$$p = p(t = 0) \exp\left(-\frac{t}{\tau}\right)$$

where

$$\tau = \frac{V}{RT_a k_a} \ .$$

Here T_a denotes ambient temperature, k_a the reaction rate constant at ambient temperature and R the gas constant. Fig. 2.18 displays plots of this equation, using experimental results obtained with two different hydrogen storage beds containing uranium powder at initial H/U ratios of either zero or one at ambient temperature. The rate of pressure change for both beds appears to be independent from the initial H/U ratio. Rate constants can be calculated from the slopes applying a least square fit.

Several researchers [Mal58; Wic62; Tan79a; Hei93] determined dissociation pressures of isotopic uranium hydrides. The decomposition of uranium hydride takes place with zero order rate [Sta79]. Enthalpy of formation, entropy of formation and free energy of formation of uranium hydrides are tabulated in Table 2.27. As apparent, the agreement between the results from various investigations is - with exceptions - rather good.

Dissociation pressures of uranium hydride, deuteride or tritide can be calculated from the general equation

$$\log p = -\frac{A}{T} + B$$

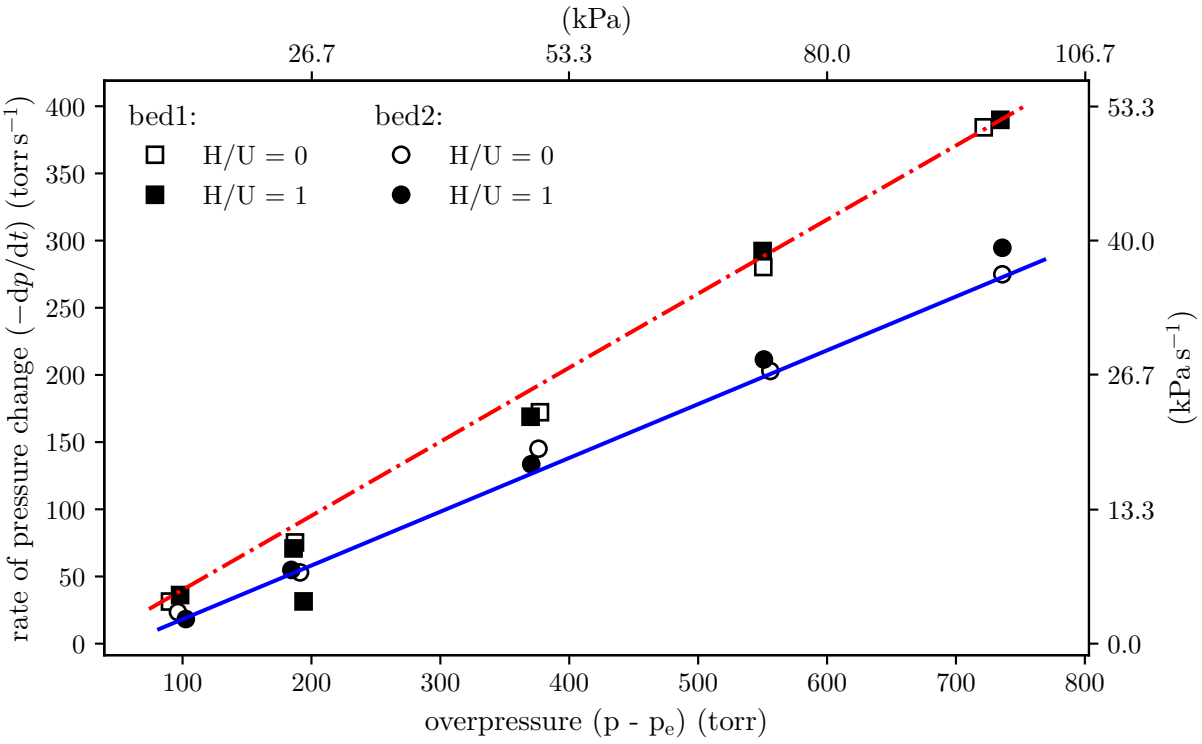


Figure 2.18: Comparison of the rate of hydrogen pressure change in two different small storage getter beds containing uranium powder as function of overpressure (after [Khe89]).

where p is the pressure in mbar and T the temperature in K. Good fit equations obtained from values in the literature determined with three hydrogen isotopes are [Flo51; Mal58; Wic62; Nor75]

$$p_{UH_3} = 10^{-(\frac{4525}{T})+9.27} \cdot 1.33$$

$$p_{UD_3} = 10^{-(\frac{4500}{T})+9.40} \cdot 1.33$$

$$p_{UT_3} = 10^{-(\frac{4471}{T})+9.46} \cdot 1.33 \ .$$

Dissociation pressures of uranium hydride, deuteride and tritide are plotted as function of inverse temperature in Fig. 2.19. As apparent, at a given temperature the highest dissociation pressure is that of uranium tritide.

Tanabe et al. [Tan79a] reported, in good agreement with previous work, that the dissociation pressure of UD_3 at 573 - 703 K is higher than that of UH_3 both in the decomposition as well as in the formation mode by a factor of about two.

Table 2.27: Thermodynamic properties of uranium hydrides*.

UH_3			UD_3			UT_3			Ref.
ΔH_f^0	ΔS_f^0	ΔG_{f298}^0	ΔH_f^0	ΔS_f^0	ΔG_{f298}^0	ΔH_f^0	ΔS_f^0	ΔG_{f298}^0	
−127.0	−182.5	−72.63	−129.9	−195.8	−71.46	−130.4	−201.1	−70.41	[Flo84]
−125.2	−179.2	−71.58	−131.9	−195.9	−73.35				[Tan79a]
			−118.9			−116.0	−174.6		[Car75]
−127.7	−181.3	−73.67	−129.4	−187.1	−73.67				[Wic62]
−121.8	−177.9	−68.65	−126.0	−176.2	−73.67				[Des62]
−127.0			−129.8			−130.3			[Kol10]

*$\Delta H_f^0, \Delta S_f^0and\Delta G_{f298}^0$ are given in kJ mol^{-1}, J K^{-1} mol^{-1} and kJ mol^{-1}, respectively.

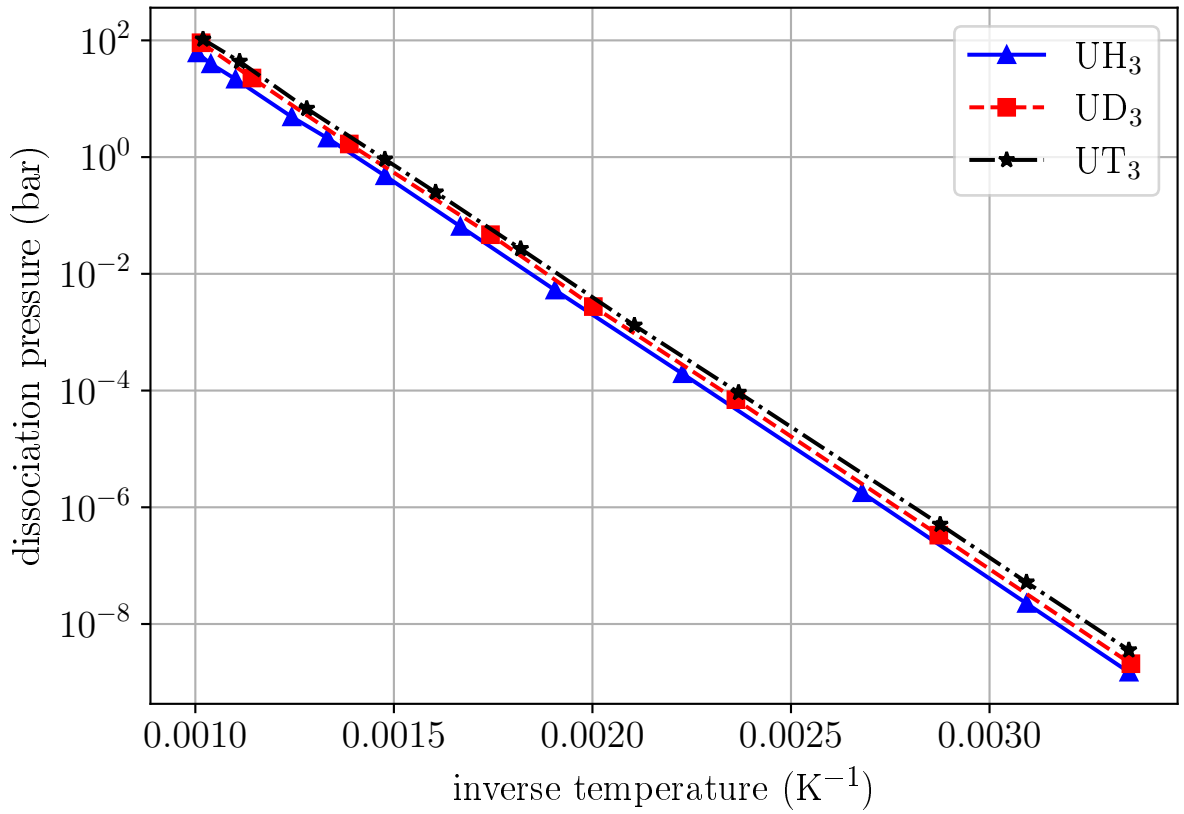


Figure 2.19: Dissociation pressures of uranium hydride, uranium deuteride and uranium tritide as function of inverse temperature.

The separation factor, α, defined by expression

$$\alpha = \frac{[\mathrm{D/H}]_{(\mathrm{gas\,phase})}}{[\mathrm{D/H}]_{(\mathrm{solid\,phase})}}$$

was determined from mixed hydride in equilibrium with its dissociation gas mixture and calculated to be about 1.3, irrespective of temperature or pressure. It should be noted, that the decomposition pressure of an equimolar UH_3/UD_3 mixture is intermediate between that of UH_3 and UD_3 but not simply equal to the arithmetic mean.

Early studies on dissociation pressures of the hydrogen - uranium system were carried out both in the hydriding as well as in the de-hydriding mode at very high temperatures up to 923 K and pressures up to 30 bar by Libowitz and Gibb [Lib57]. At 723 K the differences between hydriding and dehydriding isotherms were non-discernible, in other words negligible hysteresis. The pressure-composition plots in the range $0.001 < \mathrm{H/U} < 0.299$ show typically wide and almost completely flat plateaus (see also Fig. 3.25). When hydrogen is removed from the fully hydrided hydride the pressure falls sharply until a constant pressure plateau is reached. At this point, uranium hydride commences to dissociate and two solid phases, i.e. β-uranium hydride and α-uranium, are formed. Once nearly all hydrogen has been removed, the hydride phase disappears and the pressure decreases again sharply indicating formation of a single solid phase consisting of uranium containing dissolved hydrogen.

The isotherms plotted in Fig. 2.20, depict pressure-composition diagrams obtained under isochoric conditions by Manchester [Man95] and Kolasinski et al. [Kol10]. As apparent, as soon as the plateau limit at high H/U ratio is reached (it signalizes full conversion of uranium into its hydride), every small increase in hydrogen inventory causes sudden and steep rise of pressures up to high values. Analogous isotherms but for the uranium-uranium tritide system at T/U compositions of up to 2.99, temperatures in the range 723 - 840 K and pressures up to $\sim$ 20 bar were reported by Carlson [Car75].

Principal factors influencing the rate of hydrogen uptake by uranium in a getter bed were enumerated by Shmayda and Mayer [Shm84]. They are: i) gas overpressure, ii) initial bed capacity, iii) bed temperature, iv) bed orientation, v) helium content of the gas stream and vi) pore size of in line filters.

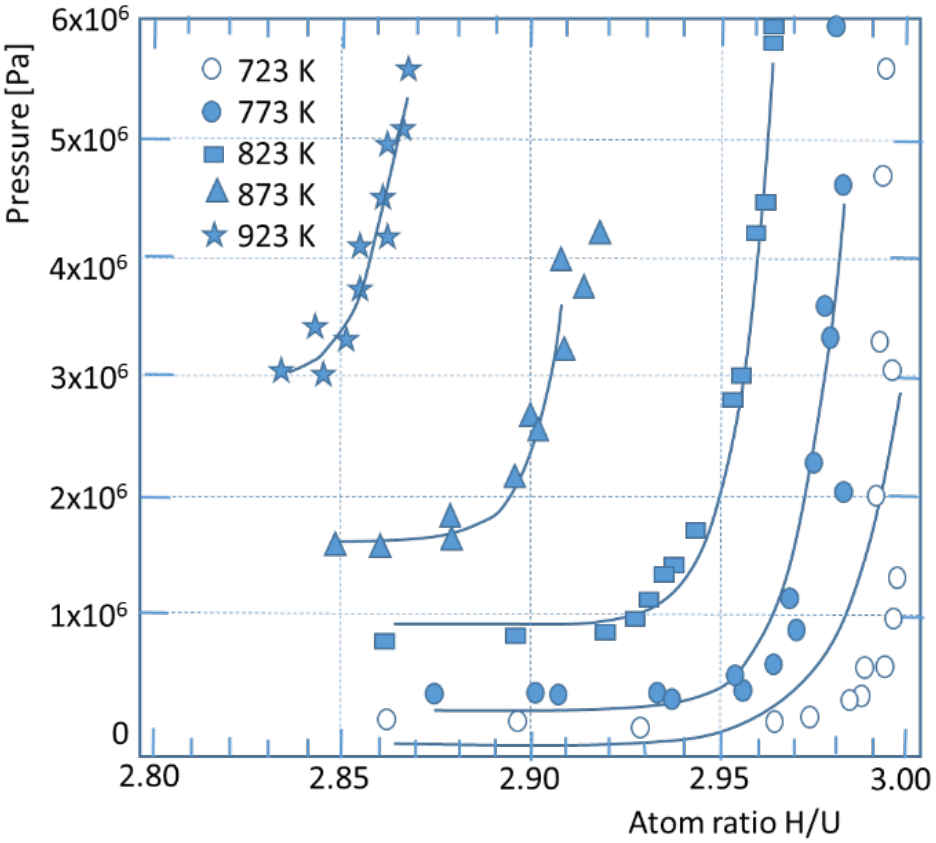


Figure 2.20: Pressure-composition isotherms of the hydrogen-uranium system (only the highest H/U atom ratios are displayed) (after [Kol10]).

With respect to the initial hydrogen to metal ratio it was shown by Kherani and Shmayda [Khe87] that the rate of hydrogen uptake decreases significantly with increasing H/U ratios. Likewise, a reduction in pore size of the sintered filters placed at inlet and outlet of the bed down to values of 5 µm or less brought about strong reduction of the hydrogen uptake rate. In order to maintain a double contained storage bed at low temperature during hydriding the annulus is usually backfilled with gas [Hei88b]. The influence of the type of gas on the cooling rate of a storage bed containing 3 kg uranium is illustrated in Fig. 2.21. As apparent, replacing argon by helium in the annulus brings about a 4.8-fold improvement in heat transport from the primary to the secondary vessel when compared to that of an evacuated annulus.

Condon and Larson [Con73; Con75] studied the decomposition of UH_3 under high vacuum at 343 - 473 K. According to these investigators, the reaction proceeds with an activation energy

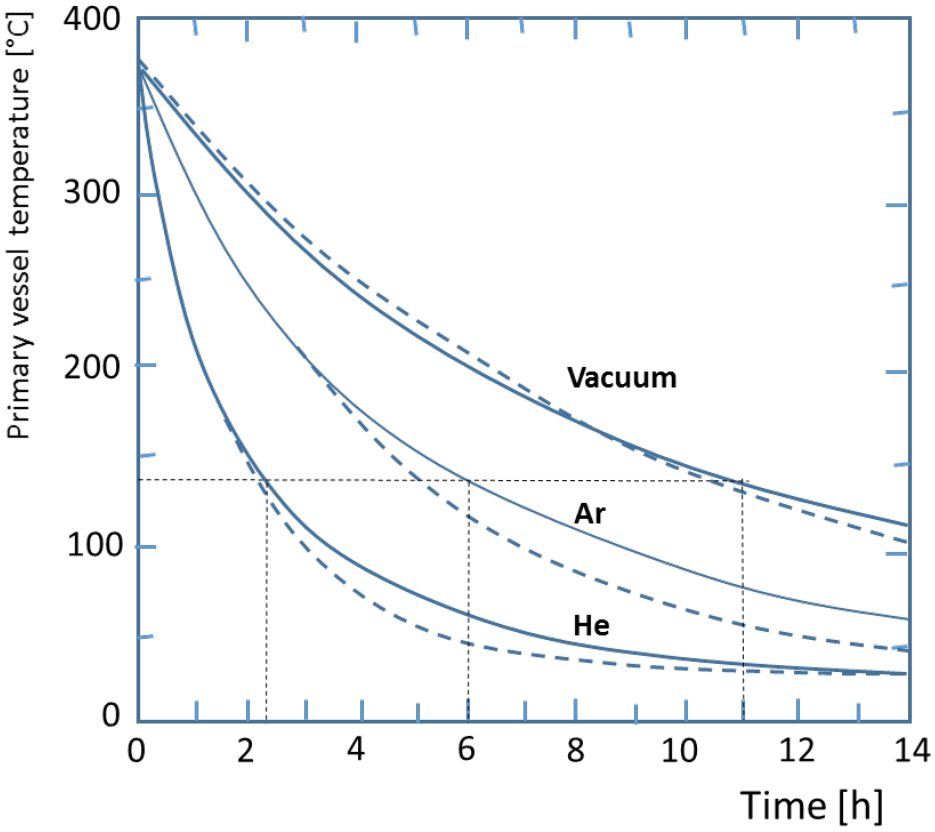


Figure 2.21: Cooling of a primary vessel holding 3 kg of uranium in a double-contained storage bed either under vacuum or with the annulus backfilled with argon or helium (broken line = theory and solid line = experiment) (after [Hei88b]).

of 72.9 kJ mol^{-1}. Lindner [Lin90] deduced from experiments carried out at 648 - 789 K that the isothermal decomposition of uranium hydride

$$UH_3 \longrightarrow U + \frac{3}{2} H_2$$

is governed by the rate of expansion of the boundary between the metal core and metal hydride phase on the surface. Consequently, the reaction fraction α can be calculated from the expression

$$\alpha = 1 - [1 - k(T, P)t]^3$$

where t is the time and $k(T,p)$ a temperature and pressure dependent kinetic coefficient. The latter is given by

$$k(P,T) = k_0 \exp\left(-\frac{E_\mathrm{a}}{RT}\right) \log\left(\frac{P}{P_0(T)}\right)$$

where P_0 denotes the hydrogen plateau pressure as function of temperature [Con75; Lin90; Sal13]. The activation energy of the decomposition reaction, E_a, was determined to be $79.1\,\mathrm{kJ\,mol^{-1}}$. P_0 can be calculated from the expression

$$\log(P_0) = -\frac{4700}{T} + 9.47 \ .$$

Lindner furthermore pointed out that plateau pressures determined with a dynamic procedure differ significantly from plateau pressures measured by adding or removing hydrogen aliquots from the system.

Salloum and Gharagozloo [Sal13] based their calculations on the physical model proposed by Lindner. They fitted data from several investigators with an Arrhenius type equation using an empirical model for the decomposition kinetics of uranium hydride (see Fig. 2.22). By this procedure, a larger temperature range was covered and hence many experimental results could be compared. A general conclusion was that the pressure build-up in the storage bed (filter obstructs gas relieve) as well as the thermal barrier represented by the bed wall retard delivery of hydrogen.

Kurz [Kur84] calculated the pressure reduction caused by sinter filters installed in a tritium storage bed employing the expression

$$\Delta P = \frac{f s \delta}{A \alpha}$$

where ΔP is the pressure reduction in $\mathrm{N\,m^{-2}}$, f the flow rate in $\mathrm{m^3\,s^{-1}}$ at $\mathrm{P_2}$, s the wall thickness of the sinter filter in m, δ the dynamic viscosity of the gas in $\mathrm{N\,s\,m^{-2}}$, A the area of the filter in $\mathrm{m^2}$ and α the permeation coefficient of the sintered filter in $\mathrm{m^2}$. When calculated results were compared with experimental values the deviations were found to be larger at the lower pressures, which is actually in accordance with expectations.

Impurities in hydrogen like $\mathrm{O_2}$ [Lei61; Ben75; Rit81; Rit84; Hay92c], $\mathrm{H_2O}$ [Kon64; Bak66; Wil66; Kon74; Jac77; Rit81; Rit86a; Rit86b], $\mathrm{N_2}$ [Mal55; Ali66], $\mathrm{NH_3}$ [Ali66], $\mathrm{CH_4}$ [Lit48],

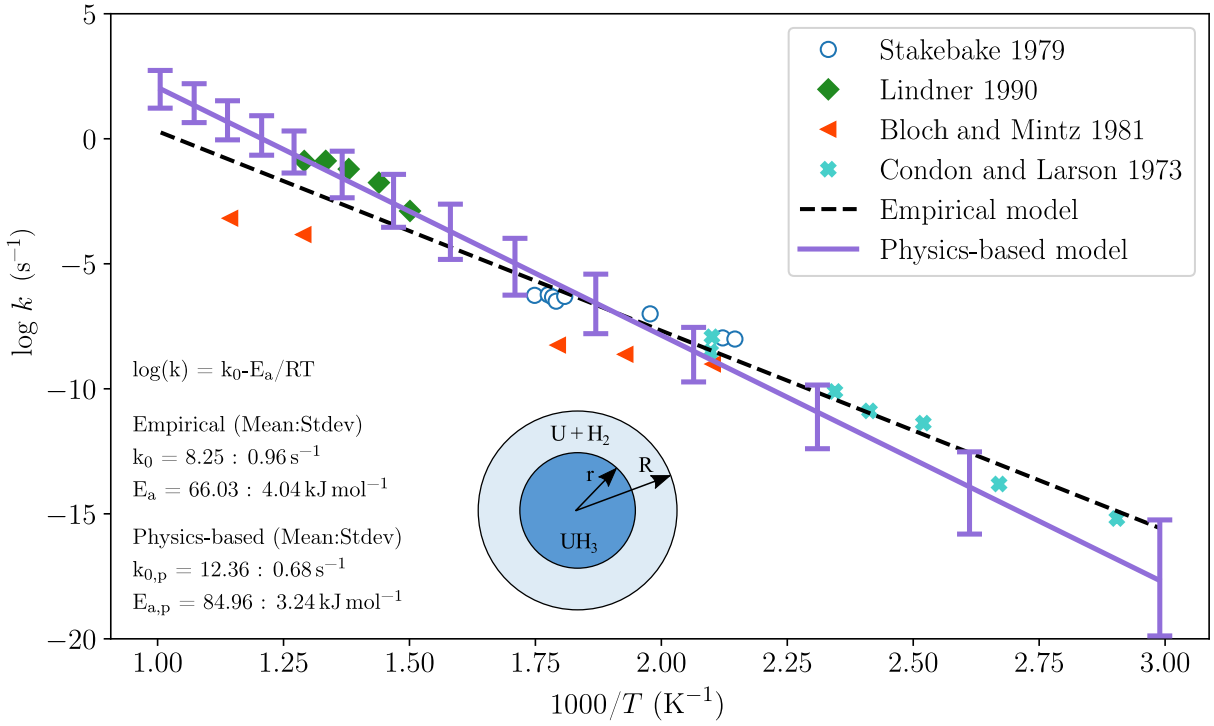


Figure 2.22: Plot of data (k in s^{-1}) on the decomposition of uranium hydride from four researchers and calculations with an empirical- as well as a physical - based model. The insert represents the decomposition of an idealized UH_3 spherical particle illustrating the transition from an UH_3 core into a $(U + H_2)$ phase on the periphery (after [Sal13]).

O_2/H_2O [Rit86a] or CO, CO_2 [Sto66; Hol86b] react with uranium to yield stable reaction products on the surface such as uranium oxides, uranium nitrides and uranium carbides. Approximate values of the heats of formation for UO, UO_2 and U_3O_3 have been reported to be 850 kJ $mol^{-1}_{O_2}$ and the ones for UN, U_2N_3 and UN_3 of the order of 600 kJ $mol^{-1}_{N_2}$. Product build-up occurs predominantly on the surface of the getter, which henceforth progressively displays worse hydrogen sorption properties and reduced absorption capacity. Correspondingly, the rate of hydrogen liberation will also be reduced when impurities accumulate on the surface [Tet01].

Uranium hydride is known to react with ammonia at ambient temperature to yield UN_2, U_2N_3 and UN [Ale62]. After rapid formation of a nitride monolayer on the hydride, the reaction is controlled by slow chemisorption of ammonia on the film.

Uranium hydride may also undergo deflagration by reaction with water vapour [New49]

$$UH_3 + 2\,H_2O \longrightarrow UO_2 + \frac{7}{2}\,H_2 \ .$$

Jackson et al. [Jac77] studied the rate of the reaction of uranium with water vapour at partial pressures of 383 Pa, 1586 Pa and 2853 Pa and temperatures of 353 K, 375 K and 423 K. Hydrogen, argon or argon-oxygen mixtures were used as carrier gas for water vapour. The reaction, which is of considerable practical significance when utilizing uranium getter beds for either tritium storage or the removal of tritium from gaseous streams [Tan83], showed complex dependency from temperature and partial pressures of water vapour, hydrogen or oxygen.

The isothermal reaction of uranium powder with steam at elevated temperatures, i.e. 773 - 1873 K, follows a parabolic rate law of the kind typical for the reaction of hydrogen with metals [Wil66].

When tritium is stored as uranium tritide for an extended period of time decay helium, i.e. ^{3}He, builds up in the solid bulk. After accumulation of helium in the lattice primarily in form of bubbles, it desorbs from solid uranium at lower temperatures than tritium. Tritium is more resistant to thermal release because it resides in lattice sites. Once bubbles reach grain or particle boundaries helium will be released rapidly. The rate of helium-3 liberation from a uranium tritide bed has been determined at ambient temperature over periods lasting up to 1200 days by Malinowski and Coronado [Mal76], Carlson [Car75] and Bowman [Bow77b]. According to the observations of Malinowski and Coronado during the first 280 days less than 2 % of the accumulated decay ^{3}He escapes the matrix. Thereafter, the rate increases swiftly approaching the rate of generation from radioactive decay after approx. 1000 storage days (see Fig. 2.23). It was postulated by Bowman that the release rate is influenced by the size of the uranium particles[16]. However, the BET surface areas of the uranium particles employed by Malinowski and Coronado (0.4 - 0.9 $m^2\,g^{-1}$) or by Bowman (0.6 $m^2\,g^{-1}$) were essentially the same which does not support this presumption. A comparison between the helium-3 release data of Malinowski and Coronado and of Bowman is displayed in Fig. 2.23. As apparent, whereas Bowman claims that the retention of ^{3}He remains very high up to ageing periods of 700 days Malinowski and Coronado see the

[16] Bowman [Bow77a] observed that the release of helium-3 at ambient temperature from UT_3 having a BET surface area of 0.6 $m^2\,g^{-1}$ was 4 % after 650 days and from UT_3 of BET surface area 3 $m^2\,g^{-1}$ after the same period of ageing 21 % (high surface areas are the result of numerous hydriding/dehydriding cycles).

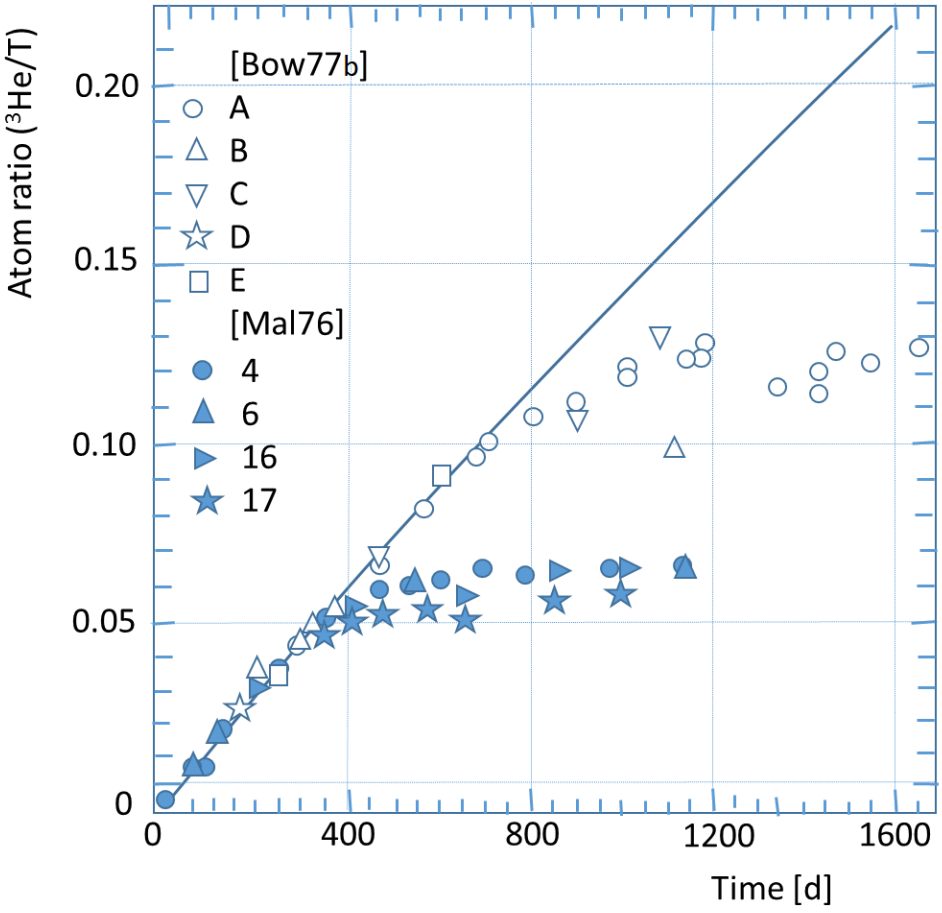


Figure 2.23: Release rate of decay helium from uranium as function of ageing time. Comparison of the results of Bowman [Bow77b] and Malinowski [Mal76]. Letters and numbers indicate different specimens used for the measurements. The solid line gives the calculated 100 % retention of helium (after [Kol10]).

beginning of release already after 400 days of storage. To elucidate the significant difference in onset time at which rapid release of ^{3}He begins, more long-term investigations with uranium tritide are needed. In fact, in a recent review of the literature dealing with the experimental and modelling database of the uranium hydride system Kolasinski et al. [Kol10] identified a number of gaps in the existing database concerning tritium storage in uranium getter beds. The authors evaluated current knowledge and recommended further research on topics such as i) ^{3}He release rate from uranium tritide, ii) consequences of surface contamination on hydrogen uptake, iii) thermal desorption properties of the hydrides and iv) kinetics of hydride phase formation.

Helium generated by decay of tritium in interstitial positions of uranium does not have enough energy to cause lattice damage but sufficient energy to perform several jumps before its energy

has been dissipated. At ambient temperature, helium will therefore migrate through the lattice with an activation energy of the order of 0.2 eV until it encounters another helium atom. Once helium atoms become clustered, the probability of formation of a vacancy will be enhanced significantly. Calculations provide evidence that in body centered cubic (bcc) metals every time five interstitial helium atoms are clustered together they spontaneously drive a metal atom off its lattice site creating a Frenkel-pair (ionic displacement) and consequently a vacancy sequestrating the five helium atoms[Bis80]. These helium atoms are deeply bound in the vacancy eventually precipitating the formation of bubbles (helium-helium self-trapping). This explains why virtually all ^{3}He remains in the metal lattice during room temperature storage until - after some critical time has elapsed - helium is released at about the same rate at which it is generated by decay. It should be noted that the presence of helium in a vacancy tends to lower the binding strength of hydrogen.

The rate of generation of helium-3 in tritium is such that already after ten days molecular tritium will contain 0.3 % helium [Car75]. Because of the "blanketing effect", this ostensibly insignificant amount of noble gas can cause almost insuperable problems in a static system utilized for trapping of tritium by a gas-solid reaction or purification of tritium from helium-3. For both purposes, a dynamic system comprising a blower rather than a pump is mandatory. Pumps, which operate with flip valves, are not recommended because they will cease to pump at pressures below a threshold value.

Attempts to improve the tritium storage properties of uranium getter by doping with other metals like Ti, Zr, Al, Si or Fe have not kept up with expectations [Yam88; Yam90; Yam91].

A number of physical properties of uranium and uranium hydride with implications to handling and storage of tritium have recently been compiled and discussed by Kolasinski et al. [Kol10]. Within this frame, they also tabulated the effective thermal conductivities, K, of solid uranium, uranium powder, and uranium hydride (see Table 2.26).

2.11.2 Palladium

One more getter material used for storage and handling of tritiated hydrogen is palladium. At ambient temperature the dissociation pressure of the tritide is approx. 67 mbar when T/Pd $\sim$ 1.4. The plateaus of the desorption isotherms of palladium hydrides, deuterides and tritides

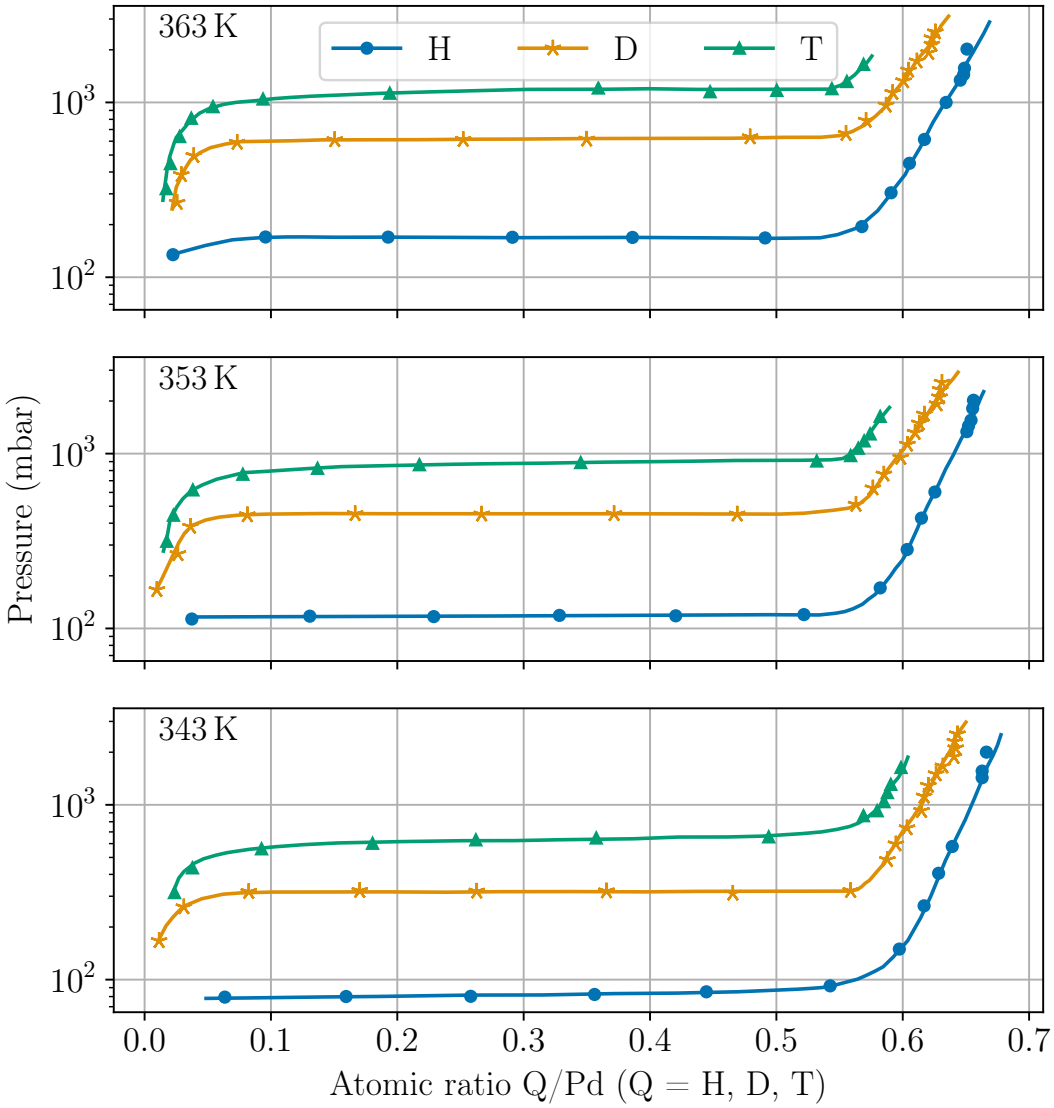


Figure 2.24: Desorption isotherms of protium, deuterium and tritium at 343 K, 353 K and 363 K from the respective palladium hydrides (after [Lae87]).

are nearly flat; the dissociation pressures at low temperatures comparatively high (see Fig. 2.24). As can be seen, the isotope effect is rather pronounced. For a given temperature and hydrogen concentration in the metal the decomposition pressure of palladium tritide is higher than that of the deuteride and that of the latter notoriously higher than of the hydride.

Dissociation pressures of isotopic palladium hydrides can be calculated from the relationship

$$\log p = -\frac{A}{T} + B \ ,$$

where p is the pressure in mbar, A and B are constants and T is the temperature in K.

On the basis of literature data, the following good fit equations were recommended for the hydride, deuteride and tritide of palladium [Lae83]

$$\log p_{\mathrm{PdH}} = -\frac{2075}{T} + 4.90$$
$$\log p_{\mathrm{PdD}} = -\frac{1899}{T} + 5.00$$
$$\log p_{\mathrm{PdT}} = -\frac{1742}{T} + 4.80 \ .$$

Advantageously, palladium is much less reactive towards gaseous impurities than uranium. When tritium is absorbed statically by palladium in a getter bed, impurities will mainly manifest by the so called "blanketing effect". This effect becomes noticeable when an inert gas or a slowly reacting impurity progressively accumulates inside of the bed near the getter surface. Under such conditions, the partial pressure of the gaseous impurity above the getter will gradually increase turning more and more into a diffusion barrier that will eventually retard considerably the absorption of tritium.

Ageing of palladium tritide for periods up to 755 days decreases the pressures of the desorption isotherm plateaus and shifts the α-phase zone of the isotherms towards higher T/Pd values [Nob92]. ^{3}He generated by decay of tritium is trapped in palladium powder in form of high pressure nano bubbles and dislocation loops [Tho83; Cow05]. Decay helium was only released from palladium tritide ($PdT_{0.6}$) at ambient temperature after aging periods exceeding 5000 days, i.e. when the helium/palladium atom ratio reaches values of the order of 0.5 [Abe90b]. This observation was corroborated by Emig et al. [Emi92],who followed the behaviour of palladium specimens loaded with deuterium and tritium over a rather extensive period of time. The initial low-level liberation of helium, i.e. 0.01 mol % after 500 days, is attributed to helium generated near surfaces which is liberated via the porosity connected to the surface. Subsequent release takes place when the solid fractures. This occurs once the He/Pd ratio attains values of the order of 0.6 and the bubble density becomes higher than 3×10^{24} bubbles/m^3.

Comparison of the helium release rate from two palladium tritide beds and two uranium tritide beds stored for hundreds of days under equal conditions provided evidence that the former traps helium much more strongly [Cor88]. This is in good agreement with earlier observations

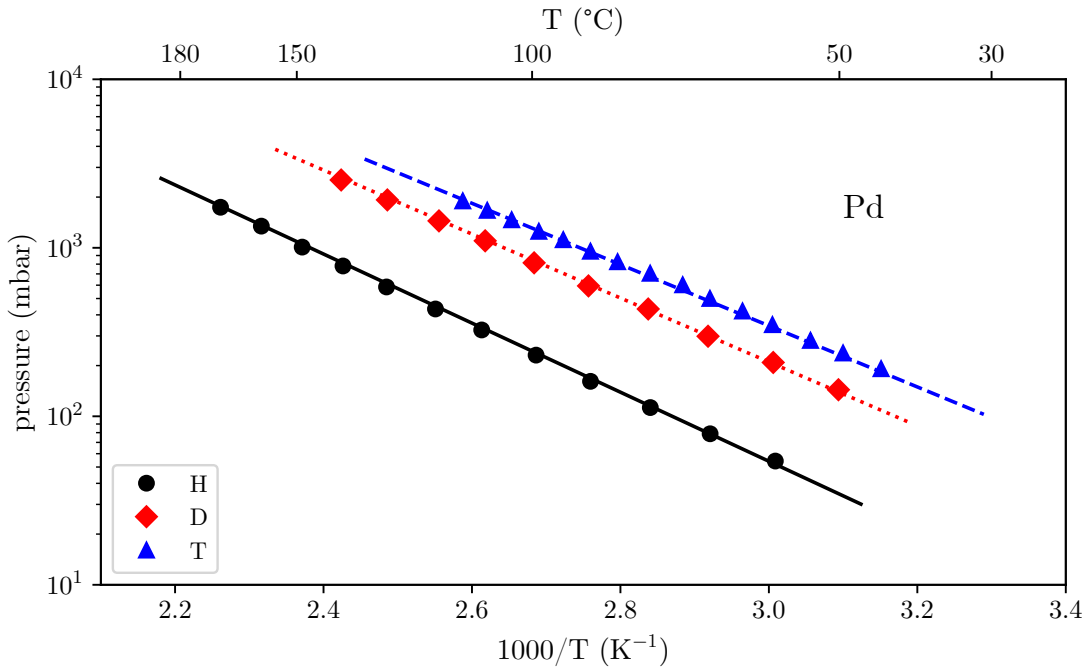


Figure 2.25: Desorption plateau pressures of protium, deuterium and tritium in the α+β two-phase region of palladium as function of inverse temperature.

reported by Bowman et al. [Bow77a]. They compared the ^{3}He release rate from LiT, UT_3, $TiT_{1.7}$ and $PdT_{0.6}$ and found that by far the slowest was that from palladium tritide. Rapid release was not detected even after an ageing period of 3.56 years (1300 days). With respect to tritium handling and storage, the principal disadvantages of palladium are its comparatively high hydrogen isotope pressures at ambient or low temperatures (little inherent safety) and its relatively high cost.

Lässer and Klatt [Lae83] measured the solubility of hydrogen isotopes in palladium at pressures within the range 0.1 - 2.0 bar, compositions covering the range $0.02 \leq x \leq 0.65$ (where $x = \mathrm{H/Pd}$) and temperatures within the range 308 - 398 K. As apparent from Fig. 2.25, at given temperatures $p_\mathrm{T} > p_\mathrm{D} > p_\mathrm{H}$.

Equation

$$\ln p = -(12.0 \pm 3.6) + ((20.4 \pm 6.1)) \cdot x$$

describes the relationship between the pressure in bar and the concentration x of tritium in the β phase of PdT_x at 343 K.

A Pd−C phase characterized by well-defined properties was found to be formed on the metal surface when palladium is heated in an atmosphere of ethylene, acetylene or carbon monoxide [Zie87]. This phase formation takes place after a carbonaceous layer is deposited on the palladium surface. Carbon atoms appear to migrate by activated diffusion from the layer on the surface into the palladium lattice eventually generating palladium carbide. Once a $PdC_{0.15}$ phase builds up the formation of β-PdH is completely suppressed [Zie85a; Sta85; Zie87].

Another palladium-based getter material developed and scrutinized at Savannah River Site, USA, consists of 50 % palladia supported on diatomaceous earth (kieselgur) [Sha99]. To prepare this getter palladium is first deposited on the kieselgur matrix from a $PdCl_2$ or $(NH_3)_4Pd(NO_3)_2$ solution which subsequently is subjected to thermal decomposition at elevated temperature. The resulting supported palladium exhibits a considerable increase of the surface to volume ratio (S/V). It was hoped that this increased S/V ratio would improve the aging properties of palladium, i.e. promote the release of helium-3. However, this did not turn out to be the case. On the other hand, kieselgur coated with palladium was found to have beneficial properties for other applications like pumping and purifying of hydrogen isotopologues [Ort85]. The favourable properties of palladium supported on kieselgur are i) inertness towards impurities (especially air), ii) hydrophobic character, iii) small protium content capable of binding tritium via isotopic exchange and iv) high reactive surface area which contributes to rapid absorption of hydrogen.

2.11.3 Titanium

Titanium reacts with hydrogen to yield a hydride whose stoichiometry is described by TiH_2. The hydride is a black powder less prone to spontaneous ignition with air than the metal powder. Interestingly, hydrogen nuclei are more densely packed in titanium di-hydride than in solid hydrogen. To activate titanium sponge for hydriding, the material is rinsed consecutively with water, acetone and alcohol and thereafter heated under vacuum at 1173 K. By this treatment, the oxide layer on the surface diffuses into the bulk and sites for the dissociation of hydrogen become available for fast reaction with molecular hydrogen.

Pressure-concentration-temperature relationships for the titanium-hydrogen system are well known since many years [McQ50; Nog81] (see Fig. 2.26). For the titanium hydride stoichiometry

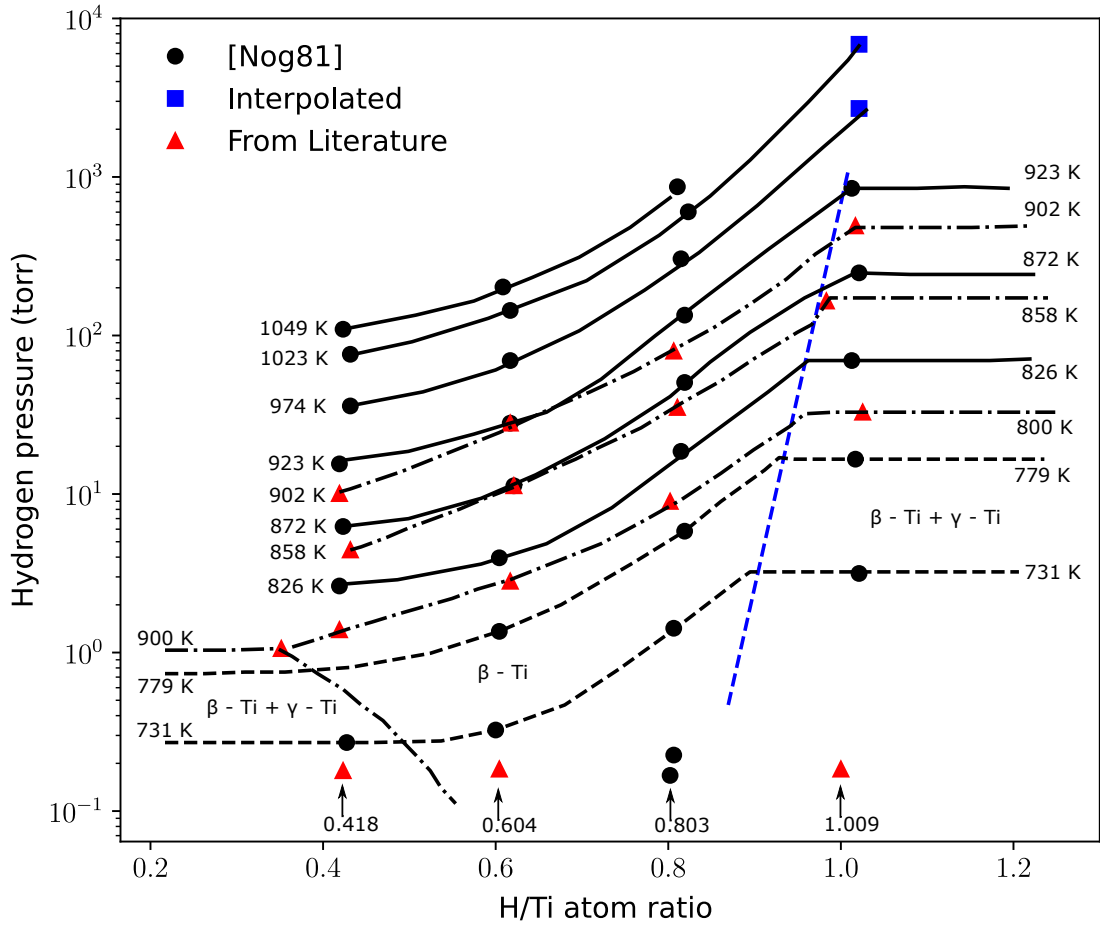


Figure 2.26: PCT data of the hydrogen-titanium system showing boundary locations (after [Nog81]).

$TiH_{1.009}$ the equilibrium dissociation pressure dependence from temperature can be calculated from expression

$$\ln p(\text{mbar}) = -\frac{19401}{T} + 28.02$$

where T is in Kelvin [Nog81]. Equilibrium p vs T data at other hydrogen concentrations can be calculated from relationships:

$$\ln p_{\mathrm{TiH}_{0.418(\beta)}} = -\frac{14871}{T} + 19.03$$
$$\ln p_{\mathrm{TiH}_{0.418(\alpha+\beta)}} = -\frac{12255}{T} + 15.74$$
$$\ln p_{\mathrm{TiH}_{0.604(\beta)}} = -\frac{15299}{T} + 21.84$$
$$\ln p_{\mathrm{TiH}_{0.803(\beta)}} = -\frac{15400}{T} + 21.84\ .$$

The effect of oxygen on the uptake of hydrogen was investigated systematically by Yamanaka et al. [Yam89]. Metallic specimens were prepared by vacuum annealing mixtures of Ti and TiO powders. With the obtained samples the uptake of hydrogen, deuterium and tritium by pure titanium and titanium containing 10, 20 or 30 [at%] oxygen was compared employing a constant volume method at temperatures in the range 873 - 1123 K. The attained results were well described by a Sieverts type expression

$$\ln \frac{c}{\sqrt{p}} = A + \frac{B}{T}$$

in which c is the solubility of hydrogen expressed in H/Ti atom ratio, p the equilibrium pressure in Pa and T the temperature in K. Values of the parameters A and B are listed in Table 2.28 together with enthalpies of solution. The data reveal higher solubility of hydrogen in titanium as well as in its oxides than deuterium or tritium. Increasing the oxygen content in titanium is associated with a decrease in hydrogen solubility. Conversely, the enthalpy of solution is only slightly affected by the presence of oxygen.

Aiming at developing long-term storage for tritium, Holtslander and Yaraskavitch [Hol81; Hol82] compared in a comprehensive investigation the reaction rate of hydrogen with titanium and zirconium in various metallic states of aggregation and researched the effect of annealing temperature, partial pressure of helium, gas re-circulation rate and the consequences of the presence of air. The evaluation included methods for packaging metal hydrides during transportation and options for a recoverable storage. Another examined topic pertained leaching of deuterium from

Table 2.28: A and B parameters and enthalpy of solution of hydrogen isotopes in pure Ti and Ti containing oxygen [Yam89].

Oxygen content at %	isotope	A	B	ΔH_{soln} kJ/g−atom
0	H_2	−11.6	5487	45.64
	D_2	−11.5	5198	43.12
	T_2	−11.5	5137	42.71
10	H_2	−11.9	5677	47.31
	D_2	−11.9	5472	45.64
	T_2	−11.9	5405	44.80
20	H_2	−12.4	5590	46.47
	D_2	−12.4	5512	46.10
	T_2	−12.3	5409	45.22
30	H_2	−13.2	5496	45.64
	D_2	−13.1	5313	44.38
	T_2	−13.1	5259	43.96

zirconium or titanium deuterides into solutions of $CaCl_2$, NaCl or $NaHCO_3$. For the leach tests the International Atomic Energy Agency leach test method was followed as closely as possible. Leach rates into all tested solutions were in the range 10^{-8} - $10^{-9}\,\mathrm{cm\,d^{-1}}$ [Hes71].

One obvious disadvantage of titanium is the relatively high dissociation temperature of titanium tritide. For this reason, titanium is normally not recommended for routine operations with tritium. On the other hand, it is exactly this property that makes titanium attractive for the long-term safe storage of tritium. The best stoichiometry for the purpose of long-lasting storage as tritide appears to be Ti:T = 1:1.

Miller and Cantlon [Mil82] carried out experiments to investigate the effect of gaseous helium and oxygen on the kinetics of hydrogen uptake by titanium sponge. According to their observations, oxygen concentrations in hydrogen of up to 0.6 % by volume have no effect on the rate of hydriding. Concentrations of helium in hydrogen exceeding 1 % by volume slow the reaction rate down significantly but only in a static mode of operation.

Titanium retains helium-3 generated by decay of immobilized tritium up to concentrations of 0.3 atoms He per atom Ti. Trapping of helium in titanium takes place most probably in form of microscopic gas bubbles [Rod71; Bow77a; Bow78; Sch89a]. Bubbles developing in α-titanium and δ-titanium showed characteristic differences. In α-titanium they were of low concentration, uneven spatial distribution and sizes displaying no discernible changes during specimen ageing at ambient temperature. Bubbles in the δ-tritide phase, on the other hand, were large in number (about 5×10^{23} bubbles/m^3) and small in size. During the course of up to 1000 d aging at ambient temperature they did not appear to change in number but exhibited linear mean size increase with $t^{1/3}$ (t = time) as helium was generated by tritium decay [Sch89a].

2.11.4 Zirconium

Zirconium hydride generated by reaction of hydrogen with the metal sponge was shown to have rather similar properties to titanium hydride especially with respect to thermal stability and resistance towards leaching. Hence, both metal sponges are considered suitable candidates for the long-term safe immobilisation of tritium in solid form [Bri81; Nog81; Ebe85; Ben87]. Titanium tritide is of the two the preferred matrix option for long-term storage because of its higher dissociation pressures. The advantage of higher pressures is faster and more efficient recovery of tritium.

2.11.5 Zirconium cobalt

The hydrogenation reaction of ZrCo

$$\mathrm{ZrCo} + \frac{3}{2}\,\mathrm{H_2} \longrightarrow \mathrm{ZrCoH_3}$$

is associated with appreciable volume expansion of the inter metallic compound. As opposed to uranium, which quickly disintegrates into a rather fine powder, the hydride obtained from zirconium cobalt ingot first converts into small flakes and then, after numerous loading/de-loading cycles, into a coarse powder. The densities of ZrCo powder and ZrCo hydride were determined to be 7.33 g cm^{-3} and 6.35 g cm^{-3}, respectively [Hay94]. The volume expansion of ZrCo induced by hydrogenation is considerably smaller than that of uranium (see Table 2.25).

The temperature dependence of the equilibrium pressure in the plateau region of a given hydrogen/metal ratio can be calculated from the van´t Hoff equation

$$\log p = -\frac{A}{T} + B$$

where A and B are empirical parameters, p is given in Pa and T in K. Some experimentally obtained values for A and B for the $ZrCoQ_x$ (Q = H, D, T) system are displayed in Table 2.29. The coefficients determined by several investigators using - at least partly - diverse techniques are in good agreement.

From Tables 2.25, 2.29 as well as Appendix D it is evident that at temperatures around ambient the equilibrium pressure of hydrogen over ZrCo hydride is higher than that over uranium hydride but still sufficiently low to meet the requirements demanded from a getter material proposed for safe storage of tritium [Pen90]. Conversely, tritium immobilized in zirconium cobalt is released at somewhat lower temperature than from uranium, which constitutes a small advantage when it comes to tritium re-cycling.

Typical $p-c$ isotherms of the ZrCo–H_2 system have been plotted as function of n_H/n_{ZrCo} ratio in Fig. 2.27 (left figure). As opposed to the rather flat $p-c$ isotherm plateaus characteristic of the U–H_2 system [Wic62], the ones of the ZrCo–H_2 system show a marked sloping behaviour with increasing n_H/n_{ZrCo} ratio. Also plotted in the figure is an isotherm at 773 K, which initially follows "normal" behaviour until at 43.5 kPa the n_H/n_{ZrCo} ratio becomes 0.1. If under these conditions the temperature and pressure are kept constant, a slow progressive decrease in hydrogen pressure is observed which after about 16 hours reaches a value of 26.9 kPa. At this point the composition of the solid reaches a value of $n_H/n_{ZrCo} = 0.98$. Once this condition is attained, additional supply of hydrogen up to a pressure of 120 kPa under isothermal conditions brings about no further uptake of hydrogen by the solid. This behaviour is explained by slow hydrogen-induced disproportionation of the original ZrCo hydride into Zr hydride and $ZrCo_2$ (only Zr binds hydrogen, the dissociation pressure of zirconium hydride at 773 K is rather small in comparison to that of ZrCo hydride and, last not least, hydrogen neither reacts with $ZrCo_2$ nor is it significantly soluble in this material).

Fig. 2.27 (right figure) illustrates the hysteresis of the zirconium-cobalt-hydrogen system during absorbtion/desorption cycles. Loading and de-loading isotherms at 573 K of the ZrCo–H_2

Table 2.29: Van´t Hoff parameters of the $ZrCoQ_x$ (Q=H, D, T) system.

Q	x	A	B	Validity range	Temp. at which P = 10^5 Pa	Ref.
				K	K	
H	0.8	3986	11.21	403 - 573	642	[Nag86]
H	0.8	4408	12.04	423 - 573	626	[Irv80]
H	0.8	6086	13.94	523 - 623	681	[Kos80]
H	3.0	5704	-	-		[Kos80]
D	0.8	4260	11.16	503 - 588	692	[Kos80]
D	3.0	5179	-	-		[Kos80]
H	0.8	4751 ± 183	12.74 ± 183.00	473 - 573	682	[Wil88]
H	0.8 - 2	4330 ± 152	12.05 ± 0.29	473 - 573	674	[Wil88]
H	0.8	4266	11.80	423 - 573	627	[Pen90]
H	0.8 - 2	4261 ± 85	11.93 ± 0.14	423 - 573	615	[Pen90]
D	0.8	4537	12.46	423 - 573	608	[Pen90]
D	0.8 - 2	4571 ± 42	12.65 ± 0.12	423 - 573	598	[Pen90]
H	0.8	3959	10.81	373 - 623	681	[Hei92]
H	1.5	3828	10.76	373 - 623	665	[Hei92]
T	0.8	3880	10.86	373 - 623	662	[Hei92]
T	1.5	3843	11.02	373 - 623	638	[Hei92]
H	1.0	2856	9.075	323 - 573	700	[Bek00]
D	1.0	3477	10.36	323 - 573	648	[Bek00]

and ZrCo−D_2 systems reveal significant isotope effect. Fukada and Mitsuishi [Fuk93] developed semi-empirical expressions based on thermodynamic considerations for the calculation of pressure-composition of the zirconium-cobalt-hydrogen system during hydrogenation and de-hydrogenation. Their model was shown to predict correctly the experimental hysteresis results.

Devillers et al. [Dev93] determined the solubility of molecular hydrogen and molecular deuterium in ZrCo at compositions within the range $2 \times 10^{-3} < (n_{\mathrm{H}} \text{ or } n_{\mathrm{D}})/n_{\mathrm{ZrCo}}) < 10^{-1}$ and temperatures in the range $473 < T < 773\,\mathrm{K}$. Sieverts' constants and $(K_S)_{\mathrm{H}}/(K_S)_{\mathrm{D}}$ ratios at several temperatures are compiled in Table 2.30. The ratio was found to be reasonably constant and equal to 1.18 ± 0.04. The $(K_S)_{\mathrm{H}}/(K_S)_{\mathrm{D}}$ ratio is furthermore comparable to that of titanium,

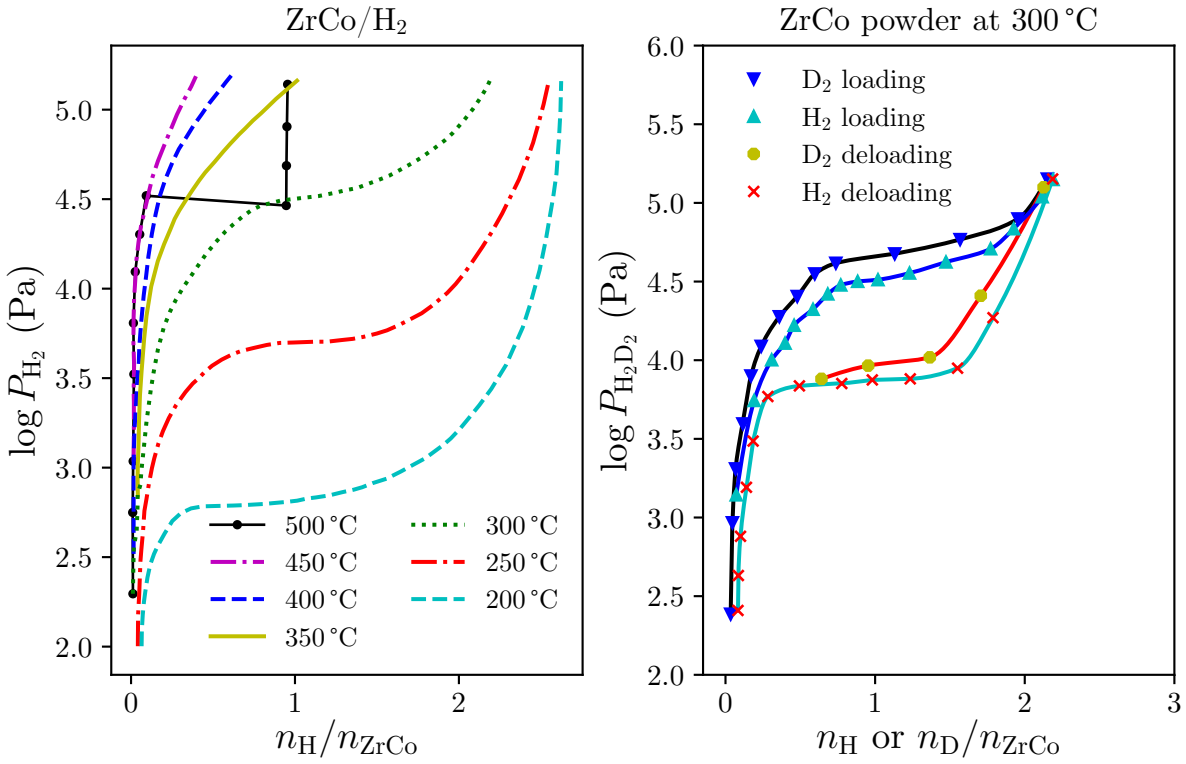


Figure 2.27: Uptake and release of hydrogen isotopologues from ZrCo at several temperatures. The left figure shows P-c isotherms of the ZrCo–H_2 system including a pressure-composition isotherm at 773 K which establishes after 16 hours of disproportionation at the concentration $n_H/n_{ZrCo} = 0.98$. An increase in hydrogen pressure does not change the hydrogen concentration in the solid because disproportionation is completed [Dev92]. The right figure illustrates the hysteresis of the ZrCo–H_2 and ZrCo–D_2 systems at 573 K [Nag86; Dev89; Pen90].

zirconium, or hafnium. The relative molar enthalpies and excess entropies for hydrogen and deuterium in infinitely diluted solution were determined to be $\Delta\bar{H}^{\infty}_{H} = -28.2\,\mathrm{kJ/mol_H}$ and $\Delta\bar{H}^{\infty}_{D} = -27.7\,\mathrm{kJ/mol_D}$ and $\Delta\bar{S}^{\infty}_{H} = -73.5\,\mathrm{J/K/mol_H}$ and $\Delta\bar{S}^{\infty}_{D} = -74.2\,\mathrm{J/K/mol_D}$, respectively.

Disproportionation proceeds via reactions such as

$$2\,\mathrm{ZrCoH_3} \longrightarrow \mathrm{ZrH_2} + \mathrm{ZrCo_2} + 2\,\mathrm{H_2}$$

$$2\,\mathrm{ZrCo} + \mathrm{H_2} \longrightarrow \mathrm{ZrH_2} + \mathrm{ZrCo_2}\ .$$

Table 2.30: Sieverts´ constants (K_S) for the solubility of hydrogen (H) and deuterium (D) in zirconium cobalt (ZrCo) [Dev93]

Temperature K	10^4 K_S(H) atom ratio $Pa^{-1/2}$	10^4 K_S(D) atom ratio $Pa^{-1/2}$	K_S(H)/K_S(D)
473	70.84	58.32	1.215
523	35.86	30.21	1.187
573	19.88	16.34	1.217
623	12.36	10.35	1.194
673	8.172	7.333	1.114
723	5.953	5.072	1.174
773	4.470	3.814	1.172

These reactions are accelerated by concomitantly occurring elevated hydrogen pressures and temperatures. Konishi et al. [Kon95a] confirmed this observation but noted that disproportionation is extremely slow at temperatures under 673 K. A quantitative reproportionation, i.e. full re-conversion of ZrH_2 and $ZrCo_2$ into ZrCo and gaseous hydrogen, was found to be achievable by vacuum annealing at elevated temperatures [Dev92; Kon95b]. Bekris et al. [Bek99; Bek00] provided further evidence for quantitative reproportionation by heating at 773 K under vacuum over a period of several hours.

Hara et al. [Har00] showed in a systematic study on the kinetics of the disproportionation reaction of zirconium-cobalt induced by hydrogen that the disproportionation rates increase with temperature until about 815 K are attained. Above this temperature the rates commence to drop again, which was explained by gradually increasing contributions of the reproportionation reaction (see also [Koo15]). Hara et al. postulated that the rate of disproportionation is controlled by a combined nucleation and nuclei growth mechanism such as proposed by Avrami et al. [Avr39; Avr40]. The probability of nucleation was assumed to be proportional to a nucleation constant and to the concentration of hydrogen dissolved in the zirconium cobalt matrix. The latter was evaluated from Sieverts' law data reported by Devillers et al. [Dev93].

To describe the disproportionation mechanism the following equations, given here in much simplified form, were proposed

$$-\ln(1-x) = k_{\mathrm{ov}} K P(t)^{1.5} t^{1.4} \ ,$$

where

x = extent of reaction

K = Sieverts´ constant = $5.45 \times 10^{-6} \exp\left(-\frac{3386}{T}\right)$

k_{ov} = overall disproportionation rate constant = $Ck^3 3$

C = proportionality constant = 9.0×10^{-7}

$k = \frac{(k_{\mathrm{d}} - k_{\mathrm{r}})}{0.13}$

k_{d} = disproportionation rate constant = $A_{\mathrm{d}} \exp\left(-\frac{E_{\mathrm{d}}}{RT}\right)$

k_{r} = reproportionation rate constant = $A_{\mathrm{r}} \exp\left(-\frac{E_{\mathrm{r}}}{RT}\right)$

and

$P(T)$ = equilibrium hydrogen pressure over $ZrCoH_x$ at T

Experimentally determined frequency factors (A) and activation energies (E) for the calculation of disproportionation and reproportionation rates induced by hydrogen or deuterium are compiled in Table 2.31. The comparatively large activation energy of the rate of reproportionation explains why re-proportionation sets in suddenly when the temperature is gradually augmented. That in spite of negligible differences in activation energies and pre-exponential factors (see Table 2.31) the observed isotope effect is large, i.e. $k_{\mathrm{ov}}(H)/k_{\mathrm{ov}}(D) = 2$, is ascribed to the large differences in solubility of hydrogen and deuterium in ZrCo as well as to the third power of the overall disproportionation rate constant in the equation given above. While the disproportionation rate induced by tritium has not yet been determined, it can be prognosticated that it will be even slower than that induced by deuterium.

At a given temperature the equilibrium pressure of hydrogen isotopes over ZrCo exhibits the pressure isotope effect $p_{\mathrm{H_2}} < p_{\mathrm{D_2}} < p_{\mathrm{T_2}}$ [Pen90; Hei92]. However, there are indications for an

Table 2.31: Arrhenius parameters for disproportionation and reproportionation of ZrCo induced by hydrogen isotopes [Har00].

Type of reaction	A	E
	$\mathrm{Pa^{-0,5}min^{-0.5}}$	$\mathrm{kJ\,mol^{-1}}$
Disproportionation (H)	2.7×10^4	65
Disproportionation (D)	2.7×10^4	66
Re-proportionation (H)	7×10^{12}	208
Re-proportionation (D)	7×10^{12}	208

inverse isotope effect at temperatures below 223 K, i.e. a crossover of activation energies [Bek00]. In view of this, at low temperatures the deuterium-ZrCo system appears to be more stable than the hydrogen-ZrCo system, the tritium-ZrCo system being the most stable of all. Analogous inverse isotope effects have been observed for other metal-hydrogen systems [Wis72]. Under this premise, tritium is released less easily than deuterium or hydrogen at temperatures below 223 K and more readily at temperatures exceeding 223 K. From the point of view of tritium storage, this constitutes a favourable property of ZrCo.

Shim et al. [Shi08a] investigated the extent of disproportionation in a ZrCo bed subjected to ITER relevant operation conditions in terms of pressure, temperature and number of cycles. Utilizing the model proposed by Hara et al. [Har00] they calculated the degree of disproportionation and verified their results. They were able to show experimentally and theoretically that disproportionation of ZrCo can be minimized if temperatures higher than 623 K and pressures above 3.1 kPa are consistently avoided.

ZrCo reacts irreversibly at temperatures above 523 K with trace impurities like methane, carbon monoxide, carbon dioxide, oxygen, nitrogen and water, all conceivably arising in the fusion fuel cycle. Presumed reaction products are oxides, carbides and nitrides [Pen91b]. The decrease in absorption rate and capacity of the getter for hydrogen isotopologues depends on the extent of reaction with these impurities.

Hayashi et al. [Hay92a; Hay94] followed the release of decay helium-3 from zirconium cobalt tritide in a storage bed over a period of up to 3.5 years. They noticed a slow but steady increase of pressure inside of the bed. With tritides having tritium concentrations in the range 0.3

< T/ZrCo < 1.5 and ZrCo getter material subjected prior to tritium-exposure for up to ten hydrogenation/dehydrogenation cycles, they found that at temperatures maintained within the range $293 < T < 523$ K during the first two years of aging the fraction of ^{3}He released was less than 3 % of that generated by radioactive decay. Beyond this period, i.e. when the ^{3}He/ZrCo ratios exceeded values of 0.15, the released fraction of helium increased rapidly up to values of 25 %. Heating aged zirconium cobalt tritide up to 823 K caused liberation of most of the immobilized tritium but only of a small fraction of the accumulated helium. It follows that beds using ZrCo getter in the Storage and Delivery System of ITER will have to be designed for fairly high temperatures if they are to comply with the requirement of periodical purification from decay ^{3}He. This purification treatment is indispensable for the supply of high purity hydrogen isotopes and to preserve the gettering properties of zirconium cobalt at high level. The presence of high concentrations of helium bubbles in the getter bulk increases the tritium equilibrium pressure over the getter (see below).

Ageing of zirconium cobalt tritide for a period of about 64 months is associated with a substantial accumulation of ^{3}He in in the getter. In spite of expected considerable stress to the crystal structure, calorimetric determinations of tritium carried out with freshly loaded and aged material gave no indication that this actually takes place [Hay05]. This unexpected behaviour should be further investigated.

Maynard et al. [May95] aged three zirconium cobalt specimens initially containing tritium at T/ZrCo ratios of 1.51, 1.44 and 2.15, respectively. The final T/ZrCo ratios determined after 3.2 years, 3.0 years and 3.1 years were found to be 1.26, 1.22 and 1.80, respectively, which are essentially the values expected after subtraction of tritium decay. The equilibrium tritium pressures in the temperature range 373 - 573 K, on the other hand, did approximately triplicate with respect to those over pristine specimens. Another consequence of ageing was that at temperatures as high as 773 K and above about 98 [%] of the generated decay ^{3}He remained in the bulk. The ZrCo alloy with the highest concentration of helium, i.e. ^{3}He/ZrCo = 0.35, released only 1.5 [%] of the total helium after numerous absorption/desorption cycles at 573 K. In view of the above it may be concluded that the results of Maynard et al. [May95] and Hayashi et al. [Hay94] are by and large consistent. In spite of this, more systematic quantitative research on the consequences of decay helium accumulation in ZrCo or in other potential storage getters on the absorption/desorption properties of tritium appears to be necessary.

Comparison of the pyrophoric properties of zirconium-cobalt with those of uranium leads to the conclusion that the former is safer because the amount of energy released per mol during exposure of zirconium-cobalt to air amounts to only about one third of that released when uranium reacts with air [Lon88].

As discussed above, under equilibrium conditions, the hydrogen isotope effect, i.e. $p_{H_2} < p_{D_2} < p_{T_2}$, displayed by the zirconium cobalt hydride system is substantial at any given temperature. Because of this, accurate knowledge of the actual composition of hydrogen isotope mixtures delivered by a getter bed under ITER relevant conditions, i. e. rapidly heated storage bed under prevailing non-equilibrium conditions, is of much relevance for an efficient performance of the ITER Storage and Delivery System (SDS). Hence, experimental data on possible dynamic composition changes during steady release of an isotopologue hydrogen mixture from a ZrCo bed were found necessary. A few studies devoted to this problem will be discussed below [Bes02b; Bel05b; Hay07b].

Fig. 2.28 displays fast release of hydrogen gas from a bed initially containing $ZrCoQ_{2.44}$ (Q = H, D) of a nearly equimolar hydrogen – deuterium mixture. The bed was heated up to 673 K with the maximum possible heating rate achievable with four heaters delivering a total of 9.1 kW [Bel05b]. While initially, the concentration of released deuterium was found to be higher than that of hydrogen, after about 8 min the isotope effect started to reverse, eventually crossing over and becoming increasingly notorious. Under these experimental conditions, deviations of up to 20 % from the initial concentration, i.e. H_2 25 % and D_2 25 %, were registered after about 30 min of getter heating. These observations are in line with earlier findings by Besserer et al. [Bes02b], who reported enrichment of the heavier isotopologue in the gas released from zirconium cobalt originally containing a mixture consisting of 10 % deuterium and 90 % tritium.

To achieve rapid release of hydrogen isotopologues from a loaded ZrCo bed Hayashi et al. [Hay07b] tried another approach. They first closed the bed, heated it up to a predetermined temperature and then opened the exhaust valve while swiftly extracting the released gas with the help of a suitable pump. To simulate more realistically gas supply at SDS, the heat of dehydrogenation, which caused an immediate temperature drop of about 40 degrees in the bed, was not compensated by supplementary heating. In experiments with a ZrCo bed loaded with hydrogen up to the ratio Q/ZrCo = 1.8 (Q = H, D, T) the getter was heated either up to 573 K or up to 623 K and the overall release rate of hydrogen isotopes determined at these two

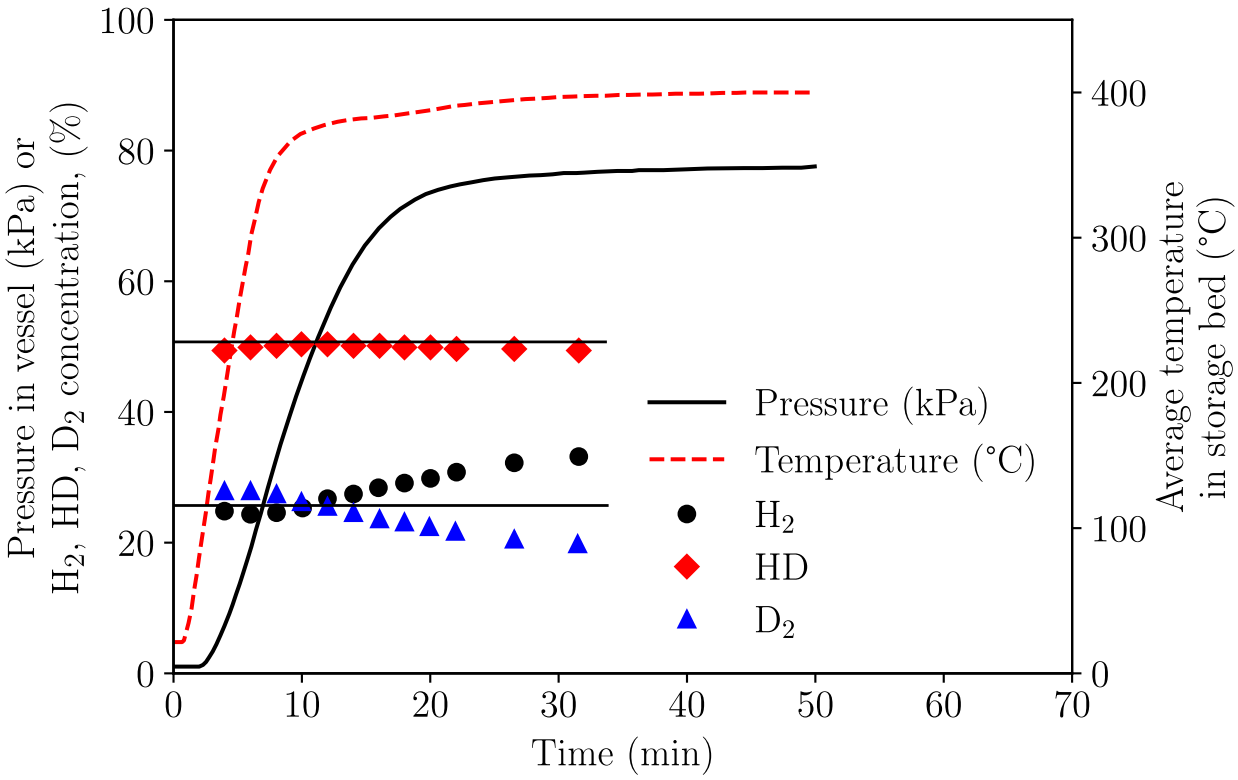


Figure 2.28: Desorption of a nearly equimolar hydrogen-deuterium mixture from a ZrCo bed (after [Bel05b]). The horizontal straight lines give the initial concentrations of H_2 (25 %), D_2 (25 %) and HD (50 %) in the bed.

temperatures. The composition of the liberated hydrogen isotope mixture was analysed in short intervals using a quadrupole mass spectrometer. Under conditions of fast release, the isotopic composition of H:D hydrogen mixtures having initial ratios of 1:9, 1:1 or 9:1 did not change significantly during the whole period of release, i.e. the isotopic ratio remained largely constant even after 95 % of the original loading had been liberated. During release, the rate progressively decreased from an initial maximum of about 0.8 l(STP)/min down to much lower values. The change in chemical composition of the hydrogen isotopes extracted from the bed has been plotted as function of remaining loading (Q/ZrCo) in Fig. 2.29. The highest deviation from the original 1:1 isotopic ratio was of the order of 5 % during the final stages of the release. Evidently, at high release temperatures the zirconium cobalt matrix promotes rapid isotopic scrambling.

Based on the results from their investigations, Hayashi et al [Hay07b] recommended replacing some of the currently rapid fuel delivery getter beds contemplated for ITER by appropriately sized fuel supplying tanks. Their advice was to incorporate fuelling tanks into the ITER Storage

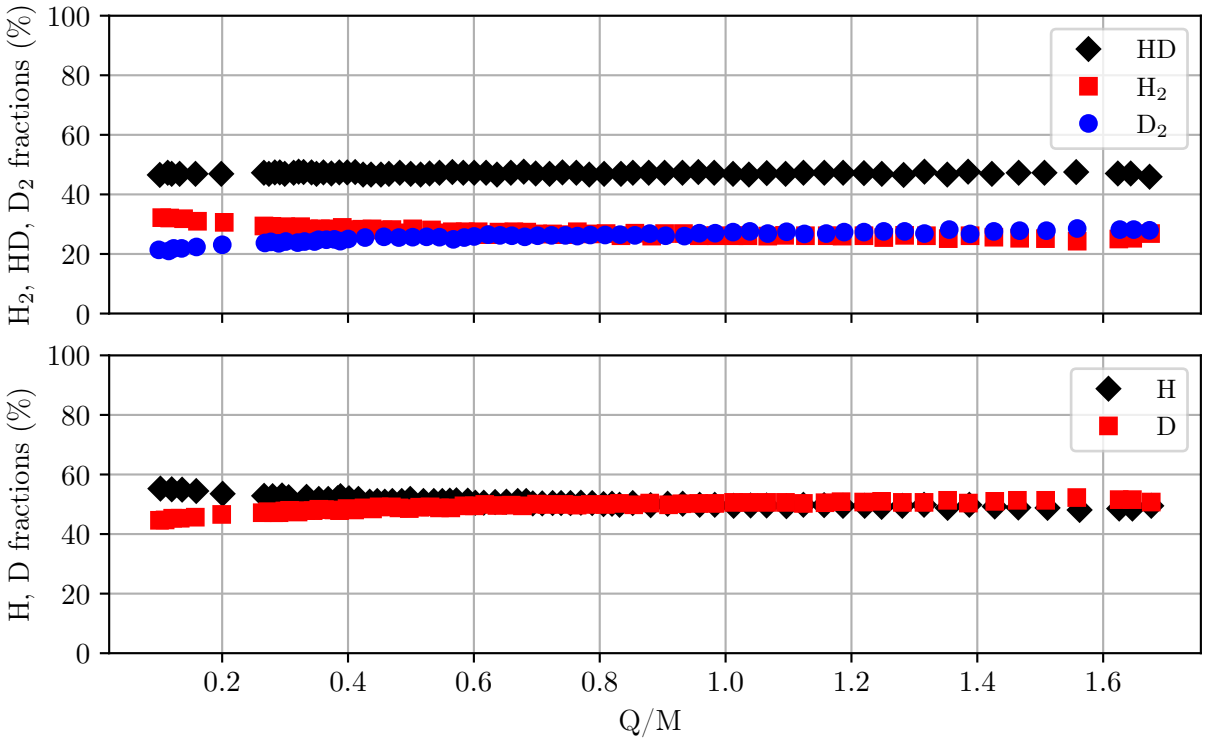


Figure 2.29: Hydrogen isotopologue release from a ZrCo bed initially loaded with a D:H = 1:1 mixture (after [Hay07b]). Fractions of H_2, HD and D_2 (upper figure) and of H and D atoms (lower figure) progressively being released at 623 K from a ZrCo bed under approximately isothermal conditions.

and Delivery System not only to comply with current fuelling demands but also from the point of view of tritium accountancy. They presumed that reduced manufacture costs of fuel delivery beds adhering to less stringent construction demands could eventually compensate for the extra costs arising from added fuelling tanks and analytics (additional analytical efforts were assumed to become necessary for isotope composition adjustments in the tanks).

Propitious properties of the reversible hydrogen getter ZrCo are: i) dissociation pressure at ambient temperature low enough to warrant safe interim tritium storage, ii) acceptable getter volume expansion by hydrogenation, iii) release of tritium at moderate temperature, iv) relatively low pyrophoricity, v) aged ZrCo retains the majority of decay ^{3}He within the bulk even at elevated temperature and vi) handling of ZrCo is not subject to national or international restrictions. Among the disadvantageous properties of ZrCo are the need to avoid disproportionation at high pressures of hydrogen and temperatures exceeding 623 K and the necessity of high temperatures for periodic release of decay helium from the matrix. Disproportionation can be minimized by

remaining under critical pressures and temperatures during loading/deloading. Disproportionated material can be returned in situ into the original composition by straightforward evacuation at elevated temperature.

2.11.6 Lanthanum nickel and its alloys

One more type of getter material successfully employed for handling and storing of tritium are compounds of lanthanum and nickel such as $LaNi_5$ or $LaNi_5$-based alloys doped with Al or Mn. These solids react reversibly with hydrogen at ambient temperature, quickly fragmenting from initially a solid material into a fine hydride powder [Wul86; Shi88; Jos89]. As typical for other metallic getters, the kinetics of absorption accelerates considerably with increasing number of absorption/desorption cycles, which is attributed to the augmenting reactive surface area of the powdering getter [Uch84].

The sorption rates of the powder appear to be essentially independent from hydrogen pressure, at least between 1 [bar] and 5 [bar] and show independency from direction, i.e. absorption or de-sorption. Rate-constrolling surface reactions are disregarded because the desorption of hydrogen does not follow the characteristic parabolic law which signalizes recombination of two hydrogen atoms into a hydrogen molecule. Because the activation energy of sorption, i.e. 31.82 [kJ/mol of H_2], agrees closely with the energy of formation of $LaNi_5H_6$, it was postulated that phase transformation during hydrogen sorption constitutes the rate controlling step [Bos76].

The absorption of hydrogen by the inter-metallic lanthanum nickel getter is described by equation

$$LaNi_5 + 3\,H_2 \longrightarrow LaNi_5H_6\ .$$

The maximum hydrogen uptake observed experimentally can actually be supra-stoichiometric, i.e. $LaNi_5H_{6.7}$. During hydride formation the solid solution phase and the full hydride phase remain hexagonal, but the reaction is accompanied by a lattice expansion of approx. 25 % [Ive81; Aki87]. As with other inter metallic compounds, a hysteresis of about 0.1 MPa is observed between the sloping isotherms for hydride formation and those for hydride decomposition [Kui71]. The plateau pressure at ambient temperature of the tritide is of the order of 2.2 bar (the exact value depends on the T/M ratio where M = inter metallic compound). Hydrogen and deuterium

plateau pressures for absorption and de-sorption have been determined as function of $LaNi_5Q_x$ (Q = H, D, T) hydride composition by Kuijpers et al. [Kui71], Biris et al. [Bir76] as well as by Boser [Bos76].

Pressure-composition isotherms of the $LaNi_5$ – hydrogen system at pressures of up to about 100 bar are provided in a review by Reilly [Rei79].

Dust clouds of $LaNi_5$ (particle size $< 74\,\mu m$) or $LaNi_5H_6$ (average particle size $12\,\mu m$) display ignition temperatures in air of 693 and 593 K, respectively. These two compounds are thus much safer than the dusts of uranium or uranium hydride both igniting already at ambient temperature [Rei79].

With progressing number of absorption/desorption cycles beyond those causing powdering, the amount of absorbed hydrogen gradually decreases and the kinetics degrade considerably [Par82; Goo83; Han89a; Han89b; Wer92]. Experimental evidence points to the occurrence of an intrinsic degradation, i.e. permanent changes of the molecular structure resulting from hydrogen absorption rather than from oxidation or poisoning by active impurities. According to Cohen et al. [Coh80a; Coh80b] will pressure-cycled material degrade faster than thermal-cycled one. Nomura et al. [Nom85] concluded from their experiments that the higher the annealing temperature prior to an absorption study the higher are the pressures of the absorption isotherms and larger the hysteresis. They remarked that a sequence of consecutive thermal cycling disproportionation steps of lanthanum nickel leads to the formation of the parent metals, i.e. nickel and lanthanum. However, re-activation appears to be possible by heating at approx. 373 K under low vacuum [Sch80].

Wermer [Wer92] observed, that storage beds containing $LaNi_{5-x}Al_x$ exposed repeatedly to tritium will gradually incorporate increasing amouts of irreversibly bound tritium (or "heel"). Once the "heel" exceeds a certain level, the storage capacity and pumping performance of the bed becomes unacceptable. At this point, the bed needs to be replaced. While the "heel" cannot be removed by simple heating and desorption, it can be reduced to very low levels by exchange reaction with deuterium.

Carbon monoxide chemisorbs on $LaNi_5$ forming a monolayer that deactivates the nickel atom sites on which catalytic dissociation of molecular hydrogen takes place. This effectively reduces the hydrogen absorption capacity of the getter [Han89b]. Sandrock and Goodell [San84] investigated the effect of impurities in hydrogen such as CH_3SH, CO, CO_2, O_2, NH_3, CH_4, C_2H_4

and N_2 on the cycle life of $LaNi_5$ at 298 K. While NH_3, CH_4, C_2H_4, and N_2 were found to be essentially innocuous other impurities caused either poisoning (rapid decrease in hydrogen capacity, e.g. CH_3SH), retardation (reduction in absorption kinetics without significant loss of capacity, e.g. NH_3), retardation-recovery (at least partial recovery, e.g. O_2), or reaction (bulk corrosion with irreversible loss of capacity, e.g. O_2 after extended cycling). $LaNi_5$ getter exposed to hydrogen contaminated by CO displayed a dependence of magnitude and type of interaction from temperature.

Thermal desorption of hydrogen from $LaNi_5H_x$ shows spectra which consist of a single peak for $x \leq 6$ which developes into a two-peak structure for $x = 6.7$ [Res87]. The rate determining step for desorption was found to be diffusion at $T < 175$ K and either diffusion or phase transformation at higher temperatures.

Nickel and lanthanum atoms on the surface of $LaNi_5$ generate by reaction with molecular oxygen or moisture a fairly thick oxide film. The oxides are complex and disproportionate by surface diffusion yielding nickel clusters in stable La_2O_3 or $La(OH)_3$ [San80]. Pre-coverage is associated with formation of β-phase $LaNiH_6$, which in a composition/pressure plot becomes apparent as sloping plateaus. The formation of β-phase $LaNi_5H_6$ begins with adsorption of hydrogen molecules on the surface and their conversion into hydrogen atoms. Only after the $LaNi_5$ lattice becomes saturated with hydrogen atoms (α-phase) will β-phase formation set in. The rate of phase transformation reaction depends on pressure and temperature [Bel81; Goo83; Miy83b].

When nickel in $LaNi_5$ is partially substituted by aluminium, e.g. $\mathbf{LaNi_{4.25}Al_{0.75}}$, alloys of improved storage properties are obtained Among the enhancements the following can be cited: i) sub-atmospheric isothermal plateau pressures at ambient temperature, ii) capability to generate pressures of more than 1 bar at intermediate temperatures and iii) stabilization of the material towards impurities, pressure/temperature cycling and tritium ageing effects [Ort85; Hoe94]. According to Goodell [Goo84] $LaNi_{4.7}Al_{0.3}$ exhibits practically no disproportionation even after 1500 cycles with hydrogen at 358 K. Also, the resistance of the alloy towards CO is much improved by partial replacement of nickel by aluminium. Actually, $LaNi_{4.25}Al_{0.75}$ alloys show no strong reaction with carbon monoxide [Han89b], or with air - even at higher temperatures [Lon88].

Favourably, tritium desorbed from aged lanthanum nickel tritide is practically free from helium-3. For example, tritium liberated from $LaNi_{4.25}Al_{0.75}$ tritide after 3.9 years of storage contained less than 10 ppm helium-3 (detection limit) [Ort90]. However, once the He/M ratio in the metal (M) exceeds a saturation level of 0.34, decay helium begins to be released. The rate of liberation eventually becomes equal to that of its generation [Sha03a].

Getter beds utilizing $\mathbf{LaNi_{4.25}Al_{0.75}}$ have been successfully implemented for tritium service at Savannah River Site **Replacement Tritium Facility** [Wer93], where much experience has accumulated over the course of 25 years of intermittent operation with tritium. Applications of beds containing $LaNi_{4.25}Al_{0.75}$ have been: i) replacement of mechanical compressors, ii) recovery-pumping, iii) isotope separation, iv) purification of hydrogen isotopes and v) tritium accountability in large storage beds of 1500 l capacity [Kle02b].

During ageing of lanthanum-nickel-aluminium tritide decay helium-3 accumulates in the lattice and induces changes of the thermodynamic properties of the getter [Nob92; Wer93; Hoe94; Wer94; Sha03a]. These changes comprise i) decrease in total storage capacity, ii) decrease of isothermal plateau pressure (and therefore of desorption pressure), iii) increase in slope of the isothermal plateaus and iv) gradual build-up of firmly sequestered tritium.

In a thermo gravimetric study coupled with mass spectrometry employing tritium aged $LaNi_{4.25}Al_{0.75}$ previously exchanged with deuterium in order to reduce the tritium content, it was observed that decay helium is released in two steps: first at 493 K together with hydrogen isotopes (T_2, DT, D_2) and then mostly singly at about 763 K [Sta15]. For these experiments, a sample aged for almost three decades and passivated by constrained reaction with air was used. After oxidation of $LaNi_{4.25}Al_{0.75}$, the released gas quantities provided information on the degree of hydrogen or helium retention loss by the getter.

Prior to disposal, the tritium heel can be extracted to a large extent by high temperature isotopic exchange using either protium or deuterium. By this way of proceeding it was possible to generate solid waste of little tritium content ($< 8 \times 10^{11}\,\mathrm{Bq\,kg^{-1}}$).

In spite of the low cost of $LaNi_{4.25}Al_{0.75}$ for instance in comparison to palladium, the trade-off is the more frequent replacement of storage beds once they have lost a substantial fraction of their hydrogen isotope storage capacity.

Another lanthanum/nickel getter material potentially suitable for tritium handling and storage has the general formula $\mathbf{LaNi_{5-x}Mn_xH_y}$ [Ide88; Ide90]. Substitution of nickel in $LaNi_5$ by

manganese was found to bring about a significant reduction in plateau pressure of hydrogen, i.e. two orders of magnitude for x values within the range $0 < x < 1$ [Lar79]. Following screening tests with seven intermetallic compounds of compositions within the range $LaNi_5$–$LaNiMn_4$, a getter of composition $LaNi_3Mn_2$ was selected for further studies [Ide88]. Hydrogen absorption isotherms plotted as function of tritium/alloy ratio yielded sloping plateaus with pressures of either a few Pa or hundreds of kPa at temperatures of either 298 or 573 K, respectively. At given temperature and hydrogen isotope concentration, the dissociation pressures of hydrides, deuterides and trititides were found to increase in the order $p_{T_2} > p_{D_2} > p_{H_2}$.

It should be noted that inter metallic compounds of the series $LaNi_5$–$LaNi_{5-x}Mn_x$ exhibit considerable catalytic activity for hydrogenation of carbon monoxide into methane and higher hydrocarbons [Bar83].

2.11.7 Zirconium nickel

Another reversible intermetallic compound employed to supply and retrieve tritium is zirconium-nickel. A monohydride, ZrNiH, and hyper stoichiometric hydrides of composition $ZrNiH_{4-x}$ have been identified [Wes80b]. Even though these compounds also show tendency to disproportionate according to reactions

$$3\,ZrNi + 2\,H_2 \longrightarrow 2\,ZrH_2 + ZrNi_3 \quad \text{or}$$
$$3\,ZrNiH_3 \longrightarrow 2\,ZrH_2 + ZrNi_3 + \frac{5}{2}\,H_2$$

they appear to be considerably more resistant towards this phenomenon than zirconium cobalt [Wat95]. In fact, Bowman et al. [Bow85] alleged that $ZrNiT_3$ retains its stoichiometry indefinitely. Ample information on the thermodynamic properties, equilibrium pressure/concentration isotherms, absorption/desorption hysteresis, and van´t Hoff plots of plateau pressures of the ZrNi–H_2 system are provided by Dantzer et al. [Dan01]. The loading capacity was found to be 15 - 20 $g_{H_2}\,kg^{-1}$ and the volume expansion of ZrNi upon uptake of hydrogen comparable to that of ZrCo, i.e. 18 % [Bar79a]. Advantageous properties of ZrNi in view of tritium storage are the high absorption rate, e.g. 13.3 mbar D_2 in a 1.2 l vessel can be pumped at 298 K down to 1.33×10^{-4} mbar in 200 s and rapid decomposition kinetics. Because tritium can be released from ZrNi tritide already at 473 K, losses by permeation are minimal [Nak85]. NMR measurements

have provided evidence that decay helium is captured in microscopic bubbles. One reason why this getter has received less attention than ZrCo is that the pressure – composition isotherms display two plateau regions: one at the limiting composition ZrNiH and another at $ZrNiH_{4-x}$ [Lib58; Wat91], see also Appendix D. In spite of this drawback, the getter has been used extensively and without contingencies at HRC, Toyama, for supply and recovery of tritium in a number of diverse experiments [Mat98; Mat02b; Tor04; Pen06].

Watanabe et al. [Wat10] investigated the kinetics of the decomposition of methane in the presence of Zr-Ni alloys. They postulated that the reaction proceeds via a sequence of reactions such as

$$CH_4\,(g) \longrightarrow CH_3\,(a) \longrightarrow CH\,(a) \longrightarrow C\,(\text{carbon deposit})$$

taking place on active adsorption sites of the alloy. Released hydrogen atoms were presumed to be absorbed by the metallic getter.

2.11.8 Getters contemplated for the Storage and Delivery System of ITER

After comparison of the physical and chemical properties of a number of getters of potential application in the Storage and Delivery System of ITER ZrCo and U were selected for the Detailed Design Report (DDR) of ITER 15 years ago. Both getters have by and large comparable properties permitting pressureless storage at ambient temperature and release at intermediate temperatures. For decades now the two materials have been subjected worldwide to rather extensive testing with hydrogen, deuterium, and relevant amounts of tritium and most pertinent properties required for a decision are now sufficiently known. After careful examination of all available data, zirconium cobalt was chosen as reference material with uranium as back-up. This decision has currently been reverted at ITER.

The most important properties that constituted the basis for the decision are discussed and summarized below.

Salient features of **zirconium cobalt** [Dev90; Pen90] are i) low dissociation pressure at ambient temperature, ii) release of tritium at moderate temperatures, iii) good compatibility with structural materials at elevated temperature, iv) low pyrophoricity (possibly due to the larger size of activated ZrCo particles in comparison to the typical 1 µm grain size of uranium powder),

v) comparatively small volume expansion upon tritium uptake, vi) commercial availability and vii) a comprehensive data base. Of overriding importance for the decision of recommending zirconium cobalt was that this intermetallic compound, unlike uranium, is not subjected to national or international control of any kind. Concerns with this getter arise from the lack of flat tritium pressure/composition plateaus and the tendency to disproportionate at high temperatures and concomitant high pressure of hydrogen. The good news is that disproportionation can be ameliorated significantly by judicious process conduction and already disproportionated material can be completely regenerated by simply baking in situ at moderate temperature under vacuum.

While the construction of ZrCo storage beds for interim storage and transport of large inventories of tritium has been demonstrated with tritium and is by now well documented, that of fast delivery beds of the kind presumably needed for the Storage and Delivery System of ITER is not. This was the incentive for more stringent tests with technical-sized ZrCo getter beds under conditions more closely resembling those relevant for ITER [Lae01b; Hay07a; Bel08b]. Within this frame, the design of "conventional" storage beds was modified aiming at improving the release rates of deuterium and tritium up to values approaching those stipulated for ITER. At TLK a new tritium storage bed was designed, manufactured and tested having the following special characteristics: i) storage bed compactness, ii) throughout optimized heat transport, iii) optimized sinter filter configuration to improve gas conduction, v) upgraded overall insulation, vi) sufficient heating power, etc. [Lae01b; Lae03a]. Even though these measures contributed to improve the rate of hydrogen delivery, the enhancements were far from meeting expectations [Bel08b]. Therefore, complementary work is indispensable. One more drawback that emerged from these experiments was the high tritium heel remaining in ZrCo getter even after extensive heating at 750 K while pumping with a dedicated pumping system[17]. In view that pumping is also needed to recover from disproportionation, it was concluded that a committed pumping system will be necessary for the ITER Storage and Delivery System. This will be associated with increased costs and a design of higher complexity.

Physical chemical and chemical properties of the **tritium/uranium system** are rather well known. What is more, there is a vast body of experience accumulated in numerous and diverse

[17] It should be noted that 750 K is about the highest design temperature of conventional storage beds. The heel will therefore have to be extracted by high temperature isotopic exchange with protium or deuterium.

facilities worldwide on handling of tritium using uranium beds on which to base the design of the Storage and Delivery System for ITER.

Favourable properties of uranium are [Wic62; Nor75]: i) extremely small dissociation pressure of the tritide at ambient temperature, ii) liberation of tritium from uranium tritide at moderate temperature, iii) no concern about disproportionation, iv) extremely flat pressure/composition isotherms over a broad composition range and v) thermal release of tritium from uranium tritide at 750 K is fast and quantitative without the aid of pumps. The capability of highly safe trapping and fast release of tritium by uranium within a comparatively small temperature span is considered an important advantage. In spite of the high pyrophoricity of uranium, it appears possible to cope with this problem by appropriate construction measures. Largest concern with uranium is the restricted handling of this material. Because possession, usage and transport of uranium underlies strict international control, handling is only permitted in licensed installations.

2.11.9 Encapsulation of hydrogen in molecular sieves

Fraenkel and Shabtai [Fra77] encapsulated molecular hydrogen in type NaA, KA, RbA and CsA zeolite. Zeolites were heated up to temperatures in the range 573 - 673 K and loaded with hydrogen at pressures of up to 9.2×10^7 Pa. Prior to loading, the specimens were freshly activated by thorough outgassing. After completion of loading the zeolite specimens were quenched at 298 K, the pressure relieved, and thereafter evacuated to remove adsorbed gas. In case of type NaA zeolite, the encapsulation takes place only in β-cavities (17 % of the total void volume) because the apertures of the α-cavity are larger than the kinetic diameter of molecular hydrogen (see Fig. 3.41). When, however, Na cations are replaced by larger cations like K^+, Cs^+ or Rb^+ encapsulation also becomes possible in the large α-cavities. Accordingly, high encapsulation yields were observed in type KA, RbA and type NaA zeolite containing 2.5 Cs^+ cations per unit cell. Regretably large cations have a large own volume, which reduces the void space of the α-cavity. Therefore, progressively increasing the number of Cs^+ ions in the unit cell from zero up to 2.5 Cs^+ ions first causes an abrupt increase in loading that gradually becomes smaller again as the number of Cs^+ cations is further increased. Hydrogen loading in type NaA containing 2.5 Cs^+ cations was found to be $2.2 \times 10^{-3}\, g_{H_2}\, g^{-1}_{Zeolite}$ when the zeolite was exposed to a hydrogen pressure of 920 bar for 15 min[18]. The obtained encapsulate was stable up to a temperature of

[18] Assumed zeolite density $\sim 2\,g\,cm^{-3}$ [Bre74].

513 K. For comparison, a hydrogen loading of $2 \times 10^{-3}\, g_{H_2}\, g^{-1}_{Zeolite}$ was achieved in the sodalite cages of NaX zeolite at 410 K and 1 bar hydrogen [Efs90].

A comprehensive review on storage options for hydrogen isotopologues in materials like zeolites, clathrate or nano tubes manufactured from carbon or boron nitride, is provided in a paper by van den Berg and Areán [Ber08].

2.12 Interaction of tritium with selected organic and inorganic materials commonly used in tritium handling facilities

In this section the physical-chemical and chemical properties of organic materials frequently encountered in tritium facilities are discussed from the perspective of their interactions with tritium. They include i) elastomers used for gaskets, membranes, insulation or gloves, ii) organic construction materials installed in tritium-handling facilities, iii) organic materials utilized inside of glove boxes and iii) diverse paints of the kind applied to protect concrete and structural materials.

2.12.1 Interaction of molecular tritium or tritiated water with polymers

2.12.1.1 General remarks

Pumps, valves, flow meters, etc. used in commercial high vacuum equipment are often furnished with different kinds of polymers for sealing, gas conduction or other special purposes. Polymers are also encountered in instrumentation used for the analysis of gases, e.g. gas chromatographs, optical spectrometers, etc. In principle, when this kind of equipment is installed in glove boxes destined to tritium handling, all polymeric gaskets and tubing that may come in direct contact with tritium should be replaced by metallic seals and tubing. Polymeric elastomers should only be tolerated when no metallic alternatives are available and/or the expected concentrations of tritium are very low. This is for instance the case in primary confinements, such as glove boxes or tritium retention systems servicing glove boxes. Nonetheless, possible direct permeation of tritium across polymers, e.g. gloves, into ambient needs to be contemplated from a safety point of view. As well known, permeation of molecular tritium or tritiated water through elastomers can take place with appreciable rate even at ambient temperature. In general and as opposed to

metals, tritiated water, i.e. T_2O or HTO, permeates more readily across organic materials (and skin) than molecular tritium, i.e. T_2, DT or HT.

Polymers are also used as insulation material of electrical cables belonging to the instrumentation installed in glove boxes. Though there is usually no concern about the resistance of these polymers to the low concentrations of tritium prevailing in glove boxes - even for extended periods of time - they constitute a source of delayed release once they have incorporated tritium via permeation and isotopic exchange. Delayed release from these polymers may retard significantly the decontamination rate of a glove box.

The **degradation of polymers** exposed to tritium has been widely investigated by numerous researchers. Radiation-induced property changes of polymeric material manifest as i) softening (degradation) or hardening, ii) embrittlement, iii) ductility loss, iv) colour change, v) dimensional change and vi) gas evolution. Some of the more egregious products generated during the degradation of halogenated polymers are gaseous hydrogen chloride and hydrogen fluoride. They can be highly corrosive for many metals (pit corrosion) especially in the presence of water vapour.

While beta rays may penetrate directly into the bulk of polymers, their degree of penetration is dependent on the type of material. In most cases, penetration of radiation will be less than one tenth of a mm. However, because molecular tritium and tritiated water can diffuse into the polymer bulk and accumulate there to a degree that is governed by temperature and solubility, radiation damage which usually commences on the polymer surface will gradually progress towards inner regions. Diffusing tritium atoms may be incorporated firmly into polymer molecules via radiochemical reactions or exchange reactions with bonded hydrogen atoms. Beta-radiation emitted by tritium atoms dissolved or integrated into polymer chains is close enough to the surrounding material to cause bond breaking and hence polymer degradation.

Recapitulating, despite of the rather low energy of tritium beta rays and their small range of penetration, the degradation of polymers will not be limited to the surface region but will also manifest deep in the bulk because of tritium permeation.

Inert additives like glass or graphite may improve the overall radiation-resistance of polymers, but they will not modify the radiation resistance of the polymeric material itself. What is more, it cannot be ruled out that inert additives incorporated into the bulk of polymers be released into ambient leading to dispersion of radioactive particulate matter of undefined chemical composition.

Antioxidants have also been shown to improve the radiation resistance of polymers, but here again the potential of unwanted side effects cannot *a priori* be ruled out [Sha07].

In general, when the application of polymers in tritium handling equipment or other systems is unavoidable, the following facts should be taken into account for material selection: i) polymers that harden should be preferred over those that soften, ii) partial pressures of tritium and exposure time to the gas should at all times be maintained at a minimum, iii) the resistance of polymers towards radiation can be improved by protection from oxygen, air and moisture [Iwa15], iv) high operation temperatures should be avoided as temperatures exceeding 373 K tend to accentuate radiation-induced molecular damage, v) in case of foreseeable need for component replacements, provisions to allow their easy access, manipulation and substitution should be taken and vi) polymers impregnated with diffused tritium may display considerable gas evolution resulting from desorption or delayed radiolysis reactions.

2.12.1.2 Properties of single polymers and their potential for application in tritium systems

2.12.1.2.1 General remarks

A number of commercial valves, equipment and instrumentation installed in tritium handling facilities containing polymers and/or elastomers have been tested in tritium service sometimes for a number of years. Additionally, single components have been examined worldwide in dedicated experiments under conditions designed to simulate those anticipated in future applications [Voo70; Dou81a; Zap82; Hem89a; Dic92]. From these activities, a vast body of data on the interaction of radioactive gases, including tritium, with many polymers and elastomers has accumulated [Hen66; Cra68; Cra75]. The properties of several polymers commonly used in a tritium environment have been reviewed recently by Fox et al. [Fox17].

The radiation resistance of polymers has frequently been investigated employing a cobalt-60 source because γ-rays are photons without mass or charge that can penetrate relatively deep into matter before being absorbed. Hence, even though gamma rays generate less ionization than beta rays, they may by virtue of their greater penetration power, cause significant damage much beyond the surface. The relative radiation resistance of a number of common polymers is tabulated in Appendix E (data supplied to Technische Dichtungssysteme GmbH, Frankfurt/M, Germany, by CEA). As already discussed, the small penetration of beta rays emitted by tritium

is counteracted by diffusion of tritium atoms deep into the bulk of organic materials. Beta rays emitted profoundly in polymeric matter can interact directly with molecular bonds causing degradation of the solid. Complementary information on the effect of irradiation obtained from compression tests is provided at the end of this chapter [Zap82]. Recapitulating, there is now a vast body of results and experience on which to base the selection of equipment with incorporated polymers. To achieve a tolerable safety standard the so called "veritable tritium compatibility" is sometimes used. This compatibility level is determined by the highest prevailing tritium level and other factors such as temperature, duration of contact, presence of additional reactive impurities, pH, co-existing mechanical stress, type of material(s), area of exposure, etc.

2.12.1.2.2 Assessment of single elastomers

Some of the experience gained worldwide with frequently utilized hard and elastomeric polymers exposed purposely or operationally to molecular tritium or tritiated water in a number of laboratories is succinctly summarized below.

Vespel® is a polyimide polymer used as stem tip of normal or automatic valves. The chemical formula of Vespel® is depicted in Fig. 2.30. Clark and Shanahan [Cla07] exposed specimens of this material to 10^5 Pa of pure gaseous tritium for periods between three months and up to 2.3 years. The effect of radiation was investigated by dynamic mechanical analysis and a characterization of the gas phase, i.e. change in total pressure and determination of the composition of the radiolysis products. According to their observations prolonged exposure had neither an effect on the total gas pressure nor on the dynamic modulus [Cla11]. The occurrence of significant interaction between gaseous tritium and Vespel® only became apparent by a large increase of the protium concentration in the supernatant gaseous tritium in the container, i.e. up to 50 %. In comparison to ultra-high molecular weight polyethylene (UHMWPE) Vespel® was found to possess the higher resistance towards exposure to tritium.

Valves fitted with Vespel® stem tips have been installed throughout the Active Gas Handling System of JET. After cycling tests of more than 5×10^4 cycles they displayed no detectable leak across the valve seat [Hem89a]. It was concluded that Vespel® is a highly radiation-resistant (up to 10^7 Gy), greatly heat resistant and resilient organic material that can be utilized incessantly for a prolonged period of time provided the temperature does not exceed 473 K [Hem89a].

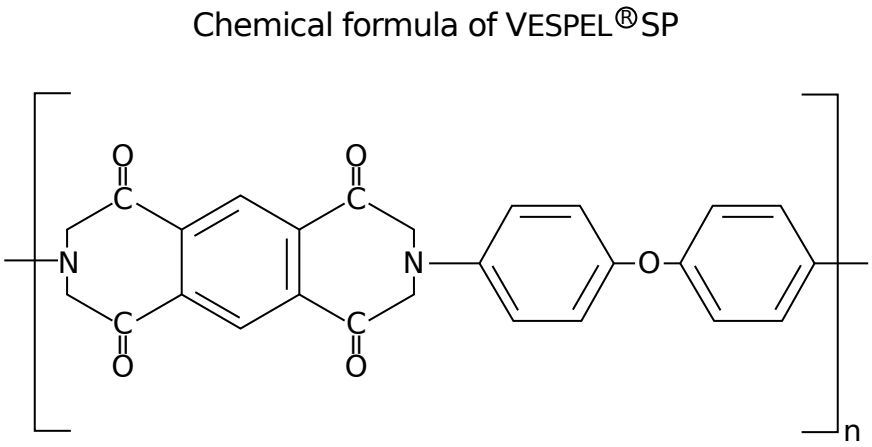


Figure 2.30: Monomer of Vespel® [Sha07].

Hollow-filament **polyimide** membranes were proposed by Hayashi et al. [Hay95b] for the development of a compact and cost-effective system for the extraction of tritium from air or nitrogen atmosphere. Criteria for the selection of a polyimide separation membrane were i) much higher permeability of water and hydrogen than that of nitrogen or air and ii) a reported good resistance towards degradation by tritium. Within the frame of parametric studies, it was shown that i) the H_2/N_2 permeation coefficient ratio is higher than 160, ii) the HTO/HT permeation coefficient ratio is about 100 and iii) low permeate/feed ratios (low permeate pressures achieved with an efficient pump) significantly contribute to improve the recovery of tritium. Under the latter conditions the recovery of HT and HTO became comparable.

Ultra-high molecular weight polyethylene (UHMW-PE) is utilized as stem tip in commercial Swagelok valves. The polymer displays low friction coefficient, is abrasion resistant and possess uniquely high toughness. After exposure to 10^5 Pa of pure gaseous tritium for 570 d a significant increase in total pressure was observed [Cla07]. When subjected to extended contact with tritium UHMWPE became brittle, dark and shrinked [Sha07]. After about 2 years the pressure increased about nine-fold, the majority of the produced gas being protium [Cla11]. This was attributed to radiation-induced cross-linking followed by an overall polymer degradation with liberation of molecular hydrogen. Additionally, the frequency dependence of the dynamical properties was drastically reduced. It was concluded that UHMWPE can only be considered acceptable for applications in which tritium is present at very low partial pressures.

Low density polyethylene (LDPE) ($0.92\,\mathrm{g\,cm^{-3}}$) and **high-density polyethylene (HDPE)** ($0.95\,\mathrm{g\,cm^{-3}}$) without additives were exposed for up to 73 hours to pure molecular tritium (up to 10^6 Pa) at 296 K and 352 K by Ema and Izumi [Ema02]. The results revealed slightly higher uptake by the low-density polymer. The degree of tritium incorporation was nearly proportional to the time of exposure. Tritium incorporation was further enhanced by increasing the temperature. Additives like biphenyl or benzophenone, known to stabilize polymers, showed no discernible effect on uptake. Tritium induced cross-linking and cracking. In a tritium environment both polymers became brittle. Hence, they do not appear to be promising for tritium applications.

Polypropylene is a hydrophobic material often used for packaging of radioactive materials. The permeability of tritiated water through polypropylene was found to be 1.5×10^{-12} STP $\mathrm{cm^3 cm/cm^2/s/Pa}$ at 296 K [Tog11]. Values of the same order of magnitude were reported by Metz et al. [Met05] or Sangaj and Malshe [San04]. Under ambient conditions the solubility of water in polypropylene was determined to be 6×10^{-5} STP $\mathrm{cm^3/cm^3/Pa}$. The experimental results were interpreted with a one-dimensional diffusion model.

Ethylene propylene diene monomer (EPDM) is an elastomer that has been employed successfully in tritium handling facilities because of its comparatively high resistance towards radiation. Experimentally it was shown that the radiation resistance of EPDM is higher than that of butyl rubber. Because of the relatively good performance of this elastomer in tritium service, it has been utilized for low pressure flange gaskets and O-rings.

Polytetrafluoroethylene (PTFE, trade name Teflon) shows considerable degradation in tritium service. When PTFE was exposed to 10^5 Pa of pure gaseous tritium for more than nine months the material became too weak to be handled [Cla07; Cla11]. The total pressure decreased only slightly most probably due to formation of tritiated hydrofluoric acid which condenses on the wall of the container. The change of properties such as storage modulus (instantaneous elastic constant), loss modulus (time-dependent viscoelastic deformation) and storage modulus/loss modulus ratio were obtained from Dynamic Mechanical Analysis (DMA) measurements. The tests showed that the dynamic modulus increased and the frequency dependence as well as the loss module decreased. Since HF may cause pit corrosion of stainless-steel, PTFE is neither acceptable as stem for valves nor as O-ring in tritium applications.

An endurance test of a hydrophobic catalyst-packing mixture was carried out in a liquid phase catalytic exchange (LPCE) column by Cristescu et al. [Cri06]. Hydrophobic properties are conferred to this catalyst by polytetrafluoroethylene. After six months of continuous operation using tritiated water having a specific tritium content of $44.4\,\mathrm{GBq\,kg^{-1}}$ no significant change in separation performance of the column was registered.

Permeation (P) and diffusion (D) of tritiated hydrogen across **Teflon** in the temperature range 347 - 423 K can be estimated from equations [Sto00]

$$P_{\mathrm{HT}} = 8.38 \times 10^{-9} \exp\left(-\frac{16.7}{RT}\right)$$
$$D_{\mathrm{HT}} = 1.39 \times 10^{-7} \exp\left(-\frac{14.9}{RT}\right) ,$$

where the permeation coefficient and diffusion pre-exponential coefficients are in $\mathrm{m^2\,s^{-1}}$ and the activation energies in $\mathrm{kJ\,mol^{-1}}$. More permeation and diffusion equations were reported for Viton, Santoprene, ethylene propylene diene monomer (EPDM), as well as for Noryl.

When surface compliance, high lubricity, non-stick characteristics and/or a low coefficient of friction are necessitated in tritium handling equipment PTFE has been replaced by either UHMW-PE, high density polyethylene or Vespel® [Fox17].

Iwai et al. [Iwa05] examined the resistance of a **tetrafluoroethylene-propylene co-polymer (AFLAS®)** resin rubber gasket towards gamma radiation at doses of up to 500 kGy. This gasket is utilized in solid polymer electrolyte water electrolyzers. Whereas the tensile strength[19] increased with radiation dose the softness remained unchanged up to a dosis of 500 kGy.

Nafion® (Dupont) is a sulfonated tetrafluoroethylene-based fluoropolymer-copolymer with ionic properties that qualifies for selective permeation of water. Because of this special property **Nafion®** finds application in analytical instrumentation and as proton exchange membrane in electrolyzers designed for the processing of tritiated water. The resistance of **Nafion®** towards radiation was recently examined experimentally by several researchers which tested the material either by exposing specimens to an external gamma radiation source [Iwa05; Fox10] or by submerging membranes into liquid tritiated water (intrinsic beta-radiation) [Cri06; Mic08].

Iwai et al. [Iwa05; Iwa08] researched comprehensively the effect of gamma radiation from a cobalt-60 source on a **Nafion®** ion exchange membrane as well as on **FEP** (fluorinated ethylene

[19] Specimens were cut and examined according to Japanese Standards for tensile tests (ASTMD-1822L).

propylene co-polymer) and **PFA** (per fluoro alkoxy ethylene co-polymer) materials[20]. Specimens were submerged in water saturated with oxygen and irradiated with a cobalt-60 gamma source at ambient temperature. It was estimated that 9.2 TBq kg^{-1} of gamma radiation would simulate 2 years[21] of exposure inside of an electrolysis cell. This is equivalent to a dose of 530 kGy. Degradation of the test materials was evaluated with tensile strength measurements, changes of the ion exchange capacity, variation in water uptake, liberation of fluorine, release of ions, etc. With increasing dose the tensile strength of Nafion experienced a marked decrease, i.e. about halved at 500 kGy. The ion exchange capacity, on the other hand, decreased only slightly when exposed to a dose of up to 600 kGy and further when subjected to an even higher dose of 850 kGy. From these observations it was concluded that the side branches of the polymer that end up in hydrophilic sulfonic acid groups are more radiation-resistant than the main polytretrafluroethylene branches. Expectedly, the dependence from radiation dose of the loss of water uptake capacity was found to correlate with the loss of ion exchange capacity. Because the insulators lost their tensile strength at 200 kGy and 300 kGy, respectively, the authors recommended to replace them in the electrolyzer by the polyimide resin Vespel®. The radiation resistance of this material is well documented.

Fox et al. [Fox10] also irradiated **Nafion®** with a ^{60}Co source either under air or submerged in de-ionized water at two dose rates and varying total dosages. According to their observations membrane degradation is strongly dependent on the dose rate as well as on total dose. From infrared measurements it was concluded that with increasing radiation dosages CF=CF bonds are formed and the amplitude of S−O stretching bonds decrease. These findings constitute evidence for defluorination of the polymer and loss of acid groups. They recommended further studies to permit final evaluation of this crucial electrolyzer component of isotope separation systems.

Clark et al. [Cla11] studied the effect of beta and gamma radiation on **Nafion®** after exposure to similar doses of these two types of radiation[22]. Assuming an absorption by the polymer of 3.7×10^{11} Bq cm^{-3} and a density of Nafion® of 2 g cm^{-3} it was possible to calculate the deposition dose, i.e. 16.9 rad s^{-1}. On the basis of such calculations they could compare the effect of both

[20] FEP and PFA are used as insulators in commercial electrolyzers.
[21] According to ITER planning the replacement of electrolysis cells is foreseen every 2 years.
[22] While many studies deal with the effect of either tritium or gamma irradiation on polymers, in only very few investigations has the effect of both irradiations been compared on the same material.

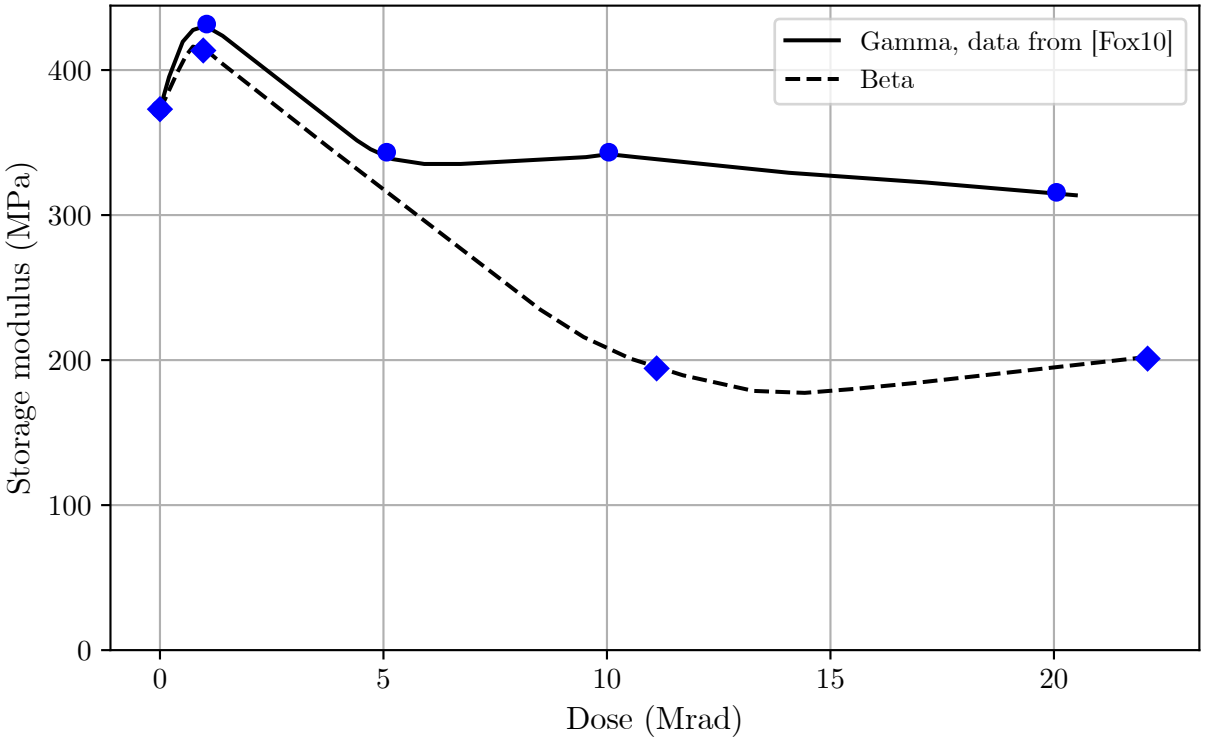


Figure 2.31: Effect of dose on storage modulus of Nafion® films at 333 K after exposure to either gamma radiation from a ^{60}Co source or beta radiation emitted by tritium (after [Cla11]).

irradiations on the storage modulus (elasticity) (see Fig. 2.31). The initial rise in storage modulus was attributed to increasing cross-linking and the subsequent decrease to ruptures of the polymer structure. Within this frame, the decrease in storage modulus induced by exposure to 1 bar tritium was found to be significantly larger than that induced by gamma irradiation. Evidently, beta radiation from tritium sequestered in the film causes more secondary damage to the matrix than gamma radiation which rather penetrates through the film. The lesson learned is, that a comparison of the effect of both forms of radiation on Nafion® films is not trivial.

Cristescu et al. [Cri06; Mic08] operated continuously two stand-alone electrolysis cells both equipped with a **Nafion®** polymer membrane. One cell contained tritiated water of 44.4 GBq kg^{-1} and the other demineralised water. For safety reasons the cell containing tritiated water was operated in close loop mode. To allow recombination of the electrolysis gases a noble metal catalyst was integrated into the loop. The cell containing demineralised water served as reference and was operated under nearly identical conditions. To uncover possible effects of tritium-

radiation on the performance of the cells the period of investigation was extended to about six months. After completion of the experiment, it was observed that the change in tensile strength and elongation of both polymer membranes, i.e. the one tested in the presence of tritiated water and the other one submerged in demineralised water, decreased, the extent of decrease differing only marginally. From this it was inferred that under the conditions of the test tritium will have no major detrimental effects on the performance of the cells. During the course of close loop operation, cations (Al, Ca, Fe, etc.) and anions (chloride, sulphate, fluoride, and phosphate) were released into the water. Most of the release occurred within the first two months of operation.

Michling et al. [Mic08] complemented the research of Cristescu et al. by performing long-term experiments with two industrial electrolyzers equipped with **Nafion®** membranes and two small electrolyzers furnished with **Nafion®117**. Prior to the tests, the industrial electrolyzers were adapted to the requirements of tritium service, i.e. plastic tubing and gaskets were replaced by metallic ones, the size of the buffer vessels was reduced to minimize the inventory of tritium, the integral leak rate was trimmed to less than $10^7\,\mathrm{Pa\,m^3\,s^{-1}}$, etc. The specific tritium activity of water in these electrolyzers was about $0.4\,\mathrm{GBq\,kg^{-1}}$. As practiced by Cristescu, one electrolysis cell contained tritiated water (specific activity $3.7\,\mathrm{GBq\,kg^{-1}}$) and the other demineralised water. The electrolyzers were operated for about one year. After completion of the experiment the cells were disassembled and the Nafion® membranes subjected to close examination. For this purpose they were first decontaminated and then cut into stripes. The reference membrane (exposed to demineralised water) and a pristine membrane were also cut into stripes and thereafter subjected to mechanical tests. When the tensile strength and elongation of Nafion® stripes pre-exposed to tritium were compared with the ones obtained from pristine material a reduction was observed, which is indicative of loss of membrane flexibility. When, however, tritium-exposed stripes were compared with stripes obtained from the reference membrane tested for the same period of time the changes in elongation were non-discernible. The tensile strength, on the other hand, decreased much less in the presence of tritium than in its absence. Both the tritium-exposed and the reference Nafion® showed reduced swelling in water. A scanning electron microscope investigation provided no evidence for tritium-induced surface modification of the membrane. Comparison between the chemical composition of the water before and after 12 month of testing showed significant differences and, as evidenced by the presence of iron, nickel and chromium ions, occurrence of structural stainless-steel corrosion induced by tritium and halogens. On the

whole, the two investigations arrived at a similar conclusion: the degradation in performance of the electrolyzers remained tolerable, in spite of prolonged operation with tritium.

Perfluoroalkoxyethylene co-polymer (PFA) and **fluorinated ethylene propylene co-polymer (FEP)** are used as electric insulators of electrolyzers integrated into water detritiation systems. PFA and FEP were irradiated with a cobalt-60 gamma source and found to lose their firmness at radiation levels of 200 kGy and 300 kGy, respectively [Iwa05]. Iwai et al. therefore recommended to replace PFA or FEP by polyimide resin Vespel®) insulators [Iwa05; Iwa08].

Viton A® is a fluorinated material used in vacuum technology for instance for the manufacture of O-rings. The maximum operating temperature of Viton A is 473 K [Wen77]. Viton® used in tritium service progressively undergoes embrittlement. Good experience with this material has only been achieved when prevailing radiation levels are very low. Kherani and Shmayda [Khe92a] determined the permeability, diffusivity, and solubility of hydrogen in Viton within the temperature range 336 - 402 K. The obtained results are summarized by the following equations

$$P = 2.7 \times 10^{-4} \exp\left(-\frac{5900}{T}\right) \text{ m}^2\,\text{s}^{-1}$$
$$D = 1.2 \times 10^{-5} \exp\left(-\frac{3300}{T}\right) \text{ m}^2\,\text{s}^{-1}$$
$$S = 2.1 \times 10^{1} \exp\left(-\frac{2600}{T}\right) \text{ (atm cm}^3\text{ (STP)cm}^{-3}\text{ atm}^{-1}\text{)}$$

where T is given in Kelvin. The hydrogen permeability at 293.15 K, P_{293}, obtained from the above equation, i.e. $5 \times 10^{-13}\,\text{m}^2\,\text{s}^{-1}$, agrees moderately well with that given in the literature, i.e. $3.5 \times 10^{-12}\,\text{m}^2\,\text{s}^{-1}$ [Hol74].

Polychloro trifluoro ethylene (Kel-F) degrades by exposure to tritium gas and is therefore not recommended for tritium-handling equipment. Numerous Kel-F flap valves installed in a detritiation plant leaked in flow direction after several years in tritium service [Pau88]. Following extended operation with tritium the flaps were 30 % destroyed and KelF had become transparent. What is more, valves exposed to tritium showed pit corrosion in the vicinity of the seat (probably caused by hydrogen fluoride).

2.12.1.3 More results on the resistance of polymeric elastomer materials towards tritium

Elastomers are polymers characterized by good viscous (ability to flow) and elastic (ability to stretch and return back) properties. Among the known elastomers, **butyl rubber** (used for gloves of glove boxes) and **ethylene propylene diene monomer (EPDM)** (used for O-rings and gaskets) have found ample application in tritium service [Fox17]. When the resistance towards tritium of butyl rubber was compared with that of Buna-N (nitrile rubber) the properties of the first were found to be superior. The degree of radiation damage experienced by a number of elastomeric materials with potential for application in tritium service was investigated by techniques such as i) off-gas measurements, ii) mass spectrometric analysis of the radiolysis products, iii) infrared spectroscopy, iv) tritium absorption kinetics, and v) autoradiography measurements [Zap82]. For the quantitative evaluation of the radiation resistance of the polymers itemized in Table 2.32 cylindrical specimens of **ethylene-propylene rubber, Viton B® V494-70**, and seven other elastomeric materials were exposed to gaseous tritium containing 7 % deuterium at a pressure of 83 kPa for more than 125 d. Control specimens were stored under air at ambient temperature for the same period of time. Subsequently, they were subjected to a standard test method (**compression set test**) recommended by the American Society for Testing and Materials (ASTM) [AST68]. According to this test, when compressive displacement is applied to a specimen, the compression set is defined as the percentage not recovered after 30 min following removal of the compression load. The degree to which an elastomer is permanently deformed will depend upon the type of elastomer, temperature, time, and interactions with chemicals or radiation. The difference between the final dimensions of the tritium-exposed elastomer after the load is released and the dimensions of the original compressed O-ring kept under air (both submitted to prolonged mechanical pressure) is defined as the **compression set**. The determined total compression set values are displayed in Table 2.32 in increasing order. A compression set of 75 % or more under the test conditions was considered to be an inadequate seal material.

According to another evaluation technique employed by Zapp [Zap82], the progress of the radiation-induced degradation was obtained from tritium off-gassing carried out in a flow system equipped with an appropriate tritium monitor, e.g. Kanne monitor. A mass spectrometric

Table 2.32: Tritium tests of elastomers exposed to 93 % tritium (balance deuterium and helium) for more than 4 month at ambient temperature (after [Zap82]).

Elastomer	Total Compression %	Radiation induced compression Set %	Tritium off gassing rate $cm^3(STP)/s$
Ethylene propylene rubber	52	44	3.6×10^{-7}
Styrene butadiene	75	68	9.1×10^{-7}
Kalrez® 1018	83	34	1.1×10^{-6}
Viton® B V494-70	88	42	1.1×10^{-6}
Viton® E60C V747	93	69	2.0×10^{-6}
Ethylene acrylic A936-70	93	77	3.9×10^{-6}
Nitrile N741-75	97	90	1.4×10^{-6}
Urethane P642-70	98	77	1.4×10^{-5}
Silicone S604-70	99	90	1.2×10^{-5}

analysis of the supernatant gases provided indirectly the amount of tritium incorporated into the specimens and the amount of protium concomitantly released into the gas phase.

In brief, all elastomers tested by Zapp displayed significant radiation damage, some becoming hard and brittle. The results are indicative of rather high radiation-induced compression set and reveal substantial off-gassing rates of tritium (see Table 2.32). Tritium outgassing measurements provided a relative indication of the solubility of tritium in the elastomers and thus of the experienced radiation dose. The solution of tritium in the bulk of elastomers was substantial. Of nine elastomers tested, i.e. ethylene propylene, styrene butadiene, VitonA® , Kalrez®.

Talcott et al. [Tal93] subjected 18 valves sealed with elastomer O-rings consisting either of **Viton A®**, **Buna-N** or **ethylene propylene diene monomer (EPDM)** to tritium pressures of either 1.33, 53.3 or 533 mbar. The initial leak rates for hydrogen of all valves were below $10^{-5}\,cm^3(STP)/s$. The valves were opened and closed 1100 times during 11 d while under constant exposure to tritium. In subsequent experiments this type of cycle was sustained for all valves over a total period lasting about 200 d. After completion of cycling a leak test was performed. The leak rates, determined after cycling in the presence of 53.3 mbar tritium, are plotted as function of time from the first exposure to tritium in Fig. 2.32. As evident, best performance in

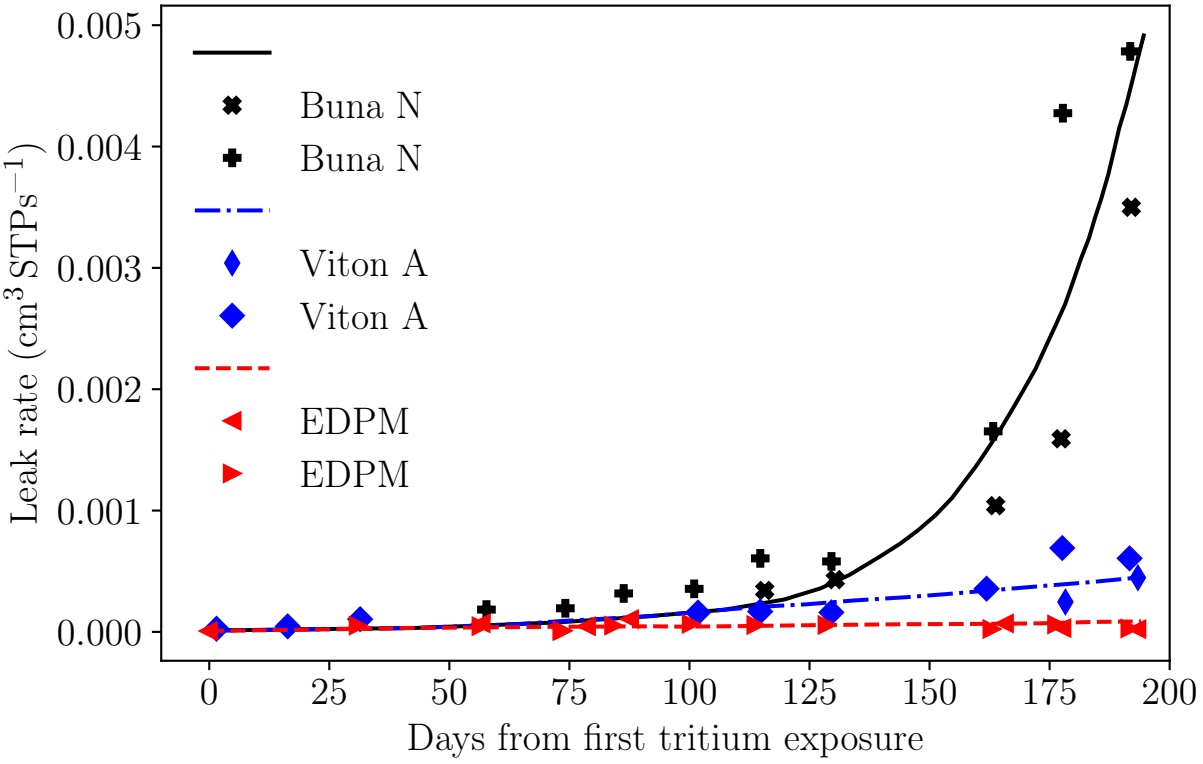


Figure 2.32: Leak rate across valves furnished with O-rings of either Buna N, Viton A, or EDPM exposed to 53.3 mbar tritium as function of time (after [Tal93]). Two specimens of each elastomere were used for the runs.

a tritium environment is displayed by **EDPM** and poorest by **Buna N**. The results show good reproducibility. They provide evidence that frequent cycling in the presence of gaseous tritium markedly decreases the lifetime of elastomers. Only the EDPM O-rings retained their physical integrity for the duration of the tests.

2.12.1.4 Effect of fillers on the radiation resistance of polymers

Clark et al. [Cla08; Cla11] exposed samples consisting of four preparations comprising the **EPDM elastomers Nordel® 1440** or **Royalene® 580H**, each either with or without carbon black filler, in closed stainless-steel containers to initially one atmosphere of tritium gas at ambient temperature for a period lasting more than one year (see Fig. 2.33). The interaction with tritium conducted to the formation of HT and to a lesser extent to H_2, DTO and CT_4. Initially, dynamic mechanical analysis revealed no change of glass transition temperature and no variation of glass transition temperature with polymer grade or the presence of filler. After about

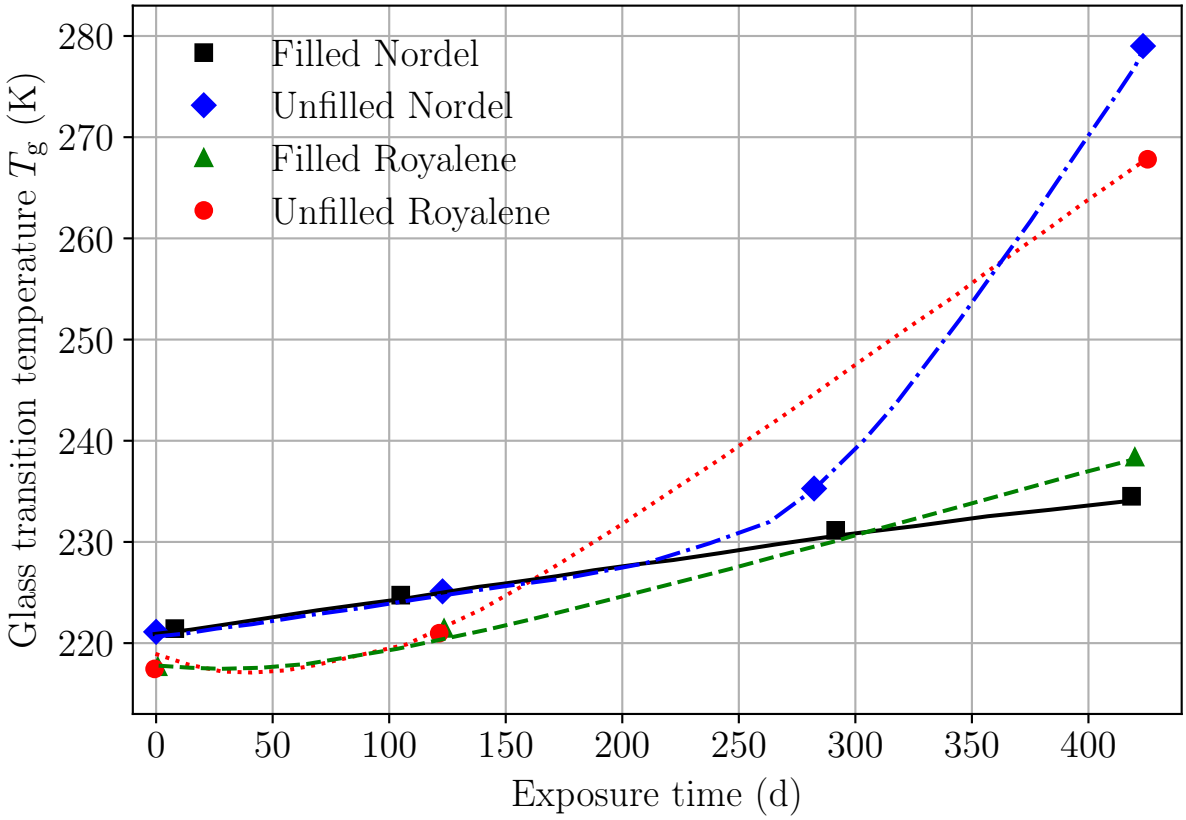


Figure 2.33: Evolution of the glass transition temperature, T_g, of elastomers expressed in Kelvin with time of exposure to 10^5 Pa gaseous tritium. Tests were carried out with four ethylene propylene diene monomer (EPDM) elastomers of which only two contained carbon black filler (after [Cla11]).

half a year of exposure to tritium the **glass transition temperature** (T_g)[23] of the samples without filler increased significantly (see Fig. 2.33). What is more, following the same period of time all samples displayed brittleness during a bend test. As evident from the experimental results, carbon black filler can mitigate the radiation-induced degradation of elastomers [Cla11].

2.12.1.5 Glove materials

Diffusivities, solubility's and permeability's of HTO vapour at (312 ± 1) K through elastomeric polymers frequently employed for the manufacture of gloves attached to glove boxes have been reported by Doughty et al. [Dou81b; Dou81a]. Their results are compiled in Table 2.33. As apparent, while the diffusion coefficients vary only by a factor of three, the differences in solubility

[23] T_g is the temperature below which the physical properties of a plastic change in a manner similar to that of a crystalline state and above which plastics behave like rubbery materials.

Table 2.33: Diffusivity, solubility and permeability of water vapour across glove materials at (312 ± 1) K [Dou81b; Dou81a].

Material	Thickness	Temp.	RH	D	S	P
	mm	K	%	$\mathrm{cm^2\,s^{-1}}$	$\frac{\mathrm{STP\,cm^3}}{\mathrm{cm^3\,Pa}}$	$\frac{\mathrm{STP\,cm^3 cm}}{\mathrm{cm^2\,s\,Pa}}$
Butyl rubber, glove	0.51	312	78	3.3×10^{-9}	0.0034	6.67×10^{-12}
Butyl rubber, Norton Co.	0.51	313	84	3.1×10^{-9}	0.0023	5.15×10^{-12}
Neoprene	0.48	312	83	3.2×10^{-9}	0.035	1.25×10^{-10}
Hypalon	0.43	311	80	9.0×10^{-9}	0.0097	8.76×10^{-11}
EPDM butyl rubber, laminated glove	0.89	310	69	5.1×10^{-9}	0.00085	5.66×10^{-12}
Hypalon/Neoprene, laminated sample	0.89	311	65	6.2×10^{-9}	0.023	8.83×10^{-11}

RH = relative humidity

and therefore in permeability are much more pronounced, i.e. up to a factor of 40. Because radiation damage takes place in the vicinity of tritium atoms, the extent of tritium damage depends strongly on the solubility of tritium and its tendency to undergo isotopic exchange.

More diffusivity, solubility and permeability constants for HT and HTO through rubber materials of the kind used for gloves as well as for protective suits have been compiled in Table 2.34. Permeation coefficients through butyl rubber were found to be largely insensitive to variations in relative humidity. For additional technical information on such properties as dynamic mechanical analysis, puncture testing, thermogravimetric analysis, tensile properties, etc. the report of Korinko and Breakiron [Kor13] should be consulted.

Two of the elastomer materials most frequently employed for the manufacture of gloves attached to glove boxes in tritium service are discussed in more detail below:

Butyl rubber is an elastomer characterized by low permeation rates for gaseous molecular tritium and tritium water vapour. This property, which is propitious for radiation protection, constitutes the main reason for recommending this material for the manufacture of gloves mounted on glove boxes. Beneficial is likewise that butyl rubber resists swelling and the attack by many solvents or oxidizing chemicals. Conversely, it is not particularly resistant to damage by radiation.

Here, however, the presumption holds that gloves will only be confronted with rather low levels of tritium [Dou81b; Dou81a].

Neoprene, also known as polychloroprene, is another material habitually employed for the manufacture of gloves for glove boxes and for gaskets to seal windows onto glove boxes. The elastomer offers high tensile strength and flexibility and is ideal for work which requires good sensitivity and dexterity. Neoprene should not be used for long-term contact with high concentrations of tritium because corrosive tritiated hydrochloric acid is one of the degradation products. In addition, incorporation of tritium into Neoprene via exchange with loosely bound elastomeric hydrogen has been noticed. For values of HT and HTO permeability constants refer to Tables 2.33 and 2.34. Neoprene gloves can be strengthened by an outer film of Hypalon. **Hypalon** is used because of its resistance towards ozone, oxidizing chemicals, and against abrasion.

Table 2.34: Permeability constants of HT and HTO through rubbers.

Polymeric material	HT $\frac{\text{STP cm}^3\,\text{cm}}{\text{cm s Pa}}$	HTO	Reference
Neoprene[a]	-	12.1×10^{-12}	[Dou81b]
Polypropylene	-	15×10^{-12}	[Tog11]
Latex	3.5×10^{-12} (H_2)	-	[Ste75][f]
Latex	3.0×10^{-12} (D_2)	-	[Ste75]
Latex	2.9×10^{-12} (T_2)	-	[Ste75]
Buna N (nitraded butadiene gum)	0.55×10^{-12} (D_2)	-	[Ste75]
Buna N	0.44×10^{-12} (T_2)		[Ste75]
Kapton (Polyimide)	0.13×10^{-12} (H_2)	-	[Ste75]
Kapton	0.13×10^{-12} (D_2)	-	[Ste75]
Kapton	0.18×10^{-12} (T_2)	-	[Ste75]
Mylar (polyethylene tera phtalate)	0.04×10^{-12} (H_2)	-	[Ste75]
Mylar	0.04×10^{-12} (D_2)	-	[Ste75]
Saran (vinyliden chloride)	0.36×10^{-12} (H_2)	-	[Ste75]
Saran	0.23×10^{-12} (D_2)	-	[Ste75]
Butyl rubber[b]	-	9.0×10^{-12}	[Rog72]
Butyl rubber[c]	-	8.0×10^{-12}	[Yas75]
Butyl rubber[d]	-	5.0×10^{-12}	[Kas74]/[Dou81b]
Butyl rubber[e]	-	6.0×10^{-12}	[Dou81b]

[a] RH 83 % and 312 K, [b] RH 90 % and 303 K, [c] RH 0 - 90 % and 310.5 K, [d] RH 66 % and 309 K, and [e] RH 80 % and 312 K, and[f] all measurements in [Ste75] performed at approx.298 K

RH = relative humidity

2.12.2 Interaction of tritiated water with organic construction materials employed in areas of restricted access

Kobayashi et al. [Kob07a] exposed in a semi-empirical study acrylic resin, butyl rubber and epoxy paint to tritiated water vapour for one day and determined desorption rates at ambient temperature under different experimental conditions. Specimens were loaded in closed loop tests and decontaminated in once-through mode sweeping either with dry nitrogen or nitrogen

containing 60 - 7000 ppm moisture. Desorption rates from the three materials did not differ markedly. Moisture was found to enhance significantly the release rate of tritium.

Ono et al. [Ono92b] determined the amount of tritiated water sorbed by neoprene rubber, linoleum and acrylic resin from a wet purge gas at a constant temperature of 303 K during a period of two hours (see Table 2.35). The experiments were carried out in a 1.5 l chamber, whose inner wall was gold-plated to minimize water adsorption. The concentration of tritium on the surface at constant partial pressure of moisture showed proportionality to the concentration of tritium in the supernatant gas. The adsorption coefficient was found to increase slightly with contact time. This was attributed to bulk penetration or trapping by sites of higher activation energy. Sorption coefficients were defined as the ratio of the equilibrium amount adsorbed, S_0, divided by the amount of HTO dissolved in the material, C_0. Adsorption coefficients increased in the order acryl resin, linoleum and neoprene rubber, all being up to two orders of magnitude smaller than the coefficient for cement. Values of the adsorption coefficients obtained for the examined organic materials were similar to those measured for paints. Desorption rate constants of HTO from linoleum, rubber or acryl resin, on the other hand, were slower by about an order of magnitude than those from silicone paint or epoxy paint.

Dickson and Miller [Dic92] as well as Ono et al. [Ono92b] investigated the adsorption of HT and HTO on such polymeric construction materials as vinyl floor tile, linoleum, and Arborite (a composite material manufactured in Canada with properties comparable to those of Formica). In accordance with expectations, the adsorption of HTO on these materials was substantially higher than on metals.

Table 2.35: Comparison of sorption coefficients of water on organic construction materials, common paints and cement (after [Ono92b]).

Material	Temperature	Total concentration C_0	Adsorption coefficient S_0/C_0	Vapour pressure	Reference
	K	$Bq\,cm^{-3}$	cm	Pa	
Linoleum	303	276	3.3	866	[Ono92b]
Neoprene rubber	303	271	5.9	866	[Ono92b]
Acrylic resin	303	278	1.2	866	[Ono92b]
Cement	303	43	180	866	[Ono92b]
Epoxy paint	303	284	9.7	866	[Ono92b]
Silicon paint	303	45	4.3	866	[Ono92a]
Epoxy paint	303	44	3.0	866	[Ono92a]
Vinyl floor tile	296	1.1×10^5	0.63	547	[Dic92]

C_0 = total tritium concentration in the material

S_0 = adsorbed HTO

2.12.2.1 Interaction of tritiated water with paints

Under certain circumstances it can be beneficial to design a tritium handling facility with walls capable of efficiently absorbing and retaining tritium. This is for instance the case when no tritium removal system is available and hermetic isolation of the facility from the environment is possible. Under these conditions, in the event of an accidental release of tritium, effective retention by the walls can contribute significantly to ameliorate releases into the environment [Num92].

Conversely, when an emergency clean-up system services a facility and hermetical sealing is not possible, walls that retain little tritium are preferable. Reduction of bleeding from the walls during clean-up may contribute significantly to reduce the time needed for the decontamination of the atmosphere of the facility. To provide a data base, the diffusivity, solubility and permeability at ambient temperature of tritiated water in several paints commonly employed in tritium installations have been investigated systematically by a number of researchers. Some of their results are compiled and compared in Table 2.36.

Table 2.36: Diffusivities, solubilities and permeabilities of tritiated water of various paints at ambient temperature.

Paint	Diffusivity $cm^2\,s^{-1}$	Solubility cm^3/cm^3 paint	Permeability $cm^3\,cm\,cm^{-2}\,s^{-1}$	Reference
Silikaluc N° 100 (silicon)	3.1×10^{-9}	2.9×10^{3}	9.0×10^{-6}	[Ono92a]
Epicon RF Topcort (epoxy)	8.4×10^{-10}	2.0×10^{3}	1.7×10^{-6}	[Ono92a]
Fluorex (fluorine)	4.5×10^{-9}	7.8×10^{2}	3.5×10^{-6}	[Ono92a]
Epoxi resin	3×10^{-11}	-	-	[Eda12]
Glid-Guard (epoxy)	3.3×10^{-10}	1.4×10^{4}	5.2×10^{-6}	[Bra85]
Carboline (epoxy)	5.9×10^{-10}	1.4×10^{4}	8.1×10^{-6}	[Bra85]
Vinyl	7.7×10^{-11}	8.1×10^{4}	6.2×10^{-6}	[Bra85]
Interthane (urethane)	3.9×10^{-10}	1.2×10^{4}	4.5×10^{-6}	[Bra85]
TFTR (acrylic-based)	4×10^{-9}	7.4×10^{2}	3.0×10^{-6}	[Hol95]
Aquapon (water-based)	1×10^{-10}	1.1×10^{3}	1.1×10^{-7}	[Hol95]

Ono et al. [Ono92a] investigated the sorption and de-sorption of tritiated water by acryl-, silicone-, epoxy-, and fluorine-based paints (thickness layer approx. 50 µm) applied on a stainless-steel plate (see also previous section). Additionally, the permeability, solubility and diffusivity of tritiated water was determined using films or membranes (thickness 45 - 220 µm) of these paints suspended in a thermostatized stainless-steel chamber. In spite of comparatively high residual tritium in protecting epoxy coatings of high pigment/binder ratio they concluded that this covering is the most adequate for protecting concrete in tritium-handling facilities. Their recommendation was mostly based on the fact that epoxy paints show the lowest permeability for gaseous and liquid tritiated water.

Edao et al. [Eda12; Eda15] covered concrete pellets with hydrophobic layers of either acrylic-silicon resin paint, acrylic urethane resin or epoxy resin paint. Using these specimens, they studied uptake as well as release of tritiated water and compared the results with similar tests performed with cement paste alone. Their findings corroborated the high permeability of tritiated water across silicon coatings (mostly through pores and voids) and the tritium enrichment of epoxy paint films. They also noticed a considerable retarding effect of paints on tritium uptake by concrete thus substantiating the findings of Ono et al. [Ono92a]. Data obtained with

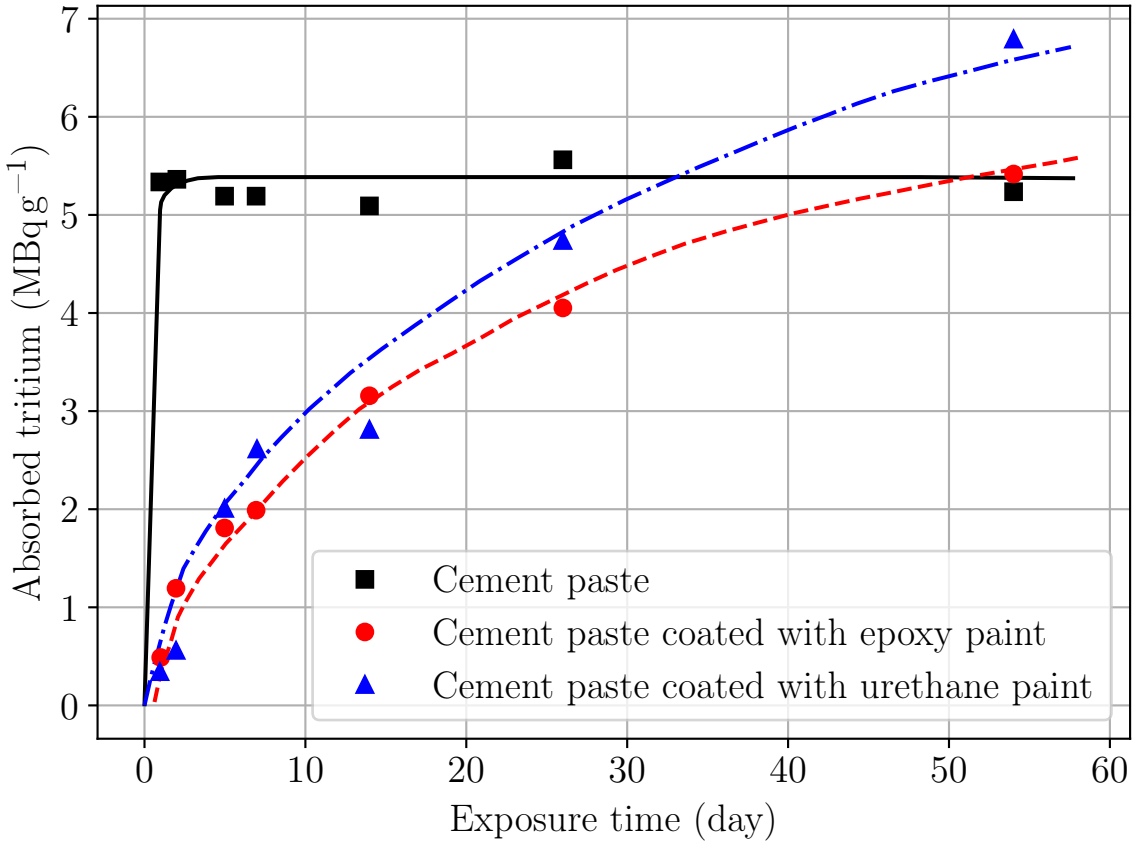


Figure 2.34: Absorption of HTO (650 - 700 Bq cm^{-3}) by cement paste, cement paste coated with epoxy paint and cement paste coated with urethane paint (after [Eda15]).

specimens exposed to an atmosphere having a relative humidity of 43 - 48 % and containing 650 - 700 Bq cm^{-3} of HTO at temperatures within the range 291 - 296 K are displayed in Fig. 2.34. As evident, whereas bare cement paste saturates after only 1 - 2 d, this process takes considerably longer with specimens coated with of 0.1 mm of paint. The increased uptake beyond that of saturation in cement paste was explained by substantial trapping of tritium on surface and bulk of the paint. Hence, hydrophobic paints will only effectively delay deep penetration of tritium into the concrete wall but not constitute an efficient long-term barrier. What is more, the degree of surface contamination may eventually exceed that of cement saturation.

Braun and Williamson [Bra85] determined diffusion and solubility constants of HTO for two epoxy, one vinyl and one urethane protective coating. The reported values were found to be of similar order of magnitude than measured for other paints by other investigators (see Table 2.36).

Sorption rates of gaseous tritium were up to four orders of magnitude larger than of tritiated water. However, because of the rather large solubility of tritiated water in the investigated coatings, permeability's of HT and HTO were not too different. The desorption rates of tritiated water from the four investigated coatings were boosted by high humidity (60 %). This was explained by an isotopic exchange process. Analogous findings with acrylic resin, butyl rubber and epoxy paint were published by Kobayashi et al.[Kob07a].

Holland and Jalbert [Hol86a] compared inside of a 0.96 m^3 test cell with a total inner surface area of 5.6 m^2 the interaction of HTO and HT with walls consisting either of bare aluminium foil or aluminium foil coated with an oil-based or a water-based epoxy paint (paint thickness in the range 0.1 - 0.2 mm). Room air clean-up in closed loop operation was simulated with a 0.54 $m^3\,hour^{-1}$ flow of clean air corresponding to one volume change in 2 hours. A semi log plot of the decrease in concentration of elemental tritium vs. time yielded a straight line which indicates that HT is neither absorbed on the metal nor on the paint. In case of HTO the same type of plot showed an initial peak, which was attributed to some conversion of HT into HTO[24] in the chamber and thereafter a curve that slowly became flatter, which was rationalized by slow release of tritiated water absorbed by the chamber walls. The experimental results were simulated with a model based i) on the release itself, ii) the conversion of elemental tritium into tritiated water, iii) the solubility and diffusion constants of HTO in the paints and iv) continuous removal of tritium by a dedicated clean-up system. According to their conclusions, outgassing from painted walls greatly prolonged the time required for decontamination from tritium of the atmosphere in a containment or caisson via a Tritium Removal System. Consequently, painted metal surfaces should either be completely avoided or the paint be applied very thinly in order to minimize tritium out-gassing. Another conclusion pertained persistency of contamination, i.e. much longer decontamination periods were necessary after an exposure to HTO than to HT. Another conclusion was that whereas Latex paints retain more tritium than epoxy paints the release of tritium from the former takes place in less time.

In a further experiment carried out at TSTA, approx. 5.4×10^9 Bq of DT were released on purpose into the main cell of this facility (volume 2900 m^3) and held there for a period of 29 min [Bar89]. The cell contained glove boxes, equipment and altogether eight stationary tritium

[24] Because total tritium in the cell acts as catalyst to the conversion reaction, this reaction is second order in concentration of tritium.

monitors. The walls of the cell were coated with an oil-based epoxy paint. The highest momentary concentration of tritium registered was $2 \times 10^7\,\mathrm{Bq\,cm^{-3}}$ and the equilibrium concentration that established after a period of 10 min was $1.9 \times 10^6\,\mathrm{Bq\,m^{-3}}$. Subsequently, the ventilation system was restarted and tritium released via stack. Under these conditions and in basic agreement with previous results obtained by Holland and Jalbert [Hol86a], tritium was removed from the cell even faster than anticipated from calculations assuming an ideal rate of removal. Three days after the release no residual air contamination was detectable. What is more, one month after the release, no contamination removable from the surfaces of the walls was measurable.

2.12.2.2 Interaction of tritium with concrete

Concrete is composed of cement, cement constituting materials (fly ash), aggregates (sand), water and chemical admixtures. It solidifies and hardens in a chemical process called hydration. The chemical process that takes place can grossly be described by equation

$$2\,\mathrm{Ca_3SiO_5} + 7\,\mathrm{H_2O} \longrightarrow 3\,(\mathrm{CaO})\,2\,(\mathrm{SiO_2})\,4\,(\mathrm{H_2O}) + 3\,\mathrm{Ca(OH)_2}\ .$$

In addition to significant amounts of structural water, this material contains some water trapped in pores. Numata et al. [Num90b; Num92] studied the adsorption, permeation and depth profiles of tritiated water across concrete as function of porosity and density. The depth profile evolution of tritium was calculated as function of time assuming that tritiated water diffuses through liquid water sequestered in cement pores. It was further supposed that during diffusion tritiated water undergoes exchange reactions with hydrogen bound in concrete. Several fractions of HTO released thermally from hardened cement paste at temperatures within the range 473 - 1123 K are described in Table 2.37. To determine the adsorption of tritiated water by concrete cylindrical specimens were exposed to water vapour ($2.5 \times 10^7\,\mathrm{Bq\,m^{-3}}$) at 296 K while keeping the relative humidity constant at 93 %. The total amount adsorbed was obtained by heating the specimens up to 1123 K. Slicing of the specimens and heating each slice as described above delivered depth profiles. Permeation experiments were performed at 296 K with liquid tritiated water containing $3.7 \times 10^9\,\mathrm{Bq\,m^{-3}}$ using 5 mm thick cement specimens saturated with water.

About 80 % of airborne tritiated water penetrated into concrete was found in free liquid water. The uptake of tritiated water revealed dependency from porosity. In fact, when the porosity

Table 2.37: Water released thermally from hardened cement paste (after [Num90b]).

Group	Temperature K	Fraction %	Type of water
I	473	65	Liquid water (free and capillary water)
II	473 - 723	20	Crystallization water
III	723 – 823	12	Decomposition of calcium hydroxide
IV	823 - 1123	3	Decomposition of calcium silicate hydrides

was increased from 0.07 to 0.28 the diffusion coefficient of tritiated water through concrete increased from 3.2×10^{-12} up to $11.3 \times 10^{-12}\,\mathrm{m^2\,s^{-1}}$. Analysis of the data showed that the inherent diffusion coefficient of tritiated water, D_i, at ambient temperature is nearly proportional to porosity, ϵ, as described by equation

$$D_i = 3.55 \times 10^{-11} \epsilon^{0.947}$$

in which D_i is given in $\mathrm{m^2\,s^{-1}}$ and ϵ in $\mathrm{cm^3\,cm^{-3}}$. Analogous measurements carried out by Terashima and Kumaki [Ter76] at 293.15 K on the diffusion of liquid tritiated water through cement materials were basically in line with the results reported by Numata [Num92]. Combining results of both investigations yielded the diffusion equation

$$D_i = 5.62 \times 10^{-11} \epsilon^{1.067}\ .$$

A one-dimensional diffusion model was used to predict tritium depth profiles in cement materials [Num90a]. The equilibrium between tritiated water vapour and liquid water on the cement surface was well described by Raoult´s law. However, two different diffusion coefficients, one for a slow diffusion ($2 \times 10^{-11}\,\mathrm{m^2\,s^{-1}}$) and another for a faster diffusion ($5.2 \times 10^{-11}\,\mathrm{m^2\,s^{-1}}$), were necessary to explain the observed profiles.

To estimate the degree of penetration of tritium into concrete walls enclosing a restricted area, concrete saturated with water at constant ambient temperature of 296 K was assumed to prevail [Num92]. Additionally, it was supposed that the concentration of tritiated water in the

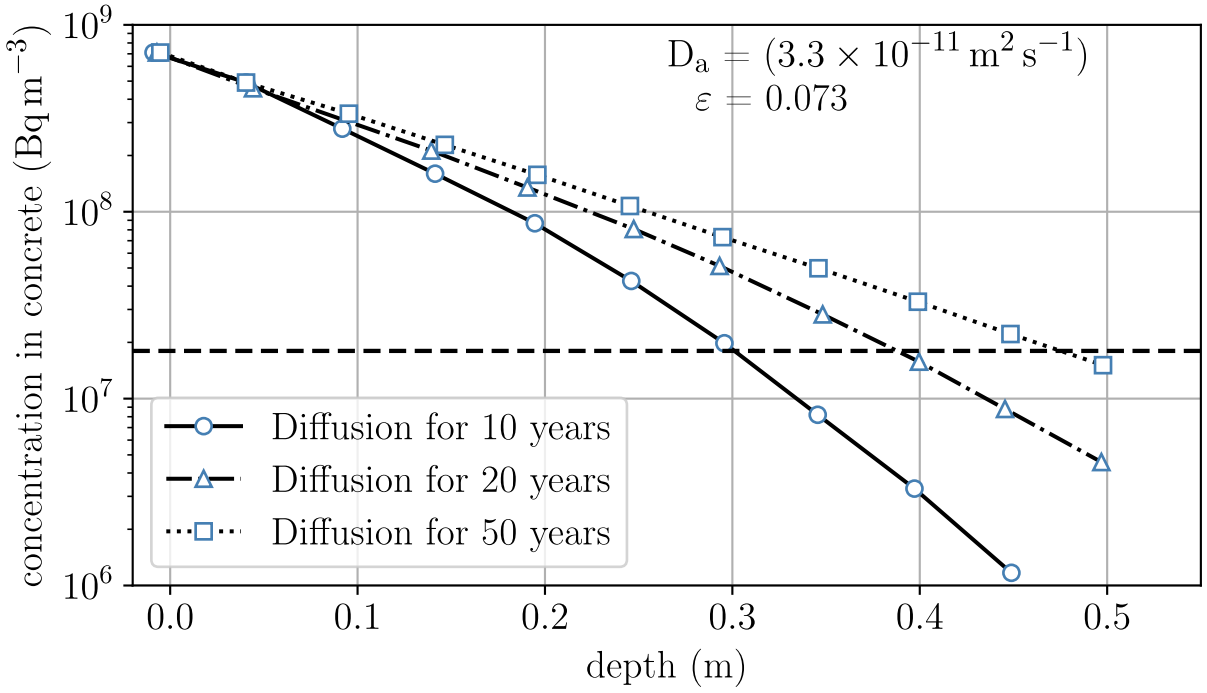


Figure 2.35: Calculated depth profiles of tritiated water in concrete exposed to air containing 2.1×10^5 Bq m^{-3} of tritium as function of exposure time (after [Num92]). The horizontal broken line gives the concentration of tritium on the concrete outer surface that equilibrates with the limit concentration of tritium in ambient air.

restricted area remained constant at 2×10^5 Bq m^{-3} [25] over the period in question (it was taken for granted that all windows, doors, and other openings of the restricted area remained closed) and it was assumed that the pore structure of concrete and the diffusion coefficient of tritiated water through the wall remained unchanged. Under these conditions the penetration of tritiated water was calculated for hypothetical periods of 10 years, 20 years and 50 years. As apparent from Fig. 2.35, after 50 years permeation through a 50 cm thick concrete wall the concentration of tritium on the outside surface reaches values of less than 1.8×10^7 Bq m^{-3} of concrete (see Fig. 2.35). According to calculations by Numata et al., this concentration of tritium on the outer concrete surface equilibrates with the limit concentration of tritium in ambient air, which at the time was 5×10^3 Bq m^{-3} of concrete. Therefore, in the event of a major accidental release of tritium into a building protecting tritium-handling activities a 0.5 m thick concrete wall will constitute a rather prolonged safe confinement.

[25] This concentration constitutes the regulatory limit in Japan.

Natalizio [Nat94] developed at **TSTA** a simple model to investigate the contribution of walls enclosing a vented building interacting with accidentally released tritium. The proposed model is applicable to a building in which the initial concentration of tritium confined in the building, C_0, is reduced either by straight forward one-way ventilation or by means of closed loop operation with an integrated Emergency Tritium Clean-up System. In the latter case the concentration decrease can be described by the expression

$$C = C_0 \exp\left(-\frac{Q}{V} + \frac{Ad}{V}\right)$$

where Q is the purge flow, V the volume of the building, A the total inner surface area of the building and d the averaged deposition rate of tritium on the various surfaces of the building. If a $1000\,\mathrm{m}^3$ building having a bare concrete surface area of $600\,\mathrm{m}^2$ is assumed, it can be shown that only for a fairly leak tight room is the effect of the surface significant. At leakage rates of the order of $0.1\,\%\,\mathrm{d}^{-1}$ or higher the contribution of the building walls is of only minor consequence. Hence, surfaces of a building will only play a role in the attenuation of the airborne concentration of HTO and ultimately protect the environment from releases, when the time of interaction with the walls is long enough, i.e. the leak rate is comparable to the deposition rate. On the other hand, Nishikawa et al [Nis06] concluded from their investigations on the permeation rate of gaseous tritium through concrete that tritiated hydrogen, in contrast to tritiated water, will probably permeate rather rapidly through the walls of a tritium handling building. The diffusion coefficient of gaseous tritium through dried cement paste tube (water/Portland cement = 0.6) tested inside of a quartz tube was found to be only $1/30^{\mathrm{th}}$ lower than that through air [Mar72]. The diffusion coefficient of hydrogen through dried cement was found to follow expression

$$D_{\mathrm{H_2}} = 1.21 \times 10^{-10} T^{1.25}\,\mathrm{m^2\,s^{-1}}$$

where T is the temperature in K.

The physisorption of water, q_p ($\mathrm{g_{H_2O}\,g^{-1}}$), on cement paste was assessed by Takata et al. [Tak05]. The data followed a Langmuir expression of the kind

$$q_\mathrm{p} = \frac{3.84 \times 10^{-8} P \exp\left(\frac{22.4\,\mathrm{kJ}}{RT}\right)}{\left(1 + 8.83 \times 10^{-7} P \exp\left(\frac{22.4\,\mathrm{kJ}}{RT}\right)\right)}\ \mathrm{g_{H_2O}\,g^{-1}}$$

where P (Pa) is the partial pressure of water vapour, R the gas constant ($\mathrm{kJ\,mol^{-1}\,K^{-1}}$) and T the temperature in K. The chemical adsorption of water, q_c ($\mathrm{g_{H_2O}\,g^{-1}}$), was observed to be essentially independent from the partial pressure of water and described by equation

$$q_\mathrm{c} = \frac{3.31 \times 10^{-7} \exp\left(\frac{52.5\,\mathrm{kJ}}{RT}\right)}{\left(1 + 4.54 \times 10^{-6} \exp\left(\frac{52.5\,\mathrm{kJ}}{RT}\right)\right)}\ .$$

The amount of structural water, q_s, was calculated from

$$q_\mathrm{s} = q_\mathrm{all} - q_\mathrm{p} - q_\mathrm{c}$$

and found to be $q_\mathrm{s} = 0.09\ \mathrm{g(H_2O)/g_{cement\,paste}}$. Here q_all represents the total amount of water retained by cement.

Takata et al. [Tak08b] determined likewise concentration depth profiles of tritium in cement paste, mortar, and concrete after exposure to tritium-bearing water vapour. In their approach, all outer surfaces except the one on the top of cement, mortar, or concrete cylinders of 100 mm diameter were covered with a layer of epoxy paint. The objective of the layer was to limit the penetration of tritium to only the upper surface of the cylinders. To determine depth profiles, the painted cylindrical specimens were placed inside of a glove box and exposed to 10^3 Pa water vapour containing 740 - 1110 $\mathrm{Bq\,cm^{-3}}$ tritium at 288 - 298 K. Total exposure time was six months. After completion of the exposure, core cylinders (3 cm) were cut from the painted cylinder center employing a core drill. Five or six discs were then cut from each core cylinder, each dropped into water and – after equilibration – the concentration of tritium in the supernatant water determined by liquid scintillation counting. By this rather simple procedure the penetration of tritium into the three examined materials was determined up to a depth of about 10 cm. Under comparable tritium-exposure conditions the penetration decreased in the order cement paste, mortar, concrete. The respective diffusion coefficients were $1.3 \times 10^{-10}\ \mathrm{m^2\,s^{-1}}$, $6.3 \times 10^{-11}\ \mathrm{m^2\,s^{-1}}$

Table 2.38: Tritium sorption on concrete or cement after exposure to HTO [Dic92].

Material	HTO in air $Bq\,m^{-3}$	Exposure time hour	rel. humidity %	Total desorbed tritium* $Bq\,m^{-2}$	Reference
Concrete	3.8×10^{10}	22	33	4.7×10^{10}	[Dic92]
Concrete	2.3×10^{10}	1.9	31.9	1.3×10^{10}	[Dic92]
Concrete	1.1×10^{11}	3.2	18.5	0.9×10^{10}	[Dic92]
Cement	4.3×10^{7}	2.0	-	0.8×10^{10}	[Ono92b]

*Desorption per unit geometric area

and $4.3 \times 10^{-11}\,m^2\,s^{-1}$. After exposure of concrete to initially 86.4 Pa HTO for six months the experimentally determined penetration was only small, i.e. 5 cm.

Using the above described experimental results, a model was developed to calculate the uptake of tritium by five 0.1 m thick concrete walls enclosing a $1000\,m^3$ room. It was assumed that the walls were initially uncontaminated, all released tritum was converted into tritiated water via isotopic exchange, gases were perfectly mixed, and the temperature remained constant at 298 K. It was further supposed that after one day of contamination a Tritium Removal System is taken into operation for one whole day in order to remove most of the tritium in the ambient air. The calculated tritium depth profile in the concrete after one day of exposure is displayed in Fig. 2.36a (solid line). The amount of tritium trapped as non-diffusive water (broken line) was estimated to be about 68 % and that physically adsorbed (dotted line) about 32 %. If after one day of exposure tritium is removed from the room atmosphere, the concentration on the concrete surface will progressively decrease induced by the resulting tritium concentration gradient (see Fig. 2.36b). What is more, during the course of one year a fraction of tritium in the wall will permeate deeper into the bulk and gradually distribute more evenly. Takata et al. estimated that under these conditions about 90 % of the tritium will remain in the concrete because of the high trapping capacity of this material. The release into ambient takes place very slowly.

Dickson and Miller [Dic92] determined sorption of HTO on concrete at ambient temperature. After exposure times of up to 22 hours to tritium-contaminated air containing up to 3.8×10^{10} $Bq\,m^{-3}$, concentrations of tritium on the surface of up to $5 \times 10^{10}\,Bq\,m^{-2}$ were registered (see Table 2.38). In good agreement with other investigators, they reported that tritiated water

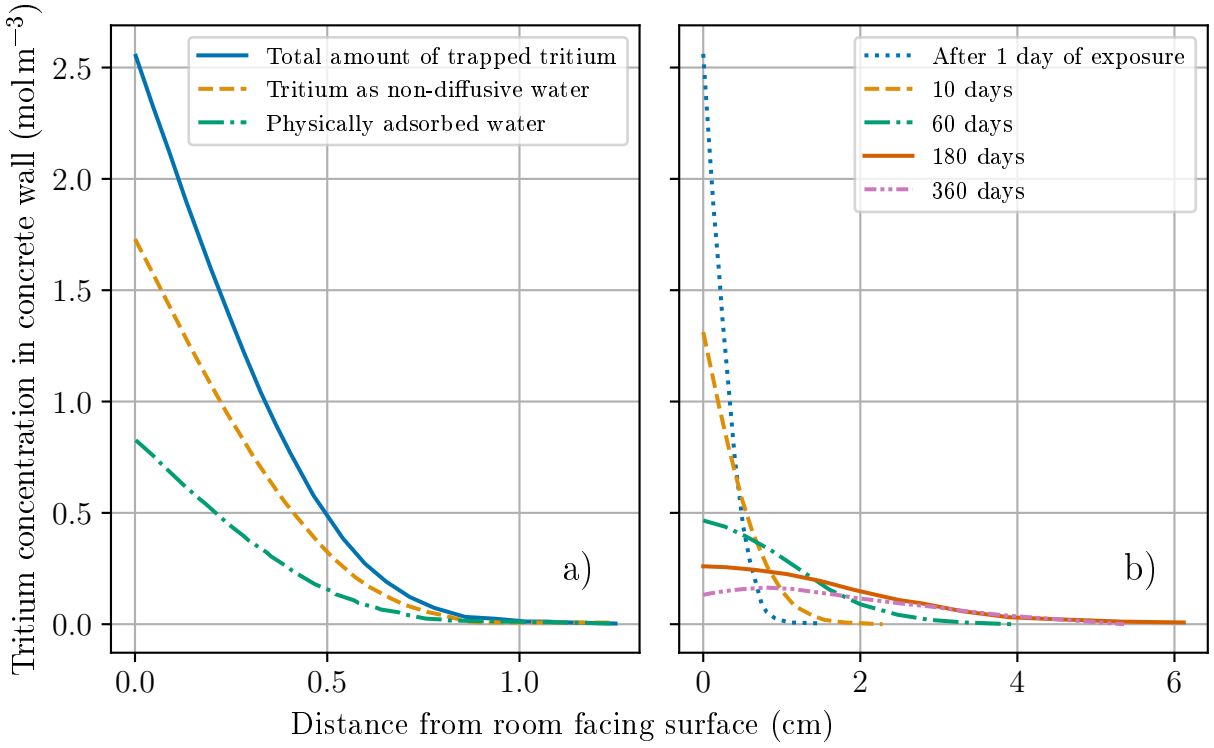


Figure 2.36: Modelling of the tritium concentration profile in concrete after exposure to air contaminated by tritiated moisture. Figure a) gives the depth profile after one day of exposure and figure b) the subsequent evolution of the profile in the bulk as function of time after the contaminated air has been fully removed (after [Tak08b]).

is generally sorbed much more readily on concrete than tritiated hydrogen and is also much more difficult to desorb than HT. When the uptake of unpainted concrete was compared with that of other materials like stainless-steel, vinyl floor tiles, glass or porcelain, the level of HTO sorption on concrete was found to be orders of magnitude higher. The rate constant of tritium desorption from cement by wet purging gas at 303 K, on the other hand, was distinctly slower than that from other organic materials. Conversely, sorption of HTO or HT on porcelain tiles was observed to be minimal and conversion of HT into HTO low. For this reason, **porcelain tiles** were considered to be an adequate barrier for the protection of concrete walls in a tritium handling facility. A limitation is that the porous grouting between the tiles - unless properly impermeabilized - may sorb more tritium than the tiles themselves.

Ono et al. [Ono92b] performed research on the adsorption of HTO at 303 K on a number of different materials including cement. The selected equilibration time of two hours was probably too short for the achievement of reproducible results. Dickson and Miller [Dic92] carried out similar experiments exposing a variety of construction materials to either HT or HTO at 296 - 298 K for periods within the range 22 - 68 hours. A notorious high level of HTO sorption by unpainted concrete, i.e. 0.9×10^{10} - 4.7×10^{10} Bq m^{-2} was registered after exposure to 0.2×10^{11} - 1.1×10^{11} Bq HTO/m^3. The obtained water adsorption coefficients increased in the order acryl resin, linoleum, and rubber. Adsorption coefficients for cement were more than an order of magnitude larger [Ono92b].

2.12.2.3 Cladding of concrete with a tritium impermeable barrier

When dealing with construction materials it is necessary to distinguished between cement and concrete: **Cement** is the binder that holds other materials tightly together and **concrete** is a mixture of materials like sand, gravel, small stones, water, and cement as binder. The standard material used for the construction of walls, floors, and ceilings of tritium handling facilities is reinforced concrete. Reinforcement commonly consists of steel bars embedded in the concrete before it solidifies and sets.

In the event of an accidental tritium release, concrete would be exposed to HT and HTO. Hence, concrete uptake and subsequent delayed release will lastly determine personnel safety. What is more, releases from building materials will determine the time delay between atmosphere clean-up and personnel access.

In order to efficiently reduce the uptake of HT and HTO by concrete, protective coatings consisting of organic or inorganic sealants applied directly onto the surface - if possible penetrating the porosity, or cladding the concrete by an impervious barrier - have been proposed. These coatings should ideally fulfil some or most of the following criteria:

- Formation of a pore-free finish
- High adhesion to concrete
- Very low water solubility and permeability values
- Excellent resistance to radiation

- Excellent resistance to solvents
- High build-up capability
- High hardness and durability
- Easy cleaning

Standard protective coatings like paints are considered to be only partially effective because of their relatively high solubility for tritium-bearing hydrogen and water. A more promising option for concrete appears to be **cladding** with glazed, highly dense ceramic tiles. They are characterized by high durability, high covering and comparatively small uptake of tritiated hydrogen or tritiated water, and easy cleaning [Sel92]. These hydrophobic materials not only improve the cleaning properties of surfaces but also mitigate the consequences of tritium absorption which is normally associated with delayed releases after completion of an emergency clean-up of the atmosphere of a facility. One remaining problem is tritium uptake through the grouting between the tiles, which constitutes about 2 % of the total surface. To cope with this problem, standard hydrated grout often associated with gas evolution is replaced by a surface fusible inorganic grout of small thermal expansion. The advantage of this material is that it keeps the separation between tile edge and grout small upon cooling. Several grouts applied by plasma spraying utilizing inorganic binders that cure retaining strength while exhibiting low shrinkage after dehydration were examined experimentally. For the experiment's grouts were selected whose surface fuses into a glassy layer by the plasma flame impinging on the surface on and between the tiles. In addition, a plasma sprayed glass layer was also tested. Glassy permeation barriers were achieved with fused silica or borosilicate powders and ethyl or sodium silicate binders. Plasma spraying porcelain enamel caused problems such as tile cracking, drying shrinkage, insufficient adhesion, lack of deposition efficiency, etc. Evidently, complementary research is necessary to further develop these techniques up to readiness for extensive technical application.

2.13 Interaction of hydrogen isotopes or helium with glass

Molecular hydrogen dissolves in glass at temperatures below 423 K. The solubility of hydrogen is generally endothermic and directly proportional to the pressure of hydrogen. At 300 K the solubility is of the order of 1 - 10 cm^3 (STP) cm^{-3} atm^{-1}. At higher temperatures, hydrogen "dissolves" atomically and the solubility becomes proportional to the square root of the hydrogen pressure. When mixtures of hydrogen and tritium are used, the latter species is incorporated not only by physical sorption but also via reaction through disruptions of Si – O – Si bonds and formation of bound tritium species such as Si – OT, Si – T bonds or tritides [She77a; Sae84]. In addition, tritium may undergo isotopic exchange with hydroxyl groups pre-existing in the glass network [Sae84]. Obviously, all these processes are associated with persistent contamination of the glass by tritium. Leaching of tritium from glass into water was found to be a rather slow process [Hir83]. According to Dickson and Miller [Dic92] the sorption of tritium on glass at ambient temperature after 22 hours of exposure to 3.7×10^{10} Bq m^{-3} of HTO in air of 33 % relative humidity containing 1.5 % HT attains a value of 1.5×10^5 Bq m^{-2} once equilibrium is established (see Table 2.39). Among a large variety of different metallic, organic, and inorganic materials, the sorption of HTO on glass was found to be particularly small. Permeability data of protium, deuterium, and tritium deuteride in silicate glasses and soda lime glasses at elevated temperatures (< 1500 K) were determined by Steward [Ste83]. Shelby[She77a] performed measurements on permation, diffusion and solubility of deuterium with several types of vitreous silica at temperatures within the rang 273 - 1073 K. The results provided evidence that isotope exchange takes place between diffusing deuterium and structural hydoxyl groups at temperatures above 573 K and a reaction yielding deuteroxyl groups at temperatures exceeding 873 K. Under the assumption that the solubilities of H_2 and D_2 are essentially the same, it was possible to obtain a generally valid expression for the solubility of deuterium at pressures covering the range 0 - 1400 atm and temperatures within the range 0 - 1073 K. The expression is the result of a combination of two models, one treating the dissolved deuterium atom as a harmonic oscillator, and the other, by contemplating the isothermal hydrogen isotope solubility as a Langmuir type of adsorption isotherm.

Vitreous silica is a commercially available high temperature, single component glass. It has superior chemical resistance, displays low thermal expansion, and has excellent optical transmission from UV up to the near infrared.

Table 2.39: Tritium sorption by glass exposed to humid air containing HTO and HT [Dic92]

HTO and HT in humid air $\mathrm{Bq\,m^{-3}}$	Exposure time h	Rel. humidity %	HT %	Total desorbed tritium* $\mathrm{Bq\,m^{-2}}$
3.8×10^{10}	22	33.0	1.5	1.5×10^{5}
2.3×10^{10}	1.9	31.9	4.0	5.9×10^{5}
11×10^{10}	3.2	18.5	8.6	37.0×10^{5}

*Desorption per unit geometric area

Helium diffuses through the walls of fused silica[26] vessels at much higher rate than any other gas but does not diffuse through soft glass [Gho48]. Diffusion coefficients (D) and solubilities (S) of helium in fused quartz were determined by Swets et al. [Swe61] both at a low and a high temperature range of 297 - 573 and 573 - 1307 K, respectively. The corresponding temperature dependencies are

$$D_{\mathrm{l}} = 3.04 \times 10^{-8} \exp\left(-\frac{23.36}{RT}\right)$$
$$D_{\mathrm{h}} = 7.40 \times 10^{-8} \exp\left(-\frac{27.69}{RT}\right)$$
$$S_{\mathrm{l}} = 1.99 \times 10^{17} \exp\left(\frac{2.85}{RT}\right)$$
$$S_{\mathrm{h}} = 1.28 \times 10^{17} \exp\left(\frac{4.92}{RT}\right)$$

where l and h denote low and high temperature range, respectively. In these equations, diffusion coefficients are given in $\mathrm{m^2\,s^{-1}}$, solubilities in $\mathrm{atoms\,cm^{-3}}$, and activation energies in $\mathrm{kJ\,g^{-1}\,atom^{-1}}$. Interestingly, the activity of a tritium oxide sample in a hermetically closed silica container can be determined by collecting and measuring volumetrically pure decay helium permeating the walls into a vacuum-tight outer containment.

[26] The glassy form of quartz.

Borosilicate glass exposed to neutrons generates tritium by a neutron capture reaction with boron [Miy83a]. Tritium released thermally from a borosilicate vessel at temperatures within the range 473 - 973 K is almost completely liberated as water (HTO or T_2O). The diffusion coefficient obtained for tritium in borosilicate glass at temperatures exceeding 573 K was reported to be

$$D = 5.34 \times 10^{-4} \exp\left(-\frac{127.8\,\mathrm{kJ\,mol^{-1}}}{RT}\right)\ \mathrm{cm^2\,s^{-1}}\ .$$

2.14 Interaction of tritium with steel, welds and several pure metals that find application in tritium handling facilities

In this section, the status of technical understanding of materials behaviour in the presence of hydrogen isotopologues is evaluated with emphasis on special effects resulting from the presence of tritium. Attention is directed primarily to materials already recognized as having high probability of utilization in tritium handling facilities. Within this frame, factors like permeation, dissolution, adsorption, desorption, trapping, effect of impurities, bulk helium generation, hydrogen-induced material embrittlement and decay-accelerated corrosion are discussed. In many metals and alloys relevant to tritium technology, hydrogen transport is determined by the properties and condition of the surface. The consequences of prolonged exposure to high partial pressures of gaseous tritium-bearing species or to tritium-rich liquids, particularly under conditions of elevated temperature of pure and alloyed metals is insufficiently understood and needs to be further investigated.

The uptake of hydrogen by strong hydride-forming metals like lithium, titanium, niobium, etc., proceeds to a large extent by dissolution of metal hydride in the metal. In case of metals and alloys, that do not form hydride phases, hydrogen is dissolved in the interstices of the metal lattice. The solubility of hydrogen in strong hydride-forming metals tends to decrease with increasing temperature because the hydride itself becomes progressively unstable. Conversely, the solubility of hydrogen in metals dissolving hydrogen in interstices frequently tends to increase with augmenting temperature.

A number of topics of direct impact to fusion technology concerning the interaction of hydrogen with first wall materials of fusion machines, like for instance hydrogen recycling on metallic walls,

control of recycling, reflection coefficients, thermal and stimulated desorption that still require additional research efforts have been discussed by several authors [Pic84; Fed01b; Cau02; Ski08]. The selection of type, thickness, and location of plasma-facing and plasma-shadowed armour materials has significant consequences on the i) quality of plasmas, ii) initial and long-term inventory of tritium in the machine, iii) plasma-induced formation rate and location of deposits consisting of dust, flakes, and other debris capable of trapping hydrogen isotopologues, iv) retrieval easiness of mobile and immobile tritium accumulated in the machine (important to remain below the administratively authorized tritium inventory limits), v) tritium breeding ratio, vi) kind, amount, and degree of contamination of tritiated waste, vii) extent of protection of the breeder blanket from radiation, viii) tritium permeation into cooling system, etc.

Not only the interaction of first wall materials with plasmas and within this frame the recycling of tritium needs to be examined but also the consequences of the incorporation of hydrogen into metals on their physical properties. Metals may be classified into endothermic (positive partial molar enthalpy of solution ΔH^0) and exothermic (negative ΔH^0) absorbers of hydrogen. This means that metals for which $\Delta H^0 < 0$ the solubility will decrease with increasing temperature and metals for which $\Delta H^0 > 0$ will show the opposite behaviour. Hydrogen dissolved in metals mostly occupies interstitial lattice positions, e.g. octahedral sites in Pd, $\alpha-$Fe, NiH_6 or tetrahedral sites in metals like Ta, Nb, V, $\beta-$Ti and $\beta-ZrH_2$ causing expansion of the metal lattice [Sch87]. The mobility of hydrogen in metals and the effect of lattice imperfections on the mobility is discussed in detail in a well referenced review paper published by Oriani [Ori93]. Reduction of hydrogen diffusivity on account of interactions with lattice defects such as the ones generated by cold work are examined in the light of a trapping theory. The generation and relaxation of mechanical stress by dislocations created when hydrogen penetrates into metals are also treated. Metals exhibiting a positive partial molar volume of hydrogen show an attractive interaction between dissolved hydrogen and dislocations which leads to a highly concentrated distribution of hydrogen along the dislocation and to smaller excess concentrations in the tensile stress region about the dislocation. The ubiquitous effect of hydrogen on metals is, however, **embrittlement** which arises mainly because of the ability of hydrogen to lessen binding forces between metal atoms [Woo16]. An important consequence of embrittlement is a reduction of the work needed to cause mechanical failure for a given load time duration. Other consequences are i) reduction in tensile elongation to cause failure, ii) decrease of the static load sustainable by a metal, iii)

increase in the rate of crack propagation and iv) decrease in the number of loads - no load cycles. Whereas in some metals like high strength steels part per million concentrations of hydrogen suffice for the development of catastrophic embrittlement, in others like Nb or Ta the resistance towards embrittlement by hydrogen is much higher.

The type of mechanism by which hydrogen diffuses through metals is dependent on temperature [Ale78]:

- At the lowest temperature hydrogen is delocalized as band state.
- At intermediate temperatures hydrogen atoms, mostly localized at specific interstitial positions, require energy for a change in location. Change in location can either occur by tunnelling from one interstitial site to another or by hopping with an activation energy sufficiently high to overcome the energy barrier between sites (classical diffusion mechanism)
- At the highest temperature hydrogen will populate states above the energy barriers and diffusion will become like through a dense gas or a liquid.

2.14.1 Interaction of molecular hydrogen isotopologues with stainless-steel

2.14.1.1 Hydrogen content of as-received stainless-steel

It is of interest to know that pure stainless-steel in **as-received** condition contains hydrogen in the bulk (or in bulk and surface layer). A result of 0.8 ppm by weight was achieved by outgassing at 973 K [Ake96]. Mine et al. [Min11] reported hydrogen concentrations within the range 1.9 - 4.7 ppm for stainless-steel´s type SUS304, SUS 316, SUS316L, SUS 310S, and SUH660 (see also section 2.14.1.11).

Zajec and Nemanic [Zaj01] extracted hydrogen from stainless-steel SS304 at temperatures as high as 1273 K and determined by quadrupole mass spectrometry the gases released during almost 60 hours of induction heating at progressively increasing temperatures. While after prolonged outgassing at up to 873 K the specimen seemed free of hydrogen, raising the temperature further up to 1273 K caused liberation of another “huge” amount of hydrogen. The total amount extracted was 5.1×10^{19} atoms H /cm^3 or 614 ppm by weight (assumed molecular weight of stainless-steel was 55.8 g mol^{-1}). This result is considerably higher than the value reported by [Ake96]. It is also higher than the value obtained from the known solubility of hydrogen in

stainless-steel calculated for ambient temperature. The higher value of [Zaj01] was explained by the more stringent outgassing conditions employed by this investigator and possible differences between specimens employed by both research teams [Ake96] and [Zaj01].

2.14.1.2 Factors influencing uptake and release of tritium from stainless-steel

A large number of publications [Lou75c; Mor77; Mon78; Gil80; Ell80; Ell81; Wer96; Nem01; Zaj01; Lon07] and review articles [Bea73c; Mar78; Mar79; Ada83; Ste83] have dealt with topics related to the interaction of tritium with containment and structural materials used for handling this gas. The passive nature of stainless-steel is generally attributed to a very adherent protective layer of "ceramic" chromium oxide, i.e. Cr_2O_3. Other elements typically present on the stainless-steel surface are iron, nickel, carbon and to a lesser extent molybdenum, manganese and calcium [Bea73c; Cas77; Ada83; Hir90c; Hat95; Han02]. Whereas the outermost surface of un-oxidized stainless-steel consists predominantly of chromium, iron and nickel, after oxidation under air at 773 K the main constituent of the surface was found to be iron, i.e. 90 %. When there is need to minimize tritium uptake, the optimal bake out temperature for stainless-steel lies in the range of 470 - 770 K. Evidently, after heating in a dry atmosphere the fraction of OH groups on the metal surface becomes comparatively small.

According to Beavis [Bea73c], annealing stainless-steel type 304 at high temperature in the presence of oxygen practically eliminates oxides of iron from the surface. Such modified surface possesses a significantly reduced ability to generate water by reaction with molecular tritium. In agreement with this observation, Hirabayashi et al. [Hir90c] detected by XPS analysis a substantial enrichment of iron on the topmost surface of stainless-steel type 316 when heating this material under air at 773 K for two hours.

Gaseous hydrogen can be incorporated into stainless-steel either via **gas-driven or plasma-driven permeation**. In the former case, hydrogen molecules are first adsorbed on the metal surface (a monolayer coverage is estimated to be of the order of 8.5×10^{14} molecules/cm^2). Adsorbed species will dissociate on the surface and diffuse into the bulk, the degree of penetration - at least at ambient temperature - being fairly small. In case of plasma-driven (also ion-driven) implantation, energetic hydrogen ions or charge exchange nuclear particles will enter the stainless-steel bulk with much higher effectiveness. They will penetrate considerably deeper into the metal

bulk at comparatively larger permeation rate than in case of gas-driven permeation [Mye82; Hol83; Ker84; Nak98].

Okuno et al. [Oku88] designed an experiment at TPL to investigate the ion-induced permeation of tritium through relevant first-wall materials of a fusion device. Employing a tritium ion source, it was possible to subject heated materials to implantation with ions having energies within the range 20 - 1400 eV. The experiment was equipped with Secondary Ion Mass Spectroscopy (SIMS) and Auger Electron Spectroscopy (AES) for the characterization of metal surfaces and with quadrupole mass spectrometry for the analysis of gases.

Another Tritium Plasma Experiment (TPE) conceived to simulate the interaction of ITER-relevant plasmas with pertinent first wall materials, was first installed and operated at Sandia National Laboratory and thereafter relocated in upgraded form in a glove box of TSTA in Los Alamos, NM [Cau90a; Tay95]. This fairly sophisticated experiment was furnished with a Langmuir probe to determine the properties of plasmas. The achievable electron temperature ranged from 5 - 10 eV, the electron density could be varied from 5.0×10^{16} - $2.5 \times 10^{18}\,\mathrm{m^{-3}}$, and the ion flux density be adjusted between 5.0×10^{20} - $2.5 \times 10^{22}\,\mathrm{m^{-2}\,s^{-1}}$ along the center line of the plasma. From the above it follows, that most ion flux densities and electron densities conditions to which plasma-facing materials of ITER will presumably be exposed could be simulated with this experimental facility [Cau02; Shi11b; Shi11a].

Ion-driven permeation of deuterium (incident ion energy < 2.0 keV) across iron followed a linear relationship between incident ion flux and permeation flux [Shu93a]. The activation energies for the recombination coefficient of deuterium on the incident side were estimated to be $-27.7\,\mathrm{kJ\,mol^{-1}}$ and $-23.9\,\mathrm{kJ\,mol^{-1}}$ for incident ion energies of 0.3 keV and 1.0 keV, respectively.

Nagasaki et al. [Nag93] performed more measurements on the plasma-driven permeation rate of deuterium across an iron membrane employing a deuterium ion beam of even higher energy, i.e. 5 keV $D_3{}^+$ (1.0×10^{15} D atoms $\mathrm{cm^{-2}\,s^{-1}}$) and temperatures within the range 303 - 1323 K. According to their observations, the permeation flux was roughly constant at temperatures below 423 K (transport limited by bulk diffusion at injection and back side of the specimen) and increasing at temperatures exceeding 473 K (transport-limited by recombinative desorption at the injection side and bulk diffusion at the back side of specimen). Similar temperature dependencies of the permeation flux have been reported for nickel, copper and silver.

Models describing ion-driven permeation have been published by Doyle et al. [Doy85] as well as by Shu et al. [Shu93a].

Plasma-driven uptake mechanisms play an important role in the vacuum chamber of fusion machines. At least three comprehensive reviews on all aspects of the interaction of plasmas with first wall materials have appeared in recent years [Cau02; Fed05; Ski08]. A model dealing with trapping of hydrogen in steel was developed by Krom and Bakker [Kro00]. They distinguished between reversible, saturable traps like a dislocation core and unsaturable, reversible traps like voids or cracks. Trapping increases the solubility of hydrogen and decreases the diffusivity of hydrogen until saturation is attained.

Myers and Wampler [Mye82; Mye84] investigated trapping of deuterium in helium-pre-implanted stainless-steel type 304 and 310. Samples of both materials were first implanted with $6 \times 10^{16}\,\mathrm{atoms\,cm^{-2}}$ of 750 keV ^{3}He, then with $4 \times 10^{16}\,\mathrm{atoms\,cm^{-2}}$ of 15 keV ^{4}He and finally, after cooling to below 170 K, with $2 \times 10^{16}\,\mathrm{atoms\,cm^{-2}}$ of 15 keV deuterium ions. Under these conditions Gaussian peaks in helium concentration were noticed in stainless-steel at depths of 0.07 µm and 1.2 µm and of deuterium at a depth of 0.13 µm. Differences in trapping behaviour of the two stainless-steel materials were non-discernable. Additionally, two kinds of steel surfaces were compared: i) surface oxidized by electro polishing under exposure to air and ii) a surface whose oxide layer was sputtered in situ by Fe ions. In both cases was the surface release of molecular deuterium proportional to the square of the concentration of D dissolved in the matrix, i. e. of second order kinetics. This was the case irrespective of temperature or the presence or not of an oxide permeation barrier. The recombination coefficient from the sputtered surface was found to be about 100 times larger than that from the oxidized one. Deuterium was bound to irradiation defects with a binding energy of 0.23 eV relative to solution sites. Helium bubbles of 1 nm diameter trapped D with a binding energy of 0.42 eV.

Deuterium strongly trapped in small 1 nm helium bubbles is possibly bound to the bubble surface by some form of chemisorption. The presence of bubbles was confirmed by transmission electron microscopy. Bubbles capable of trapping hydrogen isotopologues can also be generated by the radioactive decay of tritium, by neutron-induced transmutation or ion implantation. Trapping in irradiation defect traps - probably vacancies - is comparatively weak showing only half the binding energy of helium associated traps. Helium bubbles are characterized by much

larger thermal stability than similar irradiation defects. It follows that it may be difficult to avoid helium associated trapping of hydrogen isotopologues in structural steel of fusion devices.

Compelling experimental evidence attests molecular tritium the capability of penetrating into the bulk of stainless-steel even at ambient temperature [Hir84a; Sur88b; Wer96]. An early case in point was provided by Hirabayashi and Saeki [Hir84a] who exposed stainless-steel specimens to 13.3 kPa HT at 293 K for 35 d and determined the depth profile of tritium by chemical etching. The results indicated that even under such rather mild conditions tritium had penetrated up to 40 µm into the steel bulk. The fraction of removable tritium was determined by soaking charged specimens in water.

Wermer [Wer96] cut specimens from the wall of a 50 l transport vessel that had been utilized over decades for the transport of isotopically diluted as well as of pure tritium and determined the total tritium content in these specimens. Additionally, they measured the fraction of tritium leaching into water. The results of both measurements are compiled in Table 2.40. For comparison, a specimen exposed to gaseous tritium at elevated temperatures [Pen06] has also been included in the Table. As apparent, nearly all tritium incorporated into stainless-steel at ambient temperature can be removed by leaching, provided the time allocated for tritium penetration into stainless-steel is not too long, i.e. a few days [Hir84a]. In case of tritium in specimens cut from the transport vessel examined by Wermer, which had formerly been exposed to high levels of tritium during the course of years but always at ambient temperature, the observed leaching fraction was much smaller. Evidently, once tritium has penetrated deep into the stainless-steel bulk at elevated temperatures, e.g. 573 K, it is no longer easily removable by soaking into water or other liquids at room temperature [Pen06]. Hence, the deeper the penetration of tritium, the smaller the fraction of tritium removable from the metal surface by abrasive or chemical means . The results document the importance of detailed knowledge on the previous temperature/pressure/composition history and exposure sequence to tritium of materials for the selection of the most efficient decontamination procedure from the perspective of waste disposal.

Interestingly, stainless-steel SS316 specimens of 0.5 nm width submerged into **tritium-bearing water** (1.5 GBq cm^{-3}) at ambient temperature incorporated tritium and displayed concentrations of 5 - 10 kBq cm^{-3} at the centre after a contact time of 150 d [Tor15b]. Evidence for tritium penetration was obtained from step-by-step chemical etching. According to present understanding,

chemical reactions on the metal surface lead to the formation of atomic hydrogen which then diffuses into the bulk. Torikai et al. [Tor15b] also showed that the release rates of tritium at 573 K into vacuum or a stream of argon are non-discernible. Seemingly, both release paths are controlled by the same diffusion process[27]. The composition of the liberated gas, on the other hand, was quite different, being predominantly tritiated water when released into argon and mostly tritiated hydrogen when liberated into vacuum. Polishing the stainless-steel surface had a retarding effect on the rate of tritium release.

Stainless-steel exposed thermally to tritium-bearing hydrogen shows invariably a thin tritium-rich layer on the surface whose concentration exceeds by far that in the bulk. According to a number of researchers the width of this layer is of the order of 0.1 µm [Ell74; Hat95; Tor04; Tor07; Ots08; Pen10]. Another feature of the layer is a largely non-homogeneous distribution of tritium on the surface [Ots08]. This was rationalized by absorption/adsorption of water on surface oxides followed by formation of fairly stable –OT groups[28]. A tritium-rich layer was also observed on the reverse side of a stainless-steel specimen recoil-doped with tritium only on avers side [Aus73]. In this case, tritium diffusion to the unexposed side of the specimen had probably taken place via comparatively rapid diffusion through the grain boundary system.

Physical removal of the tritium-rich layer either by abrasion or chemical etching is only transitory because the layer on the surface reappears [Tor05b; Tor07]. Figure 2.37 provides experimental evidence for i) very high initial concentrations of tritium on the specimen top surface (almost 10^{10} Bq cm^{-3}), ii) very good reproducibility of the depth profiles of two specimens loaded under identical conditions, iii) almost complete removal of surface tritium by etching (according to BIXS measurements the tritium concentration remaining immediately after etching is only 0.7 % of that prevailing initially (compare Figs. 2.37a and 2.37b, note the different scales), iv) full recovery of surface tritium after short immersion into water and sweeping with argon for 700 hours as determined by etching (see left Fig. 2.37), and v) a second etching depth profile up to 150 µm from the surface revealing considerable loss of tritium during 4500 hours ageing under a stream of argon (see left Figure 2.37). After prolonged ageing with simultaneous chronic release for 4500 hours the surface activity determined by BIXS reappeared to a concentration of 83 kBq cm^{-2}, which is about half as high as the original value (see Fig. 2.37c).

[27] The same holds when comparing the release rate of tritium into water and the gas phase [Pen06].
[28] Surfe tritium survived 100 hours in a scintillation cocktail.

Table 2.40: Fraction of tritium leaching into water from stainless-steel exposed to gaseous tritium at ambient or elevated temperature.

Material	Dimensions mm	Gas: T in H	Exposure conditions: Pressure/Temperature/Duration	Total conc. MBq/spec	Fraction of tritium removable with H_2O^* %	Reference
SS316	10x30x1.25	3.1 % T	13.3 kPa/298 K/7 d	0.624	Incr. from initially 50 to 90 % in 5 d	[Hir84a]
50 l SS304 shipment vessel	25x25x2.0	from a few to 100 % T	$\leq$ 100 kPa/298 K / years of discontinuous exposure	1082	28.8	[Wer96]
SS316	15x15x0.5	24 % T	1.2 kPa/573 K/3 hours	18.52	3	[Pen06]

*The remaining tritium fraction can only be released by full dissolution in a strong acid mixture, e.g. $HCl + HNO_3$.

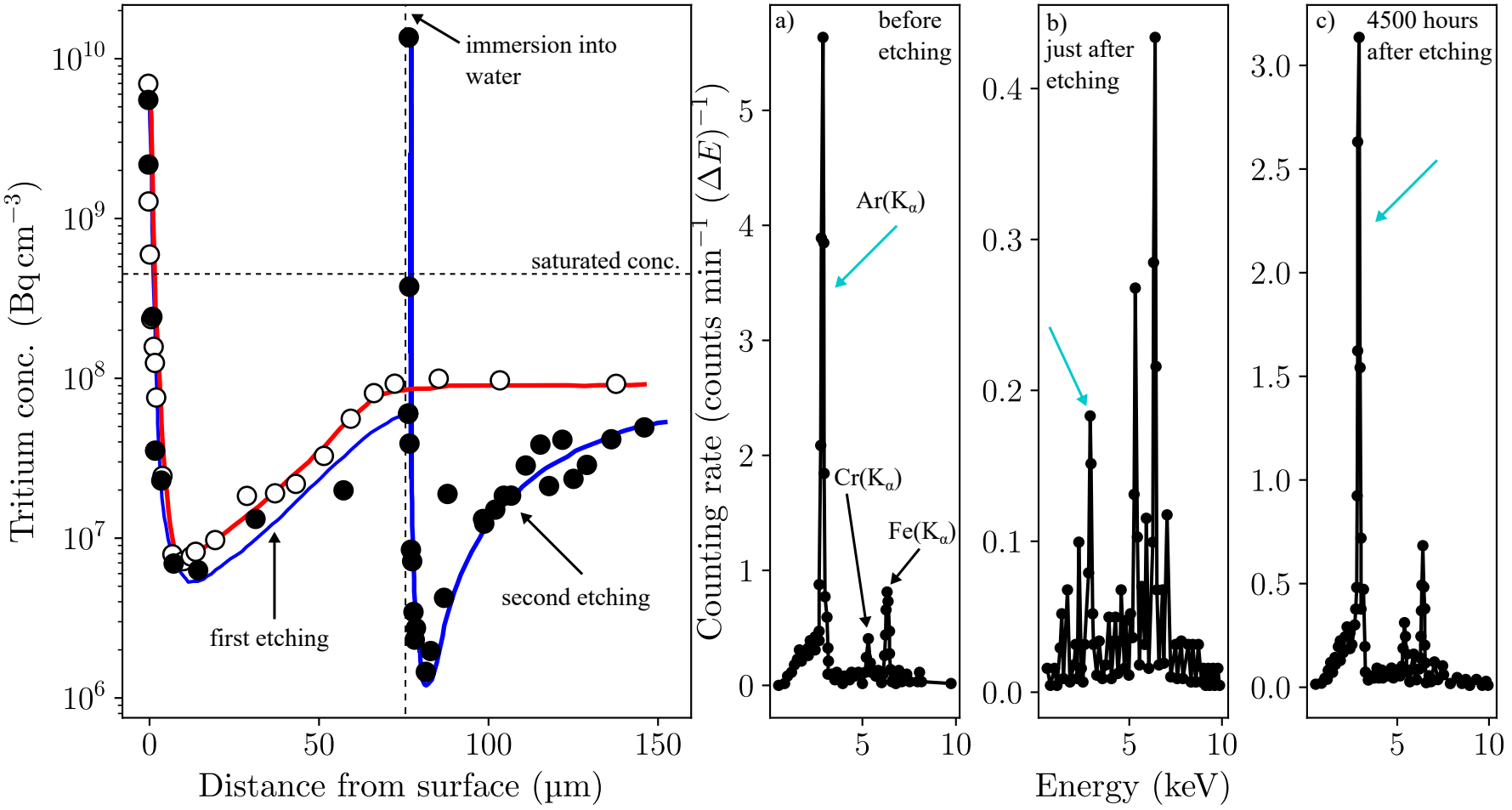


Figure 2.37: Tritium distribution between surface and bulk of stainless-steel SS316. Left figure: Tritium depth profile of two SS316 specimens loaded under identical conditions: (i) reference specimen etched only once and (ii) specimen used for BIXS and chronic release measurements and etched twice .The second depth profile was obtained after quick submersion of the etched specimen into water and subsequent sweeping with Ar for 700 hours (required for BIXS measurements). The horizontal broken line gives the calculated solubility prevailing at loading conditions. Right figure: BIXS results a) before etching, surface activity 158 kBq cm^{-2}, b) immediately after first etching, surface activity 1.1 kBq cm^{-2}, and c) after first etching and subsequent 4500 hours of chronic release, surface activity 83 kBq cm^{-2} (after [Tor07]).

Besides reappearance of tritium on the top surface, a slow and nearly constant long-term chronic release of tritium, predominantly as HTO, was detectable at ambient temperature or above using cooled bubblers containing water [Tor07]. The rate of tritium egress is essentially unaffected by the nature of the ambient medium, i.e. type of gas or liquid [Pen06]. Evidently, diffusion of tritium from the bulk to the surface governs the rate of tritium liberation and not the transfer from the metal surface to the surrounding ambient. Concurrently to the progressive release of tritium from the metal, the depth profile of tritium in the bulk reflects the diminishing tritium inventory. More on this below.

The kinetics of hydrogen transport across stainless-steel is influenced by trapping in the surface oxide film and by the existence of short-circuit diffusion paths [Aus73; Lou75c]. Austin et al. [Aus73] as well as Abraham et al. [Abr78] provided evidence by autoradiography that grain boundaries constitute a fast tritium diffusion path. The contribution of grain boundaries to the overall permeation rate is, however, small because of the low solubility of tritium within this path. According to Austin and co-workers, the diffusion of tritium through stainless-steel relies on three mechanisms: i) bulk diffusion, ii) rapid grain boundary diffusion and iii) trapping on the metal oxide surface. According to these researchers, a consequence of these distinctive diffusion paths is that inventory estimations based solely on a diffusion-controlled mechanism can lead to inaccurate results.

The uptake of tritiated hydrogen by stainless-steel is a function of temperature and pressure. Dissolution shows square root dependence from hydrogen pressure. Factors enhancing (or at least not retarding [Pow70]) the uptake of hydrogen are cold work and fine grain size [Lou75c]. A retarding effect is generally attributed to the presence of oxides on the surface, which may additionally have densified during a baking step [Lou75c; Sto84; Hir85b; Hir84b; Hir89; Hir90b; Hir90c; Hir90a; Hir91a]. The incorporation of tritium into stainless-steel can be retarded by covering the metal surface with a chromium layer, for instance by submersion into a chromium powder/ammonium chloride/alumina powder bath at 1173 K [Hir90b; Hir91a].

Louthan et al. [Lou72] noticed that stainless-steel absorbs more tritium from the gas phase when the steel is deformed. Autoradiography provided evidence that tritium was enriched at slip lines. It was shown that the drag of hydrogen by dislocations moving in response to stress was due to enhanced transport and not to easier surface entry.

2.14.1.3 Annealing

As a consequence of **cold working**, hardness, tensile strength, and electrical resistance of materials increase while ductility decreases. Additionally, cold working may increase the number of dislocations and cause planes of the crystal structure to become severly distorted. To return these materials into a strained-free structure, they are annealed, which essentially consists in the application of heat. Annealing is also necessary for materials that have undergone exposure to elevated temperatures, welding, machining involving elevated temperature or material displacement, etc. Goal of the annealing process is a material of higher ductility and reduced hardness.

Annealing can be subdivided into three stages performed at increasing temperatures: **Recovery** (also known as stress relief annealing) is primarily a low temperature process whose principal effect is relief of internal stresses caused by cold working. Main consequences are stress corrosion cracking prevention and minimization of distortion.

Recrystallization is usually carried out at a temperature higher than that for recovery and even higher than that of recrystallization but lower than for grain growth. The temperature of recrystallization is the temperature at which a highly cold worked material fully recrystallizes in one hour. For example, the recrystallization temperatures of copper, aluminum, and low carbon steel are 394, 352, and 811 K, respectively.

Grain growth is a high temperature process in which the grain boundary growth reaches the original grain size. To achieve this growth, the material must be heated at the proper temperature for an appropriate period of time and then cooled slowly at a specified rate. Annealing of AISI 321 stainless-steel at 1253 K for one hour in an oxidating atmosphere generated a 300 - 500 µm thick oxide layer consisting of Cr_2O_3 and Fe_3O_4 [Boc15].

2.14.1.4 Mechanism of hydrogen/water conversion on the surface of metals

Hydrogen dissociates on many metal and alloy surfaces subsequently diffusing and dissolving as atomic species in the solid substrate. As already pointed out, when this tritium is again released from stainless steel (or from several other metals) at ambient or higher temperature into air or other gases the predominant species is tritiated water. This takes place regardless of the temperature at which tritium-bearing molecular hydrogen was incorporated into steel (or metals)

[Aus72; Bea73c; Hir84a; Sur88b; Dic92; Cor92; Tor05b; Pen06; Tor07; Lon08; Oya12; Pen12; Pen13a; Sha16].

To understand the mechanism responsible for the conversion of absorbed tritiated hydrogen into released tritiated water it may be postulated that conventional pre-treatments of stainless-steel does not suffice to generate a completely oxygen-free surface. If this holds, iron and chromium oxides remaining on the surface could promote oxidative formation of water. However, the direct reaction of hydrogen with chromium oxides can be discarded on thermodynamic grounds. According to Chu and Rahmel [Chu79],Cr_2O_3 can only be reduced by pure and dry hydrogen at temperatures above 1300 K with a rate proportional to the square root of the pressure of hydrogen that decreases with increasing pressure of water vapor. In addition, X-ray photoelectron spectroscopy and UV photoemission measurements have shown that water readily dissociates already at ambient temperature on thin films of Fe_3O_4 [Jos00; Cut08; Boc15]. Therefore, a more plausible explanation for the formation of water is provided by the presence of hydrogen isotopes on the thermally conditioned stainless-steel surface chemisorbed as $-$OQ or $-$OOQ (Q = H, D, T) groups [Cor92; Tan08]. Oxyhydroxide species such as FeOOQ and CrOOQ (Q = H, D, T) have actually been identified in the surface layer region of stainless-steel by X-ray photoelectron spectroscopy [Oku09; Pen13a]. When these oxyhydroxide species are tritiated, they can be considered precursors of HTO generating this species by exchange reactions with ambient moisture adsorbed on the uppermost surface. Their high concentration at the surface explains the initial enhancing effect on detritiation displayed by moisture in a sweep gas. Replenishment of released tritium takes place by interaction of the metal surface with tritium migrating to the surface from the bulk. For this reason, the release of tritium into the gas phase is principally governed by the diffusion rate of tritium atoms to the surface. A rough estimation shows that the number of collisions of residual water molecules present in a dry carrier gas or in vacuum exceeds the flux of tritium atoms reaching the metal surface from the bulk. Consequently, isotopic exchange between OT groups on the metal surface and ambient moisture appears to be a likely mechanism.

Tritium is discharged at high Q_2O/Q_2 (Q = H, D, T) ratios when stainless-steel type SS316 previously loaded thermally with tritium is heated isothermally at temperatures of 573 or 673 K under a noble gas carrier [Pen12]. When the noble gas is replaced by air the Q_2O/Q_2 ratio becomes noticeably higher. Only initially is the rate of tritium release enhanced by moisture or

molecular hydrogen in the carrier gas because loosely bound physisorbed tritium on the topmost surface undergoes exchange reactions with hydroxyl or oxi-hydroxyl species on the steel surface. With progressing depletion of surface tritium, the enhancing effect of moisture and/or molecular hydrogen diminishes because then re-supply of tritium to the surface via slow diffusion from the bulk becomes rate determining for tritium release [Tor07]. While the kind of sweep gas, e.g. air or inert gas, may significantly influence the Q_2O/Q_2 ratio of the liberated tritium, the impact on the overall amount of released tritium is only minor [Pen12]. The fraction of total tritium incorporated thermally into stainless-steel which is liberated isothermally at 477, 573 or 673 K was found to be about 18, 63 - 80 or 78 - 94 %, respectively [Pen10; Pen12]. Thus, quantitative release of tritium is only possible at temperatures clearly surpassing 700 K.

Desorption of hydrogen from stainless-steel in the molecular form via recombination of neighbouring hydroxyl groups on the metal surface takes place only at elevated temperatures. Penzhorn et al. [Pen12] heated isothermally stainless-steel SS316 specimens of 6 mm width loaded with a mixture of hydrogen and tritium at several increasing temperatures. The results provided indirect evidence for the existence of a transition temperature in the vicinity of 650 K: at this temperature, the initially almost exclusive discharge as tritiated water gradually gives way to release of molecular tritiated hydrogen.

Oya et al. [Oya12] performed a thermal release study using several specimens of the same material but subjected to different pre-treatment and loading conditions. They noticed in experiments with progressively increasing temperatures that at first tritium is released almost entirely as tritiated water. When, however, the temperature was further increased, the released species became mostly molecular tritiated hydrogen. The change-over temperature was estimated to be within the range 450 - 600 K. The results of these two investigations are in good agreement with similar observations reported previously by Åkermark et al. [Ake96]. These researchers outgassed stainless-steel SS316 specimens under vacuum while increasing the temperature in hundred-degree steps in intervals of 30 min (see Fig. 2.38). As apparent from the sharply increasing mass spectrometric hydrogen peak, which persists as main peak during further high temperature outgassing (see Fig. 2.38a) and the abruptly decreasing outgassing water peak shown in Fig. 2.38b, the change over temperature lies within the range 590 - 680 K. Åkermark et al. therefore postulated that while at low temperatures the main released species is water, at temperatures above 600 K water reacts with the metal surface according to reaction

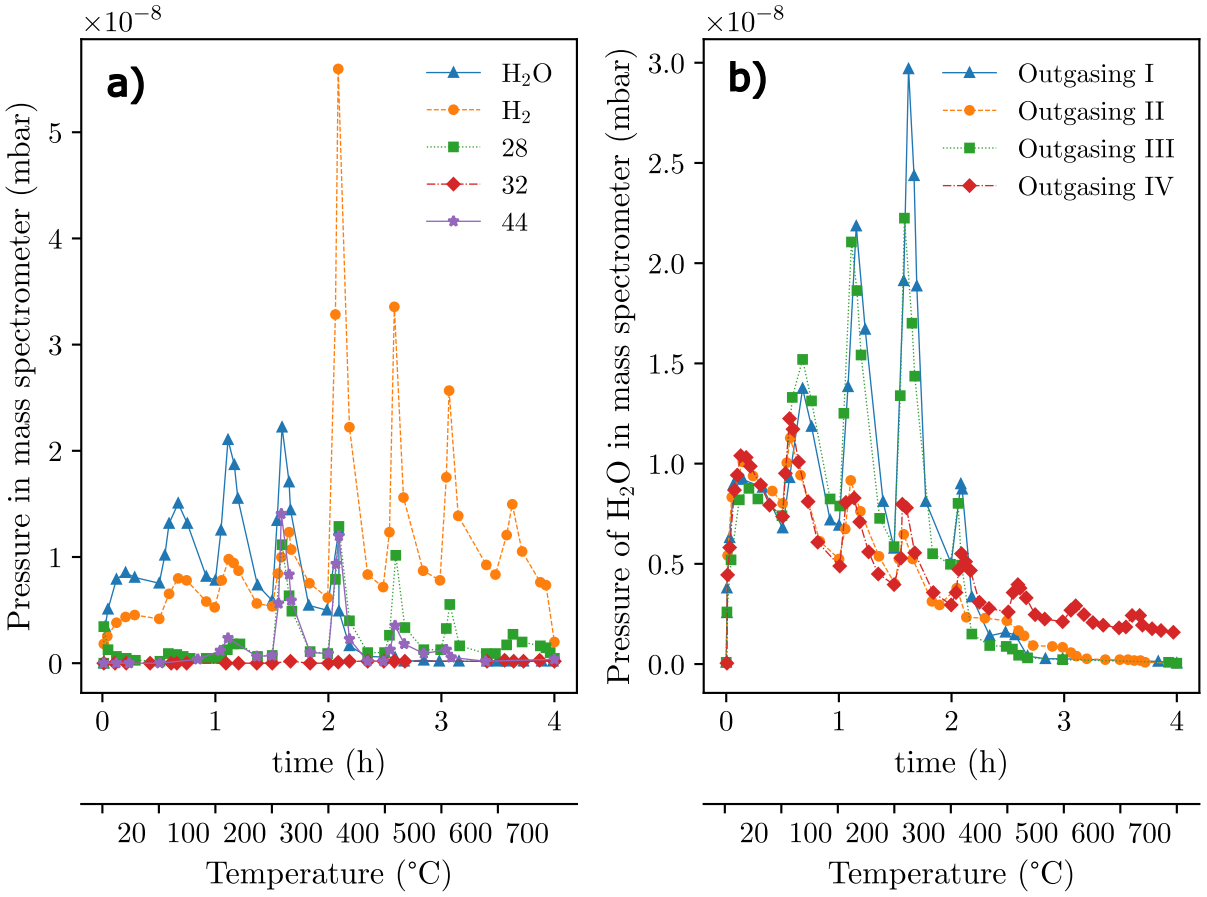


Figure 2.38: Outgassing of differently pre-treated SS316 specimens in consecutive 100-degree steps: (a) mass spectrometrically determined total outgassing and (b) outgassing of water (after [Ake96]).

$$x\,\mathrm{Me} + y\,\mathrm{H_2O} = \mathrm{Me}_x\mathrm{O}_y + y\,\mathrm{H_2}\ .$$

generating molecular hydrogen.

The formation of oxides was supported by i) X-ray photoelectron spectroscopy measurements which revealed an increase of the oxide layer on the SS316 stainless-steel surface by about 3 nm and ii) a simultaneous decrease of the partial pressure of water at temperatures exceeding 600 K (see Fig. 2.38b).

Åkermark et al. also carried out outgassing runs with stainless steel SS316 under vacuum at temperatures up to 973 K in which they compared the H_2O release characteristics following mechanical grinding of the surface with SiC paper and ultrasonic cleaning in ethanol with that

after exposure of previously outgassed specimens to ambient air having a relative humidity of 30 - 40 % for only 5 minutes. Purpose of the runs was to discern between the gas liberated from the bulk of surface of the specimens. As apparent, the water outgassing spectrum displayed by SS316 specimen subjected to the sequence surface preparation/outgassing or outgassing/air exposure (runs I and III in Fig. 2.38b) is very similar suggesting absence of water in the bulk. The concentration of hydrogen in the bulk of stainless steel SS316 obtained after degassing at temperatures up to 973 K was determined to be 0.8 ppm by weight.

Sharpe et al. [Sha16][29] postulated a mechanism of tritium migration from the bulk of aluminum 6061, oxygen-free high conductivity copper (OFHC) or stainless steel 316 to generate a tritium-rich water layer on the surface of the metals, which is broadly in line wth observations reported formerly by Austin [Aus72] and Penzhorn et al. [Pen13a]. Sharpe et al. hypothesized that "water layers" on metal surfaces constitute reservoirs of significant storage capacity for tritium, the concentration ratio across the water layer- metal surface being uniquely determined by the ratio of solubility's across this interface. While the isotopic composition of the hydroxyl layer is influenced strongly by the type of substrate metal this is only marginally the case for the isotopic composition of the outer water layers. Arguably, such a water/hydroxyl layer will have a rather large retention capacity for tritium. At equilibrium conditions, the concentration of hydrogen isotopologues in the metal is simply given by the solubility at the prevailing temperature. The actual number of outer water layers will depend on the substrate metal, the prevailing temperature and the partial pressure of water vapour to which the metal is exposed. The water layer was assumed to consist of hydroxyl groups bound to an ever-present metal oxide layer on the metal surface (non-mobile) as well as of adsorbed water molecules on the top outer surface (mobile water) [Thi87; Car12; Pen13a]. Experimentally, the tritium-rich water layers on the loaded metal specimens were removed by short exposures to a series of argon plasmas. Between exposures to plasmas water layers on the specimens suspended in a 2 l vacuum chamber purged with argon were quickly replaced by tritum-free water. During the dwell period, tritium was expected to migrate into the newly adsorbed water layers. It was postulated that the migration rate of tritium to the surface could only take place by one of three mechanisms:

[29] There are indications that water layers are present on the surface of most metals [Thi87; Car12; Pen13a]

(i) The removable tritium residing in the water/oxide layer reequilibrates within these layers during the dwell period.

(ii) Tritium migrates from the bulk into the surface layer at a constant rate.

(iii) Surface layers are replenished with tritium by diffusion from the bulk.

Because the first two options grossly underpredicted the experimental results it was concluded that during the dwell period between plasma exposures tritium atoms are transferred from the bulk to the water layer by Fickian diffusion. Hence, the sample recovers from each plasma exposure by re-populating the tritium deficient water layer from tritium in the bulk near the interface. Because the tritium migration rate is diffusion-limited, the tritium concentration in the water layer can not return to its original value within the short dwell period of only 2 s. Therefore, the amount of tritium released decreased regularly with each exposure to plasma. It was furthermore shown in sequential exposures to plasmas utilizing normalized data that the trend of activity removal does neither depend on loading conditions nor on the storage time of the loaded specimens (after charging with tritium the specimens were stored under helium for different periods).

According to the model, a perturbation of the water layer + surface/bulk system, for instance by diminution of the tritium concentration in the water layer via exchange with atmospheric moisture, will cause generation of a concentration gradient which in term will promote migration of tritium from the bulk to the surface. Because the migration is determined by diffusivity of tritium through the metal it will strongly depend from the prevailing temperature. Conversely, exposure of metals to gaseous tritium will rapidly saturate the water layer on the metal surface. Thereafter the bulk will accept tritium from the water layer at a rate which is determined by the excess concentration in the water layer with respect to that of the solubility and diffusivity of hydrogen in the base metal [Sha16]. Once exposure is terminated, the concentration of tritium on the surface will again decreases to a value essentially determined by the solubility of hydrogen in the metal. What is more, tritium transport from the bulk to the surface can be stimulated by replacing the tritium-rich water layers on the surface by tritium-deficient layers. Model predictions suggest that the equilibration time for the tritium concentration within the water layer is significantly shorter than that expected from diffusivity in the metal bulk [Sha16]. The impact on the detriation of stainless-steel is, however, only minor [Tor04].

From the known bulk solubility of hydrogen in metals, S_{bulk}, it was possible to calculate the surface solubilities of hydrogen, S_{surface}, on aluminium 6061, copper (OFHC), and SS316 employing the relationship

$$S = \frac{S_{\mathrm{surface}}}{S_{\mathrm{bulk}}} = \frac{[\mathrm{HTO}]}{[\mathrm{T}]} = K_{\mathrm{eq}}$$

To obtain the amount of tritium in the surface layer a series of subsequent plasma exposures were carried out. They provided evidence that after about 10 exposures the tritium concentration in the surface dropped to a very low level while the overall inventory in the specimen remained essentially unchanged. Hence, the total amount of tritium released in a series of plasma exposures was taken to constitute the surface tritium. In accordance with expectations, the surface solubilites on the three metals were found to be comparable, i.e. $(53 \pm 2)\,\mathrm{kmol\,m^{-3}}$, $(50 \pm 1)\,\mathrm{kmol\,m^{-3}}$ and $(17.5 \pm 0.3)\,\mathrm{kmol\,m^{-3}}$ for Al, Cu, and SS316, respectively. The respective surface thicknesses were reported to be 0.54 nm, 0.54 nm and 0.92 nm.

In conclusion, in spite of much recent work shedding light on the mechanism describing tritium uptake and release from metallic surfaces, further research is necessary for a conclusive elucidation of the various single processes.

2.14.1.5 Transport of tritium across stainless-steel's commonly employed in tritium handling systems

Most diatomic gases dissolve in metals following previous dissociation. Sieverts law states that the amount of a diatomic gas dissolved in a solid is proportional to the square root of the prevailing pressure. The expression that relates the amount of hydrogen dissolved in a metal, S, with the absolute temperature, T and the hydrogen pressure, P, is known as Sieverts law

$$S = K_{\mathrm{S}}\sqrt{P}$$

where K_{S} is the Sieverts constant. The temperature dependence of this constant is obtained from relationship

$$K_{\mathrm{S}} = K_{\mathrm{S}}^{0} \exp\left(-\frac{Q_{\mathrm{S}}}{RT}\right)$$

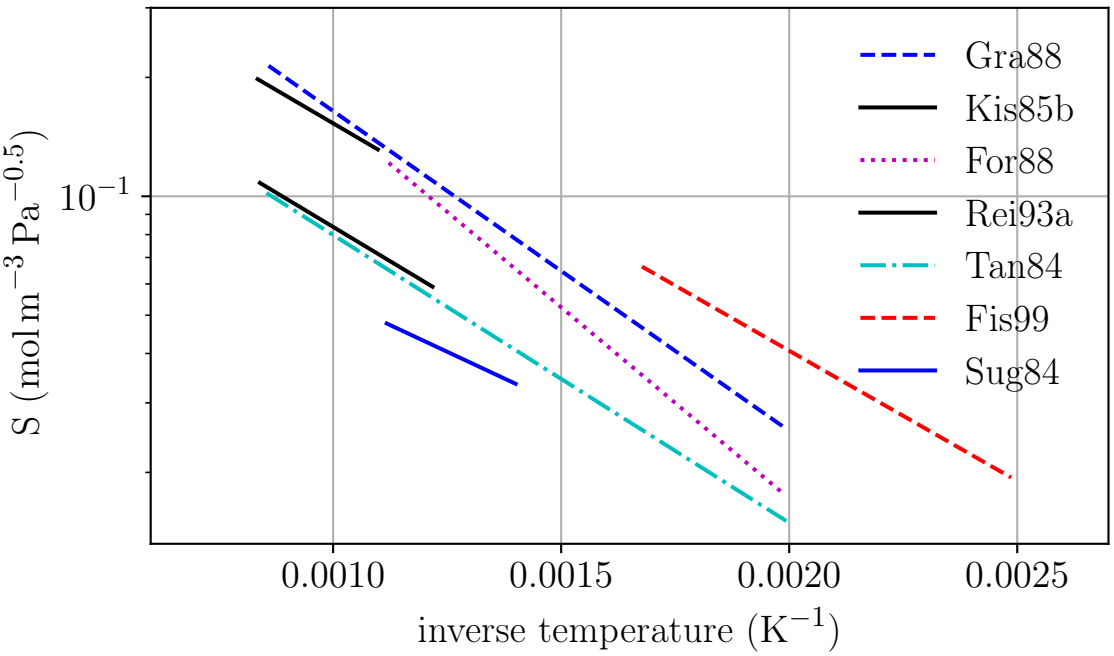


Figure 2.39: Comparison of Sieverts constants determined for hydrogen and tritium in type SS316 and SS316L stainless-steel as function of inverse temperature by several investigators (for further details and references refer to Table 2.41).

in which K_S^0 is the Sieverts pre-exponential factor in mol m^{-3} Pa$^{0.5}$, Q_S the heat of solution, T the absolute temperature in Kelvin and R the gas constant. Sieverts constants for the solubility of hydrogen isotopes in several types of austenitic steels and nickel alloys frequently employed in tritium installations or contemplated for ITER have been compiled in Table 2.42. The indicated temperature ranges are the ones used in the respective experimental studies.

Sieverts constants for hydrogen and tritium in stainless-steel type SS316 and SS316L are plotted in Fig. 2.39. The data show that in spite of considerable differences in experimental approach, type of sample and kind of pre-treatment scattering is moderate.

Diffusion coefficients of all tree hydrogen isotopes through ITER relevant stainless-steel's as well as through a selected number of nickel alloys are compared in Table 2.41. As seen, a rather consistent set of data published by numerous researchers using a variety of experimental techniques has emerged over the past fourty years. Stainless-steel types 304 and 316 show essentially the same diffusion coefficients for hydrogen [Aus72; Gra88]. The good agreement between results obtained by several investigators for type SS316 and 316L is illustrated in

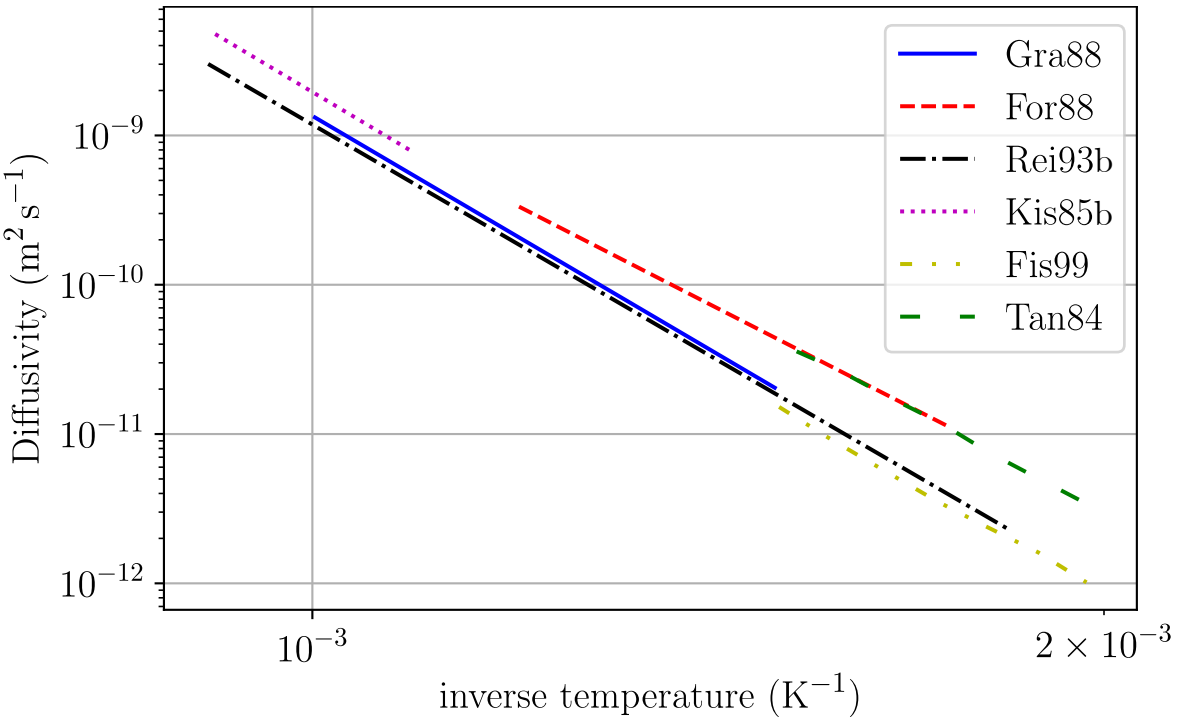


Figure 2.40: Comparison of hydrogen and tritium diffusivities across stainless-steel type 316 and SS31L as function of inverse temperature determined by different research teams (references are assinged in Table 2.42).

Fig. 2.40. The plot does not include the diffusivities determined by Shan et al [Sha91] and by Hirabayashi and Saeki [Hir84a] which depart strongly from the general trend.

Longhurst investigated the permeation of tritium through stainless-steel at ambient and elevated temperature. He reported that HT converts relatively easily into HTO on the metal surface particularly at higher temperatures (773 K) [Lon07]. Under the assumption that the conversion of HT into HTO is a surface process, the fraction of non-converted HT can be obtained from expression

$$\frac{C}{C_0} = \exp\left[-1.987 S \exp\left(-\frac{62,840}{RT}\right) t\right] ,$$

where C is the concentration of HT in m^{-3}, C_0 the initial concentration of HT in m^{-3}, S the surface to volume ratio of the system in m^{-1}, R the universal constant in $J\,mol^{-1}\,K^{-1}$, T the temperature in K and t the time in min. From an Arrhenius plot of the experimental results the activation energy was calculated to be 62.84 kJ mol^{-1}.

Table 2.41: Sieverts constants for hydrogen isotopes in several austenitic stainless-steels and nickel alloys.

Material	Hydrogen isotope	K_S^0	Q_S	Temperature range	Ref.
		mol $m^{-3}Pa^{-0.5}$	kJ mol^{-1}	K	
304	H	0.443	9.03	473 - 703	[Fis99]
304	H	0.384	9.60	373 - 873	[Nel73]
304L	H	0.180	5.86	400 - 714	[Lou75a]
316	T	0.19	10.2	703 - 903	[Sug84]
316	H	0.43	13.9	500 - 1200	[Tan84]
304	H	0.76	15.7	500 - 1200	[Tan84]
316	H	1.11	15.7	500 - 910	[Gra88]
316L*	H	1.50	18.5	523 - 873	[For88]
316L**	H	0.46	20.9	523 - 873	[For88]
316L	H	0.71	12.6	873 - 1173	[Kis85b]
316L	T	0.41	13.1	773 - 1473	[Rei93b]
316L	H	0.81	12.47	473 - 703	[Fis99]
304L	H	0.31	20.9	573 - 673	[Jon65]
16Cr-15Ni3Mo-Ti***	T	0.077	5	760 - 1090	[Dol00]
Inconel 600	H	1.61	21.3	873 - 1173	[Kis85b]
Inconel 750	H	0.63	11.6	873 - 1173	[Kis85b]
Nimonic 80A	H	0.76	11.6	873 - 1173	[Kis85b]
Hastelloy X	H	1.83	21.3	873 - 1173	[Kis85b]

* Commercial

** Heat treated

*** Austenitic steel

Remarkably, practically no difference could be detected between HTO and elemental tritium gas (HT) as permeation driving force through stainless-steel at equal initial partial pressures and elevated temperature, i.e. 773 K [Lon07]. Permeation of HTO was explained by dissociation of water molecules on the hot stainless-steel surface. The experimental evidence suggests adsorption of molecular water on the surface as first step followed by dissociation and isotopic exchange of

Table 2.42: Diffusion coefficients of hydrogen isotopes through ITER-relevant austenitic stainless-steels and nickel alloys.

Type of SS	Hydrogen isotope	D_Q^0	ΔE	Temperature range	Ref.
		$m^2\,s^{-1}$	$kJ\,mol^{-1}$	K	
304	T	1.8×10^{-6}	58.9	298 - 495	[Aus72]
304	H	2.72×10^{-6}	54.4	373 - 873	[Nel73]
304	H	1.2×10^{-6}	54.9	600 - 1000	[Gra87]
304	H	6.4×10^{-7}	53.40	473 - 703	[Fis99]
304	H	8.3×10^{-7}	49.7	500 - 1200	[Tan84]
304	T	1.29×10^{-6}	58.7	373 - 573	[Cha70]
304L	H	4.7×10^{-7}	54.0	400 - 714	[Lou75c]
304L	H and D	2.1×10^{-7}	59.4	573 - 673	[Jon65]
316	T	1.8×10^{-6}	52.9	298 - 495	[Aus72]
316	H	7.3×10^{-7}	52.4	500 - 910	[Gra88]
316	H	6.3×10^{-7}	47.8	500 - 1200	[Tan84]
316L	H	1.3×10^{-6}	54.1	873 - 1173	[Kis85b]
316	H	7.3×10^{-7}	52.4	500 - 833	[Gra88]
316L	H	4.8×10^{-7}	51.6	473 - 703	[Fis99]
316L	T	5.9×10^{-7}	51.9	500 - 1200	[Rei93b]
316L*	H	3.8×10^{-7}	45.5	523 - 873	[For88]
316L**	H	7.7×10^{-7}	42.5	523 - 873	[For88]
16Cr-15Ni3Mo-Ti***	T	1.2×10^{-5}	85.0	760 - 1090	[Dol00]
Inconel 600	H	4.9×10^{-7}	42.5	873 - 1173	[Kis85b]
Inconel 750	H	1.6×10^{-6}	53.1	873 - 1173	[Kis85b]
Nimonic 80A	H	1.4×10^{-6}	53.1	873 - 1173	[Kis85b]
Hastelloy X	H	4.9×10^{-7}	43.5	873 - 1173	[Kis85b]

* Commercial

** Heat treated

*** Austenitic steel

tritium with surface bound water. The observations of Longhurst [Lon07] are in good agreement

with results from other studies on the interaction of tritium with stainless-steel [Tor05b; Pen12; Tor15b; Sha16].

For a given isotope of hydrogen and a given temperature, the permeability of a metal is simply obtained from the product of diffusion, D, and solubility, S, i.e.

$$P = D \cdot S = P_0 \exp\left(\frac{E_\mathrm{P}}{RT}\right) \ .$$

LeClaire [Cla91] and Shiraishi et al. [Shi99] compiled permeation constants for hydrogen isotopes through austenitic stainless-steels type SS304 and SS316. Reiter et al. [Rei85] provided averaged Arrhenius equations (10 papers) for the solubility, diffusivity and permeability of all three hydrogen isotopes across stainless-steel 316L in the temperature range 600 - 900 K and pressures in the range 10^2 - 10^5 Pa (see Table 2.43). As apparent from the compilation in the table the agreement between results for protium, deuterium and tritium obtained by numerous investigators, which to a large extent used different techniques, is surprisingly good. Permeability's of hydrogen across austenitic steels seem to be relatively insensitive to bulk composition. LeClaire [Cla91] was able to show that within a factor of 1.5 the permeation results of about 30 investigations on steel containing 15 - 26 % chrome and 6 - 28 % nickel the permeation of hydrogen across SS316 can be calculated using the permeation constant $P_\mathrm{m}(T)$

$$P_\mathrm{m}(T) = 3.26 \times 10^{-7} \exp\left(-\frac{66.2\mathrm{kJ\,mol^{-1}}}{RT}\right)$$

where $P_\mathrm{m}(T)$ has units of $\mathrm{mol_{H_2}\,m^{-1}\,s^{-1}\,Pa^{-0.5}}$.

Care must be exercised when employing "as-received materials or only mildly conditioned materials" for the manufacture of components utilized in tritium service. Calculations performed with data from Tables 2.41 – 2.43 for the design of components may deviate significantly from reality because coefficients given in these tables were mostly obtained with materials subjected to rather stringent pre-conditioning treatments.

One reason for gross differences in permeation rates determined by different authors is that surface impurities on stainless-steel type SS316L can modify the boundary processes by which hydrogen isotopes adsorb on and diffuse into metals. In addition, internal trapping sites can in some cases promote and in others retard dissolution and diffusion of hydrogen in metals.

Dislocations, interstitial vacancy clusters, surface and interstitial impurities, grain boundary effects, voids and gas bubbles have all been shown to influence considerably the migration profile of hydrogen isotopes across metals.

The steady state permeation rate or rate of flow per unit area, J, through a slab of thickness d when a pressure p_1 of gas is maintained at one side and a lower pressure p_2 subsists on the other, is given by **Richardson´s law**, i.e.

$$J = \frac{DK_{\mathrm{S}}}{d}\left(p_1^{1/2} - p_2^{1/2}\right) \ .$$

For the Richardson equation to hold it is required that the rate of solution of adsorbed atoms into solid solution, i.e. molecular adsorption and dissociation, must be much greater than the rate of flow J. If this is not the case J is lower than calculated from Richardson law but still proportional to $\sqrt{p}$.

The changeover from a diffusion-controlled Richardson law type of permeation to a slower, surface-rate controlled permeation P_{s} occurs over two or three orders of magnitude range of pressures centered on a value given by

$$P_{\mathrm{s}} = \left(\frac{2P_1}{Ad}\right)^2$$

where A is a constant describing the arrival rate of atoms on adsorption sites on the metal surface [Cla91]. As a consequence, it is not possible to predict accurately permeation rates at very low pressures. On the other hand, the "diffusion controlled" permeability predicted by the Richardson law will always give the maximum rate of steady state permeation, which is important to know, particularly when dealing with tritium.

Table 2.43: Pre-exponential factors and activation energies for solubility, diffusivity and permeability of hydrogen isotopologues across SS316L.

Gas	Sieverts´ constants		Diffusivity		Permeability		Ref.
	$mol\,m^{-3}\,MPa^{-0.5}$	$kJ\,mol^{-1}$	$m^2\,s^{-1}$	$kJ\,mol^{-1}$	$mol\,m^{-1}\,s^{-1}\,Pa^{-0.5}$	$kJ\,mol^{-1}$	
H	4.27×10^2	13.9	0.63×10^{-6}	47.8	2.7×10^{-7}	61.7	[Tan84]
H	-	-	-	-	2.4×10^{-7}	63.5	[Dev80b]
H	-	-	-	-	4.2×10^{-7}	67.3	[Shi99]
H	-	-	0.73×10^{-6}	52.4	8.1×10^{-7}	68.1	[Gra88]
H	1.5×10^3	18.51	0.38×10^{-6}	45.5	1.8×10^{-7}	64.0	[For88]
H	7.15×10^2	12.6	1.3×10^{-6}	54.1	8.8×10^{-7}	66.7	[Kis85b]
H	-	-	-	-	1.52×10^{-7}	60.9	[Has85]*
D	-	-	-	-	3.5×10^{-7}	68.7	[Shi99]
D	1.80×10^2	5.86	0.47×10^{-6}	54.0	8.5×10^{-8}	59.8	[Lou75a]
T	1.31×10^2	8.24	5.9×10^{-7}	51.90	2.06×10^{-7}	63.6	[Rei93b]**
T	-	-	-	-	3.44×10^{-7}	68.1	[Bel79a]

* used SUS316, the Japanese designation for type SS316 stainless-steel

** Tritium properties were calculated by application of quantum statistical partition functions to solution and diffusion data

The bulk permeability of hydrogen through stainless-steel has been determined employing **palladium coated stainless-steel** specimens [Swa79]. For this purpose, specimens of several steel´s were first sputter-cleaned and subsequently sputter-coated on both sides with a thin palladium film ($< 100\,\text{nm}$). Palladium was not only selected because of its ability to protect the sputter-cleaned surface from re-oxidation but also because of its good adherence, high hydrogen diffusivity and high permeability. The results showed that permeation rates through oxidized specimens are two to three orders of magnitude lower than through palladium-coated stainless-steel. Experiments with tritium and deuterium provided evidence that bulk permeabilities of three different sputter-cleaned, palladium coated steels were nearly identical in spite of their fairly different bulk composition. The same observation was made by LeClaire a few years later [Cla91]. Hence, differences in surface layer composition are largely responsible for differences in permeability observed with untreated materials. According to another interesting finding, whereas surface effects taking place on the upstream oxide side are rate determining those on the downstream side are comparatively unimportant.

Type 316 stainless-steel loaded thermally with tritiated hydrogen at 573 K shows a thin layer on the top surface with tritium concentrations by and large exceeding those in the bulk [Tor07]. In comparison to the total tritium uptake by the specimen the absolute amount of tritium trapped on the surface is small. Tritium trapped in the surface layer was found to be distinctly more resistant to thermal release than tritium incorporated into the bulk. If the surface layer is removed by chemical etching, it slowly regrows while trapping a fraction of chronically released tritium.

There is a fair body of evidence supporting the occurrence of **chronic release** (CR) of tritium from stainless-steel at ambient temperature. The evidence comprises i) tritium liberation at nearly constant rate for an extended period of time [Tor05b], ii) tritium egress into stirred water in a closed containment with nearly the same rate as into the gas phase [Pen06], iii) decrease of total tritium inventory by ageing significantly beyond that arising from radioactive decay [Pen12] and iv) characteristic and predictable evolution of the tritium depth profile in the metal bulk with ageing [Tor05b]. All these measurements deliver consistent results among each other, i.e.: i) approx. the same CR into water and into a gas stream, ii) the integral CR into a gas stream (includes decay) matches the decrease in total bulk inventory determined by full etching after

completion of an experiment and iii) evolution of the tritium depth profile correlates with the observed inventory loss.

The chronic release of tritium at ambient temperature from tritium-contaminated stainless-steel constitutes "an aging" loss of comparable importance to that of radioactive decay. It therefore impacts on i) tritium inventory determinations, ii) waste sentencing, and iii) on waste storage from a radiological point of view.

Suitable models have been developed [Nao08; Pen10] for the prediction of the long-term liberation of tritium via chronic release and simultaneous tritium loss by radioactive decay from stainless-steel contaminated either homogeneously (initially approx. same concentration throughout, see Fig. 2.41) or non-homogeneously (concentration profile going through a maximum at the subsurface of the material, see Fig. 2.42). As apparent from Fig. 2.41 the loss of tritium inventory from homogeneously loaded specimens taking place during an ageing period totalling 2.3 years can be predicted reasonably well with a one-dimensional diffusion model[30]. Surprisingly, the activity in the surface layer does not appear to diminish with ageing time. However, even in the event of tritium firmly trapped in the surface layer a slight decrease would be expected on account of radioactive decay. Since this was not the case in several specimens examined over prolonged periods, it was postulated that slow replenishment of decayed tritium takes place in the surface layer. In fact, a comparison of the O1s X-ray photoelectron spectrum of the pristine stainless-steel surface with that of a specimen aged 2.9 years revealed that the initial $O/OH > 1$ ratio reversed into a $O/OH < 1$ ratio[31] [Pen13a]. Moreover, the Cr/Fe ratio became much smaller than that of the reference material. This was attributed to an enrichment of Fe_2O_3 on the metal surface. The observed $O/(Cr + Fe)$ ratio together with the reversal of the O/OH ratio on the aged specimen could only be rationalized by the formation of hydroxides (i.e. "trapping") of the kind $Cr(OH)_3$, CrOOH, $Fe(OH)_3$ or FeOOH[32]. It was postulated that during the ageing process atmospheric moisture is incorporated into the surface layer in form of OH groups which in turn retain tritium diffusing from the bulk to the surface via an exchange mechanism.

[30] It must be considered that even though all specimens were loaded under identical conditions each inventory measurement required a different specimen. From experience it is known that under these conditions the experimentally determined loading some times show significant scattering.

[31] Y. Hatano, Personal communication, 2009

[32] The existence of OH groups and H_2O in the surface layer of stainless-steel SS316 has also been observed by other investigators [Han02; Oya03; Tan08].

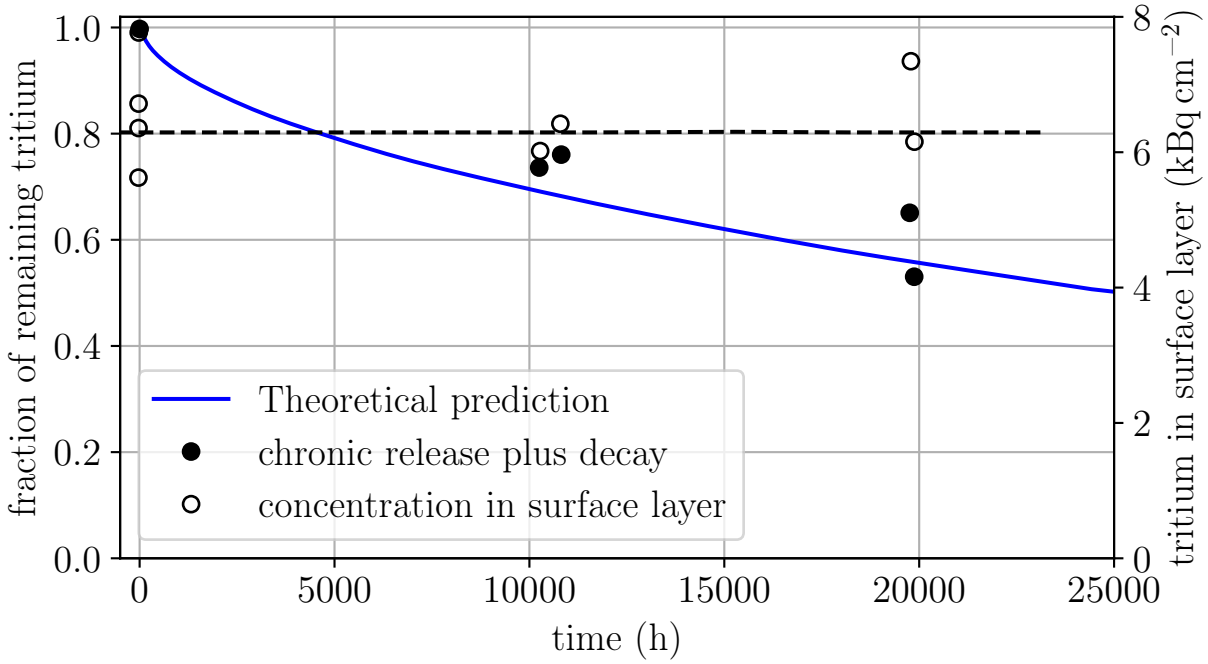


Figure 2.41: Comparison between experimentally determined total long-term loss (radioactive decay plus chronic release) at ambient temperature from stainless-steel type 316 specimens (black circle) with theoretical prediction (—). The original loading of the specimen was (0.33 ± 0.18) MBq/ specimen. The concentration of tritium in the surface layer (circle) during the same period of time remained essentially constant (broken line).

Figure 2.42 displays tritium depth profiles obtained with two type SS316 specimens supplied to HRC, Toyama by JET, already charged with tritium [Pen12]. Both specimens, whose dimensions were 6 x 15 x 15 mm^3, were loaded at JET under identical conditions. Because of their comparatively large thickness and the selected loading conditions they incorporated tritium only just beneath the surface. Both specimens were stored in a hood and aged under ambient conditions. After 2.56 years of storage one of the specimens was chemically etched. The results indicate that a fraction of tritium was liberated into ambient by chronic release (primarily from depths $< 0.02\,\mu$m) and another fraction penetrated deeper into the bulk (depths $> 0.02\,\mu$m). Etching of the other specimen after an even longer ageing period, i.e. after 4.86 years, revealed a flatter depth profile and deeper penetration of tritium into the bulk. Apparent from figure 2.42 is also a significant additional decrease of the tritium inventory remaining in the second specimen. The lost inventory is explained on one hand by chronic release into the environment and on the other by radioactive decay. After adaptation of the diffusion model to the particularities

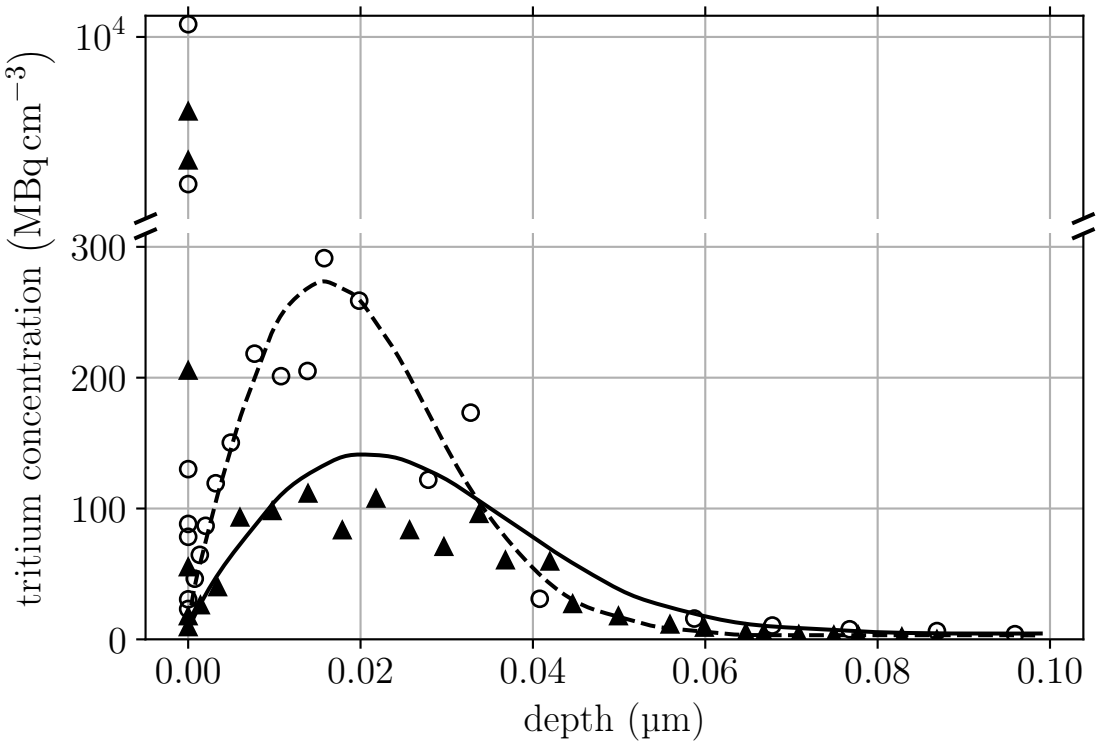


Figure 2.42: Depth profiles of tritium in non-homogeneously loaded type 316 stainless-steel specimens of 6 mm width supplied to HRC by JET. Shown are results obtained with two specimens aged either 2.56 ○ or 4.86 ▲ years at ambient temperature. Note the high concentrations of tritium at the specimen´s surface. Solid lines are theoretical predictions [Pen12].

of non-homogeneously loaded specimens, the evolution of the tritium depth profiles of both specimens could be simulated over their corresponding period of ageing [Pen12].

Recapitulating, reliable predictions of the inventory decrement induced by thermal treatment and/or chronic release requires detailed knowledge of the contamination history of the material: i) date or dates of exposure to tritium, ii) temperature and pressure at which the exposure took place including concentration of tritium prevailing in the gas phase, and iii) the achieved degree of loading. From this information the type of loading, i.e. homogeneous or non-homogeneous and the amount of tritium remaining in the material can be estimated.

Pertaining waste conditioning of materials charged non-homogeneously, it is important to realize that during a thermal treatment tritium initially incorporated just beneath the topmost

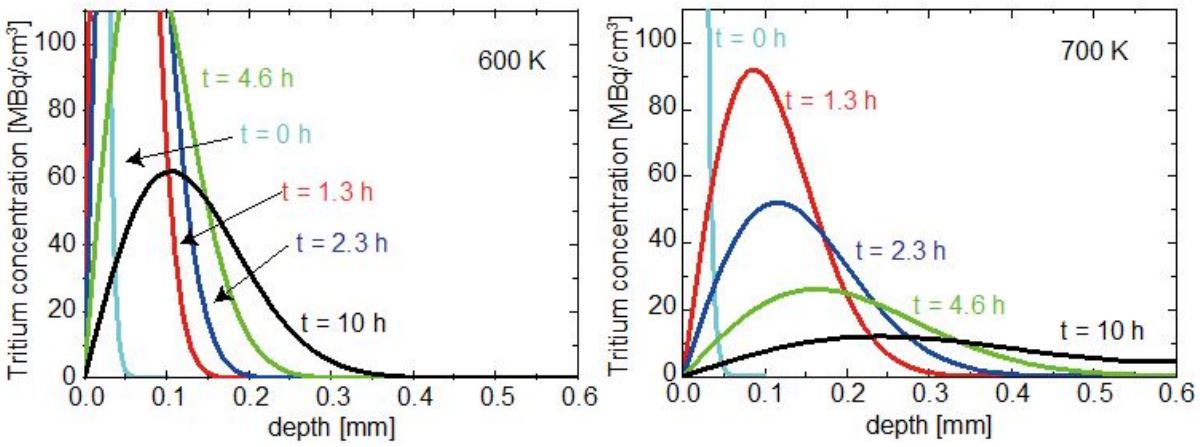


Figure 2.43: Calculated tritium depth profiles in initially non-homogeneously loaded stainless-steel 316L material heated at either 600 K (upper curves) or 700 K (lower curves) for 0.0, 1.3, 2.3, 4.6 or 10 hours [Pen12].

surface, will increasingly spread across the whole metal matrix. Hence, particularly in case of a capacious matrix, the waste will become increasingly impervious towards decontamination.

Fig. 2.43 displays calculated tritium depth profiles of a non-homogeneously charged SS316 stainless-steel specimen assumed to contain originally 57 000 MBq cm^{-3} tritium after being heated at either 600 K or 700 K for progressively increasing periods of time. The plots were predicted with a one-dimensional diffusion model [Nao08; Pen12]. As evident, heating at elevated temperature is not only associated with tritium release but also with penetration of an important fraction of tritium deep into the bulk. With increasing conditioning temperature, the degree of tritium penetration and therefore the degree of homogenization at low level increases. This trade-off needs to be considered when designing a conditioning strategy for solid waste.

2.14.1.6 Pre-treatment of stainless-steel specimens for experimental studies

Austin et al. [Aus73] as well as several other investigators [Cas77; Ada83; Sug85; Chê07; Uch08] have provided evidence that coefficients of solubility and diffusivity of hydrogen isotopologues across as received or only mildly pre-treated materials can differ substantially from coefficients gained with metals or alloys subjected to a rigorous pre-treatment. Consequently, to obtain reproducible absolute diffusivity, solubility and permeability values it has become customary to pre-treat metallic specimens under rather severe conditions. Typical pre-treatment conditions

for stainless-steel specimens consist in annealing the polished material at 1200 K for more than 2 hours [Tan84]. Reiter et al. [Rei93a] first cleaned their specimens chemically and thereafter heat-treated them under 1 bar hydrogen for 24 hours at 1300 K. This not enough, the specimens were subsequently heated under ultra-high vacuum for further 24 hours at the same elevated temperature. "As received" materials display significantly different permeation values than materials subjected to rather severe pre-treatment conditions. Therefore, substantial corrections may become necessary for the calculation of permeation rates across heated materials employed for the manufacture of components used in tritium service. In order to meet the stringent safety standards required for tritium apparatuses and in view that severe pre-treatments are not always possible, the selection of materials should not be based on "best" solubility, diffusivity, and permeation coefficients but rather on values obtained with "as received" or only mildly pre-treated materials. In critical cases, permeation experiments under realistic simulation of the anticipated conditions are recommended.

2.14.1.7 Transport of hydrogen isotopologues across a lengthy stainless-steel (or copper) pipe

In an investigation performed by Longhurst [Lon08], the concentration of deuterium highly diluted in ultrapure nitrogen that passed at low flow rates either through a stainless-steel type SS304 or a copper pipe, was determined in the exhaust stream. The pipe was up to 33 m long and had an outer diameter of 3.1 mm, i.e. $1/8^{\text{th}}$ inch. Whereas the copper pipe showed the expected breakthrough, i.e. the time lag corresponded to the one it takes for the gas to travel through the system, this was not the case with the stainless-steel pipe. This behaviour also manifested in the shape of the breakthrough curve, which in case of stainless-steel was much more like a diffusion transient than a breakthrough. At the end of the stainless-steel pipe there was strong delay with respect to the time estimated for the gas to travel from the inlet to the tube outlet point. This was considered to constitute evidence for adsorption of deuterium on and diffusion into the stainless-steel bulk as it travelled along the tube. What is more, at the downstream side of the tube it was noticed that most deuterium had converted into deuterated water. To better comprehend these observations a model essentially based on rapid hydrogen/water interconversion, classical diffusivity and Sieverts' law on solubility of molecular hydrogen in metals was developed. The model was verified by a good agreement with

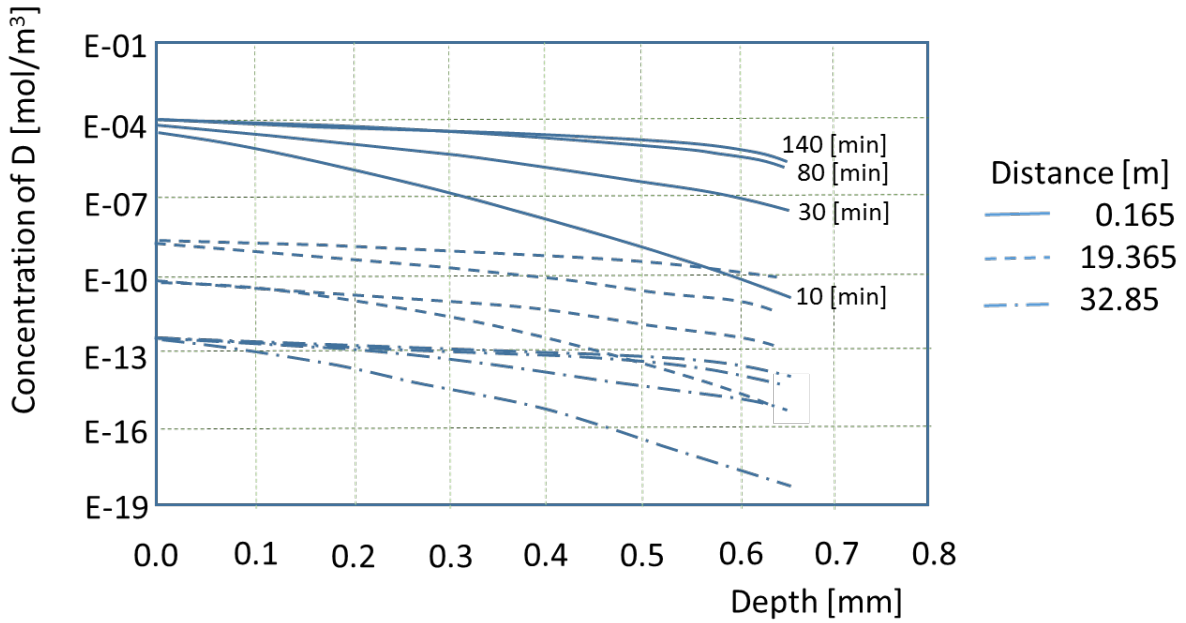


Figure 2.44: Calculated semi logarithmic plot of deuterium depth in a stainless-steel tube as function of tube length and time between injection and measurement at ambient temperature (after [Lon08]).

experimental results obtained earlier by Nishikawa et al. [Nis92a] and Shiraishi et al. [Shi97]. Calculations show that the longer breakthrough times reflect the saturation time of atomic deuterium in the pipe wall. It follows, that the concentration of highly diluted hydrogen isotopes in a long tube will depend upon factors such as length of the tube, time at which the measurement is performed, temperature, concentration of hydrogen in the carrier gas, condition of the metal surface, etc. As evident from Fig. 2.44, which shows calculated deuterium depth profiles on the inner wall of stainless-steel tubing as function of tube length and measurement time, the effect can be quite pronounced. From a practical point of view, it is apparent that this effect may be of much consequence to analytic measurements carried out with capillary tubing particularly when dealing with diluted hydrogen isotopes.

2.14.1.8 Tritium in-growth into stainless-steel containments

In-growth of tritiated protium and/or impurities such as tritiated water or tritiated hydrocarbons into tritium pre-exposed vessels containing calibrated tritium-bearing gases can modify the composition of these gases to the extent of making them useless within a relatively short time,

i.e. weeks or months [Car75; Mor77; Gil80]. Impurity in-growth may also play a role at several systems of a fusion machine. The formation of tritiated hydrogen is explained by exchange reactions between gaseous hydrogen isotopologues and dissolved or chemically bound tritium existing on the surface of stainless-steel. Tritiated hydrocarbons, e.g. tritiated methane, are generated by reaction between gaseous tritium and thin oil films or grease sticking to the inner surface of stainless-steel vessels or with carbon present on the surface or subsurface of the metal alloy.

Another equally problematic situation arises when a vessel is pre-exposed to a high level of tritium and subsequently evacuated. In case non-radioactive gases are introduced into this containment they will become contaminated. According to Carlson [Car75] "a storage tank once used for the containment of tritium will forever continue to contaminate cold gases contained within, even after numerous purges". He added "Such tank can easily add 1 ppm tritium to the contained gas" and further "It should be remembered that 40 hours per week of exposure to $6.7 \times 10^7\,\mathrm{Bq\,m^{-3}}$ of tritium (gas) or $2 \times 10^5\,\mathrm{Bq\,m^{-3}}$ of HTO is equivalent to an adsorbed dose of $5\,\mathrm{rem/y}$[33].

Off-the-shelf vessels made of 30.5 cm long stainless-steel type SS304 piping having an outer diameter of 3.8 cm and an inner diameter of 3.5 cm, a volume of $293\,\mathrm{cm^3}$, and an inner surface area of $353\,\mathrm{cm^2}$ were filled with 1.24 bar of 95 mol % tritium and examined for methane growth at ambient temperature [Mor77]. Analysis of the gas phase revealed formation of polytritiated methane. While the rate of methane formation was found to be affected by the previous surface cleaning history (comparison with an as-received test vessel previously degreased with trichlorotrifluoro ethane or trichlorotrifluoro ethylene in an ultrasonic bath followed by acetone/trichlorotrifluoroethane rinses), neither the temperature ($298 < T < 373\,\mathrm{K}$) nor the type of bake-out procedure (comparison between as-received test vessel and a test vessel baked out at423 - 433 K under vacuum for 12 hours) showed much influence. Typical concentrations of methane in the range 2 - $40\,\mathrm{cm^3}$ (STP)/$\mathrm{m^2}$ of stainless-steel surface were detected. Non-polished containers generated impurities one to two orders of magnitude more abundantly than polished vessels. It was concluded that the best method to control methane formation is to mechanically clean the surface, rinse with an adequate agent, and do not bake the surface. It appears that most of the methane formed is generated by carbon on the tubing surface arising from manufacture.

[33] Consider a tank previously exposed to tritium and thereafter opened to ambient air.

This carbon cannot be removed by degreasing. Degreasing agents were suspected to magnify the problem.

With respect to suppression of methane formation, stainless-steel first polished with a dry paper was found to be more effectively cleaned than by solvents or an electro polishing technique [Gil80]. It was concluded that methane formation can be nearly suppressed by careful cleaning of the vessel inner surface. Tritiated methane´s could also be eliminated almost completely by treating the metallic surfaces with pure tritium for 1 - 4 weeks to convert most organics into tritiated hydrocarbons and HT. After this "conditioning" procedure the vessel could be evacuated and subsequently be refilled with tritium.

Cylinders of aluminum, stainless-steel or gold ion-plated stainless-steel minimize HT ingrowth better than borosilicate glass, because of the high bulk protium content of the latter.

2.14.1.9 Heterogenous oxidation of tritium permeated up to the backside of stainless-steel

Finn and van Deventer [Fin86] investigated the oxidation of tritium permeating to the back surface of SS316 stainless-steel at temperatures within the range 623 - 823 K in a flow system using a helium stream on the back side containing oxygen in rather low concentrations, i.e. less than 10 ppm. Under these conditions the ratio of tritiated water to tritiated molecular hydrogen was found to be less than one. At higher oxygen concentrations in helium, i.e. > 50 ppm, the Q_2O/Q_2 (Q = H, T) ratio increased to more than 10. The maximum yield of tritiated water, i.e. $HTO/HT > 40$ (or 98 % conversion), was achieved at fairly high concentrations of oxygen, i.e. 1200 - 2000 ppm. The presence of 15 ppm protium in the O_2/He sweep gas at the back surface did not appear to enhance the conversion of tritium into tritiated water. Excess protium probably reduces iron oxide to iron, of which the former is needed to convert tritiated water into molecular tritium. Another possible explanation is that hydrogen occupies active sites on the metal oxide surface reducing the number of available sites for tritiated water and consequently its yield. The experimentally gained data indicate that the oxidation of tritium is half order with respect to the concentration of tritium in the metal. The oxidation to water was complicated by the fact that metal oxide formation and back reaction to form molecular tritium occur simultaneously with oxidation of tritium [Fin88]. An additional difficulty for the interpretation of the results is the multi-element composition of stainless-steel and the varying composition of bulk and

surface depending on the temperature and chemical composition of the environment to which the material is exposed.

2.14.1.10 Rudiments on corrosion of iron or stainless-steel in absence of hydrogen isotopologues

A good overview on corrosion processes exhibited by alloyed steels has recently been published by Kienzler [Kie18]. As well known, under atmospheric conditions the resistance of stainless-steel towards corrosion is significantly dependent from the chromium content of the alloy. Chromium and several other elements lead to the formation of a thin, passive protective layer, which prevents further corrosion by blocking diffusion of oxygen to the metallic surface. However, when certain conditions prevail corrosion may become perceptible. The observed effects have been classified into general and localized. **General corrosion** is characterized by a more or less uniform mass loss over the entire area exposed to the atmosphere, soil or water. In case of **localized corrosion**, the consequences are exhibited predominantly at discrete sites. Localized steel corrosion is more frequently encountered after immersion exposures rather than after contact with a gaseous environment. Typical types of localized corrosions are i) **pitting corrosion** (initiated at imperfections of the passivation layer or on an open freely-exposed surface), ii) **crevice corrosion** (occurs in crevices in which the immediate chemical environment differs from the surrounding bulk environment), iii) **contact (galvanic) corrosion** (takes place in zones in which different metals are submerged into a common electrolyte), iv) **stress corrosion** (requires simultaneous tensile stress by external loads or welding/bending) and v) **intergranular attack** (occurs when carbon diffuses to the grain boundary and precipitates as chromium carbide leaving zones of lower chromium concentration flanking the grain boundaries).

The complex chemistry of rust formation on iron or steel subjected to environmental exposure has recently been discussed by [Tam08] and [Kie18]. Initially, owing to an equilibrium establishing between stainless-steel and iron hydroxide ($Fe(OH)_2$), a dense, self-repairing rust film is rapidly formed by air oxidation at pH 9.3. Species such as FeOOH, Fe_2O_3, Fe_3O_4 and amorphous oxyhydroxides are formed in this rust (see references in [Tam08]). Once this initial corrosion ceases to progress, the film will undergo ageing which manifests visibly by rust shrinking. Partial wash out by rain and other condensates was found to have an influence on the process. Dehydration and crystallization of the rust causes iron oxyhydroxides to transform into hematite

(α-Fe_2O_3). Eventually, channels will form across the rust film linking directly the metal surface to the environment. Atmospheric moisture and oxygen can then migrate through the channels up to the metallic surface and induce crevice corrosion. The reaction products in the anode channel, i.e. Fe^{++} and cathode channel, i.e. OH^-, cannot react directly because remaining rust hinders their contact. Air oxidation of Fe^{++} in anode channels without the presence of OH^- ions results in strongly acidic solutions (pH = 1.4) which eventually lead to acid corrosion. In the presence of environmental chlorides, e.g. NaCl or $MgCl_2$, however, dissolved Fe^{++} cations are neutralized by Cl^- anions in the anode channel yielding $FeCl_2$ and OH^- is neutralized by Na^+ cations in the cathode channel yielding NaOH. Under these conditions, the dissolved metal reacts to form iron chloride. The latter may hydrolyse forming FeClOH and hydrochloric acid. Of these, the latter reduces the pH to sufficiently low values to permit initiation of crevice corrosion under the thick rust layer. For more details on the chemistry of corrosion-promoting and corrosion-protecting phases alternating on the metal surface the reader should refer to the original literature.

Maroni et al. [Mar90] investigated the chemical composition of the surface of stainless-steel type SS304 previously exposed to water at 562 K under various pH and electrochemical potential conditions by Raman spectroscopy, powder X ray diffraction, and X-ray photoelectron spectroscopy. The identified phases showed excellent correlations with the **Pourbaix diagram** for the $Fe-Cr-H_2O$ system at the temperatures selected for the experiments [Cub89; Mar90].The diagram visualizes the most stable species/phases in aqueous solution as function of potential and pH. Whereas in the potential vs pH diagram region, where $(Fe_{3-x}Cr_x)O_4$ is both predicted and found, no intergranular stress corrosion cracking was noticeable, specimens examined at potential vs pH conditions outside of the $(Fe_{3-x}Cr_x)O_4$ stability region did show evidence of this type of corrosion.

2.14.1.11 Changes of mechanical and surface properties of stainless-steel induced by hydrogen isotopologues and or helium

Stainless-steel's are susceptible to a ductility loss when placed in a hydrogen environment [Tho73; Kik78; Cas85; Mor90b; Mor90a; Rob90; Ulm90; Iga91; Ori93; Mor08]. According to Thompson [Tho73] the ductility loss of stainless-steel 304L or 309S induced by hydrogen is caused by dislocation transport of hydrogen and accumulation of hydrogen at interfaces between matrix and non-metallic inclusion particles. When hydrogen is trapped at these locations fracture takes

place by normal ductile rupture. In an experimental study performed by Grabke and Riecke [Gra00], they provided evidence that mainly mobile hydrogen and not hydrogen in deep traps is responsible for the effect of this gas on fracture. Generally, increasing concentrations of hydrogen in the bulk are associated with a regular decrease in ductility. Hydrogen in sufficiently large concentration was observed to cause a threefold increase in yield strength and normally ductile austenitic steel was found to fail by brittle cleavage rupture [Ulm90]. The presence of helium bubbles[34] from tritium decay and of tritium atoms at the grain boundaries in type 304 L and 316 stainless-steel was shown to have an enhancing effect on the low-ductility interfracture mode which went beyond that observed with pure hydrogen [Wes80a; Rob90]. These results indicate that irrespective of whether helium is incorporated by tritium decay or absorbed hydrogen is present in austenitic steel, the existence of either one in the metal causes the yield strength to increase and ductility to be reduced. Austenitic stainless-steel degradation has actually been spotted at helium concentrations in the range 200 - 700 appm. According to another finding, helium has stronger impact on the mechanical properties than hydrogen, i.e. three to four times lower concentrations of helium have the same effect on the mechanical properties than hydrogen [Wes80a].

Of all known types of stainless-steel, the effect of helium is least critical for the austenitic ones. Austenitic steels are also characterized by comparatively low hydrogen isotope permeability and high overall resistance to deleterious effects on mechanical properties induced by hydrogen [Ell80; Ell81]. Among other effects, it has been shown that fretting fatigue strength and fatigue crack growth rate of AISI 304 decrease in the presence of hydrogen [Kub06; Kan08].

Kanezaki et al. [Kan08] carried out a rather comprehensive investigation on the effect of hydrogen on the crack growth behaviour of austenitic stainless-steels. Fatigue test specimens of conventional configuration were manufactured from either SS304, SS316 or SS316L and provided with a small bore of 0.1 mm diameter and 0.1 mm depth for crack initiation. Whereas the crack growth rate of hydrogen-charged SS316L specimens was only slightly higher than that displayed by uncharged material, in tests with hydrogen-charged SS316 and SS304 specimens the crack growth rate was found to increase much more rapidly with the number of cycles than in tests performed with uncharged ones. Martensitic transformations on fatigue fracture surfaces were

[34] Helium-3 generated by tritium decay interacts only repulsively with metals and is therefore virtually insoluble in the metal matrix. It will be readily trapped in microstrucural defects or be self-trapped by other helium atoms.

detected by X-ray diffraction both in the hydrogen-charged as well as in non-charged SS316 and SS316L stainless-steel specimens. These transformations are of concern because materials with increased tendency for martensitic transformation also display increased acceleration of fatigue crack growth rates [Kan08]. A SUS304[35] specimen pre-strained at 203 K was found to contain a large fraction of martensite. This sample showed a hydrogen diffusion coefficient about 40 times higher than across SUS304 pre-strained at 302 K. This was taken as indication of rearranged martensite providing faster and more direct diffusion pathways for hydrogen. The fatigue crack growth rate of specimens pre-strained at low temperature was significantly increased by hydrogen for both SUS304 and SUS316L. While clear striations were noticed on the fatigue fracture surfaces of the uncharged SUS304 and SUS316 specimens, those on the hydrogen-charged specimens were less distinct and fewer. Complementary information was obtained by scanning electron microscopy (SEM) on the effect of hydrogen on fatigue fracture morphology.

Morgan and Lohmeier [Mor90a] exposed fracture toughness samples manufactured from SS304L and SS316 to tritium at 423 K and aged these specimens at 273 K until they contained 749 appm tritium and 440 appm of helium, respectively. With a falling load technique, they were able to demonstrate that 304L samples had lower threshold stress intensities than 316 samples and that on the average the crack growth rate of 304L was an order of magnitude faster than that of 316. This is essentially in agreement with observations of Kanezaki et al. [Kan08].

Stainless-steel 316L containing 35 appm helium and aged at 1073 K for 24 hours displayed bubbles 10 nm in diameter. Ageing the same material at 1273 K for the same length of time revealed bubbles of 20 nm in diameter. When ageing was carried out at even higher temperature, e.g. 1373 K, for only 0.083 hours the size of the bubbles was 50 - 60 nm. In general, while the bubble size increases markedly with ageing temperature, the effect of ageing time is much less pronounced [Bra94]. Bubble growth appears to occur mainly by a surface diffusion process. At 1073 and 1223 K bubbles containing helium were mostly found on matrix dislocations. Whereas a small helium content, e.g. 3.7 appm, does not impede block grain boundary motion at 1373 K, already 35 appm helium in SS316L suffice to strongly hinder the re-crystallization process. The 35 appm material aged at 1073 K displays a small density of helium bubbles. Hence, the temperature for precipitation and growth of the observable bubbles is higher than in irradiated or implanted material due to the absence of vacancy formation during tritium exposure.

[35] The Japanese JIS material designation SUS403 is equivalent to German DIN X6Cr13 or USA AISI 403.

Table 2.44: Sieverts constants of hydrogen in austenitic stainless-steels [Min11].

Material	Chromium	Hydrogen	K_0	ΔHs
	%	ppm	$\mathrm{mol_{H_2}\,m^{-3}\,MPa^{-0.5}}$	$\mathrm{kJ\,mol^{-1}}$
SUH660	13.59	1.2	38.3	1.89
SUS304	18.54-18.66	2.2	52.8	2.34
SUS316	17.01	3.4	52.8	2.34
SUS316	17.16	1.5	49.6	2.58
SUS316	24.02-24.69	2.8-4.7	59.6	1.43

Mine and Kimoto [Min11] performed a comprehensive investigation on the interaction of hydrogen with stainless-steel type SU304, SU316, SU316L, SU310S and SU660. Exposure to high pressures of hydrogen caused loss of ductility. There was also evidence for plastic deformation of the fracture surfaces. Sensitivity of ductility to hydrogen showed dependence from austenitic stability and precipitation hardening. Hydrogen diffusion through all investigated steels could be described by relationship

$$D = 1.21 \times 10^{-5} \exp\left(-\frac{63.1\,\mathrm{kJ\,mol^{-1}}}{RT}\right)\ \mathrm{m^2\,s^{-1}}$$

Solubilities, on the other hand, showed dependency from the respective alloy composition, being particularly sensitive to the content of chromium (see Table 2.44).

Stainless-steel type SS304L exposed to 62 MPa of T_2 at 423 K for 6 months and thereafter aged for 15 months showed a fracture toughness decrease to less than about 20 % of the value obtained with a pristine reference specimen due to embrittlement induced by approx. 200 ppm ^{3}He [Cas85]. Further increase in helium content had little additional effect on fracture toughness. In another study it was observed that aged specimens containing the same amount of either hydrogen or tritium displayed rather large differences in ductility [Wes80a].

Boitsov et al. [Boi08] examined the effect of decay helium on the mechanical properties and hydrogen permeability of stainless-steel type 12 Cr18 Ni10 Ti (analogue to AISI type 321H or type SS316). Specimens containing 75 or 130 appm ^{3}He were prepared by thermal exposure to tritium and selection of an ageing time calculated for the attainment of the desired concentration

of helium. Mechanical properties such as ultimate tensile strength, yield strength, reduction in area and total elongation were measured by comparing the behaviour of virgin material with that containing decay helium. According to their observations, in stainless-steel containing helium the strength characteristics of steel remained unaffected but the plasticity decreased markedly. When both hydrogen and helium were present, the samples displayed enhanced embrittlement, but the total effect was different from that given by the simple addition of both effects. Interestingly, the diffusion coefficient of hydrogen across 12 $Cr_{18}Ni_{10}Ti$ was not affected by the presence of helium but the generation of traps during the production of decay helium caused delay in kinetics and retarded measurably the attainment of the onset of steady state permanent flux.

Morgan et al. [Mor08] researched the combined effect of tritium and its decay product helium on the fracture toughness properties of stainless-steel 21-6-9 (a nitrogen-strengthened alloy) and stainless-steel type 304L weldments (for details on compositions and yield strengths refer to [Mor08]). Initially, with no tritium present, the weldments displayed fracture toughness values about three times higher than those of the base metals. This improvement was attributed to a delta ferrite phase developing in the weld microstructure. After exposure to tritium until attainment of a dissolved concentration of 1400 appm and ageing of the specimen, both weldment and base metal exhibited a reduction of fracture toughness down to about the same value. With progressing ageing, i.e. increasing decay helium concentrations within the range 50 to 800 appm, the fracture toughness properties of weldments and base metals decreased further. Weld fracture surfaces revealed tritium-induced and helium-induced embrittlement of the ductile delta ferritite phase. Hydrogen and tritium fracture surfaces were found to have smaller and more closely spaced microvoids than pristine fracture surfaces.

Bellanger and Raneau [Bel93a] performed voltametric measurements complemented by SEM studies and reported that tritium beta rays and decay helium in stainless-steel type 316L specimens, which had been exposed to tritium for several years, are detrimental to the formation of a good passivation layer on the surface. Tritium and helium induce localized stress corrosion causing embrittlement with failures of the oxide layer. It was speculated that this is due to the formation of martensite and the accumulation of helium.

Dollé [Dol87] investigated parametrically the corrosion of nickel and SS316L in the presence of fusion relevant gases like H_2, O_2, N_2, CO_2, CO, CH_4, H_2O and NH_3, at several compositions

under exposure to γ-irradiation (16.3 - 60.8 kGy) from a ^{60}Co source. Surface attack of SS316L became particularly apparent in gas mixtures containing ammonia.

2.14.1.12 Hydrogen-assisted embrittlement of stainless-steel and other metals

The interaction of hydrogen with metals can give rise either to solid solutions, solid compounds like hydrides, or gaseous compounds like hydrocarbons. The latter are formed when metals contaminated by carbon are heated in the presence of hydrogen or tritium. Atomic hydrogen, resulting from the interaction of molecular hydrogen with metals, can recombine in the metal bulk to yield molecular hydrogen. When the interaction takes place with tritium decay helium will accumulate in the bulk.

The presence of hydrogen in metals can cause **hydrogen-assisted embrittlement**. Three categories of embrittlement have been identified [Woo16]:

- **Hydrogen environmental embrittlement** (HEE): takes place when a metal is exposed to a high pressure of environmental gaseous hydrogen.
- **Internal hydrogen embrittlement** (IHE): occurs when the hydrogen source is internal (usually from manufacturing). Typical causes for IHE are an electroplating process, corrosion, cathodic charging, or thermal charging.
- **Hydrogen reaction embrittlement** (HRE): in this type of embrittlement the damage is due to an irreversible chemical reaction without external applied stress, e.g. that of iron carbide with atomic tritium

$$4\,\mathrm{T} + \mathrm{Fe_3C} \longrightarrow \mathrm{CT_4} + 3\,\mathrm{Fe}$$

  The formation and migration of methane deep in the bulk usually concentrates at grain boundaries leading to brittle rupture through a network of discontinuous micro cracks. HRE depends on the amount of carbon and carbides in the alloy.

A comprehensive, critical review of worldwide available HEE data for nickel, titanium, copper and aluminum-based alloys; for several types of austenitic, ferritic and martensitic alloys; and for nickel, iron and cobalt super alloys compiled over the past 50 years has been published as NASA report by [Woo16].

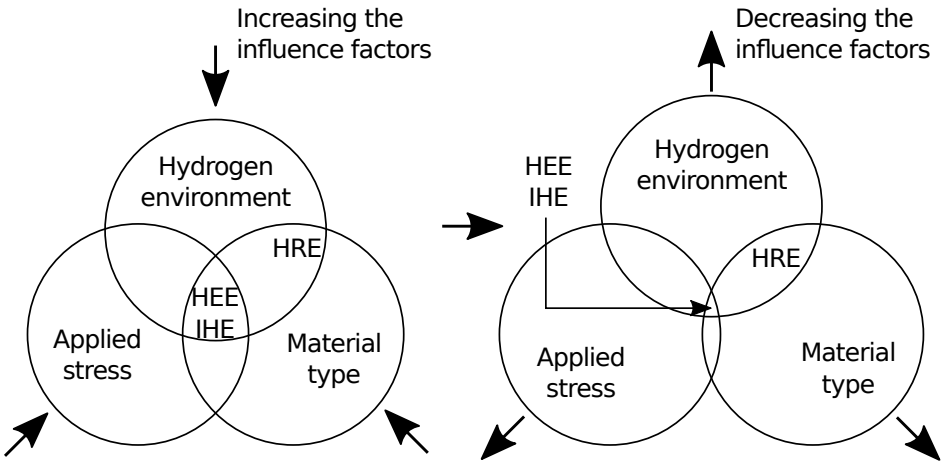


Figure 2.45: Guideline for the prevention and control of damage by hydrogen (after [Woo16]).

Fig. 2.45 depicts overlapping regions for HEE, IHE and HRE created by the intersections of three circles representing the influence factors: i) material type, ii) hydrogen environment and iii) applied stress. By selecting the proper material, employing the right pressure at the best temperature or optimizing the stress it is possible to select the best materials for diverse kinds of hydrogen applications. By reducing or removing one of these factors it is possible to alter the damaging effect for many materials.

Hydrogen-assisted embrittlement of materials like SS316 can occur from **manufacturing** or **operational use**, everywhere were the metal comes into contact with H or H_2. Processes like cathodic protection, pickling, electroplating or arc welding in which hydrogen is released from the decomposition of water may cause embrittlement. Other mechanisms of hydrogen introduction are galvanic corrosion or chemical reactions with acids. In high strength steels ppm concentrations of H_2 can sometimes suffice for the development of catastrophic embrittlement.

H_2-assisted embrittlement arises from lessening of the binding forces between metal atoms. In other words, less work is necessary for mechanical failure during load time. Small concentrations of hydrogen isotopes (or decay He) can lead to **hydrogen induced cracks (HIC)**, which manifests as loss of ductility. Other consequences of embrittlement are: i) reduction in tensile elongation to cause failure, ii) decrease of static load sustainable by a metal, iii) increase in rate of crack propagation and iv) decrease in the number of load no-load cycles. When steel

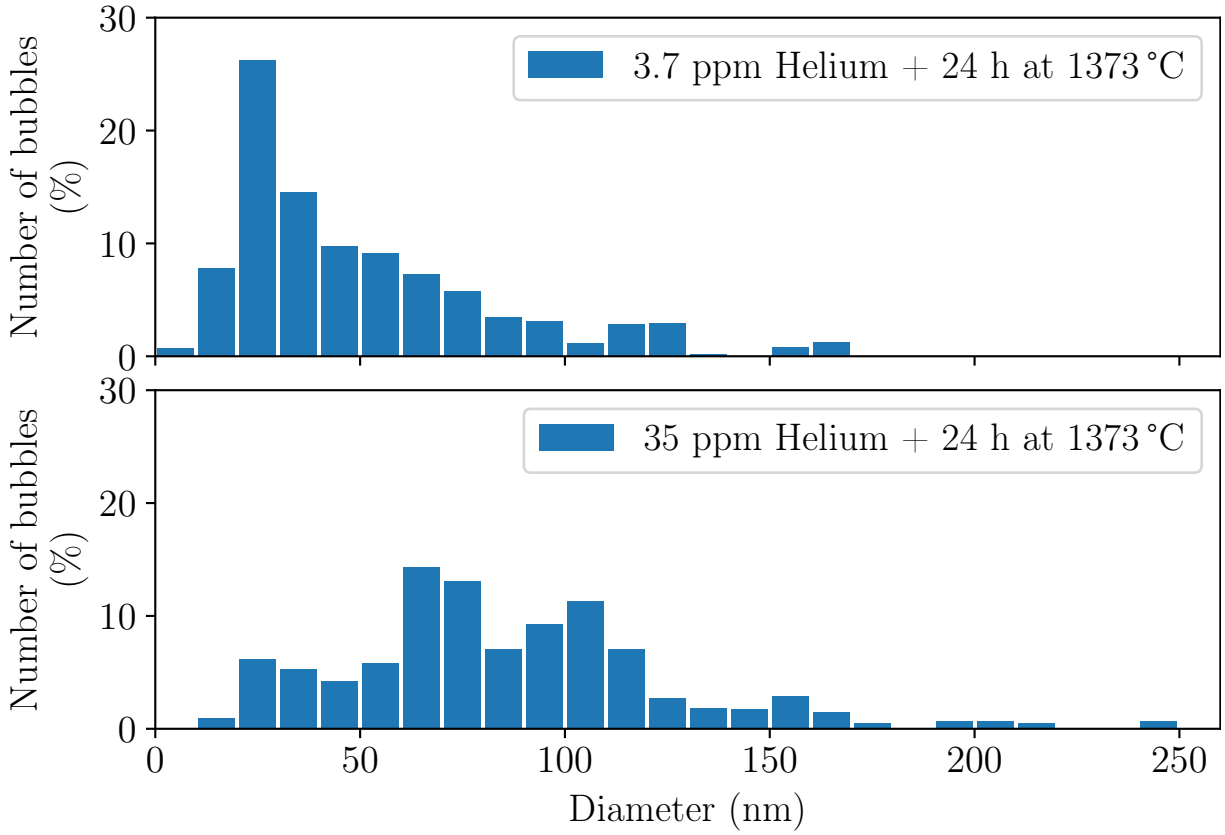


Figure 2.46: Number of bubbles in % as function of bubble diameter in nm at two helium concentrations in stainless-steel 316L (after [Hir93]).

is exposed to hydrogen at raised temperatures, pockets of methane may be formed at internal surfaces like grain or voids. This gas does not diffuse out but collects in voids at high pressure where it may initiate cracks. Decarburization of steel enhances loss of strength and ductility.

To investigate the fate of helium in stainless-steel, Hircq et al. [Hir93] exposed SS316L specimens to pure tritium at less than 25 bar over 5 hours at 723 K and thereafter aged the specimens for sufficient time to reach He concentrations of either 3.7 or 35 ppm. After baking the specimens at 1073, 1223 or 1373 K they observed coalescence in these specimens (solubility of He-3 in SS316 is very low) resulting in bubbles with mean diameters of 9 nm, 23 nm and 51 nm, respectively (see Fig. 2.46). It was concluded that the bubble size increases with helium concentration, temperature and duration of the heat treatment.

Stainless-steel type SS316 containing the same amount of either H or T exhibited significant differences in ductility [Wes80a]. Charging stainless-steel with helium caused a marked decrease of plasticity. Already 2 ppm helium in SS316 lead to a fracture toughness decrease of 20 % in comparison to that displayed by the pristine reference material [Cas85]. Further increase in helium concentration had little additional impact on fracture toughness. Consequently, decay helium enhances **hydrogen induced cracking** after it builds up bubbles.

A profuse source of information on hydrogen embrittlement of metals has been the development of earth to orbit rocket propulsion technology based on H_2 - O_2 engines [Woo16]. Within this frame, many metals resistant to hydrogen embrittlement have been identified.

Information on the possible embrittlement of beryllium assisted by hydrogen isotopologues is scarce. It is well known that **oxygen-free copper** and **oxygen-free beryllium-copper alloys** display excellent resistance towards hydrogen embrittlement [Oga17]. Conversely, beryllium-copper alloy containing oxygen displays propensity to embrittlement when exposed to hydrogen at elevated temperatures. Under these conditions, atomic hydrogen formed on the surface rapidly diffuses into the metal and reacts there with inclusions of copper oxide or oxygen to generate water which is converted to high pressure steam according to

$$Cu_2O + 2\,H = 2\,Cu + H_2O\ (g)$$

Steam collects in pressurized bubbles at grain boundaries. This type of embrittlement is called **steam embrittlement**. When oxygen-bearing copper or copper alloys are annealed or heated

in a hydrogen environment at temperatures $> 648\,\mathrm{K}$ the steam induces damage like fissures and blisters, decreasing fracture toughness and ductility of the metal.

2.14.1.13 Neutron activation of stainless-steel

Grégoire and Ladrière [Grè01] examined experimentally the activation of iron, chromium, or nickel foils, all stainless-steel base metals, by irradiation with fast neutrons. Neutrons were generated in a cyclotron by the nuclear reaction $9\,\mathrm{Be(d,n)_{10}B}$. For this purpose, a thick beryllium target was irradiated with 50 MeV deuterons; the neutron yield showing a maximum at deuteron energies of about 20 MeV. The achieved flux was estimated to be close to $10^{12}\,\mathrm{neutrons\,cm^{-2}\,s^{-1}}$. Activation results from stainless-steel type 304, 310, 316 and 316n after 10 hours exposure to radiation were reported.

An overall strategy designed to minimize the total volume of activated waste arising during power plant end of life as well as during the accumulated replacement of components was developed by Taylor et al. [Tay00b]. According to their estimations approximately 50 % of the materials resulting from the operation of a fusion power plant have the potential for clearance provided the activation levels are sufficiently low. To achieve low activation levels a careful a priori material selection is essential. The selection must be carried out keeping in mind waste volume minimization, potential for clearance and potential for recycling. It is furthermore indispensable to be aware of numerous trade-offs, like for instance efforts to reduce the maximum activation level of the first wall and the blanket may also be associated with increased activation of shield, blanket and magnets. As a result the total volume of waste material requiring repository disposal could increase significantly. Efficient material selection must therefore contemplate design requirements in all areas of significant neutron flux like the first wall, the blanket breeder, multiplier, shielding, vacuum vessel, ex vessel structures, etc. The choice of materials must be based on a comprehensive knowledge of impurity inventories supported by measured compositions.

The intense radiation environment of a fusion machine may drastically alter the material properties of plasma-facing stainless-steel. Changes are brought about by neutrons with energies of up to 14 MeV as well as by γ-rays, X-rays, tritons and deuterons. In view of the high penetrating capability of neutrons they can initiate transmutation reactions in the bulk of materials or cause crystal lattice structural damages. Capture and decay reactions induced by neutrons will introduce new impurities into the materials that, if solubility concentrations are

exceeded, will generate new phases, which may strengthen the alloy or reduce his toughness. Transmutation reactions in steel may also lead to the formation of tritium. The concentration of tritium permeated from the plasma-side into stainless-steel is estimated to be of the same order of magnitude as that arising from transmutations. In general, tritium in in-vessel steel waste is not particularly relevant from a radioactivity point of view, but of concern for waste disposal because of possible chronic gaseous release or leaching processes [Tor05b; Pen06].

A comparison of the total post-irradiation radio activities in copper and stainless-steel type 316 as function of cooling time has been provided by Butterworth and Forty [But92]. During shut down the activity of copper was estimated to be larger by a factor of two than that of stainless-steel, but already after a few days the activity of copper will fall below that of stainless-steel and then remain lower for about ten years. After elapsing of this time, the activity of copper will once again become higher but only temporarily.

2.14.1.14 Tritium permeation into blanket cooling water

With the aim of improving knowledge on the mechanism of tritium permeation into the primary cooling water of blankets, Hayashi et al. [Hay07a; Iso08] determined the permeation rate of tritium (7.4 GBq, 90 % isotopic purity) at pressures of up to 1 kPa through pure iron piping into a water jacket maintained at 423 K. The **iron pipe** was closed on one end. The water jacket, which was pressurized with 0.8 MPa helium, could be purged either with pure helium or helium containing 1 % hydrogen (hydrogen dissolved in jacket water) at a rate of 20 $cm^3\,min^{-1}$. Bubblers served to collect HTO. HT was determined by oxidation into HTO using CuO. According to their observations, the permeation rate was much smaller, i.e. about $1/5^{th}$, than that predicted from theoretical calculations. While initially a fraction of about 30 % of the permeated tritium was HT, after one day of oxide layer growth, this fraction became very small, i.e. $1/50^{th}$. The presence of 1 % hydrogen in the helium purge gas had little influence on the permeation rate or type of permeated species. Examination by autoradiography of iron used in the permeation study, which was oxidized by hot water in the jacket, revealed homogeneous distribution of tritium in the permeator material. Two oxide layers were generated: the inner layer consisting of dense

magnetite tightly adhered to the metal surface and the outer layer of loosely adherent crystalline magnetite. The growth of the outer layer is described by equations

$$\mathrm{Fe} + 2\,\mathrm{H_2O} \longrightarrow \mathrm{Fe(OH)_2} + \mathrm{H_2}$$
$$3\,\mathrm{Fe(OH)_2} \longrightarrow \mathrm{Fe_3O_4} + 2\,\mathrm{H_2O} + \mathrm{H_2}\ .$$

The concentration of tritium in the iron oxide (Fe_3O_4 = magnetite) layer on the surface was found to be comparatively small, the rate of tritium permeation remaining essentially constant irrespective of progressive oxide growth.

Hayashi et al. [Hay12] performed experiments of relevance to the design of a cooling system for the ITER tritium breeding blanket. To this effect, measurements of the permeation rate of deuterium from heavy water (D_2O) through diverse metal tubings consisting of either pure iron, nickel, stainless-steel type SS304 or pure iron covered by 10 µm gold plating were carried out. Metallic tubings were exposed on the outside to heavy water pressurized by 15 - 17 MPa helium and vacuum was maintained on the inside. All test tubes were closed on one side. The selected permeation temperature was 573 K to simulate conditions at the vacuum vessel. Build-up of molecular hydrogen isotopes on the inside of the tubing was detected and quantified with a quadrupole mass spectrometer. After several days, molecular deuterium became the major permeating species, but smaller partial pressures of HD and H_2 were also registered. Additionally, traces of H_2O, HDO and D_2O were detected. It was postulated that atomic deuterium is generated during oxidation of the metal surface with heavy water at increased temperature. Gold plating of iron was found to inhibit strongly the permeation of deuterium. The permeabilities of deuterium from heavy water at 573 K across pure iron, SS304 and nickel were determined to be $1.57 \times 10^{-11}\,\mathrm{mol\,m^{-1}\,s^{-1}\,Pa^{-0.5}}$, $1.52 \times 10^{-12}\,\mathrm{mol\,m^{-1}\,s^{-1}\,Pa^{-0.5}}$ and $1.82 \times 10^{-12}\,\mathrm{mol\,m^{-1}\,s^{-1}\,Pa^{-0.5}}$, respectively.

Surface oxide films may reduce permeation of tritium through steels by several orders of magnitude [Won84]. Within this frame, Forsyth and Thiele[For81] provided evidence that tightness, temperature stability and adherence of films formed on austenitic steel are of superior quality than those formed on ferritic steel.

2.14.1.15 Trapping of hydrogen in stainless-steel

Hydrogen trapping in stainless-steel takes place in voids, highly strained regions around crack tips, radiation damage sites, grain boundaries and by reaction with impurities [Lan84]. While impurities, dislocations, grain and phase boundaries, pores and cracks can act as traps for hydrogen and thereby have a marked influence on diffusion and effective solubility, they have little influence on permeation rates once steady state conditions have established. The rationale is that steady state is reached once all traps are occupied. For the same reason there is generally much better agreement between the permeability results obtained by different investigators than among diffusion coefficients or solubilities.

2.14.1.16 Permeation parameters of tritium through some heat resistant alloys, ferritic, and austenitic construction materials, pure stainless-steel base metals, and low permeability materials

The permeation of hydrogen and tritium across more than 30 different heat resistant alloys like Incoloys, Inconels, Nimonic and other non-commercial steels, was the research topic of Schmidt et al. [Sch85]. Permeation and diffusion measurements were carried out at temperatures in the range 1023 - 1223 K and pressures in the range 1 - 40 bar. Generally, the permeation rate of samples having a clean surface, i.e. surface without oxide layer, was found to be proportional to the square root of hydrogen pressure. Arrhenius parameters for permeability and diffusion coefficients of numerous alloys were reported.

Bell et al. [Bel79a] examined the permeation rates of tritium across several ferritic (SS406) and austenitic "clean" construction materials (Hasteloy N, Incoloy 800 and SS316) as well as of one tungsten alloy within the temperature range 573 - 973 K. The achieved results were compared with data obtained with pure iron and pure nickel under the same experimental conditions (see Table 2.45). "Clean" surfaces were generated by electroplating a 7 µm thick layer of nickel on both sides of the tubular specimens. A further advantage of electroplating was protection of the surfaces from oxidation. The absence of oxygen at the nickel-iron interface was verified by SIMS measurements. For the experiments the tube type specimens were placed inside of a metal chamber which was in turn surrounded by a furnace. Hydrogen carrier gas at 1 bar containing ppm concentrations of tritium was passed along the outside of the tube and a stream of hydrogen

in counter current at a pressure of about 20 bar inside of the tube. The latter served to collect permeated tritium. Tritium in this stream was measured with a tritium analyser. A comparison of permeabilities indicates that those of ferritic alloys are generally larger than the one´s of austenitics alloys and that the alloys have lower tritium permeabilities than iron or nickel base metals.

Hydrogen permeability's of SS321, SS316, Inconel-625 and Inconel-718 at hydrogen driving pressures in the range 10^{-3} - 10^{4} Pa and temperatures between 350 K and 1050 K, were likewise examined by Deventer and Maroni [Dev80b] (see Table 2.45). The use of active measures, i.e. delivery of hydrogen from heated uranium hydride to obtain high purity hydrogen, particularly at low pressures, i.e. < 10 Pa, was found to be important for the achievement of reliable results. Particular attention was given to low driving pressures in order to address the needs of controlled nuclear fusion. At the higher end of the pressure range all four investigated alloys displayed half power dependence of permeability on hydrogen pressure.

Kishimoto et al. [Kis84; Kis85b; Kis85a] focused in their study on the solubility and diffusivity of hydrogen through SS316L (first wall material of ITER) and nickel-rich heat resistant alloys like Inconel 600, Inconel 750, Nimonic 80A and Hastelloy X. They looked into the steady state permeation of hydrogen through austenitic steels and nickel-based materials employing a gas flow system equipped with a partial pressure analyser for the analytical measurements. The results indicate that the differences between pre-exponential terms and activation energies for the permeability of hydrogen across nickel base alloys and SS316L are not large (see Table 2.45). Differences in activation energies were attributed to the presence of titanium.

The hydrogen isotope permeability through a number of materials has been collected and compared in a review published by Steward [Ste83]. While emphasis was placed on metals of low permeability because of their importance for tritium containment, permeability's through a number of other materials of higher permeability's like iron, nickel, steels and glasses were also included. A useful list of "best" permeability values was provided for many materials.

One more literature review on the permeation of hydrogen through a large number of tritium technology relevant materials was published by Riehm et al. [Rie86]. In his work, attention is focused on **permeation-resistant barriers** for the containment of hydrogen.

Further permeation rates of hydrogen isotopes through structural materials like Ni, SS304L, Hastelloy N, Incoloy 800, Croloy T9, Croloy T22 and SS406 were determined over a wide range

of pressures but particularly at low pressures (1 - 1000 mbar) and temperatures covering the range 573 - 1073 K by Strelow and Savage [Str74]. Oxidized materials displayed a reduction of the deuterium permeation rate by a factor of one hundred or more, especially at low pressures.

Zarchy and Axtmann [Zar79] carried out a few tritium permeation experiments at ultralow pressures, i.e. driving pressure of 10^{-7} Pa, and temperatures within the range 573 - 723 K across stainless-steel 304. Aim of the work was to study deviations at very low pressures from classical behaviour (permeation rate proportional to the half power of the driving pressure) arising from a competition between permeation across the metal with that across a surface layer. The results essentially confirmed the model developed by Strehlow and Savage [Str74].

General conclusions from the data are: i) permeation rates through the alloys follow Sieverts' law, ii) perturbations by impurities, e.g. H_2O, O_2, etc., lead at low driving pressures to deviations of permeability from the $P^{1/2}$ dependence, iii) tritium permeability's through ferritic alloys are higher than through austenitic alloys, iv) austenitic alloys show lower tritium permeability's than SS406 or stainless-steel base metals like iron or nickel, v) there is still need for extending the permeation driving pressure range to values as low as 10^{-8} Pa to address all conditions that are likely in fusion relevant systems and vi) results from four investigations listed in Table 2.45 [Nel73; Bel79a; Dev80b; Kis85b] make evident that the rates of permeation through the various materials examined do not show great differences regardless of whether the surface is covered by a protective layer of nickel or not. Hence, the presence of oxygen on the metal surface does not appear to play a very important role.

Table 2.45: Tritium, deuterium and hydrogen permeation parameters through pure metals (Fe, Ni), as well as several ferritic and austenitic heat-resistant construction materials. Concentrations of main base elements are provided.

Material	Ni	Cr	Fe	Mo	P_0	ΔE	Temp. range	Ref.
	Composition (in weight%)				$\mathrm{mol\,m^{-1}\,s^{-1}\,Pa^{-0.5}}$	$\mathrm{kJ\,mol^{-1}}$	K	
Iron	-	-	100	-	0.4×10^{-7}	39.8	550 - 1000	[Bel79a]
Iron	-	-	100	-	0.8×10^{-7}	34.3	373 - 873	[Nel73]
Nickel	100	-	-	-	1.7×10^{-7}	53.1	550 - 1000	[Bel79a]
Hasteloy N	74	7	3	12	3.7×10^{-7}	66.2	550 - 1000	[Bel79a]
Hasteloy X	bal	20.7	19.7	8.9	8.9×10^{-7}	64.7	873 - 1173	[Kis85b]
Inconel 600	bal	15.9	7.0	-	8.0×10^{-7}	63.8	873 - 1173	[Kis85b]
Inconel 625	60.9	21.6	3.8	9.2	2.6×10^{-7}	60.1	500 - 1000	[Dev80b]
Inconel 718	54.0	18.4	17.5	3.0	1.0×10^{-7}	56.4	500 - 1000	[Dev80b]
Inconel 750	bal	15.3	7.0	-	10.0×10^{-7}	64.7	850 - 1250	[Kis85b]
Incoloy 800	31	23	45	-	2.76×10^{-7}	66.3	550 - 1000	[Bel79a]
Incoloy 800	-	-	-	-	3.94×10^{-8}	55.6	427 - 780	[Est02]
Nimonic 80A	bal	19.3	1.0	-	10.0×10^{-7}	64.7	873 - 1173	[Kis85b]
SS406	-	13	83	-	0.7×10^{-7}	51.1	550 - 1000	[Bel79a; Bel80]
SS316L	12.7	16.6	bal	2.1	8.8×10^{-7}	66.7	873 - 1173	[Kis85b]
SS316	13	17	65	2.5	3.4×10^{-7}	68.1	550 - 1000	[Bel79a]
SS316	13.1	16.4	bal	2.2	2.4×10^{-7}	63.5	500 - 1000	[Dev80b]

bal = balance

2.14.1.17 Interaction of tritium with advanced low activation materials and iron

Materials exposed directly or indirectly to plasmas from a fusion machine are subjected to irradiation by ions, charge exchange neutrals, electrons, neutrons and photons resulting from nuclear as well as electronic processes. For this reason, these materials should possess all or at least several of the following properties: i) low hydrogen isotope retention, ii) high thermal conductivity, iii) compatibility with ultra-high vacuum, iv) good thermomechanical properties, v) resistance towards radiation damage and vi) low activation yield with neutrons.

Materials currently under investigation for application in the vacuum vessel or blankets of future fusion machines are i) low-activation ferritic/martensitic steels known by the designations MANET , BATMAN and EUROFER (Europe)citeMarmy1991, Aiello2001, Anderoglu2013, ferritic/martensitic F82H (Japan) and 8Cr2W (Japan) [Koh96][Koh96] and iii) 9Cr-2WVT (USA) [Koh96]. Type F82H steel is under consideration for the cooling panels of the Water-Cooled Ceramic Bed Test Blanket System proposed by Japan for ITER [Gia07; Gia12]. Others are more predestined for the first wall of a fusion machine where they have to comply to a high degree with stringent thermo-mechanical and thermo-physical requirements [And13]. Materials of low susceptibility to generate activation products are attractive because they will conduct to comparatively smaller amounts of the kind of waste requiring repository disposal.

To better coordinate ongoing efforts within the European Union, Japan and USA, a collaborative working group on research and development of reduced activation materials has been established by the International Energy Agency (IEA) [Koh96; IEA01]. One important goal of this working group is to generate a reliable data base on low-activation materials. For this purpose, unirradiated and irradiated reference steels have been distributed within the frame of a **Round Robin** testing program among a number of research groups worldwide. The rather comprehensive Round Robin tests include composition optimization; fatigue, crack growth and creep fatigue tests; development of welding technologies; determination of physical properties; determination of ductile to brittle transition temperatures; examination of the thermal stability of steels and welds; studies on dynamic and static fracture toughness; modelling and theoretical studies; investigation of the compatibility with lithium; aqueous corrosion; magneto mechanical properties; etc.

Martensitic/Ferritic[36] steel **MANET** (MArtensitic for NET), known in Germany under DIN 1.4914, has been tailored to suit the requirements of first wall and structural components not only of NET but also of the next fusion machine DEMO. The material was shown to be resistant to helium embrittlement, have better thermophysical and swelling resistance properties than austenitic steel and be characterized by comparatively few activation products [Ser98]. The composition of MANET is C 0.13, Cr 10.6, Ni 0.87, Mo 0.77, V 0.22, Nb 0.16, Si 0.37, Mn 0.82, S 0.004, P 0.005, B 0.0085, N 0.020, Al 0.054, Co 0.01, Cu 0.01, Cu 0.015, Zr 0.053 and Fe the rest (all in weight %). A discussion on the impact of irradiation on the mechanical properties and behaviour of **EUROFER** supplemented by a comparison with other equivalent materials has been provided by van der Schaaf et al. [Sch03]. They delivered experimental evidence to show that this material has adequate mechanical properties even after undergoing extensive ageing. While the material has potential for application in ITER blankets its utilization can only be recommended after ultimate verification of the properties under relevant conditions. Because the existing sources of 14 MeV neutrons have a small intensity and do not allow achievement of important damage accumulation in a reasonable time, commissioning of the planned IFMIF test facility has been given high priority. Another conclusion from the work of van der Schaaf was that for the attainment of the requested extremely low impurities levels a dedicated steel making process line will have to be put into operation in time and demonstrated.

Oyaidzu et al. [Oya11c] investigated the permeation of tritium across **F82H** at four temperatures within the range 573 - 873 K utilizing on the feed side a helium carrier gas containing tritiated water. Surface analytical measurements provided evidence that the surface of F82H was covered by a layer of hematite (Fe_2O_3) containing small amounts of magnetite (Fe_3O_4). It was postulated that tritiated water when in contact with the latter tritiated water is reduced to molecular tritium. The permeability was found to be extremely slow and comparable to results published by Shestakov et al. [She02].

Saito et al. exposed F82H [Sai11b] and Ni [Sai11a] specimens to gaseous tritium at elevated temperature and obtained tritium depth profiles employing a chemical etching technique. Chronic release rates of tritium determined at ambient temperature for F82H and Ni, as well as for SS316 specimens [Nao08] all initially charged with tritium to approximately the same concentration, decreased in the order 10, 5, and 1 kBq/h respectively. Consequently, chronic release rates appear

[36] Martensite steel is characterized by a BCC α-phase and austenitic steel by an FCC γ-phase.

to correlate with the diffusivities of tritium across the respective metals or alloys. The solubility of tritium in F28H was found to be well described by the average Arrhenius expression

$$S = 0.97 \exp \frac{-22.5\,\mathrm{kJ\,mol^{-1}}}{kT} \mathrm{mol\,m^{-3}\,Pa^{-0.5}}$$

Solubilities obtained from this equation were found to be higher by almost an order of magnitude than those reported by Serra [Ser98] or Dolinsky [Dol02] (see Table 2.47). To acknowledge possible contributions from traps remaining in F82H, the solubilities of tritium provided by the above equation should be contemplated as upper limits.

Marked trapping effects at temperatures below 573 K were reported for MANET, F82H, BATMAN and EUROFER by Aiello et al. [Aie01]. A discussion of these effects together with a compilation of relevant trapping parameters for iron and martensitic steels was reported by Serra et al. [Ser98]. Permeation and diffusion of hydrogen through pre-irradiated martensitic stainless-steels or through low activation martensitic F82H decreased with increasing dose [Sch00]. The concentration of traps augmented significantly with the extent of pre-irradiation.

Several material properties of the Japanese F82H are compiled as function of temperature in Table 2.46. As apparent, some properties show perceptible dependence from temperature and others not. Wakai et al. [Wak98] examined the consequences of irradiation with up to 57 dpa on the microstructure of low-activation F82H at two temperatures, i.e. 523 K and 573 K. Irradiations were carried out at the High Flux Isotope Reactor (HFIR) and evaluation of the after-effects by transmission electron microscopy (TEM).

Otsuka and Tanabe [Ots08] examined the release of tritium from reduced-activation ferritic martensitic (RAFM) steel type **8Cr2W**. To perform experiments 8Cr2W specimens were loaded by exposure to hydrogen containing tracer amounts of tritium ($\mathrm{T/H} = 10^{-6}$) at 673 K and pressures of 0.27, 1.3 or 5.3 kPa over a period lasting 12 hours. Immediately after exposure the specimens were cooled down to liquid nitrogen temperature in order to prevent rapid release of hydrogen isotopes at ambient temperature (specimen designation GAS). The other loading procedure was electrochemical. In this case, charging was carried out by electrolysis at ambient temperature utilizing a NaOH solution containing tritium ($\mathrm{T/H} = 1.6 \times 10^{-6}$) at a current density of $1\,\mathrm{A\,m^{-2}}$. During loading, the 8Cr2W specimen was utilized as cathode while two platinum electrodes served as anodes (specimen designation EC). Irrespective of charging modus

Table 2.46: Material properties of type F82H as function of temperature.

Temperature	Thermal conductivity	Young´s modulus	Poisson´s ratio	Thermal expansion coeff.
K	$W\,mK^{-1}$	GPa		K^{-1}
298	30.3	215	0.29	-
373	34.1	215	0.29	1.0×10^{-5}
473	31.7	210	0.29	1.10×10^{-5}
573	32.2	205	0.29	1.14×10^{-5}
673	31.5	195	0.29	1.18×10^{-5}
773	32.9	190	0.29	1.21×10^{-5}
873	32.8	180	0.30	1.24×10^{-5}

a tritium-rich surface layer with concentrations much exceeding that determined in the bulk was observed. In order to measure tritium release from RAFM specimens they were directly dropped into a LSC cocktail and maintained at constant temperature while analysing the tritium content in the supernatant liquid at regular intervals. The results are plotted in Fig. 2.47. Otsuka and Tanabe then compared the accumulated total release rate from two GAS specimens with theoretical predictions utilizing a diffusion model (upper curve and data points in Fig. 2.47(a)). As evident, the agreement is quite satisfactory. The semi logarithmic plot of the amount of tritium released at 323 K as function of time suggests occurrence of three different mechanisms, each proceeding with its own rate. The corresponding diffusion constants and saturation levels of the RAFM specimens together with the contribution of each of the three stages to the total liberation are also displayed in Fig. 2.47(b). Notice that the diffusion coefficient fittings at 323 K differ from each other by nearly an order of magnitude. The two smaller diffusion coefficients were assigned to liberation from trapping sites and the larger one to release via interstitial diffusion. Examination of the tritium-bearing specimens by imaging plates revealed that tritium was not distributed homogeneously on the surface. In addition, surface tritium was found to be quite withstanding. As a matter of fact, submergence of the specimen into the LSC cocktail for 100 hours did neither alter measurably the surface distribution nor the concentration of tritium in the surface zone.

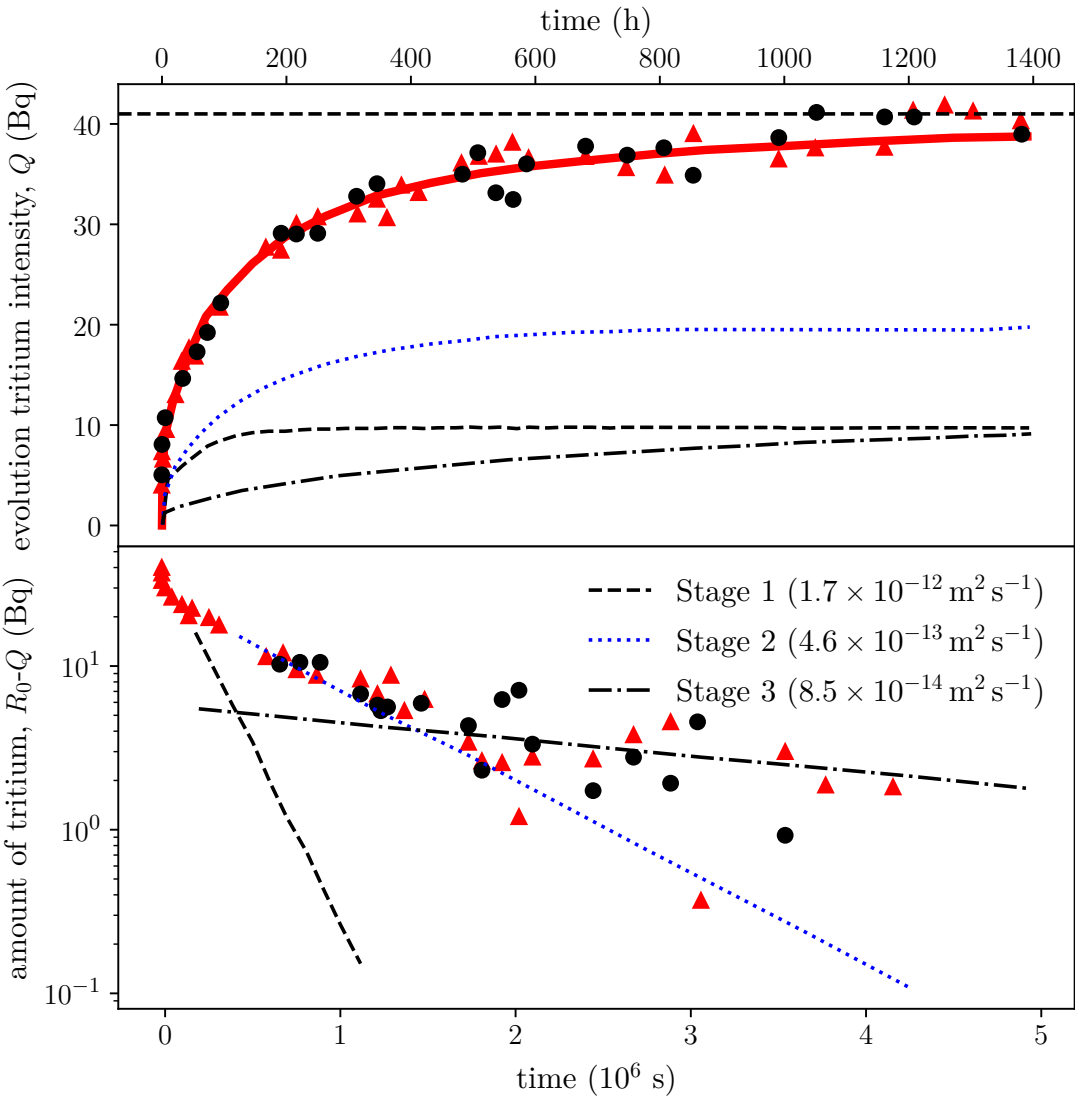


Figure 2.47: Tritium release at 323 K from two equally loaded GAS type specimens. (loaded at 673 K and 1.3 kPa). Experimental results obtained with each specimen are provided red and black symbols, theoretical predictions by dotted lines and total released tritium by the solid fat line (after [Ots08]).

Thermally and chemically very stable trapping of tritium in the very thin surface layer of stainless-steel SS316 was also noticed by Penzhorn et al. [Pen10; Pen13a]. In fact, prolonged thermal release of most tritium retained in the bulk at low temperature, e.g. 323 K, caused no discernible change of the tritium concentration in the metal surface. Evidently, the release mechanisms of tritium from surface and bulk are different. Presumably, tritium is retained atomically in the bulk and bound chemically and non-homogeneously as –OT in the metal surface layer.

The permeability of hydrogen and of deuterium through α-iron was studied by Tahara and Hayashi [Tah85] and found to be given by

$$P_{\mathrm{H}} = 1.77 \times 10^{-5} \exp\left(-\frac{31.6\mathrm{kJ\,mol^{-1}}}{RT}\right) \quad \mathrm{mol_{H_2} m^{-1}\,s^{-1}\,MPa^{-0.5}}$$

and

$$P_{\mathrm{D}} = 1.05 \times 10^{-5} \exp\left(-\frac{32.4\mathrm{kJ\,mol^{-1}}}{RT}\right) \quad \mathrm{mol_{D_2} m^{-1}\,s^{-1}\,MPa^{-0.5}}\ ,$$

respectively. Le Claire [Cla91] recommended for the calculation of the permeability of hydrogen across α-iron a similar expression

$$P_{\mathrm{H}} = 4.07 \times 10^{-5} \exp\left(-\frac{35.17\mathrm{kJ\,mol^{-1}}}{RT}\right) \quad \mathrm{mol_{H_2} m^{-1}\,s^{-1}\,MPa^{-0.5}}$$

which was estimated from results published in about twenty selected papers on the topic. In his extensive review article much additional detailed information on the permeation of hydrogen isotopes through Fe, Fe-based alloys, as well as across some commercial steels is provided. Permeability values for ferritic alloys and steels were larger than those for austenitic steels, but always smaller than for alpha-iron.

A number of diffusivity and solubility data for virgin MANET, F82H and BATMAN have been compiled in Table 2.47 together with analogous data for α-iron. All in all, the data published by various investigators are in good agreement. General conclusions concerning the solubility of hydrogen are: i) it is higher in α-iron than in MANET, F82H or BATMAN, ii) not significantly different in these three low-activation materials and iii) the results of one team differ considerably from all others i.e. [Dol00].

Table 2.47: Arrhenius constants for the diffusivity and solubility of hydrogen isotopes in "virgin" α-iron, MANET, F82H and BATMAN.

Gas	D_0	E_d	Temperature range	K_{0S}	E_S	Temperature range	Ref.
	$m^2\,s^{-1}$	$kJ\,mol^{-1}$	K	$mol\,m^{-3}\,Pa^{-0,5}$	$kJ\,mol^{-1}$	K	
				Iron			
H	3.87×10^{-8}	4.5	573 - 873	0.51	27.0	573 - 873	[For90]
H	6.20×10^{-8}	10.5	473 - 1073	0.86	23.1	473 - 1073	[Yam83]
H	4.48×10^{-8}	5.3	500 - 1000	0.44	26.3	500 - 1000	[Tah85]
H	-	-	-	0.69	24.3	473 - 1183	[Eic58]
H	7.2×10^{-8}	5.7	233 - 353				[Kiu83]
H	$1\text{-}2.5 \times 10^{-7}$	6.7 - 7.1	323 - 823				[Kiu83]
D	4.28×10^{-8}	6.5	500-1000	2.45	25.9	500 - 1000	[Tah85]
				MANET			
H	7.17×10^{-8}	13.5	523 - 873	0.41	29.6	523 - 873	[For88]
H	2.28×10^{-7}	18.0	553 - 873	0.40	28.4	553 - 8736 [Per92]	
D	1.46×10^{-7}	16.8	553 - 873	0.40	28.4	553 - 8736 [Per92]	
H	2.28×10^{-7}	18.0	553 - 873	0.66	32.0	553 - 873	[Per92]
D	1.46×10^{-7}	16.8	553 - 873	0.66	32.0	553 - 873	[Per92]
D	6.60×10^{-7}	29.0	520 - 620	0.009	10.0	520 - 620	[Dol00]
T	5.0×10^{-7}	29.0	520 - 620	0.014	12.0	520 - 620	[Dol00]
				F82H			
H	9.2×10^{-8}	13.7	473 - 723	0.63	27.4	473 - 723	
H	1.8×10^{-7}	14.1	573 - 723	0.30	25.8	573 - 723	[Ser98]
D	1.1×10^{-7}	13.9	573 - 723	0.38	26.8	573 - 723	[Ser98]
D	3.9×10^{-8}	8.0	490 - 1000	1.20	33.8	490 - 1000	[Dol02]
T	3.3×10^{-8}	7.8	490 - 1000	1.13	33.0	490 - 1000	[Dol02]
				BATMAN			
D	1.9×10^{-7}	15.2	573 - 723	0.20	24.7	573 - 723	[Ser97]

The consequences of pre-treatment on diffusivity are remarkable. Reiter et al. [Rei93a] heated MANET specimens for several days at 900 K either under vacuum or during exposure to 1 bar hydrogen and observed a strong decrease in diffusivity. When the pre-treatment was carried out under vacuum a pre-exponential factor of $8.24 \times 10^{-7}\,\mathrm{m^2\,s^{-1}}$ and an activation energy of $34.9\,\mathrm{kJ\,mol^{-1}}$ was obtained. When the samples were pre-treated at the same temperature but under 1 bar hydrogen the pre-exponential factor was found to be $1.45 \times 10^{-5}\,\mathrm{m^2\,s^{-1}}$ and the activation energy $57.8\,\mathrm{kJ\,mol^{-1}}$. Conversely, the pre-treatment procedure had no discernible influence on the solubility of hydrogen in MANET.

Average solubility values of hydrogen in iron and several other low-activation materials are plotted in Fig. 2.48. A comprehensive review on the diffusivity and solubility of hydrogen in iron has been published by Kiuchi and McLellan [Kiu83] After evaluation of 62 series of data on the diffusivity of hydrogen in iron they identified different sets of Arrhenius constants for the temperature ranges 233 - 353 and 323 - 823 K. These two sets were attributed to an increase of the fraction of H atoms hopping between octahedral rather than between tetrahedral sites with gradually increasing temperature.

Because the diffusion coefficients of the discussed advanced low activation materials do not exhibit significant differences, their selection for application in tritium relevant systems will predominantly be dependent upon the thermo-physical and thermo-mechanical properties as well as on the possibility of optimizing their chemical composition to the point where the generation of activation products is minimal.

Zhang et al. [Zha17] developed a mathematical model for the permeation of a multicomponent mixture consisting of (H_2, HT and T_2) across Reduced Activation Ferritic/Martensite (RAFM) materials like MANET II (Europe), F82H (Japan), or ARAA(Korea), in diffusion limited and surface limited regimes (for more information on multicomponent permeation across metal alloys refs. [Kiz99] and [Shi99] should be consulted). Aim of the work was to investigate the permeation of hydrogen isotopologues under conditions prevailing in a Test Blanket System for ITER, i.e. low partial pressure of tritium (<1 Pa) in a 0.1 % hydrogen in helium carrier gas across an oxidized or a bare RAFM surface. The developed model is based on classical kinetic theory involving equilibria of the gas species, and equilibria between molecular gas species and atoms dissolved in the metal.

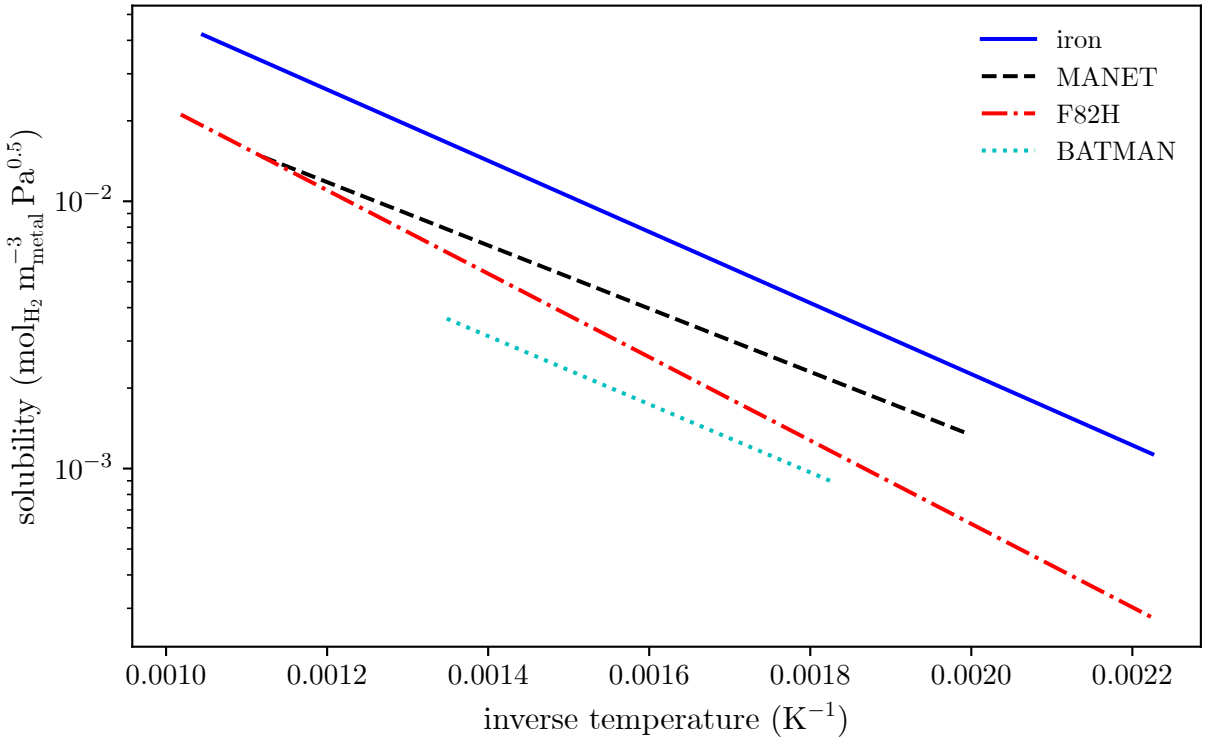


Figure 2.48: Comparison of the average solubility values of hydrogen in low-activation materials with the solubility in iron as function of inverse temperature.

The tritium atom concentration, c_T, on a metal surface under equilibrium conditions as given by the expressions

$$c_T = K_{s_T}\sqrt{p_{T2}}$$

$$K_{eq} = \frac{p_{HT}^2}{p_{H2}p_{T2}}$$

$$c_T = \frac{K_{s_T}}{\sqrt{K_{eq}(T)p_{H2}}}p_{HT}$$

is directly proportional to the partial pressure of HT and inversely proportional to the square root of the partial pressure of H_2. Because for a blanket gas stream the inequality

$$p_{H2} \gg p_{HT} \gg p_{T2}$$

holds, it is evident that the tritium equilibrium concentration on a metal will be linearly dependent from the partial pressure of HT and therefore, in accordance with the equations displayed above, the permeation flux of tritium will be significantly reduced by the presence of molecular hydrogen.

At STAR facility in Idaho National Laboratory, Idaho Falls, permeation experiments were carried out with a membrane consisting of Advanced Reduced Activation Alloy (ARAA) kept at temperatures of either 673, 723, or 773 K. The composition of the primary gas mixtures employed at Idaho for experiments with ARAA was 0.001 - 0.1 Pa T_2, 99 Pa partial pressure H_2, and 10^5 Pa He. Further permeation results with the RAFM materials MANET II and F82H were published by Serra [Ser96; Ser97]. The research at STAR and the results of Serra together with numerical simulations provided evidence that under the tested conditions the presence of hydrogen reduces the permeation rate of tritium significantly. Moreover, provided equilibrium conditions are established, it was found in line with theoretical expectations that the concentration of tritium on the metal follows a square root dependance from the T_2 partial pressure, a linear dependence from the partial pressure of HT, and is inversely proportional to the square root of the partial pressure of H_2. From the laboratory data and numerical simulations with the multicomponent permeation model under a surface-controlled regime it was concluded that the permeation flux of tritium is **reduced** by up to two orders of magnitude when the partial driving pressure of HT is reduced from 1 Pa to 0.01 Pa while the pressures of hydrogen is maintained at 100 Pa (see 2.49).

What is more, experimental data as well as simulation results indicate that the mono permeation rate across **oxidized** MANET II specimens is approximately two orders of magnitude lower than across the **bare** material, the permeation rate being proportional to pressure and square root of pressure for oxidized and clean MANET, respectively.

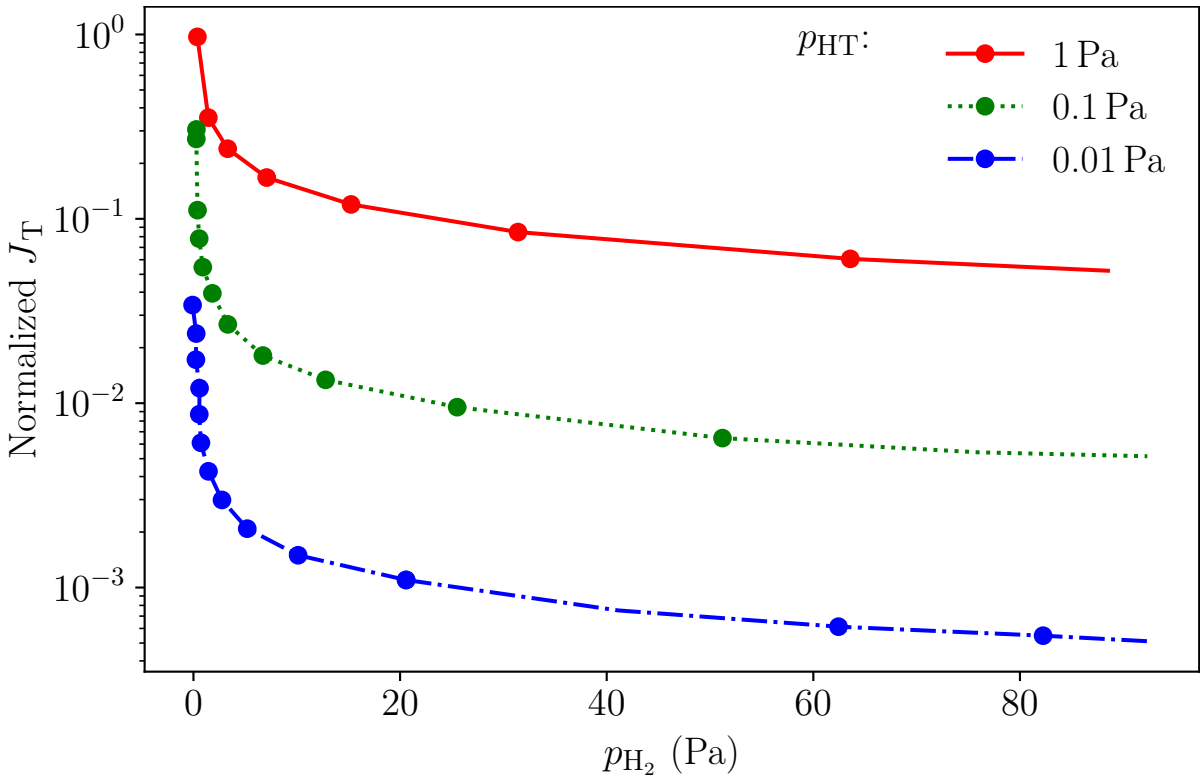


Figure 2.49: Equilibrium concentrations of tritium in a Reduced Activation Ferritic/Martensitic (RAFM) membrane as function of hydrogen partial pressure in helium (after [Zha17]). As apparent, the tritium equilibrium concentration on the metal surface is reduced by the presence of hydrogen in the carrier gas.

2.14.1.18 Interaction of tritium with welds

Ductility, elongation to failure and fracture toughness of welds are known to be reduced after exposure to tritium [Mor77]. The magnitude of the reduction increases with time as tritium penetrates by diffusion and helium is generated by radioactive decay gradually building up in the material.

The weldability of stainless-steel SS316 contaminated by tritium is discussed in some detail in 3.8.5.

2.14.1.19 Corrosion of steel induced by tritiated water

Highly tritiated water reacts aggressively with metals via peroxides formed by self-radiolysis [Pey78]. Due to this fact and in view of the much higher radiotoxicity of tritiated water in comparison to tritiated molecular hydrogen, highly radioactive tritium is preferably stored as

solid tritide. When this is not possible tritiated water can be stored under an overpressure of T_2. Under these conditions, the formation of oxygen is suppressed in the cover gas and that of peroxides in the liquid. As a result a significant reduction of corrosion can be achieved.

A time-independent correlation between the concentration of tritium in tritiated water and decreasing pH (increasing acidity) was reported by Hayashi et al. [Hay06]. In other words, whereas at tritium concentrations in the range 0.001 - 0.1 $\mathrm{PBq\,m^{-3}}$ the pH remained close to (7 ± 1), when the concentration of tritium exceeded 1 $\mathrm{PBq\,m^{-3}}$ pH values of about 3 were reached irrespective of whether the tritiated water was stored a few months or up to 5 years. According to a **Pourbaix plot** corrosive conditions establish when pH values become increasingly acidic and the oxidation-reduction potential (ORP) reaches high values. In fact, after one-year storage of highly tritiated water (10 $\mathrm{PBq\,m^{-3}}$) in a stainless-steel tank the liquid became acidic by self-radiolysis and pit corrosion was detected probably at or in the vicinity of welded zones of the containment. Induced by this kind of corrosion a leakage of radioactive liquid developed after a storage period of about one year. In view of this, these investigators recommended periodic control of the ORP of the stored water measured against a standard hydrogen electrode. Another suggested preventive measure was regular analyses of the ionic composition.

Bellanger et al. [Bel08a; Bel93a] confirmed the observations of Hayashi et al. [Hay06] which reported that stainless-steel 316L is strongly corroded by tritiated water containing chlorides or hydrogen peroxide, particularly at low pH values. The corrosion effect was markedly enhanced by temperature, which boosted the formation of defective oxides known to favour pitting and crevice (crack) corrosion. Consistently, Itoh et al. pointed out in earlier work performed in an optical glass cell containing water of 0.12 $\mathrm{TBq\,cm^{-3}}$ and maintained at ambient temperature that the total yield of radiolysis gases increased noticeably when a specimen of SS316L was introduced into the glass cell. When instead of SS316L, the test was performed with a SS304 specimen the yield of radiolysis gases increased by a factor of about four.

Ondrejcin and McLaughlin [Ond80] examined the corrosion of stainless-steel type 304L in the presence of nitric acid and hydrofluoric acid. Corrosion by HNO_3 together with HF (or TF) or by solutions of these two species together with products from the stainless-steel corrosion like ferric and dichromate ions, is particularly severe.

Because elemental tritium reacts with fluorine-containing materials like Teflon, KelF, PFA, Nafion®, or fluorinated pump oils to generate TF these materials must be strictly excluded from

tritium handling equipment [Mon78; Int91]. Inter granular stress corrosion of stainless-steel type 316 by tritium in the presence of both Teflon and moisture is reported to be acute, in particular at increased temperatures.

Experiments on the corrosion of stainless-steel SS316L by tritium (0.0007 - 0.004 mol tritium/l) - oxygen mixtures revealed a dependency of the tritium oxidation rate from the square root of the concentration of tritium, i.e. $\sqrt{c_T(t)}$. Accordingly, the following expression was formulated by Hircq and Blet [Hir93]

$$\text{rate} = K\sqrt{c_\text{T}(t)}\ \text{mol}\,\text{l}^{-1}\,\text{hour}^{-1}$$

where K is a proportionality constant described by the expression

$$K = 22.74\ c_\text{O}\ c_\text{T}\ \text{mol}^{0.5}\,\text{l}^{0.5}\,\text{hour}^{-1}.$$

This constant depends on the product $c_\text{O}(0)$ x $c_\text{T}(0)$, i.e. the initial concentrations of oxygen and tritium, respectively.

A total of twenty specimens comprising the stainless-steels SS316L, SS304, NS30, and XN26 TWS were examined under several conditions of gas composition, temperature, and exposure time to 8×10^{-4} mol tritium/l of tritiated water vapour [Hir93]. The specimens were tested either as-received, polished or welded. ESCA examination provided evidence that iron and chromium on the surface of SS316L exposed to tritiated water for 3 or 6 months at 773 K were fully oxidized generating a layer up to about 0.005 µm thick. The formation of Fe_3O_4 and Cr_2O_3 on the surface could be verified by X-ray grazing measurements. With a nuclear micro probe utilizing either the reaction $\text{T(d, n)}^4\text{He}$ or the reaction $^{16}\text{O(d, p)}^{17}\text{O}$ a tritium-rich oxide layer of up to 0.1 µm was detected. Additionally, Intergranular chromium carbide ($Cr_{23}C_6$) precipitates were observed on SS316L and SS304. From the results it was concluded that enhanced corrosion takes place in welded zones and in the presence of work-hardened martensite. Of all tested stainless-steel materials NS30 was found to possess the highest corrosion resistance.

Employing electrochemical methods (Tafel extrapolation method) Oyaidzu et al. [Oya11a] observed that tritiated water has an inhibitory effect on the passivation of stainless-steel type SUS304. This inhibitory effect manifests in highly corrosive media like 1 N H_2SO_4 or 1 N Na_2SO_4 electrolyte but not not in 1 N NaOH solution. Hence, the pH of the tritiated water determines the

occurrence of passivation inhibition. Further investigation on the effect of tritium concentration, pH, and concentration of dissolved oxygen were not straightforward [Oya11b]. To shed more light on the underlying mechanism, Oyaidzu et al. [Oya15b] performed electrochemical corrosion experiments utilizing pure chromium in a 0.01 N sulfuric acid solution. Chromium was selected because it is considered to be the main constituent of the oxidic protective layer on stainless-steel SS304. The results confirmed that self-passivation of chromium induced by dissolved oxygen was inhibited by tritium with the consequence of enhanced signs of corrosion. It was postulated that the elution of chromium induced by radiolysis products formed in highly tritiated water is responsible for the enhancement of corrosion.

2.14.2 Interaction of hydrogen isotopologues with copper and copper-based alloys

Low tritium permeability and high thermal conductivity are the salient properties of copper that confer to this metal the potential for application in tritium systems. Ancillary beneficial properties are high ductility and resistance towards hydrogen embrittlement. On the negative side are the low tolerable upper temperature and possible interactions of hydrogen with oxides on copper or oxygen dissolved in copper which may eventually conduct to material failure through intermediary formation of water (see also [Beg78] and section 3.1.3).

2.14.2.1 Physical-chemical properties

The temperature dependency of the solubility of hydrogen in metals is given by the expression

$$\ln \Sigma_{\mathrm{H}} = -\frac{\Delta\overline{H}_{\mathrm{H}}}{RT} + \frac{\Delta\overline{S}_{\mathrm{H}}}{R}$$

in which

$$\Sigma_{\mathrm{H}} = \frac{N_{\mathrm{H}}}{N_{\mathrm{M}}}$$

where $\mathrm{N_H}$ and $\mathrm{N_M}$ represent the number of hydrogen and metal atoms, respectively. The constants $\Delta\overline{H}_{\mathrm{H}}$ and $\Delta\overline{S}_{\mathrm{H}}$ stand for molar enthalpy and relative partial molar excess entropy for hydrogen in metals, respectively. Values of these thermodynamic constants are tabulated for copper in Table 2.48.

Table 2.48: Molar enthalpies and relative partial molar excess entropies for hydrogen in copper.

$\Delta\bar{H}_H$	$\Delta\bar{S}_H$	Literature
$\mathrm{kJ\,mol_H^{-1}}$	$\mathrm{kJ\,K^{-1}\,mol_H^{-1}}$	
54.9 ± 1.4	-0.037 ± 0.003	[McL73]
48.9	-0.074	[Tho67]

Data on the solubility of hydrogen in copper determined by Eichenauer and Pebler [Eic57], Thomas [Tho67], McLellan [McL73] and Penzhorn et al. [Pen11] are plotted as function of reciprocal temperature in Fig. 2.50. As evident from the plot, these results are in good agreement. The extrapolation of the high temperature data down to lower temperatures is also in line with tritium saturation concentrations measured in the sub-surface zone of copper specimens [Pen11]. Saturation concentrations were estimated from tritium depth profiles obtained by gradual chemical etching of tritium-bearing copper specimens. Substantiating previous observations by Swansiger [Swa88], rather high concentrations of tritium were detected on the top surface and sub-surface of copper, i.e. 80 - 90 % of the total incorporated tritium. The opposite is the case with stainless-steel where in spite of high concentrations on the top surface most of the total tritium, i. e. up to 99 %, resides in the bulk. On the other hand, and similar to stainless-steel, copper exposed thermally to molecular tritiated hydrogen discharges tritium at ambient temperature primarily as HTO. Specimens of this metal containing $0.25\,\mathrm{MBq\,g^{-1}}$, $1.4\,\mathrm{MBq\,g^{-1}}$ or $5.9\,\mathrm{MBq\,g^{-1}}$ of dissolved tritium displayed at 298 K chronic release rates of $120\,\mathrm{Bq\,hour^{-1}}$, $280\,\mathrm{Bq\,hour^{-1}}$ and $470\,\mathrm{Bq\,hour^{-1}}$, respectively [Pen11].

Swansiger [Swa88] determined the solubility of tritium in copper and gold at temperatures and pressures within the ranges 473 - 673 K and 3.8 - 59.2 MPa, respectively. The periods allowed for equilibration were as long as 61 days. From data obtained by acid dissolution of samples or vacuum melting with subsequent ^{3}He analysis Swansiger concluded that i) there was much more tritium on and near the surface than in the bulk of both copper or gold (see also above), and ii) surface effects contributed effectively to prolong substantially the time required for equilibration attainment with both metals. Low temperature solubilities predicted from extrapolation of data measured at > 873 K with copper by McLellan [McL73] agreed rather well with Swansiger´s

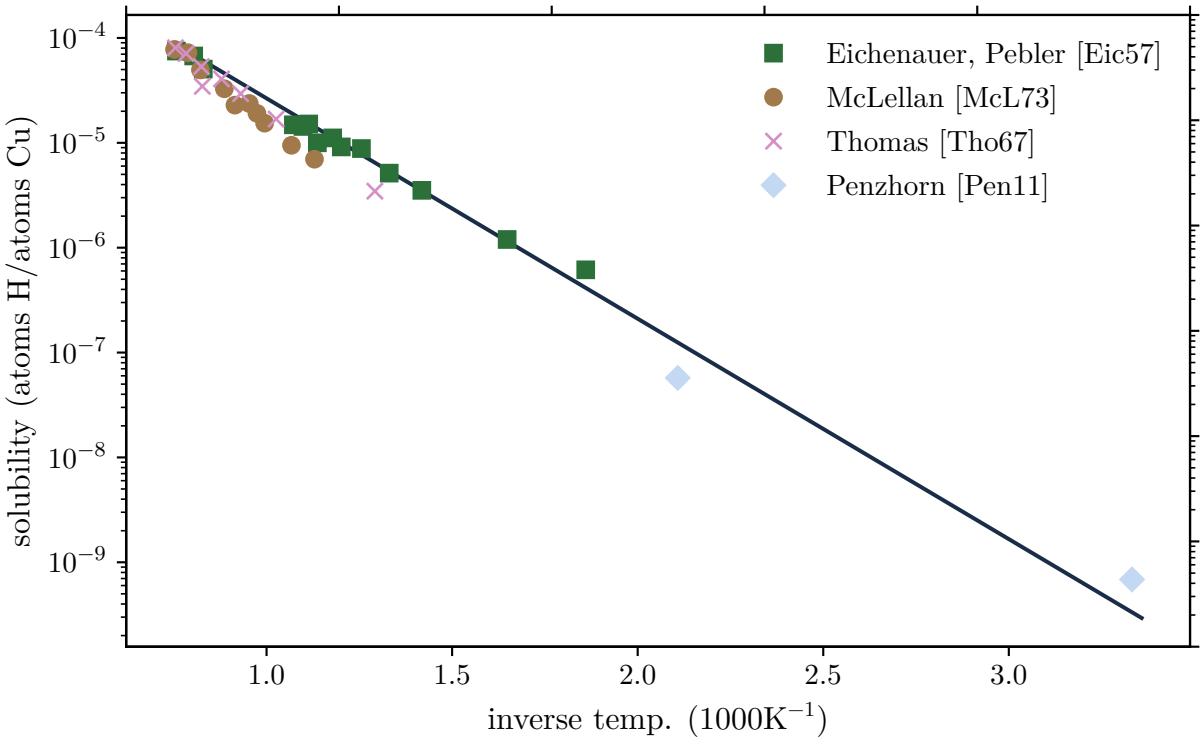


Figure 2.50: Semi logarithmic plot of the solubility of hydrogen in copper as function of inverse temperature.

measurements. In compliance with Sieverts law the solubilities at high tritium pressure showed the expected dependency from square root of fugacity.

Carnuth [Car63] noted that hydrogen diffusion coefficients in cold deformed copper were about four orders of magnitude lower, e.g. $10^{-12}\,\mathrm{cm^2\,s^{-1}}$ at 433 K, than in non-deformed copper. Conversely, the solubility of hydrogen in deformed copper increased dramatically by several orders of magnitude with respect to that in non-deformed one. From these observations it may be concluded that metal deformation bring about defects of the copper crystal framework which in turn are the cause for significant changes of hydrogen diffusion and solubility values. It is well known, that defects are responsible for substantial hydrogen atom trapping. In his comprehensive overview Balluffi [Bal78] reports that mobile defects in copper anneal to large clusters which in turn require rather high temperatures to anneal out, i. e. $\geq$ 750 K.

Diffusion coefficients of protium, deuterium and tritium in copper have been reported by Katz et al. [Kat71], Eichenauer et al. [Eic65], Birnbaum and Wert [Bir72a], as well as Tanabe et al. [Tan84]. Data in Table 2.49 show that there is reasonably good agreement between

Table 2.49: Diffusion coefficients of hydrogen isotopes in copper.

Hydrogen isotope	D_0	ΔH	Temperature range	Literature
	$m^2\,s^{-1}$	$kJ\,mol^{-1}$	K	
H_2	1.15×10^{-6}	40.8	700 - 1000	[Eic65]
D_2	6.20×10^{-7}	37.9	700 - 1000	[Eic65]
H_2	1.13×10^{-6}	38.9	700 - 1200	[Kat71]
D_2	7.30×10^{-7}	36.8	700 - 1200	[Kat71]
T_2	6.12×10^{-7}	36.5	700 - 1200	[Kat71]
H_2	2.26×10^{-7}	29.3	450 - 1200	[Tan84]
H_2	1.06×10^{-6}	38.4	473 - 713	[Gut74]
T_2	6.6×10^{-7}	37.4	943 - 1473	[Rei93b]

the coefficients determined by these investigators. Classical absolute rate theory was found to describe reasonably well the diffusion of hydrogen through copper. Mass dependences of diffusion coefficients were estimated to be $D_H/D_D = 1.55$ and $D_H/D_T = 1.85$ [Kat71]. Copper shows an inverse isotope effect, i.e. $\Delta H_H > \Delta H_D > \Delta H_T$ (ΔH = enthalpy of activation) at temperatures above 667 K and a cross over at temperatures within the range 476 - 667 K [Bai99b].

Grain boundary diffusion of deuterium through copper was first reported by Robinson [Rob60] at temperatures in the range 227 - 293 K. Maienschein [Mai88] provided several years later confirmation with experiments performed at 323 K that in unannealed copper grain boundary transport is rate determining. Following appropriate annealing, bulk processes become rate controlling provided the heat treatment has reduced sufficiently the concentration of tritium in the grain boundary.

Co-adsorbed oxygen promotes dissociation of water on gold, silver and copper by lowering the barrier to water dissociation presumably by altering the electronic structure of the surface [Hen02; Ban84]. In most investigations with copper it was found that there is no exchange reaction between hydrogen and water when water is not dissociated. Hence, surface interactions between both molecules becomes exclusively competitive for adsorption sites. In case of irreversible water dissociation, on the other hand, coadsorption of H_2O and D leads to desorption of HD.

Table 2.50: Arrhenius constants for the permeability of hydrogen across copper.

Gas	Temperature range	Pressure	P_0	E_P	Reference
	K	kPa	$\mathrm{mol\,m^{-1}\,s^{-1}\,Pa^{(0,\,-5)}}$	$\mathrm{kJ\,mol^{-1}}$	
H_2	530 - 920	-	4.1×10^{-7}	74.49	[Eic57]
H_2	620 - 770	0.15 and 0.2	8.25×10^{-9}	52.29	[Rud61]
H_2	620 - 970	0.1	5.86×10^{-7}	75.65	[Gor62]
H_2	700 - 900	0.013 - 0.1	5.2×10^{-6}	78.73	[Eic65]
D_2	700 - 900	0.013 - 0.1	3.3×10^{-6}	80.06	[Eic65]
H_2	470 - 710	0.000 13 - 0.13	8.42×10^{-7}	77.23	[Per72]
D_2	375 - 750	0.1 and 0.5	5.8×10^{-8}	71.66	[Cas76b]
H_2	470 - 700	0.000 13 - 0.13	8.8×10^{-7}	77.48	[Beg78]
T_2	323 - 443	101	4.4×10^{-8}	54	[Mai88]

Lloyd et al. [Llo97a] determined the diffusivity of deuterium across copper at 350 - 550 K. Their values were in good agreement with results obtained by other investigators at considerably higher temperatures, i.e. 800 - 1000 K. Thermal desorption studies of hydrogen adsorbed on and absorbed in Cu(111) revealed i) a high temperature peak arising from chemisorbed hydrogen, ii) a peak attributed to a large fraction of hydrogen dissolved near the surface and iii) a peak assigned to absorbed bulk species [Llo97a; Llo97b]. As common to other metals like Ni, Pd or Pt, distinct subsurface bonding sites of higher binding energy than sites in the bulk characterize hydrogen in copper. Bonding sites lying immediately below the topmost surface with higher binding energy than surface sites were also reported by Luo et al [Luo03].

Numerous investigators have studied - mostly by the membrane technique - the permeation of hydrogen isotopologues across copper (see Table 2.50). Maienschein et al. [Mai88] drew attention on the importance of gas transport along such lattice structure defects as grain boundaries. Transport through grain boundaries is essentially **independent** of **temperature** giving rise to a relatively constant flux of gas through the metal. At certain temperatures, transport by permeation can be slower than transport through defects. When this is the case, an extrapolation of high temperature data will significantly under estimate the actual permeation rate.

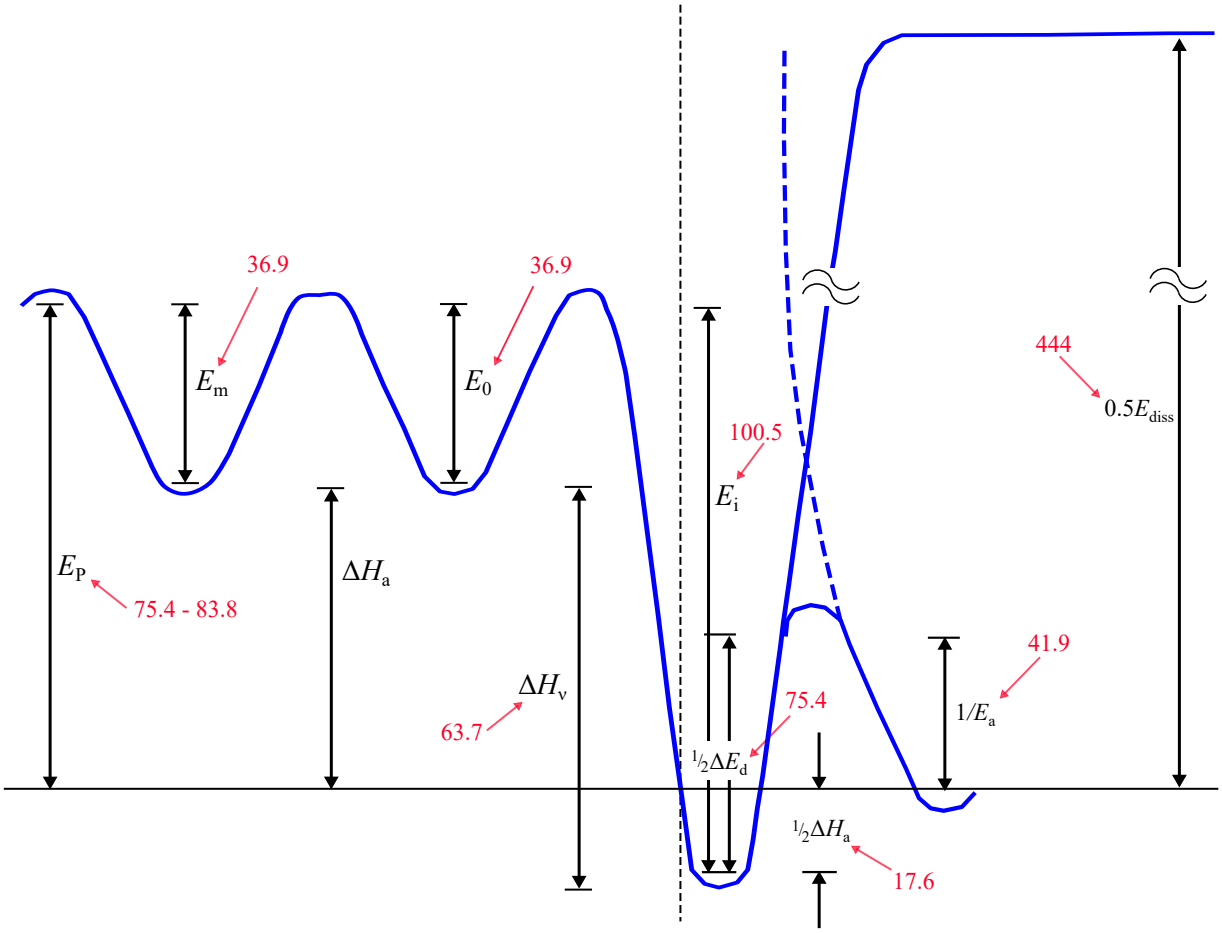


Figure 2.51: Lennard-Jones potential diagram of the deuterium/copper system (after [Llo97a]). All values are expressed in kcal mol^{-1}. The symbols E_a denote energy of adsorption, E_d energy of desorption, E_p energy of permeation, E_m energy of diffusion, E_i energy of migration into the bulk, E_o energy of migration to the surface, ΔH_a heat of adsorption, ΔH_s heat of solution, ΔH_σ heat of migration and ΔH_{dis} energy of dissociation of D_2 (thermodynamic values are shown in fat red).

On the basis of i) permeation experiments performed with an atomic deuterium source, ii) diffusion measurements and iii) results from thermal desorption studies published in the literature, Lloyd et al. [Llo97a] developed a rather noteworthy and comprehensive Lennard-Jones potential model for the deuterium/copper system. The results of the model, which are valid within the temperature range 80 - 1000 K, are displayed in Fig. 2.51.

Two distinct types of hydrogen traps, i.e. vacancies and interstitial loops, were identified in **helium-irradiated copper** increasingly loaded with deuterium atoms by a plasma-induced procedure [Tak07]. Depth profiles generated by nuclear reaction analysis were used to assign the

traps. Traps created by irradiation with a dose of $1.5 \times 10^{21}\,\mathrm{m}^{-2}$ caused the initial deuterium concentration near the plasma exposed surface to increase by a factor of 10^4.

Otsuka et al. [Ots16] investigated the release behaviour of tritium into pure water from specimens manufactured from copper, or copper alloys like CuCrZr or CuSnP utilizing the tritium imaging plate technique or liquid scintillation counting. Homogeneously loaded specimens were obtained by exposing for several hours' thin metallic samples to a pressure of 13.3 kPa tritiated hydrogen ($\mathrm{T/H} = 10^{-4}$) at 873 K for several hours. Two mechanisms of tritium release, a fast and a slow one, were identified. The fast one was attributed to the release of tritium dissolved in the bulk and the slow one to release of tritium more strongly bound on or in surface oxide layers. The slow release was found to be about two orders of magnitude smaller than the fast one from both pure copper and CuSnP. In conformity with observations by Swansiger [Swa88] and Penzhorn et al. [Pen11], imaging plate results revealed that i) the concentration of tritium on the surface and in the subsurface of copper is larger than that dissolved in the bulk and ii) tritium bound on the surface or subsurface is more strongly retained than that in the bulk. In fact, the intensities of tritium on the surface were about 30 times higher than in the bulk of copper and about 300 times higher than in the bulk of CuCrZr.

Of the metals copper, silver and gold only copper was found to chemisorb hydrogen with a noteworthy sticking probability [Chr88].

2.14.2.2 Application of copper in fusion machines

Copper based alloys containing only low concentrations of alloying elements, e.g. about 1 % by weight, are currently contemplated within the frame of the design of ITER because of their high thermal conductivity (10 - 20 times higher than of SS316) and comparatively high mechanical strength. While as rule of thumb increasing the percentage of alloying element increases the strength of copper-based alloys this will also invariably diminish the thermal conductivity of the alloy. Thus, many "improved" alloys will become less attractive for the envisaged applications. Among the negative properties of copper alloys, the following can be cited: i) relatively modest creep and fatigue parameters (60 - 80 % in comparison to those of type SS316), ii) low maximal operation temperature of only about 623 K and iii) progressive loss of electrical conductivity as transmutation products gradually accumulate during the operation of a fusion machine [Gre93].

According to competent sources, about 800 t of copper-based materials are being contemplated for ITER in components such as interlayer materials (CuCrZr) installed between armour components (CFC, W) and the divertor or between the beryllium armour and the first wall heat sink [Bar09; ITE01d]. Copper is one of the waste materials that will require detritiation during decommissioning.

A very comprehensive survey on such physical properties as yield strength, Young modulus, thermal conductivity, thermal stress factor, softening temperature, creep strength, fatigue strength of a large number of copper alloys with potential for application in fusion machines was compiled by Butterworth and Forty [But92]. The same publication also discusses property changes induced by neutron irradiation. Within this frame, it was pointed out, that copper-based materials exposed to neutron irradiation in a tokamak will become contaminated by tritium not only by permeation processes but also via transmutation reaction sequences. Christmas et al. [Chr83] as well as Wermann et al. [Wer02] investigated the branching ratios of the decay scheme of ^{64}Cu. Greenwood et al. [Gre93] calculated yields of transmutation products generated in pure copper when this material was assumed to be irradiated in the Fast Flux Test Facility (FFTF) at Pacific Northwest Laboratory, Richland, Washington (see Fig. 2.52). The principal transmutation products in order of decreasing importance were calculated to be nickel, zinc and cobalt. The rates of production of the first two products were found to be rather similar while that of cobalt was comparatively low. Calculated specific activities in 1 kg of copper after 2.5 years of irradiation with 4.1 MW m^{-2} neutrons are displayed in Fig. 2.52. As apparent, whereas initially ^{64}Cu is the dominant nuclide, during the period between 1 day and 100 years the nuclide ^{60}Co becomes the main isotope. After 100 years this role is taken over by ^{63}Ni.

Fabritsiev et al [Fab97] studied the effect of the neutron spectrum on strength and ductility properties, transmutation rate and change in electrical conductivity of pure, precipitation hardened and dispersion-strengthened copper-based alloys as function of irradiation dose and temperature. In case of precipitation-hardened alloys, the thereshold softening temperature was found to be 573 K when a dose of 5×10^{21} neutrons/cm^2 was applied.

First wall materials exposed to extremely hard neutrons carrying energies of 14 MeV will undergo a number of property changes. Neutrons will cause transmutations deep in the bulk due to their high penetrating power and concomitant high energy and generate diverse impurities including tritium. Properties are additionally modified by the effect of γ-rays, X-rays, tritons

and deuterons present in the plasma. Among other effects, these rays may trigger crystal lattice structural damages. The concentration of tritium permeated from the plasma-side into copper is estimated to be of the same order of magnitude as that resulting from transmutation reactions.

Even though the concentration of tritium in in-vessel components is not particularly relevant from the radioactivity-level-in-waste point of view, during decommissioning and the early waste management phase its impact can be rather important because of chronic release and possible leaching processes [Swa88; Pen11]. Whether the main source of tritium is pure copper or impurities in the metal still needs to be elucidated experimentally [37]. At any rate, copper is one of the materials that will necessitate detritiation during the decommissioning phase of the machine.

2.14.3 Interaction of hydrogen isotopes with copper alloys and copper-gold brazing alloys

The permeation of deuterium through several copper alloys was investigated by Begeal [Beg78] at temperatures in the range 550 - 830 K using a conventional membrane technique. Aim of the work was to extend the body of knowledge on the effect of small amounts of alloying elements on the permeability of hydrogen across copper. The results indicate that alloying copper with Sn, U, Zr, Sn/Pb/Zn/Si or Al/Fe causes only slight reduction of permeability at 573 K and shows only little effect on the permeation activation energy when compared to that of pure copper. Other alloys like copper/gold alloys revealed decreasing permeability and decreasing activation energy as the content of gold was increased. Within the frame of these activities, it was learned, that a layer of beryllium oxide can be formed on copper containing 2 % beryllium and a layer of aluminium oxide on copper containing 7 % aluminum plus 2 % silica. These oxide layers completely dominate the permeation of hydrogen. The process, which was described as "**in situ growth of a stable oxide permeation barrier**", was assumed to be initiated by high temperature reduction of the less stable oxides by hydrogen and simultaneous oxidation of the active metal. The resulting oxide layers were found to contain beryllium or aluminum but no copper.

[37] Loughlin, M. 2010. System Analysis and Standards Section, ITER. Personal communication.

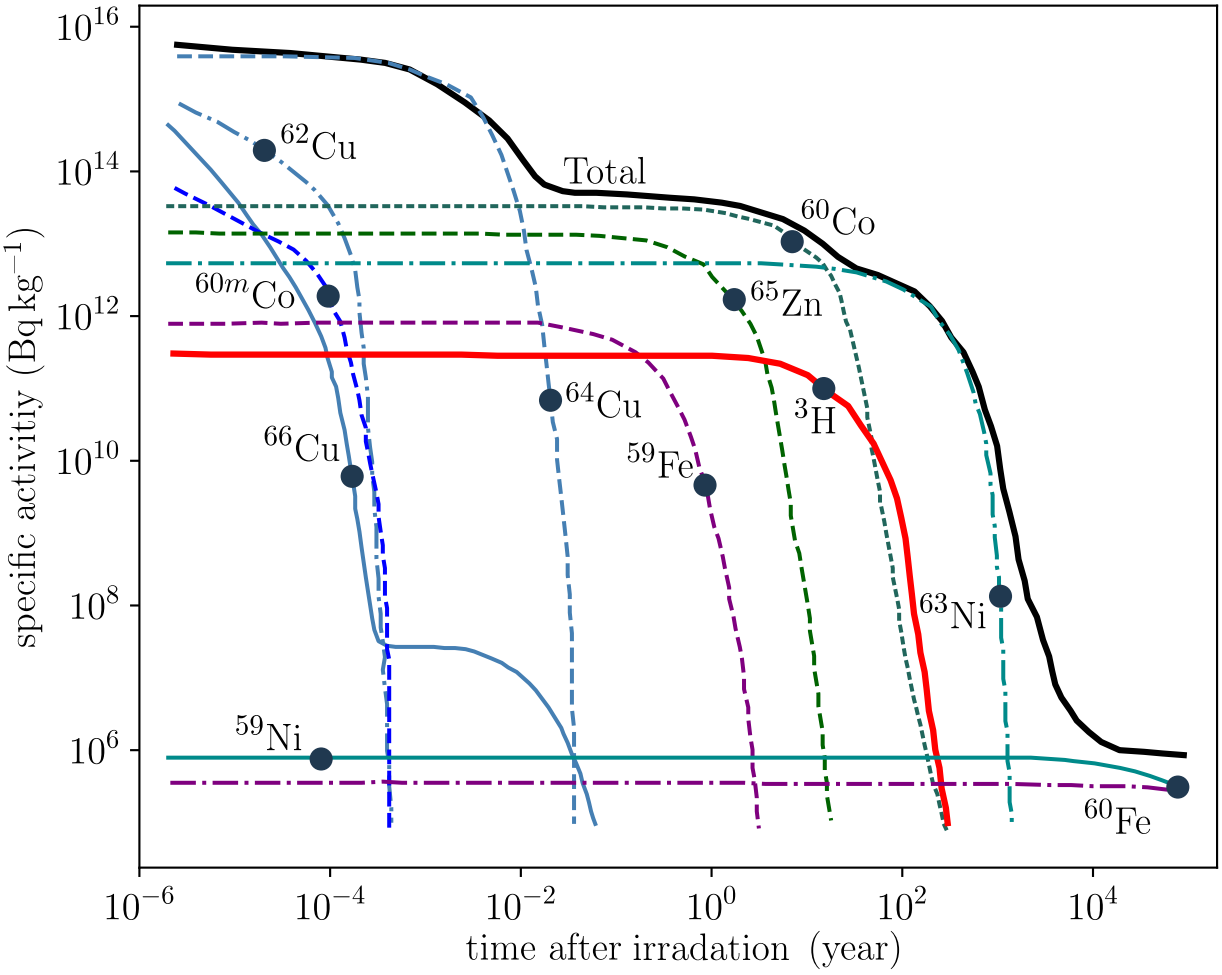


Figure 2.52: Calculated specific activities and total activity (shown in fat black) in copper after irradiation with 4.15 MW m^{-2} for 2.5 years as function of time (see also Fig. 2.2). Isotopes generated by transmutation reactions and surfacing in copper as impurities are ^{3}H (shown in fat red), ^{59}Fe, ^{60}Fe, ^{60}Co, ^{60}Co*, ^{59}Ni, ^{63}Ni, ^{62}Cu, ^{64}Cu, ^{66}Cu and ^{65}Zn (after [But92]).

2.14.4 Interaction of hydrogen isotopologues with silver and gold

Silver finds application in vacuum technology and hence in tritium handling equipment. It is an important constituent of silver-plated nickel, silver-plated copper or silver-plated stainless-steel gaskets. This type of gasket is particularly useful for equipment requiring frequent high temperature bake outs. Pure gold is used in form of wire ring gaskets or gold-plated copper gaskets in ultra-high vacuum systems. It is chemically inert, soft and ductile and can be used in flanges even at elevated temperatures. Provided it is installed properly, gold will not damage stainless-steel flanges and may be reused.

Table 2.51: Molar enthalpies and relative partial molar excess entropies for the solubility of hydrogen in silver and gold.

Metal	$\Delta\bar{H}_H$	$\Delta\bar{S}_H$	Literature
	$\mathrm{kJ\,mol_H^{-1}}$	$\mathrm{kJ\,K^{-1}\,mol_H^{-1}}$	
Ag	56.78 ± 1.76	-0.053 ± 0.004	[McL73]
	69.13	-0.035	[Tho67]
Au	27.55 ± 1.50	-0.086 ± 0.003	[McL73]
	36.22	-0.074	[Tho67]

Because of the extremely low solubilities of hydrogen isotopes in copper, silver and gold the same experimental techniques have frequently been employed to determine the solubility in all three metals. Likewise, the physical properties of these elements are often discussed together [Tho67; McL79]. This approach has also been adopted in this manual, at least for silver and gold.

Equations describing the temperature dependence of the hydrogen solubility in silver and gold have been reported by Thomas [Tho67]:

$$\text{Silver: } \log S(\text{at.}\%\mathrm{H_2}) = -0.222 - \frac{0.360 \times 10^4}{T}$$
$$\text{Gold: } \log S(\text{at.}\%\mathrm{H_2}) = -1.873 - \frac{0.188 \times 10^4}{T} \ .$$

The solubility of atomic hydrogen in a thin gold film at temperatures within the range 250 - 380 K has been discussed in a paper by Stobinski and Dus [Sto92]. The heat of solution was found to have a value of $9\,\mathrm{kJ\,mol_H^{-1}}$ and to be exothermic (as opposed to the heat of solution of molecular hydrogen). This was explained by the fact that atomic H adsorbs on gold at low temperatures and molecular H_2 does not.

Heats of solution and relative partial molar excess entropies for the solubility of hydrogen in silver and gold are provided in Table 2.51.

As can be seen in Fig. 2.53, which depicts the solubility of hydrogen and tritium in gold as function of inverse temperature, an extrapolation of the high-pressure/high-temperature results obtained by McLellan [McL73] or Thomas [Tho67] and results at high tritium pressure but

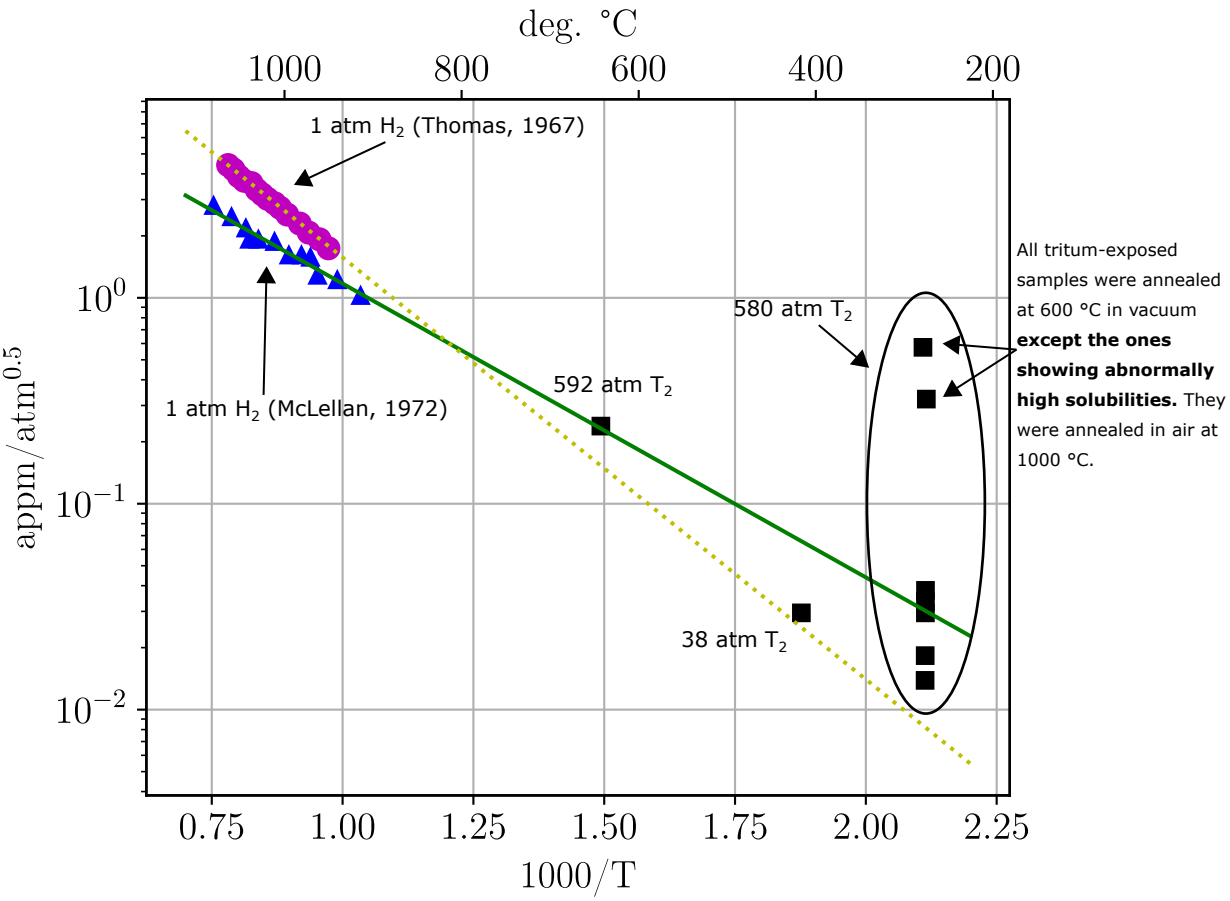


Figure 2.53: Hydrogen and tritium solubility in gold (T in K) (after [Swa88]).

low temperatures obtained by Swansiger [Swa88] are in essentially good agreement. Only gold specimens annealed in air at 1273 K exhibit much higher apparent solubilities than those annealed at 873 either under air or vacuum [Swa88]. To explain this phenomenon Swansiger postulated trapping of tritium by oxygen diffused into the matrix during high temperature annealing.

Diffusivities of hydrogen through silver are given in $m^2\,s^{-1}$ as function of temperature by expressions determined by [Eic58] or [Kat79]

$$D = 2.82 \times 10^{-7} \exp\left(-\frac{3500}{T}\right) \quad \text{(within 661 - 873 K)} \quad \text{[Eic58]}$$

$$D = (8.55 \pm 0.65) \times 10^{-7} \exp\left(\frac{3620 \pm 400}{T}\right) \quad \text{[Kat79]} \ .$$

As apparent, even though both activation energies are quite similar, the data of Katsuta are higher by a factor of about three. Eichenauer and Liebscher [Eic62] determined the diffusion coefficient

of hydrogen through gold spheres of 1.6 cm and 3 cm diameter. The obtained experimental data were well described by relationship

$$D = 5.60 \times 10^{-4} \exp\left(-\frac{5640}{RT}\right) \quad \mathrm{cm^2\,s^{-1}}$$

A number of Arrhenius parameters that can be used to calculate permeabilities of hydrogen across gold or silver are listed in Table 2.52.

2.14.5 Interaction of hydrogen isotopologues with nickel

Nickel-based alloys, like Inconel, Hasteloy, or Incoloy, are industrial materials of which nickel is the main single constituent. They are candidate structural materials for ITER as well as for the manufacture of keys and bolts [Kal00; Pia07].

Nickel has also been proposed as replacement of palladium/silver in permeators of the kind used in the plasma exhaust clean-up system of ITER where they are employed for the separation of hydrogen from impurities [Shi98; Fuk06]. Such permeators constitute crucial components of the fusion fuel cycle.

This section focusses on factors that determine the interaction of hydrogen isotopes with nickel and nickel-based alloys. Diffusivities and Sieverts´ constants of the hydrogen isotopologue - nickel system have been compiled in Table 2.53. As evident from the data collected in the table and the plots displayed in Fig. 2.54, the diffusivities determined by different investigators are fairly consistent. What is more, progress in *ab initio* computational methods has been so remarkable that in many cases the calculation of material properties has become possible with equal or even higher accuracy than obtainable from experiment [Ebi67b; Ebi67a; Lou74; Wim08].

Table 2.52: Permeability of hydrogen across gold and silver

Gas	Temperature range K	Pressure kPa	P_0 $mol\,m^{-1}\,s^{-1}\,Pa^{-0.5}$	E_P $kJ\,mol^{-1}$	Reference
			gold		
H_2	573 - 913	3 - 130	1.14×10^{-6}	114.8	[Beg78]
D_2	500 - 900	100 - 500	3.1×10^{-6}	123.0	[Cas76a; Ste83]
T_2	500 - 900	100 - 500	2.5×10^{-6}	123.0	[Cas76a; Ste83]
			silver		
H_2	-	-	2.2×10^{-7}	61.10	[Ste83]

Table 2.53: Arrhenius constants for diffusivity and solubility of hydrogen isotopes in nickel.

Gas	D_0	E_D	Temperature range	K_{0S}	E_S	Temperature range	Ref.
	$m^2\,s^{-1}$	$kJ\,mol^{-1}$	K	$mol\,m^{-3}\,Pa^{-0.5}$	$kJ\,mol^{-1}$	K	
H	7.4×10^{-7}	44.1	473 - 1073	1.0	10.7	473 - 1073	[Yam83]
H	1.9×10^{-7}	37.3	220 - 350				[Yam79]
H	3.8×10^{-6}	45.7*	298 - 1473				[Wim08]
H	7.0×10^{-7}	39.5	673 - 1273				[Kat71]
H	5.2×10^{-7}	40.0	473 - 1073	0.78	15.1	763 - 963	[Ebi67b]
H	6.7×10^{-7}	39.7	658 - 933	0.37	24.2	658 - 933	[Eic65]
H	1.1×10^{-8}	33.8	120 - 155				[Hoh82]
D	5.3×10^{-7}	38.7	673 - 1273				[Kat71]
D	3.2×10^{-7}	38.6	220 - 350				[Yam79]
D	2.4×10^{-6}	44.1*	298 - 1473				[Wim08]
D	4.3×10^{-7}	38.1	473 - 1073				[Ebi67b]
D	4.8×10^{-7}	38.5	658 - 933	0.39	28.4	658 - 933	[Eic65]
D	3.8×10^{-7}	38	550 - 1030				[Dol00]
D	8.8×10^{-8}	38.1	125 - 160				[Hoh82]
T	4.3×10^{-7}	38.1	673 - 1273				[Kat71]
T	1.8×10^{-6}	43.0*	298 - 1473				[Wim08]
T	3.7×10^{-7}	40.2	273 - 1673	0.39	12.5	273 - 1673	[Rob73]
T	2.3×10^{-7}	36	550 - 1030				[Dol00]
T	1.7×10^{-7}	38.6	125 - 160				[Hoh82]

* Result of ab initio calculations of diffusion coefficients for interstitial hydrogen isotopes.

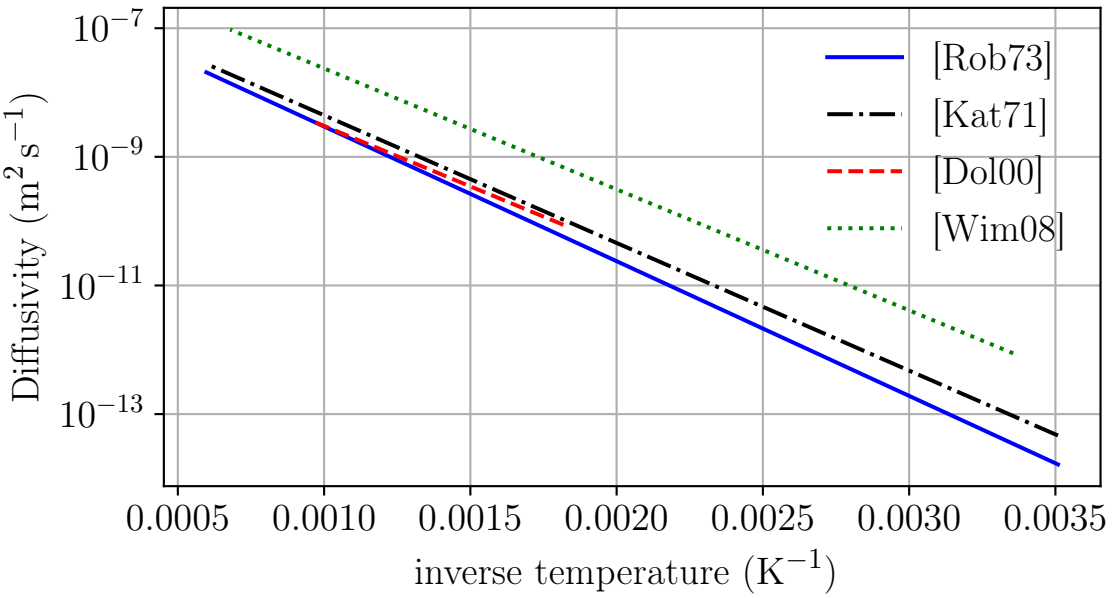


Figure 2.54: Diffusivities of tritium in nickel as function of inverse temperature.

Permeabilities of hydrogen and deuterium across nickel were determined, both singly and in mixture, by the so-called steady state method [Shi98]. They can be calculated as function of temperature from the following expressions:

$$P_{\mathrm{H}} = 4.44 \times 10^{-7} \exp\left(-\frac{54.80}{RT}\right)$$
$$P_{\mathrm{D}} = 3.81 \times 10^{-7} \exp\left(-\frac{56.20}{RT}\right) \ ,$$

where P_i (i = H or D) is given in $\mathrm{mol\,m\,m^{-2}\,s^{-1}\,Pa^{-0.5}}$ and the activation energies are in $\mathrm{kJ\,mol^{-1}}$. The determined permeations were found to be in line with results from numerous other researchers [Ebi67b; Ebi67a; Eic65; Rob73; Tan84]. A study on the permeation of single hydrogen isotopes and hydrogen isotope mixtures revealed that the hydrogen/deuterium separation factor matched the isotope effect ratio. Hence, the applied finite difference method was considered adequate for model calculations of hydrogen isotope permeation through a long nickel tube such as needed for a hydrogen permeator.

Louthan et al. [Lou74] carried out permeation experiments with single crystal nickel and polycrystalline nickel specimens. Data were obtained from the time-dependence of the permeation of hydrogen through an initially hydrogen-free nickel membrane. Another technique consisted in

a determination of the time-dependence of the outgassing of hydrogen from initially hydrogen-saturated nickel specimens. The results allowed predictions of the diffusivities of protium, deuterium, and tritium through nickel.

While diffusivities obtained from outgassing data agreed closely with values extrapolated from higher temperature experiments peformed by Katz et al. [Kat71] employing the same technique, data obtained from permeation experiments were consistently lower. This was attributed to a retention of hydrogen in metal traps like for instance dislocations. Because steady state permeation rates are not influenced by trapping, this kind of technique was preferred for the estimation of isotope effects. Satisfactory predictions were achieved with the unharmonic oscillator model as well as with the classical quantum partition function approximation.

Chemical etching results provided evidence that the concentration of tritium on the surface of nickel specimens charged thermally with molecular tritiated hydrogen was orders of magnitude higher than in the bulk. Moreover, tritium trapped on the surface was found to be much more resistant to thermal release than tritium residing in the bulk [Sai11a]. An analogous behaviour was displayed by copper [Pen11].

The transport of hydrogen across nickel is evidently influenced by trapping and short-circuited diffusion [Lou75b; Sai11a]. Accelerated diffusion of hydrogen through polycrystalline nickel at ambient temperature was reported by Brass and Chanfreau [Bra96]. The grain boundary diffusivity of hydrogen at 298 K across pure nickel was estimated to have values between two and seven times larger than for lattice diffusivity. In view of the complexity of these factors, it is quite probable that in many previous publications the contribution of intergranular diffusion to the diffusion of hydrogen across nickel has not received proper attention.

Tritium incorporated thermally into nickel is essentially liberated into a carrier gas at ambient temperature as tritiated water, probably via an exchange process with residual moisture in the flow stream [Sai11a]. The **chronic release** rate of tritium at ambient temperature can be explained by a diffusion process. Tritium depth profiles of aged nickel specimens stored under air, a stream of argon or under vacuum at ambient temperature were found to be consistent with a release mechanism based on diffusion.

A compilation of diffusivities of hydrogen isotopes through nickel is provided in Table 2.53. In early work, Katz et al. [Kat71] pointed out that the absolute rate theory provides an acceptable description of the diffusion of hydrogen isotopes through copper but fails in case

of nickel. Discrepancies between theory and experiment became particularly evident when results for all three hydrogen isotopes were compared. Yamakawa et al. [Yam77; Yam79] used a special experimental technique. It basically consists in dissolving an excess of hydrogen in thin nickel wires followed by quenching in liquid nitrogen. Hydrogen recovery was inferred from a measurement of the electrical resistivity. According to their observations, the Arrhenius pre-exponential factors and activation energies follow in the low temperature range, i.e. 220 - 340 K, the inequalities $D_0^{\mathrm{H}} < D_0^{\mathrm{D}}$ and $E_{\mathrm{H}} < E_{\mathrm{D}}$ which is contrary to expectations from classical diffusion theory.

Hohler and Schreyer [Hoh82] investigated the diffusion of hydrogen isotopes across nickel at temperatures below 300 K and distinguished between a high and a low temperature range. The low temperature range was found to be characterized by a continuous pre-exponential factor and a decrease of activation energy, the transition being gradual. For atomic hydrogen the transition begins at temperatures below ambient and continues to progress until the lowest temperatures. Moreover, for D atoms the transition sets in at much lower temperature, i.e. 170 K. In the case of tritium atoms a transition was non-discernible. More recently, Wimmer et al. corroborated experimentally these findings [Wim08]. According to their results the diffusivity of the heavier isotope is slower than that of the lighter ones, i.e. $D_{\mathrm{H}} > D_{\mathrm{D}} > D_{\mathrm{T}}$ (see Table 2.53 and Fig. 2.52). This is only true, however, for temperatures above 400 K. At lower temperatures the ordering is reversed (see insert in Fig. 2.55), which substantiates the findings of Katz et al. [Kat71], and Hohler and Schreyer [Hoh82].

Nickel surfaces exposed to deuterium plasmas generated by radio frequency revealed significant **plasma-driven permeation** [Tak91]. Depth profiles both of gas-driven and plasma-driven permeation experiments determined employing the $\mathrm{D}(^3\mathrm{He}, \mathrm{p})^4\mathrm{He}$ nuclear reaction technique brought to light concentrations of deuterium on the surface notoriously higher than in the bulk. These high concentrations were attributed to chemisorption, hydride formation, and trapping by radiation damage. Bulk concentrations were fairly constant at least up to depths of about 1 µm. Another possible reason for the high concentrations is retention of deuterium on an oxide layer existing on the metal surface. When in plasma-driven experiments the deuterium pressure was raised from 2.7 to 13 Pa the deuterium concentrations in the bulk increased from 1×10^{19} to 4×10^{19} atoms/cm^3 and the surface densities from 4.8×10^{14} up to 1.3×10^{15} atoms/cm^2, respectively.

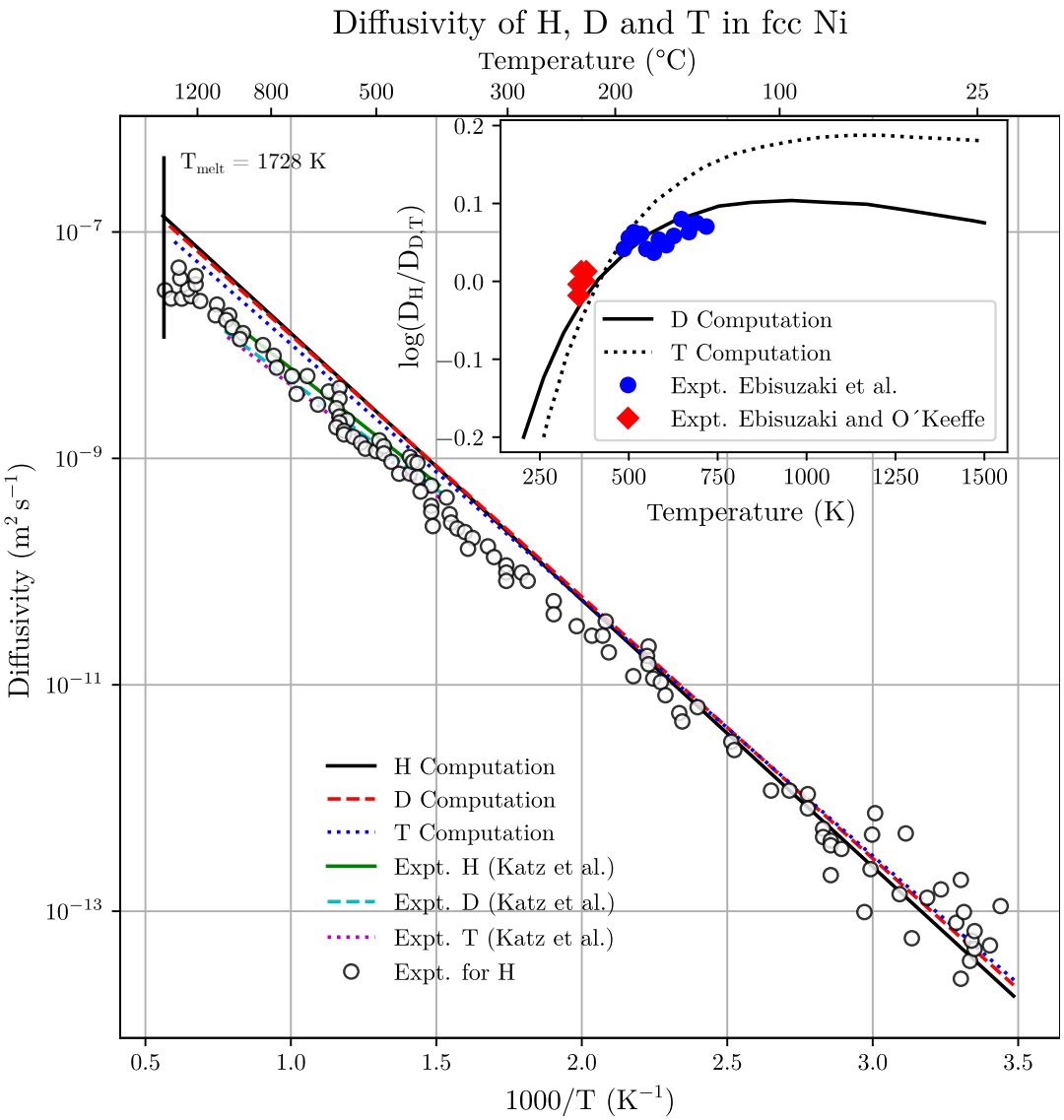


Figure 2.55: Calculated and experimental diffusion coefficients of H, D and T through Ni as function of inverse temperature (after [Wim08]). The experimental data for H (circle) were obtained by [Ale78] and the high temperature values for H, D and T by [Kat71]. Calculated ratios of the diffusivities D_H/D_D and D_H/D_T (see insert on upper right of figure) include for comparison D_H/D_D data reported by [Ebi67b] and [Ebi67a].

Gas driven permeation measurements at temperatures in the range 483 - 673 K and pressures within the range 17 - 1700 Pa followed Richard´s relationship, i.e.

$$J = k_r(C_b)^2$$

where J is the permeation rate in atoms/cm^2/s, k_r the recombination rate constant in cm^4 s^{-1} and C_b the concentration of deuterium near the surface in atoms/cm^3 [Tak91]. Deuterium concentrations in the bulk increased from 1×10^{19} to 4×10^{19} atoms/cm^3 and surface densities from 4.8×10^{14} up to 1.3×10^{15} atoms cm^{-2}, respectively, when the deuterium pressure in the plasma vessel was raised from 2.7 to 13 Pa). Experimentally obatined recombination coefficients of deuterium on nickel covered the range 10^{-21} - 10^{-23} cm^4 s^{-1}. Comparison of these results with other values in the literature disclosed scattering over several orders of magnitude. The temperature dependence of the plasma-driven permeation across nickel using 100 eV deuterium atoms was examined experimentally by Causey and Baskes [Cau87]. Plasma-driven permeation rates determined within the temperature range 473 - 773 K were found to be much higher than gas-driven rates. They agreed well with calculations carried out by Baskes [Bas80] who utilized an appropriate model.

Takagi et al. [Tak92] researched diffusion and trapping of deuterium in nickel at 523 K during and after irradiation with ^{3}He. Non-irradiated material showed no traps. Upon irradiation with ^{3}He the trap density increased as function of dose up to a saturation value. The trapped deuterium concentration at steady state permeation was 7×10^{25} m^{-3} and the typical saturated trap density at 523 K under the surface was 8.3×10^{25} m^{-3} (or 9×10^{-4} atom fraction). The highest trap density was reached at a depth of approximately 0.9 µm from the surface. Most traps were occupied by deuterium, the concentration of trapped deuterium exceeding by far that of dissolved deuterium. The depth profile of traps coincided with that of the deuterium concentration profile. Trap formation in the host metal was attributed to atomic displacements induced by ^{3}He irradiation.

The research topic of Schroeder and Ullmaier [Sch91b] was the embrittlement of iron-based alloys and nickel-based alloys induced by helium and hydrogen. According to their observations, martensitic materials are highly resistant towards helium embrittlement. Only at very high concentrations of helium, i.e. 3000 appm, did changes commence to become noticeable. In general, while there is a large body of information available on the effect of helium on tensile and creep properties after α–particle or neutron irradiation, this is not at all the case concerning the effect of helium on fatigue and fatigue crack growth. Hydrogen embrittlement in iron-based as well as nickel-based alloys is not very probable at high temperatures because of the rather high diffusivity of hydrogen through these metals when such conditions prevail. Conversely, hydrogen

distributed homogeneously in nickel-based alloys can degrade fatigue and enhance at ambient temperature the propagation of cracks even in adjacent welds. On the other hand, the fatigue properties of austenitic steels are degraded by helium at temperatures exceeding about 773 K, the degradation being promoted by increasing temperature and helium content.

Interestingly, the 30 min re-crystallisation temperature, which for nickel lies in the range 563 - 673 K, was found to be inversely proportional to the degree of cold work.

2.14.6 Interaction of hydrogen isotopes with beryllium

Beryllium is an earth alkali metal of hexagonal crystal structure. The metal has an atomic mass of 9.012 18 u, a low density of 1.848 $g\,cm^{-3}$, a high melting point of 1551.15 K and a vapour pressure at that temperature of 4180 Pa. The specific heat of beryllium is rather high, i.e. 1.825 $J\,g^{-1}\,K^{-1}$ and the heat conductivity is 201 $W\,m^{-1}\,K^{-1}$. Natural beryllium consists almost entirely of ^{9}Be. Beryllium is stable towards the atmosphere because of a protective oxide film that develops on the metal surface. Beryllium and beryllium compounds are classed as highly toxic materials because they can cause acute and chronic health problems.

2.14.6.1 Physical and physicochemical properties

At elevated temperatures the solubility of hydrogen in beryllium follows square root dependence from hydrogen pressure. At low temperatures the solubility of hydrogen in beryllium is extremely small. For this reason, in most solubility measurements hydrogen has been replaced by tritium because this radioactive element is much more sensitive to detect than other isotopes of hydrogen. When this kind of measurement is performed, great care must be taken in fully eliminating all possible contributions from tritium trapping or adsorption on the metal surface.These processes may quickly exceed the low solubility of hydrogen in beryllium. Small impurity levels, particularly of oxygen, or differences in the preparation and pre-treatment of specimens can significantly modify the properties of beryllium and eventually lead to greatly differing results. Causey et al. [Cau90b] pointed out that beryllium oxide on the surface of beryllium specimens strongly influence the permeation rate of hydrogen isotopes. Dissolution of beryllium samples after exposure to deuterium/tritium plasmas revealed that both isotopes are trapped in the metal bulk and oxide layer on the surface. Evidently, trapping has been largely responsible for the large variations in solubility and diffusivity data of hydrogen in beryllium reported in the literature

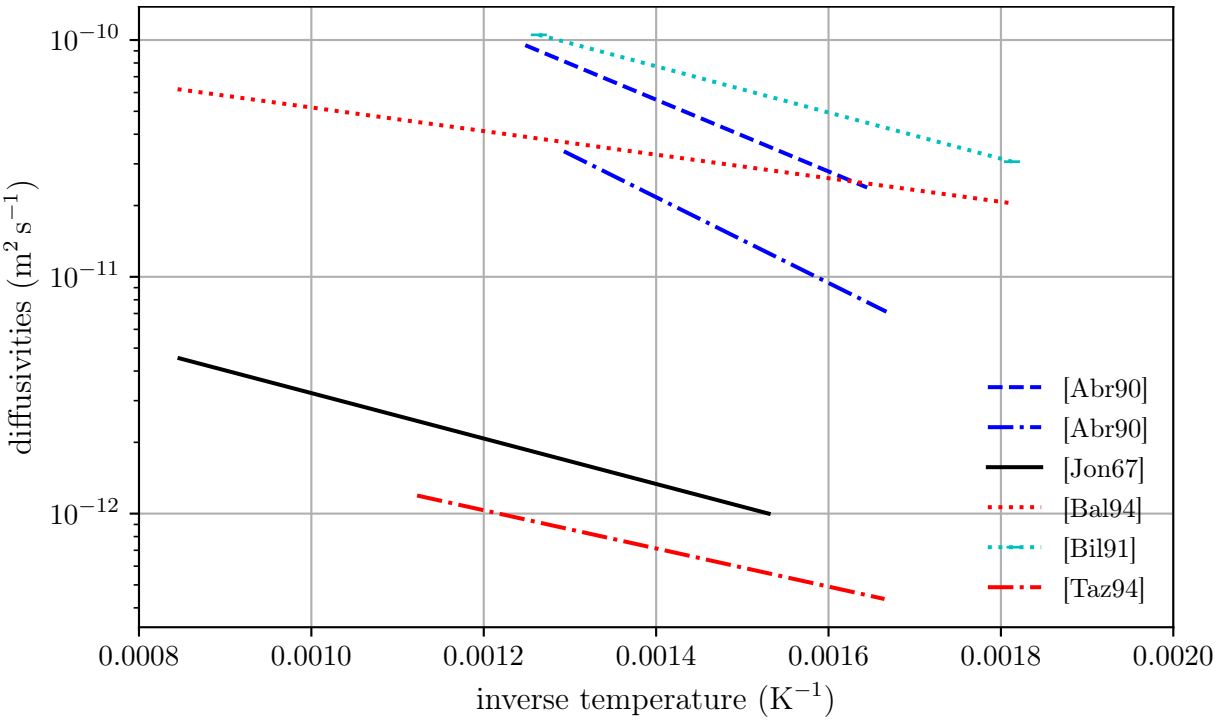


Figure 2.56: Diffusivities of hydrogen across beryllium as function of inverse temperature (see also Table 2.54).

(see Fig. 2.56 and Table 2.54). As apparent from Table 2.54, according to Jones and Gibson [Jon67] the solubility of tritium in beryllium exhibits a very small activation energy and does therefore practically not vary with temperature. Swansiger [Swa86], on the other hand, noticed a rapid decrease of tritium uptake with decreasing temperature within a small temperature range which reversed at temperatures below 623 K. This exothermic behaviour was attributed to traping effects. More work on the solubility of tritium in beryllium is needed.

Abramov et al. [Abr90] used a gas-driven permeation technique to determine the diffusivity of deuterium through beryllium. The effect of the oxide layer on permeation was accounted for by a multilayer permeation theory.

Similarly, Tazhibaeva et al. [Taz94] determined the effective diffusivity of deuterium through beryllium after correction for the diffusivity through the beryllium oxide surface layer. The result was found to be in good agreement with the diffusivity of tritium through beryllium reported by Jones and Gibson [Jon67] (see Fig. 2.56 and Table 2.54).

Table 2.54: Diffusion, solubility and permeation data of hydrogen isotopes in beryllium.

Specimen	Diffusion coefficients		Solubility coefficients		Permeation coefficients		Temp. range	Ref.
	D_0	E_D	S_0	E_S	P_0	E_P	Temp. range	Ref.
	$m^2\,s^{-1}$	$kJ\,mol^{-1}$	$mol\,m^3\,Pa^{-0.5}$	$kJ\,mol^{-1}$	$mol\,m^{-1}\,s^{-1}\,Pa^{0.5}$	$kJ\,mol^{-1}$	K	
H	3×10^{-13}	0					1123 - 1173	[Pem64]
H[1]					4.24×10^{-7}	86.96	773 - 873	[Alt81]
H[2]					3.39×10^{-11}	26.70	773 - 923	[Alt81]
H			2.24×10^{-3}	-1.82			523 - 1123	[Fro84]
D[3]	6.7×10^{-9}	28.4					620 - 775	[Abr90]
D[4]	8.0×10^{-9}	35.1					620 - 775	[Abr90]
D	9.0×10^{-12}	14.9			1.3×10^{-9}	63.5	673 - 873	[Taz94]
T	3×10^{-11}	18.5	1.96×10^{-3}	-0.00182	5.8×10^{-14}	18.5	673 - 1173	[Jon67]
T[5]	1.7×10^{-11}	3.5					573 - 1173	[Bal94]
T[6]	1.6×10^{-10}	9.5					573 - 1173	[Bal94]
T[7]	1.4×10^{-10}	11.5					573 - 1173	[Bal94]
T			7.48×10^{-4}	112.8			713 - 783	[Swa86]
T	1.73×10^{-9}	18.47					573 - 873	[Bil91]
T	1.35×10^{-10}	0					> 873	[Bil91]

TD = theoretical density, [1,2] Different types of beryllium, [3] Irradiated extra grade Be (99.8 % purity)

[4] Irradiated high-grade Be (99 % purity), [5] 81 % TD Be by cold isostatic pressing (irradiated with 2.6×10^{-21} n/cm^2)

[6] 99 % TD Be by cold isostatic pressing (irradiated with 2.6×10^{-21} n/cm^2)

[7] 100 % TD Be by hot isostatic pressing (irradiated with 5.0×10^{-22} n/cm^2)

Elleman et al. [Fow76; Fow77; Ell78b] determined diffusion coefficients for tritium across sintered (773 - 1223 K), single crystal (923 - 1473 K) and powder beryllium oxide. The corresponding temperature dependences are given by

$$D = 1.11 \times 10^{-6} \exp\left(-\frac{219.8}{RT}\right) \quad \mathrm{m^2\,s^{-1}} \quad \text{(single crystal)}$$
$$D = 7.00 \times 10^{-6} \exp\left(-\frac{203.1}{RT}\right) \quad \mathrm{m^2\,s^{-1}} \quad \text{(sintered)}$$
$$D = 3.17 \times 10^{-15} \exp\left(-\frac{70.0}{RT}\right) \quad \mathrm{m^2\,s^{-1}} \quad \text{(powder)}$$

in which the activation energies are in $\mathrm{kJ\,mol^{-1}}$. Diffusion coefficients in BeO were found to be much lower than in most metals, which implies chemical interactions between diffusing tritium and the lattice. The fraction of tritium released as water is greater for powdered specimens than for sintered or single crystal specimens [Fow77].

Permeation coefficients for hydrogen across beryllium obtained in different laboratories have been plotted in Fig. 2.57. Reasonably good concurrence between various researchers is only attained at temperatures in the vicinity of 1000 K.

The permeability coefficient of hydrogen through a thin 8 µm beryllium film deposited on EUROFER steel membranes utilizing the thermo ionic vacuum arc method was calculated to be within the range 0.23×10^{-14} and 2.3×10^{-14} $\mathrm{molH_2/m/s/Pa^{0.5}}$ at 673 K by Zajec et al.[Zaj13].This is in good agreement with results of Jones and Gibson[Jon67] Across an assumed 35 nm BeO layer the value of the permeability coefficient was much lower, i.e. about 1×10^{-17} $\mathrm{mol_{H_2}\,m^{-1}\,s^{-1}\,Pa^{-0.5}}$. Large scattering of other permeability values published in the open literature were attributed to contributions from permeation-enhancing pinholes in the beryllium layer and/or the presence of a permeation-inhibiting layer of beryllium oxide.

The build up of decay helium was simulated experimentally by pre-irradiation of beryllium with 24 keV ^{3}He ions at 300 K [Ali97; Ali01]. Irradiation with helium was shown to have strong influence on the trapping and release behaviour of hydrogen isotopologues in beryllium. Bombardment with helium ions caused formation of vacancies and bubbles. Transmission electron microscopy examination of pre-irradiated beryllium specimens subjected to deuterium implantation revealed

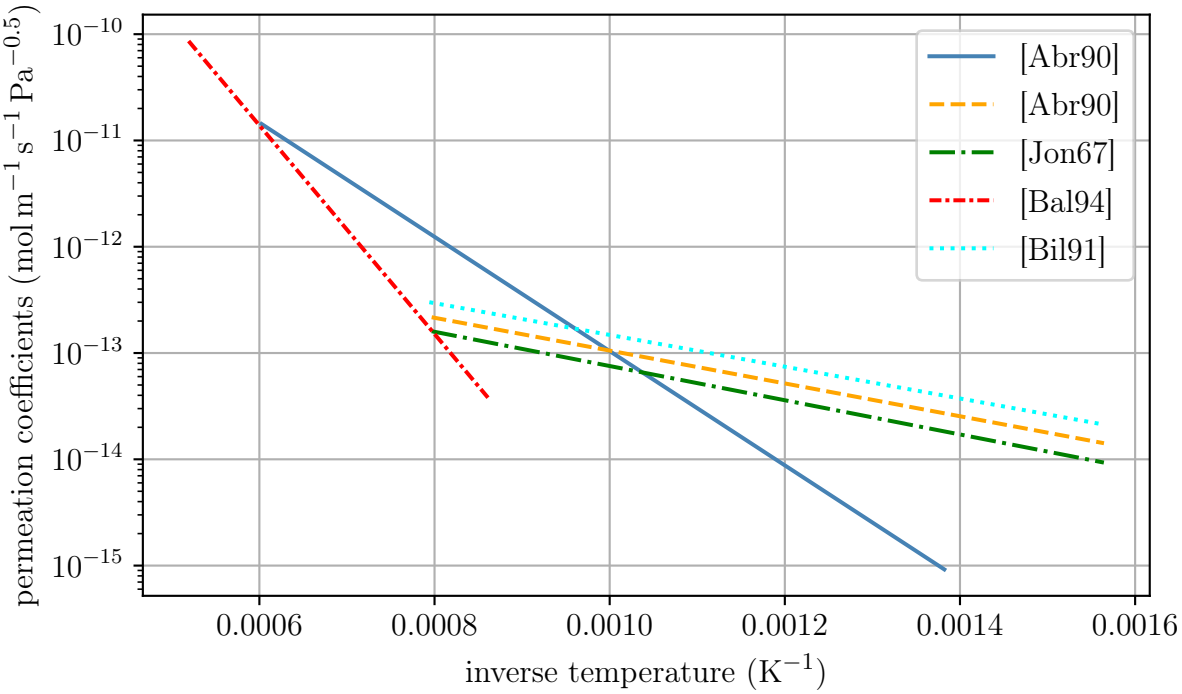


Figure 2.57: Permeation coefficients of hydrogen across beryllium as function of inverse temperature.

that D atoms were mostly trapped in vacancy type defects and D_2 molecules in gas filled cavities. The enhancement of deuterium trapping brought about by pre-irradiation was significant.

Baldwin and Billone [Bal94] determined effective tritium diffusivities in irradiated beryllium employing samples of three theoretical densities, i.e. 81 %, 99 % and 100 %, and temperatures covering the range 573 - 1173 K (see Table 2.54). The experimental evidence points to different mechanisms depending on temperature and material density. In fact, after prolonged heating at 773 K 89 % of the tritium inventory was released from the low-density beryllium and only $<$ 3.3 % from the high-density beryllium. These results suggest that i) diffusion is the predominant mechanism with small and changing contributions from surface desorption and ii) tritium release rates increase with diminishing density.

Helium production in fusion machines takes place by reactions

$$^{9}\mathrm{Be} + \mathrm{n} \longrightarrow {}^{8}\mathrm{Be} + 2\,\mathrm{n}$$

$$^{8}\mathrm{Be} \longrightarrow 2\,{}^{4}\mathrm{He}$$

2.14.6.2 Chemical properties

A direct chemical reaction between hydrogen and beryllium has not been observed even at high temperatures or hydrogen pressures [Gul50]. Hence, beryllium hydride cannot be prepared directly from the elements. A stable beryllium hydride, i.e. BeH_2, does, however, exist. This compound has to be synthesized circuitously, for instance by reduction of lithium aluminium hydride with beryllium compounds. Beryllium hydride is a white non-volatile solid stable in dry air up to a temperature of 350 K. In the presence of moisture, it decomposes rapidly even at low temperatures.

Iin fusion machines, beryllium will generate helium according to reactions

$$^{9}\mathrm{Be} + \mathrm{n} \longrightarrow {}^{8}\mathrm{Be} + 2\,\mathrm{n}$$

$$^{8}\mathrm{Be} \longrightarrow 2\,{}^{4}\mathrm{He}$$

Gulbransen and Andrew [Gul50] investigated the kinetics of the reaction of oxygen with beryllium in the temperature range 673 - 1223 K. According to these authors, the experimental data can be fitted by a parabolic rate law. In comparison to other metals and alloys the parabolic rate constant for the oxidation of beryllium, i.e. $K = 9.3 \times 10^{-17}\,\mathrm{cm^2\,s^{-1}}$, was found to be small.

The oxidation kinetics of beryllium in moist helium gas was studied by Yoshida et al. [Yos92] at temperatures in the range 823 - 1023 K using a Cahn 2000 recording micro balance. They remarked that at temperatures above 873 K the initial oxidation rate first remains constant and then, following a period of induction, begins to accelerate. The time at which acceleration sets in (break away oxidation) shortens as the temperature is raised (see Fig. 2.58). These observations were confirmed by Druyts [Dru98]. He likewise reported that oxidation takes place with parabolic kinetics by two oxidation mechanisms: one at low temperatures and another with linear accelerating kinetics at higher temperatures. The transition temperature was found to be within the range 973 - 1073 K.

Beryllium reacts exothermally with **steam** generating hydrogen via reaction [McC97]:

$$\mathrm{Be} + \mathrm{H_2O} \longrightarrow \mathrm{BeO} + \mathrm{H_2} + 608.4\,\mathrm{kJ\,mol^{-1}}\ .$$

To determine rates of hydrogen formation specimens were heated either in a furnace or by direct induction in the presence of steam. The generated gas was collected volumetrically in bubblers and analysed by gas chromatography. From a safety point of view, for instance in the event of air in-break into the vacuum vessel of a fusion machine operated at elevated temperature with beryllium as plasma facing material and water as coolant, the reaction of steam with beryllium constitutes a significant hazard [Raf97]. If enough hydrogen is produced chemically and the right amount of air is present, explosive conditions can establish.

Anderl et al. [And00] exposed beryllium pebbles at 623 - 1173 K to steam in order to obtain information on the behaviour of this metal when incorporated into tritium breeder blankets as neutron multiplier. They also exposed beryllium powder to steam at temperatures within the range 673 - 773 K in an attempt to simulate the consequences of the reaction of beryllium dust as generated by vaporization during disruptions or sputtering of beryllium constituting the surface of the first wall of fusion devices when subjected to plasmas. The experiments revealed complex reactivity determined by the prevailing temperature. The reactivity towards steam was found to be directly proportional to the specific surface area of the beryllium material. While the average generation rates of hydrogen with Be powder were in good agreement with previous work employing fully dense consolidated powder metallurgy disks and cylinders, the ones with pebbles were systematically lower [McC79]. The latter was attributed to differences in bulk and surface features of the pebbles when compared to the fully dense material. Presumably, impurities present in the surface layer of the pebbles influenced markedly the oxidation rates. Autocatalytic behaviour was noticed with 2 mm pebbles at 1173 K and with 0.2 mm pebbles at 1073 K.

Smolik et al. [Smo92] performed calculations on the rate of hydrogen production as function of temperature from an assumed fusion reactor first wall area of 300 m^2 exposed to 1 bar steam. Due to the high exothermicity of the reaction there is a strong self-accelerating effect on the production of molecular hydrogen. Consequently, reliable preventive measures were considered imperative to preclude occurrence of this reaction [Sar96].

Sarigiannis and Andritsos [Sar96] carried out another model calculation of the reaction between steam and beryllium. Beryllium was assumed to fully cover as plasma facing component an underlying first wall of ITER consisting of copper and stainless-steel. Main conclusions reached from this study were: i) the chemical energy of the oxidation reaction of beryllium with steam

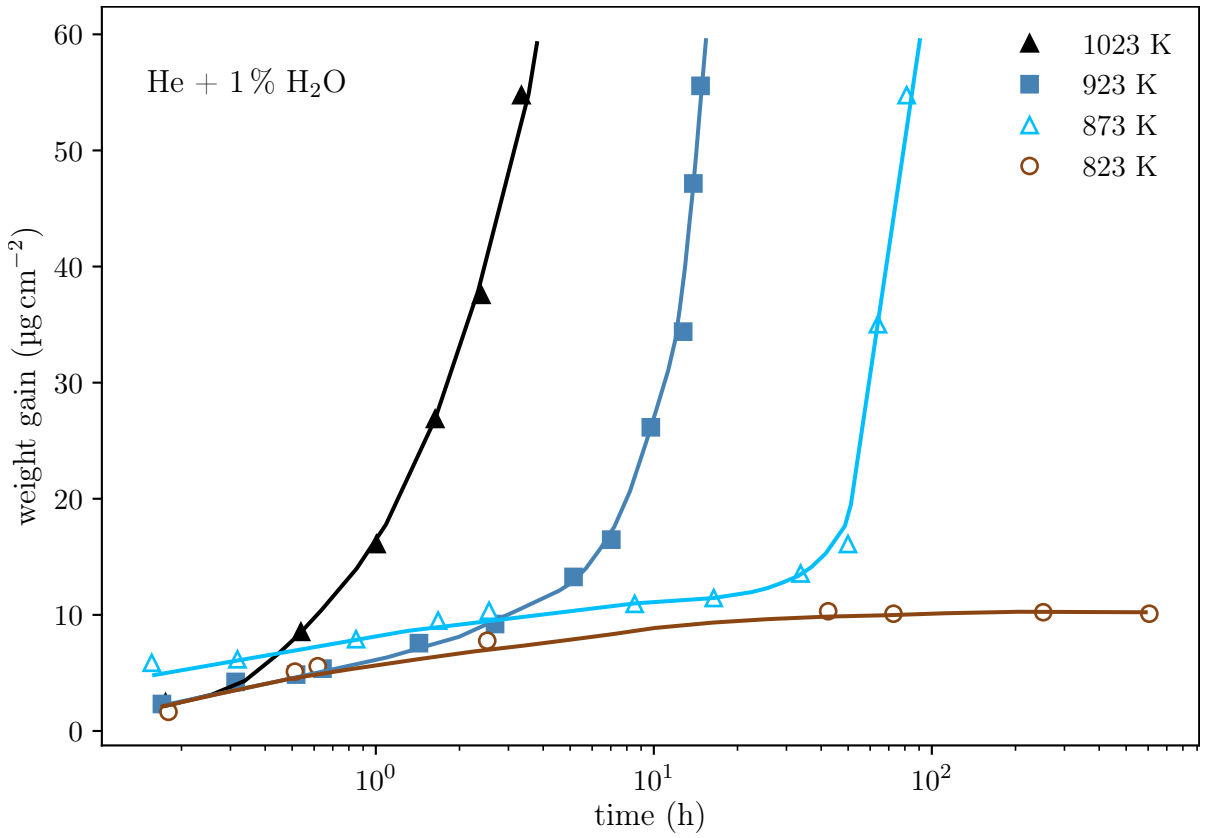


Figure 2.58: Oxidation of beryllium (weight gain) under a stream of helium containing 1 % water vapour at temperatures up to 1023 K (after [Yos92]).

is insufficient to sustain the exothermic reaction by itself, ii) in case of a hot spot (assumed to reach 1556 K) the plasma facing surface temperature will rapidly relax to temperatures close to the normal bulk first wall temperature, i.e. 633 K , iii) in the event the whole beryllium layer constituting the first wall reaches 1556 K the temperature at the reaction front will relax to only 1273 K and remain at about that value for approx. 1000 s and iv) self-ignition of beryllium is only possible if the bulk temperature rises sufficiently due to an ex-vessel LOCA (Loss of Coolant Accident) or LOVA (Loss of Vacuum Accident) event.

One more model was developed at INL for the MELCOR safety computer code contemplating the oxidation of beryllium dust during a wet bypass accident [Mer09]. This model predicts the production of hydrogen from steam reactions in beryllium dust layers on the hot surfaces inside of the vacuum vessel of a fusion machine during a LOCA accident. The model is designed to account for diffusion of steam into a beryllium dust layer, the oxidation of dust particles inside of this layer and the effective thermal conductivity of this beryllium dust layer. An important

conclusion from the model calculations was that a thermal run away of the dust layer due to the chemical heat of the beryllium - steam reaction, will not occur. In fact, it was estimated that only about 1 % of 100 kg beryllium dust will oxidize before the dust layer returns to temperatures where only little reaction is expected. The conclusion of Merrill et al. [Mer09] is in line with the results achieved by Sarigiannis and Andritsos [Sar96].

Another cause of concern is beryllium **dispersion by volatilization** via reactions such as [Stu64; Raf97; Dru98]

$$BeO\,(s) + H_2O\,(g) \longrightarrow Be(OH)_2(g)$$

For this reaction to occur the temperature must be sufficiently high. In experiments on the reaction of moisture with BeO pebbles or with other beryllium substrates like porous beryllium, plasma sprayed beryllium, fully dense beryllium or irradiated beryllium carried out at 1500 K, the generation of volatilized beryllium species depositing on the walls of downstream placed glass vessels were quantified by atomic emission spectroscopy. From the results release rates within the range 0.1 - 1.7 $\mu g\,s^{-1}$ were estimated [Con64; Stu64; McC97].

Yoshida and his co-workers [Yos92] explored experimentally the compatibility between **beryllium and stainless-steel** type 316 or 316L at temperatures in the range 673 - 973 K during extended periods of time, e.g. 26 days. At 873 K or above beryllium progressively diffuses into stainless-steel and causes redistribution of nickel in the stainless-steel surface layer. Here energy dispersive X-ray analysis revealed significant depletion of nickel. The growth rate of the overall reaction zone followed a parabolic rate law.

Roux et al. [Rou92] reserched the compatibility of beryllium with stainless-steel 316L and 1.4914 at 823 K under neutron-irradiation conditions at the SILOE reactor in Grenoble, France. The device containing the metallic specimens was additionally loaded with two different recurrently intercalated inorganic lithium ceramics, i.e. $LiAlO_2$ and Li_2ZrO_3. Irradiations were performed for 1690 hours under a helium stream containing 1 % hydrogen. The results revealed formation of oxide layers on all Be/stainless-steel touching surfaces. The observed corrosion was probably induced by water vapor in the sweep gas released from ceramics and structural materials (inspite of thorough previous degassing of the ceramics and the structural materials, the presence of

residual water could not be excluded). The oxides appear to inhibit the formation of intermetallic compounds such as observed in other laboratory experiments.

According to Hofmann and Dienst [Hof88] the compatibility between beryllium and SS3116 remains tolerable at temperatures up to 923 K. However, diffusion of Be into SS316 with formation of BeNi was observed already at temperatures of 873 K or above. Flament et al. [Fla92] provided an expression to calculate the thickness of the diffusion zone as function of time and temperature. Kawamura et al. [Kaw94] confirmed diffusion of beryllium into stainless steel with formation of BeNi at > 873 K, but identified additional products such as $Be_{21}Ni_5$, Be_2Fe and $Be_{11}Fe$ at higher temperatures, e.g. 1073 K.

Iin fusion machines, beryllium will generate helium in reactions such as

$$^{9}\mathrm{Be} + \mathrm{n} \longrightarrow {}^{8}\mathrm{Be} + 2\,\mathrm{n}$$

$$^{8}\mathrm{Be} \longrightarrow 2\,{}^{4}\mathrm{He}$$

2.14.6.3 Analysis of beryllium

Reliable and sensitive techniques for the accurate and precise detection of beryllium in a variety of solids and liquids are flame atomic absorption spectroscopy (AAS) and furnace AAS [Ell88b]. The detection limits for flame AAS and furnace AAS were reported to be $3.0\,\mu g\,l^{-1}$ and $0.08\,\mu g\,l^{-1}$, respectively. The only element causing interference with flame AAS determinations is aluminium but only at concentrations exceeding $500\,\mu g\,l^{-1}$. This interference can be overcome by the addition of 0.1 % hydrogen fluoride or of 8-hydroxiquinoline to the solution under investigation. In case of furnace AAS, possible interferences by high concentrations of molybdenum or tungsten need to be considered.

To determine **beryllium in ambient air** a defined volume of air is drawn through a filter mounted in a dust sampler. Filters of typically 0.3 µm pore size are recommended for this specific purpose. The filter supporting particles collected from an air sample is heated up to 323 K in the presence of nitric acid diluted with water (1:1) and kept at that temperature until only about $1/5^{\mathrm{th}}$ of the initial amount of acid remains. The generated beryllium oxide is subsequently dissolved in hot 3 molar sulphuric acid. The acid is maintained at 573 K until dense white fumes become visible. Thereafter the resultant solution is diluted with water and

analysed for beryllium by atomic absorption spectroscopy (AAS) at a wave length of 234.9 nm by aspirating the solution into a reducing nitrous oxide - acetylene flame. A standard beryllium solution containing beryllium at a concentration of $1000\,\mu g\,l^{-1}$ is customarily used for calibration purposes.

Cremers and Radziemski [Cre85] developed a spectrochemical laser spark technique for the semiquantitative determination of beryllium particles on filters. The sensitivity of the technique was considerered sufficient for near real-time sampling and analysis. The detection limit was found to be dependent on particle size but not the chemical form of the beryllium.

2.14.6.4 Working with and handling of beryllium

Cutting beryllium is similar to cutting cast iron. Because of the abrasive character of beryllium it is recommended to use tungsten carbide tipped tools. Blade clogging does practically not occur as beryllium tends to chip rather than bend. Hence, conventional tools such as an oscillating saw provided with a fine-toothed carbide tipped blade are suitable for beryllium. Cutting can also be performed manually with a small hacksaw. Dry cutting is recommended for beryllium to avoid contamination of the sample. The obvious hazard with this procedure is the production of beryllium dust, which must be removed quickly and thoroughly.

Plentiful operational experience on dealing with small and large quantities of beryllium in a variety of situations during hands on and remote installation as well as for the duration of maintenance activities has accumulated at the JET fusion device in Culham, Great Britain [Hai97]. Abundant and valuable information on such topics as i) safe handling of poisonous beryllium partially contaminated by radioactive species , ii) plasma spray coating, iii) hot isostatic pressing (HIP), iv) machining, v) forming and joining techniques, vi) special brazing procedures, vii) singular and routine analytics, viii) beryllium air monitoring, ix) waste conditioning and disposal, etc. are now available and accessible to ITER [Rus92; Pat03; Sca00].

2.14.6.5 Application of beryllium in fusion devices as plasma facing material or neutron multiplier in blankets

Since the early nineties approximately 3 t of beryllium have been introduced into the vacuum vessel of the JET machine while performing tests under a broad variety of operational phases [Boo91]. These research activities are well documented and have delivered much essential

knowhow on the performance of beryllium as first wall material under fusion-relevant conditions. They demonstrated that beryllium can be handled safely in a rather complex as well as radioactive environment.

Beryllium was deposited at JET over nearly all plasma facing components in form of spray evaporated layers [Dae01; Sar90; Cau02]. Beryllium sublimators manufactured by hot isostatic pressing at 1373 K were employed successfully for the purpose of spraying [Boo88; Pea91]. This technology was also developed for the *in-situ* repair of damaged beryllium (or tungsten) plasma facing surfaces [Cas97]. An identified problem concerns the high initial substrate temperature needed to achieve coatings of high strengths. In general, plasma sprayed beryllium was found to be of lower thermal shock resistance and have inferior mechanical properties than vacuum hot-pressed beryllium [Kal01].

Beryllium has also been utilized at JET as solid metal serving as limiter tiles, lower X point tiles, radio frequency screens, and X point limiters [Ber98].

The maximal tolerable temperature for beryllium handling is 923 K. This temperature limitation results from observed material swelling, degradation of mechanical properties, and the need to exclude the occurrence of a reaction with steam.

To date, the JET tokamak is the only fusion machine operated with deuterium-tritium fuel and a carbon wall fully coated with beryllium. The most important **beneficial consequences** of beryllium utilized as first wall material are: i) reduction of the impurity content in the plasmas as a result of efficient gettering of oxygen (in the plasma the oxygen concentration falls by more than an order of magnitude), ii) substitution of carbon for beryllium in the plasmas, iii) increase in density limit, iv) enhancement of the ability to control the plasma density, v) significantly improved pumping capability for hydrogen isotopes, vi) much reduced core plasma radiation, vii) in situ re-coating capability, and viii) ability to re-initiate plasma operation more rapidly after a major disruption. A design issue related to the utilization of beryllium is the behaviour under irradiation, which manifests by swelling and progressively increasing tritium inventory.

After completion at JET of the deuterium-tritium campaigns numerous tiles were removed from the inner guard and poloidal limiters as well as from the divertor. Surface and bulk analysis of the relative distributions of deuterium, tritium, carbon and beryllium of these tiles revealed C and Be erosion from the inner wall of the vacuum chamber and transport to the inner divertor [Pen01d; Pen01e; Rub03]. The mechanisms governing the transport of beryllium

and carbon do not appear to be the same [Rub03]. The results provide evidence for beryllium erosion from the main chamber and transport to plasma-exposed areas of the divertor, on whose surface they manifest as thick films rich in deuterium and tritium. Co-deposition of hydrogen isotopes together with eroded beryllium have been observed on plasma-facing and plasma-shadowed surfaces particularly when oxygen was present (formation of BeO) [Bro97]. The resulting co-deposited surface layer sometimes displayed significant hydrogenic content.

Scott et al. [Sco92] were responsible for the decontamination of the JET vacuum vessel prior to the installation of a new pumped divertor. The vessel had previously been exposed to many years of plasma operation, beryllium evaporation, and a limited operation with tritium. After testing of nine diverse decontamination techniques, the following three procedures were selected

- Abrasive linishing (sanding) machines
- Dry abrasive blasting, and
- Wet abrasive blasting

as most auspicious for further evaluation. After trials with Inconel plates covered with representative layers subsequently contaminated by tritium and beryllium, they settled for a wet abrasive blasting technique using F120 grit boron carbide. The wet technique was so effective that after its application it was possible to work in the vessel without respiratory protection.

Beryllium (and tungsten) will also constitute armour materials of ITER [Raf97; Cas97; Sca00; ITE01c; Mer11; Raf11]. It is estimated that about 13 t of beryllium will be required for the first wall of the ITER machine. Other applications are beryllium pebbles utilized as neutron multipliers (100 - 200 kg), Faraday shields (about 40 kg), RF windows, diagnostic systems, etc. Correspondingly, the total amount of operative beryllium waste through five phases is assessed of operation will be of the order of 5 t [ITE01d].

Activation and transmutation reactions of beryllium serving as first wall material in a fusion machine were investigated by Forty et al. [For98]. The following germane neutron capture reactions were identified:

$$^{9}\mathrm{Be(n,\alpha)}^{6}\mathrm{He}(\beta\text{-})^{6}\mathrm{Li(n,\alpha)}^{3}\mathrm{H}(58\,\%)$$

$$^{9}\mathrm{Be(n,}^{7}\mathrm{Li)}^{3}\mathrm{H}(33\,\%)$$

$$^{9}\mathrm{Be(n,\gamma)}^{10}\mathrm{Be}\ .$$

Therefore, first wall beryllium will turn radioactive by the formation of activation products from the interaction with plasma neutrons, trapping of tritium bred during the generation of activation products, and from tritium ions in the plasma impinging on the beryllium surface and diffusing into the bulk. Of the produced radioactive nuclides the only important ones are ^{3}H and ^{10}Be (half-life 1.6×10^{6} year, β-radiation 0.6 MeV), all others are comparatively short-lived (see Table 2.55). The resulting tritium inventory principally resides in microscopic defect sites as well as in bubbles that will also contain decay helium [And95a]. Additional radioactive elements found in irradiated beryllium (fast neutron fluency 5×10^{22} neutrons cm^{-2}) were ^{60}Co, ^{137}Cs and ^{134}Cs. Their formation was predominantly attributed to the activation of trace metallic impurities present in beryllium.

Design issues related to the utilization of beryllium are its behaviour under irradiation, which manifest by swelling and progressively increasing tritium inventory, and the resulting very high toxicity [Kum93]. Upon retrieval of beryllium from a fusion machine, this highly toxic substance is not only contaminated by tritium but also by other radioactive elements and must therefore be categorized as "mixed waste". Table 2.55 displays the specific activities of the main activation products generated in beryllium after exposure to a fluency of 0.091 MW year m^{-2} following one, ten, or one hundred years of storage. Evidently, even hundred years after exposure to numerous plasmas the activity in beryllium is still by and large dominated by tritium [ITE01d].

The rate of helium generation in beryllium was found to lie within the range of 3350 - 5300 appm per 10^{22} n cm^{-2} [Bal94]. The release rates of tritium and helium from irradiated beryllium were the subject of investigations by Baldwin and Billone [Bal94] as well as Anderl et al. [And95a]. Release data could be explained reasonably well with a diffusion model. Following irradiation of the metal with a fast neutron fluency of 5×10^{22} n cm^{-2} gases such as H_2 (6 %),

Table 2.55: Evolution as function of decay times of the specific activity of activation products generated in beryllium constituting the plasma-facing surface of a divertor following exposure to a fluency of 0.091 MW year m^{-2}(after [ITE01d]).

1 year		10 years		100 years	
Activation product	Specific activity	Activation product	Specific activity	Activation product	Specific activity
	Bq g^{-1}		Bq g^{-1}		Bq g^{-1}
Total	3.5×10^9	Total	2.1×10^9	Total	1.4×10^7
H-3	3.5×10^9	H-3	2.1×10^9	H-3	1.3×10^7
Fe-55	1.3×10^7	Fe-55	1.4×10^6	Ni-63	1.8×10^4
Co-60	3.2×10^6	Co-60	9.7×10^5	C-14	8.8×10^3
Co-57	1.4×10^6	Ni-63	3.3×10^4	**Be-10**	$\mathbf{2.2 \times 10^3}$
Mn-54	1.2×10^6	C-14	8.9×10^3	Nb-91	9.0×10^2
W-181	2.2×10^5	**Be-10**	$\mathbf{2.2 \times 10^3}$	Ar-39	8.2×10^2
W-185	1.6×10^5	Ar-39	1.0×10^3	Ni-59	2.6×10^2
Co-58	1.3×10^5	Nb-91	9.9×10^2	Mo-93	2.0×10^2
Zn-65	9.1×10^4	Mn-54	8.4×10^2	Nb-93m	1.7×10^2
V-49	4.7×10^4	Na-22	8.4×10^2	Tc-99	8.1

^{3}He (7 %), ^{4}He (81 %), HT (2 %), and T_2 (4 %) were generated. They could all be released thermally. Anderl et al. [And92b; And95a] performed isothermal release experiments using two differently pre-treated specimens. One specimen (specimen1) was first heated at 473 K for 24 hours. Subsequently the temperature was raised in 200-degree increments (annealing time 24 hours) until 1373 K were attained. This temperature is close to the melting point of beryllium, i.e. 1560 K. Under these conditions most tritium, i.e. 99.8 %, was liberated at 1073 K and only small fractions at lower or higher temperatures. The second beryllium specimen (specimen2) was first heated for 20 hours at 473 K, then at 873 K for 5 hours and thereafter first at 923 K and then at 973 K for about 20 hours. Again, no significant release was observed before the specimen reached a temperature of 923 K. At this temperature 86.3 % was liberated during an annealing period of 15 hours. Small fractions were subsequently liberated at 973 K and 1073 K. Gas was set free from both specimens mostly in form of "bursts", the release of helium and tritium being

essentially concurrent. As expected, the total concentration of tritium found in specimens 1 and 2 was nearly the same, i.e. 8.66×10^{11} Bq and 9.10×10^{11} Bq, respectively.

Pacenti et al. [Pac96] studied the release of tritium from beryllium specimens obtained from plasma-exposed JET tiles. Step-heating of Be specimens under an argon stream containing 2 % hydrogen required at least 1000 K to achieve full decontamination. This observation is well in line with the results of other investigators [Bal94; And95a]. However, when hydrogen was replaced by 2 % water, even higher temperatures were found to be necessary for a complete liberation of tritium. Enhanced resistance towards detritiation was explained by oxidation of the metal surface (see also 2.14.3).

Beryllium **implanted with deuterium** at 500 or 1500 eV at ambient temperature developed **blister domes** on the surface with a diameter of 0.4 mm [Wam84; Wam92]. At low fluencies essentially, all incident deuterium is implanted but at high fluencies the retention saturates with higher saturation levels for the higher energy implant. Annealing runs indicate that approx. 80 % of the deuterium is trapped with a binding energy of 1 eV and the remaining 20 % with an energy of 1.8 eV. The surface oxide layer was found to have a thickness of about 1.5 nm before and about 3 nm after implantation. As already discussed, the experiments suggest that tritium is trapped in bubbles together with helium with a binding energy of 2.3 eV.

Macaulay-Newcombe and Thomson [Mac94] determined the solubility of deuterium in BeO and obtained the expression

$$S = 1.4 \times 10^{-11} \exp\left(\frac{0.8\,\mathrm{eV}}{kT}\right)\left(\frac{atom fraction}{\sqrt{\mathrm{Pa}}}\right)$$

Longhurst et al. [Lon95] modified this equation by introducing data obtained by Baldwin [Bal93]. This gave rise to slightly lower pre-exponential factor 1.25×10^{-11}. Longhurst and co-workers also reported an equation for the diffusivity of hydrogen across BeO from a fit of their own experimental data

$$D = 1.33 \times 10^{-9} \exp\left(\frac{-1.335\,\mathrm{eV}}{kT}\right)\left(\frac{\mathrm{m}^2}{\mathrm{s}}\right)$$

and a hydrogen diffusivity across a damaged BeO layer on beryllium retrieved from a belt limiter tile of

$$D_{\mathrm{dam}} = 1.33 \times 10^{-15} \exp\left(-\frac{0.0025\,\mathrm{eV}}{kT}\right)\left(\frac{\mathrm{m}^2}{\mathrm{s}}\right)$$

Saturation loading of deuterium in this BeO layer was found to be described by

$$\frac{D}{BeO} = 0.33 \exp\left(\frac{92.1}{T}\right)$$

where T is in Kelvin. Because deuterium and oxygen were present in stoichiometric amounts, it was speculated that D is retained in the surface film as -OD group.

The interaction of carbon ions carrying bombarding energies of 3 - 5 keV with a clean beryllium target can be explained by implantation, reflection and sputtering processes [Gol99]. As a result, a carbon layer of increasing thickness builds up on the metal surface. After exposure to a fluency of approximately $1 \times 10^{18}\,\mathrm{cm}^{-2}$ beryllium is no longer eroded. In case of co-bombardment of C^+ and O^+, simulated in the experiment by the implantation of CO^+ ions, carbon and oxygen can accumulate in the beryllium target leading to a target of constant composition surface layers. Under these conditions the beryllium target surface is continuously eroded. Results on sputtering of beryllium by O^+ ions at energies spanning from 100 - 10 000 eV and beryllium target temperatures within the range 300 - 1000 K have been published by Wu et al. [Wu90].

Beryllium, tungsten and carbon - eventually together - are considered potential plasma facing components of ITER. Hence, the formation of co-deposits consisting of hydrogen isotopes with either on of these components or perhaps in more complex multi-component mixtures need to be contemplated [Raf97]. Mayer et al. [May96] examined the co-deposition of deuterium with targets consisting of either Be, C, or W. For this purpose, single targets were bombarded with a beam of 4.5 keV $D_3{}^+$, i.e. $1.5\,\mathrm{keV\,atom}^{-1}$. The amount of target atoms removed by sputtering was obtained from weight loss of the target. Co-deposition was only observed when the energy of the atoms or ions was sufficient for a deuterium penetration into several atom layers of the target. At ambient temperature co-deposits of deuterium with beryllium were detected having D/BeO ratios of 0.38. In case of beryllium, energetic ions were implanted into the growing BeO layer. Co-deposited deuterium could be released thermally from BeO at about 800 K. The carbon target was bombarded with up 2.8×10^{20} atoms of deuterium giving rise to a total of

3.8×10^{18} atoms of sputtered carbon. The amount of deuterium trapped together with carbon increased linearly with the amount of deposited carbon at a ratio of D/C = 0.41. Co-deposition with tungsten was not observed.

On the basis of a simple material balance model a discussion on possible co-deposition options for carbon, beryllium and tungsten under exposure to D-T plasmas was published by Hirooka [Hir97]. An analysis of the data indicated that material mixing between carbon and beryllium is much more likely than mixing of either element with tungsten.

A key difference for a detached plasma regime between carbon and beryllium is that while the former is chemically eroded and transported to shadowed areas, beryllium shows no chemical sputtering [Bro97; Coa01]. Under detached plasma regime conditions for sputtering and hence erosion of tungsten is nearly zero. Some inner divertor tiles of JET showed deposits rich in beryllium and other metals. The implication of this observation is that the greater part of the carbon incident at these areas was chemically eroded and transported efficiently to shadowed areas. The results suggest that tritium co-deposition in redeposited beryllium surfaces may be high.

One more rather important application of beryllium in fusion devices involves its utilization as **neutron multiplier** in so called **Test Blanket Modules for ITER**. A solid blanket basically consists of a combination of lithium ceramic pebble beds and beryllium pebble beds. Such blankets are currently under development for ITER in several laboratories worldwide. Out of six potential Test Blanket Systems that will be evaluated experimentally during the operational phases of ITER employing suitable mock-ups, three, i.e. the **Helium Cooled Pebble Bed** which uses low activation ferritic/martensitic steel and lithium meta titanate (Li_2TiO_3) or lithium ortho silicate (Li_4SiO_4) [Miu97], the **Water Cooled Ceramic Breeder** (Li_2TiO_3) [Miu97] and the **Helium Cooled Ceramic Breeder** (Li_4SiO_4) [Boc04] Li_4SiO_4), will rely on breeder pebbles and beryllium neutron multiplier pebbles [Gia07; Gia12]. These Test Blanket Systems will be installed at the end of each of three dedicated equatorial ITER ports. Each Test Blanket System will be equipped with its own associated ancillary equipment comprising cooling, tritium extraction, coolant purification, instrumentation, etc. For cost and space saving reasons, equipment and peripheral systems will be shared - whenever possible - between the Test Blanket Systems during their respective experimental phases.

Beryllium pebbles used as neutron multipliers in tritium breeding blankets must be of fairly uniform spherical shape and smooth surface. Their optimal sizes should remain within the range 0.3 - 1.3 mm. Such pebbles were fabricated by NGK Insulators Ltd., Hanada-shi, Japan, using the so-called rotary electrode process. To maintain activation by neutrons at acceptable levels, impurities in the pebbles such as uranium, aluminum, magnesium, iron and silicon required specification. Gelles and Heinisch [Gel92] provided complementary information on the consequences of neutron irradiation at 673 K on the mechanical and helium-retention properties of beryllium. Tensile specimens of Be were embrittled by neutron irradiation at 673 K to reach up to 8 dpa. Post irradiation examination was carried out by tensile testing, fractography, and micro structural analyses. Embrittlement at this temperature was attributed to helium bubble formation as well as c-type loop formation. When irradiations were performed at 773 K for up to 1 [dpa], helium bubbles developed in the matrix and grain boundary dislocations.

The intermetallic compound **Be-Ti** was proposed by Uchida et al. [Uch02] as candidate material for an advanced neutron multiplier. These investigators claimed that this material i) possesses good tritium release properties, ii) is characterized by reduced swelling and iii) has better mechanical properties at high temperature than other currently favoured neutron multipliers. Trade-offs are reduced neutronic performance and an incipient fabrication technology.

2.14.7 Interaction of hydrogen isotopologues with tungsten

Tungsten (W) has an atomic mass of 183.84 u, a density of 19.3 $\mathrm{g\,cm^{-3}}$, a melting point of 3695 K and a vapour pressure at that temperature of 4.27 Pa. The specific heat of W is 0.14 $\mathrm{J\,g^{-1}\,K^{-1}}$. Tungsten has a cubic centered crystalline stucture. The interest in tungsten as material for applications in high heat flux areas of fusion devicesis determined by its i) high melting point (3695 K, ii) high thermal conductivity at ambient temperature (100 $\mathrm{W\,m^{-1}\,K^{-1}}$) and iii) comparatively low retention of tritium [Ohi98]. The lower limit for the tungsten surface temperature is governed by the ductile to brittle transition temperature, which is lower than 473 K [Gia10b].

2.14.7.1 Physical-chemical properties

Hydrogen is adsorbed on tungsten atomically and molecularly in a variety of states at temperatures below 500 K. The number of adsorption states and their respective binding energies

are better defined on single tungsten crystals than on polycrystalline ones. Adsorption states are designated in order of increasing de-sorption temperature by λ (molecular), α (molecular) and β (atomic)[Kur87]. The saturation concentration of hydrogen atoms on the tungsten (100) surface was determined by Estrup and Anderson [Est66] to be $2 \times 10^{15}\,\mathrm{atoms\,cm^{-2}}$. The sticking coefficient for the initial adsorption of hydrogen on tungsten was reported to be 0.65. Adsorption of hydrogen molecules takes place via dissociation.

Hydrogen is only slightly soluble in tungsten. The equilibrium solubility (S) can be calculated from the relationship

$$S = 1.48 \exp\left(-\frac{100.5}{RT}\right)$$

in which E_0 is given in $\mathrm{kJ\,mol^{-1}}$ and S in $\mathrm{mol\,m^{-3}\,Pa^{-0.5}}$. This equation was put forward by Frauenfelder [Fra69]. A practical alternative equation is

$$logc_{\mathrm{H}} = 0.5\, logp_{\mathrm{H_2}} - 2.75 - \frac{5000}{T}$$

where c_{H} is given in at%, $p_{\mathrm{H_2}}$ in Pa and T in K [Fro84]. This second equation gives only the order of magnitude of the solubility. Hence, the two equations do not agree exactly.

The diffusion coefficient (D) of hydrogen in tungsten can be obtained from expression

$$D = 4.1 \times 10^{-7} \exp\left(-\frac{37.70}{RT}\right)\ \mathrm{m^2\,s^{-1}}$$

in which the activation energy is in $\mathrm{kJ\,mol^{-1}}$ [Fra69]. The diffusion of hydrogen in tungsten was also investigated by Ryabchikov [Rya64] at temperatures in the range 1338 - 1843 K. For the calculation of diffusion coefficients, they proposed the equation

$$D = 8.1 \times 10^{-6} \exp\left(-\frac{82.80}{RT}\right)\ \mathrm{m^2\,s^{-1}}$$

in which E_0 is given in $\mathrm{kJ\,mol^{-1}}$.

For easier comparison, a number of Sieverts' constants and diffusivity constants of hydrogen isotopes in different types of tungsten materials as pulished in the open literature are listed in

Table 2.56. In addition, a few selected diffusion coefficients have been plotted in Fig.2.59 as function of inverse temperature.

Table 2.56: Sieverts' constants and diffusivities of hydrogen isotopes in different types of tungsten materials (after [Est01]).

Gas	Solubility coefficients		Diffusion coefficients		Temperature range	Ref.
	S_0	E_S	D_0	E_D		
	$mol\,m^{-3}\,Pa^{-0.5}$	$kJ\,mol^{-1}$	$m^2\,s^{-1}$	$kJ\,mol^{-1}$	K	
H[a]	1.48	101.0	4.1×10^{-7}	37.7	1100 - 2400	[Fra69]
H[b]	1.04×10^{3}	267.9	7.2×10^{-8}	173.7	1510 - 1902	[Moo64]
H[c]	1.22×10^{-4}	2.9	6.0×10^{-4}	103.4	400 - 1200	[Zak75]
H[d]	-	-	8.1×10^{-6}	82.9	1055 - 1570	[Rya64]
H[e]	-	-	3.42×10^{-9}	37.8	308 - 385	[Ike11]
H[f]	-	-	3.0×10^{-10}	24.1	300 - 900	[Fra97]
H	2.90×10^{-2}	26.9	5.68×10^{-10}	9.3	673 - 1073	[Est01]
D	2.75×10^{-2}	28.7	5.49×10^{-10}	10.0	673 - 1073	[Est01]
T[g]	2.25×10^{-2}	27.8	5.34×10^{-10}	11.2	673 - 1073	[Est01]

[a] Sintered and rolled cylinder

[b] Filament ribbon

[c] Poly and monocristalline W tubes

[d] Commercial wire (Ø= 1 mm)

[e] Polished to mirror finish

[f] Single crystal

[g] From modelling desorption of hydrogen from pure unalloyed polycrystalline tungsten

As apparent from Table 2.56 and Fig. 2.59, the diffusivities obtained by some investigators differ by orders of magnitude. Diffusivities determined by Frauenfelder [Fra69] and Ryabchikov [Rya64] only agree at temperatures in the vicinity of 1100 K. Extrapolations of the results of [Moo64] or [Est01] up to this temperature are substantially inconsistent (see also [Lon91]). There is evidence that manufacturing processes may be of great influence on the properties of tungsten. This may explain the large discrepancies obeserved with the diffusion coefficients. Possible

reasons for the rather small effective diffusion coefficients determined by Moore and Unterwald [Moo64] have been discussed critically and in much detail by Frauenfelder [Fra69].

Esteban et al. [Est01] measured diffusivities and solubility's employing a de-sorption technique. They estimated the transport parameters of tritium across polycrystalline tungsten from experiments carried out with protium and deuterium. The results from their investigations are listed in Table 2.56.

Solubility and diffusion constants are consistent with interstitially dissolved hydrogen. However, at pressures lower than 10^{-4} mbar diffusing hydrogen is retained in sites other than interstitial ones.

Because of the rather small solubility of hydrogen isotopologues in tungsten great care must be exercised in eliminating completely traps in the specimens utilized for these measurements. To obtain more information on the influence of annealing on the eradication of traps generated during manufacture proceduresl, Nakayama et al. [Nak15] performed experiments with re-crystallized tungsten specimens annealed at progressively increasing temperatures. These specimens were then exposed at 723 K to 1.2 kPa of deuterium containing 7.2 % tritium for the duration of 3 hours. Under these conditions, specimens annealed at either 773, 873, 973, 1073, or 1173 K exhibited "apparent solubilities" of $3.6 \times 10^{-9}\, at.fr.\mathrm{Pa}^{-0.5}$, $2.0 \times 10^{-9}\, at.fr.\mathrm{Pa}^{-0.5}$, $1.9 \times 10^{-9}\, at.fr.\mathrm{Pa}^{-0.5}$, $1.1 \times 10^{-9}\, at.fr.\mathrm{Pa}^{-0.5}$ and $9.7 \times 10^{-10}\, at.fr.\mathrm{Pa}^{-0.5}$, respectively. The results revealed that even at the highest employed annealing temperature, i.e. 1173 K, the determined solubility was still higher than that obtained by extrapolation of the results of Frauenfelder [Fra69], i.e. $1.1 \times 10^{-10}\, at.fr.\,\mathrm{Pa}^{-0.5}$ (It should be noted, that Frauenfelder heated his specimens up to 2400 K and alternated between an 800 mbar hydrogen atmosphere and vacuum for respective periods of 10 hours). Moreover, and primarily for comparison purposes, an ITER grade tungsten specimen was also annealed at 1173 K and then loaded under the same conditions as the re-crystallized ones. The "apparent solubility" obtained in this case was $2.4 \times 10^{-9}\, at.fr.\mathrm{Pa}^{-0.5}$, which is more than twice that obtained when loading re-crystallized tungsten. From these results it can be concluded that while pre-heating for three hours at 1173 K under vacuum reduces the "apparent solubility" considerably, this pre-treatment is not sufficient for a complete elimination of the traps ("apparent solubility" still 1 - 3 orders of magnitude higher than that from extrapolated values of Frauenfelder).

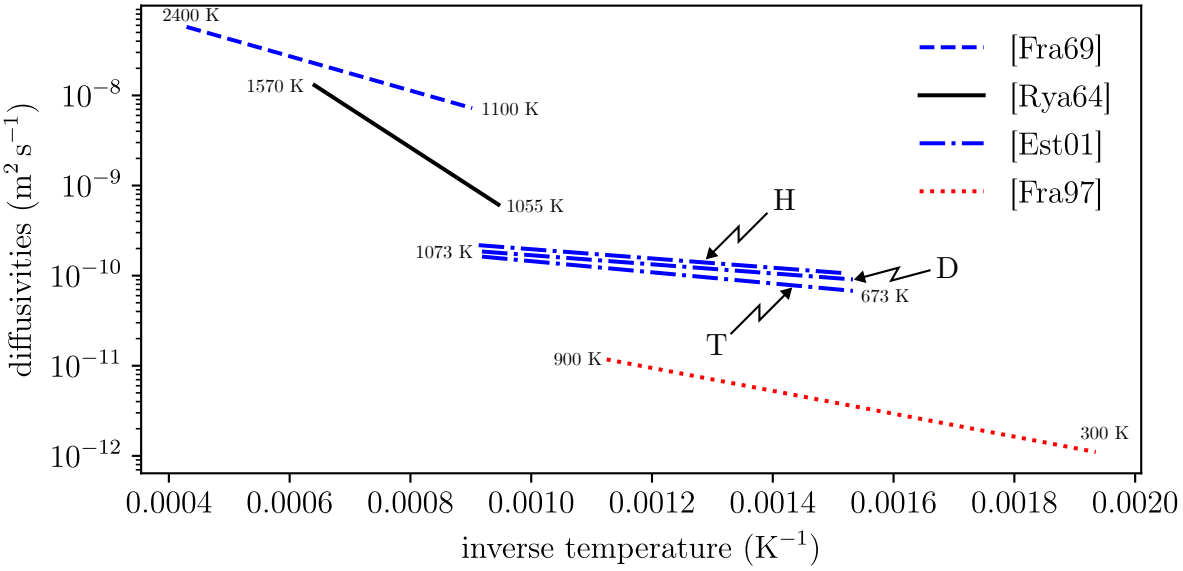


Figure 2.59: Diffusion coefficients of hydrogen isotopes in tungsten as function of inverse temperature (see also Table 2.56).

The permeation (P) of hydrogen through tungsten at pressures and temperatures covering a broad range of pressures (1.33×10^{-4} - 1.0×10^{4} Pa) and temperatures (1050 - 2400 K), was also investigated by Frauenfelder [Fra68a]. According to their findings, at pressures above 1.33×10^{2} Pa the permeation follows the equation

$$P = (7.64 \pm 2.55) \times 10^{-9} \exp\left(-\frac{131.88}{RT}\right) \text{ mol cm}^{-1}\,\text{s}^{-1}\,\text{Pa}^{-0.5}$$

where the activation energy for permeation, $E_\text{P} = 131.88$, is given in kJ mol^{-1}.

Esteban et al. [Est01] obtained for the same type of equation pre-exponential factors of 1.65×10^{-13}, 1.51×10^{-13}, and 1.20×10^{-13} mol cm^{-1} s^{-1} Pa$^{-0.5}$ and activation energies of 36.2, 38.7, and 38.9 kJ mol^{-1} for protium, deuterium and tritium, respectively. Consequently, at a given temperature the permeation increases in the order tritium, deuterium, and protium.

Nakamura et al. [Nak01] concentrated in their research on the influence of **annealing** and therefore of trapping (see also [Lon91], [Fra97], [Haa98][Haa99], [Tak11], [Tyb11], [Tor15a] on the permeation rate of implanted deuterium across tungsten specimens. The trap density in unanneled tungsten was found to be 40 ppm and the trap energy 0.9 eV. Before exposure to deuterium ions, the specimens were annealed for 3 hours at 1273 K. After this heat treatment the traps appear

to have disappeared completely. Deuterium ions were then implanted at constant temperature, constant ion energy of 1 keV, and constant incident ion flux of $9.0 \times 10^{18}\,D^+/m^2s$. The transient permeation was evaluated employing the TMAP4 code. According to their observations, the "lag time" of annealed specimens was between $1/5^{th}$ and $1/10^{th}$ smaller than of the unannealed specimens. These results are in reasonable agreement with corresponding data published by Anderl et al. [And92b]. The obtained transient permeation results could be modelled by a simple diffusion equation of deuterium across tungsten without traps.

Takagi et al. [Tak11] compared the efficiency of trap formation by hydrogen (0.2 MeV) or helium (0.8 MeV) ion beams in annealed tungsten (1173 K for 0.5 hours) and investigated the concomitant influence of temperature. Traps were visualized by the uptake of deuterium from continuous exposure to a deuterium plasma. After completion of the ion irradiation, deuterium depth profiles were determined by nuclear reaction analysis (NRA) employing the $D(^3He, p)^4He$ reaction. The measurements were carried out with a Van-de-Graaff high voltage generator. The ^3He ion energy was 1.7 MeV and the achieved probe depth 1.2 µm. According their observations, the efficiency of trap generation by irradiation with helium ions is much larger than that by hydrogen ions. Increasing the temperature from 393 to 573 K enhanced trap formation. Hence, it was postulated that primary defects in tungsten are stable at temperatures below 500 K but become mobile to yield interstitial clusters or loops at higher temperatures in the range 550 - 600 K. These interstitial clusters appear to constitute traps for hydrogen.

The permeation and transport of hydrogen across tungsten single crystal has also been calculated according to Fick´s law by first principles [Liu13]. Solubilities of deuterium at temperatures within the range 1000 - 2500 K were found to be in good agreement with Fraunfelder´s values. The temperature dependence of the dissociation coefficient of deuterium on single crystal tungsten was given to be

$$k_d = 0.21 \times 10^{39} \exp(-3.16\,eV/kT)\,(m^{-2}s^{-1}\,atm^{-1})$$

Permeation fluxes of deuterium across tungsten specimens of 21 or 50 µm thickness, were calculated to be 0.68×10^{13} and $0.34 \times 10^{14}\,atoms\,m^{-2}\,s^{-1}$, respectively.

On the basis of the present state of knowledge, the expressions for diffusivity and solubility of hydrogen in tungsten proposed by Frauenfelder [Fra69] are generally recommended. This is on

one hand justified by the reliable experimental techniques used by Frauenfelder and on the other, by the very high temperatures employed for the pre-treatment of the specimens. The latter gives reason to the assumption that in his tungsten specimens all traps were consequently eliminated [Cau02; Ski08] (see also Fig. 2.59).

Ikeda et al. [Ike11] showed with a tritium tracer technique that **plasma-driven permeation** rates and **plasma-driven diffusion coefficients** for hydrogen across tungsten are consistently higher than corresponding **gas-driven permeation rates** and **diffusion coefficients** at the same pressure and temperature conditions. Gas-driven and plasma-driven diffusion coefficients as well as permeation rates determined by Ikeda at nearly ambient temperature, were almost not influenced by trapping or surface effects. Extrapolations of permeation rates and diffusion coefficients to the high temperature gas-driven data obtained by Frauenfelder [Fra69] were largely consistent.

Frauenfelder [Fra68b] extended his studies to determinations of the permeation, diffusion and solubility of **nitrogen** in tungsten at pressures within the range 6.7×10^{-3} - 6.67×10^{4} Pa and at temperatures within the range 1373 - 2773 K. He proposed the following equations for the calculation of these quantities as function of temperature and pressure:

$$P = 8.16 \times 10^{-10} \exp\left(-\frac{217.7}{RT}\right) \text{ mol cm}^{-1}\,\text{s}^{-1}\,\text{Pa}^{-0.5}$$

$$D = 5.4 \times 10^{-4} \exp\left(-\frac{259.6}{RT}\right) \text{ m}^2\,\text{s}^{-1}$$

$$S = 15.5 \times 10^{-5} \exp\left(-\frac{41.9}{RT}\right) \text{ mol m}^{-3}\,\text{Pa}^{-0.5}$$

all activation energies being in kJ mol^{-1}. Similar measurements performed at temperatures below 2000 K by Norton and Marshall (see [Dus62]) delivered rather low values, most likely because nitrogen equilibrium concentrations were not attained in the tungsten specimens.

2.14.7.2 Chemical properties

Water vapour dissociates on the surface of tungsten. The atomic components diffuse into the metal matrix yielding solutions and oxides. The evaporation loss of tungsten increases linearly with water vapour pressure at temperatures within the range 1323 - 1548 K. The formation of hydrated tungsten oxide, i.e. $WO(OH)_2$, from the reaction of tungsten oxide (WO_3) with water

vapour may explain losses of tungsten at temperatures where the volatilization of tungsten or of its oxides is normally negligible. No stable tungsten hydrides have been reported.

2.14.7.3 Application of tungsten as plasma facing material in fusion devices

Tungsten is a material of considerable potential for application in ITER because of its low sputtering yield and excellent thermo-physical properties [Jan95]. Further advantages of this metal are low erosion under high heat loads, a very high melting point (3695 K) and boiling point (6203 K), and an extremely low vapour pressure of 4.27 Pa at this temperature. Conversely, radiation damage may lead to changes in thermal conductivity and possibly to the occurrence of radiation-induced embrittlement.

What is more, tungsten can only be employed as structural material under the condition that the operating temperature of the machine is not in conflict with the brittle to ductile transition temperature (BDTT) (see Fig. 2.60). After it was observed that the BDTT of ferritic martensitic steel increases with radiation damage [Zin00; Abe17], an analogous behaviour of tungsten was feared likely. In spite of this, there is currently only one brittle-ductile transition study of tungsten carried out by Giannattasio et al. [Gia10b]. According to their results the BDTT is associated with the kink pair mechanism for motion of screw dislocations and is furthermore highly sensitive to level and kind of impurities in the metal. The minimum operating temperature of tungsten will be determined by the BDTT attained following irradiation[38].

In view of the recent decision at ITER to use exclusively tungsten as plasma-facing material of the divertor [Pia07; Abe17], it is of much relevance for the fusion program to expand the available scarce BDDT data base by dedicated experiments that simulate to a high degree the anticipated fusion-relevant temperatures and irradiation conditions [Abe17]. What is more, because tungsten may experience at ITER a broad range of temperatures 773 - 1723 K depending on location and reactor design, these studies are considered to be quite challenging. Aggravating is the fact, that as divertor armour material, tungsten will not only be exposed to very high heat fluxes but also be subjected to the implantation of helium and hydrogen isotopes, and experience damage by neutrons.

[38] Although plasma-facing tungsten will be operated at elevated temperature a much cooler zone will prevail where this material must be joined reliably to a copper-based heat sink alloy [Abe17].
[39] Some metals that are ductile at a given temperature become brittle when the temperature is reduced.

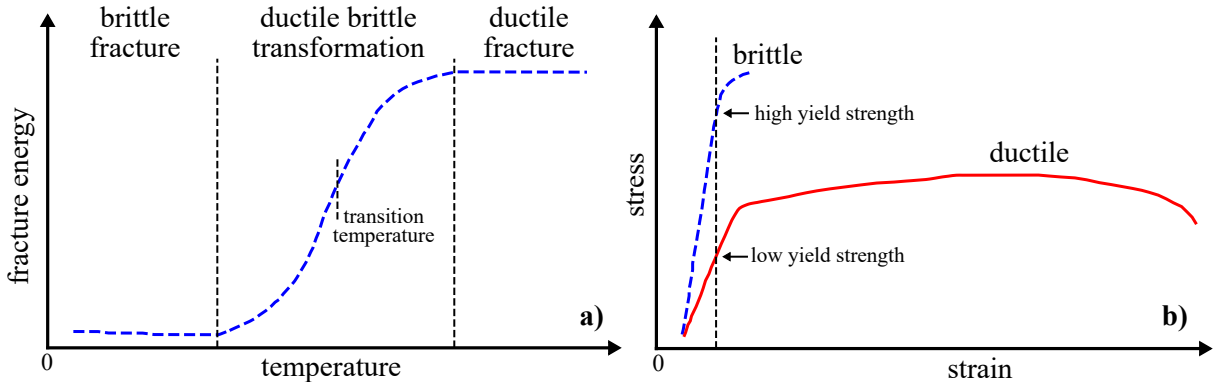


Figure 2.60: a) Brittle to ductile transformation[39] as function of temperature and b) comparison between typical brittle and ductile strain stress diagrams.

2.14.7.4 Consequences of high heat fluxes

First **high heat flux tests** employing a small-scale mock-up of the vertical divertor target of ITER were carried out employing an electron beam facility [Hir16]. Temperatures were determined with a pyrometer. They showed deviations at the periphery from calculated values at high adsorbed heat fluxes. After exposure of the mock-up to a heat load of 10 MW m^{-2} over 5000 cycles or of 20 MW m^{-2} over 300 cycles, it displayed frequent but non-systematic macro cracks in the middle of the tiles in the direction of the cooling water flow (see Figs. 2.61b, c). The appearance of macro cracks as well as of plastic strain due to compressive stress during a heating phase appears to be related to the cyclic exposure to high temperature.

Cracks were likewise detected in tungsten after exposure to hydrogen or helium plasmas under ITER relevant steady state repetitive transient conditions at temperatures within the range 670 $<$ T $<$ 1170 K [Buz17]. The tested tungsten specimens revealed i) cracking on surfaces exposed to helium and ii) strong roughening caused by plastic deformation of surfaces exposed to hydrogen. Hence, major consequences of irradiation were embrittlement of the surface and an increased tendency towards cracking. This progressive worsening of the thermal properties of the divertor surface urgently calls for further research efforts.

The applicability of tungsten as plasma facing material on **limiters** was investigated at TEXTOR by Tanabe et al. [Tan00a; Tan00b]. Three different type of tungsten limiters were tested: i) a bulk tungsten test limiter, ii) a twin test limiter one half made of bulk tungsten and the other half of graphite, and iii) main poloidal tungsten limiters. Tungsten from the bare test

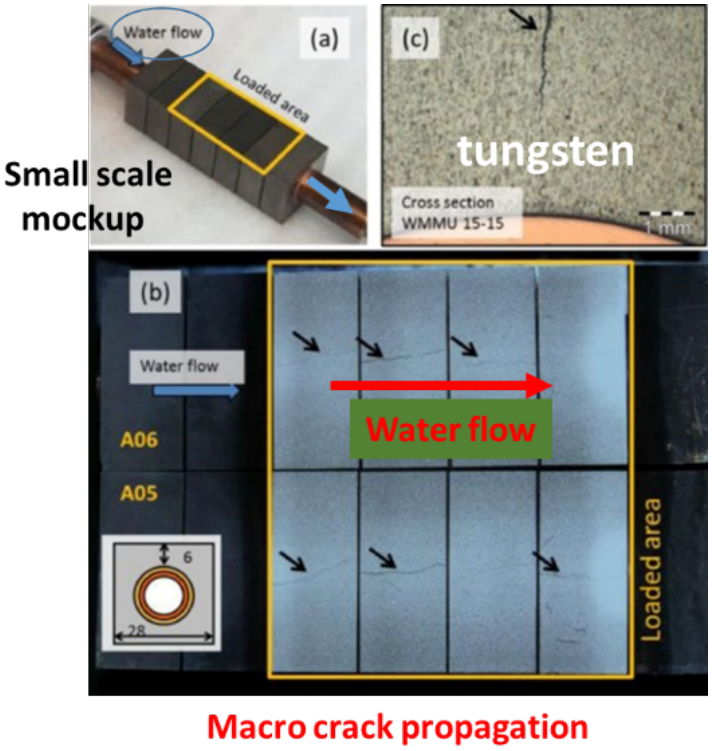


Figure 2.61: a) Small scale mock-up of the vertical divertor target of ITER supplied by EU, (b) macro crack developed in a mock up supplied by EU running parallel to the coolant pipe axis after a high heat flux test and (c) macro crack developed in tungsten after exposure to a high heat load [Hir16].

limiter was sputtered by carbon, oxygen, and by self-sputtering. However, probably owing to a prompt redeposition near the sputtered area, the accumulation of tungsten in ordinary shots was small. The half bulk tungsten/half graphite limiter was compared on one hand with respect to its impact on the plasma performance and on the other regarding qualifications of tungsten as material protecting the limiter. The results revealed that tungsten is applicable as plasma facing material provided central accumulation of the metal is avoided employing external heating systems such as Neutral Beam Injection (NBI) and/or Ion Cyclotron Resonance Heating (ICRH). Most of the hydrogen in the limiter was found to be retained in the deposited layer, the retention in deposited carbon being much higher than in deposited tungsten.

In subsequent work, a macro **brush tungsten limiter** was exposed at the TEXTOR-94 tokamak to plasmas of incident power densities of 35 - 40 $\mathrm{MW\,m^{-2}}$ [Hir03]. No indications of enhanced erosion, such as arcing in grooves (electric arc building in grooves) or intense sputtering

at the edges of brush columns were noticed. The temperature distribution was observed to be non-uniform probably because of the thermal isolation of the columns. Only minor cracks which developed perpendicularly were noticed. Crack propagation terminated at the grooves. From the results it was concluded that under plasma exposure conditions a limiter with brush configuration displays comparable performance to that of a solid tungsten limiter but is superior to the latter as far as mechanical behaviour is concerned.

Maier et al. [Mai98] investigated at ASDEX Upgrade the performance of fine grain graphite divertor tiles coated with tungsten. The metal layer was applied with a plasma spray procedure. Divertor tiles were subjected during 800 cycles to heat fluxes of up to $6\,\mathrm{MW\,m^{-2}}$ for 2 s and to lower power densities for 5 s. After these exposures, almost all tiles revealed poloidal cracks at the tungsten layer and toroidal cracks which additionally propagated into to the graphite bulk. The maximum surface temperatures of the divertor tiles were estimated to be 973 K. Because the poloidal cracks only extended throughout the coating they were assumed to start off from the mismatch between the thermal expansions of coating and substrate.

2.14.7.5 Erosion by plasma

The experience gained from the operation of ASDEX-Upgrade after the first wall of this machine was fully covered by tungsten was documented by Schleußner et al. [Sch99a] and Mayer et al. [May09]. At ASDEX it was observed that tungsten was eroded from all tiles and then transported from one location to another by plasma processes taking place within the vacuum vessel [Kri02; Neu03]. The predominant erosion source at ASDEX-Upgrade was ion impact, the eroded tungsten migrating directly through the plasma scrape off layer (SOL) without entering the confined plasma. Hence, not only tungsten but also transmutation products did show up in zones of the machine where they were not expected[40]. The deuterium inventories in plasma sprayed 200 µm thick tungsten layers and in bulk tungsten were found to be very similar. A further observation was that the carbon deposition decreased by a factor of about 15 from that observed during the operation of the original machine, whose first wall consisted entirely of carbon [May09]. Concurrently, deuterium trapped in carbon/boron co-deposited layers in the divertor decreased by up to an order of magnitude. Problems identified at the time were i)

[40] It is well known that the dominant regions of redeposition are located away from the plasma-limiter interaction regions with co-deposited films of up to µm developing in low flux regions.

difficulties with plasma start-up, ii) cooling of the plasma by tungsten particles causing loss of fusion performance in high temperature plasmas and iii) material selection.

Rooij et al. [Roo13] investigated the erosion of tungsten from the outer divertor of JET after the first wall was coated with this material primarily with the objective of simulating an ITER-like wall. The main goals were i) to estimate the chemical composition, concentration and energy of the sputtered particles and ii) to determine the fraction of particles that truly leave the surface, i.e. fraction not promptly re-deposited. Typical effective sputtering yields in the L-mode were found to be 0.001. The erosion was mainly attributed to beryllium, the dominant impurity in the plasma. The results indicated that more than 50 % of the eroded tungsten undergoes prompt re-deposition. A fraction of only 0.5 % beryllium in the target flux density was considered sufficient to explain the observed tungsten sputter signals. Another conclusion from the work was that sputtering dominates during the occurrence of ELM´s[41] rather than in between ELM´s.

As already discussed, high Z materials like tungsten, when present in the plasma in unwanted concentrations may cause substantial radiation losses and even collapse of the plasma. Tungsten can be released into the plasma either through direct grain ejection or through evaporation. The latter may take place for instance via open blister caps of insufficient thermal contact with the underlying material [Cau02].

2.14.7.6 Formation of traps and blisters in plasma exposed first wall materials

It is common knowledge that traps are generated in tungsten during manufacturing processes. The transport of hydrogen isotopes through tungsten is consequently dominated by simultaneously occurring extensive trapping [Lon91; Fra97]. Such trapping was found to take place in the material bulk at sites like vacancies, voids, surfaces, boundaries, impurity atoms, and dislocations. Trapping may be the cause for significant delays in permeation saturation and abrupt changes in permeation rate. Traps have no influence on the rate at which tritium permeates through tungsten but will increase the transient time at which steady state is established. The rate at which traps are filled or emptied is generally much faster than the rate of diffusion. It may thus be concluded that the inventory of tritium in tungsten is determined by the synergistic action of implantation, recombination, diffusion, and trapping. In the absence of traps most ions and

[41] ELM (edge-localized mode) = disruptive instability occurring in the edge region of a tokamak plasma.

neutral atoms that impinge on tungsten will either re-emerge or go through. If trapping takes place the inventory may increase significantly.

Anderl et al. [And92b] determined hydrogen trapping parameters in polycrystalline unannealed, annealed at 1273 K, and annealed at 1673 K tungsten at temperatures within the range 610 - 823 K. The experiments delivered trapping site density values of 4.4×10^{24} sites/m^3, 1.6×10^{24} sites/m^3 and 8.2×10^{23} sites/m^3 at trapping energies of 150.5 kJ mol^{-1}, 137.0 kJ mol^{-1} and 129.3 kJ mol^{-1}, respectively. From these results it follows, that trapping in polycrystalline tungsten varies inversely with pre-anneal temperature. Further trapping site densities and trapping energies of hydrogen in single crystal tungsten [Fra97], wrought tungsten [Fra97], and rolled tungsten [Pis95] have been determined at temperature within the range 300 - 900 K [Est01]. Two kinds of traps were identified in thermal desorption studies [Fra97; Ogo03]:

- Low temperature traps involving intrinsic (natural) defects with a trapping energy of 0.85 eV distributed homogeneously over the whole width of the material, and
- High temperature traps having a trapping energy of 1.45 eV, which are induced by ions and grow during implantation. Hence, they show up in the implanted zone near the surface and correlate with the implantation range.

In case of irradiation with deuterium ions the concentration of deuterium in the implantation zone greatly exceeds the value of the deuterium solubility. This causes stresses in the matrix until plastic deformations and void formations lessen these tensions. Exposure of tungsten to energetic hydrogen isotopologues, helium, and impurity particles (up to several hundreds of eV) gives rise to surface modification like blisters, nano bubbles, cracking, and metallic fuzzy nanostructures. These modifications can lead to increased erosion yield, dust formation, and worsening of the mechanical and thermal properties [Lu14; Buz17; Kaj18]. Bubble size and growth rate are closely related to the temperature of the surface. Hence, the mechanism of nano bubble formation in the near surface zone relies presumably on trapping of particles in the thermal vacancies of the material. The peak temperature of tungsten after exposure to pulsed plasmas increased by a factor of 1.3 in hydrogen and of 1.3 - 1,5 in helium plasma in comparison to the first plasma pulses, indicating an alteration of the thermal properties of the target. One conclusion is that pure helium plasma operations are likely to cause tungsten surface cracking at lower transient energy densities than would occur with hydrogen plasma.

On the ground of the extremely low solubility of hydrogen in tungsten [Fra68a], it appears that after the attainment of tritium saturation in the plasma-exposed metal surface further accumulation diminishes considerably. This is also expected on account of the short range of tritium ions in the metal and the fast diffusion of tritium at the prevailing elevated temperatures. During ITER operation most incident ions will therefore return quickly to the surface and recycle into the plasma chamber at high rates [Rot11]. Should however first wall tungsten exhibit abundant "manufacturing traps" and/or radiation-induced traps it is expected that tritium will gradually become sequestered and subsequently accrue in the bulk [Man11] (it should be noted that tritium build-up conducting to an "apparent solubility" predominantly consisting of retention in traps is notoriously apparent in metals exhibiting low solubility for tritium). Traps consisting of crystal lattice defects, dislocations, grain boundaries, or cracks are primarily produced in fusion devices by energetic deeply penetrating neutrons not constrained by magnetic fields. Energetic neutrons, generated in the D(T,n)α fusion reaction, can cause formation of traps throughout the tungsten bulk thus considerably enhancing the potential for tritium retention. Under their impact damage cascades are generated within the material giving rise to an excess of vacancies and interstitial atoms. Traps formed throughout the tungsten bulk will substantially enhance the retention of tritium much beyond solubility. A build-up of several displacements per atom may lead to changes in the microstructure as well as to modifications of the thermal and mechanical properties of the metal.

In addition to displacement damage, neutrons will also undergo **transmutation reactions** with tungsten. Principal transmutation products of tungsten are isotopes of rhenium, osmium, and tantalum. Another transmutation product is hydrogen. Even though this is only a minor product it can have significant impact on the mechanical properties of the metal if it leads to embrittlement [Abe17].

Matters of concern arising from the exposure of tungsten to plasma are i) enhanced radiation losses of plasmas contaminated by this metal [Cau02], ii) occurrence of blistering eventually leading to flakes and dust [Man11], iii) a progressive worsening of mechanical properties, and iv) impact of trapping - especially in the presence of carbon - on the transport and retention properties of tritium [Eck98; Lut00; Rot11; Tor13].

The retention of deuterium in polycrystalline tungsten foils as function of ion fluency and implantation temperature was investigated by Haasz et al. [Haa98]. They noticed that at 350

- 550 K the retention levels are higher than at ambient temperature. This enhancement was attributed to an increased diffusion coefficient which effectively translates into greater penetration. While at ambient temperature saturation appears to take place as function of fluency, this is not the case at 500 K. What is more, when ion irradiation is performed at ambient temperature most deuterium is trapped near the sub surface. If higher temperatures are selected, the deuterium levels in the sub surface zone are much lower because of diffusion towards the back of thin specimens. The retention of tritium in tungsten was found to reach a maximum at intermediate temperatures with lower retention at both higher and lower temperatures [Cau99]. Poon et al [Poo03] confirmed this observation on the basis of thermal desorption spectra. They concluded that the retention of deuterium increases with D^+ ion fluencies and decreases when implant temperatures are higher than 500 K. In fact, at $T > 700$ K retention becomes very small.

In a follow up study, Haasz et al. [Haa99] investigated the effect of ion damage on deuterium trapping in polycrystalline tungsten. Specimens of this metal were first subjected to the sequence implantation to a given damage fluency (fluency = flux integrated over time), thermal desorption, implantation to the probe fluency (10^{23} D/m^2, and finally to another thermal desorption. Experiments with 0.5 keV/D^+ ions revealed increased deuterium retention on specimens previously exposed to high fluencies in comparison to specimens exposed to only low-incident fluency implantations. The increased retention was assumed to be due to swelling-induced stresses and/or precipitation of tungsten hydrides leading to dislocations and grain cracking. Identical experiments with 1 keV/D^+ did not reveal any significant change in retention due to prior implantation. This was explained by saturation of the near surface traps the consequence being that higher fluency implantation had no further impact on trapping. In a later study, Wirtz et al. [Wir11b; Wir11a] showed that the combination of high flux hydrogen-plasma and thermal shock loading influences significantly distance, width, and depth of the resulting cracks.

O´hira et al. [Ohi98] determined the retention of hydrogen isotopes in wrought tungsten employing several irradiation sources at controlled temperatures. Annealing tungsten at 1773 was associated with a substantial reduction in retention. Thermal release of deuterium displayed correlation with modifications of the tungsten microstructure. Even with non-annealed wrought tungsten the ratio of retained atoms/incident hydrogen ions was found to be 5×10^{-5} when the metal was exposed to an incident fluence of 7×10^{25} ions/m^2 at 523 K.

The retention of deuterium and damage accumulation near the surface of **tungsten** and **molybdenum** single crystals was the research subject of Nagata and Takahiro [Nag00]. The examined parameters were i) implantation temperature, ii) incident deuterium ion energy, and iii) incident ion flux density. The experiments provided evidence that the deuterium retention near the surface of tungsten crystal was significantly higher than on molybdenum crystal at temperatures between 300 and 650 K, but particularly at ambient temperature, and up to an implantation dose of 2×10^{23} D/m^2. Trapping of D atoms in Mo and W crystals appears to take place in lattice distorsions caused by implantation-induced defects such as interstitial loops.

Hydrogen isotope implantation into tungsten at an ion fluency exceeding 10^{24} Q/m^2 (Q = H, D and T) leads to the formation of **blisters**, which strongly influence the trapping behaviour of hydrogen isotopes [Ali01; Wan01; Tok05; Luo06; Shu07; Fuk08; Buz17]. Factors determining the formation of blisters are the type of tungsten, i.e. powder metallurgy tungsten, vacuum plasma sprayed tungsten, single crystal tungsten, etc. and the temperature during irradiation [Tok05]. The blister size increases and the number of blisters decrease with ion bombardment energy [Wan01]. A strong correlation was noticed between the occurrence of blisters and blister-like features in tungsten exposed to low energy deuterium plasma and the degree of deuterium retention. Blistering actually increased the retention of deuterium. While the contribution of deuterium sequestered in blisters to the total inventory in tungsten is only minor [Man11], the pressure of deuterium inside of the blisters is mainly responsible for the expansion and rupture of these cavities.

Shimada and Nishikawa [Shi03] examined the effect of carbon concentration, beam fluency and sample temperature on blister formation on a tungsten surface. They noticed that blisters were formed when the concentrations of carbon exceeded 0.15 %. At carbon concentrations in the span 0.15 - 0.35 % the number of blisters remained small, but at higher concentrations a large number of blisters of different sizes became apparent. Up to a depth of 7 nm from the upper most surface carbon was detected either as graphite or as tungsten carbide. Increasing fluencies had an enhancing effect on the blister size.

Franzen et al. [Fra97] studied trapping and release of deuterium implanted in tungsten employing a modelling approach based on results from re-emission, thermal desorption, and isothermal desorption experiments performed at temperatures in the range 300 - 900 K. Only two type of traps were assumed to occur in the examined implanted material: i) natural traps which

depend on type and manufacture of the tungsten material whose concentration is homogeneous throughout the metal, and ii) ion-induced traps which understandably are found only in the "implantation zone". From their calculations they concluded that deuterium atoms can diffuse deep into tungsten even at ambient temperature. Under the employed experimental conditions, the depth of the resulting "diffusion zone" exceeded the "implanted zone" by more than two orders of magnitude. On the other hand, the amount of deuterium solved in tungsten was of the same order of magnitude than that trapped. The amount of solved deuterium in tungsten shows only small dependency from incident ion energy but rises with the square root of the implantation fluency [Fra97]. The relatively high amount of solved deuterium in tungsten constitutes an important difference to graphite. In case of graphite nearly all deuterium is trapped in the implantation zone, the amount dissolved being orders of magnitude lower. This property of tungsten has a marked negative impact on deuterium recycling from a tungsten first wall. Fig. 2.62 displays depth profiles of deuterium trapped in tungsten single crystals irradiated with low energy deuterium ions. As apparent, the profiles are characterized by three distinct deuterium-retention zones [Ali05; Ali08]: i) one at the surface layer at depths in the range 0.2 - 0.5 µm (the actual depth depends on the energy of the ions), ii) a second one at the sub-surface layer at depths from about 0.5 up to 2 µm and iii) a third zone in the bulk reaching depths of up to 7 µm. When the concentration of deuterium within the near-surface zone of tungsten was determined by measuring the D_2 release rate during argon sputtering, repetitive deuterium gas bursts were noticed up to completion of the analysis at a depth of 450 nm. These bursts suggest release from ruptured voids containing gaseous molecular deuterium. Blister formation at high fluencies were only observed for polycrystalline tungsten and not for single crystal tungsten.

Tungsten carbide can build up on the metal surface when the material is exposed to carbon seeded deuterium plasmas [Lut00]. Films of tungsten carbide or tungsten oxide - even when thin - will retain hydrogen isotopes efficiently. Tungsten carbide additionally serves as a barrier layer for diffusion, preventing the outward transport of tritium into the gas phase. Hence, another consequence of carbide build-up on the tungsten surface is increased retention of tritium in the bulk. Torikai et al. [Tor13; Tor15a] provided evidence that polycristalline tungsten exposed to TEXTOR plasmas of 5.4×10^{22} Deuteriumatoms/m^2/s fluence in the limiter region at 623 K, when subsequently loaded thermally with tritium, accumulates tritium in carbon deposition

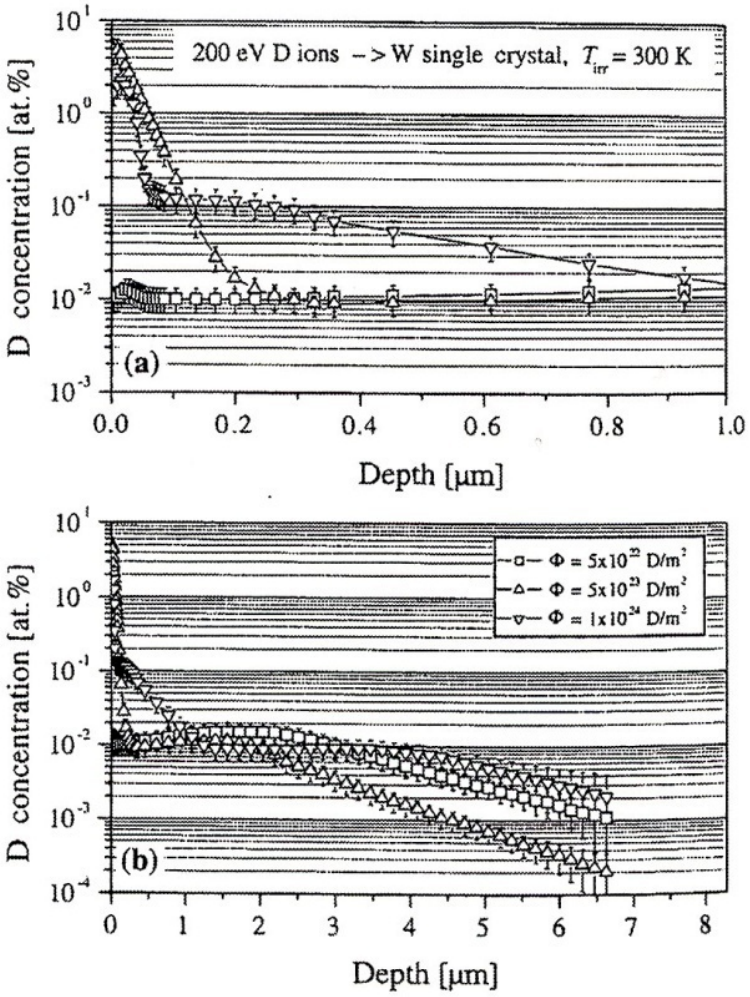


Figure 2.62: Depth profiles of deuterium (a) trapped at the top surface and (b) trapped in the bulk of single tungsten crystals after irradiation with 200 eV deuterium ions at 300 K at fluencies within the range of 1×10^{22} - 1×10^{24} D/m^2 [Ali05; Ali08].

zones existing on the surface[42]. Tritium is trapped rather firmly in these carbon depositions probably in form of carbide. It is not released from these depositions even after prolonged ageing, i.e. 513 days, at ambient temperature.

Eckstein et al. [Eck98] bombarded tungsten simultaneously with carbon and deuterium at progressing plasma edge electron temperatures using three different concentrations of carbon impurity. Their experimental results could be verified by model calculations.

[42] The rather low tritium levels prevailing in TEXTOR do not permit direct tritium visualization in tungsten

Irradiation damage of tungsten has recently been examined theoretically by first principles using pseudo potential methods [Wen17b; Wen17a]. Objective of the work was to improve understanding of the mechanisms leading to damage when tungsten undergoes plasma-exposure. A further objective was the identification of transition metals capable of enhancing the radiation resistance of tungsten. The results indicate that Zr, Mo, Hf and Re atoms have a beneficial influence on the formation of mono vacancies. Of these, Zr was found to be the most efficient promoter of mono vacancy diffusion. Alloying tungsten with rhenium appears to ameliorate significantly the occurrence of swelling induced by radiation.

The **application of a tungsten layer on surfaces** to be subjected to fusion plasmas has been carried out by one of three different techniques: i) sintering, ii) chemical-vapour deposition, or iii) plasma-spraying. Each technique introduces their own lattice imperfections. These defects, together with ion damage generated by plasmas, may act as trapping sites for hydrogen isotopologues and helium. Therefore, diffusion and solubility of hydrogen isotopologues may be substantially influenced by the selected application process and the history of interactions with plasma of the armour material.

2.14.7.7 Recovery of tritium from plasma facing tungsten

The recovery of tritium from plasma-facing tungsten constituting the first wall of ITER will possibly take place by annealing at temperatures below 623 K. To assess the effectiveness of annealing, relevant experiments were performed with pure tungsten specimens previously irradiated with negative hydrogen ions of 300 keV at < 473 K [Tsu11]. The damaged specimens were thereafter loaded with deuterium and subsequently heated for periods of 10 hours at temperatures up to 623 K. The results indicate that during annealing at 523 K only 60 % and at 573 - 623 K about 85 % of the deuterium is thermally released. The released fraction at 523 K was in line with a trapping energy of 1.29 eV, which is comparable to the vacancy trapping energy of 1.43 eV reported by van Veen et al. [Vee88] or 1.2 eV by Franzen et al. [Fra97]. It was concluded that the generated damage is consisted with vacancies.

In a further experimental study, a number of core cylinders were cut from the inner and outer CFC divertor tiles retrieved from JET. At the time, these tiles were covered by a tungsten layer on the plasma-exposed side (for details on sample history see ref. [Hei17]). From these cylinders a number of disks were sliced and singly analysed by thermal desorption spectroscopy (TDS). In

basic agreement with results presented in the previous paragraph, deuterium fractions remaining in these disks after prolonged heating at 623 K were found to be 54 % and 87 % for tungsten deposition thicknesses of 10 µm and 40 µm, respectively[43].

It is concluded that i) the fraction of deuterium remaining in the tile appears to correlate with deposition thickness, and ii) the selected temperature range was not sufficiently high for an efficient and full recovery of trapped and dissolved hydrogen isotopologues.

2.14.7.8 Formation of tungsten fuzz

Formation of fuzz was observed on the surface of tungsten when the metal was exposed to helium-containing plasmas (with a synergistic effect by hydrogen) at temperatures above 1000 K and helium fluxes of more than $10^{24}\,m^{-2}$ [Lu14; Abe17; Kaj18].

Helium presumably accumulates in clusters that grow into bubbles which eventually rupture, particularly when they are located near the surface, causing formation of the fuzz structure. In spite of the concern that tungsten fuzz could increase the degree of sputtering, experimentally it was found that the opposite is the case.

2.14.7.9 Fine spray/droplet ejection from a tungsten melt layer

At TEXTOR experiments were performed on the melt behaviour of several tungsten grades under quasi steady state melt conditions [Coe11]. The results revealed ejection of a fine spray from the tungsten melt. Sometimes, when large drops were released, the discharge was terminated. Machine operation was not obstructed by the occurrence of fine spray, but a decrease of the core temperature was registered.

2.14.7.10 Heat sink for high heat flux components

CuCrZr is a commercially available strengthened alloy of good thermal conductivity and reliable mechanical strength at low and moderate temperatures. It will be used at ITER as heat sink for high heat flux components. Weaknesses of this material are the microstructural modification and loss of mechanical strength when exposed to temperatures higher than 773 K [Pin10].

For the implementation of CuCrZr in fusion machines, it is of considerable importance to develop a durable and reliable bonding between tungsten and the copper interlayer between

[43] The annealing temperature foreseen for the tungsten covered divertor tiles of ITER is 623 K.

W and CuCrZr [Smi98]. According to one procedure, the bottom of tungsten armour is first coated with a flat and continuous layer of copper which thereafter is joined either to copper or a copper-chrome-zirconium alloy via electron beam welding or diffusion bonding. An aspect of concern is the brittle to ductile transformation of tungsten which determines the minimum operation temperature of the metal. A study is needed to uncover whether this can become critical at the interlayer between tungsten and copper. In addition, the distribution of tritium between tungsten, the copper interlayer, and the heat sink needs to be evaluated. As apparent from the figures in Appendix F, the diffusivity of tritium in copper and tungsten is similar, but the solubility in copper is orders of magnitude higher than in tungsten (the solubility of both elements increases with temperature).

Nakamura et al. [Nak00] estimated the **permeation rate** of hydrogen isotopologues through a **tungsten armoured divertor** by exposing a divertor-simulating module provided with a cavity containing water pressurized to 2.2 MPa to DT plasmas (the water coolant of ITER will be maintained 4 MPa [Mer11]. After four hours of plasma exposure break-through of tritium into the water was detected. The results were modelled employing the one-dimensional numerical analysis codes TMAP4 and TPERM. In the calculations the trap density in tungsten was taken to be 0.01 and that in copper zero.

2.14.7.11 Tungsten waste

Tungsten used as plasma-facing material in fusion machines will remain highly activated for a prolonged period of time. It will additionally be contaminated by tritium. Therefore, tungsten recovered from an operating machine must be classified as “mixed waste” (tritiated and activated waste) and dealt with accordingly. Table 2.57 provides information on the activation products generated in plasma facing tungsten retrieved from a divertor after it has been exposed to a fluency of 0.091 MW year m^{-2} and subsequently to storage for periods summing up to one, ten, or one hundred years. After a decay time of 100 years, the start of the ITER waste time scale, the activation of tungsten is due to i) products from neutron reactions with impurities and base metal isotopes, and ii) tritium resulting from transmutation reactions and interactions with plasmas [ITE01d]. Because the clearance index, even without tritium, is significantly above unity (due to hafnium and rhenium isotopes Hf-178m, Hf178n, Re-186 and Re186m) a clearance will not be possible, even if the waste is no longer contaminated by tritium (slow chronic release).

Two tons of tungsten as bulk W or W-coated CFC tiles are used at JET for ITER-like wall experiments (JET-ILW) [Bre15].

The total amount of tungsten waste arising during five operational phases planned for ITER has been estimated to be of the order of 95 tons [ITE01d].

2.14.8 Interaction of hydrogen isotopologues with palladium and alloys of palladium

Thermodynamic properties of palladium of relevance to the safe storage and handling of tritium as tritide were addressed in a previous chapter. In this section some additional properties of palladium and palladium alloys are discussed with special emphasis on those of importance to the operation and design of permeators such as used for the removal of impurities from hydrogen isotopologues and the decontamination of fusion plasma exhaust gases [ITE01d].

Table 2.57: Calculated evolution at three decay periods of the specific activity of the activation products generated in tungsten exposed in the divertor to an average fluency of 0.091 MW year m^{-2} [ITE01d].

1 year		10 years		100 years	
Activation product	Specific activity Bq g^{-1}	Activation product	Specific activity Bq g^{-1}	Activation product	Specific activity Bq g^{-1}
Total	$\mathbf{2.4 \times 10^9}$	**Total**	$\mathbf{3.0 \times 10^5}$	**Total**	$\mathbf{5.3 \times 10^2}$
^{181}W	1.3×10^9	^{179}Ta	2.8×10^5	^{91}Nb	1.4×10^2
^{185}W	1.1×10^9	^{3}H	1.4×10^4	^{178m}Hf	9.7×10^1
^{179}Ta	1.3×10^7	^{55}Fe	8.5×10^3	^{178n}Hf	9.7×10^1
^{182}Ta	9.7×10^6	^{178m}Hf	7.3×10^2	^{3}H	8.9×10^1
^{184}Re	3.3×10^5	^{178n}Hf	7.3×10^2	^{93}Mo	3.5×10^1
^{184m}Re	3.2×10^5	^{91}Nb	1.6×10^2	^{93m}Nb	3.0×10^1
^{55}Fe	8.3×10^4	^{93}Mo	3.6×10^1	^{186}Re	2.0×10^1
^{3}H	2.3×10^4	^{93m}Nb	2.2×10^1	^{186m}Re	2.0×10^1
^{181}Hf	1.1×10^4	^{186}Re	2.0×10^1	^{99}Tc	1.5
^{188}Re	1.1×10^4	^{186m}Re	2.0×10^1	^{187}Re	1.2

2.14.8.1 Physical-chemical properties

Notably, sorption of hydrogen by palladium at liquid air temperature is about ten times higher than that measured at ambient temperature and much larger than that observed for charcoal at the same cryogenic temperature. It was this particular property of palladium that contributed mostly to the development and optimization of the Thermal Cycling Absorption Process (TCAP) [Ari05] (see also section 3.18.7.4). What is more, the high permeability of hydrogen across palladium/silver alloys as well as the tolerable impact of solved hydrogen on the structural properties of palladium/silver alloys have been primary incentives for the utilization of these materials in processes destined to purification and separation of hydrogen isotopes.

Diffusion coefficients of hydrogen across pure palladium as determined by a number of independent research groups [Jos40; Dav54; Tod58; Kat60; Boh67; Kof68; Gol70; Hol70; Voe71] have been plotted as function of inverse temperature in Fig. 2.63. The length of each single plot reflects the actual temperature range employed by the respective investigators. As apparent, the data show notable consistency over a wide range of temperatures.

An averaged Arrhenius type relationship for hydrogen diffusion across palladium [Bir72a] is provided by equation

$$D = 4.5 \times 10^{-7} \exp\left(-\frac{24.07\,\mathrm{kJ\,mol^{-1}}}{RT}\right)\ \mathrm{m^2\,s^{-1}}$$

and for the diffusion of tritium [Sic71] by

$$D = 1.05 \times 10^{-6} \exp\left(-\frac{26.59\,\mathrm{kJ\,mol^{-1}}}{RT}\right)\ \mathrm{m^2\,s^{-1}}\ .$$

From these expressions it can be shown that at low temperatures diffusion through palladium follows the order hydrogen > deuterium > tritium. Because of crossover of diffusion coefficients at about 675 K this order is reversed at high temperatures [Glu06a].

Additional Arrhenius parameters for the diffusion of hydrogen across palladium as well as through five different palladium/silver alloys of increasing silver content at low hydrogen concentrations and temperatures covering the range 533 - 913 K were reported by Holleck [Hol70] (see Table 2.58). As apparent, whereas values of D_0 decrease only slightly with increasing silver content in palladium, those of the activation energy E display a clear upward trend.

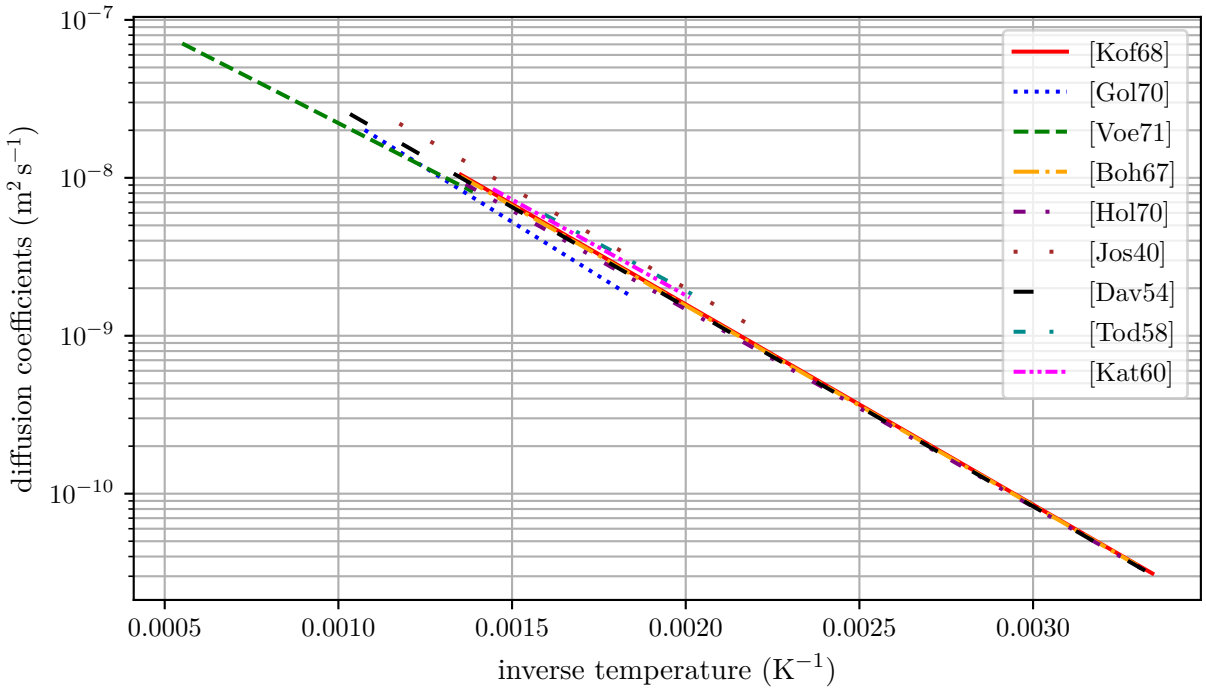


Figure 2.63: Diffusion coefficients of hydrogen through palladium as function of inverse temperature.

The dependence of the activation energy from the silver mole fraction in palladium (X_{Ag}) can be estimated from the relationship

$$E = 15.91(X_{\mathrm{Ag}})^4 + 6.28(X_{\mathrm{Ag}})^2 + 22.03 \text{ kJ} .$$

Pressure/composition isotherms of the systems hydrogen, deuterium and tritium in palladium and in palladium/silver alloys are well established [Wic64; Bro65; Fri73; Sch78; Lae83; Lae88]. Expressions for the calculation of enthalpies and entropies of solution of H, D and T in Pd have been published by Lässer and Powell [Lae86; Lae88].

The thermodynamic equilibrium between the concentration of hydrogen in the metal, x, expressed as the ratio (hydrogen atoms/palladium atoms) and the pressure of hydrogen above the metal is described by relationship [Lae85]

$$\ln \frac{p}{p_0} \left(\frac{x_{\mathrm{s}} - x}{x} \right)^2 = 2 \ln K_{\mathrm{s}}^{\mathrm{Q}} + \frac{2}{RT} \Delta\mu$$

Table 2.58: Diffusion parameters of hydrogen in palladium and palladium/silver alloys at 533 - 913 K and low hydrogen concentrations (after [Hol70]).

Material	D_o	E
	$m^2\,s$	$kJ\,mol_H^{-1}$
Pd	$(2.94 \pm 0.20) \times 10^{-7}$	22.0
Pd*	4.3×10^{-7}	23.4
Pd**	$(5.6 \pm 0.1) \times 10^{-7}$	23.2
$Pd_{0.9}Ag_{0.1}$	$(2.69 \pm 0.20) \times 10^{-7}$	22.2
$Pd_{0.8}Ag_{0.2}$	$(2.33 \pm 0.20) \times 10^{-7}$	22.3
$Pd_{0.7}Ag_{0.3}$	$(2.21 \pm 0.20) \times 10^{-7}$	24.7
$Pd_{0.6}Ag_{0.4}$	$(1.50 \pm 0.20) \times 10^{-7}$	26.4
$Pd_{0.5}Ag_{0.5}$	$(1.82 \pm 0.20) \times 10^{-7}$	33.5

* [Kat60], ** [Wan04]

in which K_s^Q is the Sieverts constant of hydrogen isotope Q, R the gas constant and $\Delta\mu$ an excess chemical potential denoting deviation from Sieverts´s law.

The temperature dependence of the desorption plateau pressure p in the $\beta \rightarrow \alpha$ phase transition region for H, D and T or for the Pd–Q or $Pd_{0.90}Al_{0.1}$–Q systems (Q = H, D or T) can be calculated from relationship

$$\ln K_s^Q = -\frac{\Delta\bar{H}_Q^{(\beta\rightarrow\alpha)}}{2RT} + \frac{\Delta\bar{S}_Q^{(\beta\rightarrow\alpha)}}{2R}$$

where $\Delta\bar{H}_Q^{(\beta\rightarrow\alpha)}$ and $\Delta\bar{S}_Q^{(\beta\rightarrow\alpha)}$ are the partial desorption enthalpy and desorption entropy of isotope Q in the $\beta \rightarrow \alpha$ phase region, respectively. Values of $\Delta\bar{H}_Q$ and $\Delta\bar{S}_Q$ for hydrogen, deuterium and tritium in palladium and in one palladium - silver alloy $Pd_{0.90}Ag_{0.1}$ are listed in Table 2.59. As can be seen, whereas the two-phase transition enthalpies show a distinct isotope effect, this is less the case for the transition entropies.

Table 2.59: Two phase transition entropies and enthalpies of the Pd-X and $Pd_{0.90}Al_{0.1}$−X systems (X = H, D, T) [Lae85].

Metal – hydrogen isotope	$\Delta\bar{H}_X^{(\beta\longrightarrow\alpha)}$	$\Delta\bar{S}_X^{(\beta\longrightarrow\alpha)}$
	$\mathrm{kJ\,mol}_{X_2}^{-1}$	$\mathrm{J\,mol}_{X_2}^{-1}$
PdH	39.0 ± 0.5	92.4 ± 1.3
PdD	35.4 ± 0.5	93.3 ± 1.3
PdT	32.3 ± 1.1	90.4 ± 3.2
$Pd_{0.90}Ag_{0.1}H$	42.4 ± 1.0	94.7 ± 2.4
$Pd_{0.90}Ag_{0.1}D$	38.9 ± 1.1	95.5 ± 2.9
$Pd_{0.90}Ag_{0.1}T$	35.8 ± 0.9	92.0 ± 2.3

Plateau pressures of H, D and T sorbed by $Pd_{0.90}Ag_{0.10}$, which is the only Pd/Ag composition showing well defined plateau pressures, can be calculated from equations [Lae88]

$$\ln p_H = -\frac{5042}{T} + 18.19\,\mathrm{mbar}$$
$$\ln p_D = -\frac{4731}{T} + 18.53\,\mathrm{mbar}$$
$$\ln p_T = -\frac{4212}{T} + 17.72\,\mathrm{mbar}$$

These expressions are strictly valid only for the temperature range 333 - 433 K. More results on the diffusion and permeation of hydrogen, deuterium and tritium through 75Pd25Ag alloys can be found in publications by Hickman [Hic69], Ackerman and Koskinas [Ack72b; Ack72a], Fujita et al. [Fuj80], Yoshida et al. [Yos85] and Nishikawa et al. [Nis96].

The effect of the annealing temperature on the solubility of hydrogen in the dilute region (α-phase) was investigated for cold-worked Pd−Ag alloys containing from 5 to 40 % Ag [Kis92a]. To this effect, pressure-composition isotherms were determined within the range $273 < T < 348$ K. The magnitude of the solubility enhancement for alloys with the same degree of cold-work was found to decrease with increasing silver content reaching zero at about 40 atom % silver.

Fujita et al. [Fuj80] determined the ratio of permeability's of hydrogen and tritium through a commercial palladium/silver alloy (Pd 80 %, Ag 15 % and Au 5 %) diffuser in the temperature range $623 < T < 823$ K at hydrogen pressures of < 1.3 bar. The permeability ratio observed at

623 K was established to be $P_H/P_T = 2.12 \pm 0.03$, which is clearly larger than $\sqrt{3}$. The P_H/P_T ratio was found to be nearly independent from temperature.

Utilizing a commercial diffuser Yoshida et al [Yos83b] measured permeation coefficients of hydrogen and deuterium across the palladium/silver alloy. The results were described by the following Arrhenius equations

$$P_H = 7.31 \times 10^{-7} \exp\left(-\frac{1370}{RT}\right) \text{ mol cm cm}^{-2} \text{ min}^{-1} \text{ kPa}^{-0.5}$$
$$P_D = 4.78 \times 10^{-7} \exp\left(-\frac{1470}{RT}\right) \text{ mol cm cm}^{-2} \text{ min}^{-1} \text{ kPa}^{-0.5} \ .$$

More recently, Wang et al. [Wan04] noticed that palladium membranes activated at 953 K have larger permeability's and are in addition more resistant to carbon monoxide poisoning than membranes oxidized in situ at 523 K. This is in line with findings by Yoshida et al. [Yos83b], who also provided evidence that the permeability of a diffuser contaminated by oil vapours recovers after baking under air at 713 K for 30 min. The specific permeability found by Yoshida et al. for hydrogen through an air baked diffuser at 0.101 MPa (the pressure used by Wang et al. [Wan04]) was 4.5×10^{-8} mol_H cm s^{-1} cm^{-2}, which is consistent with the results of Wang et al.

Tebus et al. [Teb99] performed at Bochwar All Russia Research Institute of Inorganic Materials (VNIINM) durability tests of palladium-silver alloy specimens at 623 K in the presence of gaseous tritiumum. The specimens were subjected to strain-stress tests after progressively increasing exposure times. Additionally, they were examined by electron microscopy, positron annihilation spectroscopy and X-ray structure analysis. Their results are compiled in Table 2.60. As evident from the data, palladium/silver does not lose its strength properties even after exposure to 0.8 - 0.9 MPa of an equimolar deuterium/tritium mixture over a period covering 3600 hours. The accumulation of helium was estimated under the assumption that no helium was lost to the environment from the solid during the course of the experiment. Results after prolonged exposure provided evidence for the formation of bubbles containing deuterium, tritium, and helium. While the number of bubbles remained essentially constant during the course of the experiment their size showed a tendency to increase. Actually, the average bubble diameter augmented in size from about 1 nm at about 200 appm helium content to about 3 nm at a content of about 500 appm.

Table 2.60: Long-term permeator durability tests under tritium at 623 K (after [Teb99]).

Exposure time hour	He-3 content of alloy appm	He-3 bubble concentration $cm^{-3}10^{16}$	He-3 bubble diam. nm	Lattice parameter change $\Delta a/a$ %	Tensile strength σ_u MPa	0.2 % yield stress $\sigma_{0,2}$ MPa	Elongation Δ %
0	-	-	-	-	730	570	8.2
385	73	-	-	0.07	690	530	19.7
938	205	2.7	2.4	0.05	710	480	22.5
1458	330	2.4	2.8	0.05	710	490	22.5
2003	466	1.8	3.8	0.02	725	510	20.5
3625	840	3.0	3.9	-	730	525	17.0

Lindau et al. [Lin92] implanted helium in palladium-silver tensile specimens at 573 K in order to simulate the helium build-up resulting from beta decay of tritium during long-term steady state operation of diffusors installed in plasma exhaust clean up systems of fusion machines. Implantation lead to the formation of helium bubbles, dislocation loops and stacking fault tetrahedral´s both in the bulk of grains as well as at their boundaries at all helium concentrations investigated. At about 500 appm helium in palladium/silver, the bubbles attained sizes in the range 3.3 - 5.5 nm. At this concentration of helium an increase in ultimate strength and a decrease in total elongation became noticeable. As apparent from data in Table 2.60, Tebus et al. detected bubbles of similar size at approximately the same content of helium-3 in palladium-silver after a test period lasting 3625 hours. Hence, it may be concluded that in spite of the progressive formation of helium-3 bubbles and clusters in the alloy microstructure, no significant detrimental change of the mechanical strength of the permeation membrane takes place under these conditions.

Further confirmation of the durability of palladium/silver permeators subjected to exposure of tritium is provided indirectly by numerous ITER-scale permeators that have been in tritium service without contingencies for numerous years in various tritium laboratories worldwide, e.g. TPL [Kon93; Kon94], TSTA [Wil94b; Wil95c], TLK [Glu97a] and others.

Because diffusers of different designs have been operated in several by and large diverse tritium handling facilities at germane conditions frequently using gas mixtures simulating compositions typical for the plasma exhaust clean-up system and for rather prolonged periods of time, it is fair to say that a vast body of experience is now available on which to base the design of permeators capable of complying with the demanding requirements put forward by ITER.

Dominant palladium isotope 10^5 years after final shutdown is ^{107}Pd with an estimated total activity of 1.8×10^4 Bq [ITE01d].

2.14.8.2 Applications of palladium in tritium technology

Palladium impregnated solid carriers are widely used for the separation of hydrogen isotopes via displacement gas chromatography or for the retention of tritium from gases released into the environment by tritium handling facilities.

Palladium alloys[44] formed to membranes are crucial components of the ITER fusion fuel cycle. Permeators based on palladium/silver membranes are needed for the recovery of unspent fuel from the plasma exhaust gas of a fusion device and to generate a waste gas consisting of fusion ash and impurities with an unprecedented high degree of decontamination from tritium [Bir95; Bir98a; Pen97a; Pen98; Glu00b; Glu01; Glu02b; Glu02a].

Significant amounts of palladium are needed for hydrogen isotope separation systems, the fusion fuel cycle, or tritium retention systems. The amount used in gas chromatographic columns for analytical purposes is only minor.

Palladium has been contemplated for storage and handling of tritium, but high costs and elevated pressure of the hydrides at ambient temperature are considered severe disadvantages for this application.

Zhang et al. [Zha12] investigated the release behaviour of helium-3 from palladium tritide initially containing a tritium/palladium ratio of 0.65 over extended periods of time. Measurements were performed employing either a D-T isotopic exchange technique or metal dissolution with mixture of hydrochloric and nitric acid. According to their observations, fractions of 1.7, 2.1 and 3.3 % are released after ageing periods of 604, 1265 and 2168 days, respectively.

2.14.9 Interaction of hydrogen isotopologues with metals and materials of less common application in tritium facilities

Arrhenius constants of tritium diffusivity and solubility in a number of elements like stainless-steel base metals, ferritic, austenitic construction materials or metals of immediate or marginal interest in fusion technology, which have so far not been discussed in previous sections are compiled in Table 2.61. The temperature ranges in which the experiments were performed are provided in the last column. Two alloys, i.e. **Inconel 600** and **Inconel 625**, utilized as first wall materials of the tokamaks JET, TFTR and JT60-U, are included in the table for comparison. The respective composition of each of these nickel-based alloys is:

i) Inconel 600 consists of Ni 76.0, Cr 15.8, Fe 7.2, Mn 0.2, Si 0.2, Cu 0.10, C 0.04 and S 0.007 weight %, respectively and

[44] Alloying palladium with silver is necessary to increase the resistance of permeation membranes towards embrittlement by hydrogen.

Table 2.61: Compilation of Arrhenius parameters used for the calculation of diffusivities and solubilities of tritium in metals and alloys of minor relevance to fusion (except Be and the alloys). The temperature range of validity is that of the corresponding measurement (after [Rei93b] and references therein).

Material	D_0 $m^2\,s^{-1}$	E_d $kJ\,mol^{-1}$	Temperature range K	K_{s0} at.fr. $Pa^{(0,\,-5)}$	E_s $kJ\,mol^{-1}$	Temperature range K
Be	5.5×10^{-9}	28.4	695 - 775	1×10^{-1}	100	713 - 783
Al	2.7×10^{-6}	37	898 - 1178	1.25×10^{-5}	63.9	893 - 1178
Ti	6.9×10^{-7}	49.1	873 - 1123	1.06×10^{-5}	−42.7	873 - 1123
V	5.6×10^{-8}	9.1	> 250	2.1×10^{-6}	−32.2	> 250
Ni	3.72×10^{-7}	40.2	273 - 1673	5.52×10^{-6}	12.5	273 - 1673
Ni*	2.3×10^{-7}	36	550 - 1030	-	-	-
Cu	0.66×10^{-6}	37.4	470 - 1200	3.70×10^{-5}	55.2	473 - 673
Zr	2.7×10^{-8}	24.9	-	7.7×10^{-6}	−53.5	873 - 1048
Nb	4.4×10^{-8}	12.8	> 250	3.6×10^{-6}	−33.9	-
Mo	1.38×10^{-8}	10.5	833 - 1193	1.13×10^{-4}	65.3	833 - 1193
Ta	3.7×10^{-8}	15.6	> 250	6.2×10^{-4}	−33	-
Inconel 600	2.8×10^{-7}	42.5	873 - 1173	3.46×10^{-6}	14.4	673 - 873
Inconel 625	2.2×10^{-6}	58.1	673 - 873	2.21×10^{-6}	10.6	673 - 873

* [Dol00]

D_0 = maximum diffusion coefficient at infinite temperature

ii) Inconel 625 consists of Ni 61.0, Cr 21.5, Mo 9.0, Nb 3.6, Fe 2.5, Mn 0.25, Si 0.25, Al 0.20, Ti 0.20 C 0.05 and S 0.008 weight %, respectively.

Further information on the permeability's of hydrogen isotopes through a number of pure metals, alloys and glasses are tabulated in reference [Ste83] and on the diffusion of helium and hydrogen isotopes through metals, alloys, oxides, carbides, etc. in reviews by Stickney [Sti72] and Jung [Jun92]. The former provided "recommended best values" for permeation and additionally best values for diffusivity and solubility in tungsten, molybdenum, niobium, and vanadium.

Diffusivities and solubilities of tritium in a number of fusion reactor relevant metals compiled by Reiter et al. [Rei85] have been compared in Appendix F.

2.14.10 Candidate plasma facing first wall materials for fusion machines

A comparison of some relevant properties of candidate armour materials[45] utilized to effectively protect blanket and divertor in the vacuum vessel of a fusion machine from plasmas is provided in Table 2.62. Other more specific but no less important properties are the melting thickness and surface vaporization thickness of these materials during vertical displacement events. A vertical displacement consists of a sudden plasma pressure drop, which usually is the consequence of a disruption. The plasma becomes susceptible to an asymmetric vertical instability and the non-linear evolution of this instability brings plasma of high internal energy in contact with plasma facing components which may lead to considerable wall damage [Mat96]. Melting thicknesses expressed in µm were obtained by calculation assuming a 5 mm copper substrate coated with either 10 mm of beryllium or tungsten. Exposure of such specimens to energy densities of 20 or 60 $MJ\,m^{-2}$ for 100 ms were simulated employing several pertinent computer programs (see Fig. 2.64). As apparent, the melting thickness of beryllium is significantly larger than that of tungsten. This is attributed to the lower melting point of the former. Substantial evaporation and boiling of tungsten have been observed locally at the divertor of TEXTOR in zones which attain peak temperatures of 6000 K when exposed to 20 $MW\,m^{-2}$. This can conduct to considerable erosion either as fine spray or even ejection of droplets [Coe11](see also section 2.14.10). Tungsten spraying was found to depend strongly on the material properties.

[45] Other plasma facing materials either in use or under consideration include boron carbide (B_4C), molybdenum, liquid lithium on top of graphite tiles, or a liquid lithium on tungsten-based solid.

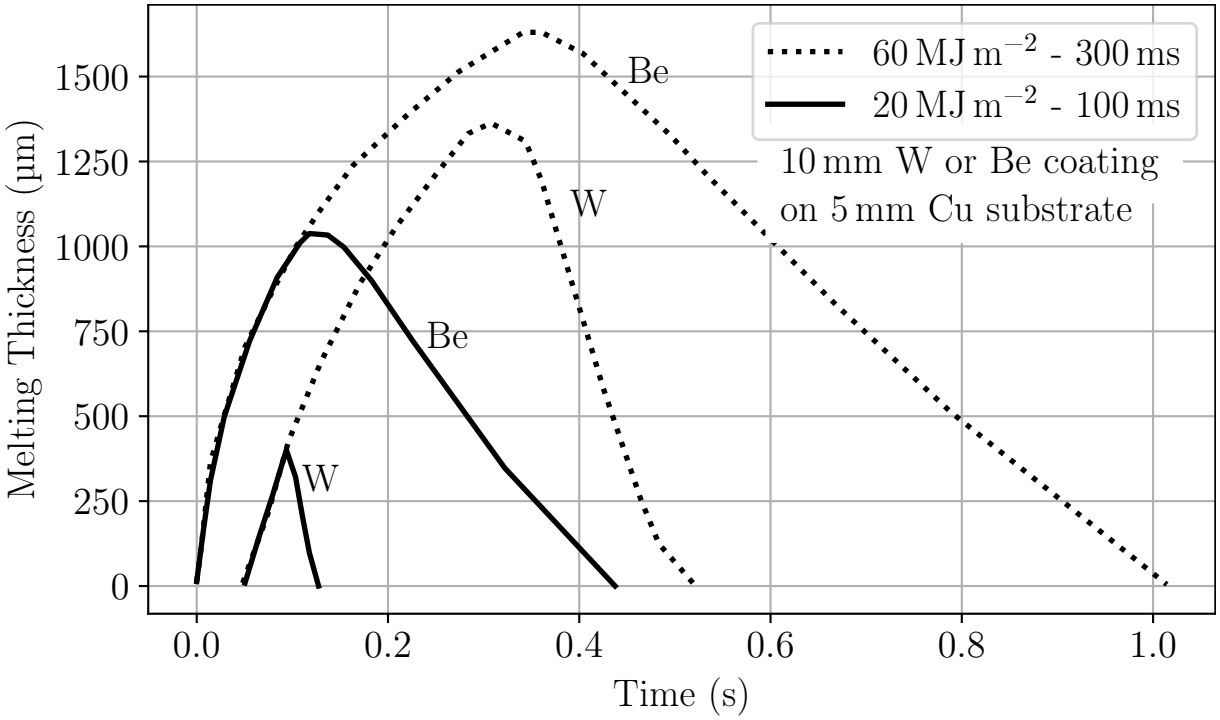


Figure 2.64: Melting thickness of Be and W calculated for vertical displacement events of 20 or 60 MJ m^{-2} 100 or 300 ms duration, respectively [Mat96].

The response of **limiters** to vertical displacement events (VDE) in a fusion device were also investigated by Mattas et al. [Mat96]. Within this frame the surface vaporizations from specimens consisting of a 5 mm thick copper substrate covered with a 10 mm layer of either Be, W or C were calculated assuming a vertical displacement event (VDE) of 60 MJ m^{-2} taking place during 300 ms. The results are displayed in Fig. 2.65. As expected, because of the lower melting point of beryllium, the degree of vaporization of this metal is considerably larger than that of tungsten or carbon.

Estimations of the temperature attained by a 5 mm copper substrate covered by either 10 mm Be, W or C after exposure to a simulated VDE of 60 MJ m^{-2} of 300 ms duration indicate that coverage by beryllium leads to a much smaller temperature rise than coverage by layers of carbon or tungsten. Evidently, high vaporization rates of beryllium consume much of the incident energy leaving only a small fraction to reach the substrate material (see Fig. 2.66).

Perevezentsev et al. [Per17] prepared specimens from representative materials to be employed for the construction of ITER like W, SS16L(n), Be, CuCrZr or three-component divertor segments.

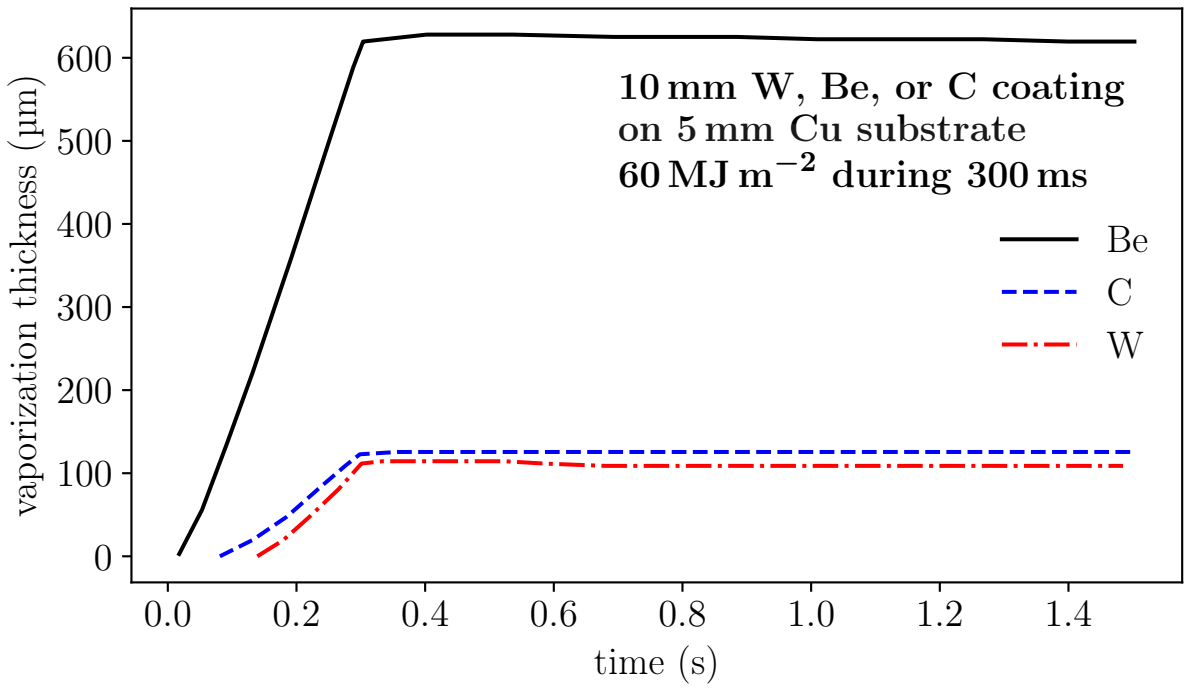


Figure 2.65: Vaporization thickness of Be, W or C calculated as function of time for a VDE event of 60 MJ m^{-2} taking place during 300 ms (after [Mat96]).

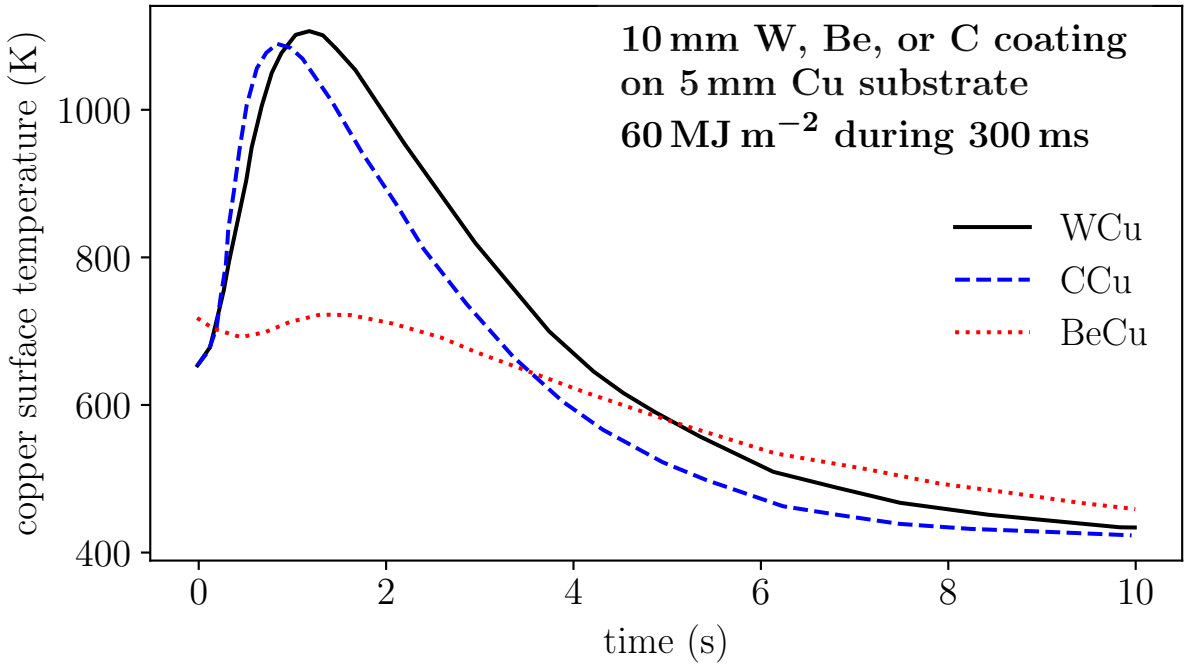


Figure 2.66: Temperature rise of a 5 mm copper substrate protected by either 10 mm thick layers of carbon, beryllium or tungsten during a 60 MJ m^{-2} VDE event lasting for 300 ms [Mat96].

Table 2.62: Comparison of relevant properties of potential armour materials [Mer11]

.

CFC	Beryllium	Tungsten
Long life time, sizable tritium inventory	Very low tritium inventory*	Very low tritium inventory*
Excellent thermal shock resistance	Oxygen gettering capability	Ref. grade: sintered and rolled
Does not melt	Comparatively low melting point	Rather high melting point
Low atomic number	Low atomic number	Intermediate atomic number
Very high thermal conductivity: $< 90\,\mathrm{MW\,m^{-2}}$	Elevated thermal conductivity: $< 20\,\mathrm{MW\,m^{-2}}$	Elevated thermal conductivity: $< 20\,\mathrm{MW\,m^{-2}}$
Very low thermal expansion at 573 K	High thermal expansion at 573 K	Low thermal expansion at 573 K
Significant sputtering	Minimal chemical sputtering	Very low sputtering

* Large difference between the true solubility of tritium and the "apparent solubility" resulting from progressive trapping.

All specimens had nearly the same dimensions[46] They were all loaded with tritium under the same pressure, temperature, and tritium concentration in deuterium (48.3 % T, 50.6 % D, and 1.1 % H) conditions. In systematic screening tests, these researchers compared the HT and HTO outgassing rates from these specimens into static air, static argon, ambient air purge gas, dry air purge gas or argon purge gas containing 5 vol % hydrogen at temperatures covering the range 293 - 323 K. Moreover, outgassing rates were also determined at a constant temperature of 1073 K. The low temperature range was considered representative of interim storage conditions and the high temperature served to estimate the achievable relative degree of decontamination. Measurements with SS316L (N), CuCrZr and W were carried out at purge gas exchange rates covering the range 0.1 - 6.0 $\mathrm{hour^{-1}}$ and those with beryllium with up to 80 $\mathrm{hour^{-1}}$. Main conclusions from their work were:

- At temperatures below 323 K the outgassing rates of tritium from SS316L (N) much exceeded those determined from CuCrZr, W or Be under all investigated conditions.

[46] Dimensions of the specimens: 20 mm width, 20 mm length, and 26 mm thickness.

- Whereas stainless-steel and CuCrZr can be decontaminated to more than 95 % by heating over 24 hours at 1073 K, the maximum achievable under the same experimental conditions with W or Be was only about 50 %.

- Exposure of specimens to about 0.05 MPa DT at 473 K for 24 hours revealed that while the rate of tritium uptake by SS316L (N) and copper alloy are comparable, those of tungsten and even more so of beryllium are significantly slower. Similar inventories were attained in copper and beryllium as well as in stainless-steel and tungsten. The highest tritium uptake rate and tritium inventory was observed in exposed metal cuttings obtained from pristine JET divertor material comprising the components tungsten, interfacial CuCrZr and stainless-steel SS316L (N).

- The outgassing rates from three-component divertor segments (1.9×10^5 Bq hour^{-1} cm^{-2}) were found to be substantially higher than the rates determined with single component materials (140 - 1380 Bq hour^{-1} cm^{-2}).

- Tritium is released from all investigated materials predominantly as HTO and to a much lesser extent as HT.

Krishna et al. [Kri12] synthezized hot rolled and annealed **CuCrZrTi** alloy in an attempt to improve the high heat flux conduction and strength properties of CuCrZr in view of the application of this material in fusion machines. One consequence of the addition of titanium to CuCrZr was further supression of the dynamic embrittlement. Titanium therefore exercises the same role in the alloy as zirconium, i.e. fixing sulphur as sulphide. The thermal conductivity of the alloy obtained from the product of specific heat, thermal diffusivity, and density was found to increase with temperature. The observed thermal conductivity increases of about 20 % from 279 W mK^{-1} at 300 K up to 379 W mK^{-1} at 873 K were explained by a kind of ageing process resulting from precipitation of excess solute. High temperatures were selected for these experiments to simulate first wall conditions in fusion devices.

POCO AXF-5Q graphite (TFTR) and carbon fibre composite (CFC) (JET) were initially tested as first wall armour materials of tokamak fusion machines to protect blanket, vacuum vessel and divertor from energetic plasma particles and high heat fluxes [Ski00; Coa06]. The same materials were also employed by JET and TFTR in campaigns carried out for the first time with

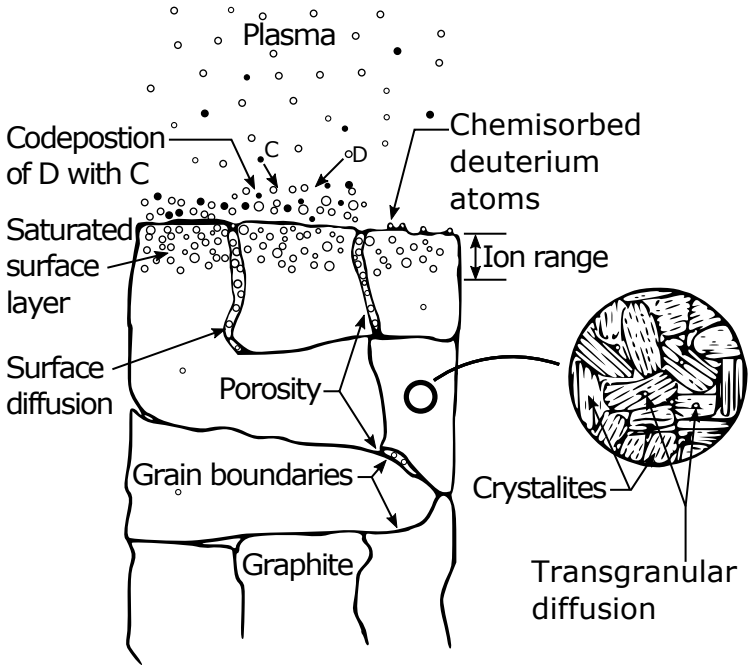


Figure 2.67: Primary mechanisms describing the interaction of energetic hydrogen particles generated in a plasma with carbon-based materials (after [Haa05]).

DT fuel. For transport, trapping and retention of energetic hydrogen (or tritium/deuterium) particles generated in plasmas in **carbon-based materials** four mechanisms can be distinguished (see Fig. 2.67) [Haa05]:

- Carbon-based material exposed to energetic hydrogen isotopologue ions generated in plasmas will first produce a saturated surface layer within the depth range of penetration of the ions.
- Sequestration of hydrogen isotopologues by co-deposition with carbon will take place concurrently on the material surface.
- Following saturation of the implantation zone, some of the mobile hydrogen isotopologue atoms will diffuse deeper into the bulk, primarily along the internal porous surfaces and grain boundaries.
- At elevated temperature a hydrogen isotopologue fraction will diffuse transgranularly deep into the bulk across the graphite lattice.

Relevant information on the **migration of first wall material** were obtained at JET while the machine was operated with a CFC plasma-facing component covered with a thin layer of beryllium applied once per operation week [Coa06]. Experiments employing tracer techniques, e.g. ^{13}C labelled methane and tiles coated with a low-Z and a high-Z marker layer, revealed significant asymmetry in the distribution of fuel and plasma impurity species between the inner (net deposition area) and the outer (net erosion) area of divertor channels. Within this frame, a layer rich in metallic species, i.e. Be\C ≈ 1, was found to deposit on the inner divertor wall tiles. On the other hand, deposition of highly hydrogenated carbon films in the Gas-Box divertor region was found to be only minor.

Another consequence of plasma-CFC interaction is the formation of high molecular weight hydrocarbons. Such species were for instance observed mass spectrometrically in the gas released when cryopumps evacuating the divertor zone of JET were warmed up[47]. The evolution of the m/e peaks of the released gases as the temperature was gradually increased points to the presence of several progressively less-volatile hydrocarbons.

A complicating issue occurring in machines operating with two or more different plasma-facing components is that flakes, dust and other debris may consist of co-deposits having a complex chemical composition as well as ill-defined tritium content. Species may occur such as i) **tungsten** and **carbon** of composition W_2C and WC and containing more than 60 % hydrogen isotopologues, ii) combinations of **beryllium** and **carbon** possibly present as a thin protective layer of Be_2C on the plasma-exposed carbon surface eventually generated by interaction of carbon with beryllium-containing plasma [Doe04; Doe07] or iii) **beryllium** and **tungsten** deposits of composition Be_2W, $Be_{12}W$ or $Be_{22}W$. These compounds have all melting points lower than that of pure W.

The retention of deuterium in self-damaged tungsten was the subject of an investigation by Tyburska et al. [Tyb09]. They exposed polycrystalline tungsten samples either directly to deuterium ions or to deuterium ions after pre-irradiation with 5.5 MeV W^{+2} ions to damage levels within the range 0.04 - 1.2 dpa with and without annealing at 1200 K for2 hours. A comparison of surface and subsurface morphology as well as of deuterium retention in pre-damaged as well as un-damaged specimens revealed an increase in radiation-induced traps with increasing dpa

[47] G. Saibene, A. Rossi, Composition of the gas released from the divertor cryopump during full warm up (LN loop), Memorandum March 10th, 1997

but deuterium retention saturation at about 0.4 dpa. According to their results, the deuterium concentration in the sub-surface region was independent from the deuterium implantation fluency. Because the detrapping temperature of deuterium from radiation-induced traps in tungsten monoblock´s is higher than 600 K, under certain conditions tungsten monoblock´s may constitute efficient tritium sinks. To study trapping of diffusing deuterium, tungsten specimens were damaged up to a depth of 2.2 µm to a level of 0.3 dpa at the rear of 25 and 500 µm thick 10 x 10 mm^2 [Tyb11]. The front side of these specimens were then exposed to deuterium plasma at elevated temperature. The results delivered information on the rate of deuterium diffusion under the prevailing conditions and showed that deuterium is retained in the traps at the rear of the specimen. Maximal implantation took place at 460 K and decreased as the temperature was further raised because of increasing thermal de-trapping.

In situ doping of carbon with beryllium (Be_2C layer) was found to reduce the chemical erosion behaviour, increase the hydrogen isotopologue retention and decrease the release temperature of the trapped species [Bal06; Doe07].

In the following the **tritium (or deuterium) inventories** measured/calculated in various research fusion machines at different operational stages are discussed.

The cumulative inventory of tritium in plasma-facing carbon components generated by the D-D reaction in the **JT-60U** machine after 5 years of operation was estimated to be 16.0 GBq [Mas96]. The inventory increased up to 170 GBq after 16 years of operation.

The deuterium isotope inventory in the **ASDEX-Upgrade** machine of 1.3 - 1.7 g was trapped in carbon/boron co-deposits on the divertor as well as in some remote areas during the carbon dominated campaigns. This inventory decreased down to 0.14 - 0.22 g during the full tungsten machine [May09]. Schleußner et al. [Sch99a] estimated the deuterium inventory remaining in the tungsten-coated divertor[48] and first wall of ASDEX-Upgrade via a deuterium material balance. According to them, the cumulative amount of deuterium introduced into the machine during the whole tungsten phase by gas puffing and neutral beam injection was 7.7×10^{24} atoms. Of this amount, 1×10^{23} (1.3 %) were retained in the tungsten divertor tiles, 0.5×10^{23} (0.7 %) in graphite tiles, and the rest, i.e 1.5×10^{23} (2.0 %), in the first wall.

[48] The tiles consisted of a graphite substrate with a 500 µm thick plasma-sprayed tungsten layer on the plasma-exposed surface.

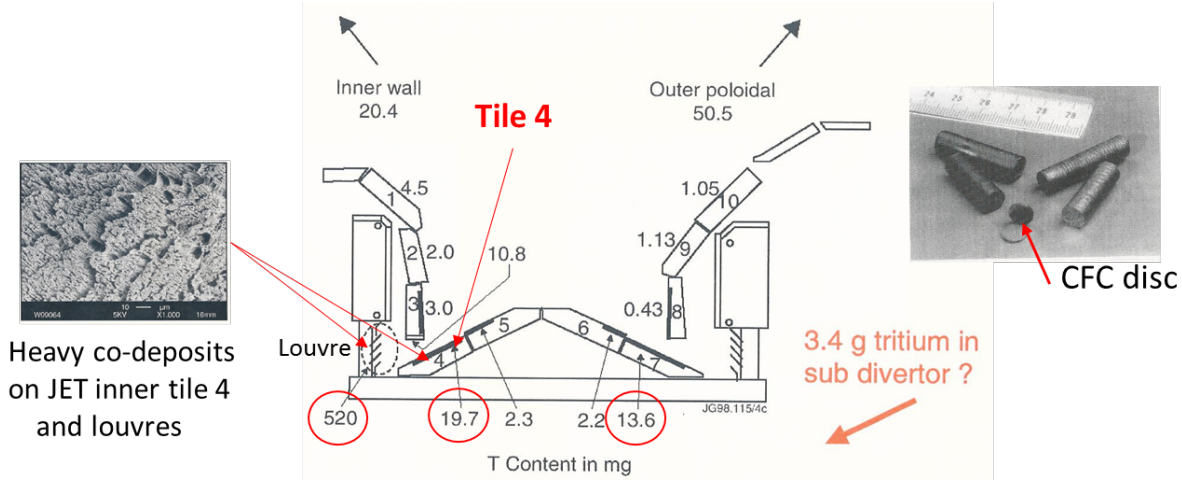


Figure 2.68: Toroidal distribution of tritium (in mg) in the divertor of JET. The divertor cross section shows heavy carbon-tritium co-deposition on inner tiles 4 and outer tiles 7 and, additionally, a particularly heavy co-deposition on the inner louvres. Much tritium-contaminated dust, flakes and other debris was detected in the subdivertor region. The insert on the left shows heavy deposits on tile and louvres and that on the right cylinders cut from tiles with a hollow drill together with one of numerous disks obtained from each cylinder [Pen00c; Pen00b].

To assess the tritium inventory of **JET** after completion of the DT1 campaign, ten divertor tiles were removed from the machine and replaced by pristine ones. A number of cylinders were then cut from these tiles at strategic positions utilizing a hollow drill (see Fig. 2.68). Subsequently, a large number of disks were cut from each cylinder and the tritium concentration in each disk determined employing a liquid scintillation counting technique [Pen00b]. By this procedure tritium concentrations i) on the plasma-exposed surface of the tile, ii) on the plasma-shadowed side of the tile (back side) and iii) in the bulk of the tile were obtained. The data delivered the approximate concentration distribution on both sides of each tile as well as a fairly resolved tritium depth profile. Based on the toroidal results of the ten tiles it was possible to estimate the poloidal inventory of tritium in the complete divertor of the machine employing a straight forward integration procedure. Total inventories of tritium in the machine were obtained from the difference between the total amount of tritium injected into and that retrieved from the machine. Similar procedures were used to estimate tritium inventories in TFTR [Ski00]. As already mentioned, very substantial quantities of tritium were found as solid carbon-tritium co-deposits in both machines. Their quantitative recovery is considered to be quite challenging.

It is interesting to compare the inventories of tritium in TFTR (graphite first wall) and JET (CFC first wall) during various phases of extended campaigns with DT fuel [Ski00]:

TFTR: The amount of tritium injected over three consecutive periods covering an interval of 3.5 year was 3.1 g via NBI and 2.1 g by gas puffing. Of this tritium, about 90 % was retained initially via wall saturation and isotope exchange. The amount of tritium remaining in the torus was estimated to be 0.85 g and the long-term retention calculated to be 12 %. The plasma interacted mainly with the bumper limiter.

JET: The amount of tritium injected into the machine over a six months period (DT1 campaign) was 0.6 g by neutral beam injection and 34.4 g by gas puffing. Of this tritium, about 40 % was retained initially by wall saturation and isotope exchange. The amount of tritium remaining in the torus was estimated to be 4.2 g and the long-term retention calculated to be 16 %. Carbon was eroded in the main chamber and chemically sputtered in the divertor. It migrated into cool plasma-shadowed areas forming thick deposits of high T/C ratios (see Fig. 2.68).

One reason for the selection of carbon as first wall material was its rather small Z value which makes it less detrimental to plasmas than other first wall materials. In spite of this and other beneficial properties, numerous campaigns without and with tritium lead to the conclusion that carbon is non-acceptable for a DT power reactor because of the rapidly increasing tritium inventory with progressing operation time [Pen00c; Pen00b; Coa01; Pen01d; Pen01e; Pen01c; Tan01b; Bek03; May07; Rot08]. Aggravating was the fact, that highly tritium-contaminated flakes (see Appendix G), dust and other debris accumulated in **inaccesible zones** like the subdivertor region, the space between tiles (see Appendix H[49]) or even the vacuum ducts [Fra99; Car00]. This tritium as well as that accruing in the bulk of the first wall was found to be very difficult to retrieve [Ski00]. On one hand, bulk heating of plasma-facing components would require unrealistic high temperatures and on the other, all alternative techniques available at the time were considered to be too slow or required vessel entry [Rot08].

Roth et al. [Rot08] compared several plasmas facing material combinations from the point of view of tritium inventory build-up as function of operation time. The upper inventory limit for tritium in the machine was fixed at 700 g. Once this limit is approached, retrieval of fuel from the

[49] Measurements carried out at TLK with the PIN diode method of the tritium concentration on six surfaces of a tile obtained from JET after the DTE1 campaign displaying substantial activities on one side of the tile. This activity is presumably due to erosion and transport of the plasma-exposed surface.

first wall would become compulsory. As apparent from Fig. 2.69, two options, i.e. all carbon or beryllium first wall and carbon/tungsten for the divertor, lead to the maximal allowable tritium inventory in a rather short operation time. Only the combinations beryllium first wall with a tungsten divertor (700 g level attained within 1500 to 5000 discharges) or metallic tungsten as the only plasma-facing material (> 18000 discharges) constitute acceptable solutions. In agreement with the prediction for a Be/W-wall, a modell calculation for ITER based on results obtained during the JET-ILW (ITER-like Wall) campaigns indicates that the fuel inventory limit is reached after 3000 or more DT-discharges [Bre15]. The longer possible period of operation without surpassing the inventory limit is ascribed to the smaller long-term fuel retention observed when an all carbon first wall is replaced by fully metallic plasma facing components. It should be noted, that progressing radiation damage of tungsten from the divertor may conduct to enhanced bulk retention of tritium and consequently to a sizeable reduction in the number of acceptable discharges.

As observed not only in JET but also in TFTR during their respective DT – campaign´s, the far too high steady state first wall erosion of carbon plasma-facing components is associated with a fairly rapidly growing fuel-carbon co-deposition. A reason for the difference in erosion behaviour is that whereas for beryllium there is an energetic threshold for physical sputtering, in case of carbon and carbon layers erosion does also take place with low energy neutrals and at ambient temperature. Furthermore, even though beryllium forms layers containing co-deposited fuel, the amount codeposited is lower than that typical for carbon layers. Moreover, measurements and calculations indicated that the tritium activity immobilized in tiles was much lower than that remaining in the JET machine as obtained from a balance between the amounts of tritium introduced and that recovered. Therefore, it appears that a large fraction of tritium is incorporated into something like a kilogram of flakes and dust such as spotted with an endoscope on flat horizontal surfaces in the subdivertor region and the louvres (see Appendix G). In the end, it was erosion and deposition that motivated the ITER-Team to replace all first wall carbon tiles by beryllium tiles and to substitute the comparatively small amounts of carbon initially contemplated for the strike point zone of the divertor by tungsten [Hir16]. Because of the high temperatures at the divertor strike point and the low ion fluxes reaching the wall of the vacuum vessel, the contribution to the tritium inventory of beryllium and tungsten at these zones is expected to be small. The main tritium inventory build-up is predicted to occur at zones of the

divertor exposed to intermediate fluxes (2×10^{23} (D+T)/m^{2}s) and maintained at intermediate temperatures (≈ 725 K).

Influence of armour material on tritium breeding ratio: Sato and Nishitani [Sat03] examined the influence of plasma-facing armour materials like tungsten and beryllium on the tritium breeding ratio (TBR) of a fusion reactor blanket. From Monte Carlo calculations of the neutron transport they concluded that for blankets containing no neutron multiplier the installation of a tungsten armour would increase the TBR. Conversely, with blankets containing neutron multiplier the introduction of a tungsten armour would bring about a decrease of the TBR. Furthermore, from the point of view of tritium breeding ratio optimization, the thinner the tungsten armour the smaller the TBR reduction. Another conclusion from the calculations was that the decrease in TBR arising from the introduction of a tungsten armour can be mitigated by increasing the ^{6}Li enrichment of lithium oxide in the blanket. In view that the thermal neutron flux behind beryllium armour is higher than behind a tungsten armour the inclusion of a beryllium armour would increase the TBR. These conclusions make evident that there is still much uncertainty as to the best configuration of the plasma facing armour –breeder blanket arrangement. Therefore, the investigators recommended critical reexamination of the effect of i) type of armour material, ii) thickness of armour material, iii) degree of lithium-6 enrichment of the breeder material, and v) presence of neutron multiplier in the blanket on the achievable TBR.

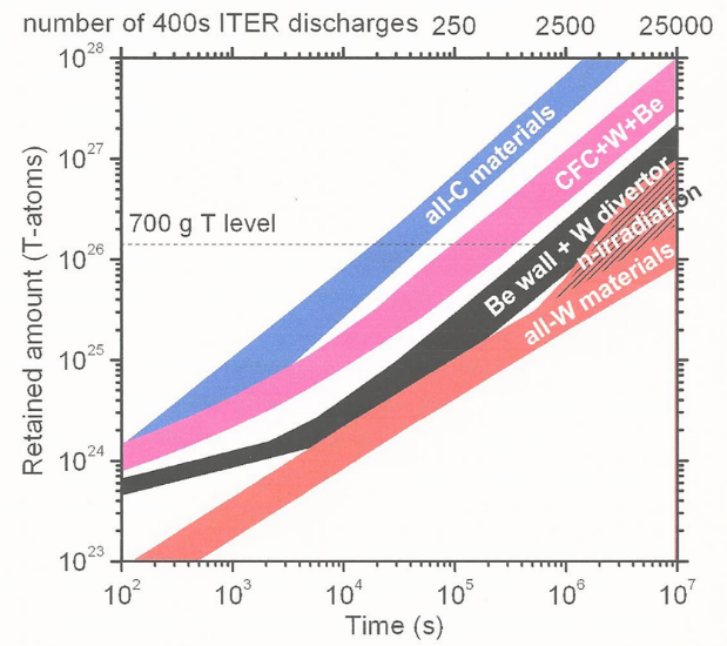


Figure 2.69: Tritium inventory increase as function of operation time calculated for ITER assuming several plasma-facing component combinations (the maximal tolerable inventory of tritium in the tokamak was taken to be 700 g)[Rot08].

2.14.11 Interaction of tritium with alumina

The properties of aluminium oxide are of particular interest for the development of barriers against the permeation of tritium through structural materials.Aluminium oxide also constitutes a good catalyst support for many industrial catalysts.It is also used as electrical insulator or as carrier for gas chromatographic analytical or isotope separation columns. In another application, low permeation alumina ceramic vessels have been used to contain and heat uranium getter powder or other getter materials up to temperatures in the range 773 - 973 K. With two ceramic vessels it was possible to purify hydrogen isotopologues diluted in an inert gas from tritium-bearing species at medium temperature in the first one and from other non-radioactive impurities at high temperatures with the second one [Hut86; Nef89; Kha15].

According to Roy and Coble [Roy67] the solubility of hydrogen in aluminum oxide is given by relationship

$$\ln X = -2.28 \pm 0.50 - \left[\frac{8024}{T} \pm 1500\right]$$

where X represents the H/Al atomic ratio and T stands for the absolute temperature. Riehm et al. [Rie86] recommended the equation

$$S = 11 \times 10^{21} \exp\left(-\frac{32.2\,\mathrm{kcal\,mol^{-1}}}{RT}\right)\ \mathrm{H\ atoms\,cm^{-3}\,Pa^{-0.5}}$$

for the same gas-solid system. A further experimental study on the solubility of hydrogen in Al_2O_3 powder in the temperature range 973 - 1173 K yielded the relationship [Ell78b]

$$S = 5.9 \times 10^{20} \exp\left(\frac{18.1\,\mathrm{kcal\,mol^{-1}}}{RT}\right)\ \mathrm{H\ atoms\,g^{-1}\,atom^{-1}}\ .$$

Diffusion coefficients of tritium across sintered and single crystal Al_2O_3 can be calculated as function of temperature within the temperature range 873 - 1173 K from equations [Fow76; Fow77; Ell78b]

$$D = 7.35 \times 10^{-2} \exp\left(-\frac{183.5\,\mathrm{kJ\,mol^{-1}}}{RT}\right)\ \mathrm{cm^2\,s^{-1}} \quad \text{(sintered)}$$
$$D = 3.26 \exp\left(-\frac{239.7\,\mathrm{kJ\,mol^{-1}}}{RT}\right)\ \mathrm{cm^2\,s^{-1}} \quad \text{(single crystal)}$$

Roberts et al. [Rob79] determined the permeability of hydrogen across high density, high purity and sintered aluminum oxide with tritium as tracer at temperatures in the ranges 1473 - 1723 K and pressures within the range 2 - 50 kPa. Temperature and pressure dependence of the permeability can be calculated from expression

$$P = \exp 48.95 \pm 0.61 \exp\left(-\frac{318.2 \pm 18.8}{RT}\right)\ \mathrm{kJ\,g^{-1}\,atom^{-1}}$$

in which P is given in units of $\mathrm{H\,atoms\,cm^{-1}\,s^{-1}\,kPa^{-0.43}}$.

Diffusivities, permeability's, and solubilities of hydrogen in aluminium oxide are compared with corresponding values determined for ceramic materials like SiC, BeO, B_4C and hot pressed Y_2O_3 in a review published by Riehm [Rie86].

2.14.12 Some fundamental aspects on the interaction of atomic hydrogen, molecular hydrogen or water with metals and oxide surfaces

Christmann [Chr88] extensively reviewed the kinetics and thermodynamics of the chemisorptive and physisorptive behaviour of atomic and molecular hydrogen interacting with solid surfaces. Characteristic to hydrogen adsorption is the high mobility of the atoms even at low temperature leading to something like a "hydrogen fog" rather than to an ordered phase. It is also for this reason that the activation energy for surface diffusion is rather small. High mobility at high temperatures is of considerably importance to heterogeneous catalysis. Substantial progress has been achieved in the area of hydrogen – surface interaction specially with respect to understanding the bonding process. The greatly improved experimental database now available is largely attributable to increasingly sophisticated spectroscopic techniques.

Thiel and Madey [Thi87] published one more rather comprehensive review on fundamental aspects concerning the interaction of water with solid surfaces of metals and their oxides. In this review, emphasis is placed on factors affecting the dissociative and associative adsorption of water on numerous well characterized metal and oxide surfaces at low coverages. The effect of extraneous atoms on the surface and imperfections of the surface on the surface chemistry of H_2O is discussed in much detail. Water, when adsorbing molecularly, shows a tendency to form three-dimensional hydrogen-bonded clusters. The so called "template effect" of the substrate determines the local orientation and long-range order of the molecules constituting these clusters. Supplementary subjects addressed in the review are the kinetics of adsorption and diffusion, strength of the water – metal bond´s, chemisorption on rough and smooth surfaces, kinetic barriers, adsorption on non-metallic surfaces, etc.

3 Basic design principles for the installation of tritium systems, typical small and large components, and key processes employed in tritium handling facilities

This chapter is dedicated to the basic design principles of tritium handling facilities, describes a number of typical small and major components, and discusses as well as evaluates many of the principal processes utilized in research and technical facilities worldwide. When appropriate, problems that manifested during the operation of equipment or while running whole processes are highlighted and the adopted solutions outlined. Employed components comprise overwhelmingly standard commercial equipment frequently modified and adapted to the requirements of a tritium environment.

A few basic principles concerning the design of systems destined to handling sizable amounts of tritium are gathered below[Int91; US 73; US 08; Poo08]:

- When tritium is handled in more than trace amounts maximum usage of glove boxes is recommended as part of a multiple barrier concept whose objective is to fully isolate tritium from the environment. While glove boxes take up considerable laboratory volume they are, on the other hand, of great benefit for the safe performance of limited or routine operations, maintenance activities, calibrations, visual and physical accessibility of components requiring repairs or replacements, etc. Additionally, they constitute an effective transitory barrier in case of an unexpected spill from a primary system. The various barriers, i.e. building, glove box, primary containment, etc. are separated from each

other by controlled pressure steps, each pressure decreasing from that of the environment down to the primary system by values in the low mbar range.

- Pressures in primary systems are normally kept below 1 bar.
- Traces of tritium released into glove boxes must be continuously removed employing either a dedicated tritium retention system or a central retention system common to several isolated glove boxes or combination of glove boxes.
- The release into the environment of tritium-bearing gases discharged from primary systems or from glove box atmospheres is only permitted after thorough recovery of tritium via a dedicated properly designed tritium retention process. At large installations, all exhaust gases can be released into the environment after passing through a Central Detritiation System. Gases exhausted from an Isotope Separation System or a Water Detritiation System shall be re-cycled.
- The utilization of a portable ventilation duct ("elephant trunk") has proven to be of invaluable benefit during maintenance, repair, upgrading, or replacement operations inside or in front of an open glove box.
- Ease of process maintenance shall be incorporated into the design of tritium systems from the very beginning.
- All minor components like valves, needle valves, flow meters, ionization chambers, etc. requiring occasional or frequent manual operation shall be easily accessible via the gloves of glove boxes and their status, i.e. open/closed, on/off, scale, etc. clearly recognizable from outside of the glove box.
- All major components installed in glove boxes that may necessitate occasional or frequent maintenance or replacement shall be easily accessible. Provisions shall be taken to allow repairs and maintenance operations without the need of glove box opening. When possible, equipment in glove boxes should be maintainable with tools that fit into pass boxes or across glove ports. Ideally, process repairs should be possible on one system while continuing the operation of other.

- High-vacuum fittings with demountable metal gaskets that do not require axial clearance for assembly/disassembly are especially convenient, as connected components are removable without disturbing the alignment of connecting tubing.

- In order to minimize tritium contamination, an adequate repair strategy should contemplate an option for pumping and purging of various piping sections of tritium primary equipment and a double valve system for components that may require replacement. The eventual replacement of components normally operating while enclosing a significant inventory of tritium should be planned well in advance considering weight and spatial configuration of the component, the replacement trajectory, the accessibility to perform connections and need for alignment, etc.

- Standardized equipment should be used whenever possible in order to minimize down time during repair activities and reduce spare part warehousing.

- Already available and tested designs should be preferred over new ones provided they are technically acceptable and fitting.

- To prevent human errors, appropriate measures at the endpoints of primary systems, e.g. double valves, pressure sensors, caps shall be taken.

- Double valves on both ends and a purge gas line or a vacuum option for the space between them shall be implemented for all components that may require replacement or frequent maintenance in order to permit isolation of the component from the process during line breaks. Of these two valves the one at the end shall be operated manually and be all metal sealed.

- Filters should not be installed in a permanent way, e.g. welded, unless safety considerations demand a high containment level.

- A multiple barrier concept between tritium primary systems and cooling or heating systems consisting of independent closed loops inter connected via heat exchangers shall assure proper isolation of tritium from the environment (ground water, sewage water, or atmosphere of the building). Accordingly, contamination of the secondary cooling or secondary heating system by tritium should only become noticeable after very prolonged time. Regular control

of the tritium levels in the secondary cooling or heating systems is mandatory (for more details see section 3.6).

- All components in glove boxes shall be fixed securely and strongly to avoid material fatigue by vibrations, opening of connections by torsion, or displacement of heavy components.
- Redundancy and diversity of all safety relevant components is necessary to comply with high safety standards.
- To exclude material stress conditions like temperature or pressure excursions, automatic shutdown procedures shall be installed.
- Vessels or other components requiring protection against overpressure shall be provided with vacuum-tight rupture disks or membranes that in the event of a pressure excursion allow expansion of gas into previously evacuated vessels or - in exceptional cases - into a Central Tritium Retention System. Relief valves are considered unacceptable because of possible tritium leaks across the valve seat seals.
- Welded joints shall be preferred over replaceable joints in primary tritium systems. If replaceable joints are compulsory, only ultra-high vacuum-tight fittings, e.g. Cajon fittings, utilizing metallic gaskets shall be permitted.
- Every primary tritium system shall undergo helium leak tests before being taken into operation. Primary equipment used for the containment of tritium shall comply with very high leak-tightness standards, e.g. total leak rate of single items $< 10^{-8}\,\mathrm{mbar\,l\,s^{-1}}$ and of systems or subassemblies $< 10^{-7}\,\mathrm{mbar\,l\,s^{-1}}$, respectively.
- Inner surfaces of calibrated tanks as well as of their associated piping should be refined, i.e. passivated by appropriate surface treatments.
- Stainless-steel type SS316L (L = low carbon, see also Appendix I) shall be preferred over stainless-steel type SS316 or SS304 because of the ability of tritium to leach carbon from the metal surface (formation of tritium-labelled hydrocarbons).
- Large inventories of tritium not immediately required for operation purposes shall be stored preferably in pressure-less form, e.g.metal tritide.

- Reliable and recurrent preventive technical and administrative measures shall be taken to exclude at all times possible formation of explosive mixtures when handling and processing tritium.
- Safety concepts and preventive measures shall be re-assessed thoroughly and frequently on a regular basis.

3.1 Materials and chemicals

Materials used for containment and processing of hydrogen isotopes must be of high standard incorporating measures necessary to adress all special effects resulting from the presence of radioactive tritium. When sizable amounts of tritium are being handled, especially under conditions of increased temperature, an evaluation of the contribution and consequences of permeation, dissolution, adsorption, desorption, radiolytical and/or chemical reactions, radiation-induced corrosion, pressurization by helium or radiolysis gas production, hydrogen embrittlement or any other degrading phenomena, etc. need to be assessed.

This section mostly focusses on materials that have already been identified as being suitable for utilization in tritium technology systems and bank on a vast body of relevant practical experience.

3.1.1 Stainless-steel

Materials commonly used for the manufacture of commercial high and ultrahigh vacuum-tight components like vessels, valves, flanges, sensors, pumps, analytical instrumentation, piping's, etc. are austenitic stainless-steels **type SS304, SS304L, SS316, SS316L** and **SS347** (L = low carbon). Modern arc-re-melted steels are considered a good choice because of their low impurity levels and therefore fewer inclusions that could promote hydrogen induced cracking eventually leading to leak paths. For a list of standardized steels ordinarily employed in tritium handling facilities and their respective composition consult Appendices I - K.

Recommended construction materials for vessels destined to tritium service are austenitic (face-centred-cubic) stainless-steel AISI **type SS316L** and **type SS304L**. Major advantage of low carbon steels are their comparatively high resistance to any effects induced by hydrogen on their mechanical properties, particularly loss of tensile ductility or hydrogen stress cracking [Ell80]. Both steels are characterized by good strength, excellent resistance towards corrosion and hydrogen embrittlement, good weldability, minor weld sensitization and therefore few inclusions by impurity particles like oxides or carbides [Chr73]. Because of their low carbon content, they display little tendency to the formation of tritium-labelled hydrocarbons when exposed to gaseous tritium. The exceptional robustness of SS316 stainless-steel has been validated in experiments with tritium at very high pressures [Cof73].

Tanaka et al. [Tan09] investigated the brittle-ductile transition (BDT) of low carbon steel plastically deformed by an incremental roll-bonding process in order to obtain fine grained specimens. Fracture toughness was determined by four-point bending tests of specimens at several temperatures and strain rates. The results revealed that specimen deformation caused fracture toughness increase and BDT temperature decrease. The observed increase in fracture toughness at low temperatures and the decrease in BDT temperature was explained in terms of grain boundaries and their refinement. The role of grain boundaries on BDT events were evaluated by molecular dynamic calculations.

Because tritium leakage has been observed in stainless-steel having poorly oriented stringers and inclusions, wrought materials are generally preferred to cast. Reason for this is that wrought materials display a more homogeneous micro structure. Specification of the forging direction of wrought components can be such that the orientation of inclusions is not in the possible tritium leak path direction. Surface treated stainless-steel, for instance mechanically polished or subjected to electro-polishing, initially displays a rapid oxidation that quickly drops to zero after formation of a very thin protective oxide film.

Worldwide much valuable, mostly positive experience has accumulated over the past decades with equipment manufactured from type SS316 stainless-steels in facilities handling small and large amounts of tritium also in the presence of other sometimes very reactive chemicals ([Bil73; Chr73; Cof73; And75; And88; Nar90; Lae99b; US 73, and other]). This experience has merged into a rather broad data base on the properties of this material. The same holds for their performance under irradiation, such as acquired during the operation of fission reactors. In short, the principal reasons for preferring **SS316L** in tritium handling facilities over other materials are its i) high stability, ii) good welding properties, iii) resistance to hydrogen embrittlement, iv) resistance towards gross martensitic transformation during thermal cycling or when subject to plastic strain at cryogenic temperatures, and last not least v) the overwhelmingly satisfactory practical experience gained in numerous installations routinely handling tritium.

Takai et al. [Tak08a] carried out a comprehensive study on the enhancement of the degradation of **Inconel 625** and iron by hydrogen. In tensile tests it was noticed that hydrogen boosts the strain-induced formation and agglomeration of vacancies, which are known to promote fracture processes. A high density of agglomerating vacancies will lead to formation of microvoids that favour crack growth. Experimental evidence was obtained employing specimens subjected to a

broad spectrum of test parameters including tensile testing under such different pre-treatment procedures as alternating unloading and reloading with and without hydrogen charging, ageing at ambient temperature or annealing at 473 K with the objective of releasing hydrogen and healing strain-induced defects (see also Fig. 2.60). The hydrogen absorption capacity increased by the hydrogen-enhanced creation of stain-induced defects and decreased by annealing at 473 K to the original capacity. Thermal desorption analysis of hydrogen was used to evaluate strain-induced defects constituting trapping sites for hydrogen. The results provided direct evidence for hydrogen-related failures of Inconel 625 and iron promoted primarily by vacancies rather than by hydrogen itself. This observation agrees well with the hydrogen enhanced strain-induced vacancy model.

In some older tritium handling facilities like TSTA, USA [And82] and Chalk River, Canada [Bok90; Ryl16] valves, pipes, fittings, expansion volumes, and manifolds were manufactured of type 300 series stainless-steels. At Chalk River the primary system of uranium storage beds was manufactured from stainless-steel type SS316L and the outer mantle from type SS304.

Type SS310 is a stainless-steel whose salient feature is good resistance towards oxidation. Even though this material is far more stable than SS304L, it is not recommended in many applications because of weld cracking problems and potential formation of brittle sigma phase [Chr73]. SS310 may, however, be considered for applications at elevated temperature when oxidation is of concern. In comparison to type SS316 stainless-steel, type SS310 has inferior creep resistance but is more resistant to oxidation.

Because of the relatively low concentration of austenite stabilizing elements, e.g. Ni, Mn, N, and C, in **type 304L** this material is not recommended under conditions of high hydrogen pressure or cryogenic temperatures. As with SS316L, low carbon content constitutes an important positive feature of SS304L because of reduced probability of hydrocarbon formation in a strong tritium environment.

High carbon grade stainless-steels **type 347H** or **type 316H** (carbon content within the range 0.04 - 0.10 %) are characterized by excellent mechanical properties. They have been employed for the confinement of tritium in components requiring strength at high temperature. Surface carbon in confinement components may, however, be detrimental because of possible formation of tritiated hydrocarbons even at ambient temperature [Mor77]. Type SS347H is known to have exceptional resistance to intergranular corrosion. Stabilized grades, such as type 347, are used in

applications where a post-weld heat treatment, which for austenitic steel takes place at about 1273 K, is not possible. This is for instance the case when a process vessel contains a reactive material like a getter or a hydride that will degrade when subjected to high temperatures.

With respect to **ITER**, a comprehensive review on the relevant properties of candidate materials for components of the first wall, blanket, or divertor of has been published by Barabash [Bar09]. The review provides the chemical composition, numerous physical properties, and plentiful data on the mechanical properties of many tokamak-relevant materials. Among them, stainless-steel **SS316L(N)**, which has been selected for the manufacture of in-vessel components of ITER, is addressed in detail. SS316L(N) is primarly used in form plates and forgings [Bar09]. Steel employed for structural and magnetic shielding purposes will constitute the bulk of activated materials. Because of this, the elemental composition of SS316L(N) is strictly specified (see Appendix K).

Some types of high strength austenitic steels usually not employed for tritium containment may be required for fasteners (such as nuts and bolts) or for mechanical joints installed in high temperature regions of ITER. This may be acceptable if the bolts are only exposed to trace amounts of tritium. These materials may also be used to contact tritium-compatible stainless-steels in order to avoid galling of mating screw contact surfaces. Typical materials used in these applications include Nitronic 60, Nitronic 50, and Nitronic 40. Nitronic materials are nickel strengthened austenitic stainless-steels, Nitronic 40 and 50 being nitrogen-stabilized.

Beryllium is not recommended as structural material because of its limited ductility at temperatures below 473 K and the high level of stress when under thermal loads.

3.1.2 Passivation of stainless-steel

Chemical or proprietary electrochemical procedures have been widely used to passivate the surface of stainless-steels [Hir89; Hir90b; Hir90c; Hir90a]. These procedures include i) enrichment in chromium of the surface oxide, ii) polishing the surface to remove oxides and reduce the effective surface area, and iii) reduction of carbon on the surface. Microstructure and surface composition changes induced electrochemically can improve the properties of vessels and components in which tritium is to be kept at high or very high purity. Passivated surfaces inhibit isotopic exchange of hydrogen isotope mixtures because of their reduced catalytic activity for the decomposition of

molecular hydrogen into atomic hydrogen (the latter is initiator of isotopic exchange). Another rather important benefit of components with passivated surfaces is that they are easier to evacuate.

Basically, a good coating should be thin, strongly adherent, of highly homogeneous composition, and show no discontinuities.

Aluminizing was found to deliver a fairly effective stainless-steel coating to reduce the rate of permeation of hydrogen isotopes through this material [For86; For87]. Pure aluminium, aluminium oxide, or aluminium nitride were shown to be effective for this purpose. During coating, which is carried out under a controlled atmosphere, aluminium reacts with the surface of stainless-steel creating inter metallic layers. Aluminium permeation barriers can be applied to rather large items provided the treatment is carried out in a fluidized bed furnace. Aluminizing can lead to a reduction of the permeation rate of three orders of magnitude for SS366L steel (when aluminizing both sides) and two orders of magnitude for type 1.4914 steel. The reduction in permeation was supposed to be the result of aluminum oxide layers forming on the aluminized surfaces. This treatment has proved to be resistant to thermal cycling.

In some applications gold is used as barrier to the permeation of hydrogen isotopes. Gold is usually applied on a thin nickel buffer layer previously vaporized onto the bulk metal after adequate conditioning of the surface [For86][For87]. A 1.5 µm thick gold layer on 316L stainless-steel reduced the hydrogen permeation rate by two orders of magnitude.

The main issues pertaining tritium permeation barriers were addressed in a review on hydrogen solid interactions by Riehm et al. [Rie86]. The compared techniques employed to inhibit tritium permeation comprised i) layered permeation barriers, ii) bulk alloy modification, iii) ion implantation, and iv) controlled surface oxidation.

Main problem with layered permeation barriers is adherence and coating integrity as well as differential thermal expansion under thermal cycling. A tin barrier layer on ferritic 410 stainless-steel was shown to reduce the permeability by four orders of magnitude. However, this effect was limited to relatively low temperatures, i.e. $< 450\,\mathrm{K}$. Aluminide and titanium ceramic coatings have been shown to provide permeation reduction factors from 10^3 to over 10^5 with a wide range of scatter. The rate controlling mechanism of hydrogen permeation may be related to the number and type of defects in the barriers [Hol95].

By so called **bulk alloy modification** a change of bulk composition is achieved by adding a new alloying element. For instance, the addition of chromium to stainless-steel will cause modification of the surface characteristics without changing significantly the bulk properties of the material. This is the case, because chromium diffuses to the surface where it is oxidized into a hydrogen-impermeable oxide layer. Similarly, the permeability of stainless-steel type SS430 could be reduced by two orders of magnitude by the addition of 2 % by weight aluminum and air oxidation [Dev80a; Tur80]. Under these conditions a highly stable layer of Al_2O_3 is formed on the surface.

Ion implantation was demonstrated to preserve bulk properties, be highly reproducible, and not associated with adhesion or interfacial problems [Mus84; Rie86]. A crucial disadvantage of ion beam techniques is the limitation to small scale samples. By implantation of aluminum ions followed by a heat treatment the permeation of hydrogen across iron could be reduced by two orders of magnitude in comparison to that across a sample coated with palladium (highest permeation rate).

Controlled surface oxidation was investigated with the aim of generating an impermeable, crack resistant, and adherent oxide barrier resitant to thermal cycling and to a hydrogen environment at elevated temperatures. A typical procedure employed to generate permeation barriers on materials used in heat exchangers consists in surface oxidation at 930 K in the presence of steam at 95 bar. The resulting thin layer reduces permeation of hydrogen by $2 - 3$ orders of magnitude [Bel78; Sto84; Rie86].

Whether the barrier inhibiting hydrogen permeation is upstream or downstream of the austenitic stainless-steel matrix is inconsequential [Roe79]. The permeation of hydrogen across oxide layers was found to obey the $\sqrt{p}$ law even in the low-pressure range.

Research efforts aimed at reducing the permeation rate of tritium through heated SS316 or F82H materials by coating their surface with a ceramic layer of low permeation coefficient for tritium were reported by a number of investigators [Hir85b; Rie86; Hir89; Hec90; Hir91a; Nak02; Kul06; Hat11; Zha10a; Zha11b; Zha11a]. Materials contemplated as **permeation barrier** passivation!permeation barrier materials for tritium are layers of oxidic ceramics like CaO, MgO, AlN (aluminum nitride), Al_2O_3, Y_2O_3, or Er_2O_3. Of these the latter has recently received special attention because of its i) high permeation reduction factor[1], ii) high thermodynamic stability

[1] Permeation reduction factors are given by the permeability ratio of uncoated to coated materials.

up to elevated temperatures (no phase transformations), iii) resistance to the presence of air, iv) good compatibility with liquid lithium, v) stable barrier properties under neutron irradiation, and vi) good electrical resistivity. Coating was carried out by running an arc discharge on an erbium cathode. During deposition on the substrate the temperature is usually maintained at 873 K in order to generate a dense erbia crystalline phase. Permeation reduction factors for tritium measured across materials such as stainless-steel SS316, SS430, EUROFER, or F82H coated with Er_2O_3 on only one side and maintained at elevated temperatures, i.e. > 773 K, were reported to lie within the range 10^3 - 10^5 [Lev07; Chi10; Oya14]. Chikada et al. [Chi11] and Mao et al. [Mao13] addressed in recent papers mechanism and computational simulation of the permeation of tritium across erbium oxide. According to these investigators, permeation appears to proceed via the grain boundary nanostructure. Further noteworthy experiments were performed employing a gas-driven deuterium permeation apparatus and utilizing F82H specimens covered either on only one side with a 2.6 µm layer or on both sides with layers of 1.3 µm thickness each. The obtained permeation reduction factors were about 10^3 for specimens covered on only one side and up to 10^5 for samples covered on both sides with only half the single layer thickness. When the thickness of the layers on both sides was increased up to 2 µm permeation reduction factors that were even up to 100 times higher were attained [Chi10; Oya14]. The activation energies derived from these studies for the permeation of deuterium through one side coverage or two side coverage of F82H with Er_2O_3 ceramic barriers were 70 - 80 and 120 - 140 kJ mol^{-1}, respectively.

Nakamichi et al. [Nak02] developed a tritium permeation barrier consisting of a $Cr_2O_3-SiO_2$ coating applied by a **chemical densification method**. To suppress the significant effect of open pores the surface was further densified by a treatment with $CrPO_4$. Deuterium permeation experiments with specimens of SS316 coated with $C_2O_3-SiO_2$ additionally treated with $CrPO_4$ displayed a permeation reduction factor of about 10^3. Similarly, a remarkable supplementary reduction of tritium permeation across a permeation barrier coating was achieved by sealing the pores by an electrochemical procedure [Zha11a].

Summarizing, the benefits of coating are limited because they will merely defer and not suppress permeation (see also sections 2.14.1.16 and 3.1.2). Therefore, solubility, which depends on coating thickness and diffusion rate of tritium across the barrier material, will determine breakthrough permeation and this only provided the surface coating is well adherent and

displays no porosity. Principal problems of engineering permeation barriers are achieving reliable, reproducible fabrication and maintaining the integrity of the barrier layer under thermal cycling.

3.1.3 Copper

Another material sometimes utilized for tritium handling equipment is copper. One especially attractive property of copper is its low permeability for hydrogen isotopologues. Copper is furthermore ductile, stable, and displays resistance towards hydrogen embrittlement because of its face-centred-cubic characteristics. The high thermal conductivity of copper is a particularly desirable property for process vessels requiring fast heat flow or constant temperature. Conversely, the following properties require attention: i) the design strength of copper diminishes rapidly when the temperature is raised above 473 K, ii) components of copper require a transition junction (normally nickel) to join to stainless-steel components, and iii) hydrogen isotopes can react at elevated temperatures with oxygen existing in solid solution with copper or with oxygen present as copper oxide precipitates. Water formed under these conditions may give rise to intergranular cavitation, cracking, and failure (the so called "**steam embrittlement**") [Sha07]. Steam embrittlement is also observed sometimes after welding. Because of this, copper used in tritium systems should be of oxygen-free grade.

3.1.4 Aluminium

In comparison to stainless-steel, aluminium has several attractive properties like low density, high thermal conductivity, and very low hydrogen isotope permeability. Aluminium is used in applications where lightweight is critical, for instance when sporadic lifting or transport inside of glove boxes, caissons, of large containers are necessary. Because aluminium is not easy to weld due to the reaction of aluminium with atmospheric moisture, which leads to porosity in the welding zone, this material is only utilized for unusual applications.

An experimental study performed by Alire et al. [Ali81], who carried out measurements on the physical properties of tritium in aluminium using the time-lag permeation technique at a

single temperature, i.e. 673 K, employing a 0.1 mm thick aluminium sheet, yielded the following relationships:

$$\begin{aligned} \text{Permeation coefficient:} \quad & P_{(673\,\mathrm{K})} = 2.5 \times 10^{-15}\,\mathrm{mol\,m^{-1}\,s^{-1}\,Pa^{-0.5}} \\ \text{Diffusion coefficient:} \quad & D_{(673\,\mathrm{K})} = 3.3 \times 10^{-15}\,\mathrm{m^2\,s^{-1}} \\ \text{Solubility:} \quad & S_{(673\,\mathrm{K})} = 25.6\,\mathrm{mol_{T_2}\,m^{-3}}\ . \end{aligned}$$

Ihle et al. [Ihl76] investigated the temperature-dependent permeability of tritium across aluminium at temperatures within the range 420 - 520 K. Their results could be interpreted with relationship

$$P = 5.8 \times 10^{-5} \exp\left(-\frac{14800}{T}\right)\ \mathrm{mol\,m^{-1}\,s^{-1}\,Pa^{-0.5}}$$

It should be noted that the surface condition of aluminium may play an important role in tritium permeability, particularly at low temperatures.

Evidence was provided by Saeki et al. [Sae92] that analogous to stainless-steel the exposure of polished or argon sputtered aluminium at 298 K for 7 days to 13.3 kPa tritium diluted either with hydrogen or deuterium for a time of 7 days causes tritium-contamination of the oxide surface. When this bound-to-the-surface tritium was released via chemical etching the majority was found to consist of HTO and the rest of HT. The degree of contamination by tritium observed on the surface of stainless-steel or aluminium is of similar order of magnitude. This suggests formation of oxi-hydroxides on the metal surface.

3.1.5 Glass, ceramics, and other non-metallic solids

Glass and ceramics are almost not permeated by tritium [Ell78b]. The much larger activation energies for diffusion and solubility of hydrogen in non-metals rather than in metal systems is attributed to the formation of chemical bonds in the lattice of the former.

Because glasses are essentially weak structural materials they should not be used for tritium containment except when needed as viewing ports or for optical spectroscopy. Even then, they must be sized with a considerable safety margin and eventually be designed by the double containment principle for safety reasons.

In spite of the rather good properties of ceramics at elevated temperatures, it is important to keep in mind that they are vulnerable to rapid changes of temperature which frequently are associated with loss of integrity.

Tritium diffusion coefficients across a number of non-metallic solids like Licalox, SiC single crystal (also aluminum doped) or pressed or vapour deposited, hot pressed Y_2O_3, pyrolytic carbon, or boron carbide have been determined by Elleman et al. [Ell78b] using a technique based on recoiling tritium into specimens and measuring the time rate of tritium release during post irradiation annealing at constant temperature (see also section 2.13).

3.1.6 Chemicals to be avoided in primary systems

Heavy metals like mercury, lead, antimony, and sulphur should be excluded from tritium primary systems. Mercury will poison metal hydride bed materials and amalgamate with aluminium, copper and silver. Sulphur, mercury, and several heavy metals are known to constitute effective catalyst poisons.

3.2 Typical small auxiliary components used in tritium handling facilities

In this section typical small components frequently employed in tritium handling facilities are described and assessed.

3.2.1 Pipes

3.2.1.1 Pipe materials

Tritium primary systems are mostly constructed employing seamless pipes. For pipes of > DN100 longitudinal seam welded pipes are acceptable. Longitudinal seams must be subjected to the same tests as round seams. Seamless capillary tubes are conventionally manufactured from stainless-steel type 304/304L, 316/316L, 316Ti, 317/317L, 321, 347, 904L, and others.

Recommended materials for pipes installed in primary systems designed for handling of hydrogen isotopologes at < 70 bar are austenitic stainless-steels type SS304, SS304L, SS316, and SS316L. Type SS316L can be subjected to thermal cycling within the temperature range 213 -

473 K. Detailed material specifications for seamless pipes and plates are compiled in references [ITE07a; ITE07b].

For high temperature applications, i.e. ≤ 1073 K, the recommended materials are type SS347 and Inconel.

Precipitation steels, e.g. 17-4 Ph or 15-5 Ph, or series 400 stainless-steels are not recommended because of their tendency to embrittlement when exposed to hydrogen.

In most tritium facilities copper pipes are used exclusively for the conveyance of water or auxiliary gases.

3.2.1.2 Pipe specifications

Pipes as well as all stainless-steel components must be of high quality and clean, so that stringers of oxide or sulphide inclusions cannot provide a leak path regardless of how parts are produced relative to grain texturing. All tubing requires ultrasonic inspection. A good surface finish is very important to get a good ultrasonic signal to noise and therefore a reliable inspection result. At Mound, USA, tubing with a defect greater than 0.005 cm deep or 0.075 cm long is rejected [Chr73].

3.2.1.3 Precautions during pipe installation

Pipes are ubiquitous components of tritium handling facilities. The most frequently installed pipes are either seamless or welded[2] and have outer diameters of 1/8 in, 1/4 in, 3/8 in, 1/2 in and 3/2 in. They are made of stainless-steel types 304 or 316 and designed for operation at temperatures of up to 377 K and pressures, depending on pipe type, that can be as high as 4134 bar (60 000 psi)[3].

Prior to the installation or assembly of pipes (this also holds for valves, equipment, and instrumentation) they should be cleaned according to procedures approved by Design Authority. A frequent cleaning procedure consists in washing sequentially with acetone, hot water, and methanol or ethanol. All austenitic stainless-steel should be free from iron oxide contaminate. Pipes should be carefully dried with nitrogen before installation [Poo08]. The ends of all open

[2] Welded pipes are generally more cost effective than seamless pipes and characterized by better surface quality on both the OD and ID when compared to hot finished seamles material. Conversely, seamless pipes have no heat-affected zone. They show better corrosion resistance, a more homogeneous grain structure, and no problem with weld seam orientation [Out11].

[3] Accessed on 23.01.2020 at 04:21 pm. http://www.swagelock.de/de-DE/product/Tubing-and-Tube-Accesories/

pipes installed or not yet installed in tritium handling systems should be covered at all times by appropriate caps to prevent entrance of dust or of other contaminants.

Hydrostatic proof or leak tests of piping are not permitted; only pneumatic testing and tritium leak testing are allowed.

If possible, pipes used in primary systems shall be maintained short in order to keep the volume of the equipment as small as possible. Pipes shall be capable of expanding freely during testing and operation and be installed relative to each other and inside of the glove box in such a way that they remain easily accessible for repair or replacement. If doable, pipes should not create zones difficult to clean. To keep the overall leak rate at the lowest possible level, the number of seams should be kept at a minimum. Joints obtained by welding should be preferred over mechanical fittings.

Long pipes should be sufficiently supported to make pipe displacements impossible. Supporting parts shall not be welded onto the pipes. Fittings of austenitic pipes should not come in contact with ferritic steels.

Process piping that could contain significant partial pressures of water vapour should be provided with heat tracing or other means of maintaining the temperature of the piping high enough to prevent water condensation. Process piping in which condensation could take place should be sloped into a vessel to avoid low points at which condensate could accumulate.

All gas supply pipes within glove boxes should either be sized or provided with appropriate flow restriction devices to limit the gas flow after a pipe rupture to values below that of the glove box bubbler capacity.

Primary system pipe connections inside of glove boxes shall be Cajon VCR threaded joints, CF flange joints, or KF flanges with ultra-sealing disk and corresponding locking ring (only for low tritium level pipes).

Tritium conducting pipes, cooled pumps, and other cooled components shall be separated from cooling water systems by a double wall barrier.

The design of piping and components shall be sized to accommodate anticipated flow capacities and account for the effect of stresses resulting from internal pressure and temperature of the flowing media.

If cryogenic liquids can be trapped between isolation devices like valves during normal or abnormal operation of a component, verification and calculations shall be provided which credibly

demonstrate that once the component reaches again ambient temperature, the resultant expansion cannot damage or exceed the design pressure of the system.

3.2.2 Vessels

Vessels in tritium service comprise tanks, fixed or mobile storage vessels, over-pressure relief vessels designed for material balance measurements, etc. Heated (or cooled) vessels of various configurations are used for getter beds, catalyst beds, adsorber beds, permeators, isotope separation systems, cryo-pumps, etc. Tritium storage tanks or other vessels shall be designed for lethal service

Tanks integrated into processes shall comply with standard requirements for fabrication, welding, leak testing, cleaning, and inspection such as approved by Design Authority. All tanks shall be accessible by a pressure transducer, vacuum gauge, thermocouple, and a mass spectrometer or any other suitable analytical instrument. At any rate, they should have at least a sample point connection, unless specifically exempted by Design Authority. PVT instrumentation must provide sufficient accuracy for the accountability of 0.1 g tritium.

Any vessel for tritium processing that is heated, cryogenically cooled, or in which a chemical reaction can conceivably cause a pressure excursion shall be protected against pressurization and uncontrolled conditions with a pressure relief device, a high temperature interlock, and a high-pressure interlock.

3.2.2.1 Surface treatments

The fabrication of vessels intended for handling calibrated tritium-bearing gases or storage of chemically pure tritium (except for He-3) require special surface treatments, like reduction of carbon and hydrogen as well as reduction and enrichment of surface chrome by an electrochemical technique (see also section 3.12). The aim of these treatments is to minimize in-growth of protium and hydrocarbons into the gas phase [Gil80]. Additional precautionary measures comprise mimization of the inner surface area of the prospective vessel and painstaking elimination from the surface of organics, oil, or grease remaining from fabrication. The latter contaminants constitute the main source of tritium-bearing hydrocarbons.

3.2.3 Valves

3.2.3.1 Design guidelines

Valves destined for tritium service should have bellows sealed with a bonnet fixed by a replaceable metal gasket. By this way of proceeding, the number of mechanical joints that must be disturbed to repair a valve is minimized. Additionally, the cost of a bonnet is lower than that of a new valve and its replacement easy and stress-free to perform. On the opposite side, complete replacement of valves requires breaking of two piping joints, which may be associated with alignment and strain problems during connection remake.

The currently preferred valve seat materials are Stellite[4] and Vespel. For low pressure process gases containing very low levels of tritium flange gaskets of ethylene propylene diene monomer (EPDM) can be used [Poo08].

3.2.3.2 Design requirement

A number of design requirements of general validity as well as some practical recommendations concerning the installation and utilization of valves in tritium service equipment are listed below [Wea94; Poo08]:

- Remotely operated valves shall be designed to revert to a safe condition in the event of a breakdown or malfunction (fail safe). Fail safe design and diversity can be of much benefit. For instance, if two valves in series perform the same function, e.g. isolation, it may be desirable to have one valve that springs to open (air pressure to close) and the other that springs to close (air pressure to open).

- All manual valves in glove boxes shall be easily accessible via the gloves of glove boxes or in justified cases by specially designed tools.

- Remotely controlled valves shall be provided with an indication system that shows status of the valve, i.e. open or closed.

- Instrumentation and equipment in tritium process systems shall be isolated by double valves to allow maintenance or replacement.

[4] Stellite is an alloy consisting of 50 % cobalt and 35 % chromium.

- Valves needed for applications at temperatures below the dew point of the facility should have a suitable stem length to accommodate thermal insulation or heating.
- Multiport outlet or gate root valves shall not be used to isolate instruments in tritium process systems unless a specific benefit makes this necessary. Root valves do not meet all criteria required in tritium service.
- Process valves shall have bellows-sealed stems with replaceable bonnets sealed with a metal gasket unless otherwise specified by Design Authority.
- Valves and check valves in tritium handling systems shall have relatively soft seats in order to achieve leakages across the seat as low as reasonably possible. Valves shall have bellows sealed bonnets to maintain a leakage across the stem at values lower than $10^{-8}\,\mathrm{cm^3\,s^{-1}}$.
- Packless valves using either metal bellows (low pressure applications) or diaphragms (high pressure applications) are more recommendable for tritium service than valves with a tritium resistant packing. Valves with no moving seals are preferable to those with packing because packing wears from normal use, is subject to radiation-induced damage, and requires periodic adjustment.
- Another wished for feature of valves destined for tritium service is the equivalent to a "secondary containment". For example, in case of Nupro bellows valves the primary sealing is constituted by the welded metal bellows and the "secondary" containment by the hose upper packing (see also Fig. 3.2 below). In this case, tritium released during a bellows failure will mostly be captured by the spring-energized Teflon seal is permeable to tritium, a comparatively small amount of tritium will continuously be liberated into the valve environment. This leak may advantageously be used for an early detection of the failed valve.
- Valves with hemispherically shaped stem tips are considered especially suitable for tritium service because they provide a particularly broad sealing area for the seat. This is important for manual valves that may show pitting and galling caused either by excessive torque or misalignment between stem and seat.

- Valves furnished with inspection ports used in conjunction with bonnet sniffer tubes are particularly recommended in critical applications. They permit direct monitoring of the bellows integrity.
- Utilization of materials of different hardness for stem and seat, e.g. seat of stainless-steel and tip of work-hardened copper, results in better sealing because the softer material may deform and adapt to the surface of the harder material. Another beneficial consequence is less galling and pitting.
- Some institutions inspect every single valve upon receipt rather than relying on a statistically based acceptance inspection program. Main objective of the inspection is the quality of the shaft alignment, because when seat and stem are not coaxial there is great tendency for leaks across the seat.
- Optimal performance requires actuator strength and closure force of remotely actuated valves to be controlled because excessive torque may lead to seat damage and leakage. To this effect, the stroke of a valve should be slowed down before closing, for instance with an air flow restrictor or intermediate actuator pressure. The aim of these measures is softer impact of the stem tips.

3.2.3.3 Stem and gasket materials

Bellows valves with either welded bellows or bellows joined to the valve body via a metal gasket have been found to be appropriate for tritium service. Silver-plated stainless-steel gaskets are the preferred option. Valves with welded bellows may be acceptable for high temperature tritium service.

Copper gaskets are customarily used for ultra-high vacuum applications.

The stem material employed for **manual valves** is typically Stellite and that for **automatic valves** Vespel or ultra-high molecular weight polyethylene (UHMWPE). For automatic Swagelok valves type HB and B series the preferred material is Vespel. For the larger valves, i.e. T and U series, Vespel is too hard to achieve an acceptable leak rate of $< 4 \times 10^{-9}\,\mathrm{STP\,cm^3\,s^{-1}}$. In this case the softer UHMWPE material is recommended.

The potential application of ethylene-propylene rubber (EPR) or high-density polyethylene (HDPE) as tip seals of piezoelectrically driven valves was investigated systematically by Gill

and Pierce [Gil85] employing a modelling study. Piezoelectrically driven valves were installed at the Tokamak Fusion Test Reactor (TFTR) in Princeton for the purpose of tritium fuelling via gas puffing. Among other criteria they were selected because of their sufficiently low elasticity moduli, resistance towards the beta-radiation of tritium, and their low content of elements other than carbon and hydrogen (minimization of high Z off-gassing).

As discussed above, automatic valves should be provided with limit switches that indicate whether the valve is open or closed. Switches can either be of plastic body (e.g. Honeywell 914CE1-3A9) (danger of breaking) or of the much sturdier and more resistant to break die-cast zinc (e.g. Micro Switch BZ-2RQ1-A2).

Ball valves (for gases of high flow rates) and **metering valves** are employed in tritium facilities for service gases streaming with coefficient of flow in the range $0.04 < \mathrm{Cv} < 015$ and carrying very low concentrations of tritium. Commercial ball valves and metering valves which use UHMWPE, polyetheretherketone (PEEK), polytetrafluoroethylene (PTFE), or Viton® (co-polymer of vinylidene fluoride and hexafluoropropylene) for seat, packing, or as O-ring material, are acceptable for these applications [Poo08].

3.2.3.4 Quality assurance

A standard test procedure for Swagelok bellows valves furnished with Cajon VCR® connectors is the one atmosphere differential helium leak test across the seat for the **seat test** and between the interior and exterior for the **envelope test**. Part of this test is also the 41.3 bar pressure test performed with nitrogen on the sub-assemblies (bellows stem and weld ring) (see Table 3.1). The latter strength test of the welds is observed for leakage and performed under water for 5 - 10 seconds (Swagelok procedure SCS-00020) [Poo08].

Table 3.1: Leak test of Swagelok valves.

Valve type	Acceptable leak rate (STP $\mathrm{cm^3\,s^{-1}}$)
B series	4×10^{-9}
HB series	4×10^{-9}
U & T series	4×10^{-9}

It is standard practice to clean and package each Swagelok valve according to Swagelok procedure SCS-00011.

The pressure and temperature ranges at which Swagelok valves can be used on the condition that the butt-welded VCR connectors have been radiographed are given in Appendix L. If the connectors have not been radiographed, the pressure ratings given in Appendix L should be reduced by 15 % in order to account for the lack of examination.

A non-standard test of the bellows valve shell (Swagelok procedure SAI-01274) is the hydrostatic pressure test using de-ionized water. With the valve open and end-plugged, the shell of the various valves is pressure-tested for one minute at the corresponding pressure given in Table 3.2.

Another non-standard procedure concerns radiography of butt-welds from the Cajon VCR connectors (Swagelok procedure SQS-00084).

Table 3.2: Hydrostatic pressure test of Swagelok valves (see also Appendix M).

Valve type	Pressure (bar)
BG series	68.9
BW series	68.9
HB series	241.2
T series	172.3

3.2.3.5 Worldwide experience with commercial valves tested in tritium service

A very large number of different commercial high and ultrahigh vacuum-tight valves made entirely of austenitic stainless-steel have been installed and used in tritium facilities sometimes handling gas of rather large specific tritium activity (see Fig. 3.1 and Appendix M) [Wea94]. Manual valves have been utilized for setting up various process configurations or the isolation of sections for the purpose of maintenance or replacement activities. Valves can either be welded or joined by mechanical fittings to stainless-steel pipes or components. Succinct informations on characteristics, applications, and performance of some typical valves commonly employed in tritium facilities are given below.

[5] http.://www.lesker.com/newweb/gas_liquid_management/. (23.07.2020)

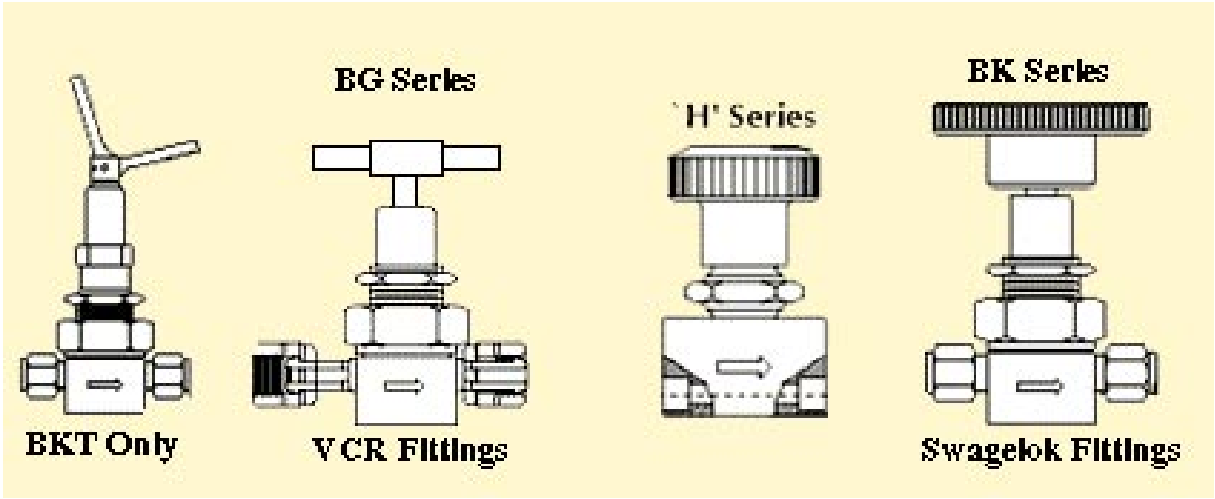


Figure 3.1: Nupro SS316 stainless-steel valves with VCR® fittings, welded fittings, or Swagelok fittings.[5]

3.2.3.5.1 Manual and automatic valves

Nupro SS-BG-V51 stainless-steel shut off valves with metal to Vespel (polyamide) stem tip seal have been used routinely in sizeable numbers, mostly over many years, for the operation of tritium primary systems. The leak rate across the seat is specified by the manufacturer to be lower than 1×10^{-9} bar cm^3 s^{-1}. The experience gained world-wide with these valves is mostly positive. Typical tritium laboratories like Chalk River [Gal05], TPL [Yam02; Yam11a], JET [Lae99b], TSTA [And82], TLK [Sch91a] and others habitually use Nupro automatic 8BK, manual 8BW, automatic 4BK, manual 4BW, 4BG, 4H, and manual UW valves (see also Fig. 3.2)[6]. Hundreds and even thousands of these valves have been installed in single tritium experiments or in large technical facilities sometimes handling besides tritium, diverse other reactive gases at different compositions, at wide ranges of pressure and temperature.

Manually operated **Nupro BW valves** of welded body have been tested in prolonged tritium service all over the world in very large numbers and found to be adequate [Cof73; Hem89a; Pen95c; Lae99b; Gal05; Yam11a]. Because they utilize a stainless-steel stem their design temperature, i.e. 773 K, and the acceptable pressures without loss of vacuum tightness are high (see Appendix M). Nupro B series valves are joined to tritium-handling equipment either by welding or, when

[6] The B series features demountable bonnets for easy maintenance or cleaning, T stands for toggle switch, K for knob and W for welded body.

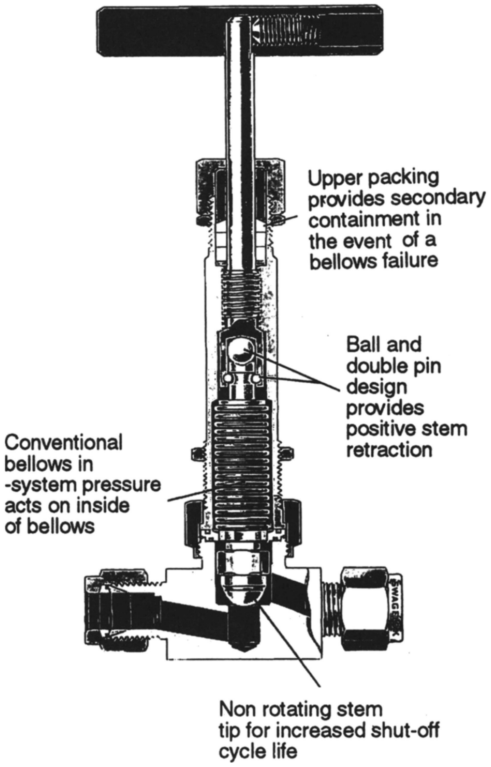


Figure 3.2: Nupro bellows valve [Wea94].

the necessity of replacement can be anticipated, utilizing all metal Cajon fittings. The vacuum tightness of these valves to the environment as well as across the seat is specified to be better than $4 \times 10^{-9}\,\mathrm{bar\,l\,s^{-1}}$. Failures of these valves occur rarely and when, merely at the seat. One exception is a failure reported by Gallagher and McCrimmon [Gal05] who detected a leak through the bellows of a sealed valve belonging to an Amersham U-bed. The failure was attributed to the fairly high temperatures the valve experienced each time the bed was heated to elevated temperatures for the thermal decomposition of uranium tritide into uranium and gaseous tritium.

Nupro SS needle valves have a metal-to-metal seal. They can be joined to a primary system either by welding or via Cajon fittings employing silver coated metal gaskets. They can also be installed in the bypass of a recirculation pump to control the pumping speed. These valves are not appropriate to isolate components in tritium process systems because their leak tightness at the seat does not meet the requirements.

Nupro type SS-4 BGV51 3C and **SS-8 BGV51 3C** are **pneumatic valves** that find application in component protection. In normal position, i.e. without forced gas pressure, they

are in closed position. Cycling tests with valves having a Stellite stem tip showed loss of leak tightness at the seat after several 100 to 2000 cycles [Hem89a]. Imide polymer (Vespel) stem inserts, on the other hand, maintained good leak-tightness even after 50 000 cycles.

Generally, valve stem tips made of Vespel continue to seal for years of operation with tritium provided they are used with not more than the specified sealing force. When valves are operated with less force than specified for the seals, leaks across valve tips have been observed, which were attributed to surface hardening.

Automatic on/off valves are normally operated pneumatically by a pilot solenoid device housed within a solenoid valve console. The normal actuating medium is nitrogen either delivered from the standard main supply of the building or from a dedicated pressurized cylinder. The latter option is employed when the required pressure is higher than that provided by the standard supply. These valves are normally of fail close type. They may be provided with a limiting switch which indicates open or closed position. Monitoring of the valve status may be needed not only for visual inspection but also for the interlock logic.

Balzers UHV 035 B valves with a metal/sapphire seal are habitually positioned between a primary tritium system and the corresponding servicing turbo molecular pump. These valves can be heated up to 673 K in closed position and up to 723 K in the open position for instance during the evacuation mode.

Balzers HPS series 145 valves, which close in 30 ms, have been utilized to protect turbo molecular pumps.

VATEC DV 81A valves, have a metal-to-metal seal. Two such valves were used as overflow bypass for infra-red cells to protect the sapphire windows of an optical cell from overpressure [Pen95c].

Good results have been obtained with all-metal gate valves (see Fig. 3.3). VAT Valves series 49 and 57 manufactured by **VAT**, headquartered in Haag, Switzerland, have been used for the pumping system of the TLK Storage System [Tri91; Tri96]. They are frequently installed in pumping systems because of their large conductance. Valves of series 57 have a nominal width of 40 mm. They close by a spring and are insulated by metal bellows. Their vacuum tightness is specified to leak rates of 10^{-10} mbar l s^{-1} both towards the environment as well as at the seat. It should be noted that seven out of eight all-metal **VAT valves** installed in JT60-U between the torus and turbo molecular pumps had to be replaced after bellows manufactured of type **SS304**



Figure 3.3: Typical UHV-tight gate valves.[7]

stainless-steel revealed signs of strain stress corrosion following about 600 cycles. Once these bellows were replaced by new ones manufactured from Inconel 625 the problem was resolved.

Ball valves are primarily employed in tritium facilities to handle service gases. However, good results have also been obtained with gases containing very low concentrations of tritium and requiring high flow rates.

Cryogenic valves featuring bellows are preferred over valves with other type of sealings. Even though bellows sometimes develop a pinhole they are still favoured because of their superior leak-tightness.

3.2.3.5.2 Variable leak and modulating valves

Manually and automatically operated Sapphire-sealed **variable leak valves** are supplied by Varian and Granville Phillips. They are compatible with ultrahigh vacuum systems and bakeable at temperatures up to 723 K. Variable leak valves are designed to deliver a controlled leak within the range 10^{-10} to 100 mbar l s^{-1}.

Modulating control valves are used in variable flow systems in which the flow must be adjusted within the range slow - full stream. They are usually electromagnetically actuated and of fail-close type. They can be controlled by an analogue signal, e.g. 4 - 20 mA that actuates the range 0 - 100 % open.

Recapitulating, there is worldwide a vast body of experience in numerous tritium installations with a large number of rather diverse valves on which to base the design of future equipment. A lesson learned is that commercial valves with packing, seats, or gaskets made of fluorinated materials such as Teflon or KelF are not tritium-compatible and should not be used in tritium

[7] http://www.lesker.com./newweb/gas_liwuid_management. 23.07.2020

handling equipment. In the presence of moisture and tritium these polymers may lead to the formation of hydrochloric and/or hydrofluoric acid, which can cause loss of sealing and hence of containment because of their highly corrosive character. Polymers such as the relatively stiff Vespel or ultra-high molecular weight polyethylene (UHMWPE) have been shown to be more radiation resistant than Teflon or KelF. In spite of this, it should be noted that full compatibility with beta radiation can only be achieved with metals.

An important degrading effect on valve performance are particulate build up on stem tips. Particles can bring about scoring and channelling on sealing surfaces.

3.2.4 Fittings, flanges, gaskets, and sinter filters

3.2.4.1 Fittings

Commercially available high vacuum-tight fittings from Swagelok and ultrahigh vacuum-tight fittings from Cajon, now all commercialized under Swagelok, with replaceable metal gaskets constitute the preferred option for equipment employed in tritium service.

Swagelok fittings can accommodate a large number of different small tube diameters, i.e. 1.6 - 50 mm, and be used in a broad range of pressures, i.e. 10^{-5} mbar to several hundred bar. Helium leak rates as low as $10^{-6}\,\mathrm{bar\,cm^3\,s^{-1}}$ are achievable. The operation up to fairly high temperatures up to 481 K is possible. They are available in broad assortment of configurations and reusable if employed according to specifications.

Cajon fittings are available for pipe sizes within the range 1.6 to 25 mm (see Fig. 3.4). The design helium leak rate of Cajon type fittings is lower than $4 \times 10^{-9}\,\mathrm{bar\,cm^3\,s^{-1}}$; their design operation temperature is equal to or less than 773 K. In tritium work, only metal gaskets should be used. Cajon fittings are applicable in pressurized systems because of their contained seal. Advantageously, these fittings are furnished with a test port for in place helium leak testing. The threads are plated for smooth turning.

Where the resilience of an elastomer or a plastic having low friction is imperative non-fluorinated materials such as polyimide are the option of choice. For obvious reasons, the surface area exposed to tritium should be reduced to a minimum [McL79].

Fittings may be attached to stainless-steel pipes by a **tungsten inert gas** (TIG) **welding** procedure [And82].

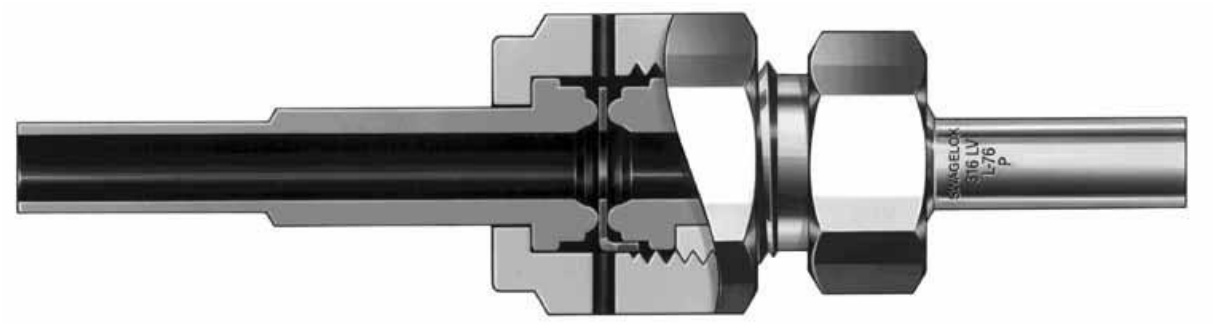


Figure 3.4: VCR® ultra-high vacuum tight assembly showing male and female nut, test ports, and side load retainer all metal gasket.[8]

3.2.4.2 Flanges

Ultra-high vacuum-tight **ConFlat** type flanges are mostly employed to connect pipes of large widths. The specified helium leak rate is lower than 10^{-10} bar cm^3 s^{-1}; the permissible operation temperature covers the range 77 - 773 K. ConFlat flanges are sealed via a knife edge employing a one-way copper gasket. ConFlat flanges are available in a broad range of fitting configurations and sizes within the range 34 - 420 mm. ConFlat flanges require testing and approval in the temperature and pressure range of use to meet tritium service requirements.

KF flanges are used for high vacuum (100 mPa - 100 nPa) sealing; they employ only aluminum gaskets. They are sealed with clamps placed around the aligned fittings. KF flanges are frequently used downstream of the exhaust side of vacuum pumps.

3.2.4.3 Gaskets

Copper, silver-plated nickel, silver plated copper, or silver-plated stainless-steel are gaskets most commonly used in the ultrahigh vacuum technology such as employed for tritium handling. Metal gaskets are normally recommended when frequent bake out is necessary. Aluminium gaskets employed many years in tritium service were found to meet specifications without contingencies [Pau88].

Wire ring gaskets consisting of pure gold or gold-plated copper have been used in high vacuum systems destined for work with tritium. Gold is chemically inert, soft, ductile and suitable for

[8] http://www.lesker.com./newweb/gas_liwuid_management. 23.07.2020

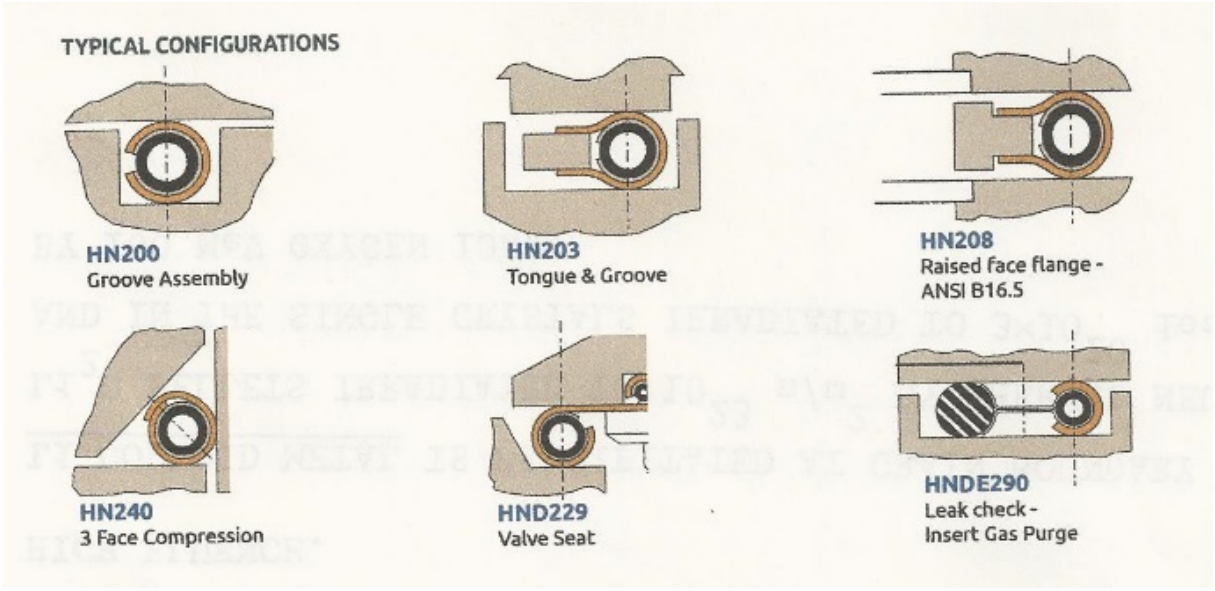


Figure 3.5: Different types of Helicoflex gaskets.[9]

high temperature applications. The metal is also attractive because it does not damage flanges and can be re-used if installed properly.

Polyimide gaskets under constant load provide good service for years. Experimentally it was observed that following exposure to tritium the hardness of polymers increased in the order Vespel (polyimide) ≈ Kalrez (perfluoro) < Viton A (perfluorated compound).

Valves furnished with Kel-F gaskets were found to be inadequate for tritium service and had to be replaced [Pau88].

Helicoflex gaskets of ring-joint, flat metal jacket, spiral wound, metal C-ring, corrugated metal jacket, or metal O-ring type, etc. can be employed at a wide range of temperatures, i.e. from cryogenic up to 873 K at a wide range of pressures from 10^{-9} mbar up to an overpressure of 10 bar. The sealing principle is based upon the plastic deformation of a jacket of greater ductility than the flange material (see Fig. 3.5). They are reusable if installed correctly. Special flanges, seals, and clamps are available for pipes of sizes within the diameter range 5/2 - 16 in.

3.2.4.4 Sinter filters

Sinter filters are fabricated by bonding powder particles through diffusion at temperatures well below the melting point. By this procedure uniformly sized pores are generated with ratings

[9] Technetics Group https://technetics.com/ (30.60.2020 09:00)

from 0.1 - 300 µm. Sinter filters have excellent temperature resistance and are of high mechanical strength. The number of materials that can be sintered is quite large, i.e. stainless-steel type SS304 or SS316, Hastelloy, titanium, Inconel, Monel, nickel, bronze, etc. Sinter filters are supplied as disks, cartridges or tubes (min. diameter 10 mm). They are employed in tritium systems for gas filtration, as spargers, or flame arresters.

A good description of the penetrability of sinter filters by particle carrying gases as function of the size of the particles and the flow dynamic characteristics of the porous medium were provided by Strauss et al. [Str13]. Experimental test results obtained with Sika filters from GKN Sinter Metals, Worcestershire, England, were provided.

3.2.5 Electrical feed-trough

Electrical feed-throughs for primary and secondary systems frequently consist of metallic-ceramic joints. A very large variety of hermetic feed-troughs are offered commercially either for dual or for single sided connecting/disconnecting plugs. They are utilized for i) coaxial cables, ii) thermocouples with multi pin thermocouple connections, iii) single or multi optical fibres, or iv) hermetically sealed high voltage wires, to name just a few. There are numerous suppliers of electrical ceramic feed-trough's.

3.2.6 connection options for components

Components in tritium systems not requiring routine maintenance are most commonly joined by full penetration welding. When occasional or frequent replacement of components is foreseeable mechanical joints are the better choice.

3.2.6.1 Joining by welding, brazing, or soldering

If possible, components integrated into primary tritium systems should be joined by welding procedures. Welds in tritium systems should be placed in a way that they remain accessible for non-destructive inspection by accepted methods like radiography or ultrasonic testing. The weld should penetrate to the inner wall of the vessel or pipe and display a smooth surface. The joining process should not create crevices or cracks in the weld joint on the interior surface of tritium containing vessels. This is important to avoid small pockets that may contain tritium generating

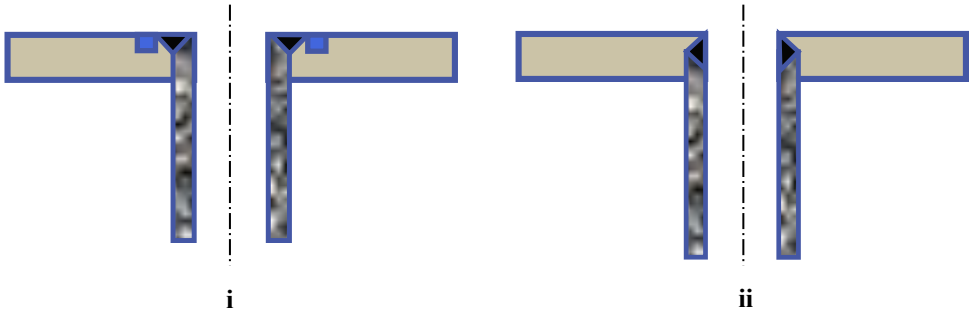


Figure 3.6: Flange to pipe welding: i) with a stress relieve groove or ii) with a thin ridge on the inside of the flange.

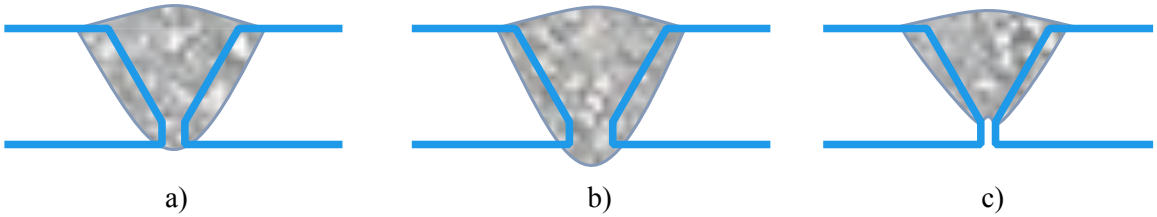


Figure 3.7: Examples of butt welding with (a) the right gap, (b) a too large gap and (c) a too narrow gap between the welded piping.

so called "**virtual leaks**". Such leaks are both difficult to outgas as well as to localise. The best joining procedure are full penetration welds. Only weld rod filler materials which harmonize with the base alloy should be chosen. Every effort should be made to reduce or eliminate welding residual stresses. A common approach to cope with this problem is to machine stress-relieve grooves into the flange before welding to the pipe (see Fig. 3.6i). Another frequently utilized approach is to machine a thin ridge on the inside of the flange (see Fig. 3.6ii).

The most reliable procedures for joining stainless-steel are Heliarc, tungsten inert gas welding (TIG) [And82], or electron beam welding. When type 300 series flanges are welded, precautions need to be taken to prevent chromium carbide precipitation during cooling after welding. The precautions include use of specific heat treatments and the utilization of low carbon steels like SS316L or SS304L [Bil73].

A common technique for joining flanges to pipes to itself consists in **circumferential butt welding** (see Fig. 3.7). To obtain an optimal weld the gap between the pipes should be 3 - 4 mm wide. If the gap is too wide the penetration will be excessive (b) and if too narrow the penetration will be insufficient (c) (possible source of virtual leaks).

Proper welding of dissimilar materials usually requires a transition junction of an intermediate material capable of accommodating differences in thermal expansion, galvanic corrosion, and other properties.

Other joining methods such as brazing or high temperature soldering are not recommended for tritium service.

3.2.6.2 Mechanical joints

All-metal mechanical joints are used to connect components in tritium systems when routine replacements are necessary or occasional repairs/replacements of failed components can be anticipated. Several commercial high vacuum tight fittings, e.g. Swagelok (only for very low concentrations of tritium), and ultra-high-vacuum tight fittings, i.e. ConFlat, Cajon, have been identified as compatible with tritium. They are all widely used in tritium installations all over the world. ConFlat flanges are predominantly utilized for joining large components and pipes. Typical gasket materials are copper, silver plated nickel, or silver-plated stainless-steel. Before installing gaskets containing silver the leachability of silver should be checked with an Environmental Compliance Authority to avoid creation of mixed waste. Properly installed one-way Cajon gaskets were shown to be quite satisfactory for tritium service.

3.2.7 Bellows and membranes

Bellows in combination with two one-way seals are used in Metal Bellows pumps for the compression of gases. Since particulate matter accumulating inside of Metal Bellows have been observed to induce mechanical rupture of the bellows, it is recommended to place filters of high conduction and good electrostatic retention at inlet and outlet of the compression zone.

Membranes are used in rupture disk devices to protect vessels from pressures exceeding design values.

High carbon steels, e.g. SS301, often used in diaphragms and membranes, should be avoided in tritium service because of possible reaction of tritium with carbon on the surface leading to the formation of volatile hydrocarbons.

3.2.8 Rupture discs

Rupture discs constitute relief devices for the protection of vessels used in tritium service that may be subjected to sudden dangerous pressurization by chemical reactions, heating, or vaporization of a cryogenic fluid. Rupture discs should be approved for tritium service and be leak-tight to better than 10^{-7} STP cm^3/s helium. Relieving systems in tritium service shall be designed in such a way that preventive maintenance is not necessary. Relieved tritium-contaminated gas should be expanded into an evacuated containment adjacent to the rupture disc. Low-carbon austenitic stainless-steel should be used for rupture discs.

3.2.9 Filters

Filters are needed at both ends of activated charcoal adsorber beds, catalyst reactors, hydrogen getter beds, hydride transport vessels, or molecular sieve dryer beds to avoid intrusion of dust into tritium processing equipment. Filtration of process gas passing through pumps or compressors is necessary to minimize particle induced corrosion, bellows damage, or rotor damage.

Fluid flow filters installed in cryogenic systems may be clogged by metal particles from iron cast pumps.

Filters should not be installed in a permanent manner unless unavoidable because of process safety. A consequential selection criterion for filters are flows dynamic requirements.

3.3 Oils and lubricants

In **oil diffusion pumps**, the oil is heated in order to generate a vapour which entrains gas molecules to the fore line port before recondensing in the boiler. These pumps, which provide high pumping speeds for light gases like helium or hydrogen, work well when the concentrations of tritium in the pumped gas are low. In the past, they were employed together with fore pumps likewise lubricated with oil or grease maintained at moderate temperature. In the presence of higher concentrations of tritium, it was observed that the vapour pressure of the oil and of the grease increased (off-gassing) and the viscosity of the oil gradually augmented. Mineral oils like Duo-Seal, consisting of saturated hydrocarbons, or silicone oils like tetramethyl tetraphenyl trisiloxane or pentaphenyl trimethyl trisiloxan whose vapour pressure is rather low, i.e. of the order of 10^{-10} mbar, displayed a tendency to polymerize and even to solidify. Oils like

polyphenyl ether oils lasted for years in tritium service but incorporated significant amounts of this radioactive gas. Also, fluorinated pump oils were tested but could not be recommended for tritium service - particularly when tritiated water was present - because the generated tritium fluoride lead to pit corrosion and damaged the equipment. To keep the pumping systems working properly cumbersome oil changes were periodically needed which sometimes were associated with environmental contamination.

The lesson learned is that direct contact of gaseous tritium with oil or grease should be completely avoided not only because of the generation of tritium-contaminated oil waste but also on account of deleterious effects on grease and oil hampering the effectiveness of the pumping system and releasing tritiated hydrocarbons. In view of the above, modern tritium installations relay for the evacuation of tritium-bearing gases almost exclusively on magnetically suspended turbo molecular pumps combined with suitable oil-free fore pumps (see section 3.14.1).

Other commercial equipment encompassing sections lubricated with oil or grease that may come in direct contact with tritium require to be upgraded in order to meet the requirements of work with tritium (see for example section 3.14.1.10).

3.4 Design of heated components

The design of heated components should compellingly minimize heat dissipation in order to avoid increased permeation losses of tritium and elevated glove box temperatures. Heated components are preferably connected to a power supply via coaxial cables. For safety reasons as well as component protection, power sources should not be over dimensioned, i.e. temperature excursions should be precluded by optimized electric design.

Thermal insulation shall be provided for heated components to minimize energy losses, prevent condensation, and warrant safe temperatures on their surfaces. Insulation of pipes is also used when there is need to avoid condensation.

Because heaters are susceptible to failure, an appropriate redundancy strategy needs to be incorporated into the design. To cope with this demand, it is advisable to install several small heaters instead of a single large one. Provisions for easy replacement of heaters belonging to critical or complex tritium-contaminated components like permeators, catalyst vessels, storage beds, etc. should be included in the design.

Components enduringly installed in glove boxes whose surface temperature may surpass 330 K should be effectively protected against inadvertent contact with burnable materials such as paper, cloth, insulation of electrical cables, plastic materials, rubber gloves, hands, etc. This can either be accomplished by engineering measures like a dedicated protective construction, and/or administrative procedures.

Selection, application, design, and installation of thermal insulation materials used for tritium-handling equipment and piping shall be in accordance with industry standards. Asbestos shall not be used for this purpose.

Insulation applications should be minimized because particulate matter from insulations tends to be small, light, and therefore readily transportable throughout facilities. Insulation type and installation procedure should be planned in advance in order to keep generation of particulates at a minimum.

3.5 Thermal insulation of heated components

Components like permeators, catalyst vessels, getter beds, adsorber beds in the regeneration mode, vaporizers, etc. operating regularly or occasionally with substantial partial pressures of tritium while at elevated temperatures, may release tritium into the glove box atmosphere via permeation through the hot outer surfaces of the primary containment. To avoid such releases these components are normally protected by a vacuum jacket, especially when the process temperature becomes appreciable. Secondary containments are habitually built to UHV-standards to allow evacuation down to very low pressures in order to minimize heat transport by gas convection. Insulation from radiation heat is achieved with thermal reflectors installed inside of the second containment in the proximity of the heat source. They usually consist of thin molybdenum sheets placed annularly as well as at bottom and top of the heat source. These measures contribute effectively to keep the temperature of the outer wall at acceptable values and tritium permeation into the glove box at tolerable levels.

Good **vacuum insulation** constitutes a very proficient barrier to heat transport from the heat source to the outer wall of the secondary containment. However, under static conditions (no enduring pumping) vacuum will quickly deteriorate if there is appreciable permeation of hydrogen isotopologues from the primary containment. This problem is habitually solved either

by continuous or intermittent evacuation of the annular space employing a suitable pump combination. While uninterrupted pumping represents the most common approach, electrical or mechanical failures of the pumping system with possible repercussions on safety cannot be excluded. Therefore, a dedicated hydrogen getter bed is considered to be an efficient, safe, and simple alternative. In fact, with a zirconium/cobalt storage bed attached directly to the isolation vacuum of a permeator operated at 623 K the isolation vacuum could be maintained constant at low lewel for several days [Pen95c]. Because permeated hydrogen is chemically rather pure it will quickly react with the metallic powder in the getter bed. To maintain the efficiency of the getter bed, periodical evacuation of decay helium, which gradually accumulates in the gas phase, is necessary.

3.6 Active cooling of tritium processing components

Heated vessels or components integrated into tritium handling equipment installed in glove boxes may release tritium across their walls via permeation. Active cooling with a re-circulating gas or with water (or other liquids like for instance glycol) in closed loop operation constitute an efficient procedure to reduce or prevent contamination of the glove box atmosphere. Since the coolant may become contaminated, appropriate precautionary measures are necessary.

3.6.1 Active cooling with chilled water

Chilled water systems should be designed so as to minimize the volume of water that potentially can undergo contamination with tritium. Whereas the volume of the secondary cooling system is usually much larger than that of the primary loop the opposite holds for the degree of contamination.

When cooling is carried out with water, possible formation of **algae** needs to be avoided. For this reason, light-transparent hoses, which are known to enhance the formation of algae, shall not be employed.

The most frequently used approach to dissipate heat from a single heated component operated with tritium consists in double walled water/gas or water/chilled water heat exchangers [Cof73; And02]. In the special case of a small primary system containing tritium at a significant partial

pressure while operated at elevated temperature, an additional third closed water loop may be necessary for enhanced safety.

Modern **local cooling systems** using **chilled water** can be placed outside of glove boxes. They are reliable, small sized, low in cost, easy to maintain and and readily available from numerous manufactures in diverse configurations. Main drawback of local cooling units running with water is their "open system" character with potential for contamination spread into the environment. Therefore they can only be employed to cool equipment handling trace amounts of tritium which perform with negligible permeation.

Research institutions are frequently equipped with dedicated heat exchangers for the removal of heat from glove boxes or experiments. Water is recirculated through heat exchangers by redundant pumps and heat dissipated into a secondary loop via a water/water heat exchanger provided with a hydraulic separation.

In larger tritium research facilities like TLK chilled water is needed to cool i) diverse components integrated into primary systems, ii) numerous adsorber beds integrated into tritium retention systems, and iii) the room air conditioning system. Chilled water (278 - 283 K) is supplied at TLK in closed loop mode from a central appropriately sized system installed in the basement of the laboratory [Sch91a]. Dependable availability of chilled water is warranted by two buffer tanks, each having a capacity of 10 m^3. These tanks are connected in series and permanently on standby. Two turbo refrigerators, each with a wattage of 800 kW, are used for cooling of the water. According to the design, in case of power supply failure, the chilled water in the buffer tanks suffices to maintain operation of all critical systems until the cause of failure has been identified and eliminated. Possible contamination of the secondary cooling loop by tritium arising from leakage or permeation across heat exchangers is detected at an early stage by routine sampling and water analysis employing conventional liquid scintillation spectrometry. Once limit values are exceeded the tritium source must be localized and eliminated. After this has been accomplished and the contaminated water been exchanged by pristine one operations may be resumed. Tritium-contaminated water is regularly fed via a direct line into a large central waste collection tank and delivered to Hauptabteilung Dekontaminationsbetriebe (Decontamination Service) of KIT following pre-established procedures.

At the tritium building of TSTA, Los Alamos [And82], primary and secondary cooling loops were cross connected via a heat exchanger. This ensured that tritium, eventually permeated

or leaked into the primary cooling loop, could not directly contaminate the secondary cooling water system. Water from the secondary cooling loop was recirculated through a cooling tower installed outside of the controlled area. Adequate provisions were necessary to prevent freezing of outdoor lines in winter. When the secondary water coolant was operated in once-through mode, the utilized water was sent to the laboratory acid waste disposal container. Because cooling of the Tritium Waste Treatment (TWT) and the Emergency Tritium Clean-up (ETC) systems of TSTA were critical, ample redundancy was provided. In the event of an emergency, switching over to the utility water supply was possible.

The far-reaching importance of the **Cooling Water System of ITER** [ITE01a] is readily understood when the list of some of the crucial safety tasks of this system is examined: i) removal of heat deposited in in-vessel components, the vacuum vessel, special heating systems, and diverse diagnostics during the burn cycle ii) safeguarding in-vessel components at less than 658 K after plasma termination to avoid beryllium - steam reactions, iii) preservation of coolant temperatures, pressures, flow rates to limit margins, iv) removal of decay heat during normal and off normal operations, v) accommodation of draining and procurement of refilling for maintenance periods, vi) maintaining water chemistry as required, v) providing confinement of radioactive inventories, vii) performing measurements of heat removal from in-vessel components and the vacuum vessel, and viii) removal of heat from plant auxiliary systems like radio frequency heating power tubes, neutral beam injectors, etc.

A **Component Cooling Water System** will be available at ITER for components like pumps, plasma heating systems, and power supply systems. Additionally, a **Chilled Water System** will provide chilled water (267 K) mainly to the heating, ventilation, air conditioning (HVAC), and detritiation systems.

3.6.2 Active cooling with gas

Coaxial cooling with inert gas is frequently utilized to cool tritium storage beds enclosing a metal tritide getter for tritium storage and delivery. Typical cooling tasks with getter beds are: i) rapid cooling of the getter after exothermal absorption of tritium, ii) storage bed cooling after tritium release, iii) support of calorimetric in-bed measurements, etc.

In case of adsorber beds, cooling is required after completion of tritium release in order to reactivate the bed.

Drawbacks of component cooling with gases are the required rather large heat exchange surface area as well as the necessary high gas throughput. Gas-to-gas heat exchangers utilizing forced gas cooling are hence not generally applicable.

3.7 Soldering

Soldered joints shall be brazed and the residual flux carefully removed by appropriate well-established procedures. Principal difference between **soft** and **hard soldering** is that the former is performed with a soldering iron and the latter with a torch, i.e. at higher temperature.

In the old days, silver brazing of copper and stainless-steel components of tritium handling equipment was common [Hol63]. All process tubing within the inert-atmosphere boxes at TSTA were of series 300 stainless-steel or deoxidized high phosphorus (DHP) copper. Copper lines integrated into the basic process loop of TSTA (151 valves) were joined by hard soldering [And82].

Soft soldering can produce - provided made correctly - strong joints at comparatively low temperatures. In spite of this, they are not permitted for tritium primary systems.

At Mound Plant in Miamisburg an older valve failed causing a release of tritium because of progressive degradation of the lead-tin soft solder joint (the break was oxidized).

3.8 Welding

The most widely employed methods for joining stainless-steel components are welding by heliarc, tungsten inert gas (TIG), or electron beam. Another frequently used welding procedure to join components is silver solder brazing. TIG welding was used at TSTA to attach fittings of metal sealed KF, Varian ConFlat, or Cajon VCR type to stainless-steel tubings [And82].

Welds must be carried out in accordance with recognized **Standards** taking into account the most recent **Explanatory Leaflets** following the latest state of the art. Only approved welders having sufficient experience with the materials to be welded should be authorized.

For the manufacture of equipment destined to tritium service careful in advance planning of all welds is compulsory in order to permit non-destructive inspection of welds and avoid

formation of crevices or cracks in weld joints of containments after their exposure to gaseous or liquid tritium (see also section 3.8.5). In view of the importance of welding for the safe enclosure of radioactive gases, this subject will be addressed in more detail below.

3.8.1 Welding procedures

Prior to welding all surfaces must be meticulously cleaned by chemical and physical means. Austenitic materials must be pickled and passivated. Welds should be continuous and have no gaps. If possible, the distance between weld seams should be larger than 30 mm. Cross seams should be avoided. Advanced welding techniques, such as electron beam welding, that do not require multiple passes, were found to be advantageous for the manufacture of tritium-exposed components.

Evidence from experience is that certain type of welds have larger tendency to crack under mechanical stress than others.

Vendors fabricating equipment for Savannah River Site (SRS), USA, a large facility that has to comply with exigent tritium standards, are asked to submit an acceptable white weld sample. The sample should be a pair of pipe caps of the same type austenitic stainless-steel as specified for the equipment item. The welded sample should be cut in two halves each marked with the purchase order number. The vendor retains one half and the other half is sent to the cognizant engineer responsible for the order. This engineer has the welded half inspected by the welding engineer before the vendor is allowed to fabricate equipment. The supplied sample is used as a guide for the white weld acceptance procedure.

Current foremost welding operations ongoing within the frame of the construction of ITER comprise: i) the base, lower cylinder, upper cylinder and top lid of the ITER cryostat, which keeps the magnets at superconducting temperature of 4.2 K, to be welded at the Tokamak site (responsibility of India), ii) three laser robots for welding double pancake of the ITER toroidal field coils in La Spezia (responsibility of Italy, Europe), and iii) current leads for the high temperature superconductor (responsibility of China) [Bal12].

3.8.2 Welding requirements

Some welding requirements for the manufacture of technical systems established over the years from experience accumulated in tritium facilities like Savannah River Site [Poo08] or TLK[10] are described below (see also Appendix N and Appendix O). The intention here is not to convey a comprehensive or consistent set of requirements, but rather to put across some of the numerous aspects requiring attention. A singular set of requirements must be specified for every institution by the pertinent authority.

- Welding procedures and welders shall be qualified by generally accepted procedures like for example Section IX of the ASME Boiler and Pressure vessel code or AD explanatory leaflets, DIN 8563, and DIN 8560.
- Preceding welding, the interior and exterior of all involved equipment shall be thoroughly cleaned.
- Stainless-steel brushes free of dirt and grease used previously only on stainless-steel shall be employed to clean between passes and on completed welds.
- Grinding wheels used for cleaning and grinding welds shall be no coarser than 60 grit and shall be new or previously used only on stainless-steel.
- Welding surfaces and a 1.3 cm band of adjacent base metal on each side of the weld shall be cleaned to bright metal immediately before assembling of welding. The equipment shall be purged with argon or helium (minimum 99.9 % purity) until the initial tack weld and subsequent welding meets inspection acceptance criteria.
- Filler materials having by and large the same chemical composition as that of the base metal shall be chosen. Only filler materials previously tested and found suitable by a recognized authority, e.g. Technischer Überwachungsverein (TÜV), Germany, shall be used. The filler material should be certified for instance according to DIN 50049/2.3. Electrodes must be dried before use. Only core-wire alloyed filler materials are allowed.
- Full penetration weld connections of stainless-steel pipes shall be carried out when using inert gas-tungsten welding (TIG) or electron beam welding procedures.

[10] Technische Liefer- und Annahmebedingungen, Kernforschungszentrum Karlsruhe, December (1987).

- Cross section reduction of a pipe due to welding must remain below 15 %.
- Root passes (first weld bead of multiple pass weld) must be carefully finished and cross welded.
- At least two passes must be welded and initial and final positions must be staggered.
- Chill/backing rings may be used for piping welds in the secondary confinement systems and service systems.
- Chill/backing rings are not authorized to be used in hot or cold nitrogen systems due to the thermal cycling load on the hot and cold segment of the system.
- Gas welding is not permitted.

3.8.3 Welding inspection

Typical, probably uncomplete welding inspection procedures such as recommended at Savannah River Site are given below for orientation [Poo08] (the responsibility remains with the respective Design Authority.):

- The back side of white tack weldings shall be visually inspected and accepted per acceptance criteria prior to welding root pass on vessel closure head weld.
- The back side of each completed root pass segment shall be visually inspected (where accessible) and accepted per acceptance criteria prior to completing the root pass. Lights, mirrors, and borescopes may be used to perform the inspection.
- Visual weld inspections shall be performed on as much as possible of the completed white weld by a certified welding inspector.
- Full penetration butt welds of piping shall be radiographed per appropriate code category, e.g. ASME B31.3. Radiograph requirements for full penetration butt welds of piping is 5 % volumetric in normal service, 20 % volumetric for category M service, and 100 % for high pressure or severe cycling service.

- All full penetration butt welds of tritium storage vessels shall be radiographed, e.g. per ASME Section VIII. Prior to making the vessel head closure weld, all required non-destructive examinations shall be performed and accepted.

Weldments can be scrutinised for surface defects by a colour contrast **dye penetrant inspection**. For this purpose, the surface must first be cleaned from loose solids and degreased. The penetrant is applied by brushing or spraying. After waiting for not less than 15 min and not more than 20 min the excess penetrant must be removed with a cloth. Immediately after the removal of the penetrant the developer is applied by spraying. Interpretation should be carried out under good light conditions within a period of 15 min following application of the developer[11].

Radiographic examination of fusion welded circumferential butt joints in steel pipework is the most frequently employed non-destructive appraisal method. Materials with thicknesses between 2 mm and 80 mm can be subjected to this technique[12]. Depending on size and shape of the pipe either i) a single wall single image (radiation passes through only one wall and merely the material on the film side is viewed), ii) a double wall single image (radiation passes through two walls of the material and only the material on the film side is viewed) or iii) a double wall double image (radiation passes through two walls of the material and both walls are viewed) examination can be carried out (see Fig. 3.8). A very fine grain film of high contrast such as Kodak AS, Agfa D7, or Fuji IX100 are habitually used. Radiographers must be certified to a minimum of "American Society for Non-destructive Testing" (ASNT) level 1 and the interpretation must also be performed by personnel with corresponding qualifications, e.g. passed Certification Scheme for Welding and Inspection Personnel (CSWIP) examination. The interpretation must be performed by a radiographic viewer in a darkened room. After the examination workpieces shall be marked lastingly with a date point that allows accurate relocation.

[11] Possible penetrant - developer combinations are either ARDOX 996P - ARDOX 9D6F or CASTROL CHECKMOR 222 - CASTROL LD-2.
[12] Further detailed information on radiographic techniques can be found in BS EN ISO 17636-2:2013 and BS EN ISO 17636-1:2013.
[13] QA Mechanical Services Ltd. South Wirral. 1990.

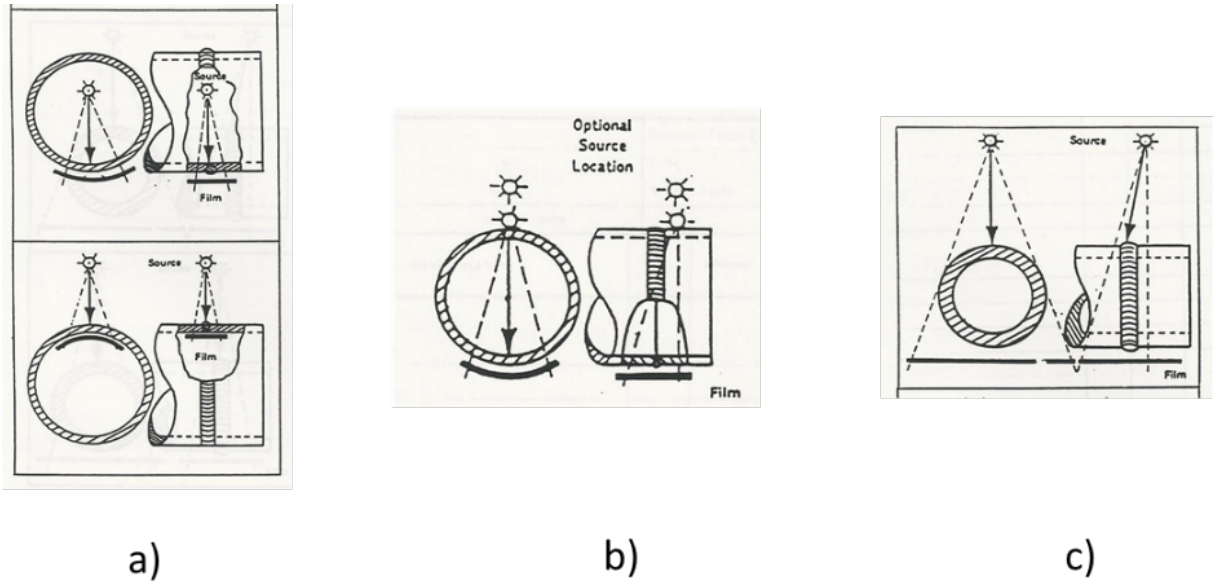


Figure 3.8: Radiographic examination techniques of butt welds. Optional procedures: a) single wall - single image, b) double wall - single image, and c) double wall - double image (note position of source in figures b) and c))[13].

3.8.4 Welding acceptance criteria

Typical welding acceptance criteria such as for example recommended at Savannah River Site [Poo08][14]:

- Rows of pores, tube pores, end crater pores, root and bonding defects as well as cracks are not permitted.
- A closure head weld on a vessel is acceptable if it has no discoloration, a straw colour, or 15 cm or less of a slight yellow-grey colour.
- A closure head weld on a vessel is unacceptable if it has blue or darker colour.
- Unless expressly requested, weld seams should not be ground.
- A pipe weld is acceptable if it has no discoloration or straw colour.
- The quality of weld seams that need to be attained is described in DIN 8563, part 3, rating group BS or BK.

[14] Responsibility for the specific requirements of each tritium-relevant project remains with the respective Design Authority

- Radiography of vessels is widely carried out according to UW51 of Section VIII of the ASME Boiler Code.
- Radiographic tests are also described in DIN 54109-54116.
- Radiography of piping is widely carried out per appropriate category ASME B31.3 code for piping.
- Qualifications of steel welders are described in DIN 8560.

3.8.5 Welding of tritium-contaminated stainless-steel

The presence of tritium and of its decay product He^3 in stainless-steel can strongly influence the mechanical and welding properties of this material [Kra68; Lin89; Hir90d; Hir90e; Goo91]. Helium enhances grain boundary cracking by formation of bubbles on carbide particles which in term reduce the amount of grain boundary sliding needed to form a void.

The weldability of stainless-steel previously subjected to contamination by tritium for an extended period of time and consequently displaying bubbles containing trapped decay helium was investigated by Hircq et al. [Hir90d; Hir90e; Hir91b; Cha91b; Hir93]. With the aim of improving understanding of the mechanism of embrittlement, an accelerated pace investigation was initiated at Centre d´Etudes de Bruyères-le-Châtel, France, by loading stainless-steel SS316 specimens with tritium at 673 K and 400 bar. Chanfreau et al. [Cha91b] exposed more SS316L and SS316 stainless-steel sheets at even higher temperature, i.e. 723 K, to nearly pure tritium at pressures within the range 10 - 25 bar for periods lasting about six hours. Under these conditions, rather homogenously loaded specimens displaying high concentrations of tritium and helium were prepared. Details on how loading was performed were not provided. The loaded specimens were subsequently subjected to ageing periods lasting for several months in order to attain accumulated concentrations of decay helium of 35 atom ppm and 66 atom ppm in SS316L and SS316 specimens, respectively. After degassing for up to 300 hours at either 723 or 1373 K under a stream of Ar or Ar/H_2 the helium-enriched specimens were welded by laser, electron beam, or argon arc. The microstructure of the welding bead and of the **heat affected zone (HAZ)** were then examined by optical microscopy, scanning electron microscopy (SEM), and transmission electron microscopy (TEM). Inspection of the welds revealed helium bubbles and cracks in the

welding bead and grain boundaries as well as intergranular decoherences in the HAZ. Bubble density and size was particularly large in specimens welded by tungsten inert gas welding (TIG). Increasing temperatures and duration of heat exposures increased the size of the bubbles. Tensile tests carried out with electron beam welded specimens containing between 6 and 24 appm helium revealed that the elastic limit increases with helium content. Examination by SEM showed ductile fracture facies in all cases. The investigators concluded that helium coalescence occurred in welds regardless of the welding techniques and even when the concentrations of helium were low. Because of the observed degradation of the mechanical properties they cautioned from welding aged stainless-steel materials pre-exposed to tritium. The dependence of helium precipitation from the type of heat treatments and microstructure were compared between welded and pristine specimens. The techniques used were optical microscopy, scanning electron microscopy, and small angle neutron scattering. Additionally, the distribution of tritium remaining in the microstructure was obtained by autoradiography measurements. The results document preferential location of tritium in the grain boundary zones. It was speculated that this may be due to intergranular precipitation of helium bubbles containing co-precipitated tritium or to an interaction between tritium and the stress field around the bubbles.

Goods and Karfs [Goo91] also studied the influence of helium on the weldability of type SS304 stainless-steel. Two types of weldings were compared: i) conventional gas metal arc (GMA) stringer bead weldings and ii) a novel GMA of very shallow penetration. Helium-3 concentrations in the range 2.7 - 85.0 appm were generated in test specimens by exposure to tritium and subsequent buildup of helium-3 by ageing. Scanning electron microscopy (SEM) revealed intergranular cracks in the HAZ of all samples containing helium and none in helium-free control specimens. The extent of cracks, i.e. total number, crack length, etc. was comparatively smaller in the novel GMA shallow penetration welds. The results lead to the conclusion, that degradation of weldability was extremely sensitive to helium concentration, the specific welding procedure, and the degree of heat input. In response to the welding process, the helium bubbles that resided at grain boundaries grew and coalesced. The coalescence of these relatively uniform arrays of grain boundary bubbles gave rise in the end to the characteristic dimple structure of the intergranular crack facets of the HAZ.

Carmichael and Haynes [Car91] applied heat with a propane torch for a short time to tritium contaminated tubing prior to welding. The objective was to drive out most of the bulk tritium.

When ends of this tubing were welded, the released HTO levels reached relatively low hazard levels of only $37\,\mathrm{MBq\,m^{-3}}$ (MPC = maximum permissible concentration of tritium oxide = $0.37\,\mathrm{MBq\,m^{-3}}$). This was considered evidence for the effectiveness of preheating. Welding was performed while continuously removing contaminated air with an "elephant trunk".

In accordance with expectations, the discussed results revealed that welding of tritium-contaminated material is associated with tritium enrichment on both sides of the weld and an intense precipitation of helium bubbles on grain boundaries. The latter induces formation of macroscopically observable severe intergranular cracking in the HAZ. Tritium depletion in the HAZ is ascribed to enhanced diffusion and solubility of tritium on account of the elevated temperature. Helium bubbles occur both inter and intra granularly; their size distribution is broad. Autoradiography performed far from the weld indicates that tritium localizes preferentially on grain boundaries, which presumably is favoured by the intergranular precipitation of helium bubbles (see also [Abr78]). In fact, precipitation of helium bubbles in austenitic steel is known to require temperatures in excess of 873 K [Kra68].

3.8.6 Remote welding

Several tools and techniques for remote welding under conditions of restricted access because of radioactive contamination were developed at JET [Tai00]. Among the alternative welding methods, autogenous overlapping spot welding was selected because of i) the simplicity and reliability of the technique, and ii) the fact that the required tool is simple and of comparably small size. This is advantageous when there is need to cope with space limitations.

3.9 Remote/automated operation of tritium handling systems

To warrant the necessary flexibility for equipment selection, process design, and process conduction of small size or technical tritium experiments still in their preliminary research phase it is generally preferable to test their performance manually. Once an experiment is well established and runs reliably, it is beneficial and as a rule much safer to operate it remotely. This holds particularly for experiments of long duration. In case of large technical experiments or laboratory infrastructure systems relying on proven technology and requiring routine operation it may likewise be advantageous to run them remotely. Important advantages of remote processing are

easiness of operation, the option of unattended process conduction, ubiquitous data recording, and last nor least enhanced safety.

Technical experiments and infrastructure systems at TLK like the complex plasma exhaust clean-up facility CAPER, the displacement isotope separation system (DISS), the water detritiation experiment TRENTA, and others, have all been equipped with dedicated Siemens Process Control Systems[15]. Six old Teleperm AS488 automation systems and their corresponding Simatic S5 servicing the laboratory infrastructure were replaced and upgraded 2012 by a Simatic PCS7-AS417. Each control system consists of an AS416 automation unit, a PCS7/OS visualization unit, and a service module based on Windows XP. For these systems, there is complete separation between hardwired modular safety circuits, computer supported process control, and monitoring systems. Safety and Diagnostic Design features systematic and progressively more specific localization of failed components. Circuit breakers comprise a separate alarm circuit and one collective message per cabinet to the process control system.

Warnings, alarms, and trips are configured at TLK in ascending order of priority. They are easily identifiable by a characteristic colour. An active alarm list comprises outstanding and not yet acknowledged alarms. Man/machine interfaces (MMI) are standardized on the basis of concepts developed for the chemical industry, e.g. NAMUR code (Normenarbeitsgemeinschaft für die Mess- und Regelungstechnik). Safe states were defined in such a way that if a single system begins to operate outside of the normal envelope an early shutdown and orderly recovery of the whole system must take place. This is considered safer than continuing with the operation of single sections. Moreover, there is normally of no major benefit when sections of a tritium system continue to operate whilst others are shut down. This safety strategy allows simple control logic and makes the need to examine consequences of possible cascade effects unnecessary. It is furthermore of significant benefit when revising existing or writing new control software for the process. In other words, changes to process control can be carried out with only few and simple software modifications without requiring a strict review of the complete shutdown sequences.

Analogously, the large and complex experimental facility JET is designed for complete remote operation from a control room using the computerized Control and Data Acquisition System (CODAS) [Sto99]. CODAS is a large UNIX-based system, custom build to JET design specifications [Sch98]. To illustrate the complexity of the control process of JET, which has been

[15] Schäfer, P. 2008. Personal communication.

operated with tritium for prolonged periods of time, a very brief description of the pertaining system is provided. As may be expected, most processes of this facility are fully automated by real time control software [Pea99b; Lae99b]. For process control the facility utilizes a commercial Distributed Control System (DCS) from Fischer and Porter connected to 3400 inputs and outputs. 414 of these inputs are analogue. Seventeen Distributed Control Units (DCU) take care of the control of the whole plant. Within these DCU´s there are 140 automated sequences and 51 analogue proportional **integral derivative controllers** (PID controllers). As well known, PDI´s have found wide and successful application in industrial control systems. Because each DCU controls a separate section of the plant, a failure in one control unit is of no consequence to the others. All DCU´s are connected to a dual ETHER-NET highway. They provide data to four PDP miniframes (DOC 2500). Each of the latter drive two operator consoles, which leads to a total number of eight consoles. Analogue inputs are recorded on 343 displays, which trend nearly one thousand points. A new DCS (SYSTEM SIX UNIX miniframe) has been connected to the ETHER-NET and has 24 displays trending ninety points. Another miniframe (CEU-2500) has also been connected to the highway. Both the AP-6400 and the CEU-2500 periodically perform calculations like conversion of measured ionisation chamber currents into tritium concentrations, estimation of tritium inventory, etc. In addition to the above, the Cryo Distillation and the Exhaust Detritiation Subsystems are controlled by two stand-alone Siemens S5-135U PLC´s, which can communicate with the Fischer and Porter system.

Summarizing, the design of safety and process control is a rather multifaceted undertaking. The assignment includes detailed specification of the whole process control structure, definition of standardized signals, specification of central and decentral operations, philosophy of operation, in particular mode and sequence of operations, display of process loops, P & I flow charts, identification of operations with confirmatory action, partitioning of cabinets, assessment of the need of reserves, standardization of signals, development of concepts for messages (warning, alarm, trips), grounding and shielding concept, etc.

3.10 Radiation protection of workers

When dealing with radioactive materials it is necessary to distinguish between **radioactivity** which is measured in Bq and **radiotoxicity** measured in Sv. Whereas radioactivity gives the number of disintegrations per unit time irrespective of the kind of radioisotope decaying and type of radiation emitted, radiotoxicity expresses the hazard potential of a dose received from radioactive material incorporated into a body. The dose depends on type and energy of the emitted rays, residence time of the radioactive material in the body, absorption path into the organism, the place of residence in the body, etc.

Workers in most tritium handling laboratories, are indirectly protected from possible contaminations by redundant tritium monitoring systems controlling the atmosphere of glove boxes, the laboratory ambient air, and the exhaust air released into the environment via stack. For example, at TLK early warning takes place via i) nearly 20 ionisation chambers monitoring the room air, ii) about the same number of monitors surveying the atmosphere of glove boxes and iii) one ionisation chamber together with a proportional counter monitoring the exhaust gas released through stack (see Fig. 3.9). Pre-alarms are transmitted solely to the Radiation Protection Service and the Control Room of the TLK, which take actions after verification of the alarm. Main alarms are additionally forwarded to the Central Alarm Station of Karlsruhe Institute of Technology.

Suspected contaminations of personnel must be reported immediately to the Radiation Protection Service and to the authorized Radiation Protection Officer responsible for the tritium handling facility. After elapsing of more than two hours from the point in time where the alleged contamination has taken place, urine samples are collected from the implicated workers and analysed for their tritium content by standardized procedures.

By way of example, incorporation of 3×10^9 Bq by a person weighting 80 kg will yield a concentration of tritium in urine of about

$$\text{conc. in urine} = \frac{3 \times 10^9}{80 \cdot 0.67} = 5.6 \times 10^7 \,\text{Bq}\,\text{l}^{-1} \ .$$

This calculation assumes that approximately two thirds of the human body consist of water.

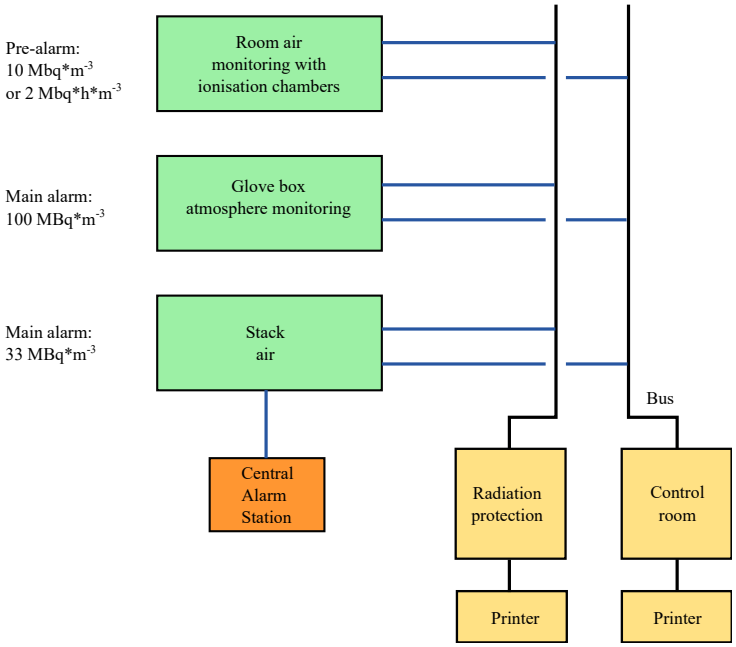


Figure 3.9: Redundant alarms from tritium monitoring at TLK.

In the event of a contamination all instructions given by the Radiation Protection Officer shall be followed.

3.11 Handling of contaminated materials or equipment

Regular and frequent wipe tests constitute a helpful radiation protection measure to determine the possible contamination of a surface. In a tritium handling facility decontamination becomes necessary once a surface contamination exceeds $50\,\mathrm{Bq\,cm^{-2}}$. Objects whose surface contamination surpasses $5\,\mathrm{Bq\,cm^{-2}}$ shall not be taken out of the controlled area. Before contaminated objects are taken out, they must be decontaminated and cleared by radiation protection.

Disposable gloves should be worn when touching or handling materials or equipment that are or could be contaminated. Inexpensive gloves made of latex or polyvinylchloride (PVC) can contribute significantly to minimize tritium uptake through the skin. They should be discarded after each use to preclude spreading of contamination. For their disposal, an adequate number of special containers should be available in the laboratory for this purpose. PVC is generally the preferred material for disposable gloves because of its low permeability to tritiated species and

high resistance to chemicals. Of concern is the potential occurrence of manufacture deficiencies or pinholes in the gloves arising when handling sharp objects.

If the floor of a tritium-handling room becomes contaminated, protective plastic overshoes should be worn and removed before exiting the contaminated area in order to avoid spreading of contamination into clean areas of the building.

All transports of radioactive materials in or out of a tritium handling facility should be documented in a special Book of Transports.

3.12 Cleaning stainless-steel surfaces to minimize formation of tritiated hydrocarbons

There is experimental evidence for the generation of tritiated water and small amounts of tritiated hydrocarbons in stainless-steel vessels containing gaseous hydrogen highly enriched in tritium. The production rate of tritiated methane was found to be roughly proportional to the surface/volume ratio of the vessel and the partial pressure of tritium. Therefore, cleaning the inner metallic surfaces of vessels used in tritium-handling systems is essential to reduce extraneous species in contained tritium.

Systematic investigations carried out by Gill [Gil80] provided evidence that cleaning the inner surface of stainless-steel vessels can significantly reduce the in-growth of tritiated hydrocarbons into pure tritium gas. Another reason for cleaning is corrosion prevention, which is of concern from a safety point of view.

Screening tests carried out at 298 K and 373 K employing SS304 specimens pre-exposed to 124 kPa of tritium revealed that the rate of methane production strongly depends on the previous cleaning history [Mor77]. In methodical experiments with a number of test vessels having a volume of 293 cm^3, the effectiveness of the following conditioning methods was compared:

- **Baking:** removal of surface carbon by baking under a vacuum of 0.1 - 0.5 Pa at 423 - 433 K for 12 hours,
- **Washing:** rinsing with trichloro-trifluoro-ethane or degreasing with trichloroethylene in an ultrasonic bath followed by rinsing with acetone and trichloro-trifluoro-ethane,

- **Mechanical treatment:** mechanical treatment either with a stainless-steel brush or by removal of 0.254 mm layer from the inner surface and
- **Heating:** extended baking at 373 K. The observed steady state methane build-up rates were found to be in the range between 2 and $> 40\,cm^3$ (STP)/m^2 of exposed surface depending on the selected conditioning method.

From the results it was concluded that the best method for minimizing methane formation was mechanical cleaning of the surface and rinsing of the surface with trichloro trifluoro ethane. Neither baking nor mere cleaning with tetrachloroethylene were found to be effective enough for the removal of carbon from the surface.

3.12.1 Cleaning austenitic steel surfaces

Generally, the type of cleaning procedure is singular to each kind of material. Surfaces of austenitic steel are first cleaned from dirt and dust with a steam jet and/or by rinsing with de-ionized water. Forging scales are removed by i) brushing with a stainless-steel brush, ii) treatment with a glass jet when the surface roughness exceeds 20 µm or iii) washing with a pickling solution that should not contain chlorides. While removal of rust and of other extraneous matter by pickling with freshly prepared 22.5 % HNO_3 (52 % in water), 2.5 % HF (40 % in water) and 75 % demineralised water at 293 K circulated for approx. 2 hours has yielded good results, this commonly applied procedure should not be utilized because of HF.

For the removal of grease from stainless-steel surfaces organic solvents should be avoided to preclude formation of a residual grease film upon evaporation of the solvent. Fluorinated and chlorinated hydrocarbons should not be used as degreasing agents because of the danger of pit corrosion. Effective results have been obtained with 3.5 % Grisiron 6729 (Hoechst Aktiengesellschaft, Frankfurt/M, Germany) and 1.5 % Grisiron 9116 diluted in 95 % demineralised water. Cleaning is performed at 333 K for approx. 30 min. After cleaning, it is necessary to rinse the surface with pure water.

Piping of less than 2.5 cm diameter and equipment of less than 0.1 m^2 surface area can be cleaned with Vertrel® MCA. Vertrel® MCA is an azeotrope of Vertrel® XF and trans-1,2 dichloroethylene ideal for utilization with a vapour degreaser machine or for manual use by wiping, spraying, or flushing through the soiled equipment. It can be used to clean from cutting

oils, gear oils, heavy grease, vacuum oils, waxes, and mineral oils; it is not classified as flammable. Knowledge on re-use, re-cycle, and disposal of Vertrel® may be of benefit [Poo08].

Steam/detergent cleaning with a water solution of Pennwalt Cleaner MC-79 (obtainable from Pennwalt Corp. in Philadelphia, PA) constitutes a frequently employed choice. For pipes larger than 7.5 cm in diameter a steam wand (rigid tube between nozzle and hose) that passes through the length of the pipe should be used. All surfaces cleaned with steam detergent must be thoroughly flushed with de-ionized water.

High pressure water blast cleaning has been found to be applicable for pipes of 2.5 cm diameter or more. High pressure water is delivered through a wand at about 3000 psig. To be effective the wand must reach all surfaces requiring cleaning. Equipment cleaned with high pressure water should be flushed with 95 % ethyl alcohol or de-ionized water.

Another surface cleaning option is electro-polishing. This treatment generates a smooth surface of reduced active metal surface area. Because hydrogen is at the same time incorporated into the metal an adverse source of protium is created that may cause contamination of pure deuterium or tritium contained in a primary system.

A very effective procedure to clean metallic surfaces incorporated into equipment destined to tritium service is treatment with oxygen plasma. Cleaning equipment such as required for oxygen plasma treatment is distributed by Compressed Gas Association Inc. (CGA G4.1) and Savannah River Laboratories. This technology serves to remove all harmful organic and inorganic materials, such as oil, greases, paper, fibre, rags, wood, coal dust, etc. It was reported that oxygen plasma is much more effective than washing of electro-polished stainless-steel with solvents. A variety of cleaning methods described in CGA G4.1 (see Appendix N) apply to diverse types of materials.

Surface passivation is conventionally performed with 15 % nitric acid containing a wetting agent such as Pril (0.1 %) at a temperature of 313 K for a period of 15 - 30 min. After cleaning and flushing it is necessary to dry the equipment. For this purpose, clean, oil-free compressed nitrogen, argon, or air are used at ambient temperature. Gases employed for drying should not contain particles larger than 50 microns.

Specific cleaning procedures recommended by various vendors for their own products should be **reviewed** and **approved** by the Design Authority to verify that they comply with all exigent demands for tritium service.

3.12.2 Cleanliness verification

Subsequent to visual inspection, a common procedure for verification of cleanliness of vessels consists in performing the following three tests: i) hydrocarbon test by infra-red spectroscopy, ii) halide test to determine the presence of chlorides, and iii) a test to determine the presence of adhered solid materials on the inner surfaces.

- For the **hydrocarbon test** the inner surface of the vessel is first flushed with 0.05 - 0.11 cm^3 of Vertrel® per cm^2 (The Chemours Co., Wilmington, USA). Then, an aliquot of the drainage is taken and analysed by infrared spectroscopy. The drained solvent shall not contain more than 100 ppm by weight of hydrocarbons.

- The **halide test** consists in flushing the inside surface of the vessel with a small amount of de-ionized water, e.g. 0.05 - 0.11 cm^3/cm^2 surface. The concentration of halides is then determined in an aliquot of the drainage by an electrical conductivity measurement (resistance of a solution between two flat electrodes separated by a fixed distance). The measured conductivity shall not exceed 10 µ mho cm. To perform quantitative measurements it is necessary to prepare calibrated solutions.

- For the determination of **adhered solids,** the surface is first washed with a known amount of water and then the drained liquid analysed for suspended solids with a turbidity meter. Turbidity is normally determined with a nephelometer. The instrument should be calibrated with a standard containing formazin polymer. A widely used unit of turbidity is the NTU (nephelometric turbidity unit). A turbidity of 5 NTU or less is acceptable.

3.12.3 Cleaning of ferritic steel

Ferritic steels to be installed in tritium handling equipment must be thoroughly cleaned and degreased. Ferritic steel surfaces have to be coated. Before coating the first treatment is blasting with quartz sand or steel shot (max. grain size 1.2 mm) until the metal becomes shiny. After removal of rust, all surfaces must be meticulously cleaned in order to eliminate blasting residues and dust. This must necessarily be carried out on the same day the surface is blasted. Immediately thereafter, a base coat is applied consisting of a two-component zinc-rich and chemically resistant paint such as manufactured by Epicote, Toronto, Canada. All hollow areas should be filled with

Epicote paste and smoothed out. Thickness of the coat after it becomes dry should lie within the range 30 - 40 µm.

Should coated material be stored for more than three months in the open air, an additional second base coat should be applied. At least 24 hours but not more than 10 days should be allowed between the first and the second base coat.

Surfaces that have already been treated and given a base coat must be provided with two top coats of two-component Epicote enamel. The thickness of the coat after it is dry should be of the order of 90 µm.

Coats should be applied following carefully the instructions provided by the manufacturer. To avoid chemical incompatibilities, base coats, pastes, and top coats should be obtained from the same manufacturer.

3.13 Leak rates

A component is considered leak-tight when its leak rate remains below the value defined for this component. Leak rates are commonly defined in $\mathrm{mbar\,l\,s^{-1}}$. A leak rate of $1\,\mathrm{mbar\,l\,s^{-1}}$ exists in a closed vessel of 1 litre when the pressure increases by 1 mbar in one second or in case of an overpressure decreases by 1 mbar in one second.

It should be kept in mind that leak rates depend on i) diameter and length of the leak, ii) initial pressure difference during the leak rate measurement, and iii) the physical properties of the gas used to carry out the measurement (particularly viscosity and molecular mass). For example, under the same pressure conditions helium flows 2.7 times faster than air. It follows that leak tests require specification of the employed gas.

A special type of leak in vacuum technology is that from holes in a vessel wall with thin connections to the vessel volume. Such holes typically result from imperfect welds, or from a not properly closed demountable joint. As opposed to leaks resulting from pinholes of the containing wall (see Fig. 3.10a), “virtual leaks” will manifest during a leak test by an initially linear pressure increase that levels off once the source of trapped gas is exhausted (see Fig. 3.10b). Of course, a vessel may also show a combination of a real leak and a “virtual leak” (Fig. 3.10c).

Depending on the magnitude of the leak, different leak detection methods are employed for their localization: i) pressure rise (fall) test (up to $10^{-2}\,\mathrm{mbar\,l\,s^{-1}}$), ii) bubble test (up to

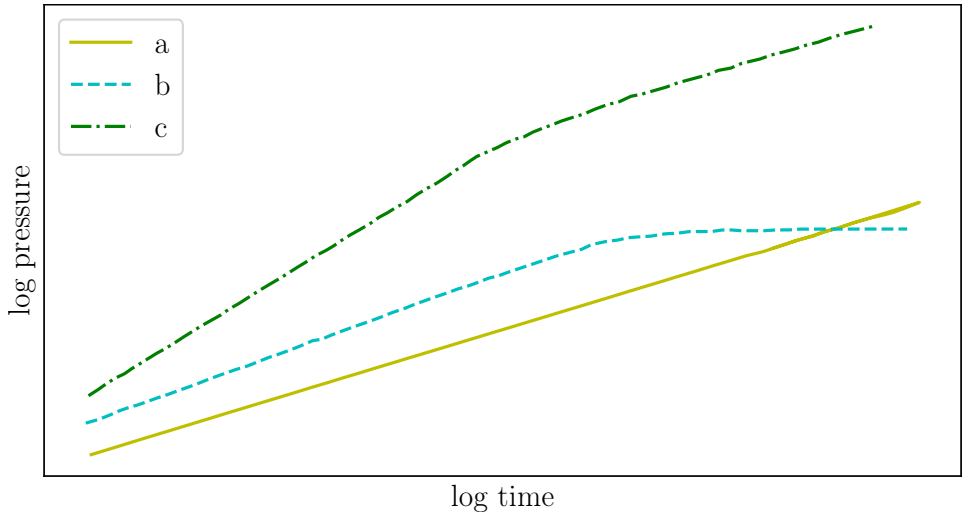


Figure 3.10: Pressure rise in an evacuated chamber caused by a) a leak, b) due to outgassing from the chamber wall, or c) a combination of leak and chamber wall outgassing.

10^{-3} mbar l s^{-1}), iii) sniffer method (10^{-7} mbar l s^{-1}), iv) detection with a helium leak detector (up to 10^{-11} mbar l s^{-1}) and v) the dye penetration method.

The **pressure-rise (fall)** method is applicable to the determination of total leak rates. In this case, the test object must be equipped with an appropriate pressure sensor. After evacuation the volume under test is closed and the pressure rise is followed in time (It is also possible to pressurize the test object and follow the rate of pressure fall).

To perform a **bubble-test** the system under examination is pressurized and the leak is searched with a soap solution applied on the outside of the suspected surface area. A regular formation of bubbles localizes the leak.

Sniff tests are principally used for the detection of small leaks. The system under test is pressurized with a **search gas** like helium, fluoro-hydrocarbons, chloro-hydrocarbons, nitrogen or a radioactive gas. For leak detection the outer surface of the system is scanned with a sniffer probe that is responsive to traces of the search gas in areas where leaks are susceptible to take place, i.e. valves, connections, welds, corrugated tubes, or feedthroughs.

For the detection of extremely small leaks a radioactive gas such as tritium is selected as search gas. It is introduced into the system and a suitable radiation sensor is utilized to sniff the surface. In view of the very low penetration of beta radiation across stainless-steel an interference during sniffing by gaseous tritium present in the system can be excluded. Because of the easy

detectability of tritium, this test is normally carried out after other sniff tests have reached their detection limit.

Helium or halogen detectors can likewise be employed as search gas but in the reverse mode to that with tritium. In this case, the detector is first integrated into to the system or section of the system under test and evacuated. Thereafter, zones of the system where the leak is suspected are sprayed with helium or a halogen-bearing search gas and traces of the search gas quantified either with a **quadrupole mass analyser** or a **sector field mass spectrometer**. The partial pressure of the search gas that establishes in the system during continuous evacuation by the high vacuum system belonging to the selected analytical instrument is then converted into a leak rate using conventional calibration methods.

To determine **total leak rates**, the equipment under test must be completely surrounded by the search gas. Either a hood or another type of plastic envelope may serve for this purpose. The hood must be made of a material strong enough to withstand, without damage, any differential pressure involved. If a flexible hood is evacuated there must be no sharp projections which might tear the hood down when it is drawn up against the equipment. If the equipment under test is leaking, the air flowing through the leak is replaced by search gas and a partial pressure of sniffer gas can build up. The leak detector responds preferentially to the gas and indicates its entry into the system.

Verification that no damage has occurred to the valves during installation of a plant requires singular helium leak tests of seat and stem seal of each valve. When measuring by the sniffer gas method the response needs to be compared with that of a certified reference leak. The search gas is applied first to the reference leak and thereafter to that of the test leak.

The **dye penetration test** is frequently used to find cracks in metals and defects in welds. It employs a low viscosity fluid of high surface migration rate. In practice, the surface under examination is painted on one side of the suspected leak site with the liquid, which after a certain time will appear on the other side of the wall.

Gas leak rates are defined by equation

$$Q = \frac{\Delta P \cdot V}{\Delta t}$$

where V is the volume of the vessel, ΔP the pressure increment, and Δt the time period in which the increment takes place. Table 3.3 shows typical leak rates of primary systems designed to contain tritium-bearing gases. In general, single helium leak rates should be lower than $10^{-9}\,\mathrm{mbar\,l\,s^{-1}}$ and total helium leak rates lower than $10^{-8}\,\mathrm{mbar\,l\,s^{-1}}$.

Table 3.3: Maximum helium leak rates of ultra-high vacuum equipment (containment volume l).

System	Max. leak rate ($\mathrm{mbar\,l\,s^{-1}}$)
Joints, valves, or fittings	1×10^{-9}
Other items (up to 10 l)	1×10^{-9}
System, subassembly (over 10 l)	1×10^{-8}
Complete installed system or assembly	1×10^{-8}

3.14 Typical components used in tritium systems

Every component utilized in experimental or technical installations handling tritium must be designed and manufactured according to very exigent standards. All tritium-enclosing components must be of fully metallic or ceramic construction and of very high leak-tightness. Plastics and elastomers as well as lubricants must be confined to zones where no or only very low concentrations of tritium are conceivable.

3.14.1 Pumps

Some of the more widely used pumping devices installed in tritium facilities all over the world under a broad spectrum of occasionally extreme conditions are described and evaluated in this section. Because pumps have been implemented in rather different applications, they are based on distinctive design concepts and cover a rather broad spectrum of diverse pumping parameters. A special feature common to all components destined to tritium service is the need to demonstrate their aptness first under representative conditions but without tritium and subsequently in its presence. Within this frame, long-term endurance tests with tritium are also of particular importance from the point of view of availability and safety. As a consequence, it generally takes several years before a new pumping concept becomes a realistic alternative.

In view of the above and because number and type of available tritium-compatible pumps is rather large and new products regularly keep appearing on the market, it is neither possible nor meaningful to attempt to generate a complete list of pumping options or to concentrate predominantly on the more recent developments. Arguably, some of the pumps discussed in this manual are rather old and some have even disappeared from the market. However, practical knowledge gained from their performance in tritium service remains valuable and applicable on one hand because the materials employed for their manufacture have not changed significantly and on the other because their basic design and working principles persist sometimes only in marginally upgraded form or a more modern design.

As already stressed, tritium-compatible pumps must operate without oil, grease, or rubber sealing's because these materials may interact with tritium either hardening or decomposing to yield products which may be deleterious not only to the pump performance but also to adjacent equipment belonging to other process steps. A fundamental requirement of all pumps destined to tritium service is rather high and enduring leak tightness. The "dead volume" of the pumps should be small in order to maintain the tritium inventory low.

3.14.1.1 Magnetically suspended turbo molecular pumps

For the evacuation of tritium-bearing gases from a primary system down to ultra-high vacuum level a combination of pumps consisting of a turbo molecular pump (TMP) equipped with magnetically levitated rotors together with a suitable roughing pump or combination of pumps have been extensively demonstrated over decades in numerous research laboratories and technical tritium facilities. The experience gained from routine operations has generally been satisfactory. Turbomolecular pumps can easily achieve vacua of 10^{-10} mbar provided the evacuated equipment is sufficiently vacuum-tight. Because these pumping systems use no lubricants, the evacuated zone is only slightly contaminated by hydrocarbons resulting from the interaction of gaseous tritium with carbon contaminating the surface of stainless-steel.

Well established manufacturers of TMPs are:

- **Balzers/Pfeiffer** manufactures pumps featuring pumping speeds in the range 50 - 1000 $\mathrm{l\,s^{-1}}$. The magnetically suspended TMH 1000 MP pump from Balzers is water cooled, has a

hydrogen pumping speed of $680\,\mathrm{l\,s^{-1}}$ and compression ratios of $k > 4 \times 10^4$ ($k = p_\mathrm{s}/p_\mathrm{e}$, where p_s is the suction pressure and p_e the exhaust pressure);

- The **Leybold model TMP-560 M** turbo molecular pump with a pumping speed of $560\,\mathrm{l\,s^{-1}}$ was recommended by Coffin [Cof82] for pumping of tritium-handling equipment to high-vacua at TSTA. This publication documents the existence of more than 40 years of experience with turbomolecular pumps using a high speed rotor. The large **Oelikon Leybold MAG TM** molecular pump was equipped with a rotor suspended in a magnetic field that can attain turbo pumping speeds for nitrogen within the range 300 - $2200\,\mathrm{l\,s^{-1}}$ and generate an ultimate vacuum of 10^{-9} mbar. This pump, which requires no lubricant, was in discontinuous operation at JT60-U facility, Japan, without contingencies over a rather extended period of time;

- **Osaka magnetically suspended vacuum turbo molecular** pumps with pumping speeds up to $2400\,\mathrm{l\,s^{-1}}$ are capable of achieving an ultimate vacuum of 10^{-10} mbar.Osaka Vacuum pump type STP300 has a compression ratio for hydrogen of 1×10^4 and a pumping speed of $300\,\mathrm{l\,s^{-1}}$.

- **Seiko-Seiki Co.**, now owned by **Edwards**, manufactures pumps with pumping speeds of up to $3000\,\mathrm{l\,s^{-1}}$. To minimize the risk of contamination by hydrocarbons and circumvent mechanical bearings or fluidic lubrication the high-speed rotor is suspended by magnetic levitation. Given that magnetic bearings are inherently cool-running, the pump requires no external cooling. The electric input to the TMP is typically accomplished through a hermetic connector. The pump casing is sealed either with an elastomer or preferably with metal O-rings. An elastomer is only tolerable when the expected partial pressures of tritium remain low. When this condition prevails, a loss of elasticity of the static seals will not necessarily manifest as a leak because possible damage is mostly restricted to the inside seal surface. In view that turbo molecular pumps may be damaged by sudden changes of pressure, they are normally equipped with safety interlocks that interrupt power allowing safe spin-down as soon as pressures become unbearably high.

- The **Edwards-Seiko type H600C** turbo molecular pump, which is equipped with magnetic bearings, has been proposed for the generation of high vacuum at the plasma exhaust

gas processing section of the ITER machine [Glu02a] . This pump necessitates a backup pressure of 0.1 mbar.

- **Mitsubishi Heavy Industries** developed in collaboration with JAERI, Japan a **turbo molecular** pumping system equipped with **ceramic rotors** ($\varnothing$ = 150 - 200 mm) supported by gas bearings [Abe90a]. Aim of the project was a ceramic pump capable of attaining a pumping speed of 1000 l s^{-1} in the vicinity of the torus. Spiral grooves starting near the centre and ending at the periphery were cut on either side of rotor and stator discs installed in each stage. Pumps based on this concept with pumping speeds of about 80 l s^{-1} (rotor width $\varnothing$ = 120 mm) and 500 l s^{-1} (rotor width $\varnothing$ = 210 mm) have now undergone extensive testing. The rotor which runs on gas bearings is operated with a 2 bar gas turbine. The bearing clearance is 50 µm. The ultimate vacuum achievable with this pump is 10^{-7} Pa; the maximum helium compression ratio being 10^4. The turbo molecular pump is operated together with a Turbovisco fore pump having a pumping speed of up to 80 l s^{-1} (rotor with $\varnothing$ = 200 mm). The pump has a clearance in axial direction of 10 µm. Stator and rotor are made of Si_3N_4 ceramic. The selected fore pump generates a vacuum of 10^{-3} Pa at an exhaust pressure of 1 bar. To accelerate the turbine, the pump requires about 6 m^3 min^{-1} gas and about 0.1 m^3 min^{-1} for the bearings. These pumps are completely oil-free. Their insensitivity to magnetic fields has been demonstrated experimentally.

3.14.1.1.1 Long-term endurance tests of turbo molecular pumps with tritium

To test the performance of turbo molecular pumps under a tritium environment, pure tritium was pumped in closed loop mode through a 150 l s^{-1} pump from Leybold modified to achieve tritium-compatibility [Hei94b]. Altogether six runs were carried out, each with a small inventory of about 2.2×10^{10} Bq of tritium. The first run was conducted using oil lubricated steel bearings and the other five using grease lubricated ceramic bearings. After 7176 hours a bearings failure was detected, which demanded pump overhauling. This failure was, however, attributed to excessive bearings loads and not to a tritium-induced cause. It was concluded from the experiments, that no pump degradation attributable to tritium developed even after accumulated 12 000 hours of operation.

Priester and Bornschein [Pri13] reported of another long-term endurance test carried out at the site of the Mainz Neutrino Mass Experiment [Kra05] with a TPU330 pump operated in the presence of an inventory of tritium of 3.7×10^{10} Bq. The pump ran discontinuously without contingencies over a period adding up to about ten years.

More recently, the same authors [Pri13] performed at TLK a major, rather pertinent and valuable endurance test with an Oerlikon Leybold® MAG W2800 pump using hydrogen consisting to more than 80 % of tritium. Salient features of this potentially tritium-compatible pump were magnetic bearings, ultrahigh vacuum CF flanges, and a comparatively small amount of oil lubricant seal at the bottom plate of the pump (see Fig. 3.11). The pump was integrated into the so called TRITOP (TRItium Test Of Pumps) closed loop, additionally equipped with a buffer vessel, a flow controller, a capacitive MKS 626B pressure gauge (0.1 mbar full scale), a fully metallic 15 $m^3\,hour^{-1}$ Normetex backup pump and a dedicated MKS type HPQ2S residual gas analyser. The pumping performance of the Oerlikon was investigated during nine runs each lasting between 6 and 96 days over an integral period of more than one year. The throughputs of these runs were varied within the range 32 and 395 g T_2, the attained cumulative tritium throughput being about 5×10^{18} Bq ($\sim$ 1.3 kg). After completion of the experiments, the pump was still running normally, performing according to specifications and showing no increased leak rate. During occasional shutdown periods usually lasting several weeks the pressure in the loop increased noticeably. Mass spectrometric analysis of the gas composition provided evidence for O-ring deterioration and epoxy resin degradation. There were also indications for the generation of small partial pessures of highly corrosive hydrogen fluoride (m/e = 20) and tritium fluoride (i.e. m/e = 22) already after 55 days of continuous re-circulation. Tritium fluoride was probably the result of the interaction of gaseous tritium with non-metallic materials like coatings and insulation layers. This observation was verified in further more careful measurements. A significant contribution to the m/e = 22 peak of species such as T_2O and CHT_3 (both m/e = 22) could be ruled out. The closed loop mode of operation enhanced isotopic exchange between gaseous tritium and protium present on the inner metallic surfaces of the pump and on other components of the loop. The exchange became apparent by a decrease of the T_2 peak and a concomitant increase of the H_2 and HT peaks. Typical for late experiments with relatively high partial pressure of tritium was the formation of hydrocarbons (mostly tritiated methane), water, tritiated water, molecular oxygen, carbon monoxide, and carbon dioxide.

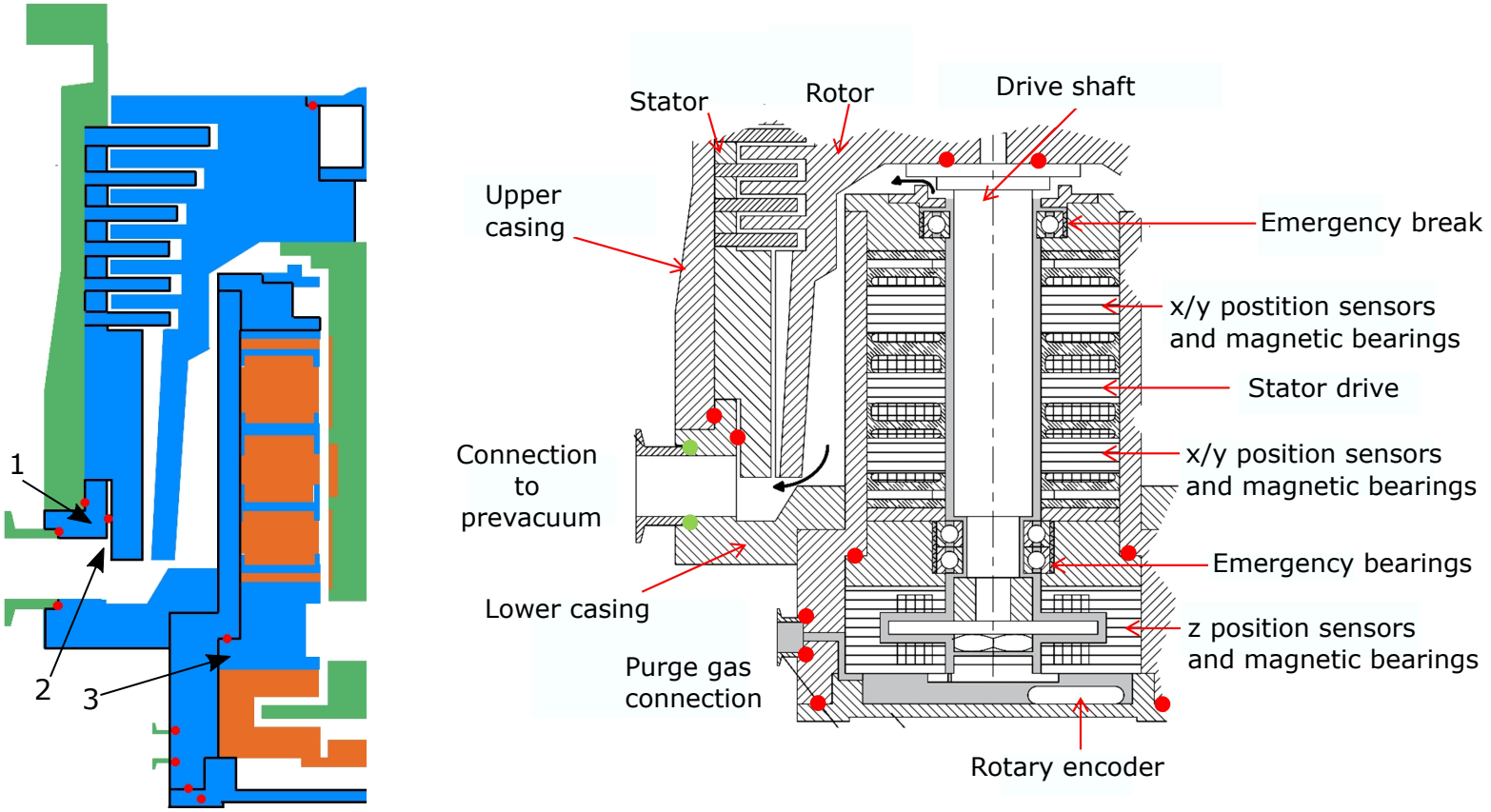


Figure 3.11: Simplified drawing of a cross section of the Leybold turbomolecular pump examined at TLK for tritium contamination. The left figure shows a cross section visualizing i) the aluminum zones (blue), ii) stainless-steel zones (green), and iii) non-metallic zones (orange). The numbers point to O-rings whose tritium activity was determined calorimetrically [Pri15]. The right figure provides some details on the operation mode of the Leybold pump. Red dots indicate positions of Viton O-rings.

Upon completion of the endurance tests, the Leybold® MAG W2800 turbomolecular pump was flushed with hydrogen for about two weeks with the objective of reducing the level of surface contamination [Pri15]. To assess possible damage caused by prolonged and dynamic exposure to gaseous tritium the pump was opened. Visual inspection revealed no damage attributable to tritium. During the subsequent dismantling stages carried out inside of the „repair glove box “of TLK (volume 5.4 m^3), the tritium levels were monitored continuously. For example, the activity rose from initially 8 up to 100 $MBq\,m^{-3}$ when removing blind flansches, up to 500 $MBq\,m^{-3}$ when removing and dismantling the magnetic bearing and up to 720 $MBq\,m^{-3}$ when opening to the shaft of the rotor. To get more information on the distribution of tritium within the pump, specimens were cut from several representative sections of the pump and analysed for tritium by calorimetry. The highest specific activities, i.e. values in the range 200 - 400 $MBq\,g^{-1}$, were found in the Viton O-rings (soft material). The degree of surface contamination of the aluminum and stainless-steel specimens was of the order of 10 - 30 $kBq\,cm^{-2}$. As would be expected, specimens from the fore vacuum section revealed higher contamination by tritium than those from the high vacuum section. This was attributed to the higher steady state pressures that probably prevailed in the low vacuum sections during the course of the test. The total tritium content in the pump after completion of the test was estimated to be several tenth´s TBq. In spite of the uncovered weak points, the tested magnetically levitated MAG W2800 Leybold turbomolecular pump was considered adequate for long-term usage in a high-level tritium environment. Because of construction and material similarity, most observations reported by Priester and Röllig on the MAG W2800 pump can be extended to other larger and smaller magnetically levitated turbomolecular pumps commercialized by Leybold.

Another evaluation of the degree of contamination experienced by turbo molecular pumps was carried out with an Edwards Seiko Seiki pump installed on the permeate side of a permeator belonging to the CAPER experiment at TLK [Cal08]. This pump was only exposed to pure hydrogen isotopologues regularly containing up to about 50 % of tritium. After 10 years of discontinuous operation the pump failed and required replacement. To this effect, the pump was transferred from the CAPER glove box into the repair glove box of TLK and completely dismantled. Prior to the transfer the pump was decontaminated by prolonged swamping with deuterium which lead to an integral release of 3.5 TBq tritium. Further 0.2 TBq were liberated while disassembling the pump inside of the repair glove box. Metallic and non-metallic specimens

taken from diverse places of the pump were analysed for tritium by a heat treatment. From the results the residual amount of tritium remaining in the pump was estimated to be about 0.3 TBq (this level of contamination is of similar order of magnitude than that reported by Priester and Bornschein [Pri13]). The highest specific activities of tritium were found in the insulation of the cables protecting the electrical connections to the motor, i.e. $0.12\,\mathrm{TBq\,g^{-1}}$. The specific activity for cable insulation plus copper was $0.025\,\mathrm{TBq\,g^{-1}}$ signalizing small tritium uptake by copper. Visual examination of the insulation evidenced significant degradation. The total activity of tritium in the pump was estimated to be 2.7×10^{11} Bq.

One more Seiko-Seiki/Edwards STP310 turbomolecular pump utilized at TLK for the PETRA and the FACT experiments also revealed malfunction. It manifested by only 50 % of the nominal rotational speed at the end of several prolonged experimental campaigns frequently utilizing aggressive gases [Wag15]. The exact cause of failure has hitherto not been identified.

3.14.1.2 Turbo molecular drag pumps

Molecular drag pumps transfer momentum from mechanical motion to gas motion employing a rapidly rotating solid surface placed closely to a fixed surface [Dan14]. In other words, the rotating solid surface imparts motion to the gas molecules. Drag pumps start pumping at a higher inlet pressure, e.g. several ten mbar, than turbomolecular pumps. Therefore, they do not require a very low backing pressure. The ultimate achievable vacuum, i.e. 10^{-6} mbar, is clearly lower than that attainable with a turbomolecular/roughing pump combination. Therefore, even though molecular drag pumps cannot replace turbomolecular pumps, they are ideally suited for certain specific applications.

The first turbomolecular pumps which combined a turbo section with a drag section were brought on the market about 30 years ago [Aud14]. More recently, turbo molecular pumps were furnished with a monolithic rotor for the high speed turbo stages as well as for the high compression ratio stages (see Fig. 3.12). Turbo drag pumps use alternating moving rotors that impart downward motion to atoms and molecules. In order to be effective, the blades must move at a velocity comparable to that of the thermal speed of the pumped molecules. The fixed stator blades are furnished with spiral grooves on both sides. They decelerate molecules for the next rotor hit and impart a directive motion creating a flow and compression towards the pump outlet. As opposed to turbo molecular pumps, which necessitate a roughing pump and a backing pump,

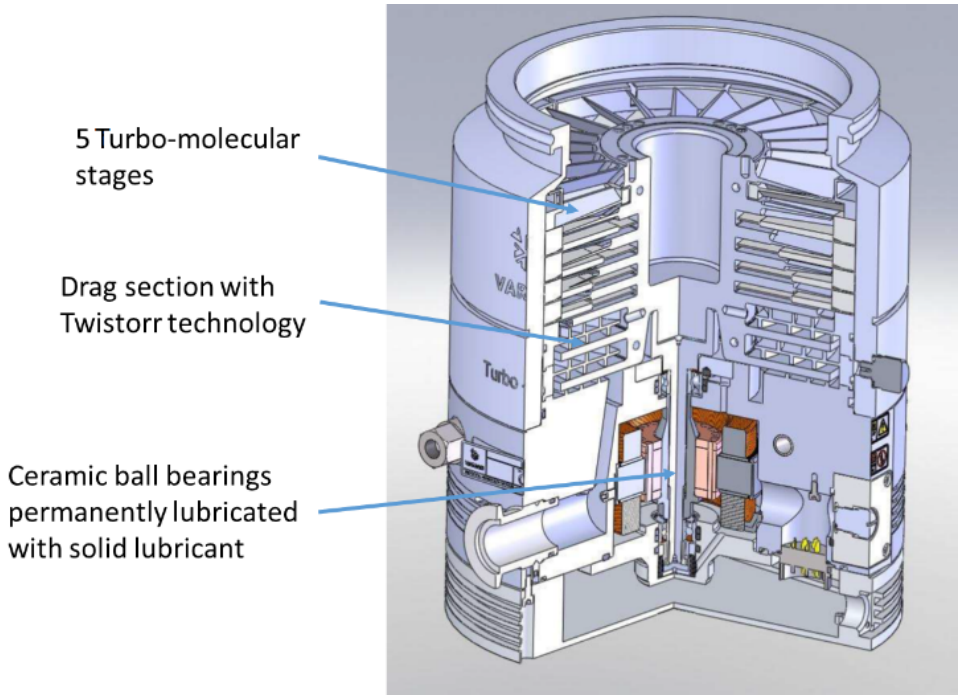


Figure 3.12: Novel Turbo-V 750/850 TwisTorr turbo drag pump from Agilent Technologies [Aud14] featuring high compression ratio, high pumping speed and compact design.

a molecular drag turbo pump can be operated with only a simple backing pump. Hence, their power consumption is comparatively small. Because molecular drag turbo pumps have a high compression ratio for light gases they are ideal for the evacuation of hydrogen isotopologues.

The JET vacuum vessel, evacuated for over 17 years with four $3500\,\mathrm{l\,s^{-1}}$ turbo molecular pumps, is now being evacuated with two **VT2000 turbo drag pumps** having a pumping speed of $2000\,\mathrm{l\,s^{-1}}$ [Pea01]. The pumps have been adapted to JET requirements for tritium service: i) all seals are metallic, ii) all poly tetra fluoro ethylene insulators have been replaced by ceramic insulators, and iii) all control electronics are installed outside of the biological shield.

Important advantages of the turbo drag pumps at JET are: i) rather prolonged lubrication of the ceramic bearings[16], ii) pumping starts at higher pressures than with turbo molecular pumps, iii) greater pumping speed possible during deuterium glow discharge cleaning, iv) capability of sustaining a backing pressure of up to 4 mbar and therefore to provide a much better isolation of the torus from the fore vacuum line.

[16] Oil lubricated bearings of turbomolecular pumps require oil renewal after 10000 hours running time.

3.14.1.3 Multistage positive displacement rotary pumps

The operation principle of the multistage positive displacement, rotary **Drystar type DP40** pump is based on a number of intermeshing rotor pairs of different profiles mounted on common shafts, which are held in correct phase relation by a pair of timing gears that do not contact each other. The Drystar pump is completely oil-free. The specified pumping speed of the Drystar pump is $52\,m^3\,hour^{-1}$; the pump can generate an ultimate vacuum of 4×10^{-2} mbar.

One application of the pump has been pumping exhaust gas of a turbo molecular pump [Pen95a]. After upgrading for tritium service, the pump performed without occurrences for a period of five years of discontinuous operation. While the pump is loud, the noise level is acceptable when the pimp is housed in a glove box.

3.14.1.4 Moving spiral (scroll) pumps

Oil-free, all metal moving spiral pumps type **NORMETEX** with specified pumping speeds of $15\,m^3\,hour^{-1}$, $18\,m^3\,hour^{-1}$, $60\,m^3\,hour^{-1}$, $150\,m^3\,hour^{-1}$, $600\,m^3\,hour^{-1}$ and $1300\,m^3\,hour^{-1}$ were manufactured at Pont-Audemer, France until recently [Cla13]. These pumps feature nutating bellows to seal the compression chamber. The pumping cavity is enclosed between two spirals, one being fixed and the other rotating uniformly within the other. The clearance between these spirals, which do not touch each other, is only about 0.1 mm. Scroll pumps have been demonstrated successfully with tritium in numerous laboratories and technical facilities worldwide under a broad variety of experimental and process conditions [Cof82; Shm87; Ort90; Hay92b; Per93b; Pen95c; Pen95a; Pen97b; Lae99b]. NORMETEX pumps were shown to be reliable and robust throughout extended, also round the clock periods of operation. They display a significant gas-type dependency exhibiting an increase in pumping efficiency in the order $H_2 < D_2 < CH_4 < C_3H_8 < He < Ne < Ar \sim air \sim N_2 \sim CO_2$ [Pen95a]. As apparent, light gases are pumped much less efficiently than heavier ones to the point that even a hydrogen isotope effect is noticeable. Gas type dependency and isotope effect are attributed to the different back diffusion rates of gases between the spirals. Similar observations were reported previously by Hayashi et al. [Hay92b], who investigated systematically the evacuation performance of scroll pumps employing hydrogen, deuterium, and tritium as test gases.

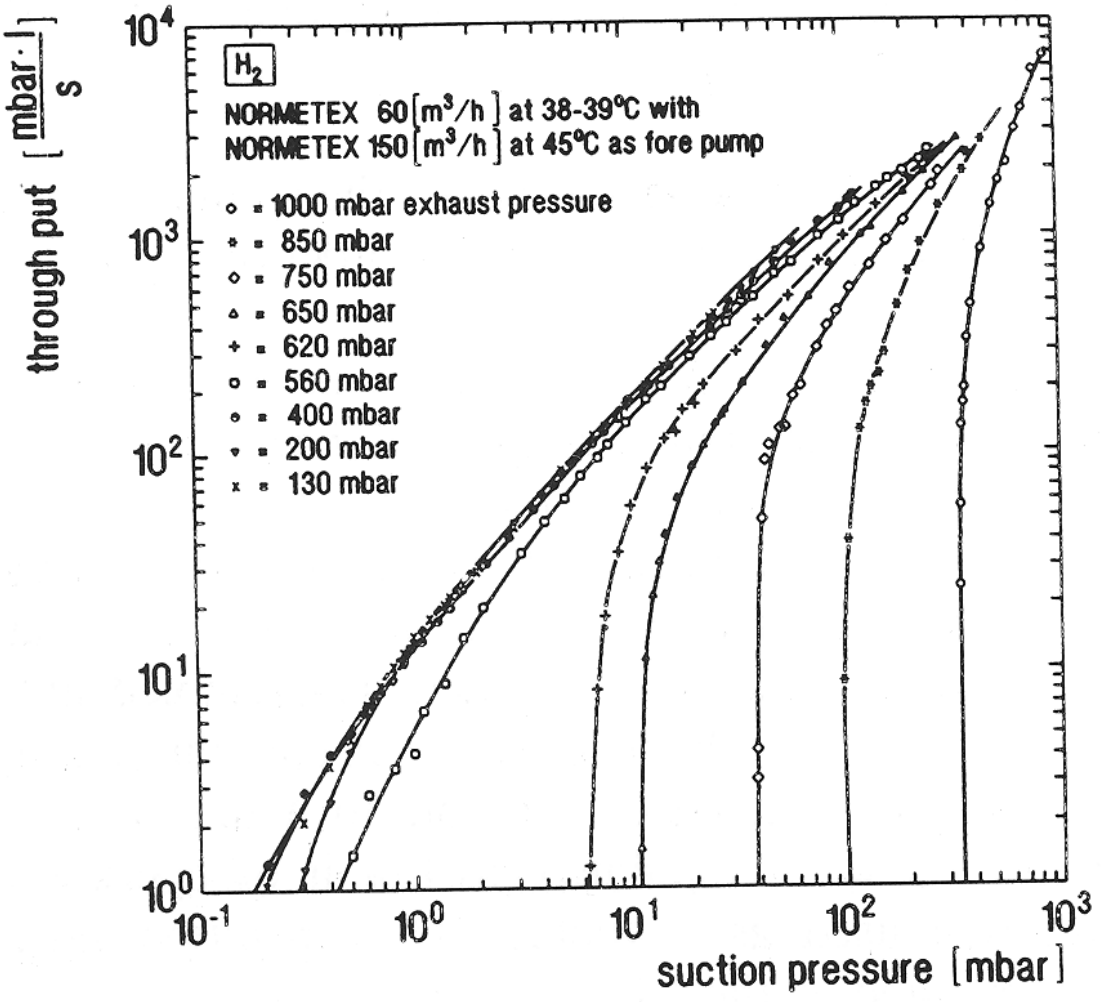


Figure 3.13: Hydrogen throughput of a 60 m^3 $hour^{-1}$ pump determined as function of increasing constant exhaust pressures [Pen95a].

Fig. 3.13 shows by way of example the hydrogen pumping characteristics of a 60 m^3 $hour^{-1}$ moving spiral pump operating at 311 - 312 K [Pen95a]. In these experiments a 150 m^3 $hour^{-1}$ NORMETEX pump served as fore pump.

The maximum specified operation pressure of the 15 m^3 $hour^{-1}$ pump is 1.5 bar and the maximum allowed static pressure 3.0 bar. The dead volume is comparatively large, i.e. 1.17 l. Because moving spiral pumps are sensitive to particulates it is recommended to install sinter filters at the pump inlet (and eventually pump outlet).

When moving spiral pumps of high compression ratio or two moving spiral pumps in series are operated in closed loop mode it is necessary for system protection to control the upstream

pressure with a dedicated pressure sensor. In case of an unexpected pressure rise, possibly arising from a leak of glove box atmosphere into a pump suction section, a Programmable Logic Controller can be used to terminate operation as soon as a safe pressure is exceeded.

One more safety measure against dangerous gas pressurization generated by a leak into the upstream section of a pump consists in a pressure release device installed downstream of the pump that re-directs the gas back into the pump suction zone. The design of a complete system capable of withstanding the maximal attainable pressure with a pump or pump combination, is difficult to accomplish.

Typical throughput curves as function of suction pressure obtained with a variety of fusion fuel cycle relevant gases using a 18 $m^3\,hour^{-1}$ NORMETEX pump operated at constant exhaust pressure of 1000 mbar are displayed in Fig. 3.14. The plotted data can also be extended to other NORMETEX pumps of different pumping speeds. Maximum pumping speeds of N_2 or Ar were achieved with the 18 $m^3\,hour^{-1}$ NORMETEX pump at suction pressures within the range 8 - 20 mbar.

Vacua achievable with typical fusion fuel cycle gases utilizing single scroll pumps of pumping speeds in the range 18 - 150 $m^3\,hour^{-1}$ operated at a constant exhaust pressure of 1000 mbar and at zero flow are compiled in Table 3.4.

Table 3.4: Vacua attainable when pumping single relevant plasma exhaust gases employing three different scroll pumps operated at zero flow rate and at constant exhaust pressure of 1000 mbar [Pen95a].

NORMETEX pump $m^3\,hour^{-1}$	Vacua mbar				
	H_2	D_2	CH_4	He	N_2
18	550	310	210	90	0.2
60	320	70		2.7	0.8
150	200	10		0.8	0.08

Maximum pumping speeds, achievable vacua, and compression ratios of several small and large NORMETEX pumps as well as of their combinations are tabulated for hydrogen and nitrogen at one exhaust pressure in Table 3.5 and for hydrogen, deuterium, nitrogen, and helium at two exhaust pressures in Table 3.6.

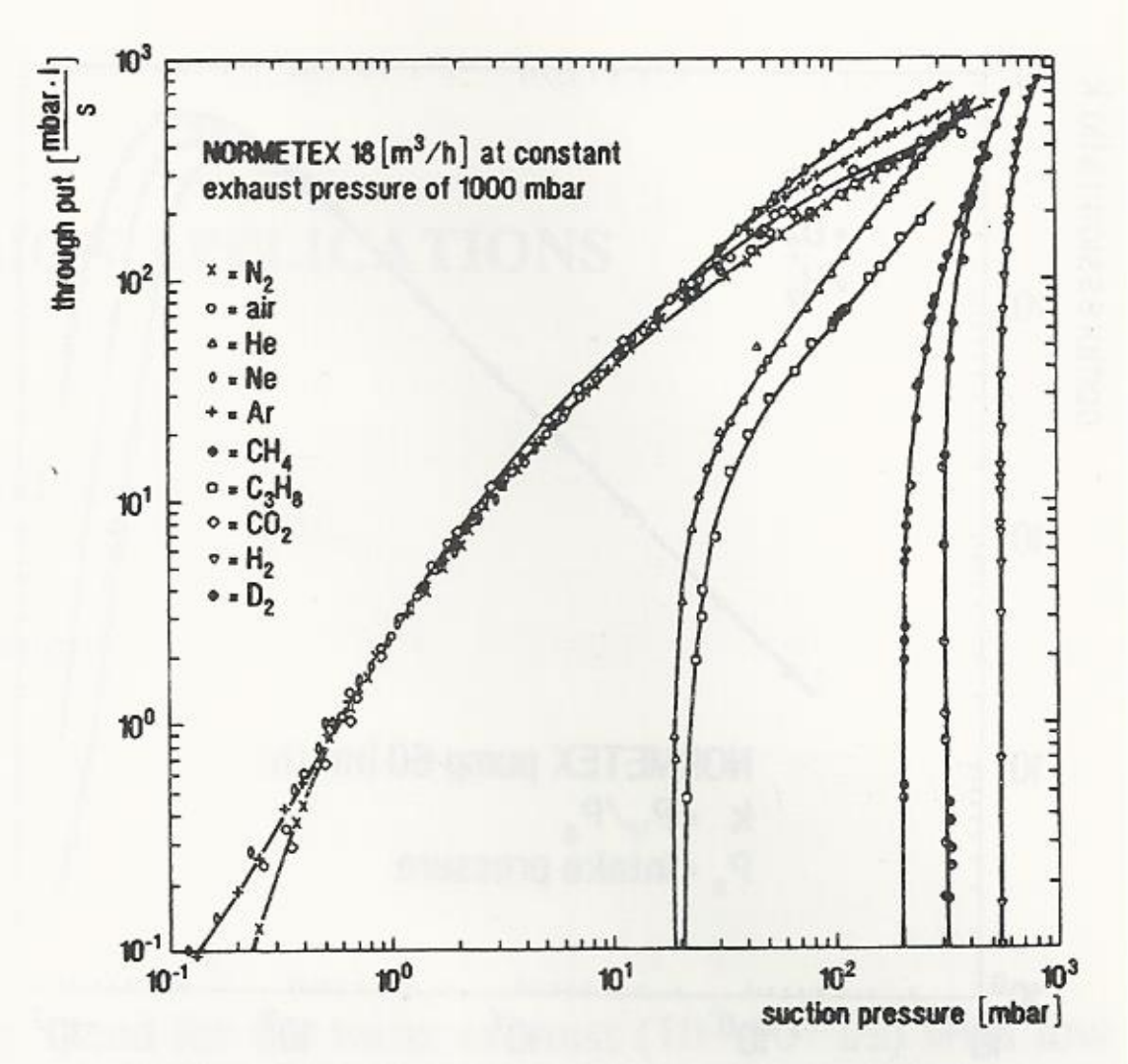


Figure 3.14: Pumping throughput of a 18 m^3 $hour^{-1}$ NORMETEX scroll pump as function of suction pressure for several gases at an exhaust pressure of 1 bar [Pen95a].

Using a test facility whose configuration was designed for experiments with single pumps as well as for pump combinations additional data for nitrogen, protium, and deuterium were obtained for rather large scroll pumps [Per93b]. The tests were carried out with combinations of several moving spiral pumps or combinations of several moving spiral pumps together with a Metal Bellows MB601 pump at constant exhaust pressures of either 600 or 1200 mbar. Obtained maximum pumping speeds, achieved ultimate vacua, and compression ratios at zero flow are tabulated in Table 3.6. The data provide evidence that vacua lower than 10^{-5} mbar are obtainable when pumping hydrogen isotopes.

Table 3.5: Pumping data of several dry mechanical NORMETEX pumps at constant exhaust pressure of 1200 mbar [Per93b].

NORMETEX Pump	Max. pumping speed $l\,s^{-1}$		Achievable vacuum mbar		Compression ratio	
	N_2	H_2	N_2	H_2	N_2	H_2
$1300\,m^3\,hour^{-1}$	220	43	1.6	3.7×10^2	7.5×10^2	3.2
$600\,m^3\,hour^{-1}$	134	41	3.5×10^{-2}	3.5×10^2	3.4×10^4	3.4
$60\,m^3\,hour^{-1}$	6	4.1	4.2×10^1	7.9×10^2	1.4×10^1	1.5
$6\,m^3\,hour^{-1}$	1	1.6	7.3×10^1	8.4×10^1	1.6×10^1	1.4×10^1

Recently, a series of pumping speed measurements performed in a collaborative effort by several Korean institutions were published by Chang et al [Cha11]. The pumping characteristic of a single MB601 HP pump (exhaust pressures in the range 30 - 600 kPa) and of a NORMETEX 15/MB601 HP pump combination (exhaust pressures in the range 30 - 100 kPa) were determined employing either nitrogen or helium as test gases. The results indicate that the pumping speeds of the MB601 HP pump with nitrogen as function of suction pressure displayed a comparable trend to that provided by the manufacturer for air. The nitrogen values, however, were consistently lower. In case of helium the deviations of the experimentally obtained pumping speeds from those supplied by the manufacturer for air were rather pronounced. Better agreement with data determined by the manufacturer on pumping speed and vacua was obtained with the MB601 HP/NORMETEX $15\,m^3\,hour^{-1}$ pump combination when tested with either gas. At suction pressures exceeding 1 kPa unfailingly higher pumping speeds were obtained with both gases when compared to values specified by the vendor (see Fig. 3.15).

The tritium compatibility of a NORMETEX PV12 scroll pump operated discontinuously for the re-circulation of gases during a period of five years within the frame of the PETRA experiment [Pen97a] and several months within the FACT experiment [Ant08a] was demonstrated experimentally. The pump worked properly according to specifications in spite of recurrent contact with high concentrations of tritium partly in the presence of carbon oxides as well as of other reactive gases [Wag15].

Table 3.6: Pump characteristics of scroll pumps in series or scroll pumps operated in series also in combination with a Metal Bellows pump [Per93b].

a) At constant 600 mbar exhaust pressure

Pump combination	Max. pumping speed $l\,s^{-1}$				Ultimate pressure mbar				Compression ratio at zero flow			
	H_2	D_2	N_2	He	H_2	D_2	N_2	He	H_2	D_2	N_2	He
Normetex 1300 + 600	270	270	275	276	1.1×10^{-3}	2.0×10^{-4}	6.0×10^{-6}	2.0×10^{-6}	5.4×10^{5}	3.0×10^{6}	1.0×10^{8}	3.0×10^{8}
Normetex 1300 + 600 + 60	272	267	276	277	1.4×10^{-5}	3.0×10^{-6}	4.0×10^{-6}	1.0×10^{-6}	4.3×10^{7}	2.0×10^{8}	1.5×10^{8}	6.0×10^{8}
Normetex 1300 + 600 + 60 + Met Bel 6	273	274	260	269	8.0×10^{-6}	5.0×10^{-6}	9.0×10^{-6}	1.0×10^{-6}	7.5×10^{7}	1.2×10^{5}	6.6×10^{7}	6.0×10^{8}

b) At constant 1200 mbar exhaust pressure

Pump combination	Max. pumping speed $l\,s^{-1}$				Ultimate pressure mbar				Compression ratio at zero flow			
	H_2	D_2	N_2	He	H_2	D_2	N_2	He	H_2	D_2	N_2	He
Normetex 1300 + 600	264	262	274	264	1.1	1.4×10^{-3}	1.1×10^{-5}	2.0×10^{-4}	1.1×10^{3}	88.5×10^{5}	1.1×10^{8}	6.0×10^{6}
Normetex 1300 + 600 + 60	270	274	276	274	3.3×10^{-3}	4.0×10^{-4}	4.0×10^{-6}	6.0×10^{-6}	3.6×10^{5}	3.0×10^{6}	3.0×10^{8}	2.0×10^{8}
Normetex 1300 + 600 + 60 + Met Bel 6	275	274	262	275	2.0×10^{-5}	3.0×10^{-4}	2.0×10^{-6}	7.9×10^{-6}	6.0×10^{7}	4.0×10^{6}	6.0×10^{8}	1.7×10^{8}

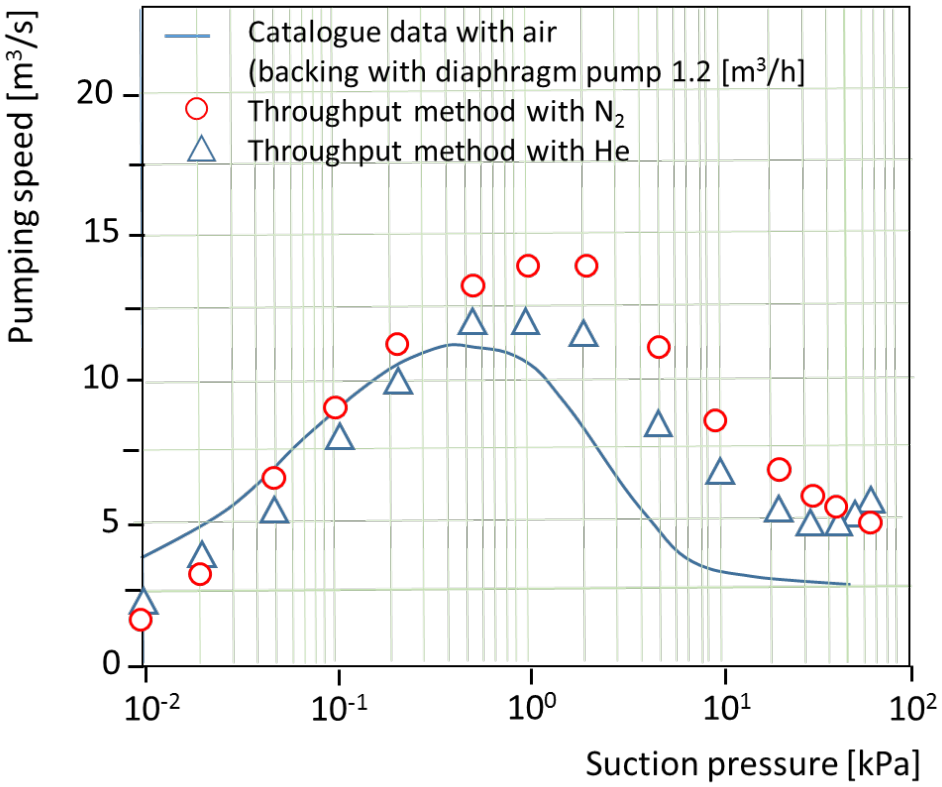


Figure 3.15: Pumping speeds for nitrogen and helium with a NORMETEX 15 scroll pump backed by a MB601 HP pump as function of suction pressure. The data for air of the manufacturer are shown for comparison, (after [Cha11]).

Fowley et al. [Fow11] performed an experimental study aimed at investigating the possible consequences of prolonged exposure to **water vapour** on the performance of a NORMETEX scroll pump. The experimental setup was rather straight forward (see Fig. 3.16). Gas from a cylinder containing compressed air was first dried and then passed through a rotameter. Water was added from a heated container through a gas regulating valve and pumped with a 15 $m^3\,hour^{-1}$ NORMETEX pump backed by a Laboport N820.3FTP dual head diaphragm pump. The water container was placed on a balance which permitted uninterrupted calculation of the water flow rate from the gradual loss of weight. Hence, the amount of supplied water was known at any point in time. The outlet pressure could be controlled by supplying air to the backside of the pump via a bypass line. The air feed stream was adjusted so that it contained 30 % water vapour at a pressure of 0.4 kPa. The apparent temperature of the NORMETEX pump throughout the course of the test, which lasted for more than two weeks, was determined to be

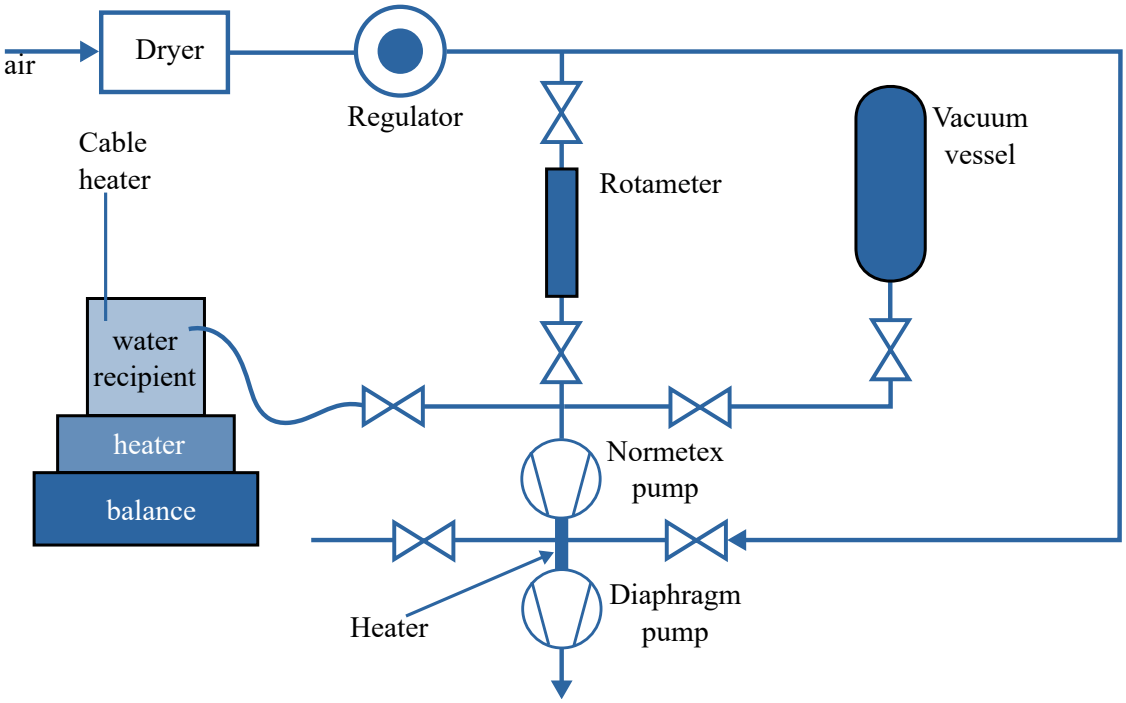


Figure 3.16: Experimental arrangement for the investigation of the influence of water vapour on the performance of a NORMETEX pump (after [Fow11]).

approx. 308 K. During the test, the conditions were such that condensed water could neither be generated inside of the pump nor in the outlet zone. The selected pressure was maintained near water condensation conditions. Fluctuations of ambient temperature were a frequent cause for instabilities. The instabilities were attributed to water condensation. After completion of the test no loss of NORMETEX pump performance was apparent when the pumping characteristics of the pristine pump were compared with those obtained after extended pumping of moist air. Water condensing in the back up pump, on the other hand, caused pressure fluctuations and a drift of operating performance.

Smaller **scroll pumps** are currently supplied by K.I. Lesker, Ideal Vacuum Products, Anest Iwata, and others. These pumps i) have pumping speeds covering the range 2 - 25 $m^3\,hour^{-1}$, ii) can achieve low ultimate pressures, iii) require no oil, and iv) are cost effective [Hay07b]. Their utilization is not recommended for flammable, explosive, toxic, or corrosive gases. Humid gases whose humidity surpasses 60 % should only be pumped with the integrated gas ballast delivered together with the pump. Typical applications of these pumps are rough pumping, turbo molecular pump backing, and gas transfers.

Table 3.7: Edwards pump with suction blanked off and utilizing a metal bellows backing pump (after [Mor13]).

Suction pressure mbar	Discharge pressure mbar	Compression ratio
Suction pipe blanked off		
0.0573	495.9	8654
0.0613	815.8	13 308
0.0665	965.1	14 513
0.0677	994.4	14 688
Inlet and discharge blanked off		
634.5	2654	4.18
974.4	2654	2.72

Because NORMETEX pumps are no longer commercially available [Cla13], Morgan and Peters [Mor13] assembled a test system for the determination of the functional performance of potential **surrogate pumps**. One identified theoretically suitable alternate is the scroll pump type nXDS15iC from Edwards. Regrettably, this lubricant-free and corrosion-resistant pump, operates with a polytetrafluoro ethylene tip seal, Chemraz® internal valves, and a perfluoroelastomer O-ring, all of which degrade in the presence of tritium. Hence, significant upgrading would be necessary if these pumps were to be installed in systems operating with tritium-bearing gases. Nevertheless, first screening experiments were carried out with a type nXDS15iC scroll pump from Edwards backed by a Metal Bellows MB-601 pump. While the suction section of the Edwards pump was blanked off the back up pump could be throttled using a bypass encompassing a ball valve to adjust the discharge pressure. The results are compiled in Table 3.7. They reveal that fairly high compression ratios can be achieved with the Edwards pump provided the suction pipe is blanked off. Increasing the discharge pressure causes the increased inlet pressure to vary slightly. When inlet and discharge pipes are blanked off the compression ratio decreases markedly if the cap closing of the suction pipe is replaced by a 100 l vessel. This is understandable when considering that the maximal discharge pressure, i.e. 2654 mbar, is independent from the volume of the suction zone but the equilibrium pressure at the suction zone will depend upon the fraction of gas compressed.

Further Normetex surrogate pumps under consideration are a Busch scroll type FO 0015A pump manufactured in Germany, and an Air Squared prototype pump from USA [Cla13].

3.14.1.5 Metal bellows pumps

Metal bellows pumps manufactured by Metal Bellows Corp., USA, have been in tritium service in large numbers at JET, Culham [Lae99b]; TFTR, Princeton [Gen95]; TLK Karlsruhe [Pen97b]; TPL, JAERI, Tokai Mura [Nar90; Yam95a]; TSTA, Los Alamos [Cof82]; Westinghouse Savannah River Company [Ort90]; and others. Twenty-six Metal Bellows pumps have been installed at the Tritium Facilities of Savannah River Site for altogether 51 years of tritium handling. The experience gained has been for the most positive. The tested pumps include rather different configurations, i.e. single containment, double containment, pumps with one to four heads, pumps of fixed speed, of variable speed, etc. To improve pumping performance two heads have been plumbed for operation in series, parallel, or independently. Some metal bellows pumps are equipped with a replaceable all-metal check valve.

For tritium handling in a primary system installed in a glove box one rather frequently utilized metal Bellows pump is **type MB151** [Ort90]. Some metal Bellows pumps feature double bellows containment with a pressure alarm between the bellows to signalize at an early stage a possible bellows rupture. Metal bellows should be protected from particles both from the outside (with a metal enclosure) and from the inside (with sinter filters), because particles have been identified as one cause for bellows rupture.

Another oil-free, double contained pump equipped with two pumping stages is the INTERATOM Metal Bellows pump manufactured by Siemens, KWU, Germany [Pen97a; Pen98]. The pump can be used for re-circulation of gases or evacuation to less than 100 mbar at an air exhaust pressure of 1 bar. The overall leak tightness of the Siemens pump is specified by the manufacturer to $< 10^{-9}\,\mathrm{mbar\,l\,s^{-1}}$; the nominal pumping speed of Model IAD pump is $4\,\mathrm{m^3\,hour^{-1}}$ at an inlet pressure of 0.1 MPa. The compression ratio is better than 10; it is not influenced by variations of the motor speed. The mass flow rate is a nearly linear function of the pumping speed. Mechanical power is transmitted from the motor to the compressor via a magnetic clutch. By this arrangement it becomes possible to adjust the pumping speed directly with an electronic speed control device. Another option is indirect pumping speed adjustment employing a bypass with integrated Nupro needle valve. As apparent from the results presented in Table 3.8, the

positive displacement INTERATOM pump is only slightly dependent from the type of pumped gas. In combination with a NORMETEX scroll pump, vacua better than 1 mbar are obtainable with hydrogen as test gas. To detect possible ruptures of metal bellows the pump is provided with a pressure sensor installed in the UHV-tight stainless-steel insulation jacket of the bellows. When a sub atmospheric pressure is maintained in the annular compartment a departure from the preset pressure will signalize a rupture. In the event of a pressure excursion, the pump can be turned off and stopped from further operation employing a Programmable Logic Controller. Altogether seven INTERATOM pumps have been installed and operated in experiments and infrastructure systems of TLK. All pumps met the program goals and provided satisfactory service with tritium over periods lasting for more than 5000 hours.

Besides a NORMETX PV12 pump, two INTERATOM Metal Bellows were also integrated into the PETRA facility of TLK and employed intermittently for the re-circulation of gases during a 5-year period within the frame of permeation and tritium storage experiments and subsequently for several months for test runs with a ferro-fluidic rotary seal (FACT experiment) [Pen97a; Ant08a]. During these two consecutive periods, the two pumps were frequently exposed to high concentrations of tritium, high partial pressures of carbon oxides, and moisture. The latter can give rise to aggressive products like formaldehyde and carboxylic acids [Wag15].

Primary tritium systems must be protected from pressurization. A dangerous pressure rise may take place when glove box atmosphere is sucked by single pumps or pump combinations during closed loop operation after development of a pinhole or another integrity loss of the system. If the process gas contains tritium the consequences may be even more severe. The most frequently utilized protection measure is a high-pressure interlock which switches off power to the pump and stops operation. An additional precaution may be a rupture disk which discharges pump exhaust gas into the pump suction pipe or into an empty vacuum tight reservoir. Important advantage of an interlock is that the destruction of the rupture disk is avoided and hence operation downtime is prevented.

Summarizing, the following protective measures need to be adhered to when installing Metal Bellows pumps in tritium handling facilities:

- The discharge of the pumps shall be provided with a rupture disk back to suction
- Pumps shall be equipped with an interlock/alarm.

Table 3.8: Vacua achievable with hydrogen isotopologues employing a single pump or a pump combimation. Results for DT with a single double-stage INTERATOM at zero flow and for H_2, D_2, or an approximately equimolar deuterium - tritium mixture with a double stage INTERATOM pump combined with a 15 $m^3\,hour^{-1}$ NORMETEX pump [Pen98].

Exhaust pressure	Suction pressure of a INTERATOM pump	Suction pressure of a INTERATOM pump backed by a NORMETEX 15 ($m^3\,hour^{-1}$) pump		
mbar	mbar		mbar	
	DT	H_2	D_2	DT*
1000	148	3.3	0.4	0.22
900	135	1.8	0.28	0.14
800	122	0.9	0.22	0.09
700	109	0.6	0.18	0.06
600	96	0.4	0.13	0.04
500	83	0.3	0.12	0.03
400	71	0.2	0.11	0.018
300	60	0.15	0.10	0.010
200	50	0.10	0.08	0.007
100	27	0.08	0.05	0.002

- The secondary containment of bellows pumps shall be backfilled and high/low alarmed.
- The installation should contemplate easy pump maintenance and replacement.
- Because accumulation of particulate matter in the folds of bellows may cause pump failure the inner surfaces of bellows should be protected from harm by sinter filters of high conduction and the outer surfaces by an appropriate containment. Pumps should preferably be installed with bellows placed in vertical position.

3.14.1.6 Vane pumps

A magnetically coupled vane pump drive was developed at Mound [Cap85] to solve the problem of tritium leakage at the shaft seals. The leak-tight type M2 vane pump attained at 750 revolutions per minute (rpm) pumping speeds of 136 l min^{-1}. Type M3 was designed to replace Toepler pumps (glass pump for the quantitative collection of gases employing mercury). This

miniaturized pump achieved a pumping speed of $5.8\,\mathrm{l\,min^{-1}}$ at 750 rpm. Vane pumps may not only find application in the low-pressure range but also serve as compressors.

3.14.1.7 Cryogenic pumps

Batch pumping of exhaust gases by cryoadsorption was first demonstrated at the Los Alamos Tandem Accelerator Facility [Sei71] employing a 2.5 l Hoke stainless-steel sampling cylinder containing about 0.9 kg of activated carbon. Cooled to liquid nitrogen temperature, the trap absorbed about 10 l of gas. Up to 1.3×10^{16} Bq of gaseous tritium were handled by this procedure without noteworthy problems.

Another spectacular cryoadsorption experiment was carried out at JET: the exhaust gases from this fusion machine were pumped with a simple "cold finger" consisting of a corrugated metal hose of 50 mm inner diameter submerged into a Dewar containing liquid helium [Hem92]. In order to pump helium charcoal was introduced into the lower end of the "cold finger". By this procedure batches of nearly 1 l solid hydrogen, i.e. 600 bar l, were pumped down to pressures of less than 0.1 Pa. The pumping speed was comparable to that of a $1200\,\mathrm{m^3\,hour^{-1}}$ roots blower. To recover the condensed gases the cold finger was simply warmed up slowly up to ambient temperature by gradually lowering the Dewar.

In practice, all Tokamak exhaust gases except helium can be pumped effectively by cryo-condensation with **cryo-pumps** furnished with **condensation surfaces** cooled to about 5 K. To include helium among the pumped gases it is necessary to furnish the cryo-pumps with appropriately designed cryo-sorption panels [Hem89a; Lae99b]. Pumps of this kind are known under the generic term **compound cryo-pump**.

Compound cryo-pumps supplied to TSTA by Lawrence Livermore National Laboratoy (LLNL) [Bat81] as well as by Brookhaven National Laboratory (BNL) [Cof79; Hse81] were first tested using either molecular sieve 5A or charcoal as adsorber material [Wal90]. After screening runs provided evidence that under comparable conditions the highest pumping speeds could be achieved with active charcoal, only this adsorber was employed in subsequent experiments. The tested LLNL pump had an inlet diameter of 400 mm and featured an outer cylindrical array comprising panels whose inner surfaces were coated with activated charcoal cooled with liquid helium (see Fig. 3.17). Concentric to this outer array was an inner chevron array likewise cooled with liquid helium. A further inner concentric array comprising a louvered shield cooled with

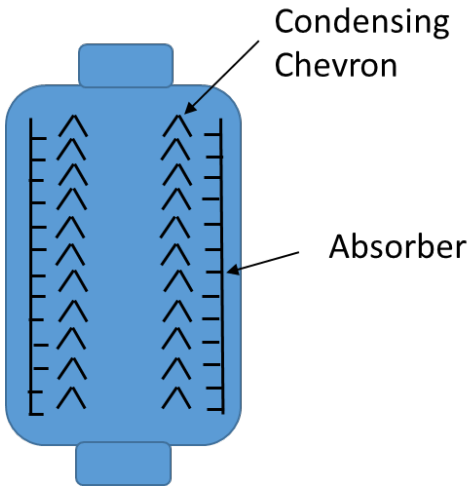


Figure 3.17: Scheme of a cryo-pump assembly showing the adsorber zone and the array of condensing Chevrons (after [Wal90]).

liquid nitrogen provided additional thermal insulation. With this configuration it became possible to pump helium and deuterium tritide separately yielding a relatively helium-free DT off-gas. Up to 7 mbar l cm^{-2} of helium were regularly sorbed on charcoal at a fairly constant speed. Pumping experiments employing a mixture consisting of 94 % deuterium tritide and 3 % helium with a pump equipped with Chevrons furnished with charcoal panels cooled with liquid helium down to 4 K delivered evidence that while tritium was predominantly condensed on the Chevrons helium was mostly adsorbed on the charcoal panels.

Sedgley et al. [Sed89] compared different types of charcoal with respect to their pumping speeds, ease of re-conditioning, capacity to accumulate pumped gas, and tolerance towards fusion environment. Concerning the pumping of helium, the screening tests revealed that high pore volume and high pore surface area, as obtained from standard measurements with nitrogen, were not necessarily the best selection criteria for a charcoal adsorber. Of all investigated charcoals, the best cryo-sorbent properties (sorption speed and capacity) for pumping of helium/deuterium and helium/tritium mixtures at 4.2 K were displayed by coconut charcoal. Based on the experiments, a cryo-pump was designed featuring a closed-end and a movable cylindrical barrier within a liquid nitrogen heat shield. The pump had a cylindrical charcoal-coated surface maintained at 4.2 K, which was surrounded by a chevron heat shield likewise maintained at 4.2 K. The barrier,

which permitted normal helium pumping during operation, could be displaced in such a way that the charcoal remained isolated during the regeneration phase.

To optimize the performance of cryo-sorption panel's, comprehensive screening tests were carried out by Perinic and his co-workers [Per93a] employing gas mixtures simulating type and composition of ITER off-gases, i.e. 0.11 Ar, 0.11 CO_2, 0.23 CO, 0.19 N_2, 0.24 O_2, 1.4 CH_4, 5.0 He and the rest H_2 (all in volume percent). At the time, the plasma-facing material was CFC. In their investigation, they compared the performance of numerous panel´s under the same experimental conditions using the specially designed TITAN test facility. The examined panel´s, all with a diameter of 430 mm, differed in i) type of sorbent (numerous different kinds of active carbons and molecular sieves), ii) type of substrate (copper, aluminium, or steel), and iii) procedure for bonding adsorbent on the panel´s (various brazes and cements mostly of high thermal conductivity). Among other conclusions, the results confirmed previous findings of Sedgley et al. [Sed89] concerning the superior properties of charcoal and molecular sieves for co-pumping of representative exhaust gas mixtures from ITER.

Complementary wide-ranging screening tests on the performance of several sorbents employing single relevant gases or representative gas mixtures were also carried out by Walthers et al. [Wal91b] and by Day et al. [Day01]. The investigated sorbent properties comprised i) pore distribution, ii) sorbent/bonding agent, iii) thermal cycling behaviour, iv) hysteresis, and others. As a result of these parametric studies activated carbon type CHEMVIRON SCII (10 - 30 mesh granules of coconut shells having BET surface areas of 1100 - 1200 $m^2\,g^{-1}$ and pore widths of 1.0 - 1.2 nm) were found to possess salient properties. Good bonding to cryo-panels was achieved with a two-component inorganic cement which displayed prolonged thermal endurance and excellent mechanical resistance to pull tests. A follow-up study on the cryo-sorption properties of CHEMVIRON-SCII, in which the pumping speed was investigated as function of i) pressure, ii) temperature, iii) adsorbent pre-load, and iv) gas composition provided further evidence that this sorbent had the potential for meeting ITER requirements.

In experiments, in which several charcoal/aluminium specimens were exposed to tritium at temperatures of about 77 K for periods lasting approximately six months, only small radiation-induced effects on the adsorption speed and adsorption capacity were registered [Sed91]. Possible effects induced by the radiation emitted by tritium were uncovered by comparing the sorption performance of specimens, i.e. pumping speed and sorption capacity prior to exposure, after

exposure to tritium for several months, and after completion of the experiment. Post irradiation tests included a qualitative and quantitative chemical analysis of supernatant gaseous tritium. Because all observed changes were only minor, it was concluded that charcoal is an adequate and reliable adsorber material.

Even though molecular sieves exhibited a number of rather attractive properties, they were discarded mainly because of their high affinity for water and other polar species. Further detrimental properties of molecular sieves are the markedly higher re-activation temperature, i.e. $> 573\,\mathrm{K}$, in comparison to that necessary for carbon, i.e. $400\,\mathrm{K}$, and the poor co-pumping performance displayed by molecular sieves for hydrogen and helium (diffusion limited).

Steady state cryo-sorption **isotheres** for helium and hydrogen (straight lines obtained from a plot of pressures vs. temperatures at constant amount of adsorbed gas) on charcoal adsorber are depicted in Fig 3.18 [Les89]. The cryo-adsorption capacity of charcoal for each of these two gases is specified by temperature, pressure, and the $(\mathrm{d}p/\,\mathrm{d}T)$ slope. Dynamic loading experiments indicated that each non-condensable has a critical temperature at which surface mobility becomes sufficiently high to clear the outer surface. At lower temperature the pores become clogged. Under these conditions, the adsorbent appears to be saturated but in reality, the adsorption capacity is below the maximal attainable value. The critical temperature is a function of the cryo-sorbent/adsorbent system, the temperature, and the rate of loading.

Day et al. [Day00; Day02; Day07] performed experiments designed to elucidate the specific pumping mechanisms of all three hydrogen isotopes on activated charcoal. According to their findings, the retention of molecular protium, deuterium, and tritium is governed by sorption, sorption together with re-sublimation, and re-sublimation, respectively. The initial sticking coefficient of helium, hydrogen, deuterium, and tritium on activated charcoal at $5\,\mathrm{K}$ were determined to be 0.4, 0.6, 0.9 and 1.0, respectively, which is in good agreement with literature values. Whereas the sticking coefficient of helium showed strong dependence from temperature, this was much less the case for hydrogen. The experiments revealed marked influence of helium on the overall pumping speed.

In another experimental study carried out by Day et al. [Day00] the poisoning effect of water and other species on the performance of ITER cryo-sorption model pumps was investigated systematically. The conclusion was that both retention and accumulation of tritiated water

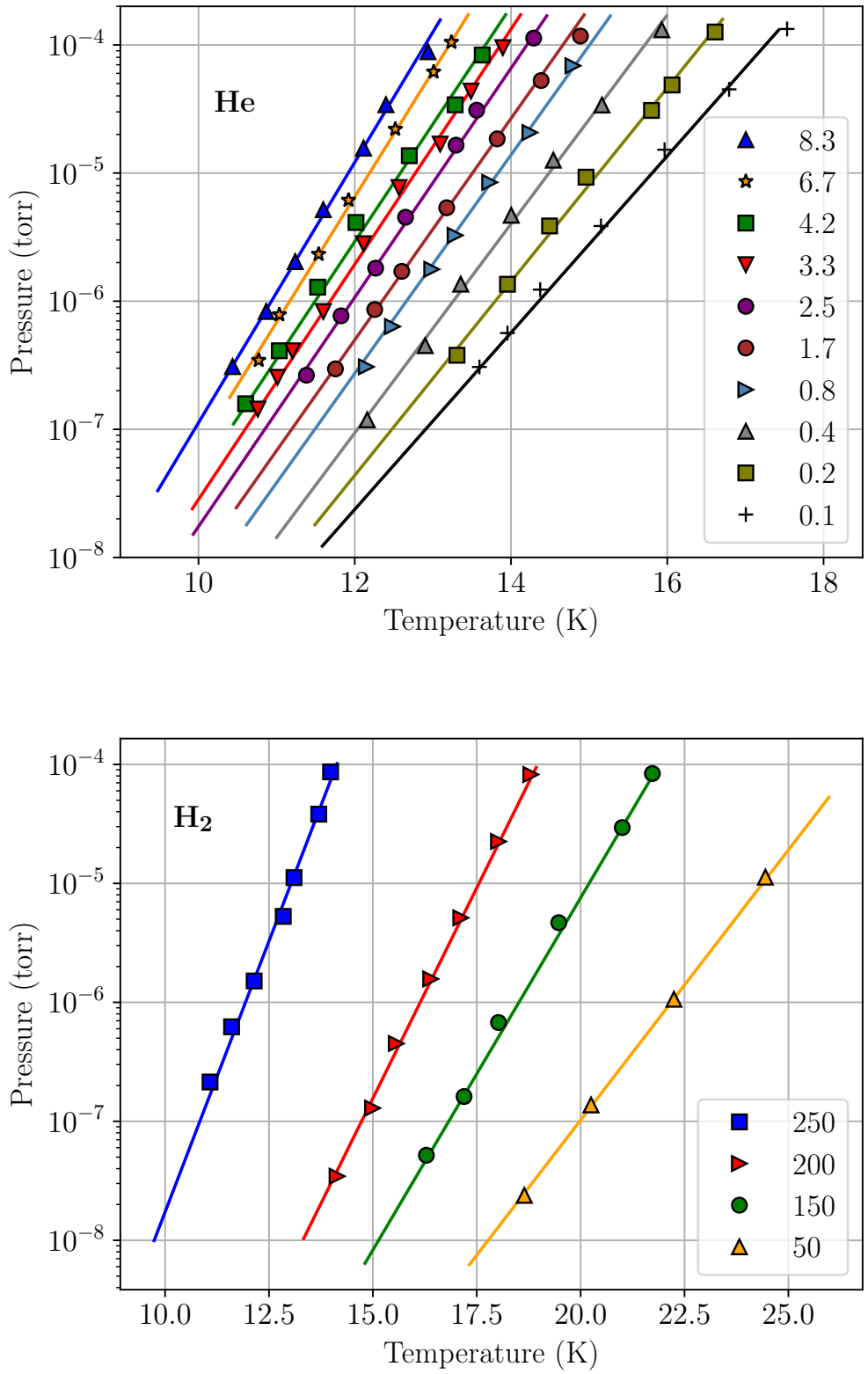


Figure 3.18: Cryo-adsorption isotheres for helium (upper figure) and hydrogen (lower figure) on charcoal. Helium and hydrogen isotheres are expressed in STP cm^3/g (after [Les89]).

as well as higher hydrocarbons on the inlet baffle system, normally maintained at 85 K, is not critical to the operation of cryo-pumps.

Precise temporal sequence of the **regeneration** temperature scheme for ITER cryo-pumps is of fundamental importance for the achievement of a clean separation of the accumulated impurities while maintaining an optimal pumping efficacy. This information is also of much importance for the design specifications of future cryo-pumps. To shed light on this issue an experimental study was performed at KIT utilizing the upgraded facility TITAN[17] [Day00; Mac01; Day09]. The results revealed that the quantitative regeneration of cryo-pumps from water is only possible by thermal means at about 400 K. In case higher polar and non-polar hydrocarbons are among the impurities in noteworthy amounts, temperatures of 450 K or even higher could become indispensable. Such high temperatures are of considerable implication to the design of pumps; they will also show up in the costs. Lower regeneration temperatures are only possible when sorbent heating is supported by efficient evacuation [Day00]. Regeneration by evacuation at insufficient temperature will probably slow down the extraction of impurities. Since the extraction efficacy will also depend on the ultimate pressure attainable with the fore pump to the cryo-pump, a high-speed fore pump was recommended by Murdoch et al. [Mur00]. It was concluded that more detailed information on type and quantity of hydrocarbons generated from plasma/wall interactions and further experimental work on the thermal desorption of impurities are still needed for the final design of cryo-pumps.

It should be noted that due to the large differences in plasma facing components of JET and ITER the composition of the exhaust gases from both machines will propably be quite different. If carbon-based plasma facing material is replaced by beryllium in the vacuum vessel and by tungsten in the divertor of ITER, the presence of higher hydrocarbons is highly unlikely in the exhaust gas of this machine [Hir16]).

The evolution of the tritium inventory in a cryo-pump during staggered operation sequences of ITER (pumping-regeneration cycles) has been examined and discussed by Murdoch et al. [Mur99]. To provide sufficient pumping speed for ITER a total of six cryopumps were considered necessary. Continuous pumping during longer pulses will make the installation of four additional cryopumps indispensable. The pumping time and therefore the time during which gases can

[17] TITAN is a test facility at KIT originally designed for the characterization of components for pumping of hydrogen isotopologues by cryo-sorption.

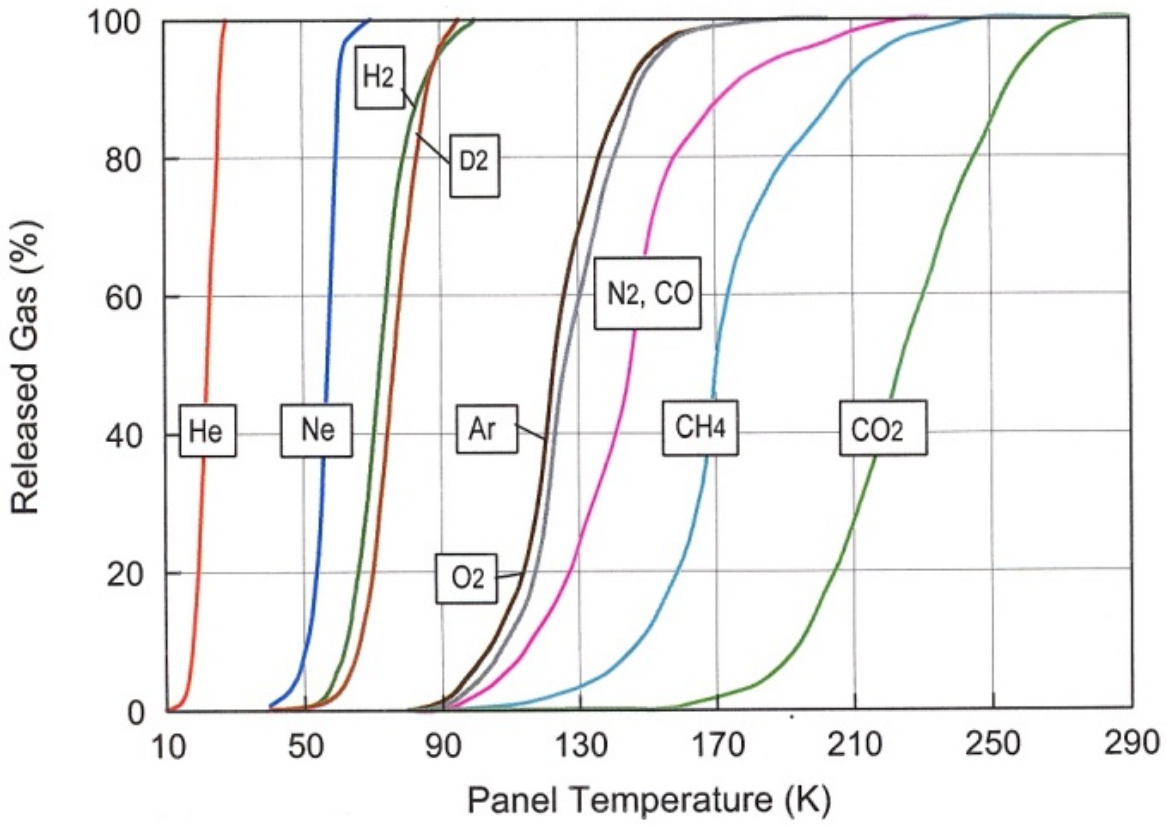


Figure 3.19: Sequential desorption of some typical plasma exhaust components as function of temperature [Day02].

accumulate in the panels has been restricted to 450 s. Thereafter, partial regeneration from hydrogen and helium is carried out at 80 - 90 K, that from air-like impurities at 300 K, and that from water-like impurities at more than 373 K [Day00; Day02] (see Fig. 3.19). With increasing number of regenerations, a fraction of the adsorbed tritium-bearing water, and/or higher tritiated hydrocarbons of high specific activity will progressively and persistently be retained in the of the cryo-pumps. Isotopic exchange and radiation-induced reactions may increase the retention of tritium. Removal of this progressively increasing contamination may require heatig of baffles, shields, and panel‘s up to temperatures of 475 K [Hau07].

During each **basic** pumping/regeneration cycle of the ITER vacuum vessel with cryopumps, the cryo-adsorption panels inside of the pumps will only be heated from 4.5 K up to 85 K in four sequential steps, each of 75 s duration. The four steps comprise i) selective release and pumping of helium, ii) rapid warm up to liberate fusion fuel gases, i.e. deuterium and tritium, iii) pump

out of these gases, and iv) rapid cool down. After about ten of these pumping/regeneration cycles, an additional special regeneration step is inserted, whose objective is the extraction of all air-like species from the panels. This regeneration is accomplished at 300 K. Because water, water-like molecules, and higher hydrocarbons, are not recovered efficiently from the baffles by pumping at 300 K, gradual and significant reduction of the sorption capacity will become apparent. Hence, a fourth regeneration step at a temperature of ≤ 473 K[18] must be performed, but at more prolonged intervals.

The fourth step is not only necessary to restore the full pumping capacity of the charcoal adsorber but also to maintain the total tritium inventory inside of the whole pump below the established limit value of 120 g [Hau07]. What is more, in order to exclude deflagration after vaporization of hydrogen isotopes adsorbed on the panel´s during a loss of vacuum accident (LOVA) (max. pressure 0.2 MPa) it is necessary to maintain the inventory of flammable gases below threshold values at all times [Wyk05]. Regular regeneration of cryo-pumps is therefore mandatory not only from an operational but also from a safety point of view [Day02; Hau07].

Heating adsorption panels of cryo-pumps up to 80 K must be accomplished in less than 75 seconds and cooling back down to 4.5 K in about the same time. This requires considerable amounts of coolant. To reduce the overall consumption of coolant, an enthalpy recovery concept is necessary. Essentially, the enthalpy from the cold panels of one pump is recovered during warm up and transferred to the panels of another pump during cool down [Bax98]. For this, both pumps need to be operated in series. In view that only 95 % of the tritium in the off-gas is in the elemental form and during routine operation the panels are solely regenerated from DT, the tritium inventory remaining in the pumps will progressively increase until the authorized safety-relevant maximum value is reached. At this point full regeneration of the sorbent can be carried out by adjoining electric resistance heaters or a forced flow of warm helium through the cooling channels of the panel´s. During tokamak operation one pump after the other will have to be regenerated from hydrogen isotopes after a pumping period of less than 600 s. For the complete release of higher molecular weight impurities longer regeneration intervals than for the fuel gases are predicted.

[18] Whereas water is almost completely released from microporous charcoal at 373 K, this may not be the case with some higher hydrocarbons.

Tests performed to determine the residual inventory of tritium in cryo-panels revealed that not only the kind of impurity gas to which the cryo-panel was exposed but also the temperature and pressure conditions at which regeneration is carried out have strong influence on the inventory [Day98; Mur07]. Specimens manufactured following ITER specifications and exposed to relevant amounts of tritium, i.e. about 2×10^{-8} Pa s, exhibited an inventory of up to 10 MBq after regeneration at ambient temperature under a vacuum of 10^{-2} Pa. This inventory is considered compatible with the constraints established for the operation of ITER cryo-pumps.

In a complementary study, the pumping performance of prototype panel´s was investigated under fairly realistic conditions utilizing the Cryogenic Fore Vacuum Subsystem of the Active Gas Handling System of JET. The performance of the panels was likewise examined under direct supply of tritium within the frame of the Trace Tritium Campaign of JET [Day05]. Pumping of tritium occurred by re-sublimation. The sticking coefficient of tritium was found to be close to unity. Post mortem examinations of aged panels have been completed. To verify the robustness of the design, long-term cycling tests under representative regeneration conditions are indispensable.

As opposed to pumps previously investigated at TSTA [Sed91] during the development of a new generation ITER pumps, much attention was given in recent research activities to the consequences of impurity accumulation and to procedures for their recurrent removal. Impurities such as water, nitrogen, oxygen, carbon dioxide, and especially higher hydrocarbons generated in the torus by plasma-wall interactions, will accumulate in the adsorption panels of the pump´s and gradually jeopardize the pumping efficiency. Within this frame, prototype cryo-pumps were configured, build, and tested at KIT (formerly KfK) to demonstrate under representative conditions high speed vacuum pumping while meeting all exigent ITER program goals [Mac98; Day01; Mac02; Day07; Hau07; Day09]. Extensive tests were carried out with a cryo-pump of 1776 mm outer diameter and total length of about 2054 mm. The need of recurrent selective impurity removal was addressed with an integrated inlet valve having a maximum stroke of 500 mm and designed to open towards the torus (see Fig. 3.20a) [Hau07]. The applications of the valve were to i) vary the pumping speed by throttling, ii) close the pump during plasma pulse operation to allow on-line regeneration, and iii) act as safety device against overpressure (opens to the torus).

At ITER, six identical large cryo-pumps will be located at divertor ports of the torus, where they will be used in intermittent batch-operation pumping/regeneration modus. A model torus

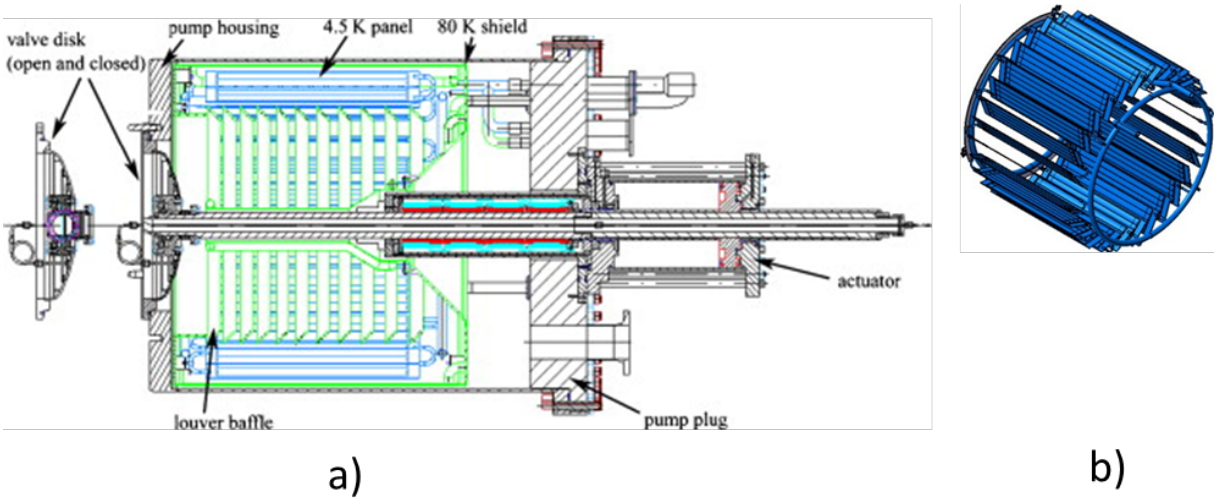


Figure 3.20: Detailed drawing of an ITER prototype cryo-pump (a) and of the integrated concentric array of 28 cryo-adsorption panel´s (b) The cryoadsorption panel´s are shown in blue in figures a) and b). The panel´s are maintained at 4.5 K with liquid helium. They are highly optimized with respect to adsorption speed and capacity [Hau07].

exhaust cryo-pump has now been built at 1:2 scale and demonstrated experimentally [Haa03]. A few numbers to illustrate the dimensions of this component: The pump has a valve head diameter of 800 mm weighing about 80 kg which travels along a 400 mm shaft stroke. A total cryo-adsorbent area of 12 m^2 is distributed over 28 cryopanels of which each has a length of 1000 mm.

3.14.1.8 Pumps based on cryo-trapping in frost layers

Another concept for helium pumping, which does not rely on condensation as solid at 4 K, is cryo-trapping in frost layers employing a chemically inert condensable gas like argon [Mur91b; Mur91a]. By adjusting (decreasing) the molar He/Ar ratio of the feed gas the vapour pressure of helium can be lowered by orders of magnitude at a given cryogenic temperature. Cryo-trapping does without a solid sorbent and therefore circumvents uncertainties concerning long-term integrity of adsorption panels during prolonged thermal cycling. For the same reason, there are no limitations to upscaling. On the other hand, the necessity of an extra dedicated process for the separation and recovery of argon is considered to be a considerable drawback, at least for ITER. In fact, argon must be recycled not only for economic considerations but also - at least in case of ITER - because of possible activation by energetic neutrons with formation of Ar-41.

Another drawback of cryo-trapping is the relatively large argon flow required and the similarity between the freezing points of argon and some tritiated organic impurities.

Recently, tritium **cryo-trapping** in argon frost layers has also found application in the KATRIN (Karlsruhe Tritium Neutrino) experiment at TLK [Ase01; Wei05; Kaz08]. Special feature of this experiment is the high luminosity Windowless Gaseous Tritium Source (WGTS) designed to inject $1.8\,\mathrm{mbar\,l\,s^{-1}}$ tritium without contamination of the spectrometer. From this source only decay electrons are guided adiabatically with the help of a magnetic transport system into the spectrometer. This is achieved in a first step employing a differential pumping section (DPS) installed downstream, which basically consists of several turbo molecular pumps (the DPS system must reduce the flow rate of tritium down $10^{-7}\,\mathrm{mbar\,l\,s^{-1}}$). To arrive at the final demanded $< 10^{-14}\,\mathrm{mbar\,l\,s^{-1}}$ value an additional Cryogenic Pumping Section (CPS) is required (see Fig. 3.21)[19]. Bearing in mind that a typical campaign of KATRIN may last about 60 days of continuous operation, a CPS was needed capable of processing an integral amount of tritium of the order of $0.5\,\mathrm{cm^3}$. Besides of this relatively "large" capturing capacity, the CPS must also be in a position of maintaining the high pumping speed throughout the campaign removing tritium effectively from the spectrometer during the whole period of operation. A further demand is quantitative recovery of tritium from CPS when this system is in the regeneration phase.

In view of the above, it was proposed to design a CPS based on argon frost technology. To investigate pumping of tritium under conditions simulating the flow regimes prevailing at KATRIN the so called TRAP (TRitium Argon frost Pump) test rig was built at TLK. The experiment utilizes a cryo-surface cooled to 4.2 K that can be covered with argon [Eic07; Eic08; Kaz08]. The cryo-surface basically consists of a 20° bent tube cooled with liquid helium whose conductance simulates that envisaged for CPS. The 20° angle prevents the so called beaming effect of the molecular flow. Separate containments for argon and tritium are employed to supply the inlet system via capillaries. Tritium exiting the device can be detected either by a calibrated residual gas analyser or a comparatively much more sensitive silicon detector. Important goals of the TRAP set up were i) demonstration of the pumping concept, ii) determination of the upper limit of the migration of tritium through the entire cryo-trap, iii) parametric investigation of the regeneration of the cryo-surface with the ultimate aim of developing an optimized regeneration

[19] B. Bornschein, TLK-Jahresvortrag: Quo Vadis KATRIN?, Presentation, 2014

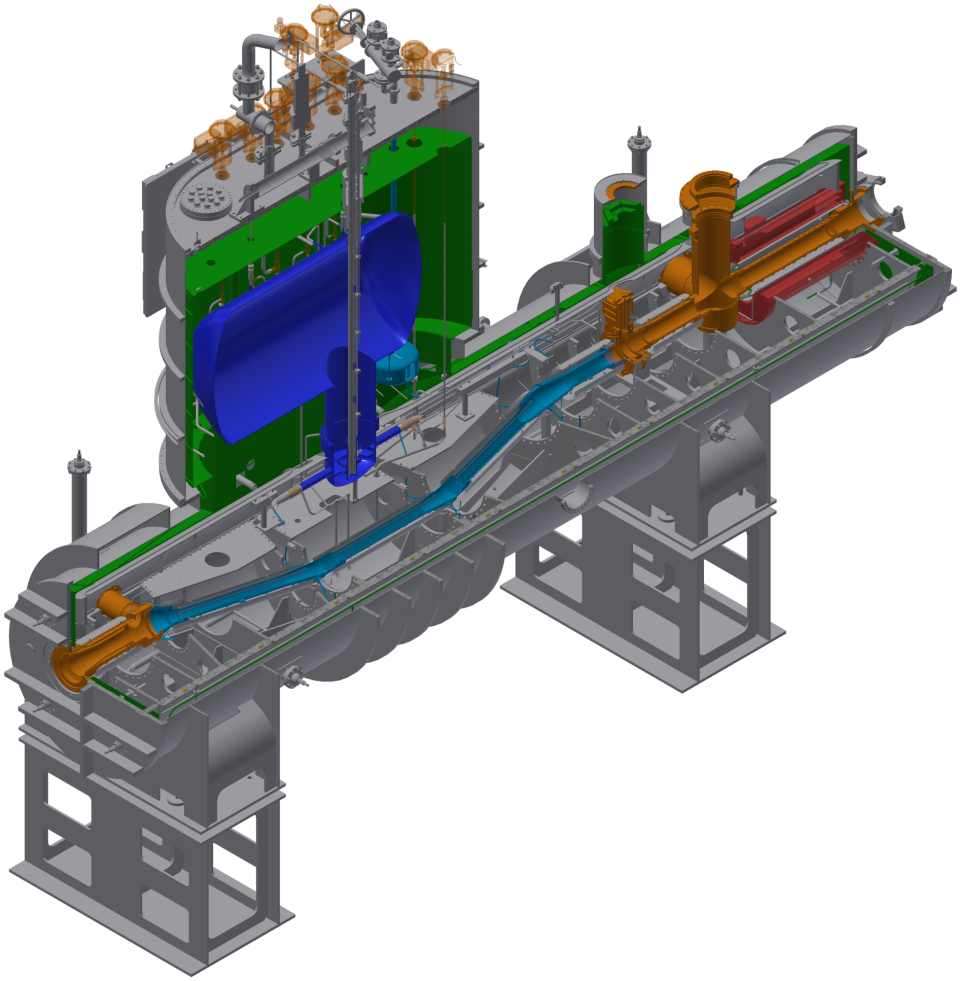


Figure 3.21: Cryogenic pumping section (CPS) of KATRIN.

procedure, and iv) experimental assessment of the possible advantages of replacing argon by krypton.

Preliminary experiments on the tritium flow rate suppression factor, F, using argon condensate as adsorbent have been reported by Eichelhardt et al. [Eic07; Eic08] and Kazachenko et al. [Kaz08]. The task consisted in spotting quantitatively tritium reaching the detection zone of TRAP downstream of the cryo-surface, here defined as Q_{Det}. Q_{Det} was taken to be the accumulation rate of tritium in the detection zone according to

$$Q_{\mathrm{Det}} = Q_{\mathrm{W}} + Q_{\mathrm{D}} + Q_{\mathrm{G}} + Q_{\mathrm{B}}$$

where

Q_{W} = adsorption rate of tritium on stainless-steel detection zone walls,

Q_{D} = adsorption rate of tritium on the detector surface,

Q_{G} = accumulation rate of tritium in the gas phase,

Q_{B} = diffusion rate of tritium into the bulk of stainless-steel.

The terms Q_{W}, Q_{D}, and Q_{G} were determined experimentally and found to be 9.6×10^4, 2.5×10^4, and 8 tritium atoms/s, respectively [Eic08]. Because at the time no technique was available for the evaluation of Q_{B} this term was assumed to be close to zero. In future experiments the inner walls of the detection system will be gold-plated in order to keep diffusion of tritium into stainless-steel walls at extremely low values.

F values, where $F = Q_{\mathrm{in}}/Q_{\mathrm{out}}$ and Q_{in} is the inflow rate of tritium and Q_{out} the outflow rate, were determined to be within the range 10^7 - 10^8. When compared to the design value of $F > 10^7$, these values were considered promising. Concerning the specific needs of KATRIN, the pre-condensed argon layer has several significant benefits: it is i) easily attachable to metallic surfaces, ii) insensitive to poisoning, and iii) straightforwardly regenerated with full recovery of tritium after each prolonged run of KATRIN. The detrimental effect of the decay heat of tritium increasingly released with progressing accumulation in the frozen argon layer has not yet been evaluated. Because the range of beta rays emitted by tritium in solids is very small, i.e. $< 4\,\mu\mathrm{m}$, most of the released energy will be deposited in the 1 - 2 µm thick cryo-adsorption layer. In view that this may lead to release and transport of tritium across the CPS into the spectrometer, further careful investigations are under way.

3.14.1.9 Roots pumps

Much relevant experience with **Roots pump´s** has accumulated with experiments carried out at the vacuum vessel of JET. The vessel has a volume of nearly $190\,\mathrm{m}^3$ and is usually maintained at a temperature of 593 K. Evacuation of this vessel is performed by four turbo molecular pumps of $3500\,\mathrm{l\,s}^{-1}$ pumping speed backed by rotary Roots pump pair´s having a pumping speed for deuterium of about $7000\,\mathrm{l\,s}^{-1}$ [Pea01].

Roots pumps with throughputs in the range 1200 - 4200 $m^3\,hour^{-1}$ were first proposed back in 1996 for the generation of rough vacuum at ITER [Lad97]. A further potential application of Roots pumps at ITER is fast regeneration of cryo-pumps.

The performance of Roots blowers with helium and hydrogen is usually inferior to that achievable with heavier gases. This is attributed to back leakage past the rotors during compression and a carry-back effect by the rotor as it returns to the high vacuum side of the chamber [Cof82]. High pumping speed, reliability, low cost, robustness, and compactness can be cited among the principal advantages of Roots blowers. However, for tritium service the elastomer O-ring body seals of commercial pumps needs to be replaced by appropriate metal seals in order to achieve the required long-term leak-tightness. A further significant upgrade to achieve full tritium-compatibility is the development of a magnetic coupling between motor and rotor. Because conventional Roots pumps provide no vacuum-tight separation between the pumping volume and the oil volume lubricating the rotating shafts, a contamination of the oil by tritium and/or a contamination of the pumped gas by oil cannot be ruled out.

Ladd et al. [Lad01] tested the pumping speed characteristics of the type EH250 and EH 1200 mechanical Roots blowers supplied by Edwards both singly as well as in combination with a backing pump. The employed test gases were N_2, He, H_2, and D_2 at inlet pressures within the range 10^{-1} - 10^4 Pa (see Fig. 3.22).

An option to solve the leak problem between pumping volume and lubricant volume could be replacement of the elastomer O-ring seals of commercial pumps by **ferro fluidic seals** [Lae02d; Ant05]. Advantages of ferro fluidic sealed feedthroughs are their capability to operate i) under ultrahigh vacuum conditions ($< 10^{-8}$ mbar), ii) at relatively high temperatures, iii) at elevated pressures, and iv) remain vacuum-tight up to tens of thousands rpm. A further advantage of this type of seal is that they are equipped with a permanent magnet that requires no extra supply of electrical power. In view of this, an investigation on the potential applicability of ferro fluidic seals as a means to upgrade Root pumps was initiated. First auspicious tests were carried out by Lässer et al. [Lae02d] under ITER-processing relevant conditions employing a prototype ferro fluidic seal capable of sustaining rotational shaft speeds of up to 1500 rpm at pressures of up to 100 kPa. Diverse parametric runs revealed that the leak rate increased slightly i) with operation time, ii) increasing rotational speed, and iii) increasing driving gas pressure. In spite of this, the leak rate remained below $10^{-9}\,Pa\,m^3\,s^{-1}$ during an integral test period of more than 4 months.

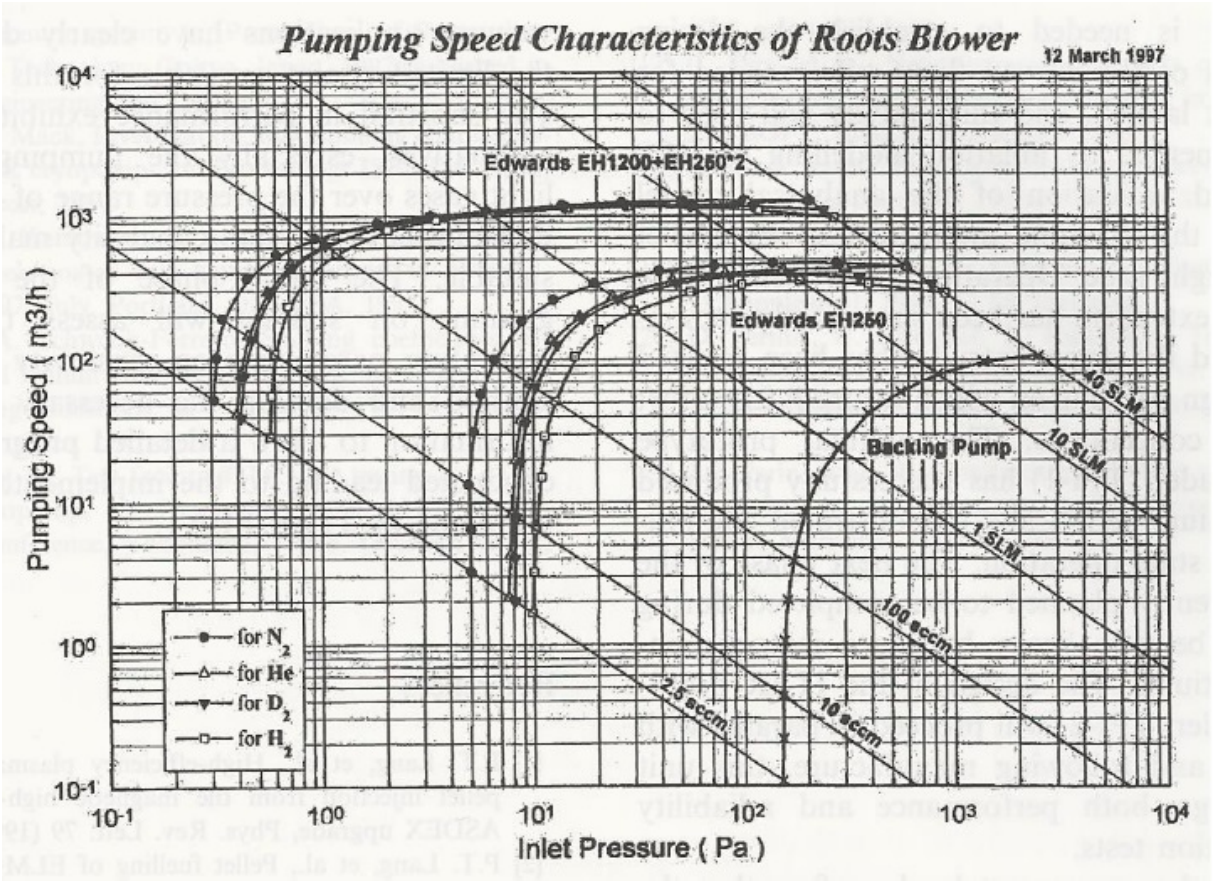


Figure 3.22: Pumping speed as function of inlet pressure of Edwards EH1200 and EH250 multistage roughing pumps [Lad01].

Under the assumption that the pressure difference remains constant at 25 kPa and the rotational speed stays constant at 1500 rpm an extrapolation of the results indicate that after six years of operation the leak rate would not increase by more than an order of magnitude. The uptake of tritium by the ferro fluidic liquid was determined to be of the order of $0.5\,\mathrm{MBq\,l^{-1}\,d^{-1}}$.

Ensuing successful testing without tritium of a ferro fluidic seal integrated into a small roots pump for an integral period of about one year, a modified ferro fluidic standard cartridge seal with six sealing teeth´s was build, integrated into the so called **Ferro Fluidic Advanced Cartridge Tritium** (FACT) facility and tested with tritium at KIT [Lae02d; Ant08a]. Two monitored volumes, one containing gaseous tritium at a pressure of 900 mbar[20] and another containing nitrogen at a pressure 400 mbar were separated from each other inside of the cartridge by the

[20] This pressure is far higher than that anticipated in an ITER roots pump, i.e. 100 mbar. The higher pressure was selected to obtain results in shorter time.

ferro fluidic material. The cartridge itself was coupled to a shaft sealed by a rotary seal operable with a brushless motor at variable speeds. The first test, which was started with a rotation speed of 1500 rpm, was planned to encompass a period of about two months. Even though initially the tritium leak rate of the ferro fluidic seal matched expectations, i. e. about $10^{-7}\,\mathrm{Pa\,m^3\,s^{-1}}$, after a short interruption of the operation, it became evident that tritium had permeated into the volume containing nitrogen. This unsuccessful result was attributed to the utilization of the wrong ferro fluid (it actually was not the one originally ordered for the tests). Because of the relevance of this experiment for the development of a fore vacuum system for ITER, a new test with a ferro fluid of optimized composition has been planned. Following preliminary compatibility tests of the chemically more robust fluid, first with hydrogen and thereafter with tritium, a cartridge containing gaseous tritium will be assembled and integrated into the FACT facility. Tests of the improved device will be conducted proceeding according to an experimental program originally developed together with Day [Day08].

3.14.1.10 SRTI pumps

SRTI wobble pumps are supplied in two basic configurations:

- **PR configuration**: comprises a completely dry leak-tight compression pump of the volumetric type in which an impeller rocks in a rotary manner within the pump chamber.
- **PBT configuration**: consists of a five cylinder volumetric pump in which a metallic bellows seals the grease lubricated drive train from the pump chamber. The cylinders are arranged vertically and in a circle.

Special features of newer versions are a ceramic/ceramic piston/cylinder contact, and two coaxial bellows totally separating the gases from the lubricants. The SRTI pump has been developed for use with radioactive and hazardous gases. The pumps are inherently gas-type independent and capable of evacuating gases down to 1 mbar at high throughput. Design pressure of the pumps is 40 bar; they must be installed in horizontal position.

SRTI pumps, now known as Thales pumps, were shown to be reliable in tritium service at Valduc, Fontenay aux Roses, and Grenoble in France [Pau88]; at TPL, Tokai Mura, Japan [Nar90]; Los Alamos Scientific Laboratory, USA [She75]; and TLK, Germany [Pen97b]. A small SRTI

pump model PR-9 was tested at Los Alamos Laboratory for the recirculation of tritium-bearing gases ($100\,\mathrm{l\,min^{-1}}$ at a pressure of $1.3 \times 10^4\,\mathrm{Pa}$) and found to deliver superb service [She75].

At Tokai-mura a double metal bellows reciprocating pump from TEC, Japan, followed by two SRTI wobble pumps were used in series to evacuate a magnetic bearing turbo molecular pump (TMP) [Nar90]. With this pump combination the fore vacuum to the TMP was determined to be 1.3 Pa. Experience at TPL with SRTI pumps type PR and PBT were not always satisfactory. This motivated closer examination of the Japanese Toyo pumps as potential replacement [Hay95a] (see below).

In one application at TLK, the hydrogen exhaust from a permeator was pumped down to 50 Pa at $10\,\mathrm{m^3\,hour^{-1}}$ pumping speed using a five-stage type PBT 105 SRTI pump.

At Laue Langevin Institute in Grenoble, France, SRTI wobble pumps type PTB 135 were used successfully in tritium service.

SRTI type PBT 105 and PMDS 63TR pumps have been proposed by Glugla et al. [Glu02a] as transfer and circulation pumps, respectively, for the exhaust gas processing system of ITER.

3.14.1.11 Sputter ion pumps

Sputter-ion pumps are used to generate ultra-high vacua, i.e. $< 10^{-11}$ mbar. For the achievement of even better vacua, e.g. 10^{-12} mbar, the sputter ion pump needs to be operated in conjunction with another pump such as a titanium sublimation pump.

Sputter ion pumps essentially consist of an anode, two cathode plates, and a permanent magnet. While the anode is usually cylindrical and made of stainless-steel, the cathode plates are manufactured from titanium. The plates are positioned on opposite sides of the anode tube where they serve as getters. The pump operates by ionizing the gas present within a magnetically confined cold cathode discharge. Electrons emitted by the cathode ionize the gas generating positive ions which are accelerated by a strong anodic potential of 3 - 7 keV to the chemically reactive cathode. For optimal operation the pressure must be lower than 10^{-4} mbar; the maximum pumping speed is reached once the vacuum reaches values of the order of 10×10^{-6} mbar. When pumping at very low initial pressures erosion of the cathode can be minimized which effectively increases the pump life time. Pumping rate and pumping capacity depend upon the type of gas that is being gettered by titanium. Heavy noble gases are pumped by ion burial. Inert gases (He) and lighter reactive gases (H_2) are initially retained by physisorption

and will eventually diffuse into the cathode material. The pumping rate will in the end be governed by the rate with which these gases are incorporated into titanium. The sputtering rate of titanium due to impacting ions depends on the ratio of the mass of the bombarding molecules to that of the mass of the cathode material. Because hydrogen is very light, its sputtering rate will be rather small. Ions impacting on the cathode will sputter material onto neighbouring surfaces. Before depositing onto the pump walls the reactive sputtered material will undergo reactions with gases such as oxygen, hydrogen, nitrogen, or carbon oxides yielding solids of low vapour pressure. Therefore, gettering is associated with a further reduction of pressure in the vessel. Energetic ions will not only sputter but a fraction of them will penetrate "deeper" into the cathode material, i.e. several atom layers, and therefore contribute additionally to a reduction of the pressure. This is particularly the case for noble gases, which cannot react chemically with titanium, as well as for light molecules like hydrogen isotopologues. The achieved pumping effect is, however, not lasting. As sputtering continues the penetrated ions will sooner or later be once again released.

Ion sputtering pumps are especially suitable for the evacuation of tritium handling systems, because they neither have moving parts nor necessitate a lubricant. Hence, they are clean, generate no vibration, need almost no maintenance, and work safely without contingencies over extended periods of time [Tor02].

Biró [Bir72b] investigated the degree of contamination by tritium of a titanium ion-getter pump installed in a neutron generator of the kind used in nuclear physics laboratories or for activation analysis. After about two years in operation a pump was dismounted and dismantled in a hood. The total activity of the tritide targets utilized in the generator was 6.2×10^{12} Bq. For more detailed information on the distribution of the contamination by tritium in the structural elements of the pump the original paper should be consulted.

3.14.1.12 Titanium sublimation pumps

Titanium sublimation pumps are similar to sputter ion pumps. They are principally used to generate ultra-high vacua. Titanium sublimation pumps basically consist of a titanium filament through which a high current is passed recurrently causing the filament to reach repeatedly sublimation temperature. Since vaporized clean titanium is very reactive it will undergo reactions with hydrogen to form a stable hydride before it deposits on the inner walls of the pump. As a

consequence, the pressure of hydrogen in the pump is reduced. The pump has several filaments that can be switched to a new filament each time one becomes exhausted. Sublimation pumps work well with reactive gases such as hydrogen, oxygen, and carbon oxides but not with inert gases like helium. Therefore, titanium sublimation pumps need to be backed up by another suitable pump.

3.14.1.13 Reciprocating compressor

An oil-free, reciprocating type of compressor with double metal bellows seal was developed at TPL, Tokai Mura, together with Toyo Engineering Co, Japan (see Fig. 3.23). The tritium compatibility of this pump was demonstrated by JAERI scientists at TSTA, Los Alamos, New Mexico [Hay91; Hay95c; Yam95a]. The pump, which comprises four-stage compression cylinders featuring carbon polyimide composite piston rings, is cooled with $5\,\mathrm{l\,min^{-1}}$ water. Each stage in each cylinder has 16 special valves. Flow fluctuations caused by the reciprocating action are eliminated by buffer tanks placed near the suction and exhaust zone. These cylinders have a diameter of 560 mm. Hence, if the the buffer tanks are included, the pump has an effective rather large dead volume of 138 l. A matter of concern has been possible release of dust from the lubricant.

With hydrogen, deuterium, tritium, helium, or nitrogen pumping speeds of up to $180\,\mathrm{m^3\,hour^{-1}}$ have been demonstrated. Tritium is pumped at a suction pressure of 5 mbar with a speed of $120\,\mathrm{m^3\,hour^{-1}}$. The pump can generate vacua of 1 mbar with nitrogen and 3 mbar with hydrogen. The ultimate suction pressure with tritium was determined to be 1.1 mbar at 667 mbar discharge pressure. The pump is specified for a maximum suction pressure and maximum discharge pressure of 1 bar and 5.8 bar, respectively. The dependency of pumping efficiency from the type of gas is small. After discontinuous operation for a period of three months with gram amounts of tritium no signs of degradation were registered [Hay95a].

The evacuation performance of the reciprocating pump improved significantly at low suction pressures after the formerly used check valves were replaced by solenoid valves [Hay11]. Under these conditions, the ultimate vacua achievable with hydrogen, helium, and nitrogen decreased from formerly 0.050, 0.063, and 0.071 to values of 0.071, 0.095, and 0.011 mbar, respectively.

With the small $1000\,\mathrm{l\,min^{-1}}$ Toyo pump vacua of about 1 mbar were attained with gases such as hydrogen, deuterium, helium, and nitrogen.

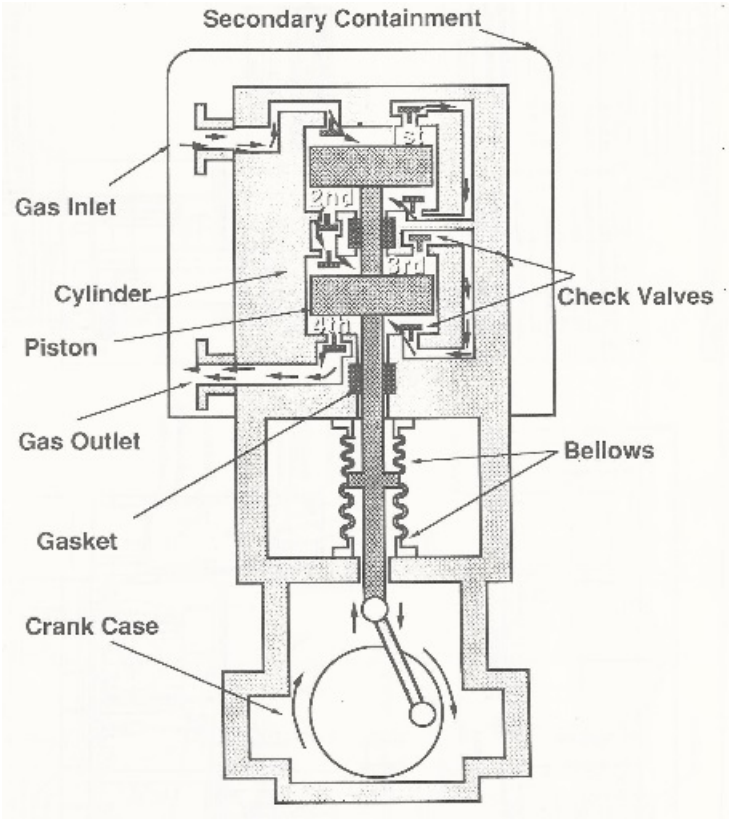


Figure 3.23: Schematic view of the oil-free TOYO/JAERI reciprocating pump with four compression stages [Hay91].

Recapitulating, an ample body of experience and literature is now available on the performance of a large variety of pumps and compressors relying on rather diverse working principles all of which have been tested in tritium service in research laboratories and technological facilities throughout the world handling between small to sizable amounts of tritium. Enough pertinent experimental data are now accessible to demonstrate that many pumps meet all criteria for an undisturbed usage in the presence of tritium.

It may further be concluded that in spite of some remaining open questions there is presently sufficient experience and pertinent literature on which to base the design of mechanical pumps required to meet the program goals of ITER.

3.14.1.14 Permeation pumps

Two diverse pumping concepts based on the selective permeation of hydrogen isotopologues are discussed below.

3.14.1.14.1 Palladium alloy membrane pump

Young [You63] was first to observe that hydrogen can be evacuated into the air from a container down to pressures of 10×10^{-8} mbar, i.e. much below the partial pressure of hydrogen in the atmosphere which is 10×10^{-3} mbar, employing a Pd or PdAg alloy diaphragm heated up to temperatures in the region 773 - 873 K. For pumping to occur, the permeate region must be oxidizing, i.e. air or oxygen. Membranes of titanium or nickel displayed similar pumping characteristics, but the attained pumping speeds were significantly lower.

Berkheimer and Buxbaum [Ber85b; Ber85a] proposed for the evacuation of hydrogen isotopologues a simple palladium-alloy membrane pump comprising a heated palladium or palladium alloy membrane and a liquid nitrogen cooled trap. Basically, hydrogen is chemisorbed and dissociated on one side of the membrane maintained at 573 K (appears to be the optimal temperature) and converted catalytically into water by reaction with oxygen on the back side. Resulting water is solidified in a liquid nitrogen trap. An obvious advantage of this membrane pump is that it operates without lubricant or moving parts. The drawback is that it only pumps hydrogen isotopologues.

3.14.1.14.2 Bilayer metal membrane pump

Shmayda et al. [Shm85] performed asymmetric permeation experiments with membranes consisting of a copper – α-iron composite. The composite was prepared by depositing copper ion vapour on α-iron to yield either columnar or equiaxed copper grains. The mean thickness of the copper layer on two equal iron substrates was determined to be either 3 or 7 µm, that of both substrates was approximately 80 µm. Gas flow across the composite was arranged in such a way that the layer with the higher product of solubility and surface recombination rate constant faced the downstream side [Shm88a]. The permeation device was found to be fully transparent to atomic hydrogen in one direction and impervious to both atomic and molecular hydrogen in the opposite direction. Gas was supplied into the upstream side of the permeation pump at a controlled rate from a tank using a leak valve. Atomic hydrogen was generated by contact dissociation employing a conventional tungsten filament held at 2000 K. Hydrogen permeation measurements of atomic hydrogen were carried out at 483 or 533 K. The measurements were performed at upstream pressures ranging from 40 µbar up to 1 bar. Pressures of up to 1 mbar

could be attained at the downstream side of the composite membranes. Under these operating conditions pumping speeds of up to 5 $l\,s^{-1}$ and compression ratios of up to 870 were shown to be possible. Compression ratios were determined by isolating the downstream vacuum pump and pumping into an evacuated downstream volume of 3.1 l. The ability of the permeation pump to compress hydrogen relies principally on the enormously different rates with which atomic and molecular hydrogen are dissolved on the two sides of the composite material.

Hydrogen concentrations lower than 0.01 % in helium could be removed from a helium stream introduced into the upstream side of the permeator. The permeant flux from a helium carrier gas containing 1 % hydrogen corresponded essentially to that observed in the absence of helium. Throughput´s were reported as high as 0.6 $mbar\,cm^3\,min^{-1}$ per square centimetre of membrane surface area.

Andrew and Haasz [And91] determined the rate of hydrogen permeation through a palladium membrane for both incident molecules and incident neutral atoms at temperatures of 300 - 570 K. As expected, covering palladium with a thin copper layer of 3 - 25 nm caused the H_2-induced permeation rate to decrease and that of atomic hydrogen to increase.

3.14.1.15 Mercury linear diffusion pump and mercury ring pump (KALPUREX process)

Giegerich and Day [Gie14] proposed continuously operating, fully tritium-compatible stainless-steel **mercury linear diffusion pumps (LDP)** and **mercury liquid ring pumps (LRP)** for DEMO to replace the batch pumping cryo-pumps selected for ITER. The latter are characterized by rather short pumping times because of rapid panel saturation. Saturation is associated with a high down time due to the necessity of recurrent regeneration[21].

To protect the metallic diffusion pumps from mercury all heated zones have been covered on the inside with a layer of glass. Advantageously, this layer also contributes substantially to reduce the permeation losses of tritium. Baffle systems maintained at 200 K are placed at the inlet and outlet zones of the pump to control the working fluid vapour and hence avoid mercury dissemination into adjacent systems.

Based on the mercury pumps, Giegerich and Day [Gie14; Gie15] proposed an advanced fuel cycle process for DEMO which carries the acronym KALPUREX (**Ka**rlsruhe **L**iquid Metal Based

[21] Whereas for JET or ITER, which can operate with burn times of the order of 75 s, cryopumps are satisfactory, this is not the case for DEMO for which about 4000 times longer burn times need to be attained.

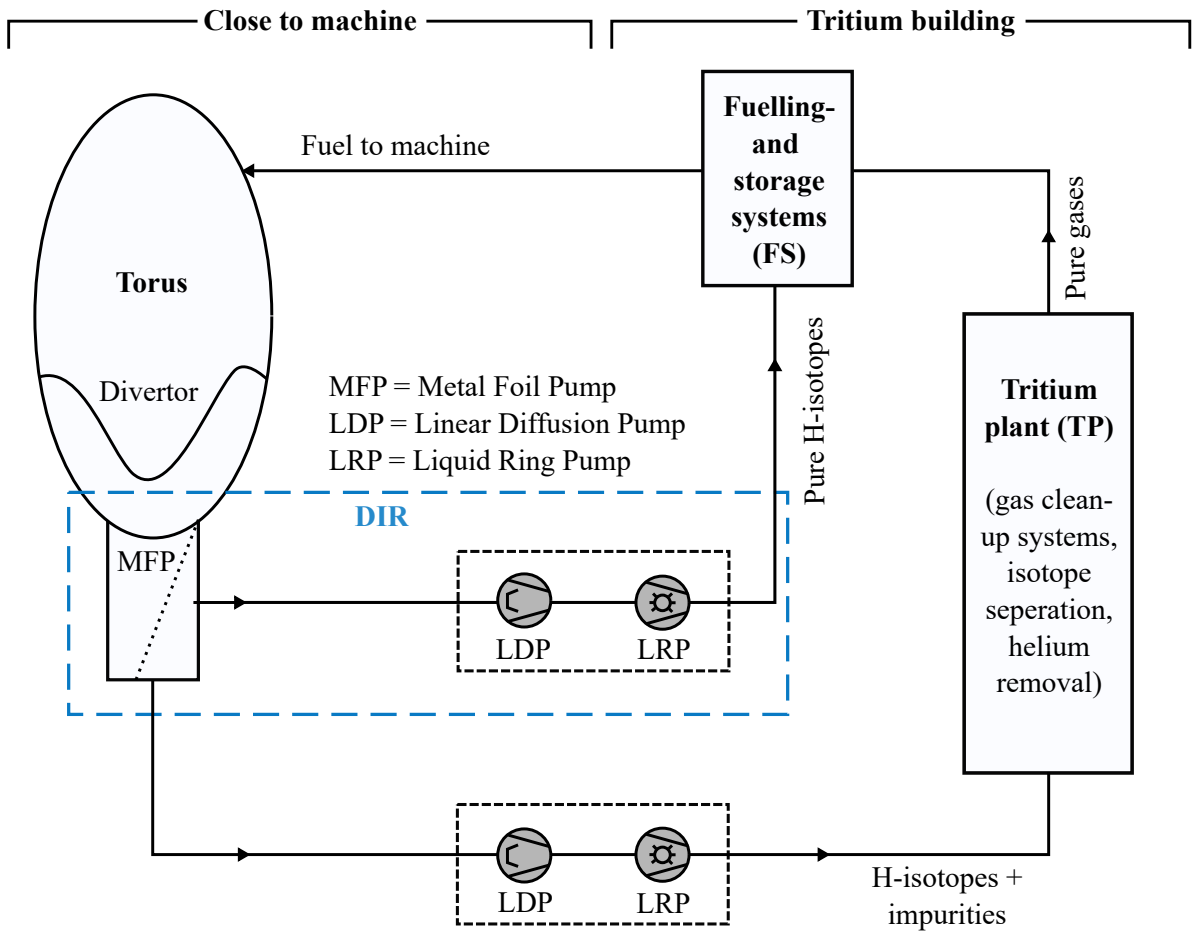


Figure 3.24: Simplified KALPUREX process proposed for the inner fuel cycle of DEMO (DIR = direct internal recycling) (after [Gie14]).

Pumping Process for **R**eactor **Ex**haust gases). It comprises three different pumping systems: i) metal foil pumps (MFP) for gas separation, ii) mercury linear diffusion pumps (LDP) as primary pumps and iii) liquid mercury ring pumps (LRP) as backing pumps (see Fig. 3.24).

The metal foils of the MFP´s are operated in the super permeability region. They are installed as close as possible to the torus, i.e. near the divertor, in order to minimize piping and conductance losses. Their ultimate function is direct recycling of unburnt fuel (D and T) into the fuelling and storage systems. Because the foils are only permeable to atomic hydrogen, they separate helium and impurities from the fuel gases deuterium and tritium. Pump train´s comprising a mercury diffusion pump and a mercury ring booster pump provide not only the necessary vacuum but also compress the permeate gas into the fuelling system (see DIR in Fig. 3.24).

Second identical pumping train´s are used for the compression of the retentate (residual gas enriched in impurities and not pumped via the foils) to the pressure required for processing at the tritium plant. Here the gas is first cleaned from helium and impurities, then subjected to isotope separation (removal of protium), and finally fed back into the fuelling system.

Currently, the principal KALPUREX components are being subjected to upgrading for tritium service, e.g. i) replacement of oil in the diffusion pump by mercury, ii) substitution of all rubber seals by metallic ones, iii) installation of mercury-compatible and tritium-compatible boilers, as well as iv) incorporation of cooled baffles at entrance and outlet of the pumps. Furthermore, a comprehensive experimental assessment program, first without tritium, is currently in progress. Supplementary, more stringent integral tests under realistic conditions, like for instance proximity to the machine, are in preparation within the frame of the next tritium campaign at JET (see [Gie15] and references therein).

3.14.1.16 Installation of pumps in glove boxes

When selecting the best and safest equipment for a given process involving tritium, pumps and compressors should be chosen on the basis of criteria like i) type of gas or gas mixture to be processed, ii) required vacua, iii) anticipated flow regimes, iv) evacuation time constraints, v) maintenance ease, vi) triboelectric effects, vii) heat generation, viii) leak-tightness, ix) possible consequences of vibrations, x) dimensions, xi) weight, xii) reliability, xiii) resistance towards corrosion, xiv) noise level, etc.

To protect equipment and personnel, the apparatus-support subjected to vibrations shall be designed to avoid resonance between the operating frequency and the natural frequency of the equipment on its support. To minimize possible damage to connections or their opening during operation of pumps, pumps should not be secured to a support but rather allow to float freely on a vibration damper. This procedure contributes appreciably to mitigate the vibration translation to other equipment [Poo08].

The vibration of all rotating equipment including high vacuum equipment shall comply with exposure levels such as accepted by industry. They are for example described in chapter 52 of ASHRAE Handbook 29.CFR 1910.95 (see Appendix N).

Pumping systems shall comply with recommended noise level criteria, such as for example given in Chapter 42 of the ASHRAE Handbook (1991) (see Appendix N).

Testing, adjusting, and balancing of pumps shall comply with accepted industrial standards, such as for example provided in chapter 57 of ASHRAE Handbook (see Appendix N).

3.14.2 Tritium storage

Pure tritium or tritium in mixtures with other hydrogen isotopes can be stored in a stainless-steel vessel as elemental gas or solidified as hydride. In the latter case, metal hydrides of low dissociation pressure at ambient temperature and high dissociation pressures at moderate temperatures are the preferred choice.

3.14.2.1 Gaseous storage of tritium

Gaseous tritium or mixtures with other hydrogen isotopologues can be stored inside of a glove box in spherical or cylindrical austenitic stainless-steel vessels connected to i) an ultrahigh vacuum-tight gas handling system equipped with diverse and complementary manometers, ii) a suitable high vacuum pumping system eventually linked to one or more calibrated volumes, and iii) analytical instrumentation. Main advantage of gaseous storage is the immediate availability of the tritium-bearing gas without necessity of prolonged heating of a metal getter or lengthy cooling of a storage bed. From a safety point of view, there is always the potential of an insidious leak of radioactive gas across the seat of valves which close the storage vessel or of incorrect opening of valves, i.e. human error. A leak may cause spread of substantial amounts of gaseous tritium into non-evacuated or evacuated equipment and from there be associated with other hazards. Other drawbacks of gaseous storage are the i) comparatively large size of the required storage vessels, ii) the need of a compressor or heated/cooled getter bed for gas pressurization, and iii) the necessity of a dedicated loop for the separation of tritium from decay helium.

Stainless-steel vessels have been utilized routinely for more than forty years for the terrestrial transport of gaseous tritium between tritium handling facilities [Wer96; US 08; US 94; US 15]. During transport of tritium at approx. ambient pressure or below, the vessel must be protected by a suitable over-pack capable of withstanding extreme heating in case of accidental exposure to an open fire. Modelling of standard transport systems have revealed that once steady state conditions have established in a hypothetical fire accident comprising extended heating at elevated temperatures, the permeation rate of tritium will remain small even after 12 hours

provided the temperature remains under 573 K, but will become rather large already after two hours at 1100 K [Ell81].

3.14.2.2 Storage in getter beds

Storage of tritium as metal tritide constitutes a rather effective and safe procedure because of i) pressureless storage, ii) high achievable volume density of tritium, iii) thermal release of tritium with very high chemical purity (separation of tritium from decay helium possible provided the conditions, i.e. type of getter, temperature, and degree of loading, are selected carefully), iv) tritium release at a pre-determined pressure by selection of the appropriate release temperature (pressures are basically predictable because of rapid release kinetics and flat pressure/composition isotherms), v) tritium retrieval into the getter by absorption at ambient temperature, and vi) intrinsically safe storage during stress situations.

3.14.2.2.1 Getters

The subject of metal hydrides is highly developed. A vast body of experience and pertinent literature is now available on which to base the design of tritium storage beds for ITER. The effectiveness of hydrogen storage as metal hydride is best validated by the fact that the hydrogen density achievable in some metal getters at maximum loading is higher than that of liquid or solid hydrogen. For example, the density of hydrogen in TiH_2, UH_3, and $LaNi_5H_6$ is respectively 2.1, 2.1, and 1.7 times higher than that of liquid hydrogen, i.e. $4 \times 10^{22}\,\mathrm{atoms\,cm^{-3}}$ [Wen82; Pen90].

The relevant fundamental chemical and physical properties of a variety of getter materials proposed for handling and storage of tritium have already been discussed in chapter 2.11. A comparison of storage-relevant properties of the most promising getters is provided in Table 2.25. Key criteria for the selection of getter materials are the dissociation pressure at ambient temperature and the temperature at which the release of hydrogen becomes sufficiently rapid. Getters requiring exceedingly high release temperatures cause design problems like i) challenging selection of structural materials, valves, or heaters, etc.; ii) excessive permeation into the isolation vacuum; iii) thermal agglomeration of the getter; iv) increased potential for interaction between getter and structural materials; etc.

Auspicious metal getters currently recommended for interim storage and handling of tritium at ITER are uranium, zirconium-cobalt, and lanthanum nickel alloy. Titanium hydride constitutes only an option for prolonged "unattended" storage [Col78; Hol81; Hol82; Ebe85]. The reasons for this are on one hand the extremely low dissociation pressure of titanium tritide at ambient temperature and the other the high thermal stability of this tritide even at very high temperatures. Hence, exceptional safety is warranted even during a fire accident.

3.14.2.2.2 Design and safety aspects of getter beds employed for tritium handling

Beds directly joined to a tritium handling facility and containing uranium or zirconium cobalt getter as powder are ideally suited for safe interim storage of hydrogen isotopes at ambient temperature. Additionally, they can routinely be utilized for tritium supply, tritium recovery, and purification of tritium from helium. They may also be employed for the emergency storage of tritium during shut down for repair or upgrading purposes. In principle, however, storage beds containing U or ZrCo are not intended for prolonged unattended storage.

The rate of hydrogen uptake by a getter bed is determined by the i) type of getter material, ii) history of the getter material, e.g. fine powder or granules, iii) type and degree of contamination by nitrogen, oxygen, or carbon of the getter surface and bulk, iii) overall design and flow conductance of the bed, iv) pressure and purity of supplied hydrogen isotopes, v) initial bed capacity, i.e. the hydrogen/metal ratio at the beginning of the hydrogen uptake, vi) initial temperature of the getter material, and vii) effectiveness of heat transport from the zone where the exothermic hydriding reaction takes place and ambient.

Several design peculiarities and safety related aspects requiring attention when constructing and operating getter beds are discussed in some detail below:

a) Effect of gas pressure

The number of hydrogen moles immobilized in a getter bed within a given time interval is not directly related to the pressure of the supplied gas. For instance, with getters like uranium, which have rather flat pressure/composition isothermal plateaus, increasing the gas supply to the bed at a given temperature causes first hydrogen to be dissolved in the metal until saturation is attained. Once this is the case, supply of more hydrogen to the bed will

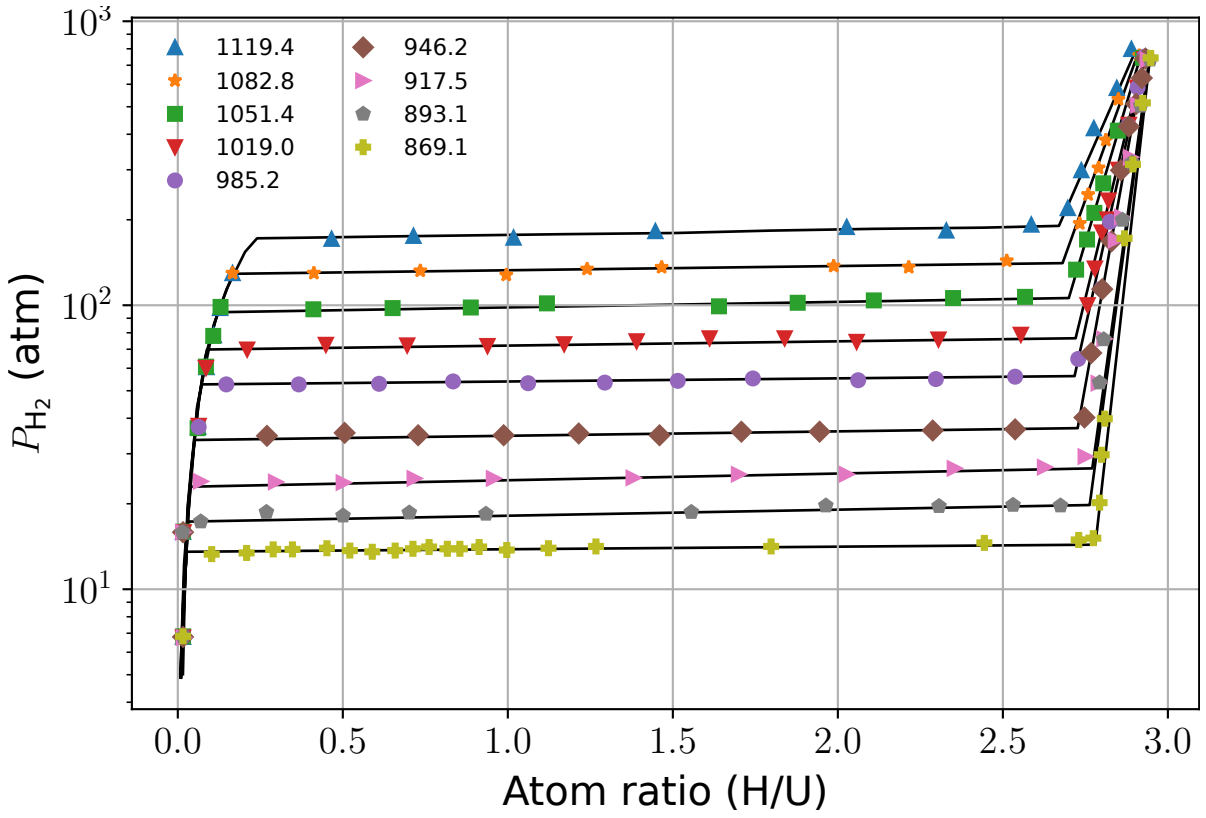


Figure 3.25: Isotherms showing the dependence of pressure in the U - H_2 system from composition expressed in H/U atom ratio. Temperatures are given in Kelvin (after [Nor75]).

not increase the pressure in the bed because of the gradual formation of uranium hydride (plateau region with coexistence of two solid phases). As apparent from Fig. 3.25, all plateaus are only slightly sloping. With progressing supply of gas to the bed substantial amounts of hydrogen are incorporated into the getter. Once, at a given temperature, equilibrium establishes between the pressure of hydrogen and the hydride, a third region becomes apparent in which the pressure of hydrogen in the bed and the concentration of hydrogen in the bed increases almost linearly with the amount of supplied gas (solubility of hydrogen in uranium hydride region).

b) Hysteresis

Another effect that needs to be contemplated when loading and deloading hydrogen isotopes from a uranium bed is hysteresis. Hysteresis is defined by the expression $\Delta P/p_{\mathrm{d}}$, where ΔP is the pressure difference between that of the isotherm of hydride formation, p_{f}, and that of the

isotherm of hydride decomposition, p_d. The hysteresis of uranium displays marked dependency from temperature. For example, at 630 K and 642 K the ratio $\Delta P/p_d$ has values of 0.067 and 1.7, respectively [Wic62].

c) Getter swelling

Hydrogen absorption is generally associated with significant swelling of the getters. For instance, uranium, whose metallic density is $19\,g\,cm^{-3}$, will rapidly expand to reach a final density of about $3\,g\,cm^{-3}$ when fully hydrided. The volume expansion upon hydrogen uptake is described by the $\frac{V_{hydride} - V_{metal}}{V_{metal}} \cdot 100$ ratio, in which V is either the volume of the hydride or the metal. For the hydrides UH_3, $ZrCoH_3$, TiH_2, and $LaNi_5H_{6,7}$ these ratios were determined to be 75 %, 20 %, 13 % and 35 %, respectively (see also Table 2.25). As evident, the degree of volume expansion is significantly dependent from the type of getter. Getter swelling is of concern because it may cause agglomeration of powder and even damage of screen plates, fins, filters, or other structural parts inside of the storage vessel. Swelling has also consequences on the absorption properties of getters. To cope with this problem, appropriate design measures must be taken. They include i) allowance of sufficient free space above the getter[22], ii) horizontal positioning of the whole getter bed, and iii) compartmentalization of the getter material inside of the bed in order to minimize densification by gravity (compartmentalization has the additional benefit of improved heat transport between bed structure and powder via the metallic screen plates).

d) Metallic filters

Metallic filters need to be installed at inlet and outlet of getter beds to prevent spreading of fine powder - most probably contaminated with tritium - into adjacent tritium handling equipment and instrumentation. Getter powder deposited on surfaces may undergo interaction with hydrogen isotopologues (incorporate or release) depending on temperature and partial pressure of the gas. Hence, the presence of getter powder on inner surfaces of tritium handling systems may i) influence the isotopic purity of gases, ii) affect the material balance of tritium, and iii) contaminate metallic waste with a highly reactive and radiotoxic mobilizable dust. What

[22] The free space that must be allowed above uranium - including an additional safety margin - is considerably larger than that required above zirconium cobalt.

is more, getter dust may i) plug capillary tubing or instrumentation like flow meters, ii) cause damage of metal bellows, iii) bring about valves to leak if the powder is deposited in the seat region, and iv) pile up for instance on optical windows or on the mirror of a mirror hygrometer affecting the accuracy of measurements.

An experimental comparison between the pressure-drop measured across different SIKA sintered filters (nominal pore sizes 1, 3, 5 or 20 µm) from GKN Sinter Metals Filters of the kind used to compartmentalize uranium powder inside of a technical scaled uranium getter bed was performed systematically by Kurz [Kur84]. His results agreed acceptably well with theoretical predictions.

Filters mounted in tritium storage beds should preferably be of high conductance and at the same time possess good electrostatic particle retention properties. Such filters are especially important for getters like ZrCo, because during liberation of hydrogen isotopes, when high temperatures and high pressures of hydrogen prevail, fast pumping of hydrogen through the exhaust filter is essential to minimize the risk of thermally induced zirconium cobalt hydride disproportionation.

Because a change in porosity has a dramatic impact on the conductance of filters, it is necessary for the achievement of high flow conductance to perform some screening tests prior to the manufacture of storage beds [Khe89]. From an investigation on the effect of filter porosity varied within the range 0.5 - 10 µm) on the rate of hydrogen uptake by a uranium bed it was noticed that filters with porosities of less than 5 µm displayed essentially the same filtering efficiency [Shm90b].

At Savannah River Site multi-element filters were selected to equip hydride beds [Poo08]. The filters are fitted above the fill level of the getter to prevent particle plugging of the filter. Good experiences were made with filters supplied by Mott Corporation, Farmington, USA.

e) Heat dynamics

Fast admission of hydrogen into a technical-sized bed containing a getter causes considerable release of thermo-chemical reaction heat and a concomitant elevation of the temperature in the centre of the bed [Khe89; Tam92; Tam93]. For the reason that this temperature increase reduces the absorption capacity of the getter, provisions must be taken for good thermal coupling between getter powder and the heat sink (or supply of power).

Electrical heaters are normally installed in axial central position surrounded by a concentric gas cooling arrangement. Numerous nickel or copper fins are used to compartmentalize the total getter load. Getter is deposited between the fins which themselves also serve for heat transfer from the getter powder to the core or viceversa [Ser95]. Tritium storage beds can be installed in a glove box either horizontally or vertically.

Fig. 3.26 illustrates an experiment on the pressure development in a vessel containing pure hydrogen evacuated by a connected immediately adjacent getter bed [Khe89]. As evident, the consequence of very poor heat removal from the getter material (bed with evacuated insulation jacket) on the equilibrium pressure that establishes after only a few seconds is significant. In fact, the equilibrium pressure is almost one order of magnitude higher than that calculated for the case in which the exothermicity of the hydride formation reaction is efficiently removed by cooling. For completeness, the pressure evolution calculated for the bed working under fully isothermal conditions, i.e. efficient heat removal, is also displayed in the figure.

Improved rates of heat transport from the hydrogen/getter reaction zone to the body of the getter bed have been accomplished with a series of parallel copper fins confining the getter material [Khe89] and mixing of the getter powder with copper grains [Hay95c; Hay95a]. Copper grain contribute considerably to improve the gettering properties of the bed because they augment the overall thermal conductivity within the getter zone and additionally provide a local rapid heat sink for the heat of hydrogenation.

Rapid cooling is usually required immediately after a tritium delivery operation or when an in-bed calorimetric determination of the tritium inventory is performed. For rapid cooling of the primary getter containment a stream of helium is passed through the vacuum guard zone. This helium may also serve to purge tritium permeated into the secondary containment. Tritium in the purge gas stream can be recuperated with an activated getter bed containing zirconium cobalt or uranium and attached in closed loop mode. After decontamination of the helium, the guard zone is ready for renewed evacuation.

Between the primary and secondary containment metallic heat shields (thermal reflectors) contribute substantially to minimize the necessary wattage of the heater and to reduce the heat transport to the outer containment. The latter is important as it serves significantly to keep tritium permeation into the glove box at low levels.

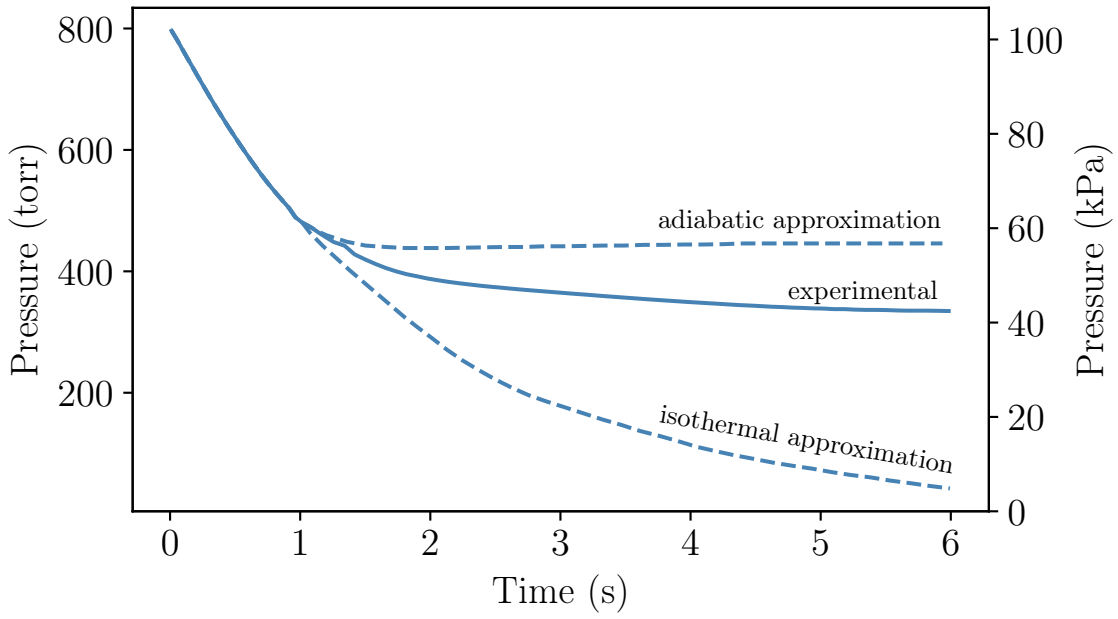


Figure 3.26: Effect of isothermal, adiabatic, or non-coooled/non-evacuated operation of a getter bed on the pumping efficiency of hydrogen. The solid line shows the pressure drop in a vessel containing pure hydrogen attached to a getter bed whose insulation jacket is neither cooled nor evacuated. For comparison, the calculated adiabatic pressure drops (getter bed thermally insulated from the environment by evacuation) and the isothermal pressure drop (bed with very efficient cooling) are also displayed (after [Khe89]).

f) Effect of impurities in hydrogen

Gaseous impurities present in the supplied hydrogen can either be i) chemically inert like noble gases, or ii) reactive like oxygen, carbon oxides, hydrocarbons, nitrogen, etc. Inert gases may slow down considerably the uptake of hydrogen by the so called “blanketing effect” while reactive gases may modify the getter surface chemically and therefore reduce the uptake rate of hydrogen isotopologues.

Less than 1 % noble gas in hydrogen suffice to induce a marked decline and even stand still of the rate of hydrogen adsorption under static conditions. This so called “blanketing effect” is attributed to progressive accumulation of non-reactive gas in the vicinity of the getter material essentially acting as a diffusion barrier. The problem is best solved by re-circulating

the hydrogen/noble gas mixture through the bed in closed loop operation until all hydrogen is completely gettered[23].

Reactive impurities will generate oxides, nitrides, and carbides on the surface of the getter material causing surface passivation and jeopardizing its sorption properties. To ameliorate this problem the getter must occasionally be reactivated by subjecting it to prolonged heating (order of hours) at elevated temperatures. This treatment promotes diffusion of species on the surface into the bulk. While with each treatment the surface is reactivated, the sorption capacity of the getter will progressively and irrevocably diminish.

g) Air ingress

Air-ingress into a tritium storage bed installed in an inert gas glove box can be considered highly improbable under normal operation conditions. For air-ingress to occur several consecutive or simultaneous failures, like a large air leak into the inert gas glove box concurrently with the rupture of a gas line, must take place. This can only happen in case of a major accident.

Within the frame of discussions on safe storage of tritium in portable getter beds this topic was, nonetheless, a matter of much concern because of the very high reactivity of fine getter powder with air. Calculations showed that spontaneous ignition of uranium powder can give rise to temperatures as high as 2000 K [Lon88; Tam93; Heu95c]. It was feared that gas/solid reactions could lead to a significant accident with eventual destruction of the getter bed and concomitant massive release of tritium. In view of this, a number of experimental studies were performed to shed more light on this subject.

Small scale laboratory experiments performed by Pervezentsev et al. [Per95b; Per95a] revealed that the reaction of uranium with air commences at much lower temperature than with zirconium cobalt or other intermetallic getters of potential application for tritium storage. This difference becomes increasingly smaller as the initial temperature is increased.

Representative simulation experiments involving air ingress into three different technical-sized beds containing fully activated uranium (up to 12 mol) at initial temperatures spanning from 294 - 824 K provided evidence, that the maximum temperature develops predominantly in the getter

[23] A technical problem arises when the noble gas impurity concentration is small because many re-circulation pumps fail to work at very low pressures.

material itself and not in the bed structure[24] [Lon92; Tam93]. The maximum temperatures actually measured were found to be much lower than estimated from a full oxidation of the getter. For instance, a bed containing 500 g of uranium developed a temperature of "only" 473 K when subjected to direct air ingress [US 73] but showed practically no temperature increase when the uranium was hydrided[25] [Heu95d; Heu95c]. One possible explanation for the incomplete oxidation of uranium is passivation due to formation of oxides and nitrides on the getter surface. Another reason could be "blanketing" by i) a non-reactive air component like argon (or nitrogen), or ii) by a reactive gas like hydrogen. To explain the formation of these gaseous barriers the following grounds were given: i) accumulation of argon from air (normal content 0.9 %) after extensive chemical consumption of oxygen and nitrogen at elevated temperature, ii) non-consumed nitrogen after extensive chemical consumption of oxygen, or iii) accumulation of hydrogen liberated thermally from the getter after substantial chemical energy is generated during the reaction of oxygen with the metal (or alloy). Thus, only in case of air ingress in flow modus through an activated uranium bed may temperatures of more than 1273 K develop with possible damage of the tritium storage vessel [Tam93]. Highest temperatures are predicted in storage beds in which the getter powder is dumped horizontally and is not compartmentalized in the zone between bed inlet and outlet [Per95a]. From the above it follows that vertical installation of a compartmentalized bed will confer the highest safety to the bed.

A reliable preventive measure against air ingress into beds containing metal tritide for instance during maintenance or repair operations with open glove box consists in backfilling it with an inert gas up to atmospheric pressure and subsequently keeping it closed.

Summarizing, even though the reasons for the unexpectedly low temperatures observed experimentally in several uranium beds deliberately subjected to air ingress experiments have not yet been irrefutably elucidated, it can be concluded from all performed tests, that air ingress into an activated getter bed does not constitute an unacceptable hazard. Massive release of tritium into the environment after such an accident has not been observed. Only in the event of a continuous air stream passing through the uranium storage bed may temperatures be reached capable of damaging the containment.

[24] J.L. Hemmerich, Air exposure test of a JET AGHS uranium bed, JET report JH/emi/018, 17th August (1990), unpublished.
[25] Hemmerich J.L., Air exposure test of a JET AGHS uranium bed, JET report JH/emi/018, 17 August (1990).

h) Tritium permeation into the insulation vacuum

The most common way to heat getter beds is axially with suitable[26], preferably replaceable heaters, installed in close contact with a heat transfer fin system that optimizes heat conduction to the getter material. Heat bridges between the actual primary getter bed and the secondary containment should be minimized in order to maintain heat conduction losses to the environment at the lowest possible level.

During the operation of a getter bed tritium will inevitably permeate through the heated primary vessel into the protective vacuum containment and deteriorate the vacuum. Since even a slight loss of vacuum will rapidly boost heat transport to the outer wall of the getter bed, measures need to be taken to maintain during each heating cycle the high vacuum insulation intact. This can be done either with a vacuum pump combination that exhausts into a tritium retention system or with an open uranium or zirconium cobalt getter bed attached directly to the heated bed and maintained at ambient temperature. Advantages of the latter approach are passive removal of tritium, i.e. no power supply, no moving parts, and no active safety devices required. Additionally, permeated tritium becomes recoverable rather than constituting waste.

For example, the partial hydrogen isotope pressure in the insulation vacuum of a permeator operated continuously for more than one week at 623 K could be maintained constant at approx. 0.025 mbar utilizing a ZrCo bed [Pen95c].

i) Measures against temperature excursions

To exclude dangerous temperature excursions the maximum installed power should be limited to a getter temperature only moderately exceeding that actually needed to drive off all tritium, i.e. about 700 K. The necessary power is determined primarily by the i) selected getter material; ii) the mass and molar heat capacity of all structural materials of the bed, getter powder, and copper grains or spheres; and iii) heat losses to the secondary containment. Additional aspects requiring attention are i) the heating rates to achieve the required hydrogen isotope delivery rates, and ii) the necessity to compensate for the heat consumed by the endothermicity of the decomposing hydride.

j) Measures against pressure excursions

[26] The design heat capacity of the heater must consider the total heat capacity of the vessel (including that of the getter powder under hydrogen isotope release conditions).

To cope with pressure excursions in a tritium storage vessel containing metal getter the standard approach is to limit the inventory of hydrogen isotopologues in the bed either by restricting the amount of getter or limiting administratively the amount of hydrogen supplied to the bed[27]. The latter is performed safely by limiting the pressure in a supply vessel of an appropriately selected volume. Another option is to design the bed to pressures capable of withstanding those of a potential excursion. The drawback of this approach is the resulting high heat capacity with negative consequences on heat transport during heating, cooling, or calorimetric measurements. The easiest and safest approach is to limit the maximum attainable temperature in the bed by judiciously dimensioning the heater (s).

k) Formation of eutectics

Uranium can form a eutectic with stainless-steel at temperatures above 980 K. Eutectic formation may be the cause for loss of physical integrity of the primary containment. Hence, preventive measures need to be taken to guarantee that this temperature cannot be attained anywhere in the bed.

l) Stress/strain analysis

The strain developing in storage vessels due to the volume expansion when getter material incorporates hydrogen can be measured with strain gauges [McK92]. Measurements on a horizontally installed bed indicate that the largest stress occurs at locations close to the side of the bed, where the bed is completely occupied by getter powder. When hydrogen is removed from the bed the stress on the walls rapidly falls to zero.

A safety stress analysis performed by O´Hira et al. [Ohi99] to qualify a sizeable package designed at JAERI for the transport of large quantities of tritium, i.e. 250 g, provided evidence that the bed complied with requirements such as stipulated in IAEA regulations. Within this frame a package must also safely withstand a hypothetical accident consisting of dropping the package from a height of 9 m on a hard ground. Additionally, calculations confirmed that the package could resist the pressures expected when the package is dropped into the deep sea to a depth of 9000 m.

[27] According to current ITER safety guidelines the amount of tritium in a bed shall not exceed 100 g.

m) Replacement of failed heating elements or thermocouples

For high availability, the storage bed must be equipped with heating elements and thermocouples that are either redundant or replaceable with moderate effort. Good accessibility is achieved by joining inlet and outlet pipes of the inner primary getter bed vessel to inlet and outlet pipes (tritium supply and cooling gas supply) mounted on the flange that serves to close the secondary vessel. Accordingly, when the secondary vessel is dismantled and lowered, the complete primary system remains fully suspended from the top flange by four pipes and connected to all feedthroughs servicing thermocouples and heaters. Assuming the top flange to be fixed and sufficient space under the bed to accommodate the secondary vessel, it becomes possible to perform repairs or component replacements.

Because of the expected high degree of contamination of the outer walls of the primary containment arising from tritium permeation, the replacement of all tritium-contaminated thermocouples inserted into the primary system or of heating elements introduced into the primary system must be carried out inside of a closed glove box. This can only take place swiftly if certain provisions are taken in advance. They comprise: i) allowance of enough free space under the storage bed to accommodate the secondary containment, ii) if necessary, availability of an appropriate lifting device for the displacement of heavy components, iii) sufficient proximity between the storage vessel and the glove ports to permit execution of all foreseeable activities utilizing gloves, iv) availability of vacuum-tight containments to discard contaminated waste, and v) availability of dedicated tools. Special tools should be manufactured and tested beforehand under realistic conditions.

n) Dependence of storage bed design on type of getter material

A conclusion from the discussions above is that the design of an optimized universal storage vessel compatible with all potential getter materials will be rather difficult because of the great differences in physical and chemical properties of the various getters. The consequence is that the ultimate design of ITER storage beds will only become possible after a final decision on the best getter material has been taken.

3.14.2.2.3 Technical storage bed

A thorough description and technical characterization of a water cooled medium sized storage vessel designed at **Forschungszentrum Jülich (FZJ)**, **Jülich**, **Germany**, has been provided by Kurz [Kur84]. Under the assumption that the outer temperature of the bed stays constant by water recirculating through the outer annular volume and the vacuum in the second containment remains below 10^{-4} mbar, it was possible to estimate the tritium inventory in the vessel under static conditions. To this effect, the temperature rise of the bed was followed until a constant temperature difference established. The actual temperature difference was shown to be directly dependent from the "tritium" inventory in the bed and the specific heat transport properties of the bed. Determination of absolute tritium inventories required careful calibration using the heater installed for the thermal decomposition of uranium hydride.

The properties of the bed were characterized by measurements like the i) heating behaviour under different conditions, i.e. helium or vacuum in the secondary containment, insertion of different heating elements, etc., ii) stationary permeation of tritium, iii) various temperature gradients inside of the bed, iv) pressure drop across sintered filters, v) memory effects, vi) gas flow characteristics, vii) absorption performance of hydrogen in mixtures with helium, etc.

For the long-term storage as well as transport of tritium a medium sized container based on zirconium or titanium hydrides having a capacity of 19 PBq was developed at **Chalk River Nuclear Laboratories** [Hol81]. The volume of the primary stainless-steel container was 4.5 l. It was equipped with two valves to permit gas recirculation. Safety enhancement during transport was achieved with special protectors for the valves and a carbon steel shipping drum containing packing and insulation materials.

Lässer designed at **TLK** a self-assay, **Fast Delivery Hydride** bed specified for hydrogen supply rates of the order of 200 Pa m^3 s^{-1}. A further basic design requirement was the capability of accepting either zirconium cobalt or uranium as hydrogen getter material. Lässer described in hierarchical, uniquely detailed way all the various construction phases of the bed [Lae01a; Lae02b; Lae03a] (see Fig. 3.27). The storage bed was manufactured for the most in workshops of KIT (formerly KfK). Within this frame, Lässer also described ex professo all dedicated tools needed for assembly and filling of the bed, explained in detail all brazing procedures, and discussed the

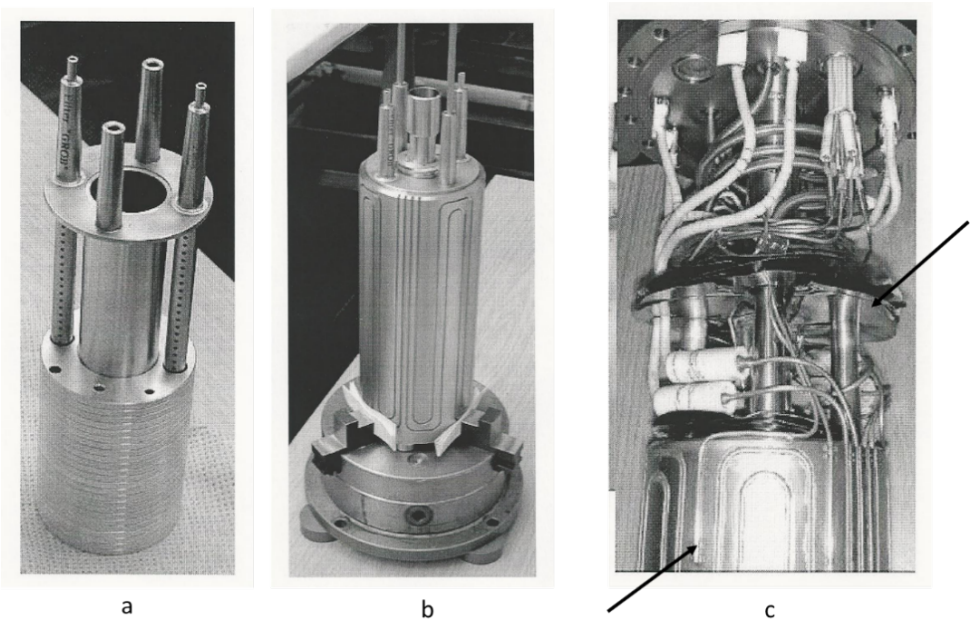


Figure 3.27: Fast delivery storage bed fabricated at KIT. The figure shows three assembly stages: a) two sinter filters each protected by a thin tube with numerous perforations installed inside of the primary vessel; also displayed are numerous copper fins stapled at the lower end, b) the primary containment with an inner stainless-steel tube in the middle, and c) electrical connections and pipes between the primary system and the top CF-150 flange used to close the outer secondary containment. The stainless-steel radiation shields between the primary containment and the CF-150 flange (upper arrow) protect the latter from excessive heat. Three thermocouples were mounted on the surface of the primary containment (one is identified by an arrow on the left lower side of the primary containment)[Lae03a].

encountered difficulties as well as the adopted solutions. Long sinter filter tubes inside of the bed served for the supply of particle-free gas to and release from a total of 44 compartments each containing equal amounts of getter material. Average inlet and outlet mesh values of the filters were 20 and 5 µm, respectively. Each sinter filter was protected by a thin tube displaying numerous small perforations created by laser cutting (see Fig. 3.27a).

Metal hydride powder was filled successively into each of 44 compartments resulting from stapling equidistantly 45 copper fins one on top of the other. The mass of powder introduced into each compartment was accurately determined by weighting. Filling was carried out with a specially designed tool having a funnel on top and utilizing a vibrator to increase filling efficiency. The powder was added after the bed had been almost completely assembled. In order to facilitate welding, top and bottom compartments were loaded with 3 mm stainless-steel balls whose function was to protect the powder from the welding zones. To circumvent oxidation

of the getter, powder loading was performed in a glove box of pure argon atmosphere. Two thermocoax heaters (3150 W each) were wound into machined grooves and fitted into the inner copper block. Two further thermocoax heaters (2000 W each) were fitted into the outer cylinder. The total installed power was calculated to be sufficient for the achievement of a hydrogen isotopologue release rate[28] of 200 $Pa\,m^3\,s^{-1}$. Pressurized nitrogen is utilized for fast axial cooling of the bed. Cooling is needed during tritium accountancy measurements and for the effective removal of the absorption heat liberated during reaction of hydrogen with the getter. To attain the design storage capacity of 100 g tritium (16.7 mol) 1.91 kg of zirconium cobalt (12.7 mol) were distributed in amounts of 44.5 g into each of the 44 compartments of the bed. Following completion of the bed, pressure tests of the primary containment and of the outer containment were carried out with nitrogen at 21 bar. Helium leak tests of the primary containment yielded values of less than 10×10^{-10} $mbar\,l\,s^{-1}$.

Replacement of ZrCo powder by another getter powder, e.g. uranium, was considered possible with a specially tailored vacuum cleaner.

To investigate the performance of the bed, it was connected to two appropriately equipped loops: i) an accountancy loop for calorimetric measurements and ii) a pVT-loop for volumetric measurements [Lae03a]. First screening tests of the fast delivery storage bed were performed with deuterium by Beloglazov et al [Bel05b; Bel08b]. According to their observations the hydrogen supply rate of the bed remained much below expectations, e.g. on the average only 10 $mbar\,l\,s^{-1}$. Because the pressure inside of the bed was determined to be about four times higher than at the bed outlet zone (pump inlet), the small gas supply rate was attributed to the high flow resistance of the outlet filter. The rate of hydrogen uptake by the bed also evidenced strong influence by the conductance of the inlet filter (perhaps aggravated by blanketing). What is more, under the test conditions the effect of active cooling by pressurized air on the rate of hydrogen uptake was non-discernible from runs without cooling. In conclusion, a modification of the configuration of the Storage and Supply System (SDS) was put forward to approach the required supply rate for ITER. To improve the delivery rates, it was proposed to join supply and loading lines of two or more beds via manifolds. In addition, screening tests with a broad spectrum of sinter filters

[28] Approximately the same amount of heat is generated during hydrogen absorption and therefore needs to be removed by fast cooling.

were found necessary in order to identify filters of sufficient conductance and concomitant high particle retention capability.

Twenty efficient tritium storage beds each containing 18 mol of ^{238}U powder, i.e. 4.28 kg, and qualified for storing up to 20.3 mol tritium were designed, manufactured, and operated with tritium at JET over several decades [Hem89a; Hem96b]. The **axially heated and cooled beds**, met the specifications of the American Society of Mechanical Engineers (ASME) code. The beds are furnished with tubular Inconel 600 filters reaching from top to bottom of the bed. Their porosities have values of 20 µm and 5 µm at inlet and outlet, respectively. To provide good gas conductance and to account for the large volume increase of uranium during hydrogen uptake, the beds were constructed in tubular form and installed horizontally. When loaded with tritium the temperature of the primary containment was limited to temperatures of less than 828 K. This constitutes a standard safety measure to exclude possible formation of eutectics between uranium and structural stainless-steel [Han58].

A genuine comparison between the properties of ZrCo and U was carried out at the **Central Storage System** of **TLK** [Bes02a; Bes02b]. This technical-sized infra structure system comprises ten beds of identical construction, of which nine contain uranium and one zirconium cobalt. This permitted a comparison of the properties of both getter materials under closely matching conditions. A typical plot displayed in Fig. 3.28 compares the fraction of deuterium released from each of four uranium deuteride beds with that from one zirconium cobalt deuteride bed all subjected to the same temperature ramp (the temperature of the getters could not be determined accurately because of the prevailing dynamic conditions). As apparent, the four uranium beds reveal comparable behaviour. The comparatively higher dissociation pressures of the ZrCo deuteride, on the other hand, causes much earlier and faster release of deuterium than from uranium deuteride. Another substantial difference is the residual deuterium inventory of 14 % remaining in the ZrCo bed.

Within the frame of the PETRA experiment, the same type of storage bed employed routinely in tritium-service at JET was demonstrated in operation with tritium at **TLK** using zirconium cobalt instead of uranium [Pen95c]. The results fully confirmed previous observations with smaller amounts of this getter. For instance, numerous tritium loading/de-loading cycles of ZrCo did not reduce measurably the loading capacity of the getter. Disproportionation during de-loading could effectively be minimized by removing hydrogen isotopes from the bed immediately after

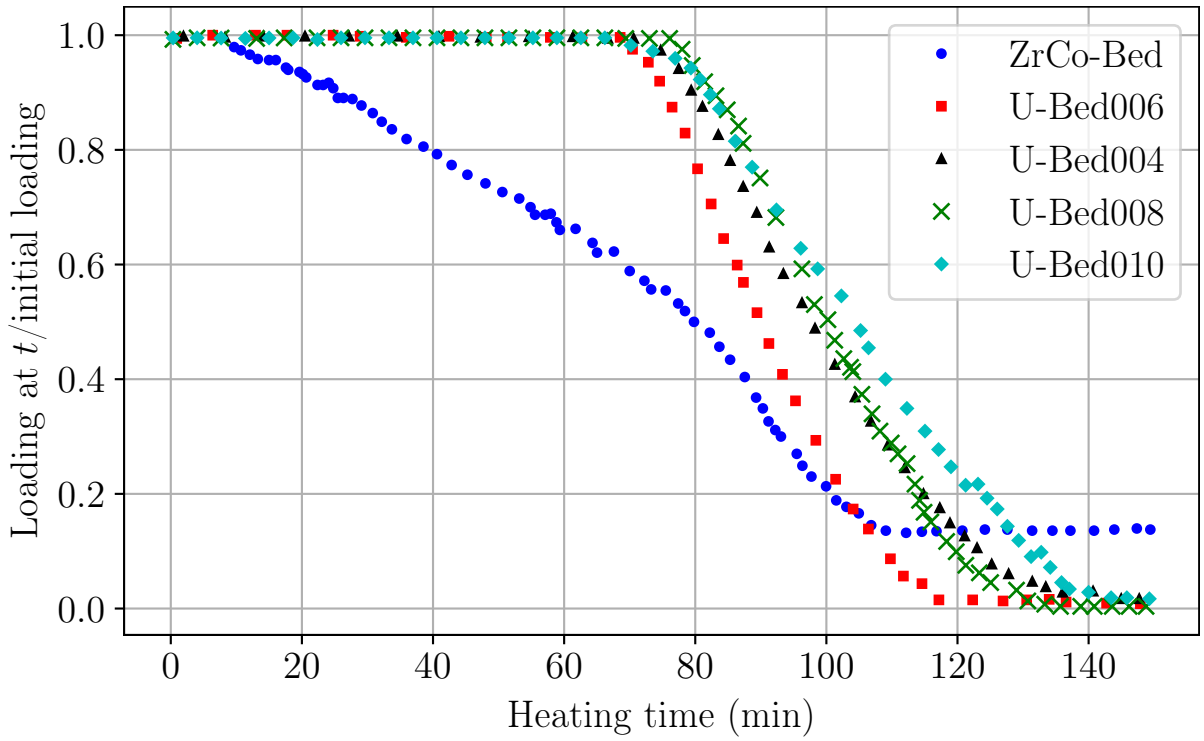


Figure 3.28: Comparison between the release rate of deuterium expressed as loading fraction at time t from each of four beds containing uranium deuteride ($UD_{2.66}$) with that from one bed containing zirconium cobalt deuteride ($ZrCoD_{1.8}$). All five beds are from the same manufacturer and of identical configuration and dimensions [Bes02a].

their thermal release from the getter with a pump combination, i.e. a NORMETEX scroll pump backed by a Siemens Metal Bellows fore pump. While absorption runs with molecular hydrogen containing reactive impurities gradually reduced the loading rate of ZrCo, it was possible to reverse the passivation of the surface of the getter by heating the bed for several hours at 673 K under constant evacuation. Evidently, this treatment promoted the expected diffusion of surface contaminants into the getter bulk.

Decay helium accumulating in the bulk of the intermetallic compound needs to be removed periodically from the storage bed by extended baking (see [Hay92a; Hay94])[29]. If the bed is integrated into a closed loop comprising an additional getter bed of low degree of loading and a pump for gas re-circulation, the thermally released gas can be transferred into the supplementary bed. Remaining slightly contaminated decay helium can be evacuated and released via stack

[29] Whereas already at 523 K about 8 % of the tritium is released, at 873 K only 16 % of He-3 accumulated in ZrCo following an ageing period of 6 months is liberated. This shows how firmly trapped He-3 is in the intermetallic getter [Hay92a].

after passing through a Tritium Retention System. For quantitative release of trapped decay helium prolonged heating at more than 873 K was found to be necessary [Hay92a].

Savannah River Site (SRS), currently sole supplier of tritium in the Unites States, designed and constructed a number of storage and transport vessels for tritium [Heu95a]. A simple transport vessel containing 493 g of depleted uranium was manufactured from two SS374H pipe caps [Heu95c]. SS374H steel was used to circumvent the necessity for heat treatments after welding. A storage bed with a hold up of 18 g tritium was first tested with protium and deuterium and subsequently with tritium.

Based on the results, another storage vessel concept was developed that proofed adequate for large amounts of pulverized getter. It basically consists of a horizontally installed double walled stainless-steel pipe with pipe caps welded on both sides (see Fig. 3.29). The selected pore size of the stainless-steel filter elements was about 5 µm. Smaller pore sizes reduced the flow rate markedly and larger ones did not confine the fine getter particles sufficiently. Back flushing contributed effectively to reduce filter clogging. The heating/cooling options tested were: i) electrical heater - cold nitrogen cooling (small beds),ii) large flows of either hot or cold nitrogen through the isolated jacket of large getter beds, and iii) axial electrical heater introduced into a dedicated heater well for direct heating of the metal hydride. A major drawback of the SRS concept was that gas re-circulation was not contemplated. This favoured blanketing and reduced the effectiveness of the reaction between tritium and the getter. Getter materials tested and compared included depleated uranium, titanium sponge, palladium deposited on Kieselguhr and $LaNi_{4.25}Al_{0.75}$.

Over the past three decades much experience on the routine operation of technical-sized tritium storage beds utilizing $LaNi_{4.25}Al_{0.75}$ getter has been gathered at **Savannah River** [Ort90; Kle02b; Kle02a]. The most employed beds contain up to 12.6 kg of the getter material and have a storage capacity of up to 390 g of tritium. These beds are horizontally installed and powered by 126 W. They are used at SRS for process gas absorption/desorption operations as well as for interim storage and supply of tritium (compression).

As commented above, in the early days absorption and desorption of hydrogen isotopes with getter beds was carried out by passing cold or hot nitrogen (glove box gas) at high flow rates through an insulation jacket (see Fig. 3.29). This process conduction improved considerably

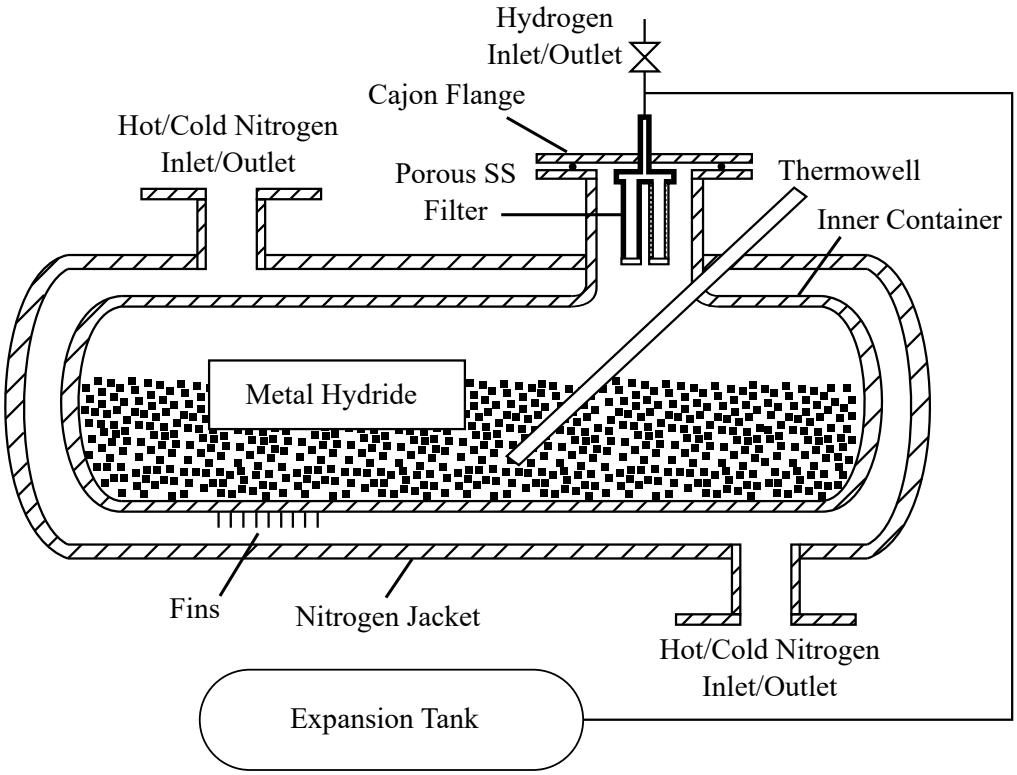


Figure 3.29: Schematic drawing of the SRS hydride storage bed [Heu95a].

when a forced cooling atmosphere was passed at high flow rates through U-tube heat exchangers inserted into the bed. A further benefit of this procedure was considerable reduction of errors during determination of the tritium inventory in the bed [Kle05a]. An extensive experimental parametric investigation on the effect of forced convection and forced air cooling as well as on coatings applied to minimize permeation losses lead to the development of much optimized storage systems [Kle05b]. The accumulation of helium-3 in the lattice of $LaNi_{4.15}Al_{0.85}$ was found to be associated with a decrease in desorption pressure and a slight diminution of storage capacity.

To investigate the tritium storage material properties of titanium sponge and rods, several hydride storage vessels were manufactured that complied with the following design principles: i) tritium capacity within the range 200 - 500 g, ii) storage life of 7 to 10 years, iii) total weight of vesse lbelow 22.7 kg in order to remain transportable by a single person, iv) diameter and length of 38.1 and 63.5 cm, respecively, to fit into a glove box passbox and v) tritium recuperation either by external heating of the vessel and/or isotopic exchange. Each vessel displayed a long

inlet tube submerged into the getter up to almost bottom of the vessel, and a short oulet tube. Both tubes were provided with a filter cup of 5 µmporosity fitted to their end. The vessels were designed to withstand a pressure of 7.00 MPa at 394 K, 1.43 MPa at 1033 K and full vacuum at same temperature. It was concluded, that 4.4 kg of titanium sponge can be activated, and loaded at ambient temperature at moderate gas flow rates without exceeding the design temperatures of the vessel and desorbed down to moderately low inventories at 973 K under evacuation.

Forde et al. [For07] developed a reliable and experimentally verified kinetic correlation for the design of large storage units. Absorption and desorption experiments performed within the temperature span 550 - 591 K constituted the experimental basis for the model. Activation energies for absorption and desorption were found to depend on whether the process occurred i) stepwise, ii) by full hydrogenation without thermal ballast, or iii) by full hydrogenation with thermal ballast. $LaNi_5$ was used as reference getter material. On the basis of the results a semi empirical heat and mass transfer modelling correlation was developed which according to the authors permits improved engineering design of large metal hydride storage units.

At **JAERI** [Kon89; Ohi99] a large tritium transport bed designed for safe storage of up to 25 g tritium on zirconium-cobalt getter material distributed between several sintered stainless-steel tubes was build and tested with tritium. The program was primarily aimed at the development of international transport procedures for the supply of ITER with tritium fuel. The 25 g transport bed was successfully employed twice for an international transport. Up to twenty-five absorption/desorption cycles had little impact on the pumping speed of the getter, but caused a slight reduction in storage capacity [Kon87; Kon88]. This observation was confirmed years later by other investigators [Bek99]. In view that for ITER and even more so for future fusion devices a 25 g transport vessel is definitely too small, a rather detailed conceptual design of a compact transport package having ten times as much storage capacity for tritium was published by O´Hira et al. [Ohi99] (see also section 8.6). The design was complemented by a comprehensive safety analysis. The primary tritium containing capsule was constructed to withstand 57.7 kPa at 353 K under normal conditions and 95.6 kPa at 437 K under accidental conditions. Calculations showed that the design remained intact when a package of this kind is i) dropped from an elevation of 9 m on a hard surface, ii) exposed to a thermal event of 30 min duration at 1073 K or iii) accidentally plunged into the deep sea to depths of up to 6000 m.

An experimental and engineering program aimed at developing a tritium Storage and Delivery System (SDS) for ITER utilizing depleated uranium as getter material is currently well under way at **KAERI**, Korea [Chu15; Yun15]. The planned SDS shall meet all requirements of the fusion fuel cycle including the capability for periodic extraction of decay helium.

Recapitulating, on present days there is worldwide a considerable body of information in the open literature on handling of tritium in small sized as well as technical-scale tritium storage beds containing diverse getter material. Particularities and long-term performance of the selected getters are well documented. Conversely, only vague and incomplete information's are available on the optimal design and manufacture of technical getter beds meeting all requirements essential for ITER. What is more, only few systematic experimental investigations are available on the performance and optimization of filters needed for the getter beds [Kur84; Khe89; Shm84; Shm90b; Shm90a]. Therefore, especially from an engineering point of view, some complementary research efforts are still considered necessary.

3.14.2.2.4 Further applications of getter beds

Uranium metal beds maintained at 973 K have been used to purify hydrogen from gaseous impurities like N_2, NQ_3, CQ_4, and O_2 (Q = H, D, T) [Car75]. At this rather high temperature the reaction kinetics of uranium with impurities is fast and the degree of tritium retention by the getter fairly low. One more benefit of the high temperature is that N, C, and O atoms trapped on the metal surface readily diffuse into the bulk. As a consequence, the metal surface remains reactive.

Getters have likewise served to strip tritium and other hydrogen isotopologues from noble gases or nitrogen streams. Within this frame, frequent applications are the removal of tritium from glove box atmospheres or tritium stripping from vacuum pump exhaust streams. Shmayda [Shm93] provided a good introduction on theory and operation of scavenger beds utilized for stripping tritium from carrier gas streams. For the decontamination of gaseous streams, two scavenger beds in series where proposed, i.e. a uranium bed for the retention of the majority of the tritium (and eventually for tritium recovery) and a second bed containing **St198 alloy getter** for the retention of remaining traces of tritium. With this process arrangement a degree of decontamination in line with that required for direct discharge into the environment could be

achieved.[30] In fact, with the St198 alloy, which is characterized by rather high reactivity towards tritium and impurities, decontamination factors of the order of 2×10^5 were experimentally verified [Shm88b].

One more application of getters is the incessant evacuation of the guard vacuum vessel of heated components such as getter beds, permeators, catalyst beds, etc. Boffito et al.[Bof87] studied and discussed the performance of a gettered Dewar jacket. According to their observations, the incorporation of two **ST707 getter pills** weighting 1.2 g each into the jacket of a Dewar reduced the total pressure in the insulation vacuum by more than two orders of magnitude. The jacket had previously been thoroughly evacuated and heated in order to remove moisture from the Dewar walls and to activate the getter. Advantageously, ST707 getter material can be reactivated recurrently. The sorption properties of the ST707 getter material for hydrogen remained essentially unaffected by the vicinity of liquid nitrogen filling the Dewar. On the other hand, sorption of carbon monoxide increased at cryogenic temperature probably because of physisorption.

With a zirconium/cobalt bed maintained at ambient temperature it was possible to keep the hydrogen isotope partial pressure in a 50 l vacuum jacket protecting a permeator operated round the clock at 623 K nearly constant at 0.025 mbar for at least a period of one week. Because under these conditions the steady state equilibrium pressure of tritium in the vessel is rather low, most decay helium is generated in the bulk of the getter. Thus, blanketing effects are small. Hence, a pump combination can be substituted by a static bed which neither depends on a power source nor requires maintenance. A major benefit of this approach is enhanced safety. The need to evacuate periodically decay helium is not considered to be a major drawback [Pen95c].

Non-evaporable getters like Zr – Al have been shown to pump gaseous hydrocarbons like alkenes, alkadienes, and cyclo-alkanes at temperatures spanning from 358 to 918 K. The pumping speed of non-saturated hydrocarbons was found to be much faster than of saturated ones [Eme87].

3.14.2.3 Metal hydrides as compressors

Metallic getter beds have been utilized for the pressurization of hydrogen isotopologues [Heu95a]. Getters tested were palladium on kieselguhr, $LaNi_{4.7}Al_{0.3}$, $Ca_{0.2}M_{0.8}Ni_5$ (M denoting a mis-

[30] The St198 bed consists of Zr_2Fe getter pills placed within two concentric sintered tubes. The bed is normally operated at 623 K.

chmetal), and $TiCr_{1.8}$. Compressions of tritium up to 136 bar becomes feasible with a sequence of two compression stages [Ort90]. Short intermittent exposures to tritium revealed no detrimental effect on the compression properties of the examined metal alloys, i.e. $LaNi_{4.7}Al_{0.3}$ (first stage) and $Ca_{0.2}M_{0.8}Ni_5$ (second stage). Purities of released tritium above 99 % were regularly achieved with the first compressor stage. Tritium from the second stage, on the other hand, showed contamination by decay helium after a storage period approaching 200 days.

Palladium supported on kieselguhr containing about 50 % of the metal has been used as pump/purifier to feed hydrogen isotopes from large gas tanks directly into a cryogenic still [Nob91]. The pump/purifier vessels were cooled by external Freon coils. Several heaters were used for hydrogen isotope desorption. The primary vessel was pressure-protected by rupture disks. Temperature- and pressure-activated interlocks were installed to turn off power to the heaters of the bed in case temperatures and/or pressures exceeded design values.

3.14.2.4 "In-bed" calorimetry

In the early days, the tritium content of a getter bed was obtained volumetrically employing a large evacuated calibrated vessel. To this effect, the metal tritide was fully decomposed by prolonged heating at sufficiently elevated temperature. An accurate measurement demanded, in addition, the determination of i) the volume of the tubing between the bed and the vessel, ii) the "heel" remaining in the getter bed (see section 3.18.12.2) and iii) an analysis of the isotopic composition of the released hydrogen. Essential for a volumetric determination are a high vacuum pumping system, calibrated vessels, and pressure sensors covering a broad pressure range.

A better option is transfer of tritium from a getter bed installed in a glove box into a small portable getter bed and determination of the tritium inventory in the latter employing a calorimeter installed outside of the glove box. An effective transfer of tritium requires sweeping with inert gas across donor and receiver bed in closed loop modus. Once the transfer into the transport vessel is completed, the transport vessel needs to be disconnected from the vessel, removed from the glove box through an air lock, transported to the calorimeter, and subjected to one or more measurements. A mandatory precaution is verification that the outer surface of the transport bed is not contaminated (contamination can take place by direct contact of the transport bed with the contaminated atmosphere of the glove box as well as from tritium diffusing to the outer surface if the transport vessel has previously been heated for tritide dissociation).

Subsequent to calorimetry, the transport vessel must be returned into the original glove box via the air lock, be attached to the primary system, evacuated, and tritium returned from the externally heated transport vessel into the storage bed.

A consequence of prolonged heating at fairly high temperatures to achieve complete release of tritium from a transportable bed is considerable contamination of the outer surface of the bed and of the glove box atmosphere. To elude these contaminations while at the same time enhancing safety and accuracy much effort has been invested worldwide into the development of "in-bed" calorimetry.

In the next section, several distinct, experimentally demonstrated "in-bed" options for the direct determination of tritium inventories in storage beds are briefly described and commented:

3.14.2.4.1 Static gas method

A fast-transient measurement of the initial rate of pressure increase in the jacket surrounding a heated metal hydride bed has been correlated with the amount of tritium in the bed. This technique was, however, not followed any further because the results showed a dependency from the number of absorption /desorption cycles as well as from the composition of the gas in the metal hydride [Kle92] (see also [Kur84]).

3.14.2.4.2 Adiabatic/isothermal calorimetry with vacuum insulation

Adiabatic/isothermal calorimetry with vacuum insulation was researched by Walters and Jenkins [Wal94] as well as by Serio et al. [Ser95]. Measurements were performed at JET utilizing one of four tritium storage beds containing uranium as tritium getter. Each primary tritium containment at JET is mounted inside of a secondary containment which in turn is installed together with three other identical assemblies inside of an evacuated tertiary containment (instead of a glove box). During calorimetric runs the secondary and tertiary containments are evacuated to less than 10^{-7} mbar in order to isolate the U bed from the environment and delineate the heat conduction path along the central tube while the primary containment was filled with 100 mbar helium to achieve a better transfer from the heaters to the structure. Under these conditions the inventory of tritium in the storage bed can be obtained from a determination of the temperature rise, provided the heat capacity of the complete structure and the heat flow through

the containment walls are known. Heat transport through the evacuated secondary and tertiary containments takes place mostly by radiative heat loss and to a lesser extent by conduction through the support structures. The temperature rise is related to the tritium inventory by the energy balance equation

$$C_P \frac{\mathrm{d}T}{\mathrm{d}t} = q - A(T - T_0) - B(T^4 - T_0^4)$$

where q is the total amount of heat generated by the tritium inventory, T the temperature of the uranium bed, T_o the temperature of the environment, A a heat conduction coefficient, B a heat radiation coefficient, C_P the heat capacity of the bed, and t the time. The unknown parameters C_P, A and B are obtained by fitting. The procedure adopted was to apply increasing test powers within the range 0.5 ($\simeq$ 1.5 g T_2) – 10 ($\simeq$ 31 g T_2) W while cooling with gas for altogether 12 hours. The different selected power levels simulate the decay heat of tritium. After 12 hours, gas cooling was stopped while keeping the electric power on. A fixed time later, i.e. 3 hours, the temperature derivative was determined. Typical temperature evolution curves at different power levels obtained after the cooling gas flow was off are plotted in Fig. 3.30a. As apparent, after stopping the gas flow, the temperature first increases steeply and then progressively levels off until isothermal equilibrium is established. A plot of the heat capacity three hours after start of heating revealed that the effective heat capacity was a function of the heating power. The results from a number of calibration measurements are plotted as function of heating power in Fig 3.30b.

Experimentally it was noticed that data taken during the transition from adiabatic (initially) to isothermal (equilibrium) were least affected by ambient temperature changes or conductivity losses originating from deterioration of the insulation vacuum. The reproducibility of the results obtained with this empirical method was found to be better than 1 % or ±0.1 W.

3.14.2.4.3 Flowing gas procedure

This method has been propagated at **Savannah River** by Klein and co-workers [Kle92; Kle95; Kle02b] using storage beds containing $LaNi_{4.25}Al_{0.75}$ and at **TPL** by Hayashi et al. [Hay05] using beds loaded with ZrCo. The method basically consists in determining the steady-state

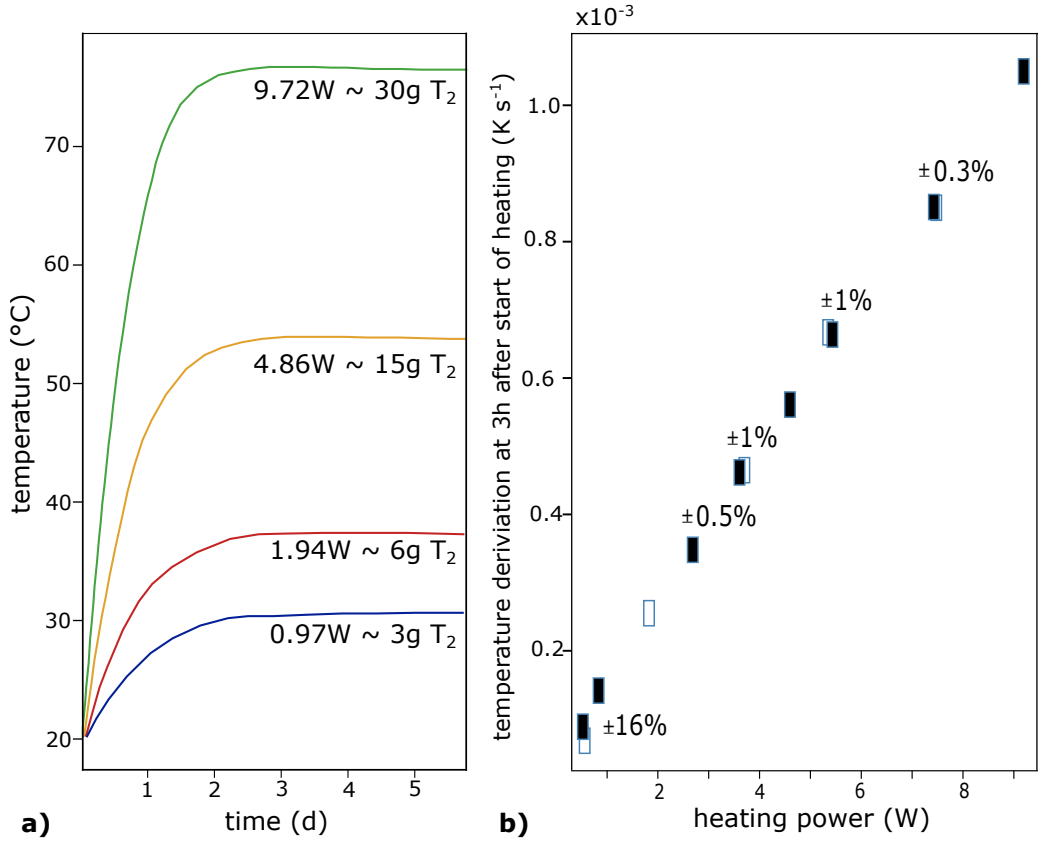


Figure 3.30: Temperature evolution as function of time in a JET uranium tritium storage bed at several heating powers simulating tritium inventories of 3 - 30 g T_2 (a). Empirical calibration results with one of JET storage beds (b) (after [Ser95]).

temperature difference between inlet and outlet of a secondary helium stream flowing through a jacketed metal hydride storage bed under carefully controlled conditions.

A typical experimental arrangement is illustrated in Fig. 3.31a. It shows schematically a bed containing 0.7 kg of ZrCo mixed with 1.1 kg of copper spheres having a diameter of 1 mm. The experiments at TPL were performed with 25 g of tritium. The power generated by tritium decay is on one hand carried away by the flowing gas and on the other by conduction from the primary containment via metallic bridges towards the secondary and tertiary systems from where it reaches the surroundings at ambient temperature. Because of the complexity of the storage bed system, heat dynamics are difficult to evaluate theoretically. Hence, empirical calibrations were selected. To this effect, calibration curves were determined employing a heater in the primary vessel designed to simulate the decay heat of tritium. To perform tritium accountancy the insulation jacket was first evacuated and then helium re-circulated through the secondary loop

(see Fig. 3.31b). Once heat equilibration was established the temperature difference between inlet and outlet of helium was measured and the result plotted to obtain a calibration curve. At least one day was found to be necessary for an inventory measurement. For a zirconium cobalt bed with a tritium capacity of 25 g the initial sensitivity was estimated to be 0.05 g and the accounting accuracy found to be 0.15 % at full capacity [Hay95b]. This result meets ITER specifications.

Hayashi et al. [Hay05] furthermore provided evidence that the initial sensitivity and accuracy of the calorimeter remained unchanged over at least a period of eight years. Besides production and accumulation of helium-3 no other ageing effect induced by the incessant presence of tritium, particularly no damage to the mass flow controller or deterioration of the Resistance Thermo Device (RTD) were detected. Uninterrupted evacuation of the vacuum jacket of the ZrCo bed was considered to be the most consequential technical measure for a good accountancy determination.

At **Replacement Tritium Facility** of Savannah River Technological Center accountancy by in-bed calorimetry was developed employing storage beds containing $LaNi_{4.25}Al_{0.75}$ metal alloy [Kle92; Kle95; Kle02b; Kle05b; Kle11]. Salient features of in-bed calorimetry are i) determination of tritium inventories without requiring knowledge of the composition of the gas sequestered as hydride and ii) cumbersome prolonged procedures for the release and return of radioactive gas from the solid matrix are circumvented.

In early runs, protium was used as hydriding isotope and electric heaters to simulate the decay heat generated by hypothetical tritium inventories captured in the getter alloy [Kle92]. Before engaging in extended measurement campaigns, several in-bed calorimetric techniques were compared among each other. **Static gas methods** such as hydride pressure, hydride bed temperature or hydride bed temperature rise above that of the glove box were soon discarded after it was observed that inspite of being fast, these techniques displayed dependency from the number of absorption/desorption cycles by the getter and from the composition of the gas constituting the metal hydride. Good results were achieved instead with a **flowing gas method** with which tritium inventories in a metal hydride are obtained from the steady state temperature rise of a gas stream flowing across the annular jacket of a metal hydride bed (see Fig. 3.32).

The power Q generated by the metal alloy tritide is dissipated according to the energy balance expression

$$Q = WC_{\mathrm{P}}K_{\mathrm{W}}\Delta T + UA\Delta T_{\mathrm{UA}}$$

in which W is the gas flow rate in standard $\mathrm{l\,min^{-1}}$, K_{W} a conversion factor, ΔT the temperature difference between the gas at the inlet and outlet of the bed, C_{P} the average heat capacity of the gas between T_{o} and T_{i}, UA the product of the average overall heat transfer coefficient times the area of heat transfer and ΔT_{UA} the average temperature difference between that of the flowing gas stream and ambient. Obviously, the first term in the above equation describes the energy carried away by the flowing gas and the second one the energy that undergoes exchange with the surroundings maintained at temperature T_{s}. Under steady state (SS) conditions and provided $T_{\mathrm{i}} \neq T_{\mathrm{s}}$ it can be shown that

$$\Delta T_{gas} = \frac{K_{\mathrm{T}}}{WC_{\mathrm{P}}K_{\mathrm{W}} + \frac{UA}{K_{\mathrm{UA}}}}(T/M)$$

where K_{T} is a constant that converts T/M into power and

$$K_{\mathrm{UA}} = ln\frac{T_{\mathrm{o}} - T_{\mathrm{s}}}{T_{\mathrm{i}} - T_{\mathrm{s}}}.$$

Loading of the alloy is expressed as the atomic ratio of tritium/metal (T/M). To calculate M, the molecular weight of $\mathrm{LaNi_{4.25}Al_{0.75}}$ was taken to be $408.62\,\mathrm{g\,mol^{-1}}$. It was further assumed that each mol hydride contains six mol metal. For the initial experiments, the alloy was loaded with precisely known amounts of protium employing a calibrated volume and evaluating the delivered inventory by volumetric procedures. The helium or protium pressure in the jacket was controlled by pressure regulators. From experiments designed to estimate the minimum time required to obtain reliable ΔT data of sufficient accuracy it was concluded that at least 14 hours are necessary. The gathered calibration data permitted in about 14 hours the determination of tritium inventories in the storage bed with an accuracy of $\pm$ 1.6 % within a confidence interval of 95 %.

In a next step, several five-point and nine-point data sets of steady state ΔT vs. T/M calibration plots were obtained utilizing a heater as power source and a stream of helium or hydrogen passed through the bed jacket [Kle95]. Regression model calculations indicated that

the steady state ΔT versus T/M data for hydrogen or helium at standard 65 l min^{-1} did not differ sigficantly. It was shown, that for values of $T/M < 0.7$ the steady state temperature rises of a gas stream passing at constant flow rate and pressure through the annular jacket surrounding the metal hydride bed correlates directly with the amount of heat generated by an electric heater simulating immobilized tritium. The generated calibration curves provided the information needed for the calculation of tritium inventories. Employing either helium at a flow rate of standard 70 l min^{-1} and 101 kPa in the bed jacket or protium at flow rates of 50, 60, 70 or 80 standard l min^{-1} virtual inventories of tritium inside of a full metal hydride storage bed with a loading of $T/M = 0.7$ could be calculated in 14 hours measuring time. Inventories with an accuracy of ± 1.6 % of a fully loaded bed were reported with a confidence level of 95 % [Kle92].

Further verification of cold runs was carried out employing tritium. Within this frame, six-point tritium in-bed accountability calibration curves were obtained utilizing two $LaNi_{4.25}Al_{0.75}$ metal hydride storage beds both designed for 390 g tritium [Kle05a]. The two tritium beds were of similar design and comparable external insulation to the ones used for cold tests but without integrated heater wells. The difference between the inlet gas temperature and the glove box temperature was maintained at ± 2 °C or less. Prior to loading with tritium, the hydride bed under test was heated at 413 K for several hours under a vacuum of less than 133 Pa. In agreement with previous results, linear correlation between steady state ΔT and the power generated by the decay of tritium was observed for T/M values lower than 0.7. Based on regression analysis six calibration points were considered sufficient for in-bed calibrations. The results with the two large-scale tritium beds provided evidence that steady state ΔT in-bed accountancy data correlate better with an actual tritium inventory in a bed than with values simulated by a heater. To investigate the effect of temperature, runs were conducted at $T/M = 0.42$ and 70 standard l min^{-1} at inlet air temperatures ranging from 296 - 353 K. Under these conditions, no significant effect of the inlet temperature on UA was detected. The influence of variations in gas flow rate within the range of standard 50 - 80 l min^{-1} on the calibration straight lines was likewise researched systematically. Tritium inventory errors at the 95 % confidence level ranged from ± 7.3 - 8.6 g for the protium/heater calibrations and from ± 4.2 - 7.5 g for beds calibrated with tritium. The 1 % tritium measurement error required for the storage vessels of ITER, was thus approached. Experiments designed to develop in-bed accountability for large storage beds such as operated at **Replacement Tritium Facility (RTF)** were carried out

with two hydride storage beds of distinctly different sizes [Kle02a]. One bed loaded with 12.6 kg of $LaNi_{4.25}Al_{0.75}$ alloy when accepting tritium up to a T/M atomic ratio of 0.7 is loaded with a tritium inventory of 1451 standard litres or 391 g and another consisting of an array of four interlinked storage beds of the same geometrical size as the previous ones but loaded with only 10.54 kg of the $LaNi_{4.25}Al_{0.75}$ alloy. When the four beds are taken together and each is loaded up to $T/M = 0.7$, the total loading amounts to standard 4856 l (the array is referred to as 5000 l) or 1307 g of tritium. As practiced in cold runs, storage beds were first evacuated and thereafter the highest amount of tritium to be employed in calibration measurements introduced into the metal alloy bed from a calibrated tank of 1500 litres volume. The tank is equipped with a high accuracy pressure transducer. The amount of injected tritium was precisely determined by pVTc procedures including mass spectrometric analysis of the chemical and isotopic composition of the delivered tritium (Note: gas analysis is only required for the accurate determination of the tritium supplied to the bed and not for in-bed calibrations!). For pVTc error calculations of the inventories in the hydride bed the sequence was to load the bed to the foreseen highest T/M loading and subsequently remove several fractions of that gas in order to obtain the next lower loadings. When complying with this constraint, ΔT_{gas} measurements were found to be exclusively dependent on the amount of tritium and not from gas pressure or gas composition within the bed. The inventory error achieved by in-bed accountability using steady state ΔT_{gas} vs. T/M data was within the range 0.7 - 2.6 %. Getter-ageing did not affect the inventory measurement. The achieved error of 1.3 % tritium at a confidence level of 95 % for a technical sized bed loaded with tritium up to a ratio of $T/M = 0.6$ approached the ITER requirement of 1 %.

Upgraded storage beds containing the same type and mass of $LaN_{4.25}Al_{0.75}$ alloy carrying the designation PAssively Cooled Electrically (PACE) heated hydride beds were also tested at Savannah River Site Tritium Facilities. These beds utilize electrical heating for desorption and much-reduced forced atmosphere cooling flow rates than previously tried out storage beds [Kle05a; Kle05b; Kle11]. The evacuated jacket leads to decreased heat losses and lower uncertainties. When the in-bed accountancy gas flow is sent through an internal and lengthy U-tube inserted into a 1.2 m long vessel smaller inventory errors are possible in comparison to the previously used gas flow through the jacket. Increasing the gas flow rate through the PACE U-tube permitted faster equilibration times and reduced tritium measurement uncertainties. Changes in vacuum jacket pressure affect significantly the ΔT values. Higher jacket pressures are associated with

increased heat transfer from the bed which leads to lower in-bed accountancy ΔT values and therefore to underestimation of the tritium inventory. For a bed fully loaded up to $T/M = 0.6$ the relativ error was determined to be 0.9 %.

Recapitulating: At Replacement Tritium Facility (RTF) in-bed calorimetric steady state ΔT_{gas} vs. T/M data were obtained both in cold tests using four single beds provided with heaters and in hot tests with tritium employing eight similar beds without heater. All twelve beds were charged with $LaNi_{4.25}Al_{0.75}$. The eight beds are used for tritium supply or gas evacuation. Within this frame, an in-bed accountability steady state flowing calorimetric method was qualified for large single beds containing approximately 1500 l of tritium as well as for a manifolded configuration of four large beds of the same dimensions but of lower single inventory to yield a total of 4856 lof tritium. Maximum tritium inventory errors ranged from 0.7 to 2.6 % for a full bed. Other measurement techniques like T_{bed}, ΔT_{bed} or $\log p_{\mathrm{bed}}$ vs. T/M displayed lower inventory measurement accuracy. To achieve accuracies better than the target accuracy for ITER, i. e. 1 %, it is necessary to i) control inlet and outlet temperatures to ± 0.1 K, ii) regulate the mass flow rate of about 60 l $\mathrm{min}^{-1}$to ± 0.3 %, and iii) control the outside temperature of the external insulation mantle to ± 0.1 K. Such exigent demands on temperature and flow control procedures were considered to be a substantial drawback of the flowing gas method [Hem95].

3.14.2.4.4 Isothermal calorimetry

Isothermal calorimetry was proposed by Hemmerich [Hem95]. He employed a horizontally installed cylindrical tritium storage bed of the type available at JET. The tested bed contained 4.3 kg of uranium and possessed a storage capacity for 121.5 g tritium. The insulation of the bed consisted of a very efficient micro porous thermal material, i.e. Microtherm, which is maintained under a hydrogen atmosphere of 1 bar. The conductivity of this material is nearly independent of temperature and has almost exactly the correct value for the envisioned application. A cross section of the configuration of the bed is displayed in Fig. 3.33. To obtain an effectively averaged temperature for the non-homogeneously distributed uranium inside of the bed and to account for a possibly non-homogeneous distribution of tritium in the uranium several Pt100 resistors were installed over the whole length of the bed on the source surface and outermost surface. The low conductivity of the insulation helps to retard the transport of heat to the outer containment and therefore coerces the attainment of equilibrium inside of the bed core.

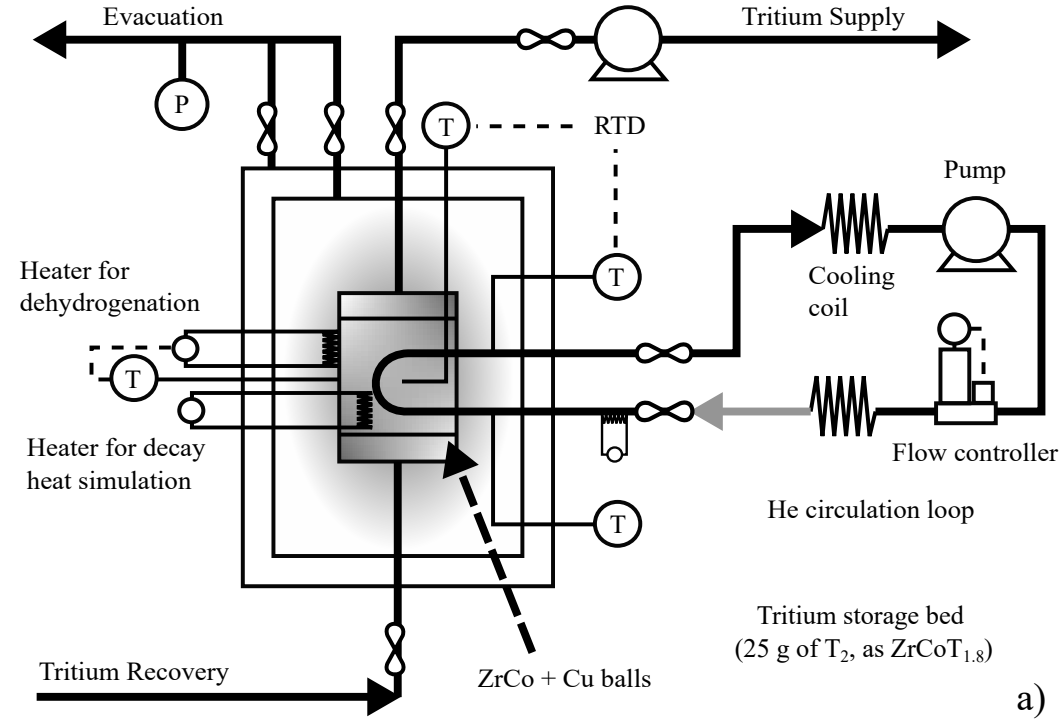
Heat transport from the cylindrical bed core to the bed surface is described by the simple relationship

$$\frac{\partial T}{\partial t} C_{\mathrm{P}} = Q - \frac{2\pi\lambda L}{\ln(D_0/D_i)}(T - T_0)$$

where t is the time, C_{P} the average heat capacity of the bed, Q the power source, λ the temperature-independent thermal conductivity of the insulation, L the length of the bed, D_i and D_0 are the inner and outer diameter of the insulation, and T and T_0 are the temperature of the core and the outer bed surface, respectively. After attainment of equilibrium, i.e. $\partial T/\partial t = 0$ and $T = T_{\mathrm{e}}$, the relationship simplifies to

$$Q = \frac{2\pi\lambda}{\ln(D_0/D_i)}(T_{\mathrm{e}} - T_0)$$

where T_{e} is the equilibrium temperature. From this equation it follows that only the temperature difference $T_{\mathrm{e}} - T_0$ needs to be determined to calculate the power Q of the source. To achieve a precision of less than 1 % a measurement time of the order of 22 hours was found to be necessary. This measurement time can be shortened if the bed is heated (or cooled) to a temperature close to that of the equilibrium value. An accuracy of the calorimetric assay of ± 0.1 % is possible provided the temperature difference measurement can be carried out with a resolution of ± 0.1 K and the ambient reference temperature, e.g. 300 K, is kept stable to within ± 0.1 K.



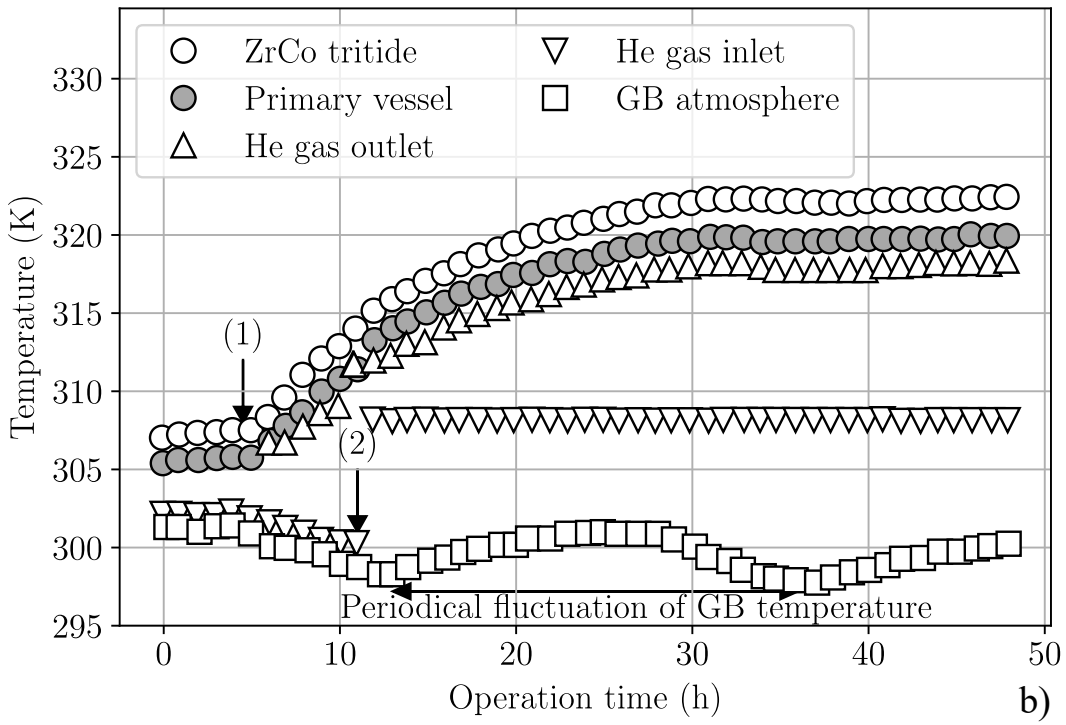


Figure 3.31: Simplified diagram of a tritium storage bed designed for "in bed" calorimetry (RTD = Resistance Thermo Device inserted into the He loop) (a). Typical temperature evolution during an inventory measurement where (1) denotes beginning of evacuation and (2) denotes beginning of gas circulation for calorimetric measurement (GB = glove box) [Hay05].

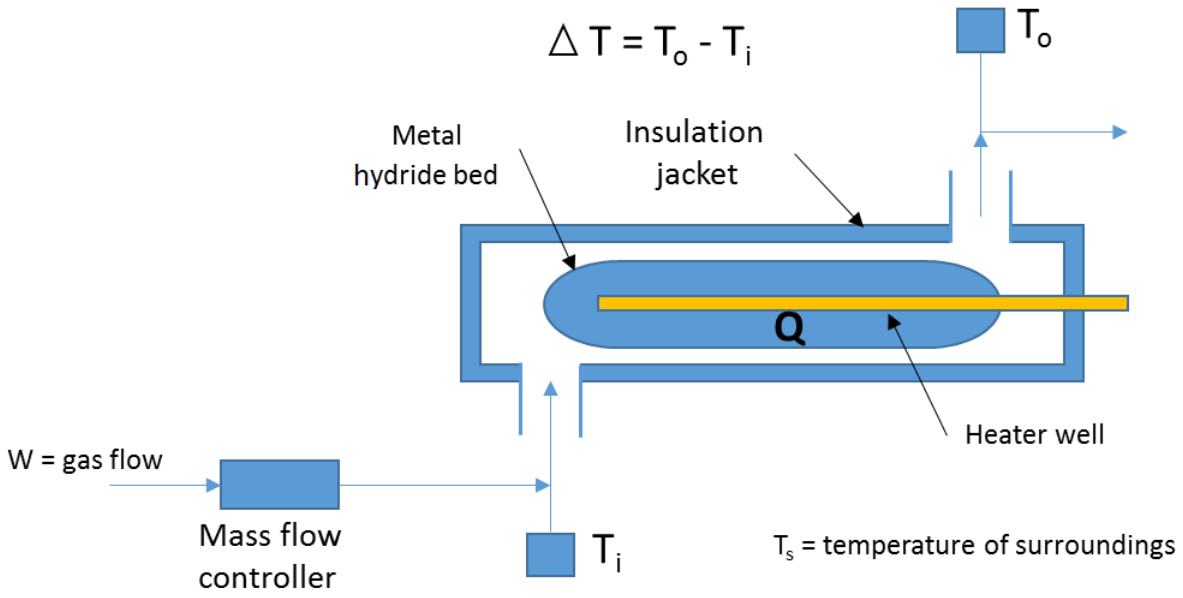


Figure 3.32: Metal hydride flowing gas calorimeter (T_i = inlet temperature and T_o = outlet temperature) (after [Kle92]).

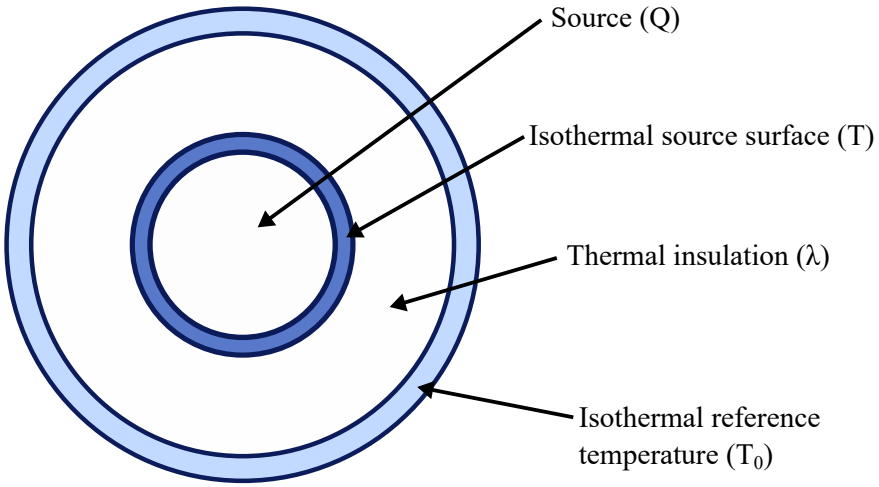


Figure 3.33: Cross section of a tritium storage bed with "in-bed" calorimetry (after [Hem95]).

3.14.3 Permeator as purifier

a) Permeator properties

A commercial permeator is a device designed to purify molecular hydrogen from other gases. It takes advantage from the property of hydrogen isotopes to easily and exclusively permeate through a heated thin walled membrane of palladium/silver alloy when a pressure difference is applied as driving force.

For the **Industrial purification of hydrogen**, the feed gas is passed through the Pd/Ag tubes at fairly elevated pressures, e.g. more than 30 bar, from the outside into the inside in order to warrant their integrity [Con62]. There is no evidence that any gas other than hydrogen diffuses across palladium-silver at the conditions employed for hydrogen isotope purification [Con62; Got70]. Impurities detected in the permeated gas at sub [ppm] concentrations are probably generated by thermal outgassing of palladium/silver membranes and other structural materials.

Diffusion and permeation data for hydrogen, deuterium, and tritium across Pd-Ag alloys have already been discussed in a previous section. Lässer and Powell [Lae88] published solubility data for all three hydrogen isotopes in various palladium-silver alloys and gave expressions for the calculation of pressures in the well-defined plateau regions of $Pd_{0.9}Ag_{0.1}$ (see also section 2.14.8).

While operating permeators it is important to keep in mind that the heated Pd/Ag membrane possesses strong **catalytic activity**. For instance, on the surface of the membrane a rapid reaction between oxygen and hydrogen generates water vapour, ammonia is decomposed into nitrogen and hydrogen, and carbon monoxide is converted into methane, carbon dioxide, and water upon reaction with hydrogen.

It is furthermore important to note, that palladium exposed at moderate temperatures, i.e. $> 333\,K$, to a stream of unsaturated hydrocarbons like ethylene or acetylene or to carbon monoxide will react to form of a new solid phase. This phase has been identified as an interstitial solution of carbon in palladium which causes lattice expansion and suppression of hydride formation upon subsequent exposure to hydrogen [Sil68; Zie85a; Zie85b; Zie87]. The structural change can be reversed by heating of the "corroded" palladium under air. Formation of a Pd-C phase has also been observed during the hydrogenation of acetylene over a palladium catalyst [Sta85; Bor99].

High separation efficiency between hydrogen and impurities is habitually achieved with a bundle of manifolded palladium/silver tubes. The tubes usually have an outer diameter of 3 mm,

are closed on one end, and have a wall thickness of approximately 100 µm. To expedite the separation, all tubes are heated up to a temperature of the order of 623 K utilizing multi sectioned heaters. By this approach, it is possible to achieve a rather homogeneous temperature profile along the permeation zone and at the same time facilitate the replacement of heaters when they are damaged. Feed gas is introduced into nearly the bottom of each Pd/Ag tube of the bundle by inserting an equal number of manifolded long capillary tubes into the Pd/Ag tubes.

In case of tritium-bearing gases the preferred gas flow direction is from the inside into the outside. Pressures of tritiated hydrogen isotopologues must be kept below 1 bar to warrant integrity and hence safety. A concentration gradient is provided by pumping continuously the gas permeated from the inside of the Pd/Ag tubes employing a suitable pump combination. To avoid tritium permeation across the outer wall of the heated permeator into the glove box the complete device is introduced into a stainless-steel vessel. During permeator operation this jacket vessel must be continuously evacuated in order to maintain the insulation vacuum at very low level and eventually recover the permeated gas. To minimize permeation into the glove box, the outside temperature of the protecting vessel shall be limited to 333 K. This is achieved on one hand by sustained evacuation and on the other by an array of heat shields placed strategically around the heated section inside of the second containment. Introduction of the permeator into a jacket vessel has the additional advantage that only the jacket vessel needs to be qualified for tritium service. Qualification of a commercial permeator is doubtless much more challenging.

The separation of hydrogen isotopes from impurities utilizing permeation across palladium-silver alloy membranes has been examined experimentally and theoretically by a number of investigators [Cha65; Tan79b; Izu81; Bon83; Eva83; Pen97a; Glu06a]. The operational experience gained at Savannah River Site over several decades partly comparing several diverse commercial permeators featuring different separation performances has been discussed in detail by Clark et al. [Cla95b]. Good long-term operation with high reliability was achieved with a permeator comprising six palladium-silver coiled tubes in a single chamber arranged in parallel to reduce the pressure drop. Each coil was heated by a single replaceable heater cartridge mounted in a well (see Fig. 3.34). By this approach, failed heaters could be exchanged without interruption of operation. To protect the permeator, the feed gas was passed first through a sacrificial uranium bed and then through a second bed containing palladium supported on alumina. Objective of the first bed was removal of excess moisture and of the second removal of all other impurities. One

more important supportive safety measure consisted in the analysis of the feed gas composition into the diffuser utilizing a mass spectrometer. Main objective of this measure was to prevent feeding of flammable mixtures. A useful and simple design improvement was a coiled feed inlet tube so arranged that the feed gas could be efficiently pre-heated. As common practice in other tritium facilities, permeators were introduced into qualified single-wall ultra-high vacuum-tight outer containments to circumvent the need to qualify a commercial permeator for tritium service.

Foster et al. [Fos08] described and tested a commercial permeator manufactured by Johnson-Matthey, West Chester, PA, USA. Its operation out in with hydrogen was carried in "inside-out" modus. Gaseous feed was supplied via a manifolded line connected to the inlet of five stapled open-ended palladium/silver coils each of 3.5 m length, 0.076 mm wall thickness and 0.0333 m^2 inner surface area. The total permeation area was thus 0.1665 m^2. Heating occured axially employing an 1800 W cartridge fitted into a heater well. A Normetex scroll pump combined with a Metal Bellows MB-601 pump served to pump permeating hydrogen. Investigated parameters were i) type of inert gas, i.e. helium or nitrogen, ii) feed gas composition, iii) varying pressure in Pd/Ag tubes, and iv) method for temperature regulation, i.e. control of temperature or of power. In accordance with expectations, the rate of permeation was found to be proportional to the difference in square root partial pressure of hydrogen in feed and permeate. Bleed flow rate vs. feed flow rate plots yielded hydrogen breakthrough curves into the bleed gas at feed flow rates within the range 3 - 4 $l_{STP}\,min^{-1}$. Similar findings were reported earlier by other investigators [Pen97a; Glu06b]. In experiments with hydrogen feed gas containing either 25 % helium or 25 % nitrogen, the breakthrough of hydrogen into the bleed stream occurred at higher feed flow rates when helium was present. This behaviour was attributed to a 13 kPa lower pressure in the tube observed when helium was used instead of nitrogen. A conclusion from these experiments is that the type of inert gas present in hydrogen affects both the permeate pressure as well as the permeation rate. Under constant power input conditions, the temperature of the shell remained unchanged within the range (673 ± 20) K, showing only a slight drift. This was also the cause for flow rate and permeate pressure drifts. When in place of constant power a temperature control technique was used to maintain the shell temperature constant, an irregular random drift was observed. Reactivation of the permeator contributed significantly to either eliminate or at least reduce this drift. Once breakthrough occurred, a higher permeation

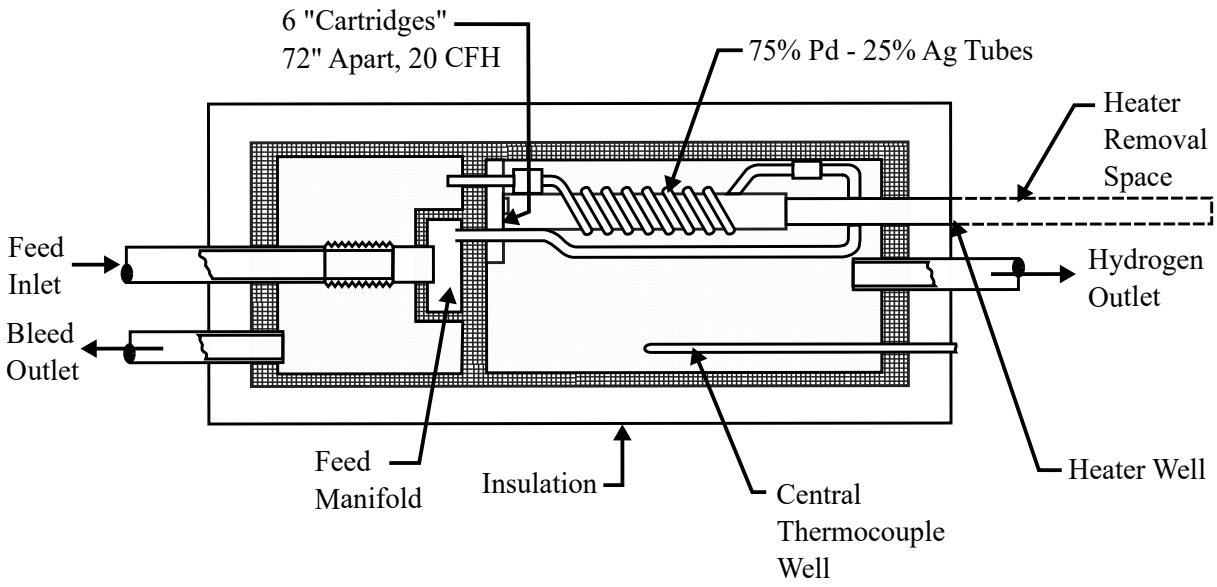


Figure 3.34: Diffuser from Resource Services Incorporated [Cla95b].

of hydrogen was observed when using constant power input control instead of temperature-control.

b) Modelling

Yoshida et al. [Yos83b] were first to propose a complete new fuel clean-up concept for processesing of the off-gas of a fusion machine employing a palladium/silver permeator as key component. To describe the operation of the permeator, a mathematical model was developed. The model is based on the assumption of a continuous stirred tank reactor comprising N volume elements, each containing perfectly mixed fuel and impurity gases. Feasibility of the preliminary design and of the underlying model were verified experimentally in a rather comprehensive study performed at TSTA, Los Alamos.

A refined model describing the separation of tritium from impurities was developed by Willms et al. [Wil93]. Willms et al. assumed the permeator to operate in plug flow mode and also supposed permeation taking place without axial or radial concentration gradients in each of the single volume elements, i.e. good gas mixing and no diffusion within the volume elements. After corroborating the efficiency of the model by comparison with experimental data, itl was considered suitable for the evaluation, understanding, and prediction of permeator performances as well as for the design of advanced components.

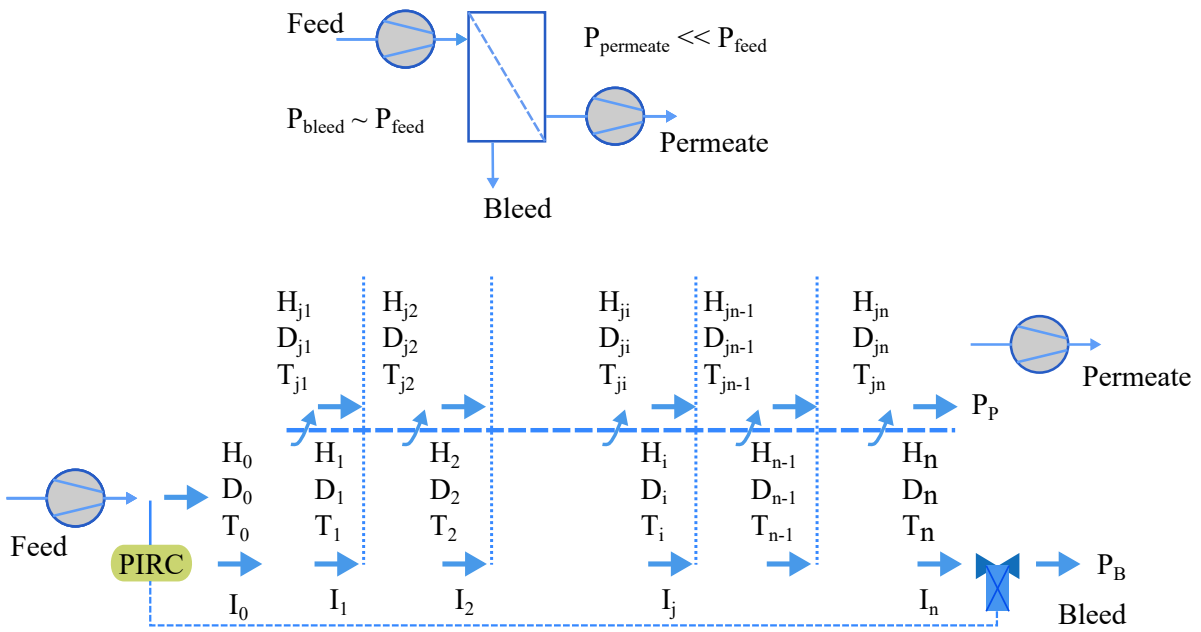


Figure 3.35: Model of a permeator cascade. Selected operation mode showing a permeator and its servicing pumps in the cascade including the corresponding servicing pumps (upper figure) and mathematical model of the flow of hydrogen isotopes (H_i, D_i, and T_i) and impurities (I_i) through each virtual element of the cascade (lower figure) (after [Glu06b]).

Glugla et al. [Glu06b] discussed a permeation concept comprising the separation of hydrogen isotopes from impurities combined with simultaneous fusion fuel (D, T) enrichment. The concept basically consists of a cascade of five permeators. Results of calculations were systematically verified by experiments. For the mathematical treatment permeate and feed flows through a permeation membrane were divided into n equal elements as illustrated in Fig. 3.35. The feed gas was assumed to consist of a mixture of hydrogen isotopes containing several impurities, I_n. Permeation flow rates were computed for each volume element taking into account the corresponding mass balance.

Under these conditions, it is possible to calculate the bleed flow rates and permeate flow rates of the separated species. Model calculations provided evidence that separations with a palladium/silver permeator strongly depend on operational parameters such as feed flow rate, feed gas pressure, permeate gas pressure, and composition of the feed gas. In fact, there is a trade-off between process efficiency and conditions that optimize the separation like high feed pressure, low permeate pressure, and low impurity levels. The plot displayed in Fig. 3.36 demonstrates the complexity of the separation.

Calculated results were obtained under the assumption of a hydrogen carrier gas containing 2 - 20 % of several typical plasma exhaust gas impurities which was passed through a palladium/silver permeator having a membrane of 100 µm thickness, a permeation area of 1 m^2 and held at 673 K. Feed and permeate pressures were assumed constant at 250 and 10 kPa, respectively. At initially small feed flow rates, the bleed gas consists almost exclusively of impurities. With increasing feed flow rate the bleed flow rates increased linearly. As apparent, once the permeation capacity for hydrogen of the permeator is attained at feed flow rates of the order of 80 - 100 mol $hour^{-1}$ a breakthrough takes place. The breakthrough conditions are determined by the prevailing impurity partial pressures. Any further increase of the feed flow rate will progressively augment the degree of contamination of the bleed gas by not-permeated hydrogen isotopes and hence decrease the separation factor. In a dynamic system a complication for process conduction is caused by the shift of breakthrough´s to higher or lower feed flow rates depending on whether the concentrations of impurities in the feed gas increase or decrease. The difference in permeability coefficients of H, D and T was found to have no strong influence on the T/D isotope ratio in bleed and permeate stream at flow rates below breakthrough. Significant tritium enrichment was only apparent at feed flow rates close or beyond to breakthrough. The highest separation efficiency of 1.6 times in the bleed flow was observed at about the breakthrough feed flow. Hence, when operating a cascade of five permeators, the simultaneous optimization of all conditions, i.e. feed flow rates, feed and permeate pressures and feed gas composition, become quite challenging. According to the calculations, optimal fuel recycling conditions, i.e. separation of impurities from fusion reactor fuel, are achieved, when operating conditions and sizing of the permeation membrane are selected that permit impurity removal without breakthrough.

The need of several extra compressors and vacuum pumps requiring control constitutes an additional difficulty. In general, conditions that favour isotope separation in the bleed, like low impurity content, high feed pressure or low permeate pressure, always reduce process efficiency. Consequently, technological separation of hydrogen isotopes from impurities simultaneously with separation of hydrogen isotopes based on permeation is less promising than other currently envisaged processes.

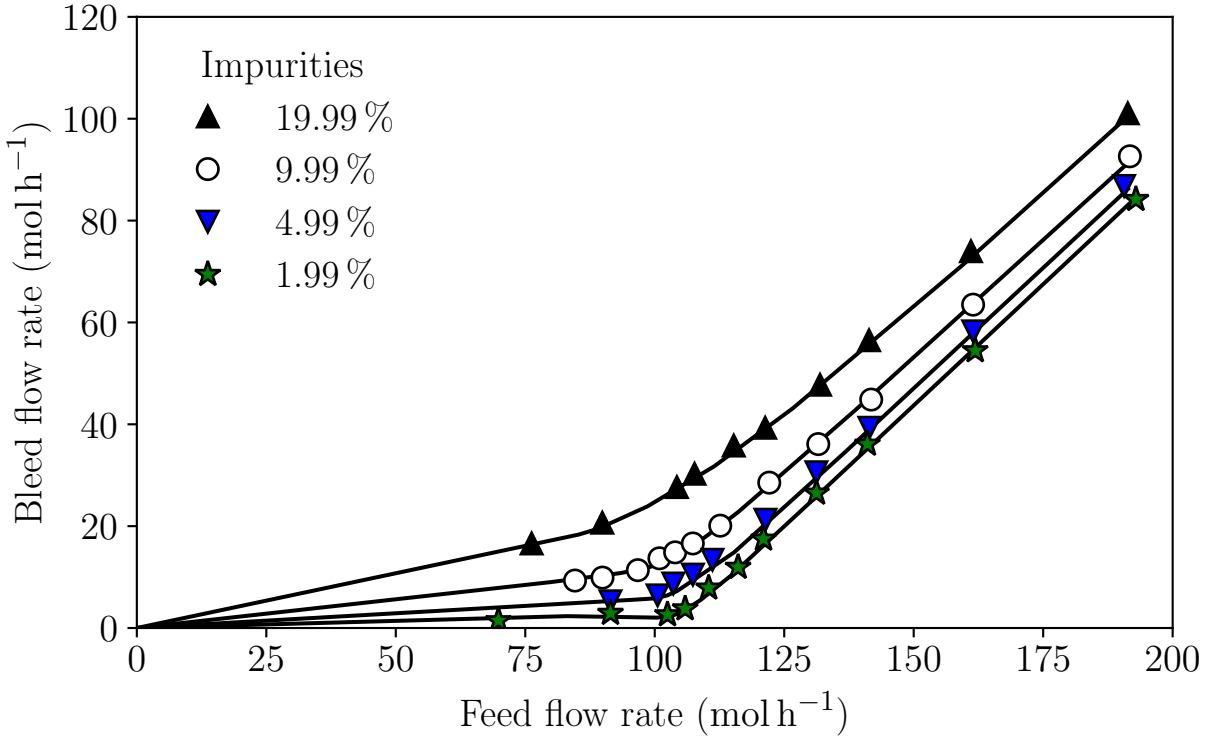


Figure 3.36: Calculated permeation of a D:T = 1:1 mixture containing impurities in the range 2 - 20 % across a 1 m² Pd/Ag membrane maintained at 673 K (after [Glu06a]). Feed and permeate pressures were maintained at 250 kPa and 10 kPa, respectively.

c) Effect of impurities on permeator performance

The effect of impurities conceivable in the fuel cycle of a fusion machine using carbon fibre composite (CFC) in the first wall on the permeation rate of hydrogen isotopes through palladium-silver membranes was examined experimentally by Yoshida et al [Yos83a], Chabot et al. [Cha89; Cha88a], Penzhorn et al. [Pen97a], and Morgan [Mor11]. Of the impurities studied, i.e. CH_4, CO_2, and CO, the latter gave rise to the strongest poisoning (see Fig. 3.37) [Cha89; Cha88a]. Poisoning started to occur at 573 K and rapidly increased further as the temperature was reduced. At temperatures in the range 573 - 650 K no poisoning was observed even after the concentration of CO was increased. This was in excellent agreement with results published earlier by Yoshida et al. [Yos83a]. When the temperature was increased up to 650 K or above a small fraction of carbon monoxide reacts with hydrogen to form methane, water, and carbon dioxide (see also section 2.11.2). The reaction is catalysed by the palladium/silver membrane.

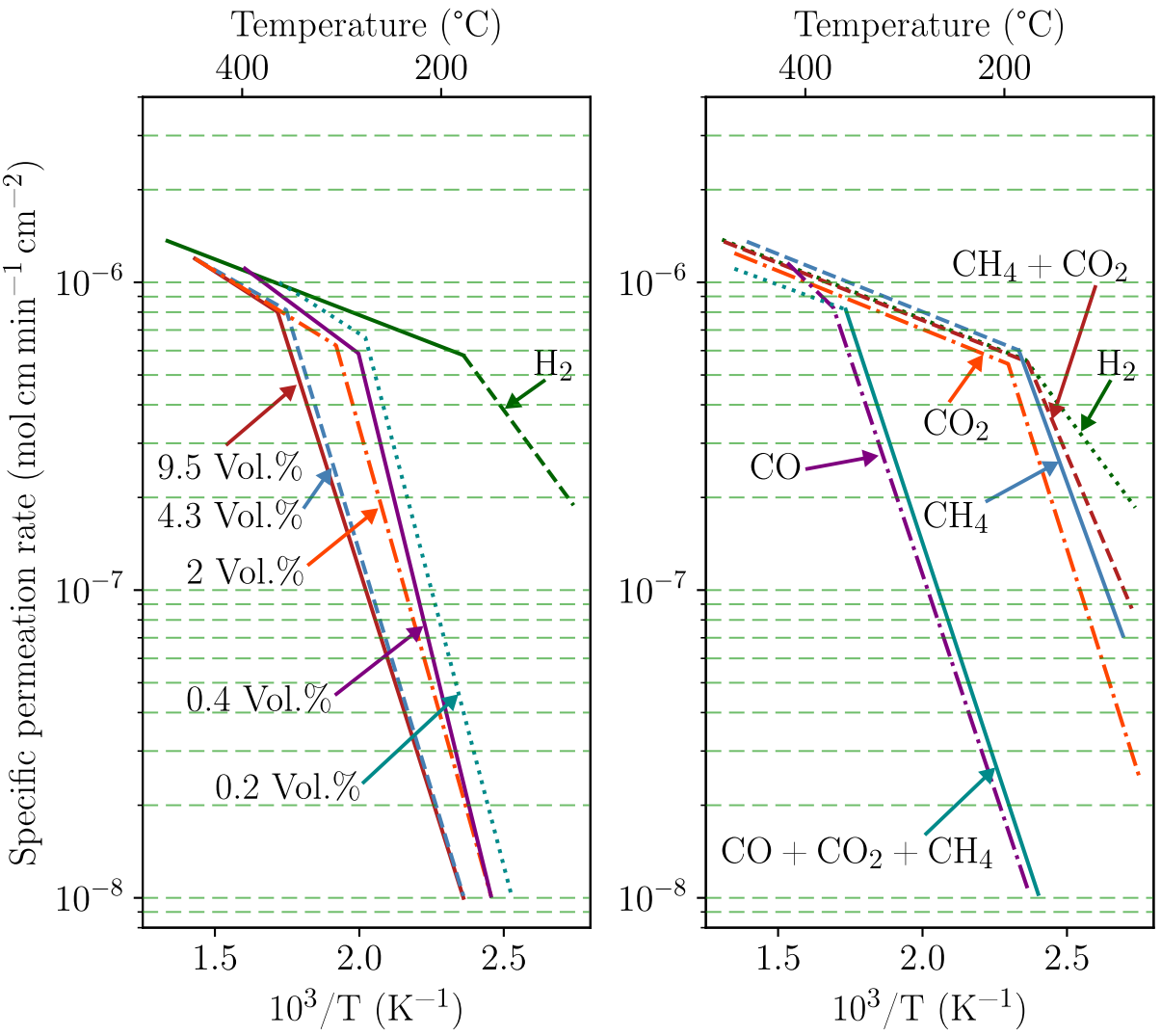


Figure 3.37: Semi logarithmic plot of the effect of increasing partial pressures of CO in hydrogen on the specific permeation rate of hydrogen through a Pd - Ag (23 % by weight) membrane as function of inverse temperature (left figure). Specific permeation rate of pure hydrogen and of hydrogen in the presence of CO_2, CH_4, $CH_4 + CO_2$, CO, and $CO + CH_4 + CO_2$ through a palladium/silver membrane plotted semi logarithmically as function of inverse temperature (after [Cha88a]) (right figure).

Experimental evidence indicates that poisoning is considerably accelerated when hydrogen in hydrocarbons is substituted by tritium. Poisoning of the membrane can be fully reversed by a heat treatment in the presence of air or heating under vacuum at $> 523\,\mathrm{K}$ [Pen97a]. Oil vapours also reduce the permeation rate of hydrogen. This effect can be eliminated by baking under air followed by reduction in the presence of hydrogen [Yos83a].

The work conducted by Morgan [Mor11] on the impact of impurities on the performance of Pd/Ag diffusors essentially confirmed observations reported by previous investigators.

d) Permeator failures

Konishi et al. [Kon91] performed permeation experiments with tritium and tritium-carbon monoxide mixtures for extended periods of time at low temperatures, e.g. 423 - 573 K. Low temperatures (minimization of helium-3 desorption) were selected to uncover possible effects of helium-3 accumulation in the palladium silver. The permeability rate of tritium was found to be approximately half that of hydrogen. While after one year of running with tritium no significant loss of overall performance was noticed a degradation of 10 % of the permeation became apparent already after 6 months of operation with a T_2-CO mixture. The observed degradation could be fully reverted by an oxidation/reduction treatment. The loss of permeability was attributed to contamination of the surface of the Pd/Ag membrane.

Palladium and palladium-silver alloy **tube failures** have mostly been attributed to steam attack by hydrogen isotopes reacting with excess oxygen in the palladium alloy or with oxygen present in the process gas as impurity [Cla95b]. As a consequence of the reaction, molecular water is formed in the grain boundaries of the alloy.

In order to improve heating of the permeator, the tolerance between the heater cartridge and its well was reduced to a minimum. The minimum tolerance depended from the occurrence of warping at the well and/or heater cartridge. When this phenomenon manifested, repairs or replacement become difficult or impossible. After optimization of the tolerance, replacement of cartridges remained possible and heating became more effective.

It was mentioned above, that thermocouples and heaters constitute in a permeator a recurring and frequent source of malfunction. Because their replacement from a contaminated permeator is rather arduous and probably accompanied by considerablereleases of tritium, permeator designs normally contemplate either easily replaceable thermocouples and heaters or the installation of spares.

One more source of failures is the brazing between palladium and stainless-steel.

On the other hand, failures of palladium-silver coils due to hydride formation during inadverted cooling of the permeator have not been reported.

Jimenez et al. [Jim16] informed in a comprehensive study that no alteration of the mechanical properties (tensile strength, ductility, micro hardness) and no **hydrogen embrittlement** takes place when palladium-silver (25 weight%) alloy is subjected to hydrogen absorption/desorption cycling. In contrast, the mechanical properties of pure well-annealed palladium were significantly altered and extensive embrittlement (loss of elongation) was observed when this metal was exposed to hydrogen irrespective of the experimental conditions employed in the tests.

In the past, palladium permeators were cooled with water, which eventually conducted to localized stress corrosion and cracking. Additionally, polymer O-ring seals frequently failed because of embrittlement prompted by high temperatures. Embrittlement-resistant palladium silver (25 % silver) coiled tubes installed in more advanced models lasted in tritium service between 4 months and 5.5 years. Because in the early days many observed failures were caused by mercury spread from mercury pumps, this type of pump was banned completely from tritium systems.

Caldwell-Nichols et al. [Cal08] embarked on a thorough **post mortem** examination of the principal permeator integrated into the CAPER facility of TLK. This permeator had been the key component in an experimental program involving numerous diverse research activities performed over a long period of time partly employing chemically aggressive gas mixtures of compositions largely representative of the plasma exhaust fuel clean-up of ITER, e.g. 1 : 1 = deuterium : tritium mixtures containing impurities such as carbon monoxide, carbon dioxide, methane, and water. The retrieval of the permeator after eight years of discontinuous operation was motivated by a failure to open circuit of the coaxial heaters, which was verified by capacitance measurements. In spite of extensive evacuation and swamping of the permeator prior to disassembly a strong release of tritium, i.e. 235 GBq, was registered after the main flange of the permeator was opened inside of the **repair glove box** available at TLK. At the time, the atmosphere of this glove box was air. Because tritium released from the permeator into the glove box could only be removed efficiently with a copper catalyst at temperatures exceeding 523 K, it was presumed that a significant fraction of the liberated tritium consisted not only of HT and HTO but also of low molecular weight tritiated hydrocarbons, which are known to be comparatively resistant towards oxidation. Visual inspection of the opened permeator revealed that the heaters had lifted in some places about 0.5 mm from the grooves in the permeator body. There was furthermore evidence for large distortions of the inlet zone of the heaters. These distortions were most probably the

cause for the observed failures. Another observation concerned the sheaths of the heaters: they had become notoriously brittle.

Amongst the measures taken to prepare the permeator for final waste disposal, numerous samples were cut from representative zones of the permeator and their tritium content determined employing a full combustion technique [Van79]. While permeator wall, inlet zone wall, palladium/silver tubes, pre-heater tube section, sections of heater cables, stainless-steel foils from heaters, or mineral wool insulation displayed activities within the span 2×10^7 - 3×10^9 Bq g^{-1}, the activities found in loose black powder and at the inlet zone of the inserted nickel capillary tubes were orders of magnitude higher fluctuating within the range 4×10^{10} - 3×10^{11} Bq g^{-1}. The total residual activity in the dismantled permeator was estimated from the concentration of tritium in the various specimens and their respective masses in the component to total about 3000 GBq. The black powder presumably consisted of carbon generated from cracking of hydrocarbons. It seemingly contained some nickel impurity carried away from the catalyst. Black powder also coated the capillary tubes inserted into the palladium/silver tubes of the CAPER permeator. It was likewise observed, but to a lesser extent, on other permeator surfaces. A rough estimation indicates that approximately half of the total activity remaining in the permeator was trapped in the loosely adhered black powder.

Interactions within a stack between carbon black particles are frequently facilitated by formation of hydrogen bonds between adjacent OH groups. Because the outer surface of carbon black displays significant concentrations of OH groups, they will control the aggregation of primary spherical particles into larger aggregates which eventually constitute the actual structure of carbon black [Ert08]. In case of the black powder carbon found in the permeator of CAPER abundant OH groups (to high degree present as OT groups) in bulk and surface may explain the observed high level of contamination[31].

3.14.4 Catalysts and catalyst beds

Primary vessels containing heated catalysts must be provided with a secondary containment consisting of a protective evacuated shell. In case the primary system is operated at elevated temperatures a multilayer superinsulation in the interspace is additionally necessary. This

[31] Persistent contamination of the black powder by tritium takes place to a large extent by isotopic exchange reactions with tritium in the gas phase.

measure contributes to maintain the external temperature of the jacket low, reduces the power required to heat the catalyst, and lessens permeation of tritium into the glove box. Of much importance is the necessity to furnish catalyst vessels with suitable inlet and outlet filters. They prevent spreading of fine tritium-contaminated catalyst powder into adjacent sections of the equipment. Heaters and thermocouples should either be redundant or replaceable with moderate effort.

Catalysts are by and large employed in form of spheres or pellets. If employed at low temperatures, they may possess substantial adsorption capacity for water. If the water is tritiated, the catalyst is contaminated by mobile tritium, an aspect that needs to be considered when giving catalysts to waste. A contaminated catalyst may readily undergo isotopic exchange with ambient moisture.

Catalysts exposed to tritium should not contain chlorides, fluorides, sulphides, phosphorus, or metals like mercury, lead, cadmium, selenium, arsenic or barium. Organic materials also need to be excluded. It is good practice to examine catalysts for these species **before introducing** them into the catalyst bed.

The exposure of palladium catalysts to unsaturated hydrocarbons or carbon monoxide at temperatures above 373 K should be avoided to prevent formation of a PdC phase which causes complete suppression of β-PdH phase formation [Sta85].

Nishikawa et al. [Nis89a] examined the kinetics and thermodynamics of the interaction of tritiated water and tritiated hydrogen with **noble metal on molecular sieve catalysts**. In their modelling, they contemplated the i) catalytic oxidation of molecular tritiated hydrogen, ii) adsorption of tritiated water, and iii) isotope exchange reactions between gaseous tritium (HT or HTO) and adsorbed or structural water in the catalyst.

Exposure of a platinum catalyst/packing mixture ($\sim$ 1 % noble metal) to the beta radiation emitted by tritium in preliminary dynamic and static experiments lasting for up to six months revealed no long-term change of key catalytic properties [Mur07]. However, more results when in contact with high specific activities are needed.

Catalysts constitute safety devices that can effectively contribute to reduce the explosion risk in the event of a major accident in nuclear plants. In fact, they can effectively prevent the accumulation of molecular hydrogen generated during a spill, the radiolysis of water, or reactions of metals with water vapour at high temperature. As a consequence, the occurrence

of detonations with damage of equipment or even entire containments when they happen to enclose an air atmosphere can be averted [Mor04]. Within this frame, Iwai et al. [Iwa12] compared the performance of commercial **granular hydrophylic** and **hydrophobic noble metal catalysts** for the oxidation of tritium in humid air at 293 K and 423 K. At 423 K both catalysts retained their respective activity even in the presence of gases such as generated from burning low-halogen cables. At 293 K, on the other hand, considerable increase in catalytic activity was observed initially with both catalysts due to the effect of produced hydrogen. With progressing reaction time, the reactivity first decreased and then gradually recovered up to the original values. Therefore, to avoid this loss of catalytic effectiveness by water generated during the oxidation of hydrogen[32], noble metal catalysts bed should be maintained at a temperature of at least 500 K (if the accident could be associated with a loss of electric power, appropriate measures should be taken).

A significantly improved hydrophobic platinum catalyst supported either on **stainless-steel honeycomb** or **silicon carbide ceramic** Honeycomb was recently proposed by JAEA [Iwa15] (see Fig. 3.38, left). The catalytic metal consists of nanometer sized platinum particles firmly adhered to the honeycomb surface. Screening tests revealed that within the temperature range 263 - 500 K the honeycomb catalyst is relatively insensitive to temperature. This constitutes an improvement with respect to granular catalysts which display a marked decrease of hydrogen oxidation reaction rate constant when the temperature is reduced from 500 K to about half that value (see Fig. 3.38, right). Concerning the hydrogen concentration in the feed gas, the honeycomb catalyst exhibited the lowest oxidation rate constant at about 100 ppm. At higher or lower partial pressures of hydrogen the oxidation rate constant went up again.

Recapitulating, honeycomb catalysts are essentially as effective at ambient temperature as conventional granular hydrophobic catalysts at 473 K. Hence, honeycomb catalysts can be installed without the necessity of permanent supply of electric power [Kim18]. This makes honeycomb catalysts intrinsically safer and superior to granular ones. What is more, according to Iwai et al. [Iwa15], the catalyst is resistant to the consequences of fire, i.e. elevated temperature, and to gases generated during burning of low halogen cables. In fact, most of the catalytic activity of commercial hydrophilic Pt/Al_2O_3 catalysts and of commercial hydrophobic Pt catalysts operated at constant 423 K persisted under a simulated cable fire with generation of gases and

[32] Water will accumulate in the catalyst until equilibrium at the prevailing temperature establishes.

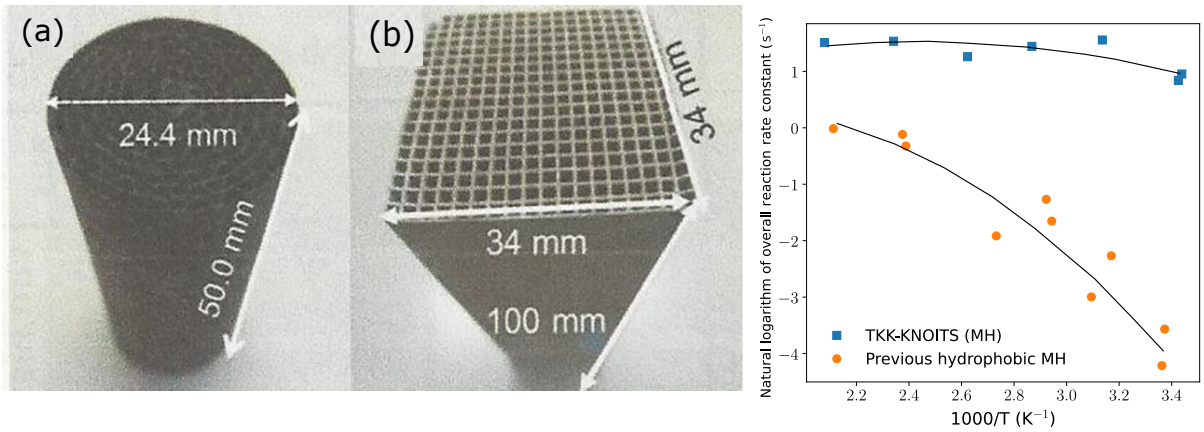


Figure 3.38: Novel platinum TKK-KNOITS catalyst applied either on a stainless-steel honeycomb carrier (a) or a silicon carbide carrier (b) (left figure). Semilog plot of the overall oxidation reaction rate constant as function of inverse temperature as determined for a honeycomb (□) and a granular (○) catalyst (right figure) (after [Iwa15]).

water [Iwa12]. Water produced by oxidation of hydrogen only had a detrimental effect on the reaction rate when the catalyst temperature was maintained at 293 K. Under these conditions water probably competed with hydrogen for the reactive catalytic sites. When the small pressure drop across honeycomb catalysts and their comparatively good thermal transport properties are taken into account they undoubtedly constitute a rather attractive option.

Conversions into water higher than 99.5 % of hydrogen at low concentration in a carrier gas were achievable at ambient temperature with an **alveolate hydrophobic catalyst** containing 1.37 % platinum. Yang et al. [Yan16] developed such a catalyst at Institute of Nuclear Physics and Chemistry, Mianyang, China. The support consists of hydrothermally treated cordierite ($2\,MgO\ 2\,Al_2O_3\ 5\,SiO_2$). The hydrothermal treatment converts the original crystalline cordierite structure into an amorphous support that completely loses its capability for water adsorption. In experiments, in which the catalyst temperature was maintained constant at 293.4 K and the relative humidity of the carrier gas kept at 59.5 %, the reaction rate constant was determined to be $0.182\,s^{-1}$ at a conversion of 48 %. The activation energy of the oxidation reaction of hydrogen was estimated to be $32.5\,kJ\,mol^{-1}$. The attained oxidation rates were found to be much faster than over a honeycomb catalyst. Claimed advantages of the alveolate catalyst were: i) low pressure drop, ii) non-burnable inorganic support, iii) efficient catalyst of small volume (beneficial

from an energetic point of view), and iv) highly effective hydrophobic performance at ambient temperature and relative humidity's covering the range of 0 - 100 %.

A novel **micro channel catalytic reactor** for the conversion of tritiated deuterium (e.g. DT) into water by reaction with gaseous oxygen has been developed and tested at KIT [San12; Dem15a]. Highly tritiated water is generated catalytically in two foils each of which is provided with 45 platinized micro channels partially coated with catalyst. The approximate dimensions of the foils are 100 µm height, 300 µm width, and 11 mm length. They are enclosed by two stainless steel plates joined together by diffusion bonding. Hydrogen and oxygen are fed into the micro channel reactor via 1/8th inch VCR connections and water exits through a 1/4th inch VCR connection. Fast reaction rates of about $8\,\mathrm{mg\,min^{-1}}$ at conversions in the range 97 - 99 % were achieved at 400 ± 10 K. At this temperature the rates are fast while permeation rates remain tolerable. A paramagnetic oxygen monitor for the detection of over stoichiometric oxygen controls the conversion and ensures safety [Men77; Tel13]. A further safety measure consists in back flow protection by non-return valves combined with automatic actuated valves relying on pressure difference measurements. The micro reactor has been tested with hydrogen in a parametric study comprising feed flow rates, composition, and temperature. It has also been demonstrated successfully with tritium utilizing the infrastructure provided by the facility CAPER operated at TLK [Dem15a]. Generated highly tritiated water was collected either in a cold trap or adsorbed on a platinized molecular sieve bed. An operation modality allowing easier process control was to introduce a mixture of helium and hydrogen isotopologues on one side and oxygen on the other into the micro reactor. Under these conditions, highly tritiated water of $1.13 \times 10^{13}\,\mathrm{Bq\,g^{-1}}$ was generated at a rate of up to $0.5\,\mathrm{g\,hour^{-1}}$. In a next step, it was shown that tritium incorporated into platinized molecular sieve can be recovered with a PERMCAT type unit by isotopic swamping with deuterium [Wel11; Par12]. An optimized swamping rate, was achieved at 327 K. The low residual activity remaining in the bed was confirmed by calorimetric measurements. From the experimental results it was concluded, that a recovery of tritium is only reasonable up to a decontamination factor of 100. Salient advantages of the micro channel reactor are i) very small inventory of tritium, ii) no generation of solid waste (in contrast to oxidation of hydrogen with a metal oxide reactor, e.g. CuO) and iii) intrinsic preclusion of explosions or detonations, i.e. reactor of micro meter dimensions.

In an attempt to explain and harmonize widely| scattered catalysis data from different researchers Ribeiro et al. [Rib97] proposed what he termed the **turnover rate (TOR)**. For the quantification of heterogeneous catalytic reactions, the TOR was defined as the number of product molecules formed per active catalysis site and unit of time. In catalysis by metals the active site may be i) a single metal atom, ii) a collective of atoms with a certain geometry, or iii) different sites with a distribution of TOR´s. In case of supported catalysts in which each surface atom constitutes an active site, the number of sites can be obtained from a straightforward chemisorption measurement. In case of large single crystals, the TOR is estimated from the geometrical area. As Fig. 3.39 illustrates, a plot of turnover rate data on the methanation of carbon monoxide with hydrogen as function of inverse temperature obtained by a large number of different investigators using different kinds of **nickel catalysts** under a variety of diverse experimental conditions yields a single straight line. Consequently, the hydrogenation of CO on nickel is largely independent from the catalyst surface structure, loading, percentage of metal exposed, and type of support. Reasonably good results were also achieved with TOR values estimated from a comparison of selected data obtained from 12 different research groups investigating the hydrogenation of CO over a wide variety of different **cobalt catalysts**.

Ribeiro et al. [Rib97] recommended a number of guidelines to investigators for collecting and reporting TOR data. They encompass: i) reaction conditions avoiding poisoning, sintering, coking, heat transfer limitations, pore diffusional restrictions, film mass transfer limitations, etc. ii) catalyst properties like preparation, pre-treatment, utilization of single crystal rather than supported metals, and iii) employment – whenever possible – of p*roven and standard methods* for catalyst characterization.

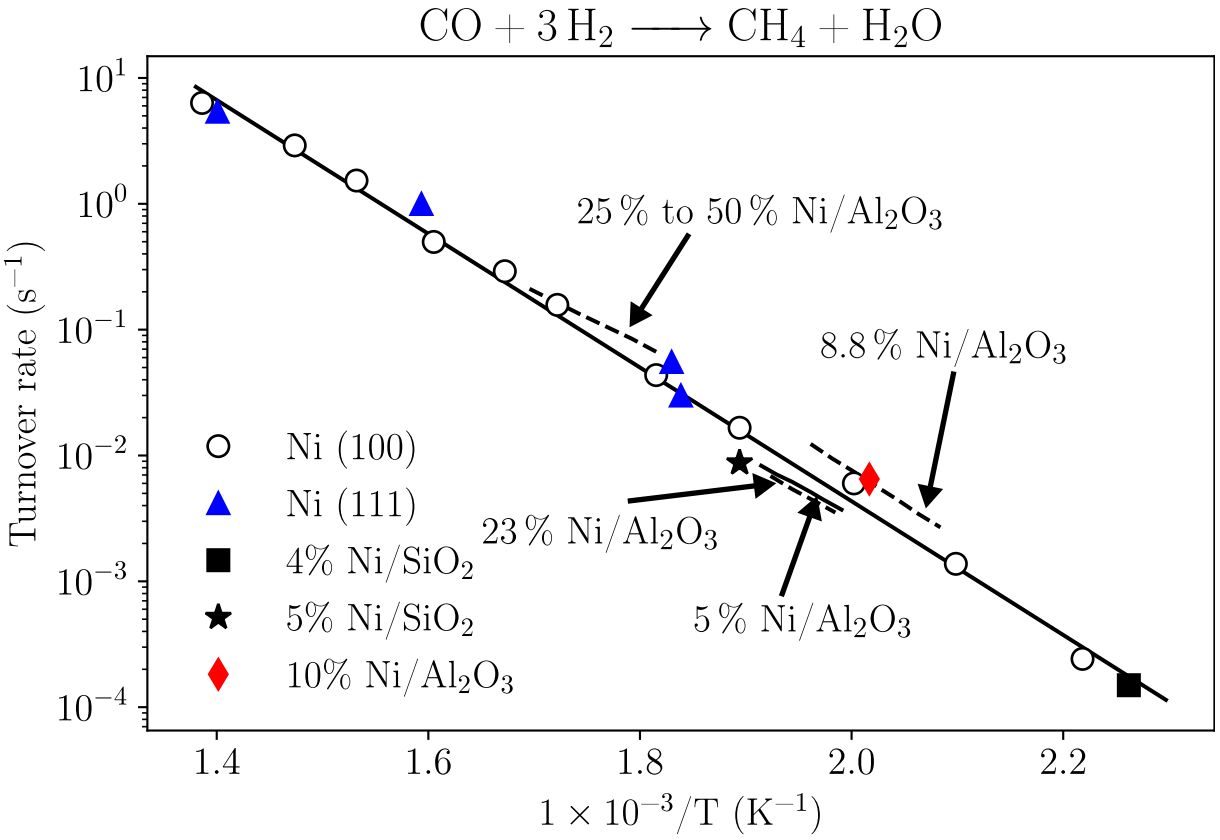


Figure 3.39: Turnover rate for the methanation of CO over diverse nickel catalysts as function of inverse temperature. The plot shows data reported by eight different research teams each employing a catalyst of singular composition, i.e.: Ni(100), Ni(111), 4 % Ni/SiO_2, 5 % Ni/SiO_2, 5 % Ni/Al_2O_3, 8.8 % Ni/Al_2O_3, 10 % $NiAl_2O_3$, 23 % Ni/Al_2O_3 or 25 - 50 % Ni/Al_2O_3 (after [Rib97]).

3.14.5 Molecular sieve beds

Beds containing molecular sieve adsorber used for the adsorption of highly radioactive species shall be jacketed if requiring thermal regeneration. Process equipment containing molecular sieves should feature suitable filters to avoid spreading of fine, tritium-contaminated material into adjacent primary system equipment.

Heated/cooled adsorber beds should not be furnished with valves because of the danger of pressurization.

Molecular sieves may be utilized as spheres or pellets. They should not contain chlorides, fluorides, sulphides, phosphorus, or metals like mercury, lead, cadmium, selenium, arsenic or barium. Organics also need to be excluded. Molecular sieves should be examined for these species before they are introduced into an adsorption bed.

The regeneration of molecular sieves previously used for the adsorptive removal of water from a gas stream is habitually carried out by a thermal procedure employing a hot carrier gas flowing in opposie direction to that in which the bed was loaded. To reduce regeneration time and hence operation cost the technical applicability for this purpose of **microwave energy** was examined systematically at Ontario Hydro by Singh [Sin84]. Adsorbers tested were zeolites type 4A and type 13X; the employed microwave radiation frequency was 2450 MHz. It was experimentally verified that microwave heating did not alter the adsorption properties of the investigated molecular sieves. Encountered problems were i) significant absorption of microwave energy by the molecular sieves leading to a continuous matrix heating, and ii) non-homogeneous distribution of temperature in the bed displaying dependency from the carrier gas flow rate. In consequence, the drying efficiency decreased and the distribution of water remaining in the conditioned zeolite became non-uniform.

Hot molecular sieves 3A, 4A, 5A 13X, or other adsorbers like silica gel when exposed to radioactive low molecular weight hydrocarbons like tritiated methane, for instance during their reactivation, may appreciably enhance the rate of formation of hydrogen, of other low molecular weight hydrocarbons (ethane, ethylene, etc.), and of carbonaceous material via radiation-induced processes [Shi83]. Carbonaceous material may deposit on adsorber surfaces and reduce their adsorptive and catalytic activity. The highest effectivity for the formation of hydrogen and

hydrocarbons of all adsorbers was exhibited by silica gel. On the other hand, this adsorber displayed the lowest rate of formation of carbonaceous material.

3.14.6 Electrolyzer

Numerous streams of tritium-contaminated water arising during the operation of fusion devices or in large tritium handling facilities must be subjected regularly to treatment in a Water Detritiation System (WDS) for decontamination from tritium and eventually tritium recycling. A WDS typically comprises a Combined Electrolysis Catalytic Exchange (CECE) process and a cryogenic distillation system. Crucial component of the CECE process is a tritium-compatible electrolyzer. The tritium inventory of electrolyzers is determined by the water hold-up, and the enrichment factor, i. e. the tritium/hydrogen ratio of the water. Because of the high tritium inventory in the electrolyzer, which is three to four times larger than that in Liquid Phase Catalytic Exchange (LPCE) columns, efforts to minimize tritium holdup in this component are of utmost importance.

A major concern with commercial electrolyzers is their insufficient tritium leak-tightness. This issue is adressed by consequent upgrading of all sealing materials (replacement of organic by metallic seals) and limiting of the total operational tritium inventory in the component. Another aspect requiring precaution measures is consequent prevention of the formation of explosive gaseous mixtures.

Electrolysis units working with a **solid polymer electrolyte** constitute at present the preferred option for ITER [Iwa02c; Cri05a; Oga05; Sug05; Cri07b; Per08]. These electrolyzers i) do not generate complex secondary waste, e.g. tritiated water containing diverse electrolytes, ii) do not contaminate catalytic exchange columns with potassium ions, and iii) have a comparatively small inventory of tritium. Two electrolysis units utilizing solid polymer electrolyte were selected for the facility TRENTA installed at TLK [Cri05a; Cri07b]. The employed electrolyzers have each a hydrogen generation rate of $1\,m^3\,hour^{-1}$. Within the frame of the upgrading activities for tritium service, the leak rate of the electrolyzer (contains tritiated water) was reduced to less than $10^{-5}\,mbar\,l\,s^{-1}$. Both electrolyzers exhibit a water holdup of about 5 l and are installed in a ventilated caisson. Tritiated hydrogen is removed from the oxygen stream generated in the electrolyzer via catalytic conversion into water which may itself be recovered by a stripping step

installed downstream. In this case, tritium is stripped from tritium/deuterium-bearing water vapour transported by gaseous oxygen into demineralized water flowing in counter current. Water collected at the bottom of the stripping column is returned to the electrolyzer for subsequent processing. Endurance tests with up to $3.7 \times 10^{12}\,\mathrm{Bq\,kg^{-1}}$ over a period of 12 months were carried out successfully [Cri07b]. After completion of these preliminary experiments, the solid polymer membrane of the electrolyzer gave no indication of deterioration. Further more stringent tests with water having an order of magnitude higher specific activity of tritium have now been completed.

To recover tritium from deuterium fuel employed for the operation of the **Large Helical Device** of the National Institute of Fusion Science (NIFS) in Nagoya, a CECE process operating at reduced pressure has been taken into operation [Sug05]. The electrolyzer, which also utilizes **solid polymer electrolyte**, constitutes the principal component of the new process. It generates gaseous hydrogen of 99.99 % purity at a rate of $1\,\mathrm{N\,m^3\,hour^{-1}}$. It was manufactured in Japan by Showa Engineering Co, Tokyo.

Another waste water detritiation facility based on the CECE concept and capable of processing $10\,\mathrm{t\,year^{-1}}$ of tritiated water, has been designed for JET [Per08; Lef15]. The average concentration of tritium in 95 t of water collected at JET during eight years of operation covers the range 1 - $100\,\mathrm{GBq\,kg^{-1}\,year^{-1}}$. Critical component of this facility is an electrolyzer featuring a proton exchange polymeric membrane as solid electrolyte. The solid electrolyte contributes considerably to a reduction of the inventory of tritiated water. A drawback of membranes is their possible degradation by radiation. Provided the specific activity of water is maintained at values below $20\,000\,\mathrm{GBq\,kg^{-1}}$ a life expectancy of the membrane of about 1 year appears plausible. The electrolyzer, which converts tritiated water into tritiated hydrogen, has a nominal holdup of 20 kg tritiated water, a maximum allowable tritium inventory of 37 TBq, and a hydrogen production rate of about $10\,\mathrm{Nm^3/hour}$.

A distinctive electrolyzer concept developed in VALDUC, France, may find application for the recovery of tritium from highly tritiated water. It consists of an electrolysis cell comprising a **hollow palladium/silver cathode** coated with porous palladium black. This component was tested with tritiated water with up to $1.2 \times 10^{13}\,\mathrm{Bq\,cm^{-3}}$. The cell employs sodium hydroxide as electrolyte and achieves a throughput of up to $20\,\mathrm{cm^3\,d^{-1}}$. The operation temperature is 353 K and the typical hydrogen flow rate $15\,\mathrm{cm^3\,min^{-1}}$ [Gir91].

A similar prototype electrolyzer was tested at VALDUC, France. The test system encompassed a tritiated water loop, a system for the elimination of anode gases, and a circuit for the recovery of tritium diffused across the cathode. The cathode features a 100 µm thin **palladium-silver thimble** supported from the inside by a porous ceramic or a fritted nickel tube. The cathode generates a highly pure hydrogen isotope stream via electrolytic decomposition of water. Hydrogen isotopes are extracted from the electrolyzer by a combination of diffusion and pumping. To minimize isotope effects the cell is operated at a temperature of 353 K and a current of 700 A m^{-2}. The raised electrolyzer temperature contributes to accelerate diffusion. The electrolyzer has been demonstrated at Valduc employing tritiated water of more than 30 TBq cm^{-3} (more than 50 % T_2O) during a total operational period surpassing 1500 hours. The production of 6 g gaseous tritium was carried out without occurrences. Main advantages of the concept are i) a highly pure hydrogen isotope product stream, i.e. not contaminated by O_2, Q_2O, etc. (Q = H, D, T), ii) high radiation tolerance of the electrolysis cell, and iii) no requirement of peripheral pressure control devices. The only shortcoming is a waste water containing sodium hydroxide [Bel99b].

A ceramic **electrolysis cell** utilizing a **stabilized zirconia tube** with platinum electrodes was developed several years ago at JAERI. The cell was demonstrated with pure tritium gas (1.4×10^{12} Bq) at TSTA, Los Alamos National Laboratory, USA [Kon83; Kon85; Kon87; Kon86]. This electrolysis cell, which was operated at 903 K, decomposes tritiated water vapour (3 % T_2O in helium) into the elements. The conversion efficiency of T_2O into T_2 was found to be 99.9 %. The cell was operated continuously in closed loop mode decomposing T_2O at a rate of 7.4×10^{14} Bq d^{-1}. Main features of the cell are i) low tritium inventory, ii) high radiation resistance, and iii) no alkali waste.

3.14.7 Cryogenic traps for the retention of water

In this section cryogenic traps developed for the retention of moisturec from an inert carrier gas are discussed. One obvious advantage of cryogenic trapping is regeneration from retained water by straightforward melting and collection by gravity without or only little heating and essentially no purge gas. The factors determining the efficiency and therefore applicability of several cryogenic traps tested in the past will be examined in some detail below because this type of trap may become a crucial component both of the Coolant Purification System and of

the Tritium Extraction System of the **Helium Cooled Pebble Bed** (HCPB) blanket which is one reference concept in the European Breeding Blanket Program for DEMO design [Boc04].

A cold trap concept highlighting a heat exchange surface consisting of a bundle of 57 vertical tubes of 11 mm internal diameter and a length of about 183 mm was build and tested at **ISPRA** [Hou97]. Moist gas was first sent downwards through a tube bundle and then upwards towards the outlet of the trap through a single large tube placed in the middle of the trap. The tube bundle was submerged in a liquid nitrogen bath positioned in a cylindrical shell itself surrounded by an evacuated vacuum-tight chamber. The chamber provided the necessary thermal insulation. Liquid nitrogen was admitted in regular pulses. Temperature sensors installed in the upper and lower region of the shell served to control the temperature. The trap was not provided with electrical heaters. In the design the carrier gas was confronted immediately at the inlet zone with rather low temperatures, which probably was the cause for enhanced formation of ice in the inlet zone near the cooled tubes. To regenerate the trap, water was first liquefied and then drained by gravity from the bottom of the trap. Of concern were two competing water retention mechanisms: one in which water vapour diffuses to cold surfaces and condenses and another consisting of the condensation of water onto ice aerosol particles. Once ice nucleation commences, vapour depletion appears to occur predominantly by particle nucleation. The consequence was enhanced release of moisture in the exhaust stream [Sch95].

Another cryo-trap concept for the retention of tritiated water from an inert gas stream was designed and tested at **TPL**, JAERI, in Tokai-mura. In order to facilitate work in a glove box the trap was cooled with Freon [Ohi93]. To increase the cooling surface area, the inside of the cold zone was packed with copper spheres of either 5 or 8 mm diameter. Further tests were carried out with deuterium employing three traps of the same kind (one in operation, another in regeneration, and a third one on standby) at TSTA, Los Alamos National Laboratory, New Mexico. During switching from one trap to another, substantial water spikes were noticed. This problem was solved experimentally by installing small molecular sieve beds at the exit of each trap. The adsorber beds were provided with filters on both ends to minimise dissemination of molecular sieve dust.

One more liquid nitrogen cooled cold trap concept with dimensions of 1500 mm overall height and 250 mm diameter was developed and tested at **Fontenay-aux-Roses** [Cha92; Cha93a; Cha93b] (see Fig. 3.40a). The water capacity of the trap was only about 12 g. The trap was

operated at a nominal carrier gas flow rate of 0.5 (STP) m^3/hour. The temperature of the gas outlet zone could be regulated within the range 70 - 100 K. Sixteen cooling fins welded on a cylindrical vessel immersed in a Dewar filled with liquid nitrogen were used to cool the process gas. Micro ice crystals were retained by a sintered stainless-steel filter placed at the exit of the trap. An automatic liquid nitrogen refilling device permitted regulation of the temperature. Process gas was introduced from the top of the trap. As it entered the trap it was sequentially cooled by heat exchange with vaporised cool nitrogen above the liquid nitrogen and then by liquid nitrogen once reaching the zone closer to the bottom. At helium flow rates across the trap in the range 200 - 1000 l $hour^{-1}$ and inlet water concentrations of up to 1000 vppm water vapour concentrations at the trap outlet of 0.5 vppm were shown to be achievable. The water retention effectiveness of the trap manifested by a progressively increasing pressure drop across the trap. The pressure plunge was attributed to clogging of the stainless-steel filter. Analysis of the experimental results suggested occurrence of progressive ice deposition primarily at very low water vapour concentrations, i.e. 30 - 40 vppm, and at flow rates exceeding 100 l $hour^{-1}$. Encountered plugging problems made modifications of the trap imperative. The release rate of condensed water could be enhanced by heating the trap body up to 523 K.

A medium sized cryogenic trap claimed to represent approximately 1/6th the size required for ITER was tested at **TLK** [Hac84; Bek01; Bek02a] (see Fig. 3.40b). Salient features of this trap are i) two separate pre-coolers, ii) electric heating coils arranged in parallel windings around the cooling tube in five separate sections of the freezing zone which permit segmental adjustment of the temperature profile, iii) operation at temperatures below 173 K to generate an exhaust gas containing less than 0.2 vppm moisture, and iv) variable helium gas throughput of up to 3 (STP)m^3/hour while maintaining relatively small linear gas velocities in the freezing zone (typically 10 cm s^{-1})[33]. A total of 22 copper cooling plates chilled with liquid nitrogen flowing through a central coil in counter current to the gas flow direction serves to condense several ten grams of water carried by the process gas. Water condenses on the plates as ice. Thirteen Pt-100 resistance thermometers are available to determine the temperature profile across the cryo-trap. Carrier gas is delivered from several 50 l pressurized cylinders containing helium with a calibrated moisture content. Three hygrometers were used to determine the humidity. The

[33] This contributes to avoid fast cooling and hence critical super-saturation, which is responsible for the formation of aerosols.

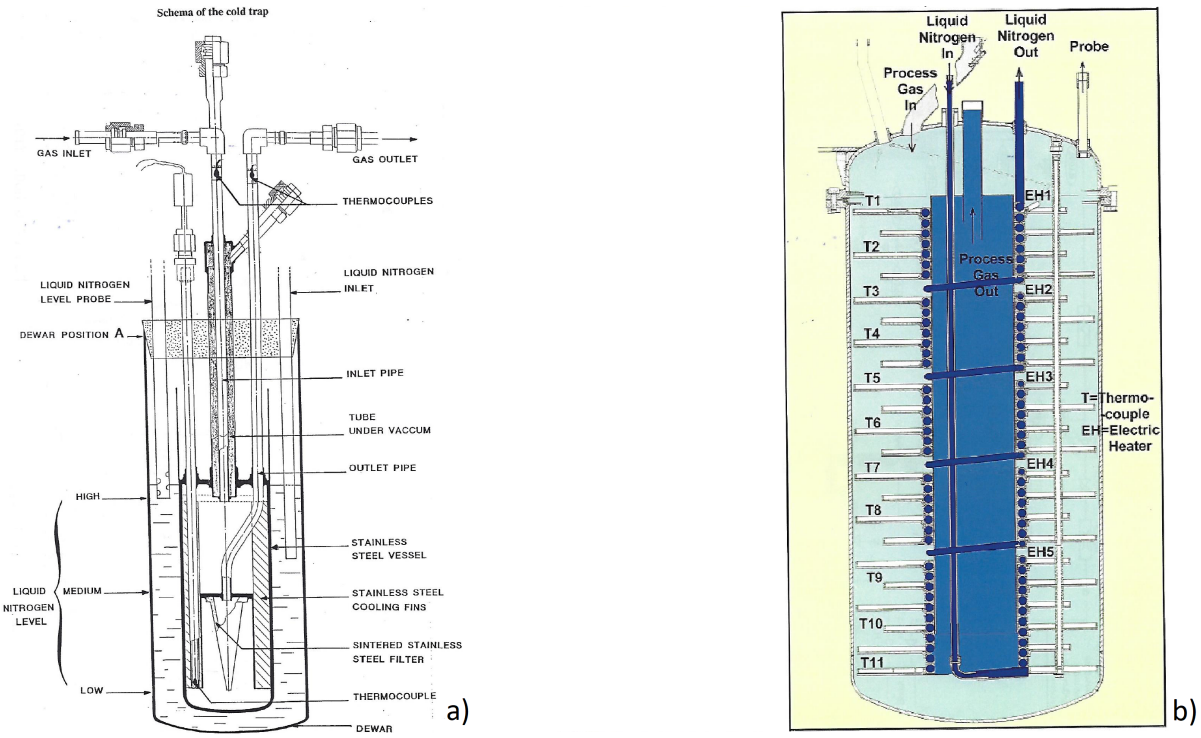


Figure 3.40: Cryogenic trap concepts for the retention of water from a helium stream tested at Fontenay-aux-Roses [Cha92] (figure a) and at TLK [Bek02a] (vacuum container not shown) (figure b).

complete trap was vacuum insulated. When the cold trap was cooled employing a constant liquid nitrogen flow of 24 lN_2 /min for about 40 hours a constant temperature as low as 191 K (water vapour concentration 0.4 ppm) could be attained. Increasing the liquid nitrogen flow rate up to 35 lN_2 /min improved the water retention efficiency of the trap considerably. Under these conditions, stable low temperatures were reached after approx. sixty hours of uninterrupted operation. The dew point reached at the trap outlet was lower than 187 K which translates into a water concentration in the exhaust stream of 0.2 ppm. At an outlet temperature of 296 K and a pressure of 2 bar the liquid nitrogen consumption was estimated to be within the range 2 - 3 lN_2 /min). This rather high liquid coolant consumption was attributed to insufficient thermal insulation of the cold trap. The average retention rate of water was determined to be 0.2 g hour^{-1}.

General conclusions from the gained experience are:

- After thermal equilibration is established in a cryogenic trap operated at helium flow rates of more than 1 m^3 (STP) /hour the water vapour concentration in the trap exhaust gas can

be reduced from initially 300 - 650 vppm to values of less than 0.02 vppm (removal factor of 15 000 - 32 500).

- Cryogenic traps displaying initial ice deposition are fully efficient (water near detection limit at trap outlet). Hence, pre-deposition of ice enhances water retention and notably reduces water concentrations at the outlet.
- Super-saturation of the carrier gas leads to formation of fine aerosols not removable by filters. Super saturation takes place when i) two saturated streams of different temperatures are mixed, ii) gases or vapours are rapidly expanded, or iii) chemical reactions generating solid products take place.
- More design details on the manufacture of technical-sized cryogenic traps are needed in the open literature.

Key remaining practical problems pertaining scalability of the traps are i) maximization of the water retention without necessity of regeneration (enhanced operation efficiency, reduced downtime, and minimisation of costs) and ii) improvement of the water retention efficiency at high process gas flow rates. Upgrade is possible by either increasing the total number of traps in operation or further design optimization of present-day traps.

3.14.8 Retention of hydrogen isotopes by cryo-adsorption trapping

There is already an ample body of information concerning the fundamental parameters required to understand the retention of hydrogen isotopes from a helium carrier gas passing through cryo-adsorption traps. The same does not hold for the design of efficient cryo-adsorption traps of the size needed for the retention and recovery of tritium bred in solid breeder blankets. According to current concepts, fusion machines are supplied with fuel by extracting with helium purge gas in closed loop operation the tritium bred in the blanket and trapping it selectively with an integrated cryogenic trap (or traps).

3.14.8.1 Basic aspects

The preferred purge gas for the extraction of bred tritium from lithium ceramics and beryllium pebbles in a fusion reactor blanket is helium. Cryogenic adsorption has been proposed for the

retention of tritium from the blanket purge gas. In most concepts hydrogen is added to the carrier gas in low concentration to enhance the release of molecular tritium. Many experimental studies on the factors that govern the cryogenic adsorption of each of the six hydrogen isotopologues or of representative mixtures utilizing molecular sieves or other adsorbers like active charcoal have been carried out. Parametric investigations of the factors determing the separation of hydrogen isotopologues are likewise of significant practical relevance.

Basmadjan [Bas60a; Bas60b] was probably the first to determine adsorption isotherms of hydrogen and deuterium on zeolites type 4A, 5A, and 13X at temperatures of 75, 80, 85 or 95 K and pressures up to 1 bar. More adsorption isotherms of hydrogen and helium on molecular sieve 5A at pressures higher than 1 bar and at 76 K were reported by Kidnay and Hiza [Kid67]. The results revealed that deuterium is adsorbed on zeolites type 4A, 5A, and 13X more efficiently than hydrogen. Stern and Di Paolo [Ste67] investigated the adsorption of N_2, He, and other gases on molecular sieves type 5A, 10X, and 13X at 77 K. While the isotherms for helium at 77 K on all three molecular sieves obeyed Henry´s law, the isotherms of nitrogen were better represented by the Dubinin-Radushkevich relationship.

A few representative results on the isobaric cryo-adsorption of hydrogen and deuterium on molecular sieves 3A, 5A, mordenite, and active charcoal at temperatures in the range 73 - 173 K are listed in Table 3.9. The data reveal that i) the highest adsorption capacity is displayed by charcoal, ii) deuterium is more strongly adsorbed than hydrogen on all tested adsorbers (see also [Kid67]), and iii) the least effective cryo-adsorber for both hydrogen isotopes is zeolite 3A (see also [Bre74]). Measurements performed by Xiao and Heung [Xia11] at liquid nitrogen temperature, agree by and large with these results. They confirm that i) zeolite 3A does practically not adsorb hydrogen at liquid nitrogen temperature, and ii) the amount of adsorbed deuterium is consistently higher than that of hydrogen for all examined adsorbers. Differences in the relative adsorption by various materials reported by Noppel (see footnote 20) and [Xia11] can be attributed to i) residual amounts of water remaining in the zeolites, ii) different temperature ranges employed by the two research groups, iii) utilization of the same type of adsorbent but from different provenience, and iv) use of materials from different manufacture charges.

A number of fundamental parameters for the operation and understanding of the cryogenic adsorption of hydrogen were determined by Xiao and Heung [Xia11] from a comparison between

[33] Noppel, H.E., IRCh, Kfk, 1996. unpublished results.

Table 3.9: Cryo-sorption of hydrogen and deuterium on different adsorbers at 1000 mbar equilibrium pressure (in cm^3 (STP) /g)[33] .

Temperature (K)	Zeolite 5A		Zeolite 3A		Mordenite	Activated charcoal	
	H_2	D_2	H_2	D_2	D_2	H_2	D_2
173	12	17	3.5	4.3	7.2	17.2	18.5
148	34	45	5.9	7.2	20	46	45
123	80	100	7.5	10.5	50	100	100
98	125	155	7.8	12.0	100	172	190
73	180	200	8.0	13.0	125	298	305

several different adsorbers like zeolites, activated carbon, silica gel, and alumina. The experiments were performed with hydrogen and deuterium at liquid nitrogen temperature. When examined under comparable conditions, zeolite 13X displayed the highest hydrogen uptake of all investigated adsorbers. Remarkably, different lots from a single vendor or materials from different vendors showed clearly noticeable differences. Some sorbents behaved differently at low and high pressure of hydrogen. The fastest adsorption rate was observed with molecular sieve type 4A followed by activated carbon, molecular sieve 5A, and molecular sieve 13X. According to ref. [Xia11], the effect of residual moisture initially present in adsorbers is particularly notorious: already 0.5 weight% moisture remaining in the adsorber following insufficient conditioning by heating under vacuum or because of adsorption of atmospheric moisture subsequent to completion of the conditioning treatment can reduce the cryo-adsorption capacity for hydrogen by up to 50 %. Poorly dried adsorbers eventually lost completely their adsorption capacity for hydrogen.

From the above it follows that at cryogenic temperatures the kinetic diameter of hydrogen isotopes is similar to that of the pore opening of zeolite 3A. For this reason, zeolite 3A can be used for the separation of hydrogen isotopes from water and other adsorbable gases. Concerning the separation of hydrogen and deuterium, the highest separation factor is achieved with zeolites 5A and 3A and the lowest with active charcoal. The increasing separation achievable with zeolite 3A with decreasing temperatures is attributed to a kinetic effect (see Figs. 3.41 and 3.42 below). An additional set of data on the cryo-adsorption of H_2 by active charcoal is provided in Appendix

P. The adsorption of hydrogen isotopes by active charcoal at 1 bar and ambient temperature is comparatively minimal.

Beloglazov et al. [Bel05a] obtained at TLK cryogenic adsorption data for hydrogen on 20 kg molecular sieve 5A cooled to 77 K using helium as carrier gas at a flow rate of $2\,m^3\,hour^{-1}$. Based on the experimental results, the adsorption capacity for hydrogen could be calculated from breakthrough curves, yielding approx. $5 \times 10^{-4}\,mol\,g^{-1}$ at a hydrogen partial pressure of 120 Pa. The mass-transfer zone of the hydrogen/5A system was found to be narrow, i.e. about 12.5 % of the molecular sieve bed height.

Separation factors are defined by the ratio between the mole fractions of the adsorbed phase, X_i, to that of the gas phase fraction, Y_i, according to

$$\alpha = \frac{\frac{X_{D_2}}{X_{H_2}}}{\frac{Y_{D_2}}{Y_{H_2}}}$$

Separation factors for the hydrogen/deuterium system at 75 K on type 4A, 5A, and 13X molecular sieves were found to be 2.54, 2.00, and 2.16, respectively [Bas60a; Mai92b]. On silica gel at 78 K the H_2/D_2 separation factor value was distinctly higher, i.e. 4.5 [Bas60a]. Additional separation factors for the binary systems D_2/HD, HD/H_2, H_2/HT, HT/T_2, D_2/H_2 on molecular sieves type 4A, 5A, 13X, and on activated carbon over a broad range of pressures were reported after rather comprehensive experiments by Enoeda et al. [Eno94], Nishikawa et al. [Nis95b], and Kotoh and Kudo [Kot02].

At low partial pressures of hydrogen, i.e. 0 - 53 mbar diluted in 1 bar helium, the adsorption data on charcoal, molecular sieve 5A, S115, UOP ZSM5, and Wessalith-DAY could be fitted using a standard Langmuir equation [Wil94b].

Blet et al. [Ble93] investigated the adsorption of binary isotopic hydrogen mixtures, i.e. (H_2 + D_2) and (D_2 + T_2), on zeolite 5A at 77 K and found that within a comparatively narrow pressure range the results could be fitted by the equation

$$\frac{Q}{Q_s} = \frac{k\sqrt{P}}{1+\sqrt{P}}$$

where Q denotes the hydrogen adsorption capacity in cm^3 (STP) /g molecular sieve at a given equilibrium pressure, Q_s is the saturation capacity at the saturation vapour pressure, and k is a constant that depends on temperature as well as on the heat of adsorption of the molecule. The experiments yielded a separation factor for hydrogen and deuterium of 1.39.

Nishikawa et al. [Nis92c; Nis94] compared the adsorption capacity for hydrogen of adsorbers like molecular sieve 3A, 4A, 5A, and 13X, activated carbon, silica gel, and volcanic ash, at a hydrogen partial pressure of 193 Pa and an adsorber temperature of 77 K. Because zeolites 4A, 5A, and activated carbon were found to be much superior to all the other, the adsorption capacities for hydrogen and deuterium of only these adsorbers were further investigated at the same temperature and partial pressures covering the range 10 - 10 000 Pa. Capacities were estimated from breakthrough curves using 1 bar helium carrier gas and flow rates within the span 0.2 - 1.5 l min^{-1}. Under these conditions the pressure drop across the adsorber bed was negligible.

Nishikawa et al. [Nis94] provided evidence that the adsorption capacities for hydrogen and deuterium on the investigated adsorbers are well described by Langmuir-type equations of the kind

$$Q_i = \frac{a_1 P_i}{1 + b_1 P_i} + \frac{a_2 P_i}{1 + b_2 P_i}$$

where Q_i denotes the adsorption capacity (in mole hydrogen per g adsorber) of species i (one of six molecular isotopologues of hydrogen), P_i stands for the partial pressure of species i (in units of Pa), and a_1 and b_1 are Langmuir coefficients for site 1, and a_2 and b_2 Langmuir coefficients for site 2 in units of mol kg^{-1} Pa^{-1} and Pa^{-1}, respectively.

Both Langmuir coefficients are interrelated by the expression

$$a_i = q_0 b_i$$

where q_0 denotes saturation adsorption in mol g^{-1}. This term depends on the type of adsorbent and adsorbate but not on temperature.

The two terms in the expression for Q_i reflect the existence of at least two different adsorption sites on the adsorber, of which each is characterised by a different adsorption energy [Nis98]. At

77 K the adsorption on site 1 contributes mostly to the adsorption in the low-pressure region and that on site 2 predominates in the high-pressure region.

From the experimental adsorption results a rather consistent and complete set of a_1, a_2, b_1, b_2 and Langmuir coefficients was calculated for all six molecular isotopologues of hydrogen on zeolite 4A, zeolite 5A, and 12 - 30 mesh active carbon at 77 K. Experiments with tritium were mostly performed at TSTA, Los Alamos, employing a volumetric technique [Kaw00]. The results are compiled in Table 3.10 [Nis94; Eno95a; Nis95b; Nis95a; Nis95c; Tan96; Nis98; Kaw00]. Whereas on type 4A and 5A the adsorption capacity of deuterium is clearly higher than that of hydrogen, i.e. large isotope effect in the low-pressure region, the adsorption capacity on active carbon is rather similar for both hydrogen isotopes. The results could be well interpreted over a pressure range of five orders of magnitude by the two-site Langmuir model discussed above. In accordance with expectations, the adsorption increased in the order H_2, D_2, and T_2.

The mass transfer capacity coefficient K obtained from breakthrough curves can be calculated from equation

$$K = \frac{\bar{u}}{Z_\mathrm{a}} \int_{C_\mathrm{B}}^{C_\mathrm{E}} \frac{\mathrm{d}C}{C - C^*}$$

where $\bar{u}$ denotes the superficial fluid velocity, Z_a is the length of the adsorption zone, C the concentration in the void space of the bed, C^* the concentration in equilibrium with the amount adsorbed on the bed, C_B the concentration at the time of breakthrough (defined as 0.9 C_i, where C_i is the concentration at the bed inlet), and C_e denotes the concentration at the time when the exhaust reaches the concentration 0.9 C_i.

Mass transfer capacity coefficients provide appreciable information on the rate of gas adsorption. Because the values obtained for hydrogen, typically 10 - 20 s^{-1}, were essentially the same as the ones for water, it was concluded that molecular sieves type 4A and 5A as well as active carbon have the potential to serve as suitable adsorbers for hydrogen isotopologues at liquid nitrogen temperature [Nis94].

Table 3.10: Langmuir constants of hydrogen isotopes (Q_i) on molecular sieves 4A and 5A, and active carbon at 77 K.

Gas	a1 ($\mathrm{mol\,kg^{-1}\,Pa^{-1}}$)	b1 ($\mathrm{Pa^{-1}}$)	a2 ($\mathrm{mol\,kg^{-1}\,Pa^{-1}}$)	b2 ($\mathrm{Pa^{-1}}$)	References
			Zeolite 4A		
H_2	$(3.7 \pm 0.6) \times 10^{-6}$	$(3.1 \pm 1.0) \times 10^{-3}$	$(3.3 \pm 0.6) \times 10^{-7}$	$(1.0 \pm 0.1) \times 10^{-4}$	[Kaw00; Nis92c; Nis98; Nis95b; Tan96]
HD	$(6.7 \pm 0.9) \times 10^{-6}$	$(6.2 \pm 1.0) \times 10^{-3}$	$(4.7 \pm 0.1) \times 10^{-7}$	$(1.4 \pm 0.1) \times 10^{-4}$	[Kaw00; Nis95b; Tan96]
D_2	$(1.4 \pm 0.3) \times 10^{-5}$	$(1.2 \pm 0.4) \times 10^{-2}$	$(6.5 \pm 0.9) \times 10^{-7}$	$(1.7 \pm 0.2) \times 10^{-4}$	[Kaw00; Nis92c; Nis95b; Nis98; Tan96]
HT	9.2×10^{-6}	8.6×10^{-3}	5.1×10^{-7}	1.5×10^{-4}	[Kaw00]
DT	2.1×10^{-5}	2.1×10^{-2}	7.8×10^{-7}	2.2×10^{-4}	[Kaw00]
T_2	3.0×10^{-5}	3.1×10^{-3}	9.2×10^{-7}	2.6×10^{-4}	[Kaw00]
			Zeolite 5A		
H_2	$(4.7 \pm 1.1) \times 10^{-6}$	$(3.3 \pm 1.0) \times 10^{-3}$	$(2.6 \pm 0.8) \times 10^{-7}$	$(1.2 \pm 0.1) \times 10^{-4}$	[Kaw00; Nis92c; Nis95b; Nis98; Nis95a; Tan96]
HD	$(7.4 \pm 1.5) \times 10^{-6}$	$(5.3 \pm 1.1) \times 10^{-3}$	$(3.2 \pm 0.7) \times 10^{-7}$	$(1.3 \pm 0.1) \times 10^{-4}$	[Kaw00; Nis95b; Tan96]
D_2	$(1.3 \pm 0.1) \times 10^{-5}$	$(9.2 \pm 0.5) \times 10^{-3}$	$(3.9 \pm 0.1) \times 10^{-7}$	$(1.2 \pm 0.1) \times 10^{-4}$	[Kaw00; Nis92c; Nis95b; Nis98; Nis95a; Tan96]
HT	$(8.7 \pm 1.2) \times 10^{-6}$	$(6.2 \pm 0.8) \times 10^{-3}$	$(3.4 \pm 0.6) \times 10^{-7}$	$(1.3 \pm 0.1) \times 10^{-4}$	[Eno95a; Kaw00; Tan96]
DT	1.6×10^{-5}	1.1×10^{-2}	4.2×10^{-7}	1.4×10^{-4}	[Kaw00]
T_2	1.9×10^{-5}	1.3×10^{-2}	4.5×10^{-7}	1.5×10^{-4}	[Kaw00]
			Active carbon		
H_2	$(6.8 \pm 1.8) \times 10^{-6}$	$(4.5 \pm 0.2) \times 10^{-3}$	$(5.3 \pm 0.6) \times 10^{-7}$	$(0.8 \pm 0.4) \times 10^{-5}$	[Kaw00; Nis92c; Nis95b; Nis98; Nis95a; Tan96]
HD	$(7.3 \pm 1.8) \times 10^{-6}$	$(4.7 \pm 0.4) \times 10^{-3}$	$(5.6 \pm 0.6) \times 10^{-7}$	$(7.6 \pm 0.3) \times 10^{-5}$	[Kaw00; Nis95b; Tan96]
D_2	$(7.0 \pm 0.1) \times 10^{-6}$	4.5×10^{-3}	5.5×10^{-7}	5.5×10^{-5}	[Nis95b; Nis92c; Nis98; Nis95a; Tan96]
HT	8.8×10^{-6}	5.1×10^{-3}	6.2×10^{-7}	1.1×10^{-4}	[Kaw00]
DT	9.6×10^{-6}	5.9×10^{-3}	6.8×10^{-7}	1.1×10^{-4}	[Kaw00]
T_2	1.0×10^{-5}	6.4×10^{-3}	7.2×10^{-7}	1.2×10^{-4}	[Kaw00]

Based on the assumption of two independent adsorption sites coexisting on the investigated adsorbers and assuming that each site has a different surface diffusivity, Tanaka et al [Tan96] succeeded in calculating breakthrough curves for the cryogenic adsorption of multi component hydrogen isotopes on molecular sieve type 4A, 5A, and activated carbon at 77 K. Breakthrough curves for binary hydrogen isotope mixtures were calculated by adapting the equations used for the adsorption of single hydrogen isotopes to two isotopes [Nis95a]. The calculated breakthrough curves agreed well with the experimental results obtained with two or even three hydrogen isotopes, also at varying partial pressures of the hydrogen isotopes.

Kotoh et al. [Kot02; Kot05] discussed an adsorption potential model for the adsorption of H_2, HD, HT, D_2, DT, and T_2 on synthetic zeolite 5A and 13X at 77.4 K, in which the difference in isotopic hydrogen adsorption is estimated from the zero-point energy difference of the hydrogen isotopologues. With the proposed model, they were able to fit adsorption data for all six molecular hydrogen isotopes making use of equilibrium pressures covering more than seven orders of magnitude, from 10^{-2} up to 10^5 Pa. In addition, Kotoh et al. determined volumetrically separation factor values for the binary systems D_2/HD, HD/H_2, HT/T_2, and D_2/H_2 on zeolite 4A, 5A, and activated carbon at 77 K as function of a rather wide range of pressures. The obtained values were in essentially good agreement with corresponding results reported previously for the systems D_2/H_2, D_2/HD, and HD/H_2 by Nishikawa et al. [Nis95b] and Enoeda et al. [Eno96] on molecular sieve 5A at the same temperature but based on the breakthrough technique.

Recently, the adsorption of hydrogen, deuterium, and of an equimolar mixture of both isotopes on zeolite 5A using a 1 or 2 m long column at liquid nitrogen temperature (77 K) was investigated experimentally by Zhang et al [Zha04; Zha06]. The authors did not compare their results with data from other investigators.

As well known, replacement of sodium ions in the zeolite 4A cage by exchange with more voluminous potassium ions is associated with a pore size reduction of the α-cages (see Fig. 3.41). This reduction takes place gradually with progressing degree of cation replacement. By increasingly incorporating potassium ions into zeolite 4A the molecular sieving properties become more and more modified up to the point where at ambient temperature the adsorption of carbon dioxide is completely suppressed. Hence, the separation of water vapour from carbon dioxide

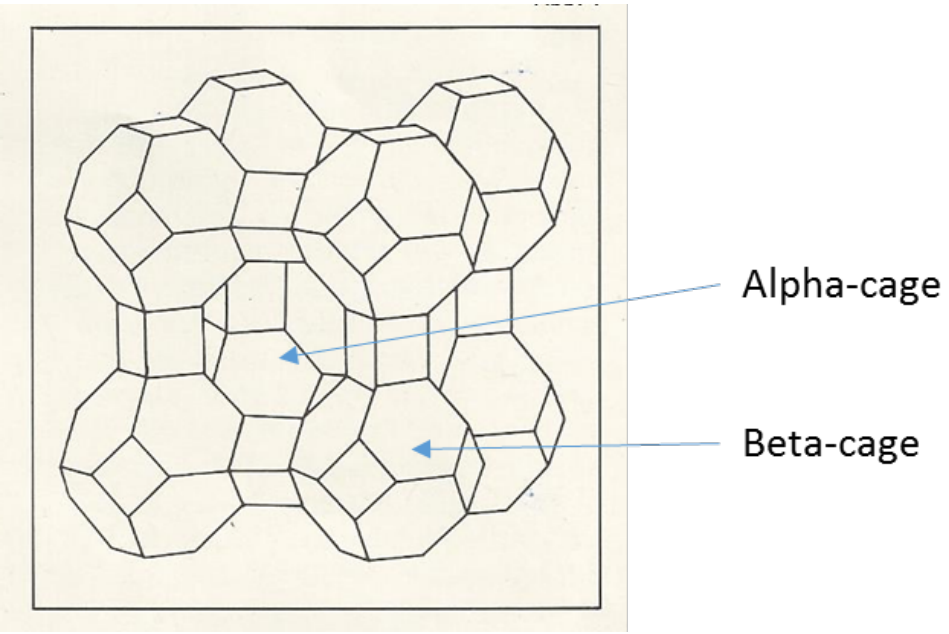


Figure 3.41: Cubic array of 8 truncated octahedrons (β-cage) in the corners of the zeolite type A framework (α-cage).

becomes possible. In addition, as first reported by scientists from Union Carbide[34], when type 3A zeolite obtained from type 4A zeolite modified by 20 % exchange with potassium ions is used as adsorber at 77 K, it becomes possible to completely suppress the adsorption of hydrogen isotopologues. Evidently, the alpha-cage pore size of potassium-exchanged type 4A zeolite is temperature dependent and - at liquid nitrogen temperature - smaller than that of molecular hydrogen. Suppression of the adsorption of molecular hydrogen has been confirmed by a number of independent research teams [Bas60b; Fla74; Nis92c; Xia11].

Flapper and Gijsman [Fla74] showed, moreover, that while nitrogen is readily adsorbed on zeolite 5A at 77 K at the same temperature there is practically no adsorption of this gas on zeolite 3A within the broad pressure range of 10^{-6} - 0.3 bar (see also [Sch68; Xia11]). These results constitute compelling evidence that hydrogen and nitrogen can be barred from adsorption on molecular sieve 3A on the ground of their molecular size. In other words, at 77 K the kinetic diameters of hydrogen, i.e. 0.29 nm, and of nitrogen, i.e. 0.36 nm, are larger than the effective pore size of zeolite 3A. The latter was actually reported to be smaller than 0.30 nm [Bre74]. The adsorption of water (kinetic diameter 0.27 nm), on the other hand, is almost not influenced by

[34] Union Carbide Corporation, Hameln, unpublished results, 1980.

substitution of sodium ions with potassium ions [Bre56]. Therefore, a separation of water from hydrogen and nitrogen is possible employing a zeolite 3A bed at cryogenic temperatures.

One more piece of innovative research is devoted to the separation of molecular hydrogen isotopologues employing **zeolite 3A** [Kot08; Kot09]. Molecular sieve 3A is obtained from synthetic zeolite 4A whose chemical formula is ($Na_{12}Al_{12}Si_{12}O_{48}$). The twelve sodium ions positioned near the six ring apertures to the α–cavity confer to this aperture an effective pore size of 0.4 nm. As already mentioned above, all type A molecular sieves have a central so called α-cavity with a free diameter of 0.66 nm (see Fig. 3.41). When a large fraction of the sodium ions are replaced via isotopoic exchange with larger potassium ions the aperture diameter is reduced to 0.3 nm which at ambient temperature can only be penetrated by i) hydrogen (kinetic rotational diameter 0.24 nm and minimum cross sectional diameter 0.29 nm), ii) water (kinetic rotational diameter 0.32 nm and minimum cross sectional diameter 0.27 nm), and iii) helium (kinetic rotational diameter 0.30 nm and minimum cross sectional diameter 0.26 nm) [Bre74]. In view that the size of the α-cage aperture depends on temperature, Kotoh et al. examined the possibility of separating hydrogen isotopologues using zeolite 3A at selected cryogenic temperatures. As nicely visualized in Fig. 3.42, depending on whether the minimum cross-sectional diameter or the kinetic rotational diameter of a diatomic molecule determine the sieving process, the adsorption will follow case (a) or case (b).

Whereas in case (a) a separation between H_2 and HD is not possible, in case (b) the isolation of HD by molecular sieving from a H_2/HD mixture should be realizable. What is more, adjustment of temperature within a fairly narrow critical range should allow separation of more or even all hydrogen isotopologues. An important experimental pre-requisite for an effective separation is a homogeneous cryogenic temperature distribution within the bed employed for the separation. In an attempt to isolate HD from a mixture of H_2, HD, and D_2, Kotoh et al. performed screening experiments with zeolite 3A maintained at three cryogenic temperatures, i.e. 130 K, 140 K and 160 K[35]. The aim was to determine the molecular sieving properties of zeolite 3A at very low temperatures (the diameter of the pore aperture decreases with decreasing temperature). The runs consisted of three sequential steps: i) sieving adsorption, ii) confinement, and iii) recovery. Experimentally obtained separation factors were found to be rather reproducible and fairly high

[35] Zeolite 3A will almost not adsorb hydrogen at 77.4 K [Bre74]. For molecular sieving to occur temperatures above 125 K are necessary [Kot08].

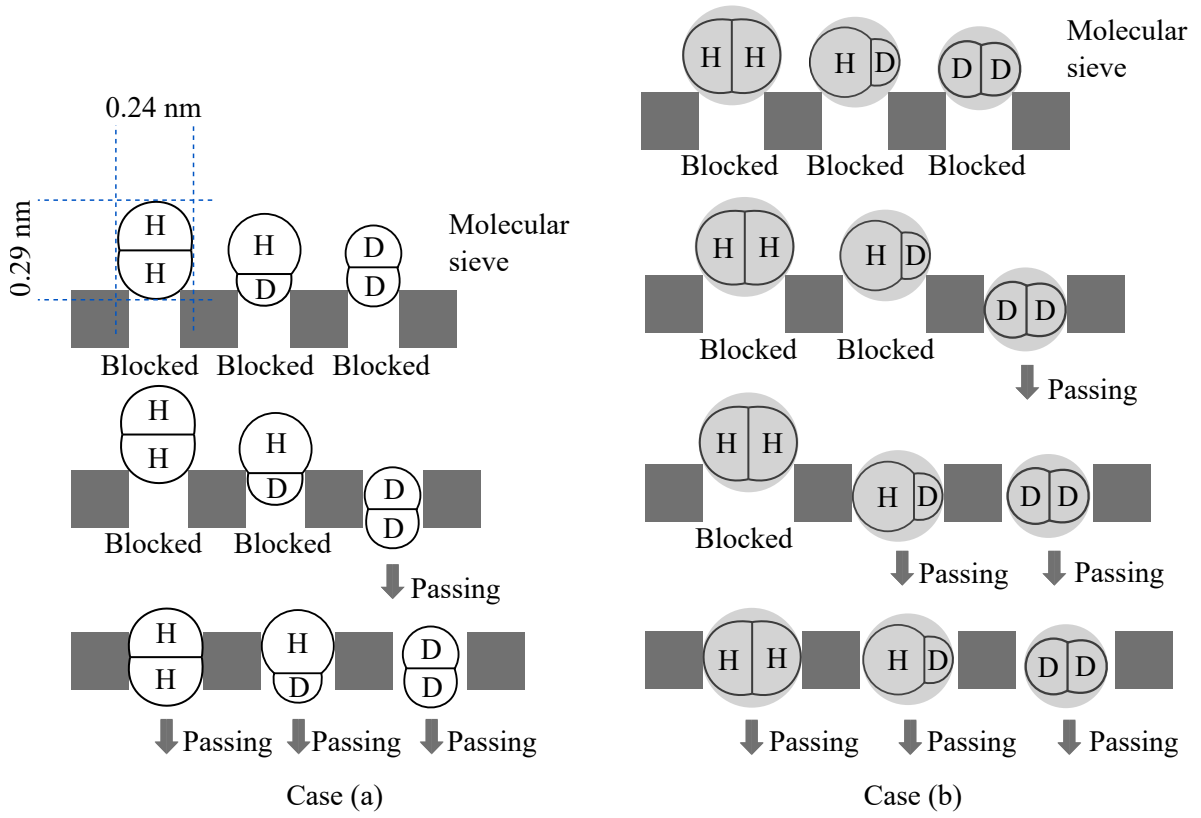


Figure 3.42: Model to explain molecular sieving of hydrogen isotopologue molecules by zeolite 3A at cryogenic temperatures. On the left based on minimum cross-sectional diameter (case (a)) and on the right based on kinetic rotational diameter (case (b)) (after [Kot09]). Temperatures increase from top to bottom.

Table 3.11: Separation factors of HD/H_2 and D_2/H_2 by molecular sieving adsorption using zeolite 3A [Kot09].

Temperature (K)	α_{HD/H_2}	α_{D_2/H_2}
130	3.19	3.71
140	2.60	3.34
160	2.20	2.24

(see Table 3.11). All $\alpha_{(HD/H_2)}$ separation factors determined from the sieving step were found to be larger than unity but smaller than the corresponding $\alpha_{(D_2/H_2)}$ separation factors. They increased with decreasing temperature. This constitutes first evidence that molecular sieving by zeolite 3A is determined by the larger dynamic diameter of rotating hydrogen molecules rather than by the minimum cross-sectional diameter.

In conclusion, a separation by molecular sieving of the species H_2, HD, HT, D_2, DT, and T_2, here given in order of decreasing width, appears to be feasible.

3.14.8.2 Experience with technical scale cryogenic adsorber traps

Enoeda et al. [Eno96] performed cryo-adsorption experiments at TPL, Tokai-mura, designed to investigate the recovery of tritium released from the first wall of a fusion machine during helium glow discharge cleaning. They simulated the gas exiting the machine with a gaseous mixture consisting of helium containing 400 ppm H_2 and 0.5 ppm HT. Flow rates during adsorption were in the range 13 - 60 l min^{-1} at a carrier gas pressure of 1000 mbar. For the retention of hydrogen isotopes, they employed a test loop featuring a 0.5 kg cryo-adsorption bed containing $1/8^{th}$ inch 5A molecular sieve pellets. The bed of dimensions 10.9 cm inner diameter and 8 cm height was submerged in liquid nitrogen. Their experimental results agreed well with model calculations. Regeneration of the bed, i.e. recovery of 75 % H_2 and 60 % HT, was achieved in 75 min. The kinetics of regeneration was enhanced by low helium purge gas pressures, i.e. 506 mbar, in the opposite direction to loading. Regeneration was the most-time-consuming step of the cyclic adsorption/regeneration operation.

Two relatively large cryogenic molecular sieve beds (CMSB), each containing 1.6 kg of type 5A zeolite immersed in liquid nitrogen (77 K), were employed at **TSTA** in a closed loop system to

investigate the retention of hydrogen present at low concentration in helium carrier gas [Wil95b]. The attained hydrogen loading capacities were found to be much lower than anticipated from previous comparable bench scale experiments [Wil94a; Nis00]. This finding was attributed to the fact that these beds had previously been in tritium service at TSTA for about eight years and had therefore experienced some radiation-induced loss of adsorption capacity (probably loss of crystallinity, i.e. amorphization). What is more, optimal regeneration temperatures could not be realized out of cryogenic bed design reasons. An important conclusion from the work was that in spite of the low partial pressure of hydrogen in the carrier gas (13 - 26 mbar) the observed hydrogen breakthrough was rather sharp even though the period of adsorption was fairly long. Because TSTA has been dismantled, much needed scalability studies are no longer possible.

A semi-technical scale cryogenic molecular sieve bed designed and manufactured at workshops of **TLK** was tested with protium in closed loop mode [Bel05a]. The bed, which contains 20 kg of molecular sieve 5A, is installed in a liquid nitrogen cooled vacuum insulated vessel that chills the molecular sieve uniformly to approx. 77 K. For regeneration of the adsorber, the bed can be heated up to 600 K using three independent electrical heaters. Breakthrough tests at flow rates of up to $2\,m^3\,hour^{-1}$ helium containing 120 Pa H_2 (2000 ppm) were performed and reported to agree with the adsorption capacity of the cryogenic molecular sieve adsorber bed. Because the mass transfer zone was found to be relatively narrow (12.5 % of bed height) a scale up to flow rates more relevant to ITER was considered possible.

3.14.8.3 Targets for cryogenic inertial fusion

Aerogels can provide a framework for holding liquid or solid deuterium – tritium mixtures without adding too much fusible material [Fea87]. Advantageously, aerogels are of rather low density. For instance, whereas the theoretical density of amorphous silica has a value of $2200\,kg\,m^{-3}$ that of open cell foams is only $150\,kg\,m^{-3}$. Aerogel targets such as needed for cryogenic inertial confinement fusion, sequestering a mixture of liquid deuterium and tritium of actual composition 25 % D_2, 50 % DT, and 25 % T_2, were prepared by Bowers et al. [Bow90]. For this purpose, the cryogenic liquid was adsorbed in small-celled foam consisting either of i) extracted polystyrene, ii) resorcinol formaldehyde, iii) carbonized resorcinol formaldehyde, or iv) a composite. The degree of filling achievable with these targets was found to be rather high. The properties of the prepared frameworks were compared among each other in an experimental study.

3.14.9 Tritium purification utilizing hot metal getter beds

The purification of hydrogen using getters is a quite developed subject on which a vast body of experience and literature is now available. The purification of hydrogen from such impurities as O_2, N_2, CO, CO_2, Q_2O and NQ_3 (Q = H, D, T) employing hot metal getter beds was investigated during the Eighties by a number of researchers. Aim of the work was to develop a tritium purification process for the plasma exhaust gas of a fusion machine as well as for the clean-up of hydrogen isotopes exhausted from primary systems in tritium handling laboratories. Within this frame, Hutter et al. [Hut86] manufactured a compartmentalized ceramic bed containing uranium powder which was designed for operation at temperatures as high as 1173 K. A ceramic reactor was chosen for the containment of uranium in order to possibilitate very high temperatures while precluding possible formation of uranium-stainless-steel eutectic.

Recently, the interest in uranium beds utilizing ceramic as structural material has resurfaced [Kha15]. Main reason for selecting ceramics was the very low hydrogen permeability of this material. Heating of the bed was carried out by high frequency induction. The advantage of this approach is very rapid heating of the getter material and hence fast liberation of tritium. However, caution must be exercised when subjecting ceramic material to large and rapid temperature changes because of its tendency to develop cracks with consecuential loss of containment.

At elevated temperatures uranium gettering of N, O, and C, regardless of whether molecular (N_2, O_2, CO, CO_2) or bound to hydrogen (NH_3, H_2O, C_xH_y, etc.) to yield nitrides, carbides, and oxides, becomes rapid and quantitative. Moreover, at high temperatures the degree of decomposition of the other reaction product, i.e. uranium hydride, into the elements is rather high. If the selected temperature is very high, the getter begins to sinter (it starts at about 773 K and becomes much more pronounced at 1173 K). A consequence of sintering is considerable reduction of the specific surface area which translates into substantial loss of getter reactivity.

Main equations describing the chemistry between uranium and typical plasma exhaust impurities are [Kur87]:

$$\mathrm{U} + \mathrm{O_2} \longrightarrow \mathrm{UO_2} \quad (773\,\mathrm{K})$$

$$3\,\mathrm{U} + 2\,\mathrm{CO} \longrightarrow \mathrm{UO_2} + 2\,\mathrm{UC} \quad (1123\,\mathrm{K})$$

$$2\,\mathrm{U} + \mathrm{CO_2} \longrightarrow \mathrm{UO_2} + \mathrm{UC} \quad (1053\,\mathrm{K})$$

$$\mathrm{U} + 2\,\mathrm{H_2O} \longrightarrow \mathrm{UO_2} + 2\,\mathrm{H_2} \quad (873\,\mathrm{K})$$

$$2\,\mathrm{U} + 1.5\,\mathrm{N_2} \longrightarrow \mathrm{U_2N_3} \quad (1023\,\mathrm{K})$$

$$2\,\mathrm{U} + 3\,\mathrm{NH_3} \longrightarrow \mathrm{U_2N_3} + 4.5\,\mathrm{H_2} \quad (1073\,\mathrm{K})$$

$$\mathrm{U} + \mathrm{CH_4} \longrightarrow \mathrm{UC} + 2\,\mathrm{H_2} \quad (1173\,\mathrm{K})$$

where the temperatures at which these reactions proceed readily are given in parenthesis.

Caron-Charles and Gilot [Car89b] performed a comprehensive theoretical analysis of the thermodynamics of all reactions between uranium and impurities and conducted selected kinetic studies of the complex reactions taking place between single gases like O_2, N_2, NH_3, and CH_4 or some of their mixtures with massive uranium. In addition, they provided kinetic equations which predicted correctly the rate of hydrogen liberation from reactions of uranium with these impurities at 973 K. On the basis of their analysis they concluded that the optimal temperature range for the removal of impurities from hydrogen carrier gas with uranium is in the range 1000 K and 1300 K. Only under these conditions is the highest product stability achieved. Lower temperatures were found to be preferable when nitrogen species (N_2, NH_3) predominate in the carrier gas and the higher ones when methane constitutes the principal impurity. Methane and nitrogen were identified as the most resistant species towards gettering. Other conclusions were: i) at high temperatures ammonia is removed in two parallel processes either via direct reaction with the solid or by catalytic decomposition into the elements and ii) typical plasma exhaust impurities influence each other's kinetics markedly during the gettering process.

To achieve a high degree of purification a sequence of two alumina beds containing uranium, one held at 773 and another at 1173 K, was proposed by Schira and Hutter [Hut86; Sch88]. Objective of the first bed was the quantitative retention of highly reactive molecular oxygen and water via irreversible formation of uranium oxide. The second bed maintained at higher

temperature served to convert residual oxygen, nitrogen, and all carbon/hydrogen-bearing species into uranium oxides, nitrides, and carbides and molecular hydrogen. The concentration of methane in hydrogen in the second bed was reduced from 1 % to less than 10 ppm. The reason why quantitative removal of impurities is not possible under these conditions is the occurrence of reverse reactions such as

$$U_2N_3 + \frac{3}{2}H_2 \rightleftharpoons 2\,UN + NH_3$$

$$UC_2 + 2\,H_2 \rightleftharpoons UC + CH_4$$

$$U_3O_8 + 2\,H_2 \longrightarrow 3\,UO_2 + 2\,H_2O$$

which promote renewed formation of methane, water, and ammonia [Nef89]. Concerning uranium hydride, Caron-Charles [Car87] provided evidence that at temperatures exceeding 700 K, this species will be fully dissociated provided the partial pressure of gaseous hydrogen is maintained below 10^5 Pa.

In order to even further improve the degree of purification of hydrogen and comply with specifications requested at the time by TLK, i.e. less than 1 ppm of remaining impurities, an additional third step was proposed consisting of a cryogenic bed containing one kg of molecular sieve adsorber maintained at 77 K with liquid nitrogen. Because this adsorption step not only increased retention of residual impurities but also retained an unacceptably large fraction of hydrogen carrier gas, a higher temperature of the cryogenic molecular sieve bed became unavoidable [Nef89]. Consequently, this route was disregarded. The finally adopted solution consisted of one stainless-steel and two ceramic beds containing uranium powder maintained at 773 K, 973 K and 1173 K, respectively, followed by a tail-end palladium/silver permeator [Tam91a; Tam92]. Objective of the first getter bed was removal of oxygen, carbon oxides, and water, of the second removal of molecular nitrogen and ammonia and of the third bed, maintained at the highest temperature, removal of residual methane. The permeator served to purify hydrogen isotopes from helium. With this combination, the concentration of impurities could be reduced to values meeting TLK (as well as ITER) specifications. However, in the end the concept was abandoned because of safety considerations, high process complexity, the generation of mixed uranium-tritium waste, and elevated operation costs.

Other getters like Zr_3Al_2 (ST101, SAES Milano, Italy) or $Zr(V_{0.83}Fe_{0.17})_2$ (ST707, SAES, Milano, Italy)) essentially displayed similar behaviour to uranium [Hei85]. Whereas nitrogen, oxygen, and carbon monoxide are effectively removed from hydrogen carrier gas at 773 K, an appreciable depletion of methane was only achievable at temperatures exceeding 873 K. Analogous to concepts utilizing uranium, waste requiring after-treatment, elevated operational costs, and safety concerns were the main shortcomings of this approach.

Recapitulating, concepts involving uranium as getter to clean-up plasma exhaust gases of a fusion machine were dropped at an early stage primarily because of the i) arising mixed waste (tritium and uranium), ii) the high operation temperatures of the getter beds, and iii) the restrictive management of uranium.

3.14.10 Organic getters for hydrogen

In laboratory experiments it was shown that certain unsaturated liquid or solid compounds with one or more carbon-carbon triple bonds like for instance

$$C_6H_5{-}C{\equiv}C{-}C{\equiv}C{-}C_6H_5$$

$$C_6H_5{-}C{\equiv}C{-}CH_2{-}CH_2OH$$

when dispersed over supported catalysts are capable of gettering hydrogen from an inert gas atmosphere at ambient temperature [Mil81; Sou82].

Attempts to extend this application to the removal of tritium at concentrations within the range 1 - 500 ppm from an air atmosphere remained below expectations. It appears that under these conditions water formation either via catalytic oxidation of hydrogen (oxygen on the catalyst) or exchange of tritium with background water are favoured over triple bond capture by hydrogenation.

3.14.11 Molecular sieve "membrane"

An advanced concept for the extraction of tritium from the helium purge gas exiting a breeder blanket is currently being investigated experimentally at TLK [Dem12]. According to this

concept, the purge gas is first cooled, compressed, and dehumidified[36] and thereafter passed through a series of separators consisting of sodalite molecular sieve applied by pore plugging on a hollow porous support consisting of α-alumina (Ircelon, France). A basic requirement is that the applied sodalite layer be homogenous throughout displaying no defects. If this is the case, the layer acts like a very thin "membrane" of $< 1\,\mu m$ thickness. The separation of hydrogen and helium is based on the cubic structure of the alumino silicate framework of sodalite. Ideally the sieve framework must be completely free from occluded species and have only six of the eight six-ring faces of the framework occupied by Na^+ ions[37]. Hence, two pores are unblocked giving access to hollow sodalite cages with a free diameter of 0.66 nm. The pores to the cages consist of a six ring with a free diameter of 0.23 - 0.26 nm [Bar71; Sch75]. In view of this, it becomes possible to separate helium (kinetic diameter 0.26 nm) from hydrogen (kinetic diameter 0.29 nm) or tritium. While nearly pure helium is recovered on the permeate side and returned directly into the blanket following a hydrogen makeup, concentrated tritium exiting the bleed side is fed into an isotope separation system and regained in pure form. Experiments are under way to further improve the permeation efficiency by optimizing the separation temperature of the "membrane" [Bre74; Dem12].

3.15 Measurement of process parameters

This section is devoted to a description of tritium-compatible instrumentation used worldwide in tritium-handling installations to measure such process parameters as temperature, pressure, vacuum, gas flow rate, moisture, radioactivity, etc. In general, measurement and control instrumentation in tritium facilities must be installed with good accessibility for maintenance, calibration, periodic on-line surveillance testing, and troubleshooting. While some instruments will require recurring calibration, others may only necessitate a first-time calibration or even be employed as received from the manufacturer.

A few general guidelines [Poo08]:

- Instrumentation and controls shall be designed to fail safe.

[36] Because sodalite readily adsorbs water (up to 13.6 % by weight) it is necessary to remove moisture effectively from the blanket purge gas with a dedicated zeolite adsorber bed before it is passed through the sodalite "membrane". Since the adsorbed water is tritiated, it will require periodic recovery.

[37] As the temperature is increased these Na^+ cations may show considerable mobility, which enhances molecular diffusion.

- Instrumentation destined for tritium handling facilities shall allow for calibration either utilizing redundant equipment or the availability of isolation/test valves that permit calibration in place.
- Modular construction is to be provided in order to permit easy replacement of failed components.
- Instrumentation shall be selected not only to cover the full range of expected normal process parameters at the required accuracy but also the range anticipated during abnormal conditions.
- Instrumentation wiring shall not be installed in the same conduit of cable trays carrying power or control wiring in order to preclude electromagnetic interferences.
- All safety related instrument loops and interlocks shall be reviewed prior to installation for electrical fail-safe design requirements.

3.15.1 Pressure and vacuum gauges

3.15.1.1 Pressure gauges

Pressure transducers from i) **Sensotec**, ii) **Lincoln/Sirus** IV, **Precise Sensors** (pressure range 0 to tens of bar), and iii) **Teledyne Hastings** TCVG (low pressures in the range 0 - 1 mbar) have been used for tritium systems installed at Savannah River Site [Poo08]. For more sensitive measurements type **Baratron**®, **Paroscientific** or ionisation pressure instruments have been employed. The latter are of high accuracy and good linearity (deviation $< 0.25\,\%$).

Absolute and differential Baratron® capacitance manometers have been used widely and for decades under a large variety of conditions in numerous tritium handling facilities in Canada [Shm87], Europe [Sch91a; Gir92; Pen95c; Pen95a; Lae99b], Japan [Mat89; Tor02; Yam02; Yam11a], USA [Rhi73; And77; And82; Gal05], and several other laboratories and countries. In these facilities pressures of gases and gas mixtures of different compositions and degrees of chemical aggressiveness containing hydrogen isotopes with up to 100 % tritium have been measured partly for rather prolonged uninterrupted periods of operation mostly without contingencies. The following advantageous properties of capacitance manometers can be listed i) comparatively

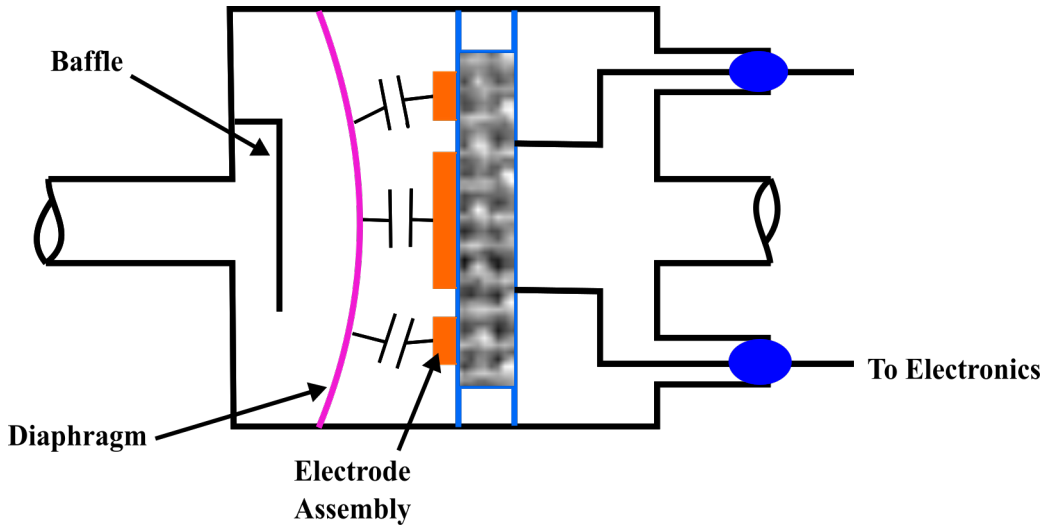


Figure 3.43: Functional diagram of a differential Baratron® capacitance manometer (MKS). The tube on the right is connected to the reference pressure.In case of absolute sensors the open tube on the right is sealed and contains a getter. Modified from https://www.mksinst.com/n/baratron-capacitance-manometers (17.06.2020).

small self-volume, ii) robustness, iii) high accuracy, iv) relatively high overpressure rating, v) fully metallic construction, vi) fairly wide pressure range, and v) very good technical support.

All-metal membrane pressure gauges used in tritium handling equipment for pressures surpassing 1 mbar should not have oil on their backside.

The operation principle of a **differential Baratron® capacitance sensor** is illustrated schematically in Fig. 3.43. The sensor is made of Inconel® and houses a diaphragm and a metal on ceramic electronic assembly. The reference right side of the diaphragm is evacuated to a very high vacuum. Pressures are deduced from the change in capacitance between the metal diaphragm and the adjacent dual electrode.

By design the sensor tolerates an overpressure twice that of the full range scale. **Absolute sensors** have a sealed tube on the right side which contains a getter that preserves an extremely low reference pressure. Some sensors are bakeable up to temperatures of 673 K. MKS sensors cover a rather broad pressure range from 10^{-5} mbar up to 33 bar. As opposed to Pirani or ion gauges, Baratron® capacitance manometers are insensitive to the kind of gas whose pressure is being measured.

3.15.1.2 Vacuum gauges

Vacua are frequently measured with cold cathode ionization vacuum gauges like type **Sensa Vac** which covers a pressure range from 10^{-8} Pa to 100 kPa. Because these gauges have no filament they are immune to air inrush. **Pirani** gauges are used for pressures higher than 0.1 Pa and **Penning** gauges for pressures below 1 Pa. The response of ion gauges and Pirani gauges is dependent from the type of gas. Fifteen years of accumulated experience with a Pirani vacuum gauge in tritium handling systems were described by Gallagher and McCrimmon [Gal05].

The **Viscovac** vacuum gauge from Leybold is a microprocessor-controlled device that relies on gas friction for pressure measurement. This gauge is particularly suitable for corrosive and radioactive gases. The sensor head is pushed over a stainless-steel sensing tube containing an easily exchangeable stainless-steel ball (diameter 4.5 mm) that is freely suspended by a magnetic field and rotates at a high speed. The pressure is obtained from an expression which is a function of the relative molecular mass of the gas or gas mixture used, the diameter of the ball, the mass density of the ball material, a friction coefficient, and the relative decrease in rotation number of the ball at the prevailing temperature. Pressure measurements with the Viscovac gauge are highly reproducible featuring an extremely low long-term drift (less than 1 %/year). The technique permits measurement and control of pressures within the range 10^{-7} - 1 mbar. The sensor is made entirely of stainless-steel, has a small volume, can be used for a continuous measurement, and requires no temperature control. The instrument is used for the determination of pressures and calibration purposes.

For the accurate determinations of low and extremely low total hydrogen pressures, e.g. 10^{-7} - 10^{-1} Pa, a **Bayard-Alpert type** ion gauge was shown to provide reliable results. Improvements of the original gauge were achieved with a screened ion gauge having a cylindrical anode [Gen85]. The upgraded V-shaped collector was made of pure gold and the cylindrical anode of a gold-plated tungsten foil with square plates at both ends. The closed-system ionisation gauge has several advantages over conventional grid gauges: i) it is independent from external electrical fields, ii) has a well-defined ionisation path for the electrons, iii) is designed to eliminate disturbing effects from adsorbed gases when operated at 523 K, iv) has a stable gold work function, and v) shows negligible ion pumping. With the sole exception of molecular tritium, the relative sensitivities for

HD, D_2, HT, and DT of Bayard-Alpert ion gauges were found to agree well with the sensitivities obtained with a quadrupole mass spectrometer [Wat87].

3.15.2 Temperature sensors

3.15.2.1 Thermocouples

A thermocouple consists of a pair of dissimilar conductors welded or fused together at one end to constitute the measuring junction and a free end to form the reference junction. Running wires across or parallel to AC lines must be carefully avoided, because induced currents may have an influence on the results. Thermocouples must be immersed deeply into the material whose temperature is to be measured. Heat conduction away from the hot junction causes low readings and must be avoided.

Thermocouples should be selected on the basis of the anticipated operating temperature range and required accuracy. NiCr-Ni thermocouples are habitually used in tritium facilities for temperatures up to 873 K. Type J, K, E, and T thermocouples are employed in tritium service for temperatures up to 1273 K. Noble metal thermocouples such as type S, R, and B are selected for temperatures up to 273 K.

Thermocouples should be designed fail-safe with proper upscale or downscale burnouts so that when a junction breaks or a wire is lifted the device alarms. A redundant thermocouple shall be provided where thermocouples are of direct immersion type, welded to the device, or safety relevant.

When high accuracy is required resistance temperature detectors are the preferred option. Pt100 resistance thermometers are employed for temperatures in the range 73 - 1170 K. To exclude self-heating these sensors are operated with only 0.1 mA.

3.15.2.2 Pyrometers

Optical pyrometers for contactless temperature measurements employ the radiation intensity emitted by a heated component in a defined interval of the spectrum. They are available for several temperature ranges and temperatures up to 3300 K.

A ratio pyrometer takes the ratio of the radiation intensities of two different, narrow ranges of the spectrum, which are close to each other. They are equipped with a chopper provided

with two interference filters and a photomultiplier. The temperature measurement of a ratio pyrometer does neither depend on the geometry of the radiating object nor from its distance to the pyrometer. Advantageously is also that the "black body" assumption required for optical pyrometers is not necessary. A common application is the determination of high temperatures, i.e. 1273 - 3273 K, on solid metals, graphite, or ceramics. An absolute accuracy of ± 12 K has been achieved at 1473 K. Ratio pyrometers are insensitive to dust, steam, and dirt on observation windows.

Pyrometers can be utilized to measure temperatures inside of glove boxes. In case of the Tritium Decontamination experiment TIDE at TLK, a borosilicate optical window was fixed with O-rings onto a hole drilled into the polycarbonate window of a glove box. Objective of the window was to determine the temperature of a tritium-contaminated CFC specimen obtained from a tile removed from the first wall of JET employing a pyrometer installed on a tripod outside of the glove box. For decontamination, specimens were subjected to rapid induction heating up to temperatures of the order of 1100 K utilizing a water-cooled hollow coil attached to a powerful high frequency generator (Fritz Hüttinger, type IG5/200 Hz, 10 kV A, heating current 65 A). In the glove box the specimen was fixed inside of a small dedicated closed box integrated into a loop and provided with a borosilicate window on one side. Because the temperatures measured with and without the two borosilicate windows were the same, it was concluded that borosilicate was essentially transparent to the radiation emitted by the carbon fibre composite (CFC) specimen. Temperatures were verified with a thermocouple fixed on the back side of the carbon specimen.

3.15.3 Hygrometers

Quantitative determinations of water partial pressures in a carrier gas are frequently necessary in tritium technology but difficult to perform accurately, because of the highly polar character of this molecule. When accurate moisture analyses are needed, it is often necessary to use trace-heated transfer lines in order to minimize water adsorption/desorption and condensation phenomena. In general, there is no universal method suited to all applications. A hygrometer must thus be selected depending upon the concentration level of moisture, chemical composition

of the carrier gas, and type of measurement to be carried out, i.e. single or repetitive. A table with dew point conversions into partial water pressures is provided in Appendix Q.

Hygrometer measuring principles are either electrolytic, capacitive, or based on a vibrating quartz crystal or a chilled mirror.

3.15.3.1 Electrolytic hygrometer

Electrolytic hygrometers are founded on the measurement of the electrolysis current through water absorbed on a hygroscopic material like a film of phosphorus pentoxide P_2O_5 or a semi permeable membrane. The number of electrolysed water molecules, which is proportional to the moisture content of the gas, is obtained from Faradays law under the premise of a properly controlled flow. Electrolytic hygrometers need to be inspected periodically to verify that neither the film has been damaged nor conducting particles on the film have caused a short circuit. For good results, rather low flow rates must be maintained to allow sufficient time for equilibration between absorbed water and moisture in the gas phase. Problems are considered to be the i) electrolytic generation of hydrogen and oxygen, both of which are released into the effluent gas, ii) long response time, and iii) sensitivity of the measurement to variations in carrier gas flow rate or pressure. Erroneous measurements may additionally result from clogging or deterioration of the sensor. The detection limit of electronic hygrometers is (1.0 ± 0.5) ppm.

3.15.3.2 Condensation hygrometer (mirror dew point)

A condensation hygrometer measures the temperature at which water condenses on a cooled metal mirror. Condensation on the temperature-controlled mirror surface is detected by an optoelectronic mechanism. Particularly advantageous is the fact that for a given carrier gas the condensation temperature depends solely on the partial pressure of water. It is important to keep in mind that gases (especially organic gases) condensing at about the same temperature as water can interfere with the measurement. The detection limit depends on the thermal conductivity of the carrier gas. For instance, a value of 0.5 ppm in nitrogen will yield 2.5 ppm in hydrogen or helium. To attain high accuracies, this type of hygrometer needs frequent cleaning of the mirror and periodic calibration.

Because the mirror dew point[38] hygrometer is considered to be one of the most accurate instruments, it is often used for calibration purposes and to verify the correct operation of process hygrometers.

3.15.3.3 Capacity humidity sensor

Capacitive humidity sensors feature a substrate of anodized aluminium which conducts to a porous layer of alumina onto which a very fine film of gold is vaporized [Pfe82]. Water vapour diffusing through the gold into the alumina pores cause changes of the impedance of the capacitor whose dielectric is constituted by the alumina. Alternatively, it is also possible to measure the effect of humidity on the dielectric constant of a polymer. Capacity humidity sensors are robust against condensation and towards a short exposure to temperatures as high as 343 K. The humidity measurement itself, on the other hand, is appreciably influenced by temperature (variations in ambient temperature are noticeable), aging effects, and contaminations. In view of this, it may be necessary to thermostatize the sensor at a temperature above ambient, e.g. 323 K. Capacitive sensors require frequent calibration because of the difficulty to account for physically adsorbed water. They are relatively insensitive to the flow rate.

Capacitive sensors normally have a very low detection limit of <1 µbar provided the sensor has been calibrated recently and is not much older than 2 years.

3.15.3.4 Vibrating quartz crystal hygrometer

A vibrating quartz crystal hygrometer measures humidity by the frequency change in the vibration of a quartz crystal covered by a hygroscopic resin. To perform a measurement the crystal is exposed alternately to gas dried over a molecular sieve bed and to the wet gas; the variation in vibration frequency is proportional to the mass of adsorbed moisture. Equilibrium is usually established in less than a minute. Problems are caused by a chemical modification or chemical contamination of the resin. The detection limit is less than 1 ppm.

[38] Dew point is the temperature at constant pressure at which a sample of moist air reaches water vapor saturation (see also Appendix Q).

3.15.3.5 Moisture meter calibration

Hygrometers require calibration in regular intervals with a gas of accurately known dew point. A way of proceeding is to generate a gas stream containing a low partial pressure of water (0.1 - 100 µbar) by passing a carrier gas through a freezer consisting of a large metallic vessel completely submerged in refrigerated methanol (see Fig. 3.44). The device contains numerous troughs covered with ice integrating to a total surface area of 1.7 m^2. Gas inlet and outlet are arranged as heat exchangers in which helium at ambient temperature heats the cool gas exiting the calibration device. This arrangement contributes to avoid condensation of moisture on the inner wall of the gas exit. The temperature of the refrigerated methanol, which can be controlled within the range 193 - 243 K, determines the sublimation temperature of ice and consequently the moisture content of the purge gas. The logarithm of the partial pressure of water is nearly linearly dependant from the ice temperature. Pfeifer [Pfe82] examined systematically the performance of PANAMETRIC moisture sensors with this device and showed that the temperature measured at the humidifier differed by not more than 1 K from that of the dew point obtained with a freshly calibrated PANAMETRIC condensation hygrometer. He attributed the small temperature difference to errors arising from Pt-100 temperature sensors submerged in methanol. Repeated calibrations carried out over an extended period of time revealed significant drift of the calibration curves. This needs to be considered for accurate measurements.

Another common technique used to produce a reference gas of precisely known moisture content is based on the catalytic conversion of a hydrogen-oxygen mixture into water. For gas transport a carrier like argon or nitrogen is appropriate. Hygrometers can be connected to this reference gas for calibration purposes via a manifold. Within a moisture concentration spanning the range 0.5 - 70 ppm the achievable accuracy is better than 3 %.

Saturated salt solutions (NaCl, LiCl, K_2SO_4, etc.) in a closed container at constant temperature constitute another option for calibrations in low precision applications. A drawback of salt solutions is the long period of equilibration.

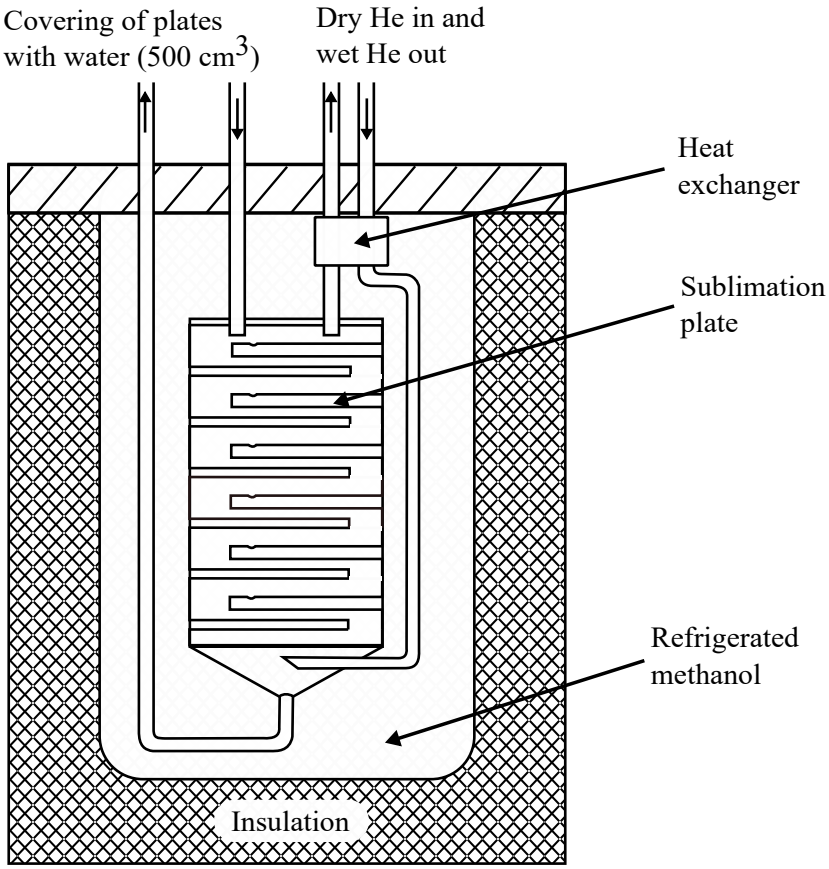


Figure 3.44: Schematic diagram of a humidifier ([Pfe82]).

3.15.4 Oxygen monitor

Oxygen is a paramagnetic gas that is attracted by a magnetic field. It can therefore influence an external magnetic field. The magnetic susceptibility of oxygen decreases inversely with temperature. These properties are used to determine the level of oxygen in a wide range of carrier gases.

Paramagnetic oxygen sensors like type PMA 45K supplied by M&C TechGroup have been tested in a tritium environment. They are utilized as preventive measure against the formation of explosive mixtures [San12; Dem15a].

3.15.5 Gas flow meters

The physical principle of all-metal mass flow meters such as manufactured by Tylan, USA, is based on the thermal conductivity of gases. The sensor uses a heat source and a differential

temperature measurement whose signal is proportional to the mass flow (see Fig. 3.45). For the protection from particles the sensor is furnished with a 20 µm mesh screen installed at the fitting inlet.

At TLK three Tylan flow meters integrated into the PETRA experiment [Pen98] were used irregularly in long-term runs during a period of more than three years to measure the flow rates of the feed gas, bleed gas, and permeate gas of a palladium/silver permeator employing a process gas consisting of a 1 : 1 = D : T mixture additionally containing carbon oxides. While no detrimental effects were noticed with the flow meter installed on the permeate side, flow meters mounted in feed and bleed sides were found to progressively clog requiring refurbishment or replacement. When these flow meters were opened to air a white polymeric material was observed to obstruct the inlet screen (not shown in Fig. 3.45). It is highly probable that the laminar flow element (secondary flow, also called restrictor bypass) displayed in Fig. 3.45 likewise clogged gradually. If this is the case, an important pre-requisite for a reliable measurement with the flow meter, i. e. constant ratio between the flows through the restrictor and the sensor, will no longer hold. Since organic polymers leading to clogging will almost certainly be highly radioactive, their removal is difficult and hazardous. Therefore, complete replacement of the flow meter was the adopted solution. Experimentally it was observed that tritium/deuterium-carbon oxide mixtures passing through a permeator generate polymers, possibly enhanced by the catalytic activity of PdAg [Bea72; Bea73a; Shu94; Ohi95; Pen00a; Wag15]. A conceivable solution of the problem could be to furnish mass flow meters installed in tritium-handling facilities with easily accessible and replaceable protective screens.

At Savannah River Site experience in tritium service was acquired with mass flow controllers and mass flow meters from Brooks Instruments, MKS, and Omega Engineering [Poo08]. At JET [Lae99a], TLK [Tri91; Pen00a], TPL [Eno94; Yam02; Yam11a], TSTA [And82; Car89a] and other laboratories large numbers of the same or equivalent flow controllers were installed and demonstrated successfully during routine operation.

According to some manufacturers, mass flow meters and mass flow controllers should not be exposed to water vapour.

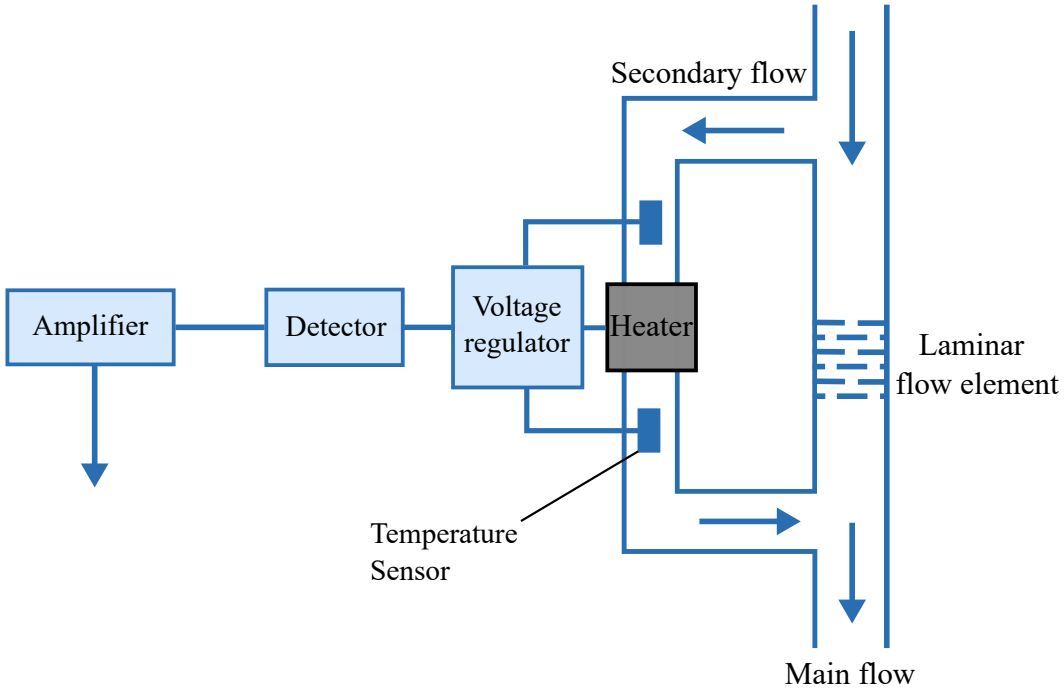


Figure 3.45: Operation principle of a mass controller[39]

3.16 Analysis of gases in tritium-handling facilities

The field "analysis of tritiated species" is highly developed. A considerable body of experience and literature is now available. Therefore, only introductory rudiments will be presented in this section. They include i) habitual techniques used for gas sampling, ii) the preparation of accurate gas mixtures, and iii) a description of some of the most common instrumental techniques recommended for the qualitative and quantitative determination of tritium-bearing species. Moreover, working principles of the recommended analytical techniques, possible occurrence of cross contaminations, achievable accuracies, will be discussed when relevant.

Caution: analytical equipment installed in the vicinity of a fusion machine may be subjected to extraneous magnetic fields.

3.16.1 Determination of volumes

Habitual methods for the determination of the volume of a containment are [Fra06]:

- **Calculation**: A volume can simply be estimated from the geometrical dimensions of the containment. This inaccurate method can only be used with containments of simple configuration having no or only few comparatively small adjacent volumes[40].

- **Weighing**: the containment is first weighted empty and then filled with water or another suitable liquid at a defined temperature. From the measured weights and the known density of the liquid at the temperature of the measurement, it is possible to calculate the volume. Drawbacks of this method are i) filling of all dead volumes without bubbles is difficult (verification of the absence of bubbles in case of non-transparent vessels impossible), ii) the need to retrieve quantitatively the liquid after the measurement, and iii) limitation to only relatively small volumes because large balances with sufficient sensitivity are frequently not available.

- **Expansion**: when gas contained in a known volume at known pressure and temperature is expanded into a previously evacuated unknown volume it becomes possible to calculate the unknown volume utilizing the ideal gas law. Constant temperature in the known vessel is achieved by thermal insulation.

Two practical methods proposed recently for the determination of the volume of small recipients are described below:

The **Continuous Variable Volume Expansion** method developed by Fratolillo [Fra06] basically consists of a variable gas-tight volume which can be connected to the unknown volume (see Fig. 3.46a). A requirement is that the capacity of the variable volume be larger than that of the unknown one. For a measurement the unknown volume is first evacuated and valve V1 is closed. Thereafter the variable volume (in red) is filled with gas, e.g. air, at a precisely determined pressure and then expanded into the unknown volume by opening valve (V1). If the variable volume is now compressed until the original pressure is re-established, the unknown volume can be read directly on a scale. A rigorous temperature constancy is not necessary with this method because measurements can be performed rapidly without having to wait for thermal equilibration. The accuracy of the method was estimated to be 0.5 %. A commercial device is now on the market (see Fig. 3.46b).

[40] Depending on the relative values of known and unknown volumes dead volumes are some times neglected.

Small volumes can likewise be determined by the so called **Discontinuous Variable Volume** expansion method proposed by Köllö et al. [Koe11]. The method is based on a modification of the conventional expansion method. Instead of calibrating a volume with a liquid of known density, a reference chamber closed by an ISO-K flange with elastomeric sealing is used, which can be opened to accomodate solid cylinders or cubes of different but well-known volumes (see Fig. 3.47). For a measurement one of two procedures can be selected: In one case the unknown volume is evacuated and the rest of the system including the reference chamber is filled with gas up to a pressure measured accurately with sensor P, e.g. MKS Baratron 120AA covering the range $10 < p < 10^5$ Pa (an additional sensor, e.g. MKS Baratron 901P is needed to verify the vacuum in the range $1 < p < 10$ Pa (not shown in the figure)). By opening the upper valve, the gas is expanded into the unknown volume. In the other case, only the unknown volume is filled with gas up to a certain pressure, the upper valve is closed and the rest of the system - including the reference chamber - is evacuated. By opening the upper valve, the gas is expanded into the rest of the system. For a volume determination at least two measurements are necessary employing either two different solid bodies or one body and the empty reference chamber.

Advantages of this procedure are that no liquid is needed and a determination of the reference volume is not necessary. For volumes within the range 10 - 1000 cm^3 the uncertainty was calculated to be lower than 1 %. This value was confirmed experimentally. For volumes of less than 10 cm^3 the uncertainty increases significantly.

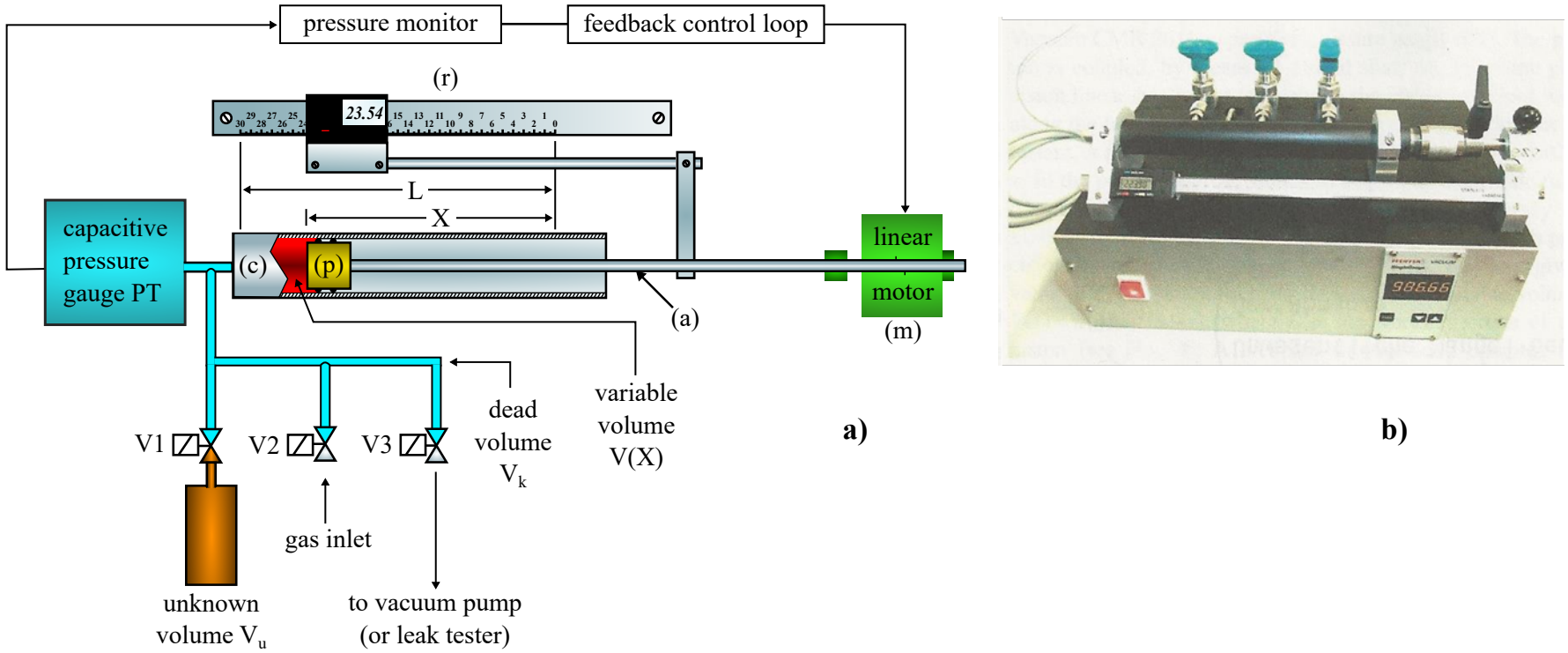


Figure 3.46: Determination of small volumes by the Variable Volume method showing (a) scheme of principle and (b) commercial device [Fra06].

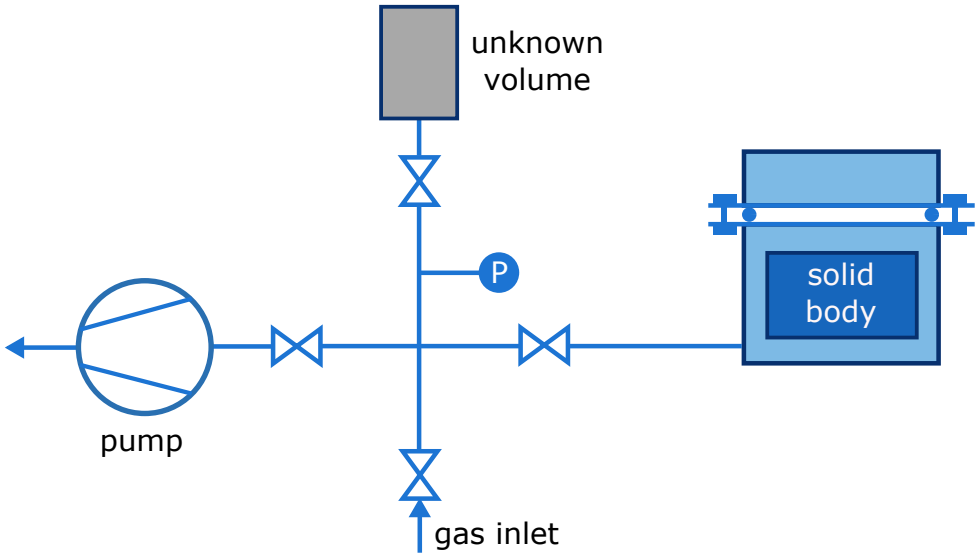


Figure 3.47: Experimental arrangement for the determination of small volumes according to the Discontinuous Variable Volume method. The volume of a reference chamber is varied by introducing solid bodies of known volume (after [Koe11]).

3.16.2 Preparation of gas mixtures for calibrations

A fundamental requirement for calibrations or acceptance tests of analytical equipment are accurate gas mixtures. In most laboratories gas mixtures are obtained by sequential addition of high purity gases into a mixing vessel beginning with the smallest amount and progressing towards the largest. The temperature of the vessel used for the preparation of mixtures needs to be measured and controlled. To ensure good mixing it is indispensable to recirculate the gases for a sufficient length of time. For a calculation of the composition of a mixture it is necessary to know accurately pressures, temperatures, and the chemical composition of the gas mixture.

The mole percentage of the i^{th} component in gas mixtures, X_i, can be calculated from the relationship

$$X_i = \frac{100 n_i}{\sum_{i=1}^{N} n_i} = \frac{100 \sum_{j=1}^{G} f_{ij} \left[\frac{p_j V}{Z_j R T_j} - \frac{p_{j-1} V}{Z_{j-1} R T_{j-1}} \right]}{\frac{p_f V}{Z_f R T_f}}$$
$$= \frac{100 \sum_{j=1}^{G} f_{ij} \left[\frac{p_j}{Z_j T_j} - \frac{p_{j-1}}{Z_{j-1} T_{j-1}} \right]}{\frac{p_f}{Z_f T_f}}$$

where n_i is the number of moles of the i^{th} component, N the total number of components in the mixture, f_{ij} the fractional abundance of the i^{th} component in the j^{th} feed gas, p_j the total pressure after the j^{th} feed gas was added, Z_j the correction factor for deviation from ideal gas law behaviour (see also section 2.5.1.7 and Appendix C), V the volume in which the mixture is prepared, R the gas constant and T_j the temperature of the gas in Kelvin at the time the pressure p_j is measured. A correction for deviations from the ideal gas law is needed when pressures exceed 1 bar significantly.

Schlösser et al. [Sch13c] prepared recently accurate mixtures of H_2, HD, and D_2 for the calibration of analytical instrumentation, e.g. Raman spectroscopy, gas chromatography, mass spectrometry, etc. HD was synthesized starting from a H_2/D_2 mixture (eventually containing some HD, for more details see sections 2.5.1.8 and 3.16.5.1) by catalysed isotopic scrambling using a catalyst consisting of 0.5 % Pt on Al_2O_3. If N_{x}^i is taken to be the initial amount of the isotopologue x (where x = H_2, HD, or D_2), then the equilibrium constant at a given temperature is obtained from

$$K(T) = \frac{(N_{\text{HD}}^i + 2\delta)^2}{(N_{\text{H}_2}^i - \delta)(N_{\text{D}_2}^i - \delta)}$$

Solving for δ one gets the expression

$$\delta_{\pm}(K) = \frac{b \pm \sqrt{b^2 - 4(K-4)(KN_{\text{H}_2}^i N_{\text{D}_2}^i - (N_{\text{HD}}^i)^2)}}{2(K-4)}$$

where

$$b = K(N_{\text{H}_2}^i + N_{\text{D}_2}^i) + 4N_{\text{HD}}^i$$

and only δ_- provides a solution. Knowing δ, it is possible to calculate the concentrations of each of the molecular hydrogen isotopes with expressions such as

$$N_{\text{H}_2}^{\text{eq}} = N_{\text{H}_2}^i - \delta$$

$$N_{\text{D}_2}^{\text{eq}} = N_{\text{D}_2}^i - \delta$$

$$N_{\text{HD}}^{\text{eq}} = N_{\text{HD}}^i + 2\delta \ .$$

In case of Raman spectroscopy, the absolute Raman signal, S_x, is related to the number of molecules of isotopologue, x, by relationship

$$S_\mathrm{x} = R_\mathrm{x} N_\mathrm{x}$$

in which R_x is a response factor characteristic for each molecular hydrogen isotope (see Fig. 3.48).

The relative Raman intensities of the three components can then be obtained from equations like

$$S^\mathrm{rel}_{\mathrm{H_2}} = \frac{R_{\mathrm{H_2}} N^\mathrm{eq}_{\mathrm{H_2}}}{R_{\mathrm{H_2}} N^\mathrm{eq}_{\mathrm{H_2}} + R_\mathrm{HD} N^\mathrm{eq}_\mathrm{HD} + R_{\mathrm{D_2}} N^\mathrm{eq}_{\mathrm{D_2}}}$$

They are shown as function of initial composition in Fig. 3.48. The absolute Raman signals S_x were obtained from the area under the respective vibrational Q_1 branch, corrected for overlaps from S_1 and O_1 lines of other isotopologues.

In case special mixtures of molecular hydrogen isotopologues other than obtainable from equilibration of H_2/D_2 mixtures are needed, it is also possible to prepare pure HD and blend this gas with other molecular hydrogen species. Pure HD can be obtained from lithium aluminum deuteride according to reaction

$$2\,\mathrm{LiAiD_4} + 4\,\mathrm{H_2O} \longrightarrow 8\,\mathrm{HD} + \mathrm{Al_2O_3} + \mathrm{Li_2O}\ .$$

After synthesizing HD by this reaction, Ellefson et al. [Ell78a] prepared highly accurate mixtures of H_2, D_2, HD, and ^{3}He and discussed the propagation of errors.

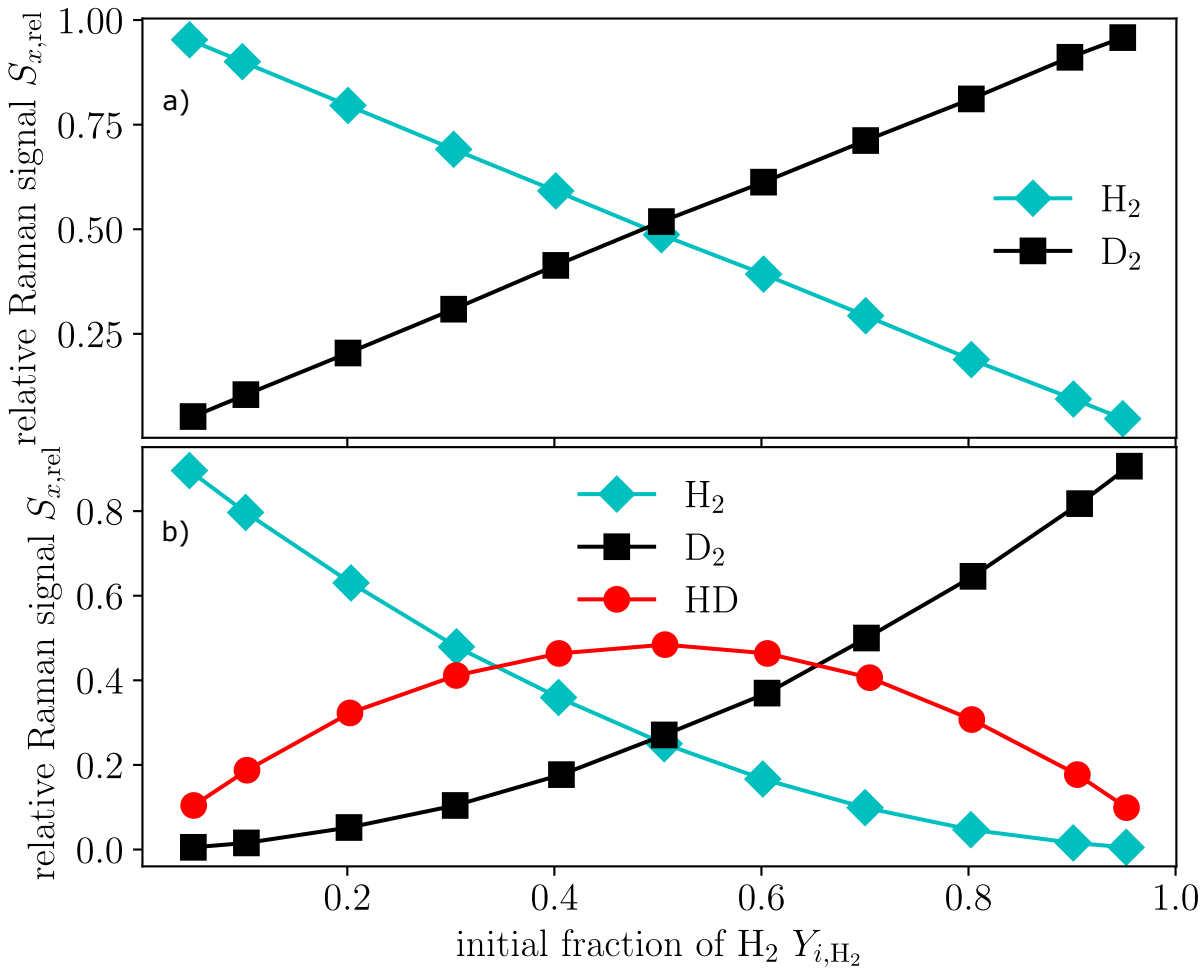


Figure 3.48: Relative Raman intensities of H_2, HD, and D_2 as function of the initial fraction of H_2 [Sch13c]. The upper plot (a) shows the intensities before catalytic equilibration and (b) the lower one, those after catalytic equilibration at 298 K.

3.16.3 Grab sampling or in-line

Sampling can be accomplished either by direct grabbing and transport of the sample to a standalone analytical instrument or via an in-line procedure. In line can either be i) continuous, e.g. a tritium air monitor or a light-absorption technique that utilizes an optical cell through which the gas is continuously re-circulated or passed in once-through modus, or ii) sporadic for instance with a mass spectrometer or a gas chromatograph directly connected to the primary system via a capillary and a sampling port.

3.16.3.1 Grab sampling

For the analysis of gases in tritium primary systems the most common approach is to expand an aliquot into a previously evacuated transportable stainless-steel gas cylinder of pre-determined volume. The cylinder must be provided with two valves in series and joined to the tritium primary system via a Cajon fitting using a one-way metallic O-ring. The sampling point needs to be equipped with one or more manometers for verification of vacuum tightness of the sampling system and quantification of the aliquot. To evacuate the sampling point an appropriate pumping system capable of discharging radioactive waste gases to a Central Detritiation System must be accessible. The pumping system serves to evacuate the sampling cylinder and all lines connecting the sampling point to the primary system prior to accepting a sample. Once the aliquot has been taken, the cylinder is transported to another glove box where it can be connected to the selected analytical instrument, e.g. gas chromatograph, optical spectrometer, mass spectrometer, etc. Two transports across glove box air locks and four if the sampling cylinder is returned into the original glove box are therefore necessary. Grab sampling from glove boxes necessitates trained personnel and eventually active support from health physics personnel. Because grab sampling is fairly time consuming, cumbersome, and always accompanied by the latent danger of i) leaks during connections and disconnections to a primary system, ii) valves leaking across the seat, iii) contamination during transfers through glove boxes and air locks (the sampling cylinder may become contaminated on the outer surface), and iv) human errors during evacuation of lines, it is evident that this technique must be restricted to exceptional measurements.

In general, grab sampling is a procedure typically employed i) during the start-up phase of experimental or technological sized tritium facilities, ii) for occasional calibrations of in-line instrumentation installed in routinely operated facilities, and iii) sporadic special analytical measurements.

3.16.3.2 In-line analysis

The most effective option for the analysis of gases in primary systems handling large quantities of tritium constitutes the direct integration of the analytical instrument into the primary system. If the analytical instrument is installed in the same glove box as the one housing the primary system a small volume pipe can be employed to connect the instrument to the primary system.

In case different glove boxes shelter primary system and analytical instrument, pipes of double containment are needed for gas transport between the two glove boxes.

In-line analytics is normally employed for continuous or repetitive rapid gas analysis. Trade-off are i) utilization of expensive glove box space, ii) inside and outside contamination of equipment (can no longer be utilized outside of the glove box unless thoroughly decontaminated), iii) eventually an additional heat source in the glove box, and iv) dealing in the glove box with equipment that increases the decontamination time constant.

In case an optical cell or a sensor is integrated into the primary system and the electronics is placed outside of the glove box, electrical and/or optical connections require appropriate feedthroughs.

Many spectroscopic techniques necessitate optical cells of advanced design to exclude accidental releases into the glove box in case of integrity loss. Because the utilization of quartz or other windows in a tritium primary system contradicts the current design philosophy requiring fully metallic tritium primary systems, optical cells have been introduced into protective stainless-steel containments equipped with optical windows and containing inert gas at a pressure different from that prevailing in the primary system [Pen95c; Ohi00b]. By this procedure, a leaking window can be recognized at an early stage utilizing a differential pressure sensor. To warrant accessibility of the cell, for instance when a defect or broken window requires replacement, cells should be joined to primary systems employing Cajon fittings with all metal gaskets.

In another approach, optical cells dsigned to withstanding rather high pressures, e.g. 2 MPa, have been manufactured [Ohi96; Ohi00b].

Worldwide, a number of laboratories dealing routinely with large amounts of tritium have employed long **capillary tubes** of low total volume for sampling from process-relevant positions of primary systems. These lines are normally connected to a manifold which is evacuated by a dedicated pumping system exhausting to a Central Detritiation System. Capillary lines are designed to conduct gas under laminar flow conditions. Accuracy and reliability of this sampling procedure has been demonstrated successfully with analytical techniques such as mass spectrometry and gas chromatography (see for example [Bil73; Lae92; Voo95]). Sampling lines of up to 60 m are not uncommon [Bil73]. Capillary tubes having inner diameters in the range 0.4 - 2.4 mm and a length of more than 40 m have likewise been validated experimentally. Gas fractionation was only observed for mixtures consisting of tritium and argon or tritium and

nitrogen, i.e. molecules of quite different molecular weight, using a pressure difference of 0.5 bar as driving force, and an extra-long capillary of 60 m. With higher driving force pressure differences or much shorter capillaries, no fractionation was noticed.

When passing a mixture consisting of highly diluted deuterium in ultrapure nitrogen through a 33 m long $1/8^{th}$ inch stainless-steel SS304 tubing a considerable delay in deuterium breakthrough was observed [Lon08] (see section 2.14.1.7 and Fig. 2.44 for more details). Thus, in critical cases careful experimental checking is advised.

3.16.4 Infrared analysis

A sizeable body of literature is devoted to infrared spectra and molecular constants of isotopically substituted species that may be encountered in gases processed within the frame of the fusion fuel cycle. Typical examples are methanes, e.g. CD_4, CT_4, CH_2T_2, CD_2T_2 [Gin35; Nie38; Jon58; Sve61; Add76], or water, e.g. T_2O, $T_2^{18}O$, THO, and TDO [Sta56; Kan84; Ich85; Kob11] (see also section 2.5.1.9).

Other impurities present in the fusion fuel cycle and identified by infrared spectroscopy are carbon monoxide, carbon dioxide, and isotopologues of ammonia. The non-overlapping infrared spectra of the most relevant non-tritiated impurities are displayed in Fig. 3.49. Because of this, infrared spectroscopy has found application for the qualitative and quantitative analysis of tritium-bearing gases in fusion-relevant tritium processes [Rev73]. Compact infrared spectrometers like type SPECTRAN or MEKOS manufactured by Perkin-Elmer, have been adapted to the requiremens of a tritum environment and used to study the kinetics of gaseous tritium with species such as CO, CO_2, and CH_4, all expected in the plasma exhaust of fusion machines having a CFC plasma-facing first wall [Pen95c; Pen00a].

The **SPECTRAN** infra-red analyser is a single beam photometer of high light intensity equipped with a bakeable, ultrahigh vacuum tight 49 cm long cell. Before penetrating into the optical cell, the broad band emitted by the light source passes a high frequency chopper. Behind the cell light passes alternatingly through a measurement interference filter and a reference interference filter fixed into holes of a rotating disk. The measurement filter is selected to coincide with an absorption band of CO and the reference filter where CO does not absorb. These filters are rotated by a step motor. The resulting internal calibration yields a very stable base line

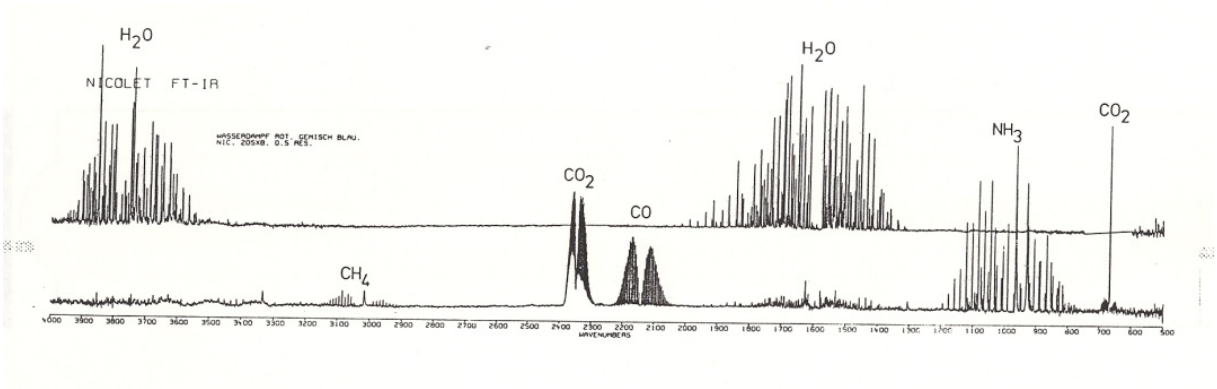


Figure 3.49: Infrared absorption bands of gases observed in the plasma exhaust of fusion machines.

which for instance permits determination of small changes in partial pressure of carbon monoxide during the course of many days. The measured extinction

$$E = -\log \frac{I_{\mathrm{mes}}}{I_{\mathrm{ref}}}$$

is almost independent from the transmission of the optical cell and in consequence from possible aerosol deposition on optical windows or from intensity changes of the radiation source. To handle safely significant partial pressures of tritium the metallic optical cell was equipped with 2 mm thick sapphire windows and directly integrated into the primary loop. As further precautionary measure against possible loss of window integrity, the cell was protected by additional sapphire windows fixed in front of both sides of the primary optical cell. The vacuum-tight inter-spaces on both sides of the cell were joined by a vacuum-tight stainless-steel line. The resulting interspace was filled with inert gas to a pressure different from that of ambient (or the primary loop). For early detection of a broken or leaking window, pressure changes exceeding set values were registered with a differential pressure sensor which delivered a signal capable of activating an alarm[41] and stopping the experiment. All optical components of the spectrometer were installed inside of the glove box and the power supply as well as read outs were fitted into an electronic rack located outside.

[41] The need for a cell with four windows becomes dispensable if the spectroscopic section is housed in a dedicated containment. In such a case an eventual window failure can be detected with an ionisation chamber.

Analogously, the **MEKOS** infrared spectrometer, which was furnished with a 13.8 cm long optical cell, served to determine in real time nearly simultaneously partial pressure changes of carbon monoxide, carbon dioxide, and methane. Quantitative determinations necessitated periodic infrared absorption calibrations to account for the effect of changes in total pressure.

In summary, MEKOS and SPECTRAN infrared spectrometers were shown to be reliable and comparatively simple analytical tools for process diagnostics, process control, and gas phase kinetic studies.

Stevens et al. [Ste61](see also references therein) investigated the analysis of heavy water in water in the 1 - 99 % concentration range utilizing double beam infrared spectroscopy furnished with an additional neutral variable transmission filter. The filter consists of two thin metal discs having identical spiral slots cut through them. When the disks are superimposed and the spirals aligned the light transmission can be varied within the range 0 - 50 % with a reproducibility of 0.1 %. From the optical densities with transmission peaks at 2700 cm^{-1} and 1900 cm^{-1} utilizing a sample thickness of only 0.25 mm the standard deviations were found to be 0.01 % at 99 % D_2O, 0.1 % at 40 % D_2O, and 0.01 % at 1 % D_2O. The transmission peak in the 1900 cm^{-1} region was determined to be the most suitable for D_2O concentrations of $\geq$ 40 % and that in the 2700 cm^{-1} region for D_2O concentrations of $\leq$ 40 %.

Another approach consists in measuring the optical densities at the wave lengths of 1645 cm^{-1}, 1460 cm^{-1} and 1220 cm^{-1}, which are the normal ν_2 vibrations of H_2O, HDO, and D_2O, respectively. The concentrations of H_2O, HDO, and D_2O are interdependent and obtainable from the equilibrium constant of the reaction

$$H_2O + D_2O \rightleftharpoons 2\,HDO\ .$$

In view that Beer´s law is obeyed and the extinction coefficients are well established, it is possible to calculate the composition of a sample from the measured optical densities. Best precisions can be obtained at low and high D_2O concentrations. In a cell of 0.025 mm thickness the standard deviation was found to be $<$ 0.15 % D_2O over the entire 1 - 99 % concentration range [Ste61].

Using conventional infrared spectroscopy at 2500 cm^{-1} and an optical cell of 25 µm path length the fraction of deuterium in water can be determined quantitatively at concentrations

in the range 1000 ppm to 5 % [Cec56; Cri02a]. At these deuterium concentrations only HDO molecules contribute to the peak, the contribution of D_2O can therefore be neglected.

Größle et al. [Gro15] recently explored at TLK a prospective application of **Fourier Transform infrared absorption spectroscopy**. Aim of the work was in-line monitoring of the concentration of deuterium in the liquid phase of the TRENTA isotope separation system. As well known, homonuclear diatomic molecules are not IR-active because of the absence of transitional dipole moments. However, certain interactions taking place in the liquid phase can induce transition dipole moments that make diatomic molecules IR-active (see Fig. 3.50a). To perform these measurements a special cryogenic cell of 52 mm absorption length was employed. Samples were liquefied at 20 - 25 K using a 250 W cryogenic system supplied by Linde. Prior to condensation, equilibration of the employed H_2 - D_2 mixture was carried out in the gas phase in the presence of a palladium catalyst (see Fig. 3.50b). With the equilibrated H_2/D_2 mixtures it was demonstrated that FTIR constitutes an adequate technique for the quantitative analysis of liquefied hydrogen isotopologues. After FTIR analysis the condensed samples were volatilized and the concentrations of the molecular isotopic hydrogen species verified by laser Raman spectroscopy. Even though first results are considered promising further research is needed for the practical implementation of the technique.

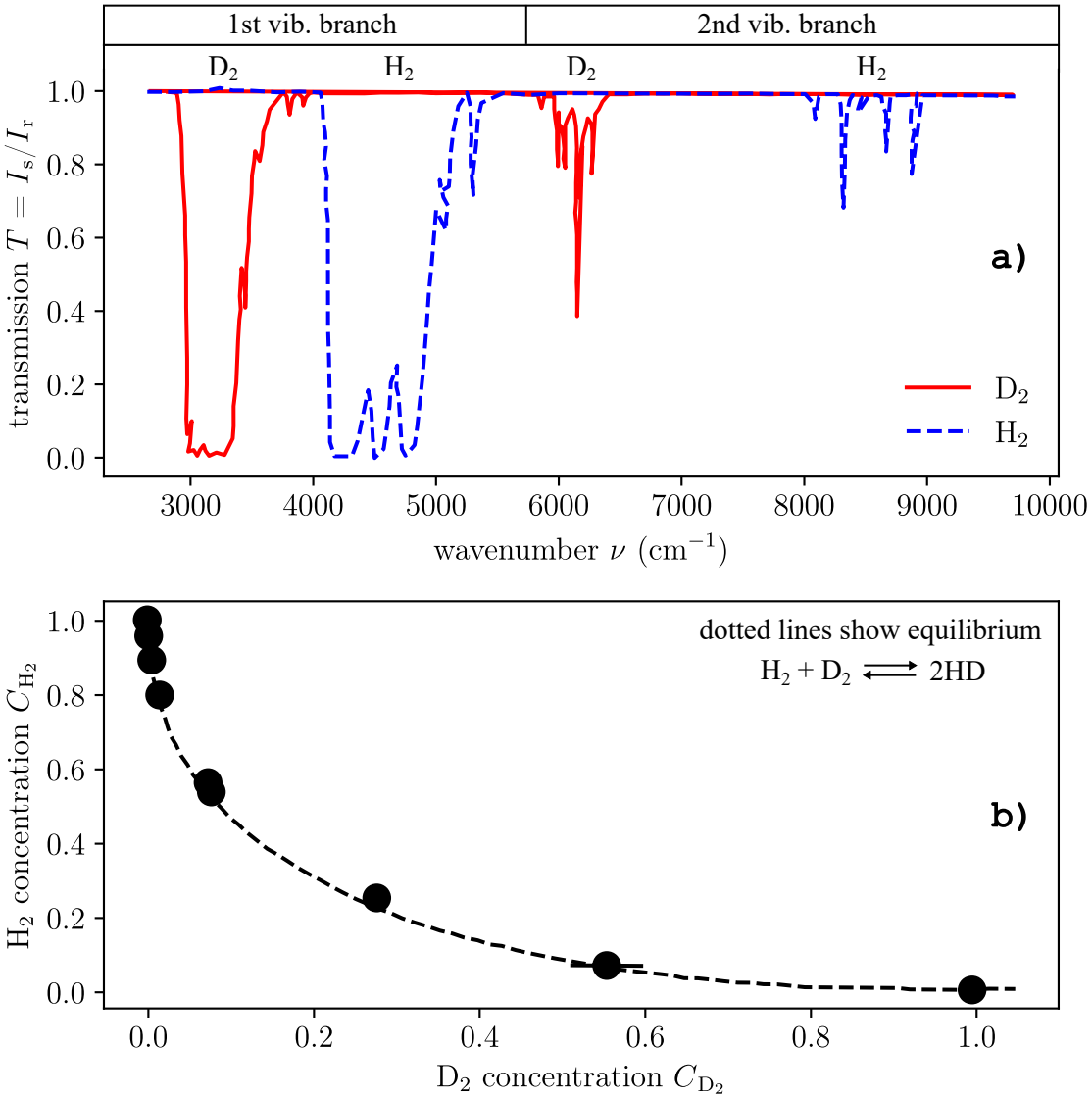


Figure 3.50: First and second vibration bands in the FTIR transmission spectra of liquid hydrogen and liquid deuterium are shown in the upper figure a) and equilibrium concentrations of hydrogen and deuterium in the gas phase are displayed in the lower figure b) [Gro15].

3.16.5 Laser Raman spectroscopy

Laser Raman (LR) spectroscopy is a potent optical analytical technique for the identification and quantitative determination of diatomic and polyatomic tritium-bearing species. The technique, which is finding many adepts in tritium technology, is based on the capability of certain molecules to scatter a beam of monochromatic light (inelastic photon-molecule collision). The fraction of scattered light that is shifted in frequency with respect to that of the incident light is known as

Raman-scattering. The allowed transitions in diatomic molecules are governed by the selection rules, i.e. $\Delta v = 0, \pm 1$ and $\Delta J = 0, \pm 2$, where v and J denote vibration and rotation quantum numbers, respectively. Spectra resulting from vibration transitions are classified into O, Q, or S branches. Q spectral lines which result from different initial rotational states (J values) are considerably stronger than O-branch or S-branch lines and therefore preferred for determinations of concentrations. As implicitly already pointed out above, laser Raman spectroscopy cannot be applied directly to the analysis of mono atomic species like He-3 or He-4.

Because laser Raman spectrometers suitable for the analysis of tritium-bearing species were not commercially available during the early Nineties, several laboratories started to assemble spectrometer systems using diverse components from different manufacturers. Within this frame, much practical experience accumulated during the development of several distinctive spectrometer concepts. Raman light was generated with argon-ion lasers operated at a wave length of 488 nm and output power of either 3 W [Ohi95], 7 W (total power of laser 15 W) [Eng92], or 8 W [She92]. To deal with the relatively low Raman scattering cross sections of the gases of interest, the intensity of the exciting radiation was enhanced by multi pass excitation using a dielectric filter arrangement and a retro Raman mirror [Eng92] (see Fig. 3.51). For the detection of Raman light, spectrometers were equipped either with i) a monochromator combined with a computer controlled multichannel image detector having 1024 elements consisting of a photodiode array and a microchannel plate image intensifier cooled by a thermoelectric Peltier element [Eng92], ii) a double monochromator coupled to a photomultiplier and a photon counting system equipped with a charge-coupled device (CCD) cooled with liquid nitrogen and a multichannel detector joined to sampling points via optical fibres [Ohi92], or iii) a camera lens imaging into a spectrometer with an intensified multichannel photodiode array detector [She92].

To meet requirements for handling highly radioactive gases, special ultra-high vacuum-tight quartz [Ohi92], silica [She92], stainless-steel [Eng92], or aluminium alloy (Dural and Invar) [She92] Raman optical cells - generally of only small dead-volume - were conceived, fabricated, and tested. Whereas the quartz and silica cells were made entirely of a single material, Raman cells of stainless-steel or alumina alloy required selection and fixation of special windows. Within this frame, i) fused silica windows sealed with an indium alloy O-ring [She92], ii) sapphire windows of one [λ] flatness sealed by solid state diffusion bonding at 773 K using either a tantalum ferrule or an aluminum interlayer [Mil91; Eng92], or iii) diffusion-bonding fused silica windows [Eng92]

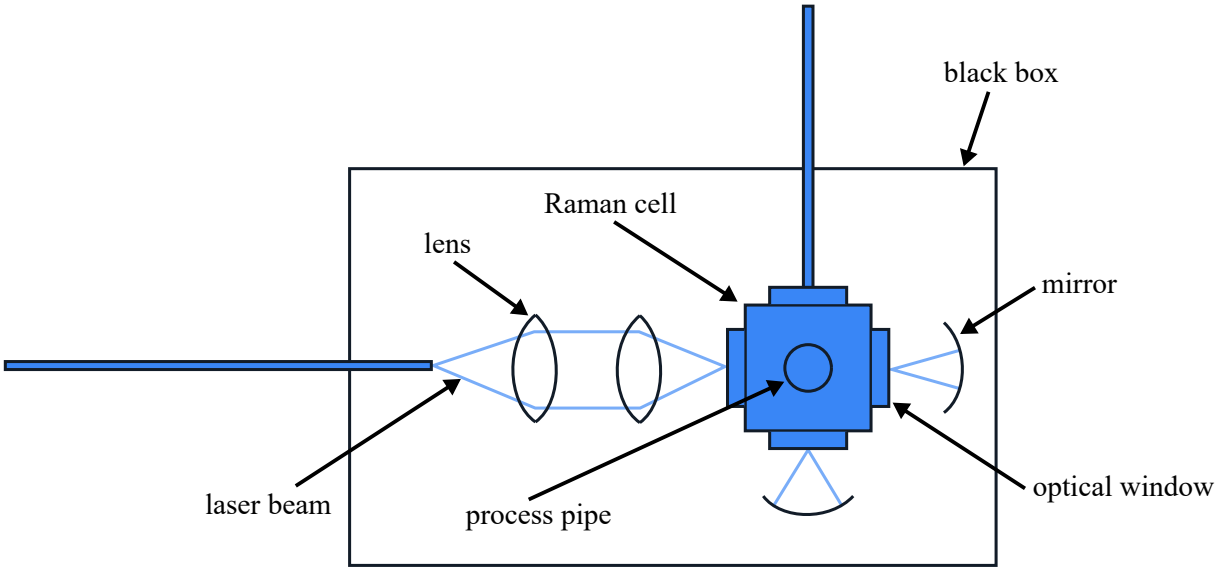


Figure 3.51: Laser Raman cell and adjacent optics housed in a black box. Only the inlet pipe connection to the process is shown on the front.

were tested and compared. To circumvent the problem of stray light originating from reflections of the laser light on the stainless-steel surface the bores were covered by a black enamel varnish [Eng92] or an anodized black coating [She92]. To ameliorate the problem of progressing window opaqueness, Sherman et al. [She92] designed slowly rotating window holders which permitted a more prolonged usage of the windows.

With respect to the application of laser Raman in tritium-handling systems, the first-generation spectrometers unveiled many problems that demanded solutions. For instance, it was realized that i) large sized and powerful cooling devices such as used for the first generation spectrometers to remove heat generated by powerful lasers were costly and necessitated too much space, ii) progressive opaqueness of windows at the incidence zone of the laser light significantly reduced their transparency, iii) the anti-reflection coating applied to the inner wall of the cell experienced irreversible damage after only a few months contact with tritium, and iv) optical benches furnished with vibrational cushioning used for the fixation of many small optical components, the monochromator, and the detector system did not fit into normal sized glove boxes.

In view of the above, Taylor et al. [Tay01] explored the suitability of a fibre-pumped frequency-doubled Nd:YVO_4 laser of single frequency output and more than 5 W power at 532 nm as light source for a laser Raman spectrometer. An important feature of this solid-

state laser was its slow and small variation in single frequencies. For the detection of Raman light, a monochromator/charged-coupled detector system (CCD) was found to be appropriate [Tay01; Stu10]. Effective enhancement of the Raman signal was achieved with an actively stabilized external resonator (ASER) boosted by retro-reflexion of the argon-ion laser light. To avoid catastrophic laser damage via mode-matched beam retro-reflexion an isolator capable of decoupling the laser from retro-reflexion was incorporated. Special features of the Nd:YVO_4 laser/ASER concept were its compactness (approximate size $0.46\,\mathrm{x}\,0.14\,\mathrm{x}\,0.11\,\mathrm{m}^3$) and small heat generation of less than 50 W. This heat was dissipated mostly by conduction into the supporting metallic optical table. Because of the above, the entire optical system comprising the laser head, the spectrometer, the charge-coupled detector, the actively stabilized external resonator, and all other optical components could be fitted on a comparatively small optical table of less than $1\,\mathrm{m}^2$ surface area placed inside of a specially designed dedicated glove box of small dimensions. The optical table was furnished with vibration cushioning generated by actively controlled air legs.

More recently, a laser Raman spectroscope for the determination of the isotopic composition of hydrogen isotopologues was mounted and taken into operation at Valduc [God11]. Fibre optics are used for the transmission of the excitation radiation from a 0.1 W diode pumped Nd-YAG laser operated at 532 nm as well as for the transmission of scattered radiation. A 1024 x 265-pixel CCD cooled to 233 K with a Peltier element constitute the detection system. For work in glove boxes a special all-metal gas probe permitting multiple reflexions of the laser beam was developed in order to increase the Raman signal intensity. The spectrometer was optimized to permit continuous monitoring of the evolution of exchange reactions taking place in a mixture of H_2, D_2, and T_2, leading to the formation of HT, DT and DH. The initial pressure of the gas mixture was 800 mbar. According to their observations, at ambient temperature the attainment of equilibrium requires about 16 hours. The detection limit at an acquisition time of 120 s was found to be approx. 0.2 % for each species.

Recapitulating, basically three different laser Raman spectroscopy (LRS) concepts have been demonstrated with tritium-bearing gases: 1) conventional LRS [Eng92; She92], 2) remote and multi sampling location LRS using optical fibres for light transmission [Ohi96], and 3) compact LRS with an actively stabilized external resonator (ASER) [Tay01; Stu10]. In all three concepts the main electronic components were installed outside of the glove box, which is advantageous from the point of view of maintenance, repair, and glove box decontamination. In options 1) and

2) the principal optical components were mounted outside of the glove box that constituted the secondary barrier to the optical cell. The laser beam entered the cell either through a window or lenses tightly sealed into the walls of the dedicated air tight optical cell box. Alternatively, optical fibres were used. Option 3) was the only one with all optical components placed inside of a small glove box. The benefit of the latter approach is that cell and spectrometer are mounted on one and the same optical table and therefore have common vibration cushioning. The detection limits achieved with the three concepts improves in the order fibre LR, conventional LR, and external resonator LR. The detection limit attainable with the ASER technique for hydrogen was demonstrated to be about 1 Pa for hydrogen and about 3 Pa for tritium after approx. 1 min acquisition time and unity signal to noise ratio. With some further improvements, such as increase of the effective laser power to more than 50 W, augmentation of the enhancement ratio, and further reduction of elastic scattering, detection limits for tritiated species of the order of 0.1 Pa appear achievable.

Raman spectra of all thermalized binary and tertiary H_2, D_2, and T_2 mixtures were recently published by Sturm et al. [Stu10] (see Fig. 3.52). These investigators used a CW Nd:YVO_4 laser of (5 W output power at 532 nm) and a high throughput (f/1.8) spectrograph coupled to a Peltier-cooled (200 K) CCD array detector of 512 x 2048 pixels. The installed equipment was considered equally suitable for measurements in a flow system as well as in a static gas cell. Examined gases were i) pure fillings of the homonuclear isotopologues H_2, D_2, and T_2, ii) equilibrated binary mixtures of H_2 + D_2, H_2 + T_2, and D_2 + T_2 which additionally provided the three heteronuclear isotopologues HD, HT, and DT, and iii) general mixtures containing all isotopologues at varying partial pressures. Dynamic range of the Raman system and detection limits of all hydrogen isotopologues were determined using gas mixtures within the total pressure range of 13 - 985 mbar (much wider pressure ranges are possible after upgrading the equipment).

Fischer et al. [Fis11] performed first long-term monitoring experiments employing a laser Raman spectroscopy system developed at TLK comprising the so-called LARA cell installed in a glove box [Tay01]. To assess the applicability of this analytical technique to the needs of the KATRIN experiment, several runs were carried out under throughput, pressure, and composition conditions relevant to this experiment. In a closed loop test with about 100 mg tritium that extended over a period of about three weeks, the occurrence of reactions between gaseous tritium and the stainless-steel tube walls were noticed. While isotope exchange reactions

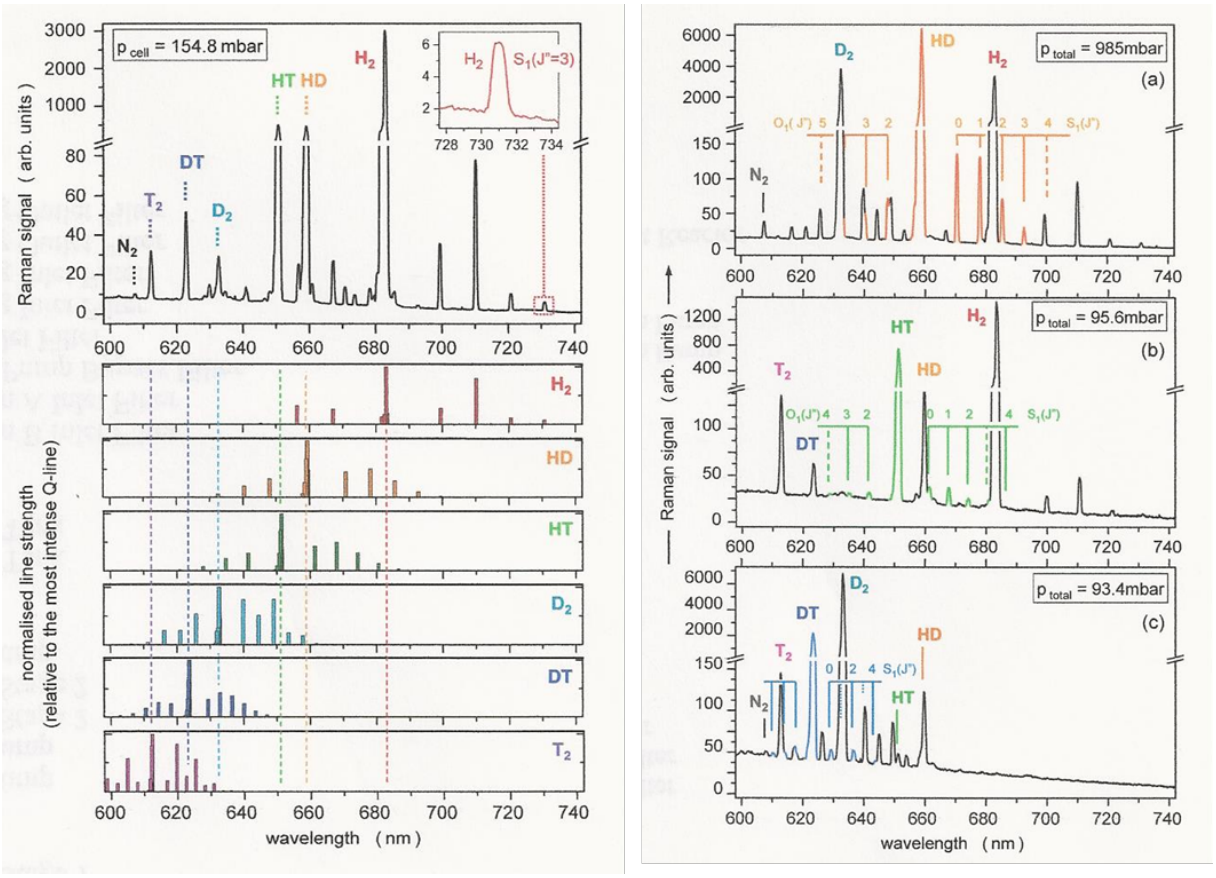


Figure 3.52: Raman spectra of equilibrated hydrogen isotopologue mixtures. The figure on the left displays Raman spectra of the equilibrated H_2 + D_2 + T_2 mixture and the figures on the right the equilibrated mixtures of a) H_2 + D_2, b) H_2 + T_2 and c) D_2 + T_2 after an accumulated measurement time of 1000 s for each spectrum, respectively [Stu10].

yielded DT and HT, chemical reactions with carbon on the surface of the structural material gave rise to the formation of tritiated methanes. The tests demonstrated the benefits of a double pass geometry which almost doubled the laser irradiance in the LARA cell but uncovered other shortages. For instance, to further improve the signal to noise ratio it was decided to try-out a new temperature-stabilized 5 W 532 nm laser.

O´hira et al. [Ohi96; Ohi00a; Ohi00b] developed a multidetection system whose salient feature is a single spectrometer capable of determining concurrently the Raman spectra of two gas mixtures comprising hydrogen isotopologues present in two different analytical points. In order to irradiate concurrently via optical fibres two Raman cells, each equipped with four sapphire windows, the laser beam of an argon ion laser was split into two equivalent beams using

a half mirror. Cells capable of withstanding pressures as high as 2 MPa were employed in these experiments. Raman scattering light was collected through a fibre array and passed first through a monochromator. After dispersion of the light with a grating of 300 or 1200 grooves/mm it was sent to a CCD array detector of four active windows cooled with liquid nitrogen. The detection limit for hydrogen isotopologues was reported to be 0.3 kPa at an acquisition time of 120 s.

An important application of "high speed", **multi-port laser Raman spectroscopy** was real-time isotopic analysis of the molecular hydrogen isotopologues H_2, HD, HT, D_2, DT, and T_2, during the operation of a cryogenic isotope separation system [Ohi92; Iwa02b]. The experimental results provided evidence that one measurement per minute of these hydrogen species is possible, with sensitivities better than 1000 ppm. The developed technology utilizes optical fibres and as in other spectrometers a multi-channel detection system equipped with a liquid nitrogen cooled CCD. The reliability of the technique was demonstrated over rather extended periods of usage [Iwa02c]. It was furthermore verified that sub-percent relative concentration sensitivities can be accomplished with only single pass excitation at relatively short acquisition times [Lew08].

Rupp et al. [Rup15] provided first evidence that the sensitivity of Raman spectroscopy can be augmented markedly when a conventional Raman cell is replaced by a silver-lined **hollow optical glass fibre** device with an inner diameter of 1 mm (see Fig. 3.53). Transmittance of the laser beam through a capillary can be almost free of losses provided the capillary is perfectly straight and the focal length has been correctly selected [Sch15]. A high reflectivity mirror at the end of the capillary reflects the laser beam back to a dichromic beam splitter. Only Raman light passes this splitter. After passing the splitter, the light is collected by two achromatic lenses and finally imaged onto a fibre bundle. The achievable limits of detection are much lower and acquisition times far shorter, i.e. 0.48 mbar in 5 s, than values reported in the literature, i.e. 4.5 mbar in 100 s [Ohi96] or 1.38 mbar in 50 s [Sal12]. Since additional enhancements of the attainable sensitivity are conceivable with further improved metal-lined hollow glass fibre cells, there is great potential for the application of this technique in special fields of tritium technology like for instance real time monitoring of flowing gases.

Schlösser et al. [Sch15] recently provided experimental evidence that **mono atomic helium** can be detected, in spite of not being Raman active, when excited by the β-radiation emitted by tritium. Fig. 3.54 shows the Raman spectrum of isotopically substituted hydrogen molecules and the radio luminescent spectrum of helium such as induced by the beta radiation of tritium when

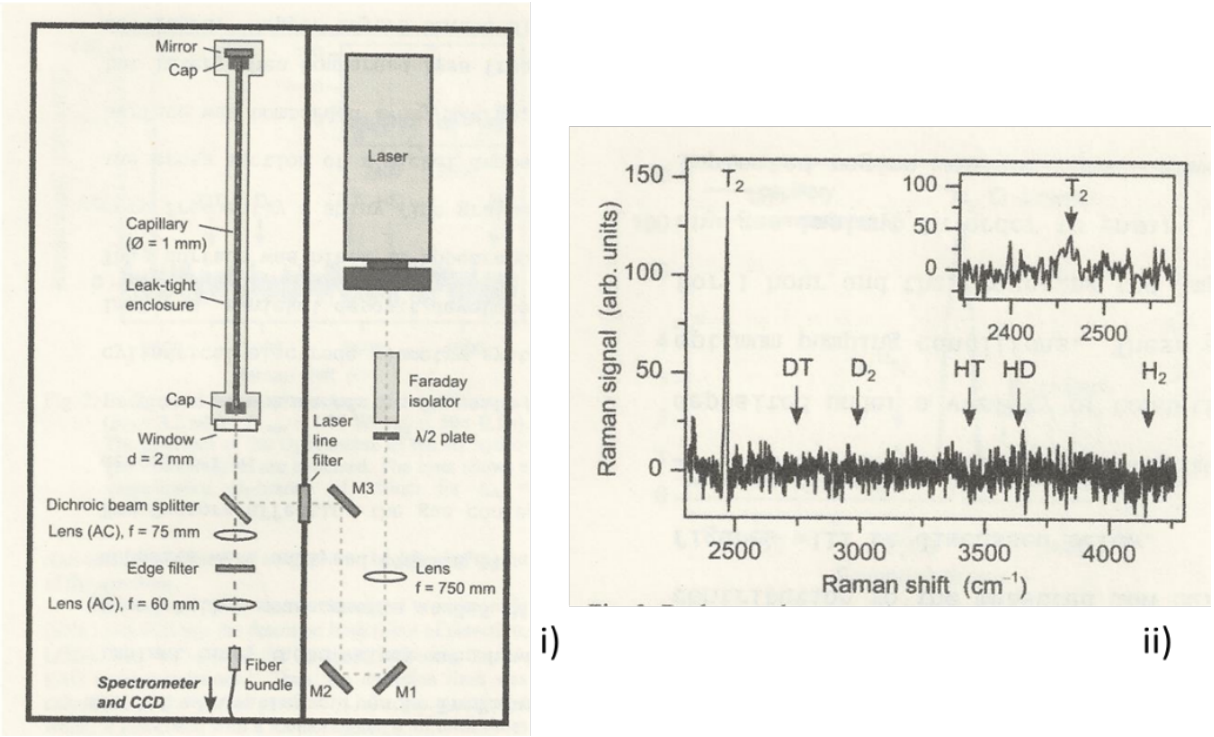


Figure 3.53: Raman spectroscopy employing a long hollow silver-lined glass fibre capillary. The figure on the left shows the optical arrangement comprising a 532 nm laser, several mirrors (M1 - M3), and a 650 mm long hollow silver-lined glass fibre. The figure on the right displays the Raman spectrum obtained with 3.4 mbar highly concentrated tritium, i.e. 93.2 % T_2, 4 % HT and 2.8 % DT [Rup15].

generated in a gaseous He/Q_2 (Q = H, D, T) mixture. For the spectrum, an excitation wavelength that delivers Raman lines in the same wave length region as that of the radio luminescent lines was selected. At the same time, it is important to choose lines which display no overlapping in both spectra. The potential applications of this new technique for the qualitative and quantitative analysis of helium is currently under further experimental evaluation.

The robustness of the optical coating applied to windows used in laser Raman spectroscopy to minimize reflection losses of the laser beam is a critical issue of much practical consequence. Fischer et al. [Fis15] carried out an experimental study of this problem. Tests were performed with a cubic Raman cell displaying four antireflection windows coated on both sides by an electron beam deposition (see Fig. 3.51). When this cell was integrated into a loop containing 200 mbar of highly purified tritium and the gas re-circulated for a period of three months severe damage of the inner side of all four windows became apparent. The damage of the coated windows

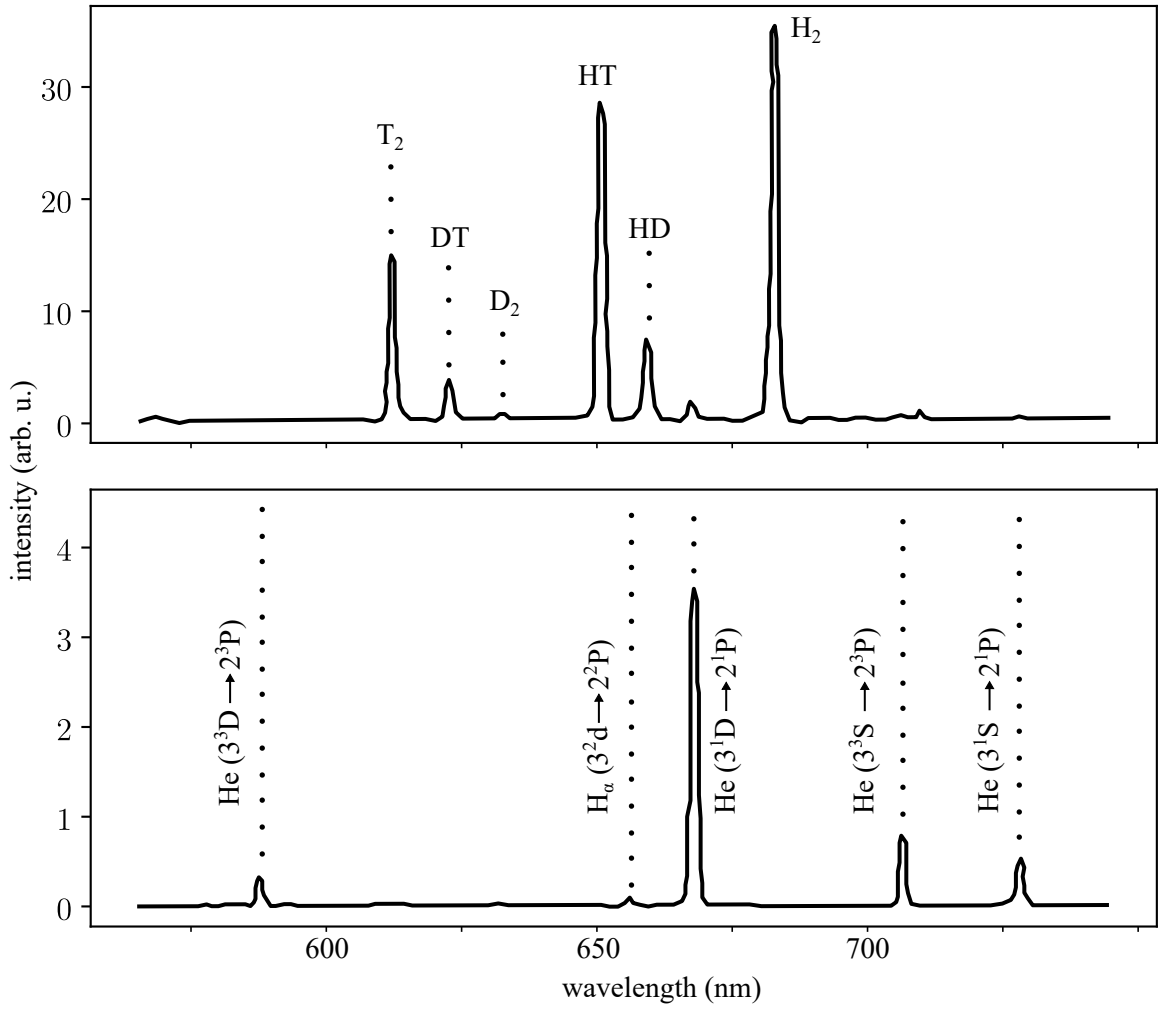


Figure 3.54: Raman spectrum of a hydrogen isotopologue mixture together with the radio luminescence lines at 587.6 nm, 667.8 nm, 706.5 nm and 728.1 nm of helium [Sch15].

resulted either from direct reactions with tritium or reactions of the coating with corrosive species generated from the interaction of structural materials in the cell with tritium. Visual inspection of the fully dismantled equipment revealed degraded poly tretrafluoroethylene (PTFE) in a valve. Accordingly, it was presumed that liberation of HF and/or HCl were responsible for the damaged coating. Repeating the experiment under complete exclusion of PTFE confirmed this supposition.

More work is currently under way to identify resistant anti reflection coatings. Preliminary experiments provided evidence that ion-assisted deposition, magnetron sputtering, and ion beam sputtering are promising coating techniques.

Besides analysis of tritium-bearing species, a further important application of laser Raman has been the elucidation of mechanism and determination of kinetics of gaseous reactions taking place between molecular tritium and other species. Typical examples are i) the exchange reaction between molecular tritium and molecular hydrogen or molecular deuterium [She92; God11], ii) the reaction of molecular tritium with carbon monoxide [Ohi93], or iii) the reaction of molecular tritium with methane [Uda92b; Uda92c; God11].

In summary, the subject laser Raman spectroscopy is highly developed and much information as well as relevant literature is now available. It is generally recognized, that the technique is particularly suitable for the simultaneous assay of all hydrogen isotopologues both under static as well as dynamic conditions [Tay01; Stu10]. The method has been demonstrated successfully for the quantitative real-time analysis of species such as carbon oxides and isotopologues of water or alkanes [Uda92b; Uda92c; Uda92a; God11]. In comparison to other analytical techniques, laser Raman i) is characterized by short response time, ii) is not associated with sample destruction, iii) can be carried out by grab sampling or in line measurements, iv) in case of in line procedures requires no optical cell evacuation and does not generate radioactive waste, v) the cost of the basic instrument is acceptable, and vi) rapid multi-port spectroscopy is possible employing one central spectrometer. Drawbacks of the technique are: i) not applicable to all gases, ii) utilization of optical windows constitutes a safety concern, iii) gradual loss of optical window transparency inflicted by powerful laser rays in conjunction with tritium, organics, and condensable species, iv) progressive deterioration of the anti-reflexion coating causing gradual loss of sensitivity, v) optical cells sensitive to vibrations, and vi) data reduction is complex.

3.16.5.1 Calibration of laser Raman systems

The accurate in-line calibration of Raman systems for non-radioactive hydrogen isotopologues has been addressed in much detail by Schlösser et al. [Sch13c] (see also section 3.16.2, 3.18.2 and refs. [Fis11; Int15]). For this purpose, accurate mixtures of H_2, D_2 and HD were prepared in a gas mixing loop provided with two mixing vessels, one for H_2 and another for D_2, and a platinum catalyst bed (see also [Kaw08]). In practice, precisely known amounts of hydrogen

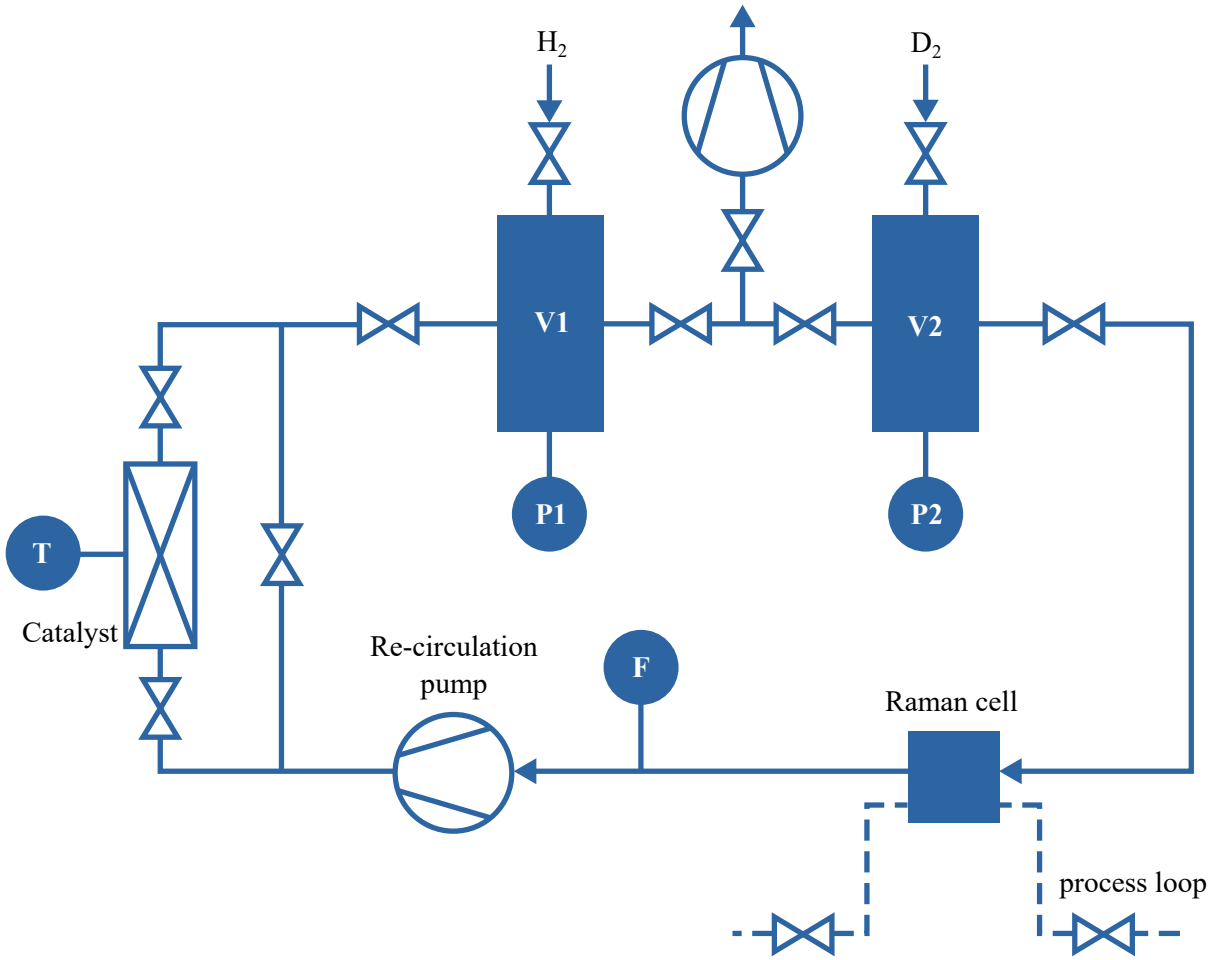


Figure 3.55: Closed loop with integrated Raman cell for the preparation of calibrated $H_2/HD/D_2$ gas mixtures (after [Sch13c]).

and deuterium were introduced separately into the two vessels by a $pVT - c$ procedure and HD prepared in situ employing a catalyst in a bypass. The Raman cell was integrated into the loop in order to circumvent sample transfers (see Fig. 3.55). From an evaluation of statistical and systematical uncertainties the calibration accuracy was found to be better than 0.4 %.

In a follow-up paper, Schlösser et al. [Sch13b] examined experimentally and theoretically the accurate calibration of a laser Raman system such as needed for the KATRIN experiment. Aim of the work was further minimization of systematic uncertainties. In the KATRIN experiment the isotopic composition of the tritium gas in the beta electron source is determined by in line laser Raman spectroscopy. When working with radioactive species special problems like possible occurrence of radiochemical and exchange reactions with the walls of the containment and with trace impurities in the parent radioactive gases require attention. Two independent

calibration methods were examined: i) a gas sampling catalytic technique of high accuracy but challenging when dealing with radioactive species and ii) an approach based on theoretical Raman signals that includes all six isotopologues. The latter method is based on theoretical Raman intensities and spectral sensitivities. *Ab initio* off-diagonal matrix elements of the polarizability were taken from the literature and verified by depolarization measurements [Jam13; Sch13a]. Because experimental values are not available for comparison, a confidence uncertainty persists. To determine the spectral sensitivity of the system, a solid fluorescent standard traceable to the US National Institute of Standards and Technology (NIST) in Gaithersburg, Md, was utilized. A cross calibration between the non-radioactive isotopologues and the relative Raman response functions yielded agreement to better than 2 %. It was concluded, that the trueness requirements for the calibration of the laser Raman system (better than 10 %) used for the species relevant to KATRIN, i.e. T_2, DT, D_2, H_2, HD and HT, will probably be exceeded .

The HYDE loop [Sch13c; Jam13] at TLK was developed 2013 to generate accurate gas mixtures of the isotopes H_2, HD and D_2 within the frame of experiments in preparation of KATRIN. Based on the same principle, an upgraded facility capable of handling tritium has recently been commissioned and carries now the acronym TRIHYDE [Nie21]. Main objectives of the enhanced system are to i) produce by manometric procedures and chemical equilibration highly accurate binary and tertiary gas mixtures of any combination of the six isotopologues of molecular hydrogen, ii) produce highly accurate mixtures of hydrogen isotopologues with other gases, iii) verify measured Raman intensities vs accurate gas mixtures of tritiated hydrogen isotopologues to yield absolute calibration factors and theoretical intensities, and iv) further reduce current calibration uncertainties.

TRIHYDE is practically a fully metallic system that displays a total leak rate of less than 10 - 8 $\mathrm{mbar\,l\,s^{-1}}$ (see Fig. 3.56). For the determination of gas inventories, the TRIHYDE facility incorporates two mixing vessels with a combined volume of 1600 $\mathrm{cm^3}$. The system can be operated within the pressure range $1 \times 10^{-3} < \mathrm{p} < 900\,\mathrm{mbar}$ and the temperature range $293 < \mathrm{T} < 473\,\mathrm{K}$ with uncertainties of $< 0.15\,\%$ of the pressure reading, $< 0.20\,\%$ of the temperature reading and $< 0.25\,\%$ of the vessel volume. The system has been installed inside of a dedicated glove box, which for safety reasons is operated with a nitrogen atmosphere. Broadly, the TRIHYDE system consists of two interlinked loops. One loop, the **P-loop**, takes advantage of several large infrastructure systems of the TLK, e.g. the Tritium Transfer System, the Tritium Storage System,

the Isotope Separation System and the CAPER Clean-up System for the processing and isotope separation of KATRIN exhaust streams contaminated with impurities. After purification and isotopic separation, the obtained pure reagents can be recycled. A dedicated intercalated "mini" loop, consisting of a turbomolecular pump, a scroll pump, a metal bellows pump, three buffer vessels and a PdAg permeator is used to accumulate waste gases in a buffer vessel for batch-wise processing in the infrastructure systems, i.e. to purify hydrogen isotopes from decay helium and other chemical impurities, and separate isotope mixtures into its homo-isotopic constituents (isotopic purity). The other loop, the **A-loop**, is designed for the preparation of i) mixtures of hydrogen isotopes, ii) mixtures of hydrogen isotopes with other gases and the iii) determination of the isotopic and chemical composition of the mixtures intended for KATRIN. To accomplish this task, the A-loop consists of analytical instrumentation, a recirculation pump, two vessels for gas mixing, a catalyst bed and a turbo molecular pumping system for evacuation. Accurate and species-independent pressure readings are carried out in each mixing vessel, apiece equipped with two capacitive pressure gauges with full scales of 1000 and 2.6 mbar, respectively. To accelerate catalysed exchange reactions and/or improve outgassing, the catalyst and the mixing vessels can be heated up to 473 K. The in-line analytical techniques incorporated into the A-loop in the order of their upstream installation at the back side of a circulating pump are: i) a wave length calibrated Raman spectroscopy system (LARA) on top light intensity calibrated by an insertable NIST SRM2242 standard for the continuous monitoring of the gaseous composition of the recirculating gas (see Fig. 3.56) ii) a binary gas analyser (BGA) based on the speed of sound (accuracy about 10^{-3}), iii) an ionisation chamber (IC) to monitor the activity of tritiated gases and iv) a beta-induced X-ray spectrometer (BIXS) for continuous activity monitoring of the circulating gas. Furthermore, an off-line residual gas quadrupole mass spectrometer analyser has been placed up-stream of the turbo molecular pump ($p < 10^{-3}$ mbar) for the assessment of impurities with $m/e > 9$. Laser Raman spectroscopy, the binary gas analyser and the residual gas analyser were also used to determine the purity of the employed gases. A particular advantage of in-line Raman spectroscopy gas analysis is the capability of analysing simultaneously several species with high sensitivity. For the evaluation procedures of laser Raman data refer to [Nie21] and references therein.

In preliminary measurements performed by circulating tritium through TRIHYDE for a period of more than 1500 hour, progressive increase of poly-tritiated methane and hydrogen tritide with

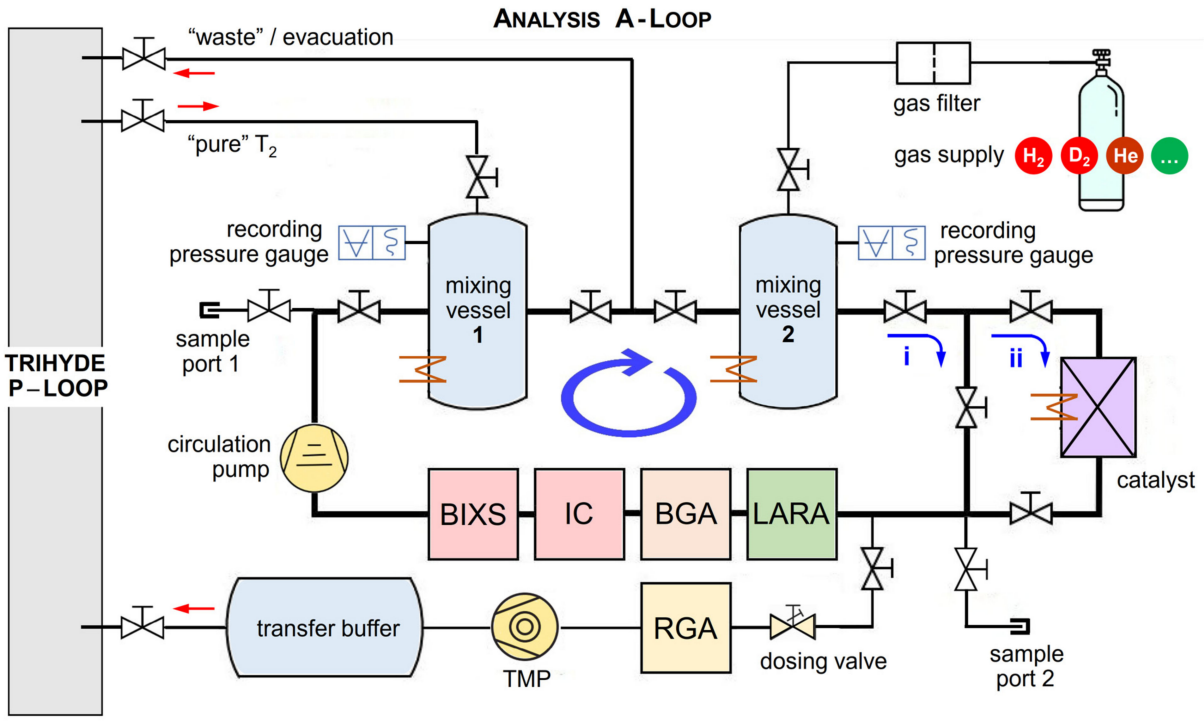


Figure 3.56: Scheme of the A-loop of TRIHYDE (for acronyms see text): The P loop is linked to the principal infrastructure systems of TLK and to a "mini loop" (not shown) for the continuous extraction of impurities in preparation of tritium recycling by batch processing.

simultaneous decrease of the partial pressure of tritium was noticed. This was attributed to reactions of tritium with hydrogen or carbon present on the surface/subsurface of the pristine stainless-steel recipient.

When either H_2 – D_2, H_2 – T_2 or D_2 – T_2 are used as starting mixtures (initial binary sample) heteroatomic radioactive species HD, HT or DT (tertiary sample after equilibration) are generated by equilibration. This can be accomplished with the TRIHYDE facility by catalysis, eventually at increased temperature. The latter is associated with a shifting of the isotopic ratio. Another option, is -induced self-equilibration with radiation emitted by tritium. Experimentally it was shown that beta-induced self-equilibration may establish in less than 72 hours depending on such process parameters as filling pressure of the mixing vessels.

The TRIHYDE facility can likewise be employed for the production of highly accurate mixtures of tritium with gases that do not contain hydrogen. Such mixtures are needed for cross-calibrations of standard tritium accountancy methods using gas chromatography, mass spectrometry or beta-induced X-ray spectroscopy or calorimetric procedures. One more option is

the preparation of accurate mixtures of tritium with rare gases, e.g. T_2 in helium, of application in research aimed at the optimizing of the extraction of tritium from the breeder blanket of fusion devices. Accurate mixtures of T_2 in argon have been valuable for investigations concerned with the performance of the purge gas in the cryogenic pumping section of KATRIN. A more basic field of application, are the kinetics and reaction mechanism of isotopic exchange reactions between organic per-tritiated molecules and gaseous H_2 or D_2. The characterization by laser Raman spectroscopy of the resulting multiple hydrogen isotope-bearing organic isotopologues are of special interest, because the Raman spectra of most of these molecules are unknown.

The theoretical LARA calibration factors based on ab-initio calculations are compared in Fig. 3.57 with derived values obtained experimentally from runs with TRIHYDE. As apparent from the plots in the figure, there is remarkably good agreement between theoretical and practical values. What is more, the uncertainties of most of the experimental relative calibration factors are lower by approximately a factor of 3 than the theoretical values. This is attributed to the high accuracy achieved for the preparation of gas mixtures with the TRIHYDE facility, which was independently verified by supplementary speed of sound measurements [Nie23].

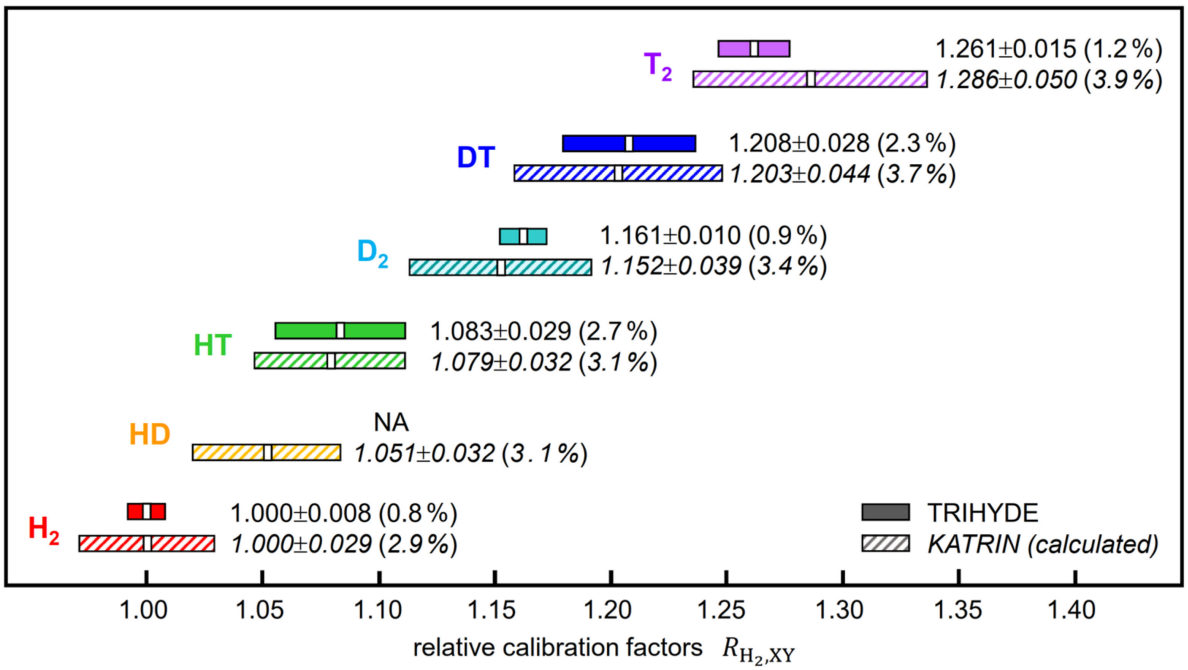


Figure 3.57: Calibration factor ratios: comparison between experimental values obtained with the facility TRIHYDE and calculated values derived from ab-initio calculations based on [Nie21], sections 3.16.2, 3.18.2 and refs. [Fis11] and [Int15]

3.16.6 Mass spectrometry

The basic physics of mass spectrometry is well established and confirmed by numerous experiments worldwide. A wide range of appropriate hardware exists commercially and special measurement systems can readily be designed and built. The technique, which is rather powerful, has been extensively applied for the qualitative and quantitative analysis of gases containing tritium [McI57; Sch71; Bea73b; Bil73; Voo95; Lae99b; Bra04]. Sufficient evidence was provided that with this technique, particularly when used in combination with gas chromatography and/or laser Raman spectroscopy, many complex and difficult analytical problems can be solved.

Basically, three different kinds of mass spectrometers have been implemented worldwide for the routine analysis of gaseous tritium-bearing species: i) sector field mass spectrometer, ii) quadrupole mass spectrometer, and iii) omegatron. In addition, a special time of flight mass spectrometer specifically designed for the investigation of the interaction of hydrogen isotopologues with the surface of solid materials deserves attention.

In the following section several mass spectrometric techniques are briefly discussed and special issues requiring attention when dealing with fuel cycle relevant gases commented. Main advantages and problems arising in their application are succinctly highlighted and - when pertinent - the adopted solutions outlined.

3.16.6.1 Sector field mass spectrometer

Experience with sector field mass spectrometers for the analysis of tritiated gases, helium, and other low molecular weight gases has accumulated with commercial instruments such as: i) MAT271 Finnigan, Balzers, ii) type MM 3001, VG Isotopes Ltd., England[42], VG 30-38 [Pri95], iii) Mode 21-201 Consolidated Engineering Corp., Pasadena, California [McI57], iv) Varian-MatCH4, Centre d´Études de Bruyères-le-Châtel [Sch71], and v) Atlas CH-4B [Bil73], to name just a few. To circumvent tritium-contaminated oil and the resulting volatile impurity species, sector field mass spectrometers have been equipped with oil-free turbo molecular pumps relying on magnetic-bearings. A gas inlet system based on a changeover valve and a 1 m long capillary with an inner diameter of 0.1 mm has been described by Brand [Bra04].

The analysis by mass spectrometry of gas mixtures comprising all or several hydrogen isotopologues, i.e. H_2, HD, D_2, HT, DT, and T_2, measuring m/e peaks within the range $1 < m/e < 6$ is rather complex, particularly when the available resolution is insufficient. The separation of ions such as D^+ and $H_2{}^+$, or T^+ and $^3He^+$ constitute specially challenging tasks. Another striking example is provided by the $m/e = 3$ peak which can be assigned to i) T^+ (arising from the isotopologues HT, DT or T_2 of which all have different ionisation probability), ii) HD^+ (arising from HD), iii) the trimer $H_3{}^+$ (arising from an ion-molecule reaction) or iv) $^3He^+$. The latter ion is practically always present eventually in high concentrations because of the radioactive decay of tritium. For the separation of the doublets $HD^+ - {}^3He^+/T^+$ of mass 3 or the doublets $HT^+ - D_2{}^+$ of mass 4 resolutions higher than 1000 are needed (see Appendix R and Fig. 3.58). For instance, the separation of HD^+ from $^3He^+/T^+$ necessitates a resolution of 500 and that to separate $H_2{}^+$ from D^+ a resolution almost three times as high, i.e. 1300. The separation of $^3He^+$ and T^+ is not really necessary because these peaks can be obtained by calculation. The appearance of trimer ions like $H_3{}^+$ (conflicts with HD^+), $D_3{}^+$ (conflicts with

[42] Specially developed for process control of a diffusion isotope separation column in Jülich, H.R. Ihle, personal communication.

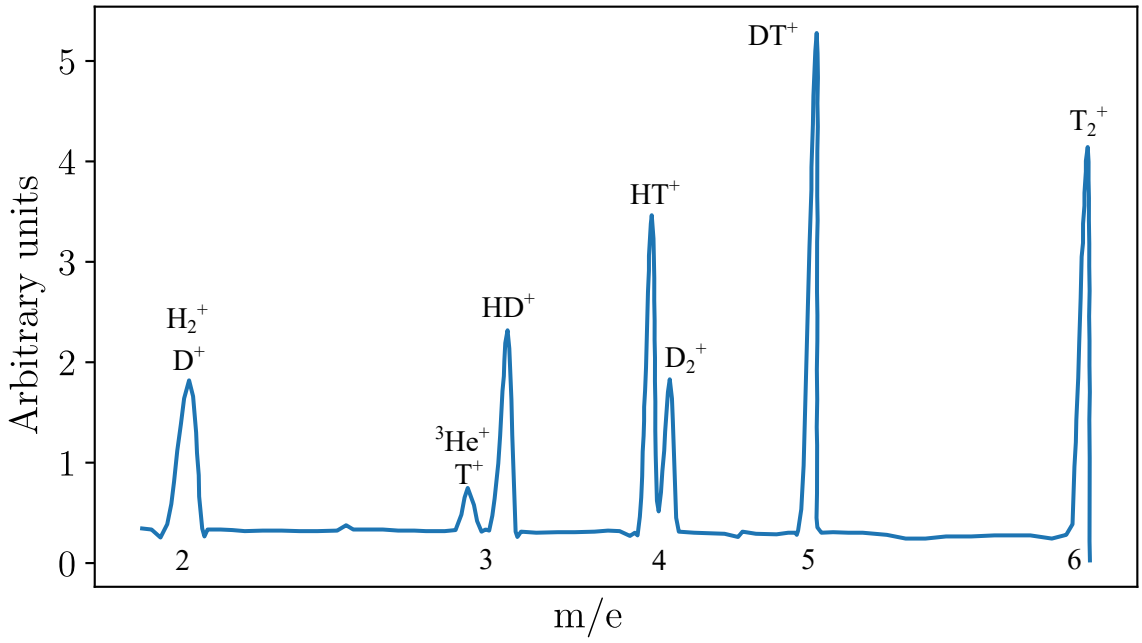


Figure 3.58: Mass spectrum of six hydrogen isotopes and ^{3}He with a resolution of 1000 (10 % valley) (after [Sch71]).

T_2^+), H_2D^+ (conflicts with D_2^+), H_2T^+ (conflicts with DT^+), or HDT^+ (conflicts with T_2^+) certainly does not make things easier.

As already pointed out, $[H_3^+]$ ions of mass $m/e = 3$ can be generated in the ion source during mass spectrometric analysis of molecular hydrogen [Bra04]. The ion – molecule reaction leading to the formation of $[H_3^+]$ ions is

$$H_2^+ + H_2 \longrightarrow H_3^+ + H \ .$$

Consequently, the amount of $[H_3^+]$ ions formed is directly proportional to the pressure of hydrogen molecules and to the number of $[H_2^+]$ ions in the ion source, which in turn is also proportional to the number of H_2 molecules in the source. Hence

$$[H_3^+] = k_3[H_2]^2$$

Likewise, the number of HD^+ ions is proportional to the number of hydrogen molecules in the ion source according to

$$[HD^+] = k_2[H_2] \ .$$

From this it follows that the intensities of $m/e = 2$ and $m/e = 3$ ions are given by expressions

$$I_2 = k_1[H_2]$$

and

$$I_3 = k_3[{H_2}^+][H_2] + k_2[H_2] \ ,$$

respectively, where I_3 results from the partial contributions of $[{H_3}^+]$ and $[HD^+]$ ions. The ratio of intensities I_3/I_2 is then

$$I_3/I_2 = \frac{[{H_3}^+] + [HD^+]}{[{H_2}^+]}$$

which conducts to

$$I_3/I_2 = \frac{k_2}{k_1} + \frac{k_3}{k_1}[{H_2}^+]$$

Accordingly, the I_3/I_2 ratio is a linear function of the mass two ion current. It therefore becomes possible to determine the ratio of constants k_3/k_1 from a plot of I_3/I_2 vs the amount of hydrogen injected into the mass spectrometer. The k_2/k_1 ratio, on the other hand, is obtained from the intercept of the straight line at the ordinate when the hydrogen pressure in the ion source approaches zero. Although the formation of trimer ions can be maintained small by proper choice of gas flow rates into the mass spectrometer, it is always prudent to verify their absence experimentally [McI57; Bea73b][43].

Another complicating factor in mass spectrometry of diatomic hydrogen isotopes are monoatomic ions generated with characteristic probabilities: e.g. ${H^+}/{H_2}^+ = 0.0082$ (0.0053), ${D^+}/{D_2}^+ = 0.0055$ (0.0040) and ${T^+}/{T_2}^+ = 0.0042$ (0.0035) [McI57] (values in parenthesis are from reference [Sch71]). The same holds for other hydrogen isotopologues, e.g. HD, HT, and DT, with the added complication that for example the ratios H^+/HD^+ and D^+/HD^+ from HD show significant differences. One more feature requiring attention are memory effects either from molecular hydrogen isotopes or species like water, isotopically substituted water, hydrocarbons,

[43] Price and Aslett [Pri95] found in the mass spectrum of pure deuterium the species ${D_2}^+$ to be 99.9969 % and ${D_3}^+$ to be 31 ppm.

etc. Hydrocarbons produce a large number of ions of different m/e ratios than of the parent ion. These ions are sometimes difficult to assign particularly when dealing with mixtures of gases. The latter is especially the case when hydrocarbons are isotopically substituted or contain other atoms like oxygen or nitrogen. It furthermore needs to be kept in mind that hydrogen isotopologues have different ionisation probabilities.

In case of an equilibrated hydrogen isotope mixture which does not contain other impurities, it is possible to calculate successively, solely on the basis of the unique mass $m/e = 5$ (DT^+) and mass $m/e = 6$ ($T_2{}^+$) and three equilibrium constants, the four other hydrogen species in the mixture (see section 2.5.1.8 and ref. [Sch71])[44].

The quantitative analysis of certain impurities in hydrogen like carbon monoxide (CO) and nitrogen (N_2) is quite challenging because of the rather high resolutions, i.e. > 3000, needed to separate the CO^+ and $N_2{}^+$ ions [Pri95].

It has been shown that the accurate determination of all components of ambient air, i.e. N_2, O_2, Ar, CO_2, and He-4 (atmospheric moisture was not removed from the samples) is possible with a VG 30-38 mass spectrometer. The detection limit for helium-4 was estimated to be 0.12 ppm.

Ions arising from natural stable isotopes of molecules present in the analysed gas mixture are on one hand complicating but may on the other be rather helpful. If judiciously used, natural isotopes may serve as reliable internal standards. While variations in the concentration of natural isotopes are usually very small, in special cases they may depart significantly from natural values. For instance, when the analysed gas is of industrial origin and the analysed gas is the product from an isotopic separation system. A further feature requiring attention is possible isotopic equilibration in the ion source.

Because the correct determination and interpretation of isotope ratios demands measurements of high precision, it is easy to understand why a high-resolution mass spectrometer together with personnel of ample germane experience on instrumental effects and their underlying causes constitute a fundamental requirement for a dependable qualitative and quantitative analysis of complex hydrogen isotope mixtures. In fact, sector field mass spectrometry is frequently used to calibrate quadrupole mass filters.

[44] Techniques used to accelerate equilibration include a hot wire, catalysts, or spark discharges, like those from a Tesla coil leak tester [McI57].

Advantages of sector field mass spectrometry for the analysis of hydrogen isotopologues are i) the high dynamic range from ppm to 100 %, ii) the possibility of identifying and analysing quantitatively all six hydrogen isotopes without the need for equilibration, iii) good commercial availability and iv) reliable maintenance service. Disadvantages are the i) high acquisition costs, ii) equipment of large overall dimension and weight, iii) need of frequent calibrations and maintenance, and iv) complexity of operation as well as of data evaluation requiring specially qualified professionals.

3.16.6.2 Quadrupole mass spectrometer

Quadrupole mass spectrometers are applied predominantly for the identification of gases having masses within the range $1 < m/e < 100$ and for the determination of their partial pressures in gas mixtures. The peripheral equipment required for the operation of a quadrupole mass spectrometer includes an ultra-high vacuum pumping system, an ion gauge, a power supply, amplifiers, controls, and a computer.

The relative sensitivities for H_2, HD, D_2, HT, DT, and T_2 of a quadrupole mass spectrometer were reported to be 1.00, 1.09, 0.99, 1.06, 0.96, and 0.88, respectively [Wat87].

At Tokamak Fusion Test Reactor (TFTR), Princeton, USA, a quadrupole mass spectrometer from Extranuclear, Pittsburgh, PA consisting of a quadrupole filter with 9.5 mm diameter rods run at 5.1 MHz and operated at an ionizing voltage of 70 eV, was used as main analytical tool [Voo95]. A Gallileo channel electron photomultiplier and a Faraday cup served for ion detection. The instrument was designed for a mass range of 70 atomic mass units. To evacuate the spectrometer to high vacuum, i.e. $< 10^{-6}$ mbar, a Leybold-Heraeus turbo molecular pump with a capacity of $120\,l\,s^{-1}$ possessing rotor bearings lubricated with grease was used. Yearly replacement of the grease was necessary to keep the pump in good running conditions.

JET Joint Undertaking, Abingdon, England, selected a quadrupole residual gas analyser from Spectra Metrics for the analysis of tritiated gases [Lae92; Lae99b]. Final vacuum in the mass spectrometer was achieved with an ion sputter pump combined with a SAES getter pump.

Extrel quadrupole, Pittsburgh, PA, mass spectrometers have likewise found application in tritium-handling laboratories [Gil88a].

At Chalk River Laboratories, Canada, a Spectramass DataQuad quadrupole mass spectrometer is employed for the analysis of the purity of T_2 (the only expected impurities are DT and D_2) [Mil95].

At HRC, Toyama, Japan, a quadrupole mass spectrometer manufactured by Anerva type M101QA-TDM was selected for tritium measurements. Ultra-high vacuum is achieved with a titanium sputter ion pump backed by a turbo molecular pump system [Tor13].

Advantages of quadrupole mass spectrometers are i) small dimension, ii) easy operation, iii) comparatively low cost, iv) low operational costs (essentially only personnel), iv) many suppliers, and v) good service. Main disadvantage is the relatively low resolution. To service numerous sampling points a sampling header and an exhaust header have been utilized successfully.

3.16.6.3 Omegatron

In an omegatron ions are generated inside of a box subjected to a strong magnetic field and an oscillating electric field orthogonal to the magnetic one. If the electric field is varied until it coincides with the cyclotron frequency of a particular ion species, these ions will singularly follow a spiral orbit with a radius that increases linearly with time until it impinges on a fixed collector. The resulting current will be a function of the partial pressure of the gas in the omegatron. The ion collector is of pure gold, the electrodes are of tungsten/gold (plated in liquid gold), and the cathode is of iridium coated with ThO_2 and has a surface area of $2\,mm^2$. Lowest detectable partial pressure is 10^{-12} mbar. The instrument can be heated up to 573 K during measurements and up to 973 K for degassing. The magnet has a 40 mm gap, pole pieces of $\varnothing = 100$ mm, and operates 0.4 T. The ion transmission is about 100 %. This instrument has been developed at University of Essen, Germany [Gen87].

Omegatron mass spectrometers have been tested successfully with tritium-bearing gases in glove boxes both at JET [Lae92] and at TLK [Gen85; Gen87; Eng91; Eng92; Cal01]. Their principal field of application is the quantitative analysis of hydrogen isotopes and helium. However, the instrument has also been applied for the investigation of the reaction between molecular tritium and carbon monoxide [Pen00a]. As apparent from the data plotted in Fig. 3.59, besides carbon dioxide a number of per-tritiated organic species could be identified among the products.

Because the resolution of the omegatron is given by the expression

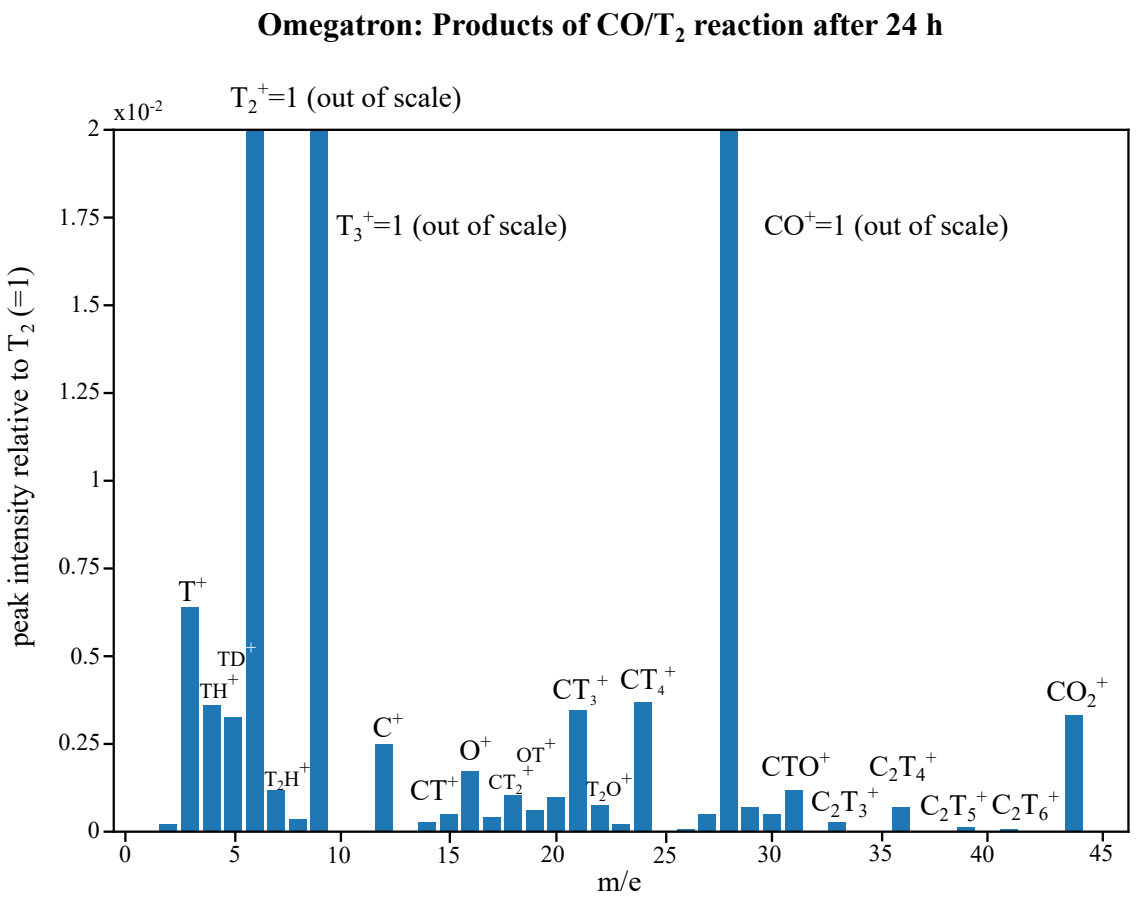


Figure 3.59: Mass spectrum of the products of the reaction of carbon monoxide with tritium obtained with an omegatron [Pen00a].

$$\frac{m}{\Delta m} = \frac{2000}{m}$$

where m is the mass of the ion, this mass spectrometer is especiallay suitable for the qualitative and quantitative determination of ions of low masses, e.g. hydrogen isotopologues, air components, helium, etc. An Omegatron can easily discriminate between all ions with $1 < m/e < 9$ except between T^+ and $^3He^+$ ions. The appearance of significant fractions of $Q_3{}^+$ trimer ions (Q = H, D, T) and of even higher mass ions in omegatrons has been attributed to peculiarities of its ion source [Cal01; Bea73c]. Whereas the $Q_3{}^+/Q_2{}^+$ ratio typical of natural hydrogen is only 3×10^{-4}, in omegatrons the same ratio reaches values almost two orders of magnitude higher, i.e. 2×10^{-2}, depending on the operation conditions. As opposed to this, a high resolution (> 1200 at $m/e = 2$) double focussing magnetic sector mass spectrometer from Fisons Instruments (VG

38-38) showed only 0.0031 % D_3^+ in 99.9969 % D_2^+ in the mass spectrum of pure deuterium [Pri95].

Advantages of the omegatron are i) rather high resolution for low masses, ii) comparatively simple operation, iii) relatively inexpensive, iv) low waste generation, v) moderate maintenance requirements, vi) low operating cost (personnel only), vii) cost of additional sampling points low, and viii) compactness. Conversely, drawbacks are: i) dependence of resolution from ion mass, ii) need of a special gas inlet system, iii) small dynamic range, iv) condensables and organics may plug capillary tubing, and v) limited commercial availability and service.

3.16.6.4 Special mass spectrometers

Gill et al. [Gil88b] developed a sophisticated time-of-flight mass spectrometric technique designed to provide information on the behaviour of hydrogen isotopes on surfaces. The technique allowed determination of the exchange rate between gaseous water vapour and hydrogen isotopes retained on the surface of solid materials. A limitation of this type of spectrometry is the comparatively low resolution.

A mass spectrometer equipped with a fixed dual collector system of only 1 l volume for the determination of ^{3}He and ^{4}He was developed by Halverson and Herzog [Hal81]. Ions were detected either with a Faraday cup or a photomultiplier. Aim of the spectrometer was the analysis of ^{3}He generated from the decay of very low concentrations of tritium in water or organic environmental samples.

Another mass spectrometer designed specifically for the quantitative determination of ^{4}He in ^{3}He within the range 2 - 100 ppm was developed and described in detail by Burton and Cornelius [Bur89].

3.16.6.5 Calibration of mass spectrometers

Mass spectrometers used in fusion-relevant tritium handlinmg installations require periodic calibration. For this purpose, either a pure gas like H_2, D_2, ^{3}He, etc. or a mixture of gases, for instance a six-component mixture consisting of H_2, D_2, ^{4}He, Ne, N_2, and Ar at equal concentrations, or T_2–D_2 mixtures of different concentrations have been utilized. Primary standards of ^{4}He in ^{3}He have been prepared gravimetrically [Bur89].

A satisfactory sequence of analysis of standards and samples to achieve high accuracy was shown to be i) vacuum background, ii) standard 1, iii) standard 2, iv) unknown sample, v) standard 1 or 2, vi) unknown sample, vii) and standard 1 or 2. With this sequence cross contamination is minimized.

Sensitivities of all analysed gases require verification on a regular basis. For example, the relative sensitivity of H_2/D_2 was determined to be 0.9392 ± 0.0035 [Pri95].

3.16.6.6 Sampling for mass spectrometry

Sizable and multifaceted processes frequently require analytical data from numerous sampling points in recurrent intervals. This can be accomplished with a fairly long line (up to 60 m) of small inner diameter connected to the sampling points through one or more remotely controlled manifolds. Analysis is then carried out centrally with a single analytical instrument like a sector field mass spectrometer, which is a fairly large and complex instrument, or with any other suitable analytical instrument like a gas chromatograph or a laser Raman spectrometer. In case of gases containing significant activities of tritium long capillaries must be protected by guard pipes. Tritium-bearing samples can be introduced sequentially into a mass spectrometer by means of remotely controlled actions. Sampling procedures as described above have been demonstrated successfully in several tritium handling facilities like TFTR [Voo95], Mound Laboratory [Bil73], JET [Lae92] and others. Surfaces of the sampling manifold and of the inlet piping to mass spectrometers have often been passivated, in order to reduce modifications of gas composition by isotopic exchange while the gas flows from the sampling location to the analytical instrument. Trace heating of pipes at ≈ 400 K contributes effectively to minimize memory effects. Because composition at various sampling points may differ substantially it is important to purge, for example with nitrogen or helium, and evacuate the sampling manifold carefully. It is advisable to isolate repeatedly the manifold for a period consistent with a typical sample drawing time to obtain a back-ground value. This may also serve to corroborate the overall vacuum tightness of the sampling zone. To obtain a representative gas sample, the first aliquot is usually evacuated with a turbo molecular pump into a disposal tank. To perform an analysis, a pre-evacuated, medium sized expansion volume, e.g. 1 - 3 l, is typically filled with a low pressure of the unknown gas ($\ll 1$ mbar). To analyse the sample quantitatively it is necessary to wait until equilibrium has established. Gas is then fed from the batch volume into the mass spectrometer either through

a gold leak or through a pinhole (molecular leak). Another commonly utilized option is a fine needle valve. To avoid demixing, it is necessary to inject the gas under molecular flow conditions. In the ion chamber of the mass spectrometer the pressure is adjusted to a value of the order of 1 mPa. Ionisation chambers of suitable dimensions can be employed to provide complementary information on the amount of tritium present in an unknown sample.

Whereas sampling lines used at JET have a diameter of 0.635 cm (1/4 in) [Lae92], the ones installed at TFTR [Voo95], Mound Laboratory [Bil73], TSTA[And75], and TLK [Lae01b] are capillary. Typically, 15 - 20 different sampling points have been identified in these facilities. In some facilities mass spectrometers are housed in a dedicated glove box and in others a containment was considered unnecessary. Rejected or already analysed samples are evacuated by an assigned vacuum system and released through a Central Detritiation System.

Capillaries contribute to minimize the inventory of mobilized tritium. Because capillaries can easily be damaged they require passive protection when installed inside of glove boxes and a protective jacket when used for the transport of tritium between glove boxes. Drawbacks of thin tubing are memory effects, possible clogging, and inefficient evacuation. Conversely, pipes having a diameter of 1/4 in are sturdy, easier to evacuate but enclose large amounts of sample. In some cases, a sizeable sample does not constitute a problem, e.g. when there is enough gas available or unused gas can be returned to the vessel of origin.

Results published by Longhurst and Cleaver [Lon08], who determined the breakthrough of deuterium when passing a mixture of highly diluted deuterium in ultrapure nitrogen through a 33 m $1/8^{\text{th}}$ inch stainless-steel SS304 tubing maintained at ambient temperature admonish to caution (see also section 2.14.1.7. A strong delay through the capillary with respect to the time estimated for the gas to travel from the tube inlet to the outlet point was noticed, which was attributed to adsorption of deuterium on and diffusion into the stainless-steel bulk as it travelled along the tube. Lengthways the path most deuterium is converted into deuterated water (see section 2.14.1.7 and Fig. 2.44). Calculations confirm the presumption that longer breakthrough times result from saturation of the tube wall by atomic deuterium. Hence, concentration and chemical form of highly diluted hydrogen isotopes passing through a long tube will depend upon tube length, time at which the measurement is performed, temperature (eventually trace heating), type of carrier gas, concentration of hydrogen in the carrier gas, condition of the metal surface, etc. An even more pronounced effect can be expected for gases carrying tritium.

In case the line is trace heated, increased migration of hydrogen into the bulk of the line and enhanced isotopic exchange need to be expected.

3.16.7 Gas chromatography

For a gas chromatographic analysis of samples of unknown composition aliquots are passed through a thermostatized separation column using helium, nitrogen, or another carrier gas maintained at constant flow rate. Each constituent of the sample is then transported through the column with a characteristic retention time. Retention times depend on a number of factors like i) type of gas being separated, ii) temperature of the column, iii) type of packing material, iv) type of carrier gas, v) carrier gas flow rate, vi) length and width of the column, etc.

Prior to qualitative and quantitative analysis of unknown samples, retention times and specific calibration factors must be determined under well-defined conditions for each species anticipated in the mixture. For the detection of tritium-bearing species exiting sequentially a separation column the most common devices are: i) helium ionisation detector (detects basically all gases except the carrier gas), ii) thermal conductivity detector (detects basically all gases except the carrier gas), and iii) small volume ionisation chambers which detects exclusively HT, T_2, DT, and all hydrocarbons or species like ammonia with one or more bound hydrogen atoms substituted by tritium. A flame ionisation detector has also been utilized primarily because of its very high sensitivity for almost all organic compounds and otherwise good properties [Lae92]. This kind of detector, however, is usually not recommended for routine work in a glove box because of safety considerations.

Gas chromatography has been since many decades a well understood analytical technique for the qualitative and quantitative analysis of gases. A vast body of relevant literature is available on the subject. In this section only topics of conventional and radio gas chromatography as well as of micro gas chromatography pertaining the requirements of tritium handling facilities will be addressed in some detail.

3.16.7.1 Conventional gas chromatography

It is common knowledge that most analytical problems posed by inorganic and organic tritium-bearing and tritium-free gas mixtures cannot be solved with a simple, one column gas chromatograph. This is particularly the case when dealing with samples consisting of several different

species covering a wide range of concentrations and boiling points. The presence of several hydrogen isotopologues constitutes an additional special challenge [Kaw08]. Therefore, for complex gaseous mixtures more than one column and more than one temperature program are often necessary to achieve sufficiently good separations of all species. In addition, sometimes more than one detector is necessary to tackle an analytical problem. Moreover, in some cases complementary analytical techniques such as mass spectrometry, Raman spectroscopy, infra-red spectroscopy, or Omegatron spectroscopy are imperative for an unequivocal component identification and quantification.

Gas chromatography is one of the most frequently employed technique for the analysis of gases. This is because of its i) simplicity, ii) easiness of routine operation, iii) comparatively low cost, iv) high sensitivity and accuracy, v) broad spectrum of analysable species, vi) small sample requirement, vii) excellent commercial availability, and viii) good maintenance service. On the negative side are i) long retention times of some species, ii) sometimes ambiguous peak assignment, iii) insufficient leak-tightness for work with radioactive gases (holds especially for a large number of required four-way Valco valves), and iv) substantial heat source when housed in a glove box.

3.16.7.1.1 Analysis of hydrogen isotopes

Hydrogen is a special molecule not only because of the existence of three isotopes of substantially different mass but also because homo nuclear hydrogens, i.e. H_2, D_2 and T_2, give rise to spin isomers: the spins of two hydrogen nuclei may either couple to form a triplet state (odd-J H_2 or ortho hydrogen) or a singlet state (even-J H_2 or para hydrogen) (see also Table 2.5).

Bachmann et al. [Bac62] were the first to show that ortho-hydrogen can be separated from para-hydrogen practically without overlapping on an iron-free[45] 5A or 13X molecular sieve column maintained at liquid oxygen temperature. At standard temperature and pressure the ratio of ortho to para is nearly 3:1. If, however, thermal equilibrium between the two forms is established, for instance in the presence of a catalyst like ferric oxide or activated carbon, the even-J H_2 form of hydrogen dominates, e.g. 89 % at 40 K.

[45] Iron catalyses the ortho-para conversion.

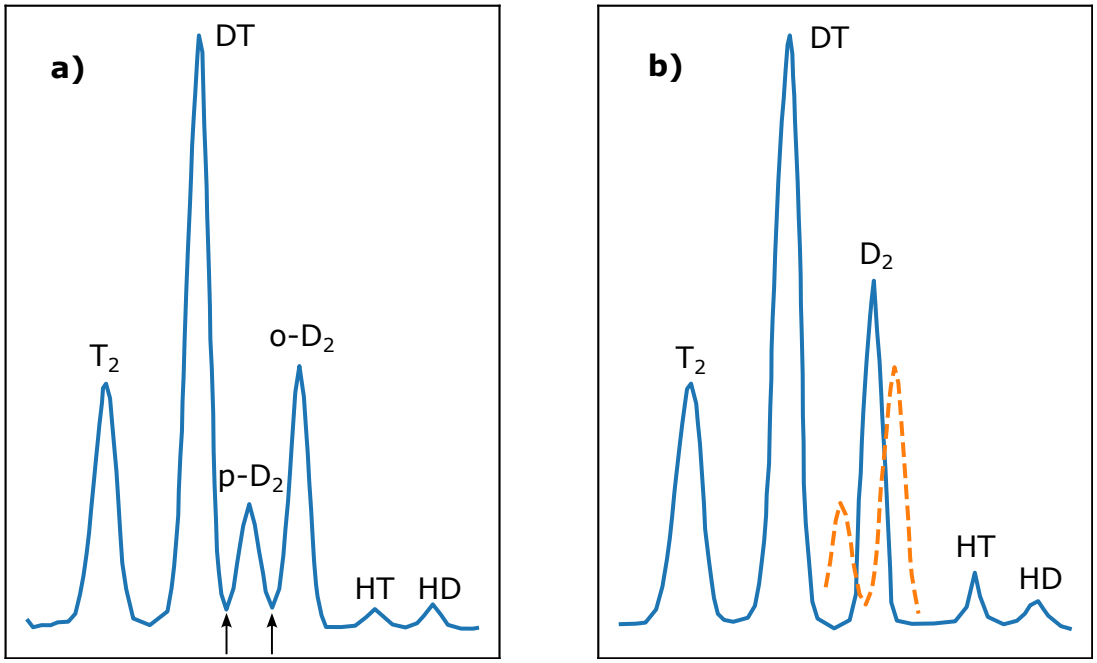


Figure 3.60: Gas chromatographic separation of a D_2, DT, and T_2 mixture consisting of 25.3 mol, 49.5 mol and 25.2 mol, respectively. All constituents of the mixture were determined with the same attenuation. The gas chromatogram on the left was obtained with a column without catalyst and the one on the right with a column doped with iron. The dotted line shows for comparison the original ortho and para hydrogen peaks. Hydrogen is only present in trace concentrations (after [War76]).

On account of the above, the gas chromatogram of a D_2, DT, and T_2 mixture passed through a catalyst-free molecular sieve column shows i) T_2 and DT peaks, ii) ortho deuterium and para deuterium peaks and iii) probably small peaks of HD and HT peaks, which originate from the presence of small amounts of hydrogen impurity in the D-T mixture (see Fig. 3.60a) (the arrows point to insufficient separation). If, however, a catalyst layer is applied on the molecular sieve surface the ortho and para peaks unite into a single peak that is perfectly well separated from the other two molecular peaks (see Fig. 3.60b) [War76].

The formation of a single peak is explained by the occurrence of a slow inter-conversion between ortho and para hydrogen

$$\text{ortho hydrogen} \rightleftharpoons \text{para hydrogen}$$

during their passage through the molecular sieve column doped with iron. Presumably, the exchange (partition) between the mobile and immobile phase of both species takes place fairly rapidly. While without interconversion each species would migrate with a retention time of its own, in case of interconversion each molecule migrates partly as ortho hydrogen and partly as para hydrogen at their corresponding characteristic retention time. The consequence is that out of two peaks a single one with a retention time somewhere between the two establishes. More details on the theoretical background of this interconversion, are provided in a paper by Keller and Giddings [Kel60].

The ortho-para hydrogen interconversion is also catalysed effectively by magnesium chloride ($MgCl_2$) on alumina [Tan88]. Stockmeyer[Sto91] employed neutron transmission measurements to show that hydrogen adsorbed on chabazite displays interconversion even at cryogenic temperatures within the range 40 – 70 K.

The first complete separation of all six hydrogen isotopes, i.e. H_2, D_2, T_2, HD, HT, and DT, by gas chromatography was successfully achieved by King [Kin63]. For the separation he used a 3 m long coiled glass column containing activated alumina covered with a layer of iron hydroxide, which was applied to avoid the presence of ortho and para hydrogen. The column was submerged into liquid nitrogen. Carrier gas was helium. To increase the sensitivity of the thermal conductivity detector, effluent hydrogen isotopes were converted into their corresponding oxides by passing them through a heated copper oxide bed. Peaks were assigned classically by comparison with the retention times of pure compounds.

Genty and Schott [Gen67; Gen70] succeeded during the late Sixties with the separation of all six hydrogen isotopes within a period of only 45 minutes using the same kind of column but first activated under vacuum at 493 K for 24 hours and then treated with carbon dioxide. They improved the overall detection capability by analysing effluent gases with a combination of thermal conductivity detector and ionization chamber. To increase the sensitivity of the thermal conductivity detection they replaced helium carrier gas by neon. Genty and Schott [Gen70] proofed experimentally that in an equilibrated mixture the concentrations of H_2, HD, and D_2 can be obtained by calculation from known concentrations of T_2, HT, and DT determined gas chromatographically utilizing an ionisation chamber. They provided evidence that mass spectrometry and gas chromatography deliver nearly the same results for all six hydrogen isotopes. For the analysis of a mixture of all hydrogen isotopes a calibration was not found to be necessary.

Vogd et al [Vog88] performed parametric studies at temperatures in the range 123 - 183 K to compare the separation effectiveness of all hydrogen isotopes with columns packed with type 3A, 4A, or 5A molecular sieves containing some charcoal as catalyst for the ortho-para hydrogen interconversion Their conclusion was that type 5A displays the best properties for analytical as well as preparative purposes.

Kawamura et al. [Kaw08] were able to achieve a good separation of hydrogen and deuterium on a mordenite column at 144 K but did not succeed with the separation of HD from these two isotopologues at the same temperature. Several GC separations were also performed at TLK using a modified mordenite column operated at 173 K and employing helium as carrier gas. An ionisation chamber of 4 cm^3 volume served as tritium detector. Calibrations were carried out with two standards containing either $(7.25 \pm 0.26) \times 10^5$ Bq cm^{-3} or $(4.51 \pm 0.22) \times 10^8$ Bq cm^{-3} of tritium. Separation of HT and DT was possible at 173 K. The detection limit for tritium in hydrogen was determined to be 1 ppm. Because of the high moisture adsorption efficiency of the GC column, the exiting carrier gas was at all times highly dry and the ionisation chamber displayed no memory effects. A column containing modified mordenite showed little peak tailing and good separation in moderate time at mild cryotemperature when compared with an aluminum oxide or molecular sieve 5A packing.

Projecting the above results to the analysis of hydrogen isotopes at ITER leads to the ascertainment that gas chromatography at cryogenic temperatures is advantageous because of: i) high accuracy, ii) good detection limit, iii) good reproducibility, iv) capability of separating HT and D_2, v) sampling points of low cost, and vi) possible analysis of He-3. Conversely, the disadvantages are: i) long overall retention times, e.g. 30 - 40 min, ii) gas chromatograph open to process lines, iii) need of confinement, and iv) generation of much expensive neon carrier gas waste (estimation for ITER of the order of 100 l d^{-1}).

3.16.7.1.2 Analysis of mixtures of hydrogen isotopes together with other species

At JET, Culham

An analytical strategy designed to solve most analytical problems expected to arise during plasma exhaust gas processing was developed at JET. It is based on two gas chromatographic (GC) systems equipped with a total of five columns and tailored to allow i) analysis of samples

covering a rather broad range of concentrations while keeping cross contaminations at a minimum, ii) conduction of quite diverse and complementary analytical separation tasks and iii) swift switching for the best detector for each single analytical task [Lae92; Lae93; Lae01b; Lae02c].

The *first GC system* is furnished with two 4-way Valco valves and four separation columns, and the *second GC system* with one 4-way Valco valve and one separation column. 4-way Valco valves are needed to switch gaseous streams from i) one separation column to another, ii) from one detector to another, or iii) directly to the exhaust detritiation system. Valco valves are likewise used to switch the injection system to the evacuation pumps. Two stainless-steel columns, packed with molecular sieve 13X, are employed for the separation of He, Q_2 (Q = H, D, T), O_2, N_2, C_xQ_y and CO; one stainless-steel column packed with HayeSepD material is predominantly employed for the analysis of water; and another column consisting of copper tubing packed with Fe-doped alumina is utilized for the separation of helium and all six hydrogen isotopes. Whereas the first three columns are maintained at 323 K in an oven, the cryogenic column, which is placed outside of the secondary confinement, is submerged into a Dewar filled with liquid nitrogen maintained at 77 K. Species that may condense or be adsorbed on the gas chromatographic column held at 77 K must be prevented from entering the column.

For sample injection (initial pressure of the order of 0.03 bar) the gas to be investigated is first expanded into one of two previously evacuated long capillary columns and then compressed with helium, nitrogen, or neon (gas best suited for the determination of He) [Lae99c]) up to a pressure of 1.4 bar into a small sampling volume of 0.1 - 0.2 cm^3 connected to a Valco valve. Pressurization increases the amount of sample ready for injection. Furthermore, pressurized samples deliver sharp gas chromatographic peaks and allow repetitive injection of identical amounts into the column. The gas in the sampling volume of the 4-way Valco valve is now ready for injection into one of the columns packed with molecular sieve and operated at 323 K. Helium and hydrogen isotopes, which exit unseparated this heated column rather rapidly, are then injected via another Valco valve into a column packed with Fe-doped alumina and maintained at 77 K. These operation conditions allow efficient separation of He, H_2, HD, HT, D_2, DT, and T_2. Gases exiting this column are analysed sequentially with a thermal conductivity detector (when H_2, HD, HT, D_2, DT, and T_2 are present at concentrations higher than 0.5 %) or a small ionisation chamber (when HT, DT, T_2 are present at concentrations of > 10 ppm) (see Fig. 3.61).

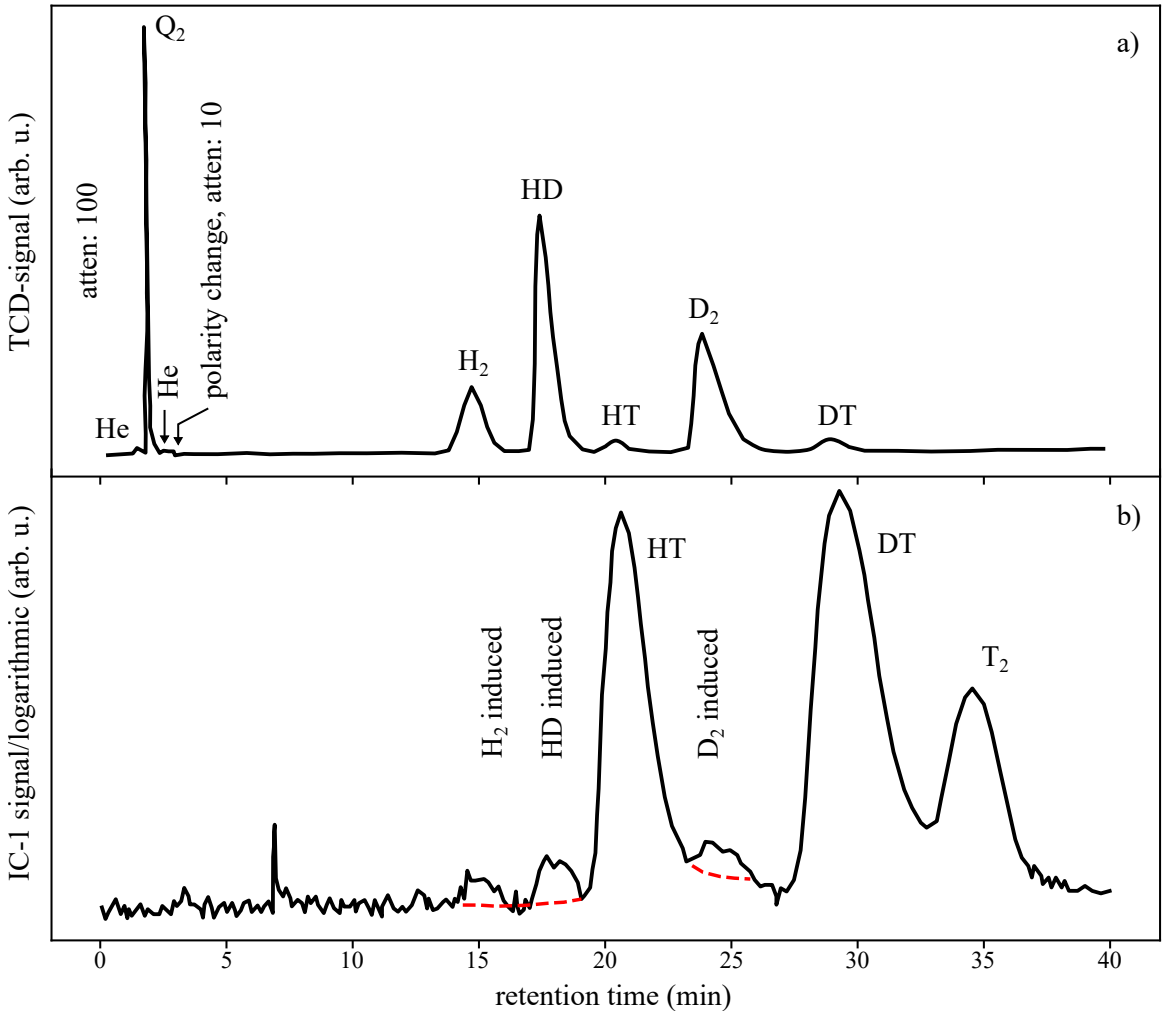


Figure 3.61: Comparison of the eluate when a mixture of six hydrogen isotopologues is injected into an iron-doped alumina column held at cryogenic temperature and analysed with two different detectors. The upper figure shows the peaks registered with a thermal conductivity detector and the lower one those with an ionisation chamber when both chromatograms have the same time scale. Note that the sensitivity of ionization chambers is far higher than that of thermal conductivity detectors [Lae99c].

The high separation efficiency of cryogenic columns takes place at the expense of retention times, i.e. they become comparatively long (more than 35 min for heavy hydrogen isotopes).

The *second gas chromatographic system* at JET is used to separate and detect CO, CO_2, tritiated and tritium-free higher molecular weight hydrocarbons (C_XQ_Y), and water (Q_2O), as well as tritiated and tritium-free hydrogens (Q = H, D, T). For this purpose, a HayeSepQ column is utilized, which if necessary may additionally be temperature-programmed to reduce the retention times of the higher hydrocarbons. Detection of separated peaks is carried out

with a flame ionisation detector, an ionisation chamber, or a flow proportional counter detector. CO and CO_2 are converted into methane with a "methanizer" that operates with a heated catalyst and a stream of hydrogen. By this procedure they become indirectly detectable with the flame ionization detector. Because these three detectors are rather quickly saturated by high concentrations, the gas chromatograph is furnished with a splitter that reduces the size of the sample by about two orders of magnitude. The flow proportional counter detector is used only sporadically because its sensitivity was found to be far too high - even behind the splitter.

The use of long stainless-steel tubing (⌀ 1/4 in) for the transport of gaseous samples between several process sampling points and the GC systems was shown to be feasible and practical at the Active Gas Handling System of JET [Lae99c]. This pipe size allows easy and fast supply of gas up to the analytical equipment and thereafter straightforward evacuation or purging. In comparison to capillaries, further advantages are ruggedness and lower memory effects. In several laboratories capillary tubing placed in guard pipes is the preferred option, e.g. Mound Laboratories [Lin87]. From the point of view of inventory minimization, gas transport is usually performed at low pressures.

At TLK (CAPER):

The semi-technical plasma exhaust processing experiment CAPER operated at TLK exemplifies to a large extent the plasma exhaust processing concept currently under realization for ITER [Glu97a; Glu98b; Glu00a; Bor05]. Hence, it is licit to argue that, just like the previously discussed analytical strategy of JET, the successfully implemented and verified gas chromatographic concept of TLK has also demonstration character. For the analysis of gases entering and exiting the main components of the three-step process CAPER a special gas chromatograph has been developed and installed inside of the main glove box [Lae02c].

Major gaseous species that need to be determined gas chromatographically together with their expected concentration ranges are:

- H_2, HD, D_2, HT, DT, T_2: 0.1 - 100 %
- O_2, N_2: 0.1 - 100 %
- Methane and higher hydrocarbons: 0.1 - 20 %
- CO and CO_2: 1 ppm – 50 %

- Tritiated inorganic and organic species: 1 ppm – 100 %
- Water vapour: > 0.1 ppm

Five different gas chromatographic systems are in use at TLK. One gas chromatograph (GC1) is part of the plasma exhaust clean-up simulating system CAPER. It is mounted in one of several glove box modules housing the CAPER facility. Two gas chromatographs (GC2 and GC3) are installed in the vicinity in glove boxes enclosing the Tritium Measurement Technique system. These gas chromatographs are equipped with several and diverse gas chromatographic columns, and are available to perform complementary analyses, partly in grab sampling modus. Further two GC´s comprise a special and a conventional micro gas chromatograph.

The gas chromatograph that predominantly is used to solve the analytical problems of the CAPER experiment is a type "Sichromat" from Siemens (GC1). This gas chromatograph was found to meet basic tightness requirements because even when handling tritium at very high concentrations the background values in the confinement remained unaffected. To re-direct gases GC1 is equipped with three 4-way Valco valves. Gases are prepared for injection into separation columns by compression with carrier gas. For this purpose, the "Sichromat" is equipped with two long capillaries each having a volume of 15 cm^3 and an inner diameter of 1 mm. For the separation and analysis of gases three columns (packing materials: Porapak Q (O_2, N_2, CO, CQ_4, CO_2, Q_2O, CnQm, Q = H, D, T), Al_2O_3 doped with Fe (helium-3 and all hydrogen isotopes), and molecular sieve 5A ($^3He + {}^4He$, Q_2, CQ_4, CnQm), all being more than 2 m long and having an outer diameter of 3 mm, are available. In addition, three thermal conductivity detectors (for concentrations in the range 0.05 - 100 %) and three small ionization chambers (for concentrations in the range 0.1 - 100 ppm) connected in series have been installed. Separations that can be performed with the GC1 gas chromatograph using three columns and 6 detectors are summarized in Table 3.12. When a gas mixture consisting of He, Q_2, O_2, N_2, CO, CQ_4, CO_2, Q_2O, and higher hydrocarbons is injected into the Porapak Q column helium and hydrogen isotopes pass through the column without separation in a rather short time while the other gases are retained. He^3 and all hydrogen isotopologues except H_2 (H_2 is added in front of the thermal conductivity detector to circumvent the anomaly in thermal conductivity of H_2–He mixtures [Han64]) are separated and quantified employing the alumina/Fe column (77 K) which is installed downstream. The separated peaks are registered with a thermal conductivity detector (catharometer) as well

Table 3.12: Gas chromatographic columns and detectors used to identify the gaseous species observed at CAPER (after [Lae02c]).

Column	Detector	Species that can be separated	Range
Porapak Q, 6 m, 243 - 373 K, He	He ionization	$O_2, N_2, CO, CQ_4, CO_2, Q_2O$, C_nQ_m	0.1 - 100 ppm
	Ionization chamber	CQ_4, Q_2O, C_nQ_m	> 0.1 ppm
Al_2O_3 with Fe, 2 m, 77 K, He	catharometer	^3He, $H_2, HD, HT, D_2, DT, T_2$	0.05 - 100 %
	Ionization chamber	HT, DT, T_2	> 0.1 ppm
Molecular sieve, 5 A, 6 m, 333 K, N_2	catharometer	$^3He + {}^4He$, Q_2, CQ_4, C_nQ_m	0.05 - 100 %
	Ionization chamber	$HT + DT + T_2, CQ_4$, C_nQ_m	> 0.1 ppm

as with an ionisation chamber connected in series. All other gases remaining trapped on the Porapak Q column are subsequently subjected to a separation under a temperature program while the eluent stream has been redirected by a Valco valve from the alumina/Fe column to the He detector and the other ionisation detector. Because trapping can lead to increased flow resistance and eventually to clogging, timely switching of gas streams with Valco valves is very important. Chromatographic signals of the six detectors are fed into a PC and analysed with a "Chromeleon" software. This software allows efficient data storage and transfer of data to other software systems for further evaluation and archiving. Exhaust gases from the columns pass through a pressure regulator which effectively contributes to circumvent pressure fluctuations caused by the downstream pumps that transfer the gases to the Central Detritiation System of TLK.

3.16.7.2 Micro gas chromatography

Besides conventional gas chromatography, good results have also been achieved with micro gas chromatographs. Within this frame, the industrial experience accumulated by the petro industry with micro gas chromatographs where they are used mostly for product control has been of much benefit. Crucial components of this technique are capillary separation columns.

In early work, Bruner et al. [Bru69] separated all deuterium and tritium substituted methane's with a 47 m long coiled glass capillary column maintained at 77 K exhibiting on the inner wall a thin layer of active silica. The carrier gas consisted of 70 % nitrogen and 30 % helium. In their experiments, a hydrogen flame detector and an ionisation chamber served for the identification and quantification of effluents.

Kawamura et al. [Kaw01] utilized a commercial micro gas chromatograph from MTI Analytical Instruments Inc. equipped with a small thermal conductivity detector for the analysis of hydrogen isotopes. This instrument is equipped with semiconductor processing technology. For work with hydrogen isotopes, they modified the instrument to allow submersion of the separation column into a Dewar containing liquid nitrogen placed outside of the chromatograph. In comparison to gas chromatographs employing conventional columns, separation in a micro GC takes place in considerably shorter time while maintaining excellent separation. Retention times measured for H_2, HD, and D_2 were found to be 43 s, 47 s and 54 s, respectively. The tubular column had a length of 4 m and an inner diameter of 0.53 mm. The inner surface of the column was covered with a 0.08 mm thick porous layer consisting of alumina with an applied $MnCl_2$ coating. Good sensitivities were achieved with neon as carrier gas. In view, that commercial micro GC´s are insufficiently vacuum-tight (leaks were detected at pumps, connecting tubing, valves, etc.) they were installed inside of a glove box when handling gases of high tritium content.

Lässer et al. [Lae03b] performed at TLK micro gas chromatographic separations utilizing a 4 m long alumina/$MnCl_2$ capillary column maintained at 77 K, a 25 m long Haysep capillary column operated at ambient temperature, and a 4 m long molecular sieve 5A capillary column held at 77 K. With these columns they were able to separate He, H_2, HD, D_2, N_2, CH_4, CO, CO_2, C_2H_6, and C_3H_8 at retention times of less than than 3 min. This illustrates the great potential of micro GC for the quantitative evaluation of isotopic composition and chemical purity of plasma exhaust gases.

Beloglazov et al. [Bel05b] employed a micro gas chromatograph manufactured by Agilent Technologies Inc. which was equipped with a 4 m long column containing alumina coated with $MnCl_2$. This column required occasional regeneration by heating at 393 K for over one hour. The micro GC was utilized to investigate the fast release of hydrogen isotopes (H_2, HD, D_2) from a heated zirconium cobalt getter bed. In spite of the comparable short separation time achievable with the capillary column, grab sampling for subsequent analysis could not be avoided because

separation and sampling time added together were longer than the experimentally required minimum sampling rate of 2 per min.

At JET, Culham, a second micro gas chromatograph furnished with a micro thermal conductivity detector proofed to be superior to conventional gas chromatographs for the analysis of the composition of plasma-off gases. Especially the analysis of higher hydrocarbons, e.g. up to decanes, was found to be rather long-lasting when using conventional chromatographs [Gru11]. To avoid contaminations by tritium, the micro GC was installed inside of a glove box. It is equipped with three modules, each provided with a different capillary column, i.e. CP-Sil 5CB, PoraPlot Q, and 5A molecular sieve. All primary containment welds of the gas chromatograph were subjected to a radiography examination. In addition, a helium leak test was carried out after assembly of the pipe work. The specified amount of injected sample was rather small: 10^{-6} - 10^{-5} dm^3. To compress the sample up to 100 kPa, which is the pressure needed for an analysis, the gas is first introduced into a previously evacuated capillary and then pressurized with the carrier gas in plug flow mode. A clean separation of a number of impurities and numerous heavy hydrocarbons generated by plasma-wall interactions at the end of the JET campaign with a carbon first wall was successfully demonstrated.

Advantages of micro gas chromatography can be summarized as follows: i) short retention times, ii) small amounts of sample and therefore minimal amounts of gaseous radioactive waste, iii) high separation efficiency, iv) equipment of small size that easily fits into a glove box, and v) comparatively low cost.

With respect to the fusion fuel cycle, micro gas chromatopraphy was shown to possess the capability for the qualitative and quantitative analysis with short retention times and sensitivities in the ppm range of most relevant gaseous species.

3.16.7.3 Calibration of gas chromatographs

Accurate pressure-volume-temperature determinations are essential for the preparation of deuterium-tritium-hydrogen mixtures of the kind needed for the calibration of gas chromatographic measurements [Sch13c; Sch13b]. Calorimetry backed up by mass spectrometry (MS) or gas chromatography (GC) has been utilized to verify pressure-volume-temperature (PVT) measurements of tritium-bearing mixtures prepared for the qualitative and quantitative analysis of all hydrogen species present in gaseous mixtures [Lin87; Koe09]. To control tritium inventory results,

Lindner et al [Lin87] filled fifty bottles with different concentrations of all three isotopes of hydrogen via pressure–volume-temperature measurements. According to their observations the amounts of tritium obtained from PVT measurements combined with mass spectrometry plus their uncertainties[46] completely overlapped the calorimetric measurements plus their respective uncertainties.

At TLK, gas chromatographs are calibrated with mixtures of hydrogen isotopologues including tritium at concentrations in the range 0 - 100 % [Koe09]. The inventory of tritium in these mixtures is determined with a calorimeter of high accuracy (better than 1 %)[47] and precision (or reproducibility) better than 0.1 %. Important advantage of the quasi isothermal calorimeter is the diverse and non-destructive character of the technique. To generate a calibration straight line, several deuterium- or hydrogen-tritium mixtures are prepared by volumetric measurements and prolongued mixing. After equilibration they are filled into stainless-steel vessels that fit into the calorimeter. The total amount of gas in each vessel and its composition is calculated from pressure-volume-temperature (PVT) measurements employing procedures developed by Köllö [Koe11] (see also section 3.16.1 or Schlösser et al. [Sch13c; Sch13b].

Statistical evaluations of several pressure–volume–temperature systems for gases such as needed for volumetric measurements employed in calibrations were carried out by Bohl and Sellers [Boh68] as well as by Lindner et al. [Lin87]. Independent errors were assumed for the analysis because all measurements were performed with different devices. The basic hypothesis was that an error in one reading does not cause errors to readings from another. It is complicating that in some cases the uncertainty can be a function of the quantity determined. In conclusion, PVT measurements of tritium with accuracies better than 0.1 % are possible, provided all parameters are carefully controlled.

While for calibrations the response of an ionization chamber is directly and only proportional to the radiation passing through the chamber [Gen70; Lae92; Lae99c], the response of catharometers depends on the nature of the gas [Gen70; Lae99c]. The sensitivities of hydrogen isotopes were found to increase in the order $H_2 > HT > T_2$ or $H_2 > HD > D_2$ [Gen70; Tan88; Lae93].

[46] The uncertainty of mass spectrometric results was highest at samples with about 50 mol % tritium because of difficulties in resolving the mass spectrometric peaks of all six isotopic molecular species.
[47] Accuracy is the degree of veracity or closeness to the actual quantity.

Calibration factors expressed relative to methane and detection limits for carbon oxides as well as for a number of hydrocarbons obtained with a flame ionisation detector were published by Lässer et al. [Lae99c].

3.17 Determination of tritium radioactivity in gases, liquids and solids

This section is devoted to a discussion of techniques frequently employed for the determination of tritium in gases, liquids, and solids. The techniques are of relevance to process analytics, process control, elucidation of radiochemical reactions and process mechanisms, safety in tritium handling facilities, etc. Methods employed for the routine surveillance of tritium in the environment are treated only marginally.

In case of liquids or gases it can be assumed that tritium will be distributed homogeneously within the diluent. Conversely, for tritium in solids it is necessary to distinguish between i) the fraction of tritium on the surface directly measurable for instance with a windowless detector[48], ii) the fraction of removable tritium which can be measured by swipes (important from a radiation protection point of view), and iii) the total amount of tritium on and in the surface as well as in the bulk (frequently distributed non-homogeneously).

3.17.1 Ionisation chamber

Ionisation chambers are well suited for monitoring tritium in air. They also find wide application for the determination of tritium in process gases, glove boxes, exhaust gas of Detritiation Systems, or as detectors in radio gas chromatography. Beta-particles passing through ion chambers generate ion pairs which are collected by an electric field applied across the chamber. Ion pairs produced outside of the chamber must be removed with a filter and an ion precipitator before reaching the chamber.

It has been estimated that about 40 GBq of tritium will generate an ionisation current of approximately 1 µA. To convert current into concentration of tritium ($\mu Ci\,m^{-3}$) a simple rule of thumb is:

$$\frac{10^{15} \cdot \text{current in Ampére}}{\text{chamber volume in litres}} .$$

[48] Because of the short range of betas emitted by tritium in solids a direct measurement will only detect the fraction of tritium present on or close to the surface

In other words, a tritium concentration of 40 kBq m^{-3} will generate an ionisation current of 1 fA in a chamber of one litre volume.

The chemical form of tritium-bearing species in a gas stream, e.g. tritiated hydrocarbon, HT, or HTO, was found to influence significantly the reading of ionisation chambers [Nis89b]. Adsorption and isotope exchange reactions between tritium in the gas phase and that adsorbed on the electrode were shown to give rise to substantial memory effects. The utilization of a copper electrode (see also above) ameliorated the problem.

As apparent from the data in Table 3.13 the degree of ionisation induced by tritium is measurably dependent on the nature of the carrier gas [Att76]. Consequently, in gaseous mixtures the current output of the chamber will be a function of composition. In fact, Rodrigo et al. [Rod92] stressed the need to calibrate ionisation chambers with representative process gases under representative operating conditions because not only the main gases but also impurities were shown to have a complex effect on measured ionization currents [Rod95b]. This is known as **Jesse effect**. For example, the effect caused by 25 ppm ethylene in argon is almost completely suppressed by 0.5 % nitrogen [Par72]. Moreover, at low concentrations of tritium the experimental calibration values were significantly higher than theoretical predictions.

In-line, compact, ultrahigh vacuum compatible, and bakeable simple ionisation chambers were developed by Kherani and Shmayda [Khe89; Khe92b; Khe94]. A parametric study provided evidence that the measured current was practically equal to the saturation current. Memory effects could be mitigated by baking as well as by diamond-polishing the inner surfaces and subsequently treating the surfaces by an electro polishing procedure. Detection limits of the order of 10^4 Bq m^{-3} were shown to be achievable.

To characterize the performance of ionisation chambers Kherani and Shmayda designed and fabricated low level (large volume = 0.99 l) and medium level (small volume = 0.085 l) ionization chambers. They proved that these chambers can provide reliable HTO monitoring results if maintained at 373 K and a carrier gas stream of 1 % relative humidity is used at ambient temperature and pressure. Calibrations were carried out with a nitrogen carrier gas containing HT, which was oxidized to HTO on CuO windings maintained at 973 K. To determine tritiated water in a gas stream water bubblers were selected as integrators. The influence of i) carrier gas flow rate, ii) pressure at two constant tritium activities, and iii) collector potential on the monitor signal was investigated parametrically. At least up to carrier gas flow rates of 35 l min^{-1} neither

Table 3.13: Ionization induced by tritium in several gases [Att76].

Gas	Ion pair/disintegration	Relative ionization
Hydrogen	132	0.69
Nitrogen	158	0.82
Helium	162	0.84
Carbon dioxide	162	0.84
Methane	193	1.00
Argon	205	1.06
Propane	218	1.13

the low level nor the medium level monitors were influenced by the flow rate. The investigated tritium concentrations covered the range from 3.7×10^{-5} - 37 GBq m^{-3}. Monitor responses were found to be directly proportional to pressure within the range 15 - 100 kPa but deviated from proportionality to higher values at lower pressures.

Small and large open wall ionisation chambers, having volumes of 15 cm^3 and 570 cm^3, respectively, were built at JET to perform tritium measurements within a broad dynamic range [Cal93]. They were mounted on Conflat flanges in order to enable their introduction into bakeable vessels. By this approach, memory effects caused by surface contamination could be efficiently minimized. While the small ionisation chambers were used to detect up to 100 % tritium, in process streams, large chambers where required to measure tritium at concentrations up to 70 GBq m^{-3} in second containments. The JET Team also performed systematic investigations on the effect of total pressure and gas composition at constant tritium content on the response of the ionisation chambers.

Small stainless-steel ionization chambers of special configuration have been employed successfully at JET for the routine determination of gaseous tritium-bearing species in sometimes rather aggressive gaseous process streams or at the exit of gas chromatographic columns [Lae99c]. The electrodes of these ionisation chambers were made of OFHC-copper (OFHC = oxygen-free high thermal conductivity) electroplated with a 1 µm layer of nickel. Teflon was used as insulation material. This fluorinated polymer was tolerable because of the involved low concentrations of tritium. Gas is introduced into the chamber between the cylindrical outer electrode and the

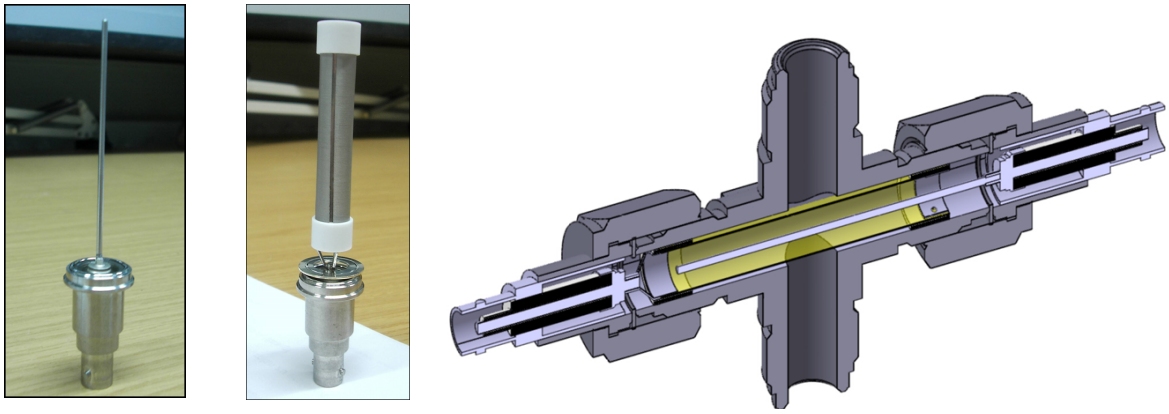


Figure 3.62: Exploded view of a TLK ionisation chamber showing a) the rod cathode, b) the anode basically consisting of a net and c) the main chamber body [Wag09].

centre electrode and leaves the chamber via a bore in the middle of the centre electrode. The outer electrode is kept at a constant voltage of 26 V. All micro gas chromatographs operated at JET were equipped with these small volume micro ionisation chambers [Lae03b].

Small volume ionisation chambers with an effective volume of $< 3\,\mathrm{cm}^3$ were likewise used routinely as tritium detectors in several tritium loops in Chalk River Nuclear Laboratories, Canada [Sur88a] and TLK [Mat91; Pen95c; Glu97a; Mun98; Lae01b; Bor03; Wag09]. They are robust, simple, ultrahigh vacuum tight, bakeable, and inexpensive. Because the housing of the chambers is manufactured from standard Cajon cross joints, they are easy to integrate into tritium-compatible primary systems of the kind currently used in most tritium facilities worldwide (see Fig. 3.62). What is more, they can tolerate elevated pressures of up to 15 bar and are bakeable at temperatures of up to 573 K using an external electric band heater. Thus, they are easy to decontaminate.

TLK ionisation chambers were found to be responsive to total pressure, gas composition, type of gas, and radiation from other nuclides. This is in good agreement with previous observations of Attala et al. [Att76], Nishikawa et al. [Nis89b] and Caldwell-Nichols et al. [Cal93]. The ionisation chambers employed at TLK were developed by M. Glugla and commercialized by Münchener Apparatebau MAB, Germany. A small version of this ionisation chamber, which was entirely manufactured at TLK workshops, served as detector for radio gas chromatographs. Installed at the exhaust stream of isotope separation columns they were used to detect tritium-bearing

species in the eluate. The output of these ionisation chambers is determined with a pico ampere meter. The sensitivity of an ionisation chamber with an effective volume of 4.7 cm^3 was reported to be 4×10^4 Bq cm^{-3} [Pen95c] and the detection limit for HT < 0.1 ppm, which is more than four orders of magnitude higher than of a gas chromatographic thermal conductivity detector.

One should be aware, that ionisation chambers will also respond to ionization generated inside of the chamber by external radiation like gamma rays, X-rays, or cosmic rays.

A detailed model describing the performance of small ionisation chambers was developed by Munakata et al. [Mun98]. The dependence of the ionization current from total pressure of nearly equimolar deuterium-tritium mixtures in the presence and absence of helium as inert diluent was examined experimentally within the pressure range 1 - 10^3 mbar and compared with theoretical calculations. The observed non-linearity of the dependence was attributed to energy losses resulting from recombination reactions taking place within the chamber volume. A best fit recombination constant determined with a least square algorithm that takes into account the recombination of positive hydrogen ions like Q_5^+ with electrons and possibly with negative ions like Q^- was included in the calculations [McC93]. This means, that energy losses such as discussed by Mueller [Mue61] and by Holliday and Sternglass [Hol57] were incorporated into the model. With these enhancements, a much better simulation of the experimental results was possible by numerical calculations. The developed experimentally validated model can provide useful information on which to base the design of improved ionization chambers.

A typical plot of the current as function of specific tritium activity in a small ionisation chamber is displayed in Fig. 3.63 [Wag09]. As apparent, the signal shows a significant dependence from total pressure in the chamber.

For the determination of **tritiated water** in the presence of other radioactive gases it is possible to split the sample gas stream into two streams, one of which is passed through an ionisation chamber and the other first through an adsorber bed and then through a second ionisation chamber. The concentration of tritiated water in the test gas and that of the other radioactive gas is obtained by subtraction. This approach has also been recommended to deal with interference by Ar-41. It must be pointed out, however, that when the Ar-41/tritium concentration ratio exceeds 10 the analysis of tritium becomes erratic and inaccurate [Wit75].

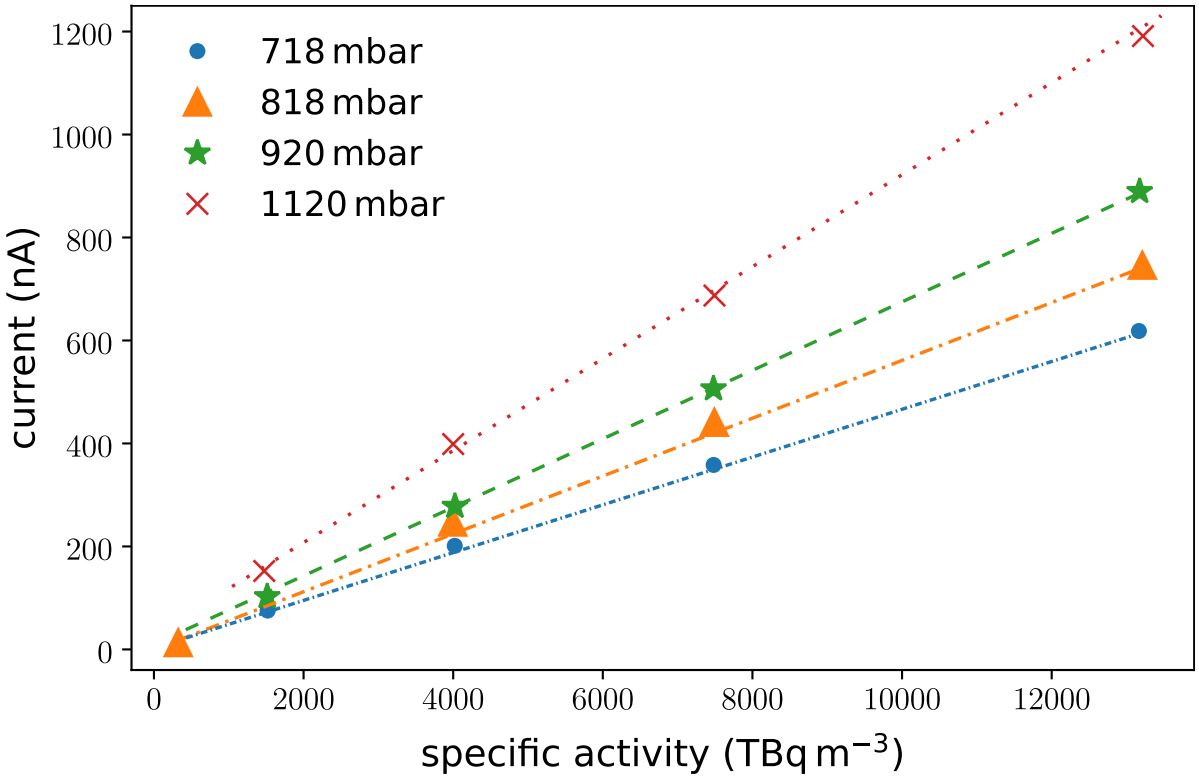


Figure 3.63: Calibration plots of current vs. specific activity of a small ionisation chamber at several total pressures (after [Wag09]).

Inside of glove boxes or room air exhaust ducts **open mesh** ionisation chambers are frequently installed. With this configuration the need of a mechanical pump is avoided and memory effects are minimized.

Monitoring of tritium in the air of tritium handling areas or buildings is carried out with air flow ionisation chambers of large volume, e.g. 10 to 50 l. The ionisation current is determined with vibrating reed electrometers or pico ampere meters; the detection limit for tritium being of the order of $< 10^5\,\mathrm{Bq\,m^{-3}}$. These ionisation chambers can be calibrated with i) a known gamma radiation source, ii) a commercial standard (tritium in nitrogen), or iii) in closed loop mode with a gas containing a known amount of tritium. When necessary, background contamination can be removed with commercial cleansers.

Major advantages of ionisation chambers are i) comparatively low cost, ii) ruggedness, iii) easy scalability, iv) good sensitivity, v) continuous detection, vi) no operation costs, vii) minimal maintenance, and viii) very broad dynamic range of detection. Drawbacks are i) their sensitivity to vibration, ii) easy contamination, i.e. pronounced memory effect, which manifest drastically

when the concentration of tritium undergoes large fluctuations, iii) inability to measure tritium after a prolonged exposure to moisture, iv) incapability of distinguishing between tritium and other radiation sources or between various tritiated species, and v) dependency of signal from pressure and type of gas [Int91].

In case very low concentrations of tritium need to be determined and a possible interference by background radon or an ambient γ-radiation is conceivable, the problem can be solved with two compensating chambers, i.e. one for the sample and ambient radiation and one more for ambient radiation only. By this procedure a significant improvement of sensitivity can be achieved. To protect an ionisation chamber from radiation penetrating into the chamber from outside, e.g. gamma radiation, the chamber can either be i) placed far away from the radiation source, ii) equipped with a compensating measuring system like two coaxially placed chambers of which only one is exposed to the tritium-containing stream, or iii) surrounded by lead shielding.

For optimized compensation many configurations have been tested with various degrees of success: i) concentric arrangement, ii) two ionisation chambers side by side, iii) switching a clean air flow and the sample flow back and forth between two identical chambers or iv) the use of two chambers on a rotating turn-table. Ideally, two chambers are needed in the same position in space and time, which is an impossible endeavour.

3.17.2 Proportional counter

Proportional counters are pulsed counting instruments that use a counting gas consisting of a commercially available argon/methane gas mixture, known as P-10 (90 % argon and 10 % methane). The inert gas is ionized by the incident radiation and the methane quench gas ensures that each pulse discharge terminates. The sample gas is mixed with the counting gas and both are injected into the counter [Int91]. The total number of electrons generated in the counting volume is proportional to the concentration of tritium. The number of ion pairs produced in the counting gas is amplified in strong electric fields surrounding the anode. The number of pulses is proportional to the concentration of tritium. By an anticoincidence technique consisting of multiwire chambers and pulse shape or height discrimination, it is possible to distinguish between beta-particles from tritium and alpha-particles or electrons generated by γ-radiation. The sensitivity of proportional counters is estimated to be $3.7 \times 10^2\,\mathrm{Bq\,m^{-3}}$ (or $10^{-8}\,\mathrm{Ci\,m^{-3}}$) of

sample gas at a counting time of one minute. This tritium detection limit is better by orders of magnitude than that of ionisation chambers.

Because of the high sensitivity of proportional counters for tritium, they are frequently employed for monitoring tritium in gases stacked to the environment. The proportional counter used at TLK to measure tritium activity in vent air has a dynamic range of 3.8×10^3 - 5×10^7 $\mathrm{Bq\,m^{-3}}$ [Vol95]. To allow quantification of tritium under all circumstances including in the event of an accident, the measuring range is expanded to values up to $5 \times 10^{11}\,\mathrm{Bq\,cm^{-3}}$ with an ionisation chamber and a tritium adsorption collector.

Among the disadvantages of proportional counters, the following can be cited: i) high operation cost, ii) an upper detection limit of about $50\,\mathrm{MBq\,m^{-3}}$ and therefore limited measurement range unless dilution of the sampling gas is possible, and iii) permanent need of a counting gas. On the positive side, proportional counters i) allow discrimination from external penetrating radiation or from other radioactive gases accompanying the tritium, and ii) have very high sensitivity for tritium.

3.17.3 Liquid scintillation counting

Liquid scintillation counting is a simple and extensively used standard technique for the determination of tritium in water and other organic or inorganic liquids. To determine the tritium content of a solid the material is dissolved in so called **bulk solvent** (see below) to form a homogeneous solution and then analysed by liquid scintillation counting.

In practice, an aliquot from the solution containing an unknown concentration of tritium is placed in a translucent plastic (e.g. polyethylene) or glass vial together with a commercial liquid scintillation "cocktail". The degree of dilution in the vial must be properly adjusted to avoid counting saturation. Usually a very large number of vials can be counted sequentially during the course of many hours in a liquid scintillation counter using automatic sample changers.

The liquid scintillation "**cocktail**" consists of i) a soluble primary scintillator such as for instance p-terphenyl, ii) a secondary scintillator (wave length shifter) which shifts the spectrum emitted by the primary scintillator to longer wave lengths nearer to those needed for an optimum performance of the photomultiplier, iii) some form of surfactant (surface active agent), and iv) a **bulk solvent**. Usually, an aromatic organic compound like toluene or xylene, which absorbs

most of the energy of the beta rays and transfers it to the primary scintillator is employed as solvent. The fluorescence light emitted by the excited scintillator is detected and counted with a photomultiplier tube (photons are emitted when excited molecules return to the ground state).

A significant reduction of noise and inherent background can be achieved with two photomultiplier tubes connected in a coincidence circuit. This circuit assures that genuine pulses, which reach both photomultipliers, are counted, while spurious pulses, which only affect one of the tubes, are disregarded. During counting the vials must be protected from ambient light. Refrigeration of the photomultiplier and of the scintillation source down to temperatures as low as 263 K, contributes effectively to reduce the thermoionic background. Another methodology to reduce the background is pulse height discrimination which allows rejection of weak noise pulses and large pulses arising from cosmic rays or gamma ray background. Counting only pulses arising from tritium increases the detection efficiency and improves the detection limit. As already mentioned, lead shielding surrounding the counting chamber can also promote a background reduction. The detection limit for tritium in water[49] under good external conditions, i. e. cave, is estimated to be $0.01\,\mathrm{Bq\,l^{-1}}$ or $0.3\,\mathrm{pCi\,cm^{-3}}$.

For very low-level tritium measurements like in hydrological applications, electrolysis is used for tritium enrichment. After enrichment the samples are usually neutralized with $PbCl_2$ and then distilled. Very low-level counting demands a particularly low and reproducible background. At the underground laboratory "Felsenkeller" in Forschungszentrum Rossendorf, Dresden, Germany, the detection limit achieved for tritium in water is in the range 1 - 1.5 TU[50,51].

Interferences: Counting efficiency is not impaired by optically dense suspended white materials. On the other hand, certain chemicals, solvents, and colorants can reduce the photoemission by a quenching process. The occurrence of chemiluminescence not generated by tritium is also possible. Therefore, samples to be analysed by liquid scintillation counting should not contain strong quenching agents, like for instance aldehydes, phenols, amines, nitro compounds, etc. If these or equivalent chemicals are present in the sample under analysis, one option is to convert them into water by an appropriate combustion procedure. Coloured substances can in some cases

[49] As term of reference, the ordinance "Verordnung über die Qualität von Wasser für den menschlichen Gebrauch" (quality of water intended for human consumption) [Bun01a] gives $100\,\mathrm{Bq\,l^{-1}}$ of tritium in water as limit value for water of human consumption.

[50] One Tritium Unit (TU) is defined as $0.118\,\mathrm{Bq/l_{water}}$ and corresponds to a T/H ratio of 10^{-18}.

[51] D. Degering, Verein für Kernverfahrenstechnik und Analytik (VKTA), Forschungszentrum Rossendorf, Dresden, personal communication (2016).

be removed with a strong adsorber such as active charcoal. All the discussed effects must be eliminated by exclusion or minimisation of the active impurities. Additionally, careful preliminary screening test measurements should be carried out.

3.17.4 Smear technique

Tritium contaminated surfaces represent a significant radiological hazard. Therefore, there is continuing need for the development of accurate and reproducible methods to measure tritium on surfaces. They are required to i) provide radiological protection, ii) contribute to mitigate contamination spread, iii) evaluate performed decontamination in order to clear on-site and off-site transports, and iv) determine tritium levels in waste to meet disposal criteria.

A comparative evaluation of several diverse instrumental techniques and swipes for the determination of surface tritium was undertaken by Surette and Wood [Sur95]. One conclusion from their work was that none of the tested instrumental techniques was more sensitive than the combination swipe/LSC. Additionally, typical practical problems linked to the diverse examined monitors, and techniques like limited dynamic range, contamination of windowless probes, requirement of large smooth flat surfaces, exceedingly long counting time, costs, transportability, etc. were critically discussed.

An extensively employed but not very accurate technique to appraise the degree of contamination arising from removable particles on surfaces is the smear technique. According to this procedure, a known surface area of typically about 100 cm^2 is uniformly scrubbed with a dry (or moist) piece of filter paper, which is thereafter introduced into a liquid scintillation counting vial previously filled with liquid scintillation cocktail. After a standing time of 10 - 20 min the vial is counted.

Because the smear procedure is associated with large uncertainty [Rod95b], particularly if the examined surface of the material is rough, is non-uniformly contaminated, or has been exposed to tritium under increased temperature and/or for an extended period of time, it is necessary to deal cautiously with the results.

An attempt to develop measurement procedures suitable for the determination of surface contaminations by tritium with international credibility was carried out by Whitlock [Whi92]. For accredited measurements, a certified source traceable to internationally accepted standard

methods was considered indispensable. Such a source has to be suitable for all kinds of diverse contamination measuring instruments. It should therefore be of high flatness and not introduce errors from a variation of surface area.

3.17.5 Tritiated water vapour determination in a gaseous stream

To determine quantitatively the concentration of tritiated water vapour in gaseous streams collection methods such as i) adsorption on silica gel or molecular sieves, ii) retention in bubblers containing water, or iii) condensation by cold trapping or freeze-out have been proposed and tested.

To measure the concentration of tritium retained in adsorbers, the adsorber is first stirred in water - eventually after adding a scintillation counting solution – and, after equilibrium between solid and supernatant water is established, an aliquot is taken for a measurement of the tritium content by liquid scintillation counting. Tritium detection limits of $24 \times 10^{-6}\,\mathrm{Bq\,cm^{-3}}$ (or $6 \times 10^{-4}\,\mathrm{pCi\,cm^{-3}}$) in airborne tritium-bearing hydrogen oxide have been reported when the flow rate is integrated over the total collection time [Osl73].

The water bubbler/LSC counting technique is especially useful in areas which are not monitored by ionisation chambers.

Shortcoming of all these techniques are their batch character and the need to integrate over the period of measurement. Hence, a pre-requisite are stable and unchanging sampling conditions during the course of the measurement. A problem with bubblers are disturbances caused by frequent aliquot sampling or loss of water due to vaporization. In case of elevated ambient temperature or changing atmospheric conditions the bubblers can be maintained in a refrigerating box at a constant temperature a few degrees below ambient.

3.17.6 Continuous aqueous tritium monitoring

Continuous monitoring of tritium in aqueous effluents of large handling tritium facilities like Savannah River Site is necessary for early warning of an unanticipated release [Hof95]. Experience accumulated over the years has shown that a fully automated system only functions well when i) rigorous water purification by micro filtration is carried out, ii) flow monitors provide accurate information on the flow rate through the water purification system, iii) ultra violet sterilization

Table 3.14: Determined water quality parameters at SRS [Hof95].

Parameter	Influent	Effluent
pH	5.6 ± 0.7	6.0 ± 0.5
Conductivity mS	91 ± 14	2.7 ± 3.0
Total dissolved solids ppm	46 ± 10	1.3 ± 2.2
Turbidity [NTU]	12 ± 9	2.8 ± 4.0
Tritium concentration $\mathrm{kBq\,l^{-1}}$	0.5 ± 0.8	0.5 ± 0.5

keeps algae formation under control, and iv) activated charcoal, ion exchange resin columns, and a phase separator are incorporated into the flow system. The complete measurement arrangement is displayed in Fig. 3.64. Filter F1 protects all downstream components; two pressure sensors monitor any pressure development in the ultraviolet sterilizer; the sterilizer destroys organisms like algae; filter F2 removes suspended debris and slime; the charcoal bed (Act, C) removes dissolved organics; the anion exchange resin (An. Ion exc.) removes anions, e.g. chlorine (chemo luminesces with tritium) and residual organics; it is followed by a strong base cation exchange resin (Cat. Ion exc.) column that retains hardness minerals like calcium; next step is a polishing bed consisting of mixed cation/anion resin (M.B. ion exc.); filters F3 and F4 remove very fine debris including possible resin particles; and finally a phase separator extracts the dissolved gases. The quality of the released water is verified with an in-line conductivity probe. Beads of plastic scintillator coupled to coincidence electronics provide adequate sensitivity, i.e. $25\,\mathrm{kBq\,l^{-1}}$, for early detection of tritium breakthrough. All water quality parameters routinely determined at SRS on the influent and effluent side of the aqueous tritium monitoring system are summarized in Table 3.14. For added independent safety, standard surveillance is carried out regularly by grab sampling in combination with liquid scintillation counting. It was concluded that the developed control procedure contributes effectively to a prevention of accidental releases.

Long-term operating experience with solid scintillating monitors has been reported by Bruyere and Cadwallader [Bru12]. Most common failures were clogged or cracked filters, pump hose ruptures, diverse pump failures, clogged flow meters, etc.

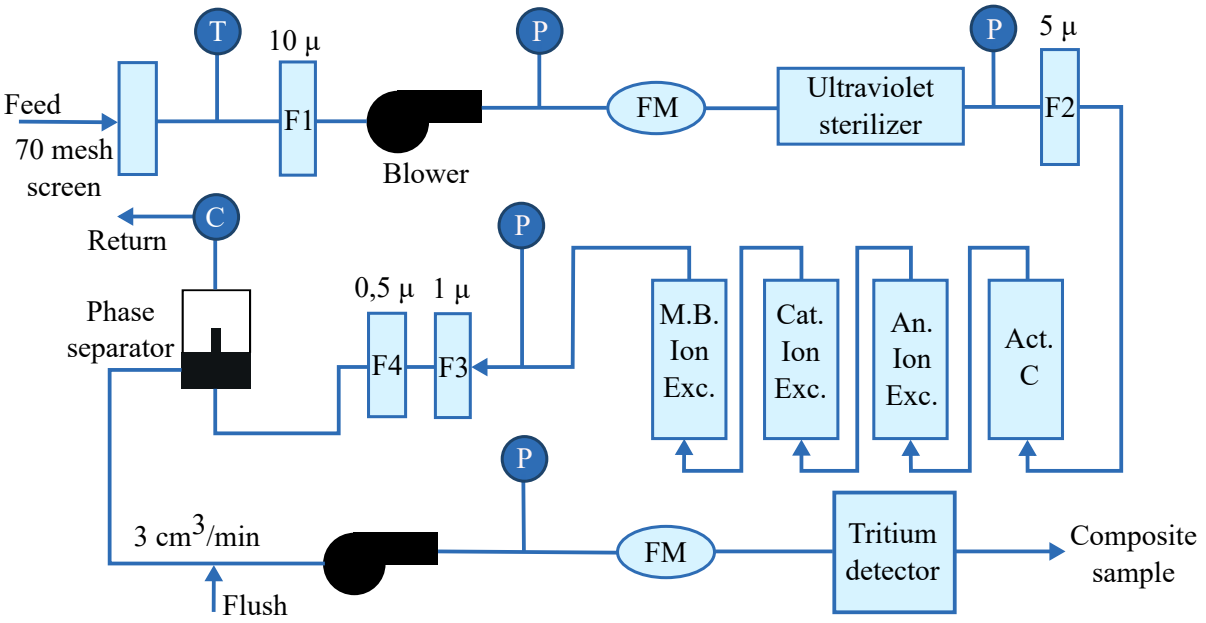


Figure 3.64: Combination of water purification and tritium monitoring of effluent water at Savannah River Site (after [Hof95]) (FM = flow monitor).

3.17.7 Beta scintillator

Beta scintillators in combination with a pressure transducer are effective for the determination of the total amount of tritium in a gaseous hydrogen isotope sample [Col74; Voo95]. Basically, a Eu doped CaF_2 crystal is immersed into a tritium-containing sample and the fluorescence induced by beta particles emitted by tritium or by any other tritiated compound is detected with a photo multiplier tube. The output current of the photomultiplier is measured with an electrometer. If the pressure of the gas is kept below 100 Pa the auto absorption of beta decay particles can essentially be neglected. The concentration in mol % of tritium in the gaseous sample is calculated from the expression

$$T_2\,\% = 100\,\mathrm{K}\frac{\Delta S}{\Delta P}$$

where constant K is a measure of the scintillator sensitivity in pressure units/V, ΔS is the scintillator signal corrected by the background signal, and ΔP the pressure corrected for the background pressure. The constant K is obtained employing standards of known concentration of tritium.

3.17.8 Accelerator mass spectrometry

Accelerator mass spectrometry (AMS) is a powerful technique of high sensitivity for the determination of depth profiles of tritium, deuterium, and beryllium in carbon or other solid materials. The technique was developed in Forschungszentrum Rossendorf (FZR), Dresden, Germany, by Friedrich et al. [Fri00b; Fri00a; Fri01]. Negative ions such as T^-, $H_3{}^-$, and HD^- are generated in the accelerator mass spectrometer employing a commercial caesium-sputtering ion source. The ions are selected with an 82.5° deflection magnet and accelerated up to 23 keV using a Tandetron whose terminal voltage is 1.5 MeV. Interfering negative helium-3 ions are not produced inside of the caesium sputtering source. In the nitrogen gas stripper of the Tandetron, most of perturbing HD and H_3 ions are split into atomic ions (see Fig. 3.65a). For sputtering a specially modified target rod characterized by a fixed supporting point and a movable end was build, with which the stationary Cs^+ ion beam can be scanned on the sample surface over a parallelogram of about $2.5 \,\mathrm{x}\, 2.5\,\mathrm{mm}^2$. In practice, this is accomplished mechanically with two off-axis discs rotating with different frequencies. Mechanical scanning eventually leads to the formation of a crater of approximately cylindrical shape. Wobbling is needed to avoid the formation of a bell-like shaped crater, which would deliver inaccurate depth profiles. To maintain the thermal release of hydrogen isotopes from the carbon matrix at very low levels, during sputtering the cathode target is cooled with liquid Freon. As already mentioned above, tritium ions are counted with a surface barrier detector. Remaining molecules are eliminated with an aluminium stopping foil positioned in front of the detector.

Because absolute measurements of tritium in carbon are rather imprecise, standards have been prepared from graphite powder and pure tritium gas (99 %) [Sta01]. After exposure of the graphite standard to tritium, the obtained concentrations of tritium were quantified by liquid scintillation counting. Typically, ratios of $T/C = 10^{-9}$ and $T/C = 10^{-10}$ were obtained. With these standards, the total amount of tritium trapped in samples of unknown composition could be calculated.

AMS was shown to be rather effective for the simultaneous determination of depth profiles of tritium, carbon, and beryllium on the surface of graphite tiles previously exposed to numerous tritium-deuterium plasmas at JET [Coa99; Fri00a; Pen00b; Pen01e] as well as for the determination of tritium depth profiles of specimens subjected to annealing at increasing temperatures

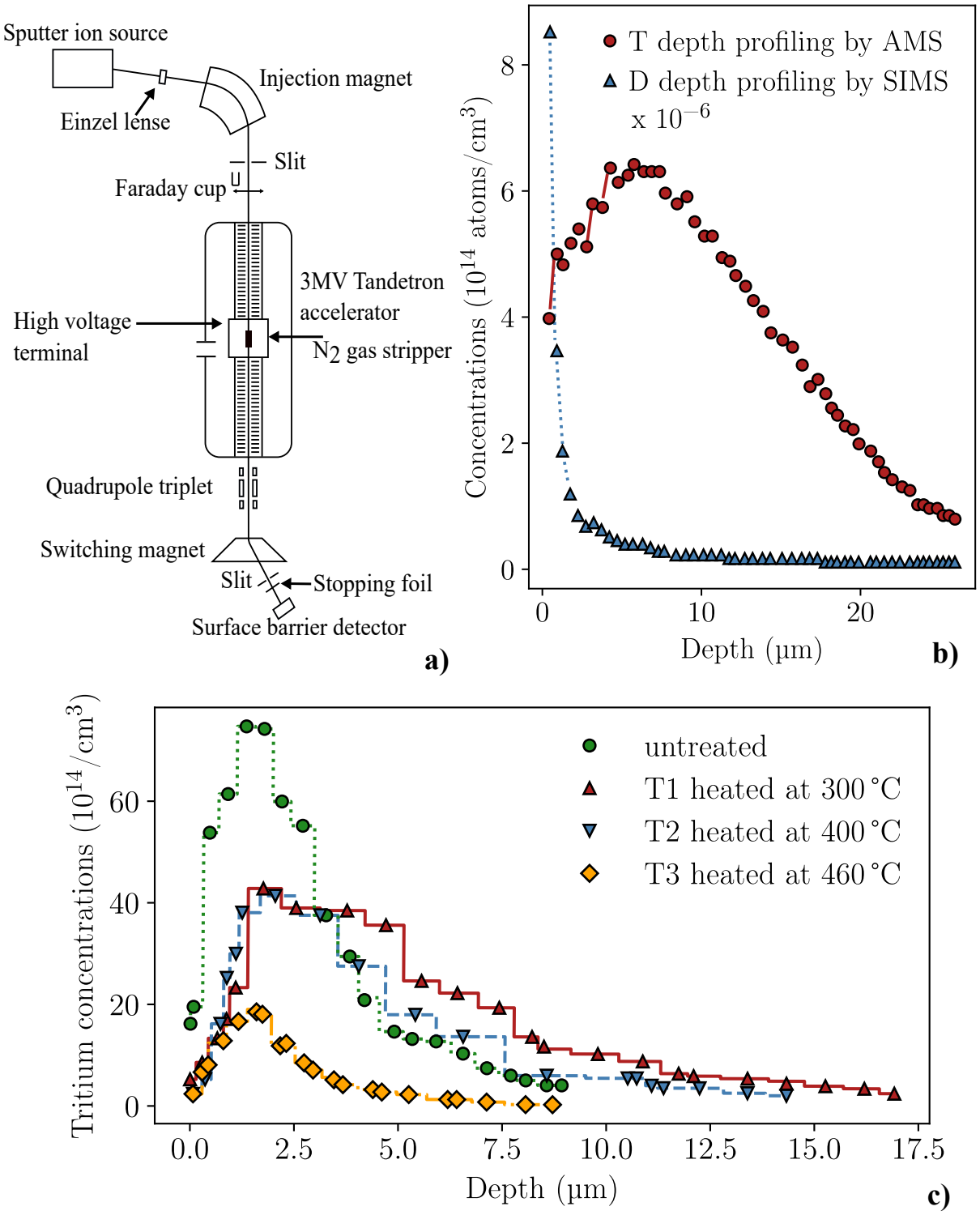


Figure 3.65: The principle of operation of the accelerator mass spectrometer in Rossendorf is presented schematically on the upper left figure a). The depth profile of tritium and deuterium in specimens supplied by ASDEX after exposure to D-D plasmas are displayed in figure b) and tritium depth profiles as function of annealing temperature of CFC specimens supplied by JET in figure c) [Sun97; Fri00b; Fri00a; Pen00b; Fri01; Pen01e].

(see Fig. 3.65c). The valuableness of the technique was also demonstrated with ASDEX Upgrade graphite tiles previously exposed to numerous deuterium–deuterium plasmas [Sun97; Fri00b; Fri00a; Fri01] (see Fig. 3.65b). In case of ASDEX tiles, the maximum concentrations of tritium were in the range 1×10^{14} - 5×10^{15} atoms cm^{-3} and the integrated amounts in the range 10^{11} - 10^{12} atoms cm^{-2} [Fri01]. The concurrent high concentration depth profile of deuterium atoms, analysed with a Faraday cup, and the low concentration depth profile of tritium atoms, determined by an AMS counting technique using a semiconductor detector, is exhibited in Fig. 3.65b. The detection limit for tritium is about 10^{11} atoms cm^{-3}.

An advantage of accelerator mass spectrometry (and of ERDA) is the concurrent determination of depth profiles of several elements. Shortcomings are the i) rather sophisticated and expensive equipment requiring considerable surface area, ii) need of highly qualified personnel, iii) eventually the need to cut small specimens from a larger object (potential dissemination of radioactive dust), iv) necessity of transport of tritium-contaminated specimens to where the AMS equipment is installed, and v) the small area of analysis. Hence, while AMS is a potent technique, it is at the same time restricted in its application.

3.17.9 Elastic recoil detection analysis (ERDA)

To determine hydrogen isotope depth distributions by ERDA on the surface of a solid specimen the surface is bombarded with 2.6 MeV ^{4}He ions, 35 MeV ^{35}Cl^{+7} ions, or some other ions at a fixed oblique incidence angle of for instance 75° [Beh00; Wie97]. With a detector positioned at 75° to the surface a recoil angle of 30° is obtained. Recoiling atoms resulting from elastic collisions of the bombarding ions are analysed for their mass and energy, of which the latter correlate with the depth from which the recoil atoms emerge. The backscattering spectrum of the incident ions can be utilized to obtain additional information on heavier components in the specimen. In order to separate the recoiling target atoms from the large flux of elastically scattered primary ions it is necessary to mount a thin stopper foil in front of the detector. Additionally, this foil serves the purpose of stopping backscattered ions. Common foil materials are Mylar, aluminium, or stainless-steel. Eventually, a correction is necessary for bombardment-induced release of hydrogen isotopes, which may occur during measurements with high incident fluency. High fluencies are for instance required with Cl ions, which are characterized by low sensitivity. Similarly, for the

reason that the sensitivity for 80 MeV ^{197}Au ions is much higher than for 210 MeV ^{127}I ions, with the former recoil spectra at much lower incident fluencies are possible.

Best results with ERDA are obtained with very flat specimens. In case of carbon fibre composite (CFC), which was an extensively used armour material in several fusion machines, even the polished surfaces are not uniform enough. Thus, there is considerable uncertainty in the depth distributions. The depth scale of ERDA is of the order of the surface roughness.

For the quantitative determination of hydrogen isotopes by ERDA, calibrated targets are necessary.

Elastic recoil detection analysis with 2.6 MeV ^{4}He ions has been shown to constitute a valuable tool for the determination of hydrogen isotope depth profiles in carbon-hydrogen isotope layers deposited on samples of tiles obtained from ASDEX Upgrade after numerous plasma discharges [Wie97].

At Forschungszentrum Rossendorf samples obtained from the inner wall tiles of JET were bombarded according to the ERDA principle with a primary beam of ^{35}Cl ions of 35 MeV. With the experimental arrangement used, recoil spectra of H, D, T, He, Be, O, and C could be determined simultaneously [Kre94; Sta01]. The recoil energy spectra delivered the data from which depth profiles of all seven elements could be calculated within depths in the µm range.

To determine depth distributions of H and D as well as of C, N, and O in an a-C : D layer at Beschleuniger Laboratorium in Garching 210 MeV ^{127}I ions were used [Ass94]. In the same laboratory, 80 MeV ^{197}Au ions were employed to measure hydrogen and deuterium depth profiles as well as hydrogen isotope concentrations in an a-C : D layer [Ber98]. These investigations constitute only examples of the wide range of application of ERDA.

3.17.10 Nuclear reaction analysis (NRA)

Nuclear reaction analysis (NRA) is a quantitative, highly sensitive, non-destructive technique that provides information on trapping and depth profiling of hydrogen isotopes in surface and subsurface of solids at depths of a few microns. Nuclear reactions are induced between the incident beam and isotopes within the target. The characteristic radiations emitted by these reactions can be used to identify the isotopes present.

Resonant reactions implemented for the analysis of hydrogen in diverse materials are:

$^{1}H(^{15}N, \alpha\gamma)\,^{12}C$ with 6.385 MeV or 13.35 MeV ^{15}N ions

$^{1}H(^{19}F, \alpha\gamma)\,^{16}O$ with 6.418 MeV or 16.44 MeV ^{19}F ions

$^{1}H(^{7}Li, \gamma)\,^{8}Be$ with 3.97 MeV ^{7}Li ions .

According to the first reaction above, a ^{15}N beam is focussed on a hydrogen-containing specimen. If the energy of the nitrogen ions equals the resonance energy, the ^{1}H and ^{15}N nuclei fuse into a ^{16}O compound nucleous. This compound nucleous undergoes immediate decay into an alpha particle and an excited ^{12}C isotope, which itself emits a gamma ray with a well-defined energy of 4.43 MeV while reaching the ground state. The gamma ray provides an unequivocal evidence for the occurrence of the reaction and hence for the presence of hydrogen in the material.

In case deuterium or lithium are also present in the sample, the sensitivity of the hydrogen measurement is reduced [Wie97].

For the simultaneous determination of deuterium, carbon, and beryllium profiles in solids like stainless-steel or divertor tiles made either of graphite or beryllium, the pertinent nuclear reactions are:

$^{12}C(^{3}He, p)\,^{14}N$

$^{9}Be(^{3}He, p)\,^{11}B$

$^{2}D(^{3}He, p)\,^{4}He$

$^{2}D(^{3}He, \alpha)\,^{1}H$

$^{2}D(d, p)\,^{3}T$.

The first four reactions are initiated by a ^{3}He beam of 2.5 MeV. Under these conditions, the secondary protons produced by the above reactions can be detected at different energies. Protons created in nuclear reactions are counted with a surface barrier detector covered with a 0.1 mm stainless-steel foil to stop 3.5 MeV ^{4}He ions from the nuclear reactions as well as ^{3}He ions backscattered from the incident beam. With deuterium, the reaction cross section reaches a maximum at 0.7 MeV. Therefore, as the ^{3}He beam passes through the surface region and loses energy it continues to react with deuterium with increasing cross section until it has slowed down to less than 0.7 MeV, which in a graphite matrix takes place at about 8 µm. When ^{3}He

ions have an energy of 0.7 MeV the bombardment-induced deuterium release is comparatively small. Along the same line, the analysis depth of carbon and beryllium has been determined to be approximately 1 µm and 1.7 µm, respectively [Rot80; Hug92a; Coa97]. The reason for this is the rapid decrease of beryllium and carbon cross sections with beam energy. In consequence, NRA analysis is dominated by concentrations on the surface. Beam energies of 2.5 MeV, which are usually employed for the detection of carbon and beryllium, are well above the threshold of the corresponding reactions, i.e. about 1.2 MeV.

An important limitation of this technique is the necessity of a complex and expensive heavy ion accelerator operated by highly qualified personnel. Concerning the technique itself, damage caused by heavy ion bombardment during sputtering is associated with release of hydrogen from the material, which may actually have significant influence on the measurement. A further drawback is the relatively small depth resolution, and small area of analysis.

3.17.11 Calorimetry

Calorimetry is a highly developed method for the quantitative determination of tritium which has already established during the early Forties. The basic principles are well understood and confirmed by experiments. A vast body of experience and pertinent literature on the subject is now available. While calorimetry was originally developed for the determination of heats of transformation, it more and more found application for the accurate determination of tritium inventories in solids, liquids, and even gases. An important reason why tritium can be determined by calorimetry so efficiently is that this radionuclide is a pure beta emitter whose released β energy is in most cases absorbed virtually to 100 % by the tritium carrier and the containment walls. Neutrinos emitted during the decay of tritium are not registered in the calorimeter as measurable energy. In terms of thermal energy release, 3.7×10^{13} Bq of tritium represent an energy source of 33.7 MW (or approx. 1.94 W mol^{-1} or 324 mW g^{-1}). Within the frame of routine activities in tritium handling facilities the most frequent application of calorimeters has been the measurement of tritium inventories in wastes, metal getters, adsorbers, structural materials, and catalysts. Calorimeters are also used irregularly for shipper/receiver comparisons within the frame of tritium acquisition actions.

Some more special applications have been i) the determination of the half-life of tritium [Luc00], ii) the evaluation of the tritium content of flakes collected from the JET vacuum vessel after the D-T campaign [Pen02][52], iii) an investigation of the palladium hydride and deuteride systems employing a pressure differential scanning calorimeter [Wag83], iv) a determination of the enthalpy of the hydride formation during reaction of hydrogen with ZrNi [Dan02], etc.

Calorimeters constitute an important tool for the assay of the tritium inventory in solid materials provided the absolute quantity of tritium in the sample is sufficient [Rhi73]. When tritium is present at very low concentrations, it must be kept in mind that all collateral adsorption and desorption processes, chemical or radiochemical reactions, or phase transformations taking place simultaneously to the decay of tritium in the containment may influence appreciably the calorimetric measurement. Of course, tritium permeated into the wall of the vessel containing the sample will also be determined by the calorimeter. Another source of disturbance during calorimetric measurements are fluctuations of ambient temperature. To cope with the latter problem, an effective measure is to install the calorimeter in a room whose ambient temperature can be maintained constant to less than one degree [Hem94; Doe05; Ale11a]. Some calorimeters, i.e. isothermal calorimeters, which are based on a special measurement principle, have been contained either by an air [Jos15] or a water cooled mantle maintained at constant temperature [Kap95; Son10].

With respect to tritium accountancy, an important advantage of modern calorimeters is the rather broad range of concentrations from about 1 µW to more than 20 W that can be subjected to analysis without sample intrusion. In spite of this, more than one calorimeter is necessary when the analysis of samples having rather diverse tritium concentrations or unusual dimensions need to be carried out. In practice, calorimetric shipper/receiver comparisons of the tritium shipped as uranium or zirconium/cobalt tritide in authorized and sealed small transport vessels can be carried out without sampling or even breaking of the transport vessel seal.

Within the frame of a collaborative **Round Robin** analysis activity Kraemer and Thornton [Kra96] compared the tritium contents of four portable Amersham MK IV getter beds containing between 3.7×10^{13} Bq and 8.5×10^{14} Bq tritium. The measurements were performed with calorimeters belonging to the shipper (Chalk River, Canada), the receiver (TLK, Germany),

[52] Measurements with flakes were performed without opening the transport containment to the atmosphere. By this way of proceeding, oxidation reactions were avoided and direct contact of workers with highly toxic, substantially tritium-contaminated fine powder consisting of carbon and beryllium could be ruled out.

and to a third independent party (ETHEL, Italy). These unique results revealed significant systematic errors of the three data sets [Tho94]. The lesson learned was that frequent calibrations using whenever possible diverse verification methods are compulsory for a reliable determination of tritium.

The amount of tritium supplied thermally from a portable tritium storage bed into a primary system can be estimated calorimetrically by straight forward comparison between the initial tritium content in a bed with that remaining after completion of the delivery. When the delivery is performed by external heating of the bed, this operation must be carried out inside of a glove box. The strong heating needed for the thermal decomposition of tritides is associated with considerable contamination of the outer surface of the vessel and of the glove box. Therefore, when the contaminated getter bed is removed from the glove box for transport to the calorimeter site it must be introduced into a protective vacuum-tight secondary containment to prevent contamination of calorimeter and environment. Of course, tritium diffused into the wall of the transportation vessel is registered calorimetrically together with that present inside as tritide.

Numerous calorimeters, some operated at rather high temperatures, e.g. $\leq 1173\,\mathrm{K}$, were built at or for Mound. They were furnished with sample volumes covering the range 0.004 - 385 l (see Table 3.15) [Chr73; Bil73]. A total of twelve **twin cup** calorimeters – six installed in glove boxes - were used to determine tritium in very diverse objects contaminated to quite different degrees. The main reason for placing several in glove boxes was to circumvent unprotected transfers of contaminated samples or transport vessels. The calorimeters were equipped with multijunction thermopiles and a copper sample chamber immersed in a bath of controlled temperature. Permanently installed resistance heaters were utilized for calibration purposes. Twin design allowed reduction of the effect of fluctuations of the bath temperature. Blanke et al. [Bla63] reported during the early Sixties that the power levels assayed at Mound with the 12 calorimeters covered the range 0.1 µW - 100 W, the attained limit accuracies and precisions for optimum power sources being of the order of 0.02 % and 0.003 %, respectively.

Two **isothermal calorimeters** of large sample volume for tritium measurements of high precision were concurrently developed at TLK and Valduc. At TLK, a calorimeter with a sample volume of 325 l was tested by Kapulla and found to have a detection limit of 100 mW [Kap92; Kap94; Kap95]. A double walled inner vessel through which water was recirculated served to maintain constant temperature. Analogously, a calorimeter with a sample volume of 380 l

encompassing two concentric cylindrical cells, one taken as reference, was built at Valduc in close collaboration with industry [Dev96]. The heat flux was determined with thermoresistance elements. The achieved detection limit was determined to be 160 mW, the time required for a full calorimetric measurement was at least 48 hours.

Another **isothermal calorimeter** concept to that developed in Valduc, comprising three instead of two concentric chambers each separated by a heat transfer media, was manufactured by Mason and Vasallo [Mas92]. Helical electrical heating coils wound around each cylinder were employed to obtain constant heat flow. Temperatures of the cylinders were controlled to better than 0.001 K. The inner, middle, and outer cylinders were maintained at progressively decreasing temperatures. Consequently, heat flowed from the inside to the outside. The time required for a routine calorimetric measurement fluctuated between 2 hours and 5 hours depending on the tritium inventory of the sample. These comparatively short measurement times were achieved with an algorithm capable of predicting the sample power from the initial data. With a tritium amount of 7.4×10^2 TBq and calibrations carried out under precise boundary conditions, accuracies of 0.2 % and 0.1 % were obtainable after 8- or 24-hours measurement time, respectively. The detection limit of tritium was reported to be 7.4 TBq after 10 hours of continuous storage bed heat output.

A **power compensation isothermal calorimeter** of comparable design to that described above is in operation at TLK [Mas95] (see Table 3.14). In this instrument the heat source is enclosed by three concentric chambers maintained throughout the calorimetric measurement at progressively lower but constant temperatures making use of servo control loops (the largest cylinder is the coldest). Whilst heating the cylinders, heat is extracted from the outer cylinder either with Peltier cooling elements or by forced air convection. When a tritium-bearing sample is introduced into the calorimeter the electrical power to the inner cylinder is reduced by the heat dissipated by the sample. This reduction in delivered electrical power is compensated by an automatic control system that preserves the constancy of the temperatures. The reduction in power constitutes a measure of the thermal energy deposition rate and therefore of the tritium inventory. Accuracy and detection limit are comparable to those of the instrument described by Mason and Vasallo in their publication of 1992 [Mas92].

Once Hemmerich and his co-workers [Hem94] became aware of the crucial importance of stable temperatures for the development of high-resolution calorimetry, a calorimeter was build

containing within its body a rectangular aluminium block weighting 6.7 kg, which served as **inertial guidance temperature control**. To demonstrate the concept, these investigators built not only a single cup calorimeter but also a more advanced **twin cell calorimeter** (see Fig. 3.66). The double cup calorimeter provided the additional advantage that it could be used not only as a differential calorimeter but also for the simultaneous measurement of two tritium-bearing samples. The metal block was surrounded by numerous heat flow sensing thermopile arrays and by an isothermal environment. Temperature fluctuations in this environment could be detected by flow sensors and corrected by conventional feedback control. A multilayer thermal insulation consisting of alternating aluminium sheets and ceramic fibre sheets served to provide a well-defined heat flow conductance of about $1\,\mathrm{W\,K^{-1}}$ and a thermal diffusivity in radial direction of only $2 \times 10^{-7}\,\mathrm{m^2\,s^{-1}}$. Salient feature of the twin cell calorimeter, whose sample volume is 0.5 l, is high thermal inertia. For this reason, the calorimeter is also denominated **inertial temperature control calorimeter** (see ITC calorimeter in Table 3.15). After the equilibrium disturbance brought about by opening and closing the calorimeter when a sample replacement is carried out, about twelve hours are required for the calorimeter to return to the initial output signal. The resolution of the ITC-calorimeter was determined to be $\pm 10\,\mu\mathrm{W}$, which corresponds to a temperature stability of $\pm 6 \times 10^{-5}\,\mathrm{K\,hour^{-1}}$ over a wide dynamic range of almost six decades, i.e. $5\,\mu\mathrm{W} - 2\,\mathrm{W}$.

With a further improved **inertial guidance vacuum calorimeter** [Hem96a; Doe05; Ale11a] accuracies of ± 100 ppm and a resolution of $\pm 0.2\,\mu\mathrm{W}$ over an even wider dynamic range of more than six decades, i.e. $3\,\mu\mathrm{W}$ - $10\,\mathrm{W}$ were demonstrated. Heat transfer by convection and conduction was minimized by evacuating the whole assembly with a turbo molecular pump backed by a rotary pump. A thermally insulated mass was used as reference to control the base temperature. The aluminum base, which holds the sample containment, rests inside the vacuum vessel only on thermoelectric heat pumps. This arrangement permits excellent control of the base temperature. The block was connected to the measurement chamber by heat flow sensors consisting of a bismuth telluride thermopile array, i.e. thermocouples connected electrically in series and thermally in parallel. Heat liberated by the sample flowing through these thermopiles generates a thermoelectric voltage directly proportional to the heat flow. The calorimeter itself was protected by conventional insulation, which further contributed to a good temperature control.

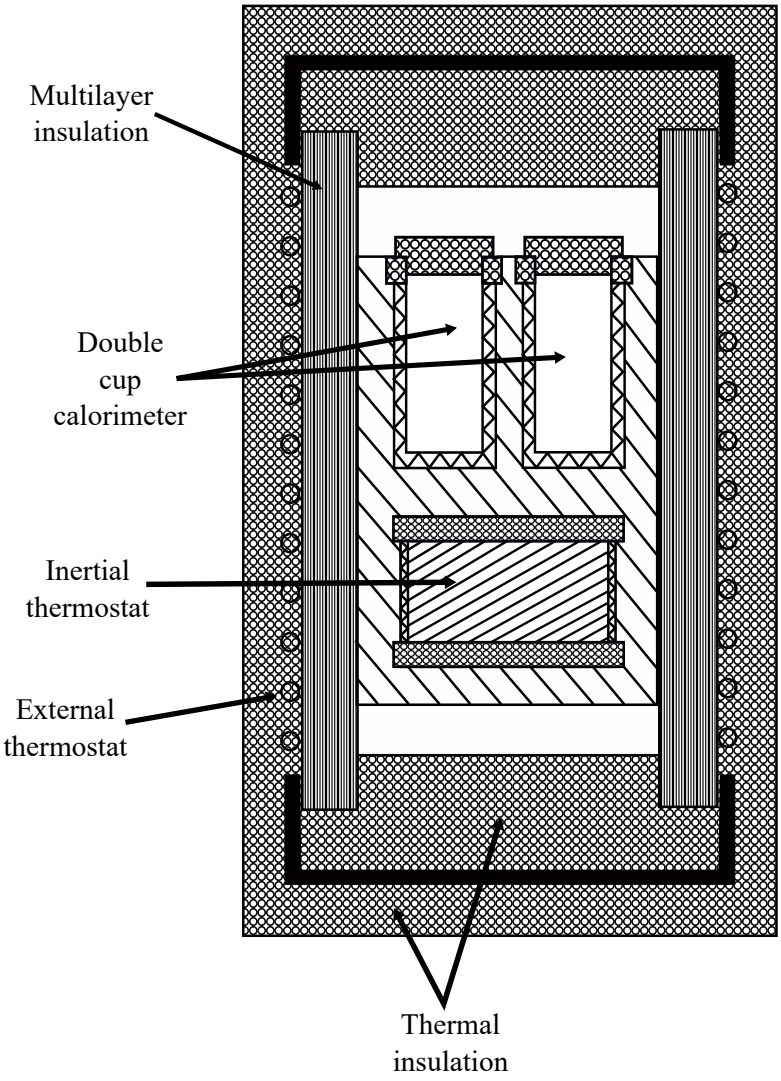


Figure 3.66: Simplified schematic drawing of a twin cell inertial temperature control (ITC) calorimeter with integrated inertial feedback control [Hem94].

Much practical experience – to a large extent based on calorimeter intercomparison - has been gained at TLK with calorimeters designed after the inertial guidance principle having a sample volume of 0.5 l and a detection limit of 1 µW (or 10^9 Bq) (see calorimeter IGC-A05 in Table 3.15). Many tritium determinations were carried out for accountancy purposes, others served analytical needs, or were performed within the frame of research activities [Lae01b]. A significant effort went into the measurement of tritium in specimens cut from graphite and CFC tiles retrieved from JET after completion of the DT1 campaign. Quantitative data obtained by calorimetry were systematically validated by comparison with results obtained from diverse

techniques such as coring/full combustion or accelerator mass spectrometric analysis of the same specimens [Pen01e; Pen01a].

An **inertial guidance large volume** calorimeter type IGC-V25 of similar detection limit as type IGC-V05 but of much larger sample capacity, i.e. 20 l, also underwent thorough testing at TLK [Doe05]. Design specifications of this calorimeter were i) sufficient sample volume to accommodate up to three first wall tiles retrieved from the JET machine, and ii) capability of determining the inventory of tritium remaining in three tiles after their decontamination by prolonged thermal outgassing. Purpose of these activities was the development of accurate, non-invasive sentencing procedures for tritium-contaminated first wall tiles of a fusion device in view either of waste disposal or interim storage for later reuse. Aim of the work was the development of sentencing techniques for the evaluation of the tritium inventory remaining in conditioned first wall components in view of disposal in a waste reporitory facility.

Excellent results were achieved with a commercial **thermoelectric vacuum calorimeter** (see IGC-V05 calorimeter in Table 3.15) largely based on the design worked out for the IGT-V calorimeter and likewise equipped with an inertial feedback control (see Fig. 3.67) [Doe05; Bue15]. This calorimeter is furnished with a 0.5 l measurement chamber connected to a thick aluminium base plate via thermopiles. Peltier heat pumps placed between the base and the support structure are controlled by Pt1000 sensors. The inertial mass consisting of a large metal block rests on thermopiles mounted on the base plate. All components are housed in an evacuated vessel. With this assembly, almost the complete heat transport takes place via the metal structure through the sensors. Therefore, the sensitivity of the calorimeter is determined by the temperature stability of the base plate. The interspace of the jacketed vacuum vessel contains a recirculating fluid that is maintained at a constant temperature of (300.0000 ± 0.0001) K by a suitable temperature controller. The calorimetric evaluation of samples requires a blank obtained from a measurement carried out with the empty calorimeter cup. For this purpose, the base line is obtained from the signal recorded before and after each measurement [Ale11a].

Reproducibility´s, accuracy´s, and precision´s achievable with four partly different calorimeters employed routinely at TLK have been measured, compared, and discussed by Alecu et al. [Ale11a]. Of the four calorimeters, three operate on an inertial guidance controlled quasi equilibrium principle and have sample volumes covering the range 0.5 - 20.6 l. The other is of power compensation isothermal type and has a sample volume of 1.3 l. With two uranium getter

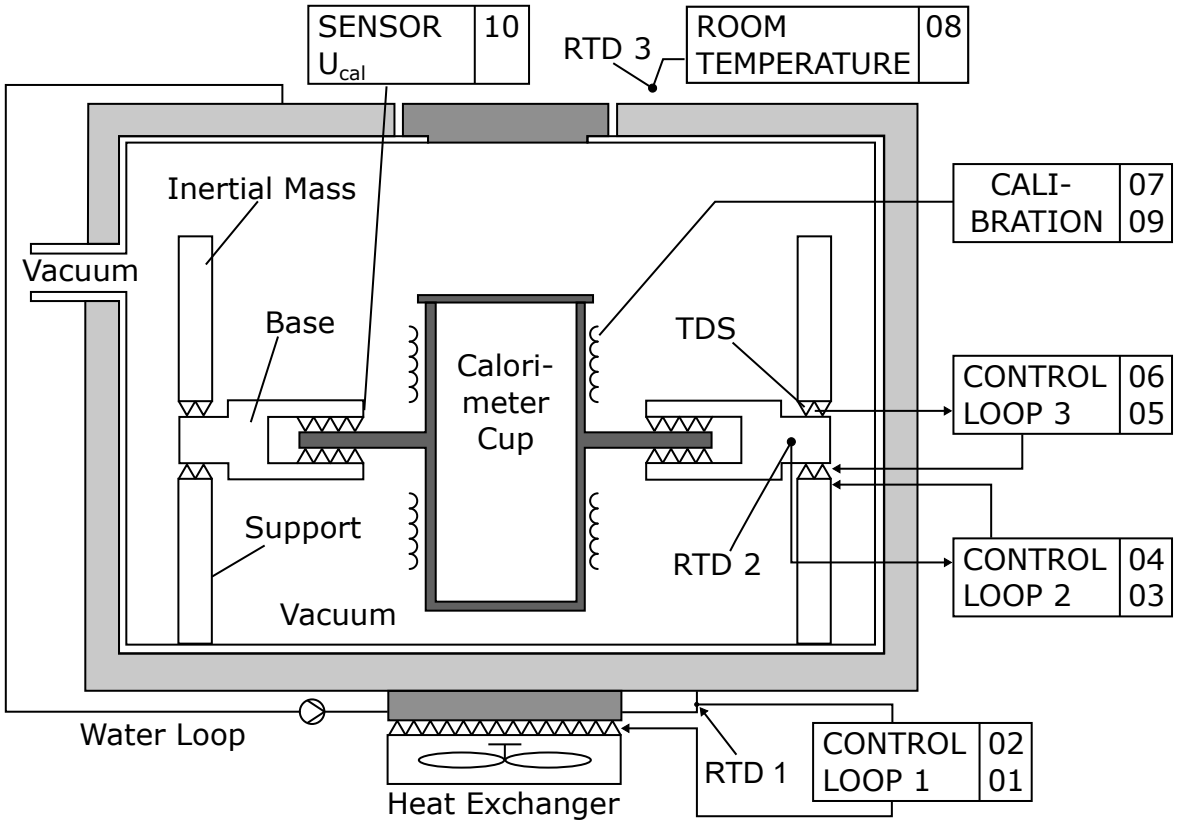


Figure 3.67: Schematic illustration of the TLK vacuum calorimeter type IGC-V05 showing the inertial mass, heat exchanger, calorimeter cup, control loops, and the water-cooled outer vessel that keeps the temperature constant at 300 ± 0.1 K (after [Doe05]).(RTD = resistance thermometer detector, TDS = thermal derivative sensor, U_{cal} = thermopile signal)

beds containing different amounts of tritium, i.e. approx. 31 or 2300 mg, up to five measurements were carried out in each of the four calorimeters. The researchers concluded from the results that the measured inventories did not differ by more than 0.6 % from each other (representative data obtained with the portable uranium tritide bed containing the larger amount of tritium are compiled in Appendix S). The obtained tritium inventories constitute evidence of the high accuracies and precisions possible with samples containing only small inventories of tritium. For example, an accuracy of 0.3 % was achieved with a getter bed containing merely 0.5 mg tritium. In comparison to other calorimeters belonging to the 20 l sample volume class, the IGC-V25 exhibits a relatively good tritium detection limit when the fairly large sample volume is considered [Bue15].

In the meantime, interface and software of three of the four calorimeters installed at TLK have been upgraded and new dedicated LabView programs have been developed and implemented to drive and control the instruments.

Within the frame of ongoing waste management activities for ITER, CEA and SETARAM engaged in a collaborative effort aimed at developing a special **large volume twin cell** calorimeter. Principal application of this calorimeter will be the waste category classification of large volume drums containing tritium-contaminated waste [Jos15]. The outer surface of the calorimeter is conventionally temperature controlled by an air bath (it was selected instead of a water bath on the ground of safety considerations) employing Peltier elements[53]. The sample volume of the calorimeter is rather large, i.e. 385 l. Measurements can be carried out within the range of 10 - 3500 mW, which corresponds to tritium inventories covering the span 0.03 - 10 g. To reduce the overall volume of the calorimeter without losing precision, a phantom reference cell was calculated that measures heat flows in three dimensions utilizing a large number of Peltier modules placed all around the sample drum. A calibration **Joule effect** device can be placed in 100 l or 200 l canisters and installed inside of the calorimeter via a connector. A Joule effect calibration measurement requires typically 2 - 3 days. The calorimeter has been designed to permit drum loading/deloading with a conventional forklift.

One more **twin cell symmetric heat flow** calorimeter was developed by SETARAM, Caluire, France, for Korea Electric Power Research Institute (KEPTL), Korea. This calorimeter features a sample volume of 18 l and has a detection range between 211 µW (0.65 mg tritium) and 20 W (62 g tritium) [Son10]. A good baseline is achieved with Peltier elements used as heat flow sensors attached to the outer surface of both cups. The temperature of the calorimeter jacket is controlled by a water bath. In addition, a thermostat controls the temperature of the electronics to (298.0 ± 0.1) K. First measurements performed with samples having a power of 9998.94 mW and 49.91 mW yielded precisions of 0.13 % and 0.28 %, respectively. A dummy bed equipped with an electrical source has been built to simulate the decay heat from a storage bed under realistic conditions.

A rather sensitive **twin cell thermal conduction** (TCTC) calorimeter has been developed in HRC, Toyama, for the determination of the concentration of tritium in water [Mat08; Mat10].

[53] Thermoelectric heat pumps (Peltier elements) cool by extracting heat from a region and thereby reducing its temperature. The extracted heat is rejected to a "heat sink" of higher temperature. Solid state heat pumps use many thermocouples made of high performance crystalline semi-conductor material.

It consists of two heat sensors, two cell holders, and a heat sink compactly packed into a vacuum chamber evacuated by a turbomolecular/fore pump combination. The volume of the sample cell is 0.024 l. Calibrations were carried out by **Joule effect** heating using a fine Manganin wire resistance wound around the outside of the sample cell holder. Input powers within the range 0.25 - 42.25 µW were generated by varying the applied voltage. The lower detection limit was determined to be 0.036 µW, which corresponds to 40 MBq tritium.

Calorimetry is nowadays a well-established technique for the quantification of tritium. The technique has been successfully validated by comparison with other diverse analytical procedures and within the frame of an international **Round Robin** measurement program. Remarkable technical progress in recent years has led to the development of advanced calorimeters capable of precise determination of very low activities in comparatively large sample volumes.

For the quantitative evaluation of the total amount of tritium in liquids or solids the plusses are plentiful: i) non-invasive assay of the total inventory, which means neither generation of secondary waste nor spreading of contamination, ii) the chemical or physical form of tritium is irrelevant, iii) distribution of tritium in solids or in viscous liquids plays no role, e.g. it is immaterial whether tritium is enriched on the surface or not distributed homogeneously in the bulk, iv) no need of complementary analytics like chemical speciation or isotopic analysis, v) impurities, even in large concentrations, have normally no influence on the determination of tritium, vi) special chemical procedures for sample preparation with the associated handling hazards are not necessary, vii) advanced calorimeters display large dynamic of six or more decades [Hem96a; Ale11a], and viii) high sensitivity as well as accuracy achievable even with large samples. Conversely, the main shortcomings are: i) fixed configuration of the sample holder volume constitutes a problem for specimens of large size or irregular geometry (this problem is usually solved by mechanical fragmentation), ii) determination of low activities may be masked by chemical, physical, or nuclear transformations proceeding with release or absorption of energy, iv) rather time consuming measurements and calibration, and v) eventual need to identify interfering radionuclides in the sample.

Table 3.15: Comparison of several calorimeters used in laboratories worldwide for the determination of tritium inventories in solid and liquid materials.

Model	Sample volume (l)	Detection range (g tritium)	Comments	Location	Ref.
TC	0.007	4.6×10^{-3} - 0.62	LLL workshop	Mound	[Chr73]
TC	2.25	0.6 - 60	LLL workshop	Mound	
TRBT	18.9	6 - 90	LLL workshop	Mound	
	0.004	3.4×10^{-6}#	LLL workshop	Mound	[Bil73]
TCTC	< 0.024	3.1×10^{-7}	HRC workshop	Toyama	[Mat08]
ISC	0.5	3.1×10^{-3} - 3.1	TLK workshop	TLK	[Kap92;
	315	3×10^{-1} - 30.1	TLK workshop	TLK	Kap94;
					Kap95]
TCC	380	0.5#	Sceres/CEA	Valduc	[Dev96]
LVTC1380	385	3.1×10^{-2} - 10.8	SETARAM	Valduc	[Jos15]
ITC	0.5	3×10^{-5} - 30.9	JET workshop	Abingdon	[Hem94]
IGT-V	0.5	1×10^{-5} - 30.9	JET workshop	Abingdon	[Hem96a]
PCI 351	1.3	3.1×10^{-3} - 15.4	Antech, UK	TLK	[Mas95]
IGC-A05	0.5	3.1×10^{-5} - 15.4	Antech, UK	TLK	[Bue15]
IGC-V05	0.5	1.5×10^{-6} - 30.9	Antech, UK	TLK	[Doe05]
TCSHF	17.9	7×10^{-4} - 62	SETARAM	KEPTL	[Son10]
IGC-V25	20.6	1.5×10^{-5} - 15	Antech, UK	TLK	[Ale11a]

# Lower detection limit
TC = Twin cup calorimeter
TRBT= Twin resistance bridge calorimeter
TCTC = Twin cell thermal conduction calorimeter
ISC = Isothermal shield calorimeter
TCC = Two concentric cells with thermo resistance sensors
LVTC = Large volume twin cell calorimeter
PCI = power compensation isothermal calorimeter
ITC = Inertial temperature control
IGT –V = Inertial guidance thermoelectric vacuum calorimeter
TCSHF = twin cell symmetric heat flow calorimeter
IGC-A = Thermoelectric inertial guidance controlled
IGC-V = Thermoelectric vacuum inertial guidance controlled

3.17.12 Bremsstrahlung counting of tritium

The determination of tritium by counting bremsstrahlung was first proposed by Matsuyama et al. [Mat89]. They employed an ultra-high vacuum tight cell having a volume of 30 cm^3 furnished with a gold-coated beryllium window through which it was possible to determine pure tritium (99 %) as well as the partial pressure of tritium in gaseous mixtures with hydrogen containing only 1 % [Mat07]. With the aim of developing the technique for quantitative determinations, it became apparent that while at pressures below 1 kPa the X-ray intensity was directly proportional to the total pressure, at pressures above 1 kPa it departed strongly from linearity. This deviation was explained by self-adsorption of beta-rays. After it was shown that the experimentally observed bremsstrahlung spectrum could be simulated by an exponential function like

$$c = afP \exp(-bP)$$

in which c is the counting rate, f the tritium fraction in hydrogen, P the total pressure, and a and b are constants depending on the counter, the conclusion was reached that the determination of partial pressures of tritium in mixtures with hydrogen isotopes is possible within the pressure range 6.7×10^{-2} - 10^3 mbar.

Matsuyama et al [Mat05] further showed in a systematic investigation on the fundamental parameters governing the bremsstrahlung counting technique, that the method can be applied to the quantitative determination of tritium in highly enriched liquid water. Once it was confirmed that the X-ray intensity depends on the volume of examined tritiated water, the volume used for measurements was fixed at 5 cm^3. The X-ray spectrum induced by tritium beta–rays emitted in water consisted almost exclusively of bremsstrahlung. The experimental arrangement comprised a 13 cm^3 ultra-high vacuum-tight stainless-steel vessel provided with a 150 µm thick beryllium window coated with gold. Under these conditions, the X-ray intensity showed linear dependency from the tritium concentrations in water at least within the range 0.004 - 40 MBq cm^{-3}. Because nickel concentrations in tritiated water exceeding 200 ppm cause a decrease in X-ray intensity, it is necessary to exclude this metal from samples under investigation. The detection limit of tritium was determined to be 2.8 kBq cm^{-3}. Background originating from electronic noise and natural radioactivity can be effectively reduced by lead shielding and an increase of the lower discrimination level. To analyse X-ray spectra, a program was developed and validated

experimentally. The program comprised i) simulation of the tritium β–ray spectrum, ii) conversion efficiency factor of β–rays to bremsstrahlung photons, and iii) single attenuation coefficients of the bremsstrahlung in tritiated water, gold coating, and beryllium plates.

In summary, especially the non-invasive character of the bremsstrahlung counting technique makes this type of measurement attractive for numerous applications concerned with high level tritium monitoring, regardless of whether the system is static or dynamic and liquid or gaseous.

3.17.13 Beta-induced X-ray spectroscopy (BIXS)

While the direct measurement of tritium beta rays can be utilized to determine the surface contamination of solid materials, the depth range of beta rays is limited to only about 1 µm for organic materials and about 0.1 µm for metals. When, however, bremsstrahlung X-rays are generated by the interaction of β-rays with the host material, it becomes possible to detect tritium, for example in stainless-steel, at depths of up to 70 µm [Mat98; Mat02b]. Accordingly, depth profiles as well as the total quantity of tritium trapped in the top surface and subsurface layers of solids like organic polymers [Mat98], boron [Nak04], ZrNi [Mat98], graphite or carbon fibre composite [Mat03; Tor05a], tungsten [Mat02a], copper [Pen11], or stainless-steel [Tor02; Tor07; Pen12] were shown to be detectable by beta-ray induced X-ray spectroscopy (BIXS).

To determine tritium in surface layers of solids the characteristic X-rays generated by the interaction of β-rays emitted by tritium trapped in the sample surface with the adjacent gas phase have been successfully employed. An effective procedure is to keep the specimen under an argon atmosphere and measure the characteristic Ar(K_α) X-rays of argon at 2.9 keV. For the analysis of tritium in the bulk of stainless-steel the characteristic X-rays of Cr(K_α) at 5.9 keV and Fe(K_α) at 6.4 keV as well as the emitted associated bremsstrahlung deliver the necessary information [Tor02; Pen12]. For the quantitative determination of tritium, the conversion efficiency of β-rays into X-rays must be determined experimentally.

Monte Carlo calculations were proposed to determine the content and depth distribution of tritium in the near surface, i.e. $0 <$ depth < 5 µm, of metals and construction materials based results obtained by β-ray induced X-ray spectrometry [An08]. Monte Carlo simulations have also provided information's on the performance of the system at higher total pressures and on the influence of different silicon drift detector (SDD) positions [Ebe16].

Röllig et al. [Roe13], Bornschein et al [Bor15], and Ebenhöch et al. [Ebe16] recently discussed and tested one more robust BIXS system for the **static determination of gaseous tritium**. Primary goal of the work was a detector that meets the exigent requirements of the KATRIN experiment at TLK. Accordingly, the detector must be capable of monitoring continuously the tritium column density of the windowless gaseous tritium source and detect instabilities of 0.1 % in less than 1000 s. For proof of principles, a first BIXS system for static experiments was build and tested. In this system, gaseous tritiated hydrogen is introduced into an evacuable vessel having a geometrical volume of approx. 2 l and an effective detection volume of 0.76 l [Roe13]. The vessel is manufactured of type 316L stainless-steel. X-ray production takes place on two beryllium windows, which are sputter-coated with a 100 nm thick gold layer. A low noise, high energy resolution silicon drift detector (SDD) maintained at 242 K employing a Peltier element allows registration of the low energy zone of the bremsstrahlung spectrum. To increase the X-ray intensity, beta decay electrons are focussed magnetically with up to 120 mT employing a coil whose core is water cooled. The integral counting rate was found to depend linearly from the tritium activity in the vessel. The range of measurement comprises about six orders of magnitude, the average conversion efficiency was determined to be 3.3×10^{-7} cps /Bq[54]. A shortcoming turned out to be a memory effect progressively increasing with the number of runs, which is probably caused by adsorption/absorption of tritium on the inner walls of the chamber. In line with this presumption, the memory effect showed dependence from the partial pressure of tritium and time of exposure to this gas. In an attempt to reduce the memory effect, tests are under way to learn more about the effectiveness of gold plating. Currently, the new device is being further improved by tests on the effect of baking of the chamber and an investigation of the consequences of saturation. Assuming that memory effects can be suppressed effectively, it may be concluded that the design of a low-cost compact measuring system to monitor tritium with a detection limit of 2.9 MBq l^{-1} is feasible.

In a next step, Ebenhöch et al. [Ebe16] manufactured a compact **flow-through** detector cell for in line and real time monitoring of gaseous tritium based on the beta-induced X-ray spectrometry (BIXS) detection principle (see Fig. 3.68a). To increase the bremsstrahlung production and reduce memory effects the inner walls of the sample chamber ① were coated

[54] For comparison, the apparent conversion efficiency of graphite plates containing implanted tritium in an argon atmosphere was determined to be 4.2×10^{-6} cps /Bq [Mat02b].

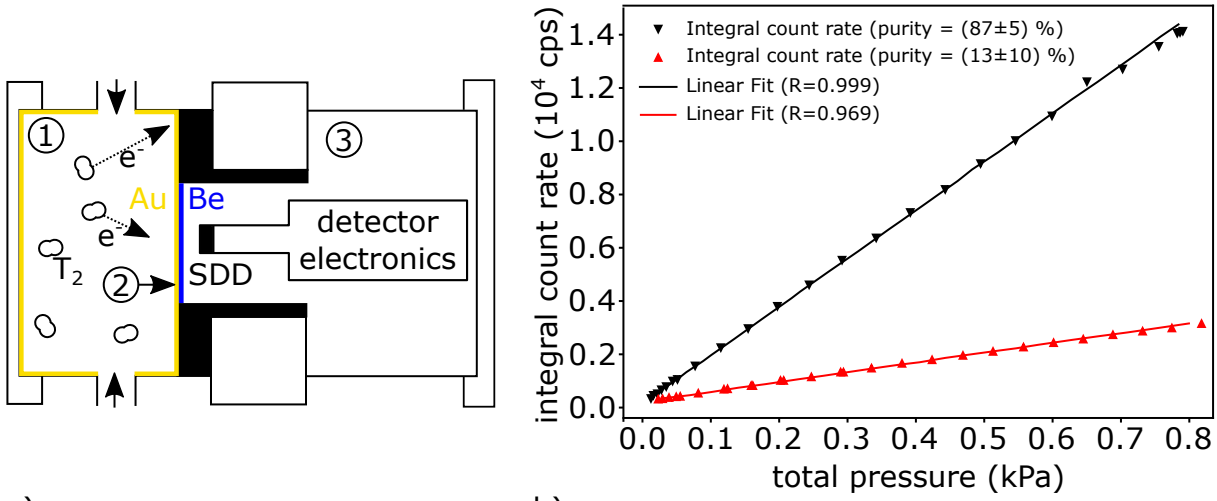


Figure 3.68: BIXS set up displaying the gold coated sample chamber ①, the gold coated beryllium window ② and the detector volume hosting the silicon drift detector (SDD) ③ (a). Plot of the integral counting rate as function of the Q_2 (Q = H, T) pressure showing two straight lines for hydrogen of different tritium content (after [Ebe16]).

with a 200 nm thick gold layer. The sample chamber was directly integrated into a process loop employing VCR connections. The loop was equipped with directly attached radio gas chromatography and mass spectrometry, which served for gas analysis. Chambers ① and ③ of the cell are separated by a 125 µm thick beryllium window (②) whose gas-exposed surface was also sputter-coated with a 100 nm layer of gold. A water-cooled coil outside of the recipient can generate a magnetic field that guides the beta decay electrons (not displayed in the figure). As in other similar systems, a silicon drift detector was used for the detection of X-rays. In closed-loop experiments the integral counting rate was found to be directly proportional to the gas pressure[55] in the cell within the range 0.01 - 0.8 kPa (see Fig. 3.68b). At higher pressures a pressure dependency was observed attributed to self-absorption of beta rays.

For KATRIN a continuous monitoring BIXS detector system was developed comprising two X-ray detectors for the measurement of bremsstrahlung. The 10^{11} beta decay electrons from the windowless gaseous tritium source of KATRIN impinge on the gold coated rear wall causing intense X-ray radiation (characteristic, continuous bremsstrahlung of up to 18.6 keV). The two X-ray detectors (silicon drift detectors with an active area of 100 mm^2) directed to the rear wall will monitor the X-ray intensity and thereby the stability of the windowless gaseous tritium

[55] The gas pressure is directly proportional to the activity.

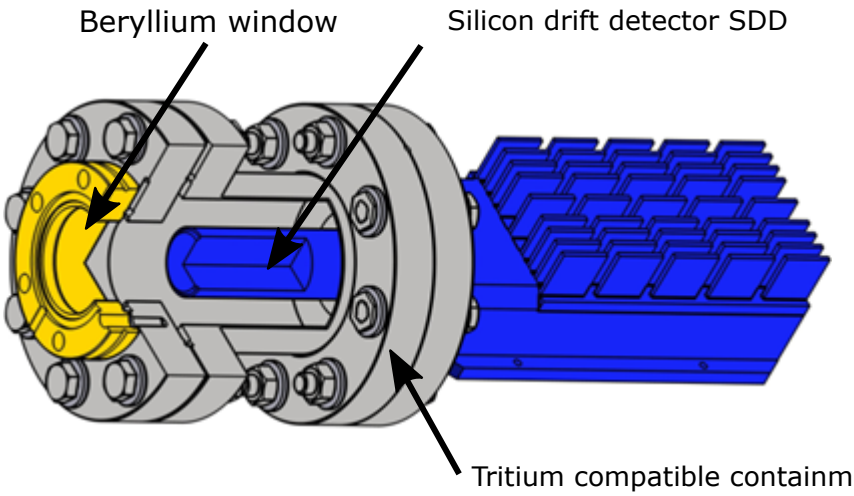


Figure 3.69: Tritium-compatible BIXS detector showing the beryllium window and the silicon drift detector utilized for the determination of HTO [Bor12].

source [Bor15]. The count rate per detector is estimated to be 10 kcps permitting detection of 0.1 % fluctuations of the windowless gaseous tritium system in about 50 s.

One more BIXS system, principally under development for in situ and continuous determination of **tritium in water** at the bottom of a LPCE column used for the detritiation of water, is presently under close examination at KIT [Nie15] (see Fig. 3.69)[56]. The measurement relies on the determination of X-rays generated by interaction of the beta radiation emitted by tritium in water. This system is also equipped with a silicon drift detector (SSD). In spite of very promising first results, supplementary improvements of the detection limit (currently only 1.4 MBq l^{-1}) are still necessary before this concept can be implemented.

In general, advantages of the BIXS technique are i) its non-destructive character, ii) the low cost, iii) equipment of small size (eventually portable), and iv) easy to operate also during an extended campaign. Drawbacks are i) the limited depth resolution and ii) the need of appropriate standards to determine the tritium beta ray conversion efficiency into X-rays. A determination of the conversion efficiency is particularly difficult for multicomponent metals like stainless-steel because of the complex assignment of a beta ray conversion efficiency for tritium to each element in the material.

[56] On present days, tritium in HTO is determined by grab sampling followed by dilution and liquid scintillation counting.

3.17.14 Autoradiography and tritium imaging plate technique

Autoradiography can detect tritium near the surface of solids employing photographic emulsions to detect primary, backscattered, and secondary electrons, Auger electrons and X-rays induced by beta decay. This analytical technique has found application in the determination of the distribution of tritium on the surface of metals like nickel or stainless-steel [Bra71; Lou75c; Tak75; Iso08]. Prior to an auto radiographic examination, the normal procedure is to polish the metal surface sequentially with 400 and then with 4000 grit SiC paper and subsequently wash and rinse the surface with ethanol. After loading with tritium, the polished surface is brought in close contact with a film, e.g. Amersham Hyperfilm, and stored at 253 K under a dry atmosphere for a period of several weeks. At this temperature losses of tritium to the environment can be minimized.

Abraham et al. [Abr78] strain-annealed type **304L stainless-steel** foils at 1323 K and either left the surfaces unpolished or electro polished and etched them. To charge the specimens they were exposed either to tritiated hydrogen for several days (exposure of both sides) or loaded by recoil injection through neutron transmutation of ^{6}Li present in form of a lithium carbonate $^{6}Li_2CO_3$ blanket in contact with only one side of the foil (exposure of one side only). Autoradiographic examinations for tritium of both sides of the foils provided evidence that inspite of the much faster diffusion paths through grain boundaries than across the lattice, the contribution of grain boundaries to the overall permeation rate is small because of tritium trapping in surface oxide films and rather low solubility of tritium in the grain boundaries.

In case of cold worked type **SS304 stainless-steel** an autoradiographic investigation revealed partitioning of tritium between phases present in the microstructures and regions of high and low defect concentrations [Bra71]. Enhanced penetration of tritium into welded regions of the same type 304 steel was also reported.

Takeuchi et al. [Tak75] injected recoil tritium into **nickel** via the $^{6}\mathrm{Li}(\mathrm{n},\alpha)^{3}\mathrm{H}$ reaction. For this purpose, the surface of the metal is first covered with a lithium layer and then irradiated with neutrons. After charging the specimens, they were washed, dried, and mounted on microscope slides. For autoradiography a Kodak AR -10 **stripping film** of thin emulsion and 2.5 µm resolution was used. After development of the emulsions the film was stripped from the specimen, floated on water, and then picked up on glass slides for microscopic observation. Electron

microscope **autoradiography** can alternatively be performed with an emulsion instead of with a film. The autoradiographical study of the tritium bearing specimens revealed accumulation of tritium in micro voids and along grain boundaries. A further finding was that tritium in lattice imperfections is highly active in catalytic reactions.

The **imaging plate (IP) technique** is an autoradiographical method that uses an imaging plate for the analysis of tritium. The technique has been applied successfully for the determination of the distribution of tritium on the surface and in the sub-surface zones of in-vessel components of fusion devices like i) graphite tiles belonging to the belt limiter of TEXTOR [Tan01a], ii) graphite tiles, dome units, and baffle plates supplied by JT60 [Tan03], iii) divertor tiles retrieved from the JET machine [Sug03], iv) metals like tungsten [Tor13; Tor15a] or molybdenum [Ots11], and v) alloys like stainless-steel or ferritic/martensitic steels like F82H or V4Cr4Ti [Has07]. These materials were either pre-exposed to i) plasmas in a fusion machine, ii) plasmas from other plasma-generating devices or iii) moist tritiated atmospheres [Tan02; Hat12]. Surface profiles of tritium on divertor tiles obtained by the imaging plate technique agreed largely with results gained by full combustion [Sug03].

To perform a measurement, the plasma-exposed side of graphite or metal tiles presumed to contain tritium is brought in close contact with imaging plates for several days in a dark room. In order to avoid cross contaminations and to discriminate the beta radiation of tritium from other radiations of energies higher than 18 keV the imaging plate is separated from the specimen by a thin film. After completion of the measurement, the plate is analysed by an imaging plate reader whose readout delivers a map of photon-stimulated-luminescence intensities [Tan01a]. One option for the determination of depth profiles deeper than the escaping depth of tritium beta particles is the utilization of thin copper, aluminum, or poly phenylene sulphide films of various thicknesses. They are placed one after the other between the contaminated surface and the detector [Sug04]. The attenuation of the detected signal intensity as function of thickness of the inserted film delivers an attenuation curve from which depth profiles can be calculated utilizing a Monte Carlo N-particle transport code.

Fig. 3.70 shows by way of example typical results obtained with tungsten stripes first subjected to TEXTOR plasmas in the limiter zone and thereafter to a 1.2 kPa mixture of deuterium/tritium at 573 K for 3 hours. Zones A (red) and B (yellow) are assigned to tritium trapped in thin tungsten carbide layers and zones C (green) and D (blue), which are found on both sides of the

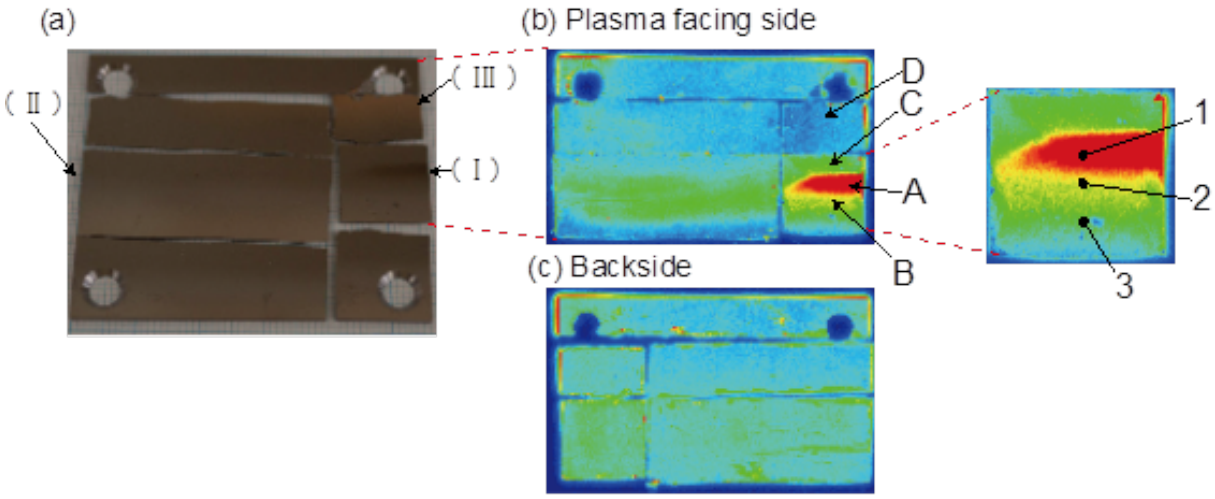


Figure 3.70: Tungsten plate cut into several smaller fragments after retrieval from the TEXTOR limiter where the plate was subjected to numerous plasmas (left). The picture in the middle shows IP images from the plasma-facing and plasma-avers side of the plate after exposure to a tritium/deuterium mixture. The picture on the right displays tritium on the surface of an amplified section of the plasma facing side of the tungsten tile. The hot spot is presumably tritium-contaminated tungsten carbide [Tor13].

plate, to zones of low concentration of tritium trapped in defects created on the surface during the course of exposure of the tungsten plate to deuterium plasmas [Lut00; Tor13; Tor15a].

Hatano et al. [Hat12] exposed Fujifilm, BAS-IP TR imaging plates for several hours to a number of water vapour samples containing tritium at increasing concentrations within the range 4 - 400 kBq cm^3. For the experiments, the 9 µm thick layer of polyethylene teraphtalate, which was placed on the imaging plate to protect the 115 µm thick layer from hygroscopic Eu-doped BaFBr phosphor, was removed. Under such conditions, tritiated water penetrated into the Eu-doped BaFBr phosphor inducing sufficient photo-stimulated luminescence (PSL) for a reliable measurement even at the lowest concentration tested, i.e. 4 kBq cm^{-3}. According to the results, the intensity of the PLS was directly proportional to the concentration of tritium in the water vapour. Since tritiated water absorbed by doped phosphor is again released from the imaging plate at ambient temperature, the plates can be reused provided the time of exposure to tritiated water does not exceed about 24 hours.

3.17.15 PIN diode

A portable, windowless PIN-photodiode detector was employed successfully for the non-destructive counting of tritium on and in the surface of graphite [Wam94; Pen01c]. Betas emitted from a specimen strike the pin photodiode and generate a current pulse which can be converted into a voltage pulse by a charge sensitive pre-amplifier. Several commercial pre-amplifiers have been identified as adequate for determinations of surface tritium. Because the energy of the beta particles emitted by tritium is low, the system noise threshold must be kept below 5.7 keV. Spurious signals to the input should be avoided by proper grounding. An accurate and reproducible spacing between detector and specimen is necessary for reproducible results. It is also important to prevent ambient light from reaching the detector. Advantageously, the attenuation of tritium betas by air was found to be small enough to allow measurement of tritium on samples without the need of sweeping with helium or applying vacuum. Rugged, portable solid-state detectors can be operated with a battery. This makes them applicable for field measurements. The depth resolution of PIN diodes is typically $< 1\,\mu m$ and the detection limit 10^9 T atoms/cm^2. A ^{63}Ni source, which emits betas with end point energy of 66 keV, was shown to be a good reference.

One further potential application of the PIN diode method is routine analysis of tritium on swipes such as carried out on a regular basis in most large tritium facilities. Swipes could be analysed much more expediently and cheaper with the PIN diode technique than is currently the case by dissolution and liquid scintillation counting. A consequential advantage of PIN diodes is that no liquid or solid (e.g. paper) tritium-contaminated waste is generated.

3.17.16 Catalytic oxidation of gaseous tritium

A prevalent technique for the determination of tritium in air carrier gas is catalytic conversion of all tritium-bearing species, i.e. hydrogen isotopologues, hydrocarbons, etc. into tritated water by oxidation on either copper oxide or a noble metal catalyst. For an expedient reaction and to rule out adsorption of water on the catalyst support, the catalytic bed is operated at rather high temperature, i.e. 773 K. Tritiated water in the effluent stream is retained in a sequence of two bubblers containing water or glycol [Tor02; Pen12; Oya15a]. Tritium collected in the bubblers is then quantified by taking an aliquot from each bubbler and analysing for tritium by

liquid scintillation counting. If high temperatures need to be avoided, it is also possible to use a hydrophobic catalyst, e.g. Pt/SiO2 pellets of 1 mm diameter, maintained at $\geq 323\,\mathrm{K}$ [Eda17]. Eventually, hydrogen can be added to the carrier gas in order to further enhance the release of tritium from the catalyst.

3.17.17 Chemical or electrochemical etching

Depth profiles and the total amount of tritium incorporated into metals like stainless-steel, iron, copper, tungsten, or nickel can be determined by incremental chemical etching or electro polishing. Etching (or electro polishing) of small specimens cut from tritium-contaminated metals is a rather simple and inexpensive though laborious procedure for the investigation of depth profiles. Main advantages of the technique are: i) depth profiles in the µm – mm range, ii) rather high detection sensitivity for tritium by liquid scintillation counting, i.e. $0.4\,\mathrm{Bq\,l^{-1}}$, iii) tritium depth profiles up to the mm range obtainable in relatively short time (in contrast to electropolishing or instrumental sputtering techniques), and iv) indirect visualization of trapping sites in the metal surface and subsurface. In comparison to other techniques, the quantification of trapped tritium by etching is particularly successful with materials displaying very low tritium solubility, e.g. copper [Pen11]. Disadvantages of the technique are i) numerous dilution steps, ii) strenuous procedure, ii) enhanced potential for contamination because of work with open radioactivity, iii) possible progressively non-uniform acid corrosion (departure from the original geometrical configuration), and iv) appreciable generation of low level tritiated liquid waste.

The first to determine tritium depth profiles in stainless-steel were probably Austin and Elleman [Aus72]. They used an electro-polishing technique employing a solution comprising 65 % H_3PO_4, 20 % H_2SO_4, and 15 % H_2O. Stainless-steel samples were loaded with tritium via the transmutation reaction $^{6}\mathrm{Li(n,\alpha)}\,^{3}\mathrm{H}$ using a surface blanket consisting of enriched ^{6}LiF and irradiating the blaket with neutrons. A special feature of the technique was one-sided loading of the metal specimen. Diffusion of tritium into the bulk was induced by annealing the specimen at constant temperature. After removing the blanket, depth profiles of tritium were obtained by progressive chemical erosion of surface layers of thicknesses in the range between 0.1 µm and 20 µm. Etching of grain boundaries was not noticed. The investigators provided evidence that tritium liberated during electro polishing quickly equilibrated with water and that less than

0.1 % of the tritium incorporated into stainless-steel was released in gaseous form (molecular tritium). To estimate the depths of eroded layers, aliquots of the electro-polish solution were analysed for ^{51}Cr. This radioisotope was chosen after it was observed that its concentration was directly proportional to the thickness of the layer removed. Released tritium was determined by distillation of the radioactive electro-polishing solution and subsequent analysis of an aliquot of the distillate by liquid scintillation counting.

Easiest approach for the determination of tritium depth profiles in metal specimens of known weight and dimensions consists in progressive removal of surface layers via chemical etching [Lou75c; Hir84a; Per02b]. Etching of stainless-steel can be carried out with a solution consisting of a concentrated acid mixture, e.g. $HCl : HNO_3 = 3 : 1$, diluted in de-ionized water [Pen06]. After an appropriate period of exposure to the etching solution, the specimen is removed from the acid, rinsed several times with a carefully known amount of de-ionized water (which is dropped into the etching solution). The released tritium is quantified by conventional liquid scintillation counting employing an aliquot from the diluted etching solution. The rate of etching can be controlled by adjusting i) the degree of acidity, ii) the duration of etching, and iii) the etching temperature. The thickness of the surface layer removed after each singular etching step is calculated from the known dimensions of the specimen and the loss of weight. Progressively etched specimens will generally lose their original geometrical shape only after they become very thin, i.e. $< 30\,\mu m$. To avoid excessive exothermicity it is important to perform etching slowly. Under these conditions an etching depth resolution of the order of $0.02\,\mu m$ is achievable. To obtain depth profiles of 15 x 15 x 6 mm^3 stainless-steel specimens the four 6 mm sides can be tightly covered with an acid resistant tape [Pen12].

The total tritium content in a specimen is obtained by full etching, i.e. complete dissolution of the specimen. In general, good agreement was obtained between tritium inventory measurements in stainless-steel specimens by complete thermal release at high temperature using a conventional flow system and the full etching technique [Pen06; Tor07]. This observation substantiates the assertion that most tritium is released from the metal as tritiated water. Actually, a number of investigators [Aus72; Hir84a; Sur88b; Per02b; Tor05b; Pen06; Pen12] have provided convincing experimental evidence for nearly quantitative release of tritium as HTO when stainless-steel is exposed to a strongly acidic etching solution.

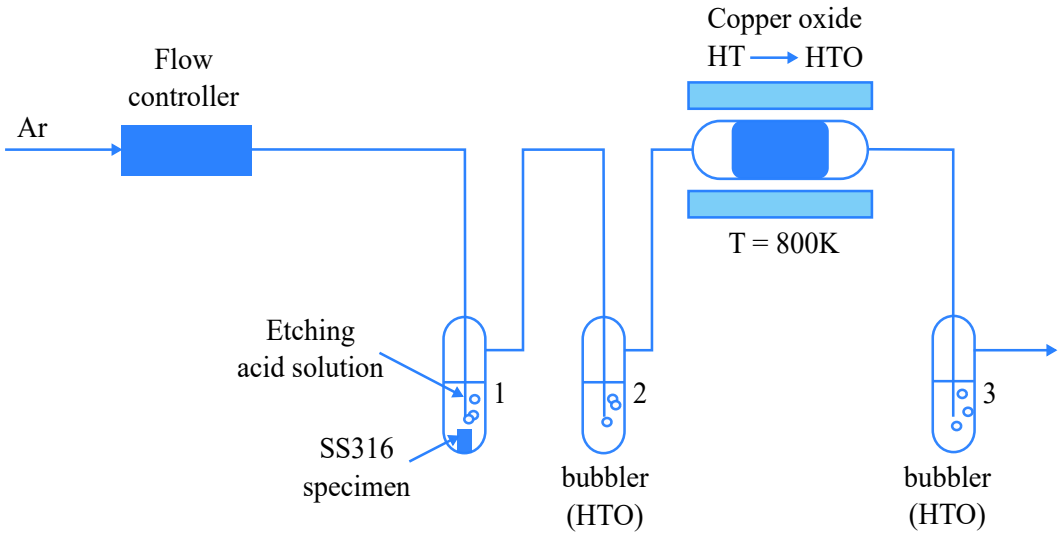


Figure 3.71: Experimental set up to investigate the chemical form of tritium released during etching of stainless-steel (after [Pen13a]).

Penzhorn et al. [Pen13a] etched in a recent complementary experiment a tritium charged SS316 stainless-steel specimen with an acid etching solution (bubbler 1) in a flow system whose total volume was purposely held as small as possible (see Fig. 3.71). A controlled flow of highly pure argon was used as carrier gas. Carrier gas exiting bubbler 1 was first passed through a bubbler containing water (bubbler 2) which retained HTO vapour. The effluent gas from the second bubbler was then passed through a CuO bed maintained at 800 K for the oxidation of HT and eventually generated tritiated hydrocarbons. Finally, the gas was passed through a third water bubbler (bubbler 3) which served to collect HTO generated by oxidation of hydrogen and hydrocarbons. Tritium accumulated in the three bubblers was quantified by liquid scintillation counting.

Following the above described procedure, a SS316 specimen charged with tritium was etched in bubbler 1 for 3 min which caused a depth-segment of about 30 µm to be dissolved from the surface of both sides of the specimen. A simple calculation revealed that the amount of hydrogen generated by reaction of acid with stainless-steel components is orders of magnitude higher than the total amount of tritiated hydrogen (HT) incorporated thermally into the specimen. Hence, it can be speculated that this hydrogen will support the transport into bubbler 3 of tritiated hydrogen generated in etching recipient 1. The findings confirm that during chemical etching 99.7 % of the tritium liberated during chemical etching remains in the first bubbler and neither

Table 3.16: Chemical form of tritium released from stainless-steel SS 316 into an etching solution at ambient temperature [Pen13a].

Exp.	Etching duration	Etched depth	Tritium released into etching soln.	Tritium into 2nd bubbler (HTO)	Tritium into 3d bubbler (HT)
	min	µm	Bq	Bq	Bq
E221	3	24.83	18 604	12.7	40.3
E223	3	29.75	9 900	20.5	10.4

HTO nor HT or tritiated hydrocarbons are released and thereafter transported in noteworthy amounts to bubblers 2 and 3 (see Table 3.16). This observation is well in line with earlier findings of Austin and Elleman who concluded that 99.9 % of the tritium released by etching remains in the etching solution [Aus72].

Etching reagents for metals: Specimens of nickel [Sai11a] or copper [Pen11] can be etched effectively at ambient or slightly higher temperature with nitric acid diluted with up to 50 % of water. An effective etching reagent for stainless-steel is a $HCl : HNO_3 = 3 : 1$ mixture diluted in de-ionized water. Tungsten is best etched with a sodium hydroxide and hydrogen peroxide solution at near ambient temperature [Nak15].

As observed with stainless-steel, the majority of tritium released during etching of tritium-contaminated copper or nickel specimens remains in the etching solution and is not liberated as gaseous tritiated hydrogen or tritiated hydrocarbons.

3.17.18 Thermal de-sorption

Employing a flow system with noble gas or nitrogen as carrier it is possible to investigate the thermal de-sorption characteristics of tritium from metals like stainless steel, copper, nickel, or tungsten and determine their total tritium content. Heating can take place either by a stepwise increase in temperature [Tor04; Pen12; Oya15a] or by a programmed linear temperature increase usually in the $K\,min^{-1}$ range (TPD = Temperature Programmed Desorption) [Hir84a; Sur88b; Hir90b; Qui08]. Installing downstream a sequence of two bubblers with a copper oxide bed placed between them and maintained at about 800 K (fast reaction rate and minimization of adsorption) it is possible to discern between liberated tritiated water and tritiated molecular

hydrogen (and/or tritiated hydrocarbons) [Tor05b; Qui08; Pen12]. Tritiated water is collected in the first bubbler and all other tritium-bearing species after their oxidation into HTO in the second bubbler. Tritium quantification occurs by liquid scintillation.

Accurate determination of the tritium inventory in metal specimens requires thermal release at rather high temperatures. For instance, stainless-steel specimens must be heated up to at least 1000 K to achieve quantitative liberation. In such a case, neither the type of carrier gas nor the partial pressure of water in the carrier gas have much influence on the liberation rate of tritium [Tor04]. The duration of heating to achieve full liberation is influenced significantly by the dimensions and surface properties of the specimen [Pen12].

Another rather simple and effective approach to determine thermally released tritium has been to sweep P-10 counting gas (90 % Ar + 10 % CH_4) over a heated tritium-bearing sample and subsequently passing the effluent gas through a gas-flow proportional counter [Aus73; Ell74].

The long-term release of tritium into the gas phase from metal specimens kept at ambient temperature ("**chronic release**") can be determined with small glass vessels provided with gas inlet and outlet [Tor05b; Pen11; Sai11b]. The vessel containing the specimen is integrated into a flow system and then introduced into an oven maintained at a constant temperature slightly above ambient. This procedure effectively contributes to reduce the influence of room temperature fluctuations. Under these conditions, nearly the only tritiated species liberated from stainless-steel, copper, or nickel is HTO. Freed tritiated water is transported from the glass vessel into two downstream, sequentially placed water bubblers using nitrogen or argon as carrier gas. The bubblers are maintained at low and constant temperature to minimize water losses by vaporization. Release rates are determined in regular intervals by liquid scintillation counting of aliquots taken from the bubblers. The total released tritium is obtained from the concentration of tritium in the bubblers and the corresponding integral collection period of tritium.

The long-term release of tritium from metallic specimens into a liquid at ambient or higher temperatures can be determined employing a number of hermetically closed glass vials each containing a specimen loaded with tritium and submerged into a well-known amount of liquid. All metallic specimens have nearly the same dimensions and are charged simultaneously under identical conditions. They are all stored under liquid at the same temperature. The amount of tritium liberated is determined by liquid scintillation counting of aliquots removed once from each vial or repeatedly from each vial at fixed intervals. Reproducible conditions are achieved

by suspending the specimen in the liquid with a platinum wire and frequently or continuously homogenizing the liquid with a magnetic stirrer. If the vials are stored in several ovens maintained at different temperatures an activation energy can be determined.

In case of stainless-steel, the rate of tritium release into water and into the gas phase were found to be nearly equal. Hence, the "chronic rate" of tritium liberation is primarily determined by the rate of diffusion from the bulk up to the surface and not by the transport rate from the surface into a liquid or gaseous phase [Pen06].

A highly developed technique with a vast body of underlying experience is **temperature-programmed desorption** (TPD) into an ultra-high vacuum tight vessel. Particularly attractive of this approach is the possibility of attaching to the vacuum vessel one or more analytical instruments capable of identifying and quantifying the released species. Within this frame, the technique was applied to measure the desorption fluxes of H_2, HD, D_2, N_2, CH_4, H_2O, CD_4, CO, and CO_2 from an amorphous deuterated carbon layer (a-C:D layer). The investigated carbon target was subjected to a linearly rising temperature ramp of $10\,\mathrm{K\,s^{-1}}$ up to a temperature of 2100 K. The released species were identified and quantified with a quadrupole mass spectrometer [Sch99b]. Heating of the specimen was carried out from the back side by electron bombardment. For the determination of partial pressures, the mass spectrometer was calibrated with corresponding pure gases. Pressures were measured with a spinning rotor gauge after correction for the sensitivity of each gas. Fluxes of desorbing gases were obtained by calculation. Integration of fluxes of the various species over the entire temperature range delivered inventories.

A large number of fundamental studies on the thermal desorption of tritium from stainless-steel type 316 samples were reported by Hirabayashi and his co-workers [Hir84a; Hir84b; Hir85a; Hir89; Mas89]. The investigations, which covered a temperature range from ambient up to 1200 K, provided evidence for the existence of several energetically quite different sorption sites.

3.17.19 Full combustion

A rather simple, reliable, but painstaking technique for the determination of surface concentrations, depth profiles, and total inventory of tritium in graphite or carbon fibre composite (CFC) tiles consists in full combustion of representative samples and collection of the released gases in water bubblers [Pen00c; Pen00b; Pen01e]. A large number of specimens were obtained by "coring"

cylinders from strategic plasma-exposed and plasma-shadowed zones of first wall divertor tiles of JET employing a hollow drill. Thin disks cut from both ends of these cylinders were used to obtain tritium surface concentrations on front and back side of the tile. The tritium content in equally thick disks cut from the rest of the cylinders eventually yielded a tritium depth profile. Coring and cutting work can only be carried out in a dedicated fully equipped glove box because of the generation of appreciable amounts of highly tritium-contaminated and beryllium-contaminated dust.

Tritium in carbon slabs can be determined quantitatively by full combustion under a stream of humidified air at temperatures higher than 1073 K. A simple quartz apparatus whose lower section can be heated externally with a small oven up to elevated temperatures is depicted in Fig. 3.72 [Van79]. During combustion species such as tritiated water, carbon oxides, eventually some tritiated hydrocarbons, and perhaps a small fraction of molecular tritiated hydrogen are generated. These species are further oxidized into tritiated water and carbon dioxide in the presence of an immediately adjacent packing of Cu/CuO wire segments. The temperature prevailing in the combustion zone and at the wire segments is the same. Tritiated water in the effluent stream is collected in a sequence of two bubblers containing either water or glycol. The arrangement is such that the vertical tube used for the transport of the effluent gas from the combustion reactor is stuck directly into the water of a first bubbler. Hence, the exhaust gas remains hot and water condensation is avoided. Aliquots from the bubblers are analysed for tritium by liquid scintillation counting. From the tritium surface and bulk concentrations in several strategically obtained coring cylinders a three-dimensional distribution of tritium in a tile can be put together.

The technique developed by Vance et al. [Van79] was originally conceived for the determination of tritium in oxides and metals. In this case, the specimens were heated in the quartz tube under a moist stream of oxygen at an even higher temperature, i.e. 1225 K. As described above, released tritium was collected in a bubbler and determined by liquid scintillation spectroscopy. It was claimed that by this procedure 1 ppb of tritium could be determined in 100 mg samples of lithium, iron, nickel, cerium, plutonium, plutonium oxide, copper foil, etc.

Truffier and Corpechot [Tru70] measured the total content of tritium in metals by the oxidation of small specimens in a quartz tube containing an over stoichiometric amount of oxygen and sealed with a burner. The quartz tube was placed inside of a steel susceptor externally isolated

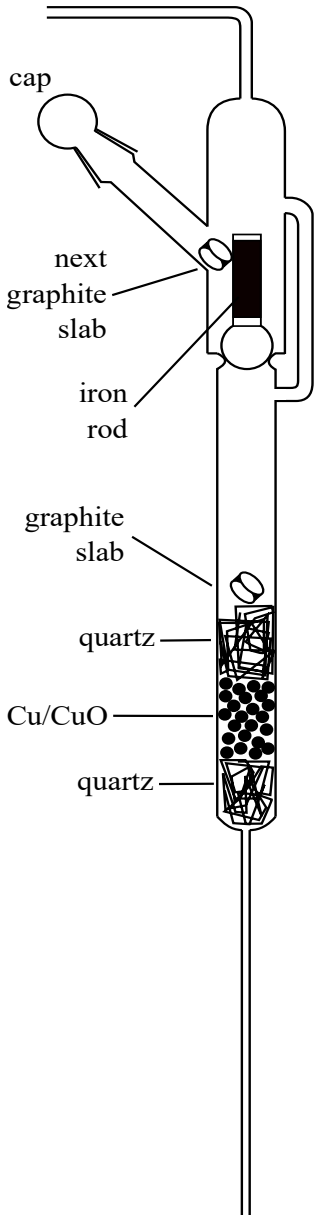


Figure 3.72: Quartz device for full combustion showing the iron rod protected by a glass envelop that can be lifted from the outside with a magnet to drop the next graphite slab into the combustion reactor. Cu/CuO is maintained in place by quartz wool. The thin tube at the bottom of the device is directly submerged into the water of the first bubbler [Van79].

by a small quartz recipient. Rapid heating up to elevated temperatures took place by high frequency induction heating. The water generated by oxidation was collected on one end of the quartz tube by submersion into liquid nitrogen. Under these conditions, the tube could be opened without loss of tritiated water. To determine tritium an appropriate solvent for tritiated water was introduced into the tube and the concentration of tritium in the water/solvent solution obtained by liquid scintillation counting of an aliquot. The procedure was demonstrated with tritium-contaminated copper, iron, and magnesium specimens.

3.17.20 Indirect determination of tritium via mass spectrometric measurement of decay ^{3}He

Demange et al. [Dem02; Dem05] determined indirectly the tritium inventory in waste drums containing low level organic waste from a measurement of the ^{3}He generated by tritium decay. Decay helium generated in the waste drum permeates across the drum O-ring sealing into a tightly closed outer containment where it was measured utilizing a mass spectrometric technique. For details consult section 8.4.9.

To determine environmental tritium in water at rather low concentrations Clarke et al. [Cla76] allowed accumulation of decay ^{3}He in degassed water sealed in glass containers. Generated ^{3}He was quantified by mass spectrometry.

3.17.21 Routine calibrations

Thermocouples, pressure transducers, flow meters, flow controllers, tritium monitors, tritium process monitors, analytical instrumentation, etc. belonging to tritium handling equipment installed in glove boxes shall be calibrated at predetermined intervals proceeding according to a fixed schedule.

Calibrated instruments or devices should be provided with a well visible sticker. The sticker should display date of calibration, person that carried out the calibration, calibration procedure, date of expiration of the calibration, range of measurement of the instrument, and whatever further information is considered to be of relevance.

3.18 Basic processes in small and large tritium-handling installations

Facilities dealing routinely with substantial amounts of tritium designed for clean-up of plasma exhaust gases, separation of hydrogen isotopes, allocation of analytical service, tritium accountancy, supply of highly pure tritium or mixtures of tritium with other hydrogen isotopes to research installations, infrastructure facilities, or large devices like fusion machines, etc. must utilize qualified process equipment installed in properly equipped secondary confinements like glove boxes, caissons, or dedicated containments.

All primary containment equipment mounted inside of glove boxes must satisfy strict safety criteria in order to meet environmental protection demands. Fabrication of primary equipment must proceed following stringent material quality specifications and adhere under all circumstances to the established rules. Basically, only tritium-compatible materials are to be employed for the manufacture of equipment destined for tritium handling utilizing only fittings furnished with metallic gaskets. Because primary containments or equipment that may require replacement will become contaminated already after the first contact with tritium, it is important that they be installed using demountable connections like Cajon VCR or Varian Conflat type and be assembled in easily accessible places inside of secondary confinements. Each primary component and tubing sub-assembly shall be pressure-proof-tested and leak-tested before installation. After completion of the primary system further leak tests are necessary to verify the overall leak-tightness. More details on manufacture procedures, equipment options, and quality control procedures are discussed in the corresponding chapters of the Tritium Manual.

Commercial equipment encompassing heated components, components of insufficient leak-tightness, or mechanically non-robust elements like quartz windows, constitute a safety risk from the point of view of tritium release via permeation, leakage, or loss of physical integrity. In order to guarantee “rock solid” tritium containment, a frequently adopted solution consists in placing vulnerable or hard to qualify components inside of a dedicated leak-tight confinement. Design requirements of this dedicated secondary confinement must meet the same standards as those of primary containments, especially if the conceivable contamination could be significant. Therefore, the vacuum tightness of dedicated secondary confinements shall be better than $10^{-9}\,\mathrm{mbar\,l\,s^{-1}}$. Qualification as tritium compatible component of an uncomplicated secondary confinement

will almost certainly be much simpler than any attempt to upgrade and qualify commercial equipment.

Dedicated secondary vessels housing heated primary components will have to be maintained under unceasing vacuum and be provided with heat shields to avoid hot outer walls and excessive heat losses by the primary component. The strategy of enclosing components or process sections in a dedicated second containment has been demonstrated successfully time and again with a large number of rather diverse and frequently very complex equipment. Good examples are: i) the preparative gas chromatographic system of JET [Lae95; Lae99a], ii) the four uranium storage beds constituting the intermediate storage system of JET [Lae99b], iii) a cryotransfer pump operated with liquid nitrogen and liquid helium at JET [Hem89a], iv) commercial palladium/silver permeators [Pen95c; Glu00b], v) a sophisticated ceramic electrolysis cell [Oku93], vi) diverse optical cells for infrared or Raman spectroscopy installed in special secondary containments provided with optical windows [Pen95c; Ohi00b], vii) a displacement isotope separation system [Doe02], etc.

Large upper Conflat flanges of dedicated secondary confinement vessels can be used for penetrations accessing enclosed components as well as for the suspension of components via minimized heat bridges. Enhanced safety can also be achieved for optical cells designed for high pressures employing a dedicated secondary vessel [Ohi96; Ohi00a; Ohi00b]. Remarkably, many crucial components installed at JET in dedicated secondary vessels handling large inventories of tritium did not require protection by a glove box or caisson.

Confinements to primary installations must be serviced either by a dedicated singular or by a Central Tritium Retention System which keeps the enclosed atmosphere constantly at slightly subatmospheric pressure and the contamination by tritium below the allowed levels.

Tools needed for repair or replacement of components shall remain - if possible - inside of the secondary confinement.

Protection of personnel, environment, and equipment demands redundant tritium monitoring devices installed in diverse and strategically selected positions.

In large installations emergency power supply must be available to cope with utility power failure. Under total failure of power or pressurized gas supply, valves and active components shall go into a safe state, systems shall be isolated, heaters turned off, and gas evolution due to loss of cryogenic cooling or chemical reaction eventually leading to pressurization be contained safely.

Safety relevant tritium monitoring of the primary system as well as glove box monitoring, room monitoring of the control area, duct monitoring, and stack monitoring shall all remain active.

Fundamental processes that constitute the basis of nearly every tritium handling research facility, of many infrastructure systems, and of the fuel cycle of fusion machines will be discussed in some detail below.

3.18.1 Evacuation

A vast body of experience with tritium has accumulated with a variety of oil-free pumps like scroll pumps, Metal Bellows pumps, roots pumps, wobble pumps, reciprocating compressors, etc. The pumps have been employed successfully often for prolonged time while processing high levels of tritium either singly or in combination to achieve **intermediate vacua** of the order of 10^{-3} mbar. When one or more of these positive displacement pumps are combined with magnetically suspended oil-free turbo molecular pumps **high vacua** in the range 10^{-3} - 10^{-7} mbar are routinely achieved. In case high vacuum systems are additionally evacuated with sputter ion pumps or titanium sublimation pumps [Pic86] **ultra-high vacua** better than 10^{-7} mbar are achievable (in practice, vacua of less than 10^{-12} mbar have been reported). However, because of cathode erosion the lifetime of sputter ion pumps is relatively short. To prolong their durability, the usual procedure is to start these pumps only after vacua better than 10^{-6} mbar already prevail.

One more option for evacuation to high and ultra-high vacua are cryo pumps which function by condensation or cryosorption. Because these pumps require liquid coolant, i.e. liquid nitrogen and/or liquid helium, and operate in batch mode, they are not suitable for the evacuation of small devices installed in glove boxes.

To exclude contamination of tritium-handling primary systems by oil in most tritium facilities oil turbo molecular pumps have been replaced by oil-free ones.

For more details on single pumps and their combination options consult sections 3.14.1 and 4.1.4. A few vacuum technology pertinent data of selected gases of relevance to the fusion fuel cycle have been compiled in Appendix T.

3.18.2 Gas re-circulation

Dry, hermetically sealed pumps like NORMETEX scroll pumps, Metal Bellows Corp. pumps, Toyo reciprocating compressors, or Siemens metal bellows pumps are suitable for re-circulation of tritium-bearing gases in closed loop operation. Organic lubricants, elastomers or fluorocarbons are not permissible for pumps in tritium service. Flow rates can be adjusted either with a bypass equipped with a needle valve or with an electronic speed control of the pump motor. In case of a leak into the primary system an interlock triggered by a sudden pressure rise should terminate operation and prevent re-initiation of operation until the problem has been identified and remedy found.

Appropriate filters against particle intake are necessary to avert pump damage.

For re-circulation of gases at low pressures blowers instead of scroll pumps or Metal Bellows pumps should be selected. While scroll pumps show considerable back streaming - particularly of light gases - through the clearance between scroll and pump body, bellows pumps with flipping seals only operate at pressures above a critical value.

3.18.3 Tritium transfer procedures

Pure gases or their mixtures can be transferred between recipients containing gases at different pressures by straightforward gas expansion. The transferred fraction will depend upon volumina and initial pressures in both recipients [Hir88]. Larger amounts of gas can be transferred under the enhancing effect of single oil-free pumps like NORMETEX moving spiral pump, Metal Bellows pump (see Tables 3.4, 3.5 and 3.8), or a reciprocating compressor (or any pump combination). The dead volume of some of these pumps may be considerable and must therefore be taken into account.

The **Sporadic transfer** of **small amounts** of tritium-bearing gases from one primary system to another (eventually installed in a different glove box) can be carried out employing UHV-tight stainless-steel transport vessels provided with two valves in series. The second valve is needed to verify the leak-tightness of the primary vessel before the transport is initiated. The vessel may be filled with gas by PVT procedures and then be transferred between glove boxes via the air locks of the donating and accepting glove box.

Occasional transfer of **larger amounts** of pure tritium-bearing hydrogen isotopes from one glove box to another can be realized with small portable uranium beds such as supplied by Amersham (now GE Healthcare). The actual transfer from glove box to glove box can take place via air locks. Because Amersham type beds are not protected by an insulation vacuum, they display considerable contamination on the outer surface due to permeation of tritium across the wall when uranium tritide is decomposed by prolonged heating at elevated temperatures (commonly performed with a heating tape)[57]. Additionally, significant contamination of the glove box atmosphere must be taken into account. Typical surface contaminations at MBq cm^{-2} level have been detected on a uranium bed. Attempts to reduce the activity of the outer surface of a GE Healthcare bed by submersion into water, cleaning by rubbing with a detergent, or even treating with water in an ultrasonic bath showed only moderate success[58].

When **frequent transfers** of **large quantities** of tritium are necessary amongst adjacent glove boxes, the preferable procedure is to utilize pipes connecting the two primary systems. Between the glove boxes the transfer pipe must be doubled walled, i.e. protected by a gas-tight jacket opened to the atmosphere of one of the two connected glove boxes, and monitored for tritium. Jacketed transfer lines between primary tritium handling systems up to 30 m long have been used regularly in numerous tritium handling installations like for example JET [Lae99b], Bruyères-le-Châtel [Hir88], TLK (CAPRICE – PERMCAT or the integration KATRIN - CAPRICE) [Doe08], etc. without contingencies.

Large tritium-handling experimental facilities like Bruyères-le-Châtel, France or TLK, Germany [Sch91a] opted additionally for a **Central Tritium Transfer System** designed to accept and distribute hydrogen isotopes within all systems of the respective laboratories. A central system is justified by activities such as i) receive tritium delivered by national or international suppliers, ii) analyse chemical purity and isotopic composition of received tritium, iii) perform shipper - receiver comparisons, iv) analyse the chemical and isotopic composition of gases utilized or transferred within the laboratory and secure information needed for tritium material balance, v) supply chemically pure hydrogen isotope mixtures to the Isotope Separation System and receive pure hydrogen isotopes from this system, vi) supply/receive chemically and isotopically

[57] Replacing uranium tritide by a getter tritide decomposing at lower temperatures, e.g. ZrCo, will only ameliorate but not solve this problem.

[58] R.-D. Penzhorn, Institute of Radiochemistry, unpublished results, Kernforschungszentrum Karlsruhe, Karlsruhe, Germany, 1999

pure gases to/from the Tritium Storage System, vii) supply chemically impure hydrogen isotopes to the Analytical System and to the Tritium Purification System, viii) supply pure tritium and mixtures of tritium with other hydrogen isotopologues to the experiments, ix) receive pure tritium or mixtures of tritium with other isotopologues from the experiments, etc.

Two gas chromatographs of complementary analytical capability (inclusive detection of radioactive eluents), and a volumetric analysis system comprising three calibrated vessels of diverse sizes have been shown to suffice to cope with most qualitative and quantitative analytical tasks. Other analytical techniques like omegatron, laser Raman spectroscopy, infrared spectroscopy, or calorimetry, partly installed in glove boxes, constitute efficient complementary analytical tools.

Chief advantages of a Central Transfer System are i) direct or indirect access to common equipment like a high vacuum pumping system, analytical instrumentation, calibrated volumina, re-circulation pumps, etc. of all infrastructure systems (and major experiments) requiring supply or disposal of tritium, ii) inter-connection of all major experiments and infrastructure systems, iii) co-ordinated, centrally managed material balance comprising tritium suppliers, experiments, and infrastructure systems, and iv) central data acquisition and archiving.

Safety considerations prompted **TLK** to perform all transfers of tritium-bearing gases following a so-called **fetch-principle** (Holprinzip). Accordingly, the system requiring tritium must become active and fetch tritium utilizing either a previously evacuated vessel, a pumping system, or a getter bed. The procedure adopted at TLK avoids pressurisation of tritium-bearing gases and minimizes the amount of tritium remaining in the line connecting systems after completion of a transfer. Because pressurisation in the receiving system is still possible in the event that glove box gas leaks into the primary system upstream of a pumping system, the involved downstream primary system should be designed to withstand the elevated pressure. The maximum attainable pressure can be estimated from the compression ratio of the transfer pump (or pump combination) with gases constituting the atmosphere of the donator glove box.

For the routine delivery of radioactive and non-radioactive gases into the JET torus during plasma pulses a complex automated system was developed by Pearce et al. [Pea99b]. Non-radioactive gases are suppled from nine different pressurized gas cylinders. The system was shown to be highly flexible and meet all major requirements of the JET machine. Before starting an experimental campaign, gas type and initial pressure of each of the introduction modules is specified and entered into the computer system CODAS. The gas cylinders connect through

a matrix of valves which allows any cylinder to connect through to any one of four transfer lines or to a vacuum line. The four transfer lines connect through to a second matrix of valves which allows for any of the ten gas introduction points to the torus to be connected to any one of the transfer lines. Verification of the purity of gases is carried out by an automated system. This was especially important in view of potential cross contaminations caused by human errors, pressurized cylinders containing impure gases, insidiously leaking valves, or control problems with the selected complex matrix for the supply of gases. The system allows detection of contaminations at ppm level.

Because of the proximity to the torus, pressure gauges compatible with radiation of up to 10^{22} neutrons of 14 MeV were selected. Absolute piezo dosing valves of all-metal seal were shown to be radiation resistant up to a dose of 10^8 rad. These valves could control a deuterium flow of up to 1500 mbar l s^{-1}. For the introduction of tritium, a separate dedicated module was installed. Tritium transfer lines from the AGHS of JET to the torus module are all secondary contained. Numerous piezo dosing valves relying on an all-metal seal combined with an isolation valve serve for gas fuelling.

After injection of many hundreds of grams of tritium into the torus and many hundreds of generated pulses there is presently abundant experience on which to base the design of future injection systems.

3.18.4 Processes for chemical purification and recycling of tritium from fusion devices

Within the frame of the fusion fuel cycle of ITER a central duty adjudicated to the plasma exhaust clean-up system consists in cleaning the gas continuously pumped from the torus and the neutral beam injection system from impurities and the helium ash generated by the fusion reaction before re-injection into the torus. A further crucial task of the clean-up system is recovery of all residual molecular and bound tritium from the impurity stream to the point of generating an exhaust gas that can be released into the environment. Such rather exigent objectives are best accomplished when all tritium-bearing species are converted at the highest degree possible into a single chemical form, i.e. either Q_2 or Q_2O (Q = H, D, T). In view that tritium oxide is biologically 25000 times more radiotoxic than molecular tritium, conversion

into the molecular form is the preferred option. Prior to re-injection into the torus, an isotopic separation is necessary in order to recover molecular deuterium and tritium and discharge or interimly store nearly completely decontaminated protium. This slightly contaminated protium can be used in several applications.

Because palladium/silver permeators purify hydrogen isotopes selectively by physical permeation the attainable degree of chemical purification is extremely high (see section 3.14.3). For this reason, this device constitutes a key component of most purification and recycling processes concepts developed to date. Operating a permeator in conjunction with appropriate catalysts, offers important advantages: i) cracking of aliphatic and olefinic hydrocarbons of low or high molecular weight into the elements, ii) enormous enhancement of the conversion of aliphatic and olefinic hydrocarbons into carbon dioxide and molecular hydrogen, and iii) the option of isotopic swamping by counter current procedures to recover quantitatively tritium from an isotopically-substituted gaseous molecular hydrogen stream.

Several process concepts based on diverse process step combinations have been demonstrated experimentally and theoretically under stringent realistic experimental conditions in the presence of relevant concentrations of tritium. Because of worldwide prolific basic and technological research activities during past decades on pertinent topics, there is now a vast body of experience on which to base design and construction of a clean-up process meeting virtually all requirements of ITER. The most promising process options that have emerged are succinctly described below.

3.18.4.1 Loop combining a nickel catalyst with a palladium/silver permeator (CAPRICE)

A rather effective process concept for the recovery of tritium from gaseous mixtures of hydrogen isotopologues containing typical plasma exhaust impurities such as helium ash and small partial pressures of carbon monoxide, carbon dioxide, aliphatic and olefinic hydrocarbons, and water vapour, was developed at Institute of Radiochemistry, FZK, during the period 1985 – 1993 [Pen91a]. First experiments designed to demonstrate the achievability of the demanded unprecedented high degree of tritium recovery were carried out during the period 1986 – 1988 [Pen88]. These and numerous other subsequent investigations performed without and with tritium culminated in a comprehensive technical scale facility planned and erected at TLK in four glove box modules by National Nuclear Corporation (NNC), United Kingdom [Nat91]. Commissioning and first experiments were performed by Glugla and co-workers [Glu95].

First step of the tritium-recycling process comprises extraction of the majority of the molecular hydrogen isotopes - tritium and deuterium - from the plasma exhaust gas using one (or several) front end palladium/silver permeator (s). Thereafter, all impurities and the remaining molecular hydrogen isotopes present in the permeator bleed are processed batch-wise in closed loop operation. Principal components of the loop are a heated nickel catalyst bed, a second palladium/silver permeator and several diverse pumps.

The chemically most resilient impurity in the plasma exhaust is methane. This hydrocarbon is decomposed reversibly on nickel catalyst into carbon and molecular hydrogen. Many experimental results are available on the mechanism of this reaction as apparent from the results published by Rostrup-Nielsen and Trimm [Ros77], McCarty and Wise [McC79], and Kuijpers et al. [Tri77; Kui81; Kui83; Kui84].

Equilibrium constants for the reaction

$$3\,\mathrm{Ni\,(s)} + \mathrm{CH_4(g)} \rightleftharpoons \mathrm{Ni_3C\,(s)} + 2\,\mathrm{H_2(g)}$$

were determined within the temperature range 499 - 558 K by Browning and Emmett [Bro52]. The temperature dependence of the rate of decomposition of methane over a Ni/SiO_2 catalyst is described by an equation obtained from investigations of Fukada et al. [Fuk04]

$$k = 3.09 \times 10^1 \exp\left(\frac{-29.5\,\mathrm{kJ\,mol^{-1}}}{RT}\right)$$

Higher saturated hydrocarbons like ethane, propane, and butane have also been shown to crack into the elements according to reaction

$$\mathrm{C}_x\mathrm{H}_y(\mathrm{g}) \underset{\text{Ni catalyst}}{\rightleftharpoons} x\,\mathrm{C\,(s)} + \frac{\mathrm{y}}{2}\,\mathrm{H_2\,(g)}$$

The same holds for unsaturated hydrocarbons [Ros77; Tri77]. As displayed in Fig. 3.73, ethylene is rapidly converted into ethane and a small fraction of methane when the reaction is carried out in the presence of nickel catalyst maintained at 443 K in a closed loop mode of operation and bypassing the permeator [Pen91d]. Raising the temperature further up to 773 K causes the equilibrium fraction of generated hydrogen to increase significantly, that of ethane to drop nearly to zero, and that of methane to become substantial. Once a heated permeator, whose permeate

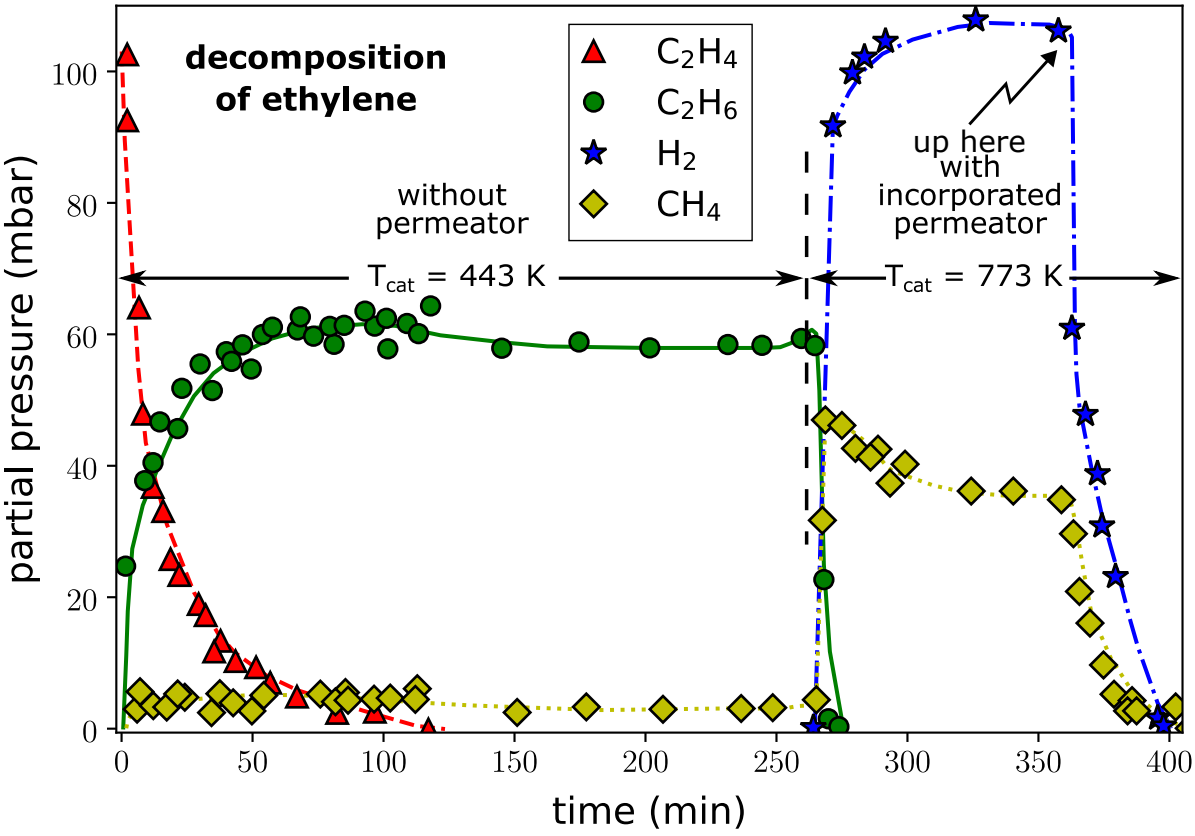


Figure 3.73: Equilibrium decomposition of ethylene on a nickel catalyst in closed loop operation mode first without and then with integrated permeator. The catalyst temperature was maintained i) at 443 K, ii) at 773 K and iii) at 773 K with concurrent removal of hydrogen from the loop via an integrated palladium/silver permeator. The initial pressure of ethylene was 102.3 mbar (after [Pen91d]).

gas is continuously pumped, is integrated into the loop, the reaction of ethylene into carbon and hydrogen rapidly shifts towards the right (removal of a gaseous reaction product) and the conversion into carbon becomes essentially quantitative.

When carbon monoxide, another potential plasma exhaust impurity, is exposed to a nickel/SiO_2 (or supported on alumina) catalyst at 550 K disproportionation takes place according to reaction

$$2\,CO \rightleftharpoons C\,(ads) + CO_2$$

which leads to carburization of the catalyst [Ros77; McC79].

Because the overall cracking rate gradually decreases with progressing deposition of carbon on the catalyst surface, occasional regeneration of the catalyst is recommended. Regeneration of the heated catalyst with hydrogen takes place according to reaction

$$Ni_3C + 2\,H_2 \longrightarrow 3\,Ni + CH_4 \ .$$

Carbon generated via aliphatic or olefinic hydrocarbon cracking deposits on the nickel catalyst i) as chemisorbed species, ii) bulk nickel carbide, iii) amorphous carbon, and iv) crystalline elemental carbon (in order of decreasing reactivity towards hydrogen). The carbon deposit produced from the decomposition of hydrocarbons on nickel catalyst reacts with hydrogen yielding almost exclusively methane [Kui81]. After completion of the reduction with hydrogen at 723 K (decarburization) only a very small amount of strongly bound carbon remains on the surface [Kui84]. In the specific case of carbon generated by disproportionation of carbon monoxide higher hydrocarbons were observed additionally to methane upon reaction with hydrogen at temperatures of 473 K.

Kuijpers et al. [Kui84] and Fukada et al. [Fuk04] demonstrated experimentally that at temperatures within the range 573 - 1073 K the original properties of the catalyst can be restored. The only regeneration products are gaseous methane and sometimes a small fraction of higher hydrocarbons. This finding is of immediate consequence to the above described plasma exhaust clean up processes because it means that the catalyst can remain in operation for prolonged time without requiring frequent replacement. This has actually been the case with the facility CAPRICE now in service with tritium at TLK for almost 30 years.

Additional reactions promoting gasification of carbon are:

$$C + O_2 \longrightarrow CO_2$$

$$C + CO_2 \longrightarrow 2\,CO$$

$$C + H_2O \longrightarrow CO + H_2 \ .$$

Easy catalyst regeneration is of consequence to the above described plasma exhaust clean up process. Because the catalyst can remain in operation for an extended period of time there is no need for frequent and cumbersome catalyst replacements. In fact, the facility CAPRICE

at TLK has been in discontinuous service with tritium for almost 30 years with one and the same catalyst. Because the nickel-catalyzed gasification of carbon by steam proceeds with the same rate as the diffusion of carbon through nickel, an increase of pressures is not expected to lead to higher rates. Regeneration with oxygen appears to be less effective than with hydrogen. The regeneration of the catalyst with carbon dioxide requires exceedingly high temperatures, i.e. 900 K [Tri77]. At temperatures above 973 K the rate of gasification decreases.

Another pertinent reaction taking place on the nickel catalyst by reaction with carbon monoxide is the conversion of tritiated water into tritiated molecular hydrogen. This so-called **water gas shift reaction** proceeds according to reaction

$$Q_2O + CO \longrightarrow Q_2 + CO_2 \quad (Q = H, D, T) \ .$$

Recapitulating, when hydrocarbon cracking and water gas shifting take place on a heated nickel catalyst in closed loop mode while continuously and quantitatively removing chemically liberated hydrogen isotopes via a permeator integrated into the loop, the reaction rate can be greatly accelerated and the degree of conversion shifts to almost 100 % [Pen91a; Glu95; Glu97a]. Therefore, an initial gas mixture consisting mostly of He ash, CO, CO_2, CxQy, Q_2, and Q_2O (Q = H, D, T) is converted into helium, carbon, carbon monoxide, and carbon dioxide. This constitutes in essence of the operation principle of the CAPRICE process.

The technical scale process CAPRICE has been demonstrated successfully with up to 90 % tritium containing 10 % deuterium and impurity gases at compositions frequently simulating those expected in the exhaust gas of the ITER machine [Bor05]. The facility has now been operated for more than twenty eight years by a fairly large number of different operators and researchers many from abroad. Besides of the constantly ongoing experimental program, aimed at developing a final clean-up process for ITER, CAPRICE, has also served reliably and without contingencies over many years for the recovery of tritium from most exhaust gases released by diverse TLK experiments as well as infrastructure systems. These exhaust gases consisted of diverse tritiated species sometimes together with other reactive or non-reactive inorganic and organic gases. The resulting off gases were decontaminated to the extent that they could be released into the environment. Therefore, CAPRICE has significantly contributed to retain tritium within the

laboratory and keep releases into ambient at levels much below those authorized for the whole laboratory.

3.18.4.2 Isotopic swamping device PERMCAT

The original PERMCAT (PERMeator/CATalyst) reactor developed at TLK is a device designed for isotopic swamping (see Fig. 3.74a). For enhanced efficiency, it combines in a single component a palladium/silver permeator with a nickel catalyst [Glu97b]. PERMCAT was conceived as final detritiation step for the extraction of very small concentrations of tritium ($< 1\,\%$) from a tritium-bearing gas mixture. It operates at 673 K. To meet the unprecedent high decontamination requirements of ITER it is necessary to strictly avoid cross contaminations between gaseous streams of the CAPRICE process with those of the subsequent PERMCAT process.

Meanwhile, more advanced PERMCAT reactor concepts based either on edge welded bellows welded to palladium/silver tubes (see Fig. 3.74b) or on a corrugated palladium/silver membrane (see Fig. 3.74c) have been developed and tested. Aim of these improvements has been to better cope with the rather significant dilation and deformation of membranes upon hydrogen uptake at elevated temperature [Glu06b; Dem10]. An additional benefit of corrugation is substantial increase of total permeation area within a given volume and significant improvement of the mechanical stability of the rather thin Pd/Ag membrane. Good corrugated palladium/silver tubes completely free of cracks were only obtainable after the material was annealed at 1273 K. These advanced devices still need to be demonstrated in tritium service over prolonged periods of time and under a variety of exigent experimental conditions before they can be recommended for implementation at ITER.

Best catalyst promoting isotopic exchange between molecular hydrogen and tritiated species like Q_2O, CQ_4 and Q_2 (Q = H, D, T) without at the same time furthering other side reactions was found to be the nickel-based NIKKI 111 catalyst commercially available in Japan and consisting of 50 % Ni on kieselguhr [Bor03; Bor05; Bor07; Dem10; Wel10][59]. The basic properties of this catalyst have now been investigated in several research laboratories [Tri77; Yos83b; Pen88; Wil94b; Wel10]. Surface area, bulk density, crush strength, and mercury porosity of the catalyst were determined to be $40\,m^2\,g^{-1}$, $1.55\,kg\,l^{-1}$, $200\,kg\,cm^{-2}$, and $0.17\,cm^3\,g^{-1}$, respectively. The

[59] Although a Pd on Al_2O_3 or SiO_2 catalyst was found to actively promote isotopic exchange, it was rejected because of its high susceptibility to poisoning by CO.

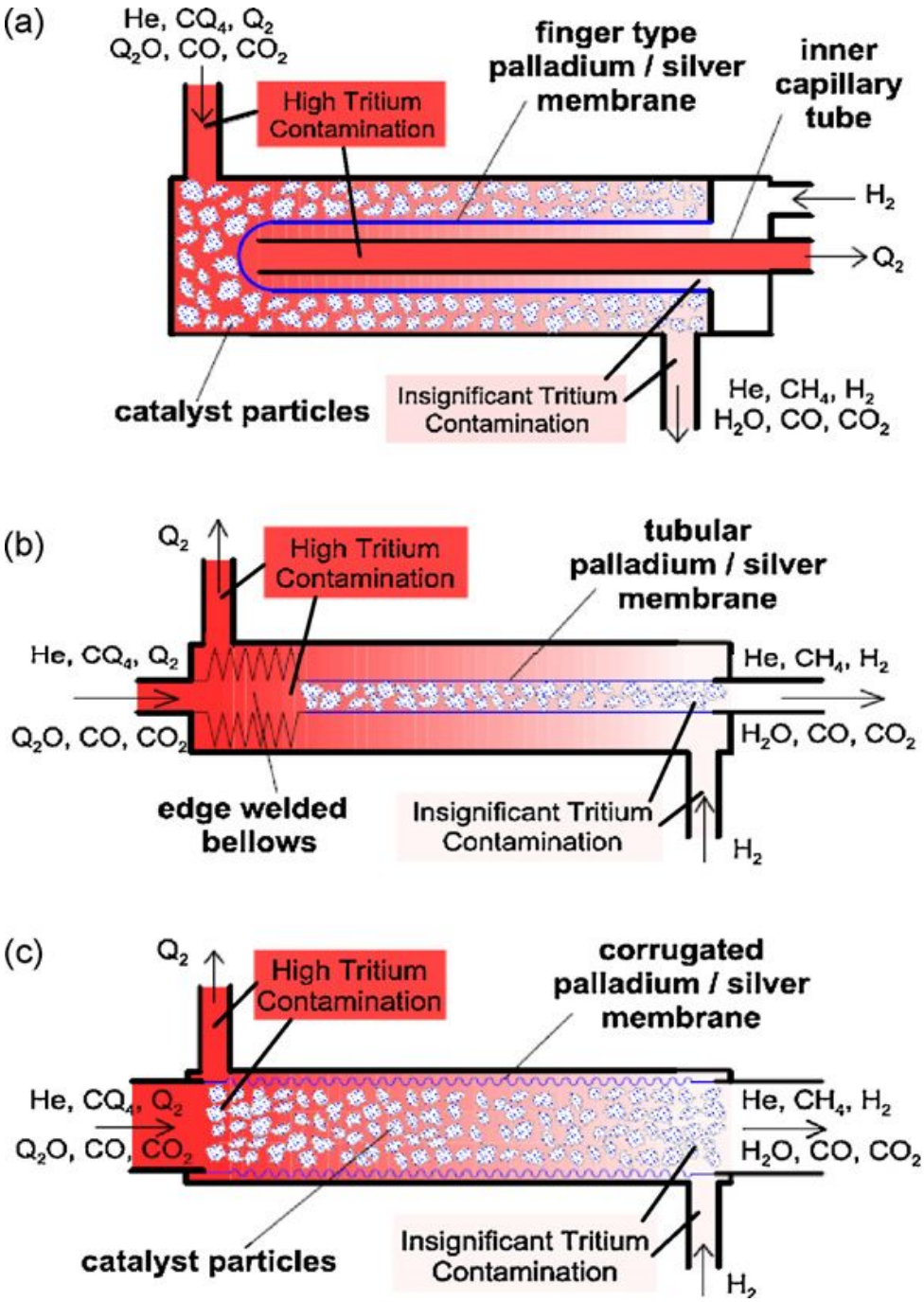


Figure 3.74: Original PERMCAT device option (a), and advanced design options (b, c) (Q=H, D, T) [Dem10].

catalyst has been employed successfully for about three decades in a variety of research and support activities at TLK with the engineering-scale facility CAPER using mostly ITER relevant gases and representative concentrations of tritium without noticeable loss of activity. As a consequence of these activities, the catalyst has been proposed as reference catalyst for the fuel clean-up system of ITER.

A numerical model of the PERMCAT swamping unit was developed by Munakata et al. [Mun05a]. The model is based on counter current one-dimensional plug flow operation across a palladium/silver membrane. Mass balance equations include catalytic reactions, isotope exchange reactions, and permeation of hydrogen isotopes through palladium/silver. Chemical species taken into account for the calculations were He, H_2, D_2, T_2, H_2O, D_2O, T_2O, CH_4, CD_4, CT_4, CO, and CO_2. The simulation of experimental results obtained with PERMCAT was considered satisfactory.

3.18.4.3 Loop combining a nickel catalyst/permeator system CAPRICE with a PERMCAT unit (CAPER)

After the original CAPRICE facility comprising two major basic consecutive steps, i.e. front-end permeator and catalysis/permeator loop, was upgraded by a third process component, i.e. a PERMCAT device, a rather sophisticated and highly efficient multistage clean-up process was obtained. The upgraded process, which is identified by the acronym CAPER (CAPRICE/PERMCAT), is illustrated in a fairly simplified block diagram in Fig. 3.75 [Glu98b; Glu00a; Bor03; Cor05].

The main body of the erected facility is depicted in Fig. 3.76. Not shown is most of the peripheral equipment comprising a large $150\,m^3\,hour^{-1}$ NORMETEX pump housed in a separate glove box, a **safety cabinet** for the pressurized gas cylinders delivering non-radioactive gases, a dedicated large Tritium Retention System, comprehensive analytics consisting of two gas chromatographs (one of which is equipped with an ionization chamber for the detection of tritiated species), etc. The good-sized secondary contained transfer line above the two glove boxes connecting the primary systems installed in each of them is displayed on the upper right of the photo. With the CAPER process it has become possible to completely recover with a very high degree of chemical purity all hydrogen isotopes from a process gas initially having a tritium concentration of $\leq 4.4 \times 10^{16}\,Bq\,m^{-3}$ and total impurities in the few percent range. At the same

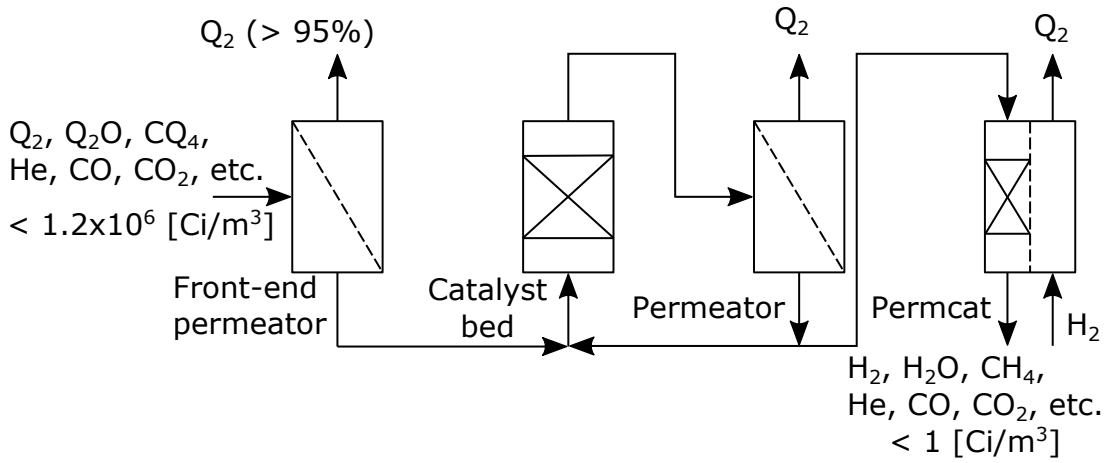


Figure 3.75: Much simplified diagram illustrating the process principle of CAPER (after [Bor05; Wel10].

time an effluent gas essentially free of tritium is generated. To achieve this goal, it is necessary to limit the tritium level in each step of the process to pre-established upper values and strictly avoid cross contaminations.

The best overall decontamination factor

$$\mathrm{DF} = \frac{\text{feed activity}}{\text{bleed activity}}$$

achieved experimentally with CAPER, i.e. 2×10^{10}, is more than two orders of magnitude higher than that currently demanded for ITER, i.e. 10^8.

The advanced counter-current isotopic swamping PERMCAT component in single bed configuration developed at TLK is much easier to fabricate than previous models and in addition more robust (see Fig. 3.77a) [Wel10]. Manufacture of the device was carried out almost completely at KIT workshops strictly adhering to quality control specifications such as described in i) Technical Terms for Delivery and Acceptance of TLK, ii) European Pressure Equipment Directive (PED 97/23/EC), iii) AD (Association for Pressure Vessel Operation) 2000 data sheets, and iv) rules and regulations related to tritium handling, occupational health and safety. Basically, the advanced PERMCAT consists of thirteen palladium/silver fingers each with a length of 350 mm, an outer diameter of 3.3 mm, and a wall thickness of 0.1 mm. They are brazed to a common cup from which the swamping gas is fed. The body of the PERMCAT catalyst bed is depicted in Fig.

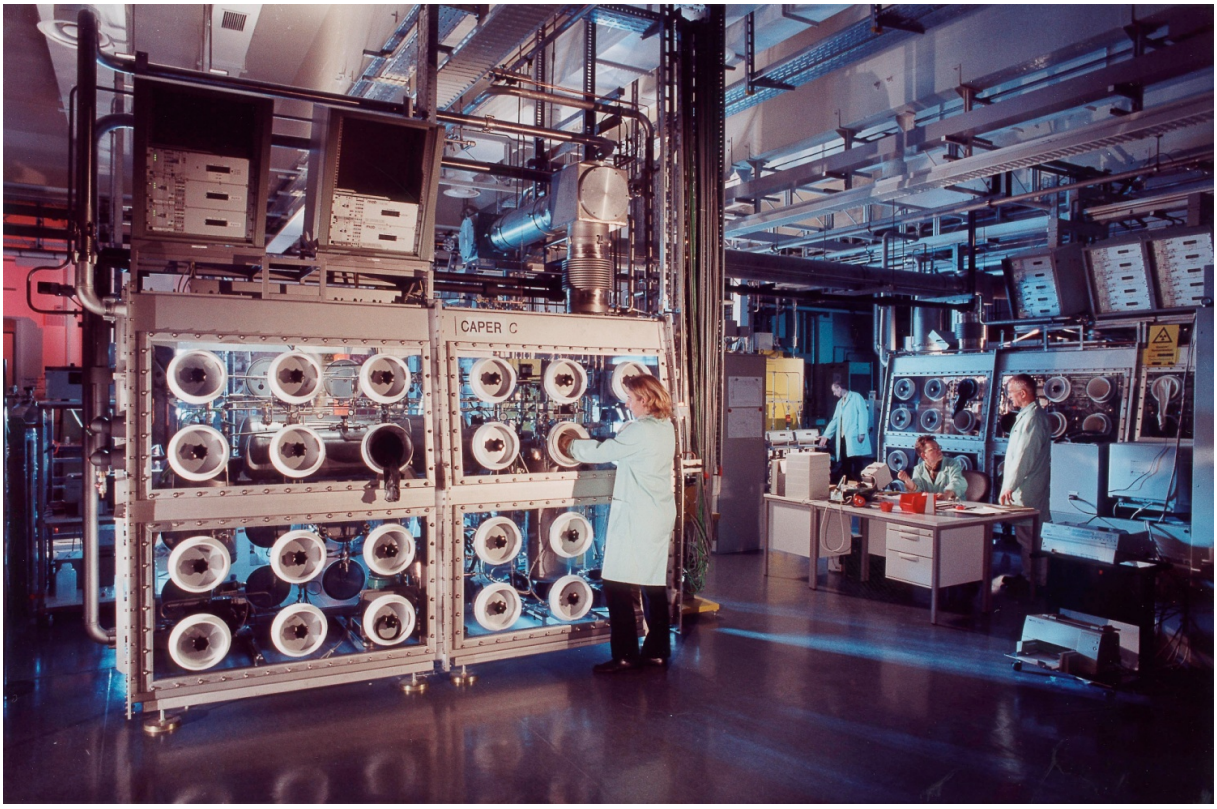


Figure 3.76: Prototype plasma exhaust cleaning facility CAPER showing the PERMCAT device (front) and the CAPRICE facility (rear right) installed in glove boxes at TLK. The confined transfer line between the PERMCAT and the CAPRICE glove boxes is shown on the right top of the photography.

3.77b). It is filled with 95 g NIKKI 111 catalyst with a grain size spanning between 500 - 800 µm. Pd/Ag membranes are kept in place by spacers. The bundle of 13 stainless-steel capillaries is joined to a stainless-steel core box connected to a CF flange for easy insertion (see Fig. 3.77c).

The crucial, upgraded facility CAPER of the TLK infrastructure is at present supplying concurrently pure tritium to the experiment KATRIN as well as to other experiments in the laboratory. In case of KATRIN, it is accepting the resulting offgas stream in order to remove impurities in provision for re-injection. KATRIN is a rather large experiment designed, erected and taken into operation for the determination of the effective electron antineutrino mass with an expected sensitivity of 0.2 eV. The measurement principle is based on a precise determination of the shape of the tritium decay sprectrum close to its end point at 18.6 keV [Bor15]. Nearly 200 scientists and operators from all over the world are currently participating in commissioning, operating and evaluating data obtained with the KATRIN experiment. One basic requirement of

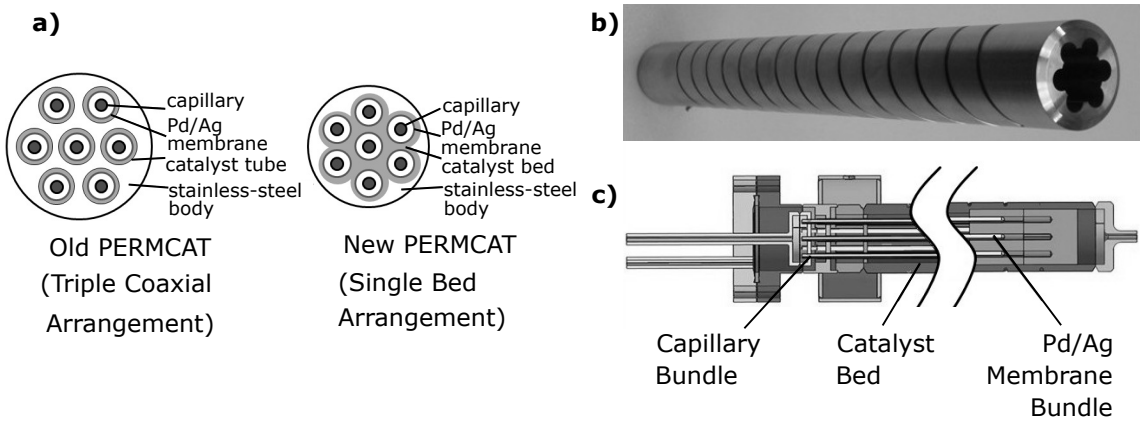


Figure 3.77: Comparison between the old and the new layout of the PERMCAT used at TLK (Note: whereas at TLK only 7 permeation units were utilized (see a)) a much higher number will be necessary at ITER.). Figure b) shows the body of the upgraded PERMCAT catalyst bed, and figure c) a longitudinal section drawing of PERMCAT [Wel10].

this experiment is the un-interrupted supply of pure tritium at a constant throughput of $40\,\mathrm{g\,d^{-1}}$ for an extended period of time. Thus, aim of the first commissioning campaign with tritium in 2016 was to demonstrate the long-term stable operation of the KATRIN source at full column density over many days [Ake20]. In this run, which was carried out without integration of the large spectrometer, a $20\,\mathrm{bar\,l}$ gas mixture consisting of 1 % DT in D_2 was recirculated for 13 days across the KATRIN inner loop comprising the windowless gaseous tritium source (WGTS). Steady state pressure conditions were maintained in the loop by compensating the small extracted offgas stream consisting of DT/D_2 contaminated by impurities with a corresponding fraction of purified DT/D_2 supplied from a pressure-controlled buffer vessel. Recirculating gas was continuously cleaned with a palladium/silver permeator exclusively permeable to hydrogen isotopes and re-injected into the WGTS of the spectrometer. Laser Raman spectroscopy integrated into the inner loop was used to monitor uninterruptedly the composition of the gas. Besides demonstration of the spectrometer stability, numerous tritium electron spectra were recorded in order to compare among potential analysis strategies, validate the calculation software and confirm the stability of the fitting parameters. After successful completion of the commissioning phase with slightly tritiated deuterium, a further campaign was performed 2019 with tritium of $> 95\,\%$ purity [Stu21]. In this case, a small bleed stream containing the impurities ^{3}He, tritiated methane and carbon monoxide was reprocessed at the CAPER facility and the purified gas collected for re-injection.

To reduce the release of impurities due to interaction of tritium with metal surfaces, the relevant section of the system was exposed statically to 680 mbar of tritium for five weeks. The success of this inertization procedure was confirmed by the absence of impurity freeze-out in the injection capillary inside of the WGTS cryostat. A remarkable conclusion from current research with the Karlsruher Neutrino Experiment employing a high purity gaseous molecular tritium source points to an upper limit of 1.1 eV (90 %) confidence level) on the absolute mass scale of neutrinos. This result improves previously obtained mass limits by almost a factor of two [Ake19; Ake20].

Recapitulating, the CAPER process has now been demonstrated in numerous short and long-term runs utilizing gases realistically simulating the expected composition of the plasma exhaust gas from a fusion machine. Experimentally it was confirmed by computer-controlled operation of CAPER that full recovery of the fuel gases is possible while generating at the same time an exhaust gas stream that qualifies for release into the environment after passing through a conventional Tritium Retention System. The CAPER process has moreover been employed routinely and successfully for the recovery of tritium from numerous rather diverse gas mixtures arising from experiments of the kind typical for a large tritium handling laboratory [Dem15b]. The TLK team engaged in operating CAPER has changed repeatedly almost completely over the past decades, it was frequently supplemented by guest scientists - recurrently from abroad. Constant enhancement of the facility itself, upgrading of the dedicated Automation System, and modernization of the Central Control System (see also section 5.7) has been carried out time and again in order to keep up with the indispensable renovation of the laboratory while complying with increasing demands posed by new experiments implemented at TLK in recent years, e.g. KATRIN. The unvarying reliability of CAPER for the supply, recovery and cleanup of tritium "process" gas used in round the clock campaigns of KATRIN can be taken as further evidence for the appropriateness of CAPER as plasma exhaust clean up process for ITER. After nearly three decades of safe experimental activities with tritium, the CAPER facility has developed into a fundamental support process of TLK. On the basis of the experience gained over the years, a reliable CAPER-like clean-up process has evolved and been designed for the fuel cycle system of ITER [Pen00b; Glu02a; Bor03; Cor05; Glu13]. The unvarying reliability of CAPER for the supply, recovery and cleanup of tritium "process" gas used in round the clock campaigns of KATRIN can be taken as further evidence for the appropriateness of CAPER for ITER.

With respect to ITER, the advanced process concept CAPER offers the following major advantages: i) low overall tritium inventory, ii) high degree of availability, iii) recovery of fuel gases in rather high chemical purity, iv) constant very high overall tritium decontamination factor ($> 10^8$), v) no major adjustment of chemical composition required, vi) rather small generation of solid waste, i.e. sporadically tritium-contaminated catalyst, vii) process based on conventional, established technology, viii) ample body of well documented basic & theoretical research, and ix) extensive operational experience partly based on advanced technology.

Note: The composition of the plasma exhaust gas at the time CAPER was planned was based on a first wall of ITER consisting mostly of CFC. With the currently foreseen first wall materials for the vacuum vessel, i.e. W and Be, the composition of the exhaust gas both with respect to type and concentration will be substantially different. In particular, fewer carbonaceous impurities present at much lower concentrations are expected.

3.18.4.4 Combination of catalyst/permeator into a single unit (PMR)

The direct combination of a permeator with a catalyst into a single unit was likewise proposed at **TSTA** and designated Palladium Membrane Reactor (PMR) (see Fig. 3.78). It consists of a permeator containing nickel metal catalyst[60] either outside of the palladium/silver permeation tubes (outside/in operation modus) (see Fig. 3.78a) or inside of a single coiled palladium/silver tube (inside/out operation modus) (see Fig. 3.78b). To accomplish plasma exhaust clean-up of a fusion machine a three-step process was proposed comprising i) a front end permeator, ii) a first stage outside/in PMR1 made up of eight 0.75 m long Pd/Ag tubes, and iii) a second stage inside/out PMR2 consisting of a single 1.5 m long coiled Pd/Ag tube packed with catalyst [Bir96; Bir98b]. Proceeding conventionally, this concept was first verified experimentally with non-radioactive reactants and subsequently employing relevant concentrations of tritium-bearing species and other impurities.

To simulate plasma exhaust gas, methane and helium were added to a stream of hydrogen isotopes obtained directly from the cryogenic isotope separation system of TSTA (see Fig. 3.79). The resulting gaseous feed stream comprised 9.7 Q_2, 0.3 CQ_4, 0.3 He, and 0.3 Q_2O l(STP)/min, respectively. The actual isotopic composition was obtained by isotopic scrambling of methane

[60] Alternatively, it is also possible to use Pt/α-Al_2O_3 catalyst [Bir96; Bir98a; Bir98b].

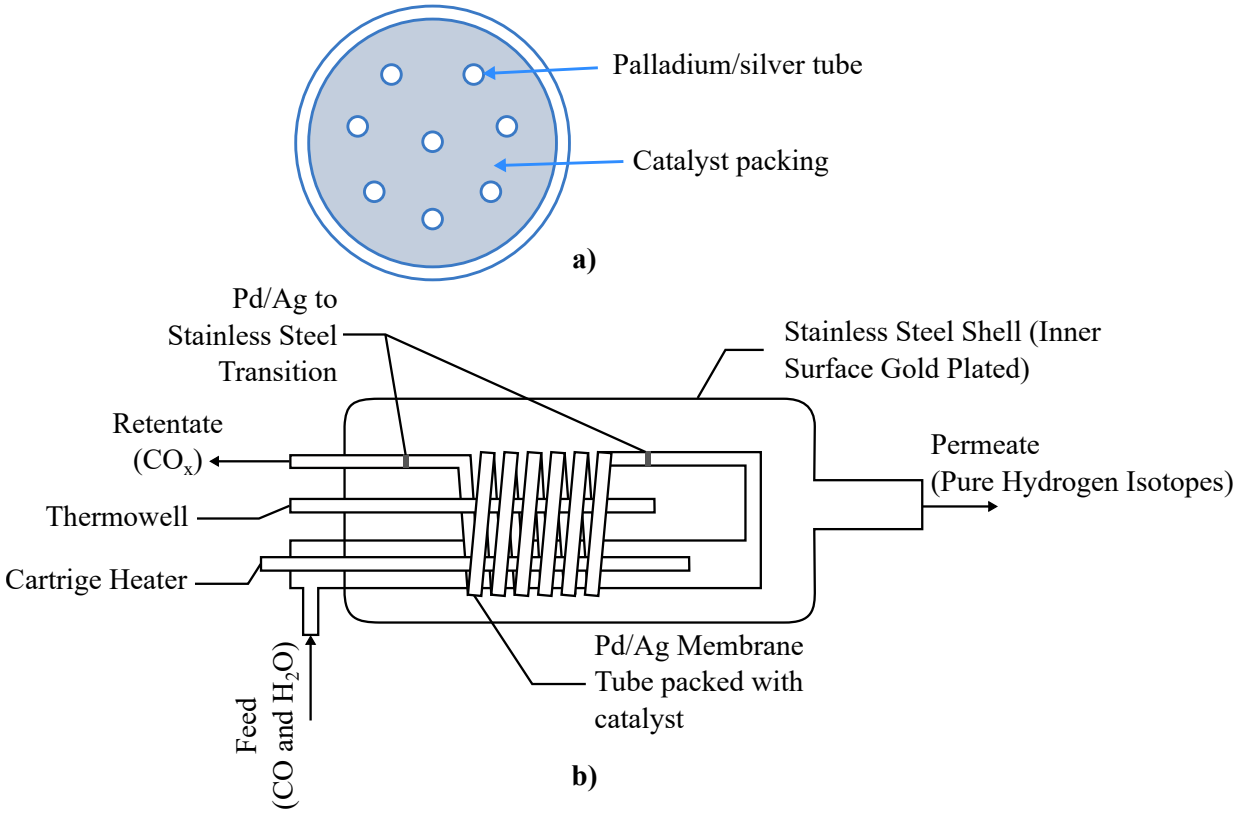


Figure 3.78: Cross section of an a) outside/in first stage PMR permeator and schematic drawing of an b) inside/out second stage PMR permeator [Wil94b; Wil95a].

and water with Q_2 (Q = H, D, T) over a nickel catalyst maintained at 673 K[61] and oxidation of Q_2 in the presence of O_2 on a Pt catalyst at 373 - 573 K (see Fig. 3.79). In order to demonstrate the proposed plasma exhaust clean-up process most of the Q_2 (simulating unburned fuel) was recovered in a first step using a front-end Pd/Ag permeator (configuration as in Fig. 3.78b but without catalyst). The design used at TSTA consisted of five coiled palladium/silver tubes, each 12 m long, 3.2 mm in diameter, and of 0.08 mm wall thickness. A metal bellows pump sufficed to remove about 98 % of permeated hydrogen, i.e. feed 9.7 STP l/min and permeate 9.5 STP l/min. Permeate hydrogen isotopes were directed back into the middle of the isotope separation system. The achieved molecular hydrogen isotope decontamination factor was estimated to be about 50.

[61] At 673 K methane is not cracked on the Ni catalyst.

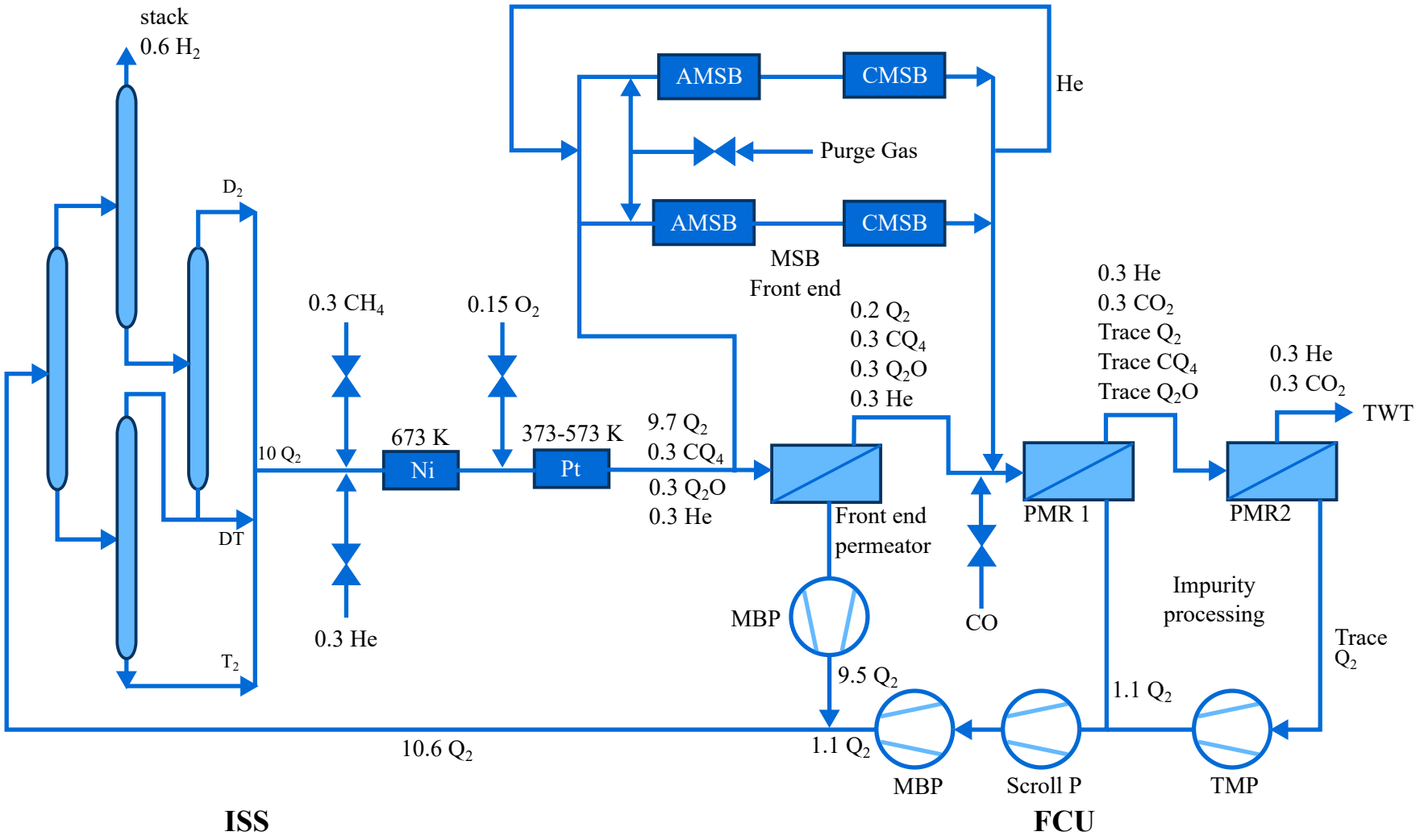


Figure 3.79: Integrated Fuel Clean-up (FCU) System and Isotope Separation System (ISS) at TSTA for testing first and second stage PMR reactors (all flows in l(STP)/min) (after [Bir98a]). TWT = Tritium Waste Treatment, AMSB = Adsorber Molecular Sieve Bed, CMSB = Cryo Molecular Sieve Bed, MBP = Metal Bellows Pump, TMP = Turbo Molecular Pump, PMR = Palladium Membrane Reactor.

Therefore, the composition of the effluent stream from the front end permeator, i.e. 0.2 Q_2, 0.3 CQ_4, 0.3 He, and 0.3 Q_2O l(STP)/min] (Q = H, D, T), respectively, comprised the remaining fraction of hydrogen isotopes and the impurities. After addition of carbon monoxide, the resulting gas mixture was processed in the first stage PMR (outside/in). Here, the impurities water and methane are converted nearly quantitatively into molecular hydrogen and other non-tritiated products like carbon dioxide and carbon monoxide via reactions such as

$$Q_2O + CO \longrightarrow Q_2 + CO_2$$

$$CQ_4 + Q_2O \longrightarrow 3\,Q_2 + CO\ .$$

These reactions are well known as the **water gas shift** and the **steam reforming** reaction, respectively. Advantageously, the large amount of catalyst present in the first stage PMR has great acceptance capacity for carbon. Provided flow meters are kept small, the pressure drop will be tolerable. Tritiated water is converted into tritium-bearing molecular hydrogen on the nickel catalyst at temperatures within the range 693 - 713 K[62]. The supply of carbon monoxide is regulated by a mass flow controller and analytical instrumentation capable of real time chemical analysis. If the ratio CQ_4/Q_2O is not within the required range either carbon monoxide or oxygen (convert hydrogen and hydrocarbons to water) must be added to the stream to achieve a good reaction performance. Because of the intimate contact between the gas and the permeator, permeated hydrogen can be extracted rather effectively with a comparatively simple scroll pump. The recovered 1.1 l(STP) /min of Q_2 is added to the front end permeate stream and re-injected into the isotope separation system. Incessant removal of permeated molecular hydrogen contributes significantly to shift the equilibrium of the two reactions displayed above towards the product side. The consequence is a very high degree of conversion. The decontamination factor attained with the first stage PMR was determined to be within the range 200 - 400. Overall size of the first stage PMR tested at TSTA was 1 m long and 10 cm diameter (excluding heater, insulation and vacuum jacket). To attain an ITER scale throughput a PMR consisting of eight Pd/Ag tubes, each with a length of 1 m, was estimated to be sufficient. If these conditions are met, a first stage PMR can process a total feed stream of 905 cm^3(STP)/min which at the time corresponded to about $1/6^{th}$ of the maximum ITER impurity design value.

[62] The Pt on α-Al_2O_3 catalyst is operated at 923 K [Bir98a; Bir98b].

Auspiciously, increasing the annular diameter of the first stage PMR from 0.50 to 0.87 cm permitted doubling the feed flow rate while maintaining full hydrogen recovery [Wil95a].

Primary task of the second stage PMR (PMR2), which operates on inside/out single-pass mode (see Fig. 3.78b), is the removal of trace amounts of hydrogen isotopes (including tritium) from the eluent impurity stream. This task is of crucial importance because it contributes significantly to increase the overall decontamination factor and hence to comply with demanded very low emissions into the environment. Consequently, whereas for the first stage PMR (PMR1) a scroll pump is sufficient, for the second stage PMR (PMR2) a turbomolecular pump backed by a scroll pump and a Metal Bellows are employed to evacuate permeated Q2 down to very low levels (see Fig. 3.79). High vacuum inside of the shell surrounding the Pd/Ag permeation tube is essential to achieve very low hydrogen isotopologue partial pressures in the eluate of PMR2. PMR2 comprises a 1.5 m long coiled Pd/Ag tube packed on the inside with nickel catalyst. It should be noted that the permeate from PMR2 consists of very low partial pressures of hydrogen isotopologues because the eluate from PMR1 is mainly composed of CO_2 and helium and only traces of Q_2, Q_2O, and CQ_4 (Q = H, D, T).

Another to some extent diverging alternative likewise proposed by researchers from TSTA, commences by adding oxygen (or carbon monoxide) to the eluate gases from the front end permeator and feeding this gas stream into one of two PMR´s arranged in parallel of which one is on line and the other on standby. Both contain Pt/α-Al_2O_3 catalyst [Bir98b; Bir98a; Bir99]. The selected process conditions are such that all hydrogen-bearing species are oxidized into tritiated water and carbon dioxide. Permeated hydrogen is pumped with NORMETEX PV-12 scroll pumps backed by Metal Bellows MB601 pumps. Advantage of this pump combination is that in the event of a pump failure the process performance will only be reduced and not stopped. Remaining traces of Q_2, as well as small partial pressures of CQ_4 and Q_2O (Q = H, D, T) are subsequently fed into a second reactor containing Pt/α-Al_2O_3 catalyst operated at 923 K where they are oxidized into water. Generated water is effectively retained in downstream placed adsorber beds each containing 22.7 kg of type 4A molecular sieve (MSB)[63]. Recyling of the hydrogen isotopologues bound to water retained by the molecular sieve can be carried out periodically either once a previously established amount of Q_2O has accumulated in the adsorber

[63] One adsorber bed is online and the other on regeneration or standby.

bed or shortly before the tritium inventory limit holding for every single component of ITER[64] is attained. Regeneration of an adsorber bed is carried out by passing carbon monoxide through the heated bed in opposite direction to that during processing. The resulting carbon monoxide/water steam exhaust gas is then passed through a PMR where water is converted into hydrogen. This hydrogen is efficiently extracted from the PMR by evacuation. The collected hydrogen isotopes are finally separated into pure hydrogen isotopologue fractions by an isotope separation system. These streams can either be re-injected into the fusion machine or stored for other applications. The overall decontamination factor achievable with this fuel clean-up process was estimated to be of the order of 10^8.

To test the process under more severe conditions a two-stage PMR system to recover tritium from tritiated water adsorbed on mobile molecular sieve beds was designed and assembled at Savannah River Site (for more details see Fig. 4.19 and section 4.3.3.2.2 below [Bir98a; Bir98b]) [Ses05]. Adsorbed tritiated water was thermally liberated from an adsorber bed as steam and transported into the PMR´s employing an inert carrier gas containing the necessary partial pressure of carbon monoxide. A mass controller serves to maintain stable process conditions. For the separation of hydrogen isotopes, the pure permeated hydrogen isotopologues are fed either into a cryogenic distillation system or a displacement gas chromatography system. In summary, the application of the two-stage PMR technology to recover tritium from adsorbed water was verified successfully at Savannah River Site.

In a further application, GE Hitachi Nuclear Energy Canada developed a process technology which is also based on a PMR component. Aim of the work was to extract tritium from gaseous and liquid tritium-contaminated waste in order to i) reduce potential environmental contaminations, ii) mitigate long-term storage issues, and iii) recover tritium for beneficial use when economically reasonable. The first Waste Treatment and Enrichment plant designed for this purpose was installed near Cardiff at the GE Healthcare manufacturing site. At this plant (formerly Amershaw), the production of a large number and quantity of a variety of tritium labelled chemicals is ongoing for many years [Bon08]). The process step sequence implemented at Cardiff which eventually leading to pure tritium is shown schematically in Fig. 3.80. Accordingly, organic waste liquids are first oxidized thermally to produce tritiated water, carbon dioxide and other gaseous impurities. Hence, the exhaust gas stream of the oxidizer contains primarily water

[64] Limit amount of tritium for every single ITER component is 100 g.

vapor, carbon dioxide and molecular oxygen not consumed during the oxidation. This gaseseous stream is quenched, further stripped from water, monitored and then released to ambient via stack. Salts resulting from oxidation are given to waste. The collected water containing about 3 ppm of tritium is purified and then subjected to water distillation for first enrichment. To achieve the necessary separation in a reasonably sized equipment, the column is packed with a highly efficient Dixon ring packing. At the top of the column a small fraction of the tritium-stripped reflux liquid is tritium-monitored by online analysis and then given to drain. Tritium-enriched water, now containing 2000 ppm tritium and having a volume reduced considerably by a factor corresponding to enrichment, accumulates at the bottom of the column. For the conversion of tritium-enriched water into molecular tritiated hydrogen, tritiated water vapor is transported by an argon stream, to which previously carbon monoxide has been added, through a PMR palladium/silver membrane reactor. In this reactor hydrogen is generated catalytically from water according to the water gas shift reaction. Tritium-enriched hydrogen is extracted across the PMR by permeation strongly accelerated by an appropriate downstream placed pump combination. PMR-bleed gases, now mostly consisting of decontaminated carbon monoxide, carbon dioxide and helium, are released through stack into the environment after first passing across a Tritium Retention System. To minimize risks for operators and the environment, a fully Distributed Process Control System (DCS), a Safety Instrumentation System (SIS), a Thermal Oxidizer Management System and a Combined Containment Access Control System were used among others for the routine operation of the facility. Other modern safety measures included forced cascade ventilation with online real-time tritium monitors for enhanced protection of operators.

The final product of the process, consisting of pure tritium of more than 99 percent purity, is obtained by isotope separation employing a thermal diffusion column. The column employed in Cardiff has been split into two smaller ones to avoid excessive height. The separation column is cooled from the outside with water and has axially a platinum wire maintained at 1373 K. Thermal diffusion is particularly advantageous for the separation of hydrogen isotopes at small scale because i) it operates with a comparatively small inventory of tritium, ii) is much simpler to operate and safer than a cryogenic distillation, iii) is of simple start up, shutdown, operation and maintenance, iv) is a process at ambient temperature, and v) of low cost for installation and operation. A drawback that requires attention is that thermal diffusion is not simple to scale up

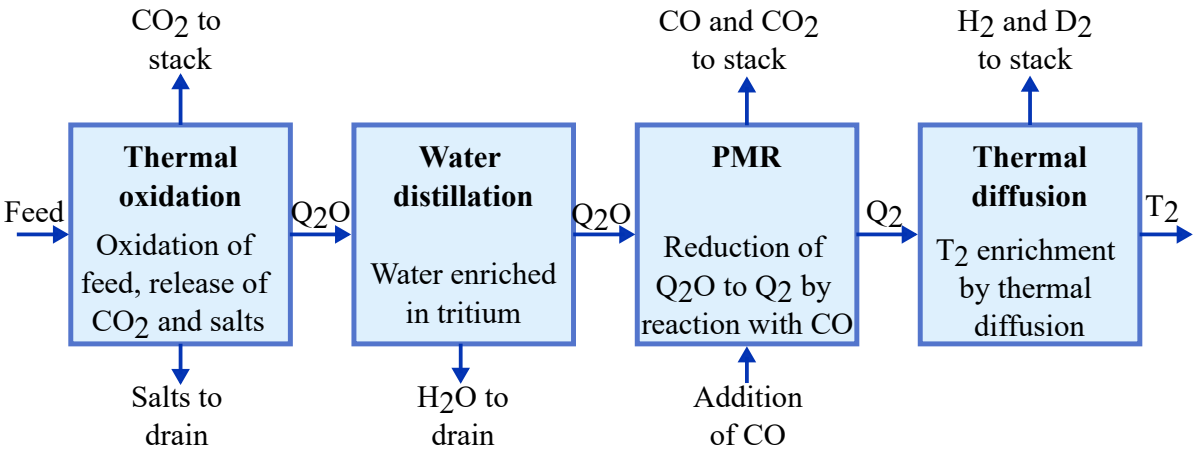


Figure 3.80: Block diagram of the basic process steps of the GE Healthcare Waste Treatment and Enrichment plant in Cardiff, UK (Q = H, D, T) (after [Bon08]).

because the columns must operate in the laminar flow regime and scale up shifts the operation towards a turbulent flow regime.

The Waste Treatment and Enrichment processes of the kind developed at GE may well be considered for application in sizeable tritium handling facilities or of large fusion experiments such as JET or ITER, when it comes to reduce discharges into the environment without perturbing the principal fuel clean-up process.

3.18.4.5 Plasma exhaust clean-up at TFTR

The Tokamak Fusion Test Reactor (TFTR) at Princeton, USA, was safely and routinely operated with tritium for several years beginning December 1993 [Sis90; Rob94; LaM94; And94b; And94a; Hal95; Mue97; Wil97]. Tritium was supplied to TFTR by Savannah River Site in approved shipping containers designed to transport between 1.9×10^{14} Bq and 7.4×10^{14} Bq of tritium. The working tritium inventory limit for TFTR was 5 g and the total quantity allowed in the vacuum vessel 2 g [Wil97]. Tritium delivered to TFTR was stored on site at ambient temperature in uranium beds. When tritium was needed to generate deuterium-tritium plasmas one or more beds were heated and the released tritium injected into the tokamak from any of twelve neutral beams or any of several gas injectors. A first trace experiment with 1 % tritium in deuterium was performed at TFTR November 1993. After successful completion of this first run, a total of almost 20 000 plasma shots including more than 841 pulses utilizing 50/50 mixtures of deuterium

and tritium were carried out during a period of three years. The performed tests released more than 1.4 GJ of fusion energy, and produced more than 4.8×10^{20} D-T neutrons and alpha particles. More than 3.2×10^{16} Bq (almost 90 g) were processed by the TFTR facility during these campaigns.

Within the frame of the TFTR activities, a **Tritium Purification System** (TPS) was integrated into the TFTR fuel cycle. The TPS of TFTR interfaced with the Gas Holding Tanks, Torus Clean-up System, Tritiated Vent System, and Tritium Storage and Delivery System. The rather compact TPS occupied only 2 m^2 of floor space for the glove boxes and 0.8 m^2 for four columns and their outer vacuum containment. Another 3 m^2 were necessary to accommodate part of the cooling system [Rob94]. The Purification System comprised i) a Feed Treatment System (FTS), which separated inert gas (nitrogen) and impurities from hydrogen isotopes, and ii) a Cryogenic Distillation System, which separated hydrogen isotopes into their pure molecular isotopologues. Prior to start of routine activities, a number of leak tests were carried out first with helium and then with tritium. Thereafter, a trial run with 3.7×10^{13} Bq followed by several integrated system tests were performed with up to ten times as high inventories of tritium.

Upon completion of plasma experiments the remaining fuel – at this point contaminated by fusion ash and other impurities - was recovered on cryo panels and subsequently transferred into a gas holding tank. Before reuse, the gas was subjected to purification by passing it through a palladium-silver permeator which permitted nearly quantitative extraction of all hydrogen isotopes from the tokamak effluent gas. The hydrogen isotopes were then separated into three almost pure streams of tritium, deuterium, and hydrogen employing a multi-stage cryogenic distillation system optimized for low tritium inventory [Sci96]. While slightly contaminated hydrogen isotopes were released via the Vent System, tritium and deuterium were stored in cold uranium beds for later recycling.

Another approach consisted in oxidation of the collected off gas and storage of the resulting tritiated water in disposable molecular sieve beds. Eventually, these beds were shipped off-site in type A containers (activity limit $< 3.7 \times 10^{13}$ Bq) either for burial in Hanford, Washington, or processing at Savannah River Site [Wil97].

3.18.4.6 Other plasma exhaust clean-up process concepts

During the early Nineties a sophisticated process concept for the recovery of tritium from the off gas of a fusion machine was developed at JAERI. It encompassed a front-end palladium/silver diffuser, a catalytic reactor for the oxidation of tritium-containing species, a battery of cold traps to retain water, and an ingenious electrolysis cell manufactured of zirconium oxide ceramic. The cell was designed for the electrolytic decomposition of tritiated water vapour and oxidation of hydrocarbons [Hay92b; Kon97; Oku97]. The loop was extensively tested at TSTA under relevant experimental conditions within the frame of a US-Japan collaboration agreement under relevant experimental conditions [Kon94]. Long-term experiments were carried out for periods lasting up to 25 days under steady state conditions employing 2 g of tritium contained in a gasesous mixture simulating composition and concentration of plasma exhaust gases [Kon94].

According to the process, the first step is conventional, i.e. extraction of most of the deuterium/tritium fuel present in the plasma exhaust stream through a front-end palladium/silver permeator operated at 573 K. Extracted hydrogen isotopes were subsequently fed directly into a cryogenic isotope separation system where a pure deuterium and a pure tritium could be isolated and protium discharged to ambient after passing through a Central Tritium Retention System (alternatively, the slightly contaminated chemically pure hydrogen could also be stored and made available for diverse other applications within the frame of the fuel cycle). The permeator bleed stream did now consist of helium ash as main component and species such as NQ_3, CQ_4, CO, CO_2, residual Q_2, as well as possibly small concentrations of several higher hydrocarbons (Q = H, D, T). This stream was further processed by adding an over-stoichiometric amount of oxygen ($< 5\,\%$) and passing it through a noble metal catalyst bed maintained at 773 K. Under these conditions, traces of hydrogen and all impurities were oxidized quantitatively to tritiated water, nitrogen dioxide, and carbon oxides. At this point, all gaseous species with the sole exception of tritiated water, were essentially tritium-free. This exiting stream was passed through a cold trap maintained at a temperature at which tritiated water could be selectively and quantitatively frozen. This was accomplished at TSTA with a Freon refrigerator [Kon92a; Kon97]. At least three cold traps were needed to permit a semi continuous operation, i.e. one in operation mode, one in regeneration mode, and a third trap in a pre-cooling mode. Programmed trap regeneration was performed at 343 K utilizing helium in reverse path to that of oxidisation as carrier gas in

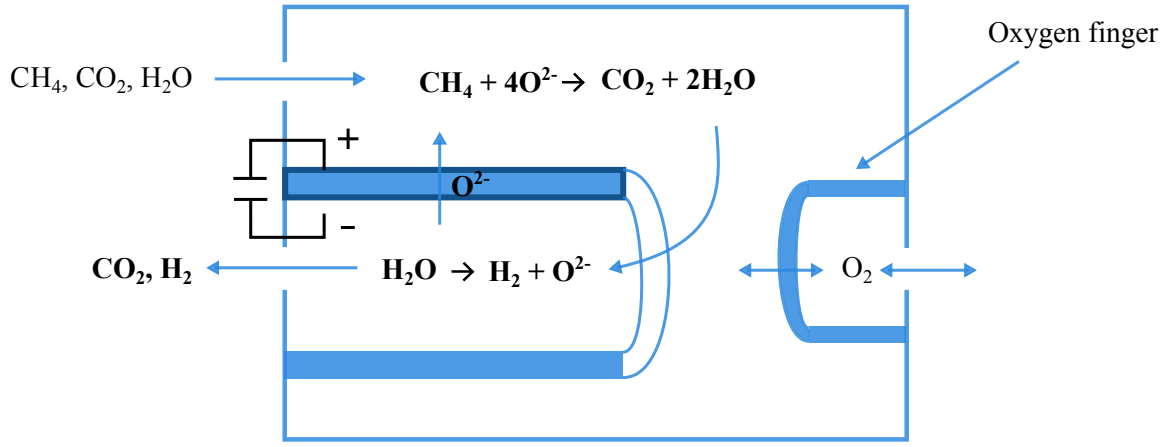


Figure 3.81: Operation principle of the zirconia electrolysis cell (after [Oku97]).

reverse direction to that of oxidation. The resulting helium stream transported tritiated water vapour through a ceramic electrolytic cell which contained ten stabilized zirconia tubes with platinum electrodes on their inside and outside.

The electrolysis cell, which replaces a catalytic reactor, is characterized by a comparatively small inventory of tritium. In the cell, water is decomposed into hydrogen on the cathode and hydrocarbons are oxidized to carbon dioxide and water on the anode. Oxygen diffuses from the cathode to the anode across the zirconia ceramic (see Fig. 3.81). Of concern is the need to maintain the electrolysis cell at a fairly high operation temperature of 870 K. The high temperature is required on one hand to attain fast kinetics and consequently high conversions, and on the other, to achieve sufficiently fast oxygen diffusion rates across the ceramic. A zirconia finger, introduced into the cell, serves to monitor and control the oxygen level in the cell. The throughput of tritiated water across the tested cell was determined to be of the order of 1.1 mol hour^{-1}. The conversion efficiency of water and methane into hydrogen and carbon dioxide was found to be better than 99.9 %.

Besides numerous test runs carried out without tritium at TPL, Japan, the electrolysis cell concept was also subjected to intensive scrutiny at TSTA, Los Alamos, within the DOE/JAERI collaborative agreement [Kon94; Kon95a; Kon98; Nis00]. Experiments were performed employing gaseous mixtures simulating composition and concentrations of plasma-exhaust gas and containing gram amounts of tritium [Kon94]. Long-term experiments were carried out for a period lasting 25 days under steady state conditions. Electrolytically generated hydrogen was continuously

extracted from the loop utilizing a permeator integrated into the loop. The only final products of the electrolytic process were tritiated hydrogen isotopologues and carbon dioxide.

Principal advantages of the electrolytical process step proposed by JAERI for the bleed stream of the front-end permeator are the i) low tritium inventory in the electrolysis cell during the water/hydrogen conversion, ii) continuous character of the process step, and iii) avoidance of solid waste. Conversely, matters of concern with the overall process concept are the i) sophisticated technology comprising several technically diferrent steps, e.g. catalytic oxidation, cryoadsorption, electrolytical processing, ii) conversion of impurities into radiotoxic and corrosive tritiated water, iii) cryoadsorption in a glove box, iv) brazing between zirconia ceramic and metal susceptible to leak or crack, v) electrolysis cell operated at high temperature may develop cracks under thermal stress, and vi) overall endurance tests under the relevant process conditions still needed.

3.18.4.7 Processes proposed for the recovery of tritium from highly tritiated water

Highly tritiated water of specific activity exceeding $10^{12}\,\mathrm{Bq\,kg^{-1}}$ will be generated at ITER in fairly large amounts i) during baking of the vacuum vessel in the presence of gaseous oxygen, ii) in the purge gas of the breeder blanket, iii) as effluent from the water detritiation system, or iv) after an accidental release of tritium [Hay06]. Highly tritiated water is normally stored in adsorbed form on molecular sieves or another adsorber. When this is not the case, i.e. tritiated water is in liquid form, it requires fast processing down to levels compatible with the CECE process because it i) is highly corrosive, ii) extremely radiotoxic, and iii) liberates radioactive gases by self-decomposition (danger of pressurization and even rupture of the containment).

In spite of a variety of process options proposed for the recovery of tritium from highly tritiated water, none has so far been validated under realistic and routine operation conditions. Some of the most promising alternatives and their associated major problems will be discussed in the following section.

3.18.4.7.1 Reduction on hot metals

Metals like uranium, magnesium, or iron, have been proposed and examined experimentally as reagents for the reduction of highly tritiated water into hydrogen.

Uranium

Tritiated water steam can be decomposed quantitatively on uranium powder at 873 K in a highly exothermic reaction according to

$$6\,H_2O + 7\,U \longrightarrow 3\,UO_2 + 4\,UH_3$$

To avoid material compatibility problems between uranium and stainless-steel and to maintain permeation losses at acceptable levels, the reaction vessel has been equipped with a disposable copper liner [Swa84; Wil66]. The temperature establishing inside of the reactor from the exothermicity of the reaction already suffices to quantitatively decompose water as well as possible impurities like methane or ammonia and to maintain hydrogen absorption by uranium at rather low levels. Disadvantages of this method are: i) uranium is a fissionable material worldwide under strictly controlled application, ii) the consumption of uranium generates highly radioactive solid mixed waste (uranium + tritium), and iii) danger of a catastrophic reaction with stainless-steel after formation of a eutectic.

Magnesium

The reaction of hot magnesium with liquid water to yield gaseous tritiated hydrogen has been employed for the recovery of tritium from low to high level tritiated waste water. Whereas highly tritiated water is habitually adsorbed on molecular sieves for enhanced safety during interim storage, most of low level water is immobilized in adsorber beds belonging to tritium stripping systems. Highly tritiated water is only released when there is need for tritium and lowly tritiated water when the adsorber bed requires re-activation. The recovery of tritium from adsorbed water is only worthwhile, when the concentration of tritium is sufficiently high. In such a case, conversion of water into molecular hydrogen and recovery of tritium via isotope separation is the habitual way to proceed. Regardless of the specific concentration of tritium in the adsorbed water, if the bed has been exposed to air, purging with inert gas is necessary before it is connected to the MgO reactor. Otherwise, a strong reaction of hot magnesium with air components, particularly oxygen, may turn into a safety problem [Ort73].

The reaction,

$$Mg + H_2O \longrightarrow MgO + H_2$$

which is exothermic by 360 kJ mol^{-1}, must be carried out at high temperature on one hand for kinetic reasons and on the other to prevent formation of magnesium hydride and hydroxide [Heu05a]. During water reduction the temperature of the metal is typically maintained at 723 - 773 K taking precautions to keep the temperature well below the melting point of magnesium, which is 923 K. Accidental melting of magnesium is associated with much magnesium vapour. Good results, i.e. up to 85 % magnesium conversion, have been obtained with a loosely packed mixture of magnesium turnings and stainless-steel springs provided the moisture content in the carrier gas is maintained within the range 3 - 20 % and the residence time kept within the range 1 - 12 s [Ort73]. Excessive water in the feed gas is detrimental to the rate of the reaction. Rate slowdown was attributed to formation of magnesium hydroxide. At least partial regeneration of the bed is possible by sweeping with hydrogen at 823 K.

A fresh magnesium bed must be conditioned for several hours at high temperature under a stream of inert gas containing hydrogen in order to remove reaction-retarding nitrogen from the metal surface. Oxidized magnesium must be given to waste. This actually constitutes a major drawback of this process option.

Iron

Iron powder reacts reversibly with water at temperatures above 700 K according to reactions [Edw95b]:

$$\mathrm{Fe} + \mathrm{H_2O} \rightleftharpoons \mathrm{FeO} + \mathrm{H_2}$$

$$3\,\mathrm{FeO} + \mathrm{H_2O} \rightleftharpoons \mathrm{Fe_3O_4} + \mathrm{H_2}\ .$$

If the conversion is performed in closed loop operation using a carrier gas like helium, it is possible to extract hydrogen from the loop in high purity either with a permeator or with a scavenging getter bed maintained at ambient temperature. Removal of a reaction product promotes shifting of the equilibria of both reactions towards the product side which increases rate and degree of conversion. Sintering of the iron powder and the formation of channels within the solidified powder have been identified as problems.

In order to minimize solid waste, it is possible to reduce periodically the produced iron oxides either with hydrogen at 873 K according to reaction

$$H_2 + FeO \longrightarrow H_2O + Fe$$

or with carbon monoxide according to reactions

$$FeO + CO \longrightarrow Fe + CO_2$$
$$Fe_3O_4 + CO \longrightarrow 3\,FeO + CO_2\ .$$

Thus, the use of iron powder can be extended beyond that of a single oxidation reaction.

Hemmerich et al. [Hem89a] proposed for the reduction of water the following sequence: iron bed, molecular sieve bed, and uranium bed operated in once-through mode. Each of the three components was placed on an electronic balance in order to follow the extent of the reaction by weight increase. Steam reacts with iron to yield iron oxide and hydrogen, non-reacted steam is retained by the adsorber, and hydrogen is collected by the uranium bed. Important upgrading achieved by this process conduction is substantial reduction of uranium waste.

Hot alloys

Examination of the factors that determine the reduction of HTO vapour over Zr–Fe–Mn alloy at temperatures exceeding 673 K in once-through modus revealed that conversion efficiencies of more than 90 % are achievable for gas residence times in the reactor of 0.7 s [Ghe95]. In comparison to other proposed metals, the reaction temperature required for Zr–Fe–Mn alloy was found to be only slightly lower. Within the ratio range $0 <$ oxygen/alloy < 2.6 conversion rates of 6 µmol min^{-1} g^{-1} alloy were attained without significant reduction in reaction rate. About 3.2 kg of Zr–Fe–Mn alloy packed between two stainless-steel filters of 20 µm rating was found to convert 1 l of vaporized water into hydrogen without significant reduction in reaction rate constant. To minimize solid waste, it is possible to increase the degree of getter conversion by performing the water reduction in closed loop operation mode.

3.18.4.7.2 Electrolysis

At SCK/CEN, Belgium, a capillary electrolysis cell for highly tritiated water was developed. The cell had a small liquid inventory of 12 cm^3, contained **sulfuric acid electrolyte**, and operated at 276 - 282 K. It relied on a porous vitreous separator and several platinum electrodes pressed against porous spacers. The cell throughput was 100 $cm^3\,d^{-1}$ [Rah87]. The process complexity is additionally increased by the necessity of purifying the electrolytically produced gas stream from HTO and SO_3 .

An electrolytic process for the conversion of tritiated water containing more than 30 $TBq\,cm^{-3}$ of tritium ($> 50\,\%$ T_2O) was equally developed at VALDUC over the past 30 years [Gir91; Bel99b; Hei03] (see also section 3.14.6). Key component is a thin Pd-Ag thimble cathode supported by a porous ceramic or fritted nickel tube. Chemically very pure tritiated hydrogen is generated by electrolysis of water at pH 14 applying a current of 700 $A\,m^{-2}$ and subsequently recovered directly via diffusion and pumping across the cathode.. Up to 6 g of gaseous tritium have been recovered from highly tritiated water within a total period of operation of 1500 hours employing a prototype electrolyzer. The occurrence of explosive mixtures in the electrolyzer is avoided by sweeping with argon.

3.18.4.7.3 PERMCAT and two stage PERMCAT

a) Screening tests

Welte et al. [Wel11; Wel12] designed single and double stage PERMCAT reactors aiming primarily at the decontamination of highly tritiated water (HTO) with molecular hydrogen in counter current mode. Manufacture of the PERMCAT reactors was carried out exclusively at the central workshops of KIT. PERMCAT reactors operate by isotopic swamping on a palladium/silver membrane in close contact with a nickel catalyst. Both, membrane and catalyst are maintained at 673 K[65]. Each PERMCAT stage consists of a bundle of 13 Pd/Ag fingers, which have a length of 350 mm, an outer diameter of 3.3 mm, and a wall thickness of 0.1 mm.

[65] It is planned to increase the number of PERMCAT stages even further in order to achieve the decontamination factor required for ITER, i.e. higher than 10^5. The aim is to reduce the activity of highly tritiated water from 10^{12} - 10^{16} $Bq\,kg^{-1}$ [Glu07] down to levels acceptable for a water detritiation facility, i.e. $\sim 10^{11}$ $Bq\,kg^{-1}$. Within this frame a three stage PERMCAT will be realized at TLK by combining a double stage with an older single stage PERMCAT.

They are brazed onto a common cup from which the swamping gas is supplied. Orbital tungsten inert gas welding was selected for all internal connections. The bundle of Pd/Ag membranes is introduced into a stainless-steel vessel and all free spaces filled with NIKKI type 111 (50 % Ni on SiO_2, grain size 500 - 800 µm) catalyst [Wel12] (see also Fig. 3.77 right). For heating purposes, each stage is furnished with two redundant 600 W thermocoax heaters.

Within the frame of screening tests intended to further optimize the flow dynamics across the PERMCAT reactor, the capillary bundle inserted into the Pd/Ag membrane tubes, whose function is to extract tritium-enriched swamping gas from the bottom of the Pd/Ag fingers, was designed and manufactured for easy replacement. Several capillary bundles each with capillaries of different diameter (0.8 mm, 1.4 mm, 2.0 mm, 2.3 mm and 2.5 mm) were one after another inserted into the permeation fingers of a double stage PERMCAT and compared among each other with respect to PERMCAT performance under standardized conditions. Feed flow rates of 50 $cm^3\,min^{-1}$, 100 $cm^3\,min^{-1}$, 150 $cm^3\,min^{-1}$ and 200 $cm^3\,min^{-1}$ employing a 1 : 1 = helium : deuterated water (D_2O) mixture were tested systematically to determine achievable decontamination factors. In the experiments, deuterated water vapour was depleated in deuterium and gaseous hydrogen enriched in deuterium. Under the test conditions, the highest decontamination factors were achieved with a bundle of cappilaries, each having 1.4 mm outer diameter and 0.2 mm wall thickness.

b) Two stage PERMCAT reactor

Subsequent to experiments with a single stage PERMCAT (effective membrane area = 0.055 m^2 [Wel11]), an upgraded two stage technical scale PERMCAT version (effective membrane area = 0.109 m^2) was tested under comparable conditions. The addition of a second PERMCAT stage doubled the total effective permeation membrane area of the device and increased considerably the decontamination factor from 89 to 3670. Suitable spacers and sinter metal disks were inserted throughout the device in order to keep catalyst and membranes in place. Measured leak rates were lower than $10^{-10}\,Pa\,m^3\,s^{-1}$. A vacuum vessel equipped with a CF-160 flange served as secondary confinement to the PERMCAT. All feedthroughs were integrated into this flange to allow easy access for quick replacement of capillaries. Upgrading of the PERMCAT design yielded a component of i) improved performance, ii) higher robustness, and iii) much easier

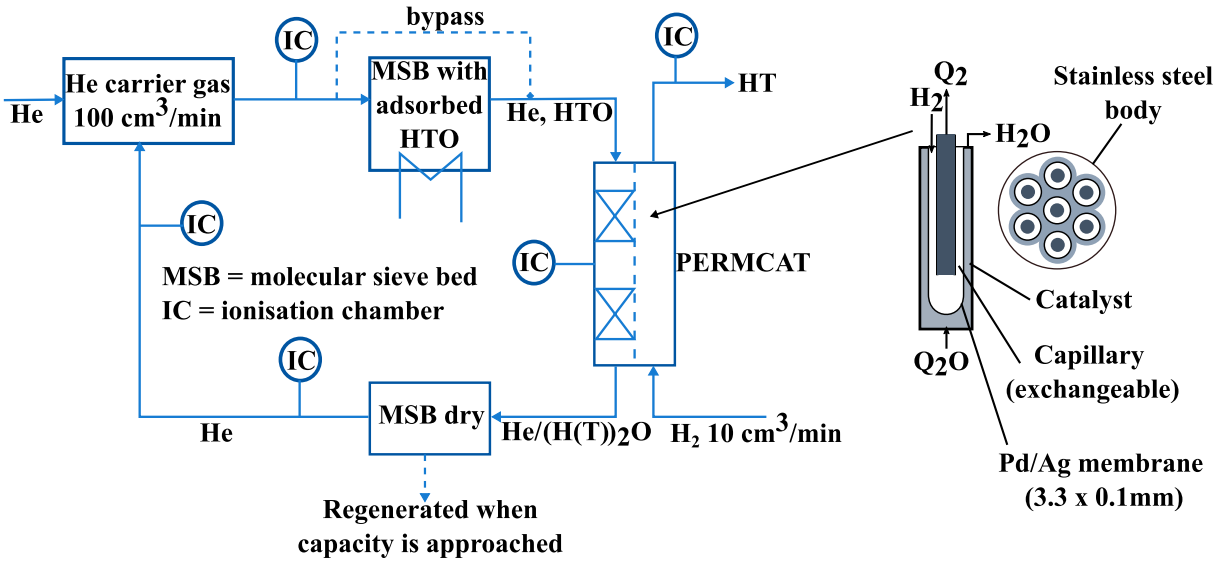


Figure 3.82: Process concept for the detritiation of highly tritiated water displaying a double stage PERMCAT. A schematic drawing of the proposed finger type PERMCAT is shown by the insert on the right (after [Wel12; Par12]).

manufacture in comparison to all formerly assembled at TLK [Glu00a; Glu00b; Dem10; Wel10; Wel12].

Parracho et al. [Par12] proposed an integral water detritiation process concept utilizing an advanced PERMCAT reactor. It was presumed that the highly tritiated water is supplied adsorbed on molecular sieve and contained in an adsorber bed equipped with two valves. Essentially, a finger type two-stage PERMCAT consisting of two reactors in series, was integrated into a closed loop furnished with three molecular sieve beds and instrumentation comprising several ionization chambers, a flow controllers, and humidity sensors (see Fig. 3.82 and ref. [Wel12]). The first molecular sieve bed (MSB) contained the tritiated water requiring detritiation and the second, installed downstream, served to trap de-tritiated water exiting the PERMCAT unit. Five ionisation chambers were employed to follow the evolution of the detritiation process. Tritiated water adsorbed by the molecular sieve bed that served for transport was released thermally by heating progressively from ambient up to 573 K. Helium was used as carrier gas for the transport of water vapour. After detritiation of the tritiated water in the double stage reactor, it was fed into the second zeolite bed where it remained adsorbed. Once loading capacity of this bed was approached, the process stream was switched to a third zeolite bed available in standby modus (not shown in Fig. 3.82). The bed saturated with de-tritiated water was regenerated thermally

in opposite direction to that of loading at 573 K again using helium as carrier gas. The activity of released de-tritiated water was now sufficiently low to allow processing in a conventional water detritiation system. Activity concentrations of HT registered with an ionisation chamber at the permeate exhaust gas stream of the PERMCAT device could be verified by radio gas chromatographic analysis. Factors contributing to optimize the release rate of water from the molecular sieve bed were obtained from a series of parametric investigations. Experiments carried out with tritiated water containing 2×10^{14} Bq kg^{-1} tritium were considered quite promising. Calorimetrically it was confirmed that the activity of the water collected in the second molecular sieve bed (originally containing approx. 120 g of dry molecular sieve type 5A) was below the detection limit of 10^9 Bq.

3.18.4.7.4 Catalyzed isotopic exchange

Shu et al. [Shu15] performed screening tests on the isotopic exchange between gaseous deuterium and highly tritiated deuterated water adsorbed alternatively on one of three different commercial platinum-bearing zeolites all of which contained 0.7 % by weight of platinum. The concentration of tritium in D_2O (0.1 - 10 %) and the temperature ($298 < T < 328$ K) were selected as main test parameters. When all relevant factors were considered the best performance at ambient temperature was obtained with Na-Y zeolite type CBV 100 CY whose water adsorption capacity is 27 % by weight. Extrapolating from the experiments, it was estimated that 2 kg of highly tritiated water can be processed with 30 kg of platinum-bearing zeolite in three days: one day for adsorption, one for exchange, and one more day for regeneration at 673 K. To achieve an exchange factor of 300, deuterium must be purged for 24 hours at a flow rate of 13 Pa m^3 s^{-1}. After detritiation, the activity of the formerly highly tritiated water met the acceptance criteria stipulated for the Water Detritiation System of ITER.

The application of platinum doped molecular sieves for the detritiation of highly tritiated water was also investigated by Demange et al. [Dem15a]. The reagent needed for these experiments, i. e. highly tritiated water, was generated in a micro channel catalytic reactor of the kind already developed and demonstrated at TLK [San12]. In this reactor DTO is produced catalytically in two foils, each of which is furnished with 45 platinized micro channels. The channels have dimensions of 11 mm length, 100 µm height and 300 µm width. They are enclosed by two stainless

steel plates joined together by diffusion bonding. While hydrogen and oxygen are fed into the reactor via small 1/8th inch VCR connections, water exits through a 1/4th inch VCR connection. An operation modality allowing easier process control was to introduce a mixture of helium and hydrogen on one side of the reactor and oxygen on the other. Under these conditions, 2 g highly tritiated water of $5.2 \times 10^{12}\,\mathrm{Bq\,g^{-1}}$ were generated at a rate of $0.5\,\mathrm{g\,hour^{-1}}$ at conversions of typically 97 - 99 %. The oxidation reaction was carried out at $(400 \pm 10)\,\mathrm{K}$. At this temperature, it was possible to achieve fast reaction rates while maintaining the rate of hydrogen permeation small.

For explosion safety reasons, a paramagnetic oxygen monitor is used to detect overstoichiometric oxygen [Men77; Tel13]. The sensor can be programmed to suppress automatically the supply of oxygen when preset values are exceeded. Further safety measures include back flow protection valves combined with automatically actuated valves relying on pressure difference measurements. The micro catalysed reactor was first tested with hydrogen in a parametric study encompassing several flow rates, process gas compositions and temperatures. It was moreover demonstrated successfully with tritium while relying on plentiful infrastructure provided by the facility CAPER at TLK [Dem15a]. In conclusion, the micro channel reactor features advantages such as i) continuous generation of a stream of tritiated water, ii) small inventory of tritium, iii) minimal generation of solid waste, iv) no renewal of solid reagent necessary, as opposed to oxidation of hydrogen when utilizing a metal oxide [Par12], and iv) inherent safety, i.e. preclusion of explosions due to the small size of the reactor.

In subsequent runs, 20 g of platinized molecular sieve (CBV 100 CY) was loaded with about 2 g of DTO containing $2.7 \times 10^{13}\,\mathrm{Bq}$ of tritium, which was generated in a micro channel catalytic reactor employing a helium-DT mixture as reagent [Wel11; Dem15a]. To recover the tritium adsorbed on the bed it was overflowed with deuterium at temperatures of less than 328 kelvin in order to promote tritium enrichment of the gas phase via catalytic isotopic exchange with adsorbed tritiated water. After several consecutive treatments, the residual activity remaining in the platinized molecular sieve bed was determined by calorimetric measurements. This determination was possible, because the adsorber bed fitted into the large sample volume of the most sensitive calorimetrer of TLK. The determined activities fluctuated within the range $4.6 \times 10^{10}\,\mathrm{Bq\,g^{-1}}$ and $27.7 \times 10^{10}\,\mathrm{Bq\,g^{-1}}$ of water. From the point of view of the required effort,

a recovery of tritium is only justifiable up to a purity of about 99 %, i. e. decontamination factor of 100. Additional efforts greatly decrease the cost effectiveness.

Alternatively, highly tritiated deuterated water can be released thermally from an adsorber bed and then fed in once-through modus into a PERMCAT unit using helium as carrier gas. In this case, tritiated water vapour, which cannot permeate across the palladium/silver membrane, is decontaminated by catalyzed exchange with freely permeating molecular deuterium flowing alongside the outside of the membrane in counter current direction [Dem10; Par12; Dem15a]. Resultant greatly decontaminated deuterated water can subsequently be adsorbed either on a platinized molecular sieve bed type CBV 100 CY, a standard molecular sieve bed or collected in a cold trap. More than 450 l of swamping gases containing in total 7.8×10^{13} Bq of tritium have been processed during the course of 3 months of continuous operation of CAPER at TLK.

3.18.5 Extraction of tritium from the blanket purge gas of a Helium Cooled Ceramic Breeder Test Blanket Module

One major test program during the D-T phase of ITER will be the experimental and theoretical evaluation as well as comparison of several concepts for the extraction of tritium from solid and liquid blankets proposed worldwide [Nis84; Yos89; Soo92; Nis94; Eno94; Eno95b; Miu97; Alb00; Bel05a; Wil93; Gia07; Cho08; Gia10a; Zha10b; Gia12]. Because to date there are almost as many solutions as there are blanket concepts, it is the aim of the ITER program to identify the most auspicious for further development and final implementation in DEMO. Only some of the more recent proposals will be discussed below mainly to draw attention on unresolved problems.

According to a proposal for the Helium-Cooled Ceramic Breeder (HCCB) Test Blanket concept [Alb00] tritium is recovered from the solid breeder by passing the helium purge gas exiting the blanket first through a cold trap maintained at less than 173 K for the retention of tritiated water and subsequently through a downstream placed molecular sieve bed kept at 78 K to adsorb hydrogen isotopes. While the recovery of tritium-bearing species without preceding conversion into a single component, i.e. HTO or HT, appears to be an attractive option, there are also drawbacks: i) two cryo traps, ii) coolant loss event of a large cryogenic adsorber bed possible, iii) conceivable accumulation of oxygen in a cryogenic adsorber bed (potential generation of ozone [Riz96]Ozone!safety), iv) inefficient and energy intensive regeneration/cooling of adsorber beds,

and v) need of an additional process step to convert all tritiated species into a single one in preparation for isotope separation.

Two Test Blanket Modules (TBM) concepts have been proposed by Korea. Of these, the status of the Helium-Cooled Solid Breeder (HCSB) module containing pebbles of lithium ortho silicate ceramic enriched in ^{6}Li up to 40 % and pebbles of beryllium as neutron multiplier was evaluated Cho et al. [Cho08]. Reduced Activation Ferrite/Martensite (RAFM) steel was adopted as structural material for the blanket. New in the proposal, is a partial replacement of some beryllium in the blanket by a graphite neutron reflector. The reflector, eventually coated with SiC to exclude reactions with air or steam, is likewise used in pebble form. Assuming a ^{6}Li-enriched ceramic, it was shown by calculations that in spite of the partial replacement of beryllium by graphite reflector, the tritium breeding ratio remains unchanged as in other TMB's at a value of about 1.3. This value is similar to that achieved in other blanket modules. To warrant fuel supply to a fusion machine, bred tritium must regularly withdrawn from the blanket. Within this frame, a concept for a Tritium Extraction System, a Helium Cooling System and a Coolant Purification System was elaborated. High pressure helium at 8 MPa at a temperature of 573 K at inlet and, depending on operating conditions, up to 773 K at outlet is used as blanket coolant. Low-pressure helium doped with 1 % hydrogen was selected as purge gas. Key components and process steps of the Tritium Extraction System comprise the sequence cooling of the blanket sweep gas, retention of water and impurities on a molecular sieve bed at ambient temperature, pre-cooling of the blanket purge gas employing a recuperator, retention of hydrogen isotopologues in a cryogenic molecular sieve bed, restoring of the original hydrogen content of the purge gas in a make up unit, and pre-heating of the purge gas before re-injecting into the blanket. Tritium retained in the cryomolecular sieve bed is released discontinuously. To this effect, the bed is heated, the released hydrogen isotopes purified with a diffuser and subsequently collected in a getter bed. Purification of the coolant takes place by converting catalytically molecular hydrogens into water and removing the generated tritiated water together with that already contaminating the helium purge with a molecular sieve bed. Filters in front and behind of all molecular sieve beds serve to avoid fine particle spreading. The tritium partial pressure in the Tritium Breeder Modulus is maintained at low values in order to minimize permeation into the Helium Cooling System.

Another recent conceptual design dealing with the extraction of tritium from a helium cooled HCCB solid breeder Test Blanket Module developed by the Chinese ITER Team is illustrated

schematically in Fig. 3.83 [Zha10b]. According to this concept, helium purge gas doped with 0.1 % hydrogen to enhance the release of tritium, is used as purge gas for the tritium bred in the blanket. Purge gas exiting the blanket now containing tritium and some impurity gases is first cooled to ambient temperature and then passed through a filter for the retention of dust. Thereafter, water in this gas stream is reduced to molecular hydrogen employing a hot metal bed. Of the proposed metals, i.e. magnesium, zinc or iron, the preferred option was the latter because the generated Fe_3O_4 can be reduced back to iron by reaction with hydrogen. After cooling the effluent gas, hydrogen isotopes are cryo-adsorbed on a molecular sieve bed placed in a vacuum insulated containment maintained at liquid nitrogen temperature. To optimize the operation, two cryogenic adsorber beds are integrated into a closed loop. Of these, one is in operation while the other is under regeneration. Hydrogen isotopes liberated during cryo-bed regeneration are extracted selectively from the loop employing a heated palladium/silver permeator also integrated into the loop. Before the carrier gas is returned to the blanket the original composition is restored by adding hydrogen up to a concentration of 0.1 % (see make up unit in Fig. 3.83/8). This complete tritium extraction system will be installed in the Tritium Building of ITER [Gia10a].

Sagawa et al. [Sag95] designed a sweep gas system for the extraction of tritium released from a blanket test mock-up. The sweep gas consisted of helium containing hydrogen, moisture, and oxygen. While the former two gases are added to enhance the liberation of tritium from the breeder material, a small partial pressure of oxygen serves as reactant for the oxidation over a palladium catalyst of all tritium species into water. Ionisation chambers, ceramic electrolytic cells (full conversion of water into gaseous species) and molecular sieve beds constituted tools for the analytical determination of total tritium, tritium in gaseous species and water species in the mock-up exhaust gas. After conversion of all tritium species into tritiated water, this component is collected in a molecular sieve bed. The bed is periodically regenerated for recycling of bred tritium. Possible consequences of the presence of oxygen in the blanket were not addressed.

Kawamura et al. [Kaw05] worked out a concept for the extraction of tritium from a DEMO blanket containing solid lithium titanate (Li_2TiO_3) ceramic breeder. It was assumed that most tritium is bred as tritiated water, of which much remains adsorbed on the breeder surface. Therefore, they selected helium doped with hydrogen and moisture as purge gas. Advantages of a partial pressure of water are enhancement of the rate of tritium liberation and thus reduction of permeation losses at the elevated average temperatures of about 870 K prevailing in the

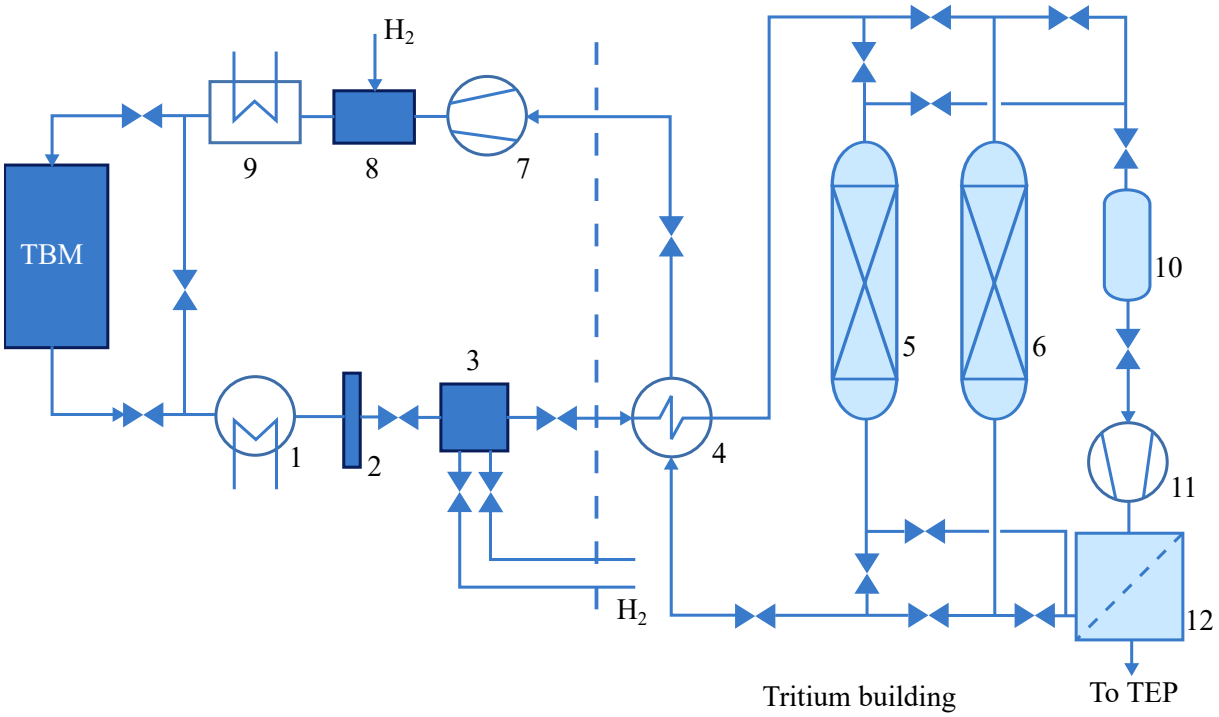


Figure 3.83: Flow diagram of the tritium extraction system of a HCCB Test Blanket Module comprising the components: cooler (1), filter (2), hot metal bed (3), heat recuperator (4), cryogenic molecular sieve beds (5,6), compressor (7), hydrogen makeup unit (8), heater (9), buffer tank (10), vacuum pump (11) and palladium/silver diffuser (12) (after [Zha10b]).

blanket. Provided the concentration of gaseous moisture in the carrier gas is about hundred times higher than that of bred tritium, quantitative liberation of tritium from the solid can be attained by isotopic exchange between gas phase H_2O and adsorbed T_2O. In view that isotopologues of water (H_2O, HTO and T_2O) constitute the main species in the purge gas, a dryer consisting of six adsorber beds each packed with 61 kg of molecular sieve 5A was proposed to retain the water present in the helium stream. These adsorber beds are considerably smaller than cryogenic molecular sieve beds such as needed in case helium is only doped with hydrogen. Adsorption takes place at ambient temperature; the release of adsorbed of water at 523 K. Because the tritium concentration in the recovered water is very high it should be converted electrolytically into tritiated hydrogen in a Water Detritiation System. Of critical importance is the radiation resistance of the solid polymer electrolyte in the electrolyzer. As alternative option it was recommended to contemplate vapor phase electrolysis using a ceramic electrolyte of the electrolyzer. Condensation of water should be avoided because of the low pH of the water

(danger of corrosion). Electrolytically generated tritiated hydrogen must be subject to isotope separation to recover molecular tritium for the re-supply of the fusion machine with fuel.

A theoretical model for the interpretation and validation of hydrogen breakthrough experiments performed with 20 kg of molecular sieve 5A adsorbent maintained at cryogenic temperatures with helium containing hydrogen or deuterium in concentrations of about 2000 vppm as carrier gas was developed by Munakata and his co-workers [Mun07]. The utilized helium flow rate of $2\,m^3\,hour^{-1}$ was about $1/6^{th}$ of that estimated necessary for the extraction of tritium from the helium cooled pebble bed Test Blanket Modules of ITER. Scale up simulations assuming a 170 kg cryoadsorber bed and a gas flow of $12\,m^3(STP)hour^{-1}$ indicated that this cryogenic molecular sieve bed can remain in operation for about 5.5 d. Under the assumption that at this point in time regeneration becomes necessary, it was concluded that the program goals for the extraction of tritium from a blanket purge gas can be met with cryo adsorber beds.

A so far neglected aspect in currently discussed concepts, is the equilibrium establishing between the solid ceramic breeder material and helium doping agent's like hydrogen and water to yield water and lithium hydroxide[66], respectively [Pen94]. Reactions describing the formation of these products at the elevated temperatures prevailing in blankets are:

$$Li_4\,SiO_4\,(cr) + xD_2 \longrightarrow Li_4\,SiO_{(4-x)}\,(cr) + xD_2\,O\,(g)$$

$$Li_4\,SiO_4\,(cr) + D_2O\,(g) \longrightarrow Li_2\,SiO_3\,(cr) + 2\,LiOD\,(g)$$

Product partial pressures as function of temperature, partial pressure of deuterium, and equilibrium constants of the relevant reactions expressed as function of temperature are provided in the reference. Under comparable conditions, the partial pressures of lithium hydroxide over lithium oxide were found to be about two orders of magnitude higher than over lithium silicate when the helium sweep gas at 1 bar carries 10 ppm water. The possible impact of LiOH formation on blanket technology requires assessment.

The potential application of a PERMCAT reactor (see Fig. 3.77c) as key component for tritium recovery from tritiated species (mostly Q_2 and Q_2O, Q = H, T) extracted from an ITER Test Blanket Module was examined critically by Bükki-Deme et al. [Bue16]. PERMCAT

[66] Lithium hydroxide is a white, hygroscopic, and highly toxic (causes severe skin burns and eye damage) crystalline strong base with a melting point of 735 K

combines a nickel catalyst, which promotes isotopic scrambling between hydrogen and tritiated species, with a palladium/silver diffusor for selective permeation of hydrogen isotopes. The reactor operation is based on isotopic swamping in counter current mode. High decontamination factors, i.e. elevated recovery of tritium, were achieved at swamping ratios exceeding 20 and low impurity flow rates. It was concluded, that the tested PERMCAT unit required significant upgrade in order to increase the rate of isotopic exchange between protium and tritiated species. Search for a more effective catalyst was also recommended.

In general, to assure high autonomy and good efficiency, each of several Test Blanket Modules to be taken into operation at ITER will be equipped with its own dedicated system for tritium recovery and processing as well as with an individual extraction system and corresponding diagnostic equipment.

Recapitulating, as of now none of the proposed tritium extraction concepts for ITER blankets has been validated in experiments carried out under representative purge gas conditions utilizing components of relevant dimensions. Several questions of much consequence to the achievement of tritium self-sufficiency for ITER remain unresolved: i) the optimization of the overall process design including selection of type, number and sequence of components, ii) demonstration of constant extraction efficiency during a prolonged period of time, iii) identification of the optimal regeneration parameters of large molecular sieve cryo-adsorber beds, iv) optimization of cryo-sorption trap design v) composition and concentrations of doping agents in the blanket sweep gas, vi) solid-gas phase chemistry in the sweep gas, etc.

3.18.6 Tritium extraction from a lead lithium breeding blanket

Besides of the solid Helium Cooled Pebble Bed (HCPB) Blanket Test Module, the second reference concept of the European Breeding Blanket Programme is the liquid Helium Cooled Lithium Lead (HCLL) Blanket Test Module. It will be discussed only very succinctly.

3.18.6.1 Helium-Cooled Lithium Lead Test Blanket Module

The Helium-Cooled Lithium Lead blanket is one of two blankets concepts selected for testing at ITER within the frame of the so-called Test Blanket Module project [Sal08; Ric11]. According to Salvay[Sal08] the extraction of tritium will take place in two steps: the first is based on a gas-liquid contactor in which tritium is stripped from the liquid metal by helium doped with

hydrogen and a second in which helium stripping gas, now containing HT + H_2, is processed to recover hydrogen isotopologues. Removal of the fuel gas from helium is carried out with a cryogenic two-bed Temperature Swing Absorption process. The cryogenic beds are regenerated for tritium-deuterium recovery by heating under vacuum. "Cleaned" helium is recirculated into the contactor.

3.18.6.2 Dual Cooled Lead Lithium breeding blanket: tritium extraction by vacuum-enhanced permeation

Another option proposed for the extraction of tritium from a lithium-lead blanket foresees permeation membranes consisting of niobium or tantalum alloys operated at high temperature ($> 1000\,\mathrm{K}$). For the extraction, PbLi is passed along the high-permeability membrane which is evacuated on the back side in order to obtain maximal driving force. A critical drawback of this concept is that these high permeability materials oxidize readily even at extremely low partial pressures of oxygen. In addition, niobium circulating in PdLi may inflict corrosion and eventually become activated in the blanket which would be detrimental when it comes to waste disposal. In view of this, Humrickhouse and Merrill [Hum15] examined the properties of reduced activation ferritic martensitic (RAFM) steel operated at much lower temperature, i.e. $700\,\mathrm{K}$, as possible alternative. As with other high permeability membranes, tritium is extracted from the liquid alloy by passing the fluid along the membrane while maintaining vacuum on the opposite side. Resistance to radial transport across the PdLi boundary layer was considered significant and hence rate determining for the efficiency of extraction. One major conclusion of their calculations was that at least twenty times larger RAFM membranes would be necessary for this material to become competitive with membranes of group 5 metals. Consequently, the authors recommended further search for materials which possess high permeability, are impervious towards oxidation and activation by neutrons, and do not display corrosive properties.

3.18.7 Isotope separation of molecular hydrogen isotopes

Many civilian and military research activities have triggered worldwide the development of technologies for the isotope purification of molecular tritium. From these research efforts several now well-established separation processes have emerged. The most advanced, i.e. cryogenic

distillation, displacement chromatography, thermal cycling absorption, and thermal diffusion will be discussed below.

3.18.7.1 Cryogenic isotope separation

Much experimental and theoretical efforts have been invested worldwide over the past 30 years into the development and optimization of cryogenic distillation systems for the separation of hydrogen isotopes. The activities have primarily been focussed on the optimization of i) condenser design and minimization of tritium inventory, ii) design of re-boilers, iii) optimization of number and location of equilibrators, iv) column dimensions, v) type and size of packing, vi) location of column interlink piping, etc. [Bar79b; Kin84; Bus88a; Ino92; LeL94; Yam94]. A vast body of experience and pertinent literature is now available on this topic.

A sizable technical cryogenic distillation facility was operated routinely with tritium in **Grenoble, France**, for several decades [Pau88; Buv93]. This plant, principally designed for the extraction of tritium and protium from the deuterated water moderator of CANDU type reactors, comprised essentially two cryogenic distillation columns operated at a pressure of 1.5 bar. Typical feed rates of the two columns were $45\,m^3$ (STP) /hour ($X_{HD} = 0.0098$, $X_{D_2} = 0.9902$, and $X_{DT} = 0.47 \times 10^{-6}$) and $0.1\,m^3$ (STP) /hour ($X_{D_2} = 0.99915$ and $X_{DT} = 8.5 \times 10^{-4}$), respectively. The total tritium holdup of the two columns was of the order of 18 g.

The Tritium Removal Facility operated in Darlington, Canada, is a large industrial plant which was erected like that in Grenoble for the extraction of tritium from heavy water,D_{20}, used in CANDU nuclear fission reactors. The Darlington plant is sized to accomplish a DF higher than $8 \cdot 10^6$. The average concentration of tritium in the heavy water from reactors is $0.4\,TBq\,kg^{-1}$ and the tritium extraction rate 1.2×10^6 TBq/a [Gug91]. With the Darlington detritiation process approx. 10^5 TBq of almost pure tritium have been extracted from 840 000 l of heavy water moderator of CANDU type reactors over a period of sixteen years. If heavy water (D_2O) is to be made available to other non-nuclear applications a removal of tritium below the level of $74\,Bq\,g^{-1}$ is required.

At **TSTA** a cryogenic isotope separation system consisting basically of four cryogenic separation columns was designed to meet the requirements of the fuel supply of a fusion machine by delivering i) a mostly tritium-free hydrogen/deuterium stream, ii) a high purity D_2 stream, iii) a stream of largely pure DT and iv) a stream of high purity T_2. A test program was carried out

in close collaboration with JAERI, Japan [Ino92]. Most important objectives of the activities were the achievement of stable conditions with respect to flows and liquid levels, and a reduction of tritium hold-up [Bel81; Eno90; Bel95b; Kve95; Yam95b; Yam96; Bai99a]. The inventory of tritium is of paramount importance because cryogenic distillation columns contain the largest mobile tritium inventory of the entire fuel cycle system of a fusion machine [Yos02].

Cryogenic hydrogen isotope distillation systems rely on the different vapour pressures of hydrogen isotopologues, which decrease in the order H_2, HD, HT, D_2, DT, and T_2. A classical separation system such as installed at **JET** is illustrated in Fig. 3.84. Because each distillation column is designed to separate adjacent species in the volatility scale, the number of pure compounds that need to be separated will determine the number of required columns. During batch distillation the columns are maintained at a temperature near the boiling point of liquid hydrogen. Therefore, the operating temperature of the columns will fluctuate between 20 K and 30 K. A reboiler at the bottom of each column provides hydrogen vapour and a condenser at the top of the column generates liquid hydrogen. Isotopic exchange takes place between the counter-current phases of down-flow liquid phase and up-flow vapour phase. The lighter isotope is enriched in the vapour phase due to its higher vapour pressure. Therefore, the lighter isotope is collected from the top of the column and the heavier one from the bottom. Since at these low temperatures isotopic exchange is negligibly slow, the separation of molecules like HT and D_2 is particularly difficult (both have almost the same molecular weight and very similar vapour pressures). Therefore, a fraction of the inventory is removed either from the bottom or the middle of a column, warmed up to ambient temperature, re-equilibrated over a noble metal catalyst (see cat 1 and cat 2 in Fig. 3.84) and reintroduced into another column. In this way the HT and DT fractions can be reduced.

The attainable purities of protium at the top of column 1 and of deuterium at the top of column 3 were found to be $> 99.9996\,\%$ and $> 99.998\,\%$, respectively, with an average tritium content of < 1 ppm. To achieve a tritium sample purity approaching 100 % a tritium inventory of more than 1 g was considered necessary. Important experimentally obtainable design parameters for cryogenic columns are i) the dependence of the **height equivalent of a theoretical plate (HETP)** from the feed rate and **reflux ratio**, and ii) the **pressure drop in a packed column**.

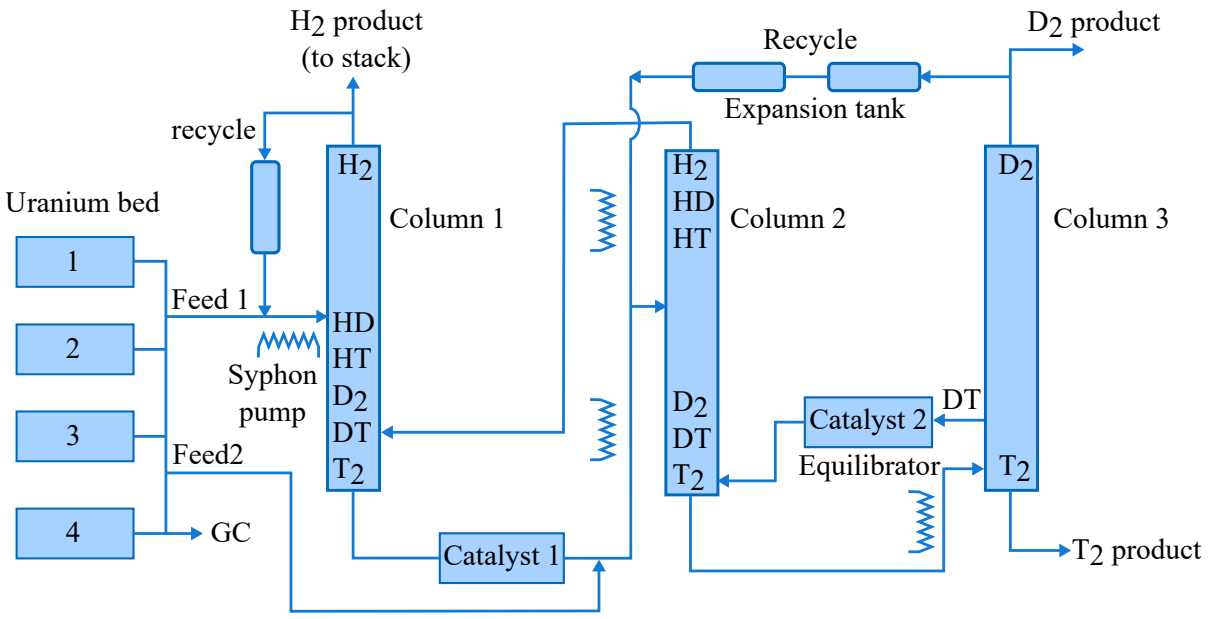


Figure 3.84: Block diagram of the cryogenic hydrogen isotope distillation system installed at JET (after [Bai99a]).

Cryogenic columns must be housed in a bakeable stainless-steel vacuum vessel kept under very high vacuum and cooled with copper coils surrounding a layer of thermal shielding through which helium at 18 K is re-circulated.

Laser Raman spectroscopy was found to be a very effective analytical tool for process control of the cryogenic distillation of hydrogen isotopes [Iwa02c]. The use of optical fibres permits remote measurements at several crucial analytical points of the isotope separation system. A data acquisition time of the order of 1 data/min was found to be possible and adequate.

The hydrogen isotope separation system of **ITER** will receive feed gases from the tokamak exhaust, the regeneration of the NBI, and gas from the water de-tritiation system. Cryogenic distillation is the most attractive process for the separation of large streams of hydrogen isotopologues because it proceeds with considerable throughput in spite of the comparatively compact size of distillation columns. The high separation performance and negligible losses of tritium by permeation at cryogenic temperatures are important further assets of this technology. On the other hand, the holdup of liquid hydrogen isotopes in distillation columns is rather large, it has been estimated to be of the order of 390 mol [Yos02].

The cryogenic isotope separation process currently envisaged for **ITER** (see Fig. 3.85) serving the water detritiation system has been developed and described by several investigators [Kve95; Mur00; Glu01; Yos02; Iwa02b; Glu06a; Glu07; Glu13]. Key components are a water detritiation process operating in combination with an isotopic separation system comprising a cascade of four cryogenic distillation columns. A conspicuous function is accomplished by seven equilibrators that serve to re-establish thermodynamic equilibrium between mixed and homonuclear isotopologues at strategic positions between the columns. Protium collected at the top of column 1 is returned to the middle of the water detritiation system in order to decontaminate tritiated water. While the tritium inventory is dominated by that present in the cryogenic distillation system, equipment size and cost are determined by the front-end water detritiation system. Adequate precautions to exclude loss of refrigerant need to be implemented because a sudden loss of cooling can lead to the evaporation of large amounts of hydrogen (and of tritium). Realistic ITER-scale simulation experiments performed by Iwai et al. [Iwa02b] have, however, provided evidence that there is enough time for the recovery of evaporating hydrogen into an adjacent safety storage system as long as the vacuum insulation remains unaffected and the reboiler heaters can be turned off fast enough.

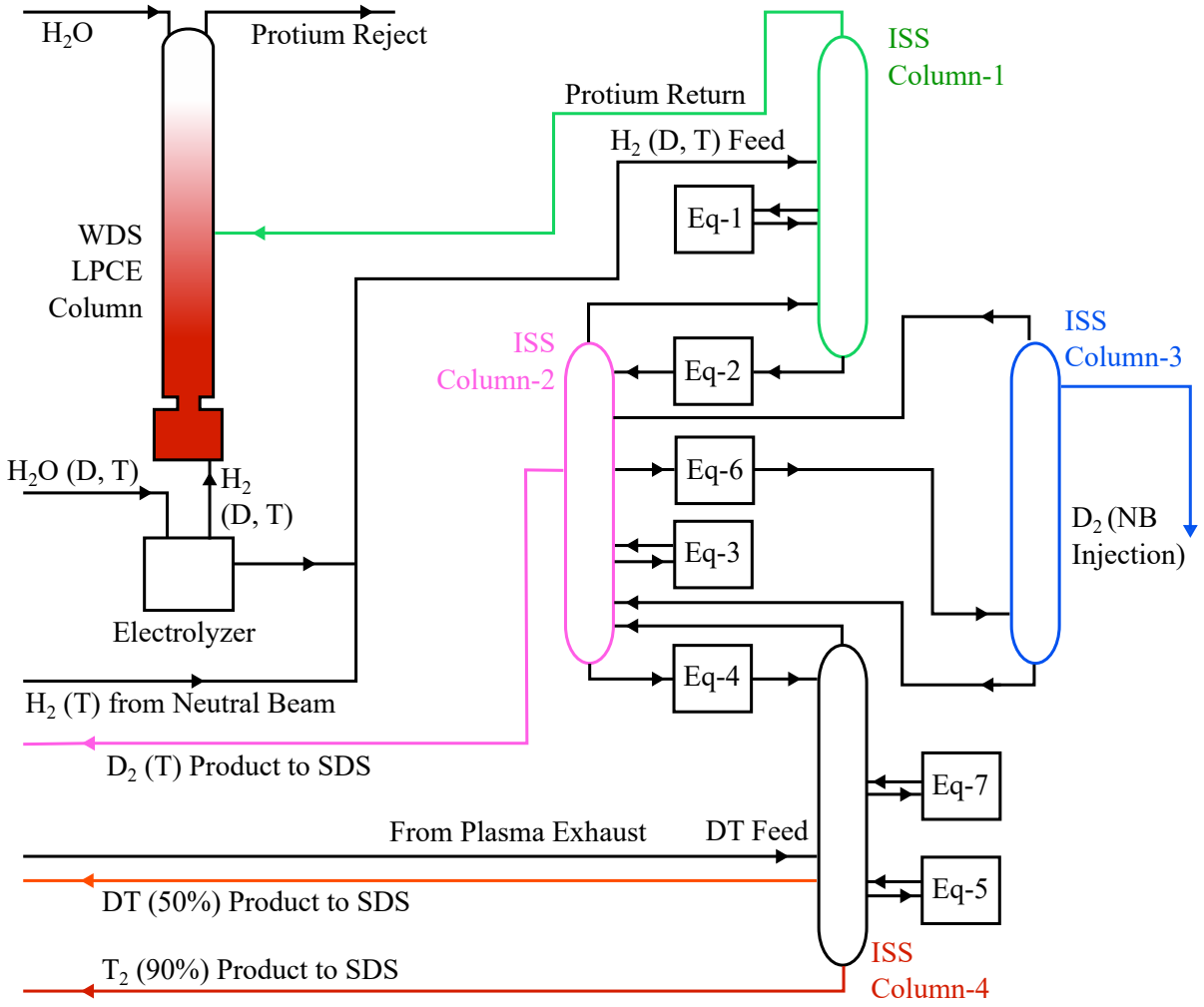


Figure 3.85: Configuration of the cryogenic isotope separation process of ITER [Glu13].

3.18.7.2 Displacement gas chromatography (DGC)

Displacement gas chromatography (DGC) is a batch process first proposed by Glueckauf and Kitt back in 1958 [Glu58]. A comprehensive theoretical discussion on procedures to determine separation factors, calculate the number of theoretical plates, and validate the results needed to interpretate the experimental results was published by Botter el al [Bot65]. Botter et al. [Bot88] were also the first to succeed with the separation and isolation by DGC of pure molecular protium, deuterium, and tritium from a hydrogen isotopologue mixture. The same investigators planned, built, and installed a DGC facility for the **Active Gas Handling System of JET** which was designed for a daily hydrogen isotope throughput of 20 mol. Besides four columns,

each loaded with five litres of a porous material impregnated with 18 % by weight of palladium, the facility encompassed four getter beds, a Metal Bellows pump, a Normetex pump, pressure regulators, diverse vessels, automatic valves, a rupture disk, etc. The sorption capacity of the packing was determined to be 1.57 Pa m^3 of hydrogen per gram of packing.

Concisely, each hydrogen isotope separation comprises the following consecutive steps: in a first step eluent hydrogen remaining from a previous separation is released from the palladium/alumina column at 473 K. Thereafter, the column is cooled to ambient temperature and filled with helium up to 100 kPa. This gas is needed to prevent initial fast and long-range diffusion. At this point the column is ready for loading with a new batch of a hydrogen isotopologue mixture. Loading is performed until approximately one quarter of the column capacity is attained. Next, hydrogen is fed at ambient temperature into the column at a flow rate of 50 or more $cm^3\,s^{-1}$ maintaining a constant pressure of 120 kPa employing a suitable pressure regulator. During the course of a separation each of the obtained pure molecular hydrogen isotope product fractions are initially collected in a dedicated vessel and thereafter fed into a uranium storage bed. Interfractions are trapped in a scavenger bed. Besides of the T-D interfraction, the scavenger bed is also used to trap the first He-T_2 front as well as residual eluent during column regeneration. The displacement separation is based on the fact that the solubility of hydrogen isotopes in palladium shows a rather large isotope effect: whereas the heavier hydrogen isotopes stay preferentially in the gas phase the lighter ones predominate in the solid phase [Lae83]. In other words, higher pressures of tritium are needed to absorb a certain amount of this gas on the palladium impregnated column than of deuterium or hydrogen (see Fig. 2.25).

Separation factors, S, are defined by equation

$$S = \frac{\left(\frac{Q_1}{Q_2}\right)_{\text{gas}}}{\left(\frac{Q_1}{Q_2}\right)_{\text{solution}}}$$

where Q_1 is the atom fraction of the heavier molecule and Q_2 that of the lighter one. Separation factors for H-D and H-T at ambient pressure and 293 K were determined to be 2 and 2.6 - 2.8, respectively [Bot88]. Even though hydrogen isotope separation factors increase with decreasing temperature, the benefit of cooling the column below ambient temperature is not sufficient to warrant the extra expense and effort.

Screening tests with nine different packings aimed at comparing their suitability for displacement gas chromatography were carried out by Rutherford and co-workers [Rut88]. For the preparation of columns, materials such as diatomaceous earth and α-alumina based commercial catalyst supports were utilized. To impregnate support material with palladium, the support material was first saturated with palladium chloride ($PdCl_2$), subsequently dried, and finally reduced employing a diluted gaseous mixture of nitrogen and hydrogen at 523 K. Best results were achieved with a packing containing 48.2 % palladium on a 20 - 50 mesh α–alumina support (surface area 0.33 $m^2\,g^{-1}$). This selection agrees well with previous findings of Botter et al. [Bot65]. Cycling experiments with the column materials indicated that all examined packings were subject to some degradation following a large number of hydriding/dehydriding cycles. Enhanced displacement kinetics was observed at 353 K. Because column packings of large surface area, e.g. 4 $m^2\,g^{-1}$, yielded broader asymmetric transition zones, i.e. long tails; they were not recommended.

In good agreement with previous results obtained by Rutherford et al. [Rut88], Gan et al. [Gan02] provided evidence that a DGC of high flow rate utilizing palladium particles of less than 100 mesh, i.e. 150 µm, constitutes a satisfactory option. A requirement was, however, that the separation be carried out at a pressure of about 4 bar because it was postulated that the decrease in displacement efficiency at high flow rates is compensated by an increase in collision frequency at higher pressures. Full activation of the packing was achieved after about 10 absorption/desorption cycles.

A **displacement GC** for the separation of tritium and deuterium from protium with a throughput of 1.25 mol d^{-1} was built at KIT workshops and demonstrated at TLK [Doe02; Doe08]. As apparent from Fig. 3.86, the basic process concept as proposed by Botter et al. 30 years before, has virtually remained unchanged. The TLK column with a total length of 6 m and a total weight of 150 kg, consists of α-alumina impregnated with 20 % by weight of palladium. Packing particles have sizes in the range 0.6 - 1.4 mm. As opposed to the carrier gas chromatography previously utilized at TLK, which separated hydrogen isotopes at liquid nitrogen temperature[67] [Nef98], the DGC column operates under rather mild conditions, i.e. temperature barely above ambient, e.g. 320 - 350 K, and a pressure close to ambient, i.e. 120 kPa.

[67] The separation of a 120 STp l hydrogen isotope batch at 3 bar required 34 hours of continuous operation and almost 2 m^3 of liquid nitrogen.

When a hydrogen isotope mixture is injected into the pre-heated column, initially containing helium, this gas is forced through the column employing a constant stream of protium. The column is equipped at inlet and outlet with thermocouples and downstream with a katarometer (TCD) as well as with an ionisation chamber (IC). These sensors serve not only to identify the displaced isotope fractions but also to provide the information needed for valve switching. Valve switching of the stream flowing through the column - either to the pure D_2 or the pure T_2 vessel - is carried out when corresponding transition bands are registered. For column regeneration after completion of a separation, all hydrogen isotopes retained by the palladium packing are fully released at 473 K and subsequently trapped in a dedicated uranium scavenger bed. A full run can be completed in only seven hours, which is within the normal working hours of a smaller sized laboratory. The eluant product consists consecutively of pure molecular tritium, pure molecular deuterium, and pure molecular protium as well as of several cross-contaminated fractions like $He-T_2$, T_2-DT-D_2, and D_2-HD-H_2.

A so called **Efficient Palladium Isotope Chromatographic (EPIC)** system was built at Mound. The EPIC system is a rapid cycling, computer operated displacement chromatography designed for unattended operation at a temperature of 353 K and a pressure of 1.5 bar [Rut88; Rut89; Emb92]. In first experiments with the EPIC system, performed employing a $2.2\,l(STP)hour^{-1}$ stream of a 1:1 deuterium/protium mixture, pure product streams of hydrogen with 99.86 % purity and deuterium with 99.992 % purity were obtained. The recommended regeneration temperature of the palladium column was 648 K. While lower temperatures were also found to be acceptable, the trade-off were significantly longer regeneration times. For the separation of all hydrogen isotopologues the EPIC system required a number of modifications like all-metal flow controllers, stainless-steel valves with Vespel stem tips, and bellows sealed with stainless-steel bonnet gaskets [Emb92].

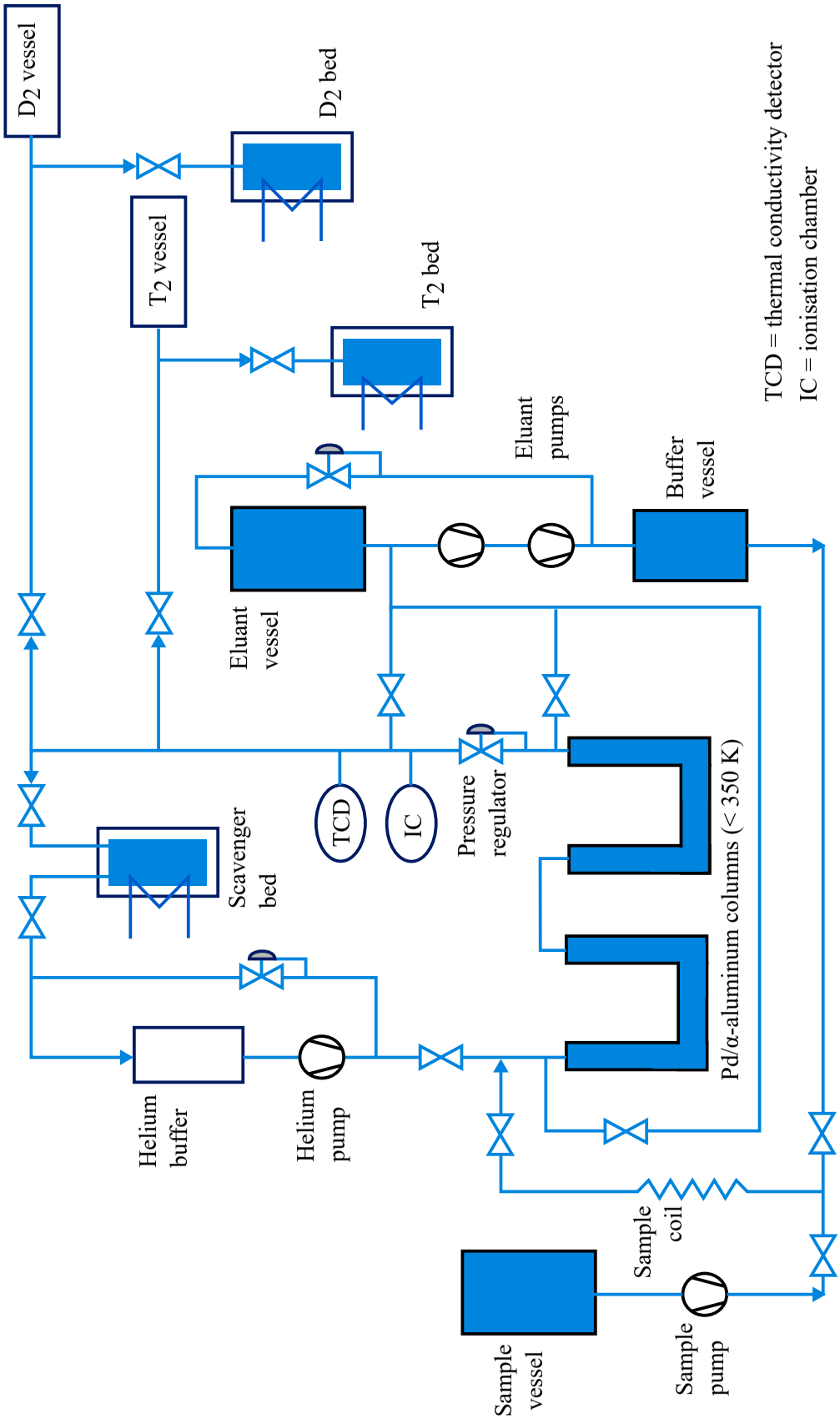


Figure 3.86: Simplified scheme of the displacement gas chromatography isotope separation system of TLK (after [Doe02]).

Recapitulating, the DGC process is particularly valuable for the separation of intermediate sized hydrogen isotope inventories, i.e. mol d^{-1} range [Bot88; Vog88; Rut89; Emb92; Fuk95; Doe08]. Displacement gas chromatography was routinely used at JET within the frame of the DTE1 campaign primarily to supplement an also available large cryogenic isotope separation system. For enhanced efficiency and reduction of costs, conventional storage beds and analytics were utilized for both separation technologies. Main duty of the DGC system of JET was to pre-enrich tritium to the point of very high isotopic purity. It operated successfully for approx. 160 runs eventually processing more than 160 g of tritium [Lae98; Lae99a]. Tritium content in the eluant was normally below 0.1 %. With a single column system, a purity of deuterium and tritium of 99.70 % and 99.96 %, respectively, was regularly achieved.

Advantages of displacement gas chromatography are i) comparatively rather high safety, ii) small space and energy requirements, iii) short time for a full separation, and iv) very high purity of the separated deuterium and tritium streams. Another valuable positive feature is that neither complex controls nor equipment are necessary. The process is not attractive for the separation of large inventories.

3.18.7.3 Thermal diffusion

Thermal diffusion is a process successfully employed for the recovery of tritium from protium or deuterium in the g d^{-1} range. Neubert et al. [Neu83] carried out experiments with a water-cooled 2.5 m high column having a centrally mounted tungsten wire maintained at 1073 K. Spacers fixing the wire axially markedly improved the separation factor, because they permitted equidistant positioning of the wire and additionally suppressed to a large extent wire vibration. Spacers were manufactured from iron with pieces of boron nitride serving for isolation. The wire was heated with a power supply providing 500 A at 20 V of alternate current; the electrical feedthroughs were water cooled. The achievable separation factor was found to depend on the length of the column and on the temperature difference between the central hot wire and the outer wall of the column. In an experiment of long duration commercial deuterium was purified from tritium (feed gas T/D = 6.9×10^{-13}, top gas T/D = 9.9×10^{-15}, and bottom gas T/D = 3.3×10^{-11}). The column was operated at a pressure of 2.3 bar. After five days of equilibration at total reflux the feed stream was kept constant at 10 l (STP) /d and half of the stream was withdrawn from the top and the other half from the bottom during a period of 8 days. Under these conditions

about 97.5 % of the tritium was stripped by the column. To prolong the lifetime of the hot wire it was recommended to employ only gas of high chemical purity. When such conditions prevailed, continuous 24 hour d^{-1} operation was possible for a period of more than eight months without any maintenance or breakdown. It was estimated that for a 1:1 mixture of deuterium and tritium a maximum separation factor of 300 can be obtained at a pressure of 1.5 bar.

Takayasu et al. [Tak81] investigated the separation of hydrogen isotopes by thermal diffusion using four Pyrex glass columns of 100 cm height and diameters of either 8, 20, 30, or 41 mm, respectively. The water jacketed columns were provided with a gas reservoir on top. A centrally mounted hot tungsten wire of 0.5 mm diameter could be maintained at constant temperatures of either 473, 523, 573, 623, 673, or 723 K. The adopted operation pressure was 1.05 bar. Feed gas was either hydrogen or deuterium containing tritium. To protect the wire, the feed gases were purified before injection into the column either with a palladium thimble or by passing them through a liquid nitrogen cooled molecular sieve bed. Furthermore, the feed gases were passed over nickel plates at 373 K for a period of two days in order to convert all tritium into either tritiated hydrogen or tritiated deuterium. When TH–H_2 or TD–D_2 mixtures were injected into the glass column tritium rapidly concentrated at the bottom. This is the case because the lighter molecules show a tendency to migrate to the centre of the column and the heavier ones to the cooler outer wall. By natural convection the hotter gas moves upwards and the cooler one downwards. Once steady state is reached, the lighter gas accumulates at the top and the heavier one at the bottom of the column. Equilibrium separation factors were determined as function of wire temperature (473 - 723 K) and column diameter ($\varnothing$ = 8 - 41 mm) and compared with predictions calculated with a modified model equation proposed by Waldmann [Wal39].

Analogous to displacement gas chromatography, the separation factor of a column, S, is obtained from equation

$$S = \frac{\left(\frac{Q_1}{Q_2}\right)_\mathrm{b}}{\left(\frac{Q_1}{Q_2}\right)_\mathrm{t}}$$

in which Q_1 is the atom fraction of the heavier molecule and Q_2 that of the lighter one. The subscripts b and t stand for bottom and top of the column. The maximum equilibrium separations factors that could be achieved with the H–T and H–D systems were 17 and 4.5, respectively.

The separation factor of a column can be significantly improved by cooling the outside wall with liquid nitrogen [Mit91; Ari02]. This was accomplished by submerging a thermal diffusion

column into a cryostat. Arita et al. [Ari02] employed either an axially placed tungsten wire with a diameter of 0.5 mm and a ceramic weight attached to its bottom or an 11 mm diameter stainless-steel sheath as heaters. The ceramic weight was used to mitigate thermal variations of the length of the wire. Spacers were employed for both type of heaters in order to minimize vibrations. The maximum separation factor attainable under these conditions with the H-T system at a feed gas rate maintained at $10\,cm^3\,min^{-1}$ was 2660 [Ari02]. While products were withdrawn from top and bottom of the column, the feed was supplied at a fairly central position. For supply and withdrawal of feed and product streams a circulation pump was utilized.

Mitsui et al. [Mit91] investigated the separation of hydrogen and deuterium using a stainless-steel column provided with a cryogenic wall and a conventional central wire of tungsten. When the wire inside of the column was heated up to 473 K the separation factor was found to be higher than when heated up to 1073 K. This effect was explained by the rapid occurrence of isotopic scrambling at elevated wire temperature, which is much slower at 473 K. In view that isotopic scrambling yields HD, it was concluded that the presence of a ternary species reduced the separation ability of the column. Another argument for the selection of a lower temperature was the consumption of liquid nitrogen, which increased markedly with increasing wire temperature, i.e.$1.0\,l\,hour^{-1}$, $3.5\,l\,hour^{-1}$ and $10.8\,l\,hour^{-1}$ when the wire was maintained at ambient temperature, 500, or 1100 K, respectively. Mitsui et al. [Mit91] additionally reported a pressure dependence of the separation factor. According to their observations, the highest separation factors for a H_2/D_2 mixture were i) 5.3 for the water-cooled wall and a wire temperature of 1273 K and a pressure of 100 kPa (theoretical prediction 96 kPa) and ii) 19.3 for the column wall at cryogenic temperature, a wire at 1073 K and a pressure of 26 kPa (the theoretical prediction is 24 kPa). As apparent, the predicted optimal pressures reflected well the experimentally determined values.

Nakamura et al [Nak92] and Matsuda et al [Mat88] carried out experiments on the separation of hydrogen isotopologues employing thermal diffusion and using either a single column or four interlinked columns. The columns used by Nakamura were 2.5 m high and had a diameter of 29.4 mm. The outer wall of the columns was cooled by chilled water maintained at a temperature of 283 K. When the experiments were performed with 4 columns the temperatures of the columns could be selected individually. The optimum pressure for the H – T system was found to be 93 kPa and that for the H – D system 106 kPa. For single column runs the selected temperature of the axial wire was 1273 K. Nakamura et al. corroborated the pressure dependence of the separation

factor observed by Mitsui et al. [Mit91] and determined maximum separation factors of 17.1 for D-T, 523 for H-T, and 74.7 for H-D when using pressures of 93 kPa, 93 kPa and 106 kPa, respectively.

In summary, large separation factors without the need of complicated equipment can be accomplished with the thermal diffusion process. Special assets of thermal diffusion are high basic safety, comparatively inexpensive equipment, and low cost of operation. On the negative side is the large height of the columns which require a custom sized second containment. What is more, because the hydrogen isotope throughput of thermal diffusion is relatively small, the process is only attractive for installations handling small amounts of tritium. Applications have been purification of tritium, purification of deuterium from tritium, and the recovery of tritium from hydrogen isotope gas mixtures released from small scale experiments.

3.18.7.4 Thermal cycling absorption process (TCAP)

A continuous gas chromatographic process for the separation of hydrogen isotopes based on **thermal cycling absorption** has been under continuous development since 1981 at Savannah River Site, South Carolina, USA [Hor92; Lee95] as well as at Valduc, France [Let98; Duc02]. The process is based on the property of palladium to absorb preferentially the lighter hydrogen isotope, i.e. more protium than deuterium or deuterium than tritium. Advantageously, absorption and concomitant separation is possible without the need of extreme temperatures. Key components of the process are two interconnected columns, one containing 40 % palladium on Kieselguhr as active packing material and another larger column filled with kieselguhr only, which allows internal gas transfer with minimal gas mixing. By repeated heating and cooling cycles, it becomes possible to separate protium, deuterium, and tritium. The palladium column is double contained and either heated to 348 K or cooled to 298 K utilizing gaseous nitrogen for heat transport. During the heating cycle gas is desorbed from the Pd-column (reaching a pressure of nearly 5 bar (pressure swing)) while transferred to the Kieselguhr column and vice versa during the cooling cycle. About 30 % of the inventory on the Pd-column is transferred during each cycle. After each cycle about 3 - 5 % of the inventory is fed into the system and about the same amount withdrawn. Tritium of more than 99.9 % purity can be produced with the TCAP process. The throughput is proportional to the total inventory in the column.

The **upgraded TCAP**process tested at Savannah River comprises a simplified column design and optimized equipment for the thermal cycling system [Heu09]. The formerly employed hot/cold gaseous nitrogen system operated by large compressors and heat exchangers has been replaced by a new thermal cycling design utilizing liquid nitrogen and electric heaters for cooling and heating, respectively [Heu08]. With the upgraded equipment a feed comprising 25 % deuterium and 75 % hydrogen was separated after approximately 60 cycles into two streams of which each had a purity higher than 99.7 %. In a further development, the performance of the thermal cycling absorption process employing a palladium/kieselguhr packed column followed by a kieselguhr packed passive plug flow reverser (TFR) was compared with that of the same palladium/kieselguhr packed column but combined with an inverse active column packed with dehydrated 4A molecular sieve [Heu11]. The palladium/kieselguhr columns were made of copper tubing. They were folded to reduce their height and trace heated. The plug flow reverser consisted of two 0.9 m long tubes filled with kieselguhr to enhance plug flow performance. Because the inverse column needs to withstand high pressures, it was manufactured for safety reasons of stainless-steel. The experimental comparison of both process configurations revealed, that the one using an inverse active column increases the throughput by more than a factor of two and delivers products of improved quality (both separated streams had purities better than 98 % at all rates tested).

Summarizing, the TCAP process is continuous, easy to control, of comparatively small size (fits into a glove box), and simple to operate within a gentle temperature range of 223 - 423 K. On the positive side are also the relatively low capital cost and straightforward scaling. Conversely, the process needs to cope with transient pressures of up to 8 bar and, depending on the demanded degree of purity, may necessitate a large number of thermal cycles, e.g. more than 50, to achieve this goal. Therefore, a complete separation may require a full working day.

More recently, Mini and Micro TCAP separation systems have been developed at SRNL. Favourably, they operate with further reduced heat load and less tritium at risk.

3.18.8 Water de-tritiation

Very substantial sources of tritium-contaminated water are heavy water moderated CANDU reactors[68] or reactors like for example the Japanese FUGEN in Tsuruga (currently being

[68] The production of tritium in heavy water of fission reactors is estimated to fluctuate within the range 7.4×10^{14} - 8.9×10^{14} Bq/GW_e/year [Bau92].

dismantled) [Kit02], which depend on natural uranium oxide or plutonium/uranium mixed oxide fuel (MOX), respectively. Tritium in the deuterated water moderator of these reactors needs to be extracted in regular intervals primarily for radiation protection reasons[69]. In point of fact, these rather large streams of tritium-contaminated water have constituted the incentive for the development of efficient detritiation processes aiming on one hand at reducing the tritium concentration in heavy water down to levels acceptable for reuse and, on the other, recovering nearly pure tritium for research or commercial purposes. Generally, only very slightly contaminated - mostly light water - is given to waste. The concentration limit of tritium in water vapour discharged into the environment is $< 3.7 \times 10^3\,\mathrm{Bq\,m^{-3}}$ [Iwa02a].

Sizeable streams of tritium-contaminated water of low-level activity, are likewise generated during the routine operation of fusion machines [Bel02; Per08; Iwa02a]. They are generated by permeation of tritium into the primary cooling water ($\sim 150\,\mathrm{m^3}$/ loop which may contain tritium at concentrations of about $2 \times 10^{12}\,\mathrm{Bq\,m^{-3}}$).

In addition, streams of highly contaminated tritiated water (mostly as DTO of $\sim 6 \times 10^{19}$ $\mathrm{Bq\,m^{-3}}$) are generated during regular baking of the vacuum vessel in the presence of oxygen. Baking is necessary in recurrent intervals to reduce the in-vessel inventory of tritium. Tritiated water can furthermore be generated in case of an accidental release (eventually of high specific concentrations of tritium) [Hay06]. Other sources are i) the oxidation of tritium-bearing exhaust gases collected as tritiated water in adsorber beds of detritiation systems, and ii) handling of tritium within the frame of activities performed at the tritium plant, the hot cell (about $20\,\mathrm{l\,d^{-1}}$ of $< 10^{14}\,\mathrm{Bq\,m^{-3}}$), or during routine maintenance work. Rationales for the recovery of tritium from these streams are i) waste volume minimization, ii) cost reduction of waste, iii) water reuse, and last not least iv) fuel economy.

Several small and major process concepts for the detritiation of water developed and demonstrated worldwide will be adressed briefly and - when pertinent - evaluated in the section below. As will become apparent, much relevant operational experience has emerged over the past decades from work on processes relevant to the detritiation of water not only in large tritium handling installations but also in smaller ones.

[69] The amount of tritium recoverable from heavy water moderator is actually large enough for commercial exploitation.

A process based on **catalytic exchange** at approx. 25 K combined with **cryogenic distillation** (CD) was developed in the late Seventies by CEA together with Sulzer Brother Ltd., Switzerland at the Laue-Langevin Institute in Grenoble, France, [Pau88]. The process was specifically tailored to the extraction of tritium and protium from heavy water. Tritium of more than 95 % isotopic purity was regularly collected and stored. Both, catalysis and distillation units were at all time operated at above-atmospheric pressure in order to exclude the possibility of oxygen accumulation in cryogenic zones (explosion risk). As further precaution, in the event of an emergency situation it was possible to sweep the affected equipment with a strong stream of nitrogen. Numerous ionization chambers served for early detection of tritium in relevant process areas. For evacuation as well as for gas transfer SRTI dry pumps manufactured in France were utilized. First generation pumps were furnished with elastomer seals which readily hardened when exposed to tritium. After replacement of these elastomer seals by metallic ones the pumps (SRTI model PBT 135) became vacuum-tight and operated without occurrences for prolonged time. With the plant at Grenoble more than 5×10^4 TBq tritium was extracted from 840 000 l of heavy water. After an extended period of operation, a negative experience was made with numerous Kel-F flap valves which developed leaks in the seat region. Once they were completely replaced by fully metallic valves equipped with aluminium flaps and indium seals the problem was resolved.

The most thoroughly investigated water detritiation process is based on the **combined electrolysis catalytic exchange** (CECE) concept, which operates in closed loop mode [Mil80; Sie88; Shi91; Ber91; Yam95b; Gra02; Mil02; Ale02; Mic08; Ale11b; Mic13; Rod13]. Very high DF´s have been achieved with the CECE detritiation technology installed either as front end to a cryogenic distillation column or as standalone process. Basically, a liquid phase catalytic exchange (LPCE) column packed with a specially developed wet-proof catalyst stimulates the isotope transfer between the liquid and the gaseous phase when operated in counter current mode. The column delivers tritium-depleted hydrogen at the top and tritium-enriched water at the bottom. Habitual operation parameters of a LPCE column are temperatures in the range 318 - 33 K and pressures in the range 100 - 120 kPa. Several types of commercial electrolyzers using either **alkali electrolyte** or **solid polymer electrolyte** [Sie88; Mic08; Mic13] have been tested together with LPCE columns.

At Monsanto Research Corporation managed by the **Mound** facility in Miamisburg, Ohio, a "tritium recovery from water" process was developed jointly with Atomic Energy of Canada Ltd (AECL) [Sie88; Shi91]. Principal components of the process are a Combined Electrolysis Catalytic Exchange System comprising two solid polymer electrolyte electrolysis cells supplied by General Electric Company and five hydrophobic exchange catalyst columns containing a catalyst developed at AECL/CRNL. The columns are arranged in series and have a combined total packed height of 15 m. The electrolyzers are operated with a water throughput of $48\,cm^3\,min^{-1}$. They generate up to $30\,l(STP)min^{-1}$ of hydrogen and $15\,l(STP)min^{-1}$ of oxygen. Detritiation of feed streams containing initially between 0.01 % and 0.1 % tritium could be accomplished successfully.

A particularly important application of the CECE process has been recycling of tritium-contaminated heavy water such as required for heavy water moderated fission reactors [Mil02]. Detritiation at **Chalk River Laboratories** was designed for a water throughput of $0.7\,kg\,hour^{-1}$ contaminated on the average by $370\,GBq\,kg^{-1}$. To upgrade contaminated heavy water, a stream is fed into a suitable point - approximately in the middle - of a LPCE column maintained at 320 K, from where it flows downwards into an electrolysis cell. The electrolysis cell is of small water hold up and hence tritium inventory. It operates with KOD electrolyte (25 percent in heavy water) and hence generates tritium-enriched deuterium. A fraction of this stream is injected into the bottom of the LPCE column where it is stripped from tritium, while water flowing down the column is enriched in the heavier isotope (see Fig. 3.87). Another tritium- enriched deuterium fraction is first subjected to a purification procedure comprising a catalyst bed to remove oxygen and an adsorber bed to retain the catalytically generated water, and subsequently a permeator, where DT is purified chemically before being trapped as metal hydride in a metal hydride storage vessel. This side stream is extracted from the process in order to keep the inventory constant. Oxygen generated in the electrolysis cell is fed into a gas phase re-combiner where it is converted into deuterated water and then passed through a vapour scrubber column whose function is to fully remove tritiated moisture. Gaseous deuterium exiting from the top of the LPCE column and the residual oxygen from the vapour scrubber column are recombined in a trickle bed (droplet) re-combiner on a wet-proof catalyst.

Graham et al. [Gra02] demonstrated with a pilot-scale CECE facility at Chalk River, Canada, that tritium can be removed from water feed streams containing $320\,GBq\,kg^{-1}$ with detritiation factors exceeding 50 000. The tritium level routinely maintained in the electrolysis cell was

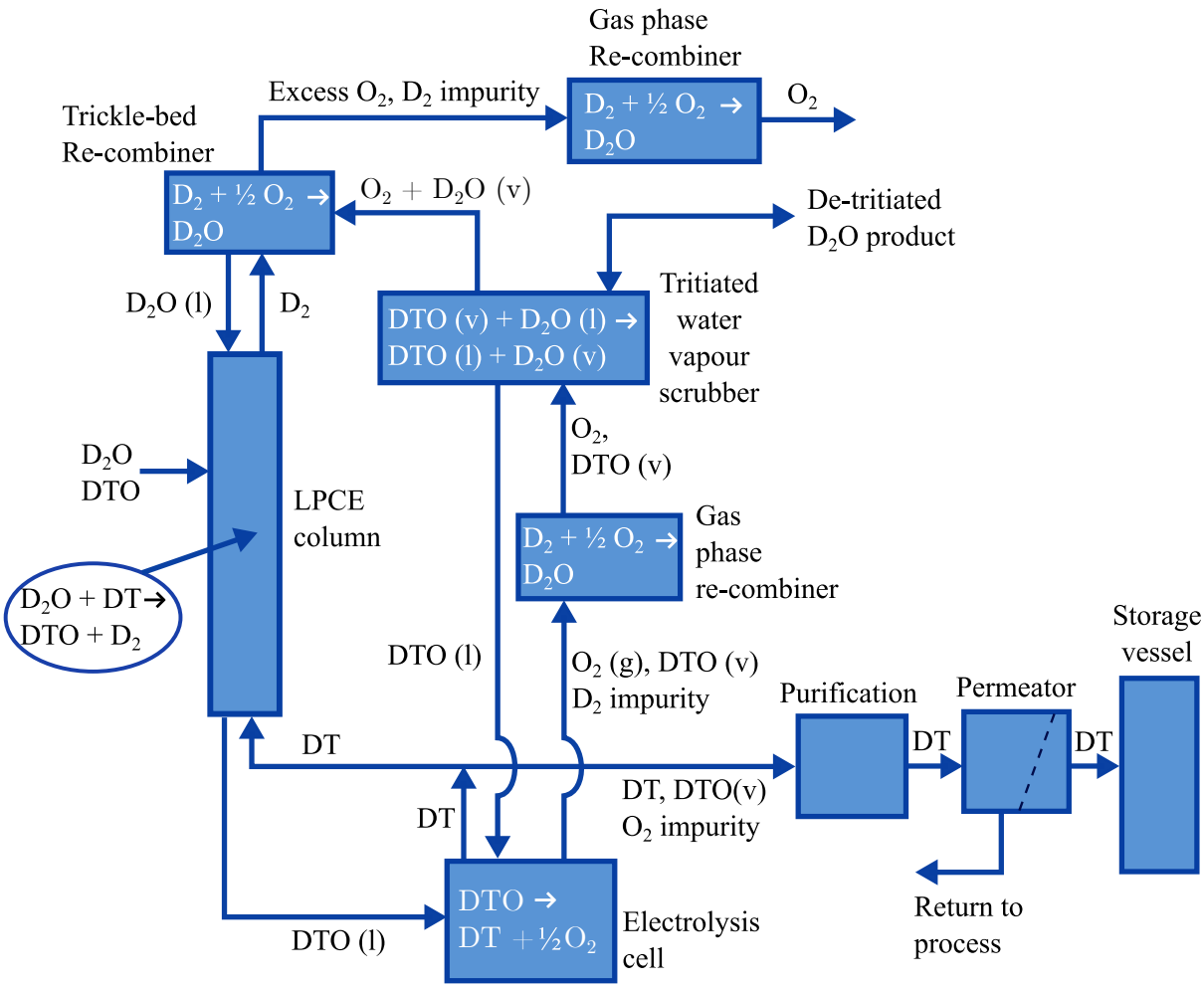


Figure 3.87: Simplified block diagram of the CECE process for recycling of tritium-contaminated heavy water operated at Chalk River Laboratories (after [Mil02]).

7.8 $TBq\,kg^{-1}$. To achieve very high overall decontamination factors a high efficiency drip bed re-combiner (catalytic converter of gaseous DT into DTO via reaction with oxygen) in support of the gas phase re-combiner was found to be essential.

The experimental industrial plant EVIO at Petersburg Nuclear Physics Institute (PNPI) in Gatchina, Russia, has been designed for the removal of tritium and protium from heavy water on the basis of the CECE isotope separation process [Ale02; Ale11b]. For research activites the plant is engaged in a close collaboration with JSC DOL, Moscow, and Mendeleyev University of Chemical Technology of Russia. Principal components of the plant are liquid phase catalytic exchange (LPCE) columns, wetproof platinum catalysts for the combustion of hydrogen, and an alcaline electrolyzer to convert water into hydrogen. The plant has operated safely since 1995 producing heavy water of 99.85 - 99.995 % purity and deuterium gas for industry and research purposes. On account of continuos upgrading (e.g. additional separation column), the plant is now capable of a daily production of reactor grade heavy water (activity 4 - 500 $MBq\,kg^{-1}$) and tritium-free heavy water of up to 35 and 9 $kg\,d^{-1}$, respectively.

Much effort has been invested at several different research institutions into the development of efficient **hydrophobic catalysts** [Fie80; Mor80; Bru82; Iso88; Shi91; Glu02b]. Some of the developed catalysts were compared experimentally among each other under similar experimental conditions to assess their potential application in LPCE columns [Cri02b; Per02a]. Particularly efficient catalysts were found to consist either of a carbon/polytretrafluoro ethylene (Teflon) or a styrene/divinylbenzene copolymer solid carrier impregnated with platinum at concentrations within the range 0.8 - 1.5 %.

A parametric test program carried out at TLK employing the TRENTA facility delivered height equivalent of theoretical plate (HETP) values for four different types of hydrophobic catalyst - packing combinations at two gas/liquid ratios [Cri02b; Cri02a; Cri07b]. The compared catalysts were those developed at i) SCK-CEN Belgium; ii) Mendeleev University, Russia; iii) Institute of Cryogenics and Isotopic Technologies, Romania; and iv) Showa Engineering, Japan [Cri02b; Cri02a]. Employing a column with a height of approx. 9 m it was experimentally demonstrated that decontamination factors in the range 5000 - 50 000 were attainable with all investigated catalyst/packing combinations.

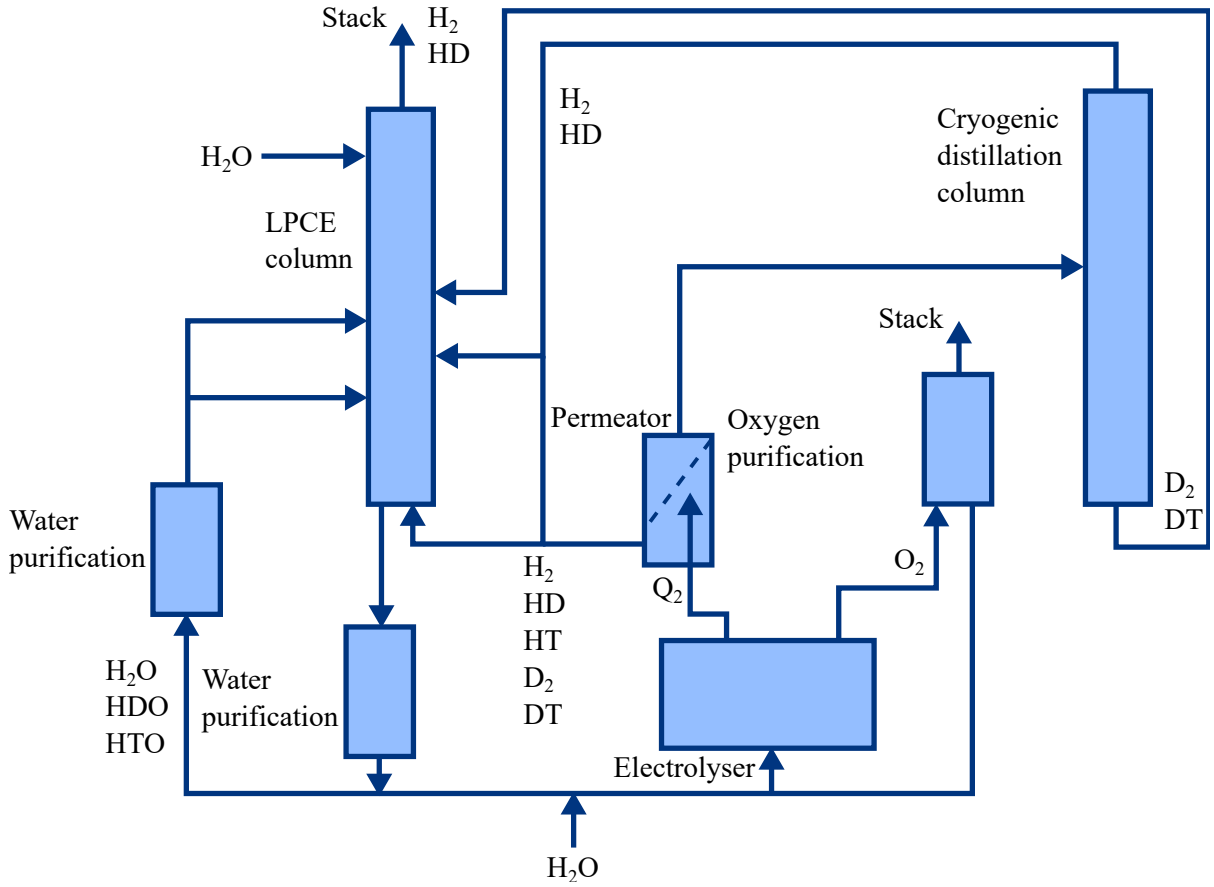


Figure 3.88: Block diagram of the facility TRENTA encompassing a Water Detritiation System and an Isotope Separation System (after [Cri07b; Cri07a]).

Frequently employed **packing materials** are mini spirals consisting of stainless-steel, bronze, or a wire mesh. Of dominant importance for a good column performance was found to be the acceptance of wetness by the packing.

Diverse amounts of tritiated water waste recurrently arising in various subsystems of the ITER Tritium Plant sporadically require the extraction of tritiumin with a Water Detritiation System (WDS) in order to reduce the volume of some times substantial amounts of low activity waste necessitating interim storage or disposal [Per08]. Main components of a typical WDS comprise several catalytic exchange towers, electrolysers, a water purification system, a pure water supply system, oxygen gas detritation dryers, several palladium/silver permeators, a hydrogen isotope separation system, a crimp metal packed flame arrester, etc. [Yos02]. The chief constituent of the cathodic gas discharged by the electrolyzer cells of the detritiation system are molecular hydrogen isotopes. The only impurity in this stream is water vapor at saturation partial pressure.

Prior to feeding the gaseous hydrogen isotopes constituting most of this stream into a cryogenic distillation column, it is necessary to remove condensable water employing a palladium/silver permeator [Iwa02c]. Design calculations performed within the frame of activities dedicated to the development of the Tokamak Exhaust Processing (TEP) System for ITER showed that in total nine permeators, each with an active permeation area of $1\,m^2$, will be necessary to extract the large inventories at comparatively high flow rates of electrolytically generated hydrogen isotopologues. Downstream of the purification step, the hydrogen isotopes are fed at about half heigth into a cryogenic distillation column.

Taking present and future needs of the TLK infrastructure into account and keeping the design of ITER in mind, it was decided at TLK to erect the facility "**TRENnung Tritium Anlage**" (TRENTA) . Key components of TRENTA were initially a liquid phase catalytic exchange column (LPCE) and an electrolyzer featuring solid polymer electrolyte (see Fig. 3.88 [Cri05a; Cri07a; Ana09; Mic13]. Subsequently, the original TRENTA system was upgraded by integrating into this system a palladium/silver permeator and a cryogenic distillation column. As in the case of ITER, while the permeator serves to extract tritiated hydrogen isotopologues from the water-saturated gas discharged by the electrolyzer cell, the task of the cryogenic distillation column is to separate the injected gas mixture into its molecular constituents. These improvements effectively support the regular operational activities at TLK by i) reducing the volume of tritiated waste water requiring storage and augmenting the autonomy of TLK by recycling tritium for the normal activities in the laboratory. In addition, the acquisition with the TRENTA facility of experimental data and operation experience concerning the dynamic interaction between all pertinent WDS subsystems may be of benefit to the design optimization and operation of the WDS for ITER.

In view that a call for tender to industry to manufacture a permeator for TRENTA of unprecedented design and throughput remained without reply, a permeator with a total membrane area of $1.2\,m^2$ was designed at TLK and assembled at workshops of KIT. To achieve exact brazing gaps the manufacture of several special tools was indispensable. The brazing procedure was qualified by standard brazing tests. The obtained permeator fully complied with all "Technical Terms of Delivery and Acceptance" required for all primary components installed in TLK. It also complied with all pertinent EU regulations like PED97/23/EC and AD2000 (see also [Wel09], section 3.18.4.3, and Appendix V). Salient features of the special permeator are 183 Pd/Ag

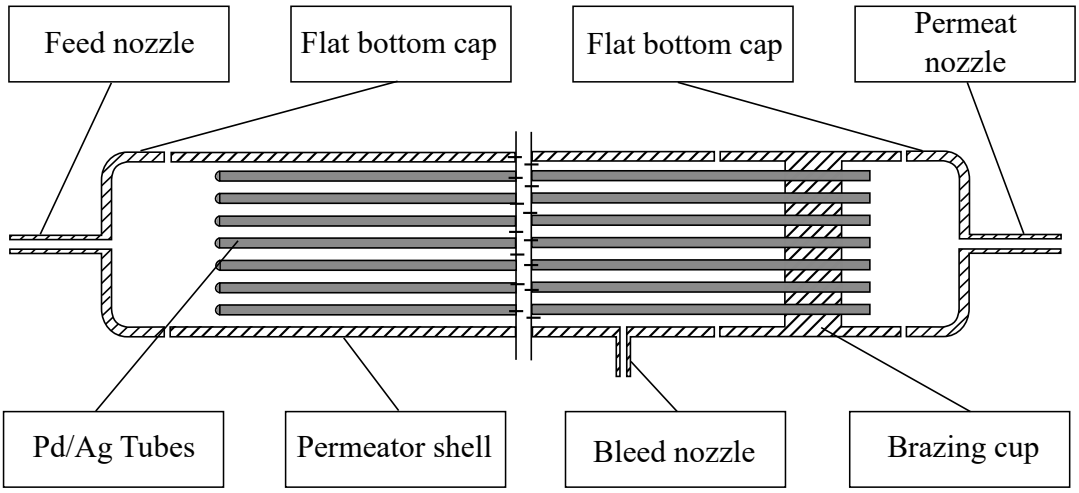


Figure 3.89: Layout of the TRENTA permeator [Wel09].

tubes each with 900 mm length, 2.3 mm diameter, and 0.1 mm wall thickness. Special vacuum brazing procedures had to be developed to join palladium/silver tubes to the brazing cup (see Fig. 3.89). The brazing procedure was also qualified by test brazing's as well as non-destructive and destructive tests. For manufacture simplicity, the permeator shown in Fig. 3.89 was designed in the filter modus. In this mode, highest priority is given to chemical purification of hydrogen rather than effective recovery of hydrogen isotopes from a gas stream, like is the case in the stripping mode of a front end permeator. The upgraded process configuration can be regarded as prototype for the combination Water Detritiation System and Isotope Separation System required for fusion machines like JET or ITER, which operate or will operate with tritium [Mur05]. Goals of the research activities at TLK are i) integration of an isotope separation system into the infrastructure, ii) systematic investigation of the effect of moisture on the permeation rate of hydrogen through a palladium silver membrane, iii) a parametric study on the interdependence between the WDS process and a cryogenic distillation unit under steady state as well as dynamic conditions and iv) further validation of the modelling software TRIMO developed at TLK.

The capability of the TRENTA waste water detritiation system (WDS) was demonstrated by processing 180 l of water containing 74 GBq tritium supplied to TLK in a single drum by JET[70]

[70] As a result of activities performed at the Active Gas Handling System of JET a total number of about 250 drums containing tritium-contaminated water with an average activity of 1.5 GBq kg^{-1} has accumulated.

[Ana09; Wel13; Mic13]. Prior to detritiation the water was purified from anions and cations to exclude possible poisoning of the WDS catalyst. During 6.5 days of continuous operation the water volume was reduced down to 6.25 l and the specific activity of tritium down to 11.9 GBq kg^{-1}. Hence, an enrichment factor of about 30 was achieved. Chemical impurities such as F^-, Cl^-, $SO_4{}^{-2}$, Fe^{+2}, Fe^{+3}, K^+, Na^+, and the pH value of the water supplied by JET before and after enrichment remained largely unaffected by the detritiation operation. Only the water conductivity increased from 2.7 to 11.0 µSv cm^{-1}. Therefore, the water quality remained largely unchanged. The analytical procedures employed for process control and understanding of fundamental parameters comprised liquid scintillation counting for the determination of tritium in liquids, ionisation chambers for the determination of tritium in gases, quadrupole mass spectrometry for the identification of species, and infra-red spectroscopy for the quantitative measurement of liquid deuterium-bearing species. Since the TRENTA facility can process up to 370 GBq kg^{-1}, enrichment factors of 250 are considered possible. From the results it was concluded, that 250 drums containing tritiated water waiting for detritiation at JET, each containing about 180 l tritiated water with an average activity of 0.5 GBq kg^{-1} (in total 22.5 TBq), could be reduced with a redesigned and upgraded TRENTA facility down to only 2 drums.

Iwai et al. [Iwa02a] proposed a concept for the detritiation of ITER waste water employing the combined electrolysis catalytic exchange (CECE) process instead of the vapour phase catalytic exchange (VPCE) procedure. This decision was taken after it was realized that the previously estimated detritiation requirements for ITER were actually less demanding than predicted[71]. The proposed CECE process encompasses a multi stage column for the isotopic exchange between natural water and tritiated hydrogen and an electrolysis cell with a solid Nafion polymer ion exchange membrane as key components. The optimal operation temperature of the column was determined to be 343 K. At this temperature, rapid equilibration between tritium in the gaseous and liquid phases establishes. The ITER electrolysis cell design is characterized by a comparatively small liquid holdup of only 1/10$^{\text{th}}$ that of an alkaline electrolyzer (see Fig. 3.90, left). Three modules, each containing 37 litres of liquid operating at a pressure of 0.15 MPa and a temperature of 349 K were proposed. The only material allowed to be in contact with liquid was titanium. According to the process the water to be detritiated is first subjected to a

[71] Permeation of tritium through the first wall of ITER is much smaller than originally thought, i.e. only 0.1 mg d^{-1} [Ise99].

front-end process whose objective is to remove negative ions, metals, and organic substances. This is carried out employing a resin bed (ion removal), a charcoal bed (retention of organics) and a filter (particle removal). Purpose of the purification is protection of catalyst and packing layer from degradation and corrosion. After this step, tritiated water is fed into about the middle of the exchange tower. Natural water is fed into the isotopic exchange column from the top. Enriched tritiated hydrogen generated in the electrolyzer is released from the bottom of the exchange column in counter current mode.

A column consists of a total number of seventy segments. Each segment comprises of 0.3 m high Dixon ring packing section and a Kogel hydrophobic catalyst section such as displayed in Fig. 3.90 (heights of packing and catalyst are 0.056 and 0.16 m, respectively). Because the total height of a CECE column amounts to 27.2 m, they were divided into two towers of only 13.6 m height, in order to fit into the building. The packing layer is completely separated from the catalyst in order to maintain stable wetting conditions (see Fig. 3.90, right). Exchange reactions taking place on the Kogel catalyst and on the packing-layer are provided on the same figure.

In the proposed concept utilizing natural water, a recombiner such as habitually employed in CECE detritiation configurations was considered unnecessary. Hence, all complex and expensive hydrogen explosion safety measures became superfluous. Oxygen produced in the electrolyzer is saturated with weakly tritiated water vapour. This stream is first passed through a condenser, where most moisture is retained, and thereafter through a molecular sieve bed for final drying. Either a side stream or all of the electrolytically released tritium-enriched hydrogen carrying water vapour is injected into a palladium/silver permeator with the objective of segregating purified hydrogen isotopologues. The isotopologues are finally separated in a cryogenic isotope separation system into pure hydrogen isotope streams.

Tritium enrichment of natural water takes place by exchange with electrolytically generated tritiated hydrogen. Tritium enriched water will eventually drop into the electrolyzer and undergo electrolysis. Reactions taking place on anode and cathode of the electrolyzer are

$$2\,H_2O \longrightarrow 4\,H^+ + 4\,e + O_2$$

and

$$4\,H^+ + 4\,e \longrightarrow 2\,H_2$$

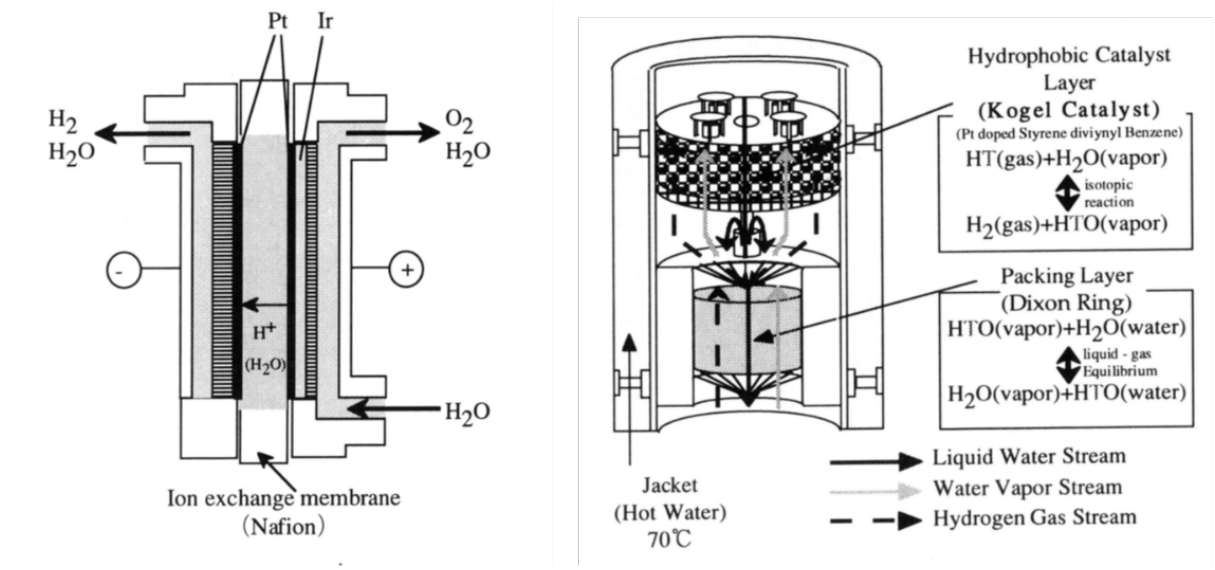


Figure 3.90: Schemes of the solid polymer electrode (left) and of a single unit of the water – hydrogen isotopic exchange column (right) (after [Iwa02a]).

respectively. Between the electrodes there is an ion exchange membrane consisting of Nafion, a material which selectively permeates hydrogen ions. Advantages of industrial electrolyzers furnished with a solid polymer electrode are i) avoidance of alkaline tritiated waste water, ii) comparatively small liquid hold-up and therefore tritium inventory, and iii) high commercial availability and good service. The life time of the membrane when exposed to tritiated water containing up to $1.85 \times 10^{13}\,\mathrm{Bq\,kg^{-1}}$ has been estimated to be of the order of 1.5 year (formation of corrosive hydrofluoric acid via radiation-induced reactions).

The hydrophobic Kogel catalyst utilized in the exchange column is manufactured by Shimizu et al. [Shi08b]. It consists of platinum doped styrene divinyl benzene. Its efficiency was demonstrated successfully at **FUGEN Nuclear Power Station**, Tsuruga, Japan, which operated during almost thirty years using MOX fuel, heavy water moderator and light water cooling [Kit98; Kit02]. A large fraction of the tritium-enriched hydrogen released from this power station first passed through a permeator for chemical purification and is then sent to isotope separation system. Another fraction is fed into the bottom of the isotopic exchange column for tritium stripping. Hydrogen decontaminated by this procedure can be released to the environment. According to the design, the facility can process $20\,\mathrm{kg\,hour^{-1}}$ of waste water having an initial

tritium content of $< 3.7 \times 10^{11}\,\mathrm{Bq\,kg^{-1}}$. The concentration of tritium in the effluent hydrogen was determined to be lower than $65\,\mathrm{Bq\,m^{-3}}$.

A detailed conceptual design of a detritiation facility has been worked out for **JET** [Per02c; Per08] (see Fig. 3.91). The task was motivated by substantial amounts of interimly stored tritiated water accumulated over the past years and displaying activity levels notoriously above the environmental discharge limit. Tritiated water was generated at JET mostly during fusion experiments with tritium, e.g. DTE1 campaign [Bel02]. The developed detritiation process concept is the result of i) a detailed assessment of key components, ii) numerical performance evaluations, iii) a large number of diverse screening experiments, and iv) a hazard and operability study.

Conventionally, the detritiation concept comprises as main components i) a commercial electrolyzer (electrolyzer 1) for the decomposition of tritiated water into the elements and concentration of water into a smaller tritium-enriched volume, ii) a LPCE column packed with a hydrophobic catalyst for the detritiation of hydrogen via isotopic exchange with liquid water, iii) a palladium silver permeator for the chemical purification of hydrogen and iv) a cryogenic distillation column for the enrichment of tritium. At JET a pressurized electrolyzer utiliizing **potassium hydroxide as electrolyte** was selected as electrolyzer 1 because of its proven high reliability. To provide supplementary protection against possible electrolyte leakage all pertinent gas flow ducts and electrolyte ducts were surrounded by water-filled channels. For the detection of potential alkali solution leakages several tritium monitors and/or electrical conductivity detectors were contemplated. Of concern are potassium hydroxide aerosols eventually generated during electrolysis. They can be removed from gaseous hydrogen with a stripping column [Sch95]. To reduce the tritium inventory in the electrolyte, a re-circulation step through the boiler was proposed. In order to transfer tritium from the vapour phase to the gas phase, water vapour generated by the electrolyzer is passed through a LPCE column together with detritiated gaseous hydrogen from the cryogenic distillation column (see Fig. 3.91). Since then, the initial concept has more recently been revised and replaced by an upgraded design that is, however, still relying on the original combined electrolysis and catalytic exchange concept [Per08]. According to the upgraded design, tritium-enriched water is first concentrated in order to achieve an additional volume reduction, allowing processing either i) off-site, ii) conversion into solid waste for direct disposal, or iii) further processing on site for full recovery of tritium.

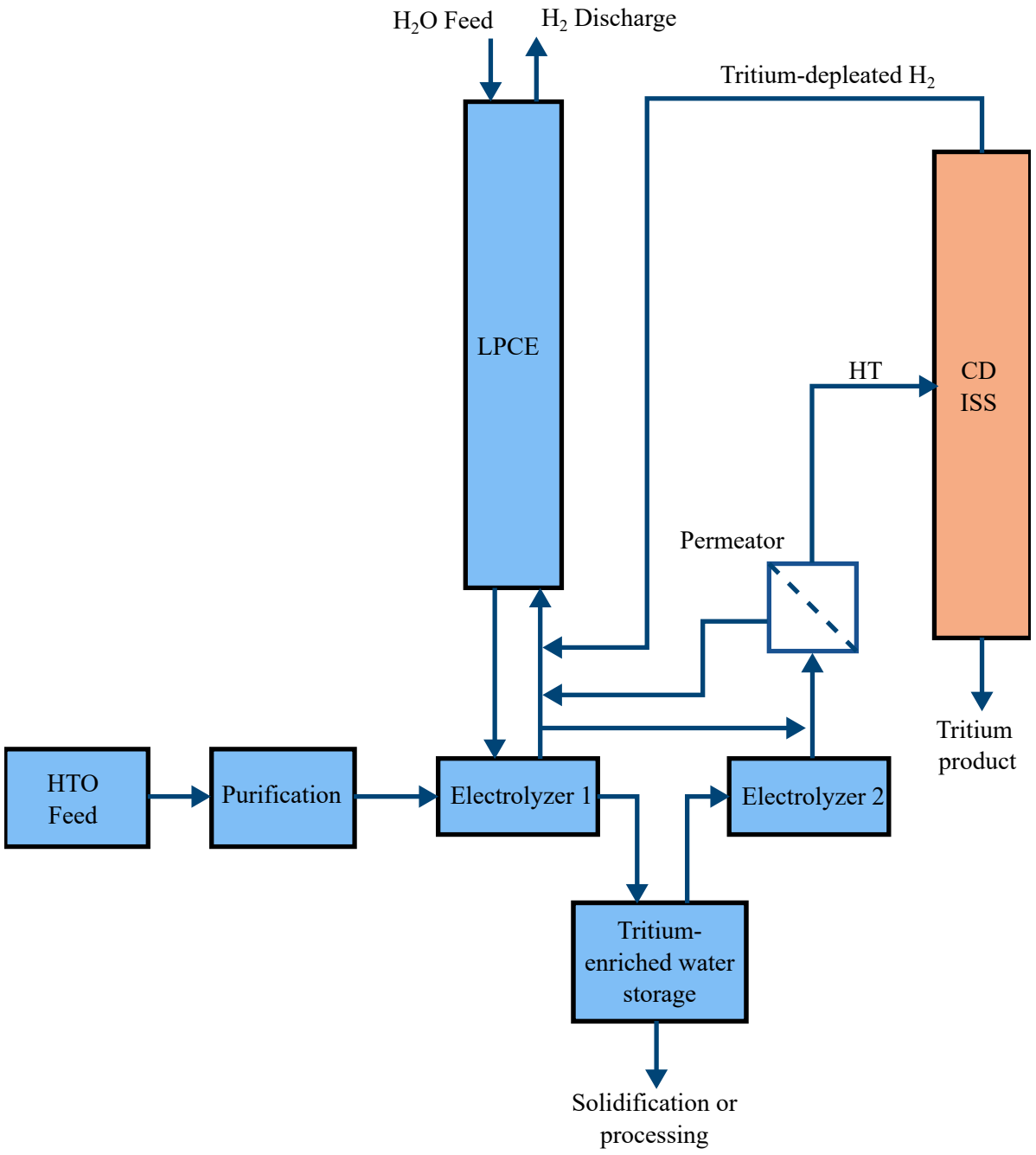


Figure 3.91: Block diagram of the water detritiation system of JET (after [Per08]).

The concentration step is considered advantageous because it copes with problems resulting from fluctuations in composition of the feed water thus ameliorating the stringency to inject into the separation column at a point where the composition of the feed matches the profile inside of the column.

The water detritiation system and the isotope separation system of the JET tritium plant must be closely integrated. To accomplish this, a second electrolyzer (electrolyzer 2) equipped with a proton exchange polymeric membrane as solid electrolyte serves to decompose tritiated water. The electrolyzer 2 is proposed at this position mainly because it operates with considerably lower tritium inventory than the alkali electrolyte electrolyzer. Once a predetermined tritium inventory has been reached in electrolyzer 1, a fraction of tritium-enriched hydrogen can be fed into the cryogenic distillation for isotope separation. Alternatively, tritiated water may be extracted from electrolyzer 1 for interim storage or subsequent processing. The ultimate aim with the facility is to extract more than 99 % of tritium present in the feed water.

At Tritium Process Laboratory (TPL), JAERI, the applicability of laser Raman spectroscopy in cryogenic hydrogen isotope separation was examined comprehensively aiming at the demonstration of the benefits of this technique for the achievement of the necessary flexibility to deal concurrently with a number of variable gas stream compositions [Ohi96; Iwa02c]. Signals from optical cells were transmitted through optical fibres to a multichannel detection system equipped with a charge-coupled detector (CCD) cooled down to liquid N_2 temperature. The results provided evidence that it is possible to determine simultaneously all six hydrogen isotopes at several positions of a column within a measurement time of only 1 min and with a detection limit of 1000 ppm. Advantageously, several Raman cells could be placed in the vicinity of the desired measuring positions inside of the ISS glove box. The electronic equipment was installed outside of the glove box for easier accessibility and protection from contamination by tritium. Pressures in the Raman cells attached to the measuring points were in the range 10 - 100 kPa and temperatures in the range 283 - 303 K. Evaluation of experimental results allowed determination of the height equivalent of a theoretical plate (HETP) value of the separation column. HETP of the employed TPL column was found to be 5 cm.

Another prospective laboratory scale technology for the extraction of tritium from aqueous waste streams has been developed at Pacific Northwest National Laboratory by Duncan and Nelson [Dun99]. In this case, tritiated water is separated from water utilizing a supported **polyphosphazene membrane** operated under counter current filtration conditions. Experiments were carried out with water containing either 4×10^2 or 1.1×10^5 Bq l^{-1} obtained from a well and a basin at Hanford site. The size of the active area of the membrane was 81 cm^2. A water feed chilled down to 278 K was supplied to the experiment at a pressure maintained

constant within the range 138 - 552 kPa. Best average depletion factors in the permeate fraction, i.e. $< 33\,\%$, were achieved with a feed containing $4 \times 10^2\,\mathrm{Bq\,l^{-1}}$ at pH = 10. The mechanism of separation is still unclear, but does not appear to be based on isotopic exchange.

Glugla et al. [Glu01; Glu02a; Glu07; Glu13], Yoshida et al. [Yos02], and Murdoch et al. [Mur00; Mur05] have discussed in detail the current tritium fuel cycle concept adopted for ITER. According to these authors, detritiation of water will be carried out with a liquid phase catalytic exchange (LPCE) column and a cryogenic isotope separation system. A cascade of four cryogenic distillation columns will deliver isotopically adjusted mixtures for fuelling of the Neutral Beam Injector (NBI) and of the Storage and Delivery System (SDS). Seven equilibrators will restore thermodynamic equilibrium between mixed and homonuclear hydrogen isotopologues via reactions such as

$$2\,\mathrm{DT} \longrightarrow \mathrm{D_2} + \mathrm{T_2}$$

(see also Fig. 3.85 in section 3.18.7.1). A de-tritiated protium stream will be routed via the Water Detritiation System (WDS) to a plant discharge point.

As already pointed out, the inventory-sensitive isotope separation system, with a steady state processing rate of $280\,\mathrm{mol\,hour^{-1}}$, has great impact on optimization and inventory minimization of the overall fuel cycle [Yos02]. Low inventory in the cryogenic distillation system is associated with much improved safety and cost savings because less tritium is tied up in the process.

A heavy water detritiation plant of industrial scale utilizing a **Liquid Phase Catalytic Exchange** (LPCE) process in combination with cryogenic distillation was recently built at Wilson site in Korea [Ahn06; Rod13]. This facility, which started operation 2007, was designed to process 100 kg of D_2O per day while achieving a detritiation factor of 35. The wet-proof noble metal catalyst used for the LPCE process retained its isotope exchange properties even in the presence of liquid water provided the operation temperature was maintained at low values within the range 293 - 333 K.

Recapitulating, the detritiation of water is now well developed and a vast body of germane knowledge and literature is available worldwide. Research on factors that determine process efficiency have reached the point where the design of a process for ITER is considered possible with a high level of reliability.

3.18.9 Modelling of fuel cycle subsystems and their interdependence

A process **simulation code** designed to analyse configuration and performance of large and complex hydrogen isotope separation systems is known under the acronym **FLOSHEET** [Bus88b; Bus88a]. This rather universal code contemplates the interaction of all major components constituting a water detritiation system like i) cryogenic distillation columns, ii) water distillation columns, iii) equilibrators, iv) stream splitters, v) stream mixers, vi) electrolyzers, vii) vapour phase catalytic exchange columns, and viii) recombiners.

One more mathematical model and computer program capable of simulating over a wide range of isotopic compositions the isotope profiles in liquid water, water vapour, and gaseous hydrogen along an LPCE column over a wide range of isotopic compositions, is that developed by **Ovcharov** et al. [Ovc09]. Realistically, this model comprises all key chemical components of a water detritiation process and furthermore takes into account homogeneous bimolecular reactions as well as reactions that occur on the surface of catalysts. To accomplish this, the model includes in the calculation´s diffusion processes taking place in the catalyst pores. Model calculations have been validated by experimental results obtained with heavy water and a 4 m high packed column operated at 315 K.

Concentration profiles in isotope separation columns under variation of diverse parameters can likewise be predicted with the so called **EVIO-4 code** worked out and verified by Alekseev and his co-workers [Ale02].

Primarily to assess the dynamic tritium holdup establishing between various subsystems of the ITER fuel cycle a software carrying the acronym **TRIMO** (TRitium Inventory MOdelling) was developed at TLK by Cristescu et al. [Cri05b]. Contemplated in the software are subsystems such as i) fuelling, ii) vacuum pumping, iii) neutral beam injector, iv) tokamak exhaust processing, v) hydrogen isotope separation, vi) water detritiation, and vii) the storage & delivery system. To increase the accuracy of the software, many of the latest improvements and modifications incorporated by the ITER-Team into the subsystems were integrated into the software. Ongoing experimental determinations of the tritium inventory interdependences between the major components of the TRENTA facility, i.e. the water detritiation system ($1/10^{\text{th}}$ of the WDS of ITER) and the isotope separation system (1/2 of the ISS of ITER), will permit a better

verification of the TRIMO software. Ultimate aim of the work is a data base and a fuel cycle software to support design activities for ITER [Cri07c].

3.18.10 Decontamination of air from tritium employing wet scrubbers

Perevezentsev et al. [Per09] proposed **wet scrubber** columns for the decontamination of air from tritiated water vapour and/or tritiated hydrogen (see Fig. 3.92). The concept is based on isotopic exchange between tritiated water vapour and liquid water in a column packed with commercial CY structured packings[72]. These packing are characterized by high throughput and good mass transfer parameters. The separation column is operated in counter flow and at ambient temperature. When the column is additionally furnished with a catalytic oxidizer it also becomes possible to remove tritiated hydrogen after its oxidation to water at slightly above ambient temperature. As opposed to a drier, which requires periodic regeneration by heating to elevated temperature, the operation of a scrubber is continuous, simple, and does without energy. Another important advantage of wet scrubbers is the comparatively small amount of generated tritiated waste water. Experiments were performed with a test system comprising humidifiers, flow controllers, water buffer tanks, and a dosing pump. From runs with tritiated water employing a wet scrubber column loaded with copper alloy packing and operated with a throughput of $1000\,m^3\,hour^{-1}$ it was concluded that a detritiation factor of the order of 1000 is achievable. It was estimated that this result can be accomplished with a column having a diameter of 0.6 m and a packing height of approx. 5 m. Because wet scrubbers do not need to be regenerated at elevated temperatures, this component has the added advantage that it will probably not be categorized by ITER as a Safety Important Component (SIC).

[72] CY type packing was developed by SULZER especially for separations that require a very large number of theoretical stages.



Figure 3.92: Wet scrubber for the decontamination of air from tritium: a) operation principle and b) gauze CY packing of low pressure drop from SULZER (after [Per09]).

3.18.11 Tritium storage and delivery

Storage and delivery systems installed in medium or large sized tritium handling facilities are usually designed for receiving, delivering, and storing tritium-bearing hydrogen gases. Such systems should additionally be capable of handling gases from i) external tritium supply sources, ii) infrastructure systems like an isotope separation system, a tritium purification system, a tritium accountancy system, an analytical system, etc., and iii) experiments. Basic equipment of these systems encompasses at least one high vacuum pumping system, several calibrated expansion volumes of different sizes designed for accountancy (thermal insulation, high quality surfaces, etc.) or gas mixing purposes, a number of gas re-circulation pumps, numerous and diverse pressure sensors, temperature sensors, flow meters, ionization chambers, etc. Moreover, several diverse and calibrated analytic instruments like radio gas chromatography, mass spectrometry, quadrupole mass spectrometry, laser Raman spectroscopy, infrared spectroscopy, or calorimetry should be available or easily accessible. By design, a storage and delivery system should be in a position of permitting the extraction of decay ^{3}He from getter beds.

Much more challenging are the requirements of the Storage and Delivery System (SDS) under construction for ITER. Major duties and safety requirements of this rather complex system have been discussed by Lässer et al. [Lae02b] and Glugla et al. [Glu07]:

- Supply of the Torus with i) tritium/deuterium mixtures (50 % tritium) or deuterium contaminated with tritium (< 0.6 % tritium) at fuelling flow rates of up to 120 Pa m^3 s^{-1} at pressures of 0.12 MPa employing up to 8 metal hydride beds, ii) 90 % pure tritium mostly to the Pellet Injection with flow rates of 50 Pa m^3 s^{-1} at a pressure of 0.12 MPa employing up to 9 metal hydride beds , and iii) deuterium contaminated with tritium (< 0.02 % tritium) to the Neutral Beam Injection at flow rates of 39 Pa m^3 s^{-1} at a pressure of 0.6 MPa via a large buffer vessel. Three storage bed batteries, each comprising three uranium storage beds, serve for storage and supply of the product gases received from ISS. With these four fractions it is possible to supply all gas mixtures of compositions such as needed for the operation of the ITER machine.

- Develop and fabricate storage beds capable of delivering hydrogen isotopologues at flow rates of up to 120 Pa m^3 s^{-1} depending on duty. Storage beds must be equipped with an evacuable secondary containment which is needed when the bed is heated or used to perform calorimetric measurements. The secondary containment may be filled with a gas during longer periods of unattended tritium storage in order to avoid build up of high core temperatures induced by tritium decay. Flow meters at inlet and outlet of the beds should be designed to permit an estimation of the approximate inventory in the bed from the time-integrated flow rate difference. Storage beds of the SDS shall be furnished with *in situ* calorimetry for in-bed tritium accountancy whenever judged necessary. Each storage bed shall be provided with software and hardware interlocks to deal with temperature and/or pressure excursions. When set values are reached the power to the heaters is switched off. Rupture disks constitute an additional safety measure. In the event of a pressurization, the gas will rupture the disk and expand into an evacuated dedicated reservoir of sufficient capacity. Storage bed batteries must be equipped for periodic recovery of ^{3}He generated by radioactive decay of tritium. By releasing tritium and helium from one bed and recirculating the liberated gases through another bed maintained at ambient temperature, only slightly contaminated helium will eventually remain in the loop. This gas can be pumped off and either be further decontaminated by a Tritium Retention System before release into the environment or be saved for other applications.

- Supply of highly pure gases like He, Ar, N_2, H_2, D_2, and He/O_2 mixtures from two batteries of 12 pressurized cylinders each connected to ring manifolds serving users. One battery is in the supply modus and the other on standby ready for replacement. Each cylinder shall contain up to 1 MPa m^3 of gas. Conventionally, at least the following equipment must be available in the design: i) connections to purge the pipework after replacement of a battery, ii) non-return valves where pertinent to exclude ingress of air, iii) rupture disks for over pressure protection, iv) hot getter beds or a palladium/silver diffuser for ultimate gas purification, and v) pressure regulators.

- Temporary safe storage of up to 1 kg tritium in ten storage beds (max. 0.1 kg/bed) of simple construction in the Long-Term Storage Vault (LTSV). These storage beds need not be equipped for in bed accountancy[73]. Temporary storage will be needed during torus maintenance, tritium recovery from first wall operations, reception of a shipment with tritium resupply, etc.

- Accurate accountancy of the tritium transported in shipping containers to and from the Storage and Delivery System. Measurements will be performed in dedicated, appropriately designed calorimeters. To avoid their contamination the transport vessel will be introduced into a special outer container.

Korea, a potential supplier of tritium for ITER, is currently responsible for the development of the Storage and Delivery System of the ITER project. Within this frame, Cho et al. [Cho11] researched the properties of the zirconium/cobalt-hydrogen system from a technical point of view to assess the applicability of this getter for storage and rapid delivery of tritium at ITER. With a plate type getter bed based on a three-tray configuration the optimization of the heating rate for rapid liberation of tritium was investigated. It was part of the same task to design, manufacture, and test a storage bed mock-up equipped with in-bed calorimetry. One more assignment within the ITER package of the Korean team was the development of a BU type international shipping containe for the safe transport of up to 50 g tritium. A further design requirement, was a bed qualifying for operation with either uranium or zirconium/cobalt as getter materials [Chu08b; Chu08a; Chu11; Chu12b].

[73] The Storage and Delivery Sytem of ITER will presumably be equipped with up to 20 storage beds and a 2 m^3 large storage vessel to handle all hydrogen isotopologues [Glu07].

From the above it is evident that SDS of ITER will necessitate plenty relatively complex peripheral equipment.

3.18.12 Tritium accountancy

Tritium accountancy is a task of fundamental importance. Principal objective is to be in a position of obtaining at all times the most accurate possible knowledge on the total tritium inventory available in a facility. To aid in tracking and reporting of tritium movements and inventories the usual way to proceed is to establish a **material balance area**. Within this frame, it is helpful to develop concurrently to the "normal" documentation for all processes or projects, notably new ones, a process flow diagram detailing type and quantity of tritium flowing into and out of every single step of a process. Radioactive material storage requirements prior and after utilization in a process should likewise be specified in advance. Techniques for measuring and/or sampling of radioactive material during the course of typical process campaigns are to be defined and a reporting scheme for processed and stored tritium be specified at an early stage. All calibration procedures required for the equipment destined to perform accountability-relevant measurements shall be described in advance. If possible, the proposed calibration methods should be traceable to a recognized institution.

Procedures for tritium safeguarding, e.g. access control policy to the material balance area, precautions during long-term storage, bookkeeping strategy, measures to control entrance and exit of materials, components, and personnel to the material balance area shall be defined and appropriately documented.

Accurate accountancy of tritium is indispensable i) from the point of view of safety, ii) for the regulatory body, and iii) for tritium economy reasons. Material control and accountability at fusion machines operating with tritium will be defined by the regulatory body at the place where the machine is operated [Kle15].

A difficult tritium accountancy problem pertains systems operating continuously in which the material to be measured is frequently not long enough stationary for a "**physical inventory taking**" (PIT).

Problems also arise when **Safety Analysis Reports** (SAR) are required for components whose tritium inventory is restricted by an upper limit. While calorimetry is considered to be a

highly sensitive and accurate technique, in many situations it is non-applicable. That is why some crucial components, e.g. tritium storage beds, have been furnished with in situ calorimetry. Sampling from non-homogeneously contaminated solids constitutes another challenge. Hence, accurate inventory determinations are often quite demanding and time consuming.

Most common tritium accountancy procedures are i) calorimetry of samples taken from components or, when this is possible, of entire components, ii) in-bed calorimetry in case of tritium storage beds, iii) scintillation counting of liquids, and iv) volumetric analysis of tritium-bearing gases in combination with analysis of the chemical and isotopic composition of the gas utilizing appropriate analytical techniques.

Significant differences between results obtained by the tritium shipper and receiver cannot be tolerated and must be resolved. The best way to accomplish this, is precise knowledge of the analytical procedures employed by the involved parties and joint comparison of results.

3.18.12.1 Accountancy of gaseous tritium

The total amount of a pure gas or a gas mixture can easily be determined from the pressure in a vessel of accurately known volume when the temperature is known and constant. For the quantification of tritium, a chemical and isotopic analysis of the gas is additionally necessary (**PVT-c procedure**). The employed analytical techniques must be suitable for the qualitative and quantitative determination over a broad range of concentrations of species such as i) helium and other noble gases, ii) all hydrogen isotopes, and iii) all other gaseous impurities like oxygen, nitrogen, carbon oxides, hydrocarbons (also the isotopically substituted ones), etc. Radio gas chromatography or radio micro gas chromatography, mass spectrometry, laser Raman spectroscopy, Omegatron, or their combination are the most frequently employed methods.

When performing volumetric measurements of small activities, the most common problems are: i) tritium trapped in catalysts, adsorbers, or hydride-forming metal particles resistant to thermal release, ii) tritium permeated into structural materials, iii), tritium incorporated chemically into non-volatile organic or inorganic liquids, or into solid compounds, and iv) accurate volumetric determination of the recipient volume. It should be remembered, that the density of tritium in hydrogenic polymeric materials may be quite significant. Of concern is also the effect of temperature causing unadverted thermal decomposition of polymers or hydrides, volatilization of tritium bearing species, etc.

While at first sight calorimetry might be considered an attractive option for the determination of the total tritium content in a gaseous mixture, the energy density of gases at low or medium pressures is in most cases insufficient.

3.18.12.2 Accountancy of tritium retained by adsorbents, catalysts, or storage beds

The majority of the tritium inventory in adsorbents, catalysts, or metal getter storage beds can be determined by total thermal desorption. However, frquently a fraction of this tritium is strongly bound in these materials and resilient to full release. The same holds for tritium-bearing water retained in catalysts or molecular sieve beds [Glu98a]. Hence, the accurate determination of the **tritium heel** in these systems is both challenging and cumbersome requiring special analytical techniques.

Several distinctive techniques have been proposed and demonstrated successfully:

Isotopic exchange:

Ellefson and Gill [Ell86; Gil86] developed an isotope exchange technique which is especially suitable for the determination of tritium in metal getter beds. The first step consists in heating the metal getter bed to an evelated temperature, e.g. 723 K, for several hours and collect the released gas in a large previously evacuated vessel of appropriated and known volume. This gas can be subjected to a volumetric determination as well as to a quantitative analysis of the chemical and isotopic composition. At this stage it may be assumed that most hydrogen isotopologues have been released and only a residual fraction X of tritium (heel) remains strongly bound in the bed. To evaluate this fraction, an accurately known amount of protium, Y mol, is introduced into the bed and after closing the bed the temperature raised to 623 K in order to facilitate isotopic scrambling. After allowing sufficient time for equilibration, the gas is released into an evacuated vessel and an aliquot is taken to determine the isotopic composition by mass spectrometry. For the calculation it is postulated that under bake-off conditions, i.e. 723 K, the released hydrogen isotope mixture has the same isotopic composition (T_1 in mol %) as that remaining in the bed. Subsequently, this procedure is repeated with a new but equal amount of protium as used for the first measurement and a second sample is taken. The amount liberated will again be Y mol and its isotopic composition T_2 in mol %. The amount of hydrogen remaining

in the bed should remain unchanged. The quantity of tritium before and after the exchange is then given by

$$X \cdot T_1 = (X \cdot T_2) + (Y \cdot T_2)$$

and

$$X = \frac{Y \cdot T_2}{T_1 - T_2}$$

where X is the number of hydrogen moles in the getter bed and $X \cdot T_2$ the total residual tritium. Main disadvantages of the dilution technique are the rather time-consuming procedure and the irrevocably altered isotopic composition of the heel. This may be of considerable disadvantage if the storage bed is subsequently used for work with isotopic pure hydrogen isotopes, e.g. D_2 or T_2.

The same technique has also been used to determine the tritium holdup in molecular sieve traps [Ell88a]. According to the method, the trap is integrated into a closed loop, heated up to 700 K while H_2 is recirculated through the trap. Under these conditions the condensable gases are distributed homogeneously throughout the whole adsorber and tritium undergoes exchange with hydrogen until after about 4 hours isotopic equilibrium is established. Repeating the treatment with the same amount of fresh hydrogen yields hydrogen containing a lower concentration of tritium. If the quantities of introduced hydrogen are known and the two concentrations of tritium are obtained by gas analysis, it is possible to estimate the holdup.

^{3}He/^{4}He ratio:

To determine the tritium inventory in an adsorber bed or a hydrogen getter bed all ^{3}He previously generated by tritium decay is removed by filling the bed with ^{4}He and pumping off several times while allowing sufficient time after each filling for equilibration [Car96; Tes05]. Four or more filling/pumping sequences are needed before an accurately known volume of ^{4}He can be introduced into the bed. After waiting for at least one month an aliquot is taken from the supernatant gas and the ^{3}He/^{4}He ratio determined by mass spectrometry. From the data, i.e. amount of ^{3}He generated during the time between the addition of ^{4}He and the determination of the ^{3}He/^{4}He ratio, it is possible to calculate the amount of residual tritium present in the bed[74]. Principal drawback of this approach is the long time needed for a result.

Direct sampling:

[74] 1 mol of gaseous T_2 generates 0.010 75 mol of ^{3}He in 35 days.

For the determination of adsorbed tritiated water preferably a large sample or - when possible - the complete adsorber bed is dropped into a known amount of water kept in a closed vessel. After allowing sufficient time for equilibration between adsorbed tritated water and liquid water (the equilibration time can be reduced by raising the temperature and shaking or stirring), a water aliquot is taken and the tritium content analysed by liquid scintillation counting. To make certain that equilibration has established, several samples of the supernatant water are taken in sufficiently long intervals. From the results the total tritium content in the adsorber can be calculated. This approach has two drawbacks: on one hand it is necessary to open the bed to grab a sample, which may be associated with contamination spread, and on the other the sample (particularly if small) is considerably modified. What is more, when sampling is carried out, accurate results can only be obtained if the tritium is homogeneously distributed in the bed, which frequently is not the case. Highest accuracy is achieved when the whole adsorber is subjected to analysis.

Controlled regeneration:

According to this procedure the adsorber bed is heated at constant temperature while purging with a noble gas. The exhaust gas is first passed across a heated magnesium bed and the isotopic composition of the resulting molecular hydrogen mixture analysed by mass spectrometry or another technique [Gil86]. The water loading of the molecular sieve bed is estimated from the temperature of regeneration, the dew point of the purge gas, and adsorption isotherm data obtained from the literature.

Bake-off profile:

Ellefson et al. [Ell88a] provided evidence that the tritium inventory in a uranium storage bed can be determined from a bake-off profile. To obtain such a profile hydrogen gas released from a U-bed at $> 800\,\mathrm{K}$ was collected with a magnetically coupled leak-tight vane pump[75] [Cap85] and measured volumetrically as function of numerous equal constant time intervals. A vane pump is recommended instead of a scroll pump because the former is capable of pumping in the low vacuum range (achievable vacuum $1.3 \times 10^{-2}\,\mathrm{mbar}$). An average flow rate is obtained from the difference of successive PVT-values divided by the time interval of collection. Fig. 3.93 shows a) the typical monotonic decrease in hydrogen flow rate while the bed is being pumped off and b) the accumulated moles of released molecular hydrogen as function of elapsed time. The bake-off

[75] Replaces the well-known glass Toepler pump which employs mercury for gas transport and compression.

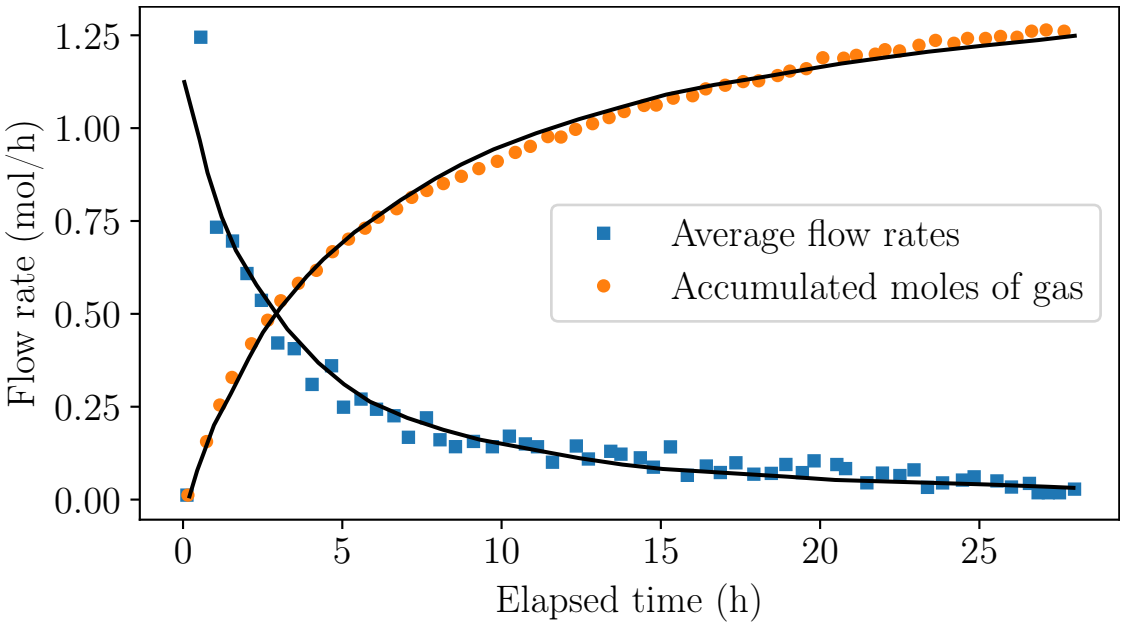


Figure 3.93: Uranium bed bake-off profile taken in 30 min intervals. The plots display experimentally obtained average hydrogen flow rates (■) in mol hour^{-1} and accumulated moles of released hydrogen (•) as function of sampling time. Solid lines are theoretical predictions obtained from fitting eqn. for $Q(t)$ given in the text. Values of the obtained fitting constants are $Q_0 = 0.19$ and $A = 0.19$ (after [Ell88a]).

end point was considered to be attained when the isotope hydrogen flow rate becomes lower than 0.02 mol hour^{-1}. As apparent, this is the case after pumping for approx. 24 hours. However, the holdup, defined as the tritium remaining in the system after a normal inventory measurement has been completed, can already be predicted after a 0.1 mol hour^{-1} flow rate is reached. To this effect the flow rate is integrated from the time at which the bake-off is stopped up to infinity.

The rate of removal, which is controlled by the viscous flow of the gas through the pumping line (Poiseuille equation), is obtained from equation

$$Q(t) = \frac{Q_0}{(At+1)^2}$$

where Q_0 is the initial flow rate, A a proportionality constant and t the time. By determining the rates at which a certain number of hydrogen moles are released in each time interval a release

curve is obtained from which Q_0 and A can be determined using a fitting procedure. With Q_0, A, and $t - \mathrm{f}$ it becomes possible to calculate the hydrogen hold-up N_{holdup} using equation

$$N_{\mathrm{holdup}} = Q_0 \int_{t_\mathrm{f}}^{\mathrm{inf}} \frac{\mathrm{d}t}{(A \cdot t + 1)^2} = \frac{Q_0}{A(At_\mathrm{f} + 1)}$$

where t_f is the time at which bake-off is stopped.

Typical holdup values in a 45 mol (270 gram) tritium capacity uranium getter bed was found to be (0.13 ± 0.09) mol tritium, i.e. 0.8 g. For this uranium storage bed, the uncertainty of the prediction was estimated to be < 1 g for pure T_2.

Calorimetry:

Calorimetry is a highly accurate, non-destructive technique capable of determining the total amount of tritium present in a transportable bed. For a measurement, the entire getter bed must be introduced into the sample chamber of the calorimeter. In case the outer surface of the bed is contaminated by tritium the getter bed must be introduced first into a second protective confinement in order to prevent pollution of the calorimeter. Because the sample chamber of most calorimeters is too small to accommodate a regular getter bed, so called in-bed calorimetry has been developed. With this technique a determination is possible inside of a glove box without necessity of bed connections/disconnections or bed transportation. Additionally, possible contamination of the glove box atmosphere when an unconfined transportable bed is externally heated to release tritium is precluded (for additional detailed information on the technique itself refer to sections 3.14.2.4 and 3.17.11).

A fundamental advantage of calorimetry is that the inventory of tritium is determined irrespective of the chemical form or state of aggregation in which this radionuclide is present in the sample. Hence, all gaseous, liquid, or solid species contaminated by tritium either chemically or via some physical process are detected. Materials like high molecular weight polymers, organic/inorganic gaskets, adsorbers, catalysts, structural materials, etc. that have incorporated tritium by permeation, isotopic exchange, or chemical reaction are all registered regardless of whether tritium is distributed in the sample homogeneously or non-homogeneously. Another great plus of calorimetry is that measurements can be carried out without sample destruction provided the sample fits into the sample holder of the calorimeter. Conversely, it is necessary to be aware that chemical reactions, physicochemical processes, e.g. adsorption/desorption

processes, phase transformations, vaporizations/condensations, etc. when associated with heat absorption or liberation, can influence the measurement - eventually in quite substantial way – when small activities are being measured. The presence of extraneous radiation sources may also constitute a source of error.

To obtain reliable measurements the rooms housing sensitive calorimeters must be maintained at fairly constant temperature, i.e. at values fluctuating no more than 3 K.

3.18.12.3 Empirical estimation of the contamination of stainless-steel by tritium

The amount of tritium incorporated into stainless-steel is often needed during decommissioning or subsequent waste disposal. A rough estimation procedure of the tritium inventory accumulated in austenitic steel after contact with gaseous tritium at 298 K has been put forward by Willms [Wil05]. According to this investigator the tritium inventory, I, can be calculated from the empirical relationship

$$I = \sqrt{503 p_{T_2} t}\exp(-0.0143t)$$

where I is given in Ci m^{-2}, t in year, and p_{T_2} in atm. In this equation the square root term accounts for the diffusion of tritium through stainless-steel and the exponential term for radioactive decay. The equation is valid within the time range $0 < t < 36$ years and pressures within the range $0.01 < p_{T_2} < 3$ atm. The model is applicable to materials exposed intermittently to tritium but not at temperatures above ambient.

4 Containment and confinement principles

Physical structures designed to prevent or control the release and dispersion of radioactive substances are defined as **containments**. Primary containment systems (**primary barrier**) consist of tanks, vessels, pumps, piping, valves, vessels and all instrumentation that is or may come in direct contact with tritium.

Confinements prevent or control releases of radioactive materials into the environment during normal operation or in case of accidents. Primary confinement barriers are mechanical systems that surround primary/secondary containments confining possible leaks or releases to the secondary confinement (building). They are designed to minimize exposures of workers to tritium. Primary confinements such as glove boxes, caissons, dedicated vessels or vacuum/gas jackets, are mandatory when significant quantities of tritium are handled particularly at temperatures above ambient. Tritium should be monitored continuously in confinements and when released from containments in the containment exhaust gas. Release into the environment should take place via an adequately sized Tritium Retention System and ideally through a stack.

When handling very small quantities of tritium hoods may be acceptable. In such a case, air should flow from areas of low to areas of higher contamination. Fume hoods use relatively high-volume rates compared to normal ventilation systems. Local ventilation contributes to the removal of airborne tritium regardless of its chemical or physical release form.

At **TSTA, Los Alamos**, all confinements were designed to contain dry nitrogen at local ambient pressure under static conditions [And82]. They were instrumented to monitor tritium in the range 3.7×10^5 - $3.7 \times 10^{10}\,\mathrm{Bq\,m^{-3}}$, oxygen in the range 0.5 - 5 % and differential pressures with respect to ambient (laboratory room atmosphere) within the range $\pm$ 500 Pa. Two fixed set point differential pressure switches (one positive and one negative) controlled the nitrogen exhaust valve (at action set point + 125 Pa the exhaust valve was opened) and supply valve (at set point - 125 Pa the nitrogen supply valve was opened) to maintain the glove box pressure

within limits. The alarm set point was set at 500 Pa. Overpressures in excess of 2 kPa were relieved by an oil bubbler system. With glove ports and bubbler port sealed, each glove box was helium leak tight to 3×10^{-9} Pa m^3 s^{-1} when internally pressurized to 2 kPa. Areas at TSTA from which tritium was excluded (zone I) were maintained at a slightly positive pressure of 0.3 mbar to minimize access of contaminated atmosphere or infiltration of dust. Areas were tritium was handled (zone II) were maintained at a slightly negative pressure of 0.3 mbar with respect to atmospheric pressure in order to minimize diffusion of tritium into the environment.

As in other tritium-handling laboratories at **TPL, Tokai-mura**, the tritium-confining glove boxes are not all equally dimensioned. They are equipped with polymetaacrylate windows, plastic glove ports and butyl neoprene rubber gloves. Similar to TSTA, glove boxes were designed to contain a nitrogen atmosphere maintained at pressures within the range ± 400 Pa with respect to that of the laboratory room by supplying nitrogen gas or pumping a small fraction of the glove box atmosphere [Nar90]. The glove box pressure control can operate individual glove boxes or groups of glove boxes simultaneously. The pressure of the air-tight laboratory is maintained at - 150 Pa below ambient pressure; the air change rate under normal conditions is maintained at 3 times hour^{-1}. Effluent gases from nitrogen glove boxes are oxidized with a catalytic oxidizer and the generated tritiated water adsorbed on an adsorber bed.

Primary confinements at **TLK, Karlsruhe** are operated either with nitrogen or with air depending on the type of experimental activity performed in the glove box. Pressures in the confinements are maintained below ambient within the range −400 - −700 Pa by a negative pressure control system. The oxygen partial pressure in nitrogen glove boxes is regulated within the range 0.5 - 1 % [Tri91; Sch91a; Bes08] (residual oxygen is needed for the effective oxidation of tritium-bearing hydrogen isotopes and hydrocarbons into water and carbon oxides). Tritium in confinements is monitored with ionisation chambers within the concentration range 5×10^5 - 5×10^{11} Bq m^{-3}. The leak rate of confinements must be smaller than 0.1 vol%h^{-1}.

The **Safety and Tritium Applied Research** facility (STAR), Idaho, with a tritium inventory limit of 1.64 g provides capability for conducting bench scale experiments as well as engineering scale tests with tritium also on hazardous materials like beryllium or molten fluoride salts [And02]. A negative pressure in the building with respect to that prevailing outside is maintained with blowers which permit at least 6 air changes hour^{-1} of once-through-air. Glove boxes are purged with dry nitrogen. Each tritium glove box is connected to a central tritium

clean up system via an overhead header. The glove box atmosphere is only routed to the tritium clean-up system when tritium concentrations in the glove box exceed a set point. When the glove box atmosphere stays below the tritium concentration set point the effluent gas is routed directly to the laboratory exhaust duct.

Besides classical confinements, there are some multipurpose special confinements like the huge **cryostat** of **ITER**. This colossal confinement surrounds the entire tokamak machine. With a diameter of approximately 30 m it will be the largest stainless-steel container ever built. Its main purpose is to provide the high vacuum and ultra-cool environment necessary for the operation of the superconducting magnets. To prevent cold zones comprising the superconducting magnets and sections of the structure attaining temperatures as low as about 4.5 K from receiving heat coming from less cool zones, numerous thermal shields held at 80 K will be installed inside of the cryostat. On top of its purely technical function, the cryostat also prevents formation of ice on cold structures. This is important to preclude generation of ozone expected when radiation from the plasma interacts with molecular oxygen condensed on the wall of the cryostat[1].

The cryostat has the following additional safety functions:

- primary confinement barrier during maintenance operations on the vacuum chamber,
- secondary confinement barrier for radioactive materials and hazardous materials possibly released from the vacuum vessel or the primary heat transfer system loops and
- secondary confinement for the separation of air from hydrogen isotopologues in the vacuum vessel.

Recapitulating, **pressure zoning** gives the assurance that tritium leaking from a primary system or a confinement will be transported from areas of lesser potential contamination to areas of greater potential of contamination where it can be monitored and retained. A basic requirement for buildings serving as secondary confinement barrier are tight doors and windows (if existing) as well as tightness of all other wall perforations of the building which house tritium handling equipment. Doors which act as pressure barriers should not be upheld open and penetrations should be regularly checked for proper sealing.

[1] Rizzello et al. [Riz96] examined possible routes leading to the formation of ozone and conditions eventually conducting to ozone explosions. While structural damage to the cryostat by ozone explosions was largely discarded, damage to the superconducting coils appeared conceivable.

In general, higher pressure differences shall be maintained in rooms in which the highest contamination by tritium is conceivable. Before sending off gases contaminated by tritium to stack the tritium must be removed.

4.1 Primary containment systems

Main function of primary containment systems enclosing tritium-bearing gases or gases contaminated by tritium is to keep this radioactive gas away from the environment. To accomplish extremely low leak rates for hydrogen isotopes standard ultrahigh vacuum stainless-steel components shall be used throughout. Employment of standard ultra-high vacuum components guarantees reliable component properties, simplifies considerably maintenance and equipment modifications, and minimizes stock-keeping.

4.1.1 Integral leak rates of primary containment

Integration over all partial leak rates of a system constitutes the integral leak rate. At **TLK** the integral helium leak rate shall not exceed 10^{-8} for primary tritium handling systems and that of single components shall be lower than $10^{-9}\,\mathrm{mbar\,l\,s^{-1}}$ [Tri91; Bes08]. Leak rates at the seat of valves must be lower than $10^{-7}\,\mathrm{mbar\,l\,s^{-1}}$.

Within the frame of inactive commissioning, all subsystems of the Active Gas Handling System of JET were leak tested employing a helium leak detector and found to display overall leaks of not more than $10^{-8}\,\mathrm{mbar\,l\,s^{-1}}$ range [Lae95; Lae99b][2]. All **JET** subsystems have been operated successfully partly with substantial amounts of tritium over extensive periods of time, without noteworthy contingencies. This fact is attributed to the persistent leak tightness of utilized commercial ultrahigh vacuum tight components. Similar observations were made in other tritium-handling facilities.

It should be kept in mind that after commissioning with helium and deuterium it is no longer possible for quite some time to determine leak rates lower than $10^{-7}\,\mathrm{mbar\,l\,s^{-1}}$ using a mass spectrometer and helium or deuterium as test gas because of significant interference by the background peak $m/e = 4$ (deuterium).

4.1.2 Transfer of hydrogen isotopologues or other gases within primary systems inside of a glove box

Transfers of hydrogen isotopologues or of other gases within a primary system or into another primary system installed in another glove box can be carried out by one the following procedures:

[2] $1\,\mathrm{mbar\,l\,s^{-1}} = 10\,\mathrm{Pa\,m^3\,s^{-1}}$.

- Pure hydrogen isotopes can be transferred from a heated getter bed installed in a primary system into a previously evacuated vessel of the same primary system by gas expansion or utilizing a pump or pump combination. Hydrogen isotopologues remaining in transfer lines of the providing vessel can be fully retrieved into the providing getter bed cooled to ambient temperature. The amount of hydrogen isotopologues received can be determined by PVT-c procedures.

- Pure hydrogen isotopes can be transferred from a heated getter bed of one primary system into the getter bed of another primary system maintained at ambient temperature. If the receiving getter bed is installed inside of another glove box than that of the providing getter bed a gas jacketed transfer line between the glove boxes is necessary. Disadvantage of this procedure is that the amount of gas transferred can only be obtained approximately from integration of the mass flow rates over the period of transfer.

- Transfer of gases from one vessel of a primary system into another previously evacuated vessel of the same primary system by direct gas expansion or with support of a single or a combination of pumps. Gas remaining in lines must be evacuated and discharged or be retrieved by reaction with a getter.

- Transfer of hydrogen isotopes or other gases can also be carried out employing a transportable vessel (getter vessel in case of tritium) attached to an evacuable line equipped with a pressure sensor and a vacuum sensor. The receiving primary system must be similarly equipped. The amount of gas transferred can be obtained from a comparison of calorimetric measurements performed before and after the transfer.

4.1.3 Supply of gases to primary systems

4.1.3.1 Inert and reagent gases

Inert gases, standard gas mixtures, or reagent gases are normally supplied to primary systems from pressurized cylinders placed in the vicinity of the glove box housing the primary system.

A few general comments:

- Conventional safety requires that all gas cylinders be properly **secured to a solid surface**.

- Pressurized cylinders containing **poisonous or explosive gases** should be accommodated in **ventilated safety cabinets** located adjacent to the glove box (see Fig. 4.7). Leaks from cylinders containing combustible gases must be meticulously avoided (control of connections, pressure reducer, etc. with a soap solution).

- Pressurized gas cylinders containing **liquid carbon dioxide** should not be used in horizontal position.

- Pressurized gas cylinders containing **oxygen** should be kept away from oil or grease (danger of fire).

- Pressurized gas cylinders should not be exposed to sun light.

- Gas bottles may be connected to a primary containment via a valve matrix from which any single bottle has access to a transfer or a vacuum line.

- Gases can be supplied directly to primary systems from **small pressurized gas cylinders** equipped with a reducing valve and mounted inside of glove boxes (without reducing valve danger of pressurization of the primary system!). A securer option is the utilization of small transportable vessels containing a known amount of gas of defined composition that fits into the pass box of the glove box. In this case, gas introduction into the primary containment takes place via an equipped sample port either into an evacuated vessel or a getter bed maintained at ambient temperature. The supplied amount of gas can be calculated from a foregoing volumetric determination.

- Combustible gases **heavier than air**, e.g. propane, may concentrate on the bottom of the glove box and constitute a source of much danger.

In case of tritium facilities requiring considerable quantities of diverse gases the installation of a well ventilated, centralized gas supply system outside of the building constitutes the most frequently implemented solution. Good accessibility of this external gas cylinder housing by the vehicles transporting the gas cylinders is of great importance for uncomplicated cylinder supply and replacement. Protection of cylinders and adjacent equipment from the elements, e.g. wind, rain, sun, etc. is important. Furthermore, sufficient and appropriate safety measures should be

taken to make certain that tritium from primary systems in the tritium facility does not find its way into the gas supply system installed outside of the building.

At ITER bundles of twelve pressurized cylinders will be employed for the supply of helium. When the gas inventory in the bundle decreases below a certain level the supply valve of the empty bundle is closed and a new full bundle is connected by opening the corresponding valve. While the new bundle begins to be used the empty one is replaced. The air in the connecting pipe work of the new bundle is flushed via a manual operation. Rupture disks protect pipe work and pressure-sensitive equipment from overpressure. **Non-return valves** prevent backstreaming of gases and contamination by tritium of the pipe work located upstream. Valves open only if the pressure in the upstream side is higher by a certain value than the pressure on the downstream side. This procedure minimizes contamination of the pipe work installed on the upstream side.

In case of tritium facilities requiring considerable quantities of diverse gases, the installation of a well ventilated, centralized gas supply system outside of the building constitutes the most frequently utilized solution. Good accessibility of this external gas cylinder housing by the vehicles transporting the gas cylinders is of great importance for uncomplicated cylinder supply and replacement. Protection of the cylinders and and adjacent equipment from the elements, e.g. wind, rain, sun, earthquakes, etc. is important. Furthermore, sufficient and appropriate safety measures should be taken to make certain that tritium from primary systems in the tritium facility does not find its way into the gas supply system installed outside of the building.

4.1.3.2 Supply of gaseous tritium

4.1.3.2.1 Supply of small inventories

Storage beds from GE Healthcare (formerly Amersham), containing approx. 100 g of depleted uranium powder have been utilized successfully in the past for the international transport of smaller amounts of tritium [Khe85; Pen97a; Lae99b; Gal05]. These beds have a nominal storage capacity for tritium of 1350 TBq in form of solid uranium tritide. Other Amersham beds like type MkIII are licensed for up to 2 PBq of tritium; they contain 100 g of depleted uranium. Beds type MkIV or MkV are licensed for 4 PBq of tritium and contain 320 g of depleted uranium

[Gal05]. Amersham beds have a design temperature of 723 K and a design pressure of 4 MPa. These design values are based on a fully loaded bed stored for up to 12 months.

Fig. 4.1 illustrates the transport strategy of GE Healthcare storage beds: a pot containing uranium tritide is packed in a vacuum-tight stainless-steel canister with an O-ring sealed lid which in turn is placed into a cork spacer fitting tightly into a galvanized stainless-steel shipping drum. After the tritium receiver has confirmed the tritium inventory declared by the tritium shipper, the tritide bed is ready for tritium acceptance by the receiver. All administrative steps and performed analyses need to be fully documented.

Before tritium is released from the transportable bed, it is first necessary to evacuate the bed at ambient temperature to remove decay helium. To accomplish this, the bed is attached to a suitable primary tritium system at a position which must be equipped with a vacuum and a pressure sensor and be connected to a high vacuum pumping system. After evacuation of all pertinent lines, leak tightness of the connection must first be verified. This is accomplished by closing the involved primary system section and controlling the persistence of good vacuum over a suitable length of time. Once leak-tightness has been confirmed, the valve to the storage bed can be opened and the bed be evacuated. Uranium tritide in the bed is subsequently decomposed thermally using a thermostated band-heater with which the bed temperature is progressively raised up to 623 K. Because of the rapid thermal decomposition of the tritide it is possible to control the liberation rate by regulating the bed heating rate. As a safety precaution against potential overheating, the heater wattage is selected to be self-limiting at a nominal unloading temperature of 623 K. Experimental evidence indicates that almost complete release of tritium is possible in about 45 min at 600 K or in about 30 min at 623 K.

Because GE Healthcare beds possess no vacuum insulation tritium will permeate into the confinement during the heating process causing a clearly detectable contamination of the glove box [Pen97a; Lae99b]. When the transport bed contains isotopically pure tritium, concentrations in a 5 m^3 glove box in the hundred MBq m^{-3} range can be expected. Additionally, the outside surface of the bed will become fairly contaminated. Therefore, appropriate precautions need be taken when removing the bed from the glove box. GE Healthcare beds can be conveniently used for accountancy purposes simply by comparing calorimetrically the amount of tritium present in the vessel before supply with that after the supply has been completed. Moreover, a calorimetric determination of the released amount can be verified by a volumetric pVT-c

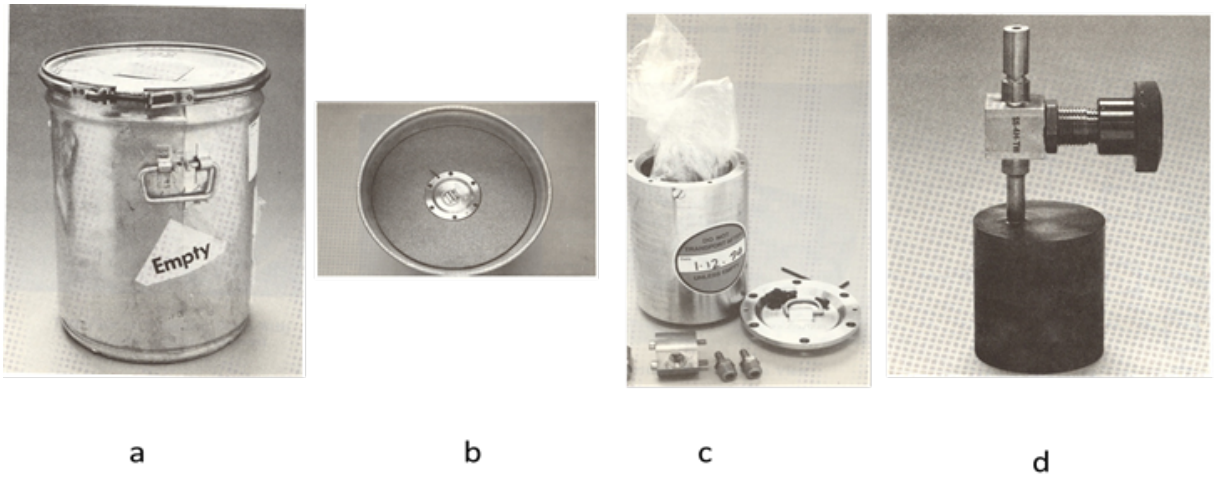


Figure 4.1: GE Healthcare tritium transport concept. Figure a) shows the stainless-steel shipping drum, figure b) the top view into the drum with the steel canister in a cork spacer, figure c) displays the opened stainless-steel canister and the tritium pot in a plastic bag and figure d) the actual tritium pot with a NUPRO 8 BK valve (after [Khe85]).

measurement performed within the receiving primary system. Because of the contaminated outer surface, the bed must be introduced into a protective vessel before placing it inside of the calorimeter. Without this preventive measure, the calorimeter may become appreciably contaminated.

A GE Healthcare uranium bed maintained at ambient temperature can also be used for the transportation of tritium from one primary system to another destination. If the receiving system comprises a getter bed and a substantial fraction of helium-3 is present in the donated tritium the tritiding reaction with the receiving getter will progressively become slower because of the so called “blanketing effect”. This effect becomes apparent when noble gas accumulates gradually in the zone adjacent to the getter where it acts as a diffusion barrier. The problem can be solved with a uranium getter bed designed for gas recirculation. To this effect, a pot of analogous configuration to the ones manufactured by GE Healthcare but furnished with two ports that can be closed manually with NUPRO 8 BK valves was manufactured at the TLK workshops. VCR couplings at the end of the two valves served to join the vessel to the tritium providing primary system or gas recirculating loop. 160 g of depleted uranium metal were introduced into the new pot and converted into powder by a number of hydriding/dehydriding cycles. The outside dimensions of this tritide bed were such that it comfortably fitted into TLK´s most

sensitive calorimeter. To avoid spreading of fine uranium powder into the contiguous primary system, filters of less than 10 µm porosity were mounted at inlet and outlet of the bed. With the modified pot it was possible to supply and retrieve tritium both quickly and quantitatively between primary systems of TLK [Bes02a].

Another tritium supply option to primary systems is the direct delivery from a **Central Tritium Transfer System** such as that of TLK using fixed gas jacketed UHV-tight stainless-steel lines. This procedure was adopted at TLK [Sch91a]. Three thermally carefully insulated vessels with volumes of 1, 15, and 100 l, respectively, are available at the receiving/delivering Tritium Transfer System for accountancy and gas mixing purposes. Tritium is supplied from one of five getter beds (four containing depleated uranium and one zirconium cobalt) installed in an immediately adjacent Tritium Storage System. Prior to a transfer, the lines and the receiving vessel are evacuated by pumps belonging to the receiving primary system (fetch principle). Upon completion of a successful leak test, the transfer can be carried out. Gas remaining in the transfer line must be directly retrieved into a storage bed or into a vessel of the receiving primary system with the assistance of pumps. In case tritium is returned from a primary system to the Tritium Transfer System, the gas is first subjected to an accountancy procedure, that may include a chemical analysis. If necessary, an isotope separation must be performed before the gas is finally forwarded to the Tritium Storage System.

4.1.3.2.2 Supply of intermediate inventories on mostly national routes

Facilities necessitating significant amounts of tritium have employed empty vessels for the transport of gaseous tritium. Westinghouse Savannah River Company (WSRC) for intance, designed a **Product Vessel** (PV)[3] with a volume of 21 l for the transport of up to 10 g (1.67 mol) gaseous tritium at pressures not higher than 1.6 bar [US 73]. The PV is equipped with a single NUPRO® SS-4HS-TW valve, has a body of type SS316 stainless-steel, and is closed with a male Cajon® SS-4-VCR-4 nut and a Cajon® SS-4-VCR-CP cap. The Product Vessel is conceived for utilization together with the UC-609 shipping package (see below).

[3] The PV vessel is designed to meet the requirements of the ASME Boiler and Pressure Vessel Code, Section VIII, Division 1, 1991 Addenda, Lethal Service, Full Vacuum to 8.5 psig (1200 torr) at 77 °F. Although the PV is designed to meet ASME code requirements it is not ASME code stamped.

Type **LP50 containers** (50 l, 1600 mbar [Gru88]) have regularly been used in the USA for shipments of molecular tritium outside of the WRSC site. For instance, Tokamak Fusion Test Reactor (TFTR) was supplied with tritium using this type of container. The LP50 is equipped with a stainless-steel valve and transported in an aluminium outer container that is also provided with a valve that serves for leak inspection. The container fits into a cemented ring of Celotex insulation moulded into a 55-gallon drum. Celotex functions not only as a shock absorber but also as heat resistant material to protect the primary transport vessel from overheating in case of fire. Currently, LP50 containers are no longer in service [Wer96; US 73].

For the shipment of tritium as uranium tritide a **Hydride Transport Vessel** (HTV) was also developed at Westinghouse Savannah River Company (WSRC) [Heu95c; US 73]. This vessel can accept up to 18 g tritium (3 mol) after reaction with 0.5 kg depleted uranium. The HTV body is formed by two welded stainless-steel type 374H pipe caps, it has a volume of 0.69 l, and is equipped with two ports each provided with a NUPRO® SS-4HS-TW valve. To prevent spreading of uranium powder, porous stainless-steel filters of 2 µm pore size are welded at inlet and outlet of seamless tubes which are themselves welded on the vessel. Tubings between valve and vessel are kept long to reduce the heat burden to the valves. As a further safety measure, the unloading temperature of the bed is limited by design to 723 K at a maximum unloading pressure of 2×10^4 Pa. To accept tritium, the receiver site must possess appropriate furnace capability.

Design requirements for shipping packages of radioactive materials are specified in packaging and transportation regulations such as 10 CFR 71.43 and 49 CFR 173.410. Among several types of shipping packages, the following are used for the transport of tritium [US 15]:

- **Type A** shipping packages are limited to the transport of gaseous or solid quantities of less than ($< 3.7 \times 10^{13}$ Bq)[US 15] tritium. Packages meeting the shipping criteria are designed by commercial manufacturers.

- **Type B** UC-609 shipping packages for tritium as gas (PV) or uranium tritide (HTV) provide the highest level of safety features of all types of radioactive material packaging. The contents are limited by the requirements of the Certificate of Compliance (CoC) for the package. Transport is possible with other than radioactive cargo either by highway, rail, water, or air. A Type B UC-609 package is limited to 150 g of gaseous or solid tritium.

Caution is advised when shipping an „emptied“ HTV because the residual heel may amount to more than 4×10^{13} Bq, which constitutes the upper limit for a type A shipment. Therefore, an „empty“ HTV still contaminated by residual heel might require a type B shipment.

In addition to terminal caps on valve ends the use of secondary containment type isolation valves is recommended for portable tritium containers [Wea94].

Supplementary information on the international transport of i) large inventories of tritium, ii) tritium-contaminated components, and iii) tritium-bearing waste is given in section 8.6 and reference [US 15].

4.1.4 Pumping systems

Pumps or pump combinations are needed in tritium handling systems for i) evacuation, ii) gas re-circulation, or iii) gas compression.

4.1.4.1 Vacuum pumping systems

The performance of individual pumps qualified for operation with tritium has been discussed in some detail in section 3.14.1. In this section the experience gained with a few pumping systems tested in small, medium, and large tritium facilities will be briefly discussed.

At **TLK** each major experiment and infrastructure system is serviced by its own high vacuum pumping system [Sch91a]. This approach confers high operational independence to the various subsystems and increases the overall availability of the laboratory. Oil-free high vacuum turbo molecular pumps (TMP) with magnetically suspended rotors are mounted in glove boxes and operated in combination with different single or combination of fore pumps. Standard evacuation is performed with TMPs of $56\,l_{N_2}/s$ or $45\,l_{H_2}/s$ suction capacity. When large volumina need to be evacuated TMPs of $200\,l_{N_2}/s$ or $180\,l_{H_2}/s$ suction capacity have been selected. Typical installed fore vacuum pumps were type NORMETEX (15 - 150 $m^3\,hour^{-1}$), Drystar (52 $m^3\,hour^{-1}$), Metal Bellows (0.3 - 7.8 $m^3\,hour^{-1}$), Siemens (7 $m^3\,hour^{-1}$), or SRTI (52 $m^3\,hour^{-1}$). Vacua achieved in conventional tritium-handling systems and within a reasonable period of time are generally not much better than 10^{-5} mbar. This is ascribed to the small conductance of pipes, valves, and of other components. A significant improvement of vacua is achieved by prolonged pumping and extensive bake out either with a heating mantle or permanently mounted resistance heaters.

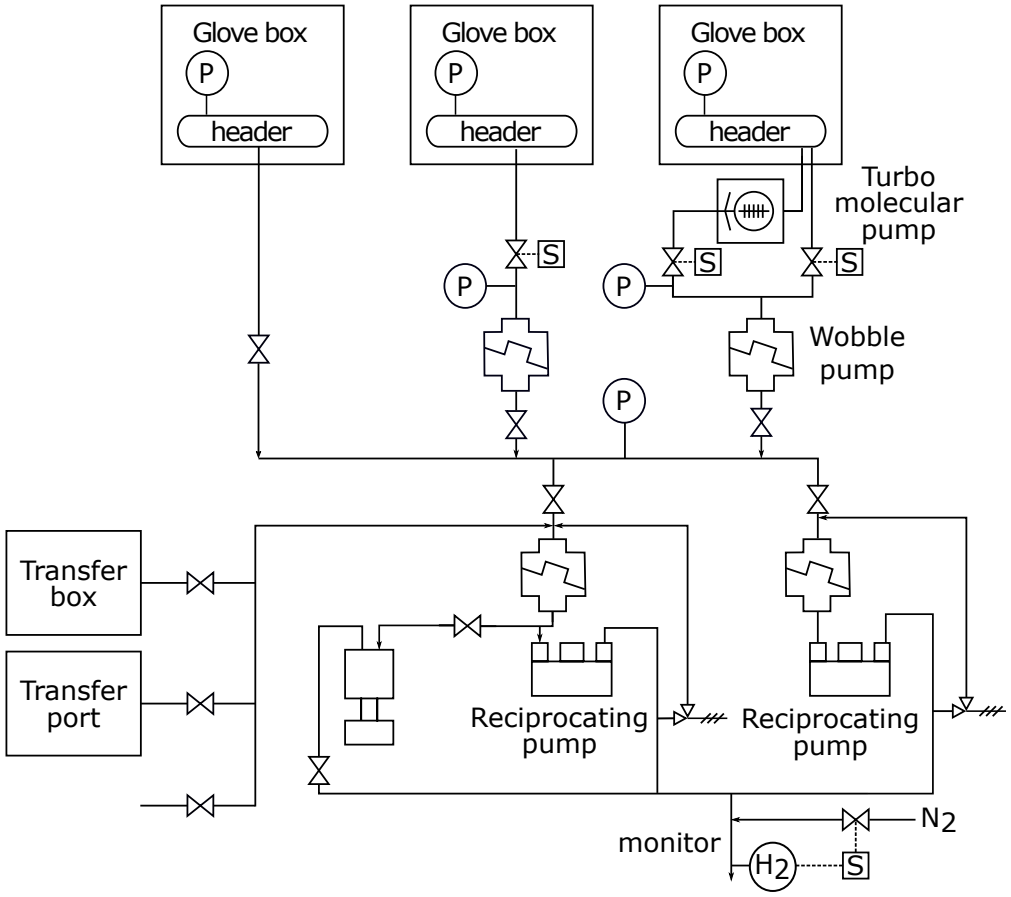


Figure 4.2: Configuration of the multi-purpose central pumping system of TPL (after [Nar90]).

An ingenuous centralized vacuum system for the evacuation of several primary subsystems as well as of transfer boxes and transfer ports was implemented at **TPL** [Nar87; Nar90]. Oil-free high vacuum pumps and oil-free fore vacuum pumps were mostly installed in hoods placed under the glove boxes. The system comprised magnetic bearing turbomolecular pumps backed by a flexible combination of secondary and tertiary wobble/piston pumps (French SRTI type PBT pumps) as well as double metal bellows reciprocating pumps (Japanese Toyo Engineering Co) (see also section 3.14.1.14). The selected pump combination was such that different quality of vacua could be generated for pass boxes and for primary systems in various glove boxes. Hence, the specific needs of each research or infrastructure activity could be satisfied by selecting the best combination and sequence of pumps (see Fig. 4.2). Drawbacks of this concept are that malfunction of the pumping system impacts on all activities and cross contaminations cannot be excluded.

In anticipation of the needs of future fusion devices, the Vacuum Facility erected at **TSTA** was equipped already during the early Eighties with three different compound cryo-pumps [Cof79; Bat81; And82; Wal90; Sed89; Sed91] capable of achieving pumping speeds of up to approx. $16\,m^3\,s^{-1}$ of DT. The cryo-pumps were connected to a torus mock-up via a 0.4 m exhaust duct and a gate valve [Wal90]; they served not only for evacuation of experimental and infrastructure systems of TSTA but also for research and development purposes of cryo-pumps meeting the requirements for the evacuation of fusion devices. The pumps were operated in batch mode, i.e. one in operation, one in regeneration, and another one on standby. Regeneration was accomplished with a pump combination consisting of a turbo molecular high vacuum pump together with an all-metal rotary scroll and a metal bellows pump. At the time, i.e. before the advent of magnetic bearing turbo molecular pumps, an important advantage of cryo-pumps was that in tritium service the cumbersome and regular replacement of tritium-contaminated lubricants could be circumvented.

Turbo molecular pumps installed and operated at the Tritium Storage and Delivery System of **TFTR** in Princeton during the early Nineties were supplied by Leybold Heraeus [Sis94]. These turbo molecular pumps, i.e. type TG-TP601/602 and TGVZ-501/502 with pumping speeds in the hundred $l\,s^{-1}$ range, were water cooled. The rotor bearings of these pumps were lubricated with grease which had to be replaced on a yearly basis. The turbo pumps were backed by mechanical sliding vane type vacuum pumps manufactured by Sergeant-Welch, whose pumping speed was of the order of $2.7\,l\,s^{-1}$. They were adapted to tritium service by replacing the original seals with glass-filled Teflon seals. In addition, original pump belt drives were substituted by electric motors directly coupled to the pump shaft. Oil changes were carried out with a specially designed device which permitted safe incorporation and removal of lubricants.

The very high efficacy of cryo-sorption was demonstrated spectacularly at **JET** during the first campaign with tritium utilizing a „cold finger“ consisting of a corrugated metal hose of 50 mm inner diameter and 60 mm outer diameter containing 100 g activated charcoal [Hug92b; Hem92]. When this finger was submerged into a 250 l capacity Dewar containing liquid He at 4 K about 600 bar l hydrogen could be pumped down to 0.1 Pa. The pumping speed was determined to be $0.35\,m^3\,s^{-1}$ at 30 Pa inlet pressure. When the Dewar was lowered the finger warmed up and the gas was released into a 345 l reservoir. In total, 50 batches were transferred by this

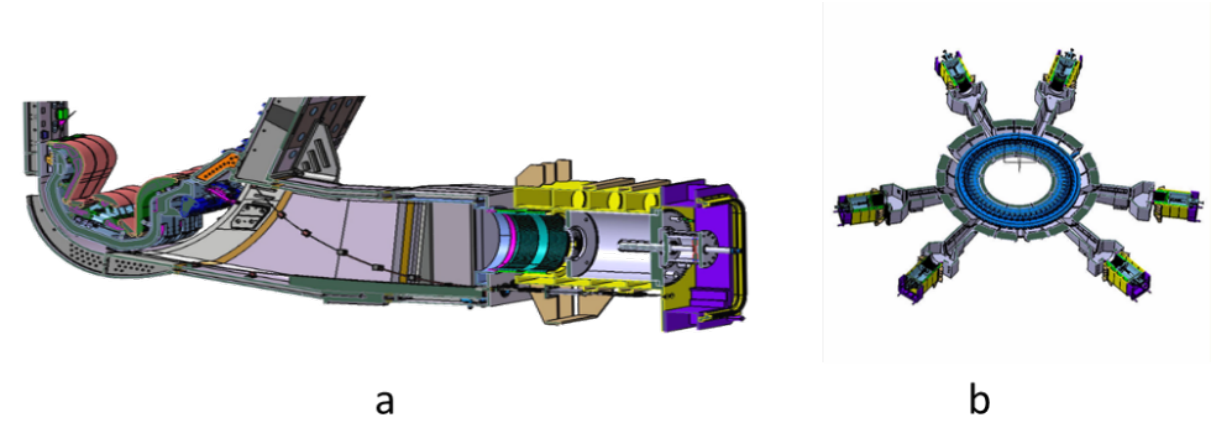


Figure 4.3: Configuration of a single cryo-pump of ITER installed at the end of a duct (a) and of six ducts with their corresponding cryo-pumps evacuating the vacuum vessel (b) ([Glu13])

procedure from the torus and the neutral beam injector to the gas recovery system. From the recovery system the hydrogen isotopologues were fed into one of two uranium beds.

The mechanical fore vacuum system of JET originally consisted of two 150 and one 600 $m^3\,hour^{-1}$ NORMETEX pumps as well as one roots pump with a pumping speed of 1000 $m^3\,hour^{-1}$ [Lae99b]. These pumps were used to evacuate the torus and the NBI cryo-pumps. They also provided backing vacuum to the turbo molecular pumps evacuating the torus.

The evacuation of the **ITER** torus with its vacuum vessel of 1330 m^3 volume, plasma volume of 837 m^3, and plasma tritium inventory of 0.2 g will be carried out with six cryo-pumps installed at the end of six ducts (see Fig. 4.3b). Each cryo-pump (see Fig. 4.3a) will operate in fast cryo cycles (pump on line 450 s) followed by fast sequential regeneration cycles which take place in 600 s [Glu07; Glu13]. The cryo panels of the cryo-pumps are covered with a layer of coconut charcoal adsorber and operate by forced cooling using supercritical helium at 4.5 K (for more details see Figs. 3.17 - 3.20). The cryo-pumps are backed by powerful roughing pumps. Duty of the roughing system is to pump i) the torus from ambient down to 10 Pa - the cryo-pump cross over pressure - and ii) the gases desorbed during the regeneration phase. The roughing pumping system must be designed for pumping speeds of up to 6000 $m^3\,hour^{-1}$.

High vacua such as needed for the plasma exhaust processing system of **ITER** will be generated with an Edwards-Seiko turbo molecular pump type H600C in combination with a NORMETEX type 9 CFM and a two-stage Metal Bellows MB601 compressor [Glu02a].

Experiments employing nitrogen, hydrogen, deuterium, and helium have been carried out with a multistage roughing system reaching nominally 25 % of the 3500 $m^3\,hour^{-1}$ pumping capacity needed for the fast regeneration of cryo-pumps [Lad01]. The study was performed with Edwards EH-1200 and Edwards EH 250 blower roots vacuum booster pumps in combination with a backing pump. In contrast to scroll pumps, which show considerable back streaming through the clearance between scroll and pump body - particularly notorious when pumping light gases - blowers operate in the inlet pressure range 0 - 1 bar. Screening tests conducted with multi-stage pump/roots blower combinations confirmed their suitability for cryo-pump regeneration. A remaining key practical problem concerns the development of a tritium-compatible shaft seal, a subject requiring further research efforts [Lae02d]. More recently obtained results on cryo-pump regeneration are presented and discussed in chapter 3.14.1.8 [Day02; Hau07].

It is generally acknowledged that the basic physics of cryo-sorption is now well established, confirmed by experiments, and documented.

4.1.4.2 Pumps for gas re-circulation

For the re-circulation of gases containing high percentage of tritium oil-free, all-metal, ultra-high vacuum-tight pumps are compulsory. Typical for this category are pumps whose operation principle is based on metal bellows such as for example pumps manufactured by Senior Aerospace Metal Bellows, USA, or Interatom, Germany. Custom features of these pumps such as explosion-proof motors, high pressure compatibility (up to 790 kPa), all metal valve design, variable speed motor, or double containment (utilize a second bellows and a welded housing as a redundant leak-tight seal to the primary pumping bellows), are optional. Senior Aerospace pumps employ welded metal bellows technology. Bellows can be manufactured from stainless-steel, Inconel®, or titanium using laser or electron beam. They are therefore rather corrosion resistant. Senior Aerospace and Interatom pumps function by the same principle. They are offered in single or dual head version. The two stage Interatom pump has a double contained metal below chamber whose central section compresses process gas by a mechanical change of volume. For gas suction and expulsion, the actual pumping space is provided with inlet and outlet flipping seals which are

alternatingly opened or closed by each gas compression and de-compression. The performance of the pump is significantly dependant from the type of gas and from pressure. For example, at 1 bar exhaust pressure the vacua achieved with air, helium, or hydrogen are 100, 113, or 156 mbar, respectively. The volume of the compression chamber is actuated externally by a magnetically coupled motor of variable speed. Accidental rupture of the primary metal bellows can be detected by a pressure sensor that registers the pressure in the secondary containment surrounding the primary bellow. To this effect the inter-space is kept at a pre-established negative pressure. It is also possible to adjust the gas re-circulation rate with a needle valve in a bypass to the pump.

For gas re-circulation at low pressures the preferred option are blowers. Blowers remain in operation even at pressures close to vacuum because they do not rely on flipping seals.

4.1.4.3 Pressurization of tritium

In most tritium handling facilities work with tritium at elevated pressures is avoided primarily out of safety considerations. However, for some special experiments pressurized tritium-bearing gases may be necessary. If the gas comprises only hydrogen isotopes the safest compression procedure consists in using a getter bed provided the involved equipment is throughout designed to withstand the final achievable pressure. When handling tritium at elevated pressure only hydrogen compatible materials should be selected for reactor, valves, valve seats, tubing as well as all other equipment that may come on contact with tritium. This holds even more if elevated temperatures are involved.

V/Ti/Fe hydrides have been utilized successfully for hydrogen compression applications [Lyn84]. The monohydride-dihydride equilibria of this material exhibits reasonably flat plateau pressures in the cast state. Within the temperature range 298 - 373 K the alloy $(V_{0.9}Ti_{0.1})_{0.95}Fe_{0.05}$ was found to display a compression ratio of about 16. Absorption/desorption cycles revealed no irreversible disproportionation of the getter. More details on other potential metal hydride hydrogen compressors are provided in a comprehensive review by Lototskyy et al. [Lot14].

Metal hydrides have been employed routinely at Savannah River site to load tritium into the reservoirs of the US nuclear weapons stockpile [Nob91]. For this purpose, tritium collected from cryogenic distillation columns is first stored in storage beds containing $LaNi_{4.15}Al_{0.85}$. Required loading pressures are generated with a two-stage metal hydride compressor system. The first

stage compressor contains $LaNi_{4.7}Al_{0.3}$ (1.4 MPa) and the second stage compressor contains $Ca_{0.2}Mn_{0.8}Ni_5$ (12.4 MPa). All storage beds are operated by external heating and cooling.

Experiments with tritium at pressures as high as 200 MPa (2000 bar) were performed by Coffin at Los Alamos Scientific Laboratories [Cof76]. Tested temperatures covered values within the range 77 - 700 K. While hydrogen (or deuterium or tritium) pressures up to a few [bar] normally constitute no problem for many materials, in case of very high pressures the induced embrittlement becomes a serious concern to which only very few materials will remain unaffected. As an example, a pressure gauge which tested safely at 34 MPa ruptured during a second test at 3.4 MPa. One material identified as suitable for work at high pressures was beryllium-copper [Oga17]. It was selected because of its good resistance towards hydrogen embrittlement. High tritium pressures were achieved with a mercury column pump actuated by application of hydraulic pressure on oil [Cof76]. An alternative pressurization procedure was to use vessels containing molecular sieve adsorber cooled to liquid nitrogen temperature. Elevated pressures of tritium were generated by removing the coolant from the tritium cryoadsorption bed. Disadvantageous with this compression procedure is that each time the whole arrangement must be sized in accordance with the pressure that is wanted. On the positive side is that cryo sorption necessitates no mechanically moving parts. In view of the potential danger of leakage or even of loss of integrity with all the associated radiation hazard, all operations including valve opening and closing were carried out remotely.

A welded diaphragm compressor comprising four stages and designed for a pressure elevation from 0.5 up to 2000 bar was likewise utilized for the densification of tritium [Cof76].

4.1.5 Alarms

Alarms are necessary for early detection of departures from normal operation of technical or research equipment. They are used effectively to prevent tritium releases into the environment and hence to protect personnel from exposure to radiation. A further high-ranking function is to avert damage from equipment. Damaged components are associated with a disruption of operations and probably with interventions like repairs or component replacement. During these operations contaminations cannot be excluded.

Typical instrumentation used to release an alarm in a tritium handling system are pressure sensors, temperature sensors, differential pressure sensors, flow meters, radiation monitors, smoke detectors, moisture meters, oxygen or nitrogen monitors, etc. Sensitive open wall (or perforated wall) radiation detectors installed in a glove box are employed to detect incipient tritium leaks or releases caused by tritium permeation.

Many early safety measures and interlocks adopted at **TLK** against over-pressures, over-temperatures, radioactivity release, power supply failure, etc. were implemented by NNC Ltd., Booths Hall, UK [Nat91], the company that erected the CAPRICE facility. The execution of alarms was assigned either to i) a Central Automation System (CAS), ii) a Local Programmable Logic Controller (LPLC) and/or iii) a hardwired Safety System (SS). From a safety point of view, primary systems and glove boxes at TLK are independent from each other or with only minimal interface. Consequently, while experimental and infrastructure primary systems at TLK are controlled by dedicated **programmable logic controllers** under operator control from an adjacent workstation, the glove box confinement systems are controlled by their own proprietary package.

Glove boxes at TLK are typically furnished with several ionisation chambers, a temperature sensor, a moisture meter, and other sensors whose selection depends on the type of glove box atmosphere and the executed tasks. When the tritium level in a glove box departs from set-point values a pre-alarm (intermittent yellow light) is released. A main alarm consisting of an intermittent red optical alarm and an acoustical alarm is released when the activity in the glove box surpasses $100\,\mathrm{MBq\,m^{-3}}$. In case a glove from a glove box ruptures a forced air flow into the glove box of $50\,\mathrm{m^3\,hour^{-1}}$ is sustained.

An electrical power failure constitutes a severe alarm. When such a failure takes place all electrically supplied components will be switched into a safe state and only safety relevant sensors and equipment, by design energized with uninterrupted power, will remain active. They provide important information on the evolution of the fundamental parameters prevailing in primary systems as well as in the confinement during all phases of the alarm.

More than 20 local **room air monitors** at TLK are provided with bubblers for activity integration[4]. They display a warning yellow intermittent pre-alarm when the activity reaches $20\,\mathrm{MBq\,m^{-3}}$ (real time) or $2\,\mathrm{MBq\,hour\,m^{-3}}$ (integral value) and a red intermittent main alarm

[4] The detection limit of TLK room air monitors is $0.5\,\mathrm{MBq\,m^{-3}}$.

light at 100 $\mathrm{MBq\,m^{-3}}$ (real time). All alarms are transmitted to the Central Control Room as well as to the Radiation Protection Service. Moreover, in case of a main alarm, acoustic and optical alarms are released in the building housing the laboratory. After verification of the alarm a general evacuation is ordered.

At TLK an ionisation chamber and a proportional counter control the activity released through stack. Together they cover the tritium concentration range 1×10^4 - 5×10^{10} $\mathrm{Bq\,m^{-3}}$. An alarm is released when the activity in the stack reaches 33 $\mathrm{MBq\,m^{-3}}$ (real time).

4.1.6 Primary containment interlocks

Tritium processing facilities and their underlying equipment are protected against hazards beyond the passive safety provided by the primary containment system and the enclosing glove box by a rigorous interlock system. The interlock system is designed to terminate and prevent further operation as soon as the protected process departs significantly from a pre-defined safe operation mode. In practice, this is accomplished by removing the driving voltage from pumps, heaters, magnetically actuated valves, sensors, etc. Sometimes, interlocks are needed for very special applications. For instance, to control the helium loop of getter beds during a tritium inventory determination.

Experiments are tripped at TLK either because of deviation from a normal control band or failure of a sensor/transducer. In case of minor deviations or transducer drift the Central Automation System (CAS) or a LPLC will initiate a warning and for larger deviations a trip to safe state A. While a safe state A cause's complete shutdown of the experiment it leaves some instrumentation energized and operational. Prior to initiation of the trip to safe state A, a warning may be given to the operator provided there is enough time to act upon. The alarm allows the operator to initiate the tripping of the hardwired system via a push bottom. If, however, the deviation of the measured value of the parameter causing the trip continues to increase a safe state A will be initiated automatically. Larger deviations or total failure of a sensor or transducer will result in a trip to safe state B. In such a case the hardwired Safety System will shut down the experiment completely leaving only safety relevant instrumentation energized and operational except where there is a source of ignition, e.g. tritium monitors, penning gauges, etc. The contactors for tripping to state A are from a different manufacturer to

contactors for tripping to state B. Because of the independence between experiment and glove box, there is no tripping of a glove box from parameters of an experiment.

For example, during the course of an experiment performed at TLK the CAS or a LPLC measures a pressure (or any other variable) with sensor 1 and monitors the pressure until it exceeds a limit value of S^+. The Safety System, on the other hand, monitors the pressure with sensor 2 until it exceeds a limit value of Z^+. Per definition $Z^+ > S^+$. Sensor 1 and sensor 2 are redundant, i.e. measure at the same location, but are when possible diverse, i.e. of different manufacturer or rely on a different measuring principle. If considered important, the CAS or the LPLC can also generate the absolute difference between sensor 1 and sensor 2, releasing a warning or a switching action when the difference surpasses a limiting value. Whereas S^+ gives first rise to a warning and then to a safety trip into an A state, Z^+ irrevocably causes a trip into a B state. In order to obtain incessant important information on the status of the facility and thereby contribute to identify possible causes of the tripping, carefully selected safety relevant sensors measuring radiation levels, pressures, and/or temperatures are connected at TLK to the uninterrupted power supply. In consequence, these sensors will remain active regardless of whether a safety trip takes place or not.

In case of the much more multifaceted situation at the **Active Gas Handling System (AGHS) of JET** a Distributed Control System is connected to 3600 inputs and outputs. In total 414 analogue inputs are recorded on trend displays [Lae99b]. The control of the plant is subdivided between 17 Distributed Control Units (DCU), each of which can control independently a section of the plant. Within these DCU´s there are 140 automated sequences and 51 PID loops. The DCU´s are connected to a dual ETHERNET highway. Additionally, a SIX UNIX DCS SYSTEM has been connected to the ETHERNET highway with 24 further trend displays. As common to all larger installations, a hard-wired interlock system has been installed for ultimate protection. These measures, here described only very succinctly, give an impression of the magnitude of the protection effort that has been put into practice for the safe operation of AGHS, the large and highly complex tritium-handling facility of JET.

The remotely operated Preparative Gas Chromatography Subsystem of the AGHS at JET, designed for the recovery of deuterium and tritium of more than 98 % purity, provides another good example for a hardwired interlock-protected tritium system [Lae99a][5]. Altogether 19 interlocks

[5] The Preparative Gas Chromatography may also be operated manually.

have been installed for this GC system. These interlocks will i) interrupt the heating power to the uranium storage beds and close inlet and outlet valves when pressures or temperatures exceed pre-established values, ii) stop pumps when pressures increase beyond a given set value in an adjacent reservoir, iii) switch off power to the oil heaters of the palladium filled gas chromatographic columns when the pressure rises beyond safe values, and iv) terminate operation and even prevent further operation when tritium concentrations surpass limit values in the nitrogen filled secondary containment (the Preparatory GC system is contained in a large stainless-steel cylindrical vessel and not in a glove box!) [Lae99b]. All interlocks are controlled at regular intervals following a pre-established scheme.

The Distributed Control System of the Preparative Gas Chromatographic system has been upgraded by a **micro Distributed Control Interface (DCI)**, which was installed primarily to achieve faster response times [Lae99a]. The upgraded DCI is capable of executing measurements, performing calculations, and carrying out correct valve switching in less than 0.3 s. Hence, the operation of valves has become possible in much shorter times than before.

4.1.7 Protective measures against over-pressure

4.1.7.1 Design guidelines

Possible internal sources of pressurization in a primary system are i) pumps or combination of pumps pumping glove box atmosphere leaking into a primary system, ii) gas release from a heated getter bed, iii) gas liberation from a warmed-up adsorber bed, iv) loss of coolant of a cryogenic adsorber bed or a cryogenic trap, v) thermal vaporization of condensed phases, or vi) exothermic chemical reactions. An over-pressure may likewise develop from a faulty pressure regulator of a compressed gas cylinder attached directly to the primary system, i.e. external source.

A reliable static preventive measure consists in limiting the power of heaters installed in primary systems in such a way that the maximum attainable temperature cannot inflict damage.

Provided no unacceptable contamination is conceivable, a pressurization induced from external sources is normally dealt with employing pressure relief valves or burst disks which discharge excess gas into the conventional off gas system. Protection against internal pressure excursions consist of burst disks which discharge tritium-contaminated excess gas into an evacuated buffer

vessel of sufficient volume to safely accommodate all of it. To allow replacement of damaged burst disks, an appropriate number of isolation valves, pressure sensors, and pumps must be accessible. The valves must be secured administratively from inadvertent closure either with a tilt over device or by temporary removal of the pertinent handles.

Two redundant and diverse pressure sensors are considered adequate to cope with pressure excursions. One is connected to an Automated Control System and the other to a hard-wired Safety System. They are installed at the exhaust zone of pumps or pump combinations. A comparison of the readings of these two independent sensors provides a healthy signal. When pressures depart from set point values all electrically supplied components and therefore the disturbed system will switch into a safe state.

Even though tremendous progress in software-based safeguarding has been acknowledged at ITER, it was still felt safer to rely on hard wired signal processing for the Tritium Plant. Consequently, departures from normal operation at the Tritium Plant will be received, registered, and responded by a Central Automated Control System together with a hard-wired Safety System. Accordingly, if pressures or temperatures depart from set-point values the operation of the pertinent tritium system is stopped and the complete affected system is brought into a safe state. This is carried out by circuit breakers which suspend power supply to heaters, pumps, and other consumers.

For obvious reasons, it is important to verify that all installed pressure and other sensors retain their physical integrity up to pressures clearly in excess of those possibly leading to rupture. Typical P&ID configurations for the protection from over-pressure of an ITER getter bed or a six-stage compressor through an Automated Control System and a Safety System have been discussed in detail in a paper by Glugla et al. [Glu05]. Even though at first sight a relief valve appears to suffice as protection against over pressurization, this option was considered not sufficiently trustworthy For the protection of pumps against over-pressure two redundant diverse pressure sensors were deemed to be more reliable. As practiced in TLK, the pressure level that activates the Safety System was set higher than that which activates the Automated Control System. Authorization for a restart of operations is granted by the responsible authority after the cause of malfunction is identified and eliminated.

Gases released by relief valves should not be discharged into pressure-controlled glove boxes without foregoing approval by the Authorized Supervisor.

4.1.7.2 Design measures against over-pressure

A list of important design measures that need to be complied with at the tritium-handling installations of SRNL is compiled below [Poo08]. A few complementary measures likewise contributing to a high level of protection against over-pressure events extend the list. The list is neither complete nor binding, it is only intended to stimulate awareness of the problems that may be encountered and that may require attention. Design measures applied in a given tritium handling installation are not necessarily the same everywhere. They are of the responsibility of the respective authorized authority.

- All pressure protection equipment must be meticulously inspected and verified. Verification records of all over-pressure protection equipment assures safety compliance and secures safe operation of the equipment.
- All vessels which are defined in U1 of ASME Boiler and Pressure Vessel Code (B&PV Code) (or any other accepted code) are stamped per Code and registered with the US National Board Inspection Code (NBI) (or with any other accepted code). Drawings and design calculations shall be made available for all code vessels.
- All Code vessels are protected by a Code-approved pressure relief device for instance as required by UG-125 to UG-136 or any other accepted code.
- Vessels for non-tritium service use pressure relief valves. Rupture disks are acceptable when the burst pressure has a differential value higher than 41.3 bar.
- All pressure relieve devices above 1.03 bar differential pressure shall be ASME B&PV B31.3 stamped.
- All rupture disks must follow ASME Code (see ASME B&PV and ASME B31.3) (see also Appendix N and Appendix O)
- Rupture disks must be located in process system zones where particulate accumulation and vapour condensation are not likely to occur. Such matter tends to cause corrosion or erosion of disks.
- Rupture disks in tritium systems (or of other hazardous gases) relieve the gas into a containment system (rupture disk, tank). Tritium process rupture disks must be helium

leak-tight to 10^{-7} STP $cm^3\,s^{-1}$ after 2 min. Only rupture disks previously approved for tritium service shall be used. The rupture disk relieving system is so designed that preventive maintenance is not required. Designs using forward buckling disks with ample operation margins (generally $> 30\,\%$ burst pressure) or reverse buckling disks with ample design margin are considered acceptable.

- Preferred material for rupture disks is low-carbon austenitic stainless-steel.
- Discharges from pressure protection devices should not be vented into the environment of personnel.
- Premature failure of a rupture disk located on the discharge side of pressure generating equipment such as pumps, compressors, or fast delivering getter beds is minimized by installing the rupture disk not directly in line with the equipment, but rather branched off the piping to lessen pressure pitches against the disk.
- Screens to avoid intrusion of insects into the vent piping shall be installed.
- Outdoor relieve discharge valves must have drains that prevent noteworthy accumulation of water.
- Pressure protection for refrigeration equipment includes conformance to ASHRAE 15 (safety standard for refrigeration equipment explaining how ASME Code is applied) (see Appendix N).

4.1.8 Protective measures against over-temperature

Temperature excursions can conduct to i) a disturbed process course, ii) pressure rise in closed recipients containing gas, iii) increased tritium permeation rates through the walls of heated vessels, iv) vaporisation of condensed phases, v) release of adsorbed gases, vi) irreversible agglomeration or hydrothermal vitrification of powders or adsorbers, vii) formation of eutectics, etc. In the event that limit design values for mechanical integrity are exceeded, catastrophic component or sensor failures may occur. Preventive active actions must therefore be taken, when departure from pre-established temperature set-point values are registered.

Two redundant and diverse temperature sensors, one connected to a Central Automated Control System and another to a hard-wired Safety System, adequately provide the required

process and component protection for the Tritium Plant of ITER. If the temperature exceeds a set-point value, the Central Automated Control System or thereafter the Safety System will turn off the electric power through a trip function [Glu05]. A comparison of the reading of two sensors provides a healthy signal.

Components like getter beds containing a significant amount of tritium are self-heating. If the bed is equipped for in-bed calorimetry it will be provided with an evacuated jacket for thermal insulation. Such a bed requires an interlock whose function is to avoid thermal insulation when the helium loop used for inventory measurements is not in operation. Otherwise the temperature of the bed may progressively increase up to the point where eventually tritium tritide is decomposed and a tritium pressure rise takes place.

4.1.9 Protective measures against tritium release from primary containments

A multi barrier concept, i.e. primary barrier (experiment or infrastructure system), secondary barrier (glove box, caisson, or dedicated confinement), and tertiary barrier (building), constitutes the established worldwide standard for handling large inventories of tritium. Accordingly, tritium released from a **primary containment** during anomalous operation or a catastrophic event either as tritiated gases (Q_2, C_xQ_y, or Q_2O, Q = H, D, T) or as radioactive dust will be retained and therefore isolated from the environment by a **primary confinement**. Specially in small instalations a dedicated, adjacent Tritium Retention System is employed not only to keep the tritium concentration inside of the secondary barrier at low levels but also to reduce rapidly the concentration of tritium in case of a major release. Tritium removal is carried out by oxidation of all tritium-bearing species into tritiated water via reaction with gaseous oxygen present in the glove box either as air component or at a constant small partial pressure in a chemically inert gas atmosphere. The oxidation proceeds readily on the surface of a noble metal catalyst operated at ambient temperature or above. Oxidized tritium is subsequently adsorbed on a molecular sieve bed maintained at ambient temperature [She77b; She79; Nar90; Sch91a; Won92; Hut95; Heu02].

To cope with a major tritium release accident in a tritium handling installation a proposed option consists in using a sequence of two separate recombiner beds under standby in preheated conditions which are automatically further activated once a release of tritium takes place. Under full operating conditions, one of these recombiners is heated up to 423 to oxidize hydrogen

isotopologues and the other up to 773 K to convert hydrocarbons (including methane) into water and carbon dioxide. For enhanced effectiveness, the exhaust gas of the first recombiner is preheated before it is fed into the second one. Drawbacks of this approach are i) significant potential for permeation releases from internally or externally heated beds, ii) shift of residual moisture adsorbed in the down stream dryer bed towards the bed outlet when air flows through the dryer bed during hot standby conditions (the consequence is a premature breakthrough of HTO), and iii) poor energy economy.

To handle the above discussed problems, an advanced catalytic recombiner/adsorber bed combination of improved design was proposed for the Active Gas Handling System by Hemmerich [Hem93]. The concept is applicable to the recovery of tritium from "minor" release sources like into primary confinements protecting tritium-handling processes or to manage releases into the atmosphere of the cryostat building after an accident at the torus vacuum vessel or the adjacent neutral beam injector. Basically, a conventional catalytic recombiner was re-designed on the principle of a counter flow heat exchanger employing a standard tube bundle partially filled with recombiner catalyst (see Fig. 4.4a). The upper end of the tubes is heated by low power heaters (< 1 kW) embedded in the catalyst itself. Therefore, during hot standby conditions the catalyst can be maintained at 773 K under minimal power consumption. Because continuous air flow is not necessary during standby there is only little relocation of water (HTO) to the adsorber bed end. Losses by permeation are almost completely eliminated by highly efficient thermal insulation. The construction is such that the potential for ignition or deflagration in the presence of high partial pressures of hydrogen is very unlikely. One further advantage of low temperatures besides optimized energy economy is that the vessel no longer needs to be build according to pressure vessel specifications. Hemmerich [Hem93] furthermore proposed a substantially improved design of molecular sieve dryer beds. As opposed to conventional dryer systems, which consist of separated dryer bed, water condenser, and heater units, in the upgraded version these units were integrated into a single component with multiple possible paths (see Fig. 4.4b). In the upgraded design the flow direction is upwards in the adsorption mode and downwards in the regeneration mode. The capability of reducing the humidity from initial 10 000 ppm down to 0.01 ppm in the exhaust gas is achieved with two dryer stages in series. At the end of regeneration, cooling is performed without air flow. By this way of proceeding deposition of HTO at the top layer of the

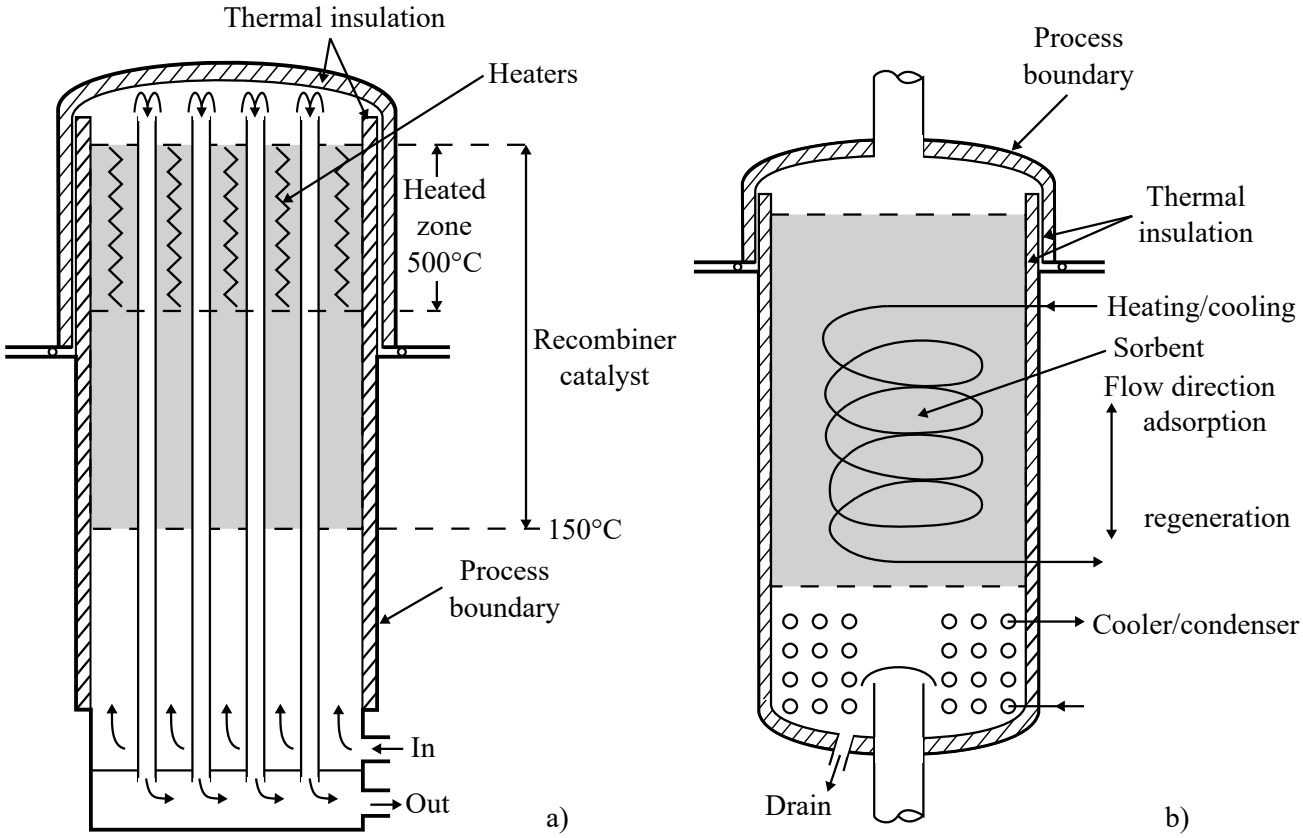


Figure 4.4: The left figure displays an upgraded recombiner design with counter flow heat exchanger featuring an integrated catalyst bed and heaters and the right figure shows an upgraded adsorber bed design with integrated condenser and a heating/cooling device submerged into the adsorber. Both components are furnished with Microtherm thermal insulation (after [Hem93]).

bed is avoided. Dryers are regenerated with dry air in counter flow mode to that of operation. Improved energy economy is achieved with a special very effective thermal insulation.

Nearly every glove box at **TLK** is equipped with a dedicated local Tritium Retention System placed in the vicinity of the glove box (see Fig. 4.5). In these systems tritiated hydrogen isotopologues and tritiated hydrocarbons contaminating the glove box atmosphere are oxidized catalytically in the presence of a heated noble metal catalyst. The generated tritiated water is conventionally adsorbed on a molecular sieve bed maintained at ambient temperature. Only one Tritium Retention System (adsorber beds were installed outside of the glove box) has been

incorporated into a glove box. The idea in back of it was to get hands on experience with this alternative option[6].

Dedicated retention systems confer high availability and process independence to the glove boxes. All local Retention Systems are backed up by a Central Tritium Retention System operating on the same principle, i.e. catalytic oxidation of tritium-bearing species in the presence of a heated noble metal catalyst followed by adsorption of generated tritiated water on a molecular sieve adsorber bed (see Fig. 4.5).

Whether air or nitrogen is selected for a glove box depends on type (flammable, catalyst poison, etc.) and amount of radioactive processed gases in the respective primary system. In some cases, it is necessary to protect burnable getters or oxygen-sensitive species from undergoing a strong reaction with oxygen.

Each **local Tritium Retention System** keeps the concentration of tritium and moisture in the adjoined glove box at very low levels. Early detection of tritium release into the glove box is recorded by ionisation chambers integrated into the inlet and exhaust pipes of the adjudicated retention system. A release can additionally be detected by an open wall ionisation chamber installed inside of each glove box. The glove box atmosphere can either be air or nitrogen (alternatively argon) containing a small partial pressure of oxygen which is regulated within set point values. Oxygen is necessary to maintain the oxidative character of the glove box cover gas.

[6] Advantage of this solution is the confinement of the Tritium Retention System; disadvantages are the increased heat load of the glove box, loss of valuable glove box space, and the external contamination of the Retention System which manifests negatively on the cover gas decontamination.

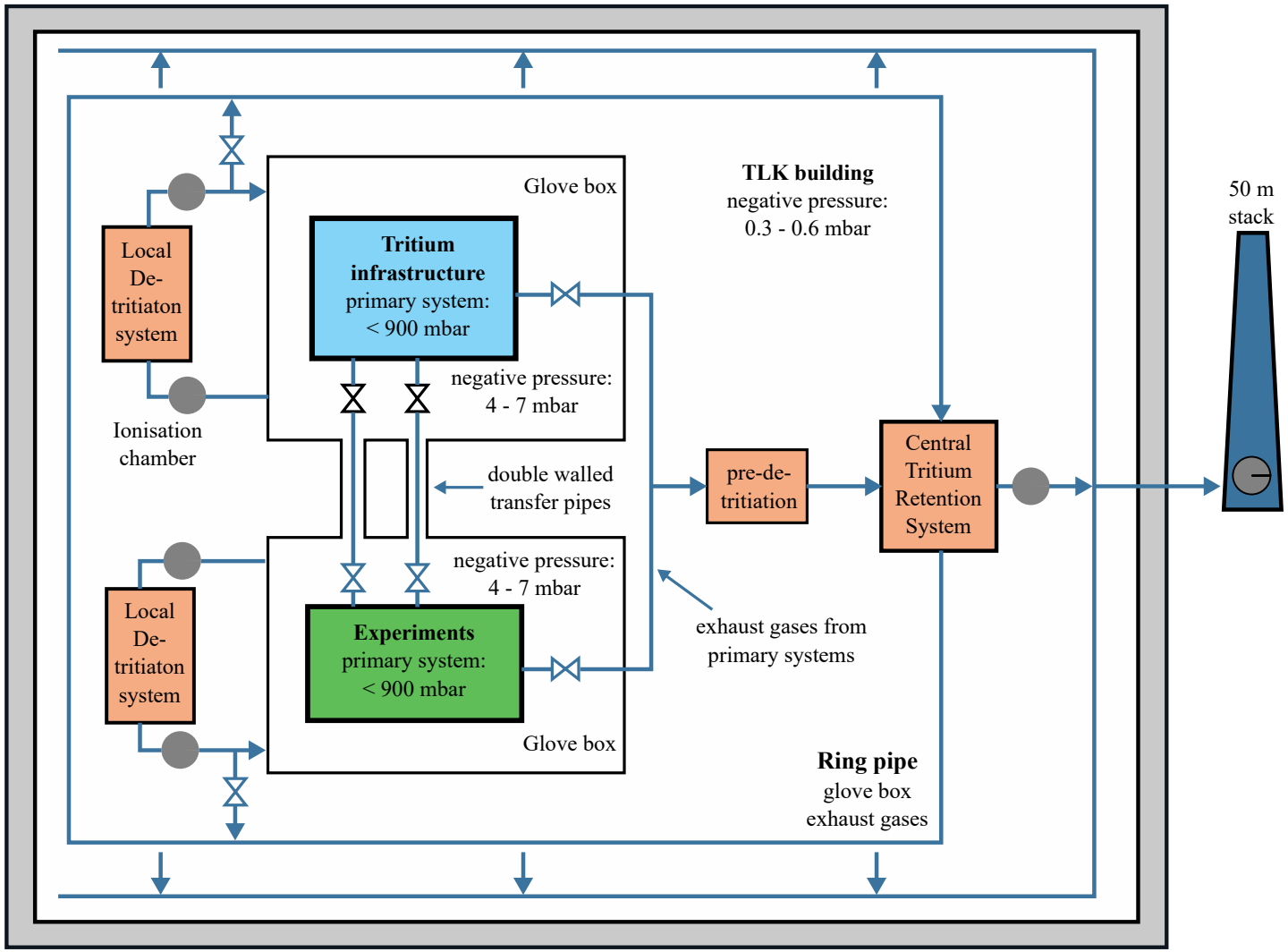


Figure 4.5: Simplified scheme of the TLK tritium removal concept from primary systems, glove boxes, and laboratory air.

The **Central Detritiation System** of TLK processes i) all exhaust gases from infrastructure and experimental primary systems, ii) enhances detritiation of the exhaust gases from primary confinement systems taking place in the Dedicated Detritiation Systems iii) removes tritium-bearing gases leaked into primary confinements in off-normal events, and iv) maintains a negative pressure in the glove boxes of 4 - 7 mbar with respect to that in the laboratory (see Fig. 3.86). Exhaust gases from all primary systems are collected in one of two buffer tanks belonging to a pre-detritiation system. These tanks are pre-filled with sufficient nitrogen to rule out formation of explosive mixtures. Pre-processing takes place in closed loop operation mode until the concentration of tritium is reduced to a level acceptable for once-through discharge via the Central Tritium Retention System. The tritium content of the gas released into the environment through a 50 m tall stack is continuously surveyed by an ionisation chamber and a proportional counter.

While the tritium retention concepts of **TPL** [Nar90; Yam11a] and TLK [Sch91a] are largely similar, a significant difference is that only TPL has a dedicated air detritiation system for the whole Controlled Area. There are three distinct tritium removal routes at TPL: i) the Effluent Tritium Removal System (ERS), ii) the Glove Box Purification System (GPS) and iii) the Air Clean-up System (ACS). The ERS removes in once-through mode tritium from the effluent streams of primary exhausts (via vacuum pumping) as well as from secondary containments; the GPS removes tritium from glove box atmospheres and maintains a negative pressure in the glove boxes; and ACS serves to process the exhaust gas generated during maintenance and repair of tritium handling systems, and the room air of the Controlled Area in case of a major off-normal event.

4.1.10 Component failure data analysis

In spite of the experience gained worldwide with a great variety of single components during operation with tritium, only very few thoroughgoing component failure analyses have been performed and reported.

Failure rates of tritium room air monitors and of other equipment installed at **TSTA** for the purpose of tritium waste treatment were analysed systematically during the period 1984 – 1990 by Cadwallader, Stolpe-Gavett, and Quintana [Cad90; Cad91a]. The results obtained were

based on failure reports, component populations, and operation demands as well as operation hours. For the analysis of the data the experience gained with the Centralized Reliability Data Organization (CREDO) system developed at ORNL for fast fission reactor failure data was found to be very valuable. Therefore, a first objective of the investigation was to adapt the CREDO procedure to the requirements of tritium technology availability and reliability programs.

Three kind of data were registered:

- One-time submission of an engineering data report describing the component as fully as possible including such data as type, model number, operating parameters, etc. A unique number was assigned to each component to allow tracking of the component through its lifetime.

- Event data describing all reportable events or failures using a unique report number for each event. Reportable events comprised component failures, events that lead to unscheduled repair or maintenance activities, and unanticipated changes from normal operating conditions caused by a component failure.

- Operation data making use of quarterly reports describing the operating period of the whole facility. From this information the time in operation of each component was deduced.

Air monitor long-term operation data collected at TSTA [Cad91a], TPL [Yam95a; Yam02], and at JET [Pin05] reveal that in general the monitors worked well. The results provide the basis for an estimation of the reliability of safety relevant monitors that also release a warning during tritium contamination situations [Cad09b; Cad09a].

To illustrate how failure rates are calculated, assume 7 monitors operated in a tritium laboratory for over 19 years, which showed 13 failures. In this case

$$\text{failure rate} = \frac{13 \text{ failures}}{7 \text{ monitors} \cdot 19 \text{ yr} \cdot \frac{8760 \text{ h}}{\text{yr}}} = \frac{1.1 \times 10^{-5}}{\text{monitor} \cdot \text{h}} \ .$$

Based on data published in the open literature an average all mode failure rate of 2.65×10^{-5} hour^{-1} per air monitor was estimated [Cad09a]. Failure events considered were those caused by mechanical faults, electrical faults, electronic faults, radiological faults, and human error. Averaged repair and maintenance times of continuous air monitors were also evaluated and

reported. The provided numbers may be useful for instance to estimate the initial number of spare continuous air monitors needed for checks and calibrations of a facility the size of ITER. A rough estimate of this spare is up to 10 % of the total number of installed monitors. The numbers may also serve to identify upgrade needs to improve the availability of equipment.

The combined failure rates of fixed monitors stopping to operate according to observations in TPL, JET, and TSTA was estimated to be $3.5 \times 10^{-6}\,\mathrm{hour}^{-1}$ per monitor. Failures taken into account for this survey comprised detectors, electronics, internal power supplies, air flow sensors, contamination, and faults of air pumps.

At TSTA **event data forms** were placed in holders and attached strategically to several systems throughout the facility for easy access of operators possibly involved in an event. By way of example, one system subjected to monitoring of failure events was the Tritium Waste Treatment System (TWT). This system was operated in batch mode. Major small and large monitored components of TWT were filters, the catalytic converter system (533 - 810 K), high- and low-pressure gas storage tanks, a molecular sieve regeneration system, radiation monitors, compressors, molecular sieve beds, an analytical system comprising two gas chromatographs, a computer control system, pressure transducers, moisture monitors, 151 remotely operated and manually operated ball valves, etc. In addition, several gases and their mixtures supplied to TWT were monitored. Most of the major components were redundantly provided with a back-up system.

For detailed lists of failure causes and consequences as well as of component populations and demand references [Cad90; Cad91a] should be consulted. Two types of failures were evaluated:

- failure rate per demand for components required upon operational demand and
- failure rate per hour for components that may fail while in operation

The comprehensive work of Cadwallader et al. lead to the conclusion that more actual failure rate data are needed for accurate fusion facility reliability and risk analyses. Feedback from field experience was considered rather valuable when planning new designs. This also pertains the development of a maintenance and replacement strategy especially inside of glove boxes.

Taylor [Tay95] provided failure modes and corresponding mitigation procedures for a large number of small and large components of the Tritium Plasma Experiment installed in a glove box of the former TSTA facility in Los Alamos, NM (see also section 2.14.1.2).

Failures of a significant number of components belonging to equipment used for tritium handling and processing at the **Tritium Process Laboratory (TPL)** were registered and evaluated systematically over the course of eleven years by Yamada et al. [Yam02] (see table 4.1). The Japanese laboratory TPL with up to 60 g tritium and facilities such as Air Clean-up System, numerous experimental and infrastructure systems in Glove Boxes, Gas Purification System, Dryer Bed Regeneration System, etc., can be considered representative for facilities currently under development and realization for ITER. Failure frequencies were defined by the ratio between the numbers of failures over the number of examined components and the integrated time of operation.

Yamanishi et al. [Yam08; Yam11a] extended the monitoring period of some of the TPL components already examined by Yamada et al. [Yam02] by doubling it up to twenty two years. Furthermore, more components of the kind frequently employed at TPL were incorporated into the list. For the extra lengthily assessed components like blowers, compressors, sampling pumps, air driven valves, electromagnetic valves or tritium room monitors they provided improved failure rates of 1.4×10^{-5}, 1.4×10^{-5}, 1.0×10^{-6}, 1.5×10^{-5}, 6.9×10^{-7} or 3.7×10^{-7} per component and hour, respectively (compare with Table 4.1).

In summary, a valuable database on the failure frequency of key components in tritium handling systems is now available. The relatively high failure frequency observed with certain valves prompted Yamanishi et al. to recommend valve redundancy in safety relevant and process critical sections.

Pinna et al. [Pin05] registered malfunctions or failures of constituents from the Active Gas Handling System and the Vacuum System of JET (in total 6259) over a prolonged period of operation of about 1.6×10^5 hours. The surveyed elements comprised large numbers of small components like air actuated and solenoid valves, catharometers, thermocouples, as well as large sized components like 150 or 600 $m^3\,hour^{-1}$ NORMETEX scroll pumps. In fact, three out of five NORMETEX pumps displayed failures after operation periods lasting between 22 000 and 29 000 hours. Defect scroll pumps frequently required replacement. Cause for malfunctions were debris accumulating in the region between the fixed and the rotating spirals or in the nutating bellows sealing of the compression chamber. Beyond AGHS, failure rates were also provided for a number of components belonging to the JET machine. A total of 4012 components pertaining the vacuum vessel were surveyed with respect to failures or malfunctions. About 600 leaks

were registered at the vacuum system during the period 1983-2002. They were classified into "installation leaks", "operational leaks" or "critical leaks" associated with machine operation stop and "non-critical leaks" without consequences to the operational activities. Representative "non-critical leaks" were small leaks, leaks that could be repaired or isolated, etc. "Critical leaks" were for instance water leaks on hot windows giving rise to window cracks.

Typical failures observed at the AGHS or the Vacuum Vessel of **JET** were:

- Bellow leaks due to fatigue induced by vibrations and differential expansion of bellows and machined components
- Flanges with damaged sealing surfaces
- Leaks of electrical feedthroughs caused by electric discharges in poorly evacuated guard vacuum
- Penning gauges giving erratic readings under the influence of strong magnetic fields or switched on under poor vacuum
- Valves clogged by debris deposited in the seat region, failed to open or close, displayed an internal leak or developed a diaphragm rupture.
- Pumps failed to start, suddenly stopped or displayed a leak
- Filters clogged
- The uninterrupted power supply lost redundancy
- Burst disk leakage
- Leaking welds

The same authors [Pin05] additionally reported on failure rate data for about 600 representative components of the fusion fuel cycle relevant tritium handling systems installed at TLK. The registered results yielded 52 failures or malfunctions for components such as:

- Generic leaks of automatic valves, ring blowers, electronic frequency converters, molecular sieve beds, ring blowers, etc.
- Heater failures of catalyst vessels and permeators. For actual failure rate data, the original literature should be consulted.

4.1.11 Planing of tritium systems incorporating maintenance

Tritium facilities should be designed and constructed in such a way that routine maintenance activities remain at a minimum [Poo08]. The design of components should incorporate measures that keep the hazard to personnel and the probability of tritium release into the environment not only during operation but also for the duration of maintenance periods as low as possible. It should be decided at an early stage whether redundant components are necessary to allow process repairs or maintenance activities on one system while continuing to operate others. Type of equipment and layout space inside of glove boxes should be planned to allow hands-on upgrading, preventive maintenance, in-service inspections, and surveillance in zones where permitted by low contamination and minimal hazard levels. The design shall allow removal, maintenance, inspection, and calibration of equipment.

Items that require frequent maintenance shall have double manual valve isolation to allow separation of the component from the process during line-breaks. The design shall provide for the possibility of evacuation and flushing of the component as well as adjudicated relevant process lines prior to performing maintenance operations.

Valves, instruments, rupture disks, and in-line heat exchangers shall have connections that are accessible for routine corrective or preventive maintenance either directly or with specially designed tools.

Provisions should be taken to permit easy calibration of transducers installed between a relief valve and a rupture disk and to allow their replacement with the same frequency as the associated relief valves.

A wide-ranging strategy of preventive maintenance procedures for systems and components should be prepared and the necessary instrumentation for surveillance during the life time of the facility be made available. Individual remedial maintenance procedures shall be outlined for each pertinent component and the interfacing systems needed to support these maintenance activities be incorporated into the system.

When recurrent calibrations of installed instrumentation or other equipment are necessary an in-place connection to calibration standards is a convenient option. Such connection may include the installation of isolation and/or test valves. All pressure instruments should either be calibrated *in situ* utilizing i) redundant, preferably diverse instruments installed on process

lines, ii) adjacent dedicated test valves, or iii) *ex situ* isolation valves particularly in case a major component replacement is necessary. Temperature loops may be calibrated either i) by comparison with redundant devices, ii) employing a decade box, or iii) a special Millivolt box for thermocouples. In case of a critical temperature, relevant temperature measurement elements should be replaced on a periodic fixed schedule

If in-place calibration of an instrument is not feasible, replacement of the expired instrument by a new freshly calibrated one may become necessary. This should preferably be carried out within the frame of maintenance activities. Routine replacement of moisture meters following prior isolation by pressure boundary valves is common practice in many installations.

At least 90 cm in front and 80 cm to other access areas should be foreseen for electrical equipment and components located outside of glove boxes in order to permit provisional utilization of tools and measuring instrumentation such as needed for maintenance or repair.

Table 4.1: Failure frequency of components in tritium service at TPL during the period April 1988 – March 1999 [Yam02].

Component	Number	Integrated operation time (hour)	Failure frequency (hour^{-1})
Blower	5	88 110	1.0×10^{-4}
		1764*	0**
Compressor	3	5417	7.4×10^{-4}
		38327*	5.2×10^{-5}**
Sampling pump	19	679885	8.8×10^{-6}
		4864*	3.5×10^{-3}**
Manual valve	307	3377*	5.9×10^{-4}**
Air driven valves	49	10780*	8.3×10^{-4}**
Electromagnetic valves	62	81840*	4.9×10^{-5}**
Tritium room monitors	7	674520	5.9×10^{-6}
Tritium process monitors	13	635079	2.0×10^{-5}
Hygrometer	9	725288	1.2×10^{-5}
Oxygen sensors	7	674520	3.0×10^{-6}
Glove boxes	10	963600	9.3×10^{-6}
Master control computer	1	96360	1.3×10^{-4}
Negative pressure control	7	636727	7.9×10^{-6}
Pre-heater	5	255629	1.2×10^{-5}
Cooling water system	1	96360	1.7×10^{-4}
Battery	1	96360	1.0×10^{-5}
Heat controller	3	289080	3.5×10^{-6}
Vacuum pump	10	67721	4.4×10^{-5}
Flow meter	26	2505360	1.2×10^{-6}
GPS	1	75474	1.3×10^{-5}
Computer software	1	96360	1.2×10^{-4}

*Integrated over the number of times operation was started
**Frequency of failure integrated over the number of times operation was started

4.2 Primary and secondary confinement options

4.2.1 Confinement options

Worldwide a multiple barrier concept has been developed and implemented successfully to ensure that gaseous tritium in a primary system is not released into the environment. Accordingly, primary systems generally consist of an ultra-high vacuum tight containment. Containments are enclosed by confinements such as glove boxes, caissons, or dedicated large vessels that prevent release into the environment of tritium that has escaped a primary system. This definition does not extend to fume hoods or tents, because they lack leak-tight boundaries. As further preventive measure against contamination spread, the level of tritium in confinements should be kept at all times as low as possible and the total pressure slightly below that of ambient, i.e. laboratory air. This is accomplished by incessant processing of a fraction of the confinement atmosphere via a Central Tritium Removal System.

According to the **multiple barrier concept**, the pressure in primary confinements is maintained a few mbar below that of a nearly gas-tight building and that of the building below that of the external ambient employing a properly designed ventilation system. The pressure will therefore decrease stepwise from ambient with the lowest concentration of tritium to that in the building to that in the primary confinement up to the primary containment, whose pressure will be lowest while the concentration of tritium will be the highest. By this approach a high level of protection for workers and environment is achieved.

To perform major repairs, maintenance or equipment replacement activities in an open glove box a provisional confinement like a tent is normally erected contiguously (see also section 4.2.1.1). For transport or short-term storage of tritium-contaminated components or equipment retrieved from the glove box they may be enveloped tightly in sealed plastic bags. Such transitory confinement represses direct contact of workers with tritium-contaminated surfaces and isolates at least temporarily outgassing tritium from the environment. Care must be exercised when selecting plastic bags because molecular tritium as well as its much more toxic oxidation product diffuse readily through plastic materials; HTO usually much faster than elemental tritium [Cof67; San04; Met05; Tog11].

Air supplied plastic suits that completely enclose the body, are widely used in facilities handling large quantities of tritium particularly when repair or refurbishment activities in open

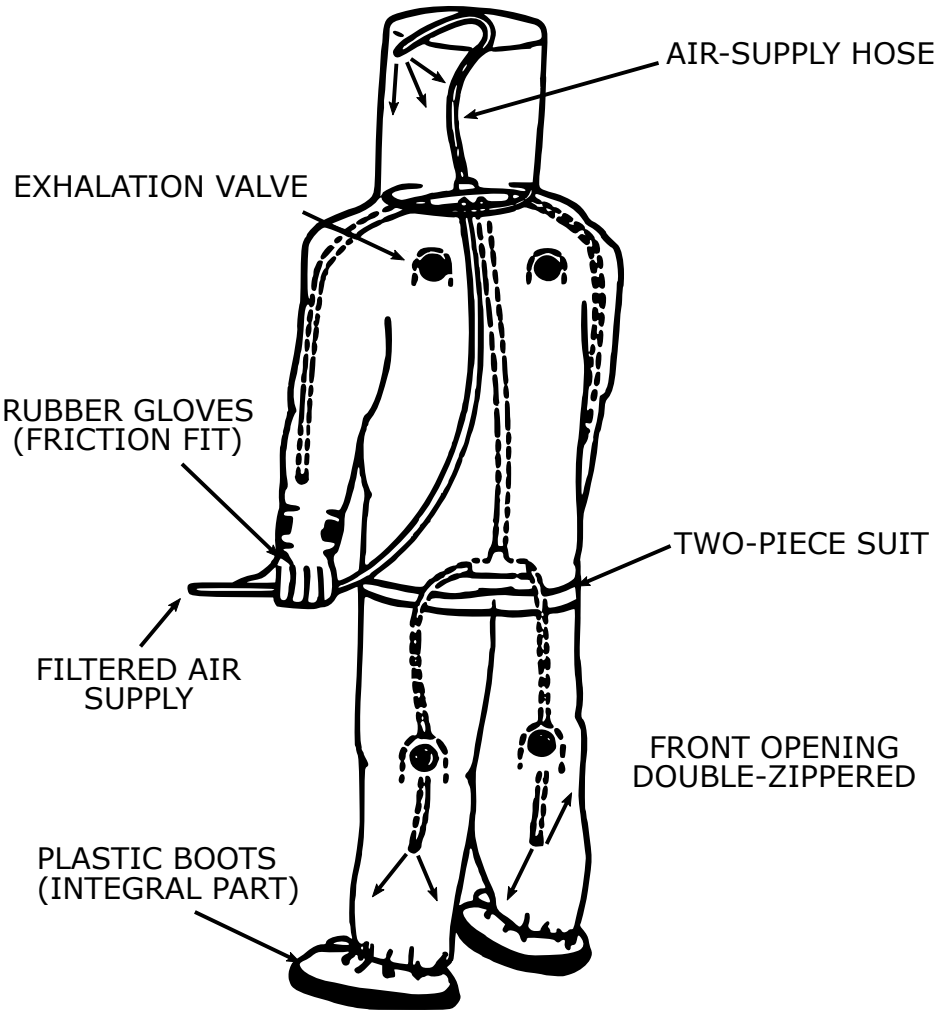


Figure 4.6: Commercial impermeable air supplied plastic suit for protection against open contamination. The suit comprises an air supply hose, exhalation valves, filtered air supply, and plastic boots. The protective suit consists of a two-piece front opened double zipped unit[7].

confinements become necessary (see Fig. 4.6). The suit is made of plastic or else of coated or impregnated fabric and maintained under positive pressure by external air supply via a flexible plastic tube. Air is distributed to the head, trunk and extremities of the worker. The supplied air serves for breathing and for cooling of the body (prolonged work in a protective suit is rather strenuous!). At high ambient temperatures extra cooling equipment may become necessary in order to refrigerate the supplied air. Of concern is the length of the hose because increasing its length increases the inlet pressure that must be supplied. This sometimes constitutes a problem.

[7] Radiation and Contamination, Radiation Protection chapter RP-2, https://de.scribd.com/document/184818297/RP-2-Radiation-and-Contamination. Last visited on 16.09.2020

For various degrees of tritium surface contamination, the following protective equipment has been recommended [Car91]:

- at $> 37\,\mathrm{kBq\,m^{-2}}$ double gloves, disposable coverall and boots over basic protection clothing which consists of underwear, coveralls and shoes worn only in radiation areas,
- at $< 1.85\,\mathrm{MBq\,m^{-2}}$ as above but with an air supplied respirator and
- at $> 18.5\,\mathrm{MBq\,m^{-2}}$ air supplied plastic suit with a disposable over suit.

The type of confinement for activities with tritium depends not only on the tritium inventory but also on size and configuration of the primary system requiring protection. A few commonly employed options are discussed below.

In addition to the implementation of confinement barriers, several administrative measures such as limitation of tritium inventory, restrictions on access time, working procedures, posting of contaminated areas, etc. can significantly contribute to further reduce the doses of workers.

Protective or anti contamination clothing is used when there is free radioactivity or radioactive particles and there is need to prevent spreading of contamination by shoes or garnments into clean areas. A mask may serve to preclude the inhalation of radioactive paricles.

4.2.1.1 Tent

In the event of maintenance, repair, corrective measures or replacement work only possible with open glove boxes all gaseous tritium must first be transferred from the primary system into a getter bed and stored safely in solid form isolated by two valves. Repair or maintenance activities on a primary containment must be performed under a strong directed stream of air, which sweeps through the open glove box and subsequently exhausts through a Central Tritium Retention System in once-trough mode before being release into the environment.

A **flexible ventilation duct** connected to the room exhaust ("elephant trunk") operated by the negative pressure system of the tritium handling facility, is frequently used, eventually together with a tent and a plastic canvas on the floor, when equipment of low or potential contamination by tritium must be exposed to ambient air for working purposes [Gen96]. A strong stream of air into the stack provides the necessary dilution in a once-through mode to reduce airborne concenration of radioactive species. Advantage of this procedure is that tritium can be removed efficientlyfrom

the potential source when the trunk is placed strategically in its vicinity. Gas sucked by the "elephant trunk" is passed across a Tritium Retention System before it is released into the environment via stack. Because the stack is monitored by radiation protection personnel this is one more though not very specific option to keep track of contaminations by tritium. Tritium contamination can also be detected at an early stage with one or more ionisation chambers positioned strategically in the vicinity of the place where the maintenance/repair/replacement work takes place. Depending on the anticipated activity level, personnel should at least wear adequate protective suits, disposable gloves and disposable shoe covers to avoid contamination spread and protect their own clothing. During the whole operation, which should be carefully planned in advance, the assistance of radiation protection personnel should be secured.

A useful alternative to the flexible ventilation duct consists of a **portable tritium clean-up system** such as developed and demonstrated successfully during the course of several years by Maienschein et al. [Mai92c] and Reitz et al. [Rei94] at Lawrence Livermore National Laboratory. The device is based on standard technology comprising a preheater, a catalytic oxidation step maintained at 720 K and a water removal step consisting of an adsorber bed containing 15 kg of zeolite 5A. Ion chambers control the radioactivity at the inlet and outlet. The whole arrangement is mounted inside of a portable cart that can be rolled into place and connected to the equipment requiring decontamination. It was designed for a nominal flow rate of $30\,\mathrm{l\,min^{-1}}$ and a decontamination factor of more than 1000. The portable system can be operated in one of three modes: i) closed loop mode only through the clean-up system itself (for instance to heat up or cool down the catalyst bed), ii) closed loop after integration into the apparatus requiring decontamination and iii) once-through mode exhausting into the facility ventilation and from there to stack.

In summary, the portable clean-up system constitutes a simple, quickly adaptable, compact, effective, versatile and reliable complementary solution.

4.2.1.2 Hood

Experiments or analytical measurements with liquids or solids of very low tritium activities are most conveniently performed in hoods which draw a strong stream of air from the laboratory and exhaust this stream via stack. The effectiveness of the directed air stream can be verified with a piece of tissue paper in the hand of an operator. Typical activities with open radioac-

tivity in a hood are weighings, aliquotings and dilutions in preparation of liquid scintillation counting, cleaning of slightly contaminated materials in an ultrasonic bath, chemical etching of tritium-contaminated metal specimens, wet analytic chemistry, etc. Activities in a hood require painstaking cleanliness in order to prevent spreading of contamination or radioactive dust. Wearing of disposable gloves is indispensable to prevent incorporation of tritium into the body via the skin.

4.2.1.3 Glove box

Glove boxes designed for handling large quantities of tritium are high integrity modular enclosures fabricated from welded stainless-steel with an appropriate number of windows and glove ports such as needed for the intended work. Corners and edges of glove boxes are rounded and stainless-steel surfaces polished to provide a smooth, easy to clean surface. Windows, usually of poly carbonate, are sealed to the glove box with soft rubber gaskets to achieve the high tightness required to meet the mandatory low leak rates.

The ideal average temperature inside of glove boxes is $(295 \pm 2)\,\mathrm{K}$. At this temperature permeation losses through the gloves are small and the instrumentation is exposed to a mild environment. Glove boxes should be equipped with an appropriate number of monitors and alarms. Monitors shall be compatible with the glove box atmosphere, easy to calibrate and be comfortably accessible for maintenance.

To cope with insidious releases and possible accidental releases of tritium into the first confinement adequate provisions must be taken for the removal of tritium-bearing species from the glove box atmosphere. Removal can be accomplished either with a Central Tritium Retention System serving several or all glove boxes in the tritium-handling installation or with a Dedicated Tritium Retention System adjacent to a glove box which operates in conjunction with a Central Tritium Retention System.

To minimize tritium leakage into the Controlled Area (fairly air-tight rooms) during routine or anomalous events a Central Tritium Retention System is employed in large tritium-handling facilities to remove tritium from the glove box exhaust stream before it is released into the environment. In the Central Tritium Retention System molecular tritium isotopologues and tritium-bearing hydrocarbons are first oxidized catalytically on a heated noble metal catalyst and converted into tritiated water vapour and carbon dioxide. Generated HTO is adsorbed

on a molecular sieve bed installed downstream of the catalytic reactor. Once saturation of the adsorber bed is approached, the bed must either be reactivated *in situ* or replaced by an activated bed. The sequence conversion into HTO and removal of this species on an adsorber bed can be accomplished with decontamination factors of about 10^4. Tritium Retention Systems additionally sustain sub-atmospheric pressure (4 - 7 mbar) inside of glove boxes [Sch91a; Won92].

In the event of a tritium spill, the affected retention systems at **TLK** will rise automatically the temperature of the noble metal recombiner in order to achieve substantial enhancement of hydrogen and hydrocarbons (especially methane) removal. In case of glove rupture, a forced flow of $50\,m^3\,hour^{-1}$ laboratory air to the Central Tritium retention system is maintained until remedy is provided [Sch91a; Won92].

Other tritium-handling institutions like **SRS** opted for an isolation of the accidentally contaminated glove box in order to avoid spreading of contamination to other glove boxes. The isolated glove box can be subjected to accelerated clean-up by circulating the affected nitrogen gas through a dedicated secondary stripper [Heu92a; Heu92b].

At **JET** [Won92; Sab01], a two stage recombiner sequence was implemented. Of these the second one was operated at high temperature to assure rapid oxidation of more resistant hydrocarbons. During tests with 1 % hydrogen and 1 percent methane in air across the two recombiners at temperatures of 413 and 773 K, respectively, the exhaust concentration of methane was found to be less than 10×10^{-4} % and that of hydrogen even much lower.

The selection of a glove box atmosphere, e.g. air or inert gas, depends primarily on the inventory of flammable gases, flammable liquids, easily oxidizable solids and from the envisaged activities with tritium:

- In case of primary systems containing small inventories of hydrogen isotopologues, other combustible gases, or gaseous tritium-bearing species, the preferred glove box atmosphere is **air** because of the less-demanding operation and comparatively lower equipment and operation costs.

- For primary systems containing elevated inventories of tritium and even more so in case of the concurrent presence of large inventories of ignitable gases or other highly reactive materials the preferred choice is an **inert gas atmosphere** like nitrogen or argon. This important safety measure addresses scenarios such as: i) considerable spill of hydrogen

isotopologues into a glove box developing into an ignitable glove box atmosphere, ii) leak[8] of glove box air into a good-sized primary containment initially containing a substantial inventory of hydrogen isotopes (or other ignitable gases) operated at pressures below that prevailing in the glove box or iii) air into a primary containment enclosing large amounts of a highly reactive solid material (e.g. fine getter powder) heating up to rather high temperatures in an exothermic oxidation reaction. In the first two cases, a dangerous large volume of a gas mixture containing more hydrogen (or any other burnable gas) than the corresponding explosion limit may result inside of a vessel or a glove box. In the third case, damage of equipment on the ground of exceedingly high temperatures is conceivable. Clearly, in all these events only an inert gas atmosphere provides "rock solid" protection against the potential development of a dangerous situation. One more though less compelling reason for replacing air by nitrogen or a noble gas, is that a significant spill of tritium into a glove box containing air may conduct to considerable partial pressures of tritiated moisture contaminating the inner walls, equipment, and electrical cables of the glove box for a prolonged time. Tritiated water permeating across rubber gloves into the skin of operators is considered to be a noteworthy radiation hazard.

To guarantee efficient catalytic oxidation of hydrogen and hydrocarbons possibly released into the inert gas atmosphere of a glove box a small partial pressure of oxygen must be sustained within a certain concentration range at all times. This is accomplished with a control system that constantly regulates the oxygen content in the nitrogen atmosphere within set point values. To assure quantitative oxidation, the range must be such that oxygen is at all times present in excess concentration to that of all tritium-bearing species that may potentially be released.

An important application of glove boxes containing an inert gas atmosphere is to preclude the oxidation of getters or other materials of reactive surface towards oxygen or moisture. To achieve an extremely inert atmosphere, i.e. very low levels of moisture and oxygen, habitually a sacrificial scavenging hot metal getter bed is used which reacts with hydrogen, moisture and other trace gases to form metal hydrides, oxides, etc. While nitrogen is a satisfactory cover gas choice from the point of view of safety and costs, it is not compatible with all purifying

[8] An air leak into a primary containment maintained at negative pressure with respect to that in the glove box can take place in case of material fatigue, break of a capillary line induced by vibrations such as generated by a pump, loosening of a connection, etc

getters, particularly when elevated temperatures are necessary to accelerate the kinetics with low molecular weight hydrocarbons. Under these conditions the reaction of the getter with molecular nitrogen may give rise to disproportionate getter consumption.

Obviously, noble gas glove boxes of highly pure atmosphere will always require a dedicated Tritium Retention System. To keep oxygen and moisture concentrations at the lowest possible level the glove box must be exceedingly leak-tight. This measure is needed to minimize irreversible consumption of active getter material. Tritium retained by the getter is usually recoverable by a thermal procedure. Exhausted getter can only be given to waste after full tritium recovery and complete oxidation. The degree of tritium removal and the completeness of oxidation needs to be verified before the material can be accepted as waste.

For the retrieval or introduction of medium-sized equipment, chemicals or small components most glove boxes are equipped with a **transfer port or pass box**, that can be evacuated and backfilled with the same gas as that of the glove box atmosphere. The pass box must be furnished with valves as well as instrumentation that allows determination and control of pressure.

Total leak rates of glove boxes should be lower than $0.1\,\mathrm{vol\%\,hour^{-1}}$ [Sch91a; Yam02]. Leak rates are determined at a pressure in the glove box of 10 mbar below ambient. Assembled glove boxes shall be tested in combination.

A useful and rather complete check list of the many issues that need to be considered when designing and manufacturing a glove box has been compiled by Frigo [Fri95] from Argonne National Laboratory.

4.2.1.4 Caisson

Caissons are primary confinements tailored to accommodate components of particularly high or unusual dimensions such as distillation columns, large pumps, large vessels, electrolyzers, complete process lines, etc. Caissons are mostly custom made from commercial components. They must comply with the same design specifications that apply to standard glove boxes, i.e. permeation resistant, mechanically sturdy, be furnished with pass boxes, meet specified leak rates, possess refined inner surfaces, etc. In principle, caissons can be serviced by the same tritium retention systems as used for other primary confinements. Because the size of caissons is often fairly large, the accessibility demanded for manually operated valves, sampling points, equipment calibration and repair activities is quite challenging.

4.2.1.5 Dedicated large stainless-steel vessels

The Active Gas Handling System of JET is one of few large tritium-handling installations that has replaced most glove boxes by confinements consisting of large cylindrical or rectangular stainless-steel vessels. One of these vessels, built as all the others to ultrahigh vacuum standards, has a diameter of 1.2 m and a height of 5 m and carries the JET designation GC-KP. This confinement vessel houses a **preparative gas chromatographic** system. The other, whose diameter is 0.7 m and height 1 m, can be evacuated and contains **four uranium beds** of the type developed at JET (JET designation HISA) [Lae95; Lup95]. One more confinement, consisting of a rectangular box with dimensions of 0.8 x 1.3 x 2.9 m^3 (JET designation GC-GL) has inert gas atmosphere and is utilized to enclose a Metal Bellows and a Normetex **pump**, an 80 l **reservoir** and diverse **support equipment** [Lae99a]. These confinements are designed to retain tritium eventually leaked or permeated from primary components. Tritium can be removed from these confinement vessels either by sweeping with inert gas or by straight forward evacuation. As opposed to glove boxes or caissons, dedicated vessels are normally not equipped with glove ports because the enclosed equipment is exclusively operated remotely.

The fairly sophisticated GC-KP confinement vessel of JET is of special configuration. It comprises an upper and a lower confinement. The upper one, which is filled with a nitrogen atmosphere of about 75 kPa, is separated from the lower one by a bulkhead. It houses inlet and outlet heads, many valves, many flanges for electrical connections, process pipes, manifolds, diagnostics and connections to GC-Gl. Additionally, the upper confinement accommodates four palladium-filled columns, pipework connecting inlet and outlet heads mounted on top of the columns, ring manifolds and a 500 l reservoir [Bot88; Lae95; Lae99a]. Each column is furnished at the inlet with a flow meter, a downstream pressure regulator, a set of thermocouples and at the outleet with a catharometer, a pressure gauge, several thermocouples, an upstream pressure regulator and an ionisation chamber. Even though by design the columns can be heated up to 573 K using recirculating silicon oil as heat transfer medium, after it was experimentally observed that a lower temperature, i.e. 473 K, sufficed for column conditioning, the full temperature range was no longer utilized. The oil, which is recirculated through concentric mantles around the columns, is supplied to the outer tubes via flexible metal hoses placed in a lower evacuated compartment. For good heat transport the columns are separated from the mantles by a helium

filled gap of only about 1 mm. Since there is no direct contact between the column and the oil there is no concern about contamination of oil by tritium. Evacuation is necessary to minimize heat losses.

Analogously, the **gas chromatographic analytical system** of JET is also confined in a protective metallic vessel [Lae93]. The confinement encloses as main components three gas chromatographic columns, a methanizer, a thermal conductivity detector, a flame ionisation detector, a flow proportional counting detector, compression capillaries, three Valco valves as well as numerous other valves. An additional column, installed outside of the main confinement in a confinement of its own, is heated externally by an oven. One more column also placed outside of the main confinement is used for the separation of hydrogen isotopes. This column is submerged in a Dewar containing liquid nitrogen. Pertinent mass flow controllers and pressure regulators are all installed outside of the confinements. Mass flow controllers and pressure regulators are all installed outside of the confinement.

The above detailed descriptions of two diverse gas chromatographic systems at JET have been included here to illustrate how glove boxes can be replaced successfully by large sized vacuum-tight stainless-steel confinements. These vessels have functioned as secondary barriers for fairly complex processes dealing with high concentrations and even significant inventories of tritium. The work demonstrated that equipment mounted inside of practically non-accessible stainless-steel containments can safely be handled remotely. Principal advantage of this containment concept is that it opens the possibility of installing tritium process components in poorly accessible zones of the machine and close to where they are needed. Drawbacks of stainless-steel confinement vessels are i) no visual contact with the equipment, ii) difficult and cumbersome access for calibration, repairs or replacements and iii) eventual spread of contamination when the latter becomes necessary.

4.3 Design of glove boxes and peripheral auxiliary equipment

4.3.1 Gases for the operation of glove boxes

Routine and abnormal operation of glove boxes necessitates regular external supply of gases to perform activities such as i) maintain the atmosphere of glove boxes at constant pressure and chemical composition; ii) actuate pneumatic valves; iii) purge sections for the entire primary system, single components, or the glove box airlock; iv) regenerate adsorber beds adjudicated to primary systems; v) carry out chemical reactions; vi) reactivate catalysts or getter beds; vii) support analytical measurements; viii) prepare gaseous mixtures; ix) condition waste; x) carry out calibrations; xi) operate in-bed calorimeters, etc.

4.3.1.1 Gases for the operation of glove boxes

Reliable, uninterrupted external supply of gases needed in significant amounts such as nitrogen, argon, helium or oxygen is usually accomplished with a battery of compressed gas cylinders placed outside of the tritium building (other options are also possible). A well-ventilated cabin, appropriately protected from the environment during all seasons and easily accessible for replacement of empty cylinders equipped with conventional control and safety instrumentation, is required.

For the supply of dry nitrogen to glove boxes sometimes the boil-off from liquid nitrogen tanks is employed [Sch91a]. This nitrogen is highly dry and readily available.

Regardless of whether pressurized cylinders are placed inside or outside of the tritium-handling facility, a contamination of the cylinders by retro-diffusion of tritium may manifest during refilling. This is a matter of concern. Therefore, to deal with this issue, reliable administrative and technical measures as well as analytical procedures need to be developed.

4.3.1.2 Gas for the operation of pneumatic valves

Remotely actuated pneumatic valves may be operated with air or nitrogen from a service line manifolded to a number of glove boxes or from gas cylinders placed close to the glove box. Gas cylinders are needed for instance to actuate large on/off valves requiring pressures higher than typical for a service line.

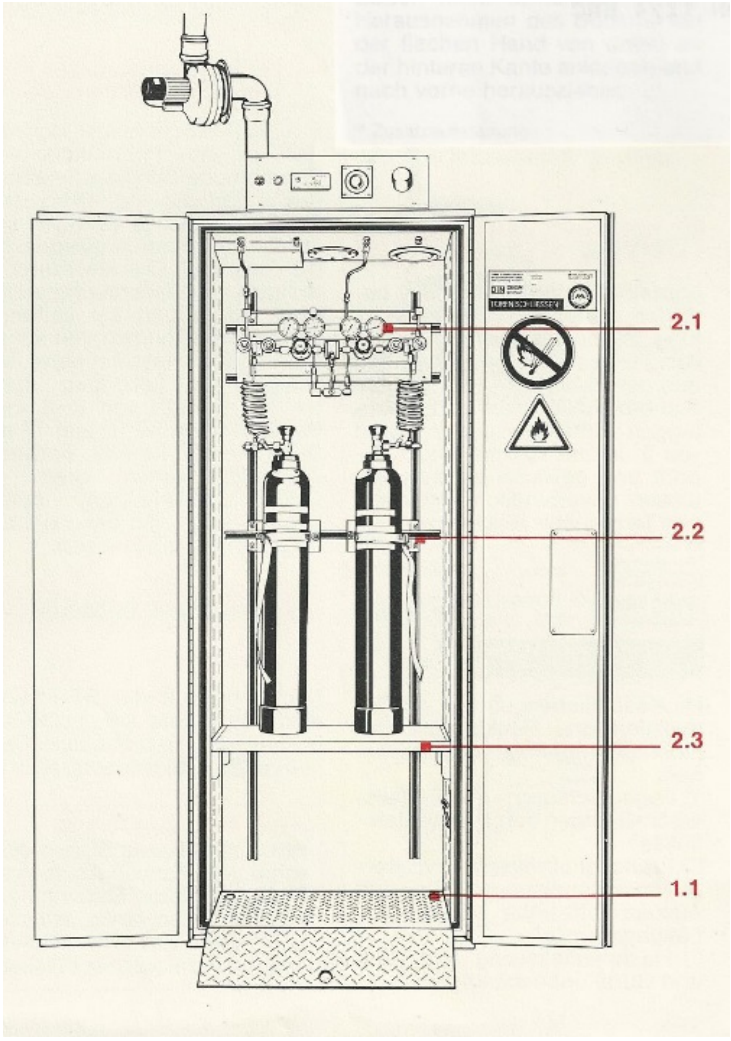


Figure 4.7: Safety cabinet for pressurized cylinders used at TLK (Düperthal).

In view, that gases actuating pneumatic valves do not come in direct contact with tritium, the risk of contamination of external gas supplying pressurized cylinders is minimal.

4.3.1.3 Gas supply to primary systems

Gases, particularly if poisonous and/or burnable, should be kept in special **safety cabinets** of the kind depicted in Fig. 4.7 and described in DIN 12925. For convenience, these cabinets are installed in the vicinity of glove boxes. Fully metallic cabinets are provided with fireproof doors and designed for easy cylinder replacement. Safety cabinets require venting. They are customarily equipped with several manometers, pressure regulators, and devices that allow firm fastening of the pressurized cylinders at adjustable heights.

Special gases needed for analytical determinations or chemical/physico-chemical measurements performed within the frame of research activities may be supplied to primary tritium systems from the inside of glove boxes. For such **exceptional cases**, small well-known quantities of gas can be supplied from small all-metal containments or so ccalled lecture bottles equipped with a pressure control. A detailed safety analysis report on which the Authorized Supervisor can base its approval is usually demanded. The report should address topics like chemical interaction of the supplied gas with tritium including potential formation of hydrogenous polymers or other solids, explosion risk, possible pressurization of the primary system or of the glove box, possible degradation of catalysts also in the event of a spill into the glove box (impairment of the Tritium Retention Systems), corrosion potential, internal/external contamination of the lecture bottle, etc. If necessary, accompanying administrative measures shall be implemented.

To permit safe connection, removal, and replacement of gas supplying containments, provisions for the evacuation of lines as well as adequate pressure and vacuum measurement instrumentation (leak test) need to be available.

4.3.2 Tritium removal systems for glove boxes

Principal functions of Tritium Removal Systems are to constantly reduce the concentration of tritium in the air or inert gas constituting the atmosphere inside of confinements while simultaneously maintaining the prevailing sub-atmospheric pressure. In addition, a Tritium Removal System must reduce at enhanced rate the concentration of tritium in the atmosphere of a glove box in the event of a tritium spill.

The layout of a Tritium Retention System depends largely on whether the atmosphere is air or chemically inert gas containing (or not) a small partial pressure of oxygen.

For the configuration of tritium confinement systems several issues require evaluation and decisions. They are:

- Type of atmosphere? When explosions can be ruled out, the most convenient atmosphere is air in combination with a catalyst/adsorber retention system. If formation of an explosive mixture is conceivable, nitrogen containing a small partial pressure of oxygen together with a catalyst/adsorber retention system is the safest option. In the event that oxygen- or moisture-sensitive materials are handled together with tritium-bearing species or when

there is potential for explosion in small tritium experiments performed in standalone glove boxes a good atmosphere option is inert gas. In such a case, oxygen, moisture, and tritium can be scavenged effectively employing a hot metal getter bed integrated into a clean-up loop of the glove box.

- Measures leading to an optimal confinement configuration include minimization of dead spaces, estimation of the most effective atmosphere turnover to keep potential contamination by tritium at low level, optimized arrangement of the purified gas inlet pipes and contaminated gas outlet pipes inside of the glove box, etc.
- Evaluation and mitigation of the impact of single components installed in the confinement on the removal efficiency of tritium (heat load, obstruction of gas re-circulation, tritium adsorbing surfaces, tritium sorbing materials, surfaces reacting with tritium, etc.).
- Evaluation of the optimum concentration ranges of oxygen and moisture in the glove box atmosphere.
- Decision on whether minimization of oxygen and humidity intrusion into the glove box is necessary.
- Decision on the most effective clean-up procedure, i.e. continuous re-circulation or batch once through. When stand-by once-through emergency systems are chosen, a temperature regime significantly above ambient may have a considerable impact on utility (permanently heated catalyst for constant rapid readiness) and capital costs (heating and cooling equipment) (see [Bix74]).
- Number, location and size of pass-throughs.
- Location and type of instrumentation.

4.3.2.1 Air atmosphere

Tritium Removal Systems servicing glove boxes confining an air atmosphere generally use a combination of noble metal catalyst (or an oxidizer catalyst like copper oxide or Hopcalite) and a drying agent consisting of molecular sieve [Bix74; She77b; Fol78; She79]. Under these conditions, molecular hydrogen, hydrocarbons, ammonia, and carbon monoxide are fully oxidized into water,

carbon dioxide, and other products provided the temperature is sufficiently high. For rapid oxidation at high conversion of all tritium-bearing species, the optimal catalyst temperature has been determined to be in the range 620 - 770 K. A high temperature is needed to make certain that methane, the hydrocarbon most resistant to oxidation, and all the other tritium-bearing species are rapidly and efficiently converted into carbon dioxide and water. Strong heating is also necessary to maintain water adsorption by the catalyst support at the lowest possible level. To protect the catalyst, all species that eventually could lead to the formation of acids, should be avoided. The feed gas to the catalyst bed must be pre-heated to assure effectual conversion and the gas effluent from the catalyst bed must be cooled down to less than 303 K to optimize adsorption of water while preventing migration of already adsorbed water and its eventual release. The adsorber used was zeolite 13X. It was conditioned by flowing moist laboratory air through the adsorber bed until the moisture content of the downstream gas was equal to that of the laboratory. Objective of this procedure was to saturate the adsorber with respect to the laboratory air moisture. Adsorber beds conditioned by this technique were found to retain efficiently tritiated water generated by catalytic oxidation.Further advantages are that the adsorber does not need to be dehydrated and homogeneous moisture levels can be sustained throughout the recirculating air loop.

The described oxidation-adsorption technology is robust and well documented. Its effectivity has been widely demonstrated in numerous tritium installations throughout the world. Drawbacks are i) conversion of molecular tritium-bearing species into the more radiotoxic tritiated hydrogen oxide form and ii) recurring necessity to regenerate or replace the molecular sieve beds and eventually oxidizer catalysts like Hopcalite.

Some experimental results on i) the identification of suitable catalysts, ii) optimized detritiation process conduction, iii) possible alternative detritiation process options, and iv) several procedures for on line and off-line regeneration of adsorber beds are described below.

Aiming at the development of an **Emergency System, Mound Laboratory** contracted Engelhard Minerals and Chemicals Corporation to construct a prototype catalytic hydrogen conversion system operated at a flow rate of $28.3\,m^3\,min^{-1}$ and designed to demonstrate a decontamination factor of 1000 for the oxidation of molecular hydrogen at very low concentrations in air, e.g. 0.5 [ppm] [Bix74]. The kinetics of the catalytic oxidation of hydrogen at such low concentrations had not been investigated previously. Tritium was selected instead of hydrogen for

the investigation because of the very high sensitivity with which this species can be detected and determined quantitatively. Experimentally, a **single pass** and a **closed loop** mode of operation were compared in order to determine decontamination factors for elemental tritium (HT) in the presence of traces of tritiated organic volatiles (presumably from pump oil degradation) diluted in air (or in any other gas mixture containing sufficient oxygen). For the conversion into water a catalyst from Engelhardt type A-16648 consisting of platinum on activated alumina was chosen. The decontamination factor (DF) achievable in single path mode with a mixture consisting of 1 ppm tritium and a tritiated hydrocarbon concentration of approximately 0.2 ppb in air was claimed to be 3.3×10^6 when the recirculating flow rate was $61.1\,\mathrm{l\,min^{-1}}$ and the average catalyst temperature 799 K [Bix74], and also [Min80; Jam88]. This DF, which is surprisingly high, may be explained by the experiment conduction. Single pass experiments with the catalyst proposed by Engelhard revealed that at 450 K or below the specified conversion of 99.9 % could not be attained. The consequence for an Emergency System would have been to maintain constantly the catalyst at a temperature higher than 500 K to keep the system in continuous state of preparedness. Such uninterrupted heating is, however, associated with significant equipment costs and substantial heating/cooling costs when compared with operation at ambient temperature but in recirculation mode. Hence, in subsequent experiments the recycling mode was examined more closely. With the finally implemented solution consisting in recycling contaminated room air via the tritium retention system and back into the contaminated room, a decontamination factor of about 1000 could be demonstrated. The merits of once-through processing and exhausting detritiated gas directly into stack on one hand with processing in recirculation mode with controlled gas release downstream and compensation of the discharged gas by introduction of fresh air into the room being detritiated, on the other, are discussed in detail in a paper by Bixel and Kershner [Bix74].

Comprehensive kinetic data describing the oxidation of tritiated hydrogen and tritiated hydrocarbons in the presence of a precious metal catalyst were reported by Bixel and Kershner [Bix74]. The rate of oxidation of molecular hydrogen over a palladium catalyst at 450 K was found to be first order, with a rate constant given by the expression

$$k = 2.27 \times 10^5 \exp\left(\frac{-29.7\,\mathrm{kJ\,g^{-1}\,mol^{-1}}}{RT}\right) \mathrm{l\,s^{-1}l_{catalyst}^{-1}}\ .$$

Values of the constant k were determined to be 1.4 and $85.0\,\mathrm{l\,s^{-1}l^{-1}_{catalyst}}$ at 300 and 450 K, respectively. Bixel and Kershner further demonstrated that tritiated hydrocarbons could be removed effectively at 588 K from an air stream using commercial Pd or Pt catalysts (whether tritiated methane was among the hydrocarbons was not explicitly mentioned).

Sherwood [She77b; She79] modified the reaction rate equation proposed by Bixel and Kershner to include diffusion and provided a theoretical treatment for the engineering design of packed-bed catalytic reactors and adsorbers. With respect to adsorbers, the shape of the equilibrium isotherm was of particular importance: if linear, the breakthrough curve was found to be spread out in time, and if of convex shape, the breakthrough curve was steep giving rise to a nearly step change (favourable). Figure 4.8 displays the unreacted fraction of hydrogen as function of catalyst temperature at several residence times and superficial velocities. The plot nicely summarizes and illustrates the reached conclusions: as apparent, the conversion of hydrogen into water on a Pt/Al_2O_3 catalyst bed is enhanced by increasing residence times. At a fixed flow rate, an increase in residence time must be balanced by augmented catalyst and pumping costs. Lower gas velocities in the bed contribute to reduce pumping costs but mass transfer and dispersion limitations reduce conversion.

Further general conclusions were gained from experimental investigations performed by Sherwood et al. [She79] and Longhurst et al. [Lon89]:

- The catalytic conversion of tritiated hydrogen into water in the presence of air is first order in tritium concentration, which is in good agreement with previous observations of Bixel and Kershner [Bix74].
- The performance of oxidation/water collection detritiation systems depends principally on the catalyst temperature and on the residence time of the processed gas in the volume occupied by the catalyst.
- Electron microscopic scans of the metal dispersed on the catalyst carrier revealed that the catalyst is deposited near the outer surface of the pellets, the concentration decreasing exponentially in radial distance from the outer edge of the pellet surface.
- The catalytic activity in the presence of air is independent of the moisture level in the glove box within the range 100 - 4000 ppm.

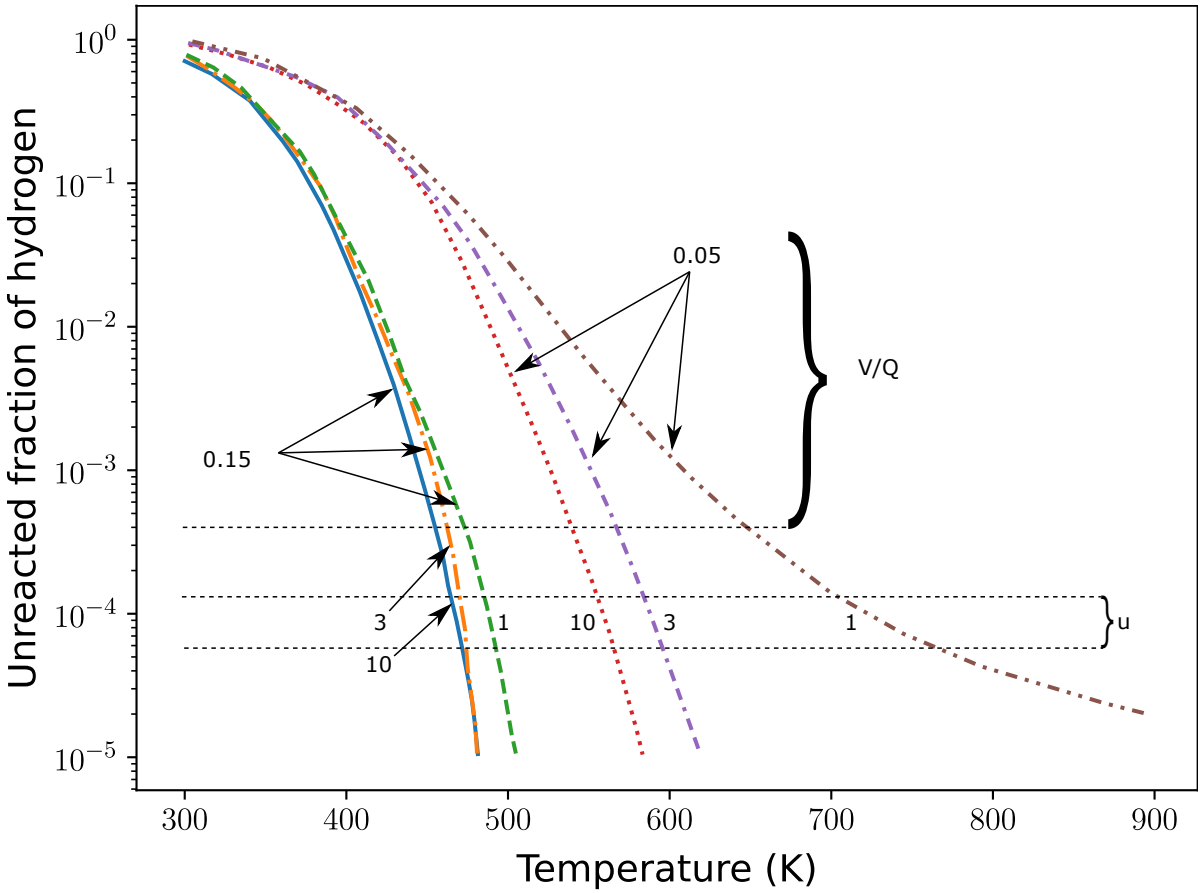


Figure 4.8: Unreacted fraction of hydrogen as function of catalyst temperature at several residence times and superficial velocities. The plot shows the influence of two residence times V/Q given in seconds (V stands for the reactor volume and Q for the flow rate), i.e. 0.05 and 0.15 s, and three superficial velocities, u, i.e. 1, 3 and 10 given in $\mathrm{m\,s^{-1}}$, on the catalytic efficiency. The three u values were calculated for HT on a Pt/Al_2O_3 catalyst of 3.18 mm diameter and a void fraction of 0.4 (after [Fol78]).

- The addition of hydrogen to the carrier gas has no significant enhancing effect. The only observed effect is that hydrogen swamping increases the catalyst temperature and consequently conversion into HTO.
- Water swamping or pre-moistening of the molecular sieve adsorber will probably reduce the fraction of HTO in the effluent gas at the expense of increased amounts of tritiated waste requiring disposal.
- A considerable range of detritiation factors has been reported for the oxidation/water collection process ($10 < \mathrm{DF} < 10^7$).

- The effectivity of the catalyst declines with time of exposure to air. Reactivation in a heated 100 % hydrogen environment effectively restores the initial catalytic activity.

Ellis [Ell92] compared reaction rates for the oxidation of methane (hydrocarbon most resistant to oxidation) in the presence of air on ten commercial catalysts, consisting of circular cylinders of Al_2O_3 impregnated with different active metals, under the same experimental conditions at temperatures in the range 573 - 873 K. Assuming the oxidation reaction of methane to be first order, rate constants K were obtained from the expression

$$K = \left(\frac{v_0}{V}\right) \ln\left(\frac{1}{1 - x_A}\right) \ ,$$

where v_0 is the total volumetric flow rate, V the volume occupied by the gas in the reactor, and x_A the conversion fraction of methane. Plots of $\ln K$ (hour^{-1}) vs T^{-1} (K^{-1}) showed catalysts impregnated with Rh, Pd, or Pt to be the most effective. At elevated temperature, i.e. 873 K, these three catalysts were practically equally efficient. However, upon exposure to air at 673 K, the catalytic activity of all three decreased with progressing time, the smallest decrease being displayed by the Rh catalyst. Increasing the reactor pressure from 100 to 700 kPa accelerated significantly the reaction rate, but this approach may be in conflict with the currently adopted safety philosophy for tritium handling systems of $p \leq 1$ bar.

Kobayashi et al. [Kob07b] addressed experimentally the special case of **SF_6** released accidentally from ITER Neutral Beam Injectors (NBI) into laboratory air. SF_6 is used as electrical insulator gas for the NBIs and may be released in case of a major accident-like fire. In order to examine the influence of this gas on the catalytic oxidation of hydrogen isotopologues by a noble metal catalyst a flow system was build comprising two pressurized cylinders one containing ambient air doped with 0 - 1 % hydrogen and another containing ambient air with 0 - 1 % SF_6. Utilizing mass flow controllers various gas mixtures were injected into two sequentially installed catalyst beds each containing catalyst of composition 0.5 % Pt on Al_2O_3. Of these two beds, the first one was held at 473 K and the other maintained at 773 K. Gas sampling was carried out before and after each catalyst bed. Analysis was performed by mass spectrometry as well as by gas chromatography. The results lead to the following conclusions: i) poisoning of the catalyst by SF_6 only takes place at temperatures exceeding 473 K, ii) at 773 K the water decontamination factor (DF) decreases from 10^4 down to about 50, and iii) the catalyst oxidation

performance fully recovers after about three days from the point in time at which the supply of SF_6 is interrupted. Gas analysis and examination of particles on the metal surface of the outlet of the second catalyst vessel by scanning electron microscopy-energy dispersive X-ray spectroscopy (SEM-EDX) delivered evidence for a mechanism based on the reaction of SF_6 with H_2O to generate corrosive and poisoning species such as HF, SF_4, SO_2F_2, SOF_2, and SO_2.

The removal rate of hydrogen released into a single empty glove box of **TLK** (volume of about 5.4 m^3) operated with an air atmosphere was investigated at catalyst temperatures within the range 373 - 723 K and constant re-circulation rates of either 30 or 60 $m^3\,hour^{-1}$ by Hutter et al. [Hut95]. The results of their experiments are plotted in Fig. 4.9. As apparent, the rate of hydrogen removal is essentially independent from temperature. Therefore, hydrogen is oxidized quantitatively on the catalyst already at 373 K or below, a conclusion that agrees well with previous studies of other researchers [Bix74; She77b; Cha88a; Cha91a]. The independence from temperature is also in line with a first order rate constant for the oxidation of molecular hydrogen in air proceeding with low activation energy such as reported by Bixel and Kershner [Bix74] (see also above). The rather pronounced effect of doubling the rate of re-circulation on the rate of hydrogen removal is a logical consequence of this. After about 40 min of re-circulation at 60 $m^3\,hour^{-1}$ the concentration of hydrogen has decreased by four orders of magnitude yielding a DF of more than 1000.

Several glove boxes or glove box combinations at TLK having volumes ranging from 6 to 32 m^3 operated with an air atmosphere are furnished with a dedicated de-tritiation system. Conventionally, all detritiation systems comprise i) a noble metal catalyst consisting of 0.5 % palladium on alumina, ii) an adsorber bed containing molecular sieves type 4A and 13X, and iii) a re-circulation pump. As in other tritium laboratories, the feed gas to the catalyst bed is pre-heated and the exhaust gas stream from each catalyst bed cooled to prevent warm effluent gas penetrating into the downstream adsorber bed already containing adsorbed tritiated water. Because these cooling systems are safety relevant, they are redundant. Consequently, in the event of a cooling breakdown an emergency cooling system takes over. Ionisation chambers installed at inlet and outlet positions of the detritiation systems serve to verify the effectiveness of the complete retention system. In most glove boxes, an open-air ionisation chamber monitors the tritium activity of the confinement atmosphere. The Central Tritium Retention System of the laboratory removes tritium from the exhaust gases of all primary systems and maintains a

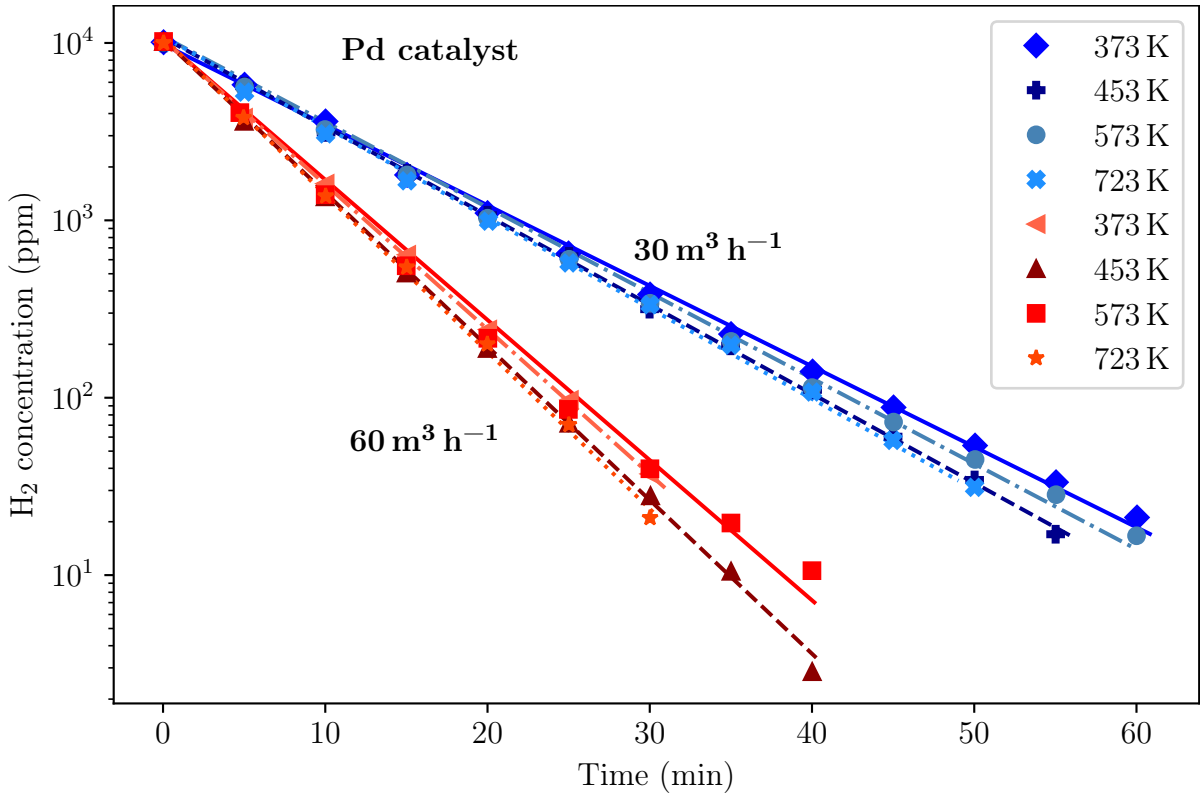


Figure 4.9: Tritium removal from a glove box with an adjacent Tritium Removal System. Effect of catalyst temperature on the time needed to reduce the concentration of hydrogen at re-circulation rates of either 30 or 60 m^3 $hour^{-1}$ in the presence of a palladium catalyst (after [Hut95]).

negative pressure in the glove boxes of experiments and infrastructure systems. To meet this demand, all boxes are interconnected via a ring pipe that extends throughout all the laboratory (see Fig. 4.5). Gases are re-circulated through this ring pipe with a rate between 110 and 120 $m^3\,hour^{-1}$. Blowers generate the specified negative pressure relative to ambient. Because of their safety relevance, these blowers as well as their related control valves are redundant. Constant operating conditions are achieved by controlled release of vent air to stack through the Central Retention System. Glove boxes are specified to a leak tightness of less than 0.1 $vol\%\,hour^{-1}$ and a negative pressure within the range 4 - 7 mbar. Under normal operation conditions, about five glove box atmosphere exchanges take place every hour.

In case of a leak or spill from a primary system into a **TLK** glove box operated with air atmosphere that leads to a rise in activity that exceeds the pre-established limit value of $5 \times 10^6\,Bq\,m^{-3}$ the temperature of the catalyst in the tritium retention system is increased automatically from 373 up to 453 K in glove boxes were tritiated hydrocarbons can be excluded and from 373 up to 723 K in glove boxes where this is not the case. Additionally, the rate of re-circulation through the affected glove box is raised up to ten glove box air exchanges per hour. The impact of these measures on the rate of tritium removal from the glove box are visualized in Fig. 4.9.

A glove box of 5.4 m^3 volume was installed at TLK exclusively for close examination and repair of highly tritium-contaminated defect components (particularly in case of emergencies). If required, the atmosphere of this glove box can be dried down to very low levels by recirculation through a large adsorber bed. Likewise, it is possible to reduce the concentration of oxygen in the glove box atmosphere to concentrations as low as 45 ppm by sweeping incessantly with pure nitrogen [Bes96]. Because such low oxygen levels can only be maintained with a flow rate of nitrogen of about 4 $m^3\,hour^{-1}$, expedient working is mandatory. .

At **TPL, Tokaimura**, Japan, glove boxes and laboratory air are serviced by three distinct detritiation systems, i.e. a Glove Box Purification System, an Effluent Tritium Removal System, and an Air Clean-up System. They are all based on the same tritium removal concept established in other tritium installations. The effluent Tritium Removal System is operated with a noble metal catalyst maintained at 773 K to warrant full oxidation of even the most oxidation-resistant hydrocarbon, i.e. tritiated methane. The Air Clean-up System was shown to be capable of

reducing the concentration of hydrogen in air from 1500 ppm down to 0.1 ppm in about 50 hours of re-circulation [Nar87].

TSTA was furnished with an automatically controlled **Emergency Tritium Clean-up System** designed to process room air in case of an accidental spill of tritium. It used a precious metal catalyst reactor for the oxidation of hydrogen isotopes into water. Water was collected by adsorption on molecular sieve. All routine gaseous effluents generated at TSTA were scrubbed from tritium employing a Tritium Waste Treatment System before release into the environment. To this effect, gaseous wastes were first collected in a holding tank, analysed, and then passed through a catalytic reactor for oxidation. The oxygen level in the holding tank was adjusted to guarantee full oxidation of the collected tritium-bearing species. After retention of the generated water, the purified exhaust gas was released into the environment.

As in other comparable tritium-handling facilities, the Exhaust Detritiation System installed at **JET**, Culham prevents tritium releases into the environment by detritiation of waste gases and provides sub atmospheric pressure in primary systems in the event of vacuum integrity loss of the Torus, the Fuelling Systems, or the Active Gas Handling Plant [Won92]. To meet these goals an airflow rate of $500\,\mathrm{m^3\,hour^{-1}}$ is maintained at ready-to-start mode. The JET detritiation system comprises a two stage recombiner in series (the first is operated at 413 and the second at 773 K) followed by three dryer units arranged in parallel (one in operation mode and the other two either in regeneration or in standby mode). The recombiner catalyst consists of activated alumina impregnated with 0.5 % palladium (BASF type RO-21). Air feed gas is first filtered from particles larger than 10 µm to 100 % and from particles larger than 2 µm to 50 %. Molecular sieves in the driers remove moisture from air to a dew point of about 213 K.

In supplementary experiments performed at AEA Harwell Laboratory, it was demonstrated that 1 % methane in the feed gas to the recombiner can be reduced to less than 10^{-4} % at the recombiner exit. This means that a DF of at least 10^4 is achievable (because the detection limit for methane was determined to be 10^{-4} %, the actual DF is probably higher). From further experimental observations, it was concluded that the oxidation of molecular hydrogen is not affected by the presence of catalyst poisons like Freon 113 and Halon 1211 (both chemicals are relevant to JET because they are used as coolants). Both poisons are of concern because they are known to react with hydrogen and water in the presence of a catalyst held at 773 K or higher

yielding HCl and HF. The oxidation rate of methane, on the other hand, was reduced appreciably by the presence of either Freon 113 or Halon 1211.

From a temperature profile determined in drier beds equipped with fifteen thermocouples separated from each other by a distance of about 100 mm it was possible to follow the de-sorption of water across the bed with progressing time [Won92] (see Appendix U). As water is de-sorbed, heat is carried away by by the air stream. This manifests by a temperature decrease of the carrier gas in the de-sorption zone. It is also possible to see that water is re-adsorbed in the dryed section of the bed downstream of the desorption zone (manifests by a temperature raise). With progressing regeneration, the characteristic temperature drop moves towards the drier exit. The results displayed in Appendix U make evident, that a simple temperature measurement can provide pertinent information on the evolution of the water breakthrough along a zeolite adsorber bed. The results also illustrate nicely that the temperature profile can be employed to distinguish between an unsaturated and a saturated drier bed.

A recent concept developed for the Tritium Retention Systems of **DEMO** contemplates i) **low temperature Detritiation Systems** (DS) for the retention of gaseous tritium as well as easily oxidizable high molecular weight hydrocarbons and ii) **high temperature Detritiation Systems** for the retention of oxidation-resistant hydrocarbons, e.g. methane [Eda16]. In view of the known downgrading effect of moisture on catalysts, hydrophobic $PtSiO_2$ catalysts were selected for both the low and the high temperature Detritiation Systems [Iwa11].

Iwai et al. [Iwa12] focussed attention on the case in which a tritium spill takes place simultaneously with a fire event. In such a case, the consequences of the generation of hydrocarbons from smoulder and/or combustion of diverse plastics such as low-halogen cables (they yield ethylene, methane, propylene, and benzene) on the performance of high temperature Detritiation Systems, needs to be examined. Under these conditions, the exothermicity of the oxidation of hydrocarbons could give rise to a sharp temperature increase in the catalytic reactor with possible negative consequences on safety. At elevated temperatures, rapid catalytic isotopic exchange reactions between tritiated hydrogen and hydrocarbons are conceivable leading among other to the formation of tritium-bearing oxidation-resistant hydrocarbons that could exit the low temperature catalytic reactor in sufficient concentration to constitute a safety hazard. Screening tests performed by Edao et al. [Eda16] employing a gas whose composition simulated that expected during a plastics and cable fire consisting of air carrier gas containing tritiated hydrogen,

moisture, and a representative mixture of saturated and unsaturated hydrocarbons provided the following preliminary results:

- The catalytic oxidation of tritiated hydrogen and the isotopic exchange reactions between tritiated hydrogen and saturated as well as unsaturated hydrocarbons at $< 403\,\mathrm{K}$ may be concurrent. When, however, these conditions prevailed a release of tritiated hydrocarbons was not observed. Therefore, oxidation reactions predominated over exchange reactions.
- With the exception of methane, most other tritiated higher saturated and unsaturated hydrocarbons present in plastic and cable fire-simulating gas undergo full oxidation in the low temperature Detritiation System. The ignition temperature was determined to be about 403 K.
- Hydrophobic catalyst´s maintained at 423 K were only slightly poisoned by hydrocarbons present in plastic and cable fire-simulating gas (hydrocarbons $\sim 1\,\%$).
- Feed gas saturated with moisture reverses catalyst poisoning
- Runaway temperatures induced by heat released from the oxidation of plastic and cable fire-simulating gas mixtures injected into the catalyst reactor at initial temperatures below 473 K were not observed.

Considerable volumina of tritium-contaminated gas may arise in large fusion installations like **ITER**, for which unusually large conventional catalyst/adsorber detritiation systems would be required[9]. To ameliorate this situation, Ito et al. [Ito92] and Hayashi et al. [Hay95b] proposed at TPL a novel and promising approach. The concept is based on the large permeation differences between hydrogen or water on one hand with those of nitrogen or air on the other across a **polyimide separation membrane** module. Feed gas is supplied by a large and powerful compressor and permeate gas extracted with a pump (see also section 2.12.1). Experiments were performed with a membrane having an effective permeation area of about $40\,\mathrm{m}^2$ at feed gas pressures of nitrogen or air up to 4 bar containing hydrogen and water at concentrations in the ranges 100 - 1000 ppm or 1000 - 10 000 ppm, respectively. Gradients between feed pressures in the range 1.6 - 3.5 bar and permeate vacua in the range 11 - 107 mbar were employed as

[9] Conceivably, the most severe accident at ITER would be the release of 100 g tritium into the $16\,000\,\mathrm{m}^3$ large stainless-steel cryostat, i.e. $2.2 \times 10^{12}\,\mathrm{Bq\,m^{-3}}$.

driving force. The effect of the feed/permeate pressure ratio at several feed pressures and of the temperature of the membrane on the recovered hydrogen fraction from nitrogen or air feed were studied parametrically. Tests performed at ambient temperature provided evidence that hydrogen can be recovered from air to more than 99 % and from nitrogen to about 97 %. The permeation rates of hydrogen and water were found to be comparable. A hydrogen isotope effect was non-discernable. Since the volume of tritium-enriched nitrogen or air permeating across a polyimide membrane is much smaller than the initial volume of tritium-contaminated gas and additionally the permeation ratio at ambient temperature can reach H_2/N_2 values as high as 160, the dimension of the tail-end catalytic oxidation/adsorption detritiation system can be downsized considerably. Even though the rate of hydrogen permeation through the module increases almost exponentially with temperature, it was recommended to maintain the membrane temperature at values not higher than 363 K to avoid membrane damage.

4.3.2.2 Chemically inert gas atmosphere

Two options for the removal of tritium-bearing species from inert gas glove boxes have been widely tested. According to the first option, nitrogen inert gas is used containing a small partial pressure of oxygen automatically maintained within a certain pressure range. The partial pressure of oxygen must exceed that necessary for the full catalytic conversion of all released tritiated hydrogen and/or hydrocarbons into oxidation products. Generated tritiated water is retained downstream of the catalytic step by an adsorber bed held at ambient temperature. As with retention systems of glove boxes confining air (see also section 4.3.2.1), the optimal catalyst temperature is within the range 620 - 770 K. The feed gas into the catalyst bed is pre-heated and the exhaust gas from this bed cooled before it is fed into the adsorber bed.

According to the second option, pure nitrogen or argon is used as glove box atmosphere. In this case, tritium-bearing species are scavenged by reaction with a hot getter bed. This approach is selected when, on top of the confinement of tritium, materials requiring protection from oxygen or moisture are handled.

In the following section the experience gained with tritium retention systems integrated into inert gas glove boxes are discussed.

4.3.2.2.1 Nitrogen or noble gas atmosphere containing a small fraction of oxygen

As already described, the oxidation of tritiated hydrogen and hydrocarbons released into an inert gas glove box is carried out on a precious metal catalyst and the generated tritiated water adsorbed on a molecular sieve bed maintained at ambient temperature. A low and approximately constant partial pressure of oxygen must be reliably regulated in the glove box atmosphere within a specified range to make certain that the ratio

$$\frac{O_2}{Q_2 + Q_2O} \gg 1 \quad Q = T, D, H$$

exceeds unity at all times.

Another frequently used oxidation catalyst has the composition 50 % MnO, 30 % CuO, 15 % Co_2O_3, and 5 % Ag_2O (other compositions have also been employed). This catalyst, known as **Hopcalite**, can oxidize molecular hydrogen and hydrocarbons in the absence of molecular oxygen. Advantageously, the exhausted catalyst can be regenerated under a stream of oxygen, but after repeated regenerations, the catalytic efficiency experiences gradual decline [Nis84]. Of importance for full and rapid oxidation of tritium-bearing species is the appropriate temperature. The temperatures at which McDonough [McD76] observed experimentally the full oxidation of gases like molecular hydrogen, aromatics, and low molecular weight hydrocarbons are displayed in Fig. 4.10. The most effective temperature for the oxidation of molecular tritium was found to be 523 K, that for the efficient oxidation of methane was significantly higher, i.e. 773 K.

Chabot et al. [Cha88b] investigated likewise the kinetics of removal of molecular tritium from dry pure nitrogen containing 4000 ppm oxygen in a 250 l stainless-steel vessel. The experiments were performed in closed loop modus employing a catalyst consisting of alumina support impregnated with either palladium or platinum and heated up to temperatures within the range 298 - 573 K. Tritium was introduced into the loop from a glass ampoule containing 2.6×10^7 Bq tritium and provided with a break seal. Generated water was retained with a cryo trap integrated into the loop and cooled with liquid nitrogen to a temperature of 93 - 98 K. A pre-heater was installed in front of the catalyst and a pre-cooler in front of the trap. Pd as well as Pt catalysts were found to remove tritium efficiently at ambient temperature down to mpc concentrations (mpc = maximum permissible concentration).

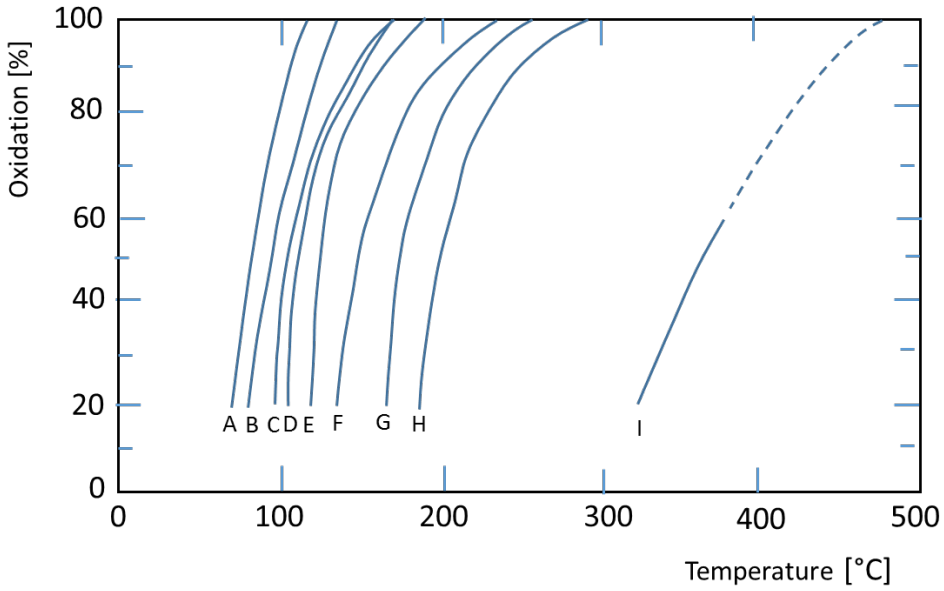


Figure 4.10: Oxidation efficiency of diverse hydrocarbons on Hopcalite as function of temperature. Assignments of the letters are: A = butene, B = hexane, C = acetylene and carbon monoxide, D = propylene, E = ethylene, F = butane, G = propane and hydrogen, H = ethane and benzene, and I = methane (after [McD76; Fol78]).

Both catalysts showed essentially the same tritium removal effectiveness. They displayed progressive loss of catalyst activity at **ambient temperature** (see also [She79]). What is more, at low catalyst temperature, i.e. below 373 K, the majority of the tritium remained adsorbed on the catalyst, evidently as HTO. When the temperature of the catalyst was increased up to 523 K, most of the moisture adsorbed by the catalyst was transported into the cold trap and the catalytic efficiency restored.

Heung et al. [Heu92a; Heu92b] interpreted the results of Chabot et al. [Cha88b] differently. These researchers postulated that at ambient temperature gaseous molecular tritium undergoes isotopic exchange with solid aluminum oxi-hydroxide groups according to

$$T_2 + 2\,AlO(OH) \longrightarrow H_2 + 2\,AlO(OT)$$

the tritium stripping mechanism being reversible and catalysed by the precious metal on the catalyst surface. This conclusion was reached after it was noticed that even when the reaction was performed under air instead of nitrogen (or argon) it still took place essentially without

formation of water. Decontamination factors as high as 10^3 were demonstrated by stripping depending on the concentration of tritium in the feed. To recover stripped tritium, it was possible to reverse the reaction by passing hydrogen over the catalyst. The retention mechanism proposed by Heung explains rather well the high concentration of tritium, which according to Chabot et al., had remained on the catalyst at low temperatures (see Fig. 4.11).

It is important to be aware of the fact that inert gas glove boxes contaminated with tritium may release tritium oxide and other tritiated species when opened to ambient air.

Every glove box or glove box combination at **TLK** operated with pure or oxygen doped inert gas (nitrogen, argon) atmosphere, is equipped with a dedicated de-tritiation system. These detritiation systems are standardized and available in three sizes, i.e. 15, 30, and 60 $m^3\,hour^{-1}$. They are housed in a cabinet placed alongside the serviced glove box. For large glove boxes, e.g. total volume 12 m^3, two de-tritiation systems can be installed in parallel. Main components of these systems are i) redundant noble metal catalysts in case of oxygen-doped atmosphere or redundant copper oxide/manganese oxide oxidizing catalyst (Hopcalite) beds in case of a pure nitrogen atmosphere„ ii) redundant molecular sieve adsorber beds, iii) ionisation chambers at glove box inlet and outlet, and iv) a re-circulation pump (see also section 4.3.2.1). The routine operation temperatures of the noble metal and the Hopcalite catalyst bed are 373 K and 473 K, respectively. These temperatures must be substantially increased if low molecular weight hydrocarbons are suspected. To detritiate the glove box atmosphere a stream is incessantly extracted, detritiated, and returned to the glove box. The feed gas into the catalyst beds is pre-heated and the feed gas into the adsorber beds cooled by gas conduction across heat exchange devices. The concentration of tritium in glove boxes is maintained at values of $\leq 4 \times 10^6\,Bq\,m^{-3}$.

Bell and Ballantyne [Bel91] worked out a **risk assessment** methodology for the Exhaust Detritiation System (EDS) of the AGHS of JET. The functions of this EDS are to i) remove tritium from the nitrogen purge gas of the AGHS valve confinements, ii) provide an air flow into the torus and AGHS openings during maintenance and emergency detritiation of the torus following a vacuum breach or over-pressurization, and iii) enable the AGHS to meet accident release targets and releases as low as reasonably achievable (ALARA) during active operation. Basic information for the assessment were the maximum tritium inventory in each physically separate unit, the time at risk, and the release frequency. With these data, the impact of the

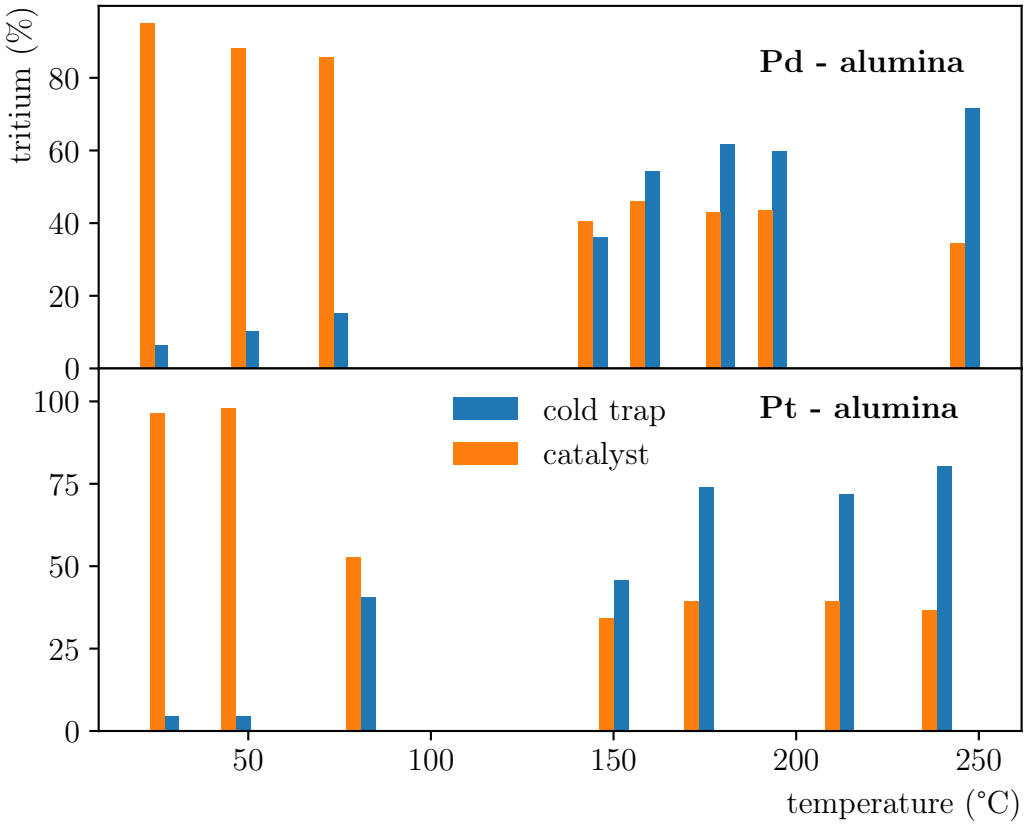


Figure 4.11: Distribution of the tritium activity between a Pd or Pt catalyst and the cold trap at several catalyst temperatures after completion of the tests (after [Cha88b]).

EDS reliability on accident consequences could be estimated. The results led to the conclusion that despite conservative assumptions for the failure rates all safety targets can be met.

Replacement Tritium Facility (RTF) at Savannah River Site (SRS) constitutes a good example for a facility requiring a rather large tritium retention system. RTF, which processes kilogram amounts of tritium each year, has been in operation since 1994 [Heu92a; Heu92b; Heu95b; Heu02] (see Fig. 4.12). Thirty glove boxes encompassing a sizeable volume of 800 m^3 serve to house all RTF relevant tritium processing equipment. The glove boxes have been separated into two groups, each supported by a primary stripper system of its own (P1 and P2). In order to recover all tritium normally released into the glove boxes each primary stripper system re-circulates nitrogen (containing 1 % oxygen) at a rate of 170 $m^3\,hour^{-1}$. The resulting

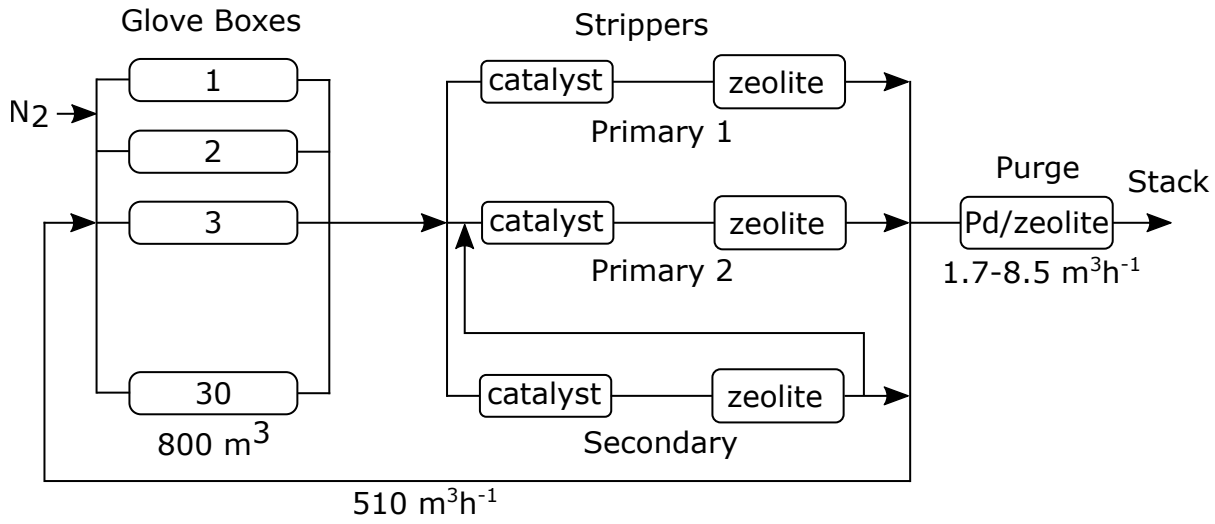


Figure 4.12: Block diagram of the two stripper systems of the Replacement Tritium Facility each servicing 15 glove boxes (after [Heu02]).

average nitrogen residence time in each group of glove boxes is about 2.4 hours. In the event of an accidental release of tritium into a single glove box, this box is isolated and a **secondary stripper** (SS) system normally on standby takes over. When this is the case, a reduction in residence time down to about 9 min takes place.

Each primary stripper system consists of a catalyst bed (residence time 1.5 s) and three smaller molecular sieve beds of which only one is on line; the other two are either in regeneration or on standby mode (see Fig. 4.13a). Every zeolite bed contains 104 kg of type 3A molecular sieve and every catalyst bed holds 130 kg of Engelhard Deoxo-D® (palladium deposited on alumina) catalyst maintained at 723 K. High temperatures are only needed when the presence of hydrocarbons is suspected. Otherwise, far lower temperatures suffice for the efficient removal of tritium [Bix74; She79; Heu92a; Heu92b]. For optimal processing, heat exchange devices preheat (pre-heater) the feed gas into the catalyst beds and cool (pre cooler) the feed gas into the adsorber beds. The impurity levels in glove boxes of nitrogen atmosphere are maintained at 1 % oxygen, 300 ppm by volume of water and less than $3.7 \times 10^3\,\mathrm{Bq\,cm^{-3}}$ of tritium.

Objective of **purge strippers** is to further reduce the concentration of tritium in purge nitrogen before it is released into the environment. A purge stripper consists of three smaller beds each containing 27 kg of zeolite type 4A impregnated with palladium and operated at ambient

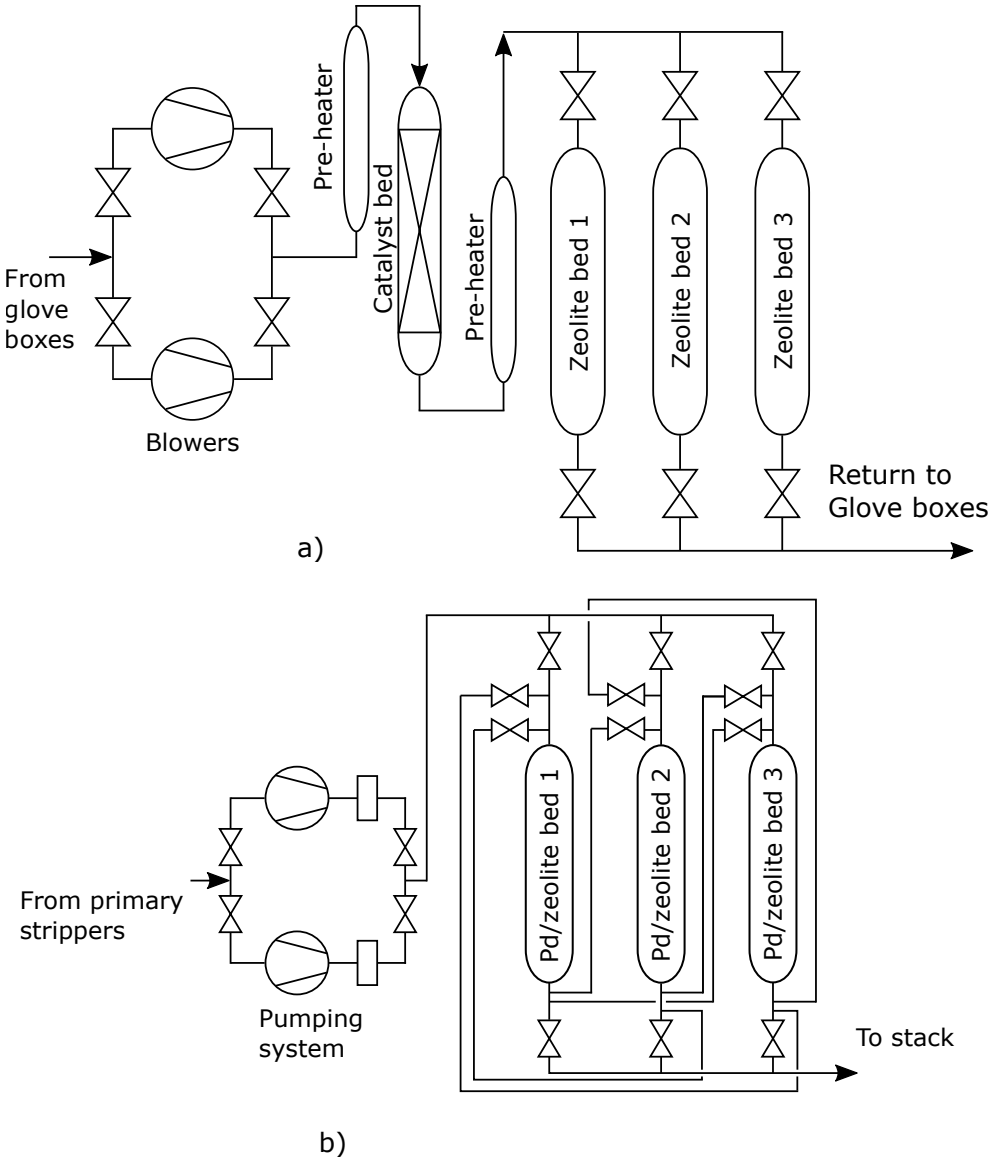


Figure 4.13: Flow diagram of the primary and secondary stripper systems of Replacement Tritium Facility (RTF) at Savannah River Site (SRS). The upper figure (a) shows the primary strippers (nitrogen circulated during normal operation in closed loop configuration). The identical secondary stripper is only used in case of a spill. Figure (b) displays the purge stripper flow diagram whose function is to further reduce the tritium contamination of the purge nitrogen (after [Heu92b]).

temperature (see Fig. 4.13b)). These beds combine the functions of the catalyst bed and the adsorber bed into a single one: palladium catalyses the oxidation of tritium and molecular sieve adsorbs the generated water. The purge rate, which is about $8.5\,\mathrm{m}^3\,\mathrm{hour}^{-1}$, is necessary to maintain the negative pressure and regulate the oxygen level in the glove boxes. Ion chambers that survey the concentration of tritium are located at the inlet to the catalyst beds, outlet of the

adsorber beds, and inside of the glove boxes. Two sets of pumps, each comprising a Normetex pump and a Metal Bellows pump connected in series, are available. Of the two pumping sets, one is in operation and the other on standby.

A simplified model describing the reduction of tritium in the glove box by the stripper system, is provided by the expression

$$\frac{C - C_e}{C_0 - C_e} = \exp\left(-\frac{Ft}{V}\right) ,$$

where C is the actual concentration of tritium in the glove box in $\mathrm{Bq\,m^{-3}}$, C_e the concentration of tritium at the outlet of the stripper in $\mathrm{Bq\,m^{-3}}$, C_0 the concentration of tritium in the glove box at time zero in $\mathrm{Bq\,m^{-3}}$, F the flow rate in $\mathrm{m^3\,hour^{-1}}$, and V the volume of the glove box in $\mathrm{m^3}$. The residence time is defined by the ratio V/F. For reasons described above, the ideal model generally gives a faster decrease in tritium concentration than observed experimentally. From the point of view of components and configuration the **secondary stripper** is identical to the primary stripper. It is only in operation during a major tritium release.

Heung and co-workers described the secondary stripper in detail based on an actual occurrence [Heu92a; Heu95b] (see Fig. 4.14). When an **accidental release** of tritium into a glove box takes place, the secondary stripper is taken automatically into operation. In such an event, the affected glove box is isolated and a fraction of the atmosphere circulated through the dedicated secondary stripper at substantially shorter residence time in the glove box, i.e. 8 - 9 min. By this procedure, the decontamination time is greatly reduced and - very important - spreading of activity into other boxes minimized. From a large tritium spill that conducted to a maximum glove box concentration of about $1.5 \times 10^{14}\,\mathrm{Bq\,m^{-3}}$ it was learned that after 150 stripping hours the tritium concentration in the glove box decreased to a bottom value of only $3.7 \times 10^{11}\,\mathrm{Bq\,m^{-3}}$. To reduce even further the tritium concentration in the glove box, i.e. back to „normal“ values of about $3.7 \times 10^{9}\,\mathrm{Bq\,m^{-3}}$, a decontamination of the inner surfaces was necessary. From these results it was concluded that the ideal stripping model required adaptation[10] to account for i) insidious releases from tritium-contaminated inner surfaces, ii) uncomplete mixing between stripper exhaust nitrogen and nitrogen in the glove box, and iii) background shifts arising from ionisation chambers of contaminated surface.

[10] While the model predicted decrease of activity after 2.5 hours down to $2 \times 10^{9}\,\mathrm{Bq\,m^{-3}}$ the actually recorded activity was much higher, i.e. $3.7 \times 10^{10}\,\mathrm{Bq\,m^{-3}}$.

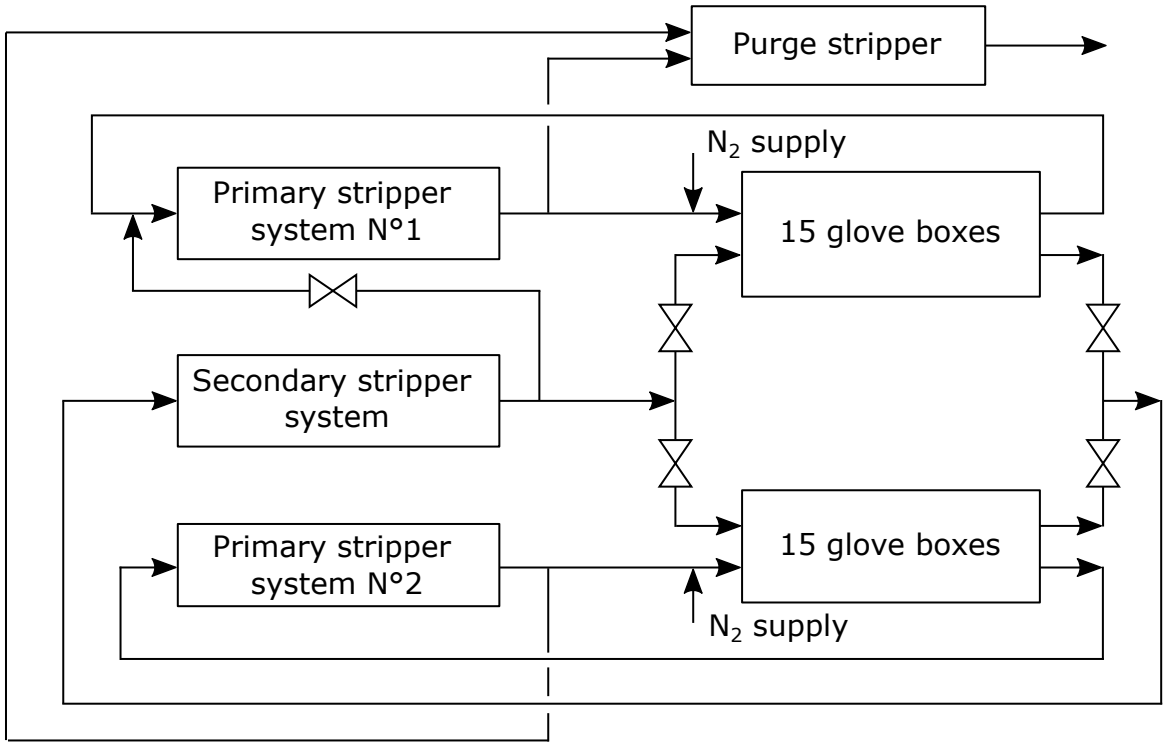


Figure 4.14: Flow diagram of the glove box stripper system at RTF (after [Heu92b]).

Remarkably, in spite of the large spill of gram quantities no appreciable release of tritium into the environment was registered. Likewise, ion chamber memory effects remained tolerable. In conclusion, when the large amount of tritium involved and the dimensions of the serviced glove box are taken into account, the design of the Replacement Tritium Facility is comparatively simple, highly effective, and cost saving.

The **Safety and Tritium Applied Research (STAR)** facility in Idaho Falls, which is authorized to handle a maximum of 6×10^{14} Bq tritium, has been equipped with exhaust/supply air blowers that maintain a negative pressure with respect to atmosphere in the building and grant, at the same time, at least six air changes per hour on a once-through basis [And02]. The output of the exhaust blowers is merged into a single duct outside of the building. This common duct is connected to another underground duct that conducts to a 76 m tall stack of the Material Test Reactor. The STAR facility is not equipped with backup power. All-welded leak-tight glove boxes constitute secondary containment to primary systems. The glove boxes are purged with dry nitrogen and furnished with ion chambers for early detection of leaked or permeated tritium. Only glove boxes using larger quantities of tritium are equipped with a dedicated clean

up system connected to the glove box via an overhead header. These clean up systems are of conventional type comprising redundant catalyst oxidizers and molecular sieve beds. They are only operated in emergencies. Ion chamber signals are used to open or close valves with the objective of incorporating or bypassing catalyst and molecular sieve beds. Accountancy is carried out by standard PVTc procedures.

4.3.2.2.2 Pure inert gas

Standalone glove boxes operated with a noble gas atmosphere (e. g. argon) have been developed to conduct work with oxygen- and/or moisture-sensitive materials [Shm93]. A successful approach to scavenge these impurities has been re-circulation of the cover gas through a heated metal or alloy getter bed. Glove boxes of this kind have also found application in research activities dealing with tritium. Gettering of species such as $O_2, N_2, Q_2, Q_2O, C_xQ_y, NQ_3$ (Q = H, D, T) eventually leaking into the glove box from a tritium-handling primary system or from the ambient circumvents oxidation of gaseous tritiated species into HTO. This is advantageous because of the i) particularly high radiotoxicity of HTO, ii) profuse and persistent adsorption of HTO on most surfaces, and iii) likely permeation of HTO across gloves (harmful to workers).

If nitrogen is selected as cover gas, a getter must be chosen that displays a very slow reaction with this gas. Otherwise, nitrogen will react with the hot metallic surface and progressively decrease its scavenging efficiency as well as absorption capacity. To cope with this problem, much effort has gone into the development of scavenger beds that react i) reversibly with hydrogen to form hydrides, ii) irreversibly and effectively with low concentrations of tritium-bearing impurities forming thermally stable nitrides, oxides, carbides, and "getter" tritide, and iv) only slowly and at elevated temperature with nitrogen. Of concern is also leaking of rapidly reacting air components like oxygen or moisture into the glove box. These species need to be effectively kept from penetrating into the glove box to prevent gradual hot getter deactivation.

Johnson et al. [Joh88] tested several heated metals like titanium sponge, zirconium sponge, uranium powder, zirconium : aluminum = 1 : 1 powder, and several tailored proprietary getters like SAES ST101 (84 % Zr + 16 % Al) and SAES ST707 (70 % Zr + 24.6 % V + 5.4 % Fe) within the temperature range 523 - 723 K and compared their respective benefits and deficiencies. The results revealed that titanium sponge, zirconium sponge, and SAES ST101 lost their activity towards tritium rapidly without recovering to an acceptable level even after conditioning at

elevated temperature. The only getter that provided satisfactory results was SAES ST707. The deactivation of hot metals and getter was attributed to an unidentified impurity - presumably sulphur - present in the glove box atmosphere in trace concentrations.

A good theoretical discussion on the applicability of cerium in fixed and fluidized bed reactors as chemical getter to scavenge tritiated contaminants such as HT and HTO (assumed initial activity 370 GBq m^{-3} or 3.8 ppm in a volume of 21 600 m^3) from an argon atmosphere has been provided by Maienschein [Mai76; Mai78]. Cerium is known to react with these species with high reactivity forming a hydride of low dissociation pressure (rather low even at 523 K). To achieve a DF of 20 000, i.e. reduction of the initial activity down to 18.5 MBq m^{-3}, it was calculated that about forty volume changes are necessary.

One more getter material manufactured by SAES Getters, Milano, Italy, and distributed under the designation ST198 (chemical composition: Zr_2Fe), was investigated rather comprehensively by Carnes[Car85] as well as by Shmayda et al. [Khe88; Hei88a; Shm92; Shm93]. This getter has a bulk density of 6.9 g cm^{-3} and a melting point in the range 1223 - 1373 K. The getter powder burns under air already at 673 K. ST198 was shown to scavenge effectively from glove box atmospheres both elemental and oxidized tritium at 573 K down to concentrations of approximately 3 MPam^{3}g$^{-1}_{\text{getter}}$. The reactivity of the getter could only be maintained at high level when the moisture content in the glove box was controlled to values below two ppm [Hei95]. In a screening test, in which 1.9×10^{10} Bq tritiated hydrogen was released intentionally into a 0.25 m^3 glove box, this species was efficiently removed in about 20 min. This corresponds to about seven system time constants. While molecular tritiated hydrogen is recoverable from the „exhausted“ bed to more than 80 % at 773 K, oxygen is bound irreversibly. An attractive advantage of ST198 is its inertness towards nitrogen at least up to temperatures of about 723 K. Hence, with limitations, ST198 is suitable for glove boxes operated with a nitrogen atmosphere. The optimal operation temperature for the getter was determined to be 623 K [Hei94b]. At this temperature, the removal rate of CO_2, CH_4, and H_2O is sufficiently fast while the rate of nitriding remains tolerable. Consequently, for a glove box containing nitrogen cover gas the temperature is critical: if too low, gettering of hydrocarbons, especially methane, is not sufficiently fast and if too high, the rate of nitriding becomes prohibitive, i.e. excessive getter consumption. The high efficiency of the getter is explained by evidence obtained experimentally, which indicates that carbides and oxides do not remain on the getter surface but rather diffuse into the bulk. If fast

removal of tritium-bearing methane's is required, a temperature close to 673 K was considered necessary. Because this temperature approaches that at which the getter begins to react swiftly with nitrogen, the best solution in such a case is to replace nitrogen by argon.

A drawback of ST198 is the rapid decrease of the purification factor with increasing hydrogen content of the bed. Therefore, provisions must be incorporated into the design of the tritium removal system for easy periodical replacement of exhausted scavenger beds by new or regenerated ones. Because metallic scavenger beds must be maintained at elevated temperature to achieve continued efficient purification, a downstream heat exchanger needs to be installed in order to keep the heat load to the glove box at acceptable levels. In view that **standalone inert atmosphere glove boxes** are operated in closed loop modus, it is necessary to furnish the glove box with a pressure monitoring and a control system to compensate for changes of ambient pressure [Shm92] (see Fig. 4.15). Bubblers providing overpressure protection to the glove box constitute an essential safety measure. Additional ancillary equipment of the tritium removal system are inlet and exhaust tritium monitors, a gas supply system, a hygrometer, a circulation pump, a flow transducer, and a bleed valve to the laboratory stack.

The scavenging efficiency of the getter bed is verified with tritium monitors installed upstream and downstream of the bed. As already discussed above, the rate at which the concentration of tritium, c, decreases with time can be calculated from the expression

$$\frac{\mathrm{d}c}{\mathrm{d}t} = \frac{F}{V}c \ ,$$

where F is the volumetric flow rate in $\mathrm{m^3\,min^{-1}}$ and V the volume in $\mathrm{m^3}$ of the glove box. From this relationship it follows that

$$c = c_0 \exp\left(-\frac{F}{V}\right) \ ,$$

where c_0 is the concentration of tritium at time zero. Accordingly, tritium is removed exponentially from the glove box atmosphere. The effective tritium removal rate is most probably slower than the exponential rate because of memory effects or gradual loss of scavenging efficiency of the getter.

Shmayda and co-workers [Shm92; Shm93; Hei94b; Hei95] developed a commercial grade, standalone glove box at CFFTP, Canada meeting tritium handling requirements (see Fig. 4.15).

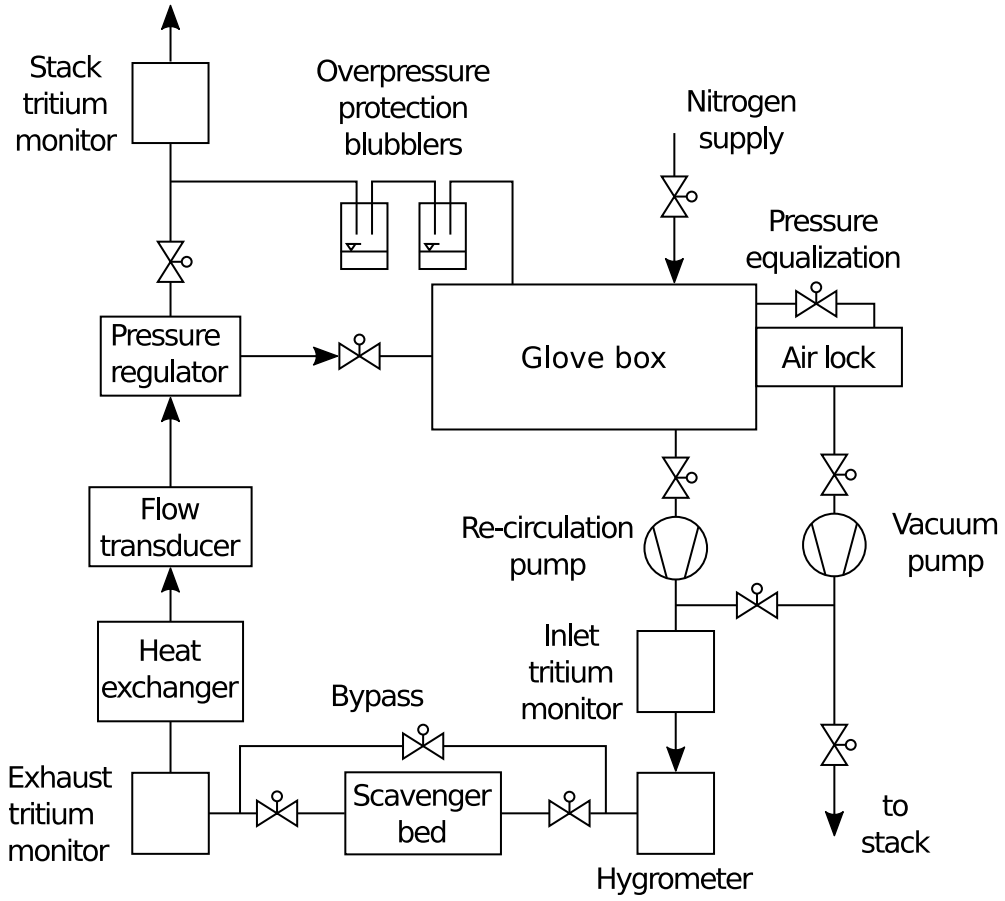


Figure 4.15: Schematic layout of a standalone inert gas glove box equipped with a getter clean-up system (after [Shm92]).

The glove boxes were designed to operate with a dry, oxygen-free, chemically inert gas atmosphere consisting either of pure nitrogen or preferably of pure noble gas. For the removal of tritium-bearing species, the selected getter material was type ST198 alloy (Zr_2Fe).

Yamanishi et al. [Yam85] carried out comprehensive theoretical studies on the removal of tritium from a noble gas atmosphere employing uranium or other getters. Of the tested getters, uranium was found to have clear advantages: i) very low dissociation pressure of the hydride at ambient temperature, ii) p-c isotherms with broad plateaus, iii) no disproportionation, and iv) straightforward recoverability of tritium at moderate temperature. However, because uranium underlies strict international controls, it is no longer contemplated for this application.

In summary, tritium removal from glove boxes containing inert gas or air atmosphere is a highly developed subject for which now a vast body of experience is available on which to base the design of confinements for a great variety of applications.

4.3.2.3 Oxygen/air supply and oxygen monitoring in glove boxes

4.3.2.3.1 Oxygen/air supply

The partial pressure of oxygen in glove boxes operated with argon or nitrogen cover gas and cleaned from tritiated species with a noble metal catalyst/adsorber system must be controlled within pre-established limits to ensure full oxidation of all leaked contaminants. The oxygen concentration is automatically adjusted by the addition of either dry air or dry nitrogen depending on whether there is deficiency or excess of oxygen. A pre-requisite is continuous analysis of the oxygen concentration in the glove box. The supply of air can be performed either with pressurized cylinders or directly with previously dried laboratory atmosphere. In the latter option,no replacements of cylinders is necessary.

4.3.2.3.2 Oxygen monitoring

Glove boxes with nitrogen atmosphere must be equipped with oxygen monitors to determine and control the oxygen concentration. Safety relevant oxygen monitors must be compatible with a tritium-contaminated nitrogen atmosphere and be energized by the uninterrupted power supply (UPS). They must be able to activate local audible (beep) and visual (blinking red light) alarms as well as an alarm at the Central Control System. Oxygen monitors shall be easy to calibrate and their sensor and electronics be of undemanding maintenance.

Oxygen monitors are installed in glove boxes at places where the oxygen concentration is most likely to rise so that an early detection becomes possible when the confinement develops a leak, for instance a pinhole in a glove. It is necessary to be aware that oxygen monitors subjected to prolonged exposure to air may give wrong readings due to cell saturation.

Another important safety relevant application of oxygen monitors is early detection of **non-respirable air**.

4.3.2.4 Catalytic exchange

A different and simple approach to remove tritium from glove boxes without excessive burden to adsorber beds was recently proposed by Heung and Staack [Heu05b]. Their approach was to operate the glove box at humidities comparable to those of ambient. Under these conditions, the driving force inducing atmospheric moisture to penetrate into secondary confinement is

minimized. Tritium bound to molecular hydrogen and moisture is removed from the glove box atmosphere by **catalytic exchange** employing protonated solids at ambient temperature. The heavier hydrogen isotope tends to enrich in the solid. Screening tests performed with 1 % platinum on alumina, 1.5 % platinum on hydrogen molecular sieve, hydrogen zeolite without Pt, and nano particle alumina coated with 2 % Pt provided evidence that from the point of view of kinetics, isotope effect, and exchange capacity hydrogen molecular sieve containing 1.5 % platinum catalyst delivers the most promising results.

Actually, the exchange capacity of this solid at 50 % relative humidity was found to be 14 mol kg^{-1}. Advantageously the molecular sieve column can be regenerated in place by sweeping with molecular hydrogen in the opposite direction to that of tritium incorporation. More work with simulation of realistic conditions is needed before this approach can be tested at technical scale and in the presence of tritium.

4.3.3 Regeneration of molecular sieves

Molecular sieves are resistant towards radiation and elevated temperatures. After saturation with tritiated water they can be regenerated numerous times either in-line or off line and be reused or subjected to interim storage.

4.3.3.1 In line regeneration

4.3.3.1.1 Replacement Tritium Facility at SRS

The Replacement Tritium Facility (RTF) at **Savannah River Site** (SRS) [Heu95b; Heu02; Heu05a] handles kilogram amounts of tritium utilizing plentiful and diverse equipment accommodated in two separate groups of thirty glove boxes (for more details see section 4.3.2.2.1). All glove boxes, whose total volume adds up to about 800 m^3, are operated with a nitrogen atmosphere. To keep tritium levels in all these glove boxes at very low concentrations, they are equipped with three stripper systems. Each of these stripper systems has three molecular sieve adsorber beds, apiece containing 104 kg of type 3A molecular sieve. In addition, there is at SRS a fourth back up stripper system comprising three smaller beds each containing 27 kg of molecular sieve type 4A.

Regeneration of these beds from tritiated water and recovery of hydrogen isotopes is accomplished with the Zeolite Bed Recovery System encompassing several beds containing 20 kg of magnesium, a furnace, several re-circulation pumps, pressure regulators, flow meters, a water trap, and a re-cycling tank (see Fig. 4.16).

Tritiated water is driven off from the molecular sieve beds requiring regeneration by gradual heating up to 523 K employing hydrogen as carrier gas. The moist exhaust hydrogen carrier gas is then passed via trace-heated lines first through a Water Retention System and thereafter through a hot magnesium (or uranium) bed heated to 723 - 773 K. The pertinent reduction reaction is

$$H_2O + Mg \longrightarrow H_2 + MgO$$

While high temperatures are necessary to suppress formation of MgH_2 or $Mg(OH)_2$ (both are tritium carriers) care must be taken to avoid approaching the magnesium melting point of 973 K to shun formation of liquefied magnesium and/or magnesium vapours. Condensation of water vapour inside of the piping is avoided by trace heating from the adsorber bed exit up to the water trap. The reducing efficiency of magnesium particles is favoured i) by large length and diameter of the bed, ii) long residence time, and iii) large surface area of the solid. With the described facility, approx. 300 l of hydrogen can be generated in 5.17 hours (or 58 STP l hour^{-1}). Once magnesium is exhausted, the bed is replaced by a fresh one and the exhausted bed disposed of as low level waste. The average amount of tritiated water processed during 10 years of operation at SRS is 6700 mol year^{-1}. Main drawbacks of this molecular sieve regeneration procedure are i) the generation of solid tritium-contaminated magnesium waste, ii) the need of elevated temperatures (possible permeation losses) and iii) use of hydrogen carrier gas.

4.3.3.1.2 Molecular Sieve Regeneration System at TSTA

At Tritium Systems Test Assembly **(TSTA)**, Los Alamos, currently a dismantled facility, the Molecular Sieve Regeneration System was integrated into the Tritium Waste Treatment System [And95c]. Beds requiring regeneration were simply valved off from the Tritium Waste Treatment System and valved into to the Molecular Sieve Regeneration System. To regenerate a molecular sieve bed the bed was heated while passing nitrogen in opposite flow direction to that of normal

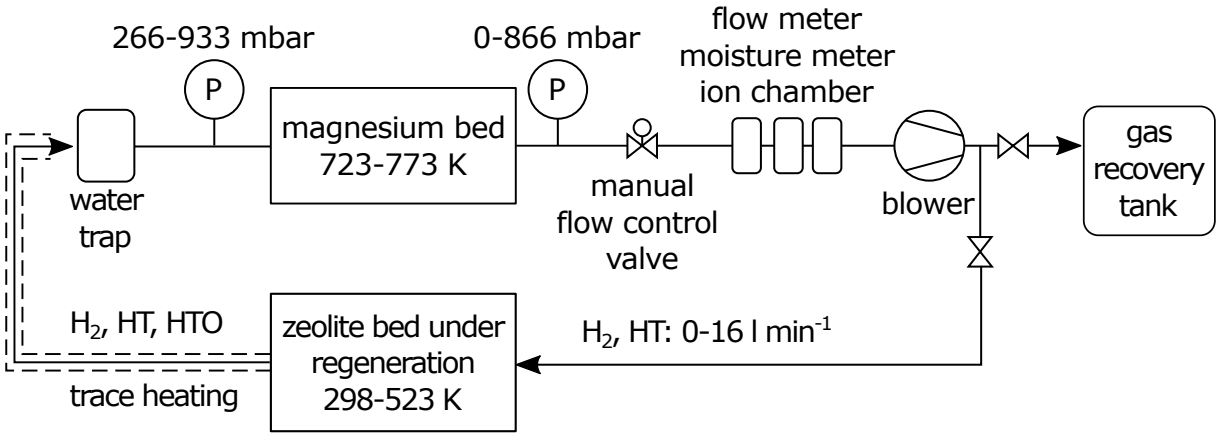


Figure 4.16: Molecular sieve regeneration process developed at SRS (after [Heu05a]).

operation [Nas92]. The steam/water mixture exiting the bed at a temperature of approximately 380 K was then passed through a heat exchanger and cooled with a chiller containing an ethylene glycol/water mixture. Gas exiting the heat exchanger at 280 K was fed into a cyclone separator optimized for the retention of condensates. Water collected in the cyclone was dropped by gravity into a holding tank. Before the carrier gas was re-introduced into the loop traces of remaining moisture were removed by passing the gas through a liquid nitrogen cooled freezer. Eventually still present particulates were retained on a filter of 5 µm porosity. Flow rate and total flow were determined with a flow meter and an integrator, respectively. The effectiveness of the regeneration was controlled with a moisture analyser.

Sporadically, tritiated wastewater was transferred into disposable molecular sieve drums for interim or long-term storage. Before transfer, the degree of tritium contamination of the water was determined either by calorimetry or liquid scintillation counting of aliquots.

4.3.3.1.3 Combined Effluent Tritium Removal Facility, Glove Box Gas Purification System, and Air Clean-up System at TPL

The Effluent Tritium Removal System (ERS), Glove Box Gas Purification System (GPS), and Air Clean-up System (ACS) at **Tritium Process Laboratory (TPL)** in Tokai-mura are designed to keep tritium everywhere in the laboratory at the lowest possible concentration level [Nar90]. During activities with tritium, a large number of primary and secondary dryers installed in these three systems require periodic regeneration (see Fig. 4.17). This is accomplished with a

directly integrated, conventional Dryer Regeneration System analogous to that implemented at TSTA. As in TSTA, regeneration is carried out by re-circulation of nitrogen in closed loop operation through the heated molecular sieve bed in opposite direction to that of normal process conduction. Blowers of max. $200\,m^3\,hour^{-1}$ flow rate are utilized for this purpose. Before the carrier gas is fed into the dryer bed it is pre-heated up to 623 K in order to enhance the release efficiency of moisture. Downstream of the beds the carrier gas is again cooled to 288 K in order to promote condensation. Condensed water is collected in a 200 l tritium receiver tank equipped with a level gauge. From here, tritiated water is first analysed and then distributed by gravity into one of three waste tanks, i.e. reserved for high, medium, or low activity concentration. The carrier gas is filtered first with a pre-filter and then with a HEPA filter. Completion of the regeneration is verified hygrometrically. For safety reasons the pressure in the loop is maintained at all times below that of the room employing a dedicated pressure control system. Important advantages of this comparatively simple process concept are that i) the dryer beds do not need to be removed for regeneration and ii) contaminated water is classified according to its specific level of contamination before disposal. This eventually manifests as cost saving.

The ample body of experience gained at **TPL** during 14 years of continuous operation with safety relevant infrastructure systems such as Air Clean-up System, Glove Box Purification System, Effluent Tritium Removal System, and Dryer Bed Regeneration System, during which the inventory of tritium in the laboratories was frequently close to 60 g, was discussed and evaluated by Yamada et al. [Yam02]. The achieved detritiation factors were 20 - 40 times higher than design values and the average concentration of tritium at stack was only $2.3 \times 10^{-5}\,Bq\,cm^{-3}$. The latter value is well below that permitted for tritiated moisture in air. During the period of evaluation, no accidental releases of tritium were registered. Failure analysis of rather different types of equipment, in total 21 items, which occurred during an accumulated period of eleven years were documented and assessed [Yam02].

Recapitulating, major advantages of in-line regeneration as developed at TPL are i) easy separation of tritium-contaminated waste water streams into low, middle, or high level, and ii) common equipment for the regeneration of molecular sieve beds installed in several different subsystems. Disadvantages are on one hand the necessity to interrupt the detritiation process during adsorber bed regeneration (unless a standby bed is available) and, on the other, handling of highly radiotoxic tritiated water.

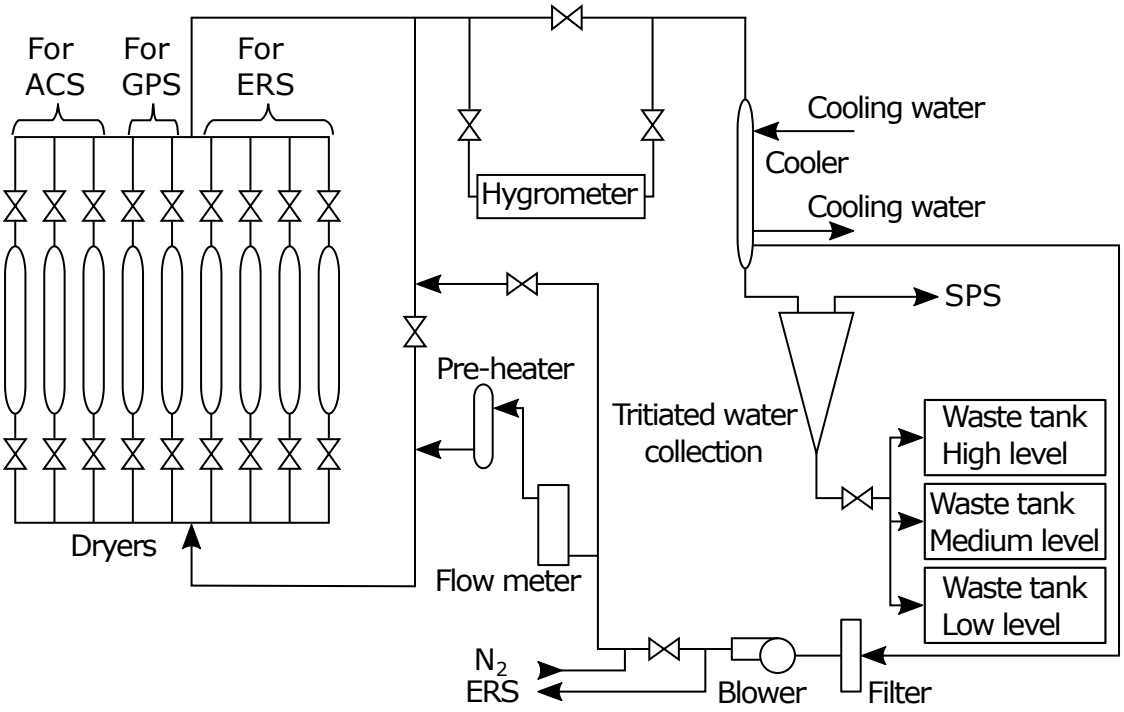


Figure 4.17: Dryer regeneration system (DRS) of TPL (for explanation of ACS, GPS, and ERS see text) (after [Nar90]).

4.3.3.2 Off-line regeneration of molecular sieve beds

As discussed in previous section 4.3.3.1.3, TPL is a tritium laboratory with experimental and infrastructural glove boxes which are serviced centrally. For this reason, in-line regeneration of exhausted molecular sieve beds was the consequential solution. In other tritium research institutions like for instance TLK, the approach is a different one: Tritium Retention Systems equipped with redundant molecular sieve beds are singly adjudicated to a large number of experimental and infrastructure glove boxes. Molecular sieve beds from these Tritium Retention Systems require replacement once loading values approach saturation (tritium detected in the effluent gas). More molecular sieve beds, also contaminated with tritiated water but from other applications - often subjected to previous interim storage - likewise require regeneration. Reactivation of such a large quantity of beds located next to glove boxes that are far apart from each other (many in different rooms) and contaminated to rather different degrees, can only be performed off-line [Sch91a].

An analogous situation was encountered at TFTR or JET. In these fusion research institutions the number of experiments performed with tritium in the fusion machine or in glove boxes was, at least in the early days, limited. Therefore, the quantity of molecular sieve beds requiring regeneration was not too large and the erection of a central in-line system for the regeneration of adsorber beds did not appear to be purposeful.

Two essentially different procedures are discussed below, which were successfully employed for off-line regeneration of adsorber beds.

4.3.3.2.1 AMOR facility at TLK

The Central Detritiation System as well as numerous dedicated Detritiation Systems installed adjacent to infrastructure and experimental glove boxes at TLK employ standardized adsorber beds. During routine operations, exhausted beds need to be replaced by pristine or regenerated ones. Retrieved beds are then either stored interimly or transported to the caisson housing the AMOR facility (Anlage zur Molekularsieb Regenerierung) where they are integrated into the loop for off-line regeneration. AMOR was developed at TLK and assembled at the workshops of KIT [Hut97] (see Fig. 4.18a)).

Adsorber beds installed in TLK detritiation systems contain about 15 kg of molecular sieve, consisting to about 85 % of $^1/_8{}^{\text{th}}$ inch mordenite 13X pellets and about 15 % of $^1/_8{}^{\text{th}}$ inch zeolite 4A pellets placed on top (see Fig. 4.18b) [Hut97]. Saturation of a molecular sieve bed is detected by humidity or radioactivity breakthrough in the exhaust gas. The actual degree of loading with water of exhausted beds is obtained from straightforward weighting of the complete bed and comparison with the original weight.

For regeneration in the AMOR facility, nitrogen carrier gas is re-circulated in closed loop mode at 10 - 20 $m^3\,hour^{-1}$ through the bed in opposite direction to that which prevailed in the Tritium Retention System. Liberation of adsorbed tritiated water takes place by slowly heating the bed up to 353 K utilizing an external heating sleeve. The bed is maintained at that temperature until most of the water has been released. Subsequently, the temperature is further raised up to 573 K and sustained at that value for several hours. It is important to note that at temperatures up to 573 K a hydrothermal amorphisation of the molecular sieve crystalline

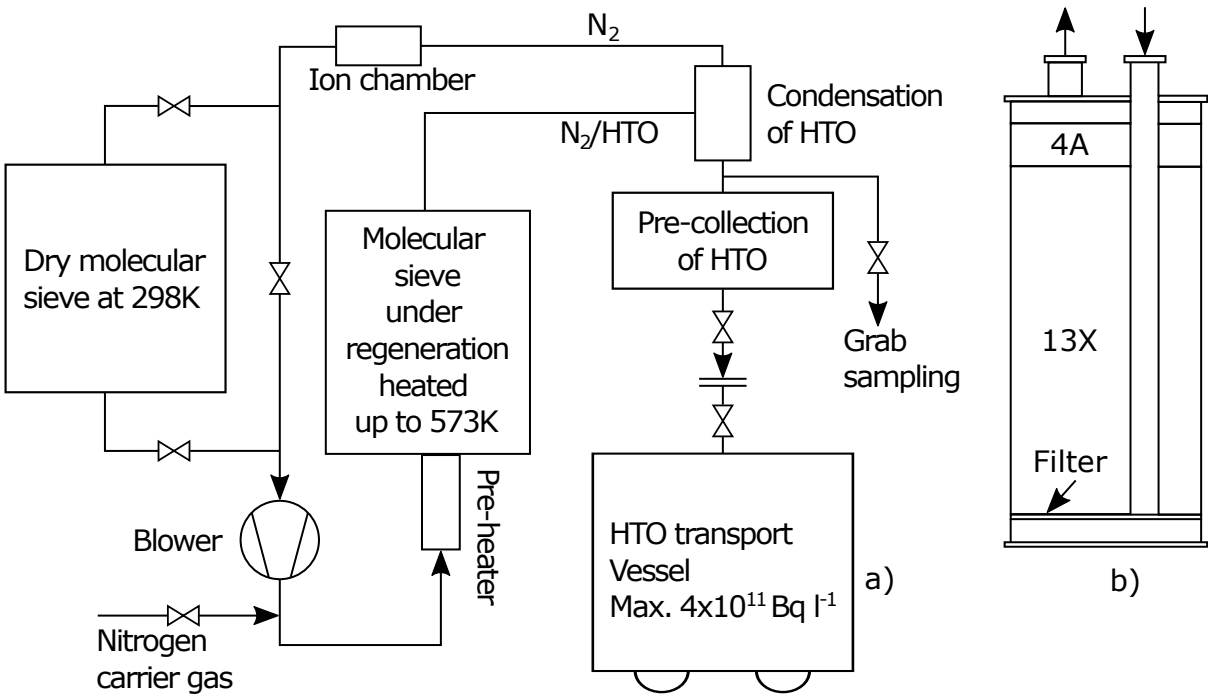


Figure 4.18: Simplified sketch of the AMOR system at TLK. Block diagram of the AMOR system operated in closed loop mode for the regeneration of molecular sieve beds retrieved from Tritium Retention Systems (see Fig.(a)). Adsorber bed from Tritium Retention Systems of TLK containing $^1/_8{}^{th}$ inch molecular sieve 4A and molecular sieve 13X pellets (see Fig.(b)).

structure does not occur[11]. Water released from the bed during gross regeneration, i.e. about 2 l, is collected in a condenser and from there dropped by gravity into a pre-collector.

For ultimate re-generation, the bed is maintained overnight at elevated temperature while re-circulating the carrier gas. To enhance decontamination the carrier gas is constantly dried using a large dry molecular sieve bed valved-in into the loop and kept at ambient temperature (see Fig. 4.18). This extra dry bed, which can be utilised for the regeneration of several exhausted beds, keeps the carrier gas dew point at rather low values. After completion of the regeneration, which is verified hygrometrically and/or with an ionisation chamber of 1 litre volume, water in the pre-collector is transferred by gravity into a transport vessel and disposed as liquid waste. The vessel is furnished with an indicator of the filling level. Some typical regeneration results obtained with the AMOR facility are tabulated in table 4.2. As apparent, achieved decontamination factors fluctuate between 10 and 100. The initial loading of „exhausted“ beds was typically of

[11] At higher temperatures and concomitant high partial pressure of moisture the crystalline structure of molecular sieve gradually vitrifies. This is associated with a considerable loss of adsorption capacity.

Table 4.2: Regeneration of molecular sieve beds with the AMOR facility.

Run number	Fraction of water remaining in bed	Tritium activity Initial	Final	DF
	%	Bq/g_{H_2O}	Bq/g_{H_2O}	
R01	1.8	5.00×10^5	9.00×10^3	56
R04	2.8	1.00×10^6	2.80×10^4	36
R09	1.3	8.70×10^5	1.13×10^4	77
R10	1.0	1.36×10^6	1.36×10^4	100
R11	7.2	2.00×10^8	1.44×10^7	14
R12	8.1	1.16×10^8	9.40×10^6	12
R13	5.1	1.64×10^8	8.36×10^6	20
R14	1.8	4.80×10^7	8.64×10^5	56

the order of 9 - 10 weight% and loading after regeneration of less than 1 weight%. A higher degree of regeneration was associated with much longer periods of re-circulation and therefore not considered worthwhile.

The simple caisson housing AMOR is serviced directly by the Central Exhaust System of TLK. The process is mostly controlled manually with complementary support of the Central Process Control System of TLK.

Advantages of off-line adsorber bed regeneration are i) short down time of Tritium Retention Systems and therefore high availability of glove boxes, ii) regeneration of exhausted beds can be performed following an independent schedule, and iii) regenerated beds can be accumulated for supply on demand. Foremost disadvantage is the necessity of connecting and disconnecting beds from Tritium Retention Systems or AMOR. However, because of the high adsorption efficiency of molecular sieve beds, these operations have nearly always been possible without detectable contamination.

4.3.3.2.2 Two stage PMR

A process based on a two-stage palladium membrane reactor (PMR) was developed at TSTA to recover tritium from mostly highly tritiated water adsorbed on molecular sieve beds stored

interimly for later conditioning. A large number of these beds had accumulated from several years of operation of the Tritium Retention Systems of TSTA each time saturated beds were replaced by pristine ones [Bir98b]. The first PMR component, which was operated in outside/in modus, had an outer diameter of 10.2 cm, and contained six palladium/silver tubes submerged in 7.22 kg of a catalyst consisting of a body of α-Al_2O_3 covered by a layer of dispersed platinum. One palladium/silver tube was aligned in the centre and the other five arranged concentrically to this tube. One end of these tubes was plugged and the other attached to a flange in such a way that the tubes could be evacuated (see Fig. 4.19a (displays only one tube)). The second PMR component was of inside/out operation modus. It contained six palladium/silver tubes of configuration such as depicted in Fig. 4.19b) (shows only one tube). They were housed in a pipe of 9.83 cm inside diameter. Each U-shaped palladium/silver tube contained 61 g of Pt/α-Al_2O_3 catalyst. For more details on the operation principle, see section 3.18.4.3.

Using the two PMR stages described above, tritium was recovered from a molecular sieve bed containing 2.05 kg of water contaminated by 4.5 g of tritium (7.9×10^{11} Bq/g_{H_2O}). To facilitate sustained operation a control method was developed that liberated automatically steam from the molecular sieve bed and fed the required amount of carbon monoxide into the stream prior to injection of the water carrier gas into the PMR1/PMR2 sequence. Inside of the PMR units, tritiated water is converted into tritiated hydrogen via the water gas shift reaction. The reverse steam reforming reaction does also take place, at least to some extent. Under these conditions, a total of about 700 standard litres of tritiated steam were processed and 1.2 g of tritium recovered within 47 hours of processing time [Bir98a; Bir98b]. In a further experiment with the two PMR stages but in combination with a cryogenic hydrogen isotope distillation system 4.5 g of tritium were recovered from 2 l of tritiated water [Bir99]. An overall decontamination factor exceeding 10^5 could be routinely achieved with the two PMR stages. Based on these positive results a demonstration system was erected and operated successfully at Savannah River Site [Ses05].

The PMR is a simple once-through process with which an efficient recovery of tritium from water adsorbed on molecular sieve is possible. Pure tritium is recovered from tritiated hydrogen, the tail-end product of the process, by isotope separation. After completion of the regeneration of the adsorber bed, it is ready for re-use. On the negative side are the need of a toxic reactant and the recurrent chemical analysis to control the feed gas composition.

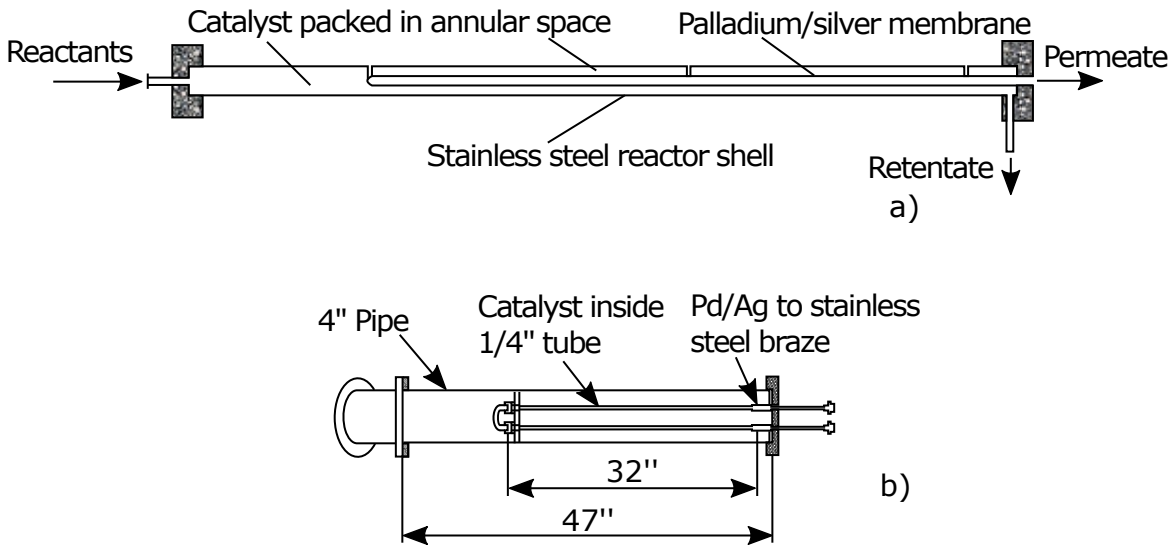


Figure 4.19: Working principle of two different palladium/silver membrane reactors (PMR) employed to demonstrate the recovery of tritium from tritiated water thermally released from molecular sieve beds. Illustration of a) outside/in and b) inside/out gas flow across a permeator tube in immediate contact with a catalyst [Wil94b; Bir98b].

R. H. Drake, Los Alamos National Laboratory [Dra96], was concerned about the fate of large amounts of tritium, i.e. 200 g in about 1800 l, stored as wastewater resulting from various DOE activities throughout the US. Los Alamos itself had accumulated about 100 g tritium in 400 l wastewater. To address the problem, he carried out a cost effectiveness analysis on the recovery of tritium from tritiated wastewater by comparing four technology options from the point of view of costs, pollution prevention, and state of technological development. The considered technology choices were: i) immobilization in cement and burial, ii) water reduction over a magnesium bed combined with cryogenic distillation, iii) two stage PMR combined with cryogenic distillation, and iv) the Canadian Detritification Services (CDS) isotope separation system from Ontario Hydro International. According to the analysis, the magnesium technology was not competitive neither on cost nor on pollution grounds (frequent and costly replacement as well as disposal of magnesium beds). While the burial technology was at the time the alternative with the lowest costs, it did nothing in the direction of pollution prevention. The PMR/ISS technology was found to be the most attractive from the point of view of pollution prevention, but of comparatively high operating costs and hence only economical when the amount of recoverable tritium in the wastewater exceeds certain threshold concentrations. From the perspective of tritium recovery,

the CDS technology was considered to be by far the most cost effective. The final price is a function of wastewater volume and concentration of tritium.

Geniesse and Stegen [Gen09] also examined the potential application of PMR technology for the recovery of trace amounts of tritium from large amounts of wastewater discharged at Hanford Site, a largely decommissioned US nuclear production complex. A principal conclusion was that the estimated costs could not be justified by the relatively small amount of recoverable tritium. Additionally, the need of handling large volumes of toxic and/or potentially explosive gas mixtures (CO, H_2) were considered to constitute a substantial safety hazard.

4.3.3.2.3 Molecular sieve regeneration at TFTR

Regeneration of molecular sieve beds used in clean up systems installed at TFTR was carried out with a Tritium Regeneration System by transferring tritium from molecular sieve beds belonging to the i) Tritium Vault Clean-up System, ii) Tritium Storage and Delivery System, and iii) Torus Clean-up System into transportable and disposable molecular sieve beds [Tuo88]. Adsorbed water was released thermally from the static molecular sieve beds in opposite direction to that of loading in closed loop operation mode and into transportable beds with the assistance of a blower. The transportable beds were handled in a fume hood furnished with glove ports. Transportable beds could readily be isolated, removed, and replaced. The amount of tritium in the transportable beds was constrained by transport and disposal site limits. The inventory in the loaded transportable beds was estimated from tritium monitor readings, process flow rates, and period of loading.

4.3.4 Tritium monitoring

Monitors normally employed for the direct measurement of airborne tritium in confinements are gas flow ionisation chambers and proportional counters (see Chapter 3.16). In order to quickly localize and identify the source of insidious or accidental releases, protect workers from incorporation of tritium, and take avoiding actions against tritium spread into the environment, these monitors must be capable of releasing optical and acoustical alarms to initiate prompt evacuation and bring about the shutdown of processes, isolate the ventilation, and enhance tritium clean-up and retention systems. To allow identification of long-term trends eventually resulting

from insidious releases, data on laboratory airborne tritium should be recorded uninterruptedly and remain accessible for evaluation.

For certain applications like maintenance, repairs, or upgrading of processes portable monitors should be available in adequate number.

Workplaces must be surveyed on a regular basis for surface contamination. The frequency of the surveys should be increased if there is potential for tritium-contaminated material spreading into other working areas. All enclosures, work surfaces, floors, equipment, doors, hoods, etc. within the work area must be examined for not strongly adhered contamination under the supervision of trained health physicists. Materials, equipment, etc. exiting the laboratory should be contamination-free. Therefore, surfaces are normally wiped (smeared) with a small paper either dry or moistened, to pick up loose tritiated material. Wipes shall typically cover an area of about 100 cm^2; they are quantified by conventional liquid scintillation.

To monitor tritium at very low concentrations, like for instance in the stack, a special sampling procedure is necessary. Stack monitoring must encompass the emissions of HT and HTO. In order to verify compliance with regulatory limits a record of the emissions into the environment must always be available for the authorities.

When using transport lines for sampling the potential for sample condensation is of concern. Outside air may warm up the condensed liquid which will then evaporate and be re-entrained. This problem is solved by trace heating in order to keep the carrier gas above its dew point.

Periodic bioassay of all personnel allowed to work in the laboratory should be carried out on a regular basis through urine sampling. During periods of increased potential for tritium-contamination, the bioassay frequency should be increased. The biological half-life of tritium in human bodies is of the order of 10 days [Wyl63; Llo86].

4.3.4.1 Ionisation chamber

All areas accessible to personnel working with tritium in a tritium-handling installation, e.g. laboratories, workshops, or other confinements, must be subjected to routine real time monitoring. Monitoring must give a prompt warning in case of abnormal tritium releases from a source such as a glove box, a tent, or a hood. Interim storage areas sheltering tritium-contaminated material and equipment must be monitored particularly if poorly ventilated, highly stocked, or often

frequented. Monitoring systems should be positioned at strategic places of the tritium-handling facility in order to allow quick localization of a source of contamination.

Spare monitors should always be available to verify contaminations or replace stationary monitors requiring repair.

Stationary ionization chambers (IC) are widely used monitoring instruments for the determination of airborne tritium, i.e. HTO and HT, in the laboratory atmosphere or in glove boxes. At TLK altogether 36 stationary monitors supplied by Berthold Technology Messtechnik and equipped with ionisation chambers manufactured by Labserco monitor a research area of about $1000\,m^2$ [Bes97]. The ionisation chambers, which have an active volume of 2 litres, are protected by filters designed to retain particles larger than $5\,\mu m$. To improve the performance of the ionisation chambers the original lithium batteries of the electrometers were replaced by equivalent electronic devices. In addition, their overall leak tightness was upgraded and the original communication software of the monitor modified to prevent bus blockades. The Brey type graphite-lubricated pumps of the monitors frequently required maintenance and sometimes replacement. Labserco ionisation chambers have a detection range for tritium of 3×10^5 - $5 \times 10^{11}\,Bq\,m^{-3}$.

Tritium monitors such as manufactured by Overhoff Technology Corporation or Berthold Technologies are used in many tritium installations worldwide. Berthold monitors have been employed for years at the **Central Tritium Retention System** of TLK to analyse gases in the ring manifold that are collected from primary systems installed in glove boxes. Because exhaust gases from pumping systems evacuating primary systems have a high probability of being contaminated by tritium, they are first accumulated for an interim period in one of three large tanks, each of $1.6\,m^3$ volume, initially containing nitrogen at 700 mbar. Nitrogen is used to exclude explosion. Once the pressure reaches 900 mbar, the gas feed is switched automatically to the next vessel. Provided the tritium concentration in the previously loaded vessel is lower than $4 \times 10^{10}\,Bq\,m^{-3}$, the gas is fed into the Central Tritium Retention System for once-through processing and subsequent release into the atmosphere. Berthold ionization chambers can activate two alarm stages when the concentration of tritium exceeds set point limiting values. If only the first limit value is reached a warning signal is sent to the Central Control System and another to the Pre-cleaning Retention System to start closed loop operation until the tritium concentration is reduced to a level below $4 \times 10^{10}\,Bq\,m^{-3}$. Once this value has been attained, the gas is fed into

the Central Retention System where the tritium concentration is further reduced in once-through mode to a level below $4 \times 10^6\,\mathrm{Bq\,m^{-3}}$. Decontamination factors of $> 10^4$ have been regularly confirmed.

Plentiful experience has accumulated during the course of decades with continuous room air monitoring of tritium in breathing air of numerous civil and military tritium-handling installations in Europe, Russia, USA, etc. A critical discussion of this subject was published by Cadwallader and Denny [Cad90]. The former Tritium Systems Test Assembly (TSTA) and the Safety and Tritium Applied Research (STAR) laboratory employed Kanne type ionization chambers that force room air through the chamber with a pump (see also section 4.3.4.3)[Hoy61; And80]. Chambers of this kind need to be controlled regularly, e.g. every week, with a standard Cs-137 source. In addition, they should routinely be subjected to a careful calibration every few years. At TSTA an artificial background setting of $1.9 \times 10^{11}\,\mathrm{Bq\,m^{-3}}$ slightly above true zero setting was used to uncover erratic readings caused by an abnormal instrument drift.

Monitors in large tritium-handling installations are usually designed to release more than one alarm level depending on the potential degree of contamination and corresponding activities that need to be exercised, e.g. partial evacuation, full evacuation, ceasing of operations, increasing of ventilation rate, etc.

All **safety relevant** tritium monitors must be energized by interruption-free power and their calibration be validated on a regular basis.

Ionization chambers installed inside of glove boxes are used to determine the concentration of tritium in the cover gas. They are usually of the open wall type, i.e. without casing, which makes a blower superfluous. It should be noted, that inside of a glove box even slightly heated components assure good gas mixing by natural convection.

Measurements carried out with stationary instruments are habitually complemented by determinations with portable, calibrated ionization chambers. Local contaminations are monitored with ionisation chambers of volumina ranging from a few tenth of a litre to a few litres, depending on the required detection limit. These rather simple devices require only a polarized chamber, suitable electronics, and a pump to expedite the gaseous sample through the chamber. Pumps constitute a frequent source of failure.

4.3.4.2 Continuous monitoring of radioactive or chemically contaminated particles in air

In case there is need to protect workers from radioactive or chemically hazardous **airborne particulates**, e.g. particles contaminated by tritium and/or beryllium such as generated in hot cells or tritium handling facilities servicing fusion experiments, continuous air monitors for sampling airborne particles must be installed in selected places [Cad09a]. Typically, a defined quantity of air, generally in the $1\,s^{-1}$ range, taken from locations representative for air respired by workers is passed across a filter paper placed on a device with a holder employing either an incorporated blower or a vacuum pump. The activity on the filter collected per defined quantity of air is then determined with an appropriate and calibrated radiation detector positioned close to the filter paper. Chemically poisonous or chemically contaminated particles usually require wet chemical analysis.

Continuous airborne particle monitors should warn workers against potential inhalation exposures and eventually be designed to actuate preventive measures.

4.3.4.3 Air sampling techniques for monitoring

Fixed **Kanne type ionisation chambers** draw room air through the chamber utilizing an integrated pump [Hoy61; And80]. The electrometer of these monitors is housed in the base plate. The Kanne configuration consists of an ionisation chamber surrounded by a closely spaced second chamber. The volume between the two chambers serves as an ionisation trap. To cancel the effect of external gamma, X-ray, or cosmic radiation either a second ionisation chamber of identical dimensions (dual configuration) or a lead shield is used.

Overhoff Technology Corporation, USA, offers ionisation chambers for airborne tritium measurements with volumes covering the ranges 0.02 to 8 l and sensitivities between 3.7×10^{-3} $Bq\,m^{-3}$ and pure tritium (see also section 4.3.4.1).

Proportional counters are pulse counting instruments in which the air sample is introduced into the counting carrier gas.

Very low levels of tritium oxide are measured using a special sampling technique, which basically consists of a combination of bubblers and cold traps or adsorbers. In the case of bubblers, air is passed at a rate of a few $l\,min^{-1}$ through either water or ethylene glycol. The

collection efficiency is virtually 100 %. Tritium collected in bubblers is analysed by conventional liquid scintillation counting of aliquots.

To determine very low levels of molecular tritiated hydrogen, air is first passed through an adsorber to retain the initially present HTO and then through a catalyst bed which converts HT into HTO. Catalytically generated tritiated water is collected with a second adsorber bed. Tritium in each of the adsorber beds (HTO) is determined by dropping the respective adsorber into water and quantifying tritium by liquid scintillation counting. It is important to allow sufficient time to achieve full equilibration between the adsorber and the supernatant water.

Nafion is a fluorinated polymer distributed by Dupont De Nemours which has been used to discriminate between the partial pressure of HT and HTO in a carrier gas. The rather effective separation is attributed to the high permeability of HTO across Nafion membranes (several thousand times that of HT). To perform a separation moist air is fed into a bundle of Nafion tubes and dry purge gas is passed in counter current along the tubes outside [How75]. By comparison between total tritium in the gas stream with that obtained after passing it through the Nafion tube bundle it is possible to calculate the concentration of HT.

4.3.4.4 Smear technique

A widely employed procedure for the approximate determination of the contamination of surfaces by tritium-bearing particles and easily removable adsorbed tritium prevailing in/on glove boxes, airlocks, floors, hoods, tables, all kinds of equipment, tools, shoes, etc. is the smear technique. Accordingly, a known surface - habitually about 100 cm^2 - is uniformly scrubbed with a dry (or moist) piece of filter paper. The swipe is then introduced into a LSC vial containing liquid scintillation cocktail and counted by LSC after a standing time of 10 - 20 minutes in order to allow for equilibration (see also section 3.17.4).

Rodrigo et al. [Rod95b] (see also references therein) compared measurements obtained by wipe-assay with results from a commercial surface contamination monitor and observed no simple correlations. Single smear measurements were actually found to be sensitive to the wipe material, surface roughness, wipe time, applied pressure, surface coverage, etc. Improvement of the accuracy were accomplished by several consecutive measurements, e.g. 3 - 5. Experimental evidence indicates that after several consecutive wipes have been taken from the same surface the amount of tritium removed by the n^{th} wipe, R_n, follows the expression [Sur88b; Rod95b; Ono95]

$$\ln R_n = n \ln(1 - f) + \ln \left(\frac{f S_0}{1 - f} \right) \ ,$$

where S_0 is the total removable activity and f an experimentally determined constant. Average values of f, obtained from plotting this equation, have been found to vary within the range 10 - 30 %. Even though a value of $f = 10\,\%$ has been widely adopted, some researchers found it to be too small [Rod95b].

Possible correlation between contaminations of surfaces inside of a glove box at ambient temperature measured by smear assay with concentrations of tritium in the glove box atmosphere were investigated systematically by Sienkiewicz [Sie85]. The type of correlation was found to depend on whether the glove box atmosphere was contaminated with HTO or HT/T_2. In case of tritium in the oxide form the degree of surface contamination y in units of dpm $\times\ 10^{-5}$ per $100\,cm^2$ was best described by equation

$$y = A \exp(Bx) \ ,$$

where A and B are constants and x is the atmospheric concentration of tritium in $mCi\,m^{-3}$. For glove boxes contaminated with molecular tritium, i.e. HT/T_2, the corresponding expression is

$$y = Ax^B \ .$$

Surette and McElroy [Sur88b] concentrated in their studies on the degree of tritium removal from surfaces by swipes. Metal specimens were first exposed to molecular tritium at ambient temperature. Thereafter, the amount of tritium removed in consecutive swipes with filter paper was determined by liquid scintillation counting. Assuming that a constant fraction of tritium r is being removed with each single swipe, it was observed that the activity S_n removed with the n^{th} swipe can be estimated from the following expression

$$S_n = r A_{n-1}$$

in which A_{n-1} is the removable activity remaining after the n^{th} swipe. From 26 swipe data obtained within a period of 15 minutes it was possible to assess the total initial amount of removable tritium and calculate a tritium removal factor.

4.3.5 Sensing primary instrumentation inside of glove boxes

Sensing instrumentation inside of glove boxes should be restricted to a minimum. Signal registration and evaluation should preferably take place outside of the glove box. Sensing instrumentation should be mounted on primary process lines utilizing Cajon VCR couplings to be accessible for repair, replacement, or calibration.

Primary sensing instrumentation should be selected based on their compatibility with hydrogen and radiation emitted by tritium. They should display very high leak tightness and be resistant to pressurization.

Primary sensing instrumentation should have small dead volume in order to minimize tritium inventory as well as zones of unreacted gases.

4.3.6 Tritium-compatible materials utilized for the manufacture of confinements

4.3.6.1 Glove box windows

There is practically no window material that satisfies all operational demands. Glass provides the greatest clarity and chemical as well as fire resistance, but is of limited impact resistance and displays poor workability. Hence, this material is not appropriate for tritium glove boxes.

Polycarbonate is the most frequently used window material for glove boxes. Poly carbonate has fair combustibility, is heat resistant, possesses excellent impact resistance, has good chemical resistance, is abrasion resistant, and displays the required workability. For example, penetrations are cut into polycarbonate windows without difficulty. On the negative side are the comparatively high costs.

Glove boxes at TPL have windows manufactured from **polymethylmetaacrylate** [Nar90]. This material has likewise excellent optics; possesses fair combustibility; displays good heat, chemical, and abrasion resistance; is remarkably resistant to impact and is characterized by flexibility and workability. The cost is lower than that of polycarbonate.

Lexan® (high impact strength), Plexiglas®, or other similar combustible materials or materials of high moisture permeability shall not be permitted for the construction of glove boxes or other confinement vessels and/or structures installed in tritium facilities.

4.3.6.2 Electrical cables inside of glove boxes

Cables installed inside of glove boxes should have a flame-retardant rating of 70 000 BTU hour^{-1}. They should not contain or else have extremely low levels of halogens like fluorine, chlorine, bromine, or iodine, and should not outgas species like sulphur or mercury. The use of armoured cables, which are protected against mechanical damage by a flexible steel covering, is not necessary inside of glove boxes. Multipair cables may terminate onto leak tight LEMO plugs and sockets at the penetration plates.

Power cables are usually multi core electrical copper cables.

Control cables or instrumentation cables are utilized for measuring, controlling, or regulating in the field of automation of sensors. They usually consist of multipair cables comprising groups of insulated conductors that are first twisted into pairs. Power cables should be clearly segregated from control cables.

Cables should be installed in glove boxes in such a way that solvents or oils cannot contact them during operation or maintenance. They should neither be located near heated or cooled zones, nor be movable along rough surfaces where they could be damaged.

Cabling materials acceptable for application in glove boxes are [Poo08]:

- *Conductor insulation materials*: ethylene propylene rubber (EPR), Tefzel (for coaxial cables only), Okonite-Okolon, Okonite´s chlorosulfonated polyethylene, polyethylene, polypropylene, cross-linked polyethylene, polyolefin (Rockbestos Company formula).

- *Jacketing materials*: ethylene propylene rubber (EPR), polyurethane, polyethylene, polypropylene, ethylene-propylene diene monomer (EPDM), chlorinated polyethylene (CPE), Okolon (CSPE).

4.3.7 Integral leak rates of confinements

All glove boxes shall be tested for leak-tightness according to accepted standards, like DIN 25412, section 2. Unless otherwise agreed, the maximum permissible total leak rate shall be 0.1 % by

volume per hour while initially at an under pressure of 10 mbar in the glove box [Yam02]. Leak rates are usually inferred from the pressure rise rate in the glove box. Connected glove boxes shall be tested together as whole assembly. Gloves constitute a frequent source of leaks because of their tendency to become brittle under the influence of ultra violet light. In some laboratories the gloves have therefore been protected from UV light by caps fixed tightly on every glove box opening. These caps also contribute to reduce permeation of ambient moisture into the glove box. Gloves must be routinely inspected and replaced following a predetermined schedule. A further obligatory safety measure is the periodical control of the overall glove box leak rate.

4.3.8 Cleaning and protection of glove box surfaces

The most common construction material of glove boxes is stainless-steel of very good surface finish. Stainless-steel provides high corrosion resistance without necessitating coating. For this reason, it requires minimum maintenance. The cleaning ability of glove boxes is important particularly after an accidental release because of the necessity to reduce the tritium background level down to acceptable values. All surfaces of a glove box should be carefully cleaned from oils, grease, and dust before installation. Austenitic materials must be pickled and passivated.

4.3.9 Assembly

The manufacturer shall supply data sheets for each glove box listing all information comprising the design, manufacture, testing, and acceptance. The data sheets should include lists of all materials used. If other materials are proposed by the contractor a written approval from the purchaser is indispensable. Where different grades of austenitic materials are used, the appropriate matching screws and nuts must be utilized. During assembly of glove boxes contact with ferritic steel parts must be strictly avoided. Screws and nuts must be treated with pure molybdenum sulphide before being assembled.

4.3.10 Weldings

All weldings must be carried out in accordance with recognized Standards or Explanatory Leaflets complying with the latest state of the art. Welding methods can be decided by the contractor but must be approved by the purchaser.

4.3.11 Drainage

When glove boxes are manufactured with a sloped bottom they must be subjected to a drainage test.

4.3.12 Airlock

Glove boxes are usually equipped with horizontal airlocks on the side and/or vertical airlocks on the bottom to facilitate i) repair or replacement of process components, ii) introduce or remove tools, iii) discharge waste, iv) retrieve contaminated equipment, v) take samples for analysis, etc. Most airlocks are of the evacuation-backfill type designed to provide access to the glove box without glove box atmosphere degradation when opening or closing the air lock. Airlocks are usually provided with vacuum service, air or inert gas flush lines, and vacuum as well as pressure gauges. Autoclave type doors are especially convenient, but simpler doors with a cross bar and screwed clamp are also adequate to seal the airlock. The dimensions of the airlock and of its door must be such that they can accommodate the largest component that is likely to require routine replacement during the life time of the tritium handling system. With its screw caps closed, an airlock must withstand either full vacuum or an over pressure of 300 mbar. A valve manifold on the airlock provides air or nitrogen (or inert gas) backfill and vacuum from the purge stripper. Airlocks open into the ambient air of a facility. When dealing with highly contaminated components an air hood (or "elephant trunk") may become necessary. Horizontal airlocks normally exhaust into the Central Exhaust System of the facility. Vertical airlocks mostly open directly into the room. In this case appropriate personnel protections measures, i.e. plastic suit, tent, radiation protection personnel, etc., may become compulsory.

4.3.13 Glove box feedtrough

i) *Electrical feedthrough*

Feedthroughs are necessary for the introduction of power cables or instrument leads into glove boxes. They should preferably be located on top of the glove box and in the proximity of the equipment with which they are connected. Utility power is usually introduced through individually sealed and insulated conductors. Multi conductor instrumentation feedthroughs are



Figure 4.20: Standard commercial feedthroughs supplied by GS Glove Box System Technik.

of the jam-nut/O-ring hermetic pin type. If possible, electrical feedthroughs should be accessible for repairs or replacements from the inside of the glove box using the gloves.

ii) *Service feedtrough*

For gas piping, process chilled water, and other services needed in glove boxes the preferred feedthrough is a welded-in stub flange. Other gasketed and flanged penetrations are also employed, provided they meet leak specifications. Tapered piped threads are not permitted for service penetrations.

Cabling within the glove shall terminate at the glove box wall. LEMO connectors can be used for penetration (see Fig. 4.20, upper right). They are available with special leak-seals to maintain glove box integrity. Penetrations should preferably be positioned on top of the glove box and in proximity of serviced equipment and instruments. Some standard electrical and service feedthroughs are depicted in Fig. 4.20.

To introduce a co-axial cable into a glove box the outer mantle is fixed to a crimp screw connection, the connection itself being fixed with an O-ring (see Fig 4.21 a)). To increase the tightness of the coaxial cable a liquid mobile glue such as Araldit two component epoxy resin

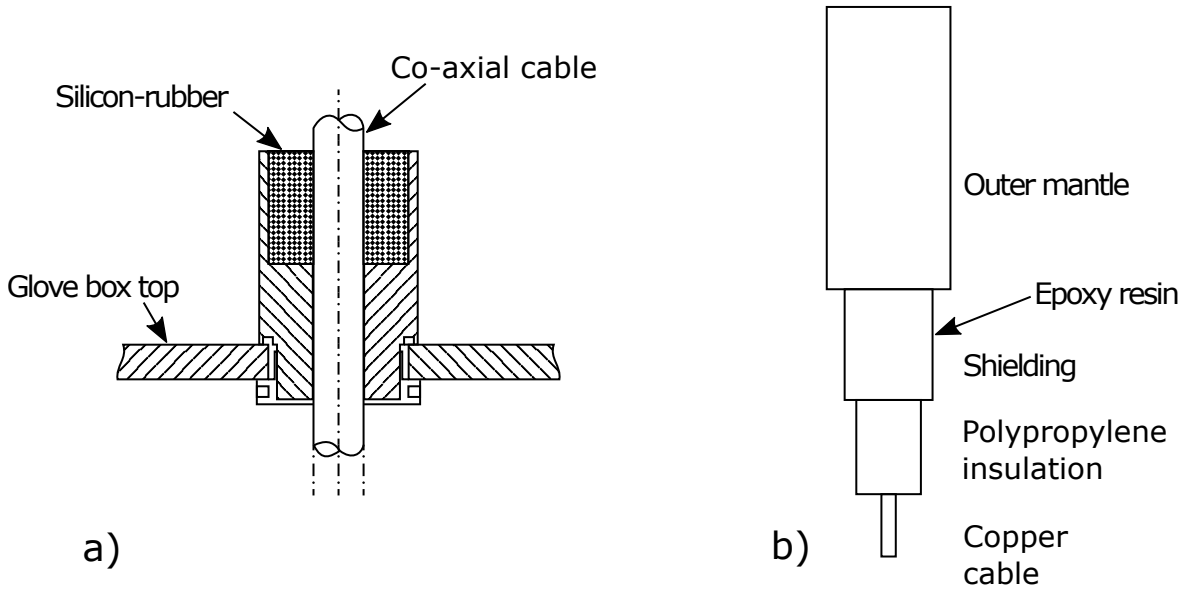


Figure 4.21: Penetration: a) crimp screw feedthrough the top of the glove box and b) coaxial cable showing where the epoxy resin is applied.

glue is poured at the end of the cable into the metallic shielding between the outer mantle and the polypropylene insulation (see Fig. 4.21 b)).

iii) *Glove box penetration for tritium conducting pipes*

A convenient glove box penetration welded on top of a glove box is displayed in Fig. 4.22 [And82; Shm90a]. A tritium line sealed into a positioning disk is depicted together with a secondary containment jacket. The penetration is sealed with an O-ring and fixed with a clamp which makes it easily demountable.

iv) *Special feedthrough*

Induction heating is sometimes employed to heat materials rapidly up to rather high temperatures inside of a glove box while keeping the electronics outside (see also section 3.15.2.2). When heating must take place inside of a glove box a metal/ceramic combination feedthrough such as manufactured by Friatec AG, Mannheim, Germany, can be welded to the glove box wall. The feedthrough is kept at low temperature by recirculating water inside of the copper induction coil.

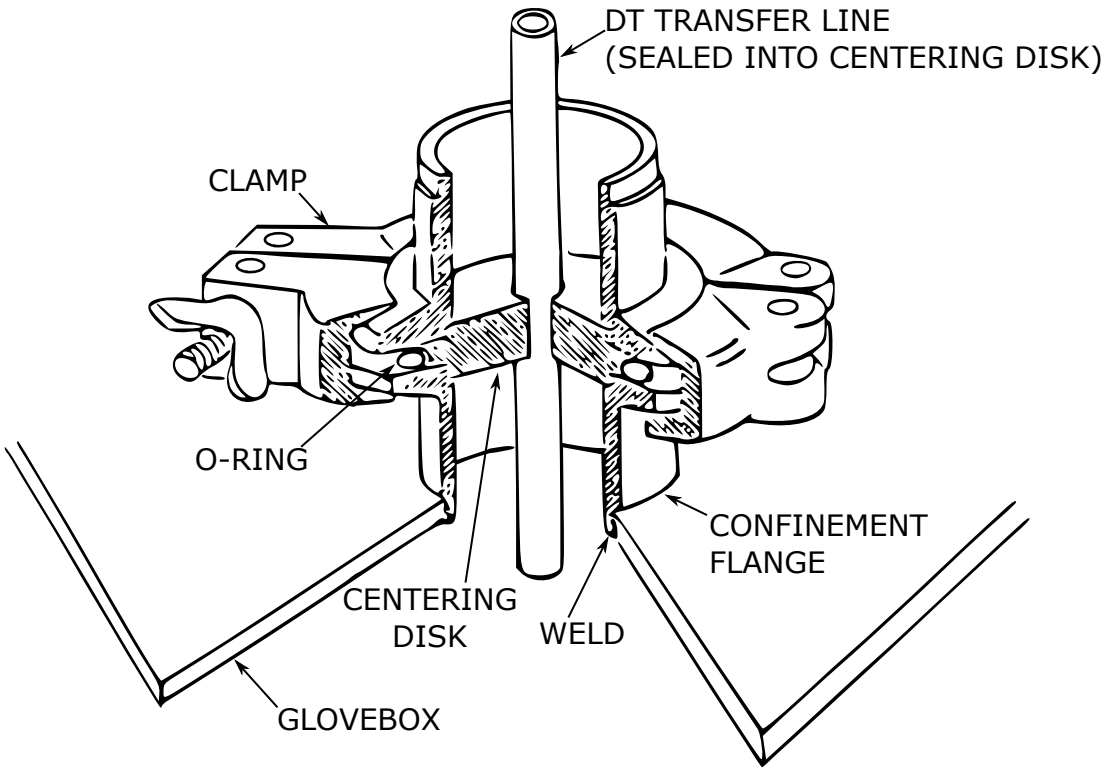


Figure 4.22: Glove box penetration for tritium pipe including confinement jacket [And82; Shm90a].

4.3.14 Glove box pressure control

The pressure in glove boxes must be maintained at all times within a fixed range and below ambient pressure in order to comply with the requirements of the multiple barrier principle. Efficient pressure regulation is also needed to cope with possible temperature changes inside of the glove box or with pressure fluctuations such as caused by workers entering or leaving the gloves. One more reason for mandatory pressure control is that the habitually used glove box windows cannot withstand pressure differences of more than 12 cm water column without undergoing leakage or even rupture.

Pressure regulation is performed automatically by pressure controllers. They regulate by switching either to admit air (or nitrogen or argon) or to evacuate via normally closed solenoid valves. The pressure-switch and gauge possess high and low set points with activated relays. Controllers are usually alarmed.

Passive pressure relief bubblers (see below) become active when pressure control failures occur.

4.3.15 Glove box pressure relief bubblers

The pressure boundary integrity of a glove box shall be protected against pressure differentials of more than ± 10 cm water column (± 9.8 mbar) with a bubbler assembly which contains oil or another equivalent liquid or device. In practice, air is admitted to the glove box by bubbling through the oil if pressure falls by more than 10 cm water column and glove box atmosphere is vented to stack if glove box pressure exceeds + 10 cm water column. The bubbler is usually designed for a 4.4 $m^3 min^{-1}$ flow through a 5 cm diameter nozzle with a relief set point of 3.8 cm water column. Most bubblers are manufactured of Plexiglas sheet or tube.

4.3.16 Glove box blowers

In case of excessive heat generation in a glove box, blowers may be installed to warrant good gas recirculation. Eventually, an acceptable average temperature of the glove box atmosphere can only be maintained with a dedicated cooling system.

4.3.17 Glove box gloves

Glove box gloves need to be of very high quality and integrity since they constitute the weakest link in the containment barrier. Selection criteria include resistance to i) wear and tear, ii) abrasion, iii) flammability, iv) ozone and other oxidants, v) solvents, vi) ultraviolet light, vii) radiation, and viii) permeability of moisture and of other gases (tritium), etc. Because of their usually large number and the need to be replaced frequently cost is also a selection criterion.

Some materials commonly employed for the manufacture of glove box gloves are: **Neoprene** [Nar90] or polychloroprene is an elastomer used in a wide variety of applications like wet suits, electrical insulation (or car fan belts). Its chemical inertness makes it well suited for gaskets, hoses, or corrosion resistant coatings. Hence, neoprene is also employed for gloves of glove boxes and as gasket to seal windows onto glove boxes [Gal05]. Neoprene has excellent tear resistance, good HTO imperviousness, and good solvent resistance but is incompatible with halogenated solvents or ketones. What is more, the dexterity (ability to move gracefully) of neoprene is poor. Therefore, neoprene should preferably be used under conditions of very mild tritium-exposure in order to exclude formation of hydrochloric acid.

Another material used for glove box gloves is **Butyl rubber**. Butyl rubber is not particularly resistant to radiation but shows low permeation coefficients for tritiated hydrogen and tritiated water vapour.

Likewise recommended for tritium service are **bonded two-layer rubber** gloves consisting of neoprene on the outside and butyl rubber on the inside [Gal05]. They combine the single advantages of each of these materials in an attempt to minimize the problem of moisture and tritium permeation[12]. The ratio of hydrogen permeability through neoprene and butyl is 3:1 and that for water permeation is 15:1. Butyl gloves are compatible with diluted acids and alkali but incompatible with petroleum products. Gloves of **butyl rubber** oxidize preferably at zones where they are stretched for instance over the glove port. If oxygen is excluded by covering the glove with a suitable thin and flexible tape or with a metallic cover this effect can be greatly ameliorated. Many elastomers including butyl rubber deteriorate in the presence of hydrocarbons. Consequently, contact with hydrocarbons should be avoided.

[12] Neoprene has good resilience and tensile strength and provides good resistance to oxidation, water, and chemicals. Advantages of butyl are gas impermeability and high flexibility.

Satisfactory results have likewise been achieved with **Hypalon** gloves from North Safety Products [Gal05]. This material is characterized by good resistance towards chemicals and against abrasion. The absorption of moisture is comparatively low. Hypalon gloves typically require replacement every 2 - 3 years.

Gloves are likely to lose integrity. Because of this, an aggressive maintenance program should be applied to exclude insidious intrusion of humid air through damaged gloves into glove boxes. In some tritium installations, gloves are replaced on a programmatic schedule and not only when a loss of integrity becomes apparent. **Increased partial pressure of oxygen** in the glove box atmosphere is often an indication of glove embrittlement.

Atmospheric moisture outside of glove boxes can permeate inside of glove boxes contributing significantly to the residual tritiated water partial vapour in the glove box. To ameliorate this problem a removable, **tightly closed metallic cover** on the glove port was shown to be beneficial. Because of their permeability gloves display a characteristic contamination on their surfaces. This needs to be kept in mind when introducing hands into them.

Important: When working with gloves all sharp objects like watch, rings, and other ornaments should be removed from hands and wrists.

4.3.18 Fabrics and insulation materials in glove boxes

Materials such as fabrics, cloths, felts, etc. should be carefully examined for particle generation capability, compatibility with other material present in the glove box, etc. before they are introduced into a glove box. Materials readily degrading, which in addition contain dyes, or residual chlorine should be avoided. If dyes are present their stability with respect to leaching should be verified in corresponding tests.

Only a minimum of flammable fabrics like tissue paper or cleaning cloths should be kept in a glove box in order to maintain the fire and combustion load low. They should be stored in the glove box in a manner such that flammability and combustion issues can be ruled out.

Insulation materials should not contain corrosives. They should be applied in a way to minimize possible detrimental effects of moisture.

4.3.19 Solvents and detergents

The use of solvents and detergents in Controlled Areas or glove boxes should be restricted to an **absolute minimum**. Solvents are of concern because of possible spilling flammability, contamination spread, attack of plastic seals causing leaks of water or oxygen into the glove box. If solvents are unavoidable for cleaning from particulates, oil, or grease they should be used judiciously preferably in form of a few drops applied to a cloth. Solvents used in glove boxes should be of low vapour pressure, high auto-ignition, high flash point, and low toxicity. Only approved solvents should be allowed. Protic reagents such as alcohols, phenols, halocarbons, and amines should be avoided. Permissible solvents should not consist of chemicals that can coke or poison stripper systems.

Important: Volatile liquids can boil and bump inside of the airlock causing a huge mess to clean and even damaging the pump. Volatile liquids should always be maintained in well sealed containments.

Very Important: It should at all time be kept in mind that a small amount of a flammable volatile solvent (amount in a tea spoon) evaporating into a closed or a semi closed glove box containing air may rapidly generate an **explosive gas mixture**!

4.3.20 Materials to be avoided in a primary tritium containment

Materials that need to be precluded from primary containment employed for handling of tritium-bearing gases are [Poo08]:

- Plain carbon steels: Even though these materials are of high strength, they are at the same time ductile and susceptible to hydrogen embrittlement. The latter is rationalized by their body centred cubic crystal structure.
- Ferritic stainless-steel (e.g. type 430); quenched and tempered ferritic steel (e.g. type 419); precipitation-hardened martensitic steels, like type 17-4PH or 13-8 MOPH; and precipitation hardened austenitic stainless-steels like type AM 350: These materials should all be precluded from tritium primary systems because of their significant susceptibility to embrittlement by hydrogen. Some commercial transducers are furnished with diaphragms of 17-4PH stainless-steel in order to improve accuracy. In case of destined for tritium service this material should be replaced by type A-286 or 300 series austenitic stainless-steels.

- Free machining grades of austenitic steels (e.g. type 303): These materials should not be used because they contain sulphur inclusions to improve their machining properties. Sulphur may undergo reactions with tritium.
- Polymers: they tend to brittle and should especially be excluded from primary systems if they contain halogens or sulphur.
- Direct contact of tritium with nitrogen and/or oxygen and moisture: beta radiation emitted by tritium induces reactions that may lead to the formation of highly corrosive gases like nitrogen oxides and/or tritiated water, hydrogen peroxide, and even highly corrosive nitric acid.
- Water and ammonia: When introduced directly or formed during the course of a chemical reaction they should be promptly removed from tritium handling systems. They tend to cause corrosion.
- Water, oxidizers, and peroxide formers: They should neither be allowed inside nor in the proximity of primary tritium containments.
- Strong acids or bases: They can cause corrosion of stainless-steel and other metals (see also section 3.17.17).
- Organic vapours: Before a containment, pipe, or any other equipment is integrated into a tritium handling system it should be thoroughly dried and freed from organic vapours, e.g. acetone, ethyl or other alcohol, etc.

4.3.21 Items to be avoided in confinements

As a precautionary measure against subtle corrosion and contamination of surfaces, the following materials should be excluded from glove boxes [Poo08]:

- Insulation, cloth, fabrics, polymers, ceramics, etc. These materials could generate tritium-contaminated particulate matter by abrasion or breakdown. They can also create clouds of contaminated dust when handled in glove boxes.
- Powders should be excluded from glove boxes. They can generate dispersing contaminated dust, which is almost impossible to remove.

- Adhesive materials should be barred from glove boxes because of their susceptibility of becoming persistently contaminated.
- Greases (e.g. Krytox® Teflon grease), oils, or pastes (e.g. SWAK Teflon paste). A possible substitute for Krytox® is the non-halogenated polyphenyl ether grease (Santovac). Friction reducing lubricants like Moly disulfide should also be excluded from tritium handling equipment.
- Flammable liquids shall be banned from glove boxes operated with air or be used in only very small quantities in closed glove boxes containing inert gas.
- Organic substances of high vapour pressures. These chemicals may cause swelling of rubber or - if flammable - lead to fire or even explosion.
- Materials or chemicals that contain halogens e.g. fluorine, chlorine, etc., sulphur, or phosphorus.
- Materials that contain carbon monoxide groups. If inevitable, they should be used very sparsely.
- Water, oxidizers, and peroxide former. These chemicals may induce corrosion. They may become adsorbed on surfaces and subsequently be contaminated by tritium.
- Materials that have not been used previously. New materials should only be introduced into a glove box after their contamination potential and material compatibility has been thoroughly evaluated.

4.3.22 Glove box atmosphere cooling

The release of heat into glove boxes should be minimized. Elevated temperature in glove boxes can cause i) increased permeation across gloves and their accelerated deterioration, ii) augmented contamination of the glove box atmosphere by volatilization of adsorbed species, and iii) destabilization and eventual damage of sensors.

Heated primary components are preferably cooled with a dedicated chilling system. Alternatively, heat can be extracted from the glove box employing a heat exchanger designed

to preclude contamination of the cooling medium. The standard approach consists in cross connected primary/secondary cooling loops.

4.3.23 Moisture control in glove boxes

The moisture level in glove boxes is habitually kept low in order to curtail contamination of the inner surfaces of the glove box and keep tritium permeation across gloves into ambient at a minimum. Low partial pressures of water are attained by i) high tightness of the glove box and ii) re-circulation of the glove box atmosphere through the molecular sieve bed belonging to a contiguous Tritium Retention System.

Because moisture readily interacts with surfaces and materials present in a glove box an accurate analysis of moisture is rather challenging. For the same reasons it is also demanding to prepare low concentration standards for calibration purposes. Glove box compatible hygrometers utilize aluminium oxide capacitors for the detection of water. Specified detection limits of these instruments are in the 0.001 - 1 ppm range. Reliable measurements necessitate calibrations at regular intervals.

4.3.24 Fire and explosion hazards

Materials having potential to trigger a fire or an explosion in a tritium facility should be stored at all times in smallest quantities. Such materials comprise hydrogen isotopes, hydrocarbons, carbon monoxide, activated getters, packing materials, paper, books, trash, flammable solvents, plastics, rubber, burnable cables, etc. The unauthorized accumulation of flammable solvents should be stringently controlled. Enforcement of these safety precautions should be verified frequently and enhanced by administrative procedures.

Hydrogen isotopes in air can become flammable in the concentration range 4 - 75 % and may give rise to detonations at concentrations within the range 18 - 59 %. For example, a dangerous situation arises when glove box air ingresses into a vessel containing hydrogen isotopes at sub atmospheric pressure or when significant amounts of hydrogen isotopes or any other flammable substance is released (or vaporized) into a closed or semi closed glove box containing air. Since the ignition energy of hydrogen is rather low, most static electricity sources can trigger an event.

It is thus necessary to introduce accompanying administrative and/or engineering measures to remain clear from such situations.

Flammable solvents of high vapour pressure, like acetone, ether, etc. should be handled with great care inside of a closed glove box containing air or in a partially opened, poorly ventilated glove box. Only small amounts of liquid, e.g. a few millilitres, evaporated into a glove box containing static air may suffice to generate a highly explosive mixture. If solvents are indispensable for a given operation, either non-flammable solvents or a **powerful portable ventilation** duct ("elephant trunk") capable of expediently diluting and removing dangerous vapours should be utilized. When in doubt, the support of knowledgeable personnel should be sought.

4.3.25 Handling of liquid cryo-coolants in glove boxes

Because glove boxes are operated at reduced pressure handling of coolants like liquid nitrogen is not straight forward - the cryogenic liquid shows strong tendency to boil and to evaporate disturbing the normal operation of the glove box. Cryo-coolants shall therefore only be used for exceptional purposes under well-defined conditions.

4.3.26 Liquid nitrogen supply

Large tritium handling facilities commonly feature a Central Liquid Nitrogen Supply System to make cryogenic coolant available to experiments and infrastructure systems. Additionally, very dry (and pure) nitrogen from the boil-off of a liquid nitrogen reservoir can be utilized i) to compensate for pressure losses experienced by glove boxes operated with a nitrogen atmosphere doped with oxygen, ii) as carrier gas for infrastructure systems like Tritium Retention Systems, and iii) as carrier or sweep gas for experiments.

Liquid nitrogen storage and supply is carried out with large Dewar vessels equipped with a liquid nitrogen level indicator, a pressure gauge, and a pressure regulating system. The integral helium leak rate of a super isolated, double walled liquid nitrogen Dewar must be lower than $10^{-8}\,\mathrm{mbar\,l\,s^{-1}}$; the permissible heat loss is specified to be less than 1.5 % per day. Direct withdrawal of liquid nitrogen to serve experiments is carried out with a flexible, shrouded metal tube. Dewars may be installed inside or outside of the tritium building.

To generate dry nitrogen the liquid nitrogen storage vessel is joined via a double jacketed line to a cold evaporator equipped with a safety valve or a rupture disk and a level indicator. The gas evaporator will generate the needed service pressure. When combined exhaust valves and safety valves are utilized they must be physically separated. To ensure that the valves remain operable at all times, they must be protected against cooling by overflowing liquid nitrogen.

In smaller sized tritium-handling installations, a Central Liquid Nitrogen System is normally not safety relevant for the operation of tritium systems. It may therefore be assembled according to conventional safety standards. If, however, tritium systems are dependent from a reliable and regular supply of large quantities of liquid N_2 like for instance a gas chromatographic isotope separation system, a cryogenic pumping system, or a cryogenic blanket experiment operated inside of glove boxes, adequate passive and active preventive measures need to be adopted to assure supply of liquid nitrogen with high safety standards and superior availability.

5 Safety philosophy in tritium handling facilities

In this section a variety of important design recommendations, ways of conduct, rules regulating work, Technical Delivery and Acceptance Terms, Applicable Manufacturing Codes, and Automated Control Systems implemented worldwide to achieve high safety standards for the operation of tritium-handling systems in Tritium Controlled Areas are discussed.

5.1 General design recommendations and advice for safe operation of tritium handling facilities

In order to keep tritium securely away from the environment a multiple barrier concept comprising a primary containment in direct contact with the radioactive gas; a primary confinement like a glove box, caisson or tent that retain tritium leaked or permeated from the primary containment; and a secondary confinement consisting of a fairly closed building constituting the Controlled Area is a worldwide accepted standard safety procedure. Introduction of tritium into a primary system is only permitted after the intactness of the primary system has been verified by leak tests and the glove box is functioning according to specifications. The latter implies that all systems pertaining the primary confinement like the tritium retention system, the under-pressure system, the system regulating the composition of the glove box atmosphere, the tritium monitoring instrumentation, etc. are in their normal state of operation.

For activities with tritium, it is generally recommended to maximize the employment of glove boxes for the confinement of primary components. This is the best solution in spite of substantial investments and considerable space requirements for glove boxes and their complementary peripheral equipment. Glove boxes constitute a reliable protection for the sporadic or continuous round the clock and even unattended operation of large and complex equipment. Diverse alarms and interlocks provide security against human errors. Advantages also manifest when it comes to perform maintenance work, calibrations, repairs or replacements. As opposed to eventually cheaper large volume metallic confinements, glove boxes offer the important advantage of permitting visual inspection of the confined equipment and immediate access to the equipment via gloves. Frequently recurring operations like calibrations of thermocouples, pressure transducers, flow meters, flow controllers, or tritium monitors are easiest and safest executed hands on via the glove box gloves. Likewise, occasional (or sometimes frequent) repairs or replacements of failed fore pumps, turbo molecular pumps, heaters, gaskets, flow controllers, flow meters, thermocouples, pressure transducers, valves, catalysts, molecular sieves, etc. are more safely performed under the protection of a glove box. Even when intrusion becomes obligatory, i.e. a whole glove box window needs to be removed, it is still possible using a provisional tent, a strong directed airflow, and eventually a protective suit to perform many activities hands on without noteworthy contamination of workers.

The utilization of organic and inorganic liquids should be avoided inside of glove boxes. These materials can deteriorate polymers, generate explosive gaseous mixtures in glove boxes operated with air and penetrate into open process systems thereby reducing the efficiency of operations. If liquids are indispensable, they shall be i) approved by the responsible authority, ii) used sparingly, and iii) unfailingly removed if no longer needed.

If unavoidable, non-burnable hydraulic, lubricating and cooling fluids may be used in places where direct contact with low partial pressures of tritium is inevitable. However, hydrogen-bearing fluids of this kind should - if possible - be precluded, especially if isotopic exchange with tritium can be expected.

Independent **air breathing systems** should be available in every large tritium-handling facility. These systems should be equipped with a dedicated oil-free compressor or with a pressurized cylinder. Breathing air should be made accessible in areas where it may be considered indispensable for workers' safety during maintenance operations. When asphyxiates like gaseous nitrogen or liquid cryogenic nitrogen or noble gas are used in large amounts, calculations should be carried out to find out whether the atmosphere could drop to values below 19.5 % oxygen. In such a case, appropriate preventive measures shall be taken to compensate for potential oxygen deficiency. When necessary, control measures comprising an oxygen monitor should be installed.

Equipment destined for work with tritium should be of high quality and therefore failsafe so as to stay away from emergencies or loss of availability. Among other, this may be achieved by incorporation of appropriate hardware and software measures.

The design should be based from the very beginning on a philosophy of **minimization of solid waste** production.

A design requirement of paramount importance for systems containing hydrogen isotopes is consequent prevention of explosive mixtures during handling, processing or storing of tritium (explosion + tritium release = double punch!).

Safety systems should be based on the principle of **redundancy, separation and diversity**. One option is to provide a redundant signal to a single actuation device and another to provide redundant signals to two independent, separate actuation devices.

Process piping joining primary systems installed inside of different glove boxes or outside of glove boxes or in hoods shall be jacketed to provide primary confinement unless the maximum tritium concentration is very small. Lines extending outside of buildings or into non-monitored

areas shall be furnished with evacuated jackets and appropriate instrumentation for early detection of leakage or jacket failure.

A comprehensive repair, component-replacement, and leak test strategy that includes evacuation, purging, and isolation of piping and components via valves - particularly in remote zones of primary equipment mounted in a glove box – should be incorporated beforehand into the design of tritium systems.

Large and complex facilities like Mound Laboratories fulfilling numerous and diverse tasks have installed a **Standards Laboratory** [Lin87]. Responsibilities of the Standards Laboratory at Mound are to i) maintain calibrated reference standards of the kind needed for the calibration of analytical instrumentation, gauges, thermocouples, radiation monitors, etc., ii) routinely calibrate instruments and sensors, and iii) return calibrated equipment to the user provided with an identification number and a calibration sticker. Along with the sticker, a certificate is handed out stating the range of application, the uncertainty and expiration date of the calibration.

Relevant plant operation data from the starting date of construction of a facility up to its date of final decommissioning shall be collected, reduced, analysed, archived, and secured. Such data are used to monitor safety levels, improve plant availability and maintainability, and provide field experience feedback for the design of new plants. Information of this kind is also of invaluable importance for i) waste management including sentencing and final waste disposal and ii) a component or equipment replacement and repair strategy.

5.2 Confinement interlocks

When glove box operation parameters like i) pressure, ii) activity level, iii) moisture level, iv) oxygen partial pressure, or v) temperature depart from pre-established upper and lower set point values interlocks will stop operations and only permit re-initiation of activities after the cause for the alarm has been identified and removed or repaired.

Open wall tritium monitors mounted inside of glove boxes alert personnel of unusual tritium releases from a primary system. These monitors will either initiate activation of a Tritium Retention System on standby or, alternatively, raise the catalyst temperature of the pertinent Tritium Retention System already in operation and simultaneously increase the rate of gas circulation to augment the atmosphere changes.

Room tritium monitors warn the staff of airborne tritium released either by integrity loss of a primary confinement or liberation from some other source. If the concentrations exceed a pre-determined value an alarm is released and evacuation of the facility (and ultimately of the building) will be announced and urged.

At the Tritium Facility of ITER concentrations of tritium in a glove box surpassing $3.5\,\mu g\,m^{-3}$ will start activation of the isolation of the glove box and of the corresponding process header [ITE01a]. It will take estimated 15 seconds between the activation signal and the complete isolation of the glove box. Room isolation and start of detritiation will be activated by tritium concentrations in the room at values exceeding $0.1\,\mu g\,m^{-3}$. Room isolation and commencement of detritiation will become active in about 30 seconds.

5.3 Fire and explosion protection

In a facility handling tritium there is much concern about the combined risk of injury and contamination by tritium of personnel following occurrence of fire or explosion. Rapid release of significant quantities of radioactive materials into the environment and damage of equipment are further possible consequences. To accomplish efficient fire and explosion prevention the implementation of a number of constructions, administrative, and monitoring measures are necessary [Bar61; And77; Vol95].

Within the frame of construction measures it is customary to compartmentalize buildings, each compartment having a separate system of ventilation and singular escape routes. In addition, actions should be taken to prevent fire and smoke from spreading into adjacent rooms.

As an example, the complex ventilation system installed at TLK is illustrated schematically in Fig. 5.1. It maintains negative pressure with respect to ambient in i) numerous large and smaller rooms and halls housing experiments and infrastructure systems operated with tritium, ii) a cold laboratory for experiments without radioactivity, and iii) the basement. Basement and ground-floor are about equal in size, i.e. $\sim 1000\,m^2$. The basement encompasses sizeable conventional infrastructure equipment. The total air throughput adds up to about $60\,000\,m^3\,hour^{-1}$.

Fire flaps installed in the ventilation air supply ducts ensure that fire cannot spread via the ventilation system (see Fig. 5.1). Flaps are released at 345 K by an integrated fusion link causing closing of the supply duct. Flaps can also be actuated manually. They are installed downstream

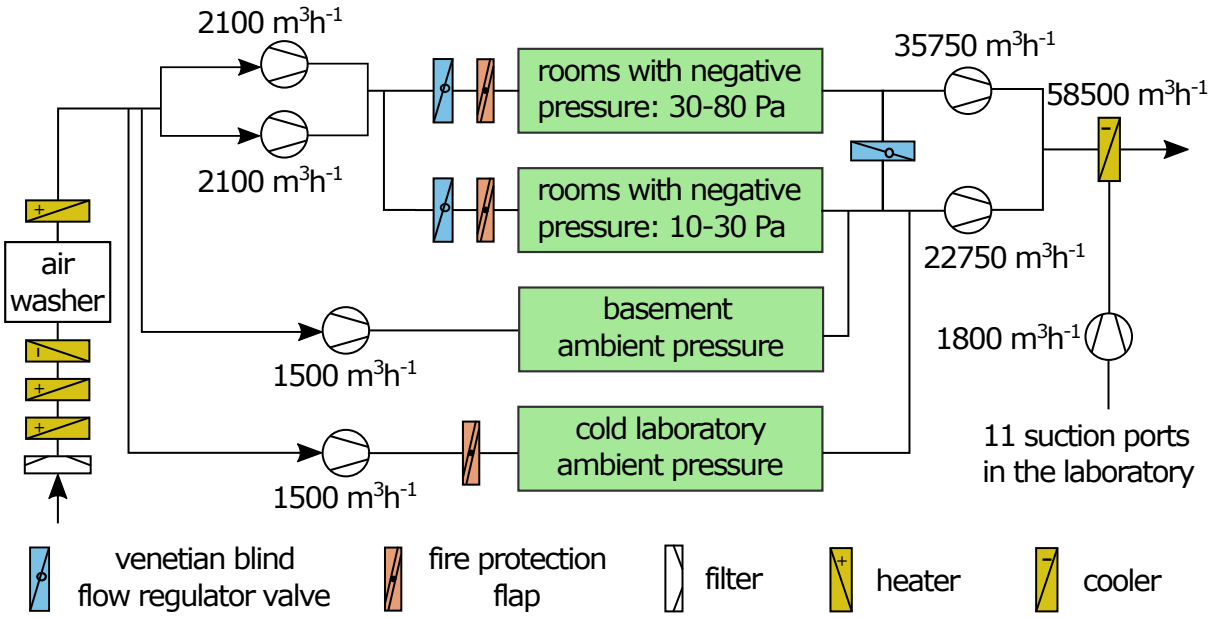


Figure 5.1: Simplified scheme of the TLK ventilation system.

of Venetian blinds inside of ducts supplying fresh air to tritium-handling rooms. Exhaust air ducts do not require fire flaps. Air ducts are designed to release contaminated air via stack. Safety relevant pumps are redundant.

The safest **fire and explosion prevention measure** for primary systems is to replace air in the glove box by an inert gas like nitrogen or argon, containing only a small partial pressure of oxygen. The oxygen content should be sufficient to warrant full catalytic oxidation of all possibly released tritium-bearing contaminants.

Relaying on the same basic principle, a fire suppression system that employs gaseous nitrogen and is designed to reduce the oxygen content of the atmosphere inside of the Biological Shield[1] from values of 21 to less than 15 % in about eight hours was installed at JET. This concentration of oxygen is neither sufficient to support normal combustion nor normal respiration [Sto99][2]. Nitrogen from the boil-off of liquid nitrogen and from an evaporator are employed for this purpose.

[1] By definition, the torus hall housing the JET tokamak with its concrete walls, doors, floor and roof constitutes the Biological Shield.

[2] The minimum acceptable value for respiration is 19.5 %. Air with only 15 % oxygen is respirable, but causes increase in pulse and breathing rate, faulty coordination, and impaired judgement, emotional upset and abnormal fatigue [Rim96]

At TLK as well as in many other equivalent tritium installations elsewhere in the world all rooms and glove boxes are strategically furnished with smoke detectors. Hence, fire detection at an early stage is warranted and fire extinguishing measures are possible soon thereafter. In case of fire at TLK the pertinent detector will instantly send an alarm to the Central Fire Alarm Station of KIT, which in turn will forward alarms to the i) Central Alarm Station of KIT Campus North, ii) the TLK Control Room, iii) the KIT Fire Brigade servicing the Campus North, and iv) the display at the entrance of the TLK building indicating the room where the alarm was released.

Cable smoulder inside of glove boxes can largely be excluded because of consistent over-dimensioning. Should in spite of this cable smoulder or cable carbonization take place, it will be detected at an early stage by smoke detectors installed in every glove box.

If considered appropriate, it is possible to install automatic fire extinguishing systems. In this context, it is important to verify that extinguishing agents be compatible with the conceivable fire sources in the tritium facility. Actions should be taken to allow expended firefighting agents such as water or others that may have become contaminated with tritium, to be containable. Within the frame of preventive measures poly vinyl chloride or other chlorine-containing organic materials should be avoided in glove boxes because of the danger of generating corrosive hydrochloric acid by reaction with tritium or during the course of the fire itself.

Only non-flammable materials should be utilized for the manufacture of glove boxes. Automated fire alarms signalling smoke by scattered light can be installed in glove boxes for early fire detection (only possible in glove boxes operated with an air atmosphere). Their number and location will depend upon the inventory of radioactive material, the potential fire load, and peculiarities of the facility. Principal aim is early detection and rapid, precise localisation of the fire source.

Glove boxes with protium or hydrocarbon lines shall have monitors and alarms with local audible and visual alarms as well as remote alarms. Sensors shall be compatible with nitrogen and low-level tritium atmospheres.

Glove boxes should be equipped with signalling lines that can be activated by push buttons to allow manual alarm release when necessary.

Of paramount importance are proper operating and emergency procedures as well as regular recurring training of all operating personnel, to assure that workers are at all time thoroughly

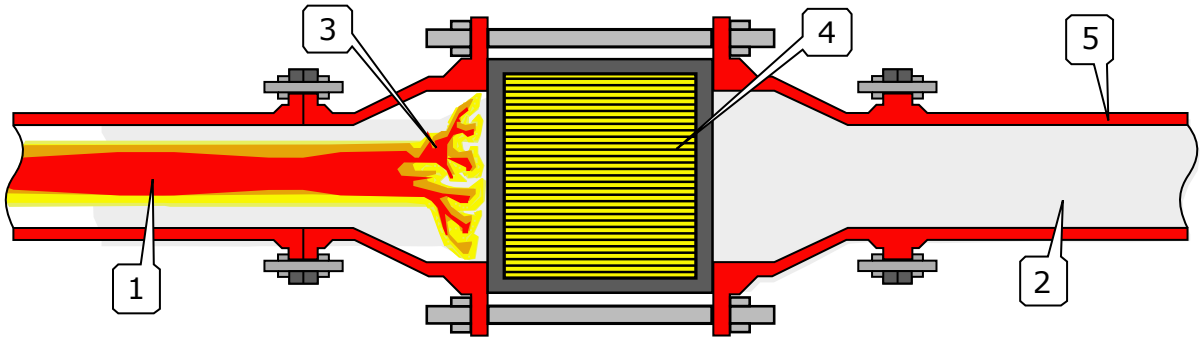


Figure 5.2: Configuration of a flame arrester. The figure shows: 1) exposed side, 2) protected side, 3) the flame stabilized by the arrester element, 4) the flame arrester element absorbing and quenching the flame front, and 5) the downstream piping. From http://www.we rmac.org/equipment/flame_arrester.html (visited on 22.01.2020).

familiar with every safety relevant procedure [US 02; US 08] (for TLK see Strahlenschutzanweisungen SAW 1 – 9 in Appendix V).

Flame arresters are installed in facilities handling flammable gases to ensure that a flame burning within a pipeline will not propagate to other equipment [Yos02]. Configuration and properties of a number of flame arresters have been discussed comprehensively in several publications [Bjo82; How82; Bro83; Pio91; Rou91]. The working principle of classical arresters is illustrated schematically in Fig. 5.2. It should be noted that of all burnable gases acetylene and hydrogen are the most difficult to arrest in practically all applications [Dav13].

According to the operation principle of a flame arrester, when the flame from a flammable gas or gas mixture enters a narrow gap between two plates it will propagate through the gaps in direction of the unburned gas. Under these conditions, heat is transferred from the flame front to the walls of the gap (or gaps). The narrower and the longer the gaps, the larger the influence of the arrester cold walls on the flame profile. In case the gap in the arrester element are sufficiently small (see 5.2), the flame front is dispersed, quenched below ignition temperature on the large surface, and the flame is extinguished.

As visualized in Fig. 5.3 for four different gases, i. e. H_2, C_2H_4, C_6H_{14} and CH_4, the **maximum experimental safe gap** (MESG) gets smaller as the pressure is raised. The appropriate gap size will depend on the reactivity of the gas/oxygen mixture. Of the four gases, the normalized MESG of gas/air mixtures containing acetylene or hydrogen is the lowest with $<$ 0.5 mm. For methane, propane, and ethylene the corresponding values are 1.14, $>$ 0.9, and 0.5 -

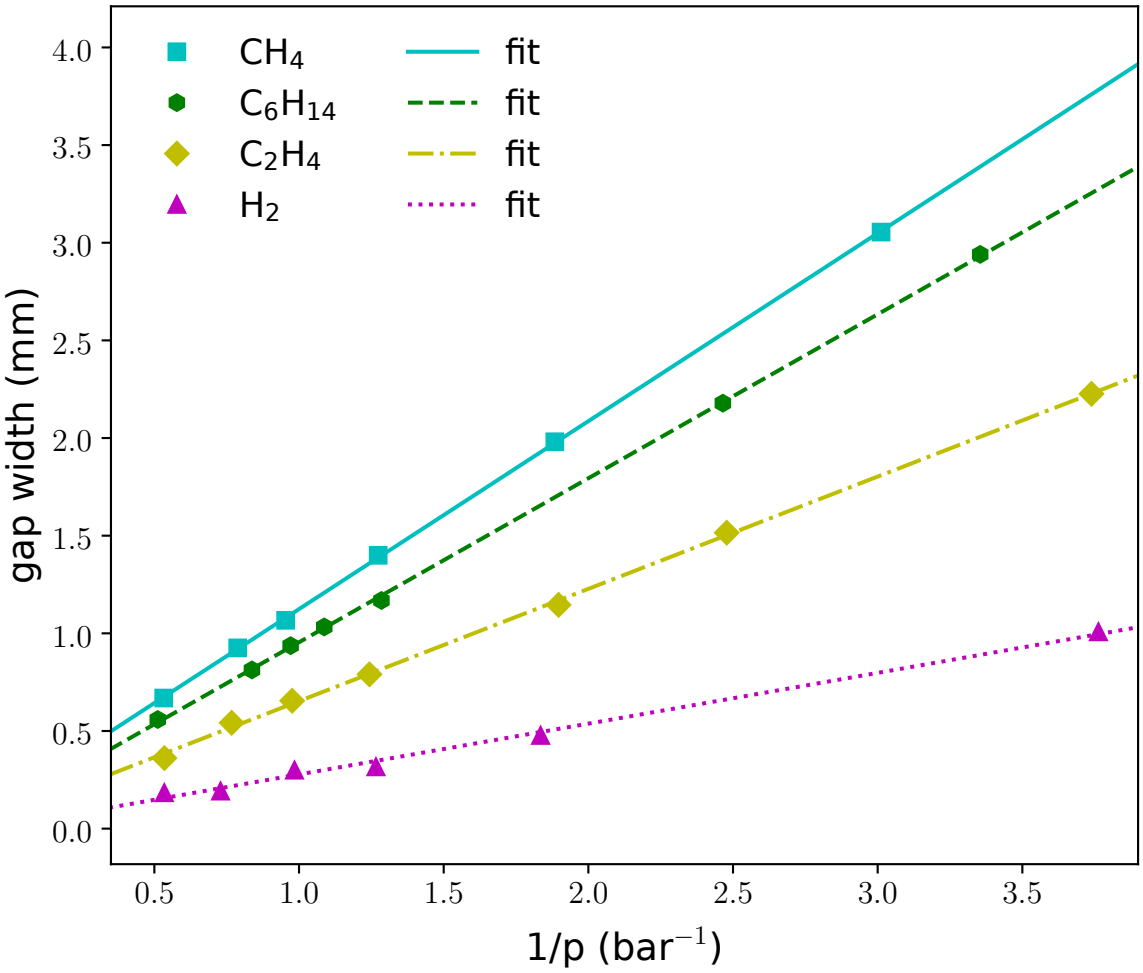


Figure 5.3: Effect of pressure on the maximum experimental safe arrester gap [Dav13].

0.9 mm, respectively. In accordance with expectations, the MESG decreases as the temperature is increased.

5.4 Basic way of conduct in Tritium Control Areas in view of radiological protective safety and safeguards

For radiological protective safety and safeguards in Tritium Control Areas it is imperative to implement and follow some well-established and generally accepted i) rules, ii) working instructions, iii) working procedures, iv) working permits, v) inspection handbooks, etc. (see for example Appendices N, O, V and references [Int91; US 94; US 73; Wel15].

Some measures and recommendations of general validity are:

- Workers handling equipment contaminated by tritium should wear protective clothing (laboratory coat, coverall), disposable gloves (usually of PVC or latex), and disposable shoe covers. By these measures, contact between bare skin and contaminated surfaces is avoided and contamination is kept away from normal clothing. Gloves may have to be replaced frequently depending on the level of contamination. It is good practice to wash hands immediately after removing the gloves.

- Tritium Controlled Areas must always maintain a high standard of cleanliness. This is important for safety reasons because components whose surface is contaminated by tritium due to chemical reaction, adsorption, or deposition of contaminated particulates can disseminate contamination ultimately even outside of the Controlled Area. Conceivably, contaminated components can be confounded with clean ones and eventually be utilized or be disposed off improperly.

- Shoe covers provide personnel protection and protection against spread of contamination to areas outside of the Controlled Area. Shoe covers must be removed and droped into a specially assigned containments before leaving the Controlled Area. In laboratories that maintain a clean environment by good housekeeping and regular smear surveys shoe covers may not be always necessary.

- Laboratory coats should be exclusively washed in a laundry approved for cleaning contaminated clothing.

- Ingestion of food or smoking in Controlled Areas is prohibited because of the risk of inadvertent contamination.

- Outer surfaces of major apparatuses, tools, small and large components, etc. in Controlled Areas should be monitored before beginning with activities in working areas. Monitoring is to be carried out by an independent Radiation Protection Service. Workplaces shall be surveyed on a regular scheduled basis. The frequency of surveys in case of an extraordinary activity will depend on the amount of tritium handled, type of operation and potential for dispersement.

- Areas contaminated (or possibly contaminated) by tritium should be posted to warn workers and constrict propagation of contamination.

- Eakins, Hutchinson and Lally [Eak71; Eak75] provided evidence that contamination of the skin with tritium eventually leads to the generation of organically bound tritium (OBT). Therefore, in case of skin contamination by tritium, decontamination should be carried out expediently. One way to prevent or minimize uptake of tritium through the skin by resorption of tritium oxide, organically bound tritium, or particulate tritides is a simple soap (or powdered detergent) wash with water. Washing should be performed two or three times for the duration of a few minutes and thereafter the skin be monitored. Washing with cool water keeps the pores of skin closed which reduces the penetration of tritium. Extensive washing is not advisable because excessive protective fat is thereby removed from the skin.

- In case of a significant tritium uptake, the water intake of the contaminated person must be increased substantially over a period of a few days in order to reduce the biological half-life [Llo86].

- Routine urine analysis (bioassay) of all personell active in the Controlled Area should be conducted on a pre-established periodic basis. This **retrospective** technique provides a very sensitive and accurate measurement of tritium in the body. An important complementary piece of information is the period of uptake.

- Evaluation of the bioassay results of all workers provides insight on the success of safety measures inside of the whole installation.

- Analyses outside of the routine program should be performed by the Radiation Protection Service whenever a release is suspected or known to have taken place. The best method to

determine whether an individual (or group of individuals) has had an uptake of tritium by contact with or inhalation of HT, HTO or any other soluble organically bound tritium is urine analysis.

- To minimize contamination spread all items contaminated with tritium should be transported depending on their degree of contaminatin either wrapped in plastics or in appropriately sealed containers.
- The staff of the tritium-handling facility should undergo a yearly health examination.
- The staff of the tritium-handling facility should experience basic theoretical education and practical training commensurate with size and complexity of the facility on the tritium safe handling practices for a broad range of tritium operations [Sis94; US 02; US 08].
- The license holder must generate and distribute admittance rules for employees, external staff and visitors.
- External visitors will require permission to perform experimental work by the Authorized Supervisor. External visitors should undergo radiological training commensurate with the site-specific hazards of the tritium facility and be handed out pertinent documentation describing the emergency plan, precautions, and safeguards needed for working in the facility. Hands on activities shall be executed following established procedures and regulations (see also section 5.5). A health examination of external staff prior to initiation of activities may become necessary.
- Visitors involved in hands-on tritium experiments are assigned to one person from the facility which will work with them in all activities involving tritium.
- Personnel planning conventional work in a Tritium Control Area shall enter only once or recurrently after explicit permission by the authorized Authority. The work should be clearly delineated.
- It is worldwide common practice to have visitor of Tritium Control Areas to sign in and out.

5.5 Some typical rules regulating work in Tritium Controlled Areas

Activities in a Tritium Controlled Area are strictly delimited by one or sometimes several specific **licenses**. A typical sequence of licenses such as granted to TLK since 1993 are discussed in detail in ref. [Wel15] (see also Genehmigung T1 – T6 and Genehmigung F in Appendix V). Responsible for the exact adherence to the granted licenses of all activities performed within the Tritium Controlled Area at TLK is the Operation Manager. In case of projects deviating from the granted license a modification of the license becomes necessary. Such modification requires a detailed and comprehensive application to the licensing authority.

Applicable exemption values, clearance levels, allowed activity concentrations and dosis coefficients at TLK have been compiled in Appendix W [Bun01b].

In most sizeable tritium-handling installations service instructions, special working instructions, and special working permits are issued so that operators can accomplish their work safely, without contaminations of the environment, or damage to property. This way of proceeding has been adopted in facilities such as TSTA [And82], TFTR [Sis94], CRL [Gal05] and TLK [Tri91; Wel15] and other (see also Appendix U).

Service instructions are issued by staff members responsible for the operation and safety of the tritium-handling installation like the Operation Manager or the Radiation Protection Officer. Service Instructions assign and distribute responsibilities and provide instructions for the conduction of operations and execution of experiments or other activities. Their objective is to keep the laboratory running securely.

Special working instructions consist of a step by step description of all allowed and limiting conditions as well as precautions to be observed during the performance of a one-time or recurring but well defined, delimited activity.

Working permits are necessary when an activity must be exercised i) in an already contaminated area, ii) in an area where a contamination cannot be excluded or iii) in an area where there is potential risk for personnel or equipment and where therefore special safety precautions must be complied with. These precautions may include wearing a protective suit, wearing respiratory protection, the installation of tritium monitoring equipment, installation of a tent, utilization of an “elephant trunk”, participation of Radiation Protection Service, or implementation of special conventional safety measures inherent to the process. A working permit

is also indispensable when personnel not belonging to the staff of the facility has to perform an activity in the supervised area.

Tritium facilities like TPL, TLK, TSTA or JET have provided thorough **Safety Descriptions** of all major infrastructure systems like Tritium Retention System, Exhaust System, Gas Supply System, Instrumentation and Control System, Storage System, Analytical System, Electrical System, etc. Similar detailed descriptions have been worked out for all key experiments. The descriptions should also document all measures and precautions taken to ensure long lasting safe operation.

The basic documentation of the tritium facility should include a comprehensive description and safety assessment of the site where the installation is erected, describe and evaluate the typical climatic and geological (e.g. seismic activity) characteristics of the site area, provide details on site access, portray at length the facility building(s), emergency plans and procedures, training programs of employees, safeguard strategy, air and water pollution control, waste handling procedures, storage and disposal strategy, etc.

An **Inspection Handbook** should contain i) a list of all inspections that need to be performed regularly, ii) an inspection calendar, ii) description of inspection procedures, iii) inspection instructions, iv) inspection protocols, etc. The results of all routine inspections shall be documented.

Complex research facilities like TPL, TLK, TSTA, etc. or the fusion experiment JET encompassing the tritium handling facility designated by Active Gas Handling System [Bel99a; Sto99], required the submission of a rather detailed and comprehensive **Safety Description** for approval of operation with tritium by competent authorities. Within this frame, it is important to be aware that regulators frequently focus primarily on the consequences of equipment faults and lines of defence for public safety rather than on whether the facility being licensed is operable.

At TFTR a special **Office of Certification and Training** was installed which among other activities organized Tritium Training Courses whose aim was to provide uniform technical and safety training to all personnel involved in operations with tritium [Sis94]. The course culminated in an examination which had to be passed by everybody. It conveyed basic knowledge on such diverse topics as physical and chemical properties of tritium; tritium compatibility with all kinds of materials, clean-up and storage of tritium; rudiments of radiation protection; diverse basic calculations related to handling of tritium; confinement principles; elements on tritium health

physics; airborne tritium monitoring; fire protection; interlocks, alarms, and controls; tritium support systems like component cooling and electrical distribution systems, etc.

For the implementation of modifications and enhancements, which are necessary in nearly all facilities, it is of utmost importance for persisting safety that clear rules be established for the **Technical Editing Process** not only of hardware but also of software. This is necessary to make certain that all modifications and enhancements i) remain traceable, ii) comply fully with every granted license, and iii) fit into the safety framework of the laboratory.

At TSTA or HRC, both representing tritium-handling laboratories without singular automated control systems, **Emergency Plans** have been implemented comprising measures to be taken in the event of i) injured or ill workers, ii) an evacuation alarm, or iii) an evacuation alarm taking place simultaneously with a fire alarm [And85; Nak11], etc. The plans included an emergency organisation structure, safety principles, a list and sequence of persons to be notified in caso of an emergency, a detailed description of the location of emergency equipment, description of evacuation procedure during or after working hours, what to do in case of loss of power, measures in case of earthquake, etc.

5.6 Technical Delivery and Acceptance Terms as well as Applicable Manufacturing Codes

Of considerable importance for safe operations with tritium is strict adherence to terms and codes such as for example the **Technical Delivery and Acceptance Terms** and **Applicable Manufacturing Codes**[3]. These terms and codes constitute important guidelines for industrial and workshop manufacturers. They establish technical standards for activities such as design, construction, and quality inspection of equipment; determination of leak rates; preparation of material surfaces; selection of pumps; choice of materials; selection of fittings, piping, and other equipment; choice of welding procedures; kind of welding inspections; certification of welders; design of metering and control equipment; guidelines for the manufacture of equipment and vessels; guidelines for the construction of glove boxes, selection and installation of electrical equipment; quality assurance techniques; radiographic and other testing procedures; accreditation of companies; procedures for writing documentation; etc.

[3] Technische Liefer- und Annahmebedingungen, Kernforschungszentrum Karlsruhe, December (1987).

A fairly comprehensive list of **Manufacturing Codes** comprising selected specifications, regulations, guidelines, handbooks and manuals applicable to US tritium facilities like Savannah River National Laboratories are listed in Appendix N [Poo08]. Another list of selected specifications, regulations, guidelines, handbooks, and manuals applicable to equipment installed at Tritium Laboratory Karlsruhe has been compiled by Welte et al. [Wel15] (see Appendix V).

Design and manufacture of components for the JET Tritium Plant must comply with requirements as stipulated in ASME VIII. Requirements exceeding this code have been demanded for i) leak tightness and ii) leak testing. Alternative national codes were permitted provided they satisfied at least ASME VIII. Some identified disadvantages of ASME codes were: i) restrictions to qualify contractors, ii) complexity of stress analysis, iii) the need of additional quality assurance (QA), and iv) lack of compatibility with vacuum and cryogenic technology.

A few supplementary codes and standards applicable to the manufacture of the Fuel Cycle of ITER are listed in Appendix X [Glu13].

For the industrial-sized cryo distillation plants at Darlington and Chalk River ASME VIII Rev 1 and AINSI B31·3 Class M and Canadian Standard CAN3-N285·0 M81 were applied. It was assumed that the dose arising to the public from a single failure would not exceed 50 mSv.

It needs to be stressed at this point that none of the above compilations are complete or up to date. They are only listed here to illustrate the complexity of the demands, draw attention on special precautions that need to be complied with during design, manufacture, installation, operation, and maintenance of facilities destined for tritium handling. They serve to illustrate what is more and more becoming international standard.

5.7 Automated Control Systems in tritium handling facilities

In modern tritium research facilities **instrumentation and control** (I&C) systems constitute the backbone to numerous safety relevant systems managed by an **Automated Control System** and backed by a hard-wired Safety Circuit. Safety Circuit trips are superimposed on trips by Automated Control Systems, i.e. the hard-wired Safety System is triggered when the Automated Control System fails to function. Set-point values of the Automated Control System are therefore slightly more stringent than those of the Safety System. Automated Control Systems allow round

the clock attended and unattended operation of a tritium facility. They take over the following duties:

- provide safety redundancy to hard-wired signal processing,
- control absolute temperature and pressure values with respect to pre-established upper and lower set points,
- control drifts between redundant and diverse safety relevant sensors to allow verification of sensor status,
- react to absence of life signal,
- perform data acquisition and collection. Acquired data can be used locally, sent to another international sub-station or to one of several data bases for use by operators, engineers, scientists, or administrations.

A widely implemented rule states that following a trip, process operation can only be re-started after complete elimination of the malfunction and authorization for re-initiation of operations by authorized staff. The latter is not possible when the system is in a low risk software solution stage.

In the following, key process control procedures implemented to achieve high safety standards in representative, rather diverse sized tritium-handling facilities devoted either to purely research activities or erected to support the operation of fusion machines are described. They exemplify - depending upon singularity and size of the facility and special characteristics of the corresponding research projects – a number of different options that have been realized successfully to accomplish this goal.

TPL: The Central Control System of TPL comprises a CENTUM unit and a YewMAC data processing system [Nar90]. The CENTUM process control system encompasses three field control stations and their corresponding terminal board cubicles, an operator station, an operator console, a universal console, and diverse printers, semi-graphic panels, etc. Control stations and terminal cubicles assume such functions as operation control, data acquisition, and data monitoring of process signals. The operator station and operator console serve as man-machine interface which manages key operations, interlocks and alarms. The universal console features buttons and

switches such as required for normal and emergency start-ups and shut-downs of operations. The semi-graphic panel visualizes essential components and their operation status. The change from normal operation into an abnormal one can be triggered manually or automatically.

TLK: The safety analysis at TLK is based on a single failure concept. In other words, it is assumed that a single failure remains without safety consequences to other sectors of a process. Hardware and software of safety relevant signals are separated at TLK from non-safety relevant signals. This approach was found to be advantageous for research activities, which necessitate higher flexibility than infrastructure systems which are of highly recurrent mode of operation. For the initial operation activities at TLK during the early Nineties, an AS3 (supporting the Tritium Transfer System) and an AS4 (supporting the Tritium Storage System) Automation System were taken into service and employed successfully over many years [Vol95]. In spite of this, it was decided to replace and adapt these ageing systems to one meeting more modern standards[4] [Bor10]. Within this frame, all older **automation systems** used for the integral operation, observation, data acquisition, conduction, and control of the major TLK tritium processing systems were completely substituted by a TelepermM AS488 Automation System from Siemens AG, Germany, complemented by a modular PCS7 library. The library was actually developed in house. The TelepermM is currently utilized for infrastructure systems such as the Tritium Storage System, the Tritium Retention System, the Isotope Separation System, the Tritium Transfer System, the Analytical System, and others. Component delivery, wiring of hardware, and assembly of the Automation System was conducted under the responsibility of Siemens AG. Specialists of TLK carried out programming and corresponding project design work. They also subjected the new software to extensive functional tests simulating all process signals. All in all, the upgraded I&C System now comprises six Automation Systems, six Programmable Control Systems and Automation Cabinets, one network cabinet for the plant and terminal bus including the corresponding optical filters, two redundant OS Servers, one Central Data Archive Server, eight Service Stations, one Engineering Station, and more than 200 I/O peripheral subassemblies. About 4.2 km of 32-wire jumper cables link these systems (see Fig. 5.4).

Consequently, the I&C now encompasses the assemblage of devices that monitor, control and protect the power system. The automation stations are centralized and connected among each other. They are also connected with the two redundant OS servers by a CS275 bus installation.

[4] Peter Schäfer, TLK, KIT, Karlsruhe, Personal communication, 2008

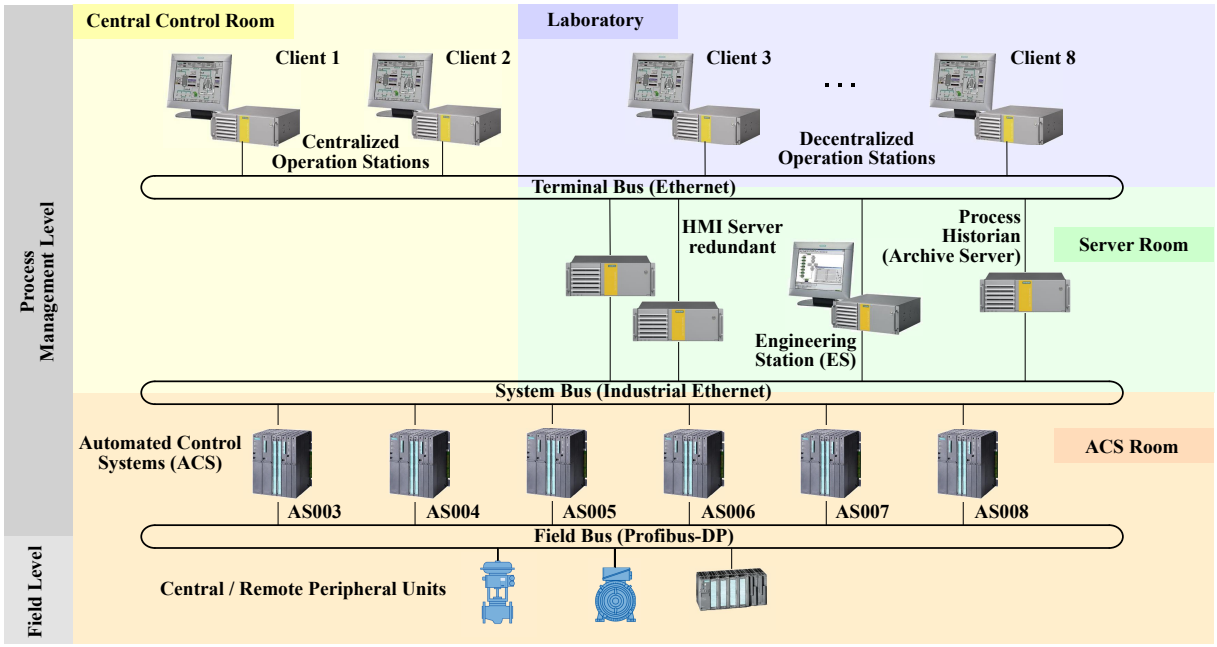


Figure 5.4: Schematic diagram of the modernized Instrumentation and Control (I&C) System of TLK[a].

Two Operation Stations are localized in the TLK Control Room, the rest is distributed decentralized as mobile units in the laboratory. Each major experiment, e.g. TRENTA, CAPER or sizable infrastructure system is equipped with its own Siemens PCST[5] Process Control System. Each Process Control System consists of a Simatic PCS7-AS417 automation, a PCS7/OS visualization unit, and a service module relying on Windows XP[6]. In case of TRENTA, two Control Systems from Rockwell Automation, each controlling one electrolyzer, were replaced by Simatic PCS7 controllers whose visualization panels could be installed close to the caisson windows enclosing the TRENTA facility[Bor10]. Because of this adaptation, they can now be operated using a glove fixed to the glove port of the caisson window.

Within the frame of the ongoing research activities it was also demonstrated that a Programmable Process Controller Simatic AG95 from Siemens can assume locally all control functions required to perform round-the-clock experiments. It was set to intervene at a lower level than the Central Control System.

Programmable process controllers can be of great help in cases such as:

[5] PCST = Public Communication of Science and Technology.
[6] Peter Schäfer, Personal communication, 2008

- **Loss of pressurized gas** causing open pressurized pneumatic valves to close (pneumatic valves are opened with pressurized air against spring tension). If such an event occurs during a running process a pressure rise in the system may be the consequence. Another after-effect is closed pneumatic valves which can only be opened after reactivation of pressurization. This can be avoided by early corrective measures, e.g. alert.

- **Loss of cooling water**: The Central Cooling Water System extracts heat from primary systems and from tritium retention systems. Loss of cooling fluid can be of considerable consequence when hot exhaust gas from a heated noble metal catalyst bed of a Tritium Retention System enters without cooling into the adsorber bed. Adsorbed tritiated water released under these conditions may significantly contaminate the gas emitted through stack. Protective measures comprise installation of one or more large reservoirs containing chilled water on standby. These reservoirs must take over the cooling function triggered by the controller until the initiating cause has been identified and removed.

- **Loss of cryogenic cooling**: When cryogenically condensed gases retained on an adsorber maintained at low temperature vaporize because of a sudden raise in temperature a rapid pressurization may occur. To prevent this, as soon as the vaporizing gas reaches a set point pressure it is expanded into an evacuated vessel by opening a valve activated by the controller. Hence, the integrity of the system is not affected. Only if the pressure surpasses an even higher set point value, shall a burst disk rupture and the gas be expanded into a safety vessel.

Mound Facility: The Tritium Emissions Reduction Facility (TERF) operated by EG&G Mound Applied Technologies for the Department of Energy, USA, is an automated process that continuously removes tritium from process gases before they are discharged into the atmosphere [Wie92]. Because automated round the clock operation is rather complex the tritium removal facility has been equipped with a Foxboro Intelligent Automation (I/A) Distributed Process Control System [Kis92b]. The control system was incorporated to increase the reliability and availability of TERF by automatically controlling the operation, assisting the operator in the diagnostic of problems, preventing maintenance, releasing alerts and alarms, generating reports and store data. The control design permits unattended operation during the day as well as round the clock unattended operation on weekdays, weekends, holidays or vacation periods. An

automatic alarm system alerts the operator outside of normal working hours. The Foxboro Fieldbus Input/Output (I/O) enclosures are located centrally together with their work stations on two process floors[7]. Hardware in the control room comprises i) an **application processor**, whose duties are first level control, process operations management, information management data collection system configuration, and management of system equipment, ii) two **workstation processors** who control display monitors (each workstation manages the information on its monitor and exchanges information with other processor modules), and iii) a **communications processor** which provides communication over the bus for all general terminals and printers. At the TERF process area zone control processors acquire input data from sensors and output control signals to the control elements via field bus modules. Approximately 400 I/O signal points are interfaced to the Foxboro system. Signal points connect to thermocouples, control valves, switches, pressure transducers, flow elements, and a variety of sensors, most of which are located inside of 14 glove boxes. Hence, the control system takes care of the i) optimization of process parameters, ii) delivery of alerts[8] and alarms to operators for better diagnosing and responding to problems, and iii) records and organizes data obtained from the process. Engineering, maintenance and operation personnel attend formal training at Foxboro and by operations personnel involved in design and implementation of the control system.

The system selected at Princeton Plasma Physics Laboratory (PPPL) for the operation with tritium at **TFTR** (now dismantled) was a D/3 Distributed Control System from Texas Instruments [Sch89b]. Three D/3 Process Control Modules were configured with redundant Micro Computer Units and a sufficient number of I/O (Input/Output) Multiplexer Chassis to accommodate the required number of digital and analogue I/O modules for its subsystem interface. All Process Control Modules were supplied with AC power by an uninterruptible power system as well as by a utility power company backed by a TFTR generator. Additionally, each Process Control Module was equipped with batteries capable of maintaining the system in operation for about 10 min in case of AC input failure. Most I/O modules supported 16 points. The configuration of the Redundant Micro Computer Units was such that one was active while the other was available as backup. Pre-programmed permissive checks and automatic sequences resided in the Process Control Modules which executed without operator intervention.

[7] TERF occupies on two floors a surface area of 225 m^2.

[8] As common to other tritium facilities, emergencies outside of normal working hours alert the operator by an automatic call-in alarm.

When necessary, operators could interact with an automatic sequence or with a process element directly. In both cases, the operator request was subjected to predefined permissive checks before actual activation became possible. In addition, certain process elements were provided with hardwired protective interlocks that had to be satisfied before a request from the Remote Control and Monitoring system could be executed. Protection against rapidly changing magnetic fields was achieved with isolation transformers installed in the AC power feed to the cabinets. This provision minimized electrical noise. All inter-area connections were executed over fibre optic links. One general conclusion was that the employment of a commercial system saved time, labour efforts, and in addition reduced costs.

Torus and peripheral equipment for the large and complex experimental device **JET** has been installed inside of a hall whose walls, floor, roof and doors were considered to constitute a complete biological shield. This shield is held at sub-atmospheric pressure using a depressurization plant that ensures positive in-leak. The biological shield also serves as fire suppression system. This is achieved by the capability of reducing in about eight hours the oxygen content of the enclosed atmosphere to less than 15 %. This concentration of oxygen will not sustain normal combustion. JET is operated with a rigorous interlock system together with a broad spectrum of safety measures that efficiently contribute to exclude tritium releases as well as damages to machine and equipment [Sto99]. The protection systems must take care of i) **pulsed operation hazards** arising from high power, high power densities, high stored energies and of ii) **continuous operation hazards** arising from the necessity for round-the-clock operation of cooling systems, cryogenic pumping systems or vessel baking systems sometimes for rather extended periods of time, i.e. up to months. The protection systems ensure that safety and integrity of JET is at all times guaranteed. Major incentives for numerous measures aimed at preventing interventions after operations with tritium and - unique to JET - beryllium, are the avoidance of machine down-time, the refrainment from lengthy and cumbersome work in a full protective suit and last not least preclusion of elevated costs. To this effect JET relies on a Programmable Logic Controller concept comprising a network of Simatic S5-110F and Simatic S5-115F PLC´s. The number of inputs from the plant and outputs to the plant of each S5-110F and S5-115F are 128 and 300, respectively. The PLC´s are self-checking. Avoidance of serious damage in pulsed operation comes primarily from high level specifications and robust design of the mechanical

and electrical systems as well as from sophisticated control systems. Complementary to active protection, much attention was given to passive protection.

Concerning prevention of tritium releases at JET all containments, pipe-work, and vessels are protected throughout by double containments. Tritium present in vessels or pipes is at all times maintained at sub-atmospheric pressure and further protected by flushing all secondary inter-space volumes with gaseous nitrogen. This gas is redirected back to the Active Gas Handling System, where it is analysed for tritium. If tritium is detected, alarms are activated and necessary corrective measures taken.

In summary, all protection systems at JET were found to be of high reliability and did not contribute significantly to down time of the overall system. The DTE1 tritium campaign of JET was executed successfully and safely, the machine protection systems working reliably at very high operational availability. However, because JET was considered to be an experimental facility sufficient standardization of the protection systems was not possible. This has conducted to unnecessary design efforts, inefficiencies in maintenance and commissioning efforts, and difficulties in analysing the safety of design solutions. These issues should be addressed in future tritium installations. In spite of this, it is without doubt that the experience gained at JET and elsewhere is providing highly valuable information for the design of the safety systems of ITER.

ITER: A very simplified block diagram of the major subsystems constituting the inner fuel cycle of ITER is displayed schematically in Fig. 5.5. As evident, all subsystems are strongly interlinked. Off gas from the torus is collected in cryo-pumps and sent to the Tokamak Exhaust Processing System (TEP), where all fuel-relevant molecular and bound tritium and deuterium is nearly completely recovered. In the Atmosphere and Vent Detritiation System (AVDS) the remaining de-tritiated gas is further de-tritiated down to extremely low levels of contamination and only then released into ambient. Recovered fuel molecules, on the other hand, are separated into molecular deuterium/tritium fractions and simultaneously freed from protium in the Isotope Separation System (ISS). Finally, fuel molecules in the Storage and Delivery System (SDS) are returned via the Fuelling System (FS) into the Torus and the Neutral Beam Injector System. The only direct gas release into the environment besides that from the Vent Detritiation System takes place from the Water Detritiation System (WDS).

Similar passive and active protection measure as successfully demonstrated at JET are being contemplated for **ITER** to assure safety and intactness of the tritium systems. Passive measures

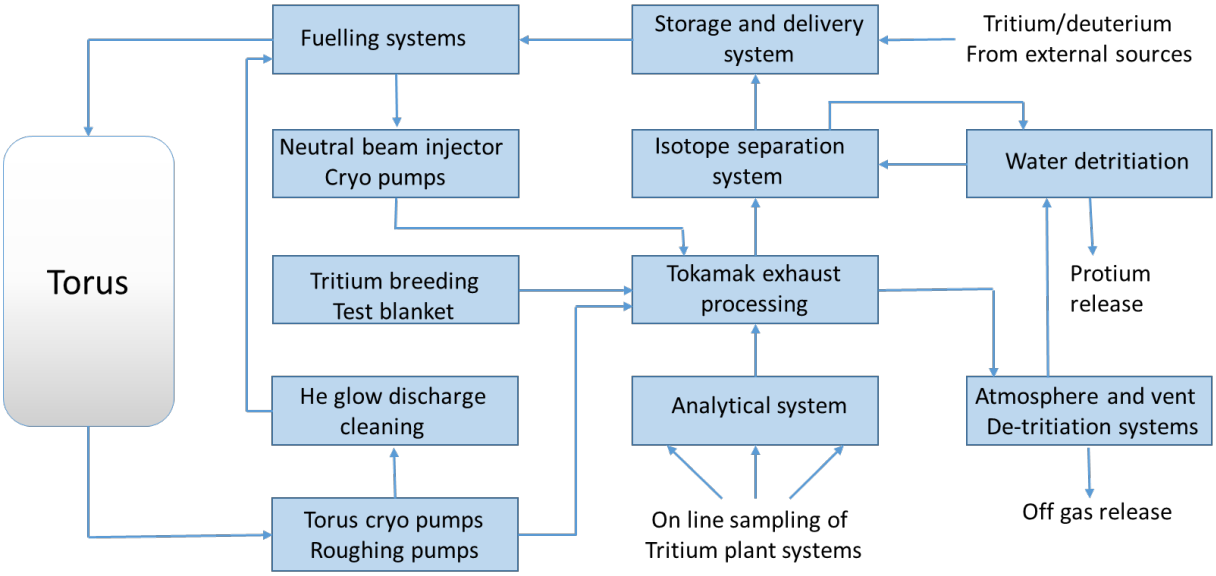


Figure 5.5: Simplified block diagram of the ITER inner deuterium/tritium fusion fuel cycle (after [Glu06c]).

comprise all-metal construction, vacuum insulation of heated components, best quality materials, high and controlled manufacture standards, second confinements, redundancy of safety-relevant sensors, burst disks, etc. Typical active measures include **Automated Control Systems**, gaseous waste treatment, pressure/temperature/radioactivity interlocks, redundant cooling fluids and pumps in safety relevant systems, uninterruptible power supply of safety-relevant sensors and components, relief valves against over-pressure, healthy signals, etc.

Because at the beginning the CAD systems of ITER-EDA did not have model management tools, it was necessary to develop own tools, which gradually evolved into the ITER **Integrated Model Management System** (IMMS) [ITE09]. Accordingly, IMMS can now handle all relevant project information's for CAD related ITER documents. ITER furthermore selected Dassault Systèmes CATIA, ENOVIA, and DELMIA to engineer reactor and plant, structure its design methodology, and warrant long-term data interoperability across the organization. CATIA V5 is used as computer aided design tool and ENOVIA V5 for product data management. A key target of the implementation of DELMIA at ITER will be the virtual verification of whether the intended plant operates according to specifications. Hence, it is now possible to test the numerous interfaces of the project before beginning of construction. The implication are rather substantial savings.

It is important to keep in mind that in the special case of ITER, design and other data must be accessible to geographically widely distributed partners and supplier locations. Typical design data comprise for instance piping and instrumentation diagrams, part design, wire frame and surface design, piping design, equipment arrangement and catalogue editor [ITE09]. Within the frame of the latter, 2D symbol catalogues and 3D part catalogues have been worked out for piping, tubing, equipment, instrumentation, electrical components, etc. using the European standard flow diagrams for process plants EN ISO 10628, the standard process measurement control functions, and instrumentation ISO3511 and the standard graphical symbols in vacuum technology DIN28401 [Laz06]. Outcomes obtained so far demonstrate that with CATIA and ENOVIA the design - which includes an extremely high number of complex critical parts inside and around the tokamak - interface without conflicting. IMMS manages and controls all ITER CATIA data assigning unique identification numbers, visualized by the IMMS tag, for which up to 70 characters can be used for individual objects. With these characters it becomes promptly possible to identify and find objects. The numbers provide information on items such as subject index, sequential IMMS number, drawing number, object type, reference or formal revision number, working revision number, model status, request for modification site and revision number, site where the object has been developed, base line (for example FEAT), date, designer, name of task officer, process title like for example isotope separation system, etc. It also becomes possible to select children or parent drawings in order to obtain information on a lower or a higher level in the development of a given drawing. Therefore, the Integrated Model Management System handles the management of the ITER CAD models and drawings processing records, tracks, updates, and replicates. It furthermore notifies on a list of addresses, indicates the status, and organizes the interchange among the joint working sites for CAD related documents. An important benefit of IMMS is that it brings together many engineering and scientific specialists who need to communicate and operate in a concurrent as well as collaborative way.

Exemplifying the kind of safety and protection measures developed for tritium systems of ITER are some typical **Pipe & Instrumentation Diagrams** (P&ID) for the Storage and Delivery System (SDS) and the Tokamak Exhaust Processing (TEP) Systems of ITER discussed in considerable detail in a paper by Glugla et al. [Glu05].

The applicability of IEC61508 (IEC = International Electrotechnical Commission), an international set of standard rules for electrical, electronic, and programmable electronic safety

frequently applied in conventional industry, to the design of ITER has been evaluated critically by Glugla et al. [Glu05]. According to IEC61508, four **Safety Integrity Levels** (SIL), i.e. SIL1, SIL2, SIL3 and SIL4, have been identified depending upon the degree of risk involved. A SIL describes the requirements over the lifetime of a plant ensuring that systems are designed, implemented, operated, and maintained in accordance with the risks involved. Therefore, after a risk evaluation on the basis of a Hazard and Operability analysis (HAZOP) and a description of all safety steps, together with their verification and validation, **Safety Instrumental Functions** (SIF) are identified and SIL´s are assigned to each SIF. While software solutions are accepted for SIL1 or SIL2, in case of SIL3 a hard ware solution is considered obligatory [9]. Safety integrity levels type SIL4 are thought to be non-acceptable for the inner fuel cycle.

Risk examples: Typical intermediate/high risk events are considered to be:

- release of tritium into a glove box,
- pressure excursion in a tritium system,
- temperature excursion of a heated component in a tritium system,
- failure of the Central Automated Control,
- failure of the hard-wired Central Safety System
- failure of power supply,
- loss of cryogenic cooling,
- failure of pressurized gas supply,
- loss of cooling water.

Occurrence of any of these events will activate the Automated Control System to immediately turn off all heaters and shut down every other electrical power consumer like pumps, blowers, etc. Pneumatic valves will close to the unactuated position. Only carefully selected **safety-relevant sensors** will remain in operation energized by the uninterrupted power supply. The information

[9] It should be noted that computer-based systems - generically referred to as programmable electronic systems - are not only used to perform non-safety functions but more and more to enact safety relevant functions.

provided by safety-relevant sensors is important to find out the cause of the event and implement the measures necessary to return the system into a safe state.

Recapitulating: Automated Control Systems collect process data via instrumentation and control devices and execute safety actions. They contribute notably to reduce the incidence of outages and shorten the duration of outages when they occur. Automated control systems, moreover, assist the operator in the diagnosis of problems, ensure preventive maintenance, and provide long-term storage of data.

6 Remote handling

Remote handling constitutes a rather important activity for the operation of fusion machines of the size of JET or ITER because, once a machine is operational, easy human access to the machine is no longer possible. This is primarily due to the high level of contamination by tritium and transmutation products that establishes soon after initiation of operation.

It has been estimated that over the years tens of thousands of tasks have been carried out at JET remotely. For example, the JET MKIIa divertor was removed and replaced with the MKII gas box divertor configuration employing almost exclusively by remote handling methods [Rol99]. Over 450 components required handling during a 15-week period throughout which work was performed about 20 hours per day and 6 days per week. Typical remote handling tasks, i.e. without personnel entering the vacuum vessel, comprise removal of defect or outdated components, installation of new components, changing of configurations, updating systems, retrieving/replacing tiles from the first wall, etc.

Even though inside of the vacuum vessel remote handling techniques represent the norm, there are always situations where remedial work can only be accomplished manually. Remote operation rates at JET were found to be similar to manual operation rates.

A specially developed **In-Vessel Training Facility** is used prior to any access to the torus to train and familiarize new operators both with manually as well as with remotely executed tasks [Edw00]. When considered necessary, objects requiring work are modelled in terms of size, weight and shape and then utilized for realistic training. Objective of the training is to keep the time the operators spend in areas contaminated by tritium and other decaying elements as short as possible. The aim is minimization of received dose during hands on work. Experience at JET indicates that maintenance activities and upgradings normally take place every 3 - 4 years and that they last from a few months to more than a year.

A comprehensive study on tritium uptake by materials and components commonly employed for the manufacture of remote handling equipment such as proposed for ITER was carried out by Higashijima et al. (see [Hig02] and references therein). They exposed the materials and components to a tritiated environment consisting of either liquid tritiated water or to an atmosphere containing 6000 - 7000 ppm moisture and about 6×10^7 Bq m^{-3} of tritium. Conclusions drawn from the experiments were: i) oxidized surface layers on metals like rust on carbon or stainless-steel, tin (Sn) coated copper and electric connectors, strongly favour contamination, ii) electric cable jackets (cross linked polyethylene) were intensely contaminated in spite of being hydrophobic because of the utilization of a white carbon filler showing large affinity for water, iii) pasted grease layers picked up tritium mostly on the exposed surface and iv) inner parts of an AC servomotor were equally contaminated as the outer surface. This was explained by a sealing gap between casing and brackets. Therefore, it was recommended to place servomotors in a leak-tight casing.

7 Occupational hygiene

Generally, conventional occupational hygiene is concerned with the prevention of hazards arising from work that may end up in injury, sickness, impaired health or significant discomfort to the working personnel or to citizens of the adjacent community. Occupational hygiene surveys comprise inspection of work places and an evaluation of the associated risks. To ensure the continued health of all workers, occupational hygiene assessments should preferably be carried out by qualified and experienced hygienists.

Workplace hazards are usually classified into physical, chemical, biological, ergonomic and psychological hazards.

Commonly occuring **physical hazards** that need to be contemplated are noise, temperature extremes, illumination extremes, vibration, ionizing or non-ionizing radiation and ergonomics. As for every other installation, the design of a tritium-handling facility must include features to facilitate for guarding of elevated surfaces or protection from fall employing fastener devices. Because falls from high locations are a leading cause of fatalities, such measures are indispensable to protect employees assigned to work under such conditions. The design of facilities encompassing hazardous energy sources must include features to facilitate the installation of lock and tag mechanisms. For example, it may be necessary to ensure that dangerous equipment be properly shut down and only restarted after completion of maintenance or repair work.

Other protective measures relate to surfaces whose temperature exceeds 333 K. They need to be secured from inadvertent contact by workers employing either engineering controls, administrative controls or suitable personnel protection devices. Much attention needs to be given to potential ignition sources. When associated with processes, they shall meet the appropriate class and division for intrinsically safe equipment. By complying with these requirements, the risk of catastrophic failure, e.g. explosion, can be avoided and personnel as well as equipment be protected.

Leaks from inert gas lines may bring about a dangerous local oxigen deficiency which can only be detected with adequate monitoring devices. Hence, occupied spaces and areas of frequent maintenance must be provided with an oxygen monitor if failure of any line in the working space could cause release of gas at a flow rate large enough to reduce the percentage of oxygen in the space to less than 19.5 %. Without corrective measures there is great potential for employee injury.

Chemical hazards requiring awareness include agents like gases, vapours, particulate aerosols, combustible dust, etc. These agents can only occur either in the air or on surfaces. More often than not, they require special analytical techniques for their identification and quantification as well as specialized sampling equipment.

Any non-radiological laboratory hoods and local exhaust systems used to control emissions of non-radiological particles, gases, vapours, mists and/or fumes in the breathing zones of workers must comply with conventional standard requirements. Ventilation is one of the primary engineering controls used to protect personnel from potential chemical exposures.

Measuring electronic devices such as required to determine noise, vibration, ionizing and non-ionizing radiation, respirable dust ($< 10\,\mu m$) and inhalable dust ($100\,\mu m$), solvents, gases, etc. are largely commercially available. Most of these devices need to be calibrated before and after use.

Biological hazards may result from biological agents like infectious microorganisms or allergens spread during work with viruses, fungi or bacteria. They can eventually be the origin of chronic infections.

Further occupational hazards that need to be kept in mind are **ergonomic deficiencies** as well as **psychological stress** situations.

In summary, tritium-handling facilities must not only comply with all safety and health standards required from a tritium-handling facility but also with all conventional occupational safety and health standards. Failure to meet with these standards would enhance the potential for workplace injuries or illness beyond those arising from radiochemical exposure.

8 Wastes

Tritium-handling laboratories and technological facilities engaged in tritium research relevant to fusion generate waste resulting from the direct exposure of solids, liquids, or gases to molecular tritium and/or other tritium-bearing species. This waste includes metals, alloys, ceramics, adsorbers, catalysts, polymers eventually of complex composition contaminated by tritium adsorption, permeation, chemical reaction, adhered tritium-contaminated dust of diverse chemical compositions. Other waste consists of tritium-bearing liquids like water, electrolytic solution, solvents, or liquid scintillation cocktail. Gaseous waste comprises primarily tritiated water vapour, molecular tritiated hydrogen isotopologues, and tritiated hydrocarbons.

The only other inherently radioactive waste generated in purely tritium-handling facilities is uranium, which is sometimes employed for storage and pressurization of gaseous tritium, or for the purification of molecular tritiated hydrogen species. Transmutation products can only be expected if materials, or components retrieved from the first wall or structures of a fusion machine have been delivered to the tritium-handling facility for research or other purposes. Kind and level of contamination of these materials/components will probably be known to a good approximation from the required way bill of transportation.

When considering radioactive waste generated during the operation of **fusion machines** the following categories need to be contemplated [ITE01d]:

- Materials turning radioactive by interaction with energetic neutrons, high energy electrons, or other particles during the operation of fusion devices with D – D or D – T plasmas. Typical radioactive species produced by fusion neutrons are ^{60}Co, ^{41}Ar or ^{14}C. Transmutation products like ^{59}Ni, ^{63}Ni, ^{93}Mo are generated from steel alloying elements. Impurity elements in stainless-steel like Co, Nb, or K also contribute to the generation of activation products. At the first wall of a fusion device tritium is not only incorporated into metals by gas-driven or plasma-driven permeation but is also generated via transmutation reactions of structural

materials like steel, beryllium, copper, and others, as well as from the impurities therein. ^{16}N is generated in the cooling water of fusion reactors by reaction of high energy neutrons with the oxygen of water molecules as they circulate through heat exchangers [Ike97]. Because this radionuclide is of very short half-life its contribution to the radioactivity of waste is only minor.

- Materials inherently radioactive like uranium. Uranium is a radioactive element whose chemical effects on the kidney are more severe than its radiotoxicity. It is particularly chemotoxic when in form of dust.

- Another naturally radioactive material is tritium . It may be present in waste in several different chemical forms like water; implanted or dissolved atomically in metals; co-deposited with carbon as dust or flakes; as tritide of reactive metals like uranium, titanium, zirconium-cobalt, or lanthanum nickel alloys; incorporated into hydrogenous organic materials like oil, membranes, paper, cloth; plastics, etc. These rather dissimilar materials have also quite different radiotoxicities.

- Typical mixed waste are tritium-contaminated beryllium or materials like carbon contaminated by tritium and beryllium (here tritium is radiotoxic and beryllium highly toxic). Uranium tritide must likewise be classified as mixed waste. If besides tritium, the waste has been exposed to energetic neutrons from D-D or D-T plasma particles a mixed waste containing transmutation products must be expected.

The design of ITER or of any other fusion machine should incorporate at an early stage measures that facilitate decommissioning, minimize occupational exposures, and keep the amount of wastes as low as possible [ITE01d]. In this respect, design guidelines should comprise i) selection of low activation construction materials, ii) employment of modular components for easy dismantling, iii) shieldings in order to maintain at low level the activation of ex-vessel components, iv) component design that keeps contamination at low levels and allows easy decontamination, and v) design that minimizes dispersion of radioactive material. Concerning the selection of materials, decommissioning strategies, and material treatments the ultimate design target of ITER should be i) minimization of the quantity of activated material requiring disposal in a repository, ii) minimization of radioactive waste material requiring transportation beyond the

site boundary, and iii) maximization of the amount of material that can be cleared for disposal as non-radioactive waste.

If possible, the generation of mixed waste should be avoided already at the source [US 02]. Within this frame, radioactive-only materials should be segregated from hazardous-only materials and if doable only non-hazardous cleaning materials should be used. In case of contaminated materials or components interimly stored for future reuse as much relevant information as possible should be documented during their active utilization. The same holds for prospective waste, for which information should be collected right from the beginning of operations in order to permit tracking of materials and components through the various processing stages until they leave the site as waste. Detailed knowledge on pressure ranges and temperature ranges and history of exposure not only to tritium but also to other chemicals are necessary for an assessment of the degree of tritium penetration into metallic surfaces. This information may be very useful during sentencing and categorization of waste.

Directive 96/29/EURATOM, known as the International Basic Safety Standards (BSS), has been applied in the EU member states beginning May 13^{th} 2000. In Germany, the "**Verordnung für die Umsetzung von EURATOM-Richtlinien zum Strahlenschutz**", which appeared July 20^{th} (2001) [Bun01b], executes this directive. A number of selected exemption values, clearance levels, allowed activity concentrations, and dosis coefficients given in this directive for tritium have been compiled in Appendix W[Bun01b]. According to the International BSS [Int14] exemption values of moderate amounts of material for reporting practices with tritium are 10^9 Bq and $10^6\,\mathrm{Bq\,g^{-1}}$. The activity of tritium corresponding to a dangerous source (D value) is 2×10^3 TBq.

In **France**, the host country of ITER, the **National Agency for Radioactive Waste Management (ANDRA)** carries the overall responsibility for all matters concerning the long-term management of radioactive wastes and repository sites [Ros10; Pam14; Can15]. ANDRA works under the authority of the Ministries for Energy, Research and the Environment. Sentencing criteria are determined in France both by the radioactivity level as well as the lifetime of the radioactive waste. Several repository sites for tritium-bearing waste are currently available in France. For very low-level waste (VLLW or tres faible activité) the repository site **Centre de la Manche** with a maximum storage capacity of $5.3 \times 10^5\,\mathrm{m^3}$ and about 50 years of operation experience is available. Another disposal facility is the **Centre de l´Aube**, which was commissioned

1992. This repository has about 50 years of operation experience and a storage capacity of $10^6\,m^3$. The site only accepts low- and intermediate-level short-lived waste (SL-ILW) (faible et moyenne activité à vie courte = FMA-VC) containing an activity of max. of $2 \times 10^5\,Bq\,g^{-1}$ and displaying a limit tritium outgassing rate of $2 \times 10^6\,Bq\,t^{-1}\,g^{-1}$. Additionally, in the vicinity of the Centre de l´Aube, a new repository for VLLW waste, i.e. **Centre Industriel de Regroupment, d´Entreposage et de Stockage (CIRES)**, with a storage capacity of $2.8 \times 10^5\,m^3$, was commissioned by ANDRA and went into operation in 2003 [Ros10].

Legal requirements concerning handling of radioactive wastes (radwastes) and the limits set on the annual exposure of employees and other persons involved in activities with radioactive isotopes need to be strictly complied with. In the UK all materials having a specific activity of $> 0.4\,Bq\,g^{-1}$ must be disposed of as radioactive waste. Up to radioactivity levels of $4\,kBq\,g^{-1}$ alpha or $12\,kBq\,g^{-1}$ beta/gamma the waste is sentenced as low-level radioactive waste (LLW) and above that level as intermediate level waste (ILW). Within the frame of legal requirements in the **United Kingdom**, handling of radioactive materials is described in the **Ionizing Radiation Regulations (IRRs)** from 1985, which deals with the approval and control of practices involving the use of radioactivity, and in the **Radioactive Substances Act** 1993 (RSA), which deals with the disposal of waste. Only LLW is accepted at the repository near Brigg in Cumbria, UK. No repository for intermediate or higher level waste is presently available in the United Kingdom.

A comprehensive literature survey on waste management options for tritium-contaminated waste was published by Mannone [Man90]. Principal topics of the review were i) origin and characteristics of tritium-contaminated wastes resulting from the operation of light water reactors, fuel reprocessing plants, and thermonuclear fusion facilities, ii) immobilization and containment of waste, iii) conditioning of liquid and solid tritium-contaminated wastes, iv) packaging of tritiated waste, and v) monitoring of tritium outgassing from waste.

Another all-embracing review of the literature was published by Clark [Cla96]. Discussed topics were i) mechanisms leading to contamination by tritium, ii) the distribution of tritium in contaminated materials, iii) assaying of tritium in liquid and solid wastes, iv) options for waste decontamination, and v) disposal choices for tritiated waste. Aim of the work were recommendations to meet demands for tritium facilities in operation at Savannah River Site. Emphasis was placed on the necessity to further assess and develop i) new methods for the removal of tritium from contaminated surfaces like plasma cleaning, combination ultraviolet

light/ozone, or lasers, and ii) the development of radiological detectors for the routine monitoring of waste.

8.1 Gaseous tritiated waste

Gaseous waste is generally not categorized. Its release into the environment depends on the chemical form and limits for discharge.

8.1.1 Inorganic gaseous tritiated waste

During the early days of tritium technology, a technical tritium extraction facility like that taken into operation 1970 at the Laue-Langevin Institute in Grenoble, France, recovered more than 7.2×10^4 TBq of tritium from over 840 000 l of heavy water and released to ambient about 1 % of the total extracted during 16 years of operation, i.e. an average of 4.5×10^{13} Bq year^{-1}. These releases were obtained from the sum of the permissible discharges and the total liberates registered during several minor incidents.

Since then it has become common practice in most laboratories to minimize the releases into the environment by passing all tritium-bearing gases exhausted from tritium handling facilities through a Central Tritium Retention System [Nar90; And95e; Vol95]. At **Tritium Laboratory Karlsruhe** waste exhaust gases released from primary systems are first collected in large vessels partially pre-loaded with nitrogen up to a pressure of 700 mbar to comply with explosion safety. Once a vessel reaches capacity and provided the concentration of tritium is sufficiently low, the gas is processed in once-through mode across a Central Tritium Retention System. In case the concentration exceeds a certain limit value, processing is carried out in closed loop operation in a so-called Pre-Treatment System until the concentration of tritium is reduced to a level acceptable for the Central Retention System, i.e. $\sim 10^{10}$ Bq m^{-3} [Sch91a; Hut95]. The pre-treatment loop relies on an oxygen donator catalyst operated at 523 K (this catalyst requires periodical regeneration), a molecular sieve bed and a gas recirculation pump (15 - 30 m^3 hour^{-1}). A few numbers may help to illustrate the performance of these systems: At TLK, which started tritium operations 1994 and increased gradually the tritium inventory during the course of the first four operational years to values of up to 23 g, the **Central Tritium Retention System** processed a total of 3×10^6 m^3 gas and retained a total of 5×10^{12} Bq of tritium. During the same period the Pre-Treatment System processed 450 m^3 of higher contaminated gases given to waste by diverse research and infrastructure primary systems and retained 2.5×10^{14} Bq of tritium [Doe98]. Releases of tritium during the period 1996 – 1999, a time in which many research activities with

large amounts of tritium like a fuel clean up loop, an isotope separation system, numerous tritium transfer devices, analytic equipment, etc. were regularly in operation, remained consistently well below the maximum authorized emission of 4×10^{13} Bq year^{-1}, i.e. 0.1 - 0.8 % of that value[1].

At **Tritium Process Laboratory** (TPL) in Tokai-mura the oxidation of tritiated species exhausted from primary systems is carried out with two sequential noble metal catalyst beds, one maintained at 473 K and the other at 773 K. Catalytically generated water is adsorbed conventionally on a molecular sieve bed [Yam11a]. Decontamination factors achievable with this catalyst/adsorber combination were found to be of the order of 10^4. During a total of 13 years of operation beginning 1988, TPL released to stack an accumulated amount of 11.1×10^{10} Bq HTO and 1.2×10^9 Bq HT. Therefore, predominantly tritiated water [Yam02]. The average concentration of tritium at stack level was estimated to be 25 Bq m^{-3}, i.e. about 200 times smaller than the authorized limit in Japan at the time. The maximum tritium inventory at TPL at the time was 60 g. During a more extended period of operation encompassing 22 years and again beginning 1988, an accumulated amount of HTO of 4.9×10^{11} Bq and of HT of 3.4×10^{10} Bq were released via stack [Yam11a]. The average concentration of tritium at stack over this longer period of time was estimated to be 71 Bq m^{-3}. Comparatively high values were only monitored during the period 2002 – 2007. This was attributed to activities related to dismantling of experimental facilities. Within this frame, the highest quantity of tritium released to stack was 73 GBq in 2005 (see Fig. 8.1). As apparent, the fraction of released HTO was at all times much larger than that of HT.

Gaseous emissions from a tritium-handling laboratory like **Ontario Hydro Research Division** erected for the purpose of supporting the **Tritium Removal Facility at Darlington Nuclear Generating Station**, Canada, were reported by Heics et al [Hei88a]. As of 1987, the emissions of tritium (HT + HTO) were restricted by the Atomic Energy Control Board of Canada to 52 GBq weeks^{-1}. This implied that concentrations of emitted tritium averaged over a one-week period were not allowed to exceed 40 kBq m^{-3}. In compliance with this restriction, the actual measured average weekly values remained 10 % below this emission limit.

It is of special interest to examine releases of tritium from **Tritium Systems Test Assembly** (TSTA). This large facility, which was devoted to tritium research in predominantly technical scale, is now dismantled. Tritium was first introduced into TSTA 1984. During the course of the

[1] Doerr, L. 2014. private communication.

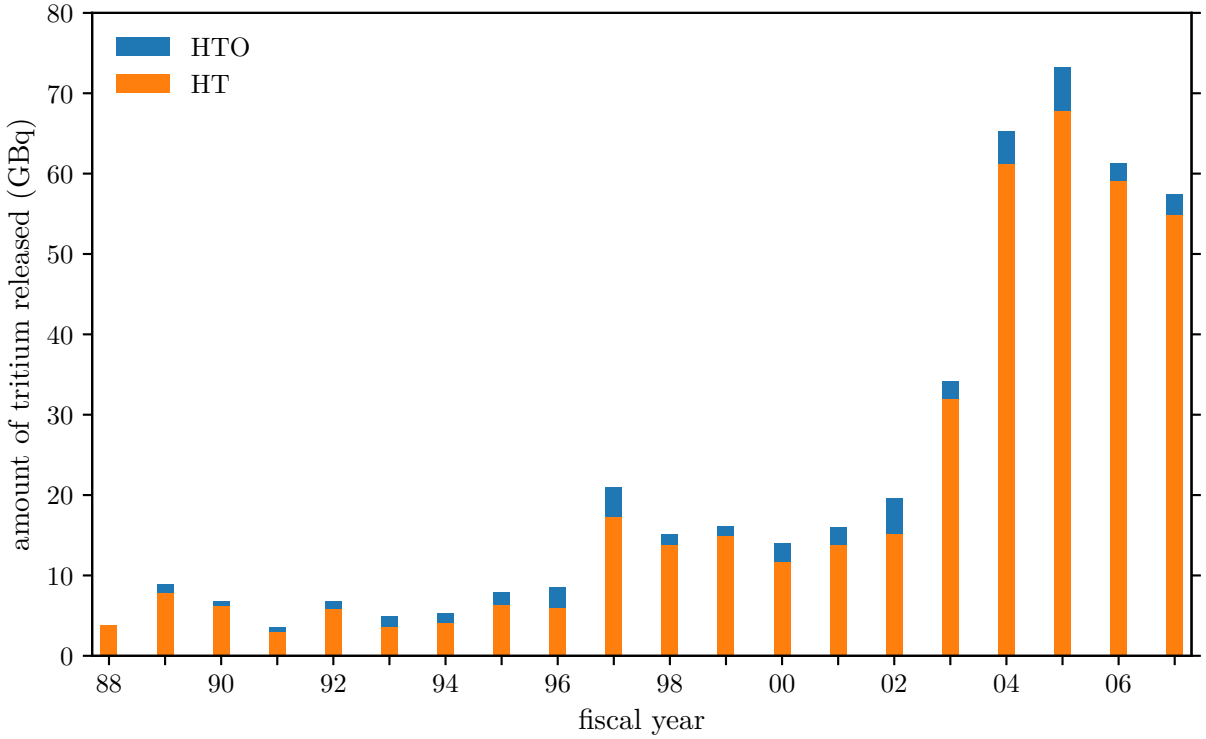


Figure 8.1: Tritium released via stack as HT and HTO from TPL during the fiscal years 1988–2007 (after [Yam11a]).

following five years the inventory progressively increased up to about 100 g. Principal components and systems available at TSTA for the research program carried out at the time were a reactor torus mock-up backed by ancillary tritium systems such as a cryogenic isotope separation system, an impurity simulation system, a number of transfer and evacuation pumps, cryo pumps, a tritium waste system, and a novel fuel clean up system. Within the frame of an ambitious investigation program as well as numerous smaller activities, up to 100 g of tritium at rates in the range 1.0 - 1.2 $\mathrm{kg\,d^{-1}}$ were processed. The limit emission into the environment was fixed at $1.5 \times 10^{12}\,\mathrm{Bq\,year^{-1}}$ [And88; Car88]. In compliance with this goal, the actual total releases after almost five years of operation with tritium remained at approximately $3.2 \times 10^{11}\,\mathrm{Bq\,year^{-1}}$. Stack monitoring performed at TSTA consistently indicated that about 80 % of the released tritium was water and the rest molecular hydrogen. This observation is well in line with measurements performed at TPL (see above). 1987 the Japan Atomic Energy Research Institute (JAERI) and the US Department of Energy (DOE) signed a collaborative agreement that constituted the basis for numerous new (no previous experience), innovative and complex tritium research

projects encompassing fundamental work on plasma exhaust clean up, tritium storage, laser Raman spectroscopy analytics, cryogenic isotope separation, cryoadsorption and tritium plasma experiments. Total releases during the period 1985 – 1990 were less than 6.3×10^{11} Bq year^{-1} [Bar90]. This value was clearly lower than the self-imposed value of 1.5×10^{12} Bq year^{-1} and well below the legal requirements holding at the time as established by the Environmental Protection Agency (EPA) or the Department of Energy (DOE).

In contrast to "normal" releases and in particular during the implementation of several exigent tritium research activities towards the end of 1988, sporadic releases of up to 3×10^{11} Bq month^{-1} (consisting of nearly three times as much HT as HTO) were registered at the TSTA stack [Bar90].

In 1991 a single tritium release of 1.5×10^{10} Bq occurred into a TSTA room which was subsequently registered at stack. Even though no personnel exposure resulted from this release, a three months shutdown period and a thorough investigation of the event was mandated by DOE [And92c]. TSTA was shut down in 2000 within the frame of a re-organization of all tritium activities ongoing in the US at the time [Wil02].

Mound Laboratories, Miamisburg, Ohio, a facility originally dedicated to nuclear weapons research, was engaged 1969 among other activities in the enrichment of tritium using a combination of cryogenic distillation and thermal cycling absorption, and in charging of diverse containers with tritium for commercial purposes. Mainly with the objective of achieving high temperature strength and exceptional corrosion resistance, all subsystem components and interconnecting pipings of this facility were fabricated from **Inconel-625**. A catalyst vessel containing 82 kg of cylindrical platinum catalyst pellets was likewise manufactured from the same material. The unprecedent implementation of this structural material was found to be quite challenging on one hand because pipings were difficult to locate and fittings commercially non-existent, and on the other, because new welding techniques needed to be developed and the spineing process (spineing a shaft means that the plane of assembly must be identified in which the shaft is most stable) did not work as expected. As a result of these activities it was concluded, that stainless-steel type 321, 347, or other would have been a better choice than Inconel-625 [Wie92]. While initially up to 10^{16} Bq were released from Mound Laboratories to the environment, the effluent discharges dropped to less than 10^{14} Bq twenty-one years later. After the prevailing Effluent Recovery System (first such system of a DOE facility) was upgraded to constitute the so-called **Tritium Emissions Reduction Facility** [Hed88; Wie92] the releases decreased even

Table 8.1: Stack concentrations of tritium-bearing species measured at JET during PTE in 1991 (in kBq m^{-3}).

Date	HTO	HT	CH_3T
18 Nov. – 25 Nov.	140	105	0.23
25 Nov. – 02 Dec.	11	258	1.52
02 Dec. – 09 Dec.	2	92	0.04
09 Dec. – 16 Dec.	1	52	0.29
16 Dec. – 23 Dec.	5	38	0.11

further and this inspite of a doubling of the tritium inventory [And92c]. This documents the extraordinary progress achieved over the years in environmental protection.

In Japan, the average annual production of tritium at **JT60-U** generated in D – D plasmas was determined to be 18 GBq and that of the cumulative production estimated to be 170 GBq. Monitoring of tritium at the stack remained below detection limit, i.e. 10^{-5} Bq cm^{-3} [Oik02].

Another example that illustrates realistically the typical release of tritium from a large physics experiment is provided by **Joint European Torus** (JET) [Hug92b; Won92; Bel95a]. In this device, work is carried out by numerous workers, technicians, engineers and scientists mostly of different nationalities employing a rather complex and voluminous fusion machine served by a tritium handling facility equipped with a huge number of valves, connections, feedthroughs, attached novel components, advanced analytical instrumentation, sophisticated diagnostics, etc. Whereas prior to 1991 only about 4 GBq year^{-1} (compare with JT60 in previous paragraph) were discharged during D-D campaigns, this amount increased to values as high as 100 GBq weeks^{-1} during the first tritium campaign of JET, i.e. Preliminary Tritium Experiment (PTE), in which 3.7×10^{13} Bq tritium was injected both into the Tokamak and into the neutral beam injector system. The total amount of tritium discharged via stack during the campaign (November 1991) was about 0.17×10^{12} Bq. In this particular case, most of the released tritium consisted of HT and much less of HTO or tritiated hydrocarbons [Bel95a] (see Table 8.1). This was attributed to the composition of the pumped carrier gas which consisted mainly of dry nitrogen to minimize explosion hazard.

From the operation of the JET machine it was learned that torus baking constitutes the largest single source of tritium release [Bel92a]. During normal operation releases occurred through ports, bellows, and other components together with small releases from diagnostic systems. Significant releases of tritium were predominantly detected during remotely performed maintenance and refurbishment campaigns of the torus wall. Permeation losses from the Tritium Processing Plant were small because all heated component are fully protected by UHV-tight secondary containments.

In general, the highest discharge rates of tritium released at JET were observed during activities performed following a machine shutdown [Sab01]. For example, during a Neutral Injector Box repair (change of valves) the Exhaust Detritiation System (EDS) collected 1780 litres tritiated water having an activity of 29 TBq. The observed total stack releases of HTO and HT taking place largely through the Active Gas Handling System (AGHS) were 2.37×10^{11} and 1.91×10^{11} Bq, respectively (see Fig. 8.2). The wide-ranging Remote Tile Exchange (RTE) operation carried out during the period May 1997 (prior to start of DET1) until February 1998 (end of DET1) constitutes another good example. In this case, 1.6×10^{12} Bq of HTO and 1.5×10^{12} Bq of HT or other tritiated gases were emitted per month through the (AGHS) across various JET stacks into the environment [Lae99b]. These values are substantially lower than the maximal monthly discharges of 2.0×10^{13} Bq for HTO and 2.5×10^{13} Bq for HT or other tritium-bearing gases authorized at the time.

Smears taken during the Remote Tile Exchange (RTE) in 1998 from known hot spots revealed values as high as 2 MBq cm^{-2}. These high values were attributed to lightly adhering particulates like dust and flakes deposited on vacuum vessel surfaces like those of the divertor carriers. Much lower values in the range 100 - 1000 Bq cm^{-2} were normal elsewhere [Edw02; Coa06].

The detritiation factor of the Exhaust Detritiation System (EDS) was obtained from a comparison between the activity at the entrance of EDS with that of the HTO activity exiting EDS via stack. Tritium measurements were carried out with ionisation chambers. Problems encountered with these sensors were i) dependance of sentivity from pressure, gas composition and flow rates, ii) memory effects, iii) sensor saturation, and iv) tritium concentration at or below detection limit. Detritiation factors ranging between 22 and up to 1700 as well as average values over two months of 123 were reported during the RTE campaign of 1997/98. These relatively low values were explained by leaks that bypassed the EDS. Detritiation factors during a shutdown

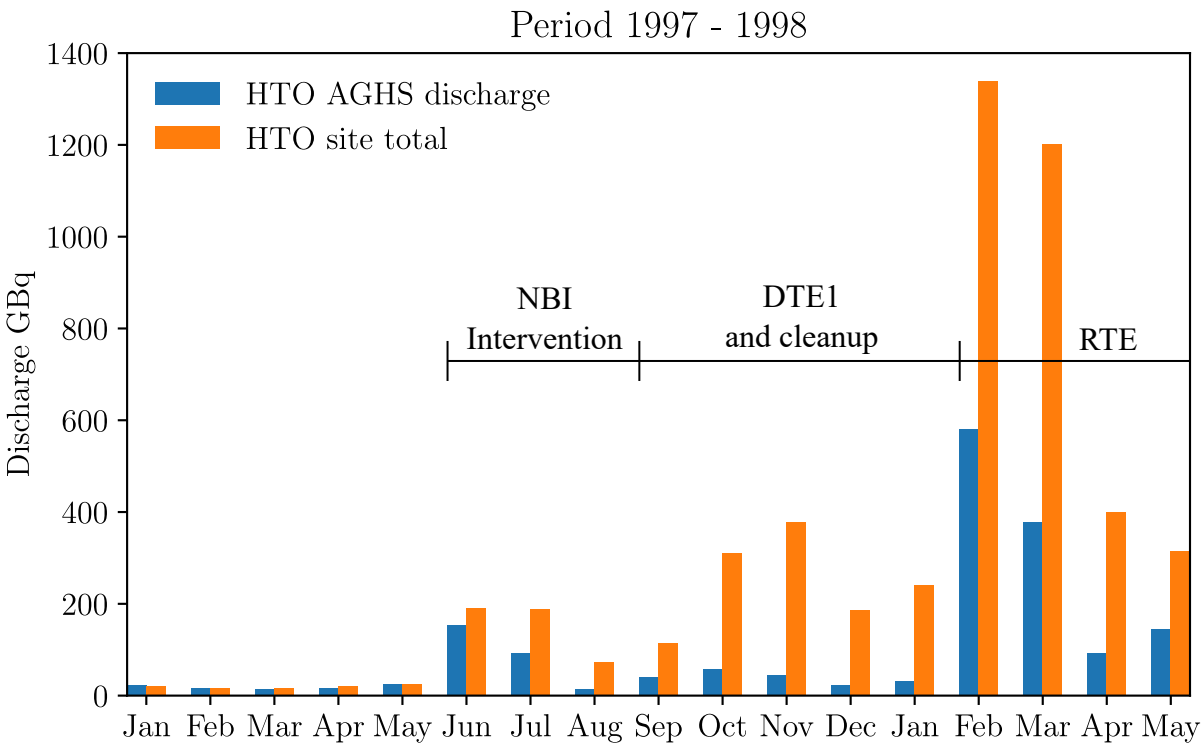


Figure 8.2: Stack discharges of HTO through the Active Gas Handling System of JET in comparison to stack releases from the site as a whole. Site releases were mainly caused by NBI = Neutral Beam Injector Box in June/August 1997, DTE1 = first Deuterium Tritium Experiment in September/January in 1997/98, and RTE = Remote Tile Exchange in February/May in 1998 (after [Sab01]).

in 2000 ranged from 6 up to 70 000. It was concluded that using the EDS for only a few hours and utilizing a dryer of very low dew point improved tritium retention efficiency very markedly. Another conclusion was that ionisation chambers are not particularly suitable for an accurate determination of detritiation factors.

The cryogenic distillation process retained practically all deuterium and tritium for re-injection into the machine and discharged protium only marginally contaminated by trace quantities of tritium. Large amounts of gas only slightly contaminated by tritium comprise those emitted from the top of the first column of the cryogenic distillation system, waste gases released from the impurity processing system, and very small amounts of frequently occurring gases sometimes containing high percentages of tritium discharged within the frame of gas chromatographic determinations or other analytical measurements. The latter small streams are mostly collected

in dedicated adsorber beds as tritiated water. This tritium is normally given to waste, because the effort that must be invested for tritium recovery is exceedingly high and hence costly.

One more case in point representative of large facilities handling sizeable amounts of tritium is the **Darlington Nuclear Generating Station (NGS), Canada**, whose authorized release **for airborne elemental** tritium is determined by so called **Derived Release Limit** (DRL). The DRL value established for the NGS for **airborne elemental tritium** is 15.6 PBq weeks^{-1} (1 PBq = 10^{15} Bq). The actual airborne elemental tritium emissions from Darlington Tritium Removal Facility were less than 0.1 % of this DRL [Rod11].

Summarizing:

- The development of advanced tritium retention technology, the enactment of pertinent administrative measures, and the implementation of modern analytical techniques have conducted to a significant decrease of gaseous tritium releases into the environment, sometimes in spite of the fact that the discharging installation augmented substantially the on-site inventory of tritium [And92c; Pet08; Gue11; Rod11].

- Gaseous effluents from JET (as well as from most tritium facilities) consist primarily of tritium oxide both at the stack as well as outside in the vicinity of the facility [Otl98]. Occasionally, however, HT/HTO ratios covering the range $1 < \mathrm{HT/HTO} < 50$ have been reported [Bar90; Otl92; Bel95a; Otl98; Rod11].

8.1.2 Organic gaseous tritiated waste

The Effluent Removal System (ERS) of Mound, a facility engaged in tritium activities since 1963, was confronted during the early days with a problem of high tritium emissions [Hed88]. Chemical analysis of the gases released via stack revealed that 99 % of the annual emissions were tritium-bearing organic compounds. It was speculated that these species were possibly generated by reactions of tritium with oils and elastomers contaminating the duct. Another explanation for the tritium-bearing hydrocarbons in the stack was that they had resisted oxidation by Hopcalite and could therefore escape into the environment. Replacing the previously used oxygen donor Hopcalite catalyst (80 % manganese dioxide and 20 % copper oxide) by a noble metal catalyst and increasing the temperature up to 873 K provided remedy [Ell92].

Other sources of trouble were i) plugging of filters with 30 µm porosity installed at the entrance of ERS and ii) corrosion by chlorine of screens installed in the exhaust of dryers, which caused dispersion of adsorbed particles. The resulting upgraded facility of improved efficiency, capacity, and reliability at Mound is known under Tritium Emissions Reduction Facility (TERF) (see also 5.7).

As discussed in previous sections, routine measurements of tritium releases from highly contaminated stainless-steel material stored at ambient temperature under a constant stream of air provided evidence that the offgas into the environment consists principally of tritiated water and usually to a smaller fraction of HT [Bel92a; Bel95a; Doe98; Rod11; Yam02; Yam11a]. Several laboratory studies on the tritium species liberated by contaminated stainless-steel exposed to ambient air are in line with this finding [Bea73c; Hir84a; Sur88b; Car91; Tor05a; Pen06; Sha16]. In view of this, most discharge monitors are designed for the assessment of only these two species.

In spite of the above, tritiated methane (CH_3T) was regularly detected together with HT and HTO at the stack of JET [Bel95a; Otl98] (see also Table 8.1). The relative specific activity concentrations of HT, HTO, and CH_3T varied from all three having approximately the same concentration to one of either three amounting to 90 % of the total. However, in most cases the dominating released species was identified to be HTO.

Another species encountered in the stack of tritium facilities is radioactive particulate matter contaminated by adsorbed tritiated organic or inorganic compounds or particulates [Moe89]. The concentration of tritium adhering on this mostly metallic substrate was found to lie within the range $0.000002 <$ (particulate tritium)/HTO < 0.0001.

Interestingly, traces of tritium-bearing organic compounds like tritiated formaldehyde (CHTO) and tritiated formic acid (HCOOT), both of which are highly soluble in water, were likewise detected in the effluent gas of several tritium handling facilities [Bel92b; Bel93b]. Both molecules are known to display high affinity for living tissues and vegetation [Bel79b]. Because tritium atoms in formaldehyde and formic acid exhibit a relatively high resistance towards isotopic exchange their chemical behavior is distinctly different from that of HTO. A technique for the detection of up to 1 Bq CHTO in 5 x 104 Bq HTO was developed by Belot et al. [Bel92b].

Basically, the procedure consists in bubbling the carrier gas at a flow rate of about $3\,l\,min^{-1}$ through distilled water containing 35 % formaldehyde. Carrier formaldehyde is needed for the precipitation of CHTO with dimedone and subsequent separation from water by filtration. In the

effluents of tritium-handling installations the concentrations of formaldehyde were found to vary within the range $0.0001 < \text{CHTO/HTO} < 0.02$. Experimentally, a median value of CHTO/HTO = 0.001 was reported [Bel93b]. In the gaseous effluents of facilities used for the interim storage of solid wastes traces of formaldehyde were likewise detected at concentrations within the range $0.0002 < \text{CHTO/HTO} < 0.003$; the median value in this case being 0.0005.

In other runs involving highly contaminated stainless-steel specimens stored under air at ambient temperature it was noticed that volatile organic tritiated carboxylate species were released in detectable amounts. The percentage of tritium in the carboxylate form was found to lie between 24 and 60 % of the total organic species [Bel93b]. This result, which still needs to be confirmed by other analytical procedures, could be of significant radiological consequence. With respect to the mechanism of formation of tritiated formaldehyde or tritiated formic acid it was speculated that they probably constitute intermediate products of the oxidation of hydrocarbons adsorbed on the surface of tritium-contaminated materials like austenitic stainless-steel type SS316 or particulate matter.

Calculations by McConville and Woods [McC95] indicate that the biological effectiveness (internal doses) of tritium beta rays escaping metallic particulate matter is much lower than had previously been prognosticated. However, this assertion still requires experimental verification.

8.2 Liquid waste

Liquid wastes are usually classified according to their degree of contamination, the number and type of chemical components, and whether they are chemically aggressive or non-aggressive, etc. From the point of view of waste conditioning and safety it is also distinguished between burnable and non-burnable liquid wastes.

8.2.1 Non-burnable liquid waste

8.2.1.1 Low contamination level

Tritium-handling facilities devoted to basic or applied research activities or large fusion machines operating with D_2 or DT fuel regularly generate tritiated water of various degrees of contamination. Exhaust streams from primary systems or resulting from analytical measurements are often of high contamination level but of relatively small volume. Thus, size and level of contamination

of these waste streams can vary quite substantially. To remove tritium-bearing inorganic and organic species from waste gases they are processed in Tritium Retention Systems (TRS) where they are first subjected to a catalytic oxidation and subsequently to quantitative adsorption on a molecular sieve bed. Catalytically generated tritiated waste water collected in adsorber beds is irregularly recovered as soon as the adsorption capacity approaches saturation. Recovery takes place by thermal release. After determination of the activity level of this tritiated water, it is either released into the environment, given to waste, or subjected to a detritiation. In case of detritiation, the resulting tritiated hydrogen isotopologue stream is processed in an isotope separation system in order to obtain pure hydrogen isotopologue streams (see section 3.18.8). Depending on the required throuput of tritiated hydrogen, an isotope separation system is chosen among thermal diffusion, displacement gas chromatography, or cryogenic distillation. Options for the extraction of tritiated hydrogen from highly tritiated waste water are isotopic exchange employing the PERMCAT process [Wel12] or catalytic reactive conversion utilizing a PMR device [Ses05].

Other regular sources of weakly contaminated water released by tritium handling facilities are i) water from cooling loops of primary components, ii) sewage water containing diluted detergents such as used for decontamination and cleaning purposes, and iii) sewage water from lavatories, showers, or toilets.

Representative for laboratories handling large inventories of tritium, i.e. up to 60 g, the **Tritium Process Laboratory** (TPL) in Tokai-mura released from April 1988 to March 2001 a total amount of 450 m^3 of tritium-contaminated waste water containing 6.6×10^9 Bq of tritium, i.e. an average of 1.5×10^7 Bq m^{-3} [Yam02]. When taken over the period 1988 - 2010, the amount of liquid water and the activity of tritium more than doubled to 1070 m^3 and 1.4×10^{10} Bq, respectively. However, the specific activity, i.e. 1.3×10^7 Bq m^{-3}, remained nearly the same [Yam11a].

Liquid effluents of low-level radioactivity from tritium-handling facilities must always be released via a separate and controlled route. For instance, at **Tritium Laboratory Karlsruhe** (TLK) sewage water is collected in two tanks, each having a useful volume of 1.9 m^3, i.e. a total volume of 3.8 m^3. Once the filling level is attained the water is automatically pumped into a sewage water collection station of Hauptabteilung Dekontaminationsbetriebe (HDB = Decontamination Service) of KIT. Tanks and collection station are in adjacent but different

buildings. Operation of pumps and adjudicated automatic valves are carried out from the Central Process Control System of TLK. The system is designed for $100\,m^3\,year^{-1}$ with a specific tritium activity not exceeding $10^{10}\,Bq\,m^{-3}$. HDB accepts up to $5 \times 10^{11}\,Bq\,m^{-3}\,year^{-1}$ of liquid inorganic wastes.

Neutron-induced **^{16}N radioactivity** generated in cooling water of fusion reactor systems necessitates special attention [Ike97]. The main nuclear reaction leading to ^{16}N, i.e. $^{16}O(n,p)^{16}N$, takes place with fusion neutrons of high average energy interacting with oxygen from water molecules. Actually, substantial radiation emitted in the vicinity of fusion machine is absorbed by cooling water as it travels to the heat exchanger and back. The decay of ^{16}N takes place with a half-life of 7.3 s generating γ-rays of energies higher than 7.6 MeV. The estimated radiation doses from ^{16}N are such that precautionary measures are considered indispensable for the protection of personnel working at the facility and to some extent also of equipment.

8.2.1.2 Intermediate and high contamination level

Throughout the operation of **Tritium Process Laboratory (TPL)** significant amounts of strongly contaminated water were generated with tritium concentrations fluctuating between a few $10^6\,Bq\,m^{-3}$ and $2 \times 10^{18}\,Bq\,m^{-3}$ [Hay06]. Some of these highly tritiated liquid water fractions with concentrations of up to $10^{12}\,Bq\,m^{-3}$ were stored at TPL within the frame of research activities - partly for fairly long periods of time. Results and experiences gained with these samples over a period of five years are described in detail by Hayashi et al. [Hay06].

A tangible example of amount and contamination degree of tritiated water generated during the operation of a fusion machine is provided by **JET**. During the operational period 1997 - 2005 a throughput between 5000 kg and 20 600 kg of intermediate level tritiated water were generated per year containing between $1\,GBq\,kg^{-1}$ and $100\,GBq\,kg^{-1}$ of tritium [Per08]. Disposal of this waste is only possible after detritiation down to levels acceptable for a repository.

Significant volumes of radioactive aqueous waste were generated at JET during shutdowns and subsequent maintenance operations. In the event of extraordinary activities like for instance during the Remote Tile Exchange (RTE) operation, which was performed after completion of the DTE1 campaign (first high power DT campaign), an average of $60\,l\,d^{-1}$ (or $1.1\,m^3$ in 10 months) of tritiated water accumulated on adsorbers in the Exhaust Detritiation System (EDS). After each operational phase, the involved personnel required showering while still under the protection

of the dressed protective clothing (pressurized suit) [Boo93]. The aqueous liquid produced during these activities, which contained tritium at concentrations within the range 0.025 - 800 TBq m^{-3}, was transitorily stored in special storage vessels [Hai99]. The concentration of tritium in this water was considered sufficient to merit a recovery of tritium!

Large amounts of tritiated water are also generated by slow permeation of tritium into the cooling water of plasma facing components and of the breeding blanket [Hay07a]. While the volume of this liquid waste is rather large, the degree of contamination is normally low (for ITER it has been estimated that about 150 m^3/loop containing approximately 2×10^{12} Bq m^{-3} will have to be dealt with) [Hay06]. As with JET, the amount of tritium present in the cooling water of ITER will be sufficiently large to justify recovery for fuel recycling purposes.

In analogy to JET, fusion machines the size of **ITER** or DEMO will generate within the frame of routine operations substantial consignments of water highly contaminated with tritium. This is especially the case during i) conditioning of the vacuum vessel by baking in the presence of oxygen (about 6 l DTO after each baking event containing approx. 6×10^{19} Bq m^{-3}), ii) recovery of tritium from the blanket (water containing approx. 10^{18} Bq m^{-3}), iii) releases from the tritium plant (less than 0.5 m^3 d^{-1} containing approx. 2×10^{16} Bq m^{-3}) and iv) discharges from research activities as well as from other miscellaneous sources [Hay06; Ito07; Ski08].

For the Darlington Nuclear Generating Station, which processes about 107 g tritium/d, the **Derived Release Limit** (DLR) for **tritiated liquid waste**, i.e. the authorized release to the environment for tritiated liquid waste, is 825 TBq weeks^{-1} [Rod11]. The actual emissions of tritiated liquid waste are less than 0.2 % of this DLR. The Tritium Removal Facility of the Darlington Nuclear Generating Station [Dav88; Gug91], which is the largest of its kind in the world, provides tritium removal services to Darlington fission reactor units as well as to several other CANDU reactors in Canada. Detritiation is based on the vapour phase catalytic exchange process (transfers tritium from heavy water to gaseous deuterium) and cryogenic distillation (separates molecular deuterium from molecular tritium and discards protium). Of the actual emission, i.e. 0.2 % of DLR, the Tritium Removal Facility contributes 30 - 35 %] to the total DTO emissions of Darlington Nuclear Generating Station. Major emission pathways of tritium are Process Vent and Tritium Immobilization Vent.

The electrolysis of tritiated water, a crucial intermediate step of many water detritiation processes, constitutes a noteworthy source of liquid tritiated waste. This waste is frequently of

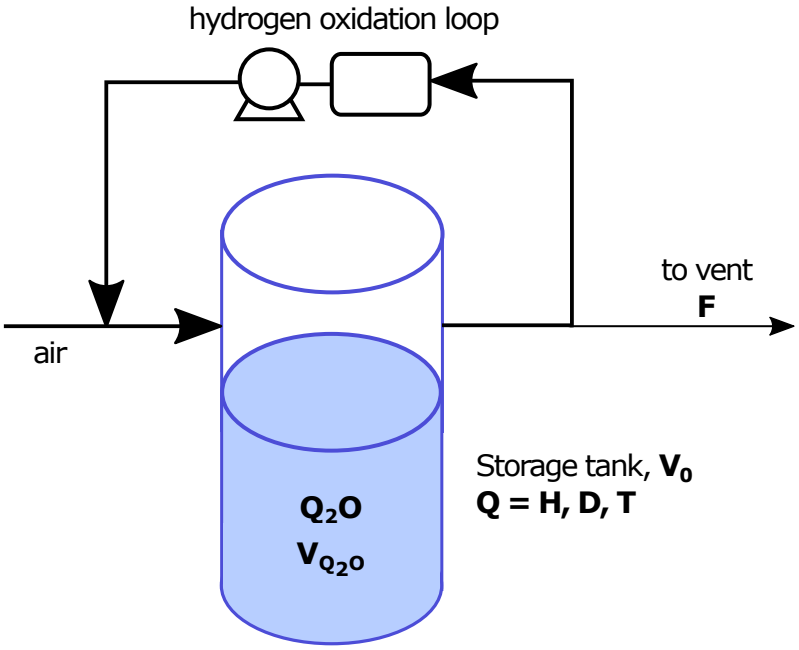


Figure 8.3: Storage tank for high level tritiated water displaying loop for the oxidation of hydrogen and a depression flow of rate F (after [Hay06]).

high specific tritium activity and simultaneously of complex chemical composition which makes it particularly corrosive and of difficult disposal.

8.2.2 Interim storage of highly tritiated water

Highly tritiated water can be stored temporarily either as liquid or immobilized on adsorbers like molecular sieves. It is classified as solid waste when adsorbed on molecular sieve or silica gel and transported in qualified transport beds.

8.2.2.1 Storage as liquid water

Hayashi et al. [Hay06] concluded from germane research activities that storage of highly tritiated water in tanks necessitates not only regular pressure release but also reconversion of the main self-radiolysis products into water. Incessant processing of cover gases can be carried out either with a small hydrophobic catalyst bed operated at about 423 K or recirculating with a pump across a bio reactor containing bacteria capable of oxidizing tritium gas [Ich05] in closed loop operation at ambient temperature (see Fig. 8.3). For efficient oxidation to occur air needs to

be injected into the loop while venting a small fractional stream F (F = flow rate of released pressure) of cover gas into a detritiation system [Hay06].

Itoh et al. [Ito07] investigated the self-decomposition of HTO as function of tritium concentrations in water within the range 16 gigaBq/cm^3 and 2 teraBq/cm^3 at storage temperatures covering the range 269 - 303 K. Experimentally determined $G(H_2)$ values for hydrogen generation were found to vary within the range 0.3 - 1.4 when the concentration of tritium in water was modified within the range 1.6×10^{10} Bq m^{-3} and 2×10^{12} Bq m^{-3}. As evident from Table 8.2, effective $G(H_2)$ values decrease with increasing concentration of tritium in water. While G values for the formation of hydrogen peroxide show the same dependence from tritium concentration, they are comparatively much smaller. The effective production rates of the radiolysis products Q_2 and Q_2O_2 (Q = H, D, T), increase with increasing temperature. In view of the above, during isochoric storage of high level tritiated water adequate precautions need to be taken to keep the concentration of hydrogen below the limit of explosion. For example, in case of a closed tank with a volume of $V_0 = 4\,m^3$ containing high level liquid water filling half the tank or $V_W = 0.5\ V_0$, i.e. $2\,m^3$, and assuming that the tritium concentration in water amounts to 20 PBq m^{-3} it was estimated that the hydrogen generation rate would reach 0.1 m^3 (STP)/d. Hence the explosion limit, i.e. 4 % hydrogen in air, would be reached in only about nine days of storage (see also section 2.10.3.2 and Fig. 2.9). Therefore, to maintain the hydrogen level below 1 % at all times, it was estimated that each tank will necessitate regular pressure release as well as gas processing at a throughput of 1 m^3 d^{-1}. Alternatively, a simple purging system could be considered but this would represent a significant burden to the detritiation system with substantial generation of diluted tritiated water. Another possibility would be to use a noble gas/oxygen mixture as cover gas. By this procedure the concentration of oxygen can be kept as low as possible and the formation of nitrates and nitrites in the water be avoided (see also below). One more choice would be to keep the temperature of the tank at < 283 K in order to reduce the generation rate of radiolytic gases down to tolerable values ([Ito07], see also below). Evidently, more research is necessary before a reliable recommendation can be made.

Peyrat [Pey78] at Centre d´Etudes de Bruyères-le-Châtel, France, was the first to show that the best way to store T_2O is in solid form at temperatures below 278 K (melting point of T_2O is 277.5 K) in a Pyrex or metallic vessel. At this temperature the evolution of radiolysis gases is smallest. This conclusion was verified by Itoh [Ito07] who found it advantageous to store HTO

Table 8.2: Effective G_{H_2} values for the self-radiolysis of tritiated water at 293 K [Hay06].

	Tritium concentration in water ($PBq\,m^{-3}$)		
	16	120	2000
$G(H_2)$	1.36	0.45	0.33
$G(H_2O_2)$	0.02	0.008	0.004

at low temperatures, e.g. 283 K when at the same time the concentration of tritium in water was of the order of a few $TBq\,cm^{-3}$. According to Itoh, the lowest rates of formation of radiolysis products occur at this temperature.

A serious concern pertaining storage of water containing more than $10^{15}\,Bq\,m^{-3}$ of tritium is corrosion. As reported by Hayashi et al. [Hay06], tritiated water stored for only a short time quickly becomes acidic, i.e. pH < 5, almost independently from the duration of storage. Peyrat [Pey78] had already observed ions such as NO_3^-, NO_2^- and H_3O^+ in the liquid phase when nitrogen is present and Fe_3^+, Ni_2^+ and Cr_3^+ ions when T_2O is stored in a stainless-steel vessel. Particularly iron, nickel and chromium ions, all major constituents of stainless-steel, are an irrefutable indication of corrosion of the metallic containment.

8.2.2.2 Storage adsorbed on molecular sieves or silica gel:

Nakashima and Tachikawa [Nak86; Nak87] investigated the radiolytic production of gaseous tritiated hydrogen either via direct self-radiolysis of tritiated water adsorbed on molecular sieve 5A or of water adsorbed on the same zeolite under exposure to external radiation from a ^{60}Co γ-source. In both cases they noticed an additional evolution of hydrogen isotopes from that calculated by straight forward self-radiolysis or gamma radiolysis of liquid water. The formation of oxygen increased with adsorbed dosis. This was, however, only the case when the radiation dosis was sufficiently high. Experiments carried out by Tadlock et al. [Tad80] or Nakashima and Tachikawa [Nak86] using silica gel as adsorber support these observations.The extra yield was attributed to some form of energy transfer between adsorber and adsorbed water molecules. The O_2/H_2 ratio was far below the stoichiomeric ratio, i.e. 0.5, and increased with increasing degree of water adsorption or of adsorbed energy.

Experiments carried out by Tadlock et al. [Tad80] or Nakashima and Tachikawa [Nak86] using silica gel as adsorber, support these observations. The extra yield was attributed to some form of energy transfer between adsorber and adsorbed water molecules. The latter researchers noticed additionally, that air inhibits significantly the production of tritiated hydrogen from tritiated water adsorbed on silica gel.

Bibler and Orebaugh [Bib77] simulated the radiolytic production of gas during long-term storage of tritiated waste solidified in concrete or of organic materials immobilized in Vermiculite placed in sealed containments. They exposed the various matrices to either beta, gamma or alpha radiation. The provenience of beta radiation was in situ trapped tritium and that of gamma radiation an external ^{60}Co source. To perform experiments with alpha radiation , ^{244}Cm was dissolved in the water used to make the concrete. The results of these runs permitted a good estimation on the effects of radiation on gas generation. For concrete, the data revealed an initial hydrogen formation rate induced by tritium beta particles of 0.1 to 0.3 molecules per 100 eV of absorbed energy. This 100-eV rate was found to decrease with hydrogen build-up because of back reactions leading to hydrogen removal. Eventually, a steady state pressure is attained which depends on the prevailing activity of tritium and the amount of water. For intensities of $< 10^5$ rad hour^{-1}, the steady state pressure was estimated to be less than 1.38 bar. While oxygen from the air sealed together with concrete was almost completely consumed, nitrogen remained unaffected. In case of organic materials sorbed on vermiculite, the gamma and alpha radiolysis results revealed formation of hydrogen as well as of traces of methane and carbon dioxide. The 100 eV yields for hydrogen from organic material exposd to radiation were found to be 4.4 for octane and and 2.2 for vacuum oil. As with concrete, in case of vermiculite only the oxygen from supernatant air was consumed during radiation exposure. Tadlock et al. [Tad80] concluded that the generation of explosive gas mixtures inside of typical tritiated waste packages from Mound facility is unlikely. This conclusion relies on the fact that the dominant gas phase product is hydrogen progressively building up to a max. pressure of less than 2.5 bar.

Walters et al. [Wal97; Wal02] examined more than thirty disposable molecular sieve beds containing tritiated water adsorbed on zeolite type 4A. These beds had been stored for periods totalling up to three years. In anticipation of pressurization arising from self-radiolysis of adsorbed tritiated water and tritium decay, the beds were designed as pressure vessels capable of resisting the theoretically maximal attainable pressure. After completion of the respective

periods of storage the chemical composition of the cover gas was analysed and the magnitude of the overpressure determined. The results provided evidence that the calculated partial pressure of decay helium was essentially attained while that of tritiated hydrogen remained in most beds clearly below the values expected from the self-radiolysis of tritiated water. These observations were explained by a quenching mechanism with molecular oxygen according to

$$H + O_2 + X \longrightarrow HO_2 + X \quad X = O_2,\ N_2,\ \text{etc.}$$

in which atomic hydrogen generated by beta radiolysis of hydroxyl groups present in molecular sieve cavities reacts with molecular oxygen in a trimolecular reaction. Gaseous oxygen was initially present in the bed cover gas (atmospheric air) and to some extent adsorbed by the molecular sieve adsorber.

The rate constant for the formation of molecular hydrogen under gamma ray irradiation and quenching by oxygen was determined employing a 10 g sample of molecular sieve type 4A containing about 15 % adsorbed water [Wal02]. The sample was irradiated for one hour up to an absorbed dosis of 5.7×10^{19} eV in the presence of different contents of molecular oxygen. From the results the value of the rate constant for the production of hydrogen under gamma ray irradiation and oxygen quenching was calculated to be $k = (19.6 \pm 4.5)\,s^{-1}$. With this constant and literature values for the third order reaction to yield HO_2 displayed above as well as with the recombination rate constant of hydrogen atoms it was shown that the reaction of oxygen with hydrogen atoms greatly reduces the production of molecular hydrogen to the extent that it becomes insignificant over the life time of tritium decay. Hence, the oxygen quenching mechanism appears to be responsible for the lack of hydrogen observed in the gas phase in disposable molecular sieve beds.

From the results of Nakashima and Tachikawa [Nak86; Nak87], Tadlock et al. [Tad80] and Walters et al. [Wal97; Wal02] it can be concluded that the mechanism of hydrogen formation from adsorbed tritiated water depends not only on the specific activity of tritium, but also and strongly from the nature of the absorber matrix and the presence of scavengers, all of which exert marked influence on the rate of radiolysis.

8.2.3 Burnable liquid wastes

Tritium-contaminated **lubricants** used in pumps, motors or other equipment with moving parts necessitating lubrication can remain in use until either the physical properties of the oil deteriorate to an intolerable level or the oil becomes excessively radioactive. At this point, replacement of the oil becomes necessary. While this operation is basically not difficult, the risk of contamination-spread during oil replacement and of possible dissemination of hydrocarbons into adjacent tritium primary systems served by the lubricated equipment is significant. This has been the motivation in tritium-handling facilities for nearly complete substitution of all oil or grease lubricated equipment by all-metal ones. Tritium-contaminated oils are categorized as burnable liquid waste.

Alcohols, acetone and other organic **solvents** used for research or cleaning purposes in tritium-handling facilities are customarily collected in plastic containers and processed following pre-established procedures. Their degree of contamination is generally not very high. At TLK several hundred litres per year of this kind of waste are collected in 50 l plastic containers and sent to Hauptabteilung Dekontaminationsbetriebe (HDB), KIT, where they are subjected to professional conditioning and disposal.

One more frequently arising burnable organic liquid waste is tritium-contaminated **scintillation cocktail**. This cocktail is used in considerable amounts for the analysis of very low concentrations of tritium in liquids or solids in practically all research institutions and industrial laboratories dealing with tritium. Because scintillation cocktail contains ignitable xylene and toluene, it is considered hazardous. Contaminated scintillation cocktails are usually collected in suitable plastic containers and shipped off-site to commercial facilities that take care of this waste by burning the cocktail in a dedicated incinerator. At TLK, tritium-contaminated liquid scintillation cocktail is collected in 10 cm^3 Kautex flasks. At the most, 100 flasks are introduced into a plastic bag and delivered to Hauptabteilung Dekontaminationsbetriebe (HDB), KIT, for their decontamination. At HDB they are incinerated together with other wastes. The maximum concentration of tritium in liquid scintillation cocktail accepted by HDB is $3 \times 10^{11}\,Bq\,m^{-3}$.

Vials contaminated during liquid scintillation measurements are also disposed of following pre-established procedures. While vial washing and reusing constitutes a feasible option, it is not a recommended procedure.

Another considerable source of tritiated organic liquids is the pharmaceutical industry. At Belgian Nuclear Research Centre SCK CEN in Mol, Belgium, tritiated organic liquids from the pharmaceutical industry consisting of 95 % methanol/water and 5 % impurities like petroleum ether, chloroform, and carbon tetrachloride as major constituents have been collected and stored over a number of years [Shm02a; Bra05]. Small quantities of glycol, formaldehyde, and hydrogen resulting from the radiolysis of methanol have also been detected. Altogether 178 l contaminated by a net tritium activity of 16.5 TBq (corrected to November 2000) have been stored at SCK CEN during the course of about 20 years in seventy 2.5 l glass containers chiefly packed inside of 12 l polyethylene containers themselves protected in 200 or 400 l drums and sometimes further secured in 600 l overpacks. The activities in the waste cover the range from 5 $\mathrm{GBq\,l^{-1}}$ to 1 $\mathrm{TBq\,l^{-1}}$.

Procedures for the conditioning of tritiated liquid waste are described in detail further down in section 8.4.2.able liquid wastes.

8.3 Solid waste

In general, early development of strategies aimed at minimizing the production of primary radioactive waste should receive high priority. Strategies should additionally evaluate and select concepts targeted on minimization of chemical reactivity, and the generation of waste with as low as possible toxicity. Another aspect requiring early consideration is development of an optimized packaging strategy for interim storage, transportation, and final waste disposal.

Frequently updated inventory determinations by analytical procedures and/or calculations constitute a fundamental requirement of good waste management [Can15].

Mixed wastes should be avoided or at least minimized. Within this frame, radioactive-only materials should be segregated from hazardous-only materials already at the source. Burnable solid waste should likewise be segregated from non-burnable solid waste at the place where the waste is generated. When possible, waste conditioning and cleaning should be carried out employing non-hazardous and non-toxic agents.

Origin and type of solid waste generated in representative fusion fuel clean up installations is a principal topic of this section. The waste has been classified into non-burnable and burnable. Major types, quantities, and the classification of waste expected from the operation of ITER are likewise discussed in some detail.

8.3.1 Non-burnable solid waste

Numerous materials utilized for the manufacture of components installed in facilities **processing tritium-bearing gases** such as stainless-steel, structural steel, copper, tungsten, ceramics, polymers, concrete, catalysts, adsorbers, palladium-silver alloy, etc. will become contaminated to various degrees after exposure to tritium. Predominant factors determining the degree of surface and bulk contamination are i) type of material, ii) chemical composition and condition of the material surface, iii) chemical composition of the gas phase, iv) integral time of exposure, v) partial pressures of tritium during exposures, and vi) temperature prevailing during each exposure. In the following some of the most common solid wastes arising in tritium handling facilities and a few methods for their decontamination are discussed.

The plasma exhaust clean-up experiment CAPER at TLK has generated waste of the kind expected from the fuel clean-up system of ITER. CAPER has been in discontinuous operation with representative amounts of tritium for about twenty years under conditions simulating to a large extent those expected to prevail at ITER. After failure of several heaters of a permeator - a crucial component of the CAPER facility - and after one of the just as essential turbo molecular pump ceased to work, it became necessary to discontinue operations. Both components were removed, dismantled, and subjected to post service examination by Caldwell-Nichols et al. [Cal08] (see also section 3.14.3). Even though prior to opening the experimental loop both components were extensively decontaminated by alternating vacuum pumping, isotopic swamping with hydrogen and vacuum pumping, they still liberated fairly rapidly large quantities of tritium when exposed to the dry air of the glove box housing CAPER.

In case of the permeator, it was observed that from the total tritium found in the permeator, i.e. 2800 GBq, nearly half, i.e. > 1350 GBq (specific activity 2.5×10^{11} Bq g^{-1}), was trapped in a black powder presumably generated during catalytic cracking of hydrocarbons. Further measurements revealed radioactivity concentrations within the range 2.1×10^{7} - 3.8×10^{10} Bq g^{-1} (total $1450 = 2800 - 1350$ GBq) in the permeator wall, inlet wall, inlet zone capillary tubes, Pd/Ag-permeation tubes, pre-heater tube section, cables, mineral wool insulation, etc.

The concentration of tritium in the disassembled turbo molecular pump body, i.e. $> 2.7 \times 10^{11}$ Bq (270 GBq), was more than one order of magnitude lower than in the permeator body. This is

understandable in view of the much higher operation temperature and tritium partial pressure in the permeator.

As apparent, waste arising from plasma exhaust clean-up equipment will contain tritium dissolved, trapped, or chemically bound in diverse materials of different chemical, physical, and radiotoxic properties. The observed highly radioactive fine dust is of particular concern. In terms of the degree of contamination, it can be expected that waste from fuel cycle components of ITER will be more contaminated than those from CAPER mainly because of the much longer exposure times to high partial pressures of tritium at temperatures between moderate and elevated.

Tritium-contaminated adsorbers and catalysts constitute only sporadically discharged wastes from tritium-handling facilities. A large fraction of their bulk tritium is considered to be mobile. Zeolites, also known as molecular sieves, are widely used adsorbers. Due to their chemical inertness, robustness against radiation and temperature cycling, as well as easy in-line or off-line regeneration they do not require frequent replacement. Because tritium is normally not distributed homogeneously in adsorber or catalyst beds, appropriate precautions are necessary when sampling for inventory determinations or sentencing purposes.

Most catalysts used in tritium systems are characterized by quite a long lifetimes. Certain catalysts require occasional re-activation, e.g. reduction or oxidation. Catalysts like methane crackers (nickel on Kieselguhr) or the water gas shift catalyst (zinc stabilized copper chromite) were found to contain of the order of 0.15 g tritium/kg catalyst and 1.2 g tritium/kg catalyst, respectively, after exposure to an equimolar gaseous mixture of hydrogen and tritium [Glu98b].

Tritium-contaminated catalysts in reduced condition as well as highly reactive solids like metallic getter powders are only acceptable for disposal in a repository after their complete oxidation has been demonstrated. Main reason for this demand is the need to rule out temperature excursions induced by exothermic reactions taking place during waste transport or storage. Demonstration of full oxidation of radioactive material is, however, difficult and cumbersome to perform. In practice, getters are oxidized in a flow system under slow, carefully controlled reaction conditions using either nitrogen or inert gas containing a small fraction of oxygen. By this procedure elevated temperatures which favour the formation of a protective oxide layer on the material surface and in addition cause getter agglomeration are avoided. As well known a protective layer and/or agglomeration may delay or even stop oxidation before completion of the reaction.

Another very significant category of non-burnable solid waste are structural materials discharged from tritium laboratories or first wall structural or armour materials generated in fusion machines. **Armour materials** are currently manufactured from low-Z elements like beryllium or carbon, or from high-Z elements like tungsten.

First wall materials exposed to plasmas become contaminated with tritium not only by gas- or plasma-induced permeation, but also by transmutation reactions mostly induced by neutrons. Plasma-facing materials may additionally become radioactive by transmutation reactions with energetic neutrons or electrons. Type and quantity of activation products will depend upon the chemical composition of the first wall (including constituent trace elements), the integral time of exposure, and the energy spectrum of the particles. Hence, besides tritium incorporated by permeation, beryllium will become progressively contaminated by radioactive isotopes of iron, cobalt, manganese, tungsten, zinc, and by a substantial fraction of tritium resulting from transmutation reactions. First wall tiles may moreover display on the surface highly toxic and radioactive loosely adhered dust. Along the same line, tungsten retrieved from a divertor will contain isotopes of tungsten, tantalum, rhenium, iron and other elements as well as permeated tritium and possibly surface contamination. From this it is clear that with respect to sentencing, transport, and final disposal these plasma-facing materials constitute a challenging type of waste.

Radionuclides generated in **Inconel** by neutron activation are ^{56}Co and ^{58}Co. Because these radionuclides have short half-lives of only 70 - 80 days, after several years of decay time the dominant nuclide will be ^{60}Co [Hai99].

Dust and flakes are waste of varying chemical composition. They are generated during the operation of the machine by erosion induced by plasmas. Dust was observed in experimental tokamak machines like JET [Fra99; Pat99; Ski00], TFTR [Ski00], DIII-D, TEXTOR [Win01] and ALCATOR C-Mod [Ski00; Car00; Gre14]. Their particle size distribution in terms of median diameter was found to be 50 % smaller and 50 % larger than the median diameter. They contaminate the surface of tiles showing up as loosely bound co-deposited materials of singular chemical composition. Eroded co-deposits may re-deposit in regions far away from the place of origin even in plasma-shadowed zones [Car00]. Co-deposited materials may consist of carbon, tungsten, beryllium, tritium and traces of numerous other radionuclides [Gol99]. Dust samples collected from the windows of an interferometer installed in TFTR displayed tritium concentration of $4.0 \times 10^{10}\,\mathrm{Bq\,g^{-1}}$ [Car00].

Flakes observed at TFTR after the carbon first wall was subjected to DT plasmas displayed a specific activity of $1.27 \times 10^{12}\,\mathrm{Bq\,g^{-1}}$. The activity was determined by calorimetry [Pat99; Fra99]. Flakes were likewise detected at JET at the time when the vacuum vessel was still protected by CFC. They were extracted from the vacuum vessel with a special vacuum cleaner. For the determination of their tritium content, they were oxidized under air at temperatures of up to 1073 K by differential thermal analysis. Depending on whether D-D or D-T was utilized as reactor fuel, the concentrations of tritium were found to be 1.5×10^{7} or $1.16 \times 10^{12}\,\mathrm{Bq\,g^{-1}}$, respectively [Bek05].

Ashikawa et al. [Ash20] examined dust removed from the JET vacuum vessel after first D-D campaigns with an ITER-like Wall (ILW) configuration beginning 2011. In this case, the divertor consisted of tungsten-coated carbon fibre composite tiles, tungsten bulk tiles and a first wall made up of beryllium blocks and beryllium coated Inconel. The tested plasmas contained a small fraction of tritium generated on one hand in D-D fusion reactions and on the other originating from tritium still remaining in the machine from previous D-T campaigns in spite of ample first wall conditioning. Vacuum cleaning of the vacuum vessel provided evidence, that the amount of dust generated in an all metal first wall machine was more than two orders of magnitude smaller than that generated when the first wall consisted of carbon fibre composite. Intriguingly, the specific concentration range of tritium in the dust did not display significant dependency from the type of first wall, i.e. 5×10^{6} - 2.6×10^{9} or 6×10^{6} - $0.8 \times 10^{9}\,\mathrm{Bq\,g^{-1}}$ with an ITER-like or a carbon wall, respectively. This was attributed to the high carbon content of the dust generated in either environment.

The chemical composition of the JET flakes was determined by i) Kleykamp and Gottschalg[2] utilizing X-ray microanalysis and X-ray diffraction and ii) Francis and Foster[Fra99] employing energy dispersive spectroscopy, electron probe microanalysis and inductive coupled plasma optical emission spectroscopy. As apparent from the results displayed in Table 8.3, whereas both investigations basically agree on the elements detected in the flakes, this is not the case for the respective concentrations, which for most elements diverge considerably. Because carbon employed for the manufacture of tiles exhibits much lower impurity concentrations for each metal

[2] Kleykamp, H. and Gottschalg, H.D. 1998. Elementaranalysen an Flakes aus dem JET in der Betriebsphase April 1996 bis Oktober 1995. Report.

Table 8.3: Chemical composition of JET flakes determined by two independent research teams(see also Appendix G.

Element	[Kle98]	[Fra99]	Element	[Kle98]	[Fra99]
	weight %			weight %	
Carbon	>80	83.6	Magnesium	0.2	0.3
Oxygen	>3	13.9	Silica	0.1	0.3
Iron	2	0.1	Beryllium	bdl	0.4
Chromium	2	<0.1	Sodium	nd	0.4
Nickel	3	<0.1	Chlorine	nd	0.6
Aluminum	5		Copper	nd	0.1

bdl = below detection limit
nd = not determined

than those found in the flakes, i.e. less than 2 ppm, the flakes are seemingly generated in a complex reaction sequence involving interaction of plasma with structural materials.

Carmack et al. [Car00] observed that the composition of the dusts collected from TFTR, DIII-D and ALCATOR C-Mod is directly related to the first wall material used in the machine, i.e. whereas the bulk of the dust material found in TFTR and DIII-D is carbon, that in the dust material from ALCATOR C-Mod consists primarily of molybdenum. Dust collected from TEXTOR consisted either of boron or mainly of iron, nickel and chromium. Dust samples from DIII-D were found to have an average specific surface area of $3.0 \pm 0.2\,m^2\,g^{-1}$. Significantly higher specific surface areas, i.e. 6.9 - $26.5\,m^2\,g^{-1}$, were obtained for dust samples collected from TFTR.

More data characterizing dust collected from the vacuum vessels of TFTR and JET after completion of corresponding campaigns with tritium are displayed in table 8.4. As apparent, the specific tritium activity and the T/C ratio of dust samples from JET and TFTR are comparable. This points to chemical similarities as well as to an analogous mechanism of formation in both machines. On the other hand, there is a notorious large difference in the BET surface area of dust collected from JET and TFTR and as expected a much lower specific activity of tritium in dust in comparison to that found in flakes. The presence of Fe, Cr and Ni strongly brings to mind erosion of structural materials.

Table 8.4: Characterization of carbon dust from TFTR and JET [Bek05]

Property	TFTR[And99]	JET[Fra99]
Tritium content ($\mathrm{Bq\,g^{-1}}$)	(2.17 ± 1.1) x10^{10}	3.92×10^{10}
BET surface area ($\mathrm{m^2\,g^{-1}}$)	13.5 ± 9.5	1000 ± 250
D/T ratio	25.1 ± 6.7	-
D/C ratio	$0.0062 \pm 0.00 \times 10^{10}$	-
T/C ratio	0.00024 ± 0.00011	0.00044
O/C ratio	-	0.094
Be/C ratio	-	0.031
Other trace elements	-	Al, Si, S, Cl, Ca, Fe, Cr, Ni, Cu
Other nuclides	-	^{7}Be, ^{60}Co, ^{137}Cs, ^{40}K

A radiological **classification methodology** of **tritiated wastes** generated at ITER, which is determined by the degree of contamination and properties of the packaging, has been proposed by Pamela et al. [Pam14]. According to this methodology, the acceptance of a waste batch is ascertained by the so called IRAS[3]

$$\mathrm{IRAS} = \sum \frac{Am_i}{10^{\mathrm{class}}} \ ,$$

in which Am_i stands for the specific activity of the radionuclide i expressed in $\mathrm{Bq\,g^{-1}}$ (waste plus packaging) and class is determined by the radiotoxicity of the radionuclide, which for tritium is 3. Therefore, waste having a specific activity of $10^3\,\mathrm{Bq\,g^{-1}}$ and being contaminated only by tritium has an IRAS value of one[4].

Within the frame of the developed methodology the following **disposal site options** for waste exclusively contaminated by tritium were identified for France [Pam14; Can15]:

- Waste complying with the acceptance criteria of very low-level waste (VLLW), i.e. $< 15\,\mathrm{kBq\,g^{-1}}$ and IRAS ≤ 1 (based on a 50-year decay period of interim storage), can be stored directly in the surface disposal facility "Centre Industriel de Regroupement, d´Entreposage et de Stockage" (CIRES) which was commissioned 2003. This facility has

[3] IRAS = Indice Radiologique d´Acceptation en Stockage.
[4] The lower the toxicity class of a radionuclide, the smaller the amount accepted in a waste package.

a storage capacity of 650 000 m^3. It is estimated that about 80 $m^3\,year^{-1}$ of this kind of waste will be generated during the operation of ITER [Pam14].

- According to the acceptance criteria of French Centre de Stockage de l´Aube (CSA) for tritiated waste the tritium activity of short-lived low and intermediate level waste (LILW-SL) must be $< 2 \times 10^5$ Bq g^{-1} and the tritium outgassing rate lower than $< 2 \times 10^6$ Bq $t^{-1}\,d^{-1}$. Waste exceeding the acceptance criteria of the CSA (facility of 1 000 000 m^3 storage capacity commissioned in 1992) may be subjected to interim storage for 50 years in any appropriate storage facility. From this it follows, that to comply with the acceptance criteria of CSA the maximum initial activity in the waste is 3 MBq g^{-1} (considering a decay period of 50 years). It is predicted that about 200 $m^3\,year^{-1}$ of this kind of waste will be generated during the operation of ITER [Pam14].

- Whenever an interim storage period of 50 years is insufficient to meet the criteria of the CSA waste disposal facility the waste must be subjected to detritiation. Therefore, in this case detritiation as well as interim storage for fifty years are necessary before the waste package can be considered apt to comply with the tritium acceptance criteria of CSA. A facility designed for the storage of long-lived intermediate level waste in a deep geological repository, i.e. 500 m under the ground, is currently being planned in France for 2025. The acceptance criteria specifications for this facility are still subject of discussions.

Waste conditioning activities for future disposals are approved by the French Nuclear Safety Authority on the basis of a pre-examination by the French national radioactive waste management agency ANDRA.

8.3.2 Burnable solid waste

Large volumes of organic material comprising full or half pressurized protective suits, gloves, protective plastic shoes, packaging materials, cellulose material, cotton, polymers, tape, paper, tissue, etc. will have to be conditioned for disposal. PVC sheets and other burnable waste generated during repair or refurbishing activities while wearing a pressurized suit, and materials used to minimize personnel exposure and contamination spread also belong to this category. This type of secondary waste arising in contaminated control areas is invariably “sentenced” as

low-level waste (LLW) and is normally removed from the control area in large plastic bags but not before the low activity has been verified for instance via an analysis of the supernatant gas employing an appropriate radiation detector.

For volume minimization the waste can be compacted and disposed in drums. A volume reduction of so called "house-keeping waste" of more than 80 % is commonly achievable. In order to minimize void spaces in the containers, it is customary - when acceptable - to blend waste arising from different activities.

Pelletier and co-workers [Pel92] compared three different process options for the decontamination of burnable organic waste, i.e. i) isotopic exchange with steam followed by dilution, ii) drying by straightforward evacuation, and iii) water extraction by "dry" vapour (non-saturated) at 333 K at a reduced pressure of 40 mbar. Of these three procedures the third one was found to require the shortest process time and deliver the smallest amount water with the highest specific activity.

When water is extracted by "dry" vapour the first step consists in a determination of the tritium activity and confirmation that no alphas (uranium) are detectable in the waste. Next, all non-organic materials like glass, metals, ceramics, etc. are segregated from the waste and given to waste separately. The organic waste is then shredded, introduced into a basket, and treated in an appropriate oven. The resulting contaminated steam is transported out by a carrier gas, passed through a water condenser, and subsequently further dried in a cryogenic unit cooled with liquid nitrogen.

Lefebvre et al. [Lef12] investigated the decontamination of low activity "house-keeping waste" of the kind arising during the operation as well as dismantling of fusion devices. To this effect, milled material was placed in a glass reactor and heated in a tubular oven at temperatures up to 423 K under a stream of argon containing 2 % oxygen. Under these conditions, decontamination takes place without combustion. The selected concentration of oxygen is such that the system as a whole remains under the flammability temperature at all times. Released tritium was trapped in a commercially available bubbling system (Tritium Sampler MARC 7000). The temperature was found to play a decisive role. At only slightly lower temperature, e.g. 393 K, the achievable degree of decontamination was found to be insufficient for waste de-classification.

Tritium-contaminated burnable waste arising from fusion machines like JET encompassed large numbers of carbon fibre composite (CFC) tiles further contaminated by beryllium and

other radioactive metals. These tiles were frequently stored transiently for the purpose of re-use. Storage must take place in special storage facilities because of chronic outgassing of tritium.

Radiotoxic dust, flakes, and other debris collected while handling burnable solid materials must receive special attention because of the danger of inhalation.

8.3.3 Operational waste from ITER

The operational solid waste of ITER resulting principally from component maintenance, repair and replacement activities has been classified in France into: i) **trés faible activité** (TFA) (very weak activity), ii) **faible et moyenne activité à vie courte** (FMA-VC) (weak and middle activity of short life time) and iii) **moyenne activité à vie longue** (MA-VL) (medium activity of long-life-time) [Ros10]. Purely tritiated waste constitutes one more special category. High level waste of long-life time[5] will not be generated at ITER.

Waste of the category MA-VL, which arises from maintenance and replacement of in vessel components belonging to the divertor, the blanket, the current drive, etc., must be handled in an especially designed hot cell facility. This facility must be equipped and configured to safely perform **remote handling** operations, cut large equipment for size reduction, detritiate large components, package large components in preparation for transport while complying with established safety standards, etc.

Disposal locations for wastes of the categories TFA and FMA-VC are presently available in France. Main constraints are the tritium concentration limits for TFA and FMA-VC waste, i.e. $10^3\,\mathrm{Bq\,g^{-1}}$ and $2 \times 10^5\,\mathrm{Bq\,g^{-1}}$, respectively. A further limitation, at least for waste of category FMA-VC, is the tritium outgassing rate which must not surpass a few $\mathrm{Bq\,g^{-1}\,d^{-1}}$. The ITER host country is furthermore planning another site for waste of the category MA-VL which is expected to be completed 2025.

Marbach et al. [Mar97] drew attention on the specific properties of metallic SS316L(N) waste generated during operation as well as dismantling of fusion machines. This waste will be contaminated by tritium and by radioactive elements resulting from transmutation reactions of energetic neutrons with constituting elements of stainless-steel such as nitrogen, manganese, iron, nickel, niobium, molybdenum, and cobalt [Pam12]. Safe storage of this type of waste requires special precautions because of chronic release of tritium. The most obvious measure is

[5] The French designation for high level waste of long lifetime is „haute activité à vie longue" (HAVL).

to detritiate the material prior to storage to an extent that suffices to generate what is defined as "conventional radioactive waste". Such type of waste, which is typical for fission nuclear plants, will only display very little chronic release of tritium. To validate this concept, a nearly technical scale process based on steel melting has been developed at CEA, Valduc [Boi97; Ros02]. Most important component of the process is a large evacuable furnace mounted inside of a glove box. With the melting technology decontamination factors of typically 900 were routinely achieved with metallic waste initially containing $3.3 \times 10^8\,\mathrm{MBq\,t^{-1}}$ of tritium. An important complementary advantage of melting is substantial reduction of waste spatial volume and consequently of specific surface area. Reduction of tritium contamination and of specific surface area will contribute considerably to ameliorate insidious chronic tritium release during long-term storage.

Preliminary calculations reveal that the high costs arising from an energy intensive waste conditioning procedure are compensated by substantial savings attained by classifying the waste in a lower category.

8.3.3.1 In-vessel radioactive operational waste

In-vessel radioactive operational waste generated in the vacuum vessel of ITER arises mostly from replacement activities of first wall materials. Stainless-steel type 316L and other structural materials contaminated by tritium and by diverse activation products will constitute the most abundant solid waste of ITER (see also previous section)[Rub10]. It has been estimated that during the first operational phase of this machine, which will be performed only with hydrogen, the amount of waste after 3000 pulses will be of the order of 4 t, 28 t, 30 t and 220 t of carbon fibre composite[6], tungsten, copper, and stainless-steel, respectively. Waste generated from replacements of divertor tiles will play a dominating role. Divertor target assemblies removed from the machine will largely be saved as spare parts rather than be discarded as waste.

Rosanvallon et al. [Ros03; Ros10] have estimated the mass of contaminated, activated and contaminated/activated **radioactive material** resulting from the operation and decommissioning of ITER to reach 34 000 t (another estimate prognosticated 31 000 t [ITE01d]). Of this amount of waste, about 10 % will be generated during the operation phase and about 90 % during the decommissioning phase. Of the total waste, about 58 % will consist of very low activity waste, 32 % of low and medium activity waste of short life time and about 10 % of medium activity waste

[6] According to current ITER design, carbon fibre composite will be replaced by beryllium as plasma-facing material.

of long-life time. Purely tritiated waste is assessed to attain about 60 t during the operational phase [Pam14] and 390 t during the decommissioning phase [Can15]. Waste of high activity and simultaneously long-life time is not expected from ITER. According to reference [ITE01d], the **mass of waste** consisting of components and component sections with a clearance index of more than unity after one hundred years following final shutdown (waste time scale of ITER) will amount to about 6100 t. This amount only holds if components or component sections having a clearance index above unity are separated from those components which have an index below that value[7] (an explanation of "clearance" is provided in section 8.4.9).

Up to about $900\,\mathrm{t\,year^{-1}}$ of tritium-contaminated and activated steels characterized by an average activity of $37\,\mathrm{MBq\,g^{-1}}$ will have to be conditioned each year. The activity of this waste must be substantially reduced to values below $19\,\mathrm{kBq\,g^{-1}}$, which means that decontamination factors[8] (DF) of the order of 2×10^3 will have to be achieved.

In another assessment, it was estimated that the total operational waste of ITER will amount to about 750 t (or $180\,\mathrm{m^3}$) [ITE01d]. Included in this waste are rather diverse constituent such as component replacements of the divertor; shielding of the blanket first wall; limiter front parts; electron cyclotron and ion cyclotron materials; wastes from the neutral beam, diagnostics, test blanket modules and the fuelling system; tritium plant equipment; remote handling equipment; hot cell equipment; etc. For the estimation of waste volumes packing fractions of about 50 % were implicated. It was further presumed that about 50 % of this waste would consist of steel. This waste will not only be contaminated by tritium but also by radioactive isotopes generated via transmutation reactions induced by neutrons. Typical radioisotopes expected in the waste 100 years after shutdown are compiled in Appendix Y. The provided specific activities pertain structural steel placed 56 mm inside of the plasma front side of the outboard shielding blanket.

Pampin et al. [Pam12] updated recently the ITER radioactive waste assessment for the major components of ITER. The evaluated components comprised the blanket including first wall and shield block, divertor, vacuum vessel and port extensions, toroidal field coils, poloidal field coils, central solenoid, cryostat and the bio shield. For the appraisal they used modern 3D models and most recent informations on materials specifications, plasma operations, maintenance and replacements schemes (more details in the list of references in [Pam12]). Activation results were

[7] Doses around $10\,\mathrm{\mu Sv\,year^{-1}}$ at maximum are considered insignificant relative to the natural background radioactivity and therefore apt for unconditional release.
[8] DF = initial activity/final activity.

obtained in a series of 22 pre-determined decay times. Three waste categories following latest French regulations were adopted: i) TFA ("trés faible activité"), ii) type A ("faible et moyenne activité vie courte") and iii) type B ("faible activité vie longe" or "moyenne activité vie longe") (see also section 8.3.3 above). A conclusion from the calculations was that only with the exception of tungsten all other plasma-facing materials, e.g. copper, beryllium, CuCrZr, SS316-LN and XM-19, classify as type B waste at shutdown on the ground of transmutation reactions of some of their constituents. Tritium is mostly encountered in Be, Cu, CuCrZr, XM-19 and SS316L(N). The respective dominant **precursor elements** in these five materials are Be; Cu and N; Cu and N; N; and N. A further conclusion was that whereas most of the materials classified as type B at shutdown remain in this category after hundred years, large amounts of materials classified as type A at shutdown decay to TFA within the same time scale. According to estimations of Pampin et al. the total amount of waste will be about 27 100 t of which after 100 years of decay about 1000 t will be of type B, 3700 t will be of type A and about 15 700 t will be classified as TFA.

Fig. 8.4 shows four plots which nicely document the consequences of plasma interaction with structural materials vulnerable to plasma exposure. Displayed are the estimated specific activities at time zero of the principal transmutation products that build up in ITER structural stainless-steel SS316L(N) at the rear (plasma shadowed side) (Fig. 8.4a) and the plasma-facing side (Fig. 8.4b) of the vacuum vessel and the concentration changes of these transmutation products as function of decay time after final shutdown. As apparent, the specific activities on the plasma-facing side are higher by about five orders of magnitude than those at the rear side. Carbon-14 is generated in steel of the vacuum vessel wall or in other in-vessel components by transmutation reactions induced by irradiation with ITER fusion neutrons. Additionally, shown in Fig. 8.4 is the evolution of the clearance indices (flat horizontal thick red lines) on both the rear side (Fig. 8.4c) and the plasma-exposed side (Fig. 8.4d) of the vacuum vessel (for an explanation of "clearance", which is based on a concept recommended by IAEA for releasing solid materials of very low radioactivity level, consult section 8.4.9). Evidently, up to about forty years after shutdown the total activity is dominated by the radionuclides Fe-55 and Co-60. It is noteworthy that the total activation at the plasma-close side is about two orders of magnitude higher on the waste time scale, i.e. 100 years after final shutdown than the clearance limit (see Fig. 8.4d) and at the rear side more than two orders of magnitude lower than the clearance level (see Fig. 8.4c).

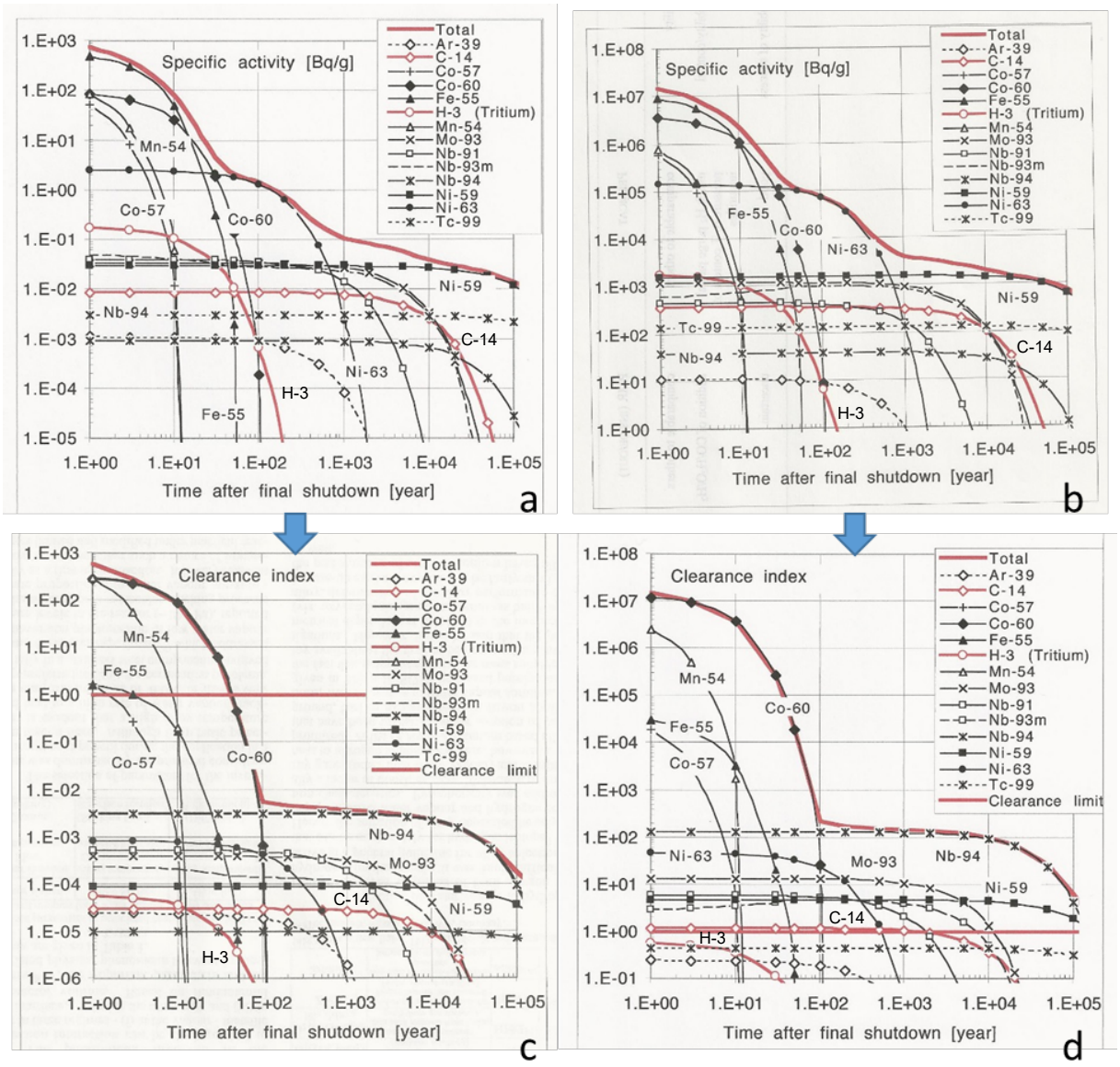


Figure 8.4: Total activity and specific activities of the principal transmutation products expected in ITER structural steel SS316L(N). It was assumed that the steel contains 0.01 wt % and 0.05 wt % of Nb and Co, respectively. Evolution of the activities at (a) the rear side surface of the outboard vacuum vessel and (b) the plasma side surface of the outboard vacuum vessel as function of decay time after shutdown. Effect of decay time after final shutdown on the clearance indices of the transmutation products at (c) the rear side surface of the outboard vacuum vessel and (d) at the plasma side surface of the outboard vacuum vessel. Shown accentuated are the evolution of tritium (–○–) (all 4 figures), carbon-14 (–◇–) (all 4 figures), the total activity (thick red line, all 4 figures) and the clearance level (flat horizontal thick red line in figures c and d) (after [Cep00; ITE01d]).

The build-up of tritium in structural stainless-steel takes place via a number of sequential (n, t)-reactions with main stainless-steel constituents as well as with impurity elements (see thick

red line in Fig. 8.4). In addition, considerable tritium contamination of the plasma-exposed structural stainless-steel will take place via plasma-induced permeation predominantly from the plasma adjacent side (contribution not displayed in the plots!).

When the plasma-facing side surface of the outboard vacuum vessel is considered and 100 years is taken as the starting waste time scale of ITER (see Fig. 8.4d), it is seen that the total clearance index is about 200 (compare with clearance limit of unity). This index only begins to decrease appreciably after elapsing of about 10000 years. Consequently, clearance of this waste will not be possible. Conversely, the total clearance index at the rear side of the vacuum vessel is more than two orders of magnitude lower than the clearance limit of unity after one hundred years (see Fig. 8.4c). Hence, in this case there is considerable potential for waste clearance.

For radioactive materials contaminated by several radioisotopes the total clearance is obtained from the addition of all constituent indices. If the resulting index is lower than unity, the material can be cleared.

8.3.3.2 Plasma-exposed non-steel metals

Hydrogen isotopes including tritium and helium will accumulate on or in non-steel armour metals like tungsten or beryllium by some or all of the following mechanisms:

- direct implantation of deuterium, tritium, or helium ions escaping the plasma (takes place predominately in shallow surface regions),
- gas-induced and plasma-induced permeation into the bulk,
- co-deposition of hydrogen isotopes with eroded carbon or beryllium on plasma facing and plasma shadowed surfaces of tiles,
- trapping in lattice disorders (defects) induced by atomic displacements. Defects may be receded or form larger defect clusters upon annealing,
- transmutation reactions with energetic neutrons and electrons,
- formation of dust and/or flakes and
- radioactive decay of tritium.

Trapping of hydrogen isotopologues and helium takes place during the operation of a fusion device when plasma-facing armour materials protecting the first wall or the divertor are exposed to γ-rays, X-rays, deuterons, tritons, α-particles and highly energetic neutrons of 14.1 MeV. After-effects of this irradiation are changes of the material crystal lattice like i) structural damages, ii) dislocations, iii) interstitial vacancy clusters, iv) pores, v) cracks, and vi) voids. When tritium, deuterium, or helium are sequestered in these traps the immediate consequence is an increase of inventory beyond solubility. Another consequence of a particle flux impinging on plasma facing components is surface erosion (reduction in thickness of the plasma facing material). What is more, eroded particles may trap tritium and redeposit on the surface of plasma facing materials (co-deposition) as well as in diverse zones shadowed from the plasma.

Neutron damage will be the main lifetime limiting phenomenon in a commercial fusion reactor (see also section 2.14.10). It is measured in displacements per atom (**dpa**). One **dpa** is defined as the number of times an atom is displaced from its postion in the lattice due to the action of an impinging particle. The dpa value is proportional to the neutron fluence. By way of example, a heat deposition of 1 MW year m^{-2} causes about 3 dpa and 10 dpa in beryllium and copper or steel, respectively [Mer11]. Characteristic consequences of neutron damage are swelling and embrittlement. Neutrons are also promoters of transmutation reactions giving rise to complex waste of non-homogeneous chemical composition and radioactivity [Rub10].

Tritium accumulates in first wall **beryllium** partly by direct implantation or trapping in defects resulting from plasma/first wall interactions and partly by breeding reactions with energetic, but uncharged neutrons that escape the plasma. In order to perform the JET-ILW (ITER like wall) research program, about 2 t of beryllium were mounted in the JET machine in form of bulk Be or Be-coated Inconel tiles [Bre15]. Chemical-assisted physical sputtering of beryllium via BeD has been identified by optical spectroscopy. At an energy of 75 eV it contributes with about 30 % to the effective beryllium sputtering yield. Chemical assisted physical sputtering is most likely caused by supersaturation of the beryllium surface by the impinging deuteron flux density. Tritium incorporated by implantation is predominantly retained near the metal surface. In case of breeding, this hydrogen isotopologue is generated throughout the metal bulk because of the great penetration power of neutrons. In the bulk, a large fraction of tritium is found sequestred in microscopic defect sites or in bubbles. Bubbles will additionally contain deuterium and helium. At the operating temperatures, the plasma-exposed beryllium surface

will mostly be covered by a thin, a few micrometers thick oxide layer intermixed with a metallic phase. Near the divertor baffles and on the divertor fins the surfaces will be essentially free from contaminants because of substantial sputtering taking place in that zone. Longhurst et al. [Lon95] performed modelling calculations for ITER on implantation, trapping, release, and permeation processes using the one-dimensional TMAP4 code and provided estimates of the maximum tritium inventories in the beryllium first wall (1.1×10^{-6} kg, 523 K, 945 m^2), the limiter (0.038 kg, up to 723 K, 130 m^2), and the divertor (2.78 kg,1023 K, 320 m^2)[9] structures exposed to plasmas. In their calculations they took into account the impact of surface layers and the mobility of beryllium through these layers, the influence of damage by ion implantation, and the effect of bubble formation. Inventories resulting from transmutations induced by neutrons in the beryllium were not included.

As with other metals, the inventory of tritium in **tungsten** is determined by implantation, re-combination, diffusion and transmutation [Buz17]. Simultaneous presence of different plasma facing armour tiles in divertor, blanket, and limiter zones will eventually lead to the formation of complex co-deposition layers of varying composition. Loosely adhered co-deposits will progressively accumulate on plasma-exposed and plasma-shadowed zones of the first wall and in the adjacent ducts.

A possible formation of mixed Be-W, W-C, and Be-C materials co-deposited with tritium was discussed in section 2.14.10. A beryllium - tungsten interdiffusion between these two metals is conceivable in the divertor region because of the prevailing high temperatures. On the other hand, retention of tritium in Be-W mixed surfaces is unlikely on account of the elevated divertor temperatures.

In carbon-tungsten mixed layers containing more than 60 atom % C hydrogen isotopologues are trapped to the same extent as on a pure carbon layer. When the surface layer contains only about 30 atom % C the retained hydrogen isotopologues are one to two orders of magnitude lower, depending on temperature, than in a pure carbon layer. The reduced retention is attributed to the formation of tungsten carbides.

[9] Calculated tritium inventories, assumed operating temperatures at the surface, and estimated plasma-exposed areas are given in parenthesis.

From the above it follows that the presence of mixed materials on the surface of first wall plasma facing waste needs to be considered when qualitative and quantitative characterization, conditioning, sentencing, and disposal of this kind of waste is carried out.

Descriptions and evaluations of design and materials of advanced plasma-facing components currently considered for ITER are provided in references [Mer11; Pit11; Tho12; Raf14; Raf17]. The present-day armoured **divertor** concept [Hir16] developed for the starting operational phase of ITER was realized end of 2013. Salient feature of this concept is that all originally planned carbon fibre composite (CFC) blocks [Car98] have been completely replaced by tungsten. However, non-systematic but frequently observed macro cracks in the direction of the cooling water flow of tungsten mock-up´s when subjected to high heat flux testing ($< 20\,\mathrm{MW\,m^2}$) constitutes a matter of concern (see Fig. 2.61) [Pit11; Wir11b; Wir11a; Hir16]. Moreover, the compared tungsten materials displayed significant differences in thermal shock behaviour, i.e. diversities in cracking distances and depths. In view of this, thermomechanical tests employing several full tungsten armoured mock-up´s are currently under way to determine their aptness for the divertor of ITER. If the new concept prevails, the ITER machine will practically contain no carbon materials.

The retention of tritium in approximately 100 t of plasma-facing beryllium and tungsten after 12000 pulses, which corresponds to an average fluency of $0.1\,\mathrm{MWy/m^2}$, has been estimated employing the TMAP4 code [Fed01a; ITE01d]. Accordingly, waste masses of approximately 95 t of tungsten (W) and 0.75 t of beryllium (Be) are expected from component replacement of ITER after several consecutive operational phases [ITE01d]. Because the lifetime of the divertor will strongly depend on the frequency of disruptions, it is important for the sake of operability to invest much effort into all sorts of measures conducting to a minimization of their occurrence[10]. The tritium inventories in the bulk of the tungsten divertor dome and in the baffle were estimated to reach values of up to 80 g and in the beryllium first wall and in the limiter values of up to 260 g. These inventories of tritium are for the most immobile.

A thermal desorption spectroscopy (TDS) study carried out with beryllium specimens obtained from **limiter** tiles retrieved from the **JET** vacuum vessel and previously exposed to deuterium plasma provided evidence that even after heating the specimens over a period of 15 hours at 513 K[11] less than 10 % of the sequestered deuterium was released [Hei17][12]. It should be noted

[10] A large number of disruptions is only expected during the initial hydrogen phase of operation.
[11] 513 K is the annealing temperature foreseen for the ITER beryllium tiles in the main chamber.
[12] Inner and outer limiter tiles are installed at about half height of the JET vacuum vessel (see [Hei17])

that these specimens were free from deposits on the surface because limiter tiles are placed in the main erosion zone of the machine. This zone is characterized by particularly high heat and particle loads. The results show that thermal conditioning of beryllium inside of the vacuum vessel will not be sufficiently effective to comply with tritium inventory restrictions or waste conditioning.

As already discussed in previous sections, tungsten and beryllium employed in fusion machines will become activated. The main activation products expected in beryllium utilized in blankets or the first wall hundred years after fusion machine shutdown are H-3, Ni-63, C-14, Be-10, Nb-91, Ar-39, Ni-59, Mo-93, Nb-93m, und Tc-99 with specific activities of 1.3×10^7, 1.8×10^4, 8.8×10^3, 2.2×10^3, 9.0×10^2, 8.2×10^2, 2.6×10^2, 2.0×10^2, 1.7×10^2 and 8.1 $\mathrm{Bq\,g^{-1}}$, respectively. The total specific activity in beryllium was calculated to be of the order of $1.4 \times 10^7\,\mathrm{Bq\,g^{-1}}$. Under the same conditions, the dominant activation products in tungsten were estimated to be Nb-91, Hf-178m, Hf-178n, H-3, Mo-93, Nb-93m, Re-186, Re-186m, Tc-99 and Re-187 with specific activities of 1.4×10^2, 9.7×10^1, 9.7×10^1, 8.9×10^1, 3.5×10^1, 3.0×10^1, 2.0×10^1, 2.0×10^1, 1.5 and 1.2 $\mathrm{Bq\,g^{-1}}$, respectively. The total activity in tungsten was calculated to be approx. $5.3 \times 10^2\,\mathrm{Bq\,g^{-1}}$.

Amounts and type of gaseous and metallic transmutation products generated in tungsten plasma-facing armour of fusion devices were recently predicted by Sawan [Saw14]. Accurate knowledge of transmutation product distribution and their respective concentration will become important for classification and sentencing of waste. The dominant transmutant in plasma-facing armour tungsten was calculated to be rhenium (in a fission reactor the main transmutation product is osmium!). Accumulation of significant amounts of gaseous (helium or tritium) and metallic products in tungsten armour needs to assessed carefully because gases sequestered in metals are the reason for deterioration of the mechanical and physical properties. Deterioration manifests predominantly by swelling and brittleness. The consequence are lowered performance and much reduced lifetime [Buz17].

Verification of transmutation product distribution calculations by pertinent experiments are currently not possible because facilities for irradiation under conditions representative for a fusion machine are worldwide not available. As of now, irradiation tests can only be performed in fission facilities, but the energy spectra of the neutrons in these facilities is considerably softer than that impacting on the first wall of fusion machines. Because the relative product distribution

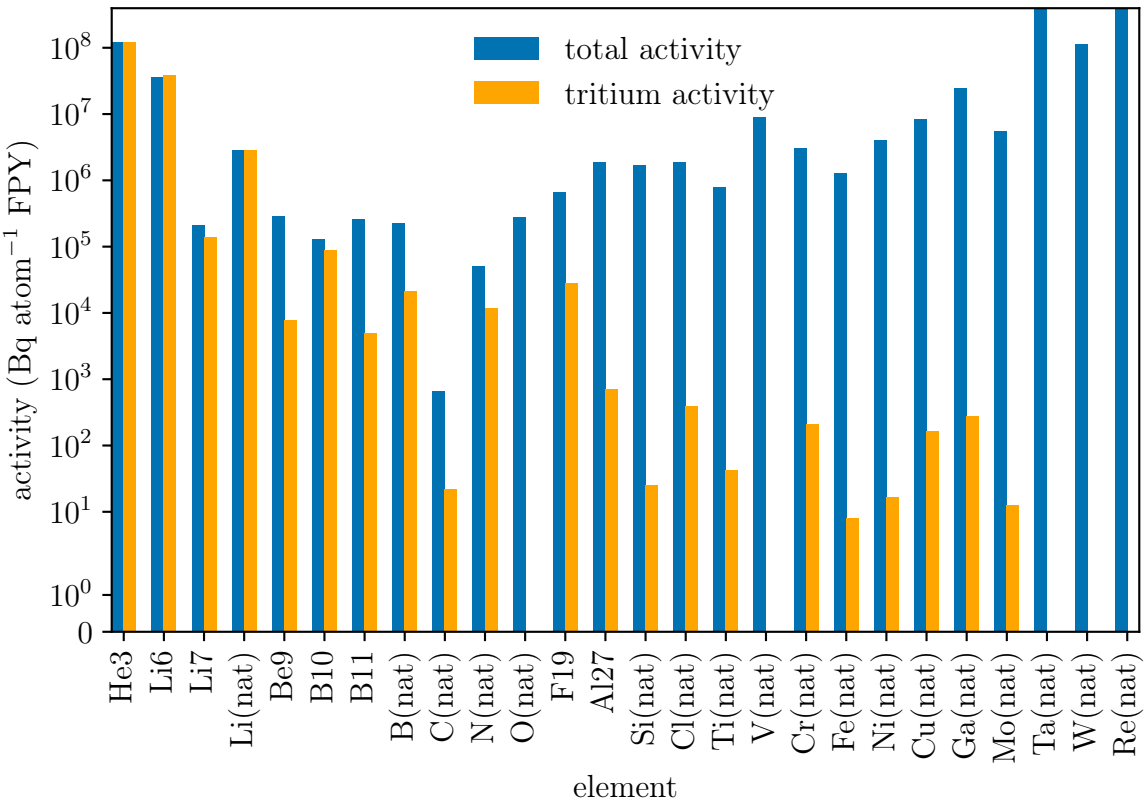


Figure 8.5: Total radioactivity and radioactivity of tritium in potential pure first wall materials after one full power year (FPY) of operation [Beh98].

strongly depends on the energy of the neutrons, an extrapolation of results obtained under "mild" conditions is usually not very meaningful. The situation will only improve when the International Fusion Material Irradiation Facility (IFMIF), presently under construction in Rokkashu, Japan, is in a position of delivering sufficiently large fluxes of 14 MeV neutrons.

Maintenance, interim storage, and disposal of first wall materials previously subjected to bombardment with 14.1 MeV neutrons in a fusion device requires special attention. Fig. 8.5 compares the total radioactivity of pure potential first wall armour materials and impurity species arising therein from the alpha, beta, and gamma decay of transmutation products and the tritium generated after one full power year (FPY) of operation. Radioactivities were calculated employing the neutron spectrum predicted to hit the first wall of ITER. For the calculations neutron transport and activation codes were used together with new revised data on neutron cross sections. Low Z elements like beryllium, boron, or carbon are favoured as plasma facing

materials because they lead to comparatively moderate radiation losses when eroded and released as impurity into the plasma. As apparent, tritium is a major contributor to the radioactivity generated by transmutations taking place in beryllium and boron. Tritium as well as helium, another abundant product of transmutation reactions, will probably accumulate in damage sites resulting from atomic displacements in the crystal lattice structure. Both gases will contribute to a deterioration of the thermophysical properties of most armour materials. In case of medium and high Z elements the major contribution to radioactivity arise from alpha and gamma radiation emitted by the transmuted atoms. The radioactivity generated by interaction of neutrons with carbon, i.e. 10^{-14} Bq/C, is notoriously low.

8.3.3.3 Plasma-facing carbon waste

Plasma-facing armour materials are installed in fusion machines for the protection of the vacuum vessel from severe particle fluxes and high thermal loads. One such material, i.e. three directional/dimensional carbon fibre reinforced carbon composite (CFC), has been developed and widely tested in several operating fusion machines [Bar91; Ara97; Coa06]. This material has also been proposed for the divertor of ITER in the vicinity of strike points and as back up for limiter and baffle on account of its excellent thermal resistance and modest radiation losses when exposed to plasmas [Bar97]. In this region tritium will not only be present in the bulk of CFC tiles but also co-deposited together with carbon ($\sim$ 0.4 T/C) as dust, flakes or other debris either on tile surfaces or dispersed into other less accessible zones of the machine. Because this material is mobilisable - particularly during accidents - the inventory of co-deposited tritium is restricted to 330 g [Pea98][13]. To accomplish this goal, regular tritium removal actions perhaps employing a specially adapted vacuum cleaner will become necessary. The maximum mass of tritiated carbon removed per cleaning by this procedure is comparatively small, i.e. 3.3 kg [ITE01d]. This highly radioactive and radiotoxic waste necessitates a singular conditioning process that has still not been thoroughly developed.

8.3.3.4 Ex-vessel solid operational waste

Waste generated in tritium handling facilities typically comprise:

[13] The maximum mobilizable tritium inventory within the ITER vacuum vessel has been limited to 450 g. This inventory results from that permissible in the cryopump (120 g) and that co-deposited on the first wall (330 g) [ITE01d]

- Catalysts; molecular sieves; activated charcoal; ion exchange resins; getters; a variety of solid reagents; process residues like dust, polymerized material; filters; column packing; insulation material; etc.
- Used or defective equipment such as rather diverse small, medium, and large pumps; analytical instrumentation; pressure sensors; hygrometers; flow meters; thermocouples; optical cells; permeators; vessels; separation columns; electrolyzers; exhausted tritium storage beds; exhausted scavenger beds; cryogenic columns; metallic and plastic piping; special items; etc. Their degree of contamination may differ considerably depending on their history of usage.
- Large numbers of small items like valves, O-rings, connections, metal gaskets, etc.
- Materials used during decontamination activities like gloves, protective clothing, breathing filters, brushes, etc.
- Glass, ceramic or plastic containers, LSC vials, etc.
- Miscellaneous laboratory specimens of diverse chemical composition and form of aggregation such as employed for analytical experimental purposes, material characterization, or post mortem evaluation.
- House-keeping trash like tissue paper, towels, etc.
- Tools, cables, seals, etc.

Surface and bulk of metallic waste are mostly contaminated with tritium to a different degree. This is particularly the case for materials heated in the presence of gaseous tritium-bearing species. Corroded metals may display on their surface loosely bound tritium-bearing oxides and hydroxides that may spread as dust. Depending on the size of the tritium-handling facility, the amount of this type of waste can be quite substantial. Interimly stored contaminated equipment will release tritium chronically. Therefore, all openings should be hermetically closed if stored interimly in a glove box. Equipment for which no immediate application can be anticipated should be transferred into a monitored dedicated storage facility.

The operation of the JET machine with large inventories of tritium required a special **Access Facility** designed exclusively for handling of diverse small, medium, and large sized highly

tritiated components. Besides tritium, some of these components were also contaminated chemically by beryllium and, if previously exposed to neutrons, by activation products [Edw02]. Depending on the degree of contamination, these components are handled either dressed in air-pressurized suits or by remote robotic procedures. As complementary safety measure to warrant low operator doses when handling such highly contaminated items, the ventilation is enhanced by an order of magnitude with respect to that of "normal operations". Activities with highly contaminated items require dedicated air monitoring and support by a Radiation Protection Service.

8.3.4 Environmental waste

It is common understanding that tritium releases should be As Low As Reasonably Achievable (ALARA). Within this frame, the size of Radiological Areas should be maintained at a minimum for better overall control and more effective decontamination.

Among others, the following issues require attention:

- All effluent air tritium monitoring systems shall be installed, tested and calibrated before initiation of operations. Prolonged testing of the effluent air monitoring system before commencement of operations is essential to establish reliable initial background values. Calibrations at regular intervals should follow.

- Airborne radionuclide emissions from tritium facilities shall not exceed Emission Standards for air pollutants.

- The radiation dose from tritium activities shall not exceed applicable dose standards, e.g. 2 mrem/hour from external radiation sources in an unrestricted area and 100 mrem/calender year from both internal and external sources [USN03].

- The potential impact of reaction products or gaseous releases resulting from i) possible chemical processes taking place in materials consisting of mixed waste and subjected to interim or prolonged storage, ii) handling of radioactive waste, iii) gaseous waste evacuation, and iv) waste minimization or volume reduction activities shall be evaluated and optimized already during the design phase.

- Every single potential hazardous and mixed waste must be characterized and approved by the responsible Authorities before it is generated.
- All new waste streams shall meet waste characterization and certification requirements of the facility where it is generated.
- Sampling of emissions consisting of particulate matter contaminated by radioactive nuclides may become necessary depending on the estimated dose. The installation of HEPA filters shall be contemplated in case processes are involved which generate radionuclide or toxic particulate matter.
- All liquid discharges from a tritium-handling facility shall be monitored for radioactive contamination.
- Hazardous metals like mercury, lead, cadmium, silver, chromium, selenium, arsenic, beryllium, and barium shall not be used unless explicitly authorized by the responsible Authority for environmental compliance.

8.4 Decontamination procedures

Radioactive waste should be decontaminated to the highest extent possible in order to achieve a reduction of waste volume and/or the lowest sentencing level achievable. For each category and type of waste the most efficient detritiation technique needs to be identified. Decontamination techniques are judged by their effectiveness, the production of secondary waste, safety, as well as on economic grounds. The latter should cover operational and disposal costs. A well equipped Detritiation Facility can contribute appreciably to this goal and hence reduce the overall disposal costs. The effectiveness and long-term impact of selected detritiation procedures should be re-evaluated frequently and critically on the basis of new results and previous experience. Eventually, a limited research activity could yield rewarding results.

8.4.1 Decontamination of stainless-steel

Surette and McElroy [Sur88b] pre-exposed as-received stainless-steel specimens to tritium at elevated temperature and observed that thermally incorporated tritium is liberated slowly

at ambient temperature with a rate of about 0.9 % d^{-1} (this value was obtained under the presumption that the release rate of tritium remains essentially constant over the duration of the measurement, which strictly taken is not the case). Stainless-steel specimens degreased before exposure to gaseous tritium displayed slower release rates, i.e. 0.2 % d^{-1} [Sur88b]. Thin SS316 specimens loaded almost homogeneously with tritium over several hours at 573 K, displayed chronic release rates of tritium at ambient temperature into the gas phase [Tor05b] and into liquid water [Pen06] over periods lasting several months. The results yielded values of the order of 0.2 % d^{-1} irrespective of the medium into which the specimens were submerged. Hence, the order of magnitude of the early observations of Surette and McElroy [Sur88b] were confirmed. The experimental data obtained by a number of investigators point to a chronic release rate at ambient temperature governed principally by thermal diffusion and the degree of loading [Sur88b; Tor05b; Pen06; Nao08; Aka08; Tor15b].

Even though mechanical abrasion, purging with hot moist air, leaching with solvents, chemical or electrochemical etching, etc. are frequently proposed as procedures for the decontamination of stainless-steel, the effectiveness of these procedures is incomplete if tritium has penetrated deep into the bulk. For example, when a type SS316 stainless-steel specimen exposed for 8 hours to 1.23 kPa HT containing 32.3 % tritium at 473 K incorporates a total of 1.35 MBq tritium, the removal by etching of a 1, 5, 10 or 50 µm thick layer from the surface of this material decreases the total activity to values of only 1.25 MBq, 1.21 MBq, 1.17 MBq and 0.67 MBq (DF = 2.0), respectively. This illustrates the inefficiency of mechanical or chemical surface treatments with stainless-steel exposed to tritium at elevated temperature. A simple surface treatment of material having a contaminated bulk will therefore not reduce substantially the chronic release at ambient temperature. To achieve effective removal of tritium penetrated deep into the bulk fairly high baking temperatures over a prolonged period of time or even melting may be required. Consequently, depending on the degree of contamination and on whether the contamination is homogeneous or heterogeneous, a decision between i) decontamination to convert the waste into a lower sentencing category, or ii) direct storage in a well-ventilated facility, eventually supported by a dedicated Tritium Retention System is necessary.

Gentile et al. [Gen05] reported on the decontamination of solids like RF feedtrough's by submersion into a solution of 3 % H_2O_2 in water for several hours at ambient temperature. The feedtrough's consisted of materials like stainless-steel, copper, and ceramic. Pre-exposure

to tritium at about ambient temperature caused a contamination of up to 17 000 Bq cm^{-2}. Under these conditions´ decontamination factors as high as 10000 were registered. It was claimed that following treatment with hydrogen peroxide the feedthrough could be utilized in a conventional non-tritium environment. In general, the technique was considered applicable to metals, ceramics, flat surfaces and soft waste. The level of surface downgrading taking place by the oxidative treatment was noticeable but considered acceptable. In a further investigation, the same researchers examined the effectiveness of bake-out to induce the release of tritium from metals, ceramics, and first wall materials like graphite tiles. Ovens were equipped with a special containment for the safe disposal of the generated radioactive ash. The selected temperatures were maintained constant at values within the range 623 - 773 K. The effluent gas was purified from ash with a separator; passed through a Venturi scrubber; de-entrained; de-contaminated by a demister; cleaned from particles with a HEPA filter, a sorption filter and an impinger; and finally passed through a molecular sieve bed before release into stack. The degree of decontamination of the material bulk was described as very good, but was not explicitly communicated.

Quinlan et al. [Qui08] focused on the development of methods for the decontamination of stainless-steel at temperatures under 573 K. Rectangular specimens of type SS316 with dimensions of 20 x 50 x 5 mm were pre-exposed to 50 kPa HT at **ambient** temperature for more than four days. Under such mild charging conditions, the tritium content of the SS316 specimens fluctuated within the range $(4.1 \pm 1.5) \times 10^7$Bq. Owing to the low loading temperature, the penetration depth of tritium into the bulk was presumably not more than a few µm [Hir84a]. When these specimens were subjected to thermal desorption under a helium carrier gas approximately 95 % was released in soluble form, i.e. HTO and the rest as molecular tritiated hydrogen. Additives to the helium carrier gas like 15 870 ppm moisture or 59 ppm hydrogen peroxide together with 6230 ppm moisture considerably enhanced the rate of tritium desorption and additionally lowered the temperature at which tritium was liberated in comparison to that required when only dry carrier gas was used. At temperatures below 473 K a rather notorious enhancement of detritiation was observed when the concentration of hydrogen peroxide in the purge gas was doubled. Consequently, stainless-steel contaminated by tritium only close to the surface can be decontaminated at comparatively low temperature when water vapour or more effectively hydrogen peroxide and moisture are added to the inert purge gas.

More experimental results pertaining the influence of temperature and water vapour on the detritiation rate of stainless-steel type SS316 loaded with tritium at **ambient** temperature for a period of only 24 hours were reported by Shmayda et al. [Shm15]. A significant release of tritium, i.e. 50 %, could be achieved simply by purging with a dry gas stream at 573 K. Hence, in agreement with the results of Quinlan [Qui08], for stainless-steel contaminated exclusively at ambient temperature, fairly moderate conditions suffice to achieve a significant degree of decontamination of the surface. In case of humid purges at 303 K, a six-fold increase in humidity from 1120 ppm to 6740 ppm, was associated with a ten-fold increase in peak outgassing rate. Increasing the humidity from 4 ppm to 1000 ppm with samples maintained at a higher constant temperature of 373 K likewise was associated with a significant raise in outgassing rate. However, because only about 15 % of the original activity present in the sample was removed by humid purges, it was argued that only tritium adhering to the stainless-steel top surface participates in the decontamination via isotopic exchange with water molecules in the purge gas. From the above, it was speculated that trapping of tritium in surface layer sites of stainless-steel restrain the liberation of tritium. Penzhorn et al. [Pen13a] provided experimental evidence for trapping of tritium on the surface layer of stainless-steel as metal hydroxides and oxihydroxides.

Stainless-steel exposed to tritium at elevated temperature, i.e. 473 - 573 K, incorporates gas into the bulk via diffusion across the surface. When eight specimens of this material all loaded under the same conditions were detritiated thermally in a flow system at the relatively low temperature of 473 K the effect of increasing partial pressures of moisture added to the carrier gas on the rate of tritium release was non-discernible (see Fig. 8.6) [Tor04]. Evidently, in this case the release takes place only by isotopic exchange between tritium on the metal surface and moisture in the gas phase. That diffusion of tritium across stainless steel is rate determining for the release of this species from the bulk could be verified by model calculations.

Corcoran et al. [Cor92] compared within the frame of activities whose final objective were the decommission of plants engaged in work with tritium the efficiency of three different procedures for the decontamination of stainless-steel, i.e. i) wet outgassing, ii) heat treatment at 323 - 673 K and iii) heat treatment at 873 - 1773 K. The purpose of the comparison was twofold: on one hand to develop a proceeding capable of reducing the activity prior to sectioning and cutting of tritium-contaminated components and, on the other, to work out a decontamination technique suitable for releasing tritium to the extent required to meet the UK landfill disposal limit for

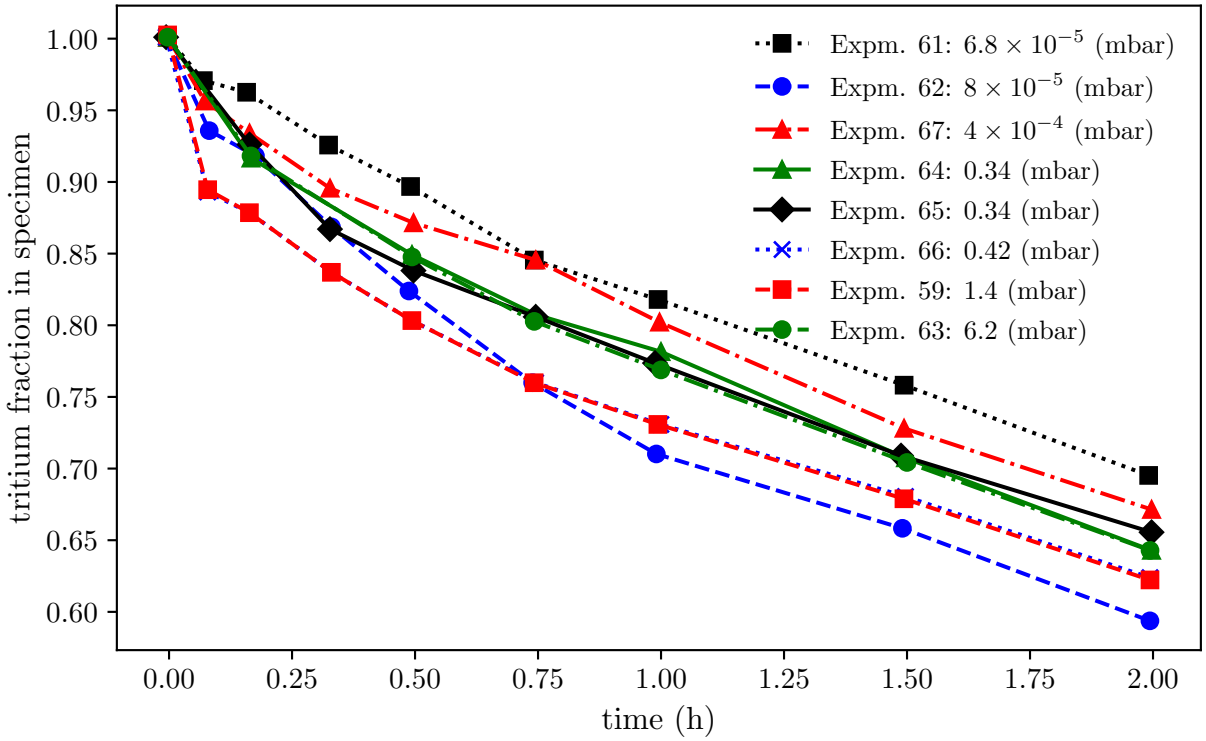


Figure 8.6: Thermal release of tritium from eight SS316 equally charged specimens at constant 473 K under an argon stream containing various partial pressures of moisture (from 10^{-6} - 0.61 kPa) [Tor04].

tritium. At the time, the limit was 1.2×10^{10} Bq t^{-1}. Specimens were obtained from two tanks, one who had experienced 10 years (tank A) and the other 20 years (tank B) of recurrent usage at tritium pressures within the range (1-2)10^5Pa **always** at ambient temperature. Of these, tank A released 7.4×10^{13} Bq of tritium and tank B 1.9×10^{14} Bq when purged with dry or moist air. These and other results led to the conclusion that the tritium inventory in storage vessel B was about 80 times higher than estimated from straight forward solubility calculations. This was attributed to the existence of a highly active surface layer retaining at ambient temperature an important fraction of the total activity. A similar observation was reported earlier by other researchers [Tor07; Pen12; Pen13a; Sha16]. When specimens from tank B were treated at 1073 K for 10 min under a stream of argon containing hydrogen a decontamination factor of $DF = 455$ was measured. A heat treatment at the melting point (1783 K) for one hour in a closed loop operation mode under atmosphere of Ar/H_2 reduced the activity from initially 2×10^{11} Bq kg^{-1} down to 5×10^7 Bq kg^{-1} yielding a DF of 4×10^3. Complementary experiments were carried out

Table 8.5: High temperature outgassing of stainless-steel at temperatures in the range 873 - 1873 K for a period of 10 min at each temperature [Cor92].

Temperature	Decontamination factor* Static conditions		Decontamination factor* Closed loop conditions	
K	Ar	Ar + 5 % H_2	Ar	Ar + 5 % H_2
873	409	692	1000	3215
1073	207	900	6120	7812
1273	193	710	5660	6912
1473	310	300	6120	4150
1873	128	67	4255	869

*Stainless-steel specimens loaded at 723 K for one hour under an atmosphere of tritium displayed initially an activity of 2.7×10^{10}Bq kg^{-1}

with specimens loaded during one hour with tritium at 723 K. Plots of decontamination factors as function of temperature revealed that the highest decontamination factors were attainable at temperatures in the range (1073 ± 200) K when argon was circulated in closed loop mode for 10 min (see Table 8.5). The DF's attained under these conditions were in the range 900 - 8000. As apparent from the results, under static conditions much lower DF´s are obtained than under dynamic conditions. What is more, the addition of 5 % hydrogen to the argon purge gas boosts considerably the rate of decontamination under static conditions, at least at temperatures under 1273 K. Even though rather high decontamination factors were obtained at temperatures below the melting point, they were still far below values needed to reach the landfill disposal limit[14].

In case of wet outgassing at ambient temperature approximately 90 % of the activity was released after 10 days and nearly 99 % after 20 days. A second wet outgassing displayed a much slower release rate. This was taken to mean that the main tritium load was already liberated after the first treatment and not replaced by diffusion of bulk tritium to the surface.

Main conclusions from the work of Corcoran et al. [Cor92] dealing with "real life" material contaminated **exclusively** at ambient temperature but over rather extended periods of time, were:

[14] The current UK landfill disposal limit for tritium is 4×10^7 Bq t^{-1}[UK 12]

- The major fraction of tritium contaminating stainless-steel storage vessels exposed to tritium at ambient temperature resides in the surface.
- Tritium is probably trapped on the stainless-steel surface in form of metal hydroxides.
- The surface fraction present in corrosion products can be removed to a large extent by prolonged (about 20 days) wet outgassing before proceeding with plant dismateling, component sectioning and heating/melting.
- A large fraction of bulk tritium (dissolved) can be released from stainless-steel by a heat treatment at 873 - 1373 K. The achievable decontamination factors remain within the range $10^3 < DF < 10^4$.

The thermal release of tritium from stainless-steel SS316 heated in several temperature steps has been the subject of a number of investigations [Car91; Won91; Ake96; Pen12]. Some results of Wong et al [Won91] are displayed in Fig. 8.7. As can be seen, at temperatures up to about 373 K only a small fraction of tritium is released as HTO and almost none as HT. When the temperature is further raised up to about 473 K, an additional substantial release of HTO takes place while the fraction of released HT still remains insignificant ($\sim 0.5\,\%$). Only when the temperature reaches 623 K does HTO commence to level off and a considerable fraction of HT but still much smaller than that of HTO, is detected. Hence, tritium is mostly liberated as HTO, i.e. $> 95\,\%$ and a substantial fraction of HT is only liberated when the temperature surpasses 500 K. The more detailed results of Akermark et al. [Ake96], which were already discussed in section 2.14.1.4, are well in line with the results reported by Wong et al. [Won91] (see also Fig. 2.38).

Penzhorn et al. [Pen12] investigated the thermal release of tritium from 6 mm thick stainless-steel 316L specimens non-homogeneously loaded at 473 K (specimens were supplied by JET). When these specimens were first heated up to 573 K, the main fraction of tritium released consisted of HTO and only a very small fraction was liberated as HT (see Fig. 8.8). Outgassing at even higher temperatures, i.e. 1073 K, caused liberation of only a small additional fraction of HTO but of a large fraction of HT which, however, was still much smaller at its maximum than the accumulated fraction released as HTO (note different scales of the ordinates). It is important to realize that as long as the temperature remained constant at 573 K no significant further

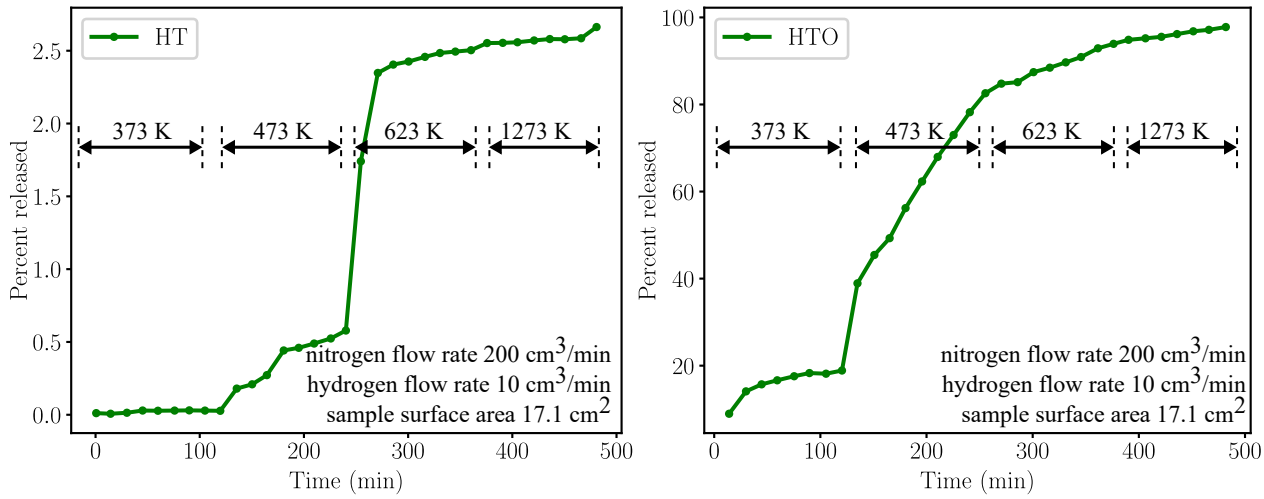


Figure 8.7: Thermal release of HTO (left) and of HT (right) from stainless-steel tubing in four consecutive thermal steps. The material was originally contaminated with 92.5 kBq m^{-2} (after [Won91], see also [Kra90; Car91]) (note the different ordinates).

release of HT took place beyond that initially liberated and in spite of continuous prolonged heating over a period lasting many hours. Only when the temperature was further raised up to 1073 K was another major fraction of HT freed but almost no additional HTO. The same behaviour was observed when the specimens were first heated up to 673 K.

Most investigators performing experiments on the release of tritium from stainless-steel SS316 within the temperature range from ambient to 1100 K agree that liberation of tritium takes place by several distinct release mechanisms depending on the prevailing temperature. However, information on these mechanisms is mostly speculative and not sufficiently proven. Hence, some ingenious studies are needed to shed more light on the subject.

There is general agreement that extended baking at temperatures above 1000 K is necessary to decontaminate stainless-steel waste from tritium down to levels low enough for waste disposal. A more radical procedure consists in **melting** [Gir92; Cla95a]. To demonstrate this procedure a semi-industrial detritiation process has been implemented at CEA, Valduc, France, designed to remove tritium from stainless-steel by complete melting under a mild vacuum of 30 - 100 mbar [Ros99; Ros00b]. If required, the contaminated stainless-steel material can be cut into pieces that fit into the crucible in which melting takes place. Melting is accomplished by induction heating up to approximately 1900 K. The process is currently being upgraded to permit in-depth sparging under vacuum using either pure noble gas (Ar) or noble gas containing a small fraction

of molecular hydrogen. Hydrogen is used to expedite the liberation of tritium by isotopic exchange [Ros02]. A model capable of predicting the release rate of tritium as function of process parameters such as i) temperature, ii) hydrogen content in argon, iii) gas flow rate, iv) initial concentration of hydrogen isotopes in the metal, v) average bubble equivalent diameter, vi) bubble velocity, etc. has been developed and verified at CEA [Ros00a; Ros00b]. Advantages of the melting process are i) reduction of waste volume, ii) disruption of the oxide layer barriers on the metal surface retarding diffusion, iii) homogeneous product of easier tritium assay, and iv) high decontamination factors. On the negative side are i) progressively increasing solubility of tritium in liquid stainless-steel with increasing temperature, ii) expensive facilities, and iii) substantial operational costs [Edw95a; Cla95a].

A **dry procedure** for the decontamination of stainless-steel or carbon steel from radioactive nuclides on the metal surface has been developed by Kameo et al. [Kam06]. The radioactively contaminated surface oxide layer on the metal surface is removed in two steps: i) coating the metal surface with a hot glass layer at 1023 K via a bead reaction and ii) removing the glass layer by thermal quenching employing blasting with dry ice at a starting temperature of 673 - 773 K. The generated secondary waste consists principally of glass scraps. It is estimated that the amount of resulting glass waste is similar to that obtained when the decontamination is performed with sulfuric acid. An advantage of the procedure is that the radioactive nuclides are stably fused into the glass scraps. The applicability and efficiency of this procedure to fusion waste has not been demonstrated.

Because of the activation levels typically attained by **Inconel** installed in fusion machines are high the containers holding this waste must be stored under concrete. To avoid spread of tritium contamination the waste containers must be accessed via an airlock.

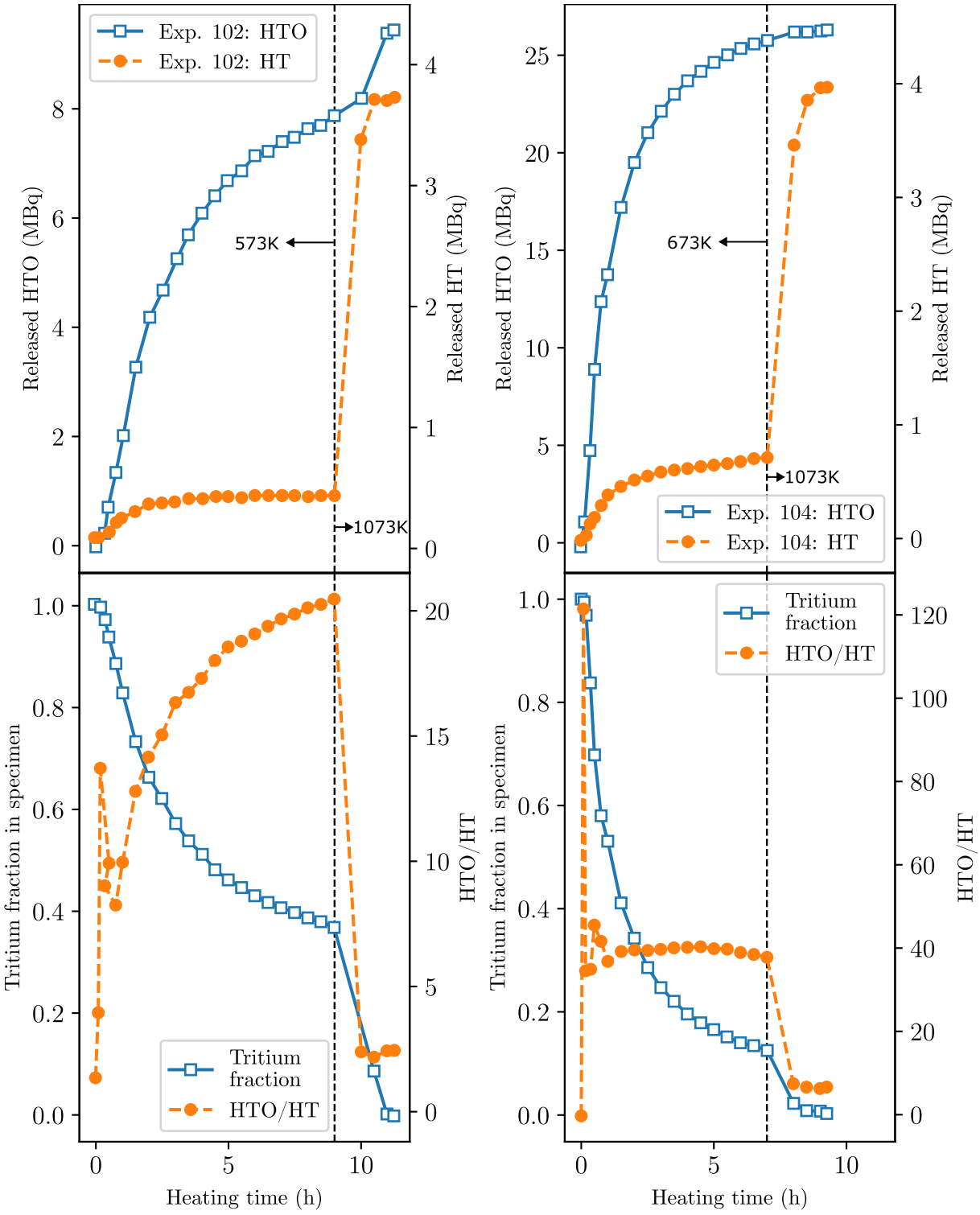


Figure 8.8: Thermal release of HTO and HT from stainless steel SS316 during prolonged heating in two consecutive steps at constant temperatures of either 573 and 1073 K or 673 and 1073 K [Pen12]. Also displayed are HTO/HT ratios. The initial loadings were Expm. 102 : 973 MBq cm^{-3} and Expm. 104 : 22.30 MBq cm^{-3}.

8.4.2 Decontamination of liquid organic wastes

A pragmatic approach to deal with tritiated organic wastes consists in converting bound tritium and dissolved tritium into tritiated water. The resulting tritiated water can be processed together with other tritiated waste water streams in a detritiation plant.

8.4.2.1 Decontamination of tritiated solvents, pharmaceuticals, and liquid scintillation cocktail

Organic tritiated solvents, tritium-contaminated liquid scintillation cocktail, or tritiated pharmaceuticals characterized by either one or more properties such as ignitability, toxicity, corrosivity, volatility, or reactivity (occurrence of radiation-induced reactions) are defined as hazardous mixed waste. Disposal of this kind of waste is tightly regulated and consequently exceptionally expensive. Accordingly, conditioning procedures are needed designed to convert this complex organic waste into a single more easily manageable product like tritiated water. From this product the recovery of tritium is straightforward.

Within this frame, Shmayda et al. [Shm02a; Shm02b] developed a **two stage high temperature reactor** comprising an atomizer nozzle and an integrated noble metal catalyst bed for the detritiatiation of liquid organic wastes such as tritium-contaminated solvents, oils, detergents, liquid scintillation cocktails, etc. Full oxidation of these species yields tritiated water and carbon dioxide (see Fig. 8.9). Initial rough oxidation of organic liquids takes place in the first stage, in which atomized solvent spray is injected into the reactor using oxygen as carrier and propellant. The whole reactor is manufactured of corrosion-impervious Hastelloy and operated at temperatures within the range 973 - 1173 K. Due to the exothermal character of the oxidation reactions, the temperature inside of the oven may exceed the design value of the oven itself. This is prevented by adjusting the external heaters, cooling with nitrogen, and regulating the reagent feed rate. The aim is to keep the maximum temperature in the oven below 1273 K and that in the catalyst bed below 1123 K. The reactor off-gas from the first oven consists of tritiated water, carbon dioxide, some unconsumed oxygen, residual unoxidized reagents and oxidized impurities. In the second stage these gases are remixed utilizing an alumina diffuser and further oxidized in the presence of a heated catalyst consisting of alumina impregnated with 0.5 % platinum. Tritiated water is collected further downstream by a demister/molecular

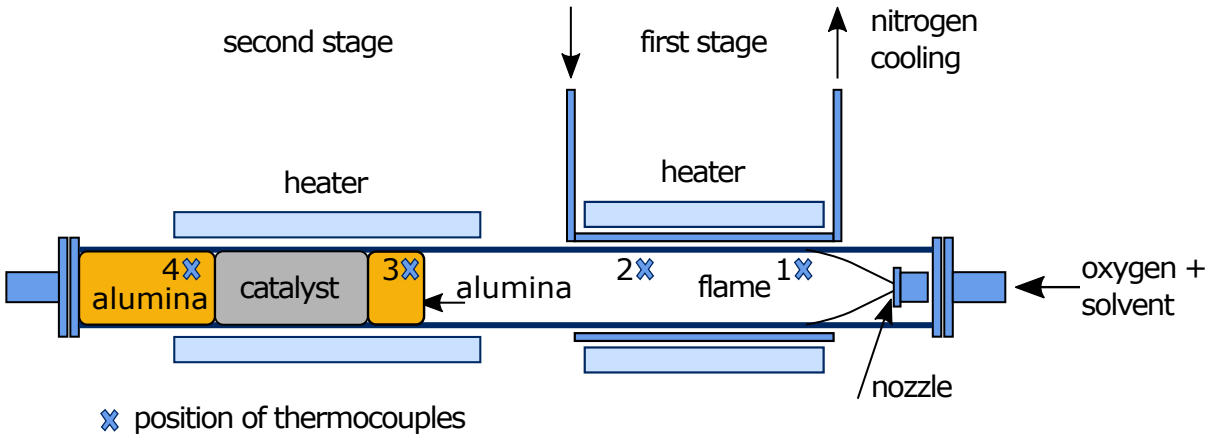


Figure 8.9: Schematic drawing of a reactor for the oxidation of tritiated solvents and reagents (after [Shm02a]). The numbers denote positions of the thermocouples, i.e. 1 injection zone, 2 flame, 3 catalyst inlet and 4 catalyst outlet.

sieve adsorber combination. After completion of the oxidation, the adsorbed water is released thermally, purified and, subjected to high-pressure electrolysis at 3 - 10 bar. Electrolytically generated hydrogen isotopologues are stripped from tritium employing a gas chromatographic isotope separation system, and stored in a getter bed for later reuse. When the waste contains chlorinated hydrocarbons special precautions are necessary, because oxidation can lead to the formation of wet and highly corrosive hydrochloric acid.

Precautions against hydrochloric acid comprise i) co-injection of methanol/water to reduce the concentration of hydrochloric acid in the condensate to values below 15 % by weight, ii) *in situ* neutralization of the HTO condensate collected in the product tank by the addition of K_2CO_3, iii) protection of the molecular sieve beds with a potassium carbonate (K_2CO_3) bed placed immediately downstream of the product tank in order to scrub HX (X = Cl, Br, F) from the effluent stream and iv) equipment manufactured entirely from highly corrosion-resistant materials like Hastelloy. A further preventive measure consists in a process conduction such as to achieve high conversion efficiency in order to guarantee low organic carbon content in the resulting tritiated water. Envisaged throughputs of contaminated organic material are in the litres per day range. Achieved conversions have exceed 99.999 %.

First cold tests in Canada and subsequent tests with tritium at SCK-CEN, Belgium, of the two-stage reactor have been carried out successfully. They were designed to demonstrate to SCK-CEN authorities that safe handling and conditioning of rather diverse tritiated solvents

and pharmaceuticals delivered for interim storage to SCK-CEN by universities and industrial installations can be processed with only negligibly small emissions [Shm02b; Bra05].

The **PMR technology** (see also section 3.18.4.3) was also shown to constitute a promising approach for the recovery of tritium from hazardous tritiated organic wastes such as generated in universities, pharmacology companies or other institutions involved in labelling operations for biomedical applications [Bir99].

In this case, steam reforming reactions between tritium-bearing alkanes, alcohols or aromatics and water vapour in a heated PMR reactor operated in closed loop mode lead to the generation of tritium-bearing molecular hydrogen according to reactions such as:

$$\mathrm{C}_n\mathrm{Q}_{2n+2} + n\,\mathrm{Q}_2\mathrm{O} \longrightarrow (2\,\mathrm{n}+1)\,\mathrm{Q}_2 + n\,\mathrm{CO} \quad (\mathrm{Q} = \mathrm{H,D,T})$$

$$\mathrm{C}_n\mathrm{Q}_{2n+1}\mathrm{OQ} + n\,\mathrm{Q}_2\mathrm{O} \longrightarrow (2\,\mathrm{n}+1)\,\mathrm{Q}_2 + n\,\mathrm{CO}$$

$$\mathrm{C}_6\mathrm{Q}_5\mathrm{CQ}_3 + 7\,\mathrm{Q}_2\mathrm{O} \longrightarrow 11\,\mathrm{Q}_2 + 7\,\mathrm{CO}$$

As soon as carbon monoxide becomes a constituent of the PMR gas, the water gas shift reaction

$$\mathrm{Q}_2\mathrm{O} + \mathrm{CO} \longrightarrow \mathrm{Q}_2 + \mathrm{CO}_2$$

needs to be taken into account. Experimental results obtained at 848 K provided evidence that more than 99 % of the injected organic compounds can be converted into molecular hydrogen and carbon monoxide by reaction with water vapour inside of a PMR type reactor (see also Fig. 3.78a). However, for the attainment of high conversion it is necessary to remove constantly hydrogen isotopologues by selective permeation (removal of a reaction product causes equilibrium to shift towards the product side). The degree of equilibrium shift and the rate of the reaction will ultimately depend on the efficiency with which hydrogen is pumped out of the reaction loop.

8.4.2.2 Decontamination of tritiated oil

The radioactivity in oil contaminated with tritium is distributed among dissolved HT, dissolved HTO, a mixture of dissolved tritiated hydrocarbons, volatile tritiated organics and non-volatile polar organics [Kra95]. The relative distribution depends on the type of oil (e.g. esters, silicone fluid, polyphenyl ethers, etc.), the degree of ageing of the oil and the level of tritium exposure. Pump oil that has been in contact with tritium for an extended period of time may contain tritium at concentrations of the order of $10\,\mathrm{TBq\,kg^{-1}}$ [Saz08]. The main contributors to this activity are polar tritiated components. These species can be removed to a rather large extent,

e.g. 95 %, with suitable polar adsorbents like faujasite NaY [Kra95; Saz08]. The rate of tritium mass transfer from the oil to the adsorber can be influenced slightly by stirring and more strongly by dilution with a high molecular weight hydrocarbon or an increase of temperature. After attainment of adsorption equilibrium, the tritium activity extracted with the solid adsorber must be released thermally and oxidized in a catalytic oxidation reactor. The objective is to convert all released organic tritium-bearing species into tritiated water and carbon dioxide. While the achievable overall reduction in radioactivity is probably not sufficient to permit declaration of the waste as non-active, a significant reduction in waste disposal costs is certainly achievable.

8.4.3 Decontamination of adsorber beds with concomitant tritium recovery

Conditioning of adsorber beds highly contaminated with tritiated water has been carried out utilizing a palladium membrane reactor (PMR) (see also section 4.3.3.2.2) [Ses05]. Accordingly, adsorbed tritiated water is thermally released using carbon monoxide as carrier gas. The resulting CO/moisture mixture is fed into a PMR reactor where conversion of water into tritiated molecular hydrogen takes place. This gas easily permeates across hot palladium/silver from which it is extracted by pumping. The most favourable steam partial pressure as well as total pressure in the reactor is achieved by dynamic optimisation. Hence, reliable real-time analytics must be available. Water condensation in process tubing or mass flow controllers is avoided by trace heating. Poisoning of the permeator by carbon monoxide needs to be addressed (see section 3.14.3).

8.4.4 Decontamination of getter beds

Klein and Hsu[Kle02b; Kle08] investigated comprehensively the conditioning of prototype tritium storage beds containing either 4.4 kg of HY-STOR 106 **titanium sponge** or 9.7 kg of **lanthanum/nickel/aluminum** by passivation with air. Objective of the research was the determination of optimized conditions for the preparation of tritium-contaminated vessels in orderto meet waste disposal exigencies. For more information on the utilization of $LaNi_{4.25}Al_{0.75}$ for tritium handling in pumping, purification, compression or storage processes including in-bed calorimetry, references[Nob91; Kle92; Kle95; Kle02b; Kle05a] may be consulted.

Attention was focussed on titanium, because this storage metal displays higher storage capacity for tritium and lower tritium equilibrium pressures than either$LaNi_{4.25}Al_{0.75}$ or ZrCo (see also Table 2.25). The preferred method for the activation of titanium sponge consisted in purging with a dry gas for several hours at temperatures progressively increasing up to 623 K and then by several heating steps at temperature steps increasing up to 873 K while constantly evacuating. Loading of the beds containing titanium sponge was performed with deuterium at flow rates within the range 5 - 20 $l\,min^{-1}$. Temperature measurements carried out a diverse positions outside of the vessel revealed that the maximum internal temperature increased with loading rate from 773 K up to 973 K at the highest flow rate tested. Within the same flow rate range the maximum external temperatures of the vessel increased from 573 K when loading at 5 $l\,min^{-1}$ and up to 673 K when at 20 $l\,min^{-1}$. To recover the immobilized gas, the vessel was heated from the outside at temperatures up to 973 K under under several vacuum conditions.

On account of the rather small temperature increase observed in the titanium bed after the first introduction of air, i.e. only 4 K, it was concluded that beds containing this storage material do not require passivation prior to disposal. The reaction with air will probably be too slow at ambient temperature to be of concern for the burial site, even in the event of a vessel breach. However, because only up to 84 % of the gas inventory in the storage vessel can be removed by thermal desorption, isotopic exchange will be necessary preceding the final vessel disposal. Conversely, storage beds containing $LaNi_xAl_y$ hydride required several successive batch-wise exposures to air to avoid an excessive temperature rise. During exposure to air, the getter undergoes oxidation, heats up, and thus releases hydrogen isotopes which subsequently need to be converted into water. Hence, a complementary oxidizing bed is necessary for the quantitative oxidation of the liberated hydrogen. A drier bed installed downstream serves to trap tritiated water.

Another decontamination procedure of getter beds consists in isotopic exchange or swamping [Mai92a; Edw95a]. To this effect, the bed is first heated under vacuum and then flushed repeatedly with deuterium or hydrogen while still at elevated temperature. The technique was applied successfully to decontaminate **palladium** and **vanadium** hydride storage beds. It was possible to remove tritium from these beds down to trace values. The analysis of the flushing gas delivered information from which the tritium remaining in the bed could be calculated. A drawback of

the **drain and flush method** is the generation of large consignments of rather diluted tritium which must be subjected to an isotope separation.

Uranium powder contaminated with tritium constitutes a special waste due to the fissionable character of the getter. Handling of this waste requires strict compliance with international control regulations. From a chemical point of view, the disposal of uranium is only possible after full oxidation. This is required in order to completely exclude the occurrence of temperature excursions in or on the way to a storage facility. Oxidation is usually performed by a cautious and stepwise increase of the temperature while purging with a stream of inert gas doped with a small partial pressure of oxygen [Hem92; Tam93]. During the oxidation of uranium, a large fraction of tritium bound to the getter is released mostly as tritiated water. The achievement of full oxidation is cumbersome, on one hand, because of the protective uranium oxide layer that builds up on the powder surface and, on the other, due to the tendency of the powder to agglomerate. It is therefore necessary to repeat the treatment alternating between hydrogenations for disruption of the agglomerates and oxidations.

Another difficulty concerns **verification of full oxidation** of the reactive waste which may be demanded by authorities prior to acceptance. A verification procedure has been developed at Kinetrics, formerly Ontario Hydro Research Division, Canada. At this institution, uranium storage beds and zirconium iron alloy (SAES St198) scavenger beds were first heated up to 823 K with the objective to remove most of the hydrogen (and tritium) still present in the metal (explosion safety) [Ant08b]. Oxidation of the getter was then performed with a stream of argon containing 20 % by volume of oxygen. As the temperature was incremented in 50-degree steps at a maximum rate of $5\,\mathrm{K\,min^{-1}}$ the oxygen partial pressure was continuously monitored to follow the progress of the oxidation. If there was no change in oxygen partial pressure the temperature was increased by a further step. This approach was continued until 823 K were reached. To verify full oxidation, the oxidized bed was exposed to hydrogen at elevated temperature. If hydrogen absorption was observed the storage bed was subjected to several hydrogen absorption/desorption cycles. After unloading the hydrogen from the last cycle, a further full oxidation was carried out following the procedure described above.

The consequences of air ingress into technical tritium storage beds containing kilogram amounts of uranium or zirconium cobalt powder have been discussed in detail in a previous section (see section 3.14.2.2.2). Doubtless, the most critical scenario is pure oxygen flowing

across the bed. The lowest temperatures at which uranium reacts in self-accelerating modus (triggered by the exothermic reaction) with oxygen and nitrogen were estimated to be 400 K and 770 K, respectively. The corresponding temperatures for ZrCo were found to be 500 K and 1000 K, respectively. Hence, from the point of view air-ingress, zirconium cobalt constitutes the safer option.

8.4.5 Decontamination of service waste

A reduction of the radioactivity on the surface of materials such as yellow polyethylene plastic bags, paper towels reinforced with plastic and yellow nuclear grade reinforced vinyl laminated Herculite® was achieved with an Oxidative Tritium Decontamination System employing ozone as principal reactive agent [Yos01; Gen02]. Screening tests were carried out with i) a rotary reaction chamber, ii) a static reaction chamber, or iii) a piston-cylinder configuration. The **rotary reaction chamber** is equipped with agitation baffles. They are utilized to maximize the exposed material surface area by eliminating dead zones within the chamber. The **static reaction chamber**, which can be heated and evacuated or pressurized to several bar, is equipped with a sapphire window of more than 70 % transmittance to vacuum ultraviolet radiation. The idea behind the **piston-cylinder-configuration** was to increase the reactant pressure and consequently the degree of ozone penetration into porous materials like carbon fibre composites and other. The design permits rapid pressure raise in the reactor up to several bar. Because purging with ozone - while known to be quite effective - was only little more efficient than ambient air it appeared that the evaporation of tritiated water contaminating the material plays a decisive role. Simultaneous exposure to ozone and irradiation with ultraviolet light of ≤ 235 nm wave length brings about a moderate synergistic effect. The slightly enhanced decontamination was attributed to splitting of ozone induced by UV radiation into molecular oxygen and highly reactive oxygen atoms. According to the researchers, the experimental results are consistent with the presumption that tritium removed by ozone is mostly residing on the material surface or perhaps in the subsurface and to a much lesser extent in the bulk. Decontamination of up to 20 kg of expendable tritium-contaminated waste down to levels permissible for free release, i.e. $16.7 \times 10^{-2}\,\mathrm{Bq\,cm^{-2}}$, were attained. Ultimate goal of the work was a cost reduction of waste disposal.

One more process for the detritiation of weakly contaminated soft **housekeeping waste** consists in heating milled waste under an argon stream containing a low partial pressure of oxygen (see also section 8.3.2). This process concept was recently proposed at Cadarache, CEA, by Lefebvre et al. [Lef12]. The partial pressure of oxygen is kept low to exclude combustion. Liberated tritiated water is either collected with a MARC 7000® bubbling system or alternatively removed from the effluent carrier gas via the catalysed exchange reaction

$$HTO + H_2 \longrightarrow HT + H_2O \ .$$

For this purpose, the effluent gas from the detritiation oven carrying the released HTO is passed through the palladium/silver tubes of a permeator containing Ni catalyst maintained at 673 K. Molecular hydrogen is fed in counter current along the outside of the tube, i.e. between membrane and reactor shell. Since hydrogen can selectively permeate the hot Pd/Ag tubes, catalytic exchange will take place with HTO. As a result, molecular hydrogen will be enriched in tritium while HTO is tritium-depleated. By proper reactor design and process conduction very high efficiency can be achieved. Tritium can be recovered from the HT stream utilizing a conventional isotope separation system. To optimize the process conditions, the influence of parameters such as i) temperature of waste detritiation (between 393 K and 423 K) ii) composition of the carrier gas, i.e. Ar with 2 % O_2, Ar with 5 % H_2 or Ar with 25 - 40 % H_2O and air, and iii) flow rate of the carrier gas within the range 300 or 450 l min^{-1} were investigated systematically. The most effective carrier gas was found to be argon containing 2 % oxygen at a reactor temperature maintained at 423 K. An important advantage of this carrier gas mixture is that it can be considered hazard-free with respect to hydrogen. Under these conditions detritiation yields of more than 50 % were achieved in little more than half a day. The optimal feed flow rate is a trade-off between waste detritiation on one hand and membrane permeability efficiency on the other.

A more drastic procedure to deal with soft housekeeping wastes was proposed by Gentile et al. [Gen05]. Waste contamination was reduced effectively down to background or nearly background levels by the sequence i) shredding, ii) grinding to pulverized particles and iii) combustion with a plasma burner to generate detritiated ash. The ash was separated by gravity in a separator and the off-gas demisted, filtered through an HEPA filter, and finally passed through a molecular sieve

bed for the quantitative retention of tritiated water. Tritiated water retained in the adsorber bed can either be given to waste or be processed in a detritiation system for tritium recovery.

8.4.6 Decontamination of the inner surfaces of glove boxes and equipment inside

A standard TLK glove box housing an integrated classical Tritium Removal System and containing much typical equipment of the kind used for research with tritium was decontaminated and refurbished. The glove box had served as confinement for two experiments with tritium, one during the period 1995 – 2000 with up to 1 g of tritium (PETRA experiment [Pen97a]) and another performed 2007 with up to 0.025 g of tritium (FACT experiment [Ant08a]). Purpose of the decontamination was to prepare the glove box together with some of the confined components for a third new research activity which is described in detail in a paper published by Wagner et al. [Wag15].

As would be anticipated, whereas wipe tests carried out on the outer surface of the glove box revealed no contamination, wipes taken from the inner surfaces of the glove box displayed contaminations of the order of 15 $kBq\,cm^{-2}$ on gloves and to about 30 $kBq\,cm^{-2}$ on the bottom below the area under the former now dismantled FACT experiment. The contamination of free cables installed inside of the glove box was obtained from leaching into water and found to be of the order of 25 $MBq\,kg^{-1}$. Turning off the Tritium Retention System integrated into the glove box caused the tritium concentration in the glove box atmosphere to increase slowly with a rate of almost 1 $MBq\,hour^{-1}\,m^{-3}$. A non-heated, single wall, strongly contaminated stainless-steel buffer vessel of 3.8 l capacity, which had been utilized for the interim storage of diverse waste gases, was repeatedly flushed with hydrogen. This treatment conducted to the recovery of approx. 200 GBq of tritium. Thereafter, the vessel was filled with hydrogen. Under these conditions, the concentration of tritium increased linearly as function of time with a steady rate of approx. 100 $kBq\,cm^{-3}\,hour^{-1}$ over a period of almost 300 days. Combining this result with regular gas chromatographic determinations of the concentration of ^3He in hydrogen, it was possible to estimate that about 40 TBq of tritium were still remaining in the vessel. This tritium was assumed to reside on the inner sub-surface of the vessel and explained by diffusional chronic release [Tor05b; Pen11].

Another non-heated single wall vessel having a volume of 6 l, which had previously been used to pepare mixtures of deuterium and tritium together with carbon oxides behaved differently when subjected to the treatment described above. Flushing with hydrogen caused only initially an increase of the tritium concentration in the gas phase. On the other hand, examination of the inner surface revealed brown-orange viscous stains which when wiped and analysed by LSC yielded comparatively high activities within the range 1.6 - 27 $MBq\,cm^{-2}$. The stains consisted presumably of a radioactive polymerized material. Valves and pipes connected directly to the buffer vessel and weighting altogether 6.9 kg exhibited a specific activity of 25 $GBq\,kg^{-1}$. Because this specific activity was determined by calorimetry it constitutes an absolute inventory. Analysis of all obtained results revealed that the activity estimated from surface measurements alone was about ten times smaller than that obtained from calorimetry. Consequently, there is indication of substantial penetration of tritium into stainless-steel structure materials even though they were maintained at all times at approximately ambient temperature (see also section 2.14.1.2).

The tritium surface contamination of a facility designed to detritiate heavy water was discussed in detail by Carmichael and Haynes [Car91].

Some lessons learned by these investigators were:

- Tubing exposed to tritium gas can display very high tritium surface contamination and release tritium oxide of very high levels of contamination,
- Materials such as flanges or tubing exposed to tritium are difficult to decontaminate because substantial tritium is incorporated into the bulk. Purging with dry or wet inert gas will only temporarily decrease the contamination of the surface. To achieve a more enduring decontamination of surfaces heating to temperatures exceeding 473 K was found to be necessary.
- Rubber gloves or plastic suits provide an effective barrier to the propagation of the surface contamination.
- Skin contamination is frequently observed when undressing from protective clothing is not done carefully.

8.4.7 Decontamination of materials constituting the first wall of a tokamak

Conditioning and decontamination from tritium of first wall materials can be performed inside of the fusion machine or, in case interim storage of tiles for future replacement or disposal is foreseen outside of the machine.

8.4.7.1 In situ decontamination

There is continuing demand for efficient and reliable procedures for the direct conditioning of the surfaces of plasma-facing components protecting the vacuum vessel of fusion devices. Conditioning and decontamination are indispensable after i) vacuum vessel venting and opening, ii) major air leaks, iii) water leaks, etc. and before beginning of plasma operation. Furthermore, it is important to reduce oxygen and nitrogen impurities in the plasma. These impurities i) lead to parasitic radiative power, ii) dilute the fuel particles, iii) accelerate the erosion rates of plasma facing materials and iv) enhance trapping and recycling of fuel particles causing the plasma to become unstable [Air11]. Moreover, the generation of high-quality plasmas is only possible after evacuation of the plasma chamber to a very low initial vacuum. In other words, to re-initiate operation base vacua as low as 10^{-7} - 10^{-8} mbar are indispensable. This is only achievable when the influx of hydrogenic species into the vacuum vessel has been sufficiently reduced.

As already discussed, one more very important reason for *in situ* decontamination of plasma-exposed and-shadowed surfaces is the necessity to meet safety and licensing demands, which means remaining below the established maximum tritium inventory. Of course, tritium economy may also play a role. Particularly challenging and difficult within this frame is the retrieval of particles, flakes, and other debris existing disseminated in plasma-shadowed sometimes poorly-accessible remote regions of the machine-like ducts, zones beneath the divertor, or on the louvers near the divertor. One more potential zone for the accumulation of co-desposit is the small gap between tiles. As apparent from tritium surface profiles obtained with a PIN diode on six surfaces of a tile retrieved from JET (tile # 004/1-44) (see Appendix H), the surface activities (here expressed in $\mathrm{Bq\,cm^{-2}}$) displayed on one lateral surface are particularly high. This can be explained by co-desposites trapped between adjacent tiles. Tritium caught between tiles will probably be rather hard to remove thermally or by any other means. As noted before,

co-desposited materials may sequester high concentrations of tritium and contain elements like carbon, beryllium or tungsten from plasma-facing components.

Presently utilized, tested or merely discussed cleaning techniques applicable inside of fusion devices [Ski03b] comprise i) thermo-oxidation with oxygen [Haa07], ii) deuterium glow discharge (GD) [Air11], iii) helium/oxygen glow discharge [Kun07], iv) laser ablation [Wat07], v) cleaning with flash lights [Cou01; Gib05] and vi) treatment by liquid wash-and-flush procedures [Mue97; Cou01; Ski08]. Regardless of the applied technique, it is always necessary to verify after completion of the cleaning action that released tritium has not been re-adsorbed or re-deposited elsewhere inside of the vacuum vessel together with other elements.

A few of the more auspicious cleaning procedures are discussed below:

Glow discharge cleaning with deuterium has been routinely applied in several fusion devices like TEXTOR, ASDEX Upgrade, or DIII-D for impurity and hydrogen recycling purposes. At JET, TFTR, and JT60-U the method has additionally been employed to recover from disruptions, a violent event that puts an end to a magnetically confined plasma.

Another conditioning procedure tested experimentally at TFTR consists in treating plasma facing materials at increased temperatures (373 - 513 K)[15] by **glow discharge** for instance with a mixture of **helium** and **oxygen** [Mue97; Kun07]. A gas of composition 80 % He and 20 % O_2 maintained at a pressure of 13.2 Pa has been successfully used to generate discharges.

The techniques adopted at TFTR for the retrieval of tritium from the vacuum vessel after completion of D-T campaigns were i) helium/oxygen glow discharge cleaning (7.9 %), ii) torus venting to 9.6×10^4 Pa air (10.1 %), and iii) bake out at 473 K combined with deuterium glow discharge cleaning (13.6 %) [Mue97]. After consecutive application of these diverse removal techniques it was possible to strip off approximately half of the tritium remaining in the machine at the end of a large number of plasma shots [Mue97; Kun07]. As apparent, none of the three options applied separately were sufficiently satisfactory.

Thermo-oxidation is predominantly utilized for the liberation of tritium from only slightly contaminated plasma-facing components like those installed in the TEXTOR vacuum vessel. Most effective agent promoting the release of tritium by this treatment was found o be oxygen. The carbon removal rate from TEXTOR was estimated from the integral rate of CO and CO_2 formation to be about $2 \times 10^{19}\,\mathrm{C\,s^{-1}}$ which translates into a removal rate of about 1 µm of

[15] The highest permissible temperature for ITER is 513 K.

co-deposit during four hours of glow discharge cleaning at 443 K [Phi07; Kun07]. Because of this, it was concluded that the enhancing effects of oxygen and temperature were not enough to make this option sufficiently attractive for utilization in fusion machines of the size of ITER.

Experiments on the thermo-oxidation of co-deposits on tiles retrieved from DIII-D revealed that the initial erosion rates are increased more effectively by elevating the temperature rather than by augmenting the pressure of oxygen [Haa07]. Experimentally it was shown that at 673 K and 79 kPa oxygen the deuterium content of co-deposits could be reduced by nearly an order of magnitude in about 15 min. An important disadvantage of thermo-oxidation are the fairly high temperatures, i.e. 500 - 700 K, necessary for an effective decrease of the inventory of co-deposited hydrogen isotopes [Phi99; Kun07]. Even under high temperature conditions, the oxidative technique is considered to be too slow for application in devices with dimensions like those of ITER. In case of ITER, the employment of deuterium and tritium as fuel gases is aggravating because of the generation of rather large quantities of T_2O and DTO[16] whose very high specific radioactivity and elevated radiotoxicity makes their handling exceptionally difficult and dangerous [Hay06; Ski08]. Conversely, in case of TEXTOR, which exclusively utilizes deuterium fuel, the employment of oxygen does not constitute a major problem because the fusion reaction generates only very little tritium.

One general negative aspect of thermo-oxidation is significant uptake of oxygen by materials facing the plasma which on one hand is associated with substantial formation and release of impurities such as oxygen and water into the plasma (plasma poisoning) and on the other with considerable passivation of the oxygen gettering property of beryllium.

Aiming at the development of procedures for the decontamination of graphite and stainless-steel inside of tokamaks some promising results were achieved by rapidly scanning over the surface of tiles retrieved from TFTR and JET with an Nd:YAG laser [Ski01; Ski02; Ski03a; Ski03b; Gen05]. Scanning of the co-deposits was performed at high speed employing galvanometer-driven mirrors. Release of tritium takes place exclusively by thermal processes when **laser-induced desorption** is carried out with the Nd laser at laser intensities below the limit for ablation or vaporization [Ski03a; Ski03b]. Under these conditions, the co-deposits adhered on tile surfaces

[16] It has been estimated that about 4.9 kg of DTO will be generated at ITER by thermo-oxidation. Since the base line processing rate at ITER is 33 g hour^{-1}, this would mean that about 6 full processing days are required to deal with this amount. Thus, a scale up of the currently considered tritiated water processing may become necessary [Ski08].

are heated under air or argon over a period of only about 10 ms with an intensity of approx. $10^4\,\mathrm{W\,cm^{-2}}$. The attained temperatures were determined with an optical pyrometer and found to be close to 2300 K. With the laser-induced desorption technique it was possible to release up to 87 % of the tritium trapped in co-deposits collected from the surface of TFTR or JET tiles. In order to detritiate flakes and other debris present in hard-to-access regions like the sub divertor, it was proposed to utilize a miniaturized rotating scan head that produces a circular region of intense heating. In spite of these promising findings, more practical experience under realistic conditions needs to be acquired and further technological developments are necessary before this technique can be implemented in a fusion device.

Some concepts developed explicitly for the removal of co-deposits inside of the vacuum vessel have been addressed in a recent comprehensive review by Skinner et al. (see [Ski08] and references therein). One such development relies on **pulsed laser ablation** combined with robotic technology. Optic fibres are employed to transmit light from an external multi kW laser beam to a scanning mirror fixed on a mobile robot. In order to reach all contaminated surfaces, the robot is circulated inside of the vacuum vessel. The technique, while auspicious, still requires considerable advancement and experimental verification.

Watanabe et al. [Wat07] proposed high power lasers, e.g. 20 ps-Nd:YAG, emitting short wave length light of 266 nm for the recovery of tritium from plasma facing material. The selected wave length was considered promising because the energy of the employed light is sufficient to break carbon-hydrogen bonds. Indeed, the Nd:YAG laser was shown to be efficient for the pulsed ablative removal of tritium from JT-60 carbon co-deposits. However, laser intensities exceeding $5 \times 10^{11}\,\mathrm{W\,cm^{-2}}$ were found to be necessary to achieve satisfactory results. Important advantages of laser ablation are the generation of only minor amounts of highly tritiated water and practically no incorporation of oxygen into the materials facing the plasma. Conversely, a significant drawback of all ablation procedures is the generation of gas and particulates highly contaminated with tritium. Even though a fraction of the generated particulates will probably be dispersed into remote and poorly accessible areas, where they are of no consequence to the plasma, it is still necessary to remove them as quantitatively as possible to comply with the imposed strict tritium inventory limitation inside of the vacuum vessel.

Tests at JET employing high power **xenon flash lights** of more than $2\,\mathrm{J\,cm^{-2}}$ revealed that these lamps are capable of removing hydrocarbon deposits on divertor tiles effectively [Cou01;

Gib05]. When cleaning by irradiation with pulses of 500 J layers of 70 - 90 µm could be detached from the tile surface. The treatment brought about release of hydrogen, diverse hydrocarbons, carbon dioxide and a significant fraction of particulates having mostly sizes of less than 20 µm. Hence, it appeared necessary to supply oxygen in combination with suction techniques to improve the efficiency. However, even with these enhancements the achieved removal rates were still too slow for application in a machine the size of ITER.

Another suggestion has been to collect ablated material with a directed gas flow **(gas blasting)** placed in the vicinity of the ablation zone and blowing the particles into a collection device or a divertor cassette. From either of these, the ablated material could be retrieved and then be subjected to de-tritiation outside of the machine.

A quite different approach for first wall cleaning was proposed by Counsell and Wu [Cou01]. They suggested installation of a **magnetically vibrated conveyor** designed for the regular collection and exhausting of fine debris (dust, aC:H films, flakes, etc.). A potential problem was seen with too heavy flakes. The principal idea in back of this concept was minimum disturbance of the operation schedule of the fusion machine.

An even more sophisticated way of proceeding consists in a liquid **wash-and-flush** cleaning technique designed to be of low impact on the evacuation conditions of the vessel [Cou01]. It was presumed that debris can be effectively removed from surfaces provided a suitable liquid is available that entrains and transports the debris to the base of the vessel for exhaust, filtering and recycling. The liquid cleaning technique has the potential for removing debris from truly inaccessible regions. The choice of liquid, however, which ideally should have properties such as i) low viscosity, ii) easy vaporization and pumping, iii) inertness to all in-vessel materials, iv) no degradation into corrosive products, etc. constitutes a major unresolved issue.

Neither the magnetically vibrated conveyor nor the wash-and-flush concept have been verified experimentally.

Regular withdrawal of mixed co-deposited dust and flakes accumulating not only on armour material but also dispersed inside of the vacuum vessel in zones at the bottom of the divertor, the vacuum ducts and other ducts, etc. is indispensable. In machines with a full or partial first wall of CFC, basically hydrocarbonaceous debris characterized by high hydrogen and therefore tritium content, was recurrently withdrawn in order to keep the machine running properly and the total inventory of tritium inside of the vacuum vessel within the limit stipulated by the

license. At JET, such sporadic withdrawals were carried out successfully with a specially designed remotely operated vacuum cleaner equipped with a cyclone collection device (see below Fig. 8.15 and [Pea00]). Evidence was provided that not only the accessible but also many poorly reachable areas could be vacuum cleaned efficaciously with this device. While this solution was adequate for JET, much higher demands would have to keep a machine like ITER clean. Among other reasons, it is because of this that ITER will most probably not include CFC as principal component of the first wall.

Other procedures that have been suggested for the removal of dust, flakes and films from the vacuum vessel are: i) **pellet blasting** (combined with suction and manipulation techniques) and ii) a so-called **water hammer** procedure which concentrates the material at the vessel floor for subsequent removal by other techniques [Cou01].

The dimension of the problem concerning the need for tritium removal from carbon plasma facing components becomes apparent when examining the tritium in-vessel inventory limits of two fusion machines furnished with carbon fibre composite or graphite first walls and operated with tritium. In case of TFTR (limit = 2 g) the maximum was reached in the vacuum vessel after about 22 months, and in the vacuum vessel and ducts of the JET machine (limit = 20 g) after approximately six months. Because both machines are research facilities and therefore operated discontinuously, these limits would be attained much earlier in a continuously running thermonuclear reactor like DEMO. These and other results eventually lead to the conclusion that high availability of fusion machines is only possible if all carbon tiles of the kind foreseen for the vacuum vessel of ITER are replaced by beryllium tiles and all carbon fibre monoblocks in the divertor substituted by tungsten monoblocks [Hir16].

In conclusion, there is still persisting need for the development of sufficiently rapid and efficient procedures for the regular decontamination from tritium of the whole vacuum vessel. Verified safe procedures are also required for the recovery of tritium from flakes, dust, and other debris retrieved from the vacuum vessel. Furthermore, *in situ* diagnostic techniques are needed for the determination of erosion and hence of the rate of formation of tritium-contaminated solid materials in a high neutron flux environment. The JET machine appears to be predestined for all of these activities because it is furnished with mostly ITER-like first wall materials.

8.4.7.2 Ex situ decontamination

During regular operation of a fusion machine some first wall materials will require replacement. Hence, materials like CFC (for ITER maybe no longer) and beryllium tiles, limiter front parts consisting of beryllium, cassettes from divertor replacements made up of tungsten with their corresponding steel support, dust, flakes, mixed co-deposits, etc. all highly contaminated by tritium and other radionuclides will recurrently be generated as waste or saved as spare parts (see also section 8.3.3.1). In order to reduce the tritium inventories in these components and hence diminish their rate of tritium outgassing, they will have to be transferred into a dedicated hot cell immediately after retrieval from the vacuum vessel. Hot cells must therefore be fully equipped for remote handling and frequent decontamination of large and heavy components. Sufficient capability for temporary storage needs to be available. In case of components intended for re-use, substantial decontamination may become necessary to lower the tritium out-gassing rates down to acceptable levels for prolonged interim storage.

Waste materials destined to a repository will necessitate considerable conditioning efforts. Sufficient and diverse analytical equipment must be on hand to meet the requirements for sentencing and qualification for storage within a radioactive waste category.

Several auspicious decontamination techniques for *in situ* application have already been described and evaluated in the previous section. However, even though in principle the same techniques are applicable for the decontamination of plasma-facing components outside of the machine, a number of adaptations are necessary. The high level of contamination by tritium and by transmutation products of the materials retrieved directly from the vacuum vessel make remote handling obligatory [Rub10]. Decontamination of single tiles or groups of tiles will be associated with distinctive technological demands and infrastructure exigencies. To avoid contamination spread, measures for the containment of loosely adherent co-deposits and other loose material are compulsory.

Schwer et al. [Sch05] released in a germane study deuterium from re-deposited carbon layers found in the TEXTOR and JET tokamaks employing localized heating with a ruby **laser**. Evaporation of the re-deposition was accompanied by the liberation of molecular hydrogen isotopologues. The results indicate that more than 80 % of the deuterium trapped in the a-C:H

layer can be desorbed by a single laser shot (average power $150\,\mathrm{kW\,cm^{-2}}$). The occurrence of evaporation was attributed to the particularly high-power density of the ruby laser spikes.

Pontau and Morse [Pon86] showed in their **thermal release** study that full liberation of hydrogen isotopologues from limiter graphite tiles requires temperatures exceeding 1273 K. This observation is in good agreement with results obtained by determining the thermal release rate of tritium from small coring specimens obtained from inner divertor tiles retrieved from the JET machine [Pac96; Pen00c; Pen01e; Bek07]. The examined tiles had previously been exposed to a large number of diverse plasmas. Quantitative liberation of tritium incorporated into specimens obtained from these tiles was only possible at temperatures higher than 1100 K. Actually, two fractions were liberated consecutively: a large one at 773 K ($\sim 86\,\%$) and a smaller one at 1373 K ($\sim 14\,\%$). Hence, effective decontamination of CFC material demands prolonged baking at rather elevated temperature. Because the design baking temperature of ITER, i.e. 513 K, is much too low for full *in situ* liberation of all tritiated species, thorough decontamination of CFC tiles is only possible outside of the machine.

In accordance with expectations, the rate of chronic release of tritium from **flakes** at ambient temperature was found to be notoriously larger than that from tiles. In measurements that lasted from a few days up to 21 months an average value of $(2.0 \pm 1.1)\,\mathrm{x}\,10^{10}\,\mathrm{Bq\,month^{-1}\,g^{-1}}$ was reported for flakes removed from the JET tokamak after completion of the DTE1 campaign [Pea98; Pen01e; Pen01a]. Chronic release experiments with these flakes performed in a glove box showed good correlation between increasing radioactivity in the argon atmosphere and simultaneously rising partial pressure of moisture. Additionally, most of the liberated activity could be removed from the glove box atmosphere by adsorption on silica gel. For all these reasons, the majority of the liberated tritium was presumably tritiated water.

Carbon fibre composite tiles or flakes, and dust generated in a CFC environment can be cautiously freed from tritium at high temperature under a stream of inert gas carrying a low partial pressure of oxygen. Because carbon is the main constituent of all these materials (see also Table 8.3) slow combustion will generate secondary waste consisting mostly of carbon oxides and tritiated water. Consequently, a process step encompassing the recovery of highly tritiated water needs to be included. Tritium can be recuperated from tritiated water via a detritiation process or, if collected water is first converted into tritiated hydrogen, by an isotope separation process. Activation products and poisonous chemicals will remain in the combustion ash or in

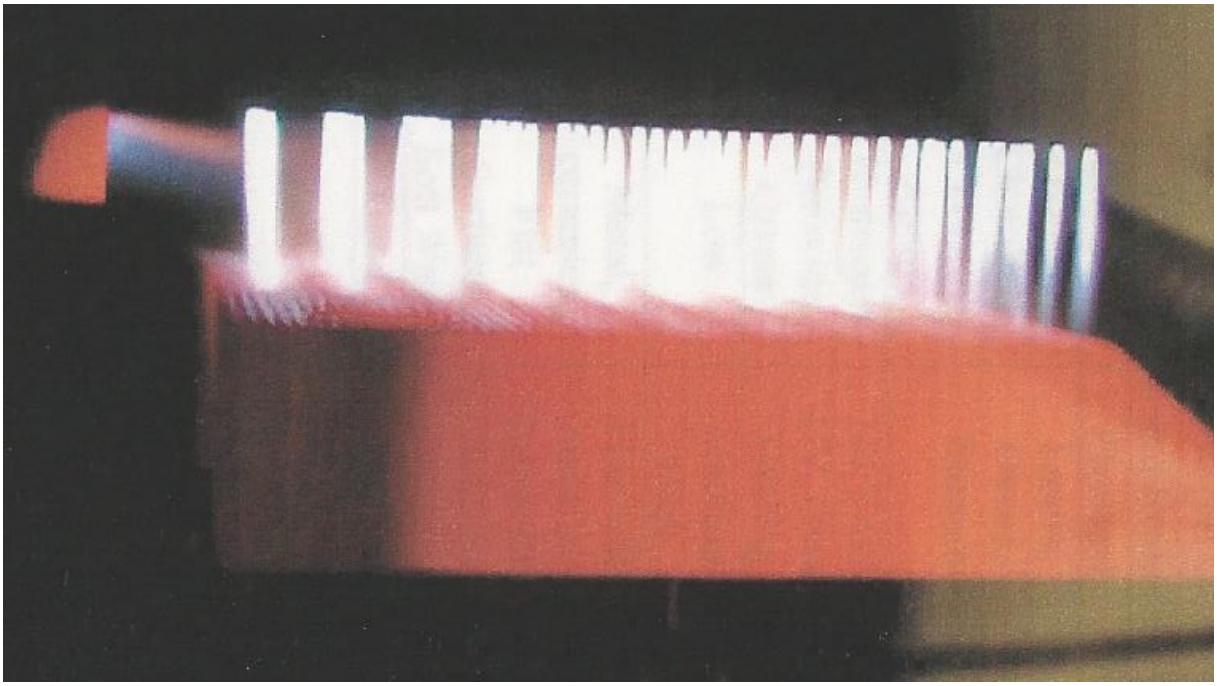


Figure 8.10: Direct decontamination of a JET tile employing an oxygen – methane burner [Gen05].

the structural materials (for instance cassettes). Following qualitative and quantitative chemical analysis and radiochemical assay of ash and structural materials, the habitual actions ahead of waste disposal can be initiated [For98; Pol05].

In screening experiments with non-contaminated segments of a CFC divertor tile of the kind installed in the JET machine, the effect of short exposures to an open oxygen/methane **flame** were examined by Bekris et al. [Bek02a]. The pyrometrically determined temperature on the material surface was about 1273 K. Further tests performed under comparable conditions using only slightly contaminated material provided evidence that decontamination factors for hydrogen isotopologues higher than 1000 are easily achievable. Additional try-outs carried out at PPPL with participation of UKAEA and TLK employing an oxygen – methane burner [Gen05] (see Fig. 8.10) and graphite tiles retrieved from the JET machine provided evidence that decontamination factors of tritium from surface and bulk of about 1000 and 60, respectively, are achievable.

8.4.7.3 First wall protective layers: boronization, molybdenumisation or siliconisation , molybdenumisation, siliconisation

To reduce co-deposition and influx of carbon, oxygen, and metallic impurities into the plasma of fusion machines while at the same time diminishing hydrogen recycling, thin films of boron or of a-B/C:H have been deposited on plasma facing surfaces by a plasma-assisted technique (**boronization**) [Win92]. Amorphous, hydrogen rich boron carbon a-B/C:H films obtained by plasma chemical vapour deposition displayed B-B and B-C bonds at a B/C = 4 ratio [Zal94]. Upon prolonged exposure to air, the oxygen content increased from 2-5 up to 15 - 20 %.

Conditioning of the first wall of TEXTOR by diborane flushing and the consequences of this treatment on plasma performance were discussed by Wienhold [Wie90].

Boronization of the first wall of the **Korea Superconducting Tokamak Advanced Research** reactor (KSTAR) was carried out with a carborane ($C_2B_{10}H_{12}$) injection system. The treatment was found to be associated with significant reduction of the impurity levels in the plasma, i.e. by factors of 3 and 10 for oxygen and carbon, respectively [Hon10]. Under this condition, temperatures of up to 10^8 degrees could be sustained for record 20 seconds.

Other first wall conditioning options comprise bulk boronized graphite or boronized carbon-carbon composite containing up to 30 wt % of boron [Hir90f]. Salient features of bulk boronized carbon-carbon composite are i) smaller plasma-induced erosion, ii) enhanced recombinative desorption of hydrogen (suppression of hydrocarbons) and iii) lower tritium inventories. Properties such as i) suppression of oxygen by gettering on boron coatings, ii) reduction of hydrocarbon formation on carbonaceous surfaces and iii) suppression of heavy metal liberation achieved by boronization were found to be associated with considerable improvement of energy confinement in the plasma. Experiments performed with the DIII-D machine confirmed these results.

ALCATOR C-Mod at Massachussets Institute of Technology, Cambridge, Massachussets is a fusion device in safe shutdown since 2016 [Gre14]. It is probably the only machine worldwide with a first wall consisting of **molybdenum tiles**. This high-Z material was chosen because of its similar properties to tungsten used for ITER. Principal aims of the work were investigation of the performance of molybdenum under a high neutron flux and elucidation of the degree of plasma core contamination under these conditions. Experiments with and without boron coating of molybdenum revealed that low Z coating appreciably reduced the concentration of

molybdenum in the plasma core which significantly contributed to optimize the confinement of energy [Lip01]. The ALCATOR C-Mod, which is characterized by high plasma density, high parallel heat flux and low divertor temperature, has demonstrated the advantages of high-Z divertor option featuring negligible erosion levels of material surfaces while maintaining hot central temperatures with low levels of radiation from metals [Lip06].

One more first wall coating material tested both at TEXTOR and ASDEX-Upgrade is silicon. **Siliconisation** was found to be highly effective in reducing the oxygen influx into plasmas. This could be particularly beneficial during the start-up phase of ITER.

8.4.8 Decontamination of walls and floors of buildings

Prior to proceeding with the decontamination of walls or floor of a building from tritium it is necessary to obtain as much information as possible on the initial degree of spatial contamination. To accomplish this, a **profiling procedure** was developed by Charters et al. [Cha05], which basically consists in drilling and sampling from concrete walls employing a specially designed drill. The drill, made of tungsten carbide, is used under hammer action to permit expedient sampling even from hard concrete. As the drill progresses through possibly contaminated concrete up to a precisely pre-determined depth it delivers powder, which is collected on an inline filter for radio analysis. Analysis for tritium is carried out by weighing a certain amount of dust, adding water, LSC cocktail, and subsequently determining the content by conventional liquid scintillation counting. The analytical results of samples taken at gradually increasing depths provide the profiling data. If activities measured in selected positions of a building are transferred to a building drawing a good characterization of the initial three-dimensional contamination of the whole building can be obtained. This knowledge can contribute significantly to the development of an efficient decontamination strategy. Excessive contaminations may eventually lead to temporary closure or even dismantling of a facility. In case of dismantling, an important benefit of profiling is rapid and effective segregation of the resulting waste after completion of the operation. As opposed to coring performed with a hollow drill, which is slow and requires further sub-sampling by cutting disks from the primary cylinders, drilling is rapid and delivers a fine powder that can be directly subjected to radio analysis.

Ablation of walls and floor surfaces with **carbon dioxide pellets** was shown to be an effective procedure for the decontamination of walls, floors and building structures [Gen05].

8.4.9 Sentencing of waste

Sentencing of radioactive waste is defined within the **clearance process** as the step in which the decision is made whether components, substances or other items which need to be given to waste are

- **Clean**: never contaminated or activated,
- **Excluded**: unlikely to be subjected to control as radioactive,
- **Exempted**: activity below exemption limits or
- **Radioactive**.

Clearance and radiological sentencing of wastes deals with principles, processes and practices that should be taken into account by management to identify, quantify and sort radioactive waste [Nuc05]. The evaluation of whether a waste may be released or not from any further control on the basis of its radioactive content is an important and sometimes difficult endeavour. In this context, approaches to segregate at an early stage radioactive substances from non-radioactive substances need to be further developed.

For the assessment of man-made radioactivity, the International Atomic Energy Agency IAEA) takes the natural background radioactivity as reference [ITE01d]. Within this frame, IAEA recommends a "clearance" process from regulatory control for releasing solid materials of very low-level radioactivity. Concerning this reference, individual doses of the order of $10\,\mu Sv\,year^{-1}$ are considered insignificant or trivial to the public. "Unconditional clearance levels" are derived from scenarios which describe the potential use of man-made solid radioactive after removal from nuclear facilities. To provide a practical definition basis, dimensionless clearance levels for single isotopes have been specified. According to this procedure a material having an index below unity can be cleared. For a material containing several isotopes the clearance indices of the radioisotopes present in a potential waste are summed up. Materials for which the total clearance index is above unity after 100 years following final shut down of ITER are designated as waste.

Information on exemption values, clearance levels, radiological free release limit values, highest allowed activity concentrations, dosis coefficients, recommendations on the transport of dangerous goods, etc. for tritium are provided in the "Verordnung für die Umsetzung von EURATOM-Richtlinien zum Strahlenschutz" [Bun01b] and in Appendix W.

Solids contaminated with tritium that could potentially contain other activated nuclides should be treated separately. Clearance and sentencing of objects and substances of this kind require determination of the content of tritium and of the other radioactive substances as accurately as possible. In order to identify all isotopes, present in objects and substances they should be subjected to radiological sampling and monitoring covering α-, β- and γ-spectroscopy. Individual sample analysis of tritium is expensive and not directly possible in the deeper bulk (low energy X-ray emitter)[17] without invasive sampling. Alternatively, the inventory of tritium can be obtained indirectly via quantitative analysis of generated decay ^{3}He (see below). Unidentified chemicals must be determined qualitatively and quantitatively before disposal.

The measurement of the specific activity of tritium in **liquid wastes** is comparatively straight forward provided the liquid is not highly viscous, dark coloured, insoluble or very corrosive. The usual procedure consists in sampling aliquots, diluting if necessary and analysing the tritium content by conventional liquid scintillation counting.

The determination of the total amount and spatial distribution of tritium in metallic or other **solid wastes**, on the other hand, may be much more time consuming. While invasive techniques are normally sufficiently sensitive they may deliver wrong results if the waste is not truly homogeneous (in mixed waste this is almost certainly the case). The easiest and most accurate method for the determination of tritium is calorimetry provided certain requisites are fulfilled such as i) sufficient radioactivity, ii) tritium decay is the only heat source and iii) the object or equivalent fragments of the object under scrutiny can be accommodated inside of the sample holder of the calorimeter. If this approach is not viable, coring at an appropriate number of strategic positions and analysis by acid dissolution together with liquid scintillation counting is a frequently employed technique to obtain tritium concentrations on the surface as well as in the bulk. Helpful complementary information is the complete history of provenance of the component under investigation together with all previously performed tritium activities that pertain the component. The latter include a location record, type of tritium species the component was

[17] A promising analytical option is BIXS (see section 3.17.10).

exposed to, exposure periods, and all other parameters which may have influenced the degree of contamination like temperature, tritium partial pressure, condition of the surface, etc. Objects belonging to process equipment previously in direct contact with tritiated molecular hydrogen or tritiated water of high specific activity for extended periods of time will probably belong to the category of intermediate or even high-level waste.

Because of the high mobility of tritium, this gas can diffuse across the surface of solids to depths that will depend on type of material, temperature, and duration of exposure. While the establishing concentrations of tritium are typically very high on the top surface and subsurface, they tend to decrease rapidly with progressing depths into the material. As a result, the contamination of the surface may be several orders of magnitude higher than that in the deep bulk. However, in case of materials or components previously exposed to tritium at elevated temperatures, especially for prolonged time, the contamination of the bulk may be dominating and eventually become homogeneous and hence approach solubility. Because of chronic release, however, in homogeneously loaded material the concentration of tritium near the surface will decrease progressively. Under these conditions, the highest concentration will be observed in the centre of the material. Furthermore, it should be kept in mind that a non-homogeneous distribution of tritium on the material surface may be the result of localized heating, corrosion limited to a small area, mechanical damage, or condition and composition of the surface.

Materials exposed to gaseous tritium at elevated temperatures will typically exhibit a special tritium depth profile in which the concentration instead of decreasing from the surface towards the bulk centre will first increase, reach a peak value and then fall towards the material middle (see for example typical tritium depth profiles in stainless-steel type SS316 displayed in Figs. 2.42 and 2.43). These profiles are attributed to tritium diffusing back into ambient across the surface during the cooling phase immediately after completion of loading (the release is enhanced by the relatively high concentration of tritium establishing in the subsurface zone and the decrease of gas pressure after comletion of loading while the material is still hot). In the long run, a slow but steady chronic release of tritium at ambient temperature will also manifests with a contribution). In addition, materials in contact with tritium will display a very thin surface layer of rather high concentration of tritium whose contribution to the total inventory will depend on the type of metal, e.g. low for stainless-steel and high for copper. As opposed to tritium in the bulk,

that trapped in the surface ceramic layer is retained rather firmly presumably as some kind of oxi-hydroxi species.

Materials like metals or concrete, when covered with a layer of paint may show concentrations of tritium in the paint diverging significantly from those in the underlying bulk. Therefore, an accurate determination of the tritium depth profile is only possible with a method of sufficient depth resolution.

Averaging is an integral part of the clearance process. Because materials released from control areas are frequently contaminated non-homogeneously, in the event of waste fragmentation segments of quite different specific activity can be generated. Hence, averaging over a sufficiently large number of specimens encompassing if possible all volume zones of the waste material is essential.

Degree and distribution of tritium contamination on the surface of flat solids can be determined with the following analytical techniques: i) imaging plate [Tan01a; Tan02; Sug03; Sug04; Ots11], ii) PIN diode [Wam94], iii) autoradiography [Tak75; Iso08] or iv) BIXS [Mat02a]]. Because tritium depth resolution of most of these techniques does not meet the requirements, their applicability for an accurate evaluation of bulk contamination is limited. In an effort to provide remedy, a new procedure to determine depth profiles employing the **imaging plate** technique was developed. For this purpose, axially bisected rods of metals previously exposed to tritium plasmas were subjected to analysis [Ots11]. Depth profiles were obtained by pressing the central flat polished surfaces of the rods onto the plates. Optimal determinations with this technique require samples of rather flat surface and prolonged measurements performed in a dark room. After exposure of the bisected rod to the plate an imaging plate reader is used for visualization and quantification of the profile.

BIXS was shown to deliver reliable quantitative surface distributions of tritium with solids of simple or singular elemental composition like boron [Nak04], carbon [Tor05a], tungsten [Mat02a] or zirconium/nickel [Mat98].

Employing a suitable programe, the contamination by tritium at depths beyond the surface and subsurface was shown to be possible when characteristic **X-rays and bremsstrahlung** induced by the interaction of tritium with metals present in the bulk are detected and evaluated [Mat02b; Mat03; Wat05; Mat16].

Reliable and reproducible depth profiles of tritium can also be obtained with an intrusive chemical **etching** technique [Pen06; Coa06]. The technique is mainly applicable to small components or to samples cut from large components like carbon fibre composite (CFC) tiles. Core cylinders are obtained with a hollow drill. The cylinders are subsequently cut into equally sized disks and each analyzed for its tritium content. With the obtained information it is possible to generate depth and surface tritium profiles. The distribution of tritium on the surface of a plasma-exposed fusion reactor tile is delivered by the tritium content of the disks cut from the plasma-facing side of the core cylinders. The number of drilled core cylinders determines the quality of the statistics. The tritium content in each disk can be accurately determined following the procedure developed by Vance [Van79] (see also section 3.17.17). Alternatively, tritium retained in disks can be completely liberated as tritiated water, tritiated molecular hydrogen, and tritiated hydrocarbons by sweeping with an inert gas while heating at elevated temperature for a prolonged period of time. Liberated molecular tritium and hydrocarbons are oxidized into water at 800 K utilizing a CuO bed and transported with a gaseous carrier up to water bubblers. To avoid HTO condensation all lines must be trace heated. Aliquots taken from the bubblers, eventually further diluted, are analysed for tritium by liquid scintillation counting (see also section 3.17.3).

The degree of loose surface contamination by tritium i) physisorbed on the surface as water, ii) absorbed in metal oxide layers in form of $-$OT groups or iii) absorbed on particles merely adhered to the metal surface, can be obtained approximately from **wet** or **dry smearing** (wiping, swabbing) [Rod95b]. Typical smear values observed on low-level waste are of the order of several $10\,\mathrm{kBq\,m^{-2}}$. The importance of the smear method is a soft correlation between the removable activity and the immediate radiological hazard. It must, however, be stressed that the removable surface contamination seldom correlates directly with the amount of tritium absorbed in the bulk of materials. Therefore, it cannot be emphasized sufficiently that for an assessment of the overall contamination of a waste by the smear method the obtained values are close to meaningless. Moreover, after removal of loose surface contamination, sufficient time should be allowed between renewed wipes. This is necessary to avoid an underestimation of the surface contamination because of likely tritium re-growth on the surface.

A simple and inexpensive **outgassing** technique that permits assessment of the tritium inventory adsorbed on incinerable waste such as cellulose materials (brown paper, wipes, cardboard,

etc.), boots, rubber and plastic or cloth gloves, was developed by Antoniazzi and Shmayda [Ant95]. They performed measurements with waste generated at diverse Canadian installations such as i) Tritium Removal Facility at Darlington Nuclear Generating Station, ii) Ontario Hydro Technologies, and iii) Shield Source Inc., a manufacturer of tritium-gas-filled lights. To determine tritium, ambient air from outside of the facility was passed at a flow rate of about $4\,\mathrm{l\,min^{-1}}$ through a bag containing the waste (volume of 120 l). The volume exchange rate was maintained at about 30 minutes and the relative humidity of the air was controlled to 33 % employing a solution of magnesium chloride ($MgCl_2$). The activity in the effluent gas was collected in bubblers containing formic acid diluted in water. Aliquots from the water in the bubbler were analysed periodically using the liquid scintillation counting technique. At least over a period of three hours the outgassed accumulated activity was found to increase almost linearly with time. For a reliable measurement a sampling time of ≥ 7 hours was found to be adequate. The results obtained with waste generated in all three installations provided evidence for a correlation between the activity of outgassed tritium, A, and the outgassing time t (see Fig. 8.11).

The results from the measurements could be fitted by the following empirical relationship

$$A(\mu\mathrm{Ci}) = 4.9 \times 10^{-14} V_0 C_0 \left[1 - \exp\left(-\frac{St}{V_0}\right) + Q_w^T t\right]$$

in which A represents the activity collected in the bubbler in $\mathrm{m^{-3}}$,V_0 the volume of the empty waste containment in $\mathrm{m^3}$, C_0 the initial concentration of tritium in the containment in $\mathrm{m^{-3}}$, S the volumetric flow rate in $\mathrm{m^3\,hour^{-1}}$, Q_w^T the pseudo steady state outgassing rate in $\mu\mathrm{Ci\,hour^{-1}}$ and t the time in hour. One general conclusion from the work was that tritium outgassing rates within the range 3.7 - $3.7 \times 10^5\,\mathrm{Bq\,kg^{-1}\,hour^{-1}}$ result from tritium concentrations in the waste covering the range 3.7×10^3 - $3.7 \times 10^8\,\mathrm{Bq\,kg^{-1}}$. Another conclusion was that of all investigated waste products paper displayed the highest specific activities of tritium.

Calorimetry is a powerful non-invasive technique successfully employed for sentencing of low-level tritium-contaminated waste stowed in large waste drums of 200 or 380 l capacity for final disposal [Kap95; Dev96]. From test measurements the lower detection limit was established to be about 100 MW. The chemical form of tritium in the waste is irrelevant because solely the decay heat of tritium is converted into tritium inventory. A drawback of calorimetry is the lack of specificity which arises from the fact that calorimetry cannot distinguish between i) different

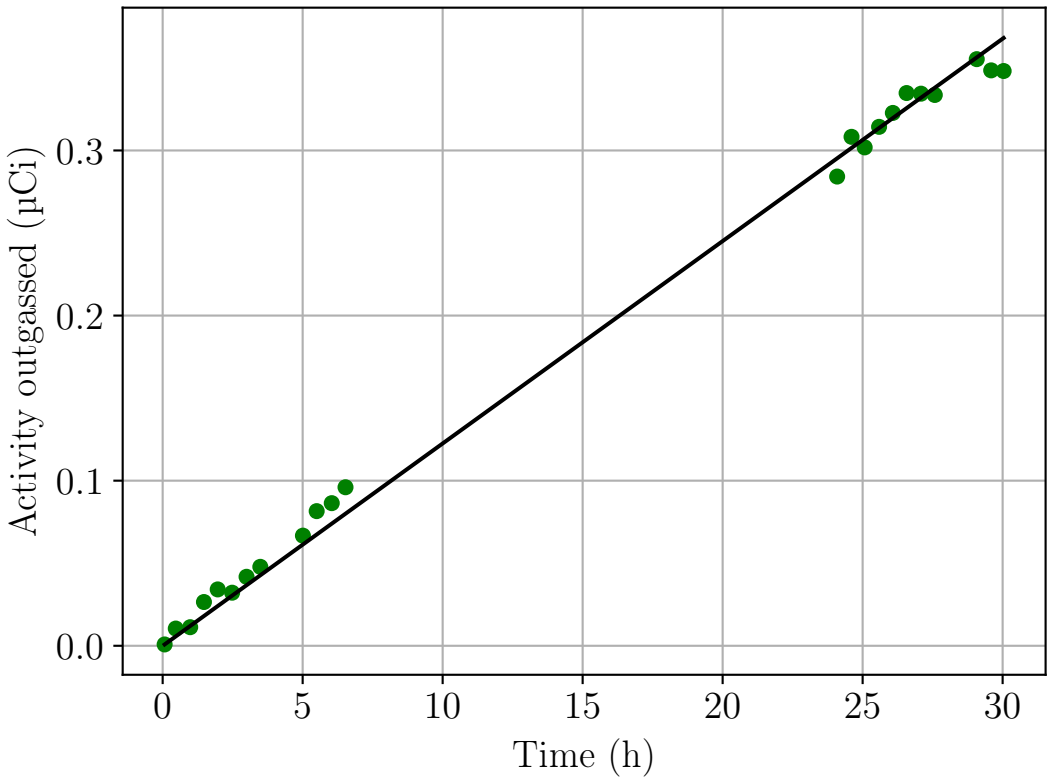


Figure 8.11: Tritium outgassing from a waste bag into a bubbler as function of time. The slope of the straight line was determined to be 11.7 nCi hour^{-1} [after [Ant95]].

decaying nuclides, ii) insidious chemical reactions or iii) phase transformations accompanied by release or absorption of energy. While from the point of view of safety, an overestimation of the tritium inventory is of little concern, it may be of negative economic impact to the institution generating the waste because of increased disposal cost. The presence of other not accounted for radioisotope (s) in the waste, on the other hand, may be associated with significant trouble with authorities.

Another proficient procedure for the determination of the total tritium inventory in drums containing low level solid organic waste, which relies on a determination of decay helium, was developed at Valduc, France [Cla76; Pia02; Rav02; Dem05; God08] The technique is only applicable to waste that **releases decay helium readily** and not to waste like metallic getters or contaminated structural materials, from which helium release is considerably delayed. Decay helium was selected as monitoring species instead of gaseous tritium because the latter is partly

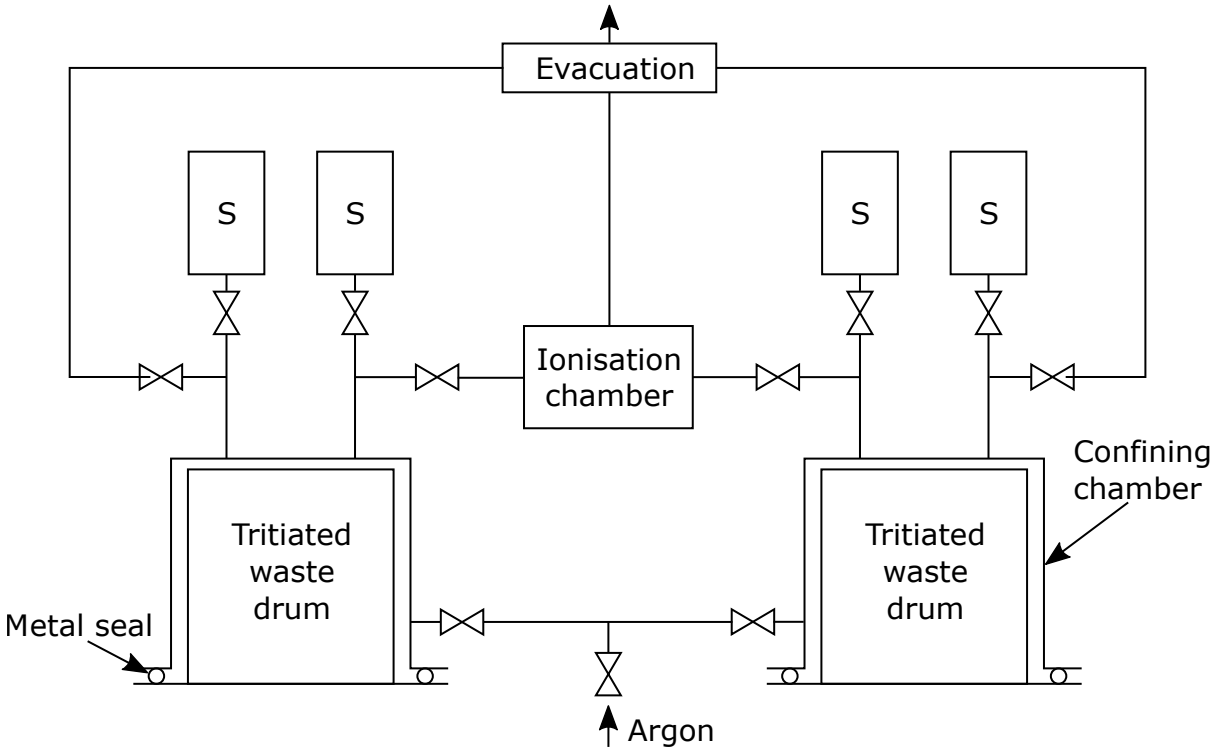


Figure 8.12: Schematic diagram of the arrangement employed for the indirect determination of the tritium inventory in two drums containing low level waste via the permeation method. Lid and polymeric O-ring of the waste drum are not displayed. Sampling cylinders are denoted by S (after [Dem05]).

adsorbed as water on many kinds of waste or firmly bound to organic material. Decay helium, on the other hand, reaches the gas phase rapidly regardless of whether generated from organically bound tritium or from adsorbed HTO. For a dependable determination, a minimum tritium inventory of 5 GBq inside of the drum containing the waste is required.

Both, direct grab sampling from a waste drum or sampling from a hermetically tight confinement into which the drum is placed have been examined experimentally and theoretically [Rav02; Dem05].

Grab sampling can be carried out with a stainless-steel cylinder of two litres volume directly connected to a 200 l drum. For this purpose, the lid of the drum requires some adaptation to warrant vacuum-tight attachment of the sampling cylinder. Reference drums containing tritium activities covering the range 0.74 - 18.5 GBq and enclosing various non-contaminated materials under argon cover gas and an accurately determined amout of tritiated water delivered normalized leak rates which allow comparison between experimental results and theoretical

calculations. Leak rates of decay ^{3}He from the waste are obtained from argon aliquots taken at regular intervals from the drum. The detection limit for tritium in a 200 l drum using the indirect procedure was estimated to be about 1.1×10^{12} Bq. More details on the analytical procedure are provided in ref. [Dem02].

The measurement arrangement employed at CEA, Valduc, France, for the determination of the **permeation of ^{3}He** from a drum into a confinement chamber is illustrated schematically in Fig. 8.12. Ideally, the ^{3}He release curves obtained as function of time from the waste evolving asymptotically up to equilibrium inside of the drum and from the leak rate into the confinement have the same shape. A comparison between direct sampling measurements and measurements of gaseous aliquots taken from the confinement chamber revealed that the former is consistently somewhat higher. This was attributed to the slow attainment of equilibrium between drum and confinement chamber [Dem05].

From a practical point of view, for a determination of the tritium inventory in low level organic radioactive waste by the **confinement method** a drum containing waste is closed by a lid employing a polymeric O-ring and stored for a period of 5 or more months. Thereafter, the drum is introduced into a confinement that is only a little larger than the drum and the confinement closed hermetically by a metallic O-ring. Air in the space between the drum and the confinement is fully displaced by purging with highly pure argon. Subsequently, the confinement is sealed vacuum-tight. Replacing air is necessary to exclude ^{4}He, an air component that limits the sensitivity of the measurement. Two gaseous aliquots consisting of argon, helium, hydrogen isotopes, and traces of air components are then taken from the confinement chamber: the first one at the beginning of the confinement and the second one after the drum has remained in the confinement - now containing pure argon - for a period of at least 5 hours. These samples are analysed by mass spectrometry using a modified low-cost mass spectrometric helium leak detector [Dem02]. Prior to each mass spectrometric analysis of the ^{3}He/^{4}He ratio, it is necessary to remove hydrogen isotopologues to avoid possible interferences by ions such as T^+ or HD^+ (both $m/e = 3$). This is accomplished by adsorbing argon and hydrogen isotopologues on 33 g of granular charcoal submerged in liquid nitrogen. Forgoing the mass spectrometric analysis, argon or a calibration gas containing purified helium is introduced into the sampling cylinder up to a pressure of 7 mbar. Sample and reference gases are injected into the helium leak detector via a conventional dosing valve. From a comparison of the initial ^{3}He/^{4}He ratio at time zero with the

ratio after elapsing of several hours it is possible to calculate the tritium activity A (in GBq) in the drum. It is given by expression

$$A = 10^{-3} \cdot V_{\mathrm{L}} \cdot \frac{P}{RT} \cdot \frac{N_{\mathrm{A}}}{t} \left[\frac{1}{\alpha_3} \left([^3\mathrm{He}]_f - [^3\mathrm{He}]_i \right) \right] = L \left[\frac{1}{\alpha_3} \left([^3\mathrm{He}]_f - [^3\mathrm{He}]_i \right) \right]$$

where V_{L} the volume between drum and confinement in l, P the atmospheric pressure in Pa, R the gas constant $8.314\,\mathrm{J\,mol^{-1}\,K^{-1}}$, N_{A} the Avogadro number, t the period of confinement, α_3 a helium enrichment factor, ^{3}He the concentration of helium in ppb at time zero (i) and at the end of the confinement (f). The term L is the normalized helium leak rate of the drum.

For the quantification of ^{3}He and ^{4}He at sub ppb concentrations three certified gas mixtures consisting of a nitrogen/oxygen matrix containing light elements at trace concentrations, i.e. (100 ± 1) ppm ^{4}He, (10 ± 1) ppb ^{3}He, or (104 ± 1) ppm H_2, are employed (it should be noted that the sensitivities of the $m/e = 2, 3$, and 4 peaks are appreciably different). With gaseous samples purified by cryogenic adsorption it was possible to determine tritium inventories in a drum containing organic waste as small as 5 GBq [Pia02].

Ravat et al. [Rav02] developed a model that simulates the permeation of decay ^{3}He from a waste drum into a leak-tight confinement chamber as function of time. The interspace between confinement and drum is kept small, e.g. 70 l, in order to minimize dilution of permeated ^{3}He. The measurement is based on the experimentally confirmed observation that decay ^{3}He generated in the drum readily permeates into the confinement across the polymeric O-ring between the lid and the drum. The results showed that while initially the concentration of ^{3}He in the drum increases linearly with time, with progressing decay the raise in concentration slows down because of the increasing permeation rate into the confinement until after about half a year an equilibrium establishes. At this point, the rate of production by tritium decay equalizes the losses in the drum by permeation into the confinement. Hence, the ^{3}He leak rate measurement becomes equivalent to a measurement of the tritium activity. Comparison between results obtained by the ^{3}He permeation method with data from other diverse destructive analytical techniques revealed that they were all within the range of standard deviations. This was considered to constitute a validation of the ^{3}He permeation method.

Currently, a fully **automated facility** relying on the indirect non-intrusive approach has been erected at Valduc for the examination of up to eight drums per day. On the average about

1500 drums are examined per year at Valduc. To further validate the helium technique more comparisons with results from conventional destructive methods appear necessary [God08]. The technique has the potential for application to other forms of tritium-contaminated waste.

Sentenced radioactive materials, components or structural items removed from the tokamak vessel, which are not usable as spares, may be cut into smaller pieces that fit into standard drums (typical drum capacity is max. 220 l). Disposal of solid waste can be carried out either by land burial [Tes05] or - if burnable - by incineration.

Segregation and sentencing systems for low level waste are offered commercially, e.g. G3400-220 from Antech. They can handle standard 340 l drums.

8.4.10 Packaging of waste

In this section methods commonly used for packaging of liquid and solid tritiated waste either for the purpose of transport, intermediate term storage or long-term storage are discussed and evaluated[Int91].

8.4.10.1 Packaging of liquid tritium-contaminated waste

Tritiated liquids of low activity level, e.g. $< 400\,\mathrm{GBq\,kg^{-1}}$], can be stored in tight containers, eventually further protected by an additional confinement depending on the actual activity and the anticipated plans for transport and storage.

Immobilisation of liquids can be achieved by **sorption** on **adsorbers** desiccants like molecular sieves, diatomaceous earth or Vermiculite. It should be noted that liquids are frequently not adsorbed homogeneously. Because under certain conditions they may desorb and condense on the walls of the enclosing containment, a tight and corrosion-resistant containment is compulsory. Within the frame of the development of disposal techniques for tritiated water employed in reprocessing plants of fission reactors an excellent review of all technical aspects related to the immobilization of water was published by McKay [McK79]. Advantages of immobilization are: i) sequestered water (or other liquids) will not spill directly into the environment in case of a sudden integrity loss of the containment and ii) experimental findings indicate that the rate of formation of radiolysis gases is inhibited by the solid matrix [Tad80; Nak86; Wal02]. It is important to keep in mind that i) pressurization will take place irrespective of whether water is stored as liquid or in immobilized form, and ii) spilled immobilized tritium is susceptible to slow

but eventually complete tritium liberation via isotopic exchange, vaporization, or leaching into environmental water. Furthermore, progressive build up of helium and of radiolysis gases inside of a solid matrix may cause weakening of the solid and consequently accelerated liberation of sorbed gases.

Another option for storage or transport of tritiated water, a major liquid waste of fusion facilities, consists in the sequestration as chemical constituent of **inorganic hydrates** or **cement** [Col75; Bib77; Wie79; Haw82; Haw84; Koe84]. Portland cement can theoretically bind up to 28 % by weight of water. A fraction of this water is evaporable and another is not. A solid block of cement has a characteristic vapour pressure which tends to decrease with time. When utilizing Portland cement, a water/cement ratio in the range 0.3 - 0.8 was found to produce the most stable solid blocks. At smaller ratios the cement is friable and at higher ones it will tend to generate a liquid phase on top of the solid.

With the aim of improving the properties of the solidified material the effect of i) additives, ii) polymer impregnation, iii) coatings, as well as iv) replacement by special cements were investigated and compared with respect to leachability, thermal stability, radiation resistance, mechanical strength and resistance towards chemicals [Col75]. Because concrete is an open structure with interconnected porosity, which develops during the curing process, the monolith becomes permeable to water and therefore susceptible to tritium loss by isotopic exchange or leaching. To cope with this problem, techniques were developed to impregnate porosity, voids and capillaries throughout the entire monolith by styrene monomer. Polymerization of the monomer was arranged to take place *in situ* [Col76]. To generate the solid matrix the first step consists in introducing dry cement into the casting container and compacting it by vibration. Waste water is dispersed into the cement powder through an injector until the water reaches the external surfaces of the cement (manifests by dampness). The injector is simply a tube with orifices along its length inserted into the cement. After withdrawing the injector, the cement is allowed to cure. Once the casting has cured, catalysed styrene monomer is introduced into the casting container and allowed to soak throughout the composite. Polymerization is induced thermally. The polymer was shown to encapsulate waste water rather effectively.

For the permament disposal of tritiated water incorporated into cement it was suggested to introduce additionally water-adsorbing solids like silica gel, clays or molecular sieves into the mix [Ben87].

In a study carried out at Mound [Mer77] burial packages consisting of tritiated water solidified in cement were surrounded by an inner polyethylene liner placed inside of a large steel drum. The drum was located inside of a still larger steel drum with Vermiculite and asphalt between them. This package effectively isolated tritium from the environment. One conclusion from the work was that safe storage was not only warranted by cement but rather by the package as a whole. In consequence, long-term storage of tritiated water immobilized in cement is only safe when utilizing a highly tight, corrosion resistant outer containment.

A reduction in volume of tritiated liquid waste via isotopic enrichment performed prior to immobilisation is desirable for economic reasons. However, the trade-offs are i) release of tritium and other gases by radiolysis, ii) pressurization from the production of decay helium-3 and iii) eventually manifestation of self-heating. These aspects need to evaluated before proceeding with waste conditioning.

As a rule, radiolysis must only be contemplated when the degree of enrichment surpasses 0.01 %. The production of ^{3}He amounts to 7.5 l STP for every g of tritium present in the vessel. Self-heating may only require preventive measures at enrichments exceeding 10 % e. g. cooling by natural convection or forced air. However, enrichments of this order are already avoided on radiolytic and corrosion grounds.

Storage of **highly tritiated liquid water** adsorbed on molecular sieve or silica gel requires special precautions. Significant progressive pressure build-up induced by the liberation of helium generated from bound decaying tritium and by gases resulting from self-radiolysis of highly tritium-enriched water when stored in a closed vessel constitutes a substantial safety issue (consult also section 2.10.3 and 2.10.4). For example, liquid water of only 1 % tritium enrichment will generate beyond radiolysis gases about 25 l STP of helium per litre of stored tritiated water. Direct venting of this helium is not possible because it will be strongly contaminated by tritiated water vapour and highly tritiated molecular hydrogen. From this it follows, that vessels containing water or other liquids of high specific tritium activity require i) a pressure measurement device to keep track of the evolution of decay and radiolysis gases, ii) a pressure relief valve that allows safe release of gases into trace heated tubing feeding into a dedicated tritium retention system and iii) a mini *ad hoc* process loop designed for periodic conversion of molecular tritium into tritiated water (see also section 8.2.2).

In summary, for the storage of liquid tritiated water enrichment levels of up to about 0.01 % are considered acceptable for storage of tritium without special precautions. While higher degrees of enrichment are thought to be manageable from the perspective of pressure rise and self-heating, relevant experimental trial runs are recommended to be on the safe side. Even though several promising solid matrices have been identified in the past, the achieved improvements in loading have generally traded off with higher costs and insufficient fixation properties for tritium. Storage of highly tritiated water necessitates not only regular depressurization of the storage vessel but also recurrent re-conversion of radiolysis gases into tritiated water [Hay06].

For the storage in solid form of **tritium-contaminated oil or tritiated octane** a dependable matrix was shown to be Vermiculite [Bib77].

8.4.10.2 Packaging of solid tritium-contaminated waste

Solid wastes only weakly contaminated with tritium can be packaged in steel drums and stored in a well-ventilated storage building equipped with suitable tritium monitoring instrumentation. The number of drums, their respective tritium content and the size of the building will determine design and throughput of the ventilation system.

If possible, tritiated solid waste should be compacted in order to minimize the number of waste containments. In case of volume reduction by shredding, the application of a **coating layer** on the surface employing adequate paints or sprays can help to ameliorate conceivable dispersion of contaminated dust and retard the release of tritium from contaminated surfaces. The volume of certain type of combustible organic solid waste can be reduced considerably by incineration.

Solidified waste of low specific activity containing less than 10 MBq tritium/g can be packaged directly in 200 l drums with a thin walled polyethylene bag as additional barrier. When the concentration of tritium in the package is within the range 10 MBq g^{-1} - 1 TBq an additional containment consisting of a rigid liner of metal or plastic is necessary. At even higher specific concentrations of more than 1 TBq per package, an additional barrier such as a rigid high-density polyethylene liner is needed. When the concentration of tritium reaches several 10 TBq per package, asphalt barriers and multiple packing, i.e. a smaller drum inside of the 200 l drum, are indispensable to keep migration of tritium under control.

Large amounts of high activity liquid tritiated waste, e.g. 30 l containing up to 1000 TBq per package, have been solidified in cement inside of a 100 l high density polyethylene liner having a wall thickness of 1 mm, which in term was introduced inside of a 110 l steel drum coated with an asphalt-bearing paint on the inner wall. A barrier of non-hardening asphalt, which was shown to be a good barrier for the migration of tritium, was placed over the top of the 100 l drum before the lid was fixed on the 110 l drum. The 110 l drum was then over-packed with a 200 l steel drum having an asphalt barrier on top and bottom. Adsorbent material placed in the annular space may constitute an additional release-retarding barrier.

Outgassing from drums containing tritium-bearing waste constitutes a waste storage problem. To **mitigate** tritium **outgassing** consisting of HTO, HT and eventually some organic tritiated species, Liger et al. [Lig15] proposed the introduction into the drums of an oxidation-promoting mixture of solid reagents consisting of MnO_2, Ag_2O and Pt together with an adsorber such as molecular sieve 4A or 5A. Laboratory screening tests with a drum filled with tritiated waste were encouraging. The data revealed a drastic reduction of the tritium release rate at ambient temperature - at least during the first months. Hence, with the aim of reducing further the long-term chronic outgassing rate of tritiated species an additional research effort is needed in order to i) identify the outgassing species, ii) understand the mechanisms of concurrent oxidation reactions of tritium-bearing species at ambient temperature, and iii) the radiolysis mechanism of adsorbed HTO.

After TSTA completed tritium activities 2001, large amounts of highly contaminated solid waste required conditioning and disposal [Tes05]. The waste comprised i) an enormous number of different small and large process components containing various degrees of incorporated tritium, ii) diverse metals holding tritium as hydride or in dissolved form, iii) molecular sieves with different amounts of adsorbed partly highly tritiated water, etc. The total inventory of tritium on site at the time TSTA ceased operations was 140 g. Disposal packages designed for the respective amount of tritium had to be developed. The amount of tritium in each singular waste unit was determined by techniques such as i) hydrogen exchange, ii) calorimetry, iii) direct sampling, iv) volumetric measurements and v) controlled thermal regeneration.

Waste buried at the radioactive waste repository site of LANL necessitated design and fabrication of special containers in some cases provided with welded over packs. Long-term storage of these over packs was carried out in special burial shafts.

8.5 Central Decontamination and Storage Facility

Large tritium-handling installations require a fully equipped Central Decontamination Facility assisted by a competent Radiological Service that guarantees high safety standards. Besides routine waste conditioning, packaging, and storage, a Decontamination Facility should simultaneously aim at the rationalization and upgrading of decontamination procedures and development of new advanced waste disposal processes.

In most large tritium-handling facilities a suitably equipped storage facility is available for the safe interim storage of large and small reusable components. Besides routine air monitoring, careful inspection at pre-established intervals of all stored components is beneficial for early detection of slowly emerging insidious tritium sources. A record as detailed as possible on the history of usage of all major components, including type of tritium-bearing chemicals the component was exposed to, partial pressures of these species during the exposure, presence of other chemicals or impurities, duration of exposures, temperature prevailing during each exposure, etc., is highly supportive for decisions on the most suitable conditioning and storage strategy. This type of information is particularly important when dealing with components of large dimensions.

8.6 National/international transport of tritium and tritium-contaminated materials

In this section several transport modalities of tritium and tritium-contaminated materials are concisely discussed mostly by way of example.

8.6.1 International transport of tritium

In the USA, the so called **Hydride Transport Vessel (HTV)** was developed at the Westinghouse Savannah River Company (WSRC),for the international transport of tritium. This vessel was designed for the shipment of up to 18 g tritium employing uranium as carrier.

With the objective of further developing vessels for the international transport of tritium, a BU type package for the shipment of up to 25 g (see Fig. 8.13a)

indexTritium, storage of elemental!storage and/or transport hydride beds!zirconium/cobalt,

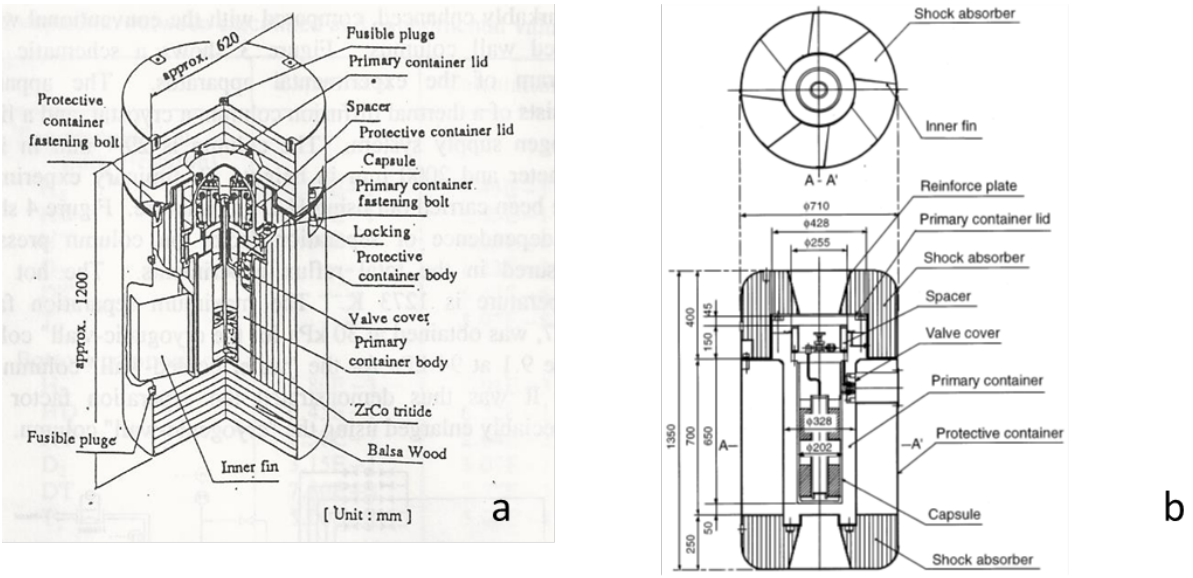


Figure 8.13: Left figure shows a detailed drawing of the TPL-92-Y-450K transport vessel of JAERI [Oku93] and the right figure the design of a transport vessel for future fusion reactors [Ohi99].

JAERI, Japan of tritium was designed at JAERI, JAPAN. The package was configured to meet the transport requirements described in Safety series N° 6 "Regulations for Safe Transport of Radioactive Materials" from IAEA[18]Safety series N° 6 "Regulations for Safe Transport of Radioactive Materials" from the IAEA , whicih are valid in Japan, USA, and Canada [Oku93; Oku95; Ohi99][. The vessel was loaded with 0.75 kg of zirconium cobalt for sequestration of the radioactive gas. The alloy was mixed with 1.2 kg of copper grains in order to improve the thermal conductivity of the bed. The total weight of the package was 450 kg and the maximum heat generation calculated to be 25 W. Assessments of the structural resistance of the package under simulation of different accidental conditions such as: i) dropping from a height of 9 m without contingencies, ii) surviving a one-meter puncture experiment, and iii) resisting a heating test carried out at 1073 K were performed and successfully completed as reported by Okuno et al. [Oku93] and O´Hira et al. [Ohi99]. The bed was employed for two international transports of up to 20 g tritium [Oku95]. Subsequently, O´Hira et al.[Ohi99] designed an even larger BU type transport package with a capacity for 250 g tritium (see Fig. 8.13b) likewise meeting the requirements stipulated by IAEA for transports of radioactive materials.

[18] Safety Series N° 6, Regulation for the Safe Transport of Radioactive Materials.

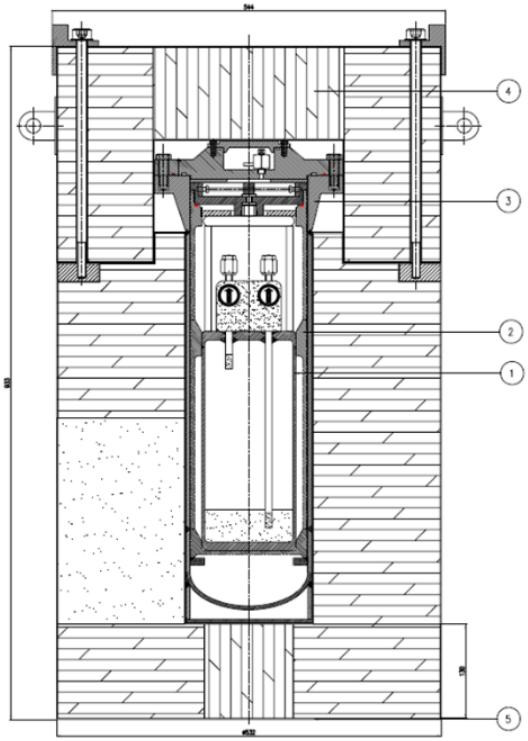


Figure 8.14: KAERI concept of BU type vessel for the international transport of tritium [Glu13].

According to IAEA Safety Standards Series No. TS-R-1 up to 335 g tritium can be transported by air, land or sea in BU type packages [Ohi99; Glu13; Lee13]. Within this frame, ITER contracted Korea Atomic Energy Research Institute (KAERI) to design a BU package for the international transport of up to 70 g tritium as uranium tritide (UT_3) (see Fig. 8.14). Among other specifications, it was requested that the container i) retain its full integrity for at least five years resisting without relief the pressure build up resulting from tritium decay into helium-3, ii) be encased in an aluminum container for ultimate contamination control and iii) be provided with an over pack for superior protection against thermal and mechanical shocks.

For additional information on the transport of small and medium inventories of tritium section 4.1.3.2 should be consulted.

8.6.2 National transport of tritium (USA)

Incoming shipments of gaseous tritium to TFTR were transported in LP-12 containers designed for medium quantities of tritium [Gru88]. LP-12 containers have a gas capacity of 12 l and are approved for air freight. The maximum allowed pressure at 298 K is 113 kPa

For transport, further processing or disposal of waste exhaust gas discharges a number of certified containers are available in the USA like the LP-12 or LP-50 containers together with its coresponding overpack. Shipment of solid waste consisting of molecular sieves containing tritiated water with up to 3.7 x 1015 [Bq] is carried out employing AL-M1-S containers. In case of solid waste additionally comprising asphalt type DOT 17H or 17C containers have been used.

8.6.3 Transport of tritium-contaminated material/waste (housekeeping waste, CFC tiles, carbon flakes, etc.)

Tritiated "housekeeping" waste such as room trash, over suits, disposable materials used to minimize personnel exposure and contamination spread, as well as slightly contaminated equipment is invariably sentenced as waste. The International Atomic Energy Agency "Regulations for the Safe Transport of Radioactive Material" established regulatory standards for international transport activities. Among five different types of packages three, i.e. type A, B and C, are qualified for the transport of radioactive substances. **Type A** packages are used for the transport of relatively small but significant quantities of radioactive material ($< 3.7 \times 10^{13}$ Bq)[US 15]. **Type B** packages are employed for the transport of highly radioactive materials ($> 3.7 \times 10^{13}$ Bq). Shippers use this type of package for materials that would represent a radiation hazard to the public or the environment if there were a major accident with concomitant release of radioactivity. Hence, this type of package must be capable of withstanding severe accident conditions without releasing radioactive materials. **Type C** packages are more robustly designed packages for the transport of highly radioactive materials by air, which must withstand a variety of transport incidents and accidents. According to the World Nuclear Transport Institute (WNTI), an international Organisation with headquarters in London dedicated to the safe, secure, efficient and reliable transport of radioactive materials, each of these three types of packages must satisfy a number of clearly defined specific tests.

Sporadically, international transports of tritium-contaminated components and wastes for instance retrieved from the vacuum vessel of a fusion machine become necessary for *post mortem* technical examination in an external or foreign laboratory. For example, after completion of the DTE1 campaign at JET, the following tritium-contaminated components and representative samples

- three outer carrier divertor tiles and six inner wall guard limiter tiles containing in total 4.33 TBq of tritium,
- seven divertor base tiles and seven poloidal graphite limiter tiles containing in total 22 TBq of tritium packed, and
- approx. 1 g of flakes and dust containing approx. 1.2×10^{12} Bq tritium

were removed from the vacuum vessel after completion of the DT1 campaign and and shipped to the Tritium Laboratory in Karlsruhe for chemical and physico-chemical *post mortem* characterization [Pen01c]. While the first and third shipment were each carried out in a single transport drum, two drums were required for the second one. Inside of the drums, the tritium-contaminated components and the highly tritium-contaminated waste were packed in hermetically tight stainless-steel vessels each provided with two valves for purging purposes (see Fig. 8.15b). Even though the transports occurred in different vessels, the safety precautions adopted by the shipper were analogous.

The dose rates on the surface of the transport vessels employed for **tiles** were of the order of $10\,\mu Sv\,hour^{-1}$; tritium was not detectable when the transport drums were opened. The release of tritium from either several single tiles packed in two concentric aluminized bags or group of several tiles packed by the same procedure reaching the inner highly tight stainless container by consecutive permeation through the bags was assessed by purging with nitrogen. Principal purpose of the sealed aluminized bags was to retard the permeation rate of tritium. The tritium concentration in the purge gas was determined employing a bubbler containing $250\,cm^3$ of water. Liquid scintillation counting of several water aliquots at progressing time revealed that about 40 kBq of tritium permeated across the aluminized bags into the free volume of the inner vessel. Each of the two bags protecting the tiles contained a small amount of silica gel adsorber in flax bags (no palladium catalyst). The outer aluminized bags in the three transport vessels

displayed surface contaminations in the range 2 - 38 Bq cm^{-2}. When outer bags placed in a 5.4 m^3 glove box were perforated, amounts of tritium between 0.1 and 1.4 MBq were released[19]. The contamination of the outer surface of inner aluminized bags spanned within the range 2 - 28 Bq cm^{-2}. When inner PVC bags were punctured, the amount of tritium released into the glove box was higher by a factor of up to four, i.e. between 0.4 - 4 MBq. It is estimated that during the time the nine tiles remained inside of the transport vessel, i.e. about seven months, the amount of loosely bound tritium which permeated into the stainless-steel vessel, the two bags, and was absorbed on silica gel was between 2 and 5 % from that initially sequestered in the tiles. Tritium depth profiles obtained from coring samples drilled at strategic zones of the tiles showed that up to 99 % of the tritium activity was concentrated in a thin 20 µm layer on the plasma exposed side of the tiles.

Summarizing, the safety measures adopted for the transport of tiles in a type A transport vessel, i.e. introduction of the tiles into two concentric sealed plastic bags each containing moisture adsorbers to capture oxidized tritium released from contaminated material were totally adequate for the intended purpose.

In the case of **flakes and dust**, the actual type A transport vessel also consisted of a heavy, hermetic, high vacuum-tight stainless-steel vessel (see Fig. 8.15b). This vessel contained the cyclone pot of the JET vacuum cleaner employed to collect flakes and other debris from the vacuum vessel of JET (see Fig. 8.15a). The collected material was kept inside of the cyclone as gathered at JET. Before introducing the pot into the transport vessel, the vessel was filled with bubble wrap packing to prevent damage of bags and cyclone. As for the tiles, two valves on the transport vessel served for purging the vessel prior to opening and hence to determine the tritium concentration in the cover gas. The cyclone pot was placed inside of a PVC bag, which in turn was protected by an aluminized bag containing silica gel in a flax bag. The atmosphere in the PVC bag was argon. This package was introduced into an additional aluminized bag which was subsquently sealed. The second bag contained pellets of a palladium catalyst/adsorber maintained in a perforated plastic bag for better contact with the gas phase. Both sealed aluminized bags served to retard the permeation rate of tritium, the catalyst converted tritiated hydrogen into tritiated water, and the adsorber kept the partial pressure of moisture at low levels.

[19] The concentration correlated with the number of tiles sealed and their specific degree of contamination.

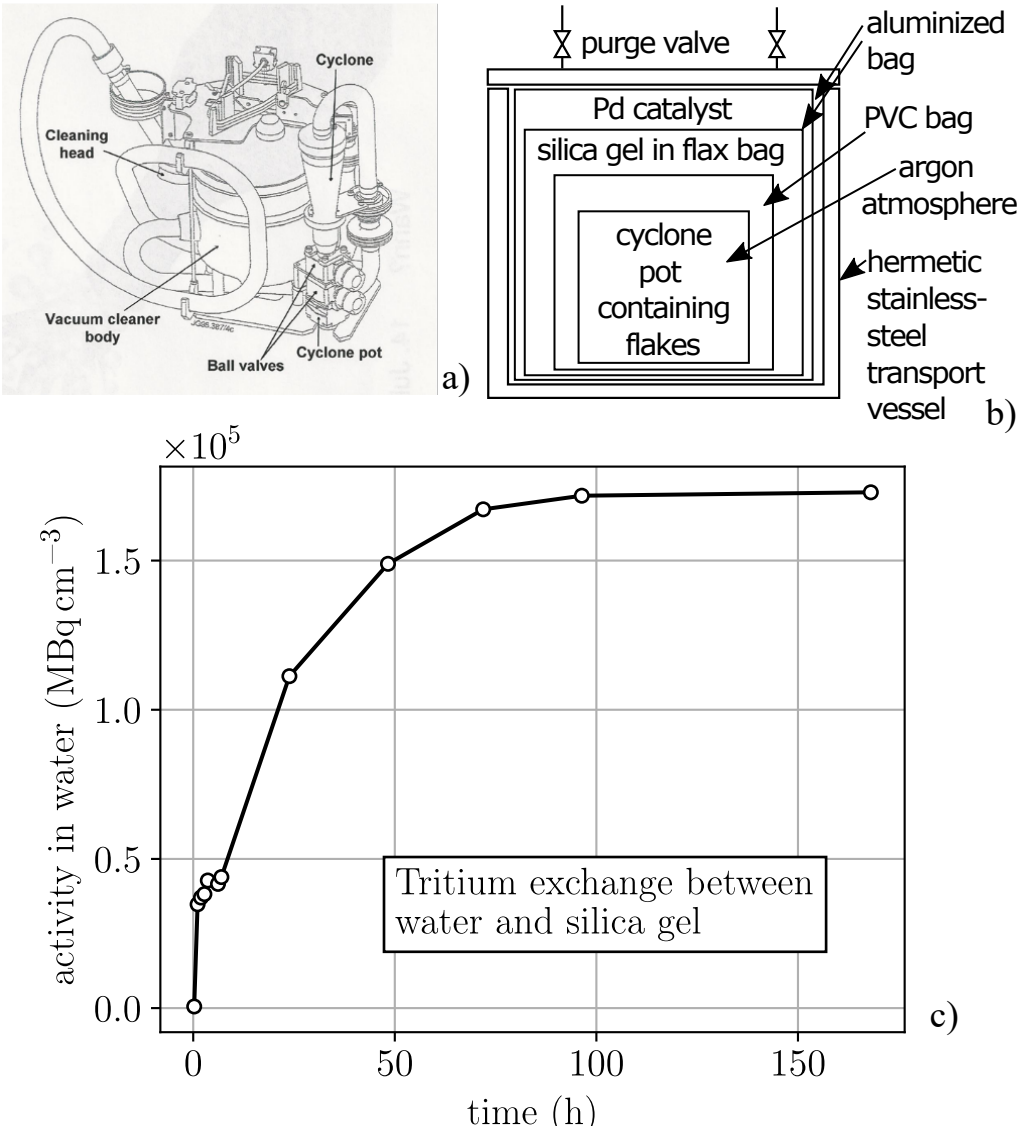


Figure 8.15: Drawing of the JET vacuum cleaner showing the cyclone pot equipped with two ball valves containing approximately 1 g flakes (a). Schematic drawing of the international transport vessel enclosing the cyclone pot packed in several bags, one containing a catalyst and another an adsorber[Pea99a; Pat99] (b). Typical results displaying the release rate of tritium from a silica gel sample containing adsorbed HTO dropped into water at ambient temperature (c)[Loh99].

When the cyclone pot was opened into a 5.4 m^3 glove box a tritium activity of approximately 0.2 TBq was liberated.

According to the results, only a minor fraction of the total tritium in the flakes, i.e. 2×10^{-4} %, permeated across the two aluminized bags containing respectively an adsorber and a catalyst/adsorber into the free volume of the stainless-steel transport vessel (see Fig. 8.15b). As evident

from figure 8.15c, some tritium was trapped in the silica gel. This amount was determined by dropping approx. 40 g of the adsorber into 1 l demineralized water. Under these conditions, slow isotopic exchange took place, full equilibration requiring about five days [Loh99].

Three flake samples obtained from JET after DTE1 weighting 0.0055, 0.0083, and 0.0051 were heated at TLK under air in a flow system at a constant temperature of 1073 K for up to 8 hours and found to contain 1.26,1.18, and 1.04 $\mathrm{TBq\,g^{-1}}$ tritium, respectively[20]. This leads to an average concentration of tritium of 1.17 $\mathrm{TBq\,g^{-1}}$. Subsequent experiments with more of these flakes (Appendix G), revealed that they released tritium chronically at a rate of approx. $2 \times 10^{10}\,\mathrm{Bq\,month^{-1}\,g^{-1}}$. Experimental evidence suggest that this tritium is primarily released as tritated water (see also section 8.4.7.2).

In accordance with expectations, the chronic release rate of tritium from tiles was much smaller than that from flakes. This is attributed to the much larger surface area of the latter.

8.7 Beryllium facility

During initial assembly of fusion machines like ITER, substantial amounts of massive beryllium must be incorporated into the first wall blanket modules. Moreover, a fair number of beryllium oxide windows must be fitted into heating systems and the lower hybrids. These activities are only possible if a dedicated special facility provides adequate protection to the work force [Boo91; Hai97; Bel98; Pam12; Raf17]. Once operation with tritium is under way and replacement or upgrading activities of the first wall become necessary, frequent handling of beryllium-contaminated components, containing tritium and other radioisotopes, can only be performed by remote handling with additional active support of a well-trained team. In view of this, the facility shall be equipped with sufficient glove boxes and analytical instrumentation to perform wet chemistry, atomic absorption spectroscopy measurements, tritium analysis, and a variety of techniques for the thermo-mechanical characterization of materials. Well-ventilated workbenches, air and particle monitoring equipment, as well as a decontamination shower are compulsory. Because of the toxicity of beryllium, a controlled drainage system will have to be installed.

All mechanical operations, decontamination activities, as well as routine and extraordinary chemical analyses, shall be carried out under the supervision and responsibility of a specially

[20] Flakes collected at TFTR contained $1.1 \times 10^{11}\,\mathrm{Bq\,g^{-1}}$ ($0.11\,\mathrm{TBq\,g^{-1}}$), i.e about 10 % of the concentration found in JET flakes.

trained staff. Medical supervision of the working staff shall be warranted. Injuries, diseases, and operational occurrences shall be reported to an independent control authority.

Many activities with beryllium will only be possible with **respiratory protective equipment** such as a full body suit supplied with pressurized air [Edw02]. In order to minimize contamination, in some situations respiratory protection equipment is worn together with a disposable overall and disposable overshoes which are removed prior to exiting the contaminated zone and disposed of as soft waste. In case of large numbers of suits and respiratory protection devices, a special service is needed for cleaning, inspection, and maintenance.

At JET, so-called **Controller Dresser Units** serving both as provisional controlled area and man access module to the torus, provide change facilities, decontamination, and monitoring for up to four operators. For emergency cases as well as when there is need to clean pressurized suites, an integral controlled air lock shower is also available.

For potentially risky activities **personal air sampling** equipment is obligatory. For this purpose workers are issued with a sampling pump capable of drawing a specified volume of air through a filter (filters of 6 µm pore size are ordinarily recommended). The pump should be maintained in the vicinity of the operator. Respiratory protection equipment is normally used only once. If not disposable, the respirator must be cleaned and sanitized before re-use.

Static air sampling devices are usually installed at specified locations within the workers environment. Health physicist will select the locations considering relevant process activities, contamination potential, and other particularities of the facility. An air volume flow of the order of $100\,\mathrm{l\,min^{-1}}$ is considered adequate for sampling.

A common procedure to assess **surface contaminations** is smearing the surface with dry filter paper and determining the amount of beryllium on the smear. For this purpose the filter paper is dissolved in a hot mixture of sulphuric acid and nitric acid. The solution is then analysed for total beryllium by atomic absorption spectroscopy. Regular comparisons with standard solutions of known beryllium concentration are important for good accuracy. For the **Beryllium Controlled Area of JET** a threshold surface contamination of $10\,\mathrm{\mu g\,m^{-2}}$ (10 % of the operational exposure limit of $100\,\mathrm{\mu g\,m^{-2}}$ was adopted [Boo91]). When this value is exceeded remedial cleaning becomes mandatory.

Large facilities handling beryllium must be equipped with a dedicated ventilation system encompassing high efficiency HEPA filters installed in the exhaust ducts. The ventilation system

must be capable of maintaining sufficient depression and achieving an adequate number of air changes per hour in the zone where work is being carried out. Environmental discharges must be assessed downstream of these filters.

A comprehensive **Code of Practice for the Safe Use of Beryllium**[Rus92; Pat03][21] applicable throughout the facility has been elaborated at JET, Culham. Among other topics, the code addresses subjects such as hazards and their control; beryllium monitoring; the medical surveillance of beryllium; training; procurement; authority to use beryllium; packaging, labelling and transport; establishment of Beryllium Controlled Areas; establishment of Respiratory Protection Zones; ventilation; cleaning; waste disposal; Health Physics Operations and Support; dealing with visitors and non-registered personnel; guidance notes for dealing with beryllium contaminated wounds for use by the medical staff and patrol service, etc.

Operations involving tritium contaminated components must be separated from other assembly work. Components containing beryllium must be delivered to site and stored in sealed containments. The outer cleanliness of the containers is responsibility of the supplier. Containers must be unpacked in a dedicated controlled area.

The limit concentration of airborne beryllium (dust) in an uncontrolled area is $0.01\,\mu g\,m^{-3}$. If beryllium is handled in a building, it is necessary to confirm by air sampling that concentrations of beryllium are below limit.

For ITER two concentration levels have been discussed:

a) $0.01 < \mathrm{Be} < 0.2\,\mu g\,m^{-3}$ for controlled areas with restricted personnel access but only basic contamination control precautions requiring air sampling and confirmation that the concentrations of beryllium are within the allowed range.

b) $\mathrm{Be} > 0.2\,\mu g\,m^{-3}$ for controlled areas with restricted personnel access, negative pressure and filtered exhaust. In this case, extensive air sampling to confirm that both inside and outside of the controlled area the concentrations are within the authorized range, are required.

At ITER a **Beryllium Management Committee** (IBCM) was constituted 2015 in charge of activities such as implementation and supervision of all applicable legislation and regulations, identification of all activities involving beryllium, coordination of all beryllium activities, identifi-

[21] Code of Practice for the Safe Use of Beryllium at the JET Laboratory, JET report SR(89)02.

cation of the best practices for safety standards, development and implementation of the training programs for handling beryllium, etc.

Facilities in Europe dedicated to fusion-relevant work with beryllium are available at JET, in Great Britain (facility area 160 m^2, the Studiecentrum voor Kernenergie in Belgium (facility area 40 m^2 and the Joint Research Center of the European Community in Ispra, Italy (facility area 26.2 m^2.

9 Building for tritium handling

Basic and technical research involving sizeable amounts of tritium can only be performed in specially designed buildings possessing the necessary infrastructure and meeting modern safety standards. Typical for this category of facilities are AGHS at JET in Abingdon [Kon92b; Lae99b]; CEA, Centre de Valduc in Valduc [Gir92]; TLK in Karlsruhe [Ach90; Sch91a; Vol95; Bes97; Pen00b]; TPL in Tokai-mura [Nar90; Yam02]; SRS in Aiken [Ort90; Poo05]; STAR in Idaho Falls [And02; And05] and several others. They all engage in research to a large extent related to the ITER fusion fuel cycle. Salient topics are i) tritium processing, ii) tritium transportation and storage; iii) hydrogen isotope purification and separation; iv) decontamination and waste; v) tritium measurement, monitoring and accountancy; vi) calorimetry, vii) material interactions; etc. Further large research facilities committed in the past to similar objectives were TSTA in Los Alamos [And88] and Princeton Plasma Physics Laboratory (PPPL) in Princeton [Hal95; Gen95; And94b]. The last two facilities have delivered quite important contributions to a broad spectrum of subjects related to tritium technology and safe handling of large inventories, but have since then been dismantled. Another large facility is the Tritium Laboratory CRL in Chalk River [Gal05], which i) offers specialized services to CANDU power stations, ii) performs tritium assay services, iii) dispenses tritium worldwide and iv) supplies certified tritium gas standards. This kind of laboratory has also provided ample knowledge on safe handling of large inventories of tritium but from a different perspective. Several medium sized facilities, like HRC in Toyama [Mat14], or Korea Atomic Research Institute (KAERI) in Korea [Chu12b], which carry out fundamental and applied research on tritium related topics, have likewise delivered noteworthy results partly within the frame of national and international collaborative efforts. The list would not be complete without mentioning tritium handling facilities dedicated to military related activities. These installations have a long tradition of safe tritium handling of large amounts of tritium [Mot92; Hir93; And95c].

In spite of rather diverse tasks and degree of technical sophistication a common feature to all these installations has been a multiple barrier safety concept consisting of progressively decreasing pressures from ambient towards the primary containments. The barriers comprise i) an ultra-high vacuum-tight all-metal primary containment, ii) a primary confinement featuring glove boxes serviced by tritium retention systems based either on catalytic oxidation followed by adsorptive removal of resulting tritiated water or scavenging from an inert gas atmosphere with a metal getter at moderate temperature and iii) a secondary confinement encompassing the building. Additional safety measures consist of double walled piping between primary containments installed in different primary confinements, vacuum jackets protecting cryogenic or heated primary components providing thermal insulation as well as a primary confinement.

Buildings are usually designed to serve as transitory confinement for tritium in case of an emergency. They are also designed to permit controlled access of visitors and personnel. While some installations are equipped with emergency air detritiation systems, this is not always the case. Buildings are generally furnished with a stack for better dispersion of emissions.

For safeguarding of nuclear materials and mobile tritium appropriate measures are implemented like controlled access, locked rooms, locked cabinets, etc.

9.1 Basic design requirements of tritium buildings

A building intended for handling of medium or large inventories of tritium should be designated as "controlled area". This means constrained access of investigators, workers, and visitors by painstaking administrative and appropriate physical control measures, e.g. access through an air lock. Withdrawal of materials or equipment from the controlled area should only be permitted after obtaining clearance from Radiation Protection. Precautionary measures are also necessary when introducing materials and equipment into the controlled area.

Facilities handling significant quantities of tritium shall be equipped with an **emergency tritium retention system** unless a safety analysis provides sufficient arguments to make such a system avertable. If an emergency system is installed, it should mitigate the consequences of a spill very markedly. In case of an accidental release of tritium into laboratory rooms, the safety systems should warrant that i) the negative pressure in all (or at least most) primary confinements remain by and large intact, ii) the contaminated air released into the ecosystem is detritiated down to acceptable levels, and iii) the tritium contamination of the affected rooms is reduced swiftly.

Further safety measures in buildings designed for tritium handling are: i) containment of the atmosphere in the tritium building employing protective flaps so that in case of an accident the room atmosphere can be cleaned from tritium before it is released into the environment, ii) strengthening of walls or sections of walls to reduce the likelihood that in case of earthquake or of any other major catastrophic event equipment is damaged causing liberation of tritium, iii) reducing the danger of the occurrence and propagation of fire with subsequent spread of contamination by regularly banning as much as possible easily combustible materials from the controlled area and by compartmentalizing the building iv) designing the building air-tight and preferably without windows to warrant undisturbed maintenance of underpressure, etc.

To reduce the amount of tritium released by a single equipment failure, the following provisions were shown to be effective: i) multiple capability for isolation of the source of tritium, ii) capability for complete isolation of areas with running tritium processes and/or with tritium handling systems from areas normally occupied by personnel not engaged in tritium work, and iii) availability of numerous strategically placed tritium monitors that allow very early detection of conditions requiring corrective or protective actions.

Facilities operating with considerable inventories of tritium employing large as well as complex equipment should be furnished with an **emergency electrical power system** to cope with a sudden loss of commercial power. Uninterruptible power supply is necessary i) to preserve health protection, radiation monitoring, and distributive control systems, ii) to orderly hold or shutdown tritium handling systems so that major equipment is not damaged and full operation can be resumed expeditiously upon restoration of commercial power, and iii) to provide important information during repair of the damaged system.

Further important functions of an emergency electrical power generation system are to keep i) the ventilation system, ii) the air detritiation system, and iii) the emergency illumination system running in relevant sections of the building.

Back-up uninterruptible power can be furnished either by an electric generator driven by a Diesel engine or by a multi battery power supply (or by both). In practice, in the event of a blackout the control system senses the utility power loss and starts the diesel engine and/or switches to the emergency battery power.

The floors of the tritium building should be strong enough to support the installed equipment. Eventually, strengthening of the floor with steel platforms may become necessary. Administrative measures should ensure that these requirements are met.

Surfaces inside of the tritium facility, e.g. walls, should be sealed with water-proof surface materials to minimize water adsorption.

Glove boxes serving as primary confinement necessitate either a dedicated or a central tritium removal system in order to safely handle tritium permeated or leaked from primary containment systems.

Containments and confinements of tritium processes should incorporate adequate engineering and manufacture measures to minimize the probability of a fire or an explosion. They should be equipped with reliable safety devices and mitigators.

Liquid nitrogen required for the operation of cryogenic systems installed in a tritium facility may be supplied from an adequately sized Dewar mounted outside of the building. The Dewar shall be easily accessible for refill and well protected from all kinds of natural and other damages. Eventually an emergency reserve Dewar may become necessary. Supply inside of the tritium handling building may take place either via a manifold or another smaller Dewar installed inside

of the building. The design should be such, that cryogenic liquid cannot be trapped between two closed valves without a release option through a relief device.

Tritium facilities should be designed to provide **cooling water** in closed loop circulation mode. Since cooling water may be critical for some systems, the necessity of redundancy needs to be contemplated. In addition, the system should be equipped with a tritium monitoring system for early detection of permeated or leaked tritium. Heat may be dissipated via a heat exchanger with a cooling loop that circulates water through a cooling tower. Cooling water used for tritium systems should not have direct contact to sewage water.

Sanitary wastes from the drainage of i) water closets, ii) lavatories, iii) showers, iv) potable water fountains, etc. shall be collected in a separate sewer system. Slightly contaminated waste water should periodically be sampled, analysed, and be subjected to disposal only after approval by authorized personnel.

The design of a tritium handling building shall contemplate monitoring for early tritium release detection and if necessary of other poisonous species, e.g. beryllium, in strategic areas like glove boxes, rooms, ducts, stack, and where radioactive materials are handled or stored.

Tritium facilities should have dedicated **ventilated rooms** for the interim storage of i) contaminated equipment, ii) contaminated wastes, iii) empty tritium shipping containments, iv) adsorber beds already decontaminated or interimly stored for re-activation, etc.

9.2 Building design guidelines

Buildings intended for the installation and execution of processes involving large quantities of tritium should provide sufficient protection against natural phenomena such as earthquake, flooding, heavy snow, and tornados. If an earthquake-proof laboratory is demanded, it will rely on walls of **reinforced concrete** [Nar90]. While there is no must for processes to remain operational after a natural phenomenon, there is a requirement of process integrity in order to keep releases of tritium at minimum levels.

A facility handling large inventories of tritium should be of **segregated layout** into functional areas. The first level of segregation should be separation of process areas from non-process areas. Further segregation criteria include i) the degree of contamination, ii) type of hazard, and iii) type of activity, such as for instance basic research, routinely operated infrastructure systems,

radiation protection activities, accountability (very low level of contamination), handling of nuclear materials, interim storage, or radiation protection and accountability (very low level contermination).

Building and equipment should be designed and operated with the constraint of minimizing potential doses to the workers on the basis of **ALARA** (As Low As Reasonably Achievable) principles. To maintain radiation exposure according to ALARA principles, all important physical design features should be based on a minimization of releasable tritium inventory. The application of the ALARA principle comprises i) correct design and operation philosophy decisions taken at an early stage, ii) utilization of already demonstrated technology whenever possible, iii) frequent, recurrent and systematic review of all critical systems, iv) early systematic evaluation and inclusion in the design of operational, repair, and replacement strategies, v) assessment of possible pathways of releases making sure that all conceivable release pathways are accounted for, and vi) continuing design improvements aimed at developing ways of additionally reducing releases and further decreasing the number of potential principal contributors.

The design of confinements and ventilation systems shall be such that i) respiratory protection is required only in areas where physical controls have been considered impossible or impractical, and ii) airborne contamination levels are maintained in accordance with ALARA principles in areas designed for worker occupancy. To control radiation exposure, appropriate administrative controls and procedures shall complement physical design features.

The **ventilation system** should be of single-pass type, and the range of ventilation rates should depend on the potential release of tritium into the breathing space of the facility, i.e. low rates at low potential releases and large ones at high potential releases. Temperature and humidity of ventilated zones should be maintained under controlled conditions in order to keep in-leakage of moisture into the glove boxes at low levels.

The ventilation ductwork of tritium handling installations should not be shared with exhaust gases released from non-tritium operations. Exhaust gases should be released into the environment through an elevated stack and at high velocity in order to ensure good and rapid mixing with the outside atmosphere.

Succinctly, the infrastructure systems of buildings housing tritium handling equipment shall at least comprise adequate ventilation, an appropriate tritium monitoring system to preclude inadvertent exposure of workers to tritium, regular service support from an independent Radiation

Protection Unit, availability of suitable relevant and calibrated analytical instrumentation (eventually redundant), and, depending upon the anticipated tritium levels, an efficient and reliable Central Detritiation System. The latter habitually also serves to generate and maintain constant negative pressure in glove boxes. In most tritium handling installations, the detritiation system is based on the catalytic oxidation of tritiated hydrogen and tritiated hydrocarbons at elevated temperature followed by retention of generated tritiated moisture in adsorber beds placed downstream.

By design, a **Central Detritiation System** should be capable of processing all effluent gases from the tritium plant both during normal as well as during emergency operations and consistently achieve decontamination factors of at least 100 in once-through operation mode.

All primary containment systems including the adjudicated instrumentation must be planed and manufactured to withstand during their lifetime all normal operations, all anticipated operational occurrences, and all design basis accidents.

9.2.1 Environmental protection concepts in representative tritium-handling facilities

The site for a large fusion machine requires careful preliminary evaluation. In case of ITER, the Technical Working Group European ITER Site Study (ESSI) evaluated within the frame of the European Fusion Develoment Agreement (EFDA) the Cadarache site. The evaluation comprised among others subjects like geological survey, electrical supply, heat sink and water supply, transportation and shipping, tritium transport and control, seismicity, external hazards and consequences on buildings, effluents and waste management, decommissioning, analysis of the socio-economic environment, population, infrastructure accommodation, scientific and industrial capabilities, educational choices, health system, labour resources, employment, cultural environment, leisure possibilities, and tourism[EFD00].

For high occupational health and safety as well as for protection of the environment diverse air detritiation concepts have been implemented and demonstrated in large tritium handling facilities. Some facilities like **Tritium Process Laboratory** in Tokai-mura, Japan [Nar90], feature an Air Detritiation System constantly in operation and others, like **TSTA**, Los Alamos [And82], utilized room air detritiation only in case of emergency events. Chief objective of the TSTA Emergency Tritium Clean-up System (ETCS) was to reduce the probability of tritium

release into the environment in the event of consecutive or simultaneous primary and secondary containment breaching [Mul78]. At the time, ETCS could be actuated either automatically, e.g. when a tritium monitor reached an upper limit concentration value, or via a computer run by an authorized operator. Conventionally, the ETCS encompassed a precious metal catalyst bed followed by several downstream placed molecular sieve drying beds. Muller [Mul78] based his calculations for the conceptual design of an Emergency Clean-up System on the building that housed the TSTA facility which had a capacity of approximately 3000 m^3 air. He assumed a maximum accidental release of the inventory on site of 100 g tritium and further supposed that processing such tritium-contaminated air through the ETCS at a rate of 0.65 $m^3 s^{-1}$ should reduce the concentration of tritium down to operational status concentrations in less than twenty-four hours. To achieve this without significant releases of tritium into the environment[1] a basic requirement was a tritium oxide decontamination factor remaining constant at a value of about 10^6. However, experience accumulated worldwide over the past decades with a variety of decontamination systems leads to the conclusion this was too optimistic.

In some laboratories like **TLK**, where most glove boxes are serviced by their own dedicated detritiation system, in the event of an accidental release of tritium the throughput across the Central Detritiation System (CDS) is increased automatically [Sch91a]. Under normal operating conditions the Central Detritiation System also maintains a negative pressure of 400 - 700 Pa below ambient pressure in all glove boxes as well as in the loop which runs through the whole laboratory comprising several rather large halls and numerous smaller rooms. The loop, which is connected to most glove boxes in the laboratory preserves a negative pressure within the range 1000 - 1800 Pa with respect to ambient[2]. The CDS processes separately gas fractions extracted i) continuously from all operating glove boxes and ii) irregularly from one of two large containers (one is on standby) which collect the primary exhaust gases released from equipment installed therein. Both containers are prefilled with nitrogen up to a predetermined subatmospheric pressure for explosion safety. The gases collected and diluted in these containers are only fed into the Central Detritiation System after a gas analysis has confirmed that the tritium concentration is below that permitted for processing in once-through modus across this

[1] Either refrigerated or dessicant absorber type air dryers were proposed.
[2] Gas in the loop is circulated at a rate of 80 m^3 $hour^{-1}$ through the main detritiation system. The loop constantly extracts a small fraction of gas from each glove box. Simultaneously a small gas fraction is extracted from the loop and released via CDS into the environment.

system (see Fig. 4.5). In the event that the diluted exhaust gases are contaminated to a degree exceeding the pre-established value they are first subjected to further pre-cleaning in closed loop operation mode until the concentration of tritium has been reduced sufficiently to allow processing in once-through modus via the Central Detritiation System and subsequent release into the environment via stack.

Tritium permeation from heated components into the cooling water system of tritium handling installations is normally extremely small because the primary cooling system is operated in close loop mode and heat dissipation takes place via a heat exchanger into a secondary closed loop. At TLK the primary cooling circuit has a temperature of 293 K at the feed point and of 300 K at the return point. The secondary loop contains water whose temperature is maintained within the range 278 - 283 K [Sch91a]. The cooling water system is continuously monitored for tritium eventually diffusing into the cooling system. A third cooling circuit is coupled to two cooling towers which cool again the secondary system with the help of refrigerators.

In case of tokamaks like ITER the situation is different. When a heat load resulting from plasma operation or during tokamak baking of the order of more than 1 MW is removed via vault coolers (throughput $< 163\,000\,\mathrm{m^3\,hour^{-1}}$) the permeation of tritium into the Tokamak Cooling Water System (TCWS) can be significant, i.e. of the order of grams.

An adequately sized Dryer Regeneration System needs to be available in tritium handling installations to allow periodic regeneration of exhausted molecular sieve beds retrieved from detritiation systems or other installations. The Dryer Regeneration System may be autonomous or integrated into a Central Detritiation System.

In facilities dealing with significant amounts of tritium and equipped with numerous tritium air monitoring systems, glove box monitoring systems and stack monitoring equipment data shall be quotidianly collected, regularly evaluated and archived. The gathered information should be transmitted separately to i) the Central Alarm Unit, ii) the Radiation Protection Team and iii) the Central Process Control System that supervises the complete facility. Read-outs and alarm panels at these stations shall complement local station alarm panels. All regularly generated data shall be archived. This way of proceeding, which is of paramount importance for the safe operation of tritium handling facilities, is already standard in most installations.

If beryllium or materials that contain this metal are handled, analytical instrumentation capable of detecting beryllium at very low concentrations must be available or at least accessible.

Appropriate beryllium monitoring should be installed in the facility for the protection of working personnel.

In large tritium facilities two or more well insulated standby tanks containing sufficient **chilled water** on standby to cope with a transitory loss of refrigeration such as caused by an interruption of utility power supply or a malfunction of refrigerator units serving safety relevant equipment should be available. The volume of standby chilled water tanks should be sufficient to permit continuation of operation during the emergency event until power supply has been restored or repairs been completed.

To protect workers and the environment from permeation and/or leakage of tritium from primary systems reaching the laboratory air after a loss of integrity of a glove box, the pressure from the environmental atmosphere to that prevailing in the laboratory, the glove boxes and the primary systems is usually reduced stepwise in decrements of a few ten Pa[3]. Under these circumstances all rooms where tritium is processed are maintained at sub-atmospheric pressure which ensures a permanent positive air in-leak into the Tritium Building and minimizes dissemination of contaminated air into the outside atmosphere as well as into other tritium-free sections of the building.

Enhanced protection of the environment from experiments utilizing large inventories of tritium was achieved at **Tritium Process Laboratory (TPL)**, Tokai, by installing glove boxes in an almost air-tight room furnished with an air-lock system [Nar90]. Such an air-tight room effectively constitutes a secondary confinement protecting the laboratory surroundings from an accidental release. When the multiple barrier concept prevails, any tritium released into the laboratory atmosphere during a simultaneous containment and confinement breach can only reach the environment via the monitored stack after it has passed through the Central Tritium Retention System. Furthermore, for added safety at TPL the experimental primary systems, the glove boxes and the air-tight main room are equipped with singular detritiation systems of different design and operation parameters. The glove box purification system (GPS) is operated at a gas flow rate of $150\,m^3\,hour^{-1}$ and a catalyst temperature of 473 K, the effluent removal system (ERS) is run at $20\,m^3\,hour^{-1}$ and a much higher catalyst temperature of 773 K, and the air clean-up system (ACS) at a gas flow rate of 50 - $300\,m^3\,hour^{-1}$ and a catalyst temperature of 473 K [Hay93] (see Fig. 9.1). As evident, to cope with more oxidation-resistant organic tritium-bearing species

[3] Exceptions to this rule demands a safety analysis and appropriate special technical precautions.

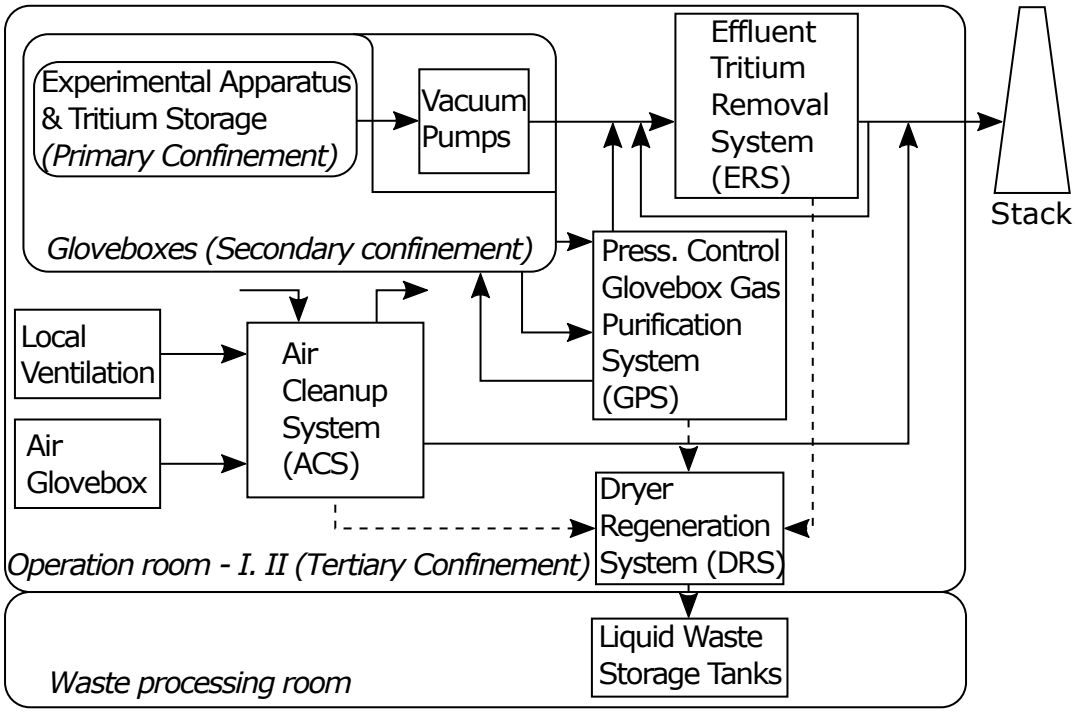


Figure 9.1: Interlinked Tritium Removal Systems at TPL (after [Hay93]).

mainly expected in primary systems (ERS), significantly higher temperatures were selected. Principal justification for separate detritiation routes is that effluents from primary containments as well as from primary, and secondary confinements generally display widely different levels of contamination and type of contaminants.

To meet **ITER** safety guidelines Yoshida et al. [Yos02] proposed for this project a concept based to a large extent on principles implemented and demonstrated at TPL. Taking process equipment and piping to constitute primary barriers, glove boxes to represent secondary barriers and buildings and/or air-tight rooms to be tertiary barriers, a dedicated detritiation system was adjudicated to each of these different classes of barriers. The complexity and diversity of ITER health and safety tasks is illustrated in very simplified fashion in Fig. 9.2 [Yos02]. Within this frame, the principal enviromental protection tasks encompass i) the ventilation and detritiation of the buildings enclosing the tokamak machine and supporting tritium systems, ii) the upkeep of the detritiation and preservation of the negative pressure in all glove boxes, and iii) the complete tokamak maintenance activities. To cope with these duties, a **Normal Ventilation** and a

Detritiation System (N-VDS 1) with a throughput of 500 $m^3\,hour^{-1}$ were proposed capable of processing in continuous mode i) the exhaust gases from all primary processing systems and therefore from all primary pumping systems, ii) all purge gas streams utilized for processing apparatuses or equipment in glove boxes, and iii) the purge gas from the Tritiated Water Holding Tank. The same N-VDS 1 system is also designed to cope in intermittent mode with i) the Fuelling Systems purge gas, ii) the air flow during maintenance operations with a portable ventilation duct ("elephant trunk") and iii) the ventilation or cover gas from the Tokamak Cooling Water System (TCWS). An additional second **Normal Ventilation Detritiation System (N-VDS 2)**, designed for a throughput of 700 $m^3\,hour^{-1}$, together with two large Standby Detritiation Systems (S-ADS and S-VDS) designed for throughputs of 4500 $m^3\,hour^{-1}$ in recirculation mode and 3000 $m^3\,hour^{-1}$ in once through mode, respectively, take care of the air detritiation of the buildings.

With the Glove Box Atmosphere Detritiation System (GDS) which is designed for a throughput of 150 $m^3\,hour^{-1}$ a recovery in 90 min of 99.9 % of the tritium is expected to be possible (the GDS system is not displayed in Fig. 9.2).

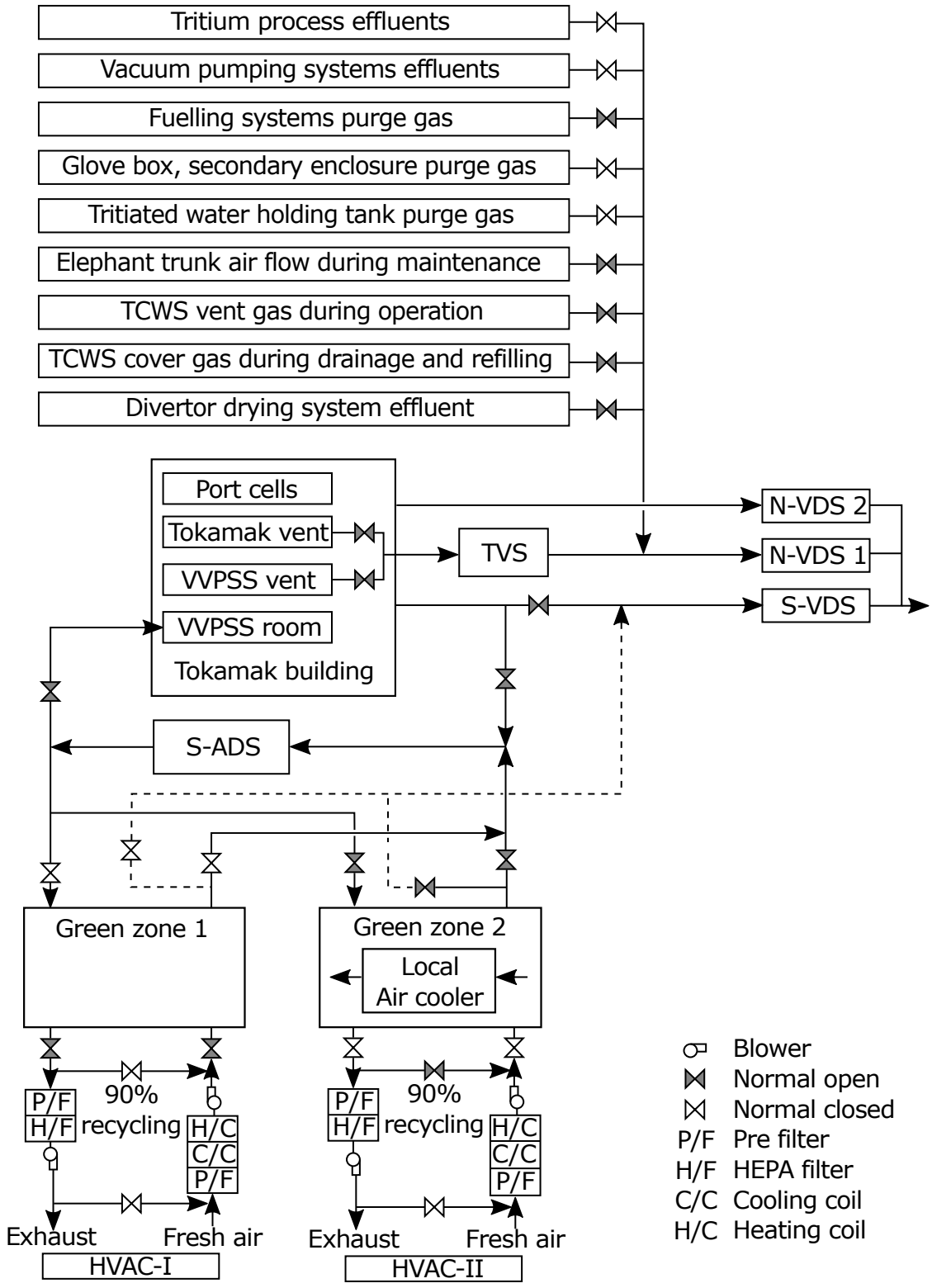


Figure 9.2: Tritium confinement and detritiation concept for the ITER tritium and tokamak buildings (after [Yos02]).

10 Compact fusion reactor

Recently, a number of early ideas on fusion confinement concepts have re-emerged. These older concepts relied on much smaller sizes than the devices currently under development which require very large tokamaks to obtain fusion power exceeding the input power needed to heat and control the plasma [Syk15]. Within the frame of the development of compact fusion General Fusion in Canada is exploring fast adiabatic compression with **merged spheromacs** [Lab08], Tri-Alpha in California, USA, is working on **merging plasmoids**, University of Washington and Lawrence Livermore in the USA are researching on the **Sustained Spheromac Physics Experiment** [Hil99; Bin10], Tokamak Energy in the UK is likewise investigating plasmas in a spherical tokamak, First Light Fusion in Oxford, UK is exploring **inertial confinement fusion** with emphasis on power generation and Lockheed Martin in California is focussing its efforts on a compact nuclear fusion machine called **high beta fusion reactor**. All these concepts are more or less funded and already undergoing ample scientific research as well as engineering testing.

The **spheromak** has perhaps the greatest potential of producing economical fusion power (see Fig. 10.1a). Conspicuous research activities are ongoing at Lawrence Livermore, California, in collaboration with Los Alamos and Sandia at the Sustained Spheromak Physics Experiment (SSPX). It generates most of the required magnetic field by driving electrical current into the plasma itself. The hot plasma is confined in a simple and compact magnetic field which uses only a small set of external stabilizing coils. Because the main magnetic field is generated by the afore mentioned plasma a substantial shrinking of the overall size of the reactor has become possible. Auspiciously, theoretical re-evaluations of older experiments provided evidence that the confinement of plasmas improves as the temperature of the plasma is increased. The energy generated in the plasma can be used for the production of electricity by heating up a coolant which in turn may spin a turbine. When compared with ITER or a stellarator the spheromak– if

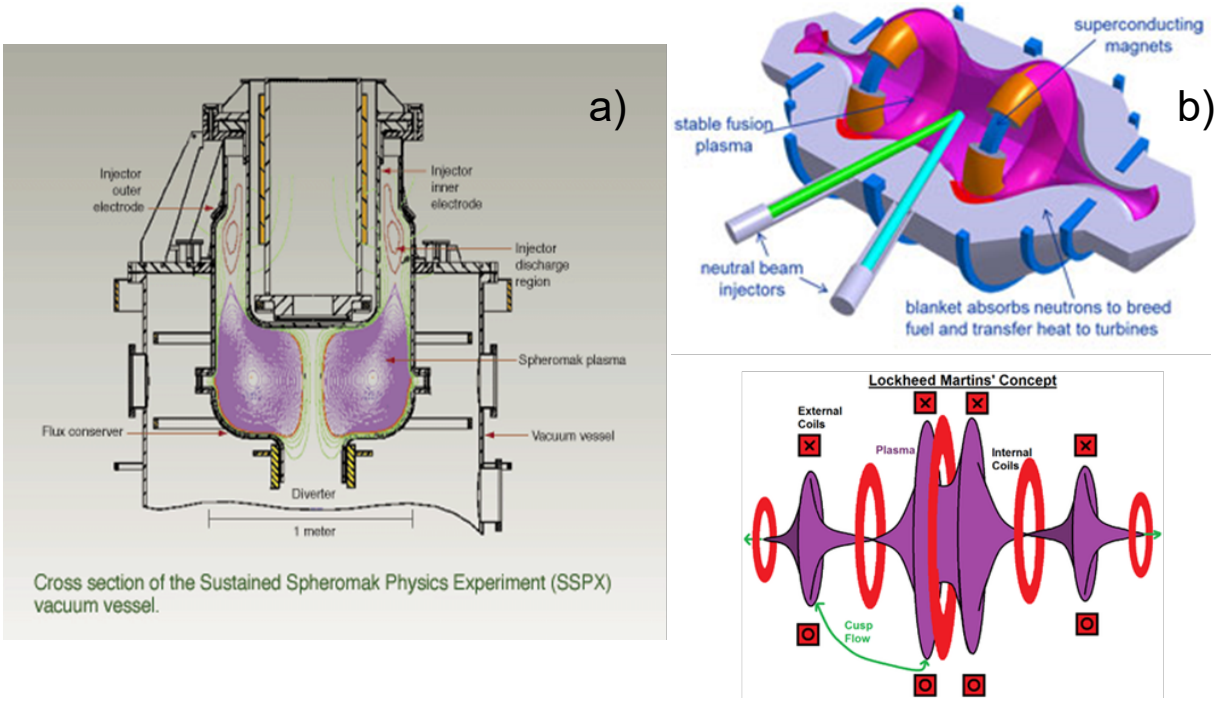


Figure 10.1: Two diverse compact fusion reactor configurations: a) spheromak and b) artists views of Lockheed Martin´s concept (after [Ras15]).

it works – could generate much more energy while at the same time being far less expensive, of considerably simpler engineering and substantially reduced in size.

The Lockheed reactor is based on a magnetic mirror confinement which contains the plasma by reflecting particles from high density magnetic fields to low density ones (see Fig. 10.1b). According to McGuire [McG07], project leader at Lockheed Martin, the newly designed reactor consists of a **cylinder** only 2 m long and 1 m wide. Hence, this design is completely different from that of a typical tokamak with its characteristic doughnut shape. It was estimated that this reactor can generate a power of up to 100 MW (enough to power a large cargo ship or an 80,000-home city. The cylindrical reactor shape is chosen to obtain strong magnetic confinement. A first prototype reactor is expected to be ready in a few years basically showing that all the physics works. There is talk of hundreds of firings with plasmas "doing what they are supposed to do". Numerous patents on these new technologies have been applied or issued.

Tokamak Energy, a privately funded UK venture engaged in nuclear fusion, claims to have heated a plasma for the first time up to 1.5×10^7 C employing a new type of reactor (ST40).

This reactor combines a **spherical tokamak** with the latest generation of high temperature super conduction magnets.

In spite of all these recent technical developments, the announcements on compact fusion reactors have not only been received with expectation but also with strong scepticism particularly with respect to their physical feasibility. For example, Günter and Lackner, Max Planck Institute for Plasma Physics, contended that the incorporation of coils into the plasma as proposed at Lockheed Martin would necessitate coil connections to the outside of the plasma vessel via fixtures. Direct contact of them with high energy plasma particles would be associated with rapid plasma cooling. An option would be superconducting coils levitating in the vessel. However, this would not solve the energy loss problem. Moreover, shielding the coils from the hot plasma and the energetic neutrons generated in the fusion reaction appears to be prohibitively difficult. The proposed configuration was thus considered unsuitable. What is more, present results fall far short of the necessary "triple product" of plasma density, temperature and confinement time (Lawson criterion) [Syk15]. From another perspective, an updated technical report shows that Lockheed´s fusion reactor may ideally be about ten times and conservatively up to hundred times larger than the originally planned version. The conservative version would weigh about 2000 tons, have a length of 18 m and a diameter of 7 m, which is much closer to a submarine than to a truck[Bes17]. Moreover, discussions on tritium issues pertaining the proposed compact fusion concepts have so far been eluded.

Maybe the day will come in which the presently favoured deuterium/tritium fuel can be replaced for example by non-radioactive and in nature sufficiently abundant protium/boron fuel. Because this reaction does only take place at much higher temperature and density than that required for DT fusion, new technology has been proposed for the creation of plasmas utilizing an ultra fast high-energy laser (peta watts in pico seconds) and for plasma confinement the magnetic field generated by a second laser ([Hor17], see also Marvel Fusion, Munich, Germany). The suggested target is nanostructured and consists of atomic proton nuclei and atomic boron-11 nuclei (HB11). Highly increased non-thermal fusion energy is supplied by avalanche-multiplication of the three $^4He^+$ ions generated in the initial HB11 fusion reaction

$$^1H + {}^{11}B \xrightarrow{3} {}^4He^+ + 8.7\,\text{MeV}.$$

The energy of the charged alpha particles can be converted directly into electricity. Advantageously, HB11 fuel is non-radiactive and all pertinent nuclear reactions proceed without neutrons. Hence, radioactive waste is not generated. For this concept to become reality at a commercial level, a procedure to accomplish every second several irradiations and ignitions using nano fuel pellets will have to be developed!

11 Concluding remarks

During the past three decades, the field of tritium technology has experienced a formidable expansion due to the continuing experimental and technological developments in plasma physics, process engineering, optimization of the fusion fuel cycle, and basic research frequently stimulated by results obtained from operating fusion machines or design activities for future devices. While for most of tritium technology much of the progress made over recent years can be categorized as consolidation and steady refinement rather than fundamental innovation, in specific areas such as plasma exhaust clean-up, cryo-pumping, water detritiation, tritium analytics, calorimetry, or isotope separation the degree of advancement has sometimes been spectacular. Another area of great progress has been the practical experience accrued worldwide on handling large quantities of tritium as well as on the interaction of this gas with diverse materials and numerous key components utilized in plasma exhaust processing. Altogether, this tritium-specific knowledge has increased significantly the reliability of planning. It has furthermore helped considerably with the selection of materials or process concepts, and will in the end contribute to improve the safety of future devices. From the above, it can be concluded that tritium technology has now reached a high degree of sophistication and maturity. This underlying know-how is of crucial importance for the successful operation of fusion machines currently under construction or the even more powerful of the future.

In order to save efforts and resources for the benefit of targeting on the expedient construction of ITER considerable research parallelism characterizing the early years of research has more and more given way to a concentration on the more promising options. Hence, most current efforts in tritium technology are dedicated to further optimization of optional process concepts and their adaptation to the specific and sometimes unprecedented demands of ITER.

With the aim of supporting ongoing activities for ITER it was decided in Karlsruhe to write a Tritium Manual dealing not only with the fundamental properties and radiochemistry of tritium

but also describing, evaluating, and reflecting on a broad range of other tritium-related topics such as process safety, tritium handling and processing, tritium production, tritium applications, tritium interactions with inorganic and organic materials relevant to tritium technology, experience with typical components used in tritium systems, tritium analytics, isotope separation, material balance issues, interim and long-term storage of tritium, design of containments and confinements, decontamination procedures, international transportation of tritium, waste treatment, waste disposal, waste categorization, and many others. Hence, the purpose of this manual is not to bring in detail all presently available information but rather to provide an overview. What is more, in spite of the current high priority of ITER, it seemed important not to limit the Tritium Manual to technology required straight away for this machine but also to gather as much as possible relevant information on technologies that were developed and tested in the past but in the end did not find their way into the present ITER design concept. This approach may be of use to researchers engaged in tritium work and eventually contribute to revive discarded ideas and efforts as ITER activities enter the experimental phase and new not yet foreseen problems require innovative solutions.

To some extent the Tritium Manual can also be contemplated as an educational supplement and practical adviser to operational personnel.

Because previously published handbooks have mostly been written from a radiological protection perspective [Int91][US 94][US 73][US 15] or have concentrated on selected tritium-related topics [Mog75], they are not superseded but rather complemented by the present Tritium Manual.

The wealth of currently available information makes it all but impossible to cover in a single manual all tritium relevant topic in appropriate length and depth. In view of this, several important topics like blankets, tritium breeder materials, radiological hazards, radiation protection, dosimetry, tritium in the environment, etc. were only treated marginally or not addressed at all. However, in its present form the Manual provides introductory information on the most important basic and technological tritium-related topics covering a wide spectrum of subjects from fully pertinent to the operation of ITER to only indirectly relevant or not applicable at all. Where considered important, topics requiring suplementary research efforts have been identified.

In writing the manual it was attempted to remain readable to beginners and useful to scientists engaged or planning research in fields related to tritium science. While emphasis was placed on

newer literature, older and occasionally very old work has also been included. Main goal of the Manual is thus to serve experts in the field by providing an expedient and broad introduction into very many topics. To those inexperienced in the subject, the Manual offers abundant information on precautions and rules that up to the present constituted the safety frame when becoming active in tritium work. For the most they have retained their validity but may require adaptation to present day state of knowledge and perception of radiation protection. The Manual may also proof useful to those designing, constructing, and operating advanced components destined to tritium service. References providing information on foregoing assemblies, eventually describing benefits and problems, achievements and failures, as well as unresolved issues of older designs are given in large number. In fact, all too frequently new components are designed and sometimes even constructed without sufficient awareness of the state of the art. The consequence are unnecessary experimental and technical efforts as well as waste of resources. If component manufacture has already progressed re-design and modifications may become necessary which constitutes considerable loss of time, effort, and resources. In this context, it is hoped that the Manual will provide a broad although unquestionably incomplete overview of the main body of tritium-pertinent literature.

Only few processes or technologies are explicitly endorsed in the Tritium Manual and detailed discussions on processes or technologies are not too frequent. Instead, it was preferred to describe as many options as possible in order to encourage the reader to select on a broad basis his own way to proceed. Sufficient references are furnished for easy search of more minutiae.

Attempts to list, discuss, or evaluate presently available commercial equipment were not considered meaningful on the ground of their enormous number, continuous rapid evolution, and frequently changing mode of commercialization. The adopted solution was to describe and evaluate the performance of representative components already subjected to prolonged tests mostly in facilities handling considerable amounts of tritium. At the same time, new promising developments were consistently evaluated for their potential application in tritium technology. Attention was likewise focused on the behaviour of materials employed for the manufacture of components already tested in a tritium environment.

A general remark pertains the Internet. While the Internet constitutes a wonderful and easy help allowing ready access to recent literature, it is at times difficult to get hold of older

references which every so often have a high standard and may still be of interest to the scientific community. Remedy should be sought by those engaged in the field.

An intrinsic difficulty with manuals is the recurrent need to keep up with a rapidly expanding literature, the development of new technologies, as well as of more modern equipment in large variety and many fields of application. An additional challenge is the continuing evolution of ITER planning with sometimes associated drastic changes in materials, components, or process specifications and conduction. In the specific case of tritium technology, the implementation of innovative equipment for routine tritium service does, however, take decades, comprising initially ample parameter testing with hydrogen/deuterium preferably by several teams and subsequently comprehensive and extended demonstration with tritium under compliance with high safety standards in one or more of only very few facilities worldwide. It is therefore more prudent for ITER to rely at least at the outset on fully proven equipment and technologies. Proven technologies and material combinations used for the manufacture of pertinent components will hence not lose quickly their validity. Sensors, analytical instrumentation, or process components whose appearance and/or peripheral electronic equipment have undergone drastic design changes but whose basic governing principles have remained unchanged will remain fully applicable. Experiences gained with such instruments and components during routine operation with tritium for extended periods of time particularly if tested by diverse research groups have been comprehensively addressed in the present Tritium Manual.

In short, it is without doubt that tritium technology for fusion has reached a high degree of development. The decision to construct ITER has moreover triggered in recent years - not only in countries directly engaged in ITER - a remarkable renaissance of new, exciting, and very promising research activities in many tritium technology areas. At the same time the realization of ITER has now reached a crucial point requiring palpable progress in the very near future. In case of major delays fusion may face loss of credibility and interest as well as of financial support. The situation right now, in which the JET machine is used to perform ITER-specific plasma-wall interaction experiments - performed with tritium under participation of highly skilled professionals from research institutions of all over the world - is highly promising for the success of the ITER project. But this situation will not endure for too long.

Note: Errors or omissions remaining in the revised Tritium Manual are the sole responsibility of the author.

The Author

Ralf-Dieter Penzhorn graduated in chemistry from the University of Chile, Santiago, Chile. After a postgraduate year at Kansas University, Kansas, USA, in the laboratories of Prof. F. Sherwood Rowland (Nobel Laureate), he received 1965 a PhD in physical chemistry from Catholic University of America, Washington DC, USA, under the guidance of Prof. Basil de B. Darwent. 1966 he performed postgraduate research together with Dr. John T. Herron and Dr. Henry Rosenstock on gas phase kinetics by mass spectrometric techniques at the National Bureau of Standards in Washington DC, USA. From 1966 to 1970 he taught physical chemistry and advanced kinetics at the Faculty for Physical and Mathematical Sciences of the University of Chile. During most of 1967 he served as scientific expert for the Development of a Science and Technology Program for Latin America at the Organization of American States (OAS), in Washington DC, USA. 1971 he emigrated into the Federal Republic of Germany, where he became Group Leader at the Institute of Radiochemistry, Nuclear Research Center Karlsruhe, Karlsruhe, researching on atmospheric chemistry (1972-1974), reprocessing of nuclear radioactive waste (1975-1985) and the development of fusion fuel cycle technology (1985-1994). He was appointed Head of the Tritium Laboratory Karlsruhe, Nuclear Research Center (1994-2001). Concurrently, he was nominated Task Force Leader for the coordination of the tritium activities at the European Union performed for JET within the frame of the European Fusion Development Agreement/Joint European Undertaking, Culham, Great Britain (1999-2001). Dr. Penzhorn was guest scientist at Hydrogen Isotope Research Center, Toyama University, Japan almost every year from 2002 to 2012, for extended periods and visited twice the School of Mathematical Science and Engineering, Chengdu University, Chengdu, China (2016, 2018). He is author/co-author of approx. 300 publications and 17 patents.

Appendices

A Miscellaneous acronyms

ADR = European Agreement on International Carriage of Dangerous Goods by Road
AECL = Atomic Energy of Canada, Ltd.
AGHS = Active Gas Handling System
ALARA = As Low As Reasonably Achievable
ALCATOR = Alto Campo Toro tokamac
ALI = Annual Level of Intake
AMU = atomic mass unit
ANDRA = Agence National pour la Gestion des Déchets Radioactifs (French national radioactive waste management agency)
ANS = Analytical System (ITER)
ASDEX = Axial Symmetric Divertor Experiment
ASER = Actively Stabilized External Resonator
ASME = American Society of Mechanical Engineers
ASN = Autorité de Sûreté Nucléaire (Nuclear Safety Authority)
ASNT = American Society for Non-destructive Testing
ASTM = American Society for Testing and Materials
AtG = Atomgesetz (German Atomic Energy Act)
BA = Broader Approach
BNL = Brookhaven National Laboratory
BSI = British Standards Institution
BSS = Basic Safety Standards
CANDU = Canada Deuterium Uranium
CAS = Central Automation System
CATIA = Computer Aided Three-Dimensional Interactive Application
CEA = Commissariat a l´Energie Atomique
CECE = Combined Electrolysis Catalytic Exchange process
CEN-Saclay = Centre d´Etudes Nucléaires de Saclay
CFC = carbon fibre composite
CFFTP = Canadian Fusion Fuels Technology Program
CFR = Code of Federal Regulations
CIRES = Centre Industriel de Regroupment, d´Entreposage et de Stockage
CODAS = Control and Data Acquisition System
CRNL = Chalk River National Laboratories
CSA = Centre de Stockage de l´Aube
CSU = Close Support Unit
CRNL = Chalk River National Laboratory
DAC = Derived Air Concentration
DCS = Distributed Control System
DEMO = Demonstration Power Plant
DF = Decontamination Factor

DIN = Deutsches Institut für Normung
DMA = dynamic mechanical analysis
DOE = US Department of Energy
DPA = displacements per atom
DRL = Derived Release Limit
EFDA = European Fusion Development Agreement
ELTL = EVEDA Lithium Test Loop
EPA = Environmental Protection Agency
EPDM = ethylene propylene diene monomer
EPR = ethylene propylene rubber
ERDA = Elastic Recoil Detection Analysis
EVEDA = Engineering Validation and Engineering Design Activities
F4E = Fusion for Energy
FMAVC = faible et moyenne activité à vie courte
FPY = full power year
FUGEN = Fugen Nuclear Power Station
FY = Fiscal Year
FZJ = Forschungszentrum Jülich
FZK = Forschungszentrum Karlsruhe
FZR = Forschungszentrum Rossendorf
G= molecules produced per 100 eV of absorbed energy
GE = General Electric
GMA welding = gas metal arc welding
HAZ = heat affected zone
HAZOP = Hazard and Operability
HCCB = Helium Cooled Ceramic Breeder
HDB = Hauptabteilung Dekontaminationsbetriebe (Decontamination Service at KIT)
HDPE = high density polyethylene
HETP = Height Equivalent of a Theoretical Plate
HMR = Hazardous Materials Regulations
HRC = Hydrogen Isotopes Research Centre, Toyama University
IAEA = International Atomic Energy Agency
I&C = Instrumentation and control
ICRP = International Commission on Radiological Protection
IEA = International Energy Agency
IEC = International Electrotechnical Commission
IEEE = Institute of Electrical and Electronic Engineers
IFMIF = International Fusion Materials Irradiation Facility
ILW = intermediate level waste
IMMS = Integrated Model Management System
INEL = Idaho National Engineering Laboratory
IPP = Max Planck Institut für Plasmaphysik
IPR = intellectual property rights
IRAS = Indice Radiologique d´Acceptation en Stockage
IRR = Ionizing Radiation Regulations
ISS = Isotope Separation System
JAEA = Japan Atomic Energy Agency
JAERI = Japan Atomic Energy Research Institute
JIS = Japan Industrial Standard

JET = Joint European Torus
JET-ILW = Joint European Torus ITER Like Wall
JT60U = Japan Atomic Energy Research Institute Tokamak 60 Upgrade
KAERI = Korea Atomic Energy Research Institute
KATRIN = Karlsruhe Tritium Neutrino experiment
KEPRI = Korea Electric Power Research Institute
KEPTL = Korea Electric Power Tritium Laboratory
KfK = Kernforschungszentrum Karlsruhe
KIT = Karlsruhe Institute of Technology
LANL = Los Alamos National Laboratory
LDPE = Low Density Polyethylene
LET = linear energy transfer
LHD = Large Helical Device
LLNL = Lawrence Livermore National Laboratory
LLW = low level waste
LOCA = loss of coolant accident
LOVA = loss of vacuum accident
LPCE = liquid phase catalytic exchange
LPLC = Local Programmable Logic Controller
LSA = low specific activity
MMI = man machine interfaces
NAMUR = Normenarbeitsgemeinschaft für die Meß- und Regeltechnik
NFPA = US National Fire Protection Agency
NIFS = National Institute of Fusion Science, Nagoya, Japan
NIST = National Institute of Standards and Technology, Gaithersburg, Maryland, USA
NNC = National Nuclear Corporation
NOMUR = Normenarbeitsgemeinschaft für die Meß- und Regelungstechnik
NRA = Nuclear Reaction Analysis
NRC = US Nuclear Regulatory Commission
OH = Ontario Hydro
ORNL = Oak Ridge National Laboratory
PCST = Public Communication of Science and Technology
PEEK = polyetheretherketone
PFC = Plasma Facing Component
PFD = Process Flow Diagram
PID = Proportional Integral Derivative controller
P&ID = Pipe and Instrumentation Diagram
PIT = physical inventory taking
PMR = Palladium membrane reactor
PNNL = Pacific Northwest National Laboratory
PPPL = Princeton Plasma Physics Laboratory
PTFE = polytetrafluoroethylene
PVC = polyvinyl chloride
QA = quality assurance
RAFM = reduced activation ferritic martensitic steel
RSA =Radioactive Substances Act
RTF = Replacement Tritium Facility, Savannah River Site
SAE = Society of Automotive Engineers
SAES = Societá Apparecchi Elettrici e Scientifici

SAR = Safety Analysis Report
SCK-CEN = Studie Centrum voor Kernenergie – Centre d´Etude de l´Energie Nucleaire
SDS = Storage and Delivery System (ITER)
SEAFP = Safety and Environmental Assessment of Fusion Power
SEM = scanning electron microscope
SIC = Safety important component
SIF = Safety Instrumental Function
SIL = Safety Integrity Levels
SNL = Sandia National Laboratory
SOL = scrape off layer
SOP = Standard Operating Procedure
SRS = Savannah River Site
SSPX = Sustained Spheromak Physics Eyperiment
STAR = Safety and Tritium Applied Research Facility
STP = standard temperature (273 K) and pressure (1 bar)
StrlSchV = Strahlenschutzverordnung (German Radiation Protection Ordinance)
TBM = Test Blanket Module
TBR = tritium breeding ratio
TEM = transmission electron microscopy
TEP = Tokamak Exhaust Processing system (ITER)
TERF = Tritium Emissions Reduction Facility
TEXTOR = Tokamak Experiment for Technology Oriented Research
TFA = tres faible activité
TFTR = Tokamak Fusion Test Reactor
TIG welding = tungsten inert gas welding
TLA = Technische Liefer- und Abnahmebedingungen
TLK = Tritium Laboratory Karlsruhe
TMP = Turbo molecular pump
TPD = temperature programed desorption
TPL = Tritium Process Laboratory
TRENTA = Trennung Tritium Anlage
TRF = Tritium Removal Facility (Darlington)
TSTA = Tritium Systems Test Assembly
TU = Tritium unit. One TU corresponds to a T/H ratio of 10^{-18}.
TÜV = Technischer Überwachungsverein (Technical Inspection Board)
UCLLL = University of California, Lawrence Livermore Laboratory
UCRL = University of California Radiation Laboratory UHMWPE = ultra high molecular weight polyethylene
UKAEA = United Kingdom Atomic Energy Authority
VDS = Vent De-tritiation System (ITER)
VNIINM = Bochwar All Russia Research Institute of Inorganic Materials
WDS = Water De-tritiation System (ITER)
WSRC = Westinghouse Savannah River Company

B Constants and conversions

$1\,\text{year} = 365.2425\,\text{d}$

$1\,\text{Ci} = 3.7 \times 10^{10}\,\text{disintegrations}\,\text{s}^{-1} = 37\,\text{GBq}$

$1\,\text{Bq} = 3.7 \times 10^{-11}\,\text{Ci}$

$1\,\text{erg} = 1 \times 10^{-7}\,\text{J} = 0.2778 \times 10^{-13}\,\text{kWh} = 6.25 \times 10^{11}\,\text{eV} = 2.390 \times 10^{-11}\,\text{kcal}$

$1\,\text{cal} = 4.1868\,\text{J}$

$1\,\text{bar} = 10^5\,\text{Pa} = 0.986\,92\,\text{atm} = 14.5\,\text{psi}$

$1\,\text{atm} = 101\,325\,\text{Pa}$

Avogadro number $= 6.023 \times 10^{23}\,\text{molecules}\,\text{mol}^{-1}$

STP conditions $\equiv 1\,\text{atm}$ and $273\,\text{K}$

1 mass unit u $= 931\,\text{MeV}$

Gas constant $= R = 8.3134\,\text{J}\,\text{K}^{-1}\,\text{mol}^{-1} = 8.3134 \times 10^{-3}\,\text{kJ}\,\text{K}^{-1}\,\text{mol}^{-1} = 1.9878\,\text{cal}\,\text{K}^{-1}\,\text{mol}^{-1}$

$= 0.08206\,\text{l atm}\,\text{mol}^{-1}\,\text{K}^{-1}$

Boltzmann constant $= k = 1.380\,66 \times 10^{-23}\,\text{J}\,\text{K}^{-1}$

Planck constant $= h = 6.626\,176 \times 10^{-34}\,\text{J s} = 6.626\,176 \times 10^{-27}\,\text{erg s}$

$1\,\text{eV} = 1.602 \times 10^{-19}\,\text{J}$

$1\,\text{cm} = 10^8\,\text{Å} = 10^7\,\text{nm}$

$1\,\text{nm} = 10\,\text{Å}$

1 TU corresponds to a T/H $= 10^{-18}$ ratio or $0.118\,\text{Bq/l}_{\text{water}}$

1 e.u. $= 4.184\,\text{J}\,\text{K}^{-1}\,\text{mol}^{-1}$

mrem = milli roentgen equivalent man

1 b (barn) $= 10^{-24}\,\text{cm}^2$

C Tritium compressibility factors at 295 K in the low-pressure range (after [US 73])

Table C.1

P (Pa)	z	P (Pa)	z	P (Pa)	z	P (Pa)	z
1.01×10^4	1.0001	3.14×10^5	1.0034	6.18×10^5	1.0068	9.22×10^5	1.0101
2.03×10^4	1.0002	3.24×10^5	1.0035	6.28×10^5	1.0069	9.32×10^5	1.0102
3.04×10^4	1.0003	3.34×10^5	1.0037	6.38×10^5	1.0070	9.42×10^5	1.0103
4.05×10^4	1.0004	3.45×10^5	1.0038	6.48×10^5	1.0071	9.52×10^5	1.0104
5.07×10^4	1.0006	3.55×10^5	1.0039	6.59×10^5	1.0072	9.63×10^5	1.0105
6.08×10^4	1.0007	3.65×10^5	1.0040	6.69×10^5	1.0073	9.73×10^5	1.0106
7.09×10^4	1.0008	3.75×10^5	1.0041	6.79×10^5	1.0074	9.83×10^5	1.0107
8.11×10^4	1.0009	3.85×10^5	1.0042	6.89×10^5	1.0075	9.93×10^5	1.0109
9.12×10^4	1.0010	3.95×10^5	1.0043	6.99×10^5	1.0076	1.00×10^6	1.0110
1.01×10^5	1.0011	4.05×10^5	1.0044	7.09×10^5	1.0078	1.01×10^6	1.0111
1.11×10^5	1.0012	4.15×10^5	1.0045	7.19×10^5	1.0079	1.02×10^6	1.0112
1.22×10^5	1.0013	4.26×10^5	1.0047	7.30×10^5	1.0080	1.03×10^6	1.0113
1.32×10^5	1.0014	4.36×10^5	1.0048	7.40×10^5	1.0081	1.04×10^6	1.0114
1.42×10^5	1.0016	4.46×10^5	1.0049	7.50×10^5	1.0082	1.05×10^6	1.0115
1.52×10^5	1.0017	4.56×10^5	1.0050	7.60×10^5	1.0083	1.06×10^6	1.0116
1.62×10^5	1.0018	4.66×10^5	1.0051	7.70×10^5	1.0084	1.07×10^6	1.0117
1.72×10^5	1.0019	4.76×10^5	1.0052	7.80×10^5	1.0085	1.08×10^6	1.0118
1.82×10^5	1.0020	4.86×10^5	1.0053	7.90×10^5	1.0086	1.09×10^6	1.0120
1.93×10^5	1.0021	4.96×10^5	1.0054	8.00×10^5	1.0087	1.10×10^6	1.0121
2.03×10^5	1.0022	5.07×10^5	1.0055	8.11×10^5	1.0089	1.11×10^6	1.0122
2.13×10^5	1.0023	5.17×10^5	1.0056	8.21×10^5	1.0090	1.12×10^6	1.0123
2.23×10^5	1.0024	5.27×10^5	1.0058	8.31×10^5	1.0091	1.13×10^6	1.0124
2.33×10^5	1.0026	5.37×10^5	1.0059	8.41×10^5	1.0092	1.14×10^6	1.0125
2.43×10^5	1.0027	5.47×10^5	1.0060	8.51×10^5	1.0093	1.16×10^6	1.0126
2.53×10^5	1.0028	5.57×10^5	1.0061	8.61×10^5	1.0094	1.17×10^6	1.0127
2.63×10^5	1.0029	5.67×10^5	1.0062	8.71×10^5	1.0095	1.18×10^6	1.0128
2.74×10^5	1.0030	5.78×10^5	1.0063	8.82×10^5	1.0096	1.19×10^6	1.0130
2.84×10^5	1.0031	5.88×10^5	1.0064	8.92×10^5	1.0097	1.20×10^6	1.0131
2.94×10^5	1.0032	5.98×10^5	1.0065	9.02×10^5	1.0099	1.21×10^6	1.0132
3.04×10^5	1.0033	6.08×10^5	1.0066	9.12×10^5	1.0100	1.22×10^6	1.0133

D Van't Hoff plots of metal hydrides with potential for application in tritium handling systems. [Pen90]

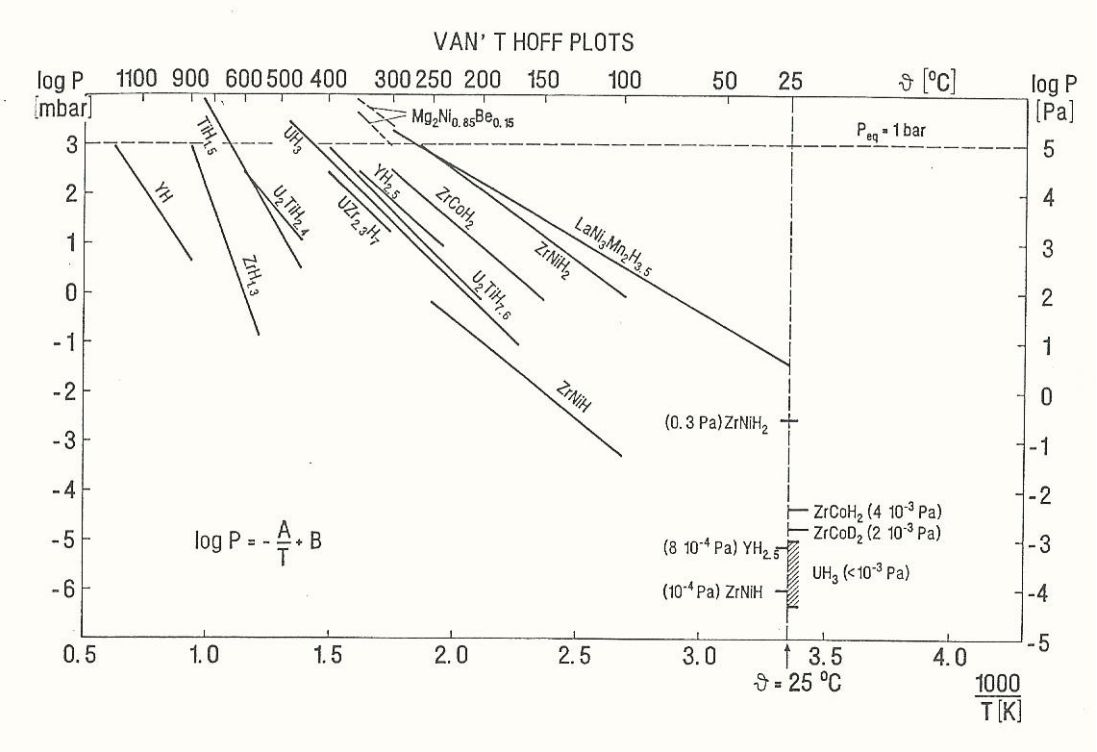


Figure D.1

E Radiation resistance of polymers (information supplied by CEA)

Table E.1

Radiation source: Co-60
Radiation intensity: 140 000 r/hour
Medium: air

Polymer material	Change in mechanical properties	Pressure deformation test	
	(less than 10 %)	γ Dosis	%
Polychloropren	1×10^5 γ	2×10^8	100
		1×10^8	95
		1×10^7	70
Butadiene copolymer	1×10^7 γ	5×10^8	100
		2×10^8	93
		1×10^8	59
Acryl nitril (Perbunam)	1×10^6 γ	2×10^8	Material becomes soapy
Polyurethane	1×10^6 γ	5×10^8	100
		1×10^8	88
Silicon	1×10^5 γ	2×10^8	100
		1×10^8	94
		1×10^7	60
Ethylene propylene	1×10^9 γ	5×10^8	55
Polytetrafluoro ethylene (Teflon)	1×10^4 γ		Material looses elastic properties
Viton B (Fluorocarbon)	1×10^4 γ	5×10^7	90

F Diffusivities and solubilities of tritium in fusion reactor relevant metals (after [Rei85])

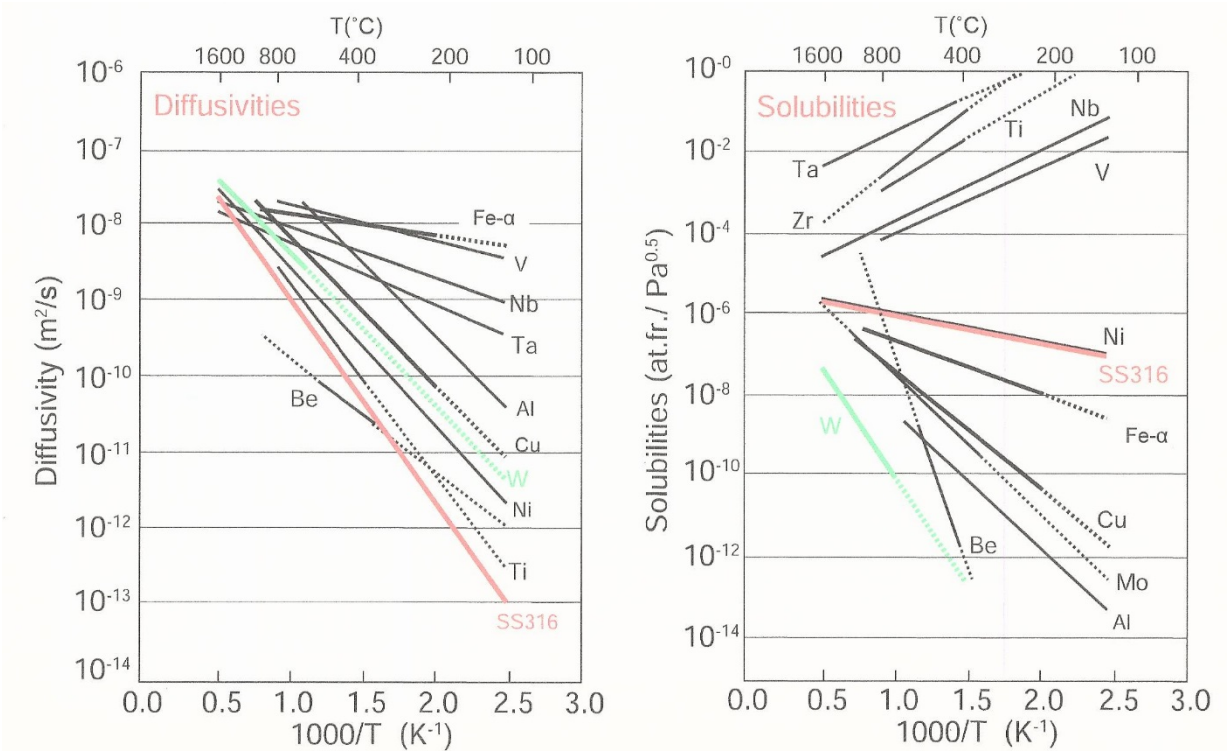


Figure F.1

G Optical microscopy of flakes from JET after DTE1

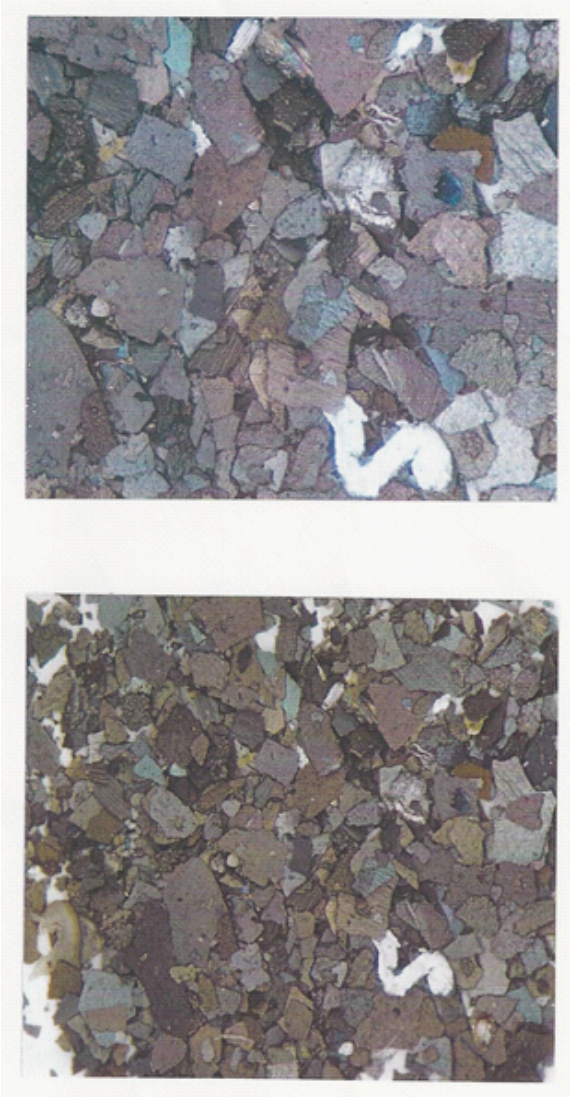


Figure G.1: (Upper figure 40:1 and lower figure 25:1)

H Tritium profiles of the plasma-exposed and plasma-shadowed sides of JET tile 004/1-44 after the DTE1 campaign

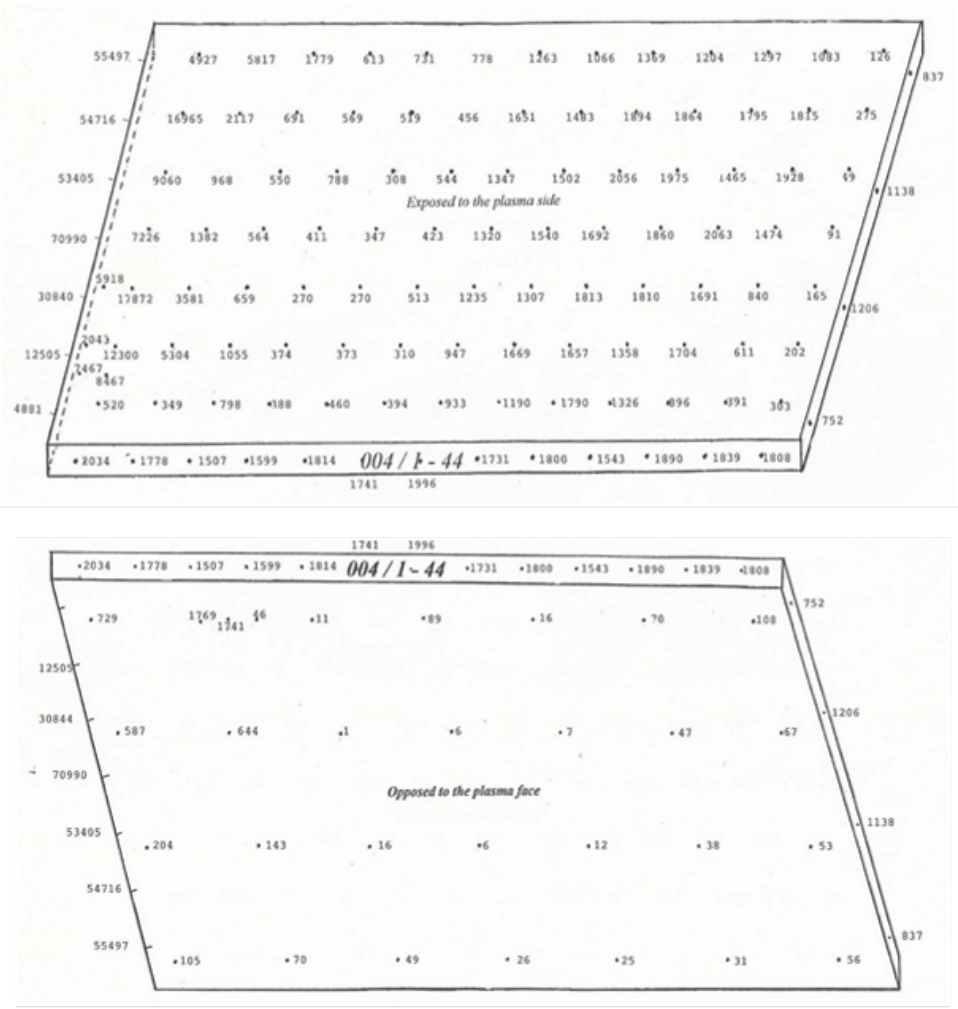


Figure H.1: Tritium distribution on the plasma-exposed (upper figure) and plasma-shadowed (lower figure) sides of JET tile 004/1-44 after the DTE1 campaign obtained with a PIN diode device on six surfaces.

I Chemical composition of austenitic stainless-steels habitually used in tritium handling systems (weight %) (after [Bar09])

Table I.1

Type	Cr	Ni	Mn	C	S	Mo
304	17.5 - 19	8 - 1	0.5 - 32	< 0.06	< 0.03	-
304L	17.5 - 19	9 - 2	0.5 - 2	< 0.03	< 0.03	-
316	16.5 - 18.5	10 - 14	0.5 - 2	< 0.07	< 0.03	2.25 - 3
316L	16.00 - 18.00	10.00 - 15.00	< 2.00	< 0.035	< 0.030	2.00 - 3.00
1.4404*	16.50 - 18.50	10.00 - 13.00	< 2.00	< 0.030	< 0.015	2.00 - 2.50
316L (N)	17.00 - 18.00	12.00 - 12.500	1.6 - 2.0	< 0.03	< 0.010	2.30 - 2.70

*EU steel number (X2CrNiMo17-12-2)

J Designations of some common standardized steels used in tritium handling facilities

Table J.1

DIN	Steel designation	SAE
1.4307	X2CrNi18-9	304L
1.4306	X2CrNi19-11	304L
1.4311	X2CrNiN18-10*	304LN
1.4301	X5CrNi18-10	304
1.4948	X6CrNi18-11	304H
1.4541	X6CrNiTi18-10	321
1.4401	X5CrNiMo17-12-2	316
1.4406	X2CrNiMoN17-12-2*	316LN
1.4432	X2CrNiMo17-12-2	316L
1.4435	X2CrNiMo18-14-3	316L
1.4436	X3CrNiMo17-13-3	316
1.4571	X6CrNiMoTi17-12-2	316Ti
1.4429	X2CrNiMoN17-13-3*	316LN

*N is an austenitic stabilizing element

K Chemical composition of structural stainless-steel specified for ITER, i.e. SS316L (N) [Bar09]

Table K.1

Element	Alloying element and impurity (weight %)	
	Min.	Max.
C	0.015	0.030
Mn	1.6	2.0
Si		0.50
P		0.025
S	0.05	0.01
Cr	17.0	18.0
Ni	12.0	12.5
Mo	2.3	2.7
Ti		0.10
Ta		0.01
Nb		0.01
Cu		0.3
B		0.0020
Co		0.05
N	0.06	0.080

L Tolerable pressure and temperature ranges of Swagelok valves with VCR® connections (for not radiographed valves the pressure ratings should be reduced by 15 %) [1]

[1] http://www.lesker.com./newweb/gas_liwuid_management. 23.07.2020

Table L.1

Material	**316 SS**	**316 SS**	**316 SS**	**316 SS**	**316 SS**	**316 SS**
Series	**BW**	**BW**	**BG**	**BG**	**BMG**	**BMG**
Temp., °F (°C)	**Working Press., psig** (VCR's radiographed)	**Working Press., psig** (VCR's not radiographed)	**Working Press., psig** (VCR's radiographed)	**Working Press., psig** (VCR's not radiographed)	**Working Press., psig** (VCR's radiographed)	**Working Press., psig** (VCR's not radiographed)
-20 (-28) to 100 (37)	1000	850	1000	850	700	595
200 (93)	830	705	830	705	610	518
300 (148)	660	561	660	561	530	450
400 (204)	500	425	500	425	450	382
500 (260)	450	382	450	382	375	319
600 (315)	400	340	400	340	300	255
650 (343)	360	306	-	-	-	-
700 (371)	330	280	-	-	-	-
750 (398)	300	255	-	-	-	-
800 (426)	260	221	-	-	-	-
850 (454)	230	195	-	-	-	-
900 (482)	200	170	-	-	-	-

Material	**316 SS**	**316 SS**	**316 SS**	**316 SS**
Series	**UW, TW**	**UW, TW**	**UG, TG**	**UG, TG**
Temp., °F (°C)	**Working Press., psig** (VCR's radiographed)	**Working Press., psig** (VCR's not radiographed)	**Working Press., psig** (VCR's radiographed)	**Working Press., psig** (VCR's not radiographed)
-20 (-28) to 650 (343)	2500	2125	2500	2125
700 (371)	2120	1802	-	-
750 (398)	1740	1479	-	-
800 (426)	1360	1156	-	-
850 (454)	980	833	-	-
900 (482)	600	510	-	-

Material	**316 SS & Vespel Stem Tips**	**316 SS & Vespel Stem Tips**		**316 SS**	**316 SS**
Series	**HB**	**HB**		**H**	**H**
Temp., °F (°C)	**Working Press., psig** (VCR's radiographed)	**Working Press., psig** (VCR's not radiographed)	**Temp., °F (°C)**	**Working Press., psig** (VCR's radiographed)	(VCR's not radiographed)
-40 (-40) to 100 (37)	3500	2975	-80 (-62) to 600 (315)	1000	850
150 (65)	3220	2737			
200 (93)	2950	2507			
300 (148)	2640	2244			
400 (204)	2400	2040			

M Nupro® shut-off SS316 valves (B series valves feature demontable bonnets for cleaning or replacement purposes)

Table M.1

Valve type	Nupro BG	Nupro BK	Nupro BKT	Nupro H
Max. pressure at 294 K bar	69	69	69	69
Temperature rating K	588	366	366	211 - 588
Flow coefficient C_v	0.39	0.39	0.36	0.28
Bonnet seal	bellows	bellows	bellows	bellows
Turns to open	2.5	2.5	n/a	1
Used for shut off	yes	yes	yes	yes
Internal volume cm^3	1.6	1.6	1.1	1.3

N Selected list of US specifications, regulations, guidelines, rules, standards, handbooks, and manuals (after [Poo08])

ACGIH, Industrial Ventilation: A Manual of Recommended Practice, 23d Edition (1998).

AGS-G001, Guidelines for Glove Boxes.

AISC LRFD, Manual of Steel Construction, Load & Resistance Factor Design, Volume I and II, Second Edition, (1994).

AISI Specification and Commentary for the Design of Cold-Formed Steel Structural Members, (1996).

ANSI Z358.1, Emergency Eyewash and Shower Equipment, (1998).

ANSI Z88.2-1992, Respiratory Protection (1992).

API RP 520, Sizing, Selection and Installation of Pressure Relieving Devices in Refineries, Part I Sizing and Selection, Sixth Edition, (1993).

API Standard 610, Centrifugal Pumps for Petroleum, Heavy Duty Chemical and Gas Industry Services, 8th Edition, (1995).

ASCE 7, Minimum Design Loads for Buildings and other Structures, (2005).

ASHRAE 15, Safety Code for Refrigeration Systems, (1994).

ASHRAE 42 Degree chilled water. Basics of Cooling Water Tower Treatment

ASHRAE 52 Standard Test Method of Commercial HVAC Filters

ASHRAE 55, Thermal Environmental Conditions for Human Occupancy (with addendum), (1992).

ASHRAE 62, Ventilation for Acceptable Indoor Air Quality (with 1990 addendum), (1989).

ASHRAE Handbooks published in a series of four volumes, one of which revised every year, ensuring that no one volume is older than four years. ASHRAE Handbook – HVAC Applications (1999), ASHRAE Handbook – Refrigeration (1998), ASHRAE Handbook Fundamentals (1997), ASHRAE Handbook HVAV Systems and Equipment (1996).

ASME A13.1, Scheme for Identification of Piping Systems, (1996).

ASME B16.34, "Valves – Flanged, Threaded End Welding End", (1996).

ASME B30.11, Monorails and Under Hung Cranes, (1998).

ASME B30.16, Overhead Hoists (Underhung), (1999).

ASME B30.2, Overhead and Gantry Cranes, Top Running Bridge, Single or Multiple Girder, Top Running Trolley Hoist, (1996).

ASME B31.1, Power Piping, (1998).

ASME B31.3, Process Piping, (1999).

ASME Boiler and Pressure Vessel (B&PV) Code Section VIII, Division 1 - Rules for Construction of Pressure Vessels, (1998).

ASME HST – 1M – 1989, (R1995), Performance Standard for Electric Chain Hoists (1989).

ASME HST – 2M – 1989 (R1995), Performance Standard for Hand Chain Manually Operated Chain Hoists (1989).

ASME HST – 4M – 1991 (R1996), Performance Standard Specification for Overhead Electric Wire Rope Hoists (1991).

ASME NOG – 1, Rules for Construction of Overhead and Gantry Cranes (Top Running Bridge, Multiple Girders), (1998).

ASME NQA – 1 – 1997, Quality Assurance Program Requirements for Nuclear Facility Applications (1997).

ASTM C450, Standard Practice for Prefabrication and Field Fabrication of Thermal Insulating Fitting Covers for NPS

Piping, Vessel Lagging and Dished Head Segments, (1994).

ASTM D5144, Standard Guide for use of Protective Coating Standards in Nuclear Power Plants, (1997).

ASTM F683, Standard Practice for Selection, and Application of Thermal Insulation for Piping and Machinery, (1997).

AWS D.1.1, Structural Welding Code, Steel, (2005).

AWS D.1.6, Structural Welding Code, Stainless-Steel, (1999).

CGA-G4.1 Cleaning equipment for oxygen service, third edition (1985)

CGA V – 1 – 1994, Compressed Gas Cylinder Valve Outlet Connections 7th Edition (1994).

CMAA 70, Specification for Electric Overhead Travelling Cranes, (1994).

HFS 100 – 1988, American National Standard for Human Factors Engineering of Visual Display Terminal Workstations, Human Factors Society (1988).

IBC, International Building Code, (2006).

IEEE 1100, Powering and Grounding Sensitive Electronic Equipment, (1993).

IEEE 141, Recommended Practice for Electric Power Distribution for Industrial Plants, (1993).

IEEE 142, IEEE Recommended Practice for Grounding of Industrial & Commercial Power Systems, (1991).

IEEE 242, Recommended Practice for Protection & Coordination of Industrial & Commercial Power Systems, (1986).

IEEE 484, Recommended Practice for Installation Design and Installation of Vented Lead Acid Storage Batteries for Stationary Applications, (1996).

IEEE 485, Recommended Practice for Sizing Lead Acid Storage Batteries for Stationary Applications, (1997).

IEEE 493, Recommended Practice for the Design of Reliable Industrial and Commercial Power systems, (1997).

IEEE 739, IEEE Recommended Practice for Energy Management in Industrial and Commercial Facilities, (1995).

IEEE 841, Standard for the Petroleum and Chemical Industry – Severe Duty Totally Enclosed Fan Cooled Squirrel Cage Induction Motors – Up to and Including 500 hp, (1994).

IEEE 845-1988, IEEE Guide to Evaluation of Man-Machine Performance in Nuclear Power Generating Stations, Control Rooms, and other Peripheries (1988).

IEEE C2, National Electric Safety Code, (1997).

IEEE C37.2, IEEE Standard Electric Power System Device Function Numbers, (1996).

IEEE C37.90, IEEE Standard for Relays and Relay Systems Associated with electric Power Apparatus, (1989) (R 19943).

IEEE C37.91, IEEE Guide for Protective Relay Applications to Power Transformers, (1985) (R 1990).

IEEE C57.12.00, IEEE Standard General Requirements for Liquid-Immersed Distribution, Power, and Regulating Transformers, (1993).

IEEE C57.93, IEEE Guide for Installation of Liquid-Immersed Transformers, (1995).

IEEE C62.11, IEEE Standard for Metal-Oxide Surge Arresters for Alternating Current Power Circuits, (1993).

IEEE C62.22, IEEE Guide for the Application of Metal-Oxide Surge Arresters for Alternating Current Systems, (1997).

IEEE C62.48, IEEE Guide on Interactions between Power System Disturbances and Surge-Protection Devices, (1995).

IEEE C95.3, Recommended Practice for the Measurement of Potential Hazardous Electromagnetic Fields – RF and Microwave, (1991).

IEEE/ANCI C95.1, Standard for Safety Levels with Respect to Human Exposure to Radio Frequency Electromagnetic Fields, 3 kHz to 300 GHz, (1991).

IESNA Lighting Handbook, 8th Edition, (1993).

ISO 14001, Environmental Management Systems – Specifications with Guidance for Use, (1996).

MSS – SP-58, Manufacturers Standardization Society, Pipe Hangers and Supports-, Materials, Design and Manufacture, (1993).

MSS-SP-69, Manufacturers Standardization Society, Pipe Hangers and Supports Selection and Application, (1996).

MSS-SP-89, Manufacturers Standardization Society, Pipe Hangers and Supports – Fabrication and Installation Practices, (1998).

NEMA 250, Enclosures for Electrical Equipment (1000 Volts Maximum), (1991).

NEMA MG 1-93, Motors and Generators, (1993) Revision 4.

NFPA 101, Life Safety Code, (2000).

NFPA 110, Standard for Emergency and Standby Power Systems, (2006).

FPA 13, Standard for the Installation of Sprinkler Systems, (1999).

NFPA 69, Standard on Explosion Prevention Systems, (2008).

NFPA 70, National Electric Code, (2005).

FPA 70E, Standard for Electrical Safety Requirements for Employee Workplaces, (2000).

NFPA 75, Standard for the Protection of Electronic Computer/Data Processing Equipment, (1999).

NFPA 801, Standard for Fire Protection for Facilities Handling Radioactive Materials, (2003).

NFPA 86, Standard for Ovens and Furnaces, (1999).

TEMA, Standards of the Tubular Exchanger Manufacturers Association, (1988), 7th Edition, Errata 1991.

TIMA, Economic Thickness Manual, Thermal Insulation Manufacturers Association ICBO, Uniform Building Code, (1997).

O Selected list of design and manufacture specifications, regulations, guidelines, rules, standards, handbooks, and manuals applied at Tritium Laboratory Karlsruhe

Planning, production, assembly and testing of equipment and vessels

AD (Association for Pressure Vessel Operation) explanatory leaflets

Accident prevention requirements (VBG)

VDE Regulations

Relevant DIN sheets

Materials sheet for steel and iron

VdTUV materials sheet

Test sheets for steel and iron

DVS explanatory leaflets

Pressure vessel regulations

Guidelines for the description and identification of KIT equipment

European Pressure Equipment Directive (PED 97/23/EC)

Fittings and components

DIN 2462 Part 1 pipes

DIN 267 Part 11 matching pairs of screws and nuts

Non-austenitic materials

DIN 17440 Surfaces of non-austenitic materials

DIN 17456 Table 6 and 8 Surface finishing

Paints

DIN 25412 Coating of ferritic steel

DIN 25415 Decontamination test of paints

Requirements for welding, qualification of welders, and preparations for welding

AD-Explanatory leaflets HPO, HP 2/1 Testing procedure

AD-Explanatory leaflets HP3 Supervision of welder, welder

AD-Explanatory leaflets HP 7/3 Heat treatment

DIN 8563 Part 3 Quality assurance of welding seam

DIN 8560 Qualification of steel welders

DIN 8558 Preparation of the weld

Din 8551 Part 1 and 4, Preparation of the welding

DIN 50049/2.3 Filler welding materials

Radiographic testing

DIN 54109 -54116 radiographic tests

DIN 54111 category B testing, quality of the image

DIN 54116 Analysis of radiographic pictures

DIN 8524, Part 1, defects in fusion welding of metals

Water pressure test for level II, III, and IV pressure vessels

AD leaflet HP30

Leak rate of glove boxes

DIN 25412

Gluing of plastics

DIN 1691

DVS leaflet 2204

Welding of plastics

DIN 1910 Part 3

DVS leaflet 2212

Radiation protection

Verordnung für die Umsetzung von EURATOM-Richtlinien zum Strahlenschutz, Bundesgesetzblatt Jahrgang 2001 Teil 1 Nr.38 am 26. Juli 2001

Safety cabinet for pressurized cylinders

DIN 12925

P Cryo-adsorption of hydrogen on active charcoal as function of temperature and pressure

Table P.1

Temp. K	248	223	198	173	148	123	98	73
P_{eq} (mbar)	1586.2	1578.4	1563.0	1531.9	1456.3	1323.6	1190.0	948.3
(cm^3 STPg^{-1})	2.7	4.3	9.7	22.3	56.9	118.8	178.4	287.9
	1388.1	1381.3	1367.3	1338.3	1283.2	1178.1	1011.7	806.0
	2.3	3.6	8.6	20.5	45.1	93.7	171.3	263.9
	1189.6	1183.6	1171.4	1146.1	1093.0	991.5	820.3	613.0
	1.9	3.1	7.4	18.0	42.0	89.6	221.3	226.4
	991.4	986.0	976.3	954.9	901.8	798.6	645.2	440.8
	2.0	3.6	7.5	16.7	41.4	90.7	163.5	259.1
	792.7	788.4	779.6	760.2	711.1	604.5	468.3	284.0
	2.4	3.5	6.7	15.4	38.4	89.9	154.6	241.0
	594.6	591.2	584.5	569.0	533.3	455.0	313.1	138.2
	2.0	3.8	6.4	13.6	30.2	68.0	137.1	221.2
	396.2	394.0	389.3	378.0	350.0	287.5	177.0	40.7
	1.6	2.3	4.0	8.9	21.2	51.5	105.4	170.8
	198.2	197.1	194.6	188.6	170.7	125.2	48.5	2.8
	0.5	0.9	1.6	4.4	12.9	35.3	73.2	94.4
	148.6	147.8	146.0	141.4	127.7	91.2	34.8	1.4
	0.25	0.5	1.2	3.2	9.8	27.8	55.8	71.5
	99.1	98.5	97.3	94.2	84.7	58.2	18.2	0.8
	0.20	0.4	0.8	2.2	6.8	20.0	39.8	47.9
	49.5	49.2	48.6	46.8	41.8	25.8	5.3	0.2
	0.10	0.25	0.46	1.3	3.7	11.7	21.9	24.1

Data are unpublished results from H.E. Noppel, 1996.

Q Dew point conversions

Table Q.1

Dew point K	Partial pressure mbar	Dew point K	Partial pressure mbar	Dew point K	Partial pressure mbar	Dew point K	Partial pressure mbar
273	6.106	247	0.5719	221	0.030 66	195	0.000 757 5
272	5.623	246	0.5169	220	0.027 02	194	0.000 644 2
271	5.172	245	0.4668	219	0.023 79	193	0.000 547 1
270	4.756	244	0.4224	218	0.020 91	192	0.000 463 8
269	4.371	243	0.3798	217	0.018 377	191	0.000 392 4
268	4.014	242	0.3420	216	0.016 117	190	0.000 331 5
267	3.684	241	0.3078	215	0.014 127	189	0.000 279 5
266	3.378	240	0.2769	214	0.012 358	188	0.000 235 3
265	3.097	239	0.2487	213	0.010 799	187	0.000 197 7
264	2.837	238	0.2233	212	0.009 431 0	186	0.000 165 8
263	2.597	237	0.2002	211	0.008 221 9	185	0.000 138 8
262	2.375	236	0.1794	210	0.007 158 2	184	0.000 116 0
261	2.172	235	0.1606	209	0.006 223 7	183	0.000 096 71
260	1.984	234	0.1434	208	0.005 405 3	182	0.000 080 47
259	1.810	233	0.1283	207	0.004 686 8	181	0.000 067 50
258	1.652	232	0.1145	206	0.004 059 0	180	0.000 055 41
257	1.506	231	0.1021	205	0.003 509 8	179	0.000 045 83
256	1.370	230	0.090 96	204	0.003 031 2	178	0.000 037 83
255	1.248	229	0.080 95	203	0.002 614 0	177	0.000 031 17
254	1.135	228	0.071 97	202	0.002 251 4	176	0.000 026 77
253	1.032	227	0.063 92	201	0.001 935 5	175	0.000 021 01
252	0.9368	226	0.056 71	200	0.001 662 3	174	0.000 017 18
251	0.8500	225	0.050 25	199	0.001 425 0	173	0.000 014 02
250	0.7707	224	0.044 48	198	0.001 220 0		
249	0.6984	223	0.039 34	197	0.001 049 9		
248	0.6322	222	0.034 75	196	0.000 889 2		

R Mass spectrometric resolutions required for the separation of the isotopes of hydrogen and helium

Table R.1

Species	Mass	Resolution m/Δm	Species	Mass	Resolution m/Δm
H	1.007276		DT	5.029500	9111.4
			H_2T	5.030052	1190.8
D	2.013500	1258.4	HD_2	5.034276	-
H_2	2.015100	-			
			T_2	6.031550	1276.2
He-3	3.015480	150774.0	HDT	6.036276	1429.0
T	3.015500	519.9	D_3	6.040500	-
HD	3.021300	5722.2			
H_3	3.021828	-	HT_2	7.038276	1666.3
			D_2T	7.042500	-
He-4	4.002050	188.1			
HT	4.023330	964.8	DT_2	8.044500	
D_2	4.027500	7296.2			
H_2D	4.028052	-	T_3	9.046500	

S Calorimetric measurements of the tritium inventory in a transportable uranium tritide vessel performed with four different calorimeters [Ale11a]

Table S.1

Measurement number	Tritium inventory mg*			
	ANTECH	IGC-A	IGC-V05	IGC-V25
1	31.83	30.81	31.10	30.98
2	31.77	30.80	31.10	30.99
3	31.00	30.85	31.16	31.21
4	31.06	30.86	31.17	-
5	30.64	30.89	31.20	-
Average	31.26	30.84	31.14	31.06
Trueness	1.54	0.10	0.09	0.10
Precision	0.52	0.04	0.05	0.13
TLK average		**31.08**		
TLK deviation		**0.18**		

Average of each calorimeter is the mean value

Trueness is accuracy determined using the average measured value

Precision is standard deviation of the results with respect to average value

TLK average is the mean value from results of all four calorimeters

TLK deviation is standard deviation of the results with respect to the TLK average

*Values corrected for decay.

T Vacuum technology relevant data of selected gases

Table T.1

Gas	Dynamic viscosity* η	Density**	Kinetic diameter	Conductance relative to air***	$C = I \times p$****
	$10^6\,\mathrm{kg\,m^{-1}\,s^{-1}}$	$\mathrm{g\,l^{-1}}$	nm	L_{gas}/L_{air}	cm mbar
H_2	9.3	0.0899	0.275	3.8	12.00×10^{-3}
D_2	13.1	0.1796	-	2.7	-
CH_4	11.8	0.7168	0.418	1.3	-
C_3H_8	8.7	2.010	-	0.8	-
He	21.0	0.1785	0.219	2.7	18.00×10^{-3}
Ne	33.1	0.900	0.259	1.2	12.30×10^{-3}
Ar	24.0	1.7878	0.366	0.9	6.40×10^{-3}
Air	19.4	1.293	0.367	1.0	-
N_2	18.7	1.251	0.378	1.0	6.10×10^{-3}
CO_2	16.2	1.977	0.466	0.8	3.95×10^{-3}

*at 1 bar and 323 K

**at 1 bar and 273 K

***for molecular flow

****C = mean free path I in cm and P in mbar at 293 K. This equation yields mean free path of various gases at pressure P.

U Temperature profile along a saturated and a non-saturated molecular sieve adsorber bed during regeneration [Won92]

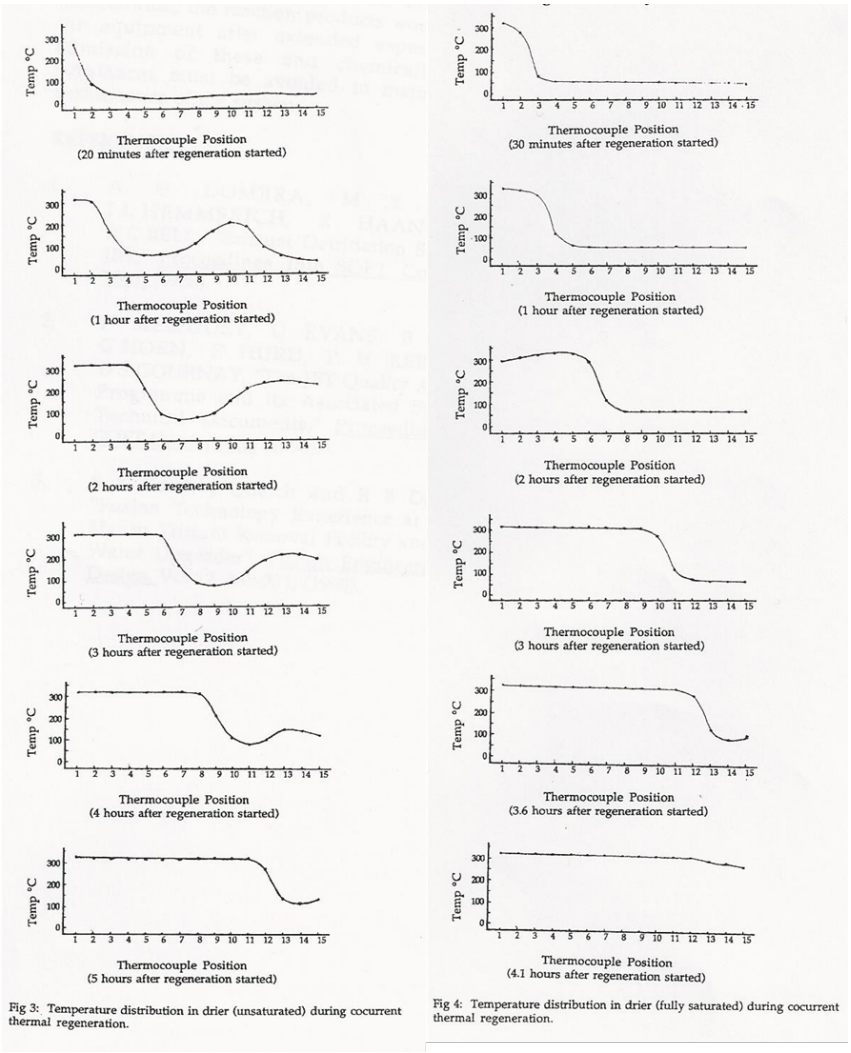


Fig 3: Temperature distribution in drier (unsaturated) during cocurrent thermal regeneration.

Fig 4: Temperature distribution in drier (fully saturated) during cocurrent thermal regeneration.

Figure U.1

V Licenses, Radiation Protection Instructions, Working Instructions, Working Procedures, Working Permits, Inspection Handbook, etc. regulating the operation of Tritium Laboratory Karlsruhe (TLK) (see also [Wel15])

TLK licenses for tritium and 100 kg ^{238}U assigned in accordance with the Radiation Protection Ordinance (Strahlenschutzverordnung (StrSchVO))

- License[1] T1/93 (3.5×10^{15} Bq)
- License T2/95 (7.0×10^{15} Bq)
- License T3/96 (7.0×10^{15} Bq)
- License T4/96 (1.4×10^{16} Bq)
- License T5/04 (^{14}C 1.0×10^{11} Bq)
- License T6/07 (1.4×10^{16} Bq plus licenses for uranium, Rb-83/84, and Kr-83)
- License F/305/89
- License diffractometer

[1] in German Genehmigung

Operation Handbook comprising 9 Radiation Protection Instructions (Strahlenschutzanweisungen (SAW))

- TLK Organisation (SAW 1)
- Radiation Protection Regulations (SAW 2)
- Handling of other Radioactive Substances at TLK (SAW 3)
- Execution of Experiments at TLK (SAW 4)
- Execution of Work at TLK (SAW 5)
- Admittance and Visitor Regulations (SAW 6 & 7)
- Alarm Regulations and Fire Protection (SAW 8 & 9)

Operation Instructions (Betriebsanweisungen)

Working Permit Radiation Protection (Arbeitserlaubnis Strahlenschutz (AES))

Working Instructions (Arbeitsanweisungen)

Inspection Manual (Prüfhandbuch)

- Inspection List (Prüfliste)
- Inspection Calendar (Prükalender)
- Inspection Procedures (Prüfanweisungen)
- Inspection Records (Prüfprotokolle)
- Inspection Proofs (Prüfnachweise)

Service Instructions (Dienstanweisungen (DAW))

Plant Technical Documentation

- Quality Documentation (Qualitätsdokumentation)
- Operator Documentation (Betriebsdokumentation)
- Safety Description (Sicherheitsbeschreibung)

Technical Terms of Delivery and Acceptance (Technische Liefer- und Abnahmebedingungen)

Technical Editing Process (Technischer Redaktionsprozess)

In addition, subsidiary General KIT Rules

- General Safety Regulations
- Terms for Acceptance of Radioactive Materials
- Regulations for Communication of Safety Relevant Incidents and Information to the Nuclear Supervisory Authority
- Official Strategies in Case of Emergencies
- Radiation Protection Instructions related to Personal Incorporation Monitoring
- Permissible Emissions for Exhaust Gases and Waste Water

W Exemption values, clearance levels, allowed activity concentration, and dosis coefficients for tritium (after [Bun01b])

Table W.1

Transport	
A1 value (ADR* class 7**)	$4 \times 10^1\,\mathrm{TBq}$
A2 value (ADR* class 7**)	$4 \times 10^1\,\mathrm{TBq}$
Exemption values	
Exemption value, activity	$1 \times 10^9\,\mathrm{Bq}$
Exemption value, activity concentration	$1 \times 10^6\,\mathrm{Bq\,g^{-1}}$
Surface contamination	$1 \times 10^2\,\mathrm{Bq\,cm^{-2}}$
Clearance levels	
Solids, liquids	$1 \times 10^3\,\mathrm{Bq\,g^{-1}}$
Rumble, break ground von $> 1000\,\mathrm{t\,year^{-1}}$	$6 \times 10^1\,\mathrm{Bq\,g^{-1}}$

Ground surfaces	$3\,\mathrm{Bq\,g^{-1}}$
Buildings for reuse or further use	$1 \times 10^3\,\mathrm{Bq\,cm^{-2}}$
Solids, liquids for disposal	$1 \times 10^3\,\mathrm{Bq\,g^{-1}}$
Buildings for demolition	$4 \times 10^3\,\mathrm{Bq\,cm^{-2}}$
Metal scrap for recycling	$1 \times 10^3\,\mathrm{Bq\,g^{-1}}$

Maximum allowed activity concentrations in radiation protection areas

In air, inhalation	$1 \times 10^2\,\mathrm{Bq\,m^{-3}}$
In water, ingestion	$1 \times 10^7\,\mathrm{Bq\,m^{-3}}$
In water, ingestion (organic)	$7 \times 10^6\,\mathrm{Bq\,m^{-3}}$

Dosis coefficients

Inhalation (water)	$1.8 \times 10^{-11}\,\mathrm{Bq\,m^{-3}}$
Inhalation (gas)	$1.8 \times 10^{-15}\,\mathrm{Bq\,m^{-3}}$
Ingestion (water and gas)	$1.8 \times 10^{-11}\,\mathrm{Bq\,m^{-3}}$
Inhalation (organically bound tritium)	$4.1 \times 10^{-11}\,\mathrm{Bq\,m^{-3}}$
Ingestion (organically bound tritium)	$4.2 \times 10^{-11}\,\mathrm{Bq\,m^{-3}}$

[1] Bundesgesetzblatt. 2001. Verordnung für die Umsetzung von EURATOM-Richtlinien zum Strahlenschutz. Report.

* ADR= European Agreement on International Carriage of Dangerous Goods by Road (Austria and Germany) (2009)

** Class 7 = radioactive substance

X Some codes and standards applicable to the design and manufacture of the ITER fuel cycle[1]

ASME Section VIII Div. 2 (vessels and its supports)

ASME B31.3 Category M (piping and its supports)

ASME B73.1M/B73.2M (pumps)

ASME B16.34 (valves)

ASME B31.3 Appendix X/EJMA (formed bellows)

EN 13445 – 2009 & (cryogenic pumps, metal flanges)

EN13445-3 Annex T (hydro formed components)

European standards for cryogenics)

[1] Glugla, M. Fuel Cycle: design, technologies and schedule, IBF/13-ITER, Buisness Forum, march 21-22, Toulou, France, 2013

Y Main isotopes in structural stainless-steel 56 mm inside of the plasma front side of the outboard shielding blanket of ITER 100 years after final shutdown of ITER [ITE01d]

Table Y.1

Radioisotope	Specific activity $\mathrm{Bq\,kg^{-1}}$	Fraction of activity %	Partial activities Bq
Ni-63	1.9×10^{10}	96	8.3×10^{14}
Ni-59	3.2×10^{8}	1.6	1.4×10^{13}
Nb-91	3.0×10^{8}	1.5	1.3×10^{13}
Mo-93	9.7×10^{7}	0.49	4.2×10^{12}
Nb-93m	8.3×10^{7}	0.42	3.7×10^{12}
C-14	6.5×10^{7}	0.33	2.9×10^{12}
Tc-99	6.5×10^{6}	0.033	2.8×10^{11}
Pt-193	4.9×10^{6}	0.025	2.1×10^{11}
H-3	4.3×10^{6}	0.022	1.9×10^{11}

Bibliography

Please note: Citations are given in numerical rather than chronological order.

[Abe17] R. G. Abernethy, Predicting the performance of tungsten in a fusion environment: a literature review, *Materials Science and Technologies*, 33 (2017) 388–399.

[Abe81] T. Abe, An assembly of tritium production experiment, *Proceedings of the US/Japan Workshop on Fusion Fuel Handling*, Oct. 13–15, 1980, Tokyo, Japan, (1981) 84–91.

[Abe90a] T. Abe, Y. Murakami, K. Hikida, H. Oshawa and S. Hata, Development of ceramic turbo molecular pumps for fusion devices, *Vacuum*, 42(7-9) (1990) 1992–1994.

[Abe90b] G. C. Abell, L. K. Matson, R. H. Steinmeyer, R. C. Bowman and B. M. Oliver, Helium released from aged palladium tritide, *Physical Review B*, 41(2) (1990) 1220–1223.

[Abr78] P. N. Abraham, T. S. Elleman and K. Verghese, Diffusion and trapping of tritium in grain boundaries of 304L stainless steel, *Journal of Nuclear Materials*, 73 (1978) 77–88.

[Abr90] E. Abramov, M. P. Riehm, D. A. Thompson and W. W. Smeltzer, Deuterium permeation and diffusion in high purity beryllium, *Journal of Nuclear Materials*, 175 (1990) 90–95.

[Ach90] H. J. Ache, M. Glugla, E. Hutter, G. Jourdan, R.-D. Penzhorn, D. Roehrig, K. Schubert, H. Sebening and H. J. E. Vetter, The Tritium Laboratory Karlsruhe: R&D work and laboratory layout, *Fusion Engineering and Design*, 12 (1990) 331–341.

[Ack72a] F. J. Ackerman and G. J. Koskinas, A model for predicting the permeation of hydrogen-deuterium/inert gas mixtures through palladium tubes, *Industrial and Engineering Chemistry Fundamentals*, 11(3) (1972) 332–338.

[Ack72b] F. J. Ackerman and G. J. Koskinas, Permeation of hydrogen and deuterium through palladium-silver alloys, *Journal of Chemical Engineering*, 17(1) (1972) 51–55.

[Ada83] R. O. Adams, A review of the stainless-steel surface, *Journal of Vacuum Science and Technologies A*, 1(1) (1983) 12–18.

[Add76] R. Addepalli and N. R. Rao, Infrared intensity analysis of molecules: Part I – CH_2D_2, CH_2T_2 and CD_2T_2 and CH_4, CD_4 & CT_4, *Indian Journal of Pure and Application Physics*, 14 (1976) 117–120.

[Agg02] S. Aggarwal, G. Charters and D. Blauvelt, Bulk building material characterization and decontamination using a concrete floor and wall contamination profiling technology, *Symposium on Waste Management*, Feb. 24–28, 2002, Tucson, AZ, USA, (2002).

[Ahn06] D.-H. Ahn, S. Paek, H.-J. Choi, K.-R. Kim, H. Chung, S. P. Yim and M. S. Lee, Development of water detritiation process using the hydrophobic platinum catalyst, *International Conference on Waste Management*, Feb. 26–Mar. 2, 2006, Tucson, AZ, USA, (2006).

[Aie01] A. Aiello, C. Fazio, I. Ricapito and G. Benamati, Hydrogen isotopes permeation through fusion oriented materials, *Proceedings of the International Tritium Workshop on Tritium-Material Interactions-Contamination and Decontamination*, Nov. 18–19, 2001, Toyama, Japan, (2001).

[Air11] A. Airapetov, L. Begrambekov, S. BrÃ©mont, D. Douaie, A. Kuzmin, Y. Sadovsky, P. Shigin and S. Vergasov, Glow discharge cleaning of carbon fiber composite and stainless steel, *Journal of Nuclear Materials*, 415 (2011) S1042–S1045.

[Aka08] K. Akaishi, Y. Torikai, D. Murata, R.-D. Penzhorn, K. Watanabe and M. Matsuyama, On the mechanism of tritium desorption from stainless steel, *Journal of Vacuum Science and Technologies A*, 26(3) (2008) 321–327.

[Ake19] M. Aker, K. Altenmueller, M. Arenz, M. Babutzka, J. Barrett, S. Bauer, M. Beck, A. Beglarian, J. Behrens, T. Bergmann, U. Besserer, K. Blaum, F. Block, S. Bobien, K. Bokeloh, J. Bonn, B. Bornschein, L. Bornschein, H. Bouquet, T. Brunst, T. S. Caldwell, L. La Cascio, S. Chilingaryan, W. Choi, T. J. Corona, K. Debowski, M. Deffert, M. Descher, P. J. Doe, O. Dragoun, G. Drexlin, J. A. Dunmore, S. Dyba, F. Edzards, L. Eisenblaetter, K. Eitel, E. Ellinger, R. Engel, S. Enomoto, M. Erhard, D. Eversheim, M. Fedkevych, A. Felden, S. Fischer, B. Flatt, J. A. Formaggio, F. M. Fränkle, G. B. Franklin, H. Frankrone, F. Friedel, D. Fuchs, A. Fulst, D. Furse, K. Gauda, H. Gemmeke, W. Gil, F. Glueck, S. Goerhardt, S. Groh, S. Grohmann, R. Groessle, R. Gumbsheimer, M. Ha Minh, M. Hackenjos, V. Hannen, F. Harms, J. Hartmann, N. Haußmann, F. Heizmann, K. Helbing, S. Hickford, D. Hilk, B. Hillen, D. Hillesheimer, D. Hinz, T. Hoehn, B. Holzapfel, S. Holzmann, T. Houdy, M. A. Howe, A. Huber, T. M. James, A. Jansen, A. Kaboth, C. Karl, O. Kazachenko, J. Kellerer, N. Kernert, L. Kippenbrock, M. Kleesiek, M. Klein, C. Koehler, L. Koellenberger, A. Kopmann, M. Korzeczek, A. Kosmider, A. Kovalík, B. Krasch, M. Kraus, H. Krause, L. Kuckert, B. Kuffner, N. Kunka, T. Lasserre, T. L. Le, O. Lebeda, M. Leber, B. Lehnert, J. Letnev, F. Leven, S. Lichter, V. M. Lobashev, A. Lokhov, M. Machatschek, E. Malcherek, K. Mueller, M. Mark, A. Marsteller, E. L. Martin, C. Melzer, A. Menshikov, S. Mertens, L. I. Minter, S. Mirz, B. Monreal, P. I. Morales Guzman, K. Mueller, U. Naumann, W. Ndeke, H. Neumann, S. Niemes, M. Noe, N. S. Oblath, H.-W. Ortjohann, A. Osipowicz, B. Ostrick, E. Otten, D. S. Parno, D. G. Phillips, P. Plischke, A. Pollithy, A. W. P. Poon, J. Pouryamout, M. Prall, F. Priester, M. Roellig, C. Roettele, P. C.-O. Ranitzsch, O. Rest, R. Rinderspacher,

R. G. H. Robertson, C. Rodenbeck, P. Rohr, C. Roll, S. Rupp, M. Ry šavý, R. Sack, A. Saenz, P. Schaefer, L. Schimpf, K. Schloesser, M. Schloesser, L. Schlueter, H. Schoen, K. Schoenung, M. Schrank, B. Schulz, J. Schwarz, H. Seitz-Moskaliuk, W. Seller, V. Sibille, D. Siegmann, A. Skasyrskaya, M. Slezák, A. Špalek, F. Spanier, M. Steidl, N. Steinbrink, M. Sturm, M. Suesser, M. Sun, D. Tcherniakhovski, H. H. Telle, T. Thuemmler, L. A. Thorne, N. Titov, I. Tkachev, N. Trost, K. Urban, D. Vénos, K. Valerius, B. A. VanDevender, R. Vianden, A. P. Vizcaya Hernández, B. L. Wall, S. Wüstling, M. Weber, C. Weinheimer, C. Weiss, S. Welte, J. Wendel, K. J. Wierman, J. F. Wilkerson, J. Wolf, W. Xu, Y.-R. Yen, M. Zacher, S. Zadorozhny, M. Zbo řil and G. Zeller, Improved upper limit on the neutrino mass from a direct kinematic method by KATRIN, *Physical Review Letters*, 123 (2019) 221802.

[Ake20] M. Aker, K. Altenmueller, M. Arenz, W.-J. Baek, J. Barrett, A. Beglarian, J. Behrens, A. Berlev, U. Besserer, K. Blaum, F. Block, S. Bobien, B. Bornschein, L. Bornschein, H. Bouquet, T. Brunst, T. S. Caldwell, S. Chilingaryan, W. Choi, K. Debowski, M. Deffert, M. Descher, D. Díaz Barrero, P. J. Doe, O. Dragoun, G. Drexlin, S. Dyba, F. Edzards, K. Eitel, E. Ellinger, R. Engel, S. Enomoto, D. Eversheim, M. Fedkevych, A. Felden, J. A. Formaggio, F. M. Fraenkle, G. B. Franklin, H. Frankrone, F. Friedel, D. Fuchs, A. Fulst, K. Gauda, W. Gil, F. Glueck, S. Grohmann, R. Groessle, R. Gumbsheimer, M. Hackenjos, V. Hannen, J. Hartmann, N. Haußmann, M. Ha-Minh, F. Heizmann, J. Heizmann, K. Helbing, S. Hickford, D. Hillesheimer, D. Hinz, T. Hoehn, B. Holzapfel, S. Holzmann, T. Houdy, M. A. Howe, A. Huber, A. Jansen, C. Karl, J. Kellerer, N. Kernert, L. Kippenbrock, M. Klein, C. Koehler, L. Koellenberger, A. Kopmann, M. Korzeczek, A. Kovalík, B. Krasch, H. Krause, B. Kuffner, N. Kunka, T. Lasserre, L. La Cascio, O. Lebeda, M. Lebert, B. Lehnert, J. Letnev, F. Leven, T.-L. Le, S. Lichter, A. Lokhov, M. Machatschek, E. Malcherek, M. Mark, A. Marsteller, E. L. Martin, F. Megas, C. Melzer, A. Menshikov, S. Mertens, M. Meier, S. Mirz, B. Monreal, P. I. Morales Guzmán, K. Mueller, U. Naumann, H. Neumann, S. Niemes, M. Noe, A. Off, H.-W. Ortjohann, A. Osipowicz, E. Otten, D. S. Parno, A. Pollithy, A. W. P. Poon, J. M. Lopez Poyato, F. Priester, P. C.-O. Ranitzsch, O. Rest, R. Rinderspacher, R. G. H. Robertson, C. Rodenbeck, P. Rohr,

M. Roellig, C. Roettele, M. Ryšavý, R. Sack, A. Saenz, P. Schaefer, L. Schimpf, K. Schloesser, M. Schloesser, L. Schlüter, M. Schrank, B. Schulz, H. Seitz-Moskaliuk, W. Seller, V. Sibille, D. Siegmann, M. Slezák, F. Spanier, M. Steidl, M. Steven, M. Sturm, M. Suesser, M. Sun, D. Tcherniakhovski, H. H. Telle, L. A. Thorne, T. Thümmler, N. Titov, I. Tkachev, N. Trost, K. Urban, K. Valerius, D. Vénos, R. Vianden, A. P. Vizcaya Hernández, M. Weber, C. Weinheimer, C. Weiss, S. Welte, J. Wendel, J. F. Wilkerson, J. Wolf, S. Wuestling, W. Xu, Y.-R. Yen, S. Zadorozhny and G. Zeller, First operation of the KATRIN experiment with tritium, *The European Physical Journal C*, 80(3) (2020) 264.

[Ake96] T. Akermark, G. Hultquist and Q. Lu, Release of water and hydrogen during outgassing of some materials, *Journal of Material Engineering and Performance*, 5 (1996) 516–520.

[Aki87] E. Akiba, K. Nomura and S. Ono, A new hydride phase of $LaNi_5H_3$, *Journal of Less-Common Metals*, 129 (1987) 159–164.

[Aku04] Y. A. Akulov and B. A. Mamyrin, Difference between the triton beta decay constants in atomic and molecular tritium measured by the helium isotope method, *Physics Letters B*, 600(1-2) (2004) 41–47.

[Aku05] Y. A. Akulov and B. A. Mamyrin, Half-life and $fT_{1/2}$ value for the bare triton, *Physics Letters B*, 610(1-2) (2005) 45–49.

[Alb00] H. Albrecht and E. Hutter, Tritium recovery from an ITER ceramic test blanket module - process options and critical R&D issues, *Fusion Engineering and Design*, 49-50 (2000) 769–773.

[Alb56] W. Albrecht and M. Mallett, Reaction of hydrogen with uranium, *Journal of the Electrochemical Society*, 103(7) (1956) 404–409.

[Alb58] W. Albrecht and M. Mallett, Reaction of hydrogen with uranium, *Journal of the Electrochemical Society*, 105(10) (1958) 610–611.

[Ale02] I. A. Alekseev, S. D. Bondarenko, O. A. Fedorchenko, A. I. Grushko, S. P. Karpov, K. A. Konoplev, V. D. Trenin, E. A. Arkhipov, T. V. Vasyanina, T. V. Voronina and V. V. Uborsky, The CECE experimental industrial plant for reprocessing of tritiated water wastes, *Fusion Science and Technology*, 41 (2002) 1097–1101.

[Ale11a] C. G. Alecu, U. Besserer, B. Bornschein, B. Kloppe, Z. Koelloe and J. Wendel, Reachable accuracy and precision for tritium measurements by calorimetry at TLK, *Fusion Science and Technology*, 60(3) (2011) 937–940.

[Ale11b] I. A. Alekseev, S. D. Bondarenko, O. A. Fedorchenko, T. V. Vasyanina, K. A. Konoplev, E. A. Arkhipov and V. V. Uborsky, Fifteen years of operation of CECE experimental industrial plant in PNPI, *Fusion Science and Technology*, 60(3) (2011) 1117–1120.

[Ale62] M. Alei, The reaction between uranium hydride and ammonia at room temperature, *Journal of Physical Chemistry*, 66(1) (1962) 145–148.

[Ale78] G. Alefeld and J. Volkl, Hydrogen in metals, Vol. 1, Springer Verlag, Berlin (1978).

[Ali01] V. K. Alimov, Deuterium retention in beryllium pre-implanted with helium ions, *Advisory Group Meeting on the "Assessment of new data for tritium retention in fusion reactor materials"*, July 2–3, 2001, Vienna, Austria, (2001).

[Ali05] V. K. Alimov, J. Roth and M. Mayer, Depth distribution of deuterium in single and polycristalline tungsten up to depths of several micrometres, *Journal of Nuclear Materials*, 337-339 (2005) 619–623.

[Ali08] V. K. Alimov, J. Roth, R. A. Causey, D. A. Komarov, C. Linsmeier, A. Wiltner, F. Kost and S. Lindig, Deuterium retention in tungsten exposed to low-energy, high-flux clean and carbon seeded deuterium plasmas, *Jounal of Nuclear Materials*, 375 (2008) 192–201.

[Ali66] R. M. Alire and J. H. McCrary, Reaction kinetics of powdered uranium and deuteroammonia, *Journal of Chemical Physics*, 45(11) (1966) 3958–3965.

[Ali70] R. M. Alire, B. A. Mueller, C. L. Peterson and J. R. Mosley, Reaction kinetics of uranium and deuterium, *Journal of Chemical Physics*, 52(1) (1970) 37–46.

[Ali81] R. M. Alire, P. E. Barry, S. A. Steward and R. K. Stump, Studies of materials exhibiting low tritium permeation rates, 9^{th} *Symposium on Engineering Problems of Fusion Research*, Oct. 26, 1981, Chicago, IL, USA, (1981).

[Ali97] V. K. Alimov, V. N. Chernikov and A. P. Zakharov, Depth distribution of deuterium atoms and molecules in beryllium implanted with D ions, *Journal of Nuclear Materials*, 243 (1997) 1047–1051.

[Alt81] R. M. Al'tovskij, A. A. Eremin, L. F. Eremina, L. A. Izhvanov, V. N. Fadeev and M. I. Urazbaev, Hydrogen permeability of beryllium, *Izvestiya Akademii Nauk SSSR*, 13(20) (1981) 73–77.

[Ami66] F. Amilhat-Caralp, L. Casahoursat and M. Destriau, Variation avec la temperature de la vitesse d'hydrogenation de l'uranium, *Bulletin de la Societe Chimique de France*, 11 (1966) 3594.

[An08] Z. An, Q. Hou and J. Long, Reconstruction of depth distribution of tritium in materials by β-ray induced X-ray spectrometry, *Nuclear Instruments and Methods in Physics Research Section B: Beam Interactions with Materials and Atoms*, 266(16) (2008) 3643–3646.

[Ana09] R. G. Ana, I. Cristescu, L. Doerr, R. Michling, S. Welte and W. Wurster, Design and experimental activities in view of water detritiation and isotopic separation systems combination in TRENTA facility, *Fusion Engineering and Design*, 84(2-6) (2009) 398–403.

[And00] R. A. Anderl, R. J. Pawelko, G. R. Smolik, F. Scaffidi-Argentina and D. Davydov, Steam chemical reactivity of Be pebbles and Be powder, *Fusion Technology*, 38(3) (2000) 283–289.

[And02] R. A. Anderl, D. A. Petti, K. McCarthy and G. Longhurst, The Safety and Tritium Applied Research Facility, *Fusion Science and Technology*, 41(3P2) (2002) 568–572.

[And05] R. A. Anderl, G. R. Longhurst, R. J. Pawelko, J. P. Sharpe, S. T. Schuetz and D. A. Petti, The Safety and Tritium Applied Research (STAR) facility: Status-2004, *Fusion Science and Technology*, 48(1) (2005) 243–249.

[And13] O. Anderoglu, T. S. Byun, M. Toloczko and M. S. A., Mechanical performance of ferritic martensitic steels for high dose applications in advanced nuclear reactors, *Metallurgical and Materials Transactions A*, 44(1) (2013) 70–83.

[And75] J. Anderson, Material Use, Tritium Operating Safety Seminar, technical report LA-6307-C, Los Alamos Scientific Laboratory, Los Alamos, NM, USA (1975).

[And77] J. L. Anderson and R. H. Sherman, Tritium Systems Test Assembly: Design for Major Device Fabrication Review, technical report LA-6855-P, Los Alamos Scientific Lab., Los Alamos, NM, USA (1977).

[And80] D. F. Anderson and R. D. Hiebert, An improved Kanne tritium monitoring system, *International Symposium on Management of Gaseous Wastes from Nuclear Facilities*, Feb. 18, 1980, Vienna, Austria, (1980).

[And82] J. L. Anderson, Tritium Systems Test Assembly: Final Safety Analysis /Report, technical report SAR-82-1F, Los Alamos National Laboratory, Los Alamos, NM, USA (1982).

[And85] J. L. Anderson, J. R. Bartlit and R. V. Carlson, Tritium Systems Test Assembly Emergency Plan, TTA-EP-100-1, RO, (1985).

[And88] J. L. Anderson, J. R. Bartlit, R. V. Carlson, D. O. Coffin, F. A. Damiano, R. H. Sherman, R. S. Willms, H. Yoshida, T. Yamanishi, T. Naito, S. Hirata and Y. Naruse, Experience of TSTA milestone runs with 100 grams-level of tritium, *Fusion Technology*, 14(2P2A) (1988) 438–443.

[And91] P. L. Andrew and A. A. Haasz, Hydrogen permeation through copper-coated palladium, *Journal of Applied Physics*, 70(7) (1991) 3600–3604.

[And92a] R. A. Anderl, M. R. Hankins, G. R. Longhurst, R. J. Pawelko and R. G. Macaulay-Newcombe, Hydrogen transport behaviour of beryllium, *Journal of Nuclear Materials*, 196-198 (1992) 986–991.

[And92b] R. A. Anderl, D. F. Holland, G. R. Longhurst, R. J. Pawelko, C. L. Trybus and C. H. Sellers, Deuterium transport and trapping in polycrystalline tungsten, *Fusion Technology*, 21(2P2) (1992) 745–752.

[And92c] J. L. Anderson, Tritium technology programs in the United States, *Fusion Technology*, 21(2P2) (1992) 226–231.

[And94a] J. L. Anderson, R. A. P. Sissingh, C. A. Gentile, R. L. Rossmassler, R. T. Walters and D. R. Voorhees, Initial testing of the tritium systems at the Tokamak Fusion Test Reactor, *Proceedings of the 15th Symposium on Fusion Engineering (SOFE)*, Oct. 11–15, 1993, Hyannis, MA, USA, (1994) 208–211.

[And94b] J. Anderson, R. Sissingh, C. Gentile, R. Rossmassler, R. Walters and D. Voorhees, Initial testing of the tritium systems at the Tokamak Fusion Test Reactor, *11^{th} ANS Meeting on Fusion Energy*, June 19–24, 1994, New Orleans, (1994) 208–211.

[And95a] R. A. Anderl, J. D. Baker, G. L. Bourne and R. J. Pawelko, Tritium and helium release from irradiated beryllium, *Fusion Technology*, 28(3P2) (1995) 1114–1119.

[And95b] J. L. Anderson and P. LaMarche, Tritium activities in the United States, *Fusion Technology*, 28(3P1) (1995) 479–490.

[And95c] J. L. Anderson and K. Okuno, Tritium handling and processing experience at the Tritium Systems Test Assembly, *Fusion Engineering and Design*, 28 (1995) 183–189.

[And95d] J. Anderson, C. Gentile, M. Kalish, J. Kamperschroer, T. Kozub, P. LaMarche, H. Murray, A. Nagy, S. Raftopoulos, R. Rossmassler, R. Sissingh, J. Swanson, F. Tulipano, M. Viola, D. Voohees and R. Walthers, Operation of the Tokamak Fusion Test Reactor tritium systems during initial tritium experiments, *Fusion Engineering and Design*, 28 (1995) 209–214.

[And95e] R. Andreani, A. Bell, D. Murdoch, R.-D. Penzhorn and G. Vassallo, Tritium related fusion R&D activities in Europe, *Fusion Technology*, 28(3P1) (1995) 449–459.

[And99] R. A. Anderl and R. J. Pawelko, BET surface area and tritium analyses for TFTR carbon dust samples, *Proceedings of the 4^{th} International Workshop on Tritium Effects in Plasma Facing Components*, May 14–15, 1998, Santa Fe, NM, USA, (1999) 20–22.

[Ant05] A. Antipenkov, C. Day, R. Laesser, A. Mack and R. Wagner, Tritium pumps for ITER roughing system, *Fusion Science and Technology*, 48(1) (2005) 47–50.

[Ant08a] A. Antipenkov, C. Day and H.-D. Adami, Tritium test of a ferrofluidic rotary seal, *Fusion Science and Technology*, 54 (2008) 35–38.

[Ant08b] A. B. Antoniazzi and C. S. Morton, Disposal pathway for tritiated reactive metals and tritiated hydrogen gas, *Fusion Science and Technology*, 54(1) (2008) 219–222.

[Ant95] A. B. Antoniazzi and W. T. Shmayda, Assessment of tritium inventory in waste by outgassing measurements, *Fusion Technology*, 28(3P2) (1995) 1457–1462.

[Ara82] Y. Aratono, E. Tachikawa, T. Miyazaki, Y. Kawai and K. Fueki, Temperature effect on recoil tritium reactions in solid alkanes at 20-300 K. Comparison of recoil tritium atoms with hydrogen(deuterium) atoms in radiolysis, *The Journal of Physical Chemistry*, 86(2) (1982) 248–251.

[Ara97] M. Araki, Y. Kude, Y. Sohda, K. Nakamura, K. Sato, S. Suzuki and M. Akiba, Development of 3D-based CFC with high thermal conductivity for fusion application, *Proceedings of the 19th Symposium on Fusion Technology (SOFT)*, Sept. 16–20, 1996, Lisbon, Portugal, (1997) 359–362.

[Ari02] T. Arita, T. Yamanishi, Y. Iwai, M. Nishi and I. Yamamoto, Experimental study for parameters affecting separation factor of cryogenic wall thermal diffusion column, *Fusion Science and Technology*, 41(3P2) (2002) 1116–1120.

[Ari05] A. A. Arias, E. N. Schmierer, D. Gettemy, D. W. Howard, J. R. Wermer and D. G. Tuggle, Thermal Cycling Absorption Process (TCAP): Instrument and simulation development status at Los Alamos National Laboratory, *Fusion Science and Technology*, 48(1) (2005) 159–162.

[Ase01] V. Aseev, A. Belesev, A. Berlev, H. Bluemer, J. Bonn, B. Bornschein, L. Bornschein, L. Doerr, G. Drexlin, K. Eitel, B. Flatt, E. Geraskin, M. Glugla, A. Golubev, C. Kraus, O. Kasachenko, R. Laesser, V. Lobashev, G. Meisel, A. Osipowicz, E. Otten, R.-D. Penzhorn, P. Plischke, J.-P. Schall, F. Schwamm, M. Steidl, T. Thuemmler, N. Titov, V. Usanov, C. Weinheimer and S. Zadoroghny, A next generation tritium beta decay experiment with sub-eV sensitivity for the electron neutrino mass, *International*

Workshop on Neutrino Masses in the sub-eV Range, June 2001, Bad Lieberzell, Germany, (2001).

[Ash20] N. Ashikawa, Y. Torikai, N. Asakura, T. Otsuka, A. Widdowson, M. Rubel, M. Oyaizu, M. Hara, S. Masuzaki, K. Isobe, Y. Hatano, K. Heinola, A. Baron-Wiechec, S. Jachmich and T. Hayashi, Determination of retained tritium from ILW dust particles in JET, *Nuclear Materials and Energy*, 22 (2020) 100673.

[Ass94] W. Assmann, P. Hartung, H. Huber, P. Staat, H. Steffens and C. Steinhausen, Setup for materials analysis with heavy ion beams at the Munich MP tandem, *Nuclear Instruments and Methods in Physics Research Section B: Beam Interactions with Materials and Atoms*, 85(1-4) (1994) 726–731.

[AST68] ASTM International, Test for Rubber Property - Compression Set Induced by Nuclear Radiation, industry norm D2309-68, (1968).

[Att76] A. Attala, C. T. Bishop, D. R. Bohl, T. L. Buxton, R. E. Sprague and D. K. Warner, Assessment of methods for analysing gaseous mixtures of hydrogen isotopes and helium, technical report MLM-2376, Mound Laboratories, Miamisburg, Ohio, USA (1976).

[Aud14] M. Audi, S. Giors and R. Gotta, The state of the art in molecular-drag turbo-pump technology, https://www.vacuum-uk.org/pdfs/vs2/VacPumps/TwisTorr.pdf, (2014), (visited on Apr. 13, 2022).

[Aus72] J. H. Austin and T. S. Elleman, Tritium diffusion in 304- and 316-stainless steels in the temperature range 25 to 222 °C, *Journal of Nuclear Materials*, 43(2) (1972) 119–125.

[Aus73] J. H. Austin, T. S. Elleman and K. Verghese, Surface effects on the diffusion of tritium in 304-stainless steel and zircaloy-2, *Journal of Nuclear Materials*, 48(3) (1973) 307–316.

[Avr39] M. Avrami, Kinetics of phase change. I General theory, *The Journal of Chemical Physics*, 7(12) (1939) 1103–1112.

[Avr40] M. Avrami, Kinetics of phase change. II Transformation-Time relations for random distribution of nuclei, *The Journal of Chemical Physics*, 8(2) (1940) 212–224.

[Aym01] R. Aymar, V. A. Chuyanov, M. Huguet, Y. Shimomura, ITER Joint Central Team and ITER Home Teams, Overview of ITER-FEAT - The future international burning plasma experiment, *Nuclear Fusion*, 41(10) (2001) 1301–1310.

[Aym97] R. Aymar, ITER overview, *Fusion Engineering and Design*, 36(1) (1997) 9–21.

[Bac62] L. Bachmann, E. Bechtold and E. Cremer, Gas-chromatographic separation of ortho- and parahydrogen on molecular sieves: Analysis, preparation, and measurement of catalytic conversion and of adsorption, *Journal of Catalysis*, 1(2) (1962) 113–120.

[Bah02] W. Bahm, G. Dammertz, M. Glugla, G. Janeschitz, P. Komarek and A. Mack, Entwicklung von Technologien fuer die Kernfusion im Forschungszentrum Karlsruhe - Teil 1, *Atw. Internationale Zeitschrift fuer Kernenergie*, 47(2) (2002) 96–106.

[Bai99a] N. Bainbridge, A. C. Bell, P. D. Brennan, S. Knipe, R. Laesser and R. Stagg, Operational experience with the JET AGHS cryodistillation system during and after DTE1, *Fusion Engineering and Design*, 47(2-3) (1999) 321–332.

[Bai99b] J. K. Baird and E. M. Schwartz, Isotope effect in hydrogen diffusion in metals, *Zeitschrift fuer Physikalische Chemie*, 211(1) (1999) 47–68.

[Bak66] M. M. Baker, L. N. Less and S. Orman, Uranium + water reaction. Part 1. - Kinetics, products and mechanism, *Transactions of the Faraday Society*, 62 (1966) 2513–2524.

[Bak68] R. T. K. Baker and R. Wolfgang, On the origin of bond-energy effects on hot hydrogen abstraction, *Journal of the American Chemical Society*, 90(16) (1968) 4473â “4474.

[Bak81] C. Baker, M. Abdou, C. Boley, A. Bolon, J. Brooks, R. Clemmer, D. Ehst, K. Evans, P. Finn, R. Fuja, Y. Gohar, J. Jung, W. Kann, R. Mattas, B. Misra, H. Schreyer, D. Smith, H. Stevens, L. Turner, D. De Freece, C. Dillow, G. Morgan, C. Trachsel, D. Graumann, J. Alcorn, R. Fields, R. Prater, J. Kokoszenski, K. Barry, M. Cherry, H. Klumpe, R. Conn, G. Emmert, I. Sviatoslavsky and D. Sze, STARFIRE: A commercial tokamak power plant design, *Nuclear Engineering and Design*, 63(2) (1981) 199–231.

[Bal06] M. J. Baldwin and R. P. Doerner, A time resolved study of the mitigation of graphite chemical erosion in deuterium plasmas containing beryllium, *Nuclear Fusion*, 46(4) (2006) 444–450.

[Bal12] A. Ballarino, P. Bauer, Y. Bi, A. Devred, K. Ding, A. Foussat, N. Mitchell, G. Shen, Y. Song, T. Taylor, Y. Yang and T. Zhou, Design of the HTS current leads for ITER, *IEEE Transactions on Applied Superconductivity*, 22(3) (2012) 4800304.

[Bal74] R. R. Baldwin, M. E. Fuller, J. S. Hillman, D. Jackson and R. W. Walker, Second limit of hydrogen + oxygen mixtures: the reaction $H + HO_2$, *Journal of the Chemical Society, Faraday Transactions 1: Physical Chemistry in Condensed Phases*, 70(12) (1974) 635–641.

[Bal78] R. W. Balluffi, Vacancy defect mobilities and binding energies obtained from annealing studies, *Journal of Nuclear Materials*, 69-70 (1978) 240–263.

[Bal93] D. L. Baldwin, Tritium release studies of irradiated beryllium, *Workshop on Beryllium for Fusion Applications*, Oct. 4–5, 1993, Karlsruhe, Germany, (1993).

[Bal94] D. L. Baldwin and M. C. Billone, Diffusion/desorption of tritium from irradiated beryllium, *Journal of Nuclear Materials*, 212-215 (1994) 948–953.

[Ban84] K. Bange, D. E. Grider, T. E. Madey and J. K. Sass, The surface chemistry of H_2O on clean and oxygen-covered Cu(110), *Surface Science*, 137(1) (1984) 38–64.

[Bar09] V. Barabash, Summary of material properties for structural analysis of the ITER internal components, technical report ITER-D-23HL7T v.3, (2009).

[Bar61] C. J. Barton, A review of glove box construction and experimentation, technical report ORNL-3070, Reactor Chemistry Division, Oak Ridge National Laboratory, Oak Ridge, NM, USA (1961).

[Bar71] R. M. Barrer and D. E. W. Vaughan, Trapping of inert gases in sodalite and cancrinite crystals, *Journal of Physics and Chemistry of Solids*, 32(3) (1971) 731–743.

[Bar79a] J.-L. Baron, A. Virot and J. Delaplace, Etude d'alliages zirconium-nickel en vue du stockage de l'hydrogene sous forme d'hydrures, *Journal of Nuclear Materials*, 83(2) (1979) 286–297.

[Bar79b] J. R. Bartlit, R. H. Sherman, R. A. Stutz and W. H. Denton, Hydrogen isotope distillation for fusion power reactors, *Cryogenics*, 19(5) (1979) 275–279.

[Bar83] J. Barrault, D. Duprez, A. Percheron-Guégan and J. C. Achard, Intermetallic compounds as catalysts for reactions of heterogeneous catalysis, *Journal of the Less-Common Metals*, 89(2) (1983) 537–543.

[Bar89] J. R. Bartlit, J. L. Anderson, R. A. Jalbert, R. V. Carlson, K. Okuno, T. Ide, H. Fukui, M. Enoeda and Y. Naruse, Dispersion and removal of tritium released into the main cell of TSTA, *Proceedings of the 13th Symposium on Fusion Engineering IEEE*, Oct. 2–6, 1989, Knoxville, TN, USA, (1989) 798–883.

[Bar90] J. R. Bartlit, The Tritium Systems Test Assembly at Los Alamos National Laboratory, *Fusion Engineering and Design*, 12(3) (1990) 393–402.

[Bar91] G. W. Barnes, A. Janos, D. Loesser, D. K. Owens and M. Ulrickson, The TFTR bumper limiter performance enhancements, *Fusion Technology*, 19(3P2B) (1991) 1761–1764.

[Bar97] V. Barabash, J. Dietz, K. Ioki, G. Janeschitz, G. Kalinin, R. Matera and K. Mohri, Materials aspects of ITER in-vessel components, *Proceedings of the 19th Symposium on Fusion Technology (SOFT)*, Sept. 16–20, 1996, Lisbon, Portugal, (1997) 347–350.

[Bas60a] D. Basmadjian, Adsorption equilibria of hydrogen, deuterium, and their mixtures. Part I, *Canadian Journal of Chemistry*, 38(1) (1960) 141–148.

[Bas60b] D. Basmadjian, Adsorption equilibria of hydrogen, deuterium, and their mixtures. Part II, *Canadian Journal of Chemistry*, 38(1) (1960) 149–156.

[Bas80] M. I. Baskes, A calculation of the surface recombination rate constant for hydrogen isotopes on metals, *Journal of Nuclear Materials*, 92(2-3) (1980) 318–324.

[Bat81] T. H. Batzer, R. E. Patrick and W. R. Call, A TSTA compound cryopump, *Journal of Vacuum Science and Technology*, 18(3) (1981) 1125–1130.

[Bau92] G. Baumgaertel, H. R. Ihle, R. Kraemer and R.-D. Penzhorn, Vorkommen, Herstellung und Verwendung von Tritium, *Tritium*, A. Fiege, editor, Kernforschungszentrum Karlsruhe GmbH, (1992), 25–42.

[Bax98] C. B. Baxi, B. Beaumont, P. Libeyre, P. Ladd, B. De Gentile and G. Claudet, Enthalpy recovery system for ITER cryo-pumps, *Proceedings of the 20th Symposium on Fusion Technology (SOFT)*, Sept. 7–11, 1998, Marseille, France, (1998) 945–948.

[Bea72] W. H. Beattie, The radiolysis of mixtures of carbon dioxide and hydrogen, *International Journal of Chemical Kinetics*, 4(4) (1972) 463–477.

[Bea73a] W. H. Beattie, The radiolysis of mixtures of carbon monoxide and hydrogen, *International Journal of Chemical Kinetics*, 5(3) (1973) 333–343.

[Bea73b] L. C. Beavis, Formation of triatomic ions of hydrogen in the ion source of gas analysers, *Journal of Vacuum Science and Technology*, 10(2) (1973) 416–417.

[Bea73c] L. C. Beavis, Interaction of hydrogen with the surface of type 304 stainless steel, *Journal of Vacuum Science and Technology*, 10(2) (1973) 386–390.

[Bee13] B. Beeler, C. Deo, M. Baskes and M. Okuniewski, First principles calculations of the structure and elastic constants of α, β and γ uranium, *Journal of Nuclear Materials*, 433(1-3) (2013) 143–151.

[Beg78] D. R. Begeal, Hydrogen and deuterium permeation in copper alloys, copper-gold brazing alloys, gold, and the in situ growth of stable oxide permeation barriers, *Journal of Vacuum Science and Technology*, 15(3) (1978) 1146–1154.

[Beh00] R. Behrisch, M. Mayer, W. Jacob, W. Assmann, G. Dollinger, A. Bergmaier, U. Kreissig, M. Friedrich, G. Y. Sun, D. Hildebrandt, M. Akbi, W. Schneider, D. Schleussner, W. Knapp and C. Edelmann, Quantitative analysis of deuterium in a-C:D layers, a Round Robin experiment, *Journal of Nuclear Materials*, 281(1) (2000) 42–56.

[Beh98] R. Behrisch, V. Khripunov, R. T. Santoro and J. M. Yesil, Transmutation of plasma facing materials by the neutron flux in a DT fusion reactor, *Journal of Nuclear Materials*, 258-263 (1998) 686–693.

[Bek00] N. Bekris, U. Besserer, M. Sirch and R.-D. Penzhorn, On the thermal stability of the zirconium/cobalt-hydrogen system, *Fusion Engineering and Design*, 49-50 (2000) 781–789.

[Bek01] N. Bekris, E. Hutter, H. Albrecht, R.-D. Penzhorn and D. Murdoch, Cold trapping of traces of tritiated water from the helium loops of a fusion breeder blanket, *Fusion Engineering and Design*, 58-59 (2001) 423–428.

[Bek02a] N. Bekris, Tritium recovery from ITER Test Blanket Module, Report Task GB8-TR6, Commission of the European Union, (2002).

[Bek02b] N. Bekris, C. Caldwell-Nichols, L. Doerr, M. Glugla, R.-D. Penzhorn and H. Ziegler, Possible techniques for the detritiation of first wall materials from fusion machines, *Journal of Nuclear Materials*, 307-311 (2002) 1649–1654.

[Bek03] N. Bekris, C. H. Skinner, U. Berndt, C. A. Gentile, M. Glugla and B. Schweigel, Tritium depth profiles in 2D and 4D CFC tiles from JET and TFTR, *Journal of Nuclear Materials*, 313-316 (2003) 501–506.

[Bek05] N. Bekris, J. P. Coad, R.-D. Penzhorn, S. Knipe, L. Doerr, R. Rolli and W. Naegele, Characterisation of flakes generated in JET after DD and DT plasma operations, *Journal of Nuclear Materials*, 337-339 (2005) 659–663.

[Bek07] N. Bekris, J. P. Coad, C. H. Skinner, C. A. Gentile, E. Damm and W. Naegele, Thermal release rate of tritium trapped in bulk and plasma exposed surfaces of carbon specimens obtained from JET divertor, *Journal of Nuclear Materials*, 367-370 (2007) 1254–1259.

[Bek99] N. Bekris, M. Sirch, U. Besserer and R. D. Penzhorn, Disproportionation of zirconium cobalt and its reproportionation, *Proceedings of the 20th Symposium on Fusion Technology (SOFT)*, Sept. 7–11, 1998, Marseille, France, (1999) 1021–1024.

[Bel02] A. C. Bell, J. Williams, J. D. Neilson and A. Perevezentsev, Detritiation processes needed for JET operation and their wider applicability, *Fusion Science and Technology*, 41(3P2) (2002) 626–631.

[Bel05a] S. Beloglazov, N. Bekris, M. Glugla and R. Wagner, Semi-technical cryogenic molecular sieve bed for the tritium extraction system of the test blanket module for ITER, *Fusion Science and Technology*, 48(1) (2005) 662–665.

[Bel05b] S. Beloglazov, M. Glugla, R. Wagner, E. Fanghaenel and S. Gruenhagen, Investigation of isotope effects in the gas streams supplied by a 1:1 ITER storage bed using a micro gas chromatography, *Fusion Science and Technology*, 48(1) (2005) 67–70.

[Bel08a] G. Bellanger, Localized corrosion of 316L stainless steel in tritiated water containing aggressive radiolytic and decomposition products at different temperatures, *Journal of Nuclear Materials*, 374(1-2) (2008) 20–31.

[Bel08b] S. Beloglazov, M. Glugla, E. Fanghaenel, A. Perevezentsev and R. Wagner, Performance of a full-scale ITER metal hydride storage bed in comparison with requirements, *Fusion Science and Technology*, 54(1) (2008) 22–26.

[Bel75] L. F. Belovodskii, V. K. Gaevoi, V. I. Grishmanovskii and N. V. Nefedov, Oxidation of tritium in air under the action of intrinsic radiation, *Soviet Atomic Energy*, 38(6) (1975) 488–491.

[Bel78] J. T. Bell, J. D. Redman, R. A. Strehlow and F. J. Smith, Tritium permeation through Incoloy 800 oxidized “in situ” by water vapor, *Proceedings of the 3^{d} Topical*

Meeting on the Technology of Controlled Nuclear Fusion, May 9, 1978, Santa Fe, NM, USA, (1978) 757–762.

[Bel79a] J. T. Bell, J. D. Redman and H. F. Bittner, Tritium permeation through clean construction alloys, *Journal of Materials for Energy Systems*, 1(3) (1979) 55–59.

[Bel79b] Y. Belot, D. Gauthier, H. Camus and C. Caput, Prediction of the flux of tritiated water from air to plant leaves, *Health Physics*, 37(4) (1979) 575–583.

[Bel80] J. T. Bell, J. D. Redman and H. P. Bittner, Tritium permeation through clean Incoloy 800 and Sanicro 31 alloys and through steam oxidized Incoloy 800, *Metallurgical Transactions A*, 11(5) (1980) 775–782.

[Bel81] L. Belkbir, E. Joly and N. Gerard, Comparative study of the formation-decomposition mechanisms and kinetics in $LaNi_5$ and magnesium reversible hydrides, *International Journal of Hydrogen Energy*, 6(3) (1981) 285–294.

[Bel91] A. C. Bell and P. R. Ballantyne, Risk assessment methodology for the JET Active Gas Handling System (AGHS) of the exhaust detritiation system and the significance in meeting design safety standards, *Proceedings of the 16th Symposium on Fusion Technology (SOFT)*, Sept. 3–7, 1990, London, UK, (1991) 1457–1461.

[Bel92a] A. C. Bell, P. Ballantyne, C. Caldwell-Nichols and M. Wykes, Routine tritium releases from JET, *Fusion Technology*, 21(2P2) (1992) 506–511.

[Bel92b] Y. Belot, H. Camus and T. Marini, Determination of tritiated formaldehyde in effluents from tritium facilities, *Fusion Technology*, 21(2P2) (1992) 556–559.

[Bel93a] G. Bellanger and J. J. Rameau, Influence of the tritium in type 316L stainless steel on corrosion, *Fusion Technology*, 24(2) (1993) 145–149.

[Bel93b] Y. Belot, H. Camus, T. Marini and S. Raviart, Volatile tritiated organic acids in stack effluents and in air surrounding contaminated materials, *Journal of Fusion Energy*, 12(1-2) (1993) 71–75.

[Bel95a] A. C. Bell, C. Caldwell-Nichols, B. Patel and L. Serio, Environmental monitoring for tritium at JET, *Fusion Technology*, 28(3P1) (1995) 821–826.

[Bel95b] D. G. Bellamy, J. R. Robins, K. B. Woodall, S. K. Sood and P. Gierszewski, ITER relevant testing of a cryogenic distillation column system, *Fusion Technology*, 28(3P1) (1995) 525–529.

[Bel98] A. C. Bell, The recycling and handling of tritium and beryllium at JET, *Fusion Engineering and Design*, 39-40 (1998) 865–873.

[Bel99a] A. C. Bell, P. Ballantyne, C. Gordont and M. A. Wright, The safety case for JET D-T operation, *Fusion Engineering and Design*, 47(2-3) (1999) 115–130.

[Bel99b] G. Bellanger and J. J. Rameau, Tritium recovery from tritiated water by electrolysis, *Fusion Technology*, 36(3) (1999) 296–308.

[Ben56] W. S. Benedict, N. Gailar and E. K. Plyler, Rotation-vibration spectra of deuterated water vapor, *The Journal of Chemical Physics*, 24(6) (1956) 1139–1165.

[Ben75] M. J. Bennett, B. L. Myatt, D. R. V. Silvester and J. E. Antill, The oxidation behaviour of uranium in air at 50 - 300 °C, *Journal of Nuclear Materials*, 57(2) (1975) 221–236.

[Ben87] R. W. Benjamin and D. C. Hampson, An Evaluation of Retention and Disposal Options for Tritium in Fuel Reprocessing, technical report DP-MS-8752, E.I. du Pont de Nemours and Co., Savannah River Laboratory, Washington, DC, USA (1987).

[Ber08] A. W. C. van den Berg and C. O. Arean, Materials for hydrogen storage: current research trends and perspectives, *Chemical Communications*, (6) (2008) 668–681.

[Ber85a] G. D. Berkheimer and R. E. Buxbaum, Erratum: Hydrogen pumping with palladium membranes, *Journal of Vacuum Science & Technology A: Vacuum, Surfaces, and Films*, 3(5) (1985) 2044–2044.

[Ber85b] G. D. Berkheimer and R. E. Buxbaum, Hydrogen pumping with palladium membranes, *Journal of Vacuum Science & Technology A: Vacuum, Surfaces, and Films*, 3(2) (1985) 412–416.

[Ber91] U. Berndt, E. Kirste, V. Prech, F. Rueckert, A. A. Sameh and H. J. Ache, Abschlussbericht zur Tritiumanreicherungsanlage, research report KFK4780, Kernforschungszentrum Karlsruhe, Institut fuer Radiochemie (IRCH), Karlsruhe, Germany (1991).

[Ber98] A. Bergmaier, G. Dollinger and C. M. Frey, A compact ΔE-E_{res} detector for elastic recoil detection with high sensitivity, *Nuclear Instruments and Methods in Physics Research Section B: Beam Interactions with Materials and Atoms*, 136-138 (1998) 638–643.

[Bes02a] U. Besserer, Tritiumspeicherung in ZrCo, PhD thesis, University of Marburg, (2002).

[Bes02b] U. Besserer, R.-D. Penzhorn and R. Brandt, The behaviour of zirconium-cobalt as a material for tritium storage, *Fusion Science and Technology*, 41(3P2) (2002) 793–796.

[Bes08] U. Besserer, L. Doerr and M. Glugla, Tritium confinement, retention, and releases at the Tritium Laboratory Karlsruhe, *Fusion Science and Technology*, 54(1) (2008) 160–163.

[Bes17] S. Best, Trouble for Lockheed's fusion reactor? Device that could "solve the world's energy crisis" is 100 times larger than first planned, www.dailymail.co.uk/sciencetech/article-4473908/Trouble-Lockheed-s-fusion-reactor.html, (2017), (visited on Apr. 4, 2023).

[Bes96] U. Besserer and K. Schmitt, Versuche zur Inertisierung der Reparaturbox (RBX), TLK report, KfK, Karlsruhe Institute of Technology, Karsruhe, Germany (1996).

[Bes97] U. Besserer, J. Dehne, L. Doerr, M. Glugla, W. Hellriegel, T. Le, F. Schmitt, K. H. Simon, T. Vollmer, J. Wendel and R.-D. Penzhorn, Tritium experience at the Tritium Laboratory Karlsruhe, *Proceedings of the 19th Symposium on Fusion Technology (SOFT)*, Sept. 16–20, 1996, Lisbon, Portugal, (1997) 1261–1264.

[Bib77] N. E. Bibler and E. G. Orebaugh, Radiolytic Gas Production from Tritiated Waste Forms, technical report DP-1459, Savannah River Laboratory, Aiken, SC, USA (1977).

[Bil73] D. R. Billing, H. S. Carden, R. S. Carlson, J. J. Dauby, D. P. Evans, P. H. Lamberger, G. F. Maul, E. A. Mershad, J. W. Reed, T. B. Rhinehammer, W. W. Rodenburg and W. W. Thomasson, Tritium Control Technology, technical report GEPP-104, General Electric Company, Neutron Devices Department, St. Petersburg, Florida, USA (1973).

[Bil91] M. C. Billone, C. C. Lin and D. L. Baldwin, Tritium and helium behaviour in irradiated beryllium, *Fusion Technology*, 19(3P2B) (1991) 1707–1714.

[Bin10] M. W. Binderbauer, H. Y. Guo, M. Tuszewski, S. Putvinski, L. Sevier, D. Barnes, N. Rostoker, M. G. Anderson, R. Andow, L. Bonelli, F. Brandi, R. Brown, D. Q. Bui, V. Bystritskii, F. Ceccherini, R. Clary, A. H. Cheung, K. D. Conroy, B. H. Deng, S. A. Dettrick, J. D. Douglass, P. Feng, L. Galeotti, E. Garate, F. Giammanco, F. J. Glass, O. Gornostaeva, H. Gota, D. Gupta, S. Gupta, J. S. Kinley, K. Knapp,

S. Korepanov, M. Hollins, I. Isakov, V. A. Jose, X. L. Li, Y. Luo, P. Marsili, R. Mendoza, M. Meekins, Y. Mok, A. Necas, E. Paganini, F. Pegoraro, R. Pousa-Hijos, S. Primavera, E. Ruskov, A. Qerushi, L. Schmitz, J. H. Schroeder, A. Sibley, A. Smirnov, Y. Song, X. Sun, M. C. Thompson, A. D. V. Drie, J. K. Walters and M. D. Wyman, Dynamic formation of a hot field reversed configuration with improved confinement by supersonic merging of two colliding high-β compact toroids, *Physical Review Letters*, 105(4) (2010) 045003.

[Bir72a] H. K. Birnbaum and C. A. Wert, Diffusion of hydrogen in metals, *Berichte der Bunsengesellschaft*, 76(8) (1972) 806–816.

[Bir72b] J. Biro, Investigation of Tritium Contamination on Titanium Ion Getter Pumps, research report KFKI-72-31, Hungarian Academy of Sciences, Central Research Institute for Physics, Health Physics Department, Budapest, Hungary (1972).

[Bir76] A. Biris, R. V. Bucur, P. Ghete, E. Indrea and D. Lupu, The solubility of deuterium in $LaNi_5$, *Journal of the Less-Common Metals*, 49 (1976) 477–482.

[Bir95] S. A. Birdsell and R. S. Willms, Modelling and data analysis of a palladium membrane reactor for tritiated impurities cleanup, *Fusion Technology*, 28(3P1) (1995) 530–537.

[Bir96] S. A. Birdsell, R. S. Willms and R. C. Wilhelm, Ultra-high tritium decontamination of simulated fusion fuel exhaust using a 2-stage palladium membrane reactor, *Fusion Technology*, 30(3P2A) (1996) 905–910.

[Bir98a] S. A. Birdsell and R. S. Willms, Design of an impurities detritiation system for ITER using a palladium membrane reactor, *Proceedings of the 20th Symposium on Fusion Technology (SOFT)*, Sept. 7–11, 1998, Marseille, France, (1998) 953–956.

[Bir98b] S. A. Birdsell and R. S. Willms, Tritium recovery from tritiated water with a two-stage palladium membrane reactor, *Fusion Engineering and Design*, 39–40 (1998) 1041–1048.

[Bir99] S. A. Birdsell and R. S. Willms, Tritium recovery from waste using a palladium membrane reactor, *Waste Management Conference (WM99)*, Feb. 28–Mar. 4, 1999, Tucson, AZ, USA, (1999).

[Bis80] C. L. Bisson and W. D. Wilson, Atomistic of tritium and helium-3 in metals, *ANS Conference on Tritium Technology in Fission, Fusion and Isotopic Applications*, 1980, Dayton, OH, USA, (1980) 78–84.

[Bix72] J. C. Bixel and C. J. Kershner, A study of catalytic oxidation and oxide adsorption for the removal of tritium from air, MLM-2140(OP), Monsanto Research Corporation Mound Laboratory, Miamisburg, Ohio, USA (1972).

[Bix74] J. C. Bixel and C. J. Kershner, A study of catalytic oxidation and oxide adsorption for the removal of tritium from air, *Proceedings of the 2^{nd} Environmental Protection Conference, US Atomic Energy Commission*, 1974, Washington, DC, USA, (1974).

[Bjo82] R. A. Bjorklund, R. O. Kushida and M. F. Flessner, Experimental evaluation of flashback flame arresters, *Plant/Operations Progress*, 1(4) (1982) 254–262.

[Bla43] J. F. Black and H. S. Taylor, Equilibrium in hydrogen-water systems containing tritium, *The Journal of Chemical Physics*, 11(9) (1943) 395–402.

[Bla63] B. C. Blanke, J. F. Eichelberger and K. C. Jordan, Applications of calorimetry, *Symposium on Research at Mound Laboratory*, June 6–7, 1963, Miamisburg, Ohio, USA, (1963).

[Ble93] V. Blet, D. Labrune, G. Moll, H. Guidon and B. Hircq, D_2 and DT gas purification by cryosorption on 5A molecular sieve, *Fusion Engineering and Design*, 18 (1993) 43–47.

[Blo69] K. Bloss, Liquid tritioammonia as a tritiating agent, *Journal of Labelled Compounds*, 5(4) (1969) 355–362.

[Blo81] J. Bloch and M. H. Mintz, Kinetics and mechanism of the U-H reaction, *Journal of the Less-Common Metals*, 81(2) (1981) 301–320.

[Blo90] J. Bloch and M. H. Mintz, The effect of thermal annealing on the hydriding kinetics of uranium, *Journal of the Less-Common Metals*, 166(2) (1990) 241–251.

[Boc04] L. V. Boccaccini, L. Giancarli, G. Janeschitz, S. Hermsmeyer, Y. Poitevin, A. Cardella and E. Diegele, Materials and design of the european DEMO blankets, *Journal of Nuclear Materials*, 329-333 (2004) 148–155.

[Boc15] W. Bochnowski, A. Dziedzic, S. Adamiak, M. Berchenko, M. Trzyna and J. Cebulski, Characterization of oxide layers produced on the AISI 321 stainless steel after annealing, *Archives of Metallurgy and Materials*, 60(3) (2015) 2327–2334.

[Bof87] C. Boffito, B. Ferrario, L. Rosai and F. Doni, Gettering in cryogenic applications, *Journal of Vacuum Science & Technology A: Vacuum, Surfaces, and Films*, 5(6) (1987) 3442–3445.

[Boh67] G. Bohmholdt and E. Wicke, Zur Diffusion von Wasserstoff und Deuterium in Palladium und Pd-Legierungen, *Zeitschrift fuer Physikalische Chemie*, 56(3-4) (1967) 133–154.

[Boh68] D. R. Bohl and D. E. Sellers, A Statistical Evaluation of a Pressure - Volume - Temperature Measurement System, research report MLM-1557, TID 4500, Mound Laboratory, Miamisburg, Ohio, USA (1968).

[Boi08] I. Boitsov, S. Kanashenko, R. Causey, E. Denisov, M. Glugla, S. Grishechkin, A. Hassanein, B. Lebedev, T. Kompaniets, A. Kurdyumov, I. Malkov and A. Yukhimchuk, Effect of radiogenic helium on stainless steel 12Cr18Ni10Ti mechanical properties and hydrogen permeability, *Fusion Science and Technology*, 54(2) (2008) 497–500.

[Boi97] L. Boisset, C. Lattaud and P. Giroux, French experience in steel de-tritiation, *Proceedings of the 19th Symposium on Fusion Technology (SOFT)*, Sept. 16–20, 1996, Lisbon, Portugal, (1997) 1697–1700.

[Bok90] S. R. Bokwa, Chalk River Tritium Laboratory, design and operation philosophy, Advanced Tritium Safe Handling Course, Handout, (1990).

[Bon08] I. Bonnett, A. Busigin and A. Shapiro, Tritium removal and separation technology developments, *Fusion Science and Technology*, 54(1) (2008) 209–214.

[Bon29] K. F. Bonhoeffer and P. Harteck, Para- and ortho hydrogen, *Zeitschrift fuer Physikalische Chemie*, B4(1-2) (1929) 113–141.

[Bon83] R. A. Bond, J. Evans, I. R. Harris and D. K. Ross, Hydrogen isotope separation using palladium alloy membranes, *Proceedings of the 12th Symposium on Fusion Technology (SOFT)*, Sept. 8–12, 1982, JÃ¼lich, Germany, (1983) 537–542.

[Boo78] T. E. Boothe and H. J. Ache, Reaction of recoil tritium with graphite. A simulation of first wall controlled thermonuclear reactor conditions, *The Journal of Physical Chemistry*, 82(12) (1978) 1362–1368.

[Boo88] M. J. van den Boogaard, Reliability and safety of the JET beryllium evaporators, JET-TN(88)01, JET, Abingdon, Oxfordshire, UK (1988).

[Boo91] S. J. Booth, G. Celentano, G. Newbert, M. Pick and A. Tesini, Beryllium related maintenance on JET, *Proceedings of the 16th Symposium on Fusion Technology (SOFT)*, Sept. 3–7, 1990, London, UK, (1991) 1383–1387.

[Boo93] S. J. Booth, D. Collins and G. Newbert, Radioactive waste management at JET, *Proceedings of the 17th Symposium on Fusion Technology (SOFT)*, Sept. 14–18, 1992, Rome, Italy, (1993) 1690–1694.

[Bor03] B. Bornschein, M. Glugla, K. Guenther, R. Laesser, T. L. Le, K. H. Simon and S. Welte, Tritium tests with a technical PERMCAT for final clean-up of ITER exhaust gases, *Fusion Engineering and Design*, 69(1-4) (2003) 51–56.

[Bor05] B. Bornschein, M. Glugla, K. Guenther, T. L. Le, K. H. Simon and S. Welte, Successful experimental verification of the Tokamak Exhaust Processing concept of ITER with the CAPER facility, *Fusion Science and Technology*, 48(1) (2005) 11–16.

[Bor07] B. Bornschein, D. Corneli, M. Glugla, K. Guenther, T. L. Le and K. H. Simon, Experimental validation of a method for performance monitoring of the impurity processing stage in the TEP system of ITER, *Fusion Engineering and Design*, 82(15-24) (2007) 2133–2139.

[Bor10] B. Bornschein, ITEP - Institute for Technical Physics, Progress Report in Research and Development, Annual Report TTA-EP-100-1, RO, (2010).

[Bor11] B. Bornschein, Between fusion and cosmology – the future of the Tritium Laboratory Karlsruhe, *Fusion Science and Technology*, 60(3) (2011) 1088–1091.

[Bor12] B. Bornschein, Ergebnisse aus Forschung und Entwicklung, Jahresbericht, Karlsruhe Institut fuer Technologie, Institut fuer Technische Physik (ITEP, Karlsruhe, Germany (2012).

[Bor15] L. Bornschein, B. Bornschein, M. Sturm, M. Roellig, F. Priester and the KATRIN collaboration, Status of the neutrino mass experiment KATRIN, *Fusion Science and Technology*, 67(2) (2015) 274–277.

[Bor99] A. Borodzinski, Hydrogenation of acetylene-ethylene mixtures on a commercial palladium catalyst, *Catalysis Letters*, 63 (1999) 35–42.

[Bos76] O. Boser, Hydrogen sorption in $LaNi_5$, *Journal of the Less-Common Metals*, 46(1) (1976) 91–99.

[Bot65] F. Botter, J. Menes, S. Tistchenko and G. Dirian, Frontal and Band Displacement Chromatography of the hydrogen isotopes on palladium columns; Chromatographies Frontale et de Deplacement de Bande des isotopes de l'hydrogene sur colonnes de palladium, *Bulletin de la Societe Chimique de France*, (11) (1965) 3374–3382.

[Bot88] F. Botter, J. Gowman, J. L. Hemmerich, B. Hircq, R. Laesser, D. Leger, S. Tistchenko and M. Tschudin, The gas chromatographic isotope separation system for the JET Active Gas Handling Plant, *Fusion Technology*, 14(2P2A) (1988) 562–566.

[Bow77a] R. C. Bowman, R. S. Carlson and R. J. DeSando, Characterization of metal tritides for the transport, storage, and disposal of tritium, *Transactions of the American Nuclear Society*, Nov. 14, 1976, Washington, DC, USA, (1977).

[Bow77b] R. C. Bowman and A. Attalla, NMR studies of the helium distribution in uranium tritide, *Physical Review B*, 16(5) (1977) 1828–1843.

[Bow78] R. C. Bowman, Distribution of helium in metal tritides, *Nature*, 271 (1978) 531–532.

[Bow85] R. C. J. Bowman, R. H. Steinmeyer, L. K. Matson, A. Attalla and B. D. Craft, Long-term behavior of the tritides formed by nickel-based intermetallic compounds, *Fusion Technology*, 8(2P2) (1985) 2337–2343.

[Bow90] J. S. Bowers, P. R. Coronado, J. A. Emig and P. C. Souers, Filling of plastic foams with liquid D-T, *Journal of Nuclear Materials*, 1(170) (1990) 121–123.

[Bra04] W. A. Brand, Mass spectrometer hardware for analysing stable isotope ratios, *Handbook of Stable Isotope Analytical Techniques*, P. A. de Groot, editor, Elsevier, Amsterdam, (2004), 835–856.

[Bra05] J. Braet and A. Bruggeman, Oxidation of tritiated organic liquid waste, *Fusion Science and Technology*, 48(1) (2005) 188–193.

[Bra71] J. D. Braun, G. L. Downs and G. W. Powell, An autoradiographic investigation of tritium in 304 stainless steel, *Metallography*, 4(3) (1971) 231–242.

[Bra85] J. M. Braun and A. S. Williamson, Permeability of protective coatings to tritium, *Fusion Technology*, 8(2P2) (1985) 2312–2317.

[Bra94] A. M. Brass, A. Chanfreau and J. Chene, Helium-3 precipitation in AISI 316L stainless steel induced by radioactive decay of tritium: Microstructural study of helium bubble precipitation, *Metallurgical and Materials Transactions A*, 25(10) (1994) 2117–2130.

[Bra96] A. M. Brass and A. Chanfreau, Accelerated diffusion of hydrogen along grain boundaries in nickel, *Acta Materialia*, 44(9) (1996) 3823–3831.

[Bre15] S. Brezinsek, Plasma-surface interaction in the Be/W environment: Conclusions drawn from the JET-ILW for ITER, *Journal of Nuclear Materials*, 463 (2015) 11–21.

[Bre56] D. W. Breck, W. G. Eversole, R. M. Milton, T. B. Reed and T. L. Thomas, Crystalline zeolites. I. the properties of a new synthetic zeolite, type A, *Journal of the American Chemical Society*, 78(23) (1956) 5963–5972.

[Bre74] D. W. Breck, Zeolite molecular sieves: Structure, chemistry, and use, John Wiley & Sons, Hoboken, NJ, USA (1974).

[Bre89] S. Brereton, Explosion hazard in liquid nitrogen cooled fusion systems, *Fusion Technology*, 15 (1989) 833–837.

[Bri81] N. J. Bridger and C. V. Freitas, Tritium Immobilisation by Incorporation in Inorganic Solids, technical report EUR 7653, European Applied Research Reports, (1981).

[Bro52] L. C. Browning and P. H. Emmett, Equilibrium measurements in the $Ni_3C-Ni-CH_4-H_2$ and $Co_2C-Co-CH_4-H_2$ systems, *Journal of the American Chemical Society*, 74(7) (1952) 1680–1682.

[Bro65] H. Brodowsky and E. Poeschel, Wasserstoff in Palladium/Silber-Legierungen, *Zeitschrift fuer Physikalische Chemie*, 44(34) (1965) 143–159.

[Bro83] G. L. Broschka, I. Ginsburgh, R. A. Mancini and R. G. Will, A study of flame arrestors in piping systems. Even officially approved flame arrestors must be used only under the exact conditions for which they were tested and approved, *Plant/Operations Progress*, 2(1) (1983) 5–12.

[Bro97] J. N. Brooks, D. N. Ruzic and D. B. Hayden, Sputtering erosion of beryllium coated plasma facing components – general considerations and analysis for ITER detached plasma regime, *Fusion Engineering and Design*, 37(4) (1997) 455–463.

[Bru12] S. A. Bruyere and L. C. Cadwallader, Operating experience review of tritium-in-water monitors, *Fusion Engineering and Design*, 87(5-6) (2012) 565–568.

[Bru69] F. Bruner, G. P. Cartoni and M. Possanzini, Separation of isotopic methanes by gas chromatography, *Analytical Chemistry*, 41(8) (1969) 1122–1124.

[Bru82] A. Bruggeman, W. Doyen, R. Leysen, L. Meynendonckx, M. Monsecour, W. Goossens, L. Baetsle, H. Belien, D. Smets and K. Van Gils, Separation of tritium from aqueous effluents (final report), *European Applied Research Reports, Nuclear Science and Technology Section*, 4 (1982) 63–109.

[Bue15] A. Buekki-Deme, C. G. Alecu, B. Kloppe and B. Bornschein, Current status of tritium calorimetry at TLK, *Fusion Science and Technology*, 67(2) (2015) 282–285.

[Bue16] A. Buekki-Deme, D. Demange, T.-L. Le, E. Fanghaenel and K.-H. Simon, PERMCAT experiments with tritium at high helium flow rates relevant for the tritium extraction systems using the CAPER facility at TLK, *Fusion Engineering and Design*, 109-111 (2016) 1331–1334.

[Bun01a] E. Bundesministerium fuer Gesundheit und Bundesministerium fuer Verbraucherschutz and B. und Bundesministerium fuer Umwelt, Naturschutz und Reaktorsicherheit, Trinkwasser Verordnung, Verordnung ueber die Qualitaet von Wasser fuer den menschlichen Gebrauch, *Trinkwasserverordnung in der Fassung der Bekanntmachung vom 10. Maerz 2016 (BGBl. I S. 459), die zuletzt durch Artikel 1 der Verordnung vom 22. September 2021 (BGBl. I S. 4343) geaendert worden ist*, (2001).

[Bun01b] Bundesministerium fuer Umwelt, Naturschutz und Reaktorsicherheit, Verordnung fuer die Umsetzung von EURATOM-Richtlinien zum Strahlenschutz, *Bundsgesetzblatt Jahrgang 2001 Teil 1, Nr. 38, Bonn am 26. Juli*, (2001), 1714–1846.

[Bur79] L. L. Burger, Distribution and Reactions of Tritiated Hydrogen and Methane, technical report IAEA-SM-232/54, International Atomic Energy Agency, Vienna, Austria (1979).

[Bur89] S. R. M. Burton and D. E. Cornelius, Improved method for determination of helium-4 in helium, Report of investigations N° 9232, United States Bureau of Mines, Pittsburgh, PA, USA (1989).

[Bus88a] A. Busigin and S. K. Sood, FLOSHEET - a computer program for simulating hydrogen isotope separation systems, *Fusion Technology*, 14(2P2A) (1988) 529–535.

[Bus88b] A. Busigin and S. K. Sood, Process simulation with microcomputers: A generalized simulation code for application to fission and fusion systems, *CNS Bulletin*, 9(3) (1988).

[But92] G. J. Butterworth and C. B. A. Forty, A survey of the properties of copper alloys for use as fusion reactor materials, *Journal of Nuclear Materials*, 189(3) (1992) 237–276.

[Buv93] J. C. Buvat, C. Latge, X. Joulia and G. Pautrot, Development of the rate-based approach for simulating hydrogen isotope separation by cryogenic distillation, *Proceedings of the 11th Symposium on Fusion Engineering (SOFE)*, Sept. 14–18, 1992, Austin, TX, USA, (1993) 1137–1141.

[Buz17] L. Buzi, G. D. Temmerman, A. E. Huisman, S. Bardin, T. W. Morgan, M. Rasinski, R. A. Pitts and G. V. Oost, Response of tungsten surfaces to helium and hydrogen plasma exposure under ITER relevant steady state and repetitive transient conditions, *Nuclear Fusion, IAEA, Vienna*, 57(12) (2017) 126009.

[Byk82] A. D. Bykov, V. P. Lopasov, Y. S. Makushkin, L. N. Sinitsa, O. N. Ulenikov and V. E. Zuev, Rotation-vibration spectra of deuterated water vapor in the 9160 - 9390 cm^{-1} region, *Journal of Molecular Spectroscopy*, 94(1) (1982) 1–27.

[Cad09a] L. C. Cadwallader and S. A. Bruyere, Continuous air monitor operating experience review, *Fusion Science and Technology*, 56 (2009) 245–251.

[Cad09b] L. C. Cadwallader and B. J. Denny, Tritium room air monitor operating experience review, *Fusion Science and Technology*, 56 (2009) 239–244.

[Cad90] L. C. Cadwallader and M. A. S. Gavett, Tritium Waste Treatment System Component Failure Data Analysis from June 18, 1984 to December 31, 1989, technical report EEG-FSP-8973, Idaho National Engineering Laboratory, Idaho Falls, Idaho, USA (1990).

[Cad91a] L. C. Cadwallader, M. A. S. Stolpe-Gavett and L. Quintana, Tritium Room Air Monitor Component Failure Data Analysis from January 1, 1984 to December 31, 1990, technical report EGG-FSP-9450, Idaho National Engineering Laboratory, Idaho Falls, Idaho, USA (1991).

[Cad91b] L. C. Cadwallander, M. A. S. Gavett and L. Quintana, Tritium room air monitor component failure data analysis from January 1, 1984 to December 31, 1990, EGG-FSP-9450, Idaho National Engineering Laboratory, Idaho Falls, ID, USA (1991).

[Cal01] C. J. Caldwell-Nichols, R.-D. Penzhorn, S. Gruenhagen, M. Sirch and J. George, Evaluation of an Omegatron mass spectrometer for use in the plasma exhaust processing of a fusion reactor, *Fusion Engineering and Design*, 58-59 (2001) 395–399.

[Cal08] C. J. Caldwell-Nichols, H.-D. Adami, N. Bekris, D. Demange, M. Glugla, F. Kramer and K.-H. Simon, Post service examination of a tritium permeator and a turbomolecular pump from the CAPER facility at the Tritium Laboratory Karlsruhe, *Fusion Science and Technology*, 54(2) (2008) 599–602.

[Cal93] C. J. Caldwell-Nichols, J. L. Hemmerich, R. Laesser and P. Milverton, The design and performance of the JET ionisation chambers for use with tritium, *Proceedings of the 17th Symposium on Fusion Technology (SOFT)*, Sept. 14–18, 1992, Rome, Italy, (1993) 1142–1146.

[Can06] Canadian Coalition for Nuclear Responsibility, www.ccnr.org, (2006), (visited on Apr. 4, 2023).

[Can15] D. Canas, C. Decanis, K. Liger, D. Dall'ava and J. Paméla, Classification methodology for tritiated waste requiring interim storage, *Fusion Science and Technology*, 67(2) (2015) 290–295.

[Cap85] F. C. Capuder, L. T. Quigley and C. K. Baker, Recent developments in magnetically coupled vane pumps for tritium service, *Fusion Technology*, 8(2P2) (1985) 2420–2422.

[Car00] W. J. Carmack, R. A. Anderl, R. J. Pawelko, G. R. Smolik and K. A. McCarthy, Characterization and analysis of dusts produced in three experimental tokamaks: TFTR, DIII-D, and Alcator C-Mod, *Fusion engineering and design*, 51 (2000) 477–484.

[Car12] J. Carrasco, A. Hodgson and A. Michaelides, A molecular perspective of water at metal interfaces, *Nature Materials*, 11(8) (2012) 667–674.

[Car63] W. Carnuth, Diffusion und Loeslichkeit von Wasserstoff in kaltverformtem Kupfer, *Zeitschrift fuer angewandte Physik*, 15 (1963) 291–295.

[Car72] R. A. Carpenter, N. M. Gailar, H. W. Morgan and P. A. Staats, The $\nu 2$ fundamental vibration-rotation band of T_2O, *Journal of Molecular Spectroscopy*, 44(2) (1972) 197–205.

[Car75] R. V. Carlson, The uranium-tritium system - the storage of tritium, *ANS Conference on Radiation Effects and Tritium Technology for Fusion Reactors*, 1975, Oak Ridge National Laboratories, TN, USA, (1975) 36–52.

[Car85] J. Carnes, Report of experiments on SAES getter, TSTA File CRM-4(2), MS A150, WX-4-7238, (1985).

[Car87] M. Caron-Charles, Hydrogen extraction from a gas mixture, *Proceedings of the 14th Symposium on Fusion Technology (SOFT)*, Sept. 8–12, 1986, Avignon, France, (1987) 1585–1590.

[Car88] R. V. Carlson, K. E. Binning, S. P. Cole, E. M. Jenkins and R. C. Wilhelm, Operating experience and procedures at the Tritium Systems Test Assembly, *Fusion Technology*, 14(2P2B) (1988) 953–957.

[Car89a] R. V. Carlson, Five years of tritium handling experience at the Tritium Systems Test Assembly, *International Atomic Energy Agency fusion reactor safety meeting*, Apr. 4–7, 1989, Jackson, WY, USA, (1989).

[Car89b] M. Caron-Charles and B. Gilot, Purification de l'hydrogene sous forme libre ou combinee dans un melange gazeux par reactions chimiques avec l'uranium, *Journal of Nuclear Materials*, 166(3) (1989) 331–341.

[Car91] A. B. Carmichael and M. J. Haynes, Radiation protection aspects of repairing a highly contaminated tritium cold box, *Health Physics*, 61(5) (1991) 665–670.

[Car96] R. V. Carlson, R. Wilhelm and K. Okuno, Studies of tritiated water absorbed on molecular sieve, *Fusion Technology*, 30(3P2A) (1996) 895–899.

[Car98] A. Cardella, S. Chiocchio, K. Ioki, G. Janeschitz, R. R. Parker, A. Lodato, R. Tivey, L. Bruno, R. Jakeman, K. Mohri, R. Raffray, G. Vieider, P. Lorenzetto, A. Epinatiev and L. Giancarli, Design of the ITER EDA plasma facing components, *Fusion Engineering and Design*, 39-40 (1998) 377–384.

[Cas62] G. J. Casaletto, L. H. Gevantman and J. B. Nash, The Self-Radiation Oxidation of Tritium in Oxygen and Air, technical report USNRDL-TR-565, U.S. Naval Radiological Defense Laboratory, San Francisco, CA, USA (1962).

[Cas75] M. Castiglioni and P. Volpe, Hot tritium reaction on ammonia: The substitution product, *Gazzetta Chimica Italiana*, 105 (1975) 247–254.

[Cas76a] G. R. Caskey and R. G. Derrick, Trapping of deuterium during permeation through gold, *Scripta Metallurgica*, 10(5) (1976) 377–380.

[Cas76b] G. R. Caskey, A. H. Dexter, M. L. Holzworth, M. R. Louthan and R. G. Derrick, The effect of oxygen on hydrogen transport in copper, *CORROSION*, 32(9) (1976) 370–374.

[Cas77] J. E. Castle and C. R. Clayton, The use of x-ray photo-electron spectroscopy in the analysis of massive layers on stainless steel, *Corrosion Science*, 17 (1977) 7–26.

[Cas85] G. R. Caskey, Tritium-helium effects in metals, *Fusion Technology*, 8(2P2) (1985) 2293–2298.

[Cas97] R. G. Castro, A. H. Bartlett, K. J. Hollis and R. D. Fields, The effect of substrate temperature on the thermal diffusivity and bonding characteristics of plasma sprayed beryllium, *Fusion Engineering and Design*, 37(2) (1997) 243–252.

[Cau02] R. A. Causey, Hydrogen isotope retention and recycling in fusion reactor plasma-facing components, *Journal of Nuclear Materials*, 300(2-3) (2002) 91–117.

[Cau87] R. A. Causey and M. I. Baskes, Plasma-driven permeation of deuterium in nickel, *Journal of Nuclear Materials*, 145-147 (1987) 284–287.

[Cau90a] R. A. Causey, Tritium plasma experiment, *Fusion Engineering and Design*, 12(3) (1990) 411–418.

[Cau90b] R. A. Causey, W. L. Hsu, B. E. Mills, J. Ehrenberg and V. Phillips, Tritium retention and migration in beryllium, *Journal of Nuclear Materials*, 176-177 (1990) 654–660.

[Cau99] R. Causey, K. Wilson, T. Venhaus and W. R. Wampler, Tritium retention in tungsten exposed to intense fluxes of 100 ev tritons, *Journal of Nuclear Materials*, 266-269 (1999) 467–471.

[Cec56] M. Ceccaldi, M. Goldman and E. Roth, Le spectre d'absorption des mélanges H_2O-D_2O a l'etat liquide entre 0.8µ et 30µ, rapport CEA NÂ° 818, Colloque Internationale Spectroscopie, Amsterdam, Netherlands (1956).

[Cep00] D. G. Cepraga, G. Gambi, M. Frisoni and R. Forrest, Radiation transport and activation calculation in support for safety analysis of ITER-FEAT, Technical Report ERG-FUS/TN-SIC 07/2000, ITER, (2000).

[Cha05] G. Charters, S. Aggarwal and D. Blauvelt, Bulk building material characterization and decontamination using a concrete floor and wall contamination profiling technology, TX76011, New Millennium Nuclear Technologies, 805 Washington Drive, Arlington (2005).

[Cha11] M. H. Chang, S. Cho, J. Y. Lim, S. B. Kang, M. K. Lee, S.-H. Yun, H.-G. Kang, K.-M. Song, D. Kim and H. Chung, Performance test of pump combination between Normetex 15 scroll and MB 601 pumps, *Fusion Science and Technology*, 60(3) (2011) 918–921.

[Cha65] S. Charalambus and K. Goebel, Enrichment of tritium by diffusion through palladium, *Zeitschrift fuer Naturforschung A*, 20(8) (1965) 1085.

[Cha70] K. F. Chaney and G. W. Powell, The diffusivity of tritium in 304 stainless steel in the temperature range 100 to 300 °C, *Metallurgical Transactions*, 1 (1970) 2356.

[Cha88a] J. Chabot, J. Lecomte, C. Grumet and J. Sannier, Fuel clean-up system: poisoning of palladium-silver membranes by gaseous impurities, *Fusion Technology*, 14(2P2A) (1988) 614–618.

1070

[Cha88b] J. Chabot, J. Montel and J. Sannier, Catalyst study for the decontamination of glove-box atmospheres containing tritium at mpc levels, *Fusion Technology*, 14(2P2B) (1988) 933–938.

[Cha88c] M. Chazalon, J.-L. Boutard, M. I. Budd, A. Cardella, W. Daenner, P. Dinner, D. Evans, M. Iseli, B. Libin, F. Moons, J. Nihoul, M. A. Vassiliadis, G. Vieider, C. H. Wu and E. Zolti, Next European Torus in-vessel components, *Fusion Technology*, 14(1) (1988) 82–144.

[Cha89] J. Chabot, J. Lecomte, C. Grumet and J. Sannier, Parametric study of hydrogen permeation rate through Pd-Ag membrane in the presence of gaseous impurities, *Proceedings of the 15th Symposium on Fusion Technology (SOFT)*, Sept. 19–23, 1988, Utrecht, Netherlands, (1989) 1272–1276.

[Cha91a] J. Chabot and J. Sannier, Catalyst study for the plasma exhaust purification process, *Proceedings of the 16th Symposium on Fusion Technology (SOFT)*, Sept. 3–7, 1990, London, UK, (1991) 708–712.

[Cha91b] A. Chanfreau, A.-M. Brass and J. Chene, Role of welding on tritium distribution and helium precipitation in an austenitic stainless steel, *Proceedings of the 16th Symposium on Fusion Technology (SOFT)*, Sept. 3–7, 1990, London, UK, (1991) 448–452.

[Cha92] J. Chabot, G. Fernandez de Grado, P. Herry and J. Sannier, Cold trap development, technical report SCECF 282, Centre d´Études Nucléaires de Saclay, France (1992).

[Cha93a] J. Chabot, G. Fernandez de Grado, P. Herry and J. Sannier, Cold trap development, technical report SCECF 303, Centre d´Études Nucléaires de Saclay, France (1993).

[Cha93b] J. Chabot, G. Fernandez de Grado, P. Herry and J. Sannier, Cold trap development, technical report SCECF 329, Centre d´Études Nucléaires de Saclay, France (1993).

[Chê07] J. Chêne, A.-M. Brass, P. Trabuc and O. Gastaldi, Role of microstructure and heat treatments on the desorption kinetics of tritium from austenitic stainless steels, *Journal of Nuclear Materials*, 360(2) (2007) 177–185.

[Chi10] T. Chikada, A. Suzuki, T. Terai, T. Tanaka, T. Muroga, T. Kobayashi and H. Maier, Deuterium permeation mechanism in erbium oxide coatings for tritium permeation barrier, *3rd China-Japan Workshop on Tritium and Tritium Blanket Technology*, June 20–23, 2010, Kunming, China, (2010) 389–393.

[Chi11] T. Chikada, A. Suzuki, H. Maier, T. Terai and T. Muroga, Modeling of tritium permeation through erbium oxide coatings, *Fusion Science and Technology*, 60(1) (2011) 389–393.

[Cho08] S. Cho, M.-Y. Ahn, D. H. Kim, E.-S. Lee, S. Yun, N. Z. Cho and K. J. Jung, Current status of design and analysis of Korean Helium-Cooled Solid Breeder Test Blanket Module, *Fusion Engineering and Design*, 83(7-9) (2008) 1163–1168.

[Cho11] S. Cho, M. H. Chang, S. H. Yun, H.-G. Kang, H. Chung, K. M. Song, D. Koo, D. Chung, D. Jeong, M. K. Lee, J. Y. Lim and D. J. Kim, R&D activities on the tritium storage and delivery system in Korea, *Fusion Science and Technology*, 60(3) (2011) 1077–1082.

[Chr73] L. Christensen, J. Fisher, C. Folkers, V. Gede, P. Landon, W. Ross, G. Snider, R. Stump and R. Tsugawa, Tritium Control Technology, WASH 1269, US Government prepared by Monsanto Research Corporation, Miamisburg, Ohio (1973).

[Chr83] P. Christmas, S. M. Judge, T. B. Ryves, D. Smith and G. Winkler, The decay scheme of ^{64}Cu, *Nuclear Instruments and Methods in Physics Research*, 215(3) (1983) 397–408.

[Chr88] K. Christmann, Interaction of hydrogen with solid surfaces, *Surface Science Reports*, 9(1-3) (1988) 1–163.

[Chu08a] H. Chung, M. Lee, C. Hong, S.-P. Yim, K.-R. Kim, S.-W. Paek and D.-H. Ahn, Development of a 500 kCi BU-type transport container, *Journal of Nuclear Science and Technology*, 45(sup5) (2008) 132–134.

[Chu08b] H. Chung, M. Shim, D.-H. Ahn, M. Lee, C. Hong, H. Yoshida, K.-M. Song, D. J. Kim, K. Jung and S. Cho, Korea's activities for the development of ITER Tritium Storage and Delivery Systems, *Fusion Science and Technology*, 54(1) (2008) 18–21.

[Chu11] H. Chung, D. Koo, D. Chung, D. Jung, S. Paek, M. Lee, S.-P. Yim, S. Lee, K.-S. Seo, S. Kim, K.-P. Hong, K.-S. Jung, Y. Jung, J. Park, D.-H. Ahn and S. Cho, Tritium research activities in KAERI, *Fusion Science and Technology*, 60(3) (2011) 1096–1100.

[Chu12a] S. Chu and A. Majumdar, Opportunities and challenges for a sustainable energy future, *Nature*, 488(7411) (2012) 294–303.

[Chu12b] H. Chung, D. Chung, J. Lee, D. Koo, J. Lee, C. Lee, K.-S. Seo, J. S. Yoon, E. H. Lee, D. W. Lee, H.-G. Kang, M. H. Chang, S. Cho, S.-H. Yun, C. S. Kim, K. J. Jung, P. Camp, S. Willms, D.-H. Ahn and H. Lee, Fusion tritium research facilities in KAERI, *Fusion Engineering and Design*, 87(5-6) (2012) 448–453.

[Chu15] H. Chung, J. Park, D. Koo, H.-G. Kang, M. H. Chang, S.-H. Yun, S. Cho, K. J. Jung and S. Paek, Direct delivery of hydrogen isotopes from a DU hydride bed, *Fusion Science and Technology*, 68(2) (2015) 368–372.

[Chu79] W. F. Chu and A. Rahmel, The kinetics of the reduction of chromium oxide by hydrogen, *Metallurgical Transactions B*, 10(3) (1979) 401–407.

[Cla07] E. A. Clark and K. L. Shanahan, Effects of tritium on UHMW-PE, PTFE, and Vespel© polyimide, *Fusion Science and Technology*, 52(4) (2007) 1007–1011.

[Cla08] E. A. Clark and G. C. Staack, Effects of tritium gas exposure on the dynamic mechanical properties of EPDM elastomer, *Fusion Science and Technology*, 54(2) (2008) 576–579.

[Cla11] E. A. Clark, E. B. Fox, M. C. Kane and G. C. Staack, Effects of tritium gas exposure on polymers, *Fusion Science and Technology*, 60(3) (2011) 1037–1040.

[Cla13] E. A. Clark, Normetex Pump Alternatives Study, technical report SRNL-STI-2013-00325, Savannah River Technology Center, Savannah River Site, Aiken, SC, USA (2013).

[Cla76] W. B. Clarke, W. J. Jenkins and Z. Top, Determination of tritium by mass spectrometric measurement of ^{3}He, *The International Journal of Applied Radiation and Isotopes*, 27(9) (1976) 515–522.

[Cla91] A. D. L. Claire, Permeation of gases through solids, *Defect and Diffusion Forum*, 33 (1991) 1–66.

[Cla95a] E. A. Clark, De-Contamination and Melt Recycling Tritium Contaminated Stainless Steel, technical report, Savannah River Technology Center, Savannah River Site, Aiken, SC, USA (1995).

[Cla95b] E. A. Clark, D. A. Dauchess, L. K. Heung, R. L. Rabun and T. Motyka, Experience with palladium diffusers in tritium processing, *Fusion Technology*, 28(3P1) (1995) 566–572.

[Cla96] E. A. Clark, Literature Survey of Tritiated Waste Characterization and Disposal (U), technical report WSRC-TR-96-0209, Westinghouse Savannah River Company, Savannah River Site, Aiken, SC, USA (1996).

[Coa01] J. P. Coad, N. Bekris, J. D. Elder, S. K. Erents, D. E. Hole, K. D. Lawson, G. F. Matthews, R.-D. Penzhorn and P. C. Stangeby, Erosion/deposition issues at JET, *Journal of Nuclear Materials*, 290-293 (2001) 224–230.

[Coa06] J. P. Coad, J. Likonen, M. Rubel, E. Vainonen-Ahlgren, D. E. Hole, T. Sajavaara, T. Renvall, G. F. Matthews and JET EFDA Contributors, Overview of material re-deposition and fuel retention studies at JET with the gas box divertor, *Nuclear Fusion*, 46(2) (2006) 350–366.

[Coa97] J. P. Coad, M. Rubel and C. H. Wu, The amount and distribution of deuterium retained in the JET divertor after the C and Be phases in 1994-1995, *Journal of Nuclear Materials*, 241-243 (1997) 408–413.

[Coa99] J. Coad, A. Andreev, M. Friedrich, D. Hole, R.-D. Makarov S.and Penzhorn and C. Wu, Hydrogen isotope analysis for films deposited in tokamaks, *8^{th} European Conference on Application of Surface and Interface Analysis*, Oct. 4–8, 1999, Sevilla, Spain, (1999).

[Coe11] J. W. Coenen, V. Philipps, S. Brezinsek, G. Pintsuk, I. Uytdenhouwen, M. Wirtz, A. Kreter, K. Sugiyama, H. Kurishita, Y. Torikai, Y. Ueda and U. Samm, Melt-layer ejection and material changes of three different tungsten materials under high heat-flux conditions in the tokamak edge plasma of TEXTOR, *Nuclear Fusion*, 51(11) (2011) 1–8.

[Cof67] D. O. Coffin, Some second thoughts on tritium contamination, *Health Physics*, 13 (1967) 1083–1086.

[Cof73] D. Coffin, R. Stoll, J. Farr and D. Vier, Tritium Control Technology, WASH 1269, US Government prepared by Monsanto Research Corporation, Miamisburg, Ohio (1973).

[Cof76] D. O. Coffin, High-pressure tritium equipment, *Tritium Operating Safety Seminar*, June 30, 1976, Los Alamos, USA, (1976).

[Cof79] D. O. Coffin and C. Walthers, Vacuum pumping of tritium in fusion power reactors, *8th Symposium on Engineering Problems of Fusion Research*, Nov. 13–16, 1979, San Francisco, CA, USA, (1979).

[Cof82] D. O. Coffin, A tritium-compatible high-vacuum pumping system, *Journal of Vacuum Science and Technology*, 20(4) (1982) 1126–1131.

[Coh80a] R. L. Cohen, K. W. West and J. H. Wernick, Degradation of $LaNi_5$ by temperature-induced cycling, *Journal of the Less-Common Metals*, 73(2) (1980) 273–279.

[Coh80b] R. L. Cohen, K. W. West and J. H. Wernick, Degradation of $LaNi_5$ hydrogen-absorbing material by cycling, *Journal of the Less Common Metals*, 70(2) (1980) 229–241.

[Col62] E. Collinson, F. S. Dainton and F. R. S. Kroh, The radiation chemistry of aqueous solutions III. The isotope effect for polonium α-particles and tritium β-particles, *Proceedings of the Royal Society of London. Series A. Mathematical and Physical Sciences*, 265(1323) (1962) 430–435.

[Col74] C. Colmenares, E. G. Shapiro, P. E. Barry and C. T. Prevo, A europium-doped, calcium-fluoride scintillator system for low-level tritium detection, *Nuclear Instruments and Methods*, 114(2) (1974) 277–289.

[Col75] P. Colombo, R. Neilson and M. Steinberg, The Fixation of Aqueous Tritiated Waste in Polymer Impregnated Concrete and in Polyacetylene, technical report BNL-20898, CONF-750989-4, Brookhaven National Laboratory, Process Technology Division, Department of Applied Science, Upton, NY, USA (1975).

[Col76] P. Colombo and M. Steinberg, Tritium Storage Development, progress report No10, BNL-50728, Brookhaven National Laboratory, Process Technology Division, Department of Nuclear Energy, Upton, NY, USA (1976).

[Col78] P. Colombo and R. Johnson, Tritium Storage Development, progress report No 15, Brookhaven National Laboratory, Upton, NY, USA (1978).

[Con62] H. Connor, Palladium alloy diffusion cells, commercial units for the production of ultrapure hydrogen, *Platinum Metal Review*, 6(4) (1962) 130–135.

[Con64] J. B. Conway, D. G. Salyards, J. Holowach and R. A. Stanley, Techniques for measuring localized corrosion rates of beryllium oxide, *Journal of Nuclear Materials*, 14 (1964) 425–433.

[Con73] J. B. Condon and E. A. Larson, Diffusion with chemical reaction and a moving boundary, *The Journal of Physical Chemistry*, 59(1973) (1973) 855–865.

[Con75] J. B. Condon, Calculated vs. experimental hydrogen reactions rates with uranium, *The Journal of Physical Chemistry*, 79(4) (1975) 392–397.

[Con80] J. B. Condon, Nucleation and growth in the hydriding reaction of uranium, *Journal of the Less-Common Metals*, 73(1) (1980) 105–112.

[Coo00] I. Cook, G. Marbach, L. Di Pace, C. Girard, P. Rocco and N. P. Taylor, Results, conclusions, and implications of the SEAFP-2 programme, *Fusion Engineering and Design*, 51-52 (2000) 409–417.

[Cor05] D. Corneli, B. Bornschein, E. Fanghaenel, M. Glugla, K. Guenther, T. L. Le and K. H. Simon, Memory effects in measurements of low tritium concentrations as required for the outlet of the TEP system of the ITER fuel cycle, *Fusion Science and Technology*, 48(1) (2005) 55–58.

[Cor88] P. R. Coronado, E. M. Fearon, R. G. Garza, J. F. Shaw, P. C. Souers, R. K. Stump and R. T. Tsugawa, ^{3}He outgassing from four working palladium and uranium beds, *Fusion Technology*, 14(2P2A) (1988) 741–743.

[Cor92] V. J. Corcoran, C. A. Campbell and P. B. Bothwell, Decontamination and decommissioning of UK tritium facilities, *Fusion Technology*, 21(2P2) (1992) 727–732.

[Cos90] M. S. Costantino, J. F. Lakner and R. Bastasz, Synthesis of monolithic uranium hydride and uranium deuteride, *Journal of the Less-Common Metals*, 159 (1990) 97–108.

[Cou01] G. F. Counsell and C. H. Wu, In-situ detection and removal of carbon debris - a challenge for the Next-Step Fusion Device, *Physica Scripta*, T91(1) (2001) 70–75.

[Cow05] D. F. Cowgill, Helium nano-bubble evolution in aging metal tritides, *Fusion Science and Technology*, 48(1) (2005) 539–544.

[Cra57] H. Craig, Distribution, production rate, and possible solar origin of natural tritium, *Physical Review*, 105(3) (1957) 1125–1127.

[Cra61] H. Craig and D. Lal, The production rate of natural tritium, *Tellus*, 13(1) (1961) 85–105.

[Cra66] A. Crane and H. P. Gush, The induced infrared absorption spectrum of solid deuterium and solid hydrogen deuteride, *Canadian Journal of Physics*, 44(2) (1966) 373–398.

[Cra68] J. Crank and G. S. Park, Diffusion in polymers, Academic Press, Cambridge, MA, USA (1968).

[Cra75] J. Crank, The mathematics of diffusion, Oxford University Press, Oxford, UK (1975).

[Cre85] D. A. Cremers and L. J. Radziemski, Direct detection of beryllium on filters using the laser spark, *Appl. Spectrosc.*, 39(1) (1985) 57–63.

[Cri02a] I. Cristescu, I.-R. Cristescu, U. Tamm, R.-D. Penzhorn and C. J. Caldwell-Nichols, Investigation of separation performances of various isotope exchange catalysts for the deuterium-hydrogen system, *Fusion Science and Technology*, 41(3P2) (2002) 1087–1091.

[Cri02b] I. Cristescu, U. Tamm, I.-R. Cristescu, M. Glugla and C. J. Caldwell-Nichols, Investigation of simultaneous tritium and deuterium transfer in a catalytic isotope exchange column for water detritiation, *Fusion Engineering and Design*, 61-62 (2002) 537–542.

[Cri05a] I. Cristescu, I. R. Cristescu, L. Doerr, M. Glugla, G. Hellriegel, O. Kveton, D. Murdoch, P. Schaefer and S. Welte, TRENTA facility for trade-off studies between combined electrolysis catalytic exchange and cryogenic distillation processes, *Fusion Science and Technology*, 48(1) (2005) 97–101.

[Cri05b] I.-R. Cristescu, L. Doerr, A. Busigin and D. Murdoch, ITER dynamic tritium inventory modelling code, *Fusion Science and Technology*, 48(1) (2005) 343–348.

[Cri06] I. Cristescu, I.-R. Cristescu, L. Doerr, M. Glugla, D. Murdoch and S. Welte, Long term performances assessment of water detritiation system components, *Fusion Engineering and Design*, 81(1-7) (2006) 839–844.

[Cri07a] I. Cristescu, I. R. Cristescu, L. Doerr, M. Glugla, G. Hellriegel, R. Michling, D. Murdoch, P. Schaefer, S. Welte and W. Wurster, Commissioning of water detritiation

and cryogenic distillation systems at TLK in view of ITER design, *Fusion Engineering and Design*, 82(15-24) (2007) 2126–2132.

[Cri07b] I. Cristescu, I. R. Cristescu, L. Doerr, M. Glugla and D. Murdoch, Integrated tests of water detritiation and cryogenic distillation in view of ITER design, *Fusion Science and Technology*, 52(3) (2007) 667–671.

[Cri07c] I.-R. Cristescu, I. Cristescu, C. Day, M. Glugla and D. Murdoch, Modeled tritium inventories within the ITER fuel cycle systems in typical fuelling scenarios, *Fusion Science and Technology*, 52(3) (2007) 659–666.

[Cub89] D. Cubicciotti, Equilibrium chemistry of nitrogen and potential-pH diagrams for the Fe – Cr – H_2O system in BWR water, *Journal of Nuclear Materials*, 167 (1989) 241–248.

[Cut08] R. S. Cutting, C. A. Muryn, D. J. Vaughan and G. Thornton, Substrate-termination and H_2O-coverage dependent dissociation of H_2O on $Fe_3O_4(111)$, *Surface Science*, 602(6) (2008) 1155–1165.

[Dae01] W. Daenner, A. Cardella, K. Ioki, R. Mattas, Y. Ohara and Y. Strebkov, ITER R&D: Vacuum vessel and in-vessel components: Shield blanket module, *Fusion Engineering and Design*, 55(2-3) (2001) 205–217.

[Dan01] P. Dantzer, P. Millet and T. B. Flanagan, Thermodynamic characterization of hydride phase growth in ZrNi – H_2, *Metallurgical and Materials Transactions A*, 32(1) (2001) 29–38.

[Dan02] P. Dantzer and P. Millet, On the accuracy of heat flux calorimetry in stable intermetallic H_2(g) systems, *Journal of Alloys and Compounds*, 330-332 (2002) 34–40.

[Dan14] P. Danielson, A Journal of Practical and Useful Vacuum Technology: Sorting out the turbo, drag, and turbo/drag pump family, http://web.gps.caltech.edu/~als/IRMS/course-materials/lecture-2---vacuum-pumps/sorting-out-turbo-drag.pdf, (2014), (visited on Apr. 14, 2022).

[Dav13] M. Davies and T. Heidermann, Protect your process with the proper flame arresters, *Chemical Engineering Progress*, 109 (2013) 16–22.

[Dav54] W. D. Davis, Diffusion of gases through metals I: Diffusion of hydrogen through palladium, US AEC report KAPL 1227, Knolls Atomic Power Laboratory, Schenectady, NY, USA (1954).

[Dav88] R. B. Davidson, P. v. Hatten, M. Schaub and D. Ulrich, Commissioning and first operating experience at Darlington Tritium Removal Facility, *Fusion Technology*, 14(2P2A) (1988) 472–479.

[Day00] C. Day, B. Kammerer and A. Mack, The influence of water on the performance of ITER cryosorption vacuum pumps, *Fusion Engineering and Design*, 51-52 (2000) 229–235.

[Day01] C. Day, The use of active carbons as cryo-sorbent, *Colloids and Surfaces A: Physicochemical and Engineering Aspects*, (2001) 187–206.

[Day02] C. Day, A. Mack, M. Glugla and D. K. Murdoch, Tritium inventories in the high vacuum pumps of ITER, *Fusion Science and Technology*, 41(3P2) (2002) 602–606.

[Day05] C. Day, D. Brennan, P. Camp, H. S. Jensen, G. Jones, A. Mack and A. Miller, Performance of ITER-relevant cryopump panels for tritiated gases, *Fusion Science and Technology*, 48(1) (2005) 29–34.

[Day07] C. Day, A. Antipenkov, M. Dremel, H. Haas, V. Hauer, A. Mack, D. K. Murdoch and M. Wykes, R&D and design for the cryogenic and mechanical vacuum pumping systems of ITER, *Vacuum*, 81(6) (2007) 738–747.

[Day08] C. Day, MEMO on the Ferrofluid rotary seal solution for ITER mechanical pumps, Institut für Technische Physik, KIT, Karlsruhe, (2008).

[Day09] C. Day and H. Haas, Experimental assessment of the ITER cryosorption pump high temperature regeneration, *Fusion Engineering and Design*, 84(2-6) (2009) 665–668.

[Day13] C. Day, Vacuum Technology, Annual Report on Results of Research and Development, Karlsruhe Institut fuer Technologie (KIT), ITEP Institute of Technical Physics, Karlsruhe, Germany (2013).

[Day98] C. Day, H. Haas, N. T. Kazakovky, A. Mack, D. K. Murdoch, D. Roehrig and G. L. Saksagansky, Summarized results of the cryosorption panel test programme for the ITER cryopumping system, *Proceedings of the 17th IAEA Conference on Fusion Energy*, Oct. 1998, Vienna, Austria, (1998) 1073–1076.

[DeF83] D. A. DeFreece, Assessment of Technical Risks and R & D Requirements for a Magnetic Confinement Fusion Fuel System: Final Report, technical report EPRI-AP–3283, Electric Power Research Institute (EPRI), St. Louis, MO, USA (1983).

[Dem02] D. Demange, M. Grivet, H. Pialot and A. Chambaudet, Indirect tritium determination by an original ^{3}He ingrowth method using a standard helium leak detector mass spectrometer, *Analytical Chemistry*, 74(13) (2002) 3183–3189.

[Dem05] D. Demange, M. Varescon, P. L. Gal, J. P. Daclin, J. C. Hubinois, C. Douche and C. Lattaud, A review of the different methods to quantify tritium inside waste drums via helium-3 mass spectrometric measurements, *Fusion Science and Technology*, 48(1) (2005) 182–187.

[Dem10] D. Demange, M. Glugla, K. Guenther, T. L. Le, K. H. Simon, R. Wagner and S. Welte, Counter-current isotope swamping in a membrane reactor: The PERMCAT process and its applications in fusion technology, *Catalysis Today*, 156(3-4) (2010) 140–145.

[Dem12] D. Demange, C. G. Alecu, N. Bekris, O. Borisevich, B. Bornschein, S. Fischer, N. Gramlich, Z. Koelloe, T. L. Le, R. Michling, F. Priester, M. Roellig, M. Schloesser, S. Staemmler, M. Sturm, R. Wagner and S. Welte, Overview of R&D at TLK for process and analytical issues on tritium management in breeder blankets of ITER and DEMO, *Fusion Engineering and Design*, 87(7-8) (2012) 1206–1213.

[Dem15a] D. Demange, I. Cristescu, E. Fanghaenel, M. Glugla, N. Gramlich, T. L. Le, R. Michling, H. Moosmann, W. M. Shu, K. H. Simon, R. Wagner, S. Welte and R. S. Willms, Micro-channel catalytic reactor integration in CAPER and R&D on highly tritiated water handling and processing, *Fusion Science and Technology*, 67(2) (2015) 312–315.

[Dem15b] D. Demange, E. Fanghaenel, S. Fischer, T. L. Le, F. Priester, M. Roellig, M. Schloesser and K. H. Simon, CAPER as central and crucial facility to support R&D with tritium at TLK, *Fusion Science and Technology*, 67(2) (2015) 308–311.

[Dep12] Department of Energy and Climate Change, Strategy for the management of solid low-level radioactive waste from the non-nuclear industry in the United Kingdom. Part 1. Anthropogenic radionuclides, Policy paper, (2012).

[Des62] M. Destriau and J. Seriot, The $U-H_2-UH_3$ and $U-4\,D_2-UD_3$ equilibria and the rate of decomposition of UH_3 and UD_3, *Comptes Rendus de l'Académie des Science*, 254 (1962) 2982–1984.

[Des73] J. Desroches, Peintures luminiscentes et lampes auto-luminiscentes, *Bulletin d'Informations Scientific et Techniques*, 178 (1973) 69–71.

[Dev80a] E. H. v. Deventer, V. A. MacLaren and V. A. Maroni, Hydrogen permeation characteristics of aluminium-coated and aluminium-modified steels, *Journal of Nuclear Materials*, 88(1) (1980) 168–173.

[Dev80b] E. H. v. Deventer and V. A. Maroni, Hydrogen permeation characteristics of some austenitic and nickel-base alloys, *Journal of Nuclear Materials*, 92(1) (1980) 103–111.

[Dev89] M. Devillers, M. Sirch and R.-D. Penzhorn, Hydrogen isotopes in pure and nitrided ZrCo*, *Zeitschrift fuer Physikalische Chemie*, 164(Part 2) (1989) 1355–1360.

[Dev90] M. Devillers, M. Sirch, S. Bredendiek-Kaemper and R. D. Penzhorn, Characterization of the zirconium-cobalt (ZrCo)-hydrogen system in view of its use for tritium storage, *Chemistry of Materials*, 2(3) (1990) 255–262.

[Dev92] M. Devillers, M. Sirch and R. D. Penzhorn, Hydrogen-induced disproportionation of the intermetallic zirconium-cobalt compound ZrCo, *Chemistry of Materials*, 4(3) (1992) 631–639.

[Dev93] M. Devillers, M. Sirch and R.-D. Penzhorn, Solubility of hydrogen and deuterium in ZrCo, *Journal of Nuclear Materials*, 207 (1993) 53–61.

[Dev96] D. Devillard, J. P. Corot and J. Y. Floricourt, Tritium accountancy in 200 litres drums by calorimetry, *Proceedings of the 19th Symposium on Fusion Technology (SOFT)*, Sept. 16–20, 1996, Lisbon, Portugal, (1996) 1249–1251.

[Dic92] R. S. Dickson and J. M. Miller, Sorption of tritium and tritiated water on construction materials, *Fusion Technology*, 21(2P2) (1992) 850–855.

[Doe02] L. Doerr, J. Dehne, M. Glugla, H. Kissel, R.-D. Penzhorn, S. Welte and J. L. Hemmerich, Upgrade of the isotope separation system at the Tritium Laboratory Karlsruhe, *Fusion Science and Technology*, 41(3P2) (2002) 1155–1159.

[Doe04] R. P. Doerner, M. J. Baldwin and K. Schmid, The influence of a beryllium containing plasma on the evolution of a mixed-material surface, *Physica Scripta*, T111(1) (2004) 75–79.

[Doe05] L. Doerr, U. Besserer, S. Gruenhagen, M. Glugla, B. Kloppe, M. Sirch and J. L. Hemmerich, High resolution vacuum calorimeter, *Fusion Science and Technology*, 48(1) (2005) 358–361.

[Doe07] R. P. Doerner, M. Baldwin, J. Hanna, C. Linsmeier, D. Nishijima, R. Pugno, J. Roth, K. Schmid and A. Wiltner, Interaction of beryllium containing plasma with ITER materials, *Physica Scripta*, T128 (2007) 115–120.

[Doe08] L. Doerr, U. Besserer, N. Bekris, B. Bornschein, C. Caldwell-Nichols, D. Demange, I. Cristescu, I. R. Cristescu, M. Glugla, G. Hellriegel, P. Schaefer, S. Welte and J. Wendel., A decade of tritium technology development and operation at the Tritium Laboratory Karlsruhe, *Fusion Science and Technology*, 54 (2008) 143–148.

[Doe98] L. Doerr, N. Bekris, U. Besserer, M. Glugla, W. Hellriegel, R.-D. Penzhorn, H.-D. Roehrig, K. Schubert, T. Vollmer and J. Wendel, Tritium operating experience at the Tritium Laboratory Karlsruhe, *Proceedings of the 20th Symposium on Fusion Technology (SOFT)*, Sept. 7–11, 1998, Marseille, France, (1998) 1015–1018.

[Dol00] Y. Dolinsky, I. Lyasota, A. Shestakov, Y. Repritsev and Y. Zouev, Heavy hydrogen isotopes penetration through austenitic and martensitic steels, *Journal of Nuclear Materials*, 283-287 (2000) 854–857.

[Dol02] Y. N. Dolinsky, Y. N. Zouev, I. A. Lyasota, I. V. Saprykin and V. V. Sagaradze, Permeation of deuterium and tritium through the martensitic steel F82H, *Journal of Nuclear Materials*, 307-311 (2002) 1484–1487.

[Dol87] L. DollÃ©, Corrosion studies, CEA report Task T.21, Centre d'Études NuclÃ©aires de Fontenay-Aux-Roses, Fontenay–aux-Roses, France (1987).

[Dor53] L. M. Dorfman and H. C. Mattraw, The exchange reaction of hydrogen and tritium, *The Journal of Physical Chemistry*, 57(7) (1953) 723–725.

[Dor54a] L. M. Dorfman, Absorption of tritium beta particles in hydrogen and other gases, *Physical Review*, 95(2) (1954) 393–396.

[Dor54b] L. M. Dorfman and B. A. Hemmer, Ion-pair yield of the tritium-oxygen reaction, *The Journal of Chemical Physics*, 22(9) (1954) 1555–1558.

[Dou55] D. L. Douglas, Tritium-carbon monoxide reaction, *The Journal of Chemical Physics*, 23(8) (1955) 1558–1559.

[Dou81a] D. H. Doughty, The measurement of water vapor permeability of glove materials using dilute tritiated water, *Journal of Nuclear Materials*, 104 (1981) 1595–1599.

[Dou81b] D. H. Doughty and L. A. West, Water Permeation through Organic Materials, technical report Sand81-3280, Sandia Laboratories, Albuquerque, NM, USA (1981).

[Doy85] B. L. Doyle and D. K. Brice, Steady state hydrogen transport in solids, *Radiation Effects*, 89(1-2) (1985) 21–48.

[Dra96] R. H. Drake, Recovery of Tritium from Tritiated Waste Water Cost-Effectiveness Analysis, technical report LA-UR-97-3767, Los Alamos National Laboratory, Los Alamos, NM, USA (1996).

[Dru98] F. Druyts, Determination of Be/air and Be/steam reactivities with TG/DTA, *Proceedings of the 20th Symposium on Fusion Technology (SOFT)*, Sept. 7–11, 1998, Marseille, France, (1998) 1597–1600.

[Duc02] D. Ducret, C. Laquerbe, A. Ballanger, J. Steimetz, V. Porri, J. P. Verdin and T. Pelletier, Separation of hydrogen isotopes by thermal cycling absorption process: An experimental device, *Fusion Science and Technology*, 41(3P2) (2002) 1092–1096.

[Dun99] J. B. Duncan and D. A. Nelson, The separation of tritiated water using supported polyphosphazene membranes, *Journal of Membrane Science*, 157(2) (1999) 211–217.

[Dus62] S. Dushman, Scientific foundations of vacuum technique, John Wiles & Sons, Inc., New York, NY, USA (1962).

[Eak71] J. D. Eakins and W. P. Hutchinson, The radiological hazard from the conversion of tritium to tritiated water in air by metal catalysts, *Tritium*, A. Moghissi and M. M.W. Carter, editors, Las Vegas, NV, USA, (1971).

[Eak75] J. D. Eakins, W. P. Hutchinson and A. E. Lally, The radiological hazard from tritium sorbed on metal surfaces, *Health Physics*, 28(3) (1975) 213–224.

[Eas83] C. E. Easterly and M. R. Bennett, Radiation catalyzed conversion of tritium gas to tritiated water, *Nuclear Technology - Fusion*, 4(2P2) (1983) 116–120.

[Eas85] C. E. Easterly, H. Noguchi and M. R. Bennett, Low concentration conversion of tritium gas to tritiated water, *Fusion Technology*, 8(2P2) (1985) 2564–2568.

[Ebe16] S. Ebenhoech, S. Niemes, F. Priester and M. Roellig, Investigations of the applicability of a new accountancy tool in a closed tritium loop, *Fusion Engineering and Design*, 109-111 (2016) 1376–1379.

[Ebe85] N. Ebeling, Die Verfestigung von angereichertem Tritium aus der Wiederaufarbeitung, PhD thesis, University of Aachen, Juelich, (1985).

[Ebi67a] Y. Ebisuzaki, W. J. Kass and M. O'Keeffe, Diffusion and solubility of hydrogen in single crystals of nickel and nickel-vanadium alloy, *The Journal of Chemical Physics*, 46(4) (1967) 1378–1381.

[Ebi67b] Y. Ebisuzaki, W. J. Kass and M. O'Keeffe, Isotope effects in the diffusion and solubility of hydrogen in nickel, *The Journal of Chemical Physics*, 46(4) (1967) 1373–1378.

[Eck98] W. Eckstein, K. Krieger and J. Roth, Erosion of W and deposition of C due to bombardment with D and CH_3, *Journal of Nuclear Materials*, 258-263 (1998) 912–916.

[Eda12] Y. Edao, S. Fukada, Y. Nishimura, K. Katayama, T. Takeishi, Y. Hatano and A. Taguchi, Effect of hydrophobic paints coating for tritium reduction in concrete materials, *Fusion Engineering and Design*, 87(7-8) (2012) 995–998.

[Eda15] Y. Edao, Y. Kawamura, R. Kurata, S. Fukada, T. Takeishi, T. Hayashi and T. Yamanishi, Measurement of tritium penetration through concrete material covered by various paint coatings, *Fusion Science and Technology*, 67(2) (2015) 320–323.

[Eda16] Y. Edao, S. K., Y. Iwai and T. Hayashi, Effect of hydrocarbons on the efficiency of catalytic reactor detritiation in an event of fire, *Journal of Nuclear Science and Technology*, 53 (2016) 1831–1838.

[Eda17] Y. Edao, Y. Iwai, K. Sato and T. Hayashi, Performance of tritium analysis system using inorganic-based hydrophobic platinum catalyst, *Fusion Engineering and Design*, 124 (2017) 818–821.

[Edw00] P. K. Edwards, A. Bell, N. Davies, R. Middleton, B. Patel, M. Pick and J. Tait, Management of combined manual and remote handling shutdowns at JET, *Proceedings*

of the 18th Symposium on Fusion Engineering (SOFE), Oct. 25–29, 1999, Albuquerque, NM, USA, (2000) 257–260.

[Edw02] P. Edwards, N. Davies, A. Loving, D. Neilson and B. Patel, Operation, maintenance and decontamination of the JET torus access facilities, *Fusion Science and Technology*, 41(3P2) (2002) 607–611.

[Edw95a] R. A. H. Edwards, Issues in tritiated waste management for fusion power reactors, *Fusion Technology*, 28(3P2) (1995) 1472–1477.

[Edw95b] R. A. H. Edwards and G. Modica, Reduction of tritiated water on a regenerable iron reactant: pilot plant design, *Fusion Technology*, 28(3P1) (1995) 586–590.

[EFD00] EFDA, ITER at Cadarache, Site Assessment Report, (2000).

[Efs90] A. M. Efstathiou, S. L. Suib and C. O. Bennett, Encapsulation of molecular hydrogen in zeolites at 1 atm, *Journal of Catalysis*, 123(2) (1990) 456–462.

[Eic07] F. Eichelhardt, B. Bornschein, L. Bornschein, O. Kazachenko, N. Kernert and M. Sturm, First tritium pumping results by a cryo-pump with a pre-condensed argon layer, *Proceedings of the 25th International Symposium on Rarified Gas Dynamics (SRGD)*, July 21–28, 2006, Saint Petersburg, Russia, (2007).

[Eic08] F. Eichelhardt, B. Bornschein, L. Bornschein, O. Kazachenko, N. Kernert and M. Sturm, First tritium results of the KATRIN test experiment TRAP, *Fusion Science and Technology*, 54(2) (2008) 615–618.

[Eic57] W. Eichenauer and A. Pebler, Messung des Diffusionskoeffizienten und der Loeslichkeit von Wasserstoff in Aluminiun und Kupfer, *Zeitschrift fuer Metallkunde*, 48 (1957) 373–378.

[Eic58] W. Eichenauer, H. Kuenzig and A. Pebler, Diffusion und Löslichkeit von Wasserstoff in α-Eisen und Silber, *Zeitschrift fuer Metallkunde*, 49 (1958) 220–225.

[Eic62] W. Eichenauer and D. Liebscher, Messung der Diffusionsgeschwindigkeit von Wasserstoff in Gold, *Zeitschrift fuer Naturforschung*, 17a (1962) 355–355.

[Eic65] W. Eichenauer, W. Loeser and H. Witte, Loeslichkeit und Diffusionsgeschwindigkeit von Wasserstoff und Deuterium in Einkristallen aus Nickel und Kupfer, *Zeitschrift fuer Metallkunde*, 56(5) (1965) 287–293.

[Eis79] M. Eisenbud, B. Bennett, R. E. Blanco, E. Compere, E. Goldberg, D. G. Jacobs, J. Koranda, A. A. Moghissi, J. H. Rust and J. K. Soldat, Tritium in the environment, NCRP Report IAEA-SM-232/62, (1979).

[El-58] M. El-Sayed, P. Estrup and R. Wolfgang, Mechanism of reaction of recoil hydrogen in the gas phase, *Journal Physical Chemistry*, 62 (1958) 1356–1363.

[Ell74] T. S. Elleman and K. Verghese, Surface effects on tritium diffusion in niobium, zirconium and stainless steel, *Journal of Nuclear Materials*, 53 (1974) 299–306.

[Ell78a] R. E. Ellefson, R. W. Baker and J. T. Gill, Gaseous Mixtures of Hydrogen, Deuterium, and Helium-3 Produced by a Partial-Pressure Mixing System, technical report MLM-2574, Mound Laboraty, Miamisburg, OH, USA (1978).

[Ell78b] T. S. Elleman, L. R. Zumwalt and K. Verghese, Hydrogen transport and solubility in non-metallic solids, *Proceedings of the 3rd Topical Meeting on the Technology of Controlled Thermonuclear Fusion*, May 9–11, 1978, Santa Fe, NM, USA, (1978) 763–770.

[Ell80] C. E. Ells, Tritium in Austenitic Stainless Steel Vessels: the Integrity of the Vessel, technical report AECL-6972, Atomic Energy of Canada Ltd, Chalk River, Ontario, Canada (1980).

[Ell81] C. E. Ells, S. A. Kushneriuk and J. H. Van Der Kuur, The Containment of Tritium in Austenitic Stainless Steel Vessels, technical report AECL-7159, Atomic Energy of Canada Ltd, Chalk River, Ontario, Canada (1981).

[Ell86] R. E. Ellefson and J. T. Gill, Tritium inventory differences: I. sampling and U-getter pump holdup, *Proceedings of the 27th Annual Meeting of the Institute of Nuclear Materials Management, New Orleans, LA, USA*, (1986).

[Ell88a] R. E. Ellefson, C. N. Lindsay and E. E. Johns, Measurement and prediction of tritium holdup, *Fusion Technology*, 14(2P2B) (1988) 1036–1040.

[Ell88b] W. G. Ellis, Determination of beryllium in liquid and solid waste samples by flame and furnace AAS, *Atomic Spectroscopy*, 9 (1988) 181–188.

[Ell92] R. E. Ellis, Catalytic oxidation of gaseous organics, *Fusion Technology*, 21(2) (1992) 556–571.

[Ema02] K. Ema and Y. Izumi, Interaction of tritium with polyethylene, *Fusion Science and Technology*, 41(3P2) (2002) 378–381.

[Emb92] M. C. Embury, R. E. Ellefson, H. B. Melke and W. M. Rutherford, Efficient palladium isotope chromatograph for hydrogen (EPIC), *Fusion Technology*, 21(2P2) (1992) 960–965.

[Eme87] L. C. Emerson, R. J. Knize and J. L. Cecchi, Pumping of hydrocarbons using non-evaporable getters, *Journal of Vacuum Science & Technology A: Vacuum, Surfaces, and Films*, 5(4) (1987) 2584–2586.

[Emi92] J. A. Emig, R. G. Garza, L. D. Christensen, P. R. Coronado and P. C. Souers, Helium release from 19-year-old palladium tritide, *Journal of Nuclear Materials*, 187(3) (1992) 209–214.

[Eml92] R. E. Emls, Catalytic oxidation of gaseous organics, *Fusion Technology*, 21(2P2) (1992) 566–571.

[Eng91] U. Engelmann, M. Glugla, R.-D. Penzhorn and H. J. Ache, Application of an omegatron type high resolution mass spectrometer for the analysis of mixtures of hydrogen and helium isotopes, *Nuclear Instruments and Methods in Physics Research Section A: Accelerators, Spectrometers, Detectors and Associated Equipment*, 302(2) (1991) 345–351.

[Eng92] U. Engelmann, M. Glugla, R.-D. Penzhom and H. J. Ache, Laser Raman spectroscopy and omegatron mass spectrometry applied to investigations of the radiochemical reactions between methane and tritium, *Fusion Technology*, 21(2P2) (1992) 430–435.

[Eno90] M. Enoeda, H. Fukui, T. Ide, K. Okuno, Y. Naruse, J. L. Anderson, J. R. Bartlit, R. H. Sherman and R. S. Willms, Separation of helium and hydrogen isotopes by ISS at the TSTA, *Proceedings of the 13th Symposium on Fusion Engineering (SOFE)*, Oct. 2–6, 1989, Knoxville, TN, USA, (1990) 630–633.

[Eno94] M. Enoeda, Y. Kawamura, K. Okuno, M. Nishikawa and K. Tanaka, Recovery of tritium by cryogenic molecular sieve bed in breeding blanket interface condition, *Fusion Technology*, 26(3P2) (1994) 664–667.

[Eno95a] M. Enoeda, Y. Kawamura, K. Okuno, K. Tanaka, M. Uetake and M. Nishikawa, Recovery of hydrogen isotopes and impurity mixture by cryogenic molecular sieve bed for GDC gas cleanup, *Fusion Technology*, 28(3P1) (1995) 591–596.

[Eno95b] M. Enoeda, T. Yamanishi, M. Yamada, S. Konishi, K. Okuno, R. S. Willms, D. J. Taylor, W. Harbin, J. R. Bartlit and J. L. Anderson, TSTA/FCU-JFCU Tritium Experiment of Breeding Blanket Interface under the Collaboration of JAERI-US/DOE, technical report JAERI research 95-034, Japan Atomic Energy Research Institute, Tokyo, Japan (1995).

[Eno96] M. Enoeda, Y. Kawamura and K. Okuno, Tritium test of cryogenic molecular sieve bed for He GDC gas cleanup by 60 SLM test loop, *Fusion Technology*, 30(3) (1996).

[Eri65] E. Eriksson, An account of the major pulses of tritium and their effects in the atmosphere, *Tellus*, 17(1) (1965) 118–130.

[Eri83] K. L. Erickson, E. P. Roth and J. F. Lakner, Thermophysical Properties of Uranium Hydride, Sandia Report SAND83-1531A, Sandia National Laboratories, Livermore, CA, USA (1983).

[Ert08] G. Ertl, H. Knözinger, F. Schüth and J. Weitkamp, Handbook of heterogeneous catalysis, 2nd edition, Wiley, Hoboken, NJ, USA (2008).

[Est01] G. A. Esteban, A. Perujo, L. A. Sedano and K. Douglas, Hydrogen isotope diffusive transport parameters in pure polycrystalline tungsten, *Journal of Nuclear Materials*, 295(1) (2001) 49–56.

[Est02] G. A. Esteban, A. Perujo, L. A. Sedano, F. Legarda, B. Mancinelli and K. Douglas, Diffusive transport parameters and surface rate constants of deuterium in Incoloy 800, *Journal of Nuclear Materials*, 300(1) (2002) 1–6.

[Est66] P. J. Estrup and J. Anderson, Chemisorption of hydrogen on tungsten(100), *The Journal of Chemical Physics*, 45(6) (1966) 2254–2260.

[Eva55] R. D. Evans, The atomic nucleus, McGraw-Hill, New York, NY, USA (1955).

[Eva75] E. A. Evans, Tritium and its compounds, 2nd edition, Butterworths, London, UK (1975).

[Eva83] J. Evans, I. R. Harris and D. K. Ross, A proposed method of hydrogen isotope separation using palladium alloy membranes, *Journal of the Less-Common Metals*, 89(2) (1983) 407–414.

[Fab97] S. A. Fabritsiev, A. S. Pokrovskii, V. R. Barabash and Y. G. Prokofiev, Neutron spectrum and transmutation effects on the radiation damage of copper alloys, *Fusion Engineering and Design*, 36(4) (1997) 505–513.

[Fai88] R. A. Failor, P. C. Souers and S. G. Prussin, Initial radiolysis effects on the tritium-oxygen gas reaction, *The Journal of Physical Chemistry*, 92(2) (1988) 429–433.

[Fai89] R. A. Failor, Kinetics of the gas phase tritium oxidation reaction, PhD thesis, University of California, (1989).

[Fea87] E. M. Fearon, P. R. Coronado, R. G. Garza, D. H. Darling and P. C. Souers, Shrinkage and opacity of $100\,\mathrm{kg\,m^{-3}}$ silica aerogel foam in liquid deuterium-tritium, *Journal of Nuclear Materials*, 149(1) (1987) 105–108.

[Fed01a] G. Federici, J. N. Brooks, M. Iseli and C. H. Wu, In-vessel tritium retention and removal in ITER-FEAT, *Physica Scripta*, 2001(T91) (2001) 76–83.

[Fed01b] G. Federici, C. H. Skinner, J. N. Brooks, J. P. Coad, C. Grisolia, A. A. Haasz, A. Hassanein, V. Philipps, C. S. Pitcher, J. Roth, W. R. Wampler and D. G. Whyte, Plasma-material interactions in current tokamaks and their implications for next step fusion reactors, *Nuclear Fusion*, 41(12) (2001) 1967–2137.

[Fed05] G. Federici and C. H. Skinner, Tritium inventory in the materials of the ITER plasma-facing components, *Nuclear Fusion Research, Springer Series in Chemical Physics*, Springer , Berlin, Heidelberg, (2005), 287–317.

[Fie80] H.-J. Fiek, J. Romaker and U. Schindewolf, Tritium-Anreicherung durch Isotopen-Austausch zwischen Wasserstoff und Wasser mittels hydrophoben Katalysators fuer die Kernbrennstoff-Wiederaufbereitung, *Chemie Ingenieur Technik*, 52(11) (1980) 892–895.

[Fin86] P. A. Finn and E. H. VanDeventer, Oxidation of tritium atoms at a stainless-steel surface, *International Symposium on Fusion Reactor Blanket and Fuel Cycle Technology*, Oct. 27–29, 1986, (1986) 5.

[Fin88] P. A. Finn and E. H. V. Deventer, Parameters important in the oxidation of tritium at a stainless-steel surface, *Fusion Technology*, 14(2P2A) (1988) 783–790.

[Fir53] E. L. Fireman, Measurement of the $(n,^3\mathrm{H})$ cross section in nitrogen and its relationship to the tritium production in the atmosphere, *Phys. Rev.*, 91 (1953) 922–926.

[Fir55] E. L. Fireman and F. S. Rowland, Tritium and neutron production by 2.2-Bev protons on nitrogen and oxygen, *Physical Review*, 97(3) (1955) 780–782.

[Fir61] E. L. Fireman and F. S. Rowland, An additional measurement of the tritium content of atmospheric hydrogen of 1949, *Journal of Geophysical Research*, 66(12) (1961) 4321–4321.

[Fis11] S. Fischer, M. Sturm, M. Schloesser, B. Bornschein, G. Drexlin, F. Priester, R. J. Lewis and H. H. Telle, Monitoring of tritium purity during long-term circulation in the KATRIN test experiment LOOPINO using laser Raman spectroscopy, *Fusion Science and Technology*, 60(3) (2011) 925–930.

[Fis15] S. Fischer, K. Schoenung, B. Bornschein, R. Rolli, V. Schaefer and M. Sturm, Investigation of durability of optical coatings in highly purified tritium gas, *Fusion Science and Technology*, 67(2) (2015) 316–319.

[Fis99] D. J. Fisher, Hydrogen diffusion in metals: A 30-year retrospective, Scitec Publications Ltd, Baech, Switzerland (1999).

[Fla74] G. L. B. F. Flapper and H. M. Gijsman, Gravimetric measurements of gas adsorption on zeolites at low temperatures, *Cryogenics*, 14(3) (1974) 150–153.

[Fla92] T. Flament, D. Herpin, L. Feve and J. Sannier, Compatibility of stainless steels and lithium-based ceramics with beryllium, *Journal of Nuclear Materials*, 191-194 (1992) 163–167.

[Flo51] H. E. Flotow and B. M. Abraham, Dissociation Pressures of Uranium Hydride and Uranium Tritide, technical report ANL-WMM 759, Argonne National Laboratory, Chicago, IL, USA (1951).

[Flo84] H. E. Flotow, J. M. Haschke and S. Yamauchi, The chemical thermodynamics of actinide elements and compounds: Part 9 the actinide hydrides, International Atomic Energy Agency (IAEA), Vienna, Austria (1984).

[Fol78] C. L. Folkers and R. J. Cena, Tritium-Containment Systems: a Tradeoff Study, technical report UCRL-52627, Lawrence Livermore Laboratory, Livermore, CA, USA (1978).

[Fon12] C. Fong, Darlington tritium removal facility (DTRF), *IAEA TRF Workshop*, Valcea, Romania, (2012).

[Fon86] J. C. Fontes, Some considerations on ground water dating using environmental isotopes, *Memories of the 18th Congress of the International Association of Hydrologists*, Sept. 8–13, 1985, Cambridge, UK, (1986) 118–154.

[For07] T. Forde, J. Maehlen, V. Yartys, M. Lototsky and H. Uchida, Influence of intrinsic hydrogenation/dehydrogenation kinetics on the dynamic behaviour of metal hydrides: A semi-empirical model and its verification, *International Journal of Hydrogen Energy*, 32(8) (2007) 1041–1049.

[For81] N. Forsyth and W. Thiele, The influence of oxide film growth on tritium permeation through steam generator tubing, *Proceedings of the 11th Symposium on Fusion Technology (SOFT)*, Sept. 15–19, 1980, Oxford, UK, (1981) 559–564.

[For86] K. Forcey, D. Ross, J. Simpson, D. Melford and A. Whitaker, Development of surface barrier layers for inhibiting the permeation of tritium through NET components, Progress Report 1.10.85 – 1.10.86 EAEC Contract Number NET/84-707, (1986).

[For87] K. Forcey, D. Ross, J. Simpson, D. Melford and A. Whitaker, Development of surface barrier layers for inhibiting the permeation of tritium through NET components, Final Report 1.10.87 EAEC Contract Number NET/84-707, Commission of the European Communities, Joint Research Center – Ispra Site, Ispra, Italy (1987).

[For88] K. S. Forcey, D. K. Ross, J. C. B. Simpson and D. S. Evans, Hydrogen transport and solubility in 316L and 1.4914 steels for fusion reactor applications, *Journal of Nuclear Materials*, 160(2-3) (1988) 117–124.

[For90] K. S. Forcey, I. Iordanova and D. K. Ross, Investigation of structure dependence of diffusivity, solubility, and permeability of hydrogen in hot rolled low carbon steels, *Materials Science and Technology*, 6(4) (1990) 357–363.

[For98] C. B. A. Forty, R. A. Forrest and G. J. Butterworth, Activation of beryllium in a fusion power plant, *Journal of Nuclear Materials*, 258-263 (1998) 793–797.

[Fos08] P. J. Foster, J. E. Klein, H. T. Sessions and G. A. Morgan, Johnson-Matthey diffuser characterization testing, *Fusion Science and Technology*, 54(2) (2008) 591–594.

[Fow11] M. D. Fowley, T. J. Steeper and J. E. Klein, A Normetex model 15 $m^3\,hour^{-1}$ water vapor pumping test, *Fusion Science and Technology*, 60(3) (2011) 910–913.

[Fow76] J. D. Fowler, R. A. Causey, D. Chandra, T. S. Elleman and K. Verghese, Abstract: Tritium diffusion in ceramic materials for thermonuclear reactors, *Journal of Vacuum Science and Technology*, 13(1) (1976) 401–402.

[Fow77] J. D. Fowler, D. Chandra, T. S. Elleman, A. W. Payne and K. Verghese, Tritium diffusion in Al_2O_3 and BeO, *Journal of the American Ceramic Society*, 60(3-4) (1977) 155–161.

[Fox10] E. B. Fox, S. D. Greenway and E. A. Clark, Radiation stability of Nafion membranes used for isotope separation by proton exchange membrane electrolysis, *Fusion Science and Technology*, 57(2) (2010) 103–111.

[Fox17] E. B. Fox, M. D. Kranjc and T. E. Skidmore, Polymer performance and aging in a tritium environment, *Fusion Science and Technology*, 71(4) (2017) 507–513.

[Fra06] A. Frattolillo, New simple method for fast and accurate measurement of volumes, *Review of Scientific Instruments*, 77(4) (2006) 045107.

[Fra68a] R. Frauenfelder, Permeation of hydrogen through tungsten and molybdenum, *The Journal of Chemical Physics*, 48(9) (1968) 3955–3965.

[Fra68b] R. Frauenfelder, Permeation, diffusion, and solution of nitrogen in tungsten and molybdenum, *The Journal of Chemical Physics*, 48(9) (1968) 3966–3971.

[Fra69] R. Frauenfelder, Solution and diffusion of hydrogen in tungsten, *Journal of Vacuum Science and Technology*, 6(3) (1969) 388–397.

[Fra77] D. Fraenkel and J. Shabtai, Encapsulation of hydrogen in molecular sieve zeolites, *Journal of the American Chemical Society*, 99(21) (1977) 7074–7076.

[Fra97] P. Franzen, C. Garcia-Rosales, H. Plank and V. K. Alimov, Hydrogen trapping in and release from tungsten: Modeling and comparison with graphite with regard to its use as fusion reactor material, *Journal of Nuclear Materials*, 241-243 (1997) 1082–1086.

[Fra99] A. C. Francis and J. Foster, Analysis Results and Data for JET In-Vessel Flakes after DTE1, JET report JET-RWMD (99) P047 AEAT, Abingdon, Oxfordshire, UK (1999).

[Fri00a] M. Friedrich, W. Pilz, G. Sun, R. Behrisch, C. Garcia-Rosales, N. Bekris and R.-D. Penzhorn, Tritium depth profiling in carbon by accelerator mass spectrometry, *Nuclear Instruments and Methods in Physics Research Section B: Beam Interactions with Materials and Atoms*, 161-163 (2000) 216–220.

[Fri00b] M. Friedrich, W. Pilz, G. Sun, R. Behrisch, C. Garcia-Rosales, N. Bekris and R.-D. Penzhorn, Tritium depth profiling in carbon samples from fusion experiments, *Nuclear Instruments and Methods in Physics Research Section B: Beam Interactions with Materials and Atoms*, 172(1-4) (2000) 655–658.

[Fri01] M. Friedrich, W. Pilz, G. Sun, R.-D. Penzhorn, N. Bekris, R. Behrisch and C. Garcia-Rosales, Tritium depth profiling by AMS in carbon samples from fusion experiments, *Physica Scripta*, T94(1) (2001) 98.

[Fri73] H. Frieske and E. Wicke, Magnetic susceptibility and equilibrium diagram of PdH_n, *Berichte der Bunsengesellschaft fuer physikalische Chemie*, 77(1) (1973) 48–52.

[Fri95] A. A. Frigo, A glove box design check list, *Proceedings of the 9^{th} Annual Conference and Equipment Exhibit of the American Glove Box Society*, July 1995, Minnesota, MN, USA, (1995).

[Fro84] E. Fromm and H. Jehn, Solubility of hydrogen in the elements, *Bulletin of Alloy Phase Diagrams*, 5(3) (1984) 324–326.

[Fuj00] M. Fujiwara, Y. Takeiri, T. Shimozuma, T. Mutoh, Y. Nakamura, S. Yamada, S. Sudo, K. Kawahata, Y. Oka, M. Sato, N. Noda, A. Iiyoshi, K. Adachi, K. Akaishi, N. Ashikawa, H. Chikaraishi, P. C. D. DeVries, M. Emoto, H. Funaba, M. Goto, K. Ida, H. Idei, K. Ikeda, S. Imagawa, S. Inagaki, M. Isobe, A. Iwamoto, S. Kado, O. Kaneko, S. Kitagawa, T. Kobuchi, A. Komori, S. Kubo, Y. Kubota, R. Kumazawa, R. Maekawa, S. Masuzaki, T. Minami, T. Mito, J. Miyazawa, T. Morisaki, S. Morita, S. Murakami, S. Muto, Y. Nagayama, H. Nakanishi, K. Narihara, A. Nishimura, K. Nishimura, A. Nishizawa, S. Ohdachi, N. Ohyabu, M. Osakabe, T. Ozaki, B. J. Peterson, K. Saito, A. Sagara, S. Sakakibara, R. Sakamoto, H. Sasao, M. Sasao, K. Sato, T. Seki, M. Shoji, H. Sugama, H. Suzuki, K. Takahata, M. Takeuchi, H. Tamura, K. Tanaka, K. Toi, T. Tokuzawa, K. Tsumori, K. Y. Watanabe, T. H. Watanabe, T. Watari, H. Yamada, I. Yamada, S. Yamaguchi, S. Yamamoto, N. Yanagi, M. Yokoyama, Y. Yoshimura, Y. Hamada, K. Itoh, K. Matsuoka, K. Murai, K. Ohkubo, I. Ohtake, M. Okamoto, S. Satoh, T. Satow, S. Tanahashi, K. Yamazaki and O. Motojima, Overview of long pulse operation in the large helical device, *Nuclear Fusion*, 40(6) (2000) 1157–1166.

[Fuj80] H. Fujita, S. Okada, K. Fujita, H. Sakamoto, K. Higashi and T. Hyodo, Ratio of permeabilities of tritium to protium through palladium-alloy membrane, *Journal of Nuclear Science and Technology*, 17(6) (1980) 436–442.

[Fuk04] S. Fukada, N. Nakamura, J. Monden and M. Nishikawa, Experimental study of cracking methane by Ni/SiO_2 catalyst, *Journal of Nuclear Materials*, 329-333 (2004) 1365–1369.

[Fuk06] S. Fukada, S. Ono and S. Suemori, Rates of methane decomposition and hydrogen permeation in catalytic-permeable Ni tube reactor, *Fusion Science and Technology*, 50(1) (2006) 99–106.

[Fuk08] M. Fukumoto, Y. Ohtsuka, Y. Ueda, M. Taniguchi, M. Kashiwagi, T. Inoue and K. Sakamoto, Blister formation on tungsten damaged by high energy particle irradiation, *Journal of Nuclear Materials*, 375(2) (2008) 224–228.

[Fuk12] S. Fukada, Y. Edao, K. Sato, T. Takeishi, K. Katayama, K. Kobayashi, T. Hayashi, T. Yamanishi, Y. Hatano, A. Taguchi and S. Akamaru, Transfer of tritium in concrete coated with hydrophobic paints, *Fusion Engineering and Design*, 87(1) (2012) 54–60.

[Fuk93] S. Fukada and N. Mitsuishi, Semi-empirical equations of pressure-composition isotherm of ZrCo-hydrogen system, *Journal of Nuclear Science and Technology*, 30(9) (1993) 956–958.

[Fuk95] S. Fukada, K. Fuchinoue and M. Nishikawa, Hydrogen isotope separation by displacement chromatography with palladium, *Journal of Nuclear Science and Technology*, 32(6) (1995) 556–564.

[Fur05] Y. Furukubo, K. Fukuda, M. Nishikawa and S. Beloglazov, Recovery method of bred tritium from solid breeders, *Fusion Science and Technology*, 48(1) (2005) 658–661.

[Gal05] C. L. Gallagher and K. D. McCrimmon, Operating experience of the Tritium Laboratory at CRL, *Fusion Science and Technology*, 48(1) (2005) 237–242.

[Gan02] L. Gan, L. Guangda and J. Guoqiang, The displacement of hydrogen-deuterium at high flow rate in palladium particle bed, *Fusion Science and Technology*, 41(3P2) (2002) 1112–1115.

[Gel92] D. S. Gelles and H. L. Heinisch, Neutron damage in beryllium, *Journal of Nuclear Materials*, 191-194 (1992) 194–198.

[Gen02] C. A. Gentile, J. J. Parker and G. L. Guttadora, Oxidative decontamination of tritiated materials employing ozone gas, *Fusion Science and Technology*, 41(3P2) (2002) 700–705.

[Gen05] C. A. Gentile, S. W. Langish, C. H. Skinner and L. P. Ciebiera, Comparison and evaluation of various tritium decontamination techniques and processes, *Fusion Science and Technology*, 48(1) (2005) 200–203.

[Gen09] D. J. Geniesse and G. A. Stegen, Evaluation of Tritium Removal and Mitigation Technologies for Waste Water Treatment, technical report DOE/RL-2009-18, Rev.0, U.S. Department of Energy, Richland, WA, USA (2009).

[Gen67] C. Genty and R. Schott, Séparation des isotopes de l´hydrogene par chromatography en phase gazeuse, *Revue du Methodes d´Analyse (GAMS)*, 2 (1967) 1–11.

[Gen70] C. Genty and R. Schott, Quantitative analysis for the isotopes of hydrogen- H_2, HD, HT, D_2 , DT, and T_2-by gas chromatography, *Analytical Chemistry*, 42(1) (1970) 7–11.

[Gen85] H. Gentsch, J. Tewes and G. Messer, An improved ion gauge with gold coated electrodes for reliable operation in reactive gases and for use as reference standard, *Vacuum*, 35(3) (1985) 137–140.

[Gen87] H. Gentsch, Inert cyclotron-resonance mass spectrometer (Omegatron), *Vakuum-Technik*, 36(6-7) (1987) 224–229.

[Gen95] C. A. Gentile, G. Ascione and J. L. Anderson, Tritium contamination experience in an operational D – T fusion reactor, *18th European Symposium on Fusion Technology (SOFT)*, Aug. 22–26, 1994, Karlsruhe, Germany, (1995) 1043–1047.

[Gen96] C. A. Gentile, S. Raftopoulos, P. LaMarche, M. Viola, T. Walters, M. Kalish, T. Kozub, H. Carnevale, D. Shaltis, S. Vinson, W. Walker, L. Ciebiera, R. Yager, M. Quigley, R. Meagher, C. Bunting, E. Rogers, M. Casey, R. Hawes, R. Raucci, D. Reeves, E. Amarescu, M. Gibson, T. Granger, S. Langish, S. Bush, J. Langford, D. Hyatt and J. L. Anderson, TFTR tritium operations lessons learned, *Fusion Technology*, 30(3P2B) (1996) 1564–1566.

[Gev64] L. H. Gevantman and C. H. Smith, The Effect of Selected Diluent Gases on the Self-Induced Isotopic Exchange between Tritium and Water Vapour, technical report USNRDL-TR-738, U.S. Naval Radiological Defense Laboratory, San Francisco, CA, USA (1964).

[Ghe95] F. Ghezzi, W. T. Shmayda, N. Venkataramani and G. Bonizzoni, Efficient HTO reduction using a Zr – Fe – Mn alloy, *Fusion Engineering and Design*, 28 (1995) 367–372.

[Gho48] J. A. Ghormley and A. O. Allen, Decomposition of Tritium Oxide under its own Radiation, technical report ORNL-128, Oak Ridge National Laboratory, Oak Ridge, TN, USA (1948).

[Gia05] L. Giancarli, V. Chuyanov, M. Abdou, M. Akiba, B. Hong, R. Laesser, C. Pan and Y. Strebkov, Breeding blanket modules testing in ITER, an international program on the way to DEMO, *7th International Symposium on Fusion Nuclear Technology*, May 22–27, 2005, (2005).

[Gia06] L. Giancarli, V. Chuyanov, M. Abdou, M. Akiba, B. G. Hong, R. Laesser, C. Pan and Y. Strebkov, Breeding blanket modules testing in ITER: An international program on the way to DEMO, *Fusion Engineering and Design*, 81(1-7) (2006) 393–405.

[Gia07] L. Giancarli, V. Chuyanov, M. Abdou, M. Akiba, B. G. Hong, R. Laesser, C. Pan and Y. Strebkov, Test blanket modules in ITER: An overview on proposed designs and required DEMO-relevant materials, *Journal of Nuclear Materials*, 367-370 (2007) 1271–1280.

[Gia10a] L. Giancarli, O. Bede, S. Beloglazov, M. Benchikhoune, K. P. Chang, V. Chuyanov, G. Dell'Orco, J. P. Friconneau, S. Gicquel, C. Gliss, C. Hansalia, M. Iseli, C. S. Kim, I. Kuehn, B. Levesy, F. T. Maluta, M. Merola, R. Pascal, L. Patisson, G. Rigoni, J. Snipes, A. Tesini and I. Yonekawa, Preparation of interfaces in ITER for integrating the test blanket systems, *Fusion Engineering and Design*, 85(10-12) (2010) 1829–1833.

[Gia10b] A. Giannattasio, Z. Yao, E. Tarleton and S. G. Roberts, Brittle-ductile transitions in polycrystalline tungsten, *Philosophical Magazine*, 90(30) (2010) 3947–3959.

[Gia12] L. M. Giancarli, M. Abdou, D. J. Campbell, V. A. Chuyanov, M. Y. Ahn, M. Enoeda, C. Pan, Y. Poitevin, E. R. Kumar, I. Ricapito, Y. Strebkov, S. Suzuki, P. C. Wong and M. Zmitko, Overview of the ITER TBM program, *Fusion Engineering and Design*, 87(5-6) (2012) 395–402.

[Gib05] K. J. Gibson, G. F. Counsell, C. Curran, M. J. Forrest, M. J. Kay and K. G. Watkins, The removal of co-deposited hydrocarbon films from plasma facing components using high-power pulsed flashlamp irradiation, *Journal of Nuclear Materials*, 337-339 (2005) 565–569.

[Gie14] T. Giegerich and C. Day, The KALPUREX process - A new vacuum pumping process for exhaust gases in fusion power plants, *Fusion Engineering and Design*, 89(7-8) (2014) 1476–1481.

[Gie15] T. Giegerich, N. Bekris, B. Butler, C. Day, M. Gethins, S. Lesnoj, X. Luo, R. Mueller, S. Ochoa, P. Pfeil and R. Smith, Conceptual design of the mechanical tritium pumping system for JET DTE2, *Fusion Science and Technology*, 68(3) (2015) 630–634.

[Gie96] P. Gierszewski, Tritium Supply for ITER, technical report CFFTP G-9616, Canadian Fusion Fuels Technology Project, Mississauga, Canada (1996).

[Gil80] J. T. Gill, Effect of container preparation on the growth of protium and methane impurities into tritium gas, *Journal of Vacuum Science and Technology*, 17(2) (1980) 645–654.

[Gil84] J. T. Gill, Investigation into the Radiation Chemistry of Tritiated Water, technical report MLM–3166, Monsanto Research Corporation, Miamisburg, OH, USA (1984).

[Gil85] J. T. Gill and C. W. Pierce, Predicted effects of tritium exposure on fast-acting piezoelectric valves for gas fueling at TFTR, *Fusion Technology*, 8(2P2) (1985) 2217–2223.

[Gil86] J. T. Gill, R. E. Ellefson and W. M. Rutherford, Tritium inventory differences: II Molecular sieve holdup, *Nuclear Materials Management*, 22-25 (1986) 94–101.

[Gil88a] J. T. Gill, R. E. Ellefson, R. P. Paulick, C. M. Colvin, R. L. Yauger, E. E. Johns, R. L. Anderson, E. L. Lewis, P. H. Lamberger and R. E. Vallee, Ammonia in tritium systems, *Fusion Technology*, 14(2P2A) (1988) 876–883.

[Gil88b] J. T. Gill, D. B. Watkins, J. N. Rigano, W. A. Clift, R. A. Watkins, A. L. Burwinkle, J. A. Schultz, L. R. Anderson and H. K. Schmidt, Time-of-flight mass spectrometer

for investigating hydrogen isotope interactions; H/D exhange rates at stainless steel and silicon surfaces, *Fusion Technology*, 14(2P2B) (1988) 1026–1035.

[Gin35] N. Ginsburg and E. F. Barker, The infrared absorption spectrum of methyl deuteride, *The Journal of Chemical Physics*, 3(11) (1935) 668–674.

[Gir91] P. Giroux, T. Pelletier and J.-F. Bressieux, Electrolysis cell for highly tritiated water, *Proceedings of the 19th Symposium of Fusion Technology (SOFT)*, Sept. 3–7, 1990, London, UK, (1991) 650–654.

[Gir92] P. Giroux, T. Pelletier and M. Maj, Strategy for management of solid tritiated wastes, *Fusion Technology*, 21(2P2) (1992) 706–713.

[Gla94] S. Glasstone and A. Sesonske, Nuclear reactor engineering: Reactor systems engineering, Springer Science & Business Media, Berlin/Heidelberg, Germany (1994).

[Glu00a] M. Glugla, R. Laesser, T. L. Le, R.-D. Penzhorn and K. H. Simon, Experience gained during the modification of the CAPRICE system to CAPER, *Fusion Engineering and Design*, 49-50 (2000) 811–816.

[Glu00b] M. Glugla, A. Perevezentsev, D. Niyongabo, R.-D. Penzhorn, A. Bell and P. Herrmann, A PERMCAT reactor for impurity processing in the JET active gas handling system, *Fusion Engineering and Design*, 49-50 (2000) 817–823.

[Glu01] M. Glugla, A. Busigin, L. Doerr, R. Haange, T. Hayashi, O. Kveton, R. Laesser, D. K. Murdoch, M. Nishi, R.-D. Penzhorn and H. Yoshida, The tritium fuel cycle of ITER-FEAT, *Fusion Engineering and Design*, 58-59 (2001) 349–353.

[Glu02a] M. Glugla, L. Doerr, R. Laesser, D. Murdoch and H. Yoshida, Recovery of tritium from different sources by the ITER Tokamak exhaust processing system, *Fusion Engineering and Design*, 61-62 (2002) 569–574.

[Glu02b] M. Glugla, T. L. Le, S. Gross, D. Niyongabo, R. Laesser and K. H. Simon, Development of specific catalysts for detritiation of gases by counter current isotopic swamping, *Fusion Science and Technology*, 41(3P2) (2002) 969–973.

[Glu05] M. Glugla, C. Caldwell-Nichols, I. R. Cristescu, L. Doerr, G. Hellriegel, R. Laesser, D. Murdoch and P. Schaefer, Protection of the primary circuits and effect on the design of the inner deuterium/tritium fuel cycle of ITER, *Fusion Engineering and Design*, 75-79 (2005) 637–643.

[Glu06a] M. Glugla, A. Antipenkov, S. Beloglazov, C. Caldwell-Nichols, I. R. Cristescu, I. Cristescu, C. Day, L. Doerr, J.-P. Girard and E. Tada, The ITER tritium systems, *24^{th} Symposium on Fusion Technology (SOFT)*, (2006).

[Glu06b] M. Glugla, I. R. Cristescu, I. Cristescu and D. Demange, Hydrogen isotope separation by permeation through palladium membranes, *Journal of Nuclear Materials*, 355(1-3) (2006) 47–53.

[Glu06c] M. Glugla, D. K. Murdoch, A. Antipenkov, S. Beloglazov, I. Cristescu, I.-R. Cristescu, C. Day, R. Laesser and A. Mack, ITER fuel cycle R&D: Consequences for the design, *Fusion Engineering and Design*, 81(1-7) (2006) 733–744.

[Glu07] M. Glugla, A. Antipenkov, S. Beloglazov, C. Caldwell-Nichols, I. Cristescu, I. Cristescu, C. Day, L. Doerr, J.-P. Girard and E. Tada, The ITER tritium systems, *Fusion Engineering and Design*, 82 (2007) 472–487.

[Glu13] M. Glugla, Fuel cycle: design, technologies and schedule, *IBF/13 - ITER Business Forum 2013*, Mar. 21–22, 2013, Toulon, France, (2013).

[Glu58] E. Glueckauf and G. P. Kitt, Gas chromatographic separation of hydrogen isotopes, *Proceedings of the International Symposium on Isotope Separation*, Apr. 23–27, 1957, Amsterdam, The Netherlands, (1958) 210–226.

[Glu88] M. Glugla, R. D. Penzhorn, J. L. Anderson and J. R. Bartlit, On the synthesis, selfradiolysis, and catalytic decomposition of tritiated ammonia and methane, *Fusion Technology*, 14(2P2A) (1988) 683–688.

[Glu95] M. Glugla, R. Kraemer, R.-D. Penzhorn, T. L. Le, K. H. Simon, K. Guenther, U. Besserer, P. Schaefer, W. Hellriegel and H. Geissler, Commissioning of the catalytic plasma exhaust clean-up facility CAPRICE and first experimental results, *Fusion Technology*, 28(3P1) (1995) 625–629.

[Glu97a] M. Glugla, R. Kraemer, T. L. Le, K. H. Simon, K. Günther, J. Wendel and R. D. Penzhorn, Results from tritium operation of the clean-up facility CAPRICE, *Proceedings of the 19th Symposium on Fusion Technology (SOFT)*, Sept. 16–20, 1996, Lisbon, Portugal, (1997) 1197–1200.

[Glu97b] M. Glugla, J. Miller, P. Herrmann, M. Iseli and R. D. Penzhorn, Tritium tests with a PERMCAT reactor for isotopic swamping, (1997) 1193–1196.

[Glu98a] M. Glugla, R. Kraemer, T. L. Le, R. D. Penzhorn, K. H. Simon and J. Wendel, Tritium inventories of catalyst beds used in torus exhaust clean-up processes, *Proceedings of the 20th Symposium on Fusion Technology (SOFT)*, Sept. 7–11, 1998, Marseille, France, (1998) 937–940.

[Glu98b] M. Glugla, D. K. Murdoch, H. Geissler, P. Herrmann, R. Kraemer and T. L. Le, Design of a catalytic exhaust clean-up unit for ITER, *Fusion Engineering and Design*, 39-40 (1998) 893–899.

[God08] A. Godot, C. Lepeytre, J.-C. Hubinois, A. Arseguel, J.-P. Daclin and C. Douche, A method to quantify tritium inside waste drums: ^{3}He ingrowth method, *Fusion Science and Technology*, 54(1) (2008) 231–234.

[God11] A. Godot, G. Coindet and J. C. Hubinois, Analysis of gases by Raman spectroscopy: Determination of isotopic composition of hydrogen mixtures (H_2, D_2 and T_2), *Fusion Science and Technology*, 60(3) (2011) 998–1001.

[Gol64] M. Goldblatt, The density of liquid T_2O, *Journal of Physical Chemistry*, 68 (1964) 147.

[Gol69] M. Goldblatt and W. M. Jones, Ionization constants of T_2O and D_2O at 25 °C from cell emf's. Interpretation of the hydrogen isotope effects in emf's, *The Journal of Chemical Physics*, 51(5) (1969) 1881–1894.

[Gol70] V. A. Gol'tzov, V. B. Demin, V. B. Khodets, G. Y. Kagan and P. V. Gel'd, *The Physics of Metals and Metallography*, 29 (1970) 195.

[Gol99] P. Goldstrass, W. Eckstein and C. Linsmeier, Erosion of beryllium and deposition of carbon and oxygen due to bombardment with C^+ and CO^+ ions, *Journal of Nuclear Materials*, 266-269 (1999) 581–586.

[Gon59] B. Gonsior, Tritium-Anstieg im atmosphaerischen Wasserstoff, *Die Naturwissenschaften*, 46(6) (1959) 201–202.

[Goo83] P. D. Goodell and P. S. Rudman, Hydriding and dehydriding rates of the $LaNi_5$ – H system, *Journal of the Less Common Metals*, 89(1) (1983) 117–125.

[Goo84] P. D. Goodell, Stability of rechargeable hydriding alloys during extended cycling, *Journal of the Less-Common Metals*, 99(1) (1984) 1–14.

[Goo91] S. H. Goods and C. W. Karfs, Helium-induced weld cracking in low heat input GMA weld overlays, *Welding Journal*, 70(5) (1991) 123–132.

[Gor62] J. K. Gorman and W. R. Nardella, Hydrogen permeation through metals, *Vacuum*, 12(1) (1962) 19–24.

[Got70] R. Goto, Hyperpure hydrogen from palladium alloy membrane permeation, *Chemical Economy & Engineering Review*, 2(11) (1970).

[Gra00] H. J. Grabke and E. Riecke, Absorption and diffusion of hydrogen in steels, *Materials Science*, 34(6) (2000) 331.

[Gra02] W. R. C. Graham, A. E. Everatt, J. R. R. Tremblay, J. M. Miller and D. A. Spagnolo, Demonstration of very high detritiation factors with a pilot-scale CECE facility, *Fusion Science and Technology*, 41(3P2) (2002) 1137–1141.

[Gra87] D. M. Grant, D. L. Cummings and D. A. Blackburn, Hydrogen in 304 steel: Diffusion, permeation and surface reaction, *Journal of Nuclear Materials*, 149(2) (1987) 180–191.

[Gra88] D. M. Grant, D. L. Cummings and D. A. Blackburn, Hydrogen in 316 steel - diffusion, permeation and surface reaction, *Journal of Nuclear Materials*, 152(2-3) (1988) 139–145.

[Grè01] O. Grègoire and J. Ladrière, Activation of stainless steel with high energy neutrons, *Journal of Nuclear Materials*, 298(3) (2001) 309–315.

[Gre14] M. Greenwald, A. Bader, S. Baek, M. Bakhtiari, H. Barnard, W. Beck, W. Bergerson, I. Bespamyatnov, P. Bonoli, D. Brower, D. Brunner, W. Burke, J. Candy, M. Churchill, I. Cziegler, A. Diallo, A. Dominguez, B. Duval, E. Edlund, P. Ennever, D. Ernst, I. Faust, C. Fiore, T. Fredian, O. Garcia, C. Gao, J. Goetz, T. Golfinopoulos, R. Granetz, O. Grulke, Z. Hartwig, S. Horne, N. Howard, A. Hubbard, J. Hughes, I. Hutchinson, J. Irby, V. Izzo, C. Kessel, B. LaBombard, C. Lau, C. Li, Y. Lin, B. Lipschultz, A. Loarte, E. Marmar, A. Mazurenko, G. McCracken, R. McDermott,

O. Meneghini, D. Mikkelsen, D. Mossessian, R. Mumgaard, J. Myra, E. Nelson-Melby, R. Ochoukov, G. Olynyk, R. Parker, S. Pitcher, Y. Podpaly, M. Porkolab, M. Reinke, J. Rice, W. Rowan, A. Schmidt, S. Scott, S. Shiraiwa, J. Sierchio, N. Smick, J. A. Snipes, P. Snyder, B. Sorbom, J. Stillerman, C. Sung, Y. Takase, V. Tang, J. Terry, D. Terry, C. Theiler, A. Tronchin-James, N. Tsujii, R. Vieira, J. Walk, G. Wallace, A. White, D. Whyte, J. Wilson, S. Wolfe, G. Wright, J. Wright, S. Wukitch and S. Zweben, 20 years of research on the Alcator C-Mod tokamak, *Physics of Plasmas*, 21(11) (2014) 110501.

[Gre93] L. R. Greenwood, F. A. Garner and D. J. Edwards, Calculation of transmutation in copper and comparison with measured electrical properties, 8^{th} *American Society for Testing and Materials symposium on reactors*, Aug. 29–Sept. 3, 1993, Vail, VA, United States, (1993).

[Gri51] E. R. Grilly, The vapor pressures of hydrogen, deuterium and tritium up to three atmospheres, *Journal of the American Chemical Society*, 73(2) (1951) 843–846.

[Gro15] R. Groessle, A. Beck, B. Bornschein, S. Fischer, A. Kraus, S. Mirz and S. Rupp, First calibration measurements of an FTIR absorption spectroscopy system for liquid hydrogen isotopologues for the isotope separation system of fusion power plants, *Fusion Science and Technology*, 67(2) (2015) 357–360.

[Gro54] A. V. Grosse, A. D. Kirshenbaum, J. L. Kulp and W. S. Broecker, The natural tritium content of atmospheric hydrogen, *Physical Review*, 93(1) (1954) 250–251.

[Gru11] S. Gruenhagen, P. D. Brennan, S. Knipe, R. Stagg and J. Yorkshades, Analysis of hydrocarbons of the JET divertor cryogenic pump at the end of the carbon wall campaign using a micro gas chromatograph, *Fusion Science and Technology*, 60(3) (2011) 931–936.

[Gru88] K. M. Gruetzmacher, R. V. Carlson, J. R. Stencel and R. A. P. Sissingh, Transportation of tritiated waste from fusion facilities, *Fusion Technology*, 14(2P2B) (1988) 966–971.

[Gue11] P. Guetat, C. Boyer, A. Tognelli and J. M. Duda, 50 years environmental tritium transfer review in the vicinity of french research centre, *Fusion Science and Technology*, 60(4) (2011) 1238–1243.

[Gug91] F. Guglielmi, G. I. Williams, J. Quelch and S. Sood, Modifications to the high tritium columns at Darlington Tritium Removal Facility, *Proceedings of the 16th Symposium on Fusion Technology (SOFT)*, Sept. 3–7, 1990, London, UK, (1991) 684–688.

[Gul50] E. A. Gulbransen and K. F. Andrew, The kinetics of the reactions of beryllium with oxygen and nitrogen and the effect of oxide and nitride films on its vapor pressure, *Journal of the Electrochemical Society*, 97(11) (1950) 383–395.

[Gut74] J. W. Guthrie, L. C. Beavis, D. R. Begeal and W. G. Perkins, Properties of hydride-forming metals and of multilayer hydrogen permeation barriers, *Journal of Nuclear Materials*, 53 (1974) 313–322.

[Haa03] H. Haas, C. Day, A. Mack and D. K. Murdoch, Performance tests of the ITER model pump, *Fusion Engineering and Design*, 69(1-4) (2003) 91–95.

[Haa05] A. A. Haasz and J. W. Davis, Hydrogen retention in and release from carbon materials, *Nuclear Fusion Research*, R. Clark and D. H. Reiter, editors, Springer-Verlag, Berlin, Heidelberg, Federal Republic of Germany, (2005), 225–248.

[Haa06] A. Haasz and J. Davis, Hydrogen isotopic effects on the erosion of carbon, *Fusion Science and Technology*, 50(1) (2006) 58–67.

[Haa07] A. A. Haasz, C. K. Tsui, J. W. Davis and R. Ochoukov, Thermo-oxidation of codeposits from DIII-D divertor tiles, *Physica Scripta*, T128 (2007) 55–59.

[Haa89] R. Haange, A. Bell, C. Caldwell-Nichols, A. Dombra, C. Gordon, J. Gowman, E. Groskopfs, J. L. Hemmerich, A. Konstantellos and E. Kussel, General overview of the Active Gas Handling System at JET, *Proceedings of the 3rd Topical Meeting on Tritium Technology in Fission, Fusion and Isotopic Applications*, May 1–6, 1988, Toronto, Canada, (1989) 461–465.

[Haa98] A. Haasz, J. W. Davis, M. Poon and R. G. Macaulay-Newcombe, Deuterium retention in tungsten for fusion use, *Journal of Nuclear Materials*, 258-263 (1998) 889–895.

[Haa99] A. A. Haasz, M. Poon and J. W. Davis, The effect of ion damage on deuterium trapping in tungsten, *Journal of Nuclear Materials*, 266-269 (1999) 520–525.

[Hac84] H. Hackfort, J. Chatzipetros and G. Assmann, Verfahren zum Ausfrieren von Xenon aus dem Aufloeserabgas von Wiederaufarbeitungsanlagen, Spezielle Berichte der Kernforschungsanlage Juel-Spez-287, Kernforschungsanlage Juelich GmbH, Juelich, Germany (1984).

[Hai97] A. D. Haigh and M. A. Pick, Operational aspects of using beryllium-safety and decontamination, *Fusion Engineering and Design*, 37(4) (1997) 531–541.

[Hai99] A. D. Haigh, R. Middleton and G. Newbert, Waste management aspects of the DTE1 and RTE campaigns, *Fusion Engineering and Design*, 47(2-3) (1999) 285–299.

[Hal81] J. E. Halverson and L. F. I. I. Herzog, Static ^{3}He/^{4}He gas mass spectrometer for low level tritium concentration measurements, *IAEA International Symposium on Methods of Low-level Counting and Spectrometry*, Apr. 6–10, 1981, Berlin, Germany, (1981) 12.

[Hal95] A. von Halle, J. L. Anderson, C. Gentile, L. Grisham, J. Hosea, J. Kamperschroer, P. LaMarche, M. Oldaker, A. Nagy, S. Raftopoulos and T. Stevenson, The tritium operations experience on TFTR, *Proceedings of the 18th Symposium on Fusion Technology (SOFT)*, Aug. 22–26, 1994, Karlsruhe, Federal Republic of Germany, (1995) 1039–1042.

[Han02] T. Hanawa, S. Hiromoto, A. Yamamoto, D. Kuroda and K. Asami, XPS characterization of the surface oxide film of 316L stainless steel samples that were located in quasi-biological environments, *Materials Transactions*, 43(12) (2002) 3088–3092.

[Han58] M. Hansen, K. Anderko and H. W. Salzberg, Constitution of binary alloys, *Journal of the Electrochemical Society*, 105(12) (1958) 260C.

[Han64] R. S. Hansen, R. R. Frost and J. A. Murphy, The thermal conductivity of hydrogen-helium mixtures, *The Journal of Physical Chemistry*, 68(7) (1964) 2028–2029.

[Han89a] J. I. Han and J.-Y. Lee, Influence of oxygen impurity on the hydrogenation properties of $LaNi_5$, $LaNi_{4.7}Al_{0.3}$ and $MmNi_{4.5}Al_{0.5}$ during long-term pressure-induced hydriding-dehydriding cycling, *Journal of the Less-Common Metals*, 152(2) (1989) 329–338.

[Han89b] J. I. Han and J.-Y. Lee, The effect of CO impurity on the hydrogenation properties of $LaNi_5$, $LaNi_{4.7}Al_{0.3}$ and $MmNi_{4.5}Al_{0.5}$ during hydriding-dehydriding cycling, *Journal of the Less-Common Metals*, 152(2) (1989) 319–327.

[Har00] M. Hara, T. Okabe, K. Mori and K. Watanabe, Kinetics and mechanism of hydrogen-induced disproportionation of ZrCo, *Fusion Engineering and Design*, 49-50 (2000) 831–838.

[Has07] K. Hashizume, J. Masuda, T. Otsuka, T. Tanabe, Y. Hatano, Y. Nakamura, T. Nagasaka and T. Muroga, Diffusional behavior of tritium in V−4 Cr−4 Ti alloy, *Journal of Nuclear Materials*, 367-370 (2007) 876–881.

[Has73] T. Hashino and Y. Okajima, Mechanism of the reaction of hydrogen with uranium, *The Journal of Physical Chemistry*, 77(18) (1973) 2236–2241.

[Has85] E. Hashimoto and T. Kino, Hydrogen permeation through type 316 stainless steels and ferritic steel for a fusion reactor, *Journal of Nuclear Materials*, 133-134 (1985) 289–291.

[Hat11] Y. Hatano, K. Zhang and K. Hashizume, Fabrication of ZrO_2 coatings on ferritic steel by wet-chemical methods as a tritium permeation barrier, *Physica Scripta*, T145 (2011) 014044.

[Hat12] Y. Hatano, M. Hara, H. Ohuchi-Yoshida, H. Nakamura and T. Yamanishi, Measurement of tritium concentration in water by imaging plate, *Fusion Engineering and Design*, 87(7-8) (2012) 965–968.

[Hat19] Y. Hatano, S. E. Lee, J. Likonen, S. Koivuranta, M. Hara, S. Masuzaki, N. Asakura, K. Isobe, T. Hayashi, J. Ikonen and A. Widdowson, Tritium distributions on W-coated divertor tiles used in the third JET ITER-like wall campaign, *Nuclear Materials and Energy*, 18 (2019) 258–261.

[Hat95] Y. Hatano, T. Maetani and M. Sugisaki, Characterization of surface barrier effect upon tritium permeation through stainless steel with Auger electron spectroscopy, *Fusion Technology*, 28(3P2) (1995) 1182–1187.

[Hau07] V. Hauer, J.-C. Boissin, C. Day, H. Haas, A. Mack, D. Murdoch, R. Laesser and M. Wykes, Design of the ITER torus prototype cryopump, *Fusion Engineering and Design*, 82(15-24) (2007) 2113–2119.

[Hau79] J. Hauck, Isotope effects for hydrogen diffusion in transition metals, *Zeitschrift fuer Physikalische Chemie, Neue Folge*, 114 (1979) 165–174.

[Haw82] S. H. Hawthorne, Conditioning of Tritiated Wastes, Part I-Tritiated Water Immobilization, technical report 82-531-K, Ontario Hydro Research Division, Ontario, Canada (1982).

[Haw84] S. H. Hawthorne, Conditioning of Tritiated Wastes: Part II-Solidification and Encapsulation, technical report 84-6-K, Ontario Hydro, Research Division, Ontario, Canada (1984).

[Haw86] J. G. Hawke, A. A. Suweda and C. A. Lukey, Spin-directed reaction of recoil tritium with hydrogen, *Journal of the Chemical Society, Chemical Communications*, (7) (1986) 499–501.

[Hay05] T. Hayashi, T. Suzuki, M. Yamada and M. Nishi, Tritium accounting stability of a ZrCo bed with "in-bed" gas flowing calorimetry, *Fusion Science and Technology*, 48(1) (2005) 317–323.

[Hay06] T. Hayashi, T. Itoh, K. Kobayashi, K. Isobe and M. Nishi, Safety handling characteristics of high-level tritiated water, *Fusion Engineering and Design*, 81(8-14) (2006) 1365–1369.

[Hay07a] T. Hayashi, H. Nakamura, K. Isobe, K. Kobayashi, T. Yamanishi and K. Okuno, Tritium behavior on the water-metal boundary for the permeation into cooling water through metal piping, *Fusion Science and Technology*, 52(3) (2007) 687–691.

[Hay07b] T. Hayashi, T. Suzuki, W. M. Shu and T. Yamanishi, Isotope effect of hydrogen rapidly supplied from the metal storage bed, *Fusion Science and Technology*, 52(3) (2007) 706–710.

[Hay11] T. Hayashi, M. Yamada, T. Suzuki and T. Yamanishi, Improvement of ultimate pressure of oil-free reciprocating pump for tritium service, *Fusion Science and Technology*, 60(3) (2011) 1101–1104.

[Hay12] T. Hayashi, H. Nakamura, K. Isobe, K. Kobayashi, M. Oyaizu, T. Yamanishi, Y. Oya and K. Okuno, Hydrogen isotope permeation from cooling water through various metal piping, *Fusion Engineering and Design*, 87(7-8) (2012) 1333–1337.

[Hay91] T. Hayashi, S. Konishi, M. Yamada, Y. Matsuda, M. Inoue, T. Nakamura, T. Takanaga, Y. Naruse and K. Okuyama, Development of large oil-free roughing pump for tritium service, *Fusion Technology*, 19(3P2B) (1991) 1663–1667.

[Hay92a] T. Hayashi, J. Amano, K. Okuno and Y. Naruse, Release behavior of decay helium from zirconium-cobalt tritide, *Fusion Technology*, 21(2P2) (1992) 845–849.

[Hay92b] T. Hayashi, S. Konishi, H. Nakamura, M. Inoue, K. Hirata, K. Okuno, Y. Naruse, J. W. Barnes, W. Harbin, R. Wilhelm, M. King, J. R. Bartlit and J. L. Anderson, Recent tritium experiments of the JAERI Fuel Cleanup System (JFCU) at the Tritium Systems Test Assembly (TSTA), *Fusion Technology*, 21(3P2B) (1992) 1979–1983.

[Hay92c] P. J. Hayward, D. G. Evans, P. Taylor, I. M. George and A. M. Duclos, Oxidation of uranium in argon-25% oxygen at 190 - 610 °C, *Journal of Nuclear Materials*, 187(3) (1992) 215–222.

[Hay93] T. Hayashi and K. Okuno, Overview of tritium safety technology at the tritium process laboratory of JAERI, *Journal of Fusion Energy*, 12(1) (1993) 21–25.

[Hay94] T. Hayashi, T. Suzuki and K. Okuno, Long-term measurement of helium-3 release behavior from zirconium-cobalt tritide, *Journal of Nuclear Materials*, 212-215 (1994) 1431–1435.

[Hay95a] T. Hayashi, M. Yamada, S. Konishi, Y. Matsuda, K. Okuno, J. E. Nasise, R. S. Dahlin and J. L. Anderson, Tritium evacuation performance of a large oil-free reciprocating pump, *Fusion Engineering and Design*, 28 (1995) 357–361.

[Hay95b] T. Hayashi, M. Yamada, T. Suzuki, Y. Matsuda and K. Okuno, Gas separation performance of a hollow-filament type polyimide membrane module for a compact tritium removal system, *Fusion Technology*, 28(3P2) (1995) 1503–1508.

[Hay95c] T. Hayashi, M. Yamada, T. Suzuki, Y. Matsuda and K. Okuno, Tritium accounting characteristics of "in-bed" gas flowing calorimetry, *Fusion Technology*, 28(3P2) (1995) 1015–1019.

[Hec90] R. Hecker, D. Stoever, H. Jonas and H. P. Buchkremer, Properties of chromia scales on high-temperature alloys used as barriers against hydrogen permeation, *Journal of Nuclear Materials*, 171(1) (1990) 84–93.

[Hed88] W. H. Hedley, P. H. Lamberger, G. E. Gibbs and C. M. Colvin, Improvements in efficiency, capacity, and reliability of Mound's Effluent Removal System, *Fusion Technology*, 14(2P2B) (1988) 1010–1013.

[Hei03] S. Heinze, P. Bussiere and T. Pelletier, French experience in tritiated water management, *Fusion Engineering and Design*, 69(1-4) (2003) 67–70.

[Hei05] S. Heinze, T. Stolz, D. Ducret and J.-C. Colson, Self-radiolysis of tritiated water: Experimental study and simulation, *Fusion Science and Technology*, 48(1) (2005) 673–679.

[Hei17] K. Heinola, J. Likonen, T. Ahlgren, S. Brezinsek, G. D. Temmerman, I. Jepu, G. F. Matthews, R. A. Pitts and A. Widdowson, Long-term fuel retention and release in JET ITER-like wall at ITER-relevant baking temperature, *Nuclear Fusion*, 57(8) (2017) 1–6.

[Hei85] H. Heimbach, H. R. Ihle and C. H. Wu, Removal of nitrogen and methane from hydrogen by metal getters, *Proceedings of the 13th Symposium on Fusion Technology (SOFT)*, Sept. 24–28, 1984, Varese, Italy, (1985) 421–426.

[Hei88a] A. G. Heics, W. T. Shmayda, K. D. Geiger and N. P. Kherani, Ontario Hydro Research Division Tritium Laboratory: Design and operating experience, *Fusion Technology*, 14(2P2B) (1988) 1277–1281.

[Hei88b] A. G. Heics, W. T. Shmayda and N. P. Kherani, Heat transport in doubly contained uranium storage beds, *Journal of Vacuum Science & Technology A: Vacuum, Surfaces, and Films*, 6(3) (1988) 1872–1875.

[Hei92] A. G. Heics and W. T. Shmayda, Tritium aging of zirconium cobalt, *Fusion Technology*, 21(2P2) (1992) 1030–1034.

[Hei93] A. G. Heics and W. T. Shmayda, Low pressure dissociation studies of uranium, *Proceedings of the 17thSymposium on Fusion Technology (SOFT)*, Sept. 14–18, 1992, Rome, Italy, (1993) 1157–1161.

[Hei94a] A. G. Heics, T. Shmayda and D. Muller, Tritium effects on the performance of turbomolecular pumps, *Proceedings of the 15th Symposium on Fusion Engineering (SOFE)*, Oct. 11–15, 1993, Hyannis, MA, USA, (1994) 73–76.

[Hei94b] A. G. Heics and W. T. Shmayda, Development of a secondary enclosure clean-up system for tritium systems, *Proceedings of the 15th Symposium on Fusion Engineering (SOFE)*, Oct. 11–15, 1993, Hyannis, MA, USA, (1994) 65–68.

[Hei95] A. G. Heics and W. T. Shmayda, Design of a second generation secondary enclosure clean-up system, *Fusion Technology*, 28(3P2) (1995) 1509–1514.

[Hem89a] J. L. Hemmerich, A. Dombra, J. Gowman, E. Groskopfs, R. Haange, A. Konstantellos, E. Kuessel, R. Laesser, P. Milverton, K. Walker and K. Walter, Key components of the JET Active Gas Handling System — experimental programme and test results, *Fusion Engineering and Design*, 11(1-2) (1989) 93–100.

[Hem89b] J. L. Hemmerich, A. Dombra, J. Gowman, E. Groskopfs, R. Haange, A. Konstantellos, E. Kuessel, R. Laesser, P. Milverton, K. Walker and K. Walter, The impurity processing loop for the JET Active Gas Handling Plant, *Fusion Engineering and Design*, 11(1-2) (1989) 557–561.

[Hem92] J. L. Hemmerich, R. Laesser and T. Winkel, Gas recovery system for the first JET tritium experiment, *Fusion Engineering and Design*, 19(2) (1992) 161–167.

[Hem93] J. L. Hemmerich, A systematic approach to the design of a large-scale detritiation system for controlled thermonuclear fusion experiments, *Fusion Technology*, 24(2) (1993) 137–144.

[Hem94] J. L. Hemmerich, L. Serio and P. Milverton, High-resolution tritium calorimetry based on inertial temperature control, *Review of Scientific Instruments*, 65(5) (1994) 1616–1620.

[Hem95] J. L. Hemmerich, Thermal design of a metal hydride storage bed, permitting tritium accountancy to 0.1 % resolution and repeatability, *Fusion Technology*, 28(4) (1995) 1732–1737.

[Hem96a] J. L. Hemmerich, J.-C. Loos, A. Miller and P. Milverton, Advances in temperature derivative control and calorimetry, *Review of Scientific Instruments*, 67(11) (1996) 3877–3884.

[Hem96b] J. L. Hemmerich, P. Milverton, G. Newbert, N. Green and A. Miller, Tritium and uranium inventory measurements with the JET AGHS precision calorimeter,

Proceedings of 16th Symposium on Fusion Engineering (SOFE), Sept. 30–Oct. 5, 1995, Champaign, IL, USA, (1996) 781–783.

[Hen02] M. Henderson, The interaction of water with solid surfaces: fundamental aspects revisited, *Surface Science Reports*, 46(1-8) (2002) 1–308.

[Hen66] B. Hennessy, J. Mead and T. Stening, The permeability of plastics films, The Plastics Institute (PI), London, UK (1966).

[Her50] G. Herzberg, Molecular spectra and molecular structure, 2nd edition, Van Nostrand Reinhold Co., New York, NY, USA (1950).

[Hes71] E. D. Hespe, Leach testing of immobilized radioactive waste solids, *Atomic Energy Review*, 9 (1971) 195.

[Heu02] L. K. Heung and M. L. Rhoden, Performance of a large-scale glovebox-stripper system, *Fusion Science and Technology*, 41(3P2) (2002) 583–587.

[Heu05a] L. K. Heung, R. H. Hsu, J. L. Rice and T. S. McGee, Performance improvements of a tritiated water recovery system, *Fusion Science and Technology*, 48(1) (2005) 435–440.

[Heu05b] L. K. Heung and G. C. Staack, Hydrogen isotope exchange properties of porous solids containing hydrogen, *Fusion Science and Technology*, 48(1) (2005) 585–588.

[Heu08] L. K. Heung, H. T. Sessions, A. S. Poore, W. D. Jacobs and C. S. Williams, Next-generation TCAP hydrogen isotope separation process, *Fusion Science and Technology*, 54(2) (2008) 399–402.

[Heu09] L. K. Heung, H. T. Sessions, X. Xiao and H. L. Mentzer, Demonstration of the next-generation TCAP hydrogen isotope separation process, *Fusion Science and Technology*, 56(4) (2009) 1471–1475.

[Heu11] L. K. Heung, H. T. Sessions and X. Xiao, TCAP hydrogen isotope separation using palladium and inverse columns, *Fusion Science and Technology*, 60(4) (2011) 1331–1334.

[Heu92a] L. K. Heung, G. W. Gibson and M. S. Ortmana, Tritium stripping by a catalytic exchange stripper, *Fusion Technology*, 21(2P2) (1992) 588–593.

[Heu92b] L. K. Heung, J. H. Owen, R. H. Hsu, R. F. Hashinger, D. E. Ward and P. E. Bandola, Tritium confinement in a new tritium processing facility at the Savannah River Site, *Fusion Technology*, 21(2P2) (1992) 594–598.

[Heu95a] L. K. Heung, Developments in tritium storage and transportation at the Savannah River Site, *Fusion Technology*, 27(2T) (1995) 85–90.

[Heu95b] L. K. Heung, Stripper system performance in the Replacement Tritium Facility, *Fusion Technology*, 28(3P1) (1995) 859–864.

[Heu95c] L. K. Heung, Tritium transport vessel using depleted uranium, *Fusion Technology*, 28(3P2) (1995) 1385–1390.

[Heu95d] L. K. Heung, Tritiated ammonia formation, *Fusion Technology*, 28(3P2) (1995) 1188–1193.

[Hic69] R. G. Hickman, Diffusion and permeation of deuterium in palladium-silver at high temperature and pressure, *Journal of the Less-Common Metals*, 19(4) (1969) 369–383.

[Hig02] T. Higashijima, K. Obara, K. Shibanuma, K. Koizumi, K. Kobayashi, Y. Oya, W. Shu, T. Hayashi and M. Nishi, Exposure to tritiated moisture and decontamination of components for ITER remote maintenance equipment, *Fusion Science and Technology*, 41(3P2) (2002) 731–735.

[Hil99] D. Hill and A. Heller, Experiment mimics nature's way of plasmas, *Science & Technology Review*, December (1999) 18–20.

[Hir03] T. Hirai, V. Philipps, A. Huber, G. Sergienko, J. Linke, T. Wakui, T. Tanabe, M. Rubel, M. Wada, T. Ohgo, A. Pospieszczyk, K. Ohya and V. Barabash, Performance and erosion of a tungsten brush limiter exposed at the TEXTOR tokamak, *Journal of Nuclear Materials*, 313-316 (2003) 67–71.

[Hir16] T. Hirai, S. Panayotis, V. Barabash, C. Amzallag, F. Escourbiac, A. Durocher, M. Merola, J. Linke, T. Loewenhoff, G. Pintsuk, M. Wirtz and I. Uytdenhouwen, Use of tungsten material for the ITER divertor, *Nuclear Materials and Energy*, 9 (2016) 616–622.

[Hir75] K. Hiraoka and P. Kebarle, Temperature dependence of third order ion molecule reactions. The reaction $H_3^+ + 2H_2 = H_5^+ + H_2$, *The Journal of Chemical Physics*, 63(2) (1975) 746–749.

[Hir83] T. Hirabayashi and E. Tachikawa, Sorption and desorption of tritium on the surface of borosilicate glass, *Radiochimica Acta*, 33(1) (1983) 61–64.

[Hir84a] T. Hirabayashi and M. Saeki, Sorption of gaseous tritium on the surface of type 316 stainless steel, *Journal of Nuclear Materials*, 120(2-3) (1984) 309–315.

[Hir84b] T. Hirabayashi, M. Saeki and E. Tachikawa, A thermal desorption study of the surface interaction between tritium and type 316 stainless steel, *Journal of Nuclear Materials*, 126(1) (1984) 38–43.

[Hir85a] T. Hirabayashi, M. Saeki and E. Tachikawa, Chemical decontamination of the tritium-sorbing surface of type 316 stainless steel, *Journal of Nuclear Materials*, 136(2-3) (1985) 179–185.

[Hir85b] T. Hirabayashi, M. Saeki and E. Tachikawa, Effect of surface treatments on the sorption of tritium on type-316 stainless steel, *Journal of Nuclear Materials*, 127(2-3) (1985) 187–192.

[Hir87] K. Hiraoka, A determination of the stabilities of $H_3{}^+(H_2)_n$ with n=1-9 from measurements of the gas-phase ion equilibria $H_3{}^+(H_2)_{n-1} + H_2 = H_3{}^+(H_2)_n$, *Journal of Chemical Physics*, 87 (1987) 4048–4055.

[Hir88] B. Hircq, General considerations for on-site tritium transfer, *Fusion Technology*, 14(3) (1988) 1299–1303.

[Hir89] T. Hirabayashi, M. Saeki, T. A. Sasaki and K.-W. Sung, Sorption of tritium on surface-modified type-316 stainless steel, *Fusion Engineering and Design*, 10 (1989) 287–291.

[Hir90a] T. Hirabayashi, S. Poosittisak, Y. Sun and M. Saeki, Tritium sorption and chemical and topographical properties of a stainless steel surface modified with chromium, *Journal of Nuclear Materials*, 173(1) (1990) 26–33.

[Hir90b] T. Hirabayashi, Y. Sun and M. Saeki, Formation of a tritium-resistant surface on stainless steel by chromium diffusion coating, *Journal of Nuclear Materials*, 175(3) (1990) 177–183.

[Hir90c] T. Hirabayashi, K.-W. Sung, T. A. Sasaki and M. Saeki, Change in tritium-sorption property of stainless steel by thermal surface oxidation, *Journal of Nuclear Materials*, 175(1-2) (1990) 78–83.

[Hir90d] B. Hircq, Materials reweldability tests, CEA report N-2644, Task Action TCP 4-2, (1990).

[Hir90e] B. Hircq, Tritium research and technology facilities for fusion inside the Bruyeres-le-Chatel Research Center of the French Atomic Energy Commission, *Fusion Engineering and Design*, 12(3) (1990) 343–347.

[Hir90f] Y. Hirooka, R. Conn, R. Causey, D. Croessmann, R. Doerner, D. Holland, M. Khandagle, T. Matsuda, G. Smolik, T. Sogabe, J. Whitley and K. Wilson, Bulk-boronized graphites for plasma-facing components in ITER, *Journal of Nuclear Materials*, 176-177 (1990) 473–480.

[Hir91a] T. Hirabayashi, Y. Sun, H. Yamamoto, Y. Toida and M. Saeki, Chemical and topographical properties of tritium-resistant stainless steel surfaces formed by chromium diffusion coating, *Journal of Nuclear Materials*, 182 (1991) 135–144.

[Hir91b] B. Hircq, Recent developments from the European Tritium Handling Programme, *Proceedings of the 16th Symposium on Fusion Technology (SOFT)*, Sept. 3–7, 1990, London, UK, (1991) 161–169.

[Hir93] B. Hircq and V. Blet, Tritium activities for fusion inside the Bruyeres-le-Châtel Center of the French Atomic Energy Commission, *Proceedings of the 17th Symposium on Fusion Technology (SOFT)*, Sept. 14–18, 1992, Rome, Italy, (1993) 1162–1166.

[Hir97] Y. Hirooka, Modeling of materials mixing behavior among beryllium, carbon and tungsten as plasma-facing materials under deuterium and tritium plasma bombardment, *Fusion Engineering and Design*, 37(2) (1997) 299–306.

[Hoe94] J. S. Hoelder, Short Term Aging of $LaNi_{4.25}Al_{0.75}$ Tritide Storage Material, technical report WSRC-MS–94-0477, Westinghouse Savannah River Company, Aiken, SC, USA (1994).

[Hof88] P. Hofmann and W. Dienst, Compatibility studies of metallic materials with lithium-based oxides, *Journal of Nuclear Materials*, 155-157 (1988) 485–490.

[Hof95] K. J. Hofstetter, Continuous aqueous tritium monitoring, *Fusion Technology*, 28(3P2) (1995) 1527–1531.

[Hoh82] B. Hohler and H. Schreyer, Diffusion of hydrogen, deuterium and tritium in face-centred cubic metals at low temperatures, *Journal of Physics F: Metal Physics*, 12(5) (1982) 857–874.

[Hol07] N. Holtkamp, An overview of the ITER project, *Fusion Engineering and Design*, 82(5-14) (2007) 427–434.

[Hol57] J. E. Holliday and E. J. Sternglass, Backscattering of 5 - 20 keV electrons from insulators and metals, *Journal of Applied Physics*, 28(10) (1957) 1189–1193.

[Hol63] B. Holmqvist and T. Wiedling, A Gas Target with a Tritium Gas Handling System, technical report AE-127, Aktie Bolaget Atomenergi, Stockholm, Nykoeping, Sweden (1963).

[Hol70] G. L. Holleck, Diffusion and solubility of hydrogen in palladium and palladium-silver alloys, *The Journal of Physical Chemistry*, 74(3) (1970) 503–511.

[Hol74] L. Holland, W. Steckelmacher and J. Yarwood, Vacuum manual, Springer, Dordrecht, Netherlands (1974).

[Hol81] W. J. Holtslander and J. M. Yaraskavitch, Tritium Immobilization and Packaging using Metal Hydrides, technical report AECL-7151, Atomic Energy of Canada Ltd, Chalk River, Canada (1981).

[Hol82] W. J. Holtslander and J. M. Miller, Immobilization and packaging of recovered tritium, technical report AECL-7757, Atomic Energy of Canada Ltd, Chalk River, Canada (1982).

[Hol83] D. F. Holland, R. A. Causey and M. L. Sattler, Implantation measurements to determine tritium permeation in first wall structures, *Nuclear Technology - Fusion*, 4(2P2) (1983) 677–680.

[Hol86a] D. F. Holland and R. A. Jalbert, A model for tritium concentration following tritium release into a test cell and subsequent operation of an atmospheric cleanup system, *Proceedings of the 17th Symposium on Fusion Technology*, Nov. 18–22, 1985, Rome, Italy, (1986) 638–643.

[Hol86b] H. Holleck and H. Kleykamp, Uranium, supplement volume C12, uranium carbides, *Gmelin Handbook of Inorganic Chemistry*, 8th edition, R. Keim and C. Keller, editors, Springer-Verlag, Heidelberg, (1986).

[Hol95] G. W. Hollenberg, E. P. Simonen, G. Kalinin and A. Terlain, Tritium/hydrogen barrier development, *Fusion Engineering and Design*, 28 (1995) 190–208.

[Hon10] S. H. Hong, K. S. Lee, H. T. Kim, G. P. Kim, J. K. Sun, H. J. Woo, J. M. Park, W. C. Kim, H. K. Kim, K. R. Park, H. Yang, H. Na and K. S. Chung, First boronization in KSTAR, *Fusion Engineering and Design*, 85(6) (2010) 946–949.

[Hor12] L. Horton, The JET programme in support of ITER, *Fusion Engineering and Design*, 87(5-6) (2012) 625–629.

[Hor17] H. Hora, S. Eliezer, G. Kirchhoff, N. Nissim, J. Wang, P. Lalousis, Y. Xu, G. Miley, J. Martinez-Val and W. McKenzie, Road map to clean energy using laser beam ignition of boron-hydrogen fusion, *Laser and Particle Beams*, 35(4) (2017) 730–740.

[Hor92] A. S. Horen and M. W. Lee, Metal hydride-based isotope separation – Large-scale operations, *Fusion Technology*, 21(2P2) (1992) 282–286.

[Hou97] C. Housiades and K. H. Schrader, Testing of a water vapour cold trap for atmospheric de-tritiation, *Proceedings of the 19th Symposium on Fusion Technology (SOFT)*, Sept. 16–20, 1996, (1997) 1217–1220.

[How04] J. How, P. Barabash and W. Spears, ITER Project Integration Document (PID), version 1.0, ITER-D-2234RH, ITER, St. Paul-lez-Durance, France (2004).

[How75] R. H. Howell, J. C. Cate and C. Wong, Separation of HT, noble gases and HTO vapor with semipermeable membranes, *Nuclear Instruments and Methods*, 124(2) (1975) 579–583.

[How82] W. B. Howard, Flame arresters and flashback preventers, *Plant/Operations Progress*, 1(4) (1982) 203–208.

[Hoy61] J. E. Hoy, Operational experience with Kanne ionization chambers, *Health Physics*, 6(2) (1961) 203–210.

[Hse81] H. C. Hseuh and H. A. Worwetz, Performance of BNL-TSTA compound cryopump, *Journal of Vacuum Science and Technology*, 18(3) (1981) 1131–1135.

[Hug92a] I. G. Hughes, R. Behrisch and A. P. Martinelli, Depth profiling of deuterium in a beryllium/carbon layer, *Nuclear Instruments and Methods in Physics Research Section B: Beam Interactions with Materials and Atoms*, 64(1-4) (1992) 434–438.

[Hug92b] M. Huguet, A. C. Bell, S. J. Booth, C. Caldwell-Nichols, A. Carmichael, P. Chuilon, N. Davies, K. J. Dietz, F. Delvart, F. Erhorn, H. Falter, B. J. Green, B. Grieveson, R. Haange, A. Haigh, J. L. Hemmerich, D. Holland, J. How, T. T. C. Jones, R. Laesser, M. Laveyry, J. Lupo, A. Miller, P. Milverton, G. Newbert, J. Orchard, A. Peacock,

R. Russ, G. Saibene, R. Sartori, L. Serio, R. Stagg, S. L. Svensson, E. Thompson, P. Trevalion, E. Usselmann, T. Winkel and M. E. P. Wykes, Technical aspects of the first JET tritium experiment, *Fusion Engineering and Design*, 19(2) (1992) 121–131.

[Hum15] P. W. Humrickhouse and B. J. Merrill, Vacuum permeator analysis for extraction of tritium from DCLL blankets, *Fusion Science and Technology*, 68(2) (2015) 295–302.

[Hut86] E. Hutter, G. Neffe and P. Schira, A ceramic container for hydrogen purification on hot uranium, *Proceedings of the 14th Symposium on Fusion technology (SOFT)*, Sept. 8–12, 1986, Avignon, France, (1986) 1559–1564.

[Hut95] E. Hutter, U. Besserer and G. Jacqmin, Treatment of tritiated exhaust gases at the Tritium Laboratory Karlsruhe, *23rd DOE/NRC Nuclear Air Cleaning and Treatment Conference*, July 25–28, 1994, Buffalo, NY, USA, (1995) 365–378.

[Hut97] E. Hutter, H. D. Adami, U. Besserer and R. D. Penzhorn, AMOR facility: regeneration of molecular sieve beds used for the retention of tritium at the Tritium Laboratory Karlsruhe, *Proceedings of 19th Symposium of Fusion Technology SOFT*, Sept. 16–20, 1996, Lisbon, Portugal, (1997) 1189–1192.

[Ich05] M. Ichimasa, S. Awagakubo, M. Takahashi, H. Tauchi, T. Hayashi, K. Kobayashi, M. Nishi and Y. Ichimasa, Tritium elimination system using tritium gas oxidizing bacteria, *Fusion Science and Technology*, 48(1) (2005) 759–762.

[Ich85] K. Ichimura, K. Watanabe, H. Kato, I. Kanesaka and K. Kawai, In situ measurement of partial pressure of tritiated water by infrared spectroscopy, *Nuclear Instruments and Methods in Physics Research Section A: Accelerators, Spectrometers, Detectors and Associated Equipment*, 241(2-3) (1985) 614–615.

[Ide88] T. Ide, F. Sakai, M. Yorozu, K. Hirata, J. Mitsui, H. Yoshida and Y. Naruse, Hydrogen isotope sorption properties of $LaNi_3Mn_2$ alloy as a candidate for the tritium storage material, *Fusion Technology*, 14(2P2A) (1988) 769–769.

[Ide90] T. Ide, K. Okuno, S. Konishi, F. Sakai, H. Fukui, M. Enoeda, Y. Naruse, J. L. Anderson and J. R. Bartlit, $LaNi_3Mn_2$ alloy as a tritium storage material, *Proceedings of the 13th Symposium on Fusion Engineering (SOFE)*, Oct. 2–6, 1989, Knoxville, TN, USA, (1990) 616–619.

[IEA01] IEA, IEA Workshop Report on reduced activation ferritic/martensitic steels, JAERI-Conf-2001-007, Tokyo, Japan (2001).

[IFM04] IFMIF International Team, IFMIF: Comprehensive Design Report, Implementing Agreement for a Program of Research and Development of Fusion Materials, International Energy Agency (IEA), Frascati, Italy (2004).

[Iga91] N. Igata, T. Fujiga and H. Yumoto, Decrease of ductility due to hydrogen in Fe–Cr–Mn austenitic steel, *Journal of Nuclear Materials*, 179-181 (1991) 656–658.

[Ihl76] H. Ihle, U. Kurz and G. Stoecklin, Permeation of tritium through aluminium in the temperature range of 25 to 2500C, *International Conference on Radiation Effects and Tritium Technology for Fusion Reactors*, Sept. 30, 1975, Gatlinburg, TN, USA, (1976).

[Ike11] T. Ikeda, T. Otsuka and T. Tanabe, Determination of hydrogen diffusivity and permeability in W near room temperature applying a tritium tracer technique, *Journal of Nuclear Materials*, 415(1) (2011) S684–S687.

[Ike97] Y. Ikeda, Y. Uno, F. Maekawa, D. L. Smith, I. C. Gomes, R. C. Ward and A. A. Filatenkov, An investigation of the activation of water by D-T fusion neutrons and

some implications for fusion reactor technology, *Fusion Engineering and Design*, 37(1) (1997) 107–150.

[Iku77] S. Ikuta, K. Okuno, K. Yoshihara and T. Shiokawa, Fragmentation by β-decay in tritium-labelled compounds, (I), *Journal of Nuclear Science and Technology*, 14(2) (1977) 131–134.

[Ino92] M. Inoue, S. Konishi, T. Yamanishi, S. O'hira, T. Watanabe, K. Okuno, Y. Naruse, R. H. Sherman, J. W. Barnes, J. R. Bartlit and J. L. Anderson, Isotope separation system experiments at the TSTA, *Fusion Technology*, 21(2P2) (1992) 293–298.

[Int14] International Atomic Energy Agency, Radiation Protection and Safety of Radiation Sources: International Basic Safety Standards, technical report IAEA Safety Standards Series No. GSR Part 3, Vienna, Austria (2014).

[Int15] International Standard Organisation (ISO), Gas analysis – Preparation of calibration gas mixtures – Gravimetric methods, industry norm ISO 6142:2005, Geneva, Switzerland (2015).

[Int91] International Atomic Energy Agency, Safe Handling of Tritium Review of Data and Experience, Technical Reports Series 324, Vienna, Austria (1991).

[Irv80] S. J. C. Irvine and I. R. Harris, An investigation of the systems $ZrCo-H_2$ and $ZrCo_{0.84}Ni_{0.16}-H_2$, *Journal of the Less-Common Metals*, 74(1) (1980) 33–43.

[Ise99] M. Iseli, Recalculation of tritium permeation, ITER-JCT memorandum, (1999).

[Iso08] K. Isobe, T. Hayashi, H. Nakamura, K. Kobayashi, T. Yamanishi and K. Okuno, Observation of tritium distribution in iron oxide with tritium micro autoradiography, *Fusion Science and Technology*, 54(2) (2008) 533–536.

[Iso11] K. Isobe, H. Nakamura, M. Nakamichi and T. Yamanishi, Radiochemical reactions between tritium and carbon dioxide at elevated temperatures, *Fusion Science and Technology*, 60(4) (2011) 1584–1587.

[Iso88] S. Isomura, K. Suzuki and M. Shibuya, Separation and recovery of tritium by hydrogen-water isotopic exchange reaction, *Fusion Technology*, 14(2P2A) (1988) 518–523.

[ITE01a] ITER, Generic Site Safety Report, Vol. II (GSSR), Safety Design, technical report G84 RI 2 01-07-02 R1.0, (2001).

[ITE01b] ITER, Generic Site Safety Report, Vol. III (GSSR), Radiological and Energy Source Terms, technical report G84 RI 3 01-07-13 R1.0, (2001).

[ITE01c] ITER, Generic Site Safety Report, Vol. IV (GSSR), Normal Operation, technical report N 24 RI 1 01-06-27 R1.0, (2001).

[ITE01d] ITER, Generic Site Safety Report, Vol. V (GSSR), Radioactive Materials, Decommissioning and Waste, technical report G84 RI 4 01-07-06 R1.0, (2001).

[ITE07a] ITER, Material Specification for the supply of 316L(N)-IG austenitic steel plates, ITER report G74 SP 1203-07-09 W0.1, ITER, St. Paul-lez-Durance, France (2007).

[ITE07b] ITER, Material Specification for the supply of 316L(N)-IG austenitic steel seamless pipes, ITER report G74 SP 1403-07-09 W0.1, ITER, St. Paul-lez-Durance, France (2007).

[ITE09] ITER, Computer Aided Design (CAD), reference manual G 74 MA 12 01-04-09 W 0.4, St. Paul-lez-Durance, France (2009).

[ITE99] ITER, ITER physics basis, *IAEA Nuclear Fusion*, 39 (1999) 2137–2659.

[Ito07] T. Itoh, T. Hayashi, K. Isobe, K. Kobayashi and T. Yamanishi, Self-decomposition behavior of high concentration tritiated water, *Fusion Science and Technology*, 52(3) (2007) 701–705.

[Ito92] H. Ito, T. Suzuki, T. Takanaga, Y. Matsuda, S. Konishi, Y. Naruse and S. Hirata, Separation of tritium using polyimide membrane, *Fusion Technology*, 21(2P2) (1992) 988–993.

[Ive81] D. G. Ivey, R. I. Chittim, K. J. Chittim and D. O. Northwood, Metal hydrides for energy storage, *Journal of Materials for Energy Systems*, 3(3) (1981) 3–19.

[Iwa02a] Y. Iwai, Y. Misaki, T. Hayashi, T. Yamanishi, S. Konishi, M. Nishi, R. Ninomiya, S. Yanagimachi, S. Senrui and H. Yoshida, The water detritiation system of the ITER Tritium Plant, *Fusion Science and Technology*, 41(3P2) (2002) 1126–1130.

[Iwa02b] Y. Iwai, H. Nakamura, S. Konishi, M. Nishi and R. S. Willms, Study on sudden loss of cryogenic coolant accident happened in the hydrogen isotope separation system for fusion reactor, *Fusion Science and Technology*, 41(3P2) (2002) 668–672.

[Iwa02c] Y. Iwai, T. Yamanishi, S. O'hira, T. Suzuki, W. M. Shu and M. Nishi, H – D – T cryogenic distillation experiments at TPL/JAERI in support of ITER, *Fusion Engineering and Design*, 61-62 (2002) 553–560.

[Iwa05] Y. Iwai, T. Yamanishi, M. Nishi, T. Yagi and M. Tamada, Durability of irradiated polymers in solid-polymer-electrolyte water electrolyzer, *Journal of Nuclear Science and Technology*, 42(7) (2005) 636–642.

[Iwa08] Y. Iwai, T. Yamanishi, A. Hiroki, T. Yagi and M. Tamada, Solid-polymer-electrolyte tritiated water electrolyzer for water detritiation system, *Fusion Science and Technology*, 54(2) (2008) 458–461.

[Iwa11] Y. Iwai, K. Sato and T. Yamanishi, Development of Pt/ASDBC catalyst for room temperature recombiner of atmosphere detritiation system, *Fusion Engineering and Design*, 86(9-11) (2011) 2164–2167.

[Iwa12] Y. Iwai, K. Sato and T. Yamanishi, Change in activity of catalysts for the oxidation of tritium during a fire event, *Fusion Engineering and Design*, 87(7-8) (2012) 946–950.

[Iwa15] Y. Iwai, H. Kubo, Y. Ohshima, H. Noguchi, Y. Edao and J. Taniuchi, Hydrophobic platinum honeycomb catalyst to be used for tritium oxidation reactors, *Fusion Science and Technology*, 68(3) (2015) 596–600.

[Izu81] Y. Izumoji, Y. Tsuzuki and Y. Osawa, Separation of hydrogen isotopes by palladium alloy membrane, *Proceedings: Tritium Technology in Fission, Fusion and Isotopic Applications*, Apr. 29–May 1, 1980, Dayton, OH, USA, (1981) 397–403.

[Jac77] R. L. Jackson, J. B. Condon and L. M. Steckel, Uranium/Water Vapor Reactions in Gaseous Atmospheres, technical report Y–2078, Oak Ridge Y-12 Plant, Union Carbide, Oak Ridge, , TN, USA (1977).

[Jal86] R. A. Jalbert, S. J. Brereton and D. F. Holland, Contamination of aluminium and painted surfaces exposed to tritium, *Fusion Technology*, 10(3P2B) (1986) 1223–1227.

[Jam13] T. M. James, M. Schloesser, S. Fischer, M. Sturm, B. Bornschein, R. J. Lewis and H. H. Telle, Accurate depolarization ratio measurements for all diatomic hydrogen isotopologues, *Journal of Raman Spectroscopy*, 44(6) (2013) 857–865.

[Jam88] B. J. James, R. L. Nolen, R. L. Hemphill and M. E. Fuehrer, Estimating the tritiated hydrocarbon decontamination factor by heavy methane, *Fusion Technology*, 14(2P2B) (1988) 939–942.

[Jan07] G. Janeschitz and W. Bahm, ITER, the 'broader approach', a DEMO fusion reactor, *Atw Internationale Zeitschrift fuer Kernenergie*, 52(8-9) (2007) 536–547.

[Jan95] G. Janeschitz, K. Borrass, G. Federici, Y. Igitkhanov, A. Kukushkin, H. D. Pacher, G. W. Pacher and M. Sugihara, The ITER divertor concept, *Journal of Nuclear Materials*, 220-222 (1995) 73–88.

[Jen84] G. A. Jensen and L. E. Leonard, Radioluminescent lighting for rural Alaskan runway lighting and marking, *Annual Conference of the IES Aviation Committee*, Nov. 1984, Charleston, SC, USA, (1984).

[Jen85] J. A. Jensen, Acceptability testing of radioluminescent lights for VFR-night air taxi operations, technical report PNL-5347 DE85 C07303, Pacific Northwest Laboratory, Richland, WA, USA (1985).

[JET89] JET Laboratory, JET Code of Practice for the Safe Use of Beryllium at the JET Laboratory, Technical Report SR(89)02, (1989).

[Jim16] G. Jimenez, E. Dillon, J. Dahlmeyer, T. Garrison, S. Darkey, K. Wald, J. Kubik, D. Paciulli, M. Talukder, J. Nott, M. Ferrer, J. Prinke, P. Villaneuva, F. Massicotte, K. Rebeiz, S. Nesbit and A. Craft, A comparative assessment of hydrogen embrittlement: palladium and palladium-silver (25 weight % silver) subjected to hydrogen absorption/desorption cycling, *Advances in Chemical Engineering and Science*, 6 (2016) 246–261.

[Joh76] Q. Johnson, T. J. Biel and H. R. Leider, Isotopic shifts of unit-cell constants of alpha-trihydrides and beta-trihydrides of uranium - UH_3, UD_3 and UT_3, *Journal of Nuclear Materials*, 60 (1976) 231–233.

[Joh88] R. E. Johnson, F. B. Gravelle and C. M. Shultz, The purification of inert glove box atmospheres using hot reactive metals, *Fusion Technology*, 14(2) (1988) 1282–1286.

[Jon52] W. M. Jones, Luminescence behaviour of tritium, *Journal of Chemical Physics*, 20 (1952) 1974.

[Jon58] L. H. Jones and M. Goldblatt, Infrared spectrum and molecular constants of CT_4, *Journal of Molecular Spectroscopy*, 2(1-6) (1958) 103–112.

[Jon65] P. M. S. Jones, R. Gibson and J. A. Evans, The Permeation and Diffusion of Hydrogen Isotopes through Stainless Steels. Part 2- EN58B Low Carbon Steel (Diffusion and Permeability of Hydrogen and Deuterium through Low-Carbon Austenitic Type Steel), technical report report N° 90/65, Atomic Weapons Research Establishment (AWRE), United Kingdom (1965).

[Jon67] P. M. S. Jones and R. Gibson, Hydrogen in beryllium, *Journal of Nuclear Materials*, 21 (1967) 353–354.

[Jon68] W. M. Jones, Vapor pressures of tritium oxide and deuterium oxide. interpretation of the isotope effects, *The Journal of Chemical Physics*, 48(1) (1968) 207–214.

[Jos00] Y. Joseph, W. Ranke and W. Weiss, Water on FeO(111) and Fe_3O_4(111): Adsorption behavior on different surface terminations, *The Journal of Physical Chemistry B*, 104(14) (2000) 3224–3236.

[Jos15] G. Jossens, C. Mathonat and F. Bachelet, Nuclear waste calorimeter for very large drums with 385 litres sample volume, *Fusion Science and Technology*, 67(2) (2015) 390–393.

[Jos40] W. Jost and A. Widmann, Diffusion von Wasserstoff und Deuterium in Palladium, *Zeitschrift fuer Physikalische Chemie*, 45B(1) (1940) 285–296.

[Jos89] Y. Josephy and M. Ron, Kinetic measurements of $LaNi_5H_x$ and $MnNi_{4.15}Fe_{0.85}H_x$ with constant pressure differentials, *Journal of the Less-Common Metals*, 147(2) (1989) 227–238.

[Jun92] P. Jung, Diffusion of helium and tritium in nuclear materials, *Diffusion Processes in Nuclear Materials*, P. Agarwala, editor, North-Holland, Amsterdam, Netherlands, (1992), 235–269.

[Kaj18] S. Kajita, S. Kawaguchi, N. Ohno and N. Yoshida, Enhanced growth of large-scale nanostructures with metallic ion precipitation in helium plasmas, *Scientific Reports*, 8(1) (2018).

[Kak02] T. Kakuta, S. Hirata, S. Mori, S. Konishi, Y. Kawamura, M. Nishi and Y. Ohara, Conceptual design of the Blanket Tritium Recovery System for the Prototype Fusion Reactor, *Fusion Science and Technology*, 41(3P2) (2002) 1069–1073.

[Kal00] G. Kalinin, V. Barabash, A. Cardella, J. Dietz, K. Ioki, R. Matera, R. T. Santoro and R. Tivey, Assessment and selection of materials for ITER in-vessel components, *Journal of Nuclear Materials*, 283-287 (2000) 10–19.

[Kal01] G. Kalinin, V. Barabash, S. Fabritsiev, H. Kawamura, I. Mazul, M. Ulrickson, C. Wu and S. Zinkle, ITER R&D: Vacuum vessel and in-vessel components: Materials development and test, *Fusion Engineering and Design*, 55(2-3) (2001) 231–246.

[Kal11] A. Kallenbach, J. Adamek, L. Aho-Mantila, S. Aekaeslompolo, C. Angioni, C. V. Atanasiu, M. Balden, K. Behler, E. Belonohy, A. Bergmann, M. Bernert, R. Bilato, V. Bobkov, J. Boom, A. Bottino, F. Braun, M. Bruedgam, A. Buhler, A. Burckhart, A. Chankin, I. G. J. Classen, G. D. Conway, D. P. Coster, P. de Marné, R. D'Inca, R. Drube, R. Dux, T. Eich, N. Endstrasser, K. Engelhardt, B. Esposito, E. Fable, H.-U. Fahrbach, L. Fattorini, R. Fischer, A. Flaws, H. Fuenfgelder, J. C. Fuchs, K. Gal, Garcia-Munoz, B. Geiger, M. G. Adamov, L. Giannone, C. Giroud, T. Goerler,

S. da Graca, H. Greuner, O. Gruber, A. Gude, S. Guenter, G. Haas, A. H. Hakola, D. Hangan, T. Happel, T. Hauff, B. Heinemann, A. Herrmann, N. Hicks, J. Hobirk, H. Hoehnle, M. Hoelzl, C. Hopf, L. Horton, M. Huart, V. Igochine, C. Ionita, A. Janzer, F. Jenko, C.-P. Kaesemann, S. Kalvin, O. Kardaun, M. Kaufmann, A. Kirk, H.-J. Klingshirn, M. Kocan, G. Kocsis, H. Kollotzek, C. Konz, R. Koslowski, K. Krieger, T. Kurki-Suonio, B. Kurzan, K. Lackner, P. T. Lang, P. Lauber, M. Laux, F. Leipold, F. Leuterer, A. Lohs, N. C. Luhmann, T. Lunt, A. Lyssoivan, H. Maier, C. Maggi, K. Mank, M.-E. Manso, M. Maraschek, P. Martin, M. Mayer, P. J. McCarthy, R. McDermott, H. Meister, L. Menchero, F. Meo, P. Merkel, R. Merkel, V. Mertens, F. Merz, A. Mlynek, F. Monaco, H. W. Mueller, M. Muenich, H. Murmann, G. Neu, R. Neu, B. Nold, J.-M. Noterdaeme, H. K. Park, G. Pautasso, G. Pereverzev, Y. Podoba, F. Pompon, E. Poli, K. Polochiy, S. Potzel, M. Prechtl, M. J. Pueschel, T. Puetterich, S. K. Rathgeber, G. Raupp, M. Reich, B. Reiter, T. Ribeiro, R. Riedl, V. Rohde, J. Roth, M. Rott, F. Ryter, W. Sandmann, J. Santos, K. Sassenberg, P. Sauter, A. Scarabosio, G. Schall, K. Schmid, P. A. Schneider, W. Schneider, G. Schramm, R. Schrittwieser, J. Schweinzer, B. Scott, M. Sempf, F. Serra, M. Sertoli, M. Siccinio, A. Sigalov, A. Silva, A. C. C. Sips, F. Sommer, A. Staebler, J. Stober, B. Streibl, E. Strumberger, K. Sugiyama, W. Suttrop, T. Szepesi, G. Tardini, C. Tichmann, D. Told, W. Treutterer, L. Urso, P. Varela, J. Vincente, N. Vianello, T. Vierle, E. Viezzer, C. Vorpahl, D. Wagner, A. Weller, R. Wenninger, B. Wieland, C. Wigger, M. Willensdorfer, M. Wischmeier, E. Wolfrum, E. Wuersching, D. Yadikin, Q. Yu, I. Zammuto, D. Zasche, T. Zehetbauer, Y. Zhang, M. Zilker and H. Zohm, Overview of ASDEX Upgrade results, *Nuclear Fusion*, 51(9) (2011) 094012.

[Kam06] Y. Kameo, M. Nakashima and T. Hirabayashi, Removal of metal oxide layers as a dry decontamination technique utilizing bead reaction and thermal quenching by dry ice blasting, *Journal of Nuclear Science and Technology*, 43(7) (2006) 798–805.

[Kan08] T. Kanezaki, C. Narazaki, Y. Mine, S. Matsuoka and Y. Murakami, Effects of hydrogen on fatigue crack growth behavior of austenitic stainless steels, *International Journal of Hydrogen Energy*, 33(10) (2008) 2604–2619.

[Kan63] R. J. Kandel, Methane-tritium system. I. mass spectra of tritium-substituted methanes, *The Journal of Chemical Physics*, 39(10) (1963) 2581–2587.

[Kan64] R. J. Kandel, Methane-tritium system. II. Kinetics of the exchange reaction, *The Journal of Chemical Physics*, 41(8) (1964) 2435–2442.

[Kan84] I. Kanesaka, M. Tsuchida, K. Kawai and T. Takeuchi, The IR spectrum of $T_2{}^{18}O$, *Journal of Molecular Spectroscopy*, 104(2) (1984) 405–413.

[Kap92] H. Kapulla, R. Kraemer and R. Heine, Tritium inventory measurements using calorimetry, *Fusion Technology*, 21(2P2) (1992) 412–418.

[Kap94] H. Kapulla, R. Kraemer and R. Heine, Calorimeter for tritium inventory measurements at TLK, *Proceedings of the 3rd ETHEL-TLK Workshop on Tritium Technology and Safety in Thermonuclear Fusion*, May 24–25, 1993, Karlsruhe, Federal Republic of Germany, (1994).

[Kap95] H. Kapulla and R. Heine, Experimental results and experience with the KfK tritium calorimeter, *Fusion Technology*, 28(3P2) (1995) 1020–1025.

[Kas11] S. Kasahara, K. Katayama, T. Fujiki, S. Ishikawa, S. Fukada and M. Nishikawa, A study on carbon and hydrogen co-deposition behavior in methane-hydrogen mixed plasma, *Fusion Science and Technology*, 60(4) (2011) 1487–1490.

[Kas74] W. Kass, Sandia National Laboratories, Memorandum, (1974).

[Kat10] K. Katayama, S. Fukada and M. Nishikawa, Direct decomposition of methane using helium RF plasma, *Fusion Engineering and Design*, 85(7-9) (2010) 1381–1385.

[Kat11] K. Katayama, S. Fukada and M. Nishikawa, Demonstration of tritium extraction from tritiated methane in helium by utilizing plasma decomposition, *Fusion Science and Technology*, 60(4) (2011) 1379–1382.

[Kat52] L. Katz and A. S. Penfold, Range-energy relations for electrons and the determination of beta-ray end-point energies by absorption, *Reviews of Modern Physics*, 24(1) (1952) 28–44.

[Kat60] O. M. Katz and E. A. Gulbransen, Permeability and diffusivity of hydrogen through a palladium tube, *Review of Scientific Instruments*, 31(6) (1960) 615–617.

[Kat71] L. Katz, M. Guinan and R. J. Borg, Diffusion of H_2, D_2, and T_2 in single-crystal Ni and Cu, *Physical Review B*, 4(2) (1971) 330–341.

[Kat79] H. Katsuta and R. B. McLellan, Diffusivity of hydrogen in silver, *Scripta Metallurgica*, 13(1) (1979) 65–66.

[Kaw00] Y. Kawamura, M. Enoeda, R. S. Willms, P. M. Zielinski, R. H. Wilhelm and M. Nishi, Adsorption isotherms for tritium on various adsorbents at liquid nitrogen temperature, *Fusion Technology*, 37(1) (2000) 54–61.

[Kaw01] Y. Kawamura, S. Konishi and M. Nishi, Development of a micro gas chromatograph for the analysis of hydrogen isotope gas mixtures in the fusion fuel cycle, *Fusion Engineering and Design*, 58-59 (2001) 389–394.

[Kaw05] Y. Kawamura, Y. Iwai, H. Nakamura, T. Hayashi, T. Yamanishi and M. Nishi, Tritium recovery from solid breeder blanket by water vapor addition to helium sweep gas, *Fusion Science and Technology*, 48(1) (2005) 654–657.

[Kaw08] Y. Kawamura, Y. Onishi, K. Okuno and T. Yamanishi, Hydrogen isotope separation capability of low temperature mordenite column for gas chromatograph, *Fusion Engineering and Design*, 83(10-12) (2008) 1384–1387.

[Kaw94] H. Kawamura, M. Kato, E. Ishitsuka, K. Nishida and M. Saito, The compatibility test between Be and SS316, *Journal of Nuclear Materials*, 212-215 (1994) 1524–1528.

[Kaz08] O. Kazachenko, B. Bornschein, L. Bornschein, F. Eichelhardt, N. Kernert and H. Neumann, TRAP - a cryo-pump for pumping tritium on pre-condensed argon, *Nuclear Instruments and Methods in Physics Research Section A: Accelerators, Spectrometers, Detectors and Associated Equipment*, 587(1) (2008) 136–144.

[Kel60] R. A. Keller and J. C. Giddings, Multiple zones and spots in chromatography, *Journal of Chromatography A*, 3 (1960) 205–220.

[Ker84] R. A. Kerst and W. A. Swansiger, Plasma driven permeation of tritium in fusion reactors, *Journal of Nuclear Materials*, 122-123(1-3) (1984) 1499–1510.

[Kha15] A. S. Khapov, S. K. Grishechkin and V. G. Kiselev, A uranium bed with ceramic body for tritium storage, *Fusion Science and Technology*, 67(2) (2015) 412–415.

[Khe85] N. P. Kherani and W. T. Shmayda, Evaluation of the Amersham International Transportable 100 g Uranium Bed, research report 827.283, Ontario Hydro Research Division, Ontario, Canada (1985).

[Khe87] N. P. Kherani and W. T. Shmayda, Bulk getters for tritium storage, *Proceedings of the Canadian Nuclear Society* 7^{th} *Annual Conference*, June 9–10, 1986, Toronto, Canada, (1987) 232–236.

[Khe88] N. P. Kherani, W. T. Shmayda and R. A. Jalbert, Tritium removal from inert gases using Zr_2Fe, *Proceedings of the 12th Symposium on Fusion Engineering (SOFE)*, Oct. 12–16, 1987, Monterey, CA, USA, (1988) 1239–1242.

[Khe89] N. P. Kherani, W. T. Shmayda and A. G. Heics, Enhancing the rate of hydriding in uranium beds, *Zeitschrift fuer Physikalische Chemie*, 164(2) (1989) 1421–1428.

[Khe92a] N. P. Kherani and W. T. Shmayda, Hydrogen Permeation through Viton, research report M92-6-K, Ontario Hydro Research Division, Ontario, Canada (1992).

[Khe92b] N. P. Kherani and W. T. Shmayda, In-line process tritium monitors, *Fusion Technology*, 21(2P2) (1992) 340–345.

[Khe94] N. P. Kherani and W. T. Shmayda, HTO monitoring using heated ion chambers, *Proceedings of the 15th Symposium on Fusion Engineering (SOFE)*, Oct. 11–15, 1993, Hyannis, MA, USA, (1994) 80–84.

[Kid67] A. J. Kidnay and M. J. Hiza, High pressure adsorption isotherms of neon, hydrogen, and helium at 76 K, *Advances in Cryogenic Engineering*, Springer US, New York, NY, USA, (1967), 730–740.

[Kie18] B. Kienzler, Corrosion processes of alloyed steels in salt solutions, *Atw Internationale Zeitschrift fuer Kernenergie*, 63(2) (2018) 104–110.

[Kik78] Y. Kikuta, T. Araki and T. Kuroda, Analysis of fracture morphology of hydrogen-assisted cracking in steel and its welds, *Fractography in Failure Analysis, ASTM STP 645*, American Society for Testing and Materials, West Conshohocken, PA, USA, (1978), 107–127.

[Kim18] C. H. Kim, J. J. Sung and P. W. Seo, Effects of airborne volatile organic compounds on the performance of Pt/TiO_2 coated ceramic honeycomb type Passive Autocatalytic Recombiner, *atw – International Journal for Nuclear Power*, 63 (2018) 457–462.

[Kin05] T. Kiniyo, M. Nishikawa, K. Katayama, T. Tanifuji, M. Enoeda and S. Beloglazov, Release behavior of bred tritium from irradiated Li_4SiO_4, *Fusion Science and Technology*, 48(1) (2005) 646–649.

[Kin63] J. King Jr, The chromatographic separation of the hydrogen isotopes including tritium, *The Journal of Physical Chemistry*, 67(6) (1963) 1397–1397.

[Kin84] M. Kinoshita, A cryogenic distillation cascade for a fusion reactor, *Fusion Technology*, 6 (1984) 629–633.

[Kir01] P. Kirkegaard and E. Bjergbakke, Chemsimul: a simulation of chemical kinetics, tech. rep. RISOR-1085, Technical University of Danmark, Roskilde, Danmark (2001).

[Kir05] P. Kirkegaard and E. Bjergbakke, Chemsimul: Chemical Kinetics Software Package, technical report Riso-R-1630, Risoe National Laboratory, Roskilde, Denmark (2005).

[Kir51] I. Kirshenbaum, Physical properties and analysis of heavy water, McGraw Hill Book Co., New York, NY, USA (1951).

[Kir99] P. Kirkegaard and E. Bjergbakke, CHEMSIMUL: A simulator of chemical kinetics, technical report RISOR-1085, Technical University of Danmark, Roskilde, Danmark (1999).

[Kis66] A. A. Kishbaugh, Extraction of Tritium from Lithium Aluminate Targets, technical report DP-1058, E. I. du Pont de Nemours and Savannah River Laboratory (SRL), Aiken, SC, USA (1966).

[Kis84] N. Kishimoto, T. Tanabe, H. Araki, H. Yoshida and R. Watanabe, Hydrogen permeation in metals during exposure to a process gas environment, *Nuclear Technology*, 66(3) (1984) 578–594.

[Kis85a] N. Kishimoto, T. Tanabe, T. Suzuki and H. Yoshida, Helium dilution effect on hydrogen permeation in 316L stainless steel and nickel-base heat-resistant alloys, *Journal of Nuclear Materials*, 127(1) (1985) 10–17.

[Kis85b] N. Kishimoto, T. Tanabe, T. Suzuki and H. Yoshida, Hydrogen diffusion and solution at high temperatures in 316L stainless steel and nickel-base heat-resistant alloys, *Journal of Nuclear Materials*, 127(1) (1985) 1–9.

[Kis92a] S. Kishimoto, N. Yoshida, T. Yao, T. Itani and T. B. Flanagan, Solution of hydrogen in cold-worked Pd–Ag alloys, *Berichte der Bunsengesellschaft fuer physikalische Chemie*, 96(10) (1992) 1477–1482.

[Kis92b] T. J. Kissner and R. E. Wieneke, A distributed process control system for the Tritium Emissions Reduction Facility, *Fusion Technology*, 21(2P2) (1992) 583–587.

[Kit02] T. Kitabata, Tritium handling experience in 165 MWE Power Generating Station, Fugen, *Fusion Science and Technology*, 41(3P2) (2002) 356–360.

[Kit98] T. Kitabata and K. Kitamura, Heavy water management and radiation protection against tritium in the Fugen nuclear power station, *Proceedings of the 19th KAIF-JAIF Seminar on Nuclear Industry*, Sept. 29–30, 1997, Seoul, South Korea, (1998) 181–198.

[Kiu83] K. Kiuchi and R. B. McLellan, The solubility and diffusivity of hydrogen in well-annealed and deformed iron, *Acta Metallurgica*, 31(7) (1983) 961–984.

[Kiz99] K. Kizu and T. Tanabe, Deuterium permeation through metals under hydrogen counter flow, *Journal of Nuclear Materials*, 266-269 (1999) 561–565.

[Kle02a] J. E. Klein, A 1600 liter tritium hydride storage vessel, *Fusion Science and Technology*, 41(3P2) (2002) 764–775.

[Kle02b] J. E. Klein, A summary of tritium in-bed accountability for 1500 liter $LaNi_{4.25}Al_{0.75}$ storage beds, *Fusion Science and Technology*, 41(3P2) (2002) 542–550.

[Kle05a] J. E. Klein, In-bed accountability development for a passively cooled, electrically heated hydride (PACE) bed, *Fusion Science and Technology*, 48(1) (2005) 416–419.

[Kle05b] J. E. Klein and J. S. Hoelder, Tritium Storage Bed Development at the Savannah River National Laboratory, a Brief History, technical report WSRC-MS-2005-00450 Rev.0, Savannah River National Laboratory, Aiken, S.C., USA (2005).

[Kle08] J. E. Klein and R. H. Hsu, Air passivation of metal hydride beds for waste disposal, *Fusion Science and Technology*, 54 (2008) 227–230.

[Kle11] J. Klein and P. Foster, Tritium in-bed accountability for a passively cooled, electrically (PACE) heated hydride bed, *Fusion Science and Technology*, 60 (2011) 964–967.

[Kle15] J. E. Klein, E. A. Clark, C. D. Harvel, D. A. Farmer, M. L. Moore, L. L. Tovo and A. S. Poorea, Tritium accountancy in fusion systems, *Fusion Science and Technology*, 67(2) (2015) 420–423.

[Kle92] J. E. Klein, M. K. Mailory and A. Nobile, Tritium measurement technique using "in-bed" calorimetry, *Fusion Technology*, 21(2P2) (1992) 401–405.

[Kle95] J. E. Klein, In-bed accountability of tritium in production scale metal hydride storage beds, *Fusion Technology*, 28(3P2) (1995) 1026–1032.

[Kle98] H. Kleykamp and H. D. Gottschalk, Elementaranalysen an Flakes aus dem JET in der Betriebsphase Oktober 1985 bis 1996, Institut fuer Materialforschung, KIT, Karlsruhe, Germany (1998).

[Kni83] R. J. Knize and J. L. Cecchi, Theory of bulk gettering, *Journal of Applied Physics*, 54(6) (1983) 3183–3189.

[Kob06] K. Kobayashi, T. Hayashi, M. Nishi, Y. Oya and K. Okuno, Sorption and desorption of tritiated water on four kinds of materials for ITER, *Fusion Engineering and Design*, 81(8-14) (2006) 1379–1384.

[Kob07a] K. Kobayashi, T. Hayashi, H. Nakamura, T. Yamanishi, Y. Oya and K. Okuno, Study for the behaviour of tritiated water vapour on organic materials, *Fusion Science and Technology*, 52 (2007) 696–700.

[Kob07b] K. Kobayashi, H. Miura, T. Hayashi, S. Hoshi and T. Yamanishi, Oxidation performance test of detritiation system under existence of SF_6, *Fusion Science and Technology*, 52(3) (2007) 711–715.

[Kob11] K. Kobayashi, T. Enokida, D. Iio, Y. Yamada, M. Hara and Y. Hatano, Near-infrared spectroscopy of tritiated water, *Fusion Science and Technology*, 60(3) (2011) 941–943.

[Koe09] Z. Koelloe, D. Demange, B. Bornschein, L. Doerr, K. Guenther and B. Kloppe, Calibrating a gas chromatograph to measure tritium using calorimetry, *Fusion Engineering and Design*, 84(7-11) (2009) 1073–1075.

[Koe11] Z. Koelloe, C. G. Alecu and H. Moosmann, A new method to measure small volumes in tritium handling facilities, using p-v measurements, *Fusion Science and Technology*, 60(3) (2011) 972–975.

[Koe84] R. Koester and H. Graebner, Konditionierung von Brennelementhuelsen und tritiumhaltigen Waessern mit hydraulischen Zementen, technical report KfK-3675, Kernforschungszentrum Karlsruhe, Karlsruhe, Germany (1984).

[Kof68] S. A. Koffler, J. B. Hudson and G. S. Ansell, Hydrogen permeation through α-palladium, *Journal Metals*, 20 (1968) 75.

[Koh96] A. Kohyama, A. Hishinuma, D. S. Gelles, R. L. Klueh, W. Dietz and K. Ehrlich, Low-activation ferritic and martensitic steels for fusion application, *Journal of Nuclear Materials*, 233-237 (1996) 138–147.

[Kol10] R. D. Kolasinski, A. D. Shugard, C. R. Tewell and D. F. Cowgill, Uranium for Hydrogen Storage Applications: A Materials Science Perspective, technical report SAND2010-5195, Sandia National Laboratories (SNL), Albuquerque, NM, USA (2010).

[Kon12] H. Kondo, T. Furukawa, Y. Hirakawa, H. Iuchi, T. Kanemura, M. Ida, K. Watanabe, H. Horiike, N. Yamaoka, I. Matsushita, E. Wakai and K. Nakamura, Completion of IFMIF/EVEDA lithium test loop construction, *Fusion Engineering and Design*, 87(5-6) (2012) 418–422.

[Kon64] T. Kondo, E. D. Verink, F. H. Beck and M. G. Fontana, Gas chromatographic and gravimetric studies of uranium oxidation mechanism, *Corrosion*, 20(10) (1964) 314t–320t.

[Kon74] T. Kondo, F. H. Beck and M. G. Fontana, A gas chromatographic study on the kinetics of uranium oxidation in moist environments, *Corrosion*, 30(9) (1974) 330–341.

[Kon83] S. Konishi, H. Ohno, H. Yoshida and Y. Naruse, Decomposition of tritiated water with solid oxide electrolysis cell, *Nuclear Technology and Fusion*, 3 (1983) 196–198.

[Kon85] S. Konishi, H. Yoshida, H. Ohno, Y. Naruse, D. O. Coffin, C. R. Walthers and K. E. Binning, Experiments on a ceramic electrolysis cell and a palladium diffuser at the Tritium Systems Test Assembly, *Fusion Technology*, 8(2P2) (1985) 2042–2047.

[Kon86] S. Konishi, H. Ohno, H. Yoshida, H. Katsuta and Y. Naruse, Solid oxide electrolysis cell for decomposition of tritiated water, *International Journal of Hydrogen Energy*, 11(8) (1986) 507–512.

[Kon87] S. Konishi, H. Yoshida, H. Ohno, T.Nagasaki and Y.Naruse, Improvements on some tritium processing components, *Proceedings of the International Symposium on Fusion Reactor Blanket and Fuel Cycle Technology*, Oct. 27–29, 1986, Tokai, Japan, (1987) 109–112.

[Kon88] S. Konishi, M. Inoue, H. Yoshida, Y. Naruse, H. Sato, K. Muta and Y. Imamura, Experimental apparatus for the fuel cleanup process in the Tritium Process Laboratory, *Fusion Technology*, 14(2P2A) (1988) 596–601.

[Kon89] S. Konishi, T. Nagasaki, N. Yokokawa and Y. Naruse, Development of zirconium-cobalt beds for recovery, storage and supply of tritium, *Fusion Engineering and Design*, 10 (1989) 355–358.

[Kon91] S. Konishi, H. Yoshida, Y. Naruse, R. V. Carlson, K. E. Binning, J. R. Bartlit and J. L. Anderson, Tritium experiments on components for fusion fuel processing at the Tritium Systems Test Assembly, *Fusion Technology*, 19(3P2B) (1991) 1668–1673.

[Kon92a] S. Konishi, T. Hayashi, M. Inoue, K. Okuno, Y. Naruse, H. Sato, H. Fukui, K. Nemoto, M. Kurokawa, J. W. Barnes and J. L. Anderson, Fabrication and installation of the JAERI fuel cleanup system, *Fusion Technology*, 21(2P2) (1992) 999–1004.

[Kon92b] A. Konstantellos, J. L. Hemmerich, A. C. Bell, J. Mart, J. Yorkshades, K. Walker, N. Skinner, G. Jones and F. Delvart, The JET active gas handling plant process control system, *Fusion Technology*, 21(2P2) (1992) 365–370.

[Kon93] S. Konishi, S. O'Hira, T. Hayashi, M. Inoue, T. Watanabe, Y. Naruse, K. Okuno, J. W. Barnes, W. Harbin, J. R. Bartlit and J. L. Anderson, Test of Palladium Diffuser in the JAERI Fuel Clean-Up System in the Tritium Systems Test Assembly, technical report JAERI-M93-088, Japan Atomic Energy Research Institute, Tokai-mura, Japan (1993).

[Kon94] S. Konishi, T. Hayashi, T. Yamanishi, H. Nakamura, Y. Naruse, K. Okuno, R. H. Sherman, R. S. Willms, J. W. Barnes, J. R. Bartlit and J. L. Anderson, Extended operation of reactor-scale fusion fuel loop under US-Japan collaboration, *Proceedings of the 15th Symposium on Fusion Engineering (SOFE)*, Oct. 11–15, 1993, Hyannis, MA, USA, (1994) 204–207.

[Kon95a] S. Konishi, M. Hara and K. Okuno, Versatile fuel cleanup system based on palladium permeation and vapor electrolysis, *Fusion Technology*, 28(3P1) (1995) 652–657.

[Kon95b] S. Konishi, T. Nagasaki and K. Okuno, Reversible disproportionation of ZrCo under high temperature and hydrogen pressure, *Journal of Nuclear Materials*, 223(3) (1995) 294–299.

[Kon97] S. Konishi, M. Enoeda, T. Yamanishi and K. Okuno, Development of a fusion fuel processing system at the Japan Atomic Energy Research Institute, *Proceedings of the 19th Symposium on Fusion Technology (SOFT)*, Sept. 16–20, 1996, Lisbon, Portugal, (1997) 1221–1224.

[Kon98] S. Konishi, T. Maruyama, K. Okuno, M. Inoue and A. Yamashita, Development of electrolytic reactor for processing of gaseous tritiated compounds, *Fusion Engineering and Design*, 39-40 (1998) 1033–1039.

[Koo15] D. Koo, J. Lee, J. Park, H.-G. Kang, M. H. Chang, S.-H. Yun, S. Cho, K. J. Jung, S. Paek and H. Chunga, Hydriding performances and modelling of a small-scale ZrCo bed, *Fusion Science and Technology*, 67(2) (2015) 435–438.

[Kor13] P. S. Korinko and Y. Breakiron, Characterization of Glovebox Gloves for the Savannah River Site, technical report SRLS-STI-2013-00027, Aiken, SC, USA (2013).

[Kos80] M. E. Kost, L. N. Padurets, A. A. Chertkov and V. I. Mikheeva, Dissociation energies in the ZrNi–$H_2(D_2)$ and ZrCo–$H_2(D_2)$ systems, *Russian Journal Inorganic Chemistry*, 25 (1980) 471.

[Kot02] K. Kotoh, T. Nishikawa and Y. Kashio, Multi-component adsorption characteristics of hydrogen isotopes on synthetic zeolite 5A-type at 77.4 K, *Journal of Nuclear Science and Technology*, 39(4) (2002) 435–441.

[Kot05] K. Kotoh and K. Kudo, Multi-component adsorption behavior of hydrogen isotopes on zeolite 5A and 13X at 77.4 K, *Fusion Science and Technology*, 48(1) (2005) 148–151.

[Kot08] K. Kotoh, K. Kimura, Y. Nakamura and K. Kudo, Hydrogen isotope separation using molecular sieve of synthetic zeolite 3A, *Fusion Science and Technology*, 54(2) (2008) 419–422.

[Kot09] K. Kotoh, S. Takashima and Y. Nakamura, Molecular-sieving effect of zeolite 3A on adsorption of H_2, HD and D_2, *Fusion Engineering and Design*, 84(7-11) (2009) 1108–1112.

[Kov16] M. Kovari, Assessment of the tritium resource available for the fusion community, *4th IAEA Technical Meeting on DEMO Programme*, Nov. 15–18, 2016, Karlsruhe, Germany, (2016).

[Kra05] C. Kraus, L. Bornschein, J. Bonn, B. Bornschein, B. Flatt, A. Kovalik, B. Mueller, E. W. Otten, J. P. Schall, T. Thuemmler and C. Weinheimer, The Mainz Neutrino Mass Experiment, *Nuclear Physics B - Proceedings Supplements*, 143 (2005) 499.

[Kra68] D. Kramer, H. R. Brager, C. G. Rhodes and A. G. Pard, Helium embrittlement in type 304 stainless steel, *Journal of Nuclear Materials*, 25(2) (1968) 121–131.

[Kra90] J. P. Krasznai and W. T. Shmayda, Decontamination Tests on Stainless Steel Tubing Removed from the Darlington Tritium Removal Facility, technical report 90-100-K, Ontario Hydro, Toronto, Canada (1990).

[Kra95] J. P. Krasznai, D. F. Mullins and R. A. Mowat, Tritiated waste management - tritiated oil packaging and decontamination, *Fusion Technology*, 28(3P2) (1995) 1540–1545.

[Kra96] R. Kraemer and M. I. Thornton, Calorimetric tritium measurements on portable getter beds, *Proceedings of the 17th Annual Symposium on European Safeguards and Research and Development Association (ESARDA)*, May 9–11, 1995, Aachen, Federal Republic of Germany, (1996).

[Kre94] U. Kreissig, R. Groetzschel and R. Behrisch, Simultaneous measurement of the hydrogen isotopes H, D, T and ^{3}He with HIERD, *Nuclear Instruments and Methods in Physics Research Section B: Beam Interactions with Materials and Atoms*, 85(1-4) (1994) 71–74.

[Kri02] K. Krieger, X. Gong, M. Balden, D. Hildebrandt, H. Maier, V. Rohde, J. Roth and W. Schneider, Erosion and migration of tungsten employed at the central column heat shield of ASDEX Upgrade, *Journal of Nuclear Materials*, 307-311 (2002) 139–143.

[Kri12] S. C. Krishna, N. Supriya, A. K. Jha, B. Pant, S. C. Sharma and K. M. George, Thermal conductivity of Cu – Cr – Zr – Ti alloy in the temperature range of 300 - 873 K, *ISRN Metallurgy*, 2012 (2012) 1–4.

[Kro00] A. H. M. Krom and A. Bakker, Hydrogen trapping models in steel, *Metallurgical and Materials Transactions, B Process Metallurgy and Materials Processing*, 31(6) (2000) 1475–1482.

[Kru70] P. Krumbiegel, Isotopieeffekte, Akademieverlag Berlin; Pergamon Press, Oxford; Vieweg und Sohn, Braunschweig, Berlin, Germany (1970).

[Kub06] M. Kubota, N. Noyama, C. Sakae and Y. Kondo, Fretting fatigue in hydrogen gas, *Tribology International*, 39(10) (2006) 1241–1247.

[Kui71] F. A. Kuijpers and H. H. van Mal, Sorption hysteresis in the $LaNi_5-H$ and $SmCo_5-H$ systems, *Journal of the Less Common Metals*, 23(4) (1971) 395–398.

[Kui81] E. G. M. Kuijpers, J. W. Jansen, A. J. D. van and J. W. Geus, The reversible decomposition of methane on a Ni/SiO_2 catalyst, *Journal of Catalysis*, 81 (1981) 429–439.

[Kui83] E. G. M. Kuijpers, A. K. Breedijk, W. J. J. W. van der and J. W. Geus, Chemisorption of methane on Ni/SiO_2 catalysts and reactivity of the chemisorption products toward hydrogen, *Journal of Catalysis*, 72 (1983) 75–82.

[Kui84] E. G. M. Kuijpers, A. J. H. M. Kock, G. J. Wermer and J. W. Geus, Carbon deposition from CH_4 and CO on Ni/SiO_2: Effects on the nickel surface structure, *Journal of Catalysis*, 88(1) (1984) 1–7.

[Kul06] T. V. Kulsartov, K. Hayashi, M. Nakamichi, S. E. Afanasyev, V. P. Shestakov, Y. V. Chikhray, E. A. Kenzhin and A. N. Kolbaenkov, Investigation of hydrogen isotope permeation through F82H steel with and without a ceramic coating of $Cr_2O_3-SiO_2$ including $CrPO_4$ (out-of-pile tests), *Fusion Engineering and Design*, 81(1-7) (2006) 701–705.

[Kul11] T. Kulsartov, I. Tazhibayeva, Y. Gordienko, E. Chikhray, K. Tsuchiya, H. Kawamura and A. Kulsartova, Study of tritium and helium release from irradiated lithium ceramics Li_2TiO_3, *Fusion Science and Technology*, 60(3) (2011) 1139–1142.

[Kum93] O. Kumberger and H. Schmidbaur, Warum ist Beryllium so toxisch?, *Chemie in unserer Zeit*, 27(6) (1993) 310–316.

[Kun07] C. L. Kunz, R. A. Causey, M. Clift, W. R. Wampler and D. F. Cowgill, Removal of the codeposited carbon layer using He – O glow discharge, *Journal of Nuclear Materials*, 367-370 (2007) 1512–1515.

[Kun70] P. J. Kuntz, E. M. Nemeth, J. C. Polanyi and W. H. Wong, Distribution of reaction products. VI. Hot-atom reactions, T + HR, *The Journal of Chemical Physics*, 52(9) (1970) 4654–4674.

[Kur84] U. Kurz, Der U/UT3-Lagerbehaelter im Tritium-Lager, Spezielle Berichte der Kernforschungsanlage Juel-Spez-258, Kernforschungsanlage Juelich GmbH, Juelich, Germany (1984).

[Kur87] W. Kurtz and H. Vanecek, Gmelin Handbook of Inorganic Chemistry: W Tungsten, Supplement volume A7, Metal, chemical reactions with metals zinc to lawrencium, 8th edition, Springer Verlag, Heidelberg, Germany (1987).

[Kve95] O. K. Kveton, H. Yoshida, J. E. Koonce, R. Haange, H. Horikiri, S. K. Sood, C. Fong, K. M. Kalyanam and A. Busigin, Design of the Water Detritiation and Isotope Separation Systems for ITER, *Fusion Technology*, 28(3P1) (1995) 636–640.

[Lab08] M. J. Laberge, An accoustically driven magnetized target fusion reactor, *Journal of Fusion Energy*, 27 (2008) 65–68.

[Lac00] K. Lackner, Der naechste Schritt zum Fusionskraftwerk, *Spektrum der Wissenschaft*, (6) (2000) 86.

[Lad01] P. Ladd, M. J. Gouge, D. Murdoch and G. L. Saksaganskiy, ITER R&D: Auxiliary systems: Fuelling and Vacuum Pumping System, *Fusion Engineering and Design*, 55(2-3) (2001) 303–311.

[Lad97] P. Ladd, H. Hurlmeier, R. Janeschitz G.and Marrs and K. Schaubel, The design of the ITER primary pumping system, *Proceedings of the 19th Symposium on Fusion Technology*, Sept. 16–20, 1996, Lisbon, Portugal, (1997) 1173–1176.

[Lae01a] R. Laesser, Development of a self-assay fast delivery tritium storage vessel, EU Report TW1-TTF/TEP13A, prepared for the Commission of the European Union, (2001).

[Lae01b] R. Laesser, C. Caldwell-Nichols, L. Doerr, M. Glugla, S. Gruenhagen, K. Guenther and R.-D. Penzhorn, Analytic of tritium-containing gaseous species at the Tritium Laboratory Karlsruhe, *Fusion Engineering and Design*, 58-59 (2001) 411–415.

[Lae02a] R. Laesser, Development of a self-assay fast delivery tritium storage bed, Intermediate Report TW1-TTF/TEP13A, prepared for the Commission of the European Union, (2002).

[Lae02b] R. Laesser, L. Doerr, M. Glugla, R.-D. Penzhorn, T. Hayashi, D. K. Murdoch and H. Yoshida, The storage and delivery system of the ITER tritium fuel processing plant, *Fusion Science and Technology*, 41(3P2) (2002) 854–858.

[Lae02c] R. Laesser, M. Glugla, S. Gruehagen, K. Guenther, R.-D. Penzhorn and J. Wendel, Use of gas chromatography in the Tritium Laboratory Karlsruhe, *Fusion Science and Technology*, 41(3P2) (2002) 515–519.

[Lae02d] R. Laesser, D. K. Murdoch and R.-D. Penzhorn, Use of ferrofluidic seals in the design of tritium compatible pumps, *Fusion Science and Technology*, 41(3P2) (2002) 621–625.

[Lae03a] R. Laesser, Design and manufacture of the storage bed: experimental plan with tabulation of proposed tests, report TW1-TTF/TEP13A, for the European Commission, (2003).

[Lae03b] R. Laesser, S. Gruenhagen and Y. Kawamura, Use of micro gas chromatography in the fuel cycle of fusion reactors, *Fusion Engineering and Design*, 69(1-4) (2003) 813–817.

[Lae08] R. Laesser, A. Antipenkov, N. B. Bekris, L. V. Boccaccini, C. J. Caldwell-Nichols, I. Cristescu, C. Day, M. Gasparotto, M. Glugla, G. Dell'Orco, F. Gabriel, O. Gastaldi, C. Grisolia, S. Knipe, A. J. Magielsen, A. Moeslang, D. Murdoch, R. Pearce, A. Perevezentsev, G. Piazza, Y. Poitevin, I. Ricapito, J.-F. Salavy, L. A. Sedano and M. Zmitko, Tritium in fusion: R&D in the EU, *Fusion Science and Technology*, 54(1) (2008) 39–44.

[Lae83] R. Laesser and K. H. Klatt, Solubility of hydrogen isotopes in palladium, *Physical Review B*, 28 (1983) 748.

[Lae85] R. Laesser, Tritium in metals, *Zeitschrift fuer Physikalische Chemie, Neue Folge*, 28(2) (1985) 748–758.

[Lae86] R. Laesser and G. L. Powell, Solubility of H, D, and T in Pd at low concentrations, *Physical Review B*, 34(2) (1986) 578–586.

[Lae87] R. Laesser, Properties of tritium and ^{3}He in metals, *Journal of the Less-Common Metals*, 131(1-2) (1987) 263–273.

[Lae88] R. Laesser and G. L. Powell, Solubility of tritium in $Pd_{1-Y}Ag_Y$ alloys (y = 0.00, 0.10, 0.20, 0.30), *Fusion Technology*, 14(2P2A) (1988) 695–700.

[Lae92] R. Laesser, C. J. Caldwell-Nichols, J. Dallimore, B. Grieveson, J. L. Hemmerich, A. Konstantellos, M. Laveyry, P. Milverton, R. Stagg and J. Yorkshades., Analytical equipment for the JET Active Gas Handling Plant, *Fusion Technology*, 21(2P2) (1992) 406–411.

[Lae93] R. Laesser, B. Grieveson, J. L. Hemmerich, R. Stagg, T. Dowhyluk, K. Torr, R. Massey and P. Chambers, The gas-chromatographic analysis system in the JET Active Gas Handling Plant, *Review of Scientific Instruments*, 64(9) (1993) 2449–2458.

[Lae95] R. Laesser, G. Jones, J. L. Hemmerich, R. Stagg and J. Yorkshades, The preparative gas chromatographic system for the JET Active Gas Handling System - inactive commissioning, *Fusion Technology*, 28(3P1) (1995) 681–686.

[Lae98] R. Laesser, N. Bainbridge, A. C. Bell, D. Brennan, J. L. Hemmerich, S. Knipe, R. Stagg and J. Yorkshades, Hydrogen isotope separation in the JET Active Gas Handling System during DTE1, *Proceedings of the 20^{th} Symposium on Fusion Technology (SOFT)*, Sept. 7–11, 1998, Marseille, France, (1998) 1005–1008.

[Lae99a] R. Laesser, A. C. Bell, N. Bainbridge, D. Brennan, L. Doerr, J. L. Hemmerich, S. Knipe and R. Stagg, The preparative gas chromatographic system for the JET Active Gas Handling System — Tritium commissioning and use during and after DTE1, *Fusion Engineering and Design*, 47(2-3) (1999) 301–319.

[Lae99b] R. Laesser, A. C. Bell, N. Bainbridge, P. D. Brennan, B. Grieveson, J. L. Hemmerich, G. Jones, D. Kennedy, S. Knipe, J. Lupo, J. Mart, A. Perevezentsev, N. Skinner, R. Stagg, J. Yorkshades, G. V. Atkins, L. Doerr, N. Green, M. Stead and K. Wilson, Overview of the performance of the JET Active Gas Handling System during and after DTE1, *Fusion Engineering and Design*, 47(2-3) (1999) 173–203.

[Lae99c] R. Laesser, A. C. Bell, B. Grieveson, J. L. Hemmerich, R. Stagg and G. V. Atkins, The analytical gas chromatographic system of the JET Active Gas Handling System — Tritium commissioning and use during DTE1, *Fusion Engineering and Design*, 47(2-3) (1999) 333–353.

[LaM94] P. H. LaMarche, J. L. Anderson, C. A. Gentile, R. J. Hawryluk, J. Hosea, M. Kalish, T. Kozub, H. Murray, A. Nagy, S. Raftopoulos, R. L. Rossmassier, R. A. P. Sissingh, J. Swanson, F. Tulipano, M. Viola, D. R. Voorhees, R. T. Walters and TFTR Team, Tritium processing and management during D-T experiments on TFTR, *Fusion Technology*, 26(3P2) (1994) 427–433.

[Lan84] R. A. Langley, Hydrogen trapping, diffusion and recombination in austenitic stainless steels, *Journal of Nuclear Materials*, 128-129 (1984) 622–628.

[Lar79] C. Lartigue, Étude structurale et thermodynamique du systeme $LaNi_{5-x}Mn_x$-hydrogéne, PhD thesis, Université du Paris, (1979).

[Las05] R. Lascola, K. E. Zeigler, C. S. McWhorter, E. Villa-Aleman, L. L. Tovo and A. E. Ward, Isotopic hydrogen analysis via conventional and surface-enhanced fiber optic Raman spectroscopy, *Proceedings of SPIE: Advanced Environmental, Chemical and Biological Sensing Technologies II*, Oct. 25–28, 2004, Philadelphia, PA, USA, (2005) 83–93.

[Laz06] A. Lazar, S. Brad, M. Zamfirache, S. Soare, N. Sofalca and M. Vijulie, Development of ITER PRM and standard parts catalogues in CATIA V5 for tritium-containing systems and components, *Progress of Cryogenics and Isotopes Separation*, 9(17-18) (2006) 105–111.

[LeC83] A. LeClaire, Permeation of gases through solids, II - an assessment of measurements of the steady-state permeability of H and its isotopes through Fe, Fe-based alloys, and some commercial steels, *Diffusion and Defect Data*, 34 (1983) 1–35.

[Lee13] S. Lee, M.-S. Lee, J.-C. Lee, W.-S. Choi, K.-Y. Kim, J.-E. Jeon, K.-S. Seo, W. Shu and M. Glugla, Development of ITER tritium transport package, *Fusion Engineering and Design*, (2013) 136–144.

[Lee60] J. K. Lee, B. Musgrave and F. S. Rowland, Hot atom reactions and radiation-induced effects in the reactions of recoil tritium with cyclo propane, *Canadian Journal of Chemistry*, 38(10) (1960) 1756–1768.

[Lee95] M. W. Lee, Hydrogen isotope separation experience at the Savannah River Site, *Fusion Technology*, 27(2T) (1995) 95–97.

[Lef12] X. Lefebvre, P. Trabuc, K. Liger, C. Perrais, S. Tosti, F. Borgognoni and A. Santucci, Preliminary results from a detritiation facility dedicated to soft housekeeping waste, *Fusion Engineering and Design*, 87(7-8) (2012) 1040–1044.

[Lef15] X. Lefebvre, A. Hollingsworth, A. Parracho, P. Dalgliesh, B. Butler and R. Smith, Conceptual design and optimization for JET water detritiation system cryo-distillation facility, *Fusion Science and Technology*, 67(2) (2015) 451–454.

[Lei61] L. Leibowitz, J. G. Schnizlein, J. D. Bingle and R. C. Vogel, The kinetics of oxidation of uranium between 125 and 250 °C, *Journal of the Electrochemical Society*, 108(12) (1961) 1155.

[LeL94] J. M. LeLann, X. Joulia, C. Latge and P. Sere-Peyrigain, Dynamic simulation of hydrogen isotope distillation unit, *18th European Symposium on Fusion Technology (SOFT-18)*, Aug. 22–26, 1994, Karlsruhe, Germany, (1994) 1059.

[Les20] K. Lesker, https://www.vacuum-uk.org/pdfs/vs2/VacPumps/TwisTorr.pdf, (2020), (visited on July 23, 2020).

[Les89] P. A. Lessard, Cryogenic adsorption of noncondensibles in the high-vacuum regime, *Journal of Vacuum Science & Technology A: Vacuum, Surfaces, and Films*, 7(3) (1989) 2373–2376.

[Let98] D. Leterq, A. Ballanger, J. Steimetz and D. Vasselin, Development of a TCAP prototype for hydrogen isotope separation, *Proceedings of the 20th Symposium on Fusion Technology (SOFT)*, Sept. 7–11, 1998, Marseille, France, (1998) 981–984.

[Lev07] D. Levchuk, S. Levchuk, H. Maier, H. Bolt and A. Suzuki, Erbium oxide as a new promising tritium permeation barrier, *Journal of Nuclear Materials*, 367-370 (2007) 1033–1037.

[Lew08] R. J. Lewis, H. H. Telle, B. Bornschein, O. Kazachenko, N. Kernert and M. Sturm, Dynamic Raman spectroscopy of hydrogen isotopomer mixtures in-line at TILO, *Laser Physics Letters*, 5(7) (2008) 522–531.

[Lew61] B. Lewis and G. von Elbe, Combustion, flames, and explosions of gases, 2nd, Academic Press Inc., Cambridge, MA, USA (1961).

[Lib57] G. G. Libowitz and T. R. P. Gibb Jr., High pressure dissociation studies of the uranium-hydrogen system, *The Journal of Physical Chemistry*, 61(6) (1957) 793–795.

[Lib58] G. G. Libowitz, H. F. Hayes and T. R. P. Gibb Jr, The system zirconium–nickel and hydrogen, *The Journal of Physical Chemistry*, 62(1) (1958) 76–79.

[Lie53] K. H. Lieser and H. Witte, Loeslichkeit von Wasserstoff in Legierungen, *Zeitschrift fuer Physikalische Chemie*, 202(1) (1953) 321–351.

[Lig15] K. Liger, P. Trabuc, X. Lefevre, M. Troulay and C. Perrais, Limitation of tritium outgassing from tritiated solid waste drums, *Fusion Science and Technology*, 67(2) (2015) 455–458.

[Lin87] C. N. Lindsay, R. E. Sprague and J. A. Brandenburg, A Measurement Control Study for Tritium Gas, technical report MLM-3441, Mound Laboratory, Miamisburg, OH, USA (1987).

[Lin89] H. T. Lin, S. H. Goods, M. L. Grossbeck and B. A. Chinl, Helium induced degradation in the weldability of an austenitic stainless steel, *Proceedings of the 14th International Symposium on Effects of Radiation on Materials*, June 27–30, 1988, Andover, MA, USA, (1989) 301–314.

[Lin90] D. L. Lindner, Isothermal decomposition of uranium hydride, *Journal of the Less-Common Metals*, 157(1) (1990) 139–146.

[Lin92] R. Lindau, A. Moeslang and R.-D. Penzhorn, Mechanical and microstructural properties of tritium permeable PdAg alloy after helium implantation, *Journal of Nuclear Materials*, 191-194 (1992) 178–182.

[Lip01] B. Lipschultz, D. Pappas, B. LaBombard, J. Rice, D. Smith and S. Wukitch, Molybdenum sources and transport in Alcator C-Mod, *Journal of Nuclear Materials*, 290-293 (2001) 286–290.

[Lip06] B. Lipschultz, Y. Lin, M. Reinke, A. Hubbard, I. Hutchinson, J. Irby, B. LaBombard, E. Marmar, K. Marr, J. Terry and S. Wolfe, Operation of ALCATOR C-Mod with high Z plasma facing components and implications, *Physics of Plasmas*, 13 (2006) 056117.

[Lit48] L. M. Litz, A. B. Garrett and F. C. Croxton, Preparation and structure of the carbides of uranium, *Journal of the American Chemical Society*, 70(5) (1948) 1718–1722.

[Liu13] Y.-L. Liu and W. Shi, Investigating permeation and transport of H isotopes in tungsten by first-principles, *Fusion Engineering and Design*, 88(5) (2013) 368–373.

[Llo86] D. C. Lloyd, A. A. Edwards, J. S. Prosser, A. A. der Maur, A. Etzweiler, U. Weickhardt, U. Goessi, L. Geiger, U. Noelpp and H. Roesler, Accidental intake of tritiated water: A report of two cases, *Radiation Protection Dosimetry*, 15(3) (1986) 191–196.

[Llo97a] P. B. Lloyd, J. W. Kress and B. J. Tatarchuk, Surface and bulk interactions of hydrogen with copper, *Applied Surface Science*, 119(3-4) (1997) 275–287.

[Llo97b] P. B. Lloyd, M. Swaminathan, J. W. Kress and B. J. Tatarchuk, Temperature programmed desorption study of the adsorption and absorption of hydrogen on and in Cu(111), *Applied Surface Science*, 119(3-4) (1997) 267–274.

[Loh99] T. Lohse, Ueberpruefung der Qualitaet des Tritiumeinschlusses in der Transportverpackung tritiierter Graphitziegel aus dem JET-Reaktor in England beim Transport ins Forschungszentrum Karlsruhe, Studienarbeit, Forschungszentrum Karlsruhe, (1999).

[Lon07] G. R. Longhurst, Tritiated Water Interaction with Stainless Steel, technical report INL/EXT-07-12584, Idaho National Laboratory, Idaho Falls, ID, USA (2007).

[Lon08] G. R. Longhurst and J. Cleaver, Interactions of hydrogen isotopes and oxides with metal tubes, *Fusion Science and Technology*, 54(2) (2008) 565–568.

[Lon88] G. R. Longhurst, Pyrophoricity of tritium-storage bed materials, *Fusion Technology*, 14(2P2A) (1988) 750–755.

[Lon89] G. R. Longhurst, R. A. Jalbert and R. L. Rossmassler, Atmospheric detritiation system performance, *Fusion Technology*, 15(2P2B) (1989) 1331–1336.

[Lon91] G. R. Longhurst, R. A. Anderl and D. F. Holland, Evidences of hydrogen trapping in tungsten and implications for plasma-facing components, *Fusion Technology*, 19(3P2B) (1991) 1799–1805.

[Lon92] G. R. Longhurst, A. G. Heics, W. T. Shmayda and R. L. Rossmassler, Experimental evaluation of the consequences of uranium bed air-ingress accidents, *Fusion Technology*, 21(2P2) (1992) 1017–1023.

[Lon95] G. R. Longhurst, R. A. Anderl, T. J. Dolan and M. J. Mulock, Modeling tritium processes in plasma-facing beryllium, *Fusion Technology*, 28(3P2) (1995) 1217–1222.

[Lot14] M. V. Lototskyy, V. A. Yartys, B. G. Pollet and R. C. Bowman, Metal hydride hydrogen compressors: A review, *International Journal of Hydrogen Energy*, 39(11) (2014) 5818–5851.

[Lou72] M. R. Louthan, G. R. Caskey, J. A. Donovan and D. E. Rawl, Hydrogen embrittlement of metals, *Materials Science and Engineering*, 10 (1972) 357–368.

[Lou74] M. R. Louthan, J. A. Donovan and G. R. Caskey, Isotope effects on hydrogen transport in nickel, *Scripta Metallurgica*, 8(6) (1974) 643–649.

[Lou75a] M. R. Louthan and R. G. Derrick, Hydrogen transport in austenitic stainless steel, *Corrosion Science*, 15(6-12) (1975) 565–577.

[Lou75b] M. R. Louthan, J. A. Donovan and G. R. Caskey, Hydrogen diffusion and trapping in nickel, *Acta Metallurgica*, 23(6) (1975) 745–749.

[Lou75c] M. R. Louthan, J. A. Donovan and G. R. Caskey, Tritium absorption in type 304L stainless steel, *Nuclear Technology*, 26(2) (1975) 192–200.

[Lu14] G.-H. Lu, Behaviours of hydrogen and helium in tungsten: new insights from modelling and simulation, *Proceedings of the Decenial IAEA Technical Meeting and Plasma Material Interaction Data for Fusion Science and Technology*, Dec. 18–19, 2014, Vienna, Austria, (2014).

[Luc00] L. L. Lucas and M. P. Unterweger, Comprehensive review and critical evaluation of the half-life of tritium, *Journal of Research of the National Institute of Standards and Technology*, 105(4) (2000) 541.

[Luo03] M. F. Luo, D. A. MacLaren, I. G. Shuttleworth and W. Allison, Preferential subsurface occupation of atomic hydrogen on Cu(111), *Chemical Physics Letters*, 381(5-6) (2003) 654–659.

[Luo06] G.-N. Luo, W. M. Shu and M. Nishi, Influence of blistering on deuterium retention in tungsten irradiated by high flux deuterium 10 - 100 eV plasmas, *Fusion Engineering and Design*, 81(8-14) (2006) 957–962.

[Lup95] J. Lupo, J. L. Hemmerich, R. Laesser, J. Yorkshades and J. L. Salanave, The impurity processing system for the JET Active Gas Handling System — Inactive commissioning, *Fusion Technology*, 28(3P2) (1995) 1347–1352.

[Lut00] J. Luthin and C. Linsmeier, Carbon films and carbide formation on tungsten, *Surface Science*, 454-456 (2000) 78–82.

[Lyn84] J. F. Lynch, G. G. Libowitz and A. J. Maeland, Hydrogen compression by metal hydrides, *Proceedings of the 5th World Hydrogen Energy Conference*, July 15–19, 1984, Toronto, Canada, (1984) 1327–1337.

[Ma14] M. Ma, UW fusion reactor concept could be cheaper than coal, https://www.washington.edu/news/2014/10/08/uw-fusion-reactor-concept-could-be-cheaper-than-coal/, (2014), (visited on Apr. 22, 2022).

[Mac01] A. Mack, C. Day, H. Haas, D. K. Murdoch, J. C. Boissin and P. Schummer, First operation experiences with ITER-FEAT model pump, *Fusion Engineering and Design*, 58-59 (2001) 365–369.

[Mac02] A. Mack, A. Antipenkov, J. C. Boissin, C. Day, S. Gross, H. Haas, V. Hauer, D. K. Murdoch and T. Waldenmaier, Design of the ITER torus cryopump, *Fusion Engineering and Design*, 61-62 (2002) 611–615.

[Mac06] D. MacMahon, Half-life evaluations for ^{3}H, ^{90}Sr, and ^{90}Y, *Applied Radiation and Isotopes*, 64(10-11) (2006) 1417–1419.

[Mac73] K. M. Mackay and M. F. A. Dove, Deuterium and tritium, *Comprehensive Inorganic Chemistry*, J. Bailar, H. J. Emeleus, C. Nyholm and A. Trotman-Dickenson, editors, Pergamon Press, Oxford, New York, Toronto, Sydney, Braunschweig, (1973), 77–116.

[Mac92] R. G. Macaulay-Newcombe, D. A. Thompson and W. W. Smeltzer, Thermal absorption and desorption of deuterium in beryllium and beryllium oxide, *Journal of Nuclear Materials*, 191-194 (1992) 263–267.

[Mac94] R. G. Macaulay-Newcombe and D. A. Thompson, The effects of surface contamination on absorption and desorption of deuterium in beryllium and beryllium oxide, *Journal of Nuclear Materials*, 212-215 (1994) 942–947.

[Mac98] A. Mack, C. Day, E. Diegele, H. Haas, S. Kraegermann, J. C. Boissin, A. Cohu, P. Schummer and D. Murdoch, ITER-primary vacuum pump, *Proceedings of the 20th Symposium on Fusion Technology (SOFT)*, Sept. 7–11, 1998, Marseille, France, (1998) 1037–1040.

[Mai76] J. L. Maienschein, Applicability of Chemical Getter Beds to Scavenge Tritium from Inert Gases, technical report UCRL-52034, Lawrence Livermore Laboratory, Livermore, CA, USA (1976).

[Mai78] J. L. Maienschein, Feasibility of chemical getter beds in scavenging tritium from inert gases, *Nuclear Technology*, 38(3) (1978) 387–404.

[Mai84] J. L. Maienschein, Radiolysis in Nitrogen-Tritium Mixtures: Formation of Ammonia in a Nitrogen Atmosphere Glove Box, technical report UCRL-90645, Lawrence Livermore Laboratory, Livermore, CA, USA (1984).

[Mai88] J. L. Maienschein, F. E. McMurphy and V. L. Duval, Increase of tritium permeation through resistant metals at 323 K by lattice defects, *Fusion Technology*, 14(2P2A) (1988) 701–706.

[Mai92a] J. L. Maienschein, F. Garcia, R. G. Garza, R. L. Kanna, S. R. Mayhugh and D. T. Taylor, Experiences with decontaminating tritium-handling apparatus, *Fusion Technology*, 21(2P2) (1992) 383–388.

[Mai92b] J. L. Maienschein, R. S. Hudson, R. T. Tsugawa, E. M. Fearon, P. C. Souers and G. W. Collins, Separation of hydrogen isotopes by selective adsorption with production of high-purity DT and T_2, *Journal of Vacuum Science & Technology A: Vacuum, Surfaces, and Films*, 10(3) (1992) 556–569.

[Mai92c] J. L. Maienschein, S. W. Wilson and F. Garcia, Design and operational experience with a portable tritium cleanup system, *Fusion Technology*, 21(2P2) (1992) 691–695.

[Mai98] H. Maier, S. Koetterl, K. Krieger, R. Neu, M. Balden and A. Upgrade-Team, Performance of tungsten coatings as plasma facing components used in ASDEX Upgrade, *Journal of Nuclear Materials*, 258-263 (1998) 921–926.

[Mal55] M. W. Mallett and A. F. Gerds, Reaction of nitrogen with uranium, *Journal of the Electrochemical Society*, 102(6) (1955) 292.

[Mal58] M. W. Mallett and M. J. Trzeciak, Hydrogen-uranium relationships, *Transactions of the American Society of Metals*, 50(981-989) (1958) 16.

[Mal76] M. E. Malinowski and P. R. Coronado, Helium release from uranium tritide, *International Conference on Radiation Effects and Tritium Technology for Fusion Reactors*, Sept. 30, 1975, Gatlinburg, TN, USA, (1976).

[Man11] A. Manhard, Deuterium inventory in tungsten after plasma exposure: a microstructural survey, PhD thesis, Mathematisch-Naturwissenschaftliche Fakultaet, Universitaet Augsburg, Augsburg, Germany, (2011).

[Man90] F. Mannone, Management of Tritium-Contaminated Wastes a Survey of Alternative Options, EU Scientific and Technical Research Reports EUR 12526 EN, Commission of the European Communities, Joint Research Centre, (1990).

[Man95] F. D. Manchester and A. San-Martin, The H – U (hydrogen-uranium) system, *Journal of Phase Equilibria*, 16(3) (1995) 263–275.

[Mao13] W. Mao, T. Chikada, A. Suzuki, T. Terai and K. Yamaguchi, Experimental and computational studies on tritium permeation mechanism in erbium oxide, *Journal Plasma Fusion Research*, 10 (2013) 27–32.

[Mar72] T. R. Marrero and E. A. Mason, Gaseous diffusion coefficients, *Journal of Physical and Chemical Reference Data*, 1(1) (1972) 3–118.

[Mar78] V. A. Maroni, Control of tritium permeation through fusion reactor structural materials, *Environmental Control Symposium*, Nov. 28–30, 1978, Washington, D. C., USA, (1978).

[Mar79] V. A. Maroni and E. H. v. Deventer, Materials considerations in tritium handling systems, *Journal of Nuclear Materials*, 85-86 (1979) 257–269.

[Mar90] V. A. Maroni, C. A. Melendres, T. F. Kassner, R. Kumar and S. Siegel, Spectroscopic characterization of oxide films on type 304 SS exposed to water at 289 °C: Correlation

with the Fe – Cr – H_2O Pourbaix diagram, *Journal of Nuclear Materials*, 172(1) (1990) 13–18.

[Mar91] P. Marmy, R. Yuzhen and M. Victoria, The tensile and fatigue properties of type 1.4914 ferritic steel for fusion reactor applications, *Journal of Nuclear Materials*, 179-181 (1991) 697–701.

[Mar96] E. Martone M., IFMIF, International Fusion Materials Irradiation Facility, Conceptual Design Activity, Final Report, ENEA Frascati Report RT/ERG/FUS/96/17, Frascati, Italy (1996).

[Mar97] G. Marbach, L. Boisset and P. Giroux, Steel reprocessing strategy for fusion reactor dismantling, *Proceedings of the 19th Symposium on Fusion Technology (SOFT)*, Sept. 16–20, 1996, Lisbon, Portugal, (1997) 1693–1696.

[Mas89] N. M. Masaki, T. Hirabayashi and M. Saeki, Study on sorption of tritium on various material surfaces and its application to decontamination of tritium-sorbing materials, *Fusion Technology*, 15(2P2B) (1989) 1337–1342.

[Mas92] J. A. Mason and G. Vassallo, Tritium measurement by isothermal calorimetry, *Fusion Technology*, 21(2P2) (1992) 425–429.

[Mas95] J. A. Mason, N. Bainbridge and J. R. Stencer, Isothermal calorimetry and tritium accountability, *Proceedings of the 18th Symposium on Fusion Technology (SOFT)*, Aug. 22–26, 1994, Karlsruhe, Federal Republic of Germany, (1995) 1087–1090.

[Mas96] K. Masaki, K. Kodama, T. Ando, M. Saidoh, M. Shimizu, T. Hayashi and K. Okuno, Tritium retention in graphite inner wall of JT-60U, *Fusion Engineering and Design*, 31(2) (1996) 181–187.

[Mat02a] M. Matsuyama, T. Murai, K. Yoshida, K. Watanabe, H. Iwakiri and N. Yoshida, Studies on retention of tritium implanted into tungsten by β-ray-induced X-ray spectrometry, *Journal of Nuclear Materials*, 307-311 (2002) 729–734.

[Mat02b] M. Matsuyama, T. Murai and K. Watanabe, Quantitative measurement of surface tritium by β-ray-induced X-ray spectrometry (BIXS), *Fusion Science and Technology*, 41(3P2) (2002) 505–509.

[Mat03] M. Matsuyama, N. Bekris, M. Glugla, N. Noda, V. Philipps and K. Watanabe, Non-destructive tritium measurements of MK IIA divertor tile by BIXS, *Journal of Nuclear Materials*, 313-316 (2003) 491–495.

[Mat04] M. Matsukawa, Recent results and modification program of JT-60 toward high integrated performance, *IEEE Transactions on Plasma Science*, 32(1) (2004) 135–143.

[Mat05] M. Matsuyama, Y. Torikai and K. Watanabe, In-situ measurement of high level tritiated water by bremsstrahlung counting, *Fusion Science and Technology*, 48(1) (2005) 324–331.

[Mat07] M. Matsuyama, Y. Torikai, M. Hara and K. Watanabe, New technique for non-destructive measurements of tritium in future fusion reactors, *Nuclear Fusion*, 47(7) (2007) S464–S468.

[Mat08] M. Matsuyama and M. Hara, Standardization of tritium measuring devices based on a high-sensitivity calorimeter, *Fusion Science and Technology*, 54 (2008) 182–185.

[Mat10] M. Matsuyama, K. Takatsuka and M. Hara, Sensitivity of a specially designed calorimeter for absolute evaluation of tritium concentration in water, *Fusion Engineering and Design*, 85(10-12) (2010) 2045–2048.

[Mat11] G. F. Matthews, M. Beurskens, S. Brezinsek, M. Groth, E. Joffrin, A. Loving, M. Kear, M.-I. Mayoral, R. Neu, P. Prior, V. Riccardo, F. Rimini, M. Rubel, G. Sips, E. V. P. de Vries and M. L. Watkins, JET ITER-like wall – Overview and experimental programme, *Physics Scripta*, T145(014001) (2011) 1–9.

[Mat14] M. Matsuyama, Progress of Tritium Measurement Techniques and Future Prospects, Annual Report 34-1, University of Toyama, Toyama, Japan (2014).

[Mat16] M. Matsuyama and S. Abe, Tracking of tritium charged into stainless steel by BIXS, *Fusion Engineering and Design*, 113 (2016) 250–254.

[Mat88] Y. Matsuda, N. Yokogawa, H. Yoshida, S. Konishi, Y. Naruse, M. Sakai F.and Yorozu, T. Ide and J. Mitsui, Experimental apparatus for thermal diffusion process in the Tritium Process Laboratory, *Fusion Technology*, 14 (1988) 585–589.

[Mat89] M. Matsuyama, H. Nakatani and K. Watanabe, In-situ measurement of tritium partial pressure by bremsstrahlung counting method, *Fusion Engineering and Design*, 10 (1989) 405–409.

[Mat91] M. Matsuyama and K. Watanabe, A small ionization chamber appropriate to tritium processing systems, *Fusion Engineering and Design*, 18 (1991) 91–96.

[Mat96] R. F. Mattas, M. Billone, A. Hassanein, N. J. Zhan, L. Green, G. D. Morgan, D. Kubik, V. D. Lee, G. Wille, E. Mogahed and I. Sviatoslavsky, U.S. ITER limiter module design, *Fusion Technology*, 30(3P2A) (1996) 558–563.

[Mat98] M. Matsuyama, K. Watanabe and K. Hasegawa, Tritium assay in materials by the bremsstrahlung counting method, *Fusion Engineering and Design*, 39-40 (1998) 929–936.

[May07] M. Mayer, V. Rohde, G. Ramos, E. Vainonen-Ahlgren, J. Likonen, A. Herrmann and R. Neu, The deuterium inventory in ASDEX Upgrade, *Nuclear Fusion*, 47(11) (2007) 1607–1617.

[May09] M. Mayer, V. Rohde, K. Sugiyama, J. L. Chen, X. Gong, C. Hopf, J. Likonen, S. Lindig, R. Neu, G. Ramos, E. Vainonen-Ahlgren and A. Wiltner, Carbon balance and deuterium inventory from a carbon dominated to a full tungsten ASDEX Upgrade, *Journal of Nuclear Materials*, 390-391 (2009) 538–543.

[May95] K. J. Maynard, W. T. Shmayda and A. G. Heics, Tritium aging effects in zirconium-cobalt, *Fusion Technology*, 28(3P2) (1995) 1391–1398.

[May96] M. Mayer, R. Behrisch, H. Plank, J. Roth, G. Dollinger and C. M. Frey, Codeposition of hydrogen with beryllium, carbon and tungsten, *Journal of Nuclear Materials*, 230(1) (1996) 67–73.

[McC79] J. McCarty, Hydrogenation of surface carbon on alumina-supported nickel, *Journal of Catalysis*, 57(3) (1979) 406–416.

[McC83a] G. T. McConville, Calculation of Charged Particle Densities in Pure Tritium Gas, technical report MLM-3097, UC34-D, Mound Laboratory, Miamisburg, OH, USA (1983).

[McC83b] G. T. McConville, D. A. Menke and R. E. Ellefson, Reaction rates of $D_2 + T_2$ mixtures at 295 K, *Journal of Vacuum Science & Technology A: Vacuum, Surfaces, and Films*, 1(3) (1983) 1441–1446.

[McC85] G. T. McConville, D. A. Menke and R. E. Ellefson, Reaction rates for the formation of deuterium tritide from deuterium and tritium, *Fusion Technology*, 8(2P2) (1985) 2245–2256.

[McC88] G. T. McConville, Effect of impurities on ions in tritium, *Fusion Technology*, 14(2P2A) (1988) 869–875.

[McC93] G. T. McConville and D. A. Menke, Exchange of dilute CH_4 in tritium gas, *Fusion Technology*, 23(3) (1993) 316–320.

[McC95] G. T. McConville and C. M. Woods, Calculation of tritium dose from insoluble particulates, *Fusion Technology*, 28(3P1) (1995) 905–909.

[McC97] K. A. McCarthy, G. R. Smolik, R. A. Anderl, R. J. Pawelko, M. A. Oates and R. S. Wallace, Chemical reactivity and mobilization of beryllium exposed to steam, *Fusion Engineering and Design*, 37(4) (1997) 543–552.

[McD76] J. H. McDonough, Detection, Reduction and Control of Gaseous Contaminants, promotional literature, Mine Safety Appliances Company, Filter Products Division, Evans City, PN, USA (1976).

[McG07] T. McGuire, Improved lifetimes and synchronization behaviour in multi-grid inertial electrostatic confinement fusion devices, PhD thesis, Massachusetts Institute of Technology, Boston, USA, (2007).

[McI57] B. B. McInteer, Analysis of H-D-T Mixtures by Mass Spectrometry, technical report LA-2086, Los Alamos Scientific Laboratory, Los Alamos, NM, USA (1957).

[McK79] H. A. C. McKay, Tritium immobilisation, *European Applied Research Report – Nuclear Science & Technology*, 1(3) (1979) 599–712.

[McK92] S. T. McKillip, C. E. Bannister and E. A. Clark, Stress analysis of hydride bed vessels used for tritium storage, *Fusion Technology*, 21(2P2) (1992) 1011–1016.

[McL73] R. B. McLellan, Solid solutions of hydrogen in gold, silver and copper, *Journal of Physics and Chemistry of Solids*, 34(6) (1973) 1137–1141.

[McL79] B. D. McLaughlin, Gasket Material Evaluation for Tokamak, technical report DPST-79-255, Technical Division, Savannah River Laboratory, Aiken, South Carolina, USA (1979).

[McQ50] A. D. McQuillan, An experimental and thermodynamic investigation of the hydrogen-titanium system, *Proceedings of the Royal Society of London. Series A. Mathematical and Physical Sciences*, 204(1078) (1950) 309–323.

[Men77] A. F. Mentink, J. O. Patterson and T. E. Hickman, Investigation of a Honeywell Dissolved Oxygen Parametric System, technical report EPA-660/4-77-023, US Environmental Protection Agency, Cincinnati, OH, USA (1977).

[Men79] M. Mendelsohn, D. M. Gruen and A. E. Dwight, Effect of aluminium additions on the thermodynamic and structural properties of $LaNi_{5-x}Al_x$ hydrides, *Advances in Chemistry*, American Chemical Sciety, (1979), 279–295.

[Mer09] B. J. Merrill, R. L. Moore and J. P. Sharpe, A preliminary assessment of beryllium dust oxidation during a wet bypass accident in a fusion reactor, *Fusion Engineering and Design*, 84(7-11) (2009) 1285–1288.

[Mer11] M. Merola, ITER in-vessel components, *Nuclear Fusion Engineering Masters*, Jan. 24, 2011, Torino, Italy, (2011).

[Mer77] E. A. Mershad, W. W. Thomasson and J. J. Dauby, Packaging of tritium-contaminated liquid waste, *Nuclear Technology*, 32(1) (1977) 53–59.

[Met05] S. J. Metz, W. Van de Ven, J. Potreck, M. Mulder and M. Wessling, Transport of water vapor and inert gas mixtures through highly selective and highly permeable polymer membranes, *Journal of Membrane Science*, 251(1-2) (2005) 29–41.

[Met68] A. Method, Compression set induced by nuclear reaction, tech.rep. American Society for Testing and Materials (ASTM), (1968).

[Mic08] R. Michling, I. Cristescu, L. Doerr, T. Fanghaenel, S. Welte and W. Wurster, Behavior of solid polymer membrane electrolyzers in use with highly tritiated water, *Fusion Science and Technology*, 54(2) (2008) 470–474.

[Mic13] R. Michling, N. Bekris, I. Cristescu, N. Lohr, C. Plusczyk, S. Welte and J. Wendel, Water detritiation processing of JET purified waste water using the TRENTA facility at Tritium Laboratory Karlsruhe, *Fusion Engineering and Design*, 88(9-10) (2013) 2361–2365.

[Mic76] R. L. Michel, Tritium inventories of the world oceans and their implications, *Nature*, 263(5573) (1976) 103–106.

[Mil02] J. M. Miller, W. R. C. Graham, S. L. Celovsky, J. R. R. Tremblay and A. E. Everatt, Design and operational experience with a pilot-scale CECE detritiation process, *Fusion Science and Technology*, 41(3P2) (2002) 1077–1081.

[Mil80] T. K. Mills, R. E. Ellis and M. L. Rogers, Recovery of tritium from aqueous waste using combined electrolysis catalytic exchange, *Proceedings of the Conference on Tritium Technology in Fission, Fusion, and Isotopic Applications*, Apr. 29–May 1, 1980, Dayton, OH, USA, (1980) 422–426.

[Mil81] H. H. Miller, E. R. Bissell, R. T. Tsugawa and P. C. Souers, Tritium gettering by acetylenes in static air, *Journal of Nuclear Materials*, 101(1-2) (1981) 238–239.

[Mil82] J. M. Miller and C. L. Cantlon, The Effect of Helium and Oxygen on the Hydriding of Titanium Sponge, technical report AECL-7698, Atomic Energy of Canada Ltd, Chalk River, Canada (1982).

[Mil91] H. J. Milton, A. A. Newton and H. H. H. Watson, Diffusion bonded windows for diagnostics of fusion plasmas, *Diffusion Bonding 2*, D. J. Stephenson, editor, Elsevier Applied Science, Dordrecht, The Netherlands, (1991), 270–292.

[Mil95] J. M. Miller and J. Quelch, Operating experience with tritium accounting and analysis systems in our tritium-handling facilities, *Fusion Technology*, 28(3P2) (1995) 1050–1054.

[Min11] Y. Mine and T. Kimoto, Hydrogen uptake in austenitic stainless steels by exposure to gaseous hydrogen and its effect on tensile deformation, *Corrosion Science*, 53(8) (2011) 2619–2629.

[Min80] J. M. Mintz and P. D. Gildea, Catalytic oxidation efficiencies for tritium and tritiated methane, industrial-scale decontamination systems, *Proceedings of the 4^{th} ANS Topical Meeting on Technol. Controlled Nuclear Fusion, SAND80-8046*, Oct. 14–17, 1980, King of Prussia, Pennsylvania, (1980).

[Mir20] S. Mirz, T. Brunst, R. Groessle and B. Krasch, Concentrated non-equilibrium HD for the cross calibration of hydrogen isopologue analytics, *Fusion Science and Technology*, 76 (2020) 284–290.

[Mit91] J. Mitsui, Y. Okada, F. Sakai, T. Die, I. Yamamoto, A. Kanagawa, K. Hirata, T. Yamanishi, K. Okuno and Y. Naruse, Separation of hydrogen isotopes by an advanced thermal diffusion column using cryogenic wall, *Fusion Technology*, 19 (1991) 1646–1650.

[Mit93] N. Mitchell, W. Daenner, P. Dinner, D. Maissonier, E. Salpietro, M. Sironi, C. Vallone and G. Vieider, Safety and Environmental Assessment of Fusion Power (SEAFP) - Specification of Technical Concepts, technical report SEAFP/R-M2(93), prepared for the Commission of the European Union, (1993).

[Miu97] H. Miura, S. Satoh, M. Enoeda, T. Kuroda, H. Takatsu, Y. Kawamura and S. Tanaka, Design of Test Blanket System for ITER Module Testing, technical report JAERI-97-051, Japan Atomic Energy Research Institute, Tokai-mura, Japan (1997).

[Miy83a] M. Miyake, H. Atsumi, Y. Nakamura, S. Yamanaka, Y. Yamamoto and K. Kitagawa, Thermal release of tritium from neutron irradiated glass, *Proceedings of the 12th Symposium on Fusion Technology (SOFT)*, Sept. 13–17, 1982, Juelich, Federal Republic of Germany, (1983) 555–560.

[Miy83b] M. Miyamoto, K. Yamaji and Y. Nakata, Reaction kinetics of $LaNi_5$, *Journal of the Less-Common Metals*, 89(1) (1983) 111–116.

[MKS14] MKS Instruments, Baratron Capacitance Manometers, www . mksinst . com / n / baratron-capacitance-manometers, (2014), (visited on Apr. 19, 2023).

[Moe06] A. Moeslang, V. Heinzel, H. Matsui and M. Sugimoto, The IFMIF test facilities design, *Fusion Engineering and Design*, 81 (2006) 863–871.

[Moe07] A. Moeslang, Irradiation facilities and the intense fusion neutron source IFMIF, *ATW*, 52 (2007) 548–557.

[Moe89] D. Moeller, The hot particle problem: a continuing challenge, IAEA report Radiation Protection Management 6:5, (1989).

[Mog75] A. A. Moghissi and M. W. Carter, editors, Tritium, Messenger Graphics, Phoenix, AZ,USA (1975).

[Mon78] B. G. Monahan, V. P. Gede, P. R. Landon, C. A. Colmenares and T. J. Biel, Materials compatibility study of 316 stainless steel at the LLL tritium facility, *3rd Meeting on the Technology of Controlled Thermonuclear Fusion*, May 9, 1978–May 11, 1987, Santa Fe, NM, USA, (1978) 9.

[Moo64] G. Moore and F. Unterwald, Thermal dissociation of hydrogen, *The Journal of Chemical Physics*, 40 (1964) 2639–2652.

[Mor04] F. Morfin, J.-C. Sabroux and A. Renouprez, Catalytic combustion of hydrogen for mitigating hydrogen risk in case of a severe accident in a nuclear power plant: study of catalysts poisoning in a representative atmosphere, *Applied Catalysis B: Environmental*, 47 (2004) 47–58.

[Mor08] M. Morgan, S. West and M. Tosten, Effect of tritium and decay helium on the fracture toughness properties of stainless-steel weldments, *Fusion Science and Technology*, 54 (2008) 501–505.

[Mor11] G. A. Morgan, Effect of impurities on the performance of a Pd−Ag diffuser, *Fusion Science and Technology*, 60(4) (2011) 1367–1370.

[Mor13] G. A. Morgan and B. Peters, SHINE Vacuum Pump Test Verification, technical report SRNL-STI–2013-00539, Savannah River National Laboratory, Aiken, SC, USA (2013).

[Mor77] G. A. Morris, Methane growth in tritium gas exposed to stainless steel, *24th Conference on Remote Systems Technology*, Nov. 14, 1976, Washington, DC, USA, (1977).

[Mor80] T. Morishita, S. Isomura, H. Izawa and R. Nakane, Tritium removal by hydrogen isotopic exchange between hydrogen gas and water on hydrophobic catalyst, *Conference*

on Tritium Technology in Fission, Fusion, and Isotopic Applications, Apr. 29–May 1, 1980, Dayton, OH, USA, (1980) 415–421.

[Mor90a] M. J. Morgan and D. Lohmeier, Threshold stress intensities and crack growth rates in tritium-exposed HERF stainless steels, *Conference on Hydrogen Effects on Material Behaviour*, Sept. 12–16, 1989, Jackson Hole, WY, USA, (1990) 459–468.

[Mor90b] M. J. Morgan and M. H. Tosten, Microstructure and yield strength effects on hydrogen and tritium induced cracking in HERF stainless steel, *Conference on Hydrogen Effects on Material Behaviour*, Sept. 12–16, 1989, Jackson Hole, WY, USA, (1990) 447–458.

[Mos76] H. Moser, Nukleare Techniken in der Hydrologie, *Kerntechnik*, 18 (1976) 461–469.

[Mot92] T. Motyka, The replacement tritium facility, *Fusion Technology*, 21 (1992) 247–252.

[Mue61] M. M. Mueller, A Calculation of the Beta Energy Adsorbed by Tritiated Gases in Spherical Vessels, technical report LAMS-2580, Los Alamos Scientific Laboratory, Los Alamos, NM, USA (1961).

[Mue97] D. Mueller, W. Blanchard, J. Collins, J. Hosea, J. Kamperschroer, P. H. LaMarche, A. Nagy, D. K. Owens and C. H. Skinner, Tritium removal from TFTR, *Journal of Nuclear Materials*, 241 (1997) 897–901.

[Mul78] M. Muller, Conceptual design of an emergency tritium cleanup system, *Proceedings of the Topical Meeting on the Technology of Controlled Nuclear Fusion*, May 9–11, 1978, Santa Fe, New Mexico, (1978).

[Mul92] D. Mullins, J. Krasznai and D. Mueller, Development of organic tritium light technology at Ontario Hydro, *Fusion Technology*, 21(2P2) (1992) 312–318.

[Mun01] K. Munakata, Y. Yokoyama, A. Baba, T. Kawagoe, T. Takeishi, M. Nishikawa, R.-D. Penzhorn, H. Moriyma, K. Kawamoto, Y. Morimoto and K. Okuno, Tritium release from catalytic breeder materials, *Fusion Engineering and Design*, 58–59 (2001) 683–687.

[Mun03] K. Munakata, A. Koga, Y. Yokoyama, S. Kanjo, S. Beloglazov, D. Ianovski, T. Takeishi, R.-D. Penzhorn, K. Kawamoto, H. Moriyama, Y. Morimoto, S. Akahori and K. Okuno, Effect of water vapor on tritium release from ceramic breeder material, *Fusion Engineering and Design*, 69 (2003) 27–31.

[Mun05a] K. Munakata, B. Bornschein, D. Corneli and M. Glugla, Numerical simulation of membrane reactor for detritiation of plasma exhaust gas, *Fusion Science and Technology*, 48 (2005) 17–22.

[Mun05b] K. Munakata, Y. Yokoyama, A. Baba, R.-D. Penzhorn, M. Oyaidzu and K. Okuno, Comparison of modelling of tritium release from ceramic breeder materials, *Fusion Engineering and Design*, 75–79 (2005) 673–678.

[Mun07] K. Munakata, S. Beloglazov, N. Bekris, M. Glugla, R. Wagner and E. Fanghänel, Experimental and simulation study on adsorption of hydrogen isotopes on MS5A at 77 K, *Fusion Engineering and Design*, 82 (2007) 2303–2310.

[Mun98] K. Munakata, U. Berndt, E. Kirste, M. Nishikawa and R.-D. Penzhorn, Experimental and computational determination of deuterium-tritium mixtures with a small volume ionization chamber, *Fusion Engineering and Design*, 39 (1998) 937–948.

[Mur00] D. K. Murdoch, M. Glugla and O. Kveton, Fuel cycle design evolution from FDR-ITER to RTO/RC-ITER, *Fusion Engineering and Design*, 49–50 (2000) 893–898.

[Mur05] D. Murdoch, R. Laesser, M. Glugla and A. Mack, ITER fuel cycle development, EU-PT activities, *Fusion Science and Technology*, 48 (2005) 3–10.

[Mur07] D. Murdoch, I. Cristescu, C. Day, M. Glugla, R. Lässer and A. Mack, Material compatibility issues in EU fusion fuel R&D and design, *Journal of Nuclear Materials*, 367 (2007) 1366–1370.

[Mur90a] D. Murdoch, J.-C. Boissin, A. Conrad and D. Perinic, Fore pumping concept for NET torus exhaust, *Fusion Technology Proceedings 16th SOFT*, London, UK, (1990) 513.

[Mur90b] T. S. Murthy and T. S. Iyengar, Applications of tritium in industry and research, *Bulletin of Radiation Protection*, 13 (1990) 173–178.

[Mur91a] D. Murdoch, J.-C. Boissin, A. Conrad and D. Perinic, Forepumping concept for NET torus exhaust, *Proceedings of the 16th Symposium on Fusion Technology (SOFT)*, Sept. 3–7, 1990, London, UK, (1991) 513–517.

[Mur91b] D. Murdoch and J. Boissin, The influence of argon cryo-trapping agent on the ITER fuel cycle design, *Fusion Engineering and Design*, 18 (1991) 85–90.

[Mur99] D. Murdoch, C. Day, P. Gierszewski, R.-D. Penzhorn and C. Wu, Tritium inventory issues for future reactors; choices, parameters, limits, *Fusion Engineering and Design*, 46 (1999) 255–271.

[Mus84] R. G. Musket, S. A. Steward, D. W. Brown and F. S. Uribe, Reduction of tritium permeation through iron using aluminium ion implantation, *Journal of Vacuum Science & Technology A 2*, (2) (1984) 723–724.

[Mye82] S. Myers and W. Wampler, Trapping and surface permeation of deuterium in helium-implanted stainless steel, *Journal of Nuclear Materials*, 111 (1982) 579–583.

[Mye84] S. Myers and W. Wampler, Trapping and surface recombination of ion–implanted deuterium in stainless steel, *Journal of Applied Physics*, 56 (1984) 1561–1571.

[Nag00] S. Nagata and H. Takahiro, Deuterium retention in tungsten and molybdenum, *Journal of Nuclear Materials*, 283–287 (2000) 1038–1042.

[Nag86] T. Nagasaki, S. Konishi, H. Katsuta and Y. Naruse, A zirconium-cobalt compound as the material for a reversible tritium getter, *Fusion Technology*, 9 (1986) 506–509.

[Nag93] T. Nagasaki, M. Saidoh, R. Yamada and H. Ohno, Ion-driven permeation and surface recombination coefficient of deuterium for iron, *Journal of Nuclear Materials*, 202 (1993) 228–238.

[Naj06] F. Najmabadi, A. Abdou, L. Bromberg, T. Brown, V. C. Chan, M. C. Chu, F. Dahlgren, L. El-Guebaly, P. Heitzenroeder, D. Henderson, H. E. S. John, C. E. Kessel, L. L. Lao, G. R. Longhurst, S. Malang, T. K. Mau, B. J. Merrill, R. L. Miller, E. Mogahed, R. L. Moore, T. Petrie, D. A. Petti, P. Politzer, A. R. Raffray, D. Steiner, I. Sviatoslavsky, P. Synder, G. M. Syaebler, A. D. Turnbull, M. S. Tillack, L. M. Waganer, X. Wang, P. West and P. Wilson, The ARIES-AT Advanced Tokamak, advanced technology Fusion Power Plant, *Fusion Engineering and Design*, 80(1-4) (2006) 3–23.

[Naj91] F. Najmabadi, R. W. Conn, C. G. Bathke, L. Bromberg, E. T. Cheng, D. R. Cohn, P. I. H. Cooke, R. L. Creedon, D. A. Ehst, K. Evans, N. M. Ghoniem, S. P. Grotz, M. Z. Hasan, J. T. Hogan, J. S. Herring, A. W. Hyatt, E. Ibrahim, S. A. Jardin, C. Kessel, M. Klasky, R. A. Krakowski, T. Kunugi, J. A. Leuer, J. Mandrekas, R. C. Martin, T.-K. Mau, R. L. Miller, Y.-K. M. Peng, R. L. Reid, J. F. Santarius, M. J. Schaffer, J. Schultz, K. R. Schultz, J. Schwartz, S. Sharafat, C. E. Singer, L. Snead, D. Steiner, D. J. Strickler, D.-K. Sze, M. Valenti, D. J. Ward, J. E. C. Williams, L. J. Wittenberg and C. P. C. Wong, The ARIES-I tokamak reactor study, *Proceedings of the 16th Symposium on Fusion Technology (SOFT)*, Sept. 3–7, 1990, London, UK, (1991) 253–257.

[Nak00] H. Nakamura, S. O´hira, W. Shu, M. Nishi, T. J. Venhaus, R. A. Causey, D. R. Hyatt and R. S. Willms, Tritium permeation experiment using a tungsten armored divertor-simulating module, *Journal of Nuclear Materials*, 283-287 (2000) 1043–1047.

[Nak01] H. Nakamura, T. Hayashi, Y. Iwai and M. Nishi, The effect of annealing on the transient deuterium permeation characteristics of tungsten, *Fusion Technology*, 39(2P2) (2001) 894–898.

[Nak02] M. Nakamichi, H. Kawamura and T. Teratani, Development of ceramic coating as tritium permeation barrier, *Fusion Science and Technology*, 41(3P2) (2002) 939–942.

[Nak04] S. Nakagawa, M. Matsuyama, H. Kodama, Y. Oya, K. Okuno, A. Sagara, N. Noda and K. Watanabe, Behavior of tritium release from thin boron films deposited on SS316, *Journal of Nuclear Materials*, 329-333 (2004) 904–908.

[Nak06] H. Nakamura, S. Sakurai, S. Suzuki, T. Hayashi, M. Enoeda and K. Tobita, Case study on tritium inventory in the fusion DEMO plant at JAERI, *Fusion Engineering and Design*, 81(8-14) (2006) 1339–1345.

[Nak07] M. Nakamichi, T. V. Kulsartov, K. Hayashi, S. E. Afanasyev, V. P. Shestakov, Y. V. Chikhray, E. A. Kenzhin and A. N. Kolbaenkov, In-pile tritium permeation through F82H steel with and without a ceramic coating of Cr_2O_3–SiO_2 including $CrPO_4$, *Fusion Engineering and Design*, 82(15-24) (2007) 2246–2251.

[Nak11] M. Nakayama and Hydrogen Isotope Research Center Staffs, Safety Handbook, International Safety Report on Work at Tritium Laboratory, Toyama, Japan (2011).

[Nak15] M. Nakayama, Y. Torikai, M. Saito, R.-D. Penzhorn, K. Isobe, T. Yamanishi and H. Kurishita, Measurement of uptake and release of tritium by tungsten, *Fusion Science and Technology*, 67(3) (2015) 503–506.

[Nak85] K. Nakamura and T. Hoshi, Supply and recovery of hydrogen isotopes in high vacuum systems using ZrNi hydride getter pumps, *Journal of Vacuum Science & Technology A: Vacuum, Surfaces, and Films*, 3(1) (1985) 34–38.

[Nak86] M. Nakashima and E. Tachikawa, Self-radiolysis of tritiated water adsorbed on silica gel, *International Journal of Radiation Applications and Instrumentation. Part A. Applied Radiation and Isotopes*, 37(6) (1986) 527–530.

[Nak87] M. Nakashima and E. Tachikawa, Radiolytic gas production from tritiated water adsorbed on molecular sieve 5A, *Journal of Nuclear Science and Technology*, 24(1) (1987) 41–46.

[Nak92] T. Nakamura, K. Hirata, T. Yamanishi, K. Okuno and Y. Naruse, Experimental study on separation characteristics of thermal diffusion columns using H – D – T system, *Fusion Technology*, 21(2P2) (1992) 942–947.

[Nak98] H. Nakamura, T. Hayashi, S. O´hira, M. Nishi and K. Okuno, Implantation driven permeation behaviour of deuterium through stainless steel type 316L, *Journal of Nuclear Materials*, 258-263 (1998) 1050–1054.

[Nao08] S. Naoe, Y. Torikai, R.-D. Penzhorn, K. Akaishi, K. Watanabe and M. Matsuyama, Transport of tritium in SS316 at moderate temperatures, *Fusion Science and Technology*, 54(2) (2008) 515–518.

[Nar87] Y. Naruse, Studies on tritium processing technology in JAERI, *International Symposium on Fusion Reactor Blanket and Fuel Cycle Technology*, Oct. 27–29, 1986, Tokai, Japan, (1987) 10–13.

[Nar90] Y. Naruse, Y. Matsuda and K. Tanaka, Tritium Process Laboratory at the JAERI, *Fusion Engineering and Design*, 12(3) (1990) 293–317.

[Nas92] J. E. Nasise, J. L. Anderson and Y. Naruse, Molecular sieve regeneration system for assaying HTO from detritation systems, *Fusion Technology*, 21(3P2B) (1992) 1974–1978.

[Nat91] National Nuclear Corporation (NNC), Basic Safety Considerations, C8322-CAPRICE, NNC document W251-SS, (1991).

[Nat94] A. Natalizio, ITER Safety Task NID-5a: On the Effect of Tritium Sorption on Building Surfaces as a Passive Mechanism for Reducing Airborne Concentrations, technical report CFFTP-G–9472, Canadian Fusion Fuels Technology Project, Mississauga, Canada (1994).

[Nef89] G. Neffe, E. Hutter, P. Schira and U. Tamm, Development work for the tritium cleanup system of the Tritium Laboratory Karlsruhe, *Proceedings of the 15th Symposium on Fusion Technology (SOFT)*, Sept. 19–23, 1988, Utrecht, The Netherlands, (1989) 1349–1353.

[Nef98] G. Neffe, U. Besserer, J. Dehne, E. Hutter, H. Kissel, R. D. Penzhorn, J. Wendel and H. Brunnader, Routine operation of the gas chromatographic isotope separation system of the Tritium Laboratory Karlsruhe, *Fusion Engineering and Design*, 39-40 (1998) 987–993.

[Nel73] H. G. Nelson and J. E. Stein, Gas-phase hydrogen permeation through alpha iron, 4130 steel, and 304 stainless steel from less than 100 °C to near 600 °C, technical note NASA-TN-D-7265, National Aeronautics and Space Administration, Washington, DC, USA (1973).

[Nem01] V. Nemanič, B. Zajec and J. Šetina, Anomalies in kinetics of hydrogen evolution from austenitic stainless steel from 300 to 1000 °C, *Journal of Vacuum Science & Technology A: Vacuum, Surfaces, and Films*, 19(1) (2001) 215–222.

[Neu03] R. Neu, A. Kallenbach, K. Krieger, V. Rohde and J. Roth, Chapter 10: Plasma-wall interaction and first-wall materials in ASDEX Upgrade, *Fusion Science and Technology*, 44(3) (2003) 692–707.

[Neu83] A. Neubert, H. Heimbach and H. R. Ihle, Design and performance of a thermal diffusion column for separation of the hydrogen isotopes, *Proceedings of the 12th Symposium of Fusion Technology (SOFT)*, Sept. 13–17, 1982, Juelich, Federal Republic of Germany, (1983) 561–566.

[New49] A. S. Newton, J. C. Warf, F. H. Spedding, O. Johnson, I. B. Johns, R. W. Nottorf, J. A. Ayres, R. W. Fisher and A. Kant, Uranium hydride II, radiochemical and chemical properties, *Nucleonics*, 4(2) (1949) 17–25.

[Nie15] S. Niemes, M. Sturm, R. Michling and B. Bornschein, High level tritiated water monitoring by bremsstrahlung counting using a silicon drift detector, *Fusion Science and Technology*, 67(3) (2015) 507–510.

[Nie21] S. Niemes, H. Telle, B. Bornschein, L. Fasselt, R. Groeßle, F. Priester, M. Schloesser, M. Sturm, S. Welte and G. Zeller, Accurate reference gas mixtures containing tritiated molecules: their production and Raman-based analysis, *Sensors*, 21 (2021) 6170.

[Nie23] S. Niemes and J. Braun, Speed of sound measurement of hydrogen isotopologues containing tritium for reference gas sample verification, *Fusion Science and Technology*, (2023) 1–5.

[Nie38] A. H. Nielsen and H. H. Nielsen, The infra-red absorption spectrum of CD_4, *Physical Review*, 54(2) (1938) 118–121.

[Nin90] H. Ninomiya, T. Ando, T. Horie, H. Horiike, K. Koizumi, T. Kushima, M. Matsukawa, Y. Neyatani and M. Yamamoto, JT-60 Upgrade device for confinement and steady state studies, *Plasma Devices and Operations*, 1(1) (1990) 43–65.

[Nis00] M. Nishi, T. Yamanishi, Y. Kawamura, Y. Iwai, K. Isobe, S. O´hira, T. Hayashi, H. Nakamura, K. Kobayashi, T. Suzuki, M. Yamada and S. Konishi, Progress of fusion fuel processing system development at the Japan Atomic Energy Research Institute, *Fusion Engineering and Design*, 49-50 (2000) 879–883.

[Nis06] M. Nishikawa, K. Furuichi and H. Takata, Study on permeation behaviour of gaseous tritium through concrete walls, *Fusion Science and Technology*, 50(4) (2006) 521–527.

[Nis12] T. Nishitani, P. Garin, M. Sugimoto, N. Nakajima, R. Heidinger, H. Kimura, K. Okano, K. Tobita, T. Yamanishi, G. Federici and N. Baluc, Progress of fusion nuclear technologies in the Broader Approach framework, *Fusion Engineering and Design*, 87(5-6) (2012) 535–542.

[Nis84] M. Nishikawa, K. Shinnai, S. Matsunaga and Y. Kinoshita, Oxidation of tritium by Hopcalite bed, *Journal of the Atomic Energy Society of Japan*, 26(8) (1984) 708–717.

[Nis89a] M. Nishikawa, K. Munakata, S. Izumi and T. Takeishi, Behaviour of tritium in a Pt-MS 5A catalyst bed, *Journal of Nuclear Materials*, 161(2) (1989) 182–189.

[Nis89b] M. Nishikawa, T. Takeishi, Y. Matsumoto and I. Kumabe, Ionization chamber system to eliminate the memory effect of tritium, *Nuclear Instruments and Methods in Physics Research Section A: Accelerators, Spectrometers, Detectors and Associated Equipment*, 278(2) (1989) 525–531.

[Nis92a] M. Nishikawa, T. Takeishi, Y. Kawamura, Y. Takagi and Y. Matsumoto, Tritium mass balance in the piping system of a fusion reactor, *Fusion Technology*, 21(2P2) (1992) 878–882.

[Nis92b] M. Nishikawa and K. Tanaka, Recovery of tritium from blanket sweep gas, *Proceedings of the International Workshop on Ceramic Breeder Blanket Interactions, Japan-US*

Workshop P195 and International Energy Agency Specialists Workshop, Oct. 26–29, 1992, Tokyo, Japan, (1992) 19–26.

[Nis92c] M. Nishikawa and K. Tanaka, Study on a method to recover tritium from blanket sweep gas, Oct. 26–29, 1992, Tokyo, Japan, (1992) 19–26.

[Nis94] M. Nishikawa, K.-I. Tanaka and M. Uetake, Study on a method to recover tritium from blanket sweep gas, *Fusion Technology*, 26(1) (1994) 17–26.

[Nis95a] M. Nishikawa, K.-I. Tanaka and M. Uetake, Mass transfer coefficients in cryosorption of hydrogen isotopes on molecular sieves or activated carbon at 77.4 K, *Fusion Technology*, 28(4) (1995) 1738–1748.

[Nis95b] M. Nishikawa, K.-I. Tanaka, M. Uetake, M. Enoeda, Y. Kawamura and K. Okuno, Adsorption isotherm and separation factor for multicomponent hydrogen isotopes in cryosorption method for recovery of tritium from blanket sweep gas, *Fusion Technology*, 28(3P1) (1995) 711–716.

[Nis95c] M. Nishikawa, M. Uetake, K. Tanaka and T. Shiraishi, Mass transfer coefficients in cryosorption of hydrogen isotopes on molecular sieves or activated carbon at 77 K, *Fusion Technology*, 28(3P1) (1995) 717–722.

[Nis96] M. Nishikawa, T. Shiraishi, Y. Kawanura and T. Takeishi, Permeation rate of hydrogen isotopes through palladium-silver alloy, *Journal of Nuclear Science and Technology*, 33(10) (1996) 774–780.

[Nis98] M. Nishikawa, K.-I. Tanaka, M. Uetake and T. Shiraishi, Isotope effect in cryosorption of tritium to molecular sieves and activated carbon at 77 K, *Fusion Technology*, 34(3P1) (1998) 234–240.

[Nob91] A. Nobile, Experience using metal hydrides for processing tritium, *Fusion Science and Technology*, 20(2) (1991) 186–199.

[Nob92] A. Nobile, J. R. Wermer and R. T. Walters, Aging effects in palladium and $LaNi_{4.25}Al_{0.75}$ tritides, *Fusion Technology*, 21(2P2) (1992) 769–774.

[Nog81] J. O. Noga, Investigations of Titanium and Zirconium Hydrides to Determine Suitability of Recoverable Tritium Immobilisation for the Pickering Tritium Removal System, technical report OH–81-368-K, Ontario Hydro Research Division, Toronto, Canada (1981).

[Nom85] K. Nomura, H. Uruno, S. Ono, H. Shinozuka and S. Suda, Effects of lattice strain on the hysteresis of pressure-composition isotherms for the $LaNi_5-H_2$ system, *Journal of the Less-Common Metals*, 107(2) (1985) 221–230.

[Nor75] C. J. M. Northrup Jr, Uranium-hydrogen system, *The Journal of Physical Chemistry*, 79(7) (1975) 726–731.

[Nuc05] Nuclear Industry Safety Directors Forum, Nuclear Industry Code of Practice on Clearance and Exemption Principles, Processes and Practices, technical report, Reading, United Kingdom (2005).

[Nuf05] Nuf Committee, Radiation and Contamination, Chapter RP-2: Radiation Protection, (2005).

[Num90a] S. Numata, H. Amano and K. Minami, Diffusion of tritiated water in cement materials, *Journal of Nuclear Materials*, 171(2-3) (1990) 373–380.

[Num90b] S. Numata, H. Amano and M. Okamoto, Tritium inventory in Portland cement exposed to tritiated water vapor, *Journal of Nuclear Materials*, 171(2-3) (1990) 350–359.

[Num92] S. Numata, Y. Fujii and M. Okamoto, Evaluation of tritiated water retention capacity of fusion reactor concrete building, *Fusion Technology*, 21(2P2) (1992) 821–826.

[Oga05] Y. Ogata, Y. Sakuma, N. Ohtani and M. Kotaka, Tritium separation by electrolysis using solid polymer electrolyte, *Fusion Science and Technology*, 48(1) (2005) 136–139.

[Oga17] Y. Ogawa, J. Yamabe, H. Matsunaga and S. Matsuoka, Material performance of age-hardened beryllium-copper alloy, CDA-C17200, in a high-pressure, gaseous hydrogen environment, *International Journal of Hydrogen Energy*, 42(26) (2017) 16887–16900.

[Ogo03] O. V. Ogorodnikova, J. Roth and M. Mayer, Deuterium retention in tungsten in dependence of the surface conditions, *Journal of Nuclear Materials*, 313-316 (2003) 469–477.

[Ohi00a] S. O'hira, T. Hayashi, H. Nakamura, K. Kobayashi, T. Tadokoro, H. Nakamura, T. Itoh, T. Yamanishi, Y. Kawamura, Y. Iwai, T. Arita, T. Maruyama, T. Kakuta, S. Konishi, M. Enoeda, M. Yamada, T. Suzuki, M. Nishi, T. Nagashima and M. Ohta, Improvement of tritium accountancy technology for ITER fuel cycle safety enhancement, *Nuclear Fusion*, 40(3Y) (2000) 519–525.

[Ohi00b] S. O'hira, K. Isobe, T. Suzuki, Y. Oya and M. Nishi, Beta induced reaction study on T_2 – CO system, *Fusion Engineering and Design*, 49-50 (2000) 905–914.

[Ohi92] S. O´hira, H. Nakamura, S. Konishi, T. Hayashi, K. Okuno, Y. Naruse, R. H. Sherman, D. J. Taylor, M. A. King, J. R. Bartlit and J. L. Anderson, On-line tritium process gas analysis by laser Raman spectroscopy at TSTA, *Fusion Technology*, 21(2P2) (1992) 465–470.

[Ohi93] S. O'hira, S. Konishi, Y. Naruse, K. Okuno, J. W. Barnes, W. Harbin, J. R. Bartlit and J. L. Anderson, Test of the Cold Traps in the JAERI Fuel Clean-Up System in

the Tritium Systems Test Assembly, technical report JAERI-M93-087, Japan Atomic Energy Research Institute, Tokai-mura, Japan (1993).

[Ohi95] S. O'hira, H. Nakamura, K. Okuno, D. J. Taylor and R. H. Sherman, Beta-decay induced reaction studies of tritium by laser Raman spectroscopy - T_2 – CO system-, *Fusion Technology*, 28(3P2) (1995) 1239–1243.

[Ohi96] S. O´hira and K. Okuno, Development of real-time and remote fuel process gas analysis system using laser Raman spectroscopy, *Fusion Technology*, 30(3P2A) (1996) 869–873.

[Ohi98] S. O´hira, A. Steiner, H. Nakamura, R. Causey, M. Nishi and S. Willms, Tritium retention study of tungsten using various hydrogen isotope irradiation sources, *Journal of Nuclear Materials*, 258-263 (1998) 990–997.

[Ohi99] S. O´hira, T. Suzuki, S. Hode and M. Nishi, Design study of a tritium transport package for future fusion reactors, *Fusion Engineering and Design*, 45(2) (1999) 187–195.

[Oik02] A. Oikawa, N. Miya, K. Kodama, T. Umehara, T. Yamazaki, K. Masaki, I. Akiyama, K. Matsushita and N. Hosogane, Tritium experience in JT-60 DD plasma operation, *Fusion Science and Technology*, 41(3P2) (2002) 612–616.

[Oka04] H. Okabe, K. Munakata, Y. Yokoyama, A. Koga, Y. Narisato, R.-D. Penzhorn and K. Okuno, Modeling of tritium release from ceramic breeder materials by focusing on transport process in breeder grain, *Journal of Nuclear Materials*, 329-333 (2004) 1309–1312.

[Oku09] K. Okuno, S. Suzuki, H. Ishikawa, T. Hayashi, T. Yamanishi and Y. Oya, Temperature dependence of oxide layer formation on hydrogen isotope retention in type 316 stainless steel, *Fusion Science and Technology*, 56(2) (2009) 799–803.

[Oku88] K. Okuno, S. O'hira, H. Yoshida, Y. Naruse, T. Suzuki, S. Hirata and M. Misumi, Experimental apparatus for tritium permeation studies in Tritium Process Laboratory, *Fusion Technology*, 14(2P2A) (1988) 713–718.

[Oku93] K. Okuno, Y. Matuda, S. Konishi, T. Yamanishi, T. Hayashi and Y. Naruse, Research and development on tritium technology at the Tritium Process Laboratory of JAERI, *Proceedings of the 17th Symposium on Fusion Technology (SOFT)*, Sept. 14–18, 1992, Rome, Italy, (1993) 1196–1200.

[Oku95] K. Okuno, Y. Matsuda, M. Ohashi and M. Hode, Development of the packaging for tritium transport, *11th International Conference on the Packaging and Transportation of Radioactive Materials (PATRAM95)*, Dec. 3–8, 1995, Las Vegas, NV, USA, (1995).

[Oku97] K. Okuno, S. Konishi, T. Yamanishi, S. O´hira, M. Enoeda, T. Hayashi, H. Nakamura, Y. Iwai, Y. Kawamura and K. Kobayashi, Tritium technology research and development at the Tritium Process Laboratory of JAERI, *Proceedings of the 19th Symposium on Fusion Technology (SOFT)*, Sept. 16–20, 1996, Lisbon, Portugal, (1997) 1277–1280.

[Ond80] R. S. Ondrejcin and B. D. McLaughlin, Corrosion of High Ni-Cr Alloys and Type 304L Stainless Steel in HNO_3-HF, technical report DP-1550, Savannah River National Laboratory, Aiken, SC, USA (1980).

[Ong08] J. Ongena and G. v. Oost, Energy for future centuries - Prospects for fusion power as a future energy source, *Fusion Science and Technology*, 53(2T) (2008) 3–15.

[Ono92a] F. Ono, S. Tanaka and M. Yamawaki, Sorption and desorption of tritiated water on paints, *Fusion Science and Technology*, 21(2) (1992) 827–832.

[Ono92b] F. Ono, S. Tanaka and M. Yamawaki, Sorption of tritiated water on organic materials and subsequent desorption, *Fusion Technology*, 21(3P2B) (1992) 1964–1967.

[Ono95] F. Ono, M. Yamawaki and S. Tanaka, Regrowth of tritium release from tritium contaminated materials, *Fusion Technology*, 28(3P2) (1995) 1250–1255.

[Ori93] R. A. Oriani, The physical and metallurgical aspects of hydrogen in metals, *Proceedings of the 4th International Conference on Cold Fusion (ICCF4)*, Dec. 6–9, 1993, Maui, HI, USA, (1993) 235–268.

[Ort73] D. A. Orth and W. J. Jacober, Tritium Control Technology, technical report WASA 1269, Mound Laboratory, Miamisburg, OH, USA (1973).

[Ort85] M. S. Ortman, T. J. Warren and D. J. Smith, Use of metal hydrides for handling tritium, *The International Journal of Applied Radiation and Isotopes*, 36(7) (1985) 589.

[Ort90] M. S. Ortman, L. K. Heung, A. Nobile and R. L. Rabun, Tritium processing at the Savannah River Site: Present and future, *Journal of Vacuum Science & Technology A: Vacuum, Surfaces, and Films*, 8(3) (1990) 2881–2889.

[Osl73] J. H. Osloond, J. B. Echo, W. L. Polzer, B. D. Johnson and A. A. Moghissi, A tritium air sampling method for environmental and nuclear plant monitoring, *Tritium*, M. W. Carter and A. A. Moghissi, editors, Messenger Graphics, Phoenix, Arizona, USA, (1973), 531–533.

[Otl92] R. L. Otlet, A. J. Walker and C. J. Caldwell-Nichols, Practical environmental, working area and stack discharge samplers, passive and dynamic, for measurement of tritium as HTO and HT, *Fusion Technology*, 21(2P2) (1992) 550–555.

[Otl98] R. L. Otlet, A. J. Walker, C. J. Caldwell-Nichols, P. Wright, A. E. Gravett, C. D. Collins, K. I. Pearce and D. C. Pryke, Discriminating samplers for the measurement of tritium as HTO, HT and CH_3T from discharge stacks and in environmental air, *Proceedings of the 20th Symposium on Fusion Technology (SOFT)*, Sept. 7–11, 1998, Marseille, France, (1998) 1657–1660.

[Ots08] T. Otsuka and T. Tanabe, Hydrogen release from ferritic/martensitic stainless steel, *Fusion Science and Technology*, 54(2) (2008) 541–544.

[Ots10] T. Otsuka and T. Tanabe, Behaviour of tritium accumulated on materials surface, *Fusion Engineering and Design*, 85(7-9) (2010) 1437–1441.

[Ots11] T. Otsuka, M. Shimada, R. Kolasinski, P. Calderoni, J. P. Sharpe, Y. Ueda, Y. Hatano and T. Tanabe, Application of tritium imaging plate technique to examine tritium behaviour on the surface and in the bulk of plasma-exposed materials, *Journal of Nuclear Materials*, 415(1) (2011) S769–S772.

[Ots16] T. Otsuka, Y. Ogawa, H. Horinouchi and K. Hashizume, Release behaviour of tritium in pure copper and its alloys into pure water at ambient temperature, *Fusion Engineering and Design*, 113 (2016) 227–230.

[Out11] Outokumpu, https://www.outokumpu.com/, (2011), (visited on Apr. 13, 2022).

[Ovc09] A. V. Ovcharov, M. B. Rozenkevich and A. N. Perevezentsev, Simulation of CECE facility for water detritiation, *Fusion Science and Technology*, 56(4) (2009) 1462–1470.

[Owe76] J. H. Owen, Equilibrium and kinetic studies of systems of hydrogen isotopes, lithium hydrides, aluminium, and $LiAlO_2$, *Proceedings of the International Conference on Radiation Effects and Tritium Technology for Fusion Reactors*, Oct. 1–3, 1976, Gatlinburg, TN, USA, (1976) 01–24.

[Oya02] Y. Oya, W. Shu, T. Suzuki, T. Hayashi, S. O´hira, M. Nishi and K. Iinuma, A study of beta-decay induced reaction on T_2O-CO_2 system, *Fusion Science and Technology*, 41(3P2) (2002) 373–377.

[Oya03] Y. Oya, Y. Makide, K. Chiba, S. Tanaka, Y. Morimoto, H. Kodama, K. Okuno, T. Kawano, Y. Asakura and T. Uda, Hydrogen adsorption behavior on stainless steel for cooling pipe in fusion reactor, *Fusion Science and Technology*, 44(2) (2003) 359–363.

[Oya11a] M. Oyaidzu, K. Isobe, T. Hayashi and T. Yamanishi, Effect of tritium and dissolved oxygen on anodic polarization of SUS304 stainless steel in sulfuric acid solution, *Journal of Nuclear Science and Technology*, 48(6) (2011) 880–884.

[Oya11b] M. Oyaidzu, K. Isobe, T. Hayashi and T. Yamanishi, Effects of tritiated water on corrosion behavior of SUS304, *Fusion Science and Technology*, 60 (2011) 1515–1518.

[Oya11c] M. Oyaidzu, K. Isobe, H. Nakamura, T. Hayashi and T. Yamanishi, Permeation behaviour of tritium through F82H steel, *Journal of Nuclear Materials*, 417(1-3) (2011) 1143–1146.

[Oya12] Y. Oya, M. Kobayashi, J. Osuo, M. Suzuki, A. Hamada, K. Matsuoka, Y. Hatano, M. Matsuyama, T. Hayashi, T. Yamanishi and K. Okuno, Effect of surface oxide layer on deuterium permeation behaviours through a type 316 stainless steel, *Fusion Engineering and Design*, 87(5-6) (2012) 580–583.

[Oya14] Y. Oya, Overview of tritium activity in Japan, *Tritium Focus Group Meeting at Idaho National Laboratory, INL*, Sept. 23, 2014, Idaho Falls, ID, USA, (2014).

[Oya15a] Y. Oya, M. Sato, K. Yuyama, M. Hara, Y. Hatano, M. Matsuyama and T. Chikada, Dynamics for HT and HTO recovery through water bubbler and CuO catalyst, *Fusion Science and Technology*, 68(2) (2015) 358–361.

[Oya15b] M. Oyaidzu, K. Isobe and T. Hayashi, Effect of tritium on corrosion behavior of chromium in 0.01 N sulfuric acid solution, *Fusion Science and Technology*, 67(3) (2015) 519–522.

[Pac96] P. Pacenti, R. Edwards and F. Campi, Detritiation of graphite and beryllium plasma-facing-components, *Proceedings of the 19th Symposium on Fusion Technology (SOFT)*, Sept. 16–20, 1996, Lisbon, Portugal, (1996) 1705–1708.

[Pae05] S. Paek, D. H. Ahn, K. R. Kim, H. Chung, S. P. Yim and M. Lee, Performance of 500 kCi tritium storage vessel for WTRF, *Fusion Science and Technology*, 48(1) (2005) 75–78.

[Pam01] J. Paméla, JET under EFDA: Organisation, recent results and prospects, *Fusion Engineering and Design*, 56-57 (2001) 19–28.

[Pam12] R. Pampin, S. Zheng, S. Lilley, B. C. Na, M. J. Loughlin and N. P. Taylor, Activation analyses updating the ITER radioactive waste assessment, *Fusion Engineering and Design*, 87(7-8) (2012) 1230–1234.

[Pam14] J. Paméla, J.-M. Bottereau, D. Canas, C. Decanis, K. Liger and F. Gaune, ITER tritiated waste management by the host state and first lessons learned for fusion development, *Fusion Engineering and Design*, 89(9-10) (2014) 2001–2007.

[Pap11] S. Papastergiou, R. Laesser, G. Piazza, P. Wikus, C. Day, H. Haas, S. Hanke, V. Hauer, J. M. Poncet, A. Antipenkov, M. Dremel, C. Mayaux, R. Pearce and F. Fellin, The european supplied components of the ITER vacuum pumping systems, *Fusion Science and Technology*, 60(3) (2011) 873–876.

[Par12] A. I. Parracho, D. Demange, S. Knipe, L. T. Le, K. H. Simon and S. Welte, Processing highly tritiated water desorbed from molecular sieve bed using PERMCAT, *Fusion Engineering and Design*, 87(7-8) (2012) 1277–1281.

[Par72] J. E. Parks, G. S. Hurst, T. E. Steward and H. L. Weidner, Ionisation of noble gases by protons: Jesse effects as a function of pressure, *Chemical Physics*, 57 (1972) 5467.

[Par82] C. N. Park and J. Y. Lee, A study on the kinetics of hydriding of the $LaNi_5$ system, *Journal of the Less-Common Metals*, 83(1) (1982) 39–48.

[Par97] R. Parker, G. Janeschitz, H. D. Pacher, D. Post, S. Chiocchio, G. Federici and P. Ladd, Plasma-wall interactions in ITER, *Journal of Nuclear Materials*, 241-243 (1997) 1–26.

[Par98] R. R. Parker, Design and issues of the ITER in-vessel components: ITER Joint Central Team and Home Teams, *Fusion Engineering and Design*, 39-40 (1998) 1–16.

[Pat03] B. Patel and W. Parsons, Operational beryllium handling experience at JET, *Fusion Engineering and Design*, 69 (2003) 689–694.

[Pat99] B. Patel, S. Knipe, P. Macheta and A. Peacock, Radiological properties of tritiated dust and flakes from the JET tokamak, *Proceedings of the 18th IEEE/NPSS Symposium on Fusion Engineering*, Oct. 25–29, 1999, Albuquerque, USA, (1999) 338–341.

[Pau88] G. P. Pautrot, The Tritium Extraction Facility at the Institute Laue-Langevin experience of operation with tritium, *Fusion Technology*, 14(2P2A) (1988) 480–483.

[Pea00] A. T. Peacock, P. A. Andrew, D. Brennan, J. P. Coad, H. Hemmerich, S. Knipe, R.-D. Penzhorn and M. Pick, Tritium inventory in the first wall of JET, *Fusion Engineering and Design*, 49-50 (2000) 745–752.

[Pea01] R. J. H. Pearce, S. Bryan, R. Cerruti and N. Green, Vacuum pumping developments on the JET tokamak, *Fusion Engineering and Design*, 58-59 (2001) 359–364.

[Pea18] R. J. Pearson, A. B. Antoniazzi and W. J. Nuttall, Tritium supply and use: a key issue for the development of nuclear fusion energy, *Fusion Engineering and Design*, 136 (2018) 1140–1148.

[Pea91] A. T. Peacock, J. P. Coad, K. J. Dietz, G. Israel, H. S. Jensen, M. A. Pick, G. Saibene and H. Bergsaker, Operational experience with the JET beryllium evaporators, *Proceedings of the 16th Symposium on Fusion Technology (SOFT)*, Sept. 3–7, 1990, London, UK, (1991) 468–472.

[Pea98] A. T. Peacock, P. A. Andrew, J. P. Coad, R. Cuhsack, F. H. Hurd, S. Mills, R.-D. Penzhorn and M. Pick, Deposites/flakes in the JET MkIIa divertor, a major source of tritium and deuterium inventory, *Proceedings of the 20th Symposium on Fusion Technology*, Sept. 7–11, 1998, Marseille, France, (1998) 233–236.

[Pea99a] A. T. Peacock, P. Andrew, P. Cetier, J. P. Coad, G. Federici, F. H. Hurd, M. A. Pick and C. H. Wu, Dust and flakes in the JET MkIIa divertor, analysis and results, *Journal of Nuclear Materials*, 266-269 (1999) 423–428.

[Pea99b] R. Pearce, S. Bryan, T. Budd, M. Gadeberg, T. Hartrampf and J. Hemmerich, The JET tokamak gas handling and introduction system, *Proceedings of the 18th Symposium on Fusion Engineering*, Oct. 25–29, 1999, Albuquerque, USA, (1999) 561–564.

[Pel92] T. Pelletier, P. Giroux and M. Maj, Reprocessing of tritiated organic products, *Fusion Technology*, 21(2P2) (1992) 560–565.

[Pem64] J. P. Pemsler and E. J. Rapperport, Hydrogen in proton-bombarded beryllium: agglomeration and diffusion, *Transactions of the Metall Society AIME*, 230 (1964) 90–94.

[Pen00a] R. D. Penzhorn, U. Berndt, C. Caldwell-Nichols, S. Gruenhagen, E. Kirste, R. Laesser and J. Wendel, Radiochemistry of an equimolar deuterium - tritium mixture or of T_2 with CO, *Fusion Engineering and Design*, 49-50 (2000) 927–937.

[Pen00b] R.-D. Penzhorn, N. Bekris, P. Coad, L. Doerr, M. Friedrich, M. Glugla, A. Haigh, R. Laesser and A. Peacock, Status and research progress at the Tritium Laboratory Karlsruhe, *Fusion Engineering and Design*, 49-50 (2000) 753–767.

[Pen00c] R.-D. Penzhorn, N. Bekris, W. Hellriegel, H.-E. Noppel, W. Naegele, H. Ziegler, R. Rolli, H. Werle, A. Haigh and A. Peacock, Tritium profiles in tiles from the first wall of fusion machines and techniques for their detritiation, *Journal of Nuclear Materials*, 279(2-3) (2000) 139–152.

[Pen01a] R.-D. Penzhorn, CFC and graphite tritiated waste, EFDA report Task TSW-001, European Fusion Development Agreement, (2001).

[Pen01b] R.-D. Penzhorn, Chronic releases of tritium from flakes and tiles at room temperature, *IAEA Advisory Group Meeting on "Assessment of New Data for Tritium Retention in Fusion Reactors Materials"*, July 2–3, 2001, Vienna, Austria, (2001).

[Pen01c] R.-D. Penzhorn, D. Adami, N. Bekris, U. Berndt, U. Besserer, M. Culcer, P. Coad, L. Doerr, W. Hellriegel, E. Kirste, A. Peacock and H. Ziegler, Chronic release of tritium from flakes and tiles at room temperature, EFDA report Task TR4, European Fusion Development Agreement, (2001).

[Pen01d] R.-D. Penzhorn, N. Bekris, U. Berndt, J. P. Coad, H. Ziegler and W. Naegele, Tritium depth profiles in graphite and carbon fibre composite material exposed to tokamak plasmas, *Journal of Nuclear Materials*, 288(2-3) (2001) 170–178.

[Pen01e] R.-D. Penzhorn, J. P. Coad, N. Bekris, L. Doerr, M. Friedrich and W. Pilz, Tritium in plasma facing components, *Fusion Engineering and Design*, 56-57 (2001) 105–116.

[Pen02] R.-D. Penzhorn, Characterization of dust and flakes generated in fusion machines after DD and DT operation, Progress report Task T438, (2002).

[Pen06] R.-D. Penzhorn, Y. Torikai, M. Matsuyama and K. Watanabe, Detritiation of type 316 stainless steel by treatment with liquids at ambient temperature, *Journal of Nuclear Materials*, 353(1-2) (2006) 66–74.

[Pen08] R.-D. Penzhorn, Natural and man-made sources of tritium: applications of tritium, *Tritium Production, Uses and Environmental Impact*, E. Tosti and N. Ghirelli, editors, Nova Science Publishers, (2008), 339–354.

[Pen10] R.-D. Penzhorn, Y. Torikai, S. Naoe, A. Perevezentsev, K. Watanabe and M. Matsuyama, Distribution and mobility of tritium in type 316 stainless steel, *Fusion Science & Technology*, 57 (2010) 185–195.

[Pen11] R.-D. Penzhorn, Y. Torikai, M. Saito, M. Hiro, A. Perevezentsev and M. Matsuyama, Uptake and distribution of tritium in copper, *Fusion Science and Technology*, 60 (2011) 1053–1056.

[Pen12] R.-D. Penzhorn, Y. Torikai, K. Watanabe, M. Matsuyama and A. Perevezentsev, On the fate of tritium in thermally treated stainless steel type 316L, *Journal of Nuclear Materials*, 429(1-3) (2012) 346–352.

[Pen13a] R.-D. Penzhorn, Y. Hatano, M. Matsuyama and Y. Torikai, Tritium interaction with surface layer and bulk of stainless-steel type 316 and consequences of ageing, *Fusion Science & Technology*, 64 (2013) 45–53.

[Pen13b] R.-D. Penzhorn, Natural and man-made sources of tritium: applications of tritium, *Tritium in Fusion: Production, Uses and Environmental Impact*, S. Tosti and N. Ghirelli, editors, Nova Science Publishers, Hauppauge, NY, USA, (2013), 3–22.

[Pen86] R.-D. Penzhorn and H. Brunner, Solidification of tritiated waste, *Proceedings 14^{th} Symposium on Fusion Technology (SOFT*, Sept. 8–12, 1986, Avignon, France, (1986) 1531–1535.

[Pen88] R.-D. Penzhorn, R. Rodriguez, M. Glugla, K. Guenther, H. Yoshida and S. Konishi, A catalytic plasma exhaust purification system, *Fusion Technology*, 14(2P2A) (1988) 450–455.

[Pen90] R.-D. Penzhorn, M. Devillers and M. Sirch, Evaluation of ZrCo and other getters for tritium handling and storage, *Journal of Nuclear Materials*, 170(3) (1990) 217–231.

[Pen91a] R.-D. Penzhorn, J. Anderson, R. Haange, B. Hircq, A. Meikle and Y. Naruse, Technology and component development for a closed tritium cycle, *Fusion Engineering and Design*, 16 (1991) 141–157.

[Pen91b] R.-D. Penzhorn, M. Devillers and M. Sirch, Storage of tritium in ZrCo alloy: Effect of pre-exposure to impurities relevant to the fusion fuel cycle, *Journal of Nuclear Materials*, 179-181 (1991) 863–866.

[Pen91c] R.-D. Penzhorn, M. Devillers, E. Willin and M. Sirch, Evaluation of getters for the interim storage of tritium, *Proceedings of the 16th Symposium on Fusion Technology (SOFT)*, Sept. 3–7, 1990, London, UK, (1991) 694–698.

[Pen91d] R.-D. Penzhorn, M. Glugla, K. Guenther, S. Kuhnmuench, T. Le and K.-H. Simon, Verfahren zur Rueckgewinnung von Tritium aus Verunreinigungen im Fusions-Brennstoffkreislauf, technical report KFK 4844, Institut fuer Radiochemie, Karlsruhe, Germany (1991).

[Pen94] R.-D. Penzhorn, Sweep gas chemistry in a lithium orthosilicate blanket, *Proceedings of the International Workshop on Ceramic Breeder Blanket Interactions*, Sept. 22–24, 1993, Paris, France, (1994) 1037–1040.

[Pen95a] R. D. Penzhorn, U. Berndt, E. Kirste, T. Le and M. Glugla, Tritium technology: performance of oil-free pumps, *Proceedings of the 18th Symposium on Fusion Technology*

(SOFT), Aug. 22–26, 1994, Karlsruhe, Federal Republic of Germany, (1995) 1115–1118.

[Pen95b] R.-D. Penzhorn, U. Berndt, E. Kirste, W. Hellriegel, W. Jung, R. Pejsa and O. Romer, Long-term permeator experiment PETRA at the Tritium Laboratory Karlsruhe: Commissioning tests with tritium, *Fusion Technology*, 28(3P1) (1995) 723–731.

[Pen95c] R.-D. Penzhorn, U. Berndt, E. Kirste, W. Hellriegel, W. Jung, R. Pejsa and O. Romer, Long-term permeator experiment PETRA at the Tritium Laboratory Karlsruhe: Commissioning tests with tritium, *Fusion Science and Technology*, 28 (1995) 723–731.

[Pen97a] R.-D. Penzhorn, U. Berndt, E. Kirste and J. Chabot, Performance of palladium/silver permeators with tritium at the Tritium Laboratory Karlsruhe, *Fusion Technology*, 32 (1997) 232–245.

[Pen97b] R.-D. Penzhorn, D. Murdoch and R. Haange, Recent results on vacuum pumping and fuel clean-up, *Fusion Engineering and Design*, 36(1) (1997) 75–89.

[Pen98] R.-D. Penzhorn, U. Berndt and E. Kirste, Long-term experiment PETRA: Qualification of components for tritium installations, EFDA report Task 332b, European Fusion Development Agreement, (1998).

[Per02a] A. Perevezentsev, A. Bell, B. M. Andreev, E. P. Magomedbekov, Y. S. Pak, M. B. Rozenkevich and Y. A. Sakharovskii, Measurement of pressure drop and HETP in columns packed with different hydrophobic catalysts for tritium isotopic exchange between water and hydrogen, *Fusion Science and Technology*, 41(3P2) (2002) 1102–1106.

[Per02b] A. Perevezentsev, K. Watanabe, M. Matsuyama and Y. Torikai, Contamination of stainless-steel type 316 by tritium, *Fusion Science and Technology*, 41 (2002) 746–750.

[Per02c] A. Perevezentsev, A. Bell, P. Brennan and J. Hemmerich, Development of a water detritiation facility for JET, *Fusion Engineering and Design*, 61 (2002) 585–589.

[Per08] A. N. Perevezentsev and A. C. Bell, Development of water detritiation facility for JET, *Fusion Science and Technology*, 53 (2008) 816–829.

[Per09] A. N. Perevezentsev, A. C. Bell, B. M. Andreev, M. B. Rozenkevich, Y. S. Pak and A. V. Ovcharov, Wet scrubber column for air detritiation, *Fusion Science and Technology*, 56(4) (2009) 1455–1461.

[Per17] A. N. Perevezentsev, L. A. Bernstein, L. A. Rivkis, I. G. Prykina, V. V. Aleksandrov, I. A. Ionessian, M. I. Belyakov and I. B. Kuprianov, Study of outgassing and removal of tritium from metallic construction materials of ITER vacuum vessel components, *Fusion Science and Technology*, 72(1) (2017) 1–16.

[Per66] A. Persky and F. S. Klein, Kinetic isotope effects in the reaction between atomic chlorine and hydrogen, *Chemical Physics*, 44 (1966) 3617.

[Per72] W. G. Perkins and D. R. Begeal, Permeation and Diffusion of Hydrogen in Ceramvar, Copper, and Ceramvar-Copper Laminates, technical report SC-DC-714493, Sandia National Laboratories, Albuquerque, NM, USA (1972).

[Per92] A. Perujo, S. Alberici, J. Camposilvan and F. Reiter, Hydrogen in the martensitic steel MANET: Diffusivity and solubility measurements, *Fusion Technology*, 21(2P2) (1992) 800–805.

[Per93a] D. Perinic, A. Mack, H. Illbruck, G. Class, D. Roehrig and D. Murdoch, Experiments on co-pumping of simulated plasma exhaust gases in a two stage cryo-pump, *Proceedings of the 17th Symposium on Fusion Technology (SOFT)*, Sept. 14–18, 1992, Rome, Italy, (1993) 334–338.

[Per93b] D. Perinic, U. Mirchhof and B. Kammerer, Testing of dry mechanical vacuum pumps for ITER, *Proceedings of the 15th Symposium on Fusion Engineering (SOFE)*, Oct. 11–15, 1993, Hyannis, MA, USA, (1993) 610–613.

[Per95a] A. N. Perevezentsev, C. Bell, R. Laesser and L. A. Rivkis, Safety aspects of tritium storage in metal hydride form, *Fusion Technology*, 28(3P2) (1995) 1404–1409.

[Per95b] A. N. Perevezentsev and R.-D. Penzhorn, Pyrophoricity of tritium storage materials, *Proceedings of the 18th Symposium on Fusion Technology (SOFT)*, Aug. 22–26, 1994, Karlsruhe, Federal Republic of Germany, (1995) 1111–1114.

[Per98] E. Perry, J. Chrzanowski, K. Rule, R. Strykowsky, M. Viola and M. Williams, Decontamination and decommissioning Tokamak Fusion Test Reactor, pamphlet of the Princeton Plasma Physics Laboratory, PO Box 451, Princeton, N.J. 08543, (1998).

[Pet08] S. R. Peterson and W. Raskob, Hystorical doses to the public from routine and accidental releases of tritium, *Fusion Science and Technology*, 54 (2008) 277–280.

[Pey78] M. Peyrat, Comportement de l'eau a forte teneur en tritium dans un system fermé, Application au Stockage CEA-R-4948, CEA, Centre d'Études de Bruyère-le-Châtel, (1978).

[Pfe82] J.-P. Pfeifer, Betriebserfahrungen mit Panametric-Feuchtefuehlern, technical report KfA-IRW-IB-12/82, Kernforschungszentrum Karlsruhe, Karlsruhe, Germany (1982).

[Phi07] V. Philipps, G. Sergienko, A. Lyssoivan, H. G. Esser, M. Freisinger, A. Kreter and U. Samm, Removal of carbon layers by oxygen glow discharges in TEXTOR, *Journal of Nuclear Materials*, 363-365 (2007) 929–932.

[Phi10] V. Philipps, P. Mertens, G. F. Matthews and H. Maier, Overview of the JET ITER-like Wall Project, *Fusion Engineering and Design*, 85(7-9) (2010) 1581–1586.

[Phi82] J. E. Phillips and C. E. Easterly, Experimental Procedure for Examining the Kinetics of Tritium Gas Conversion to Tritiated Water, technical report ORNL/TM-7670, Oak Ridge National Laboratory, Oak Ridge, TN, USA (1982).

[Phi99] V. Philipps, H. G. Esser, J. Seggern, H. Reimer, M. Freisinger, E. Vietzke and P. Wienhold, Removal of redeposited layers and hydrogen release by oxygen ventilation of TEXTOR-94, *Journal of Nuclear Materials*, 266-269 (1999) 386–391.

[Pia02] H. Pialot, D. Demange, B. Ravat and M. Grivet, Tritium activity determination in a wastes drum by helium-3 ingrowth method, *Fusion Science and Technology*, 41(3P2) (2002) 495–499.

[Pia07] G. Piazza, G. F. Matthews, J. Pamela, H. Altmann, J. P. Coad, T. Hirai, A. Lioure, H. Maier, P. Mertens, V. Philipps, V. Riccardo, M. Rubel and E. Villedieu, R&D on tungsten plasma facing components for the JET ITER-like wall project, *Journal of Nuclear Materials*, 367-370 (2007) 1438–1443.

[Pic84] M. A. Pick, The role of metal-hydrogen systems in fusion research, *Journal of the Less-Common Metals*, 103(1) (1984) 5–17.

[Pic86] R. E. Pico, Titanium sublimation pumping systems and performances on the Tandem Mirror Experiment-Upgrade (TMX-U), *Proceedings of the 11th Symposium on Engineering Problems in Fusion Research*, Nov. 18–22, 1985, Austin, TX, USA, (1986) 852–855.

[Pin05] T. Pinna, G. Cambi, S. Ciattaglia, A. L. Bue, S. Knipe, J. Orchard, R. Pearce and U. Besserer, Collection and analysis of data related to fusion machines (JET) and

TLK operating experience on component failure, *Fusion Engineering and Design*, 75-79 (2005) 1199–1203.

[Pin10] G. Pintsuk, J. Blumm, W. Hohenauer, R. C. Hula, T. Koppitz, S. Lindig, D. Pitzer, M. Rohde, P. Schoderboeck, T. Schubert, F. Tietz and O. Wouters, Interlaboratory test on thermophysical properties of the ITER grade heat sink material copper-chromium-zirconium, *International Journal of Thermophysics*, 31(11-12) (2010) 2147–2158.

[Pio91] T. C. Piotrowski, Specification of flame arresting devices for manifolded low-pressure storage tanks, *Plant/Operations Progress*, 10(2) (1991) 102–106.

[Pis95] A. A. Pisarev, A. V. Varava and S. K. Zhdanov, Ion implantation of deuterium in tungsten, *Journal of Nuclear Materials*, 220-222 (1995) 926–929.

[Pit11] R. A. Pitts, Edge physics and plasma-wall interactions, *Nuclear Fusion Engineering Masters*, Jan. 24, 2011, Torino, Italy, (2011).

[Pol05] C. Poletiko, P. Trabuc, J. Durand, B. Tormos and L. Pignoly, Dedicated procedures for the detritiation of steel and graphite, *Fusion Science and Technology*, 48(1) (2005) 194–199.

[Pon86] A. E. Pontau and D. H. Morse, Outgassing of AXF-5Q and other grades of limiter graphites, *Journal of Nuclear Materials*, 141-143 (1986) 124–130.

[Poo00] M. Poon, J. W. Davis and A. A. Haasz, Effect of carbon pre-implantation on deuterium retention in tungsten, *Journal of Nuclear Materials*, 283-287 (2000) 1062–1067.

[Poo03] M. Poon, A. A. Haasz, J. W. Davis and R. G. Macaulay-Newcombe, Impurity effects and temperature dependence of D retention in single crystal tungsten, *Journal of Nuclear Materials*, 313-316 (2003) 199–203.

[Poo05] A. S. Poore and W. D. Jacobs, New systems for waste processing of tritium-containing gases at the Savannah River Site, *Fusion Science and Technology*, 48(1) (2005) 298–301.

[Poo08] A. S. Poore and R. L. Rabun, Comments and suggestions on early version of Tritium Manual for ITER, Savannah River National Laboratory, Aiken, SC, USA (2008).

[Pow70] G. W. Powell, J. D. Braun, K. F. Chaney and G. L. Downs, Solubility and distribution of tritium in annealed and cold worked 304 stainless steel in the 100 to 300 °C temperature range, *Corrosion*, 26(8) (1970) 323–328.

[Pow91] G. L. Powell, W. L. Harper and J. R. Kirkpatrick, The kinetics of the hydriding of uranium metal, *Journal of the Less-Common Metals*, 172-174 (1991) 116–123.

[Pra61] T. H. Pratt and R. Wolfgang, The self-induced exchange of tritium gas with methane, *Journal of the American Chemical Society*, 83(1) (1961) 10–17.

[Pri13] F. Priester and B. Bornschein, TriToP - a compatibility experiment with turbomolecular pumps under tritium atmosphere, *Vacuum*, 98 (2013) 22–28.

[Pri15] F. Priester and M.Roellig, Post service examination of TMP after stress testing with kg scale tritium throughput, *Fusion Science and Technology*, 67 (2015) 539–542.

[Pri95] G. P. J. Price and T. Aslett, Performance of a VG 30-38 mass spectrometer during initial testing, *Fusion Technology*, 28(3P2) (1995) 1061–1066.

[Pyp78] J. W. Pyper and C. K. Briggs, Kinetics of the Radiation Induced Exchange Reactions of H_2, D_2 and T_2, technical report UCRL-52380, Lawrence Livermore Laboratory, Livermore, CA, USA (1978).

[Qui08] M. J. Quinlan, W. T. Shmayda, S. Lim, S. Salnikov, Z. Chambers, E. Pollock and W. U. Schroeder, Effects of H_2O and H_2O_2 on thermal desorption of tritium from stainless steel, *Fusion Science and Technology*, 54(2) (2008) 519–522.

[Qur91] M. Qureshi and K. G. Varshney, Inorganic ion exchangers in chemical analysis, CRC Press Inc., Boca Raton, FL, USA (1991).

[Raf06] A. R. Raffray, J. Blanchard, A. E. Robson, D. V. Rose, M. Sawan, J. Sethian, L. Snead, I. Sviatoslavsky and the HAPL Team, Impact of magnetic diversion on laser IFE reactor design and performance, *Journal de Physique IV (Proceedings)*, 133 (2006) 845–848.

[Raf11] A. Raffray and M. Merola, Design of the ITER first wall and blanket, *Proceedings of the 24th Symposium on Fusion Engineering (SOFE)*, June 26–30, 2011, Chicago, IL, USA, (2011) 1–6.

[Raf14] A. R. Raffray, B. Calcagno, P. Chappuis, Z. Fu, A. Furmanek, C. Jiming, D.-H. Kim, S. Khomiakov, A. Labusov, A. Martin, M. Merola, R. Mitteau, S. Sadakov, M. Ulrickson and F. Zacchia, The ITER blanket system design challenge, *Nuclear Fusion*, 54(3) (2014) 033004.

[Raf17] A. Raffray and R. Eaton, Overview of beryllium applications in ITER and role of IBMC, *Workshop on Beryllium Applications and Health & Safety Aspects for ITER*, June 28, 2017, (2017).

[Raf97] A. R. Raffray, G. Federici, V. Barabash, H. D. Pacher, H. W. Bartels, A. Cardella, R. Jakeman, K. Ioki, G. Janeschitz, R. Parker, R. Tivey and C. H. Wu, Beryllium application in ITER plasma facing components, *Fusion Engineering and Design*, 37(2) (1997) 261–286.

[Rah87] A. Rahier, R. Cornelissen and A. Bruggeman, Development of an electrolysis cell for the recovery of tritium from its oxides, *Proceedings of the 20th Symposium on Fusion Technology (SOFT)*, Sept. 7–11, 1986, Avignon, France, (1987) 1519–1522.

[Ras15] W. Rash, Lockheed Martin Claims Sustainable Fusion Is Within Its Grasp, www.eweek.com/news/lockheed-martin-claims-sustainable-fusion-is-within-its-grasp/, (2015), (visited on Apr. 13, 2022).

[Rav02] B. Ravat, D. Demange, H. Pialot and M. Grivet, Model and simulation of gaseous helium-3 exchanges with the atmosphere from a tritiated waste drum, *Nuclear Engineering and Design*, 216(1-3) (2002) 153–164.

[Ree65] L. V. C. Rees and C. J. Williams, Neutron irradiation of Linde molecular sieve 13X, *Transactions of the Faraday Society*, 61 (1965) 1481–1491.

[Rei79] J. J. Reilly, Metal hydride technology, *Zeitschrift fuer Physikalische Chemie*, 117 (1979) 155–184.

[Rei85] F. Reiter, J. Camposilvan, M. Caorlin, G. Saibene and R. Sartori, Interaction of hydrogen isotopes with stainless steel 316L, *Fusion Science and Technology*, 8(2) (1985) 2344–2351.

[Rei93a] F. Reiter, S. Alberici, J. Camposilvan, E. Serra, K. S. Forcey and A. Perujo, Diffusivity and solubility of hydrogen isotopes in the martensitic steel DIN 1.4914 (MANET) after thermal exposure at 900 K, *Zeitschrift fuer Physikalische Chemie*, 181(1-2) (1993) 151–157.

[Rei93b] F. Reiter, K. S. Forcey and G. Gervasini, A Compilation of Tritium Material Interaction Parameters in Fusion Reactor Materials, EN JRC-report EUR 15217, Commission of the European Communities, Joint Research Centre, Ispra, Italy (1993).

[Rei94] T. C. Reitz, P. A. Smuda and M. A. Benapfl, Design, operation, and application of the LLNL portable tritium processing system, *Fusion Technology*, 26(3P2) (1994) 998–1002.

[Ren94] C. Renschler, J. Gill, R. Walko, C. Ashley, T. Shepodd, S. Reed, G. Malone, L. Leonard, R. Ellefson and R. Clough, Solid state radioluminescent lighting, *Radiation Physics and Chemistry*, 44(6) (1994) 629–644.

[Res87] A. Resnik, M. Stioui, A. Grayevsky and D. Shaltiel, Thermal desorption spectra of hydrogen from $LaNi_5$, *Journal of the Less-Common Metals*, 131(1-2) (1987) 117–124.

[Rev73] G. Reversat and C. L. Clainche, Analyse de l'eau tritiée, Bulletin d'Informations Scientifique et Techniques 178, Centre d'Études Nucléaires de Saclay, Saclay, France (1973).

[Rhi73] T. B. Rhinehammer and P. H. Lamberger, Tritium Control Technology, technical report WASH-1269, Monsanto Research Corporation, Miamisburg, OH, USA (1973).

[Rib97] F. H. Ribeiro, A. E. Schach von Wittenau, C. H. Bartholomew and G. A. Samorjai, Reproducibility of turnover rates in heterogeneous metal catalysis: Compilation of data and guidelines for data analysis, *Catalysis Reviews*, 39(1-2) (1997) 49–76.

[Ric11] I. Ricapito, A. Ciampichetti, R. Laesser, Y. Poitevin and M. Utili, Tritium extraction from liquid Pb-16Li: A critical review of candidate technologies for ITER and DEMO applications, *Fusion Science and Technology*, 60(3) (2011) 1159–1162.

[Rie86] M. P. Riehm, W. W. Smeltzer and D. A. Thompson, Hydrogen-solid interactions and tritium permeation barriers, CFTP report G-86041, McMaster Institute for Energy Studies, Canadian Fusion Fuels Technology Program, Hamilton, Canada (1986).

[Rim96] Rimer Alco Northamerica, Respirable Air Handbook, AB44-COMM-60-A1, Manitoba, Canada (1996).

[Rit81] A. G. Ritchie, A review of the rates of reaction of uranium with oxygen and water vapour at temperatures up to 300 °C, *Journal of Nuclear Materials*, 102(1-2) (1981) 170–182.

[Rit84] A. G. Ritchie, The kinetics of the initial stages of the reaction of uranium with oxygen, *Journal of the Less-Common Metals*, 98(2) (1984) 193–214.

[Rit86a] A. G. Ritchie, R. C. Greenwood, S. J. Randles, D. R. Netherton and J. P. Whitehorn, Measurements of the rate of the uranium-water vapour reaction, *Journal of Nuclear Materials*, 140(3) (1986) 197–201.

[Rit86b] A. Ritchie, R. Greenwood and S. Randles, The kinetics of the uranium-oxygen-water vapour reaction between 40 and 100 °C, *Journal of Nuclear Materials*, 139(2) (1986) 121–136.

[Riz96] C. Rizzello, T. Pinna and M. T. Porfiri, Ozone hazard in the ITER cryostat, *Proceedings of the 16th Symposium on Fusion Engineering (SOFE)*, Sept. 30–Oct. 5, 1995, Champaign, IL, USA, (1996) 357–360.

[Rob30] E. J. Roberts, The ionisation constant of water at 25 °C from the electromotive force of cells without liquid junction, *Journal of the American Chemical Society*, 52(10) (1930) 3877–3881.

[Rob60] M. T. Robinson, A. L. Southern and W. R. Willis, Diffusion of deuterium in deuteron-irradiated copper, *Journal of Applied Physics*, 31(8) (1960) 1474–1482.

[Rob73] W. M. Robertson, Hydrogen permeation, diffusion and solubility in nickel, *Zeitschrift fuer Metallkunde*, 64 (1973) 436–443.

[Rob79] R. M. Roberts, T. S. Elleman, H. Palmour and K. Verghese, Hydrogen permeability of sintered aluminium oxide, *Journal of the American Ceramic Society*, 62(9-10) (1979) 495–499.

[Rob84] J. R. Robins, F. E. Bartoszek and K. B. Woodall, A Review of Tritium Conversion Reactions, technical report CFFPT-F84027, Canadian Fusion Fuels Technology Project, Ontario, Canada (1984).

[Rob90] S. L. Robinson, The effects of tritium in the flow and fracture of austenitic stainless steels, hydrogen effects on material behavior, *International Conference on the Effect of Hydrogen on the Behavior of Materials*, Sept. 12–16, 1989, Jackson Hole, WY , USA, (1990) 433–446.

[Rob94] J. R. Robins, K. B. Woodall, G. Woo, D. G. Bellamy, S. K. Sood, C. Fong, D. T. Lee, M. R. Tanaka, K. M. Kalyanam, M. Hare, A. Busigin, F. Adamek and O. K. Kveton, Tritium purification system for TFTR, *Proceedings of the 15th Symposium on Fusion Engineering (SOFE)*, Oct. 11–15, 1993, Hyannis, MA, USA, (1994) 69–72.

[Rod11] L. Rodrigo, O. El-Behairy, H. Boniface, C. Hotrum and K. McCrimmon, Tritium emissions from a detritiation facility, *Fusion Science and Technology*, 60(4) (2011) 1268–1271.

[Rod13] L. Rodrigo, H. Boniface and S. Suppiah, Overview of tritium activities at AECL - past and present, *Fusion Science and Technology*, 64(2) (2013) 333–339.

[Rod71] A. M. Rodin and V. V. Surenyants, Solid solutions of helium in titanium containing up to 30 at.% of helium, *Russian Journal Physical Chemistry*, 45 (1971) 612–614.

[Rod81] J. W. Roddy, Survey: Utilization of Zeolites for the Removal of Radioactivity from Liquid Waste Streams, technical report, Oak Ridge National Laboratory, Oak Ridge, TN, USA (1981).

[Rod92] L. Rodrigo, J. M. Miller, S. R. Bokwa, R. E. Johnson, B. M. MacDonald and J. Senchrabek, Tritium measurement and monitoring in experimental and process systems with ionization chambers, *Fusion Science and Technology*, 21 (1992) 629–635.

[Rod95a] L. Rodrigo, Effect of impurities on the measurement of tritium in inert gases with ionization chambers. Jesse effect revisited, *Fusion Technology*, 28 (1995) 1067–1072.

[Rod95b] L. Rodrigo, M. J. Ivanco, J. W. Goodale, J. A. Senohrabek, L. K. Jones and L. M. Phillipi, Measurement of tritium on surfaces, *Fusion Technology*, 28(3P1) (1995) 940–945.

[Roe13] M. Roellig, F. Priester, M. Babutzka, J. Bonn, B. Bornschein, G. Drexlin, S. Ebenhoech, E. W. Otten, M. Steidl and M. Sturm, Activity monitoring of a gaseous tritium source by beta induced X-ray spectrometry, *Fusion Engineering and Design*, 88(6-8) (2013) 1263–1266.

[Roe79] H. D. Roehrig, V. Malka, K. D. Fischmann and R. Raitz von Frentz, Studies on hydrogen isotopes behaviour in advanced nuclear systems, *Proceedings of the 10th Symposium on Fusion Technology (SOFT)*, Sept. 4–9, 1978, Padua, Italy, (1979) 685–690.

[Rog72] C. E. Rogers, M. Fels and N. Li, Separation by permeation through polymer membranes, *Recent Developments in Separation Science*, N. N. Li, editor, CRC Press, (1972), 107–155.

[Rol99] A. C. Rolfe, P. Brown, P. Carter, R. Cusack, A. Gaberscik, L. Galbiati, B. Haist, R. Horn, M. Irving, D. Locke, A. Loving, P. Martin, S. Mills, R. Minchin, J. Palmer, S. Sanders, S. G. Sanders and R. Stokes, A report on the first remote handling operations at JET, *Fusion Engineering and Design*, 46(2-4) (1999) 299–306.

[Rom09] F. Romanelli, J. Pamela, R. Kamendje, M. L. Watkins, S. Brezinsek, Y. Liang, X. Litaudon, T. Loarer, D. Moreau, D. Mazon, G. Saibene, F. Sartori and P. C. de Vries, Recent contribution of JET to the ITER physics, *Fusion Engineering and Design*, 84(2-6) (2009) 150–160.

[Roo13] G. J. van Rooij, J. W. Coenen, L. Aho-Mantila, S. Brezinsek, M. Clever, R. Dux, M. Groth, K. Krieger, S. Marsen, G. F. Matthews, A. Meigs, R. Neu, S. Potzel, T. Puetterich, J. Rapp and M. F. Stamp, Tungsten divertor erosion in all metal devices: Lessons from the ITER like wall of JET, *Journal of Nuclear Materials*, 438 (2013) S42–S47.

[Roo65] J. W. Root, W. Breckenridge and F. S. Rowland, Abstraction of hydrogen atoms by energetic recoil tritium atoms: Correlation with C−H bond-dissociation energies in hydrocarbons, *The Journal of Chemical Physics*, 43(10) (1965) 3694–3704.

[Ros00a] S. Rosanvallon and J. L. Courouau, Modelling of a steel detritiation process. Influence of experimental parameters, Association Euratom/CEA report HO-620-5010, Laboratoire de Physico-chimie et Procedes, Direction de Reacteurs Nucléaires, Cadarache, France (2000).

[Ros00b] S. Rosanvallon, G. Marbach, A. M. Brass, J.Chêne and J. P. Daclin, Steel detritiation, optimization of a process, *Fusion Engineering and Design*, 51-52 (2000) 605–609.

[Ros02] S. Rosanvallon, J. L. Courouau, G. Marbach and W. Gulden, Steel detritiation by melting with gas bubbling, *Fusion Science and Technology*, 41(3P2) (2002) 695–699.

[Ros03] S. Rosanvallon, S. Nordlinder, L. Fayette and G. Brunel, Waste management within the framework of ITER in Cadarache, *Fusion Engineering and Design*, 69(1-4) (2003) 531–536.

[Ros10] S. Rosanvallon, B. C. Na, M. Benchikhoune, J. E. Uzan, O. Gastaldi, N. Taylor and L. Rodriguez, ITER waste management, *Fusion Engineering and Design*, 85(10-12) (2010) 1788–1791.

[Ros77] J. Rostrup-Nielsen and D. L. Trimm, Mechanisms of carbon formation on nickel-containing catalysts, *Journal of Catalysis*, 48(1-3) (1977) 155–165.

[Ros99] S. Rosanvallon and F. Devitt, Steel detritiation modelling – Adaptation of a model used for dehydrogenation, Association Euratom/CEA report 99/087, Laboratoire de Physico-chimie et Procedes, Direction de Reacteurs Nucleaires, Cadarache, France (1999).

[Rot08] J. Roth, E. Tsitrone, T. Loarer, V. Philipps, S. Brezinsek, A. Loarte, G. F. Counsell, R. P. Doerner, K. Schmid, O. V. Ogorodnikova and R. A. Causey, Tritium inventory in ITER plasma-facing materials and tritium removal procedures, *Plasma Physics and Controlled Fusion*, 50(10) (2008) 103001.

[Rot11] J. Roth and K. Schmid, Hydrogen in tungsten as plasma-facing material, *Physica Scripta*, T145 (2011) 014031.

[Rot80] J. Roth, B. M. U. Scherzer, R. S. Blewer, D. K. Brice, S. T. Picraux and W. R. Wampler, Trapping, detrapping and replacement of keV hydrogen implanted into graphite, *Journal of Nuclear Materials*, 93-94 (1980) 601–607.

[Rou91] N. Roussakis and K. Lapp, A comprehensive test method for inline flame arresters, *Plant/Operations Progress*, 10(2) (1991) 85–92.

[Rou92] N. Roux, J. J. Abassin, M. Briec, D. Cruz, T. Flament and I. Schuster, Compatibility behaviour of beryllium with $LiAlO_2$ and Li_2ZrO_3 ceramics, with 316L and 1.4914 steels in SIBELIUS, *Journal of Nuclear Materials*, 191-194 (1992) 168–172.

[Roy67] S. K. Roy and R. L. Coble, Solubility of hydrogen in porous polycrystalline aluminium oxide, *Journal of the American Ceramic Society*, 50(8) (1967) 435–436.

[Rub03] M. Rubel, J. P. Coad, N. Bekris, S. K. Erents, D. Hole, G. F. Matthews and R.-D. Penzhorn, Beryllium and carbon films in JET following D-T operation, *Journal of Nuclear Materials*, 313-316 (2003) 321–326.

[Rub10] M. Rubel, Structure materials in fusion reactors: Issues related to tritium radioactivity and radiation-induced effects, *Fusion Science and Technology*, 57(2T) (2010) 474–482.

[Rud61] D. W. Rudd, D. W. Vose and S. Johnson, The permeability of copper to hydrogen, *The Journal of Physical Chemistry*, 65(6) (1961) 1018–1020.

[Rud77] C. R. Rudy and K. C. Jordan, Tritium half-life, technical report MLM-2458 UC-4, Mound Laboratory, Miamisburg, OH, USA (1977).

[Rud83] P. S. Rudman, Hydriding and dehydriding kinetics, *Journal of the Less-Common Metals*, 89(1) (1983) 93–110.

[Rum13] T. Rummel, Progress towards Wendelstein 7-X, *Fusion Science and Technology*, 64(3) (2013) 387–396.

[Rup15] S. Rupp, T. M. James, H. H. Telle, M. Schloesser and B. Bornschein, Enhanced sensitivity of Raman spectroscopy for tritium gas analysis using a metal-lined hollow glass fiber, *Fusion Science and Technology*, 67(3) (2015) 547–550.

[Rus92] R. Russ, A. Haigh and S. Booth, Beryllium safety at JET (Code of Practice for the Safe Use of Beryllium at the JET Laboratory), *Proceedings of the 14th IEEE Symposium on Fusion Engineering*, Sept. 30–Oct. 3, 1992, San Diego, Ca, USA, (1992) 596–599.

[Rut88] W. M. Rutherford, R. E. Ellis and G. C. Abell, Supported Palladium Materials for Isotope Separation, technical report MLM-3596 UC701, Mound Laboratory, Miamisburg, OH, USA (1988).

[Rut89] W. M. Rutherford, An Efficient Palladium Isotope Chromatograph (EPIC) for Hydrogen, technical report MLM-3469 UC22, Mound Laboratory, Miamisburg, OH, USA (1989).

[Rya64] L. N. Ryabchikov, Mass spectrometric investigation of degasation of molybdenum, tungsten and niobium on heating them in a vacuum, *Ukrainian Journal of Physics*, 9 (1964) 293–302.

[Ryl16] D. Ryland, Tritium activities at Chalk River Laboratories, *37th Tritium Focus Group Meeting*, Oct. 27, 2016, Rochester, NY, USA, (2016).

[Sab01] F. Sabathier, D. Brennan, N. Skinner and B. Patel, Assessment of the performance of the JET exhaust detritiation system, *Fusion Engineering and Design*, 54(3-4) (2001) 547–553.

[Sae84] M. Saeki and T. Hirabayashi, Sorption mechanisms of tritium on the surface of borosilicate glass, *Radiochimica Acta*, 35(4) (1984) 233–238.

[Sae92] M. Saeki, T. Hirabayashi, Y. Aratono, M. Nakashima, N. M. Masaki and E. Tachikawa, Chemical behavior of tritium in/on various materials, *Fusion Technology*, 21(2P2) (1992) 806–811.

[Sag95] H. Sagawa, H. Kawamura, Y. Ikejima, N. Imaizumi, R. Oyamada and K. Miura, Design study of sweep gas system for fusion blanket development in the JMTR, *Fusion Technology*, 28(3P1) (1995) 732–735.

[Sai11a] M. Saito, Y. Torikai, R.-D. Penzhorn, K. Akaishi and M. Matsuyama, On the fate of tritium in nickel, *Fusion Science and Technology*, 60 (2011) 1459–1462.

[Sai11b] M. Saito, Y. Torikai, A. Taguchi, R.-D. Penzhorn, K. Tatenuma, K. Isobe, H. Nakamura, T. Hayashi and T. Yamanishi, Tritium uptake and release behaviour of F82H, technical report ICFRM-15, Charleston, SC, USA (2011).

[Sal08] J.-F. Salavy, G. Aiello, O. David, F. Gabriel, L. Giancarli, C. Girard, N. Jonquères, G. Laffont, S. Madeleine, Y. Poitevin, G. Rampal, I. Ricapito and K. Splichal, The HCLL Test Blanket Module System: Present reference design, system integration in ITER and R&D needs, *Fusion Engineering and Design*, 83(7-9) (2008) 1157–1162.

[Sal12] R. Salter, J. Chu and M. Hippler, Cavity-enhanced Raman spectroscopy with optical feedback cw diode lasers for gas phase analysis and spectroscopy, *The Analyst*, 137(20) (2012) 4669–4676.

[Sal13] M. N. Salloum and P. E. Gharagozloo, Empirical and Physics Based Mathematical Models of Uranium Hydride Decomposition Kinetics with Quantified Uncertainties, technical report SAND2013-8540, Sandia National Laboratories, Livermore, CA, USA (2013).

[Sam99] U. Samm, Energieabfuhr in Fusionsplasmen durch Linienstrahlung von Verunreinigungen, Berichte des Forschungszentrum Juelich report Juel-3651, Forschungszentrum Juelich - Institut fuer Plasmaphysik, (1999).

[San04] N. S. Sangaj and V. C. Malshe, Permeability of polymers in protective organic coatings, *Progress in Organic Coatings*, 50(1) (2004) 28–39.

[San12] A. Santucci, D. Demange, O. Goerke, T. L. Le, P. Pfeifer and S. Welte, Inactive commissioning of a micro channel catalytic reactor for highly tritiated water pro-

duction in the CAPER facility of TLK, *Fusion Engineering and Design*, 87(5-6) (2012) 547–550.

[San80] G. D. Sandrock and P. D. Goodell, Surface poisoning of $LaNi_5$, FeTi and $(Fe, Mn)Ti$ by O_2, CO and H_2O, *Journal of the Less-Common Metals*, 73(1) (1980) 161–168.

[San84] G. D. Sandrock and P. D. Goodell, Cyclic life of metal hydrides with impure hydrogen: Overview and engineering considerations, *Journal of the Less-Common Metals*, 104(1) (1984) 159–173.

[Sao09] B. Saoutic, M. Chatelier and C. D. Michelis, Tore Supra: Toward steady state in a superconducting tokamak, *Fusion Science and Technology*, 56(3) (2009) 1079–1091.

[Sar90] R. Sartori, G. Saibene, D. H. J. Goodall, E. Usselmann, P. Coad and D. Holland, Deuterium release measurements in the Be phase of JET and determination of tritium content in the exhaust gas, *Journal of Nuclear Materials*, 176-177 (1990) 624–629.

[Sar96] D. A. Sarigiannis and F. Andritsos, Short term dynamics of the reaction between beryllium and steam on the PFCs coating of ITER, *Fusion Engineering and Design*, 31(4) (1996) 267–277.

[Sat03] S. Sato and T. Nishitani, Impact of armor materials on tritium breeding ratio in the fusion reactor blanket, *Journal of Nuclear Materials*, 313-316 (2003) 690–695.

[Saw06] M. E. Sawan and M. A. Abdou, Physics and technology conditions for attaining tritium self-sufficiency for the DT fuel cycle, *Fusion Engineering and Design*, 81(8-14) (2006) 1131–1144.

[Saw14] M. E. Sawan, Transmutation of tungsten in fusion and fission nuclear environments, *Fusion Science and Technology*, 66(1) (2014) 272–277.

[Saz08] A. B. Sazonov, G. V. Veretennikova and E. P. Magomedbekov, Interaction of tritium with oils and tritiated waste oil decontamination, *Fusion Science and Technology*, 54 (2008) 584–587.

[Sca00] F. Scaffidi-Argentina, G. R. Longhurst, V. Shestakov and H. Kawamura, The status of beryllium technology for fusion, *Journal of Nuclear Materials*, 283-287 (2000) 43–51.

[Sch00] F. Schliefer, C. Liu and P. Jung, Diffusion and permeation of hydrogen in low-activation martensitic stainless steel - effect of irradiation, *Journal of Nuclear Materials*, 283-287 (2000) 540–544.

[Sch03] B. van der Schaaf, F. Tavassoli, C. Fazio, E. Rigal, E. Diegele, R. Lindau and G. LeMarois, The development of EUROFER reduced activation steel, *Fusion Engineering and Design*, 69(1-4) (2003) 197–203.

[Sch05] B. Schweer, A. Huber, G. Sergienko, V. Philipps, F. Irrek, H. G. Esser, U. Samm, M. Kempenaars, M. Stamp, C. Gowers and D. Richards, Laser desorption of deuterium retained in re-deposited carbon layers at TEXTOR and JET, *Journal of Nuclear Materials*, 337-339 (2005) 570–574.

[Sch10] D. P. Schissel, G. Abla, S. Flanagan, L. Kim and X. Lee, The between-pulse data analysis infrastructure at the DIII-D National Fusion Facility, *Fusion Science and Technology*, 58(3) (2010) 720–726.

[Sch11] M. Schloesser, S. Fischer, M. Sturm, B. Bornschein, R. J. Lewis and H. H. Telle, Design implications for laser Raman measurement systems for tritium sample-analysis, accountancy or process-control applications, *Fusion Science and Technology*, 60(3) (2011) 976–981.

[Sch13a] M. Schloesser, T. M. James, S. Fischer, R. J. Lewis, B. Bornschein and H. H. Telle, Evaluation method for Raman depolarization measurements including geometrical

effects and polarization aberrations, *Journal of Raman Spectroscopy*, 44(3) (2013) 453–462.

[Sch13b] M. Schloesser, S. Rupp, H. Seitz, S. Fischer, B. Bornschein, T. M. James and H. H. Telle, Accurate calibration of the laser Raman system for the Karlsruhe Tritium Neutrino Experiment, *Journal of Molecular Structure*, 1044 (2013) 61–66.

[Sch13c] M. Schloesser, H. Seitz, S. Rupp, P. Herwig, C. G. Alecu, M. Sturm and B. Bornschein, In-line calibration of Raman systems for analysis of gas mixtures of hydrogen isotopologues with sub-percent accuracy, *Analytical Chemistry*, 85(5) (2013) 2739–2745.

[Sch15] M. Schloesser, O. Pakari, S. Rupp, S. Mirz and S. Fischer, How to make Raman-inactive helium visible in Raman spectra of tritium-helium gas mixtures, *Fusion Science and Technology*, 67(3) (2015) 559–562.

[Sch64] F. Schmidt-Bleek and F. S. Rowland, Recoil reactions of tritium with organic compounds, *Angewandte Chemie, International Edition in English*, 3(12) (1964) 769–776.

[Sch68] B. Schimpke and K. Schuegerl, Kryosoption von Stickstoff bei 77 K, *Chemie Ingenieur Technik*, 40(5) (1968) 207–213.

[Sch71] R. Schott and G. Beau, Analyse quantitative des isotopes de l'hydrogène par spectrométrie de masse, *Méthodes Physiques D'Analyse (GAMS)*, 7(2) (1971) 165.

[Sch75] F. Schwochow and L. Puppe, Zeolithe - Herstellung, Struktur, Anwendung, *Angewandte Chemie*, 87(18) (1975) 659–667.

[Sch78] S. Schmidt and G. Sicking, Solubility isotherms of tritium in palladium at low equilibrium pressures, *Zeitschrift fuer Naturforschung A*, 33(11) (1978) 1328–1332.

[Sch80] L. Schlapbach, A. Seiler, F. Stucki and H. C. Siegmann, Surface effects and the formation of metal hydrides, *Journal of the Less-Common Metals*, 73(1) (1980) 145–160.

[Sch85] A. S. Schmidt, F. Verfuss and E. Wicke, Studies on the permeation of hydrogen and tritium through heat resistant alloys, *Journal of Nuclear Materials*, 131(2-3) (1985) 247–260.

[Sch87] T. Schober, R. Laesser, C. Dieker and H. Trinkaus, Swelling of selected metal tritides, *Journal of the Less-Common Metals*, 131(1-2) (1987) 293–299.

[Sch88] P. Schira and E. Hutter, Tritium cleanup on hot uranium powder, *Fusion Technology*, 14(2P2A) (1988) 608–613.

[Sch89a] T. Schober and K. Farrell, Helium bubbles in α-Ti and Ti tritide arising from tritium decay: A TEM study, *Journal of Nuclear Materials*, 168(1-2) (1989) 171–177.

[Sch89b] G. Schobert, N. Arnold, D. Bashore, R. Mika and G. Oliaro, Distributed process control system for remote control and monitoring of the TFTR tritium systems, *Proc. 15th Symposium on Fusion Technology (SOFT)*, Sept. 19–23, 1988, Utrecht, The Netherlands, (1989) pp. 1663.

[Sch91a] P. Schira, E. Hutter, G. Jourdan and R.-D. Penzhorn, The Tritium Laboratory Karlsruhe: Laboratory design and equipment, *Fusion Engineering and Design*, 18 (1991) 19–26.

[Sch91b] H. Schroeder and H. Ullmaier, Helium and hydrogen effects on the embrittlement of iron- and nickel-based alloys, *Journal of Nuclear Materials*, 179-181 (1991) 118–124.

[Sch95] K. Schaber, Aerosolbildung durch spontane Phasenuebergaenge bei Absorptions- und Kondensationsprozessen, *Chemie Ingenieur Technik*, 67(11) (1995) 1443–1452.

[Sch98] V. Schmidt, The development of the JET control and data acquisition system, *IEEE Transactions on Nuclear Science*, 45(4) (1998) 2026–2032.

[Sch99a] D. Schleussner, H. Maier, P. Franzen, R. Behrisch, M. Balden, ASDEX-Upgrade Team, M. Perl, W. Knapp and C. Edelmann, Hydrogen isotope inventories in the ASDEX Upgrade tungsten coated divertor tiles, *Journal of Nuclear Materials*, 266-269 (1999) 1296–1302.

[Sch99b] D. Schleussner, D. Roesler, J. Becker, W. Knapp, C. Edelmann, C. Garcia-Rosales, P. Franzen and R. Behrisch, Temperature programmed desorption from graphite, *Journal of Vacuum Science & Technology A: Vacuum, Surfaces, and Films*, 17(5) (1999) 2785–2790.

[Sci96] R. J. Scillia, Operational experience in the recovery of tritium from TFTR plasma exhaust gases by cryogenic distillation, *Proceedings of the 16th Symposium on Fusion Engineering (SOFE)*, Sept. 30–Oct. 5, 1995, Champaign, IL, USA, (1996) 592–595.

[Sco92] S. M. Scott, H. F. Buttgereit, G. Celentano and K. Malone, Decontamination of the JET vacuum vessel from beryllium and tritium, *Proceedings of the 17th Symposium on Fusion Technology (SOFT)*, Sept. 14–18, 1992, Rome, Italy, (1992) 1216–1219.

[Sed89] D. W. Sedgley, Development and application of charcoal sorbents for cryopumping fusion devices, *Fusion Engineering and Design*, 10 (1989) 217–222.

[Sed91] D. W. Sedgley, C. R. Walthers and E. M. Jenkins, Fusion reactor high vacuum pumping: charcoal cryosorber tritium exposure results, *14th Symposium on Fusion Engineering IEEE*, Sept. 30, 1991–Oct. 3, 1980, San Diego, California, (1991) 1233–1236.

[Sei71] T. P. Seitz, R. Woods, M. Wallis and R. L. Henkel, The safe handling of large quantities of tritium gas at the Los Alamos Tandem Accelerator Facility, *Nuclear Instruments and Methods*, 93(1) (1971) 125–129.

[Sek84] M. Seki and T. Hirabayashi, Sorption mechanisms of tritium on the surface of borosilicate glass, *Radiochimica Acta*, 35 (1984) 233–238.

[Sel92] B. G. Sellars, Preliminary Assessment of a Surface Fusible Grout Concept, technical report CFFTP G-9248, Canadian Fusion Fuels Technology Project, Mississauga, Canada (1992).

[Ser95] L. Serio, J. L. Hemmerich, R. Laesser and P. Milverton, Transient adiabatic/isothermal calorimetry tests on JET uranium beds for tritium storage, *Proceedings of the 18th Symposium on Fusion Technology (SOFT)*, Aug. 22–26, 1994, Karlsruhe, Federal Republic of Germany, (1995) 1107–1110.

[Ser96] E. Serra, Hydrogen and tritium kinetics in fusion reactor materials, PhD thesis, University of Salford, Salford, Great Britain, (1996).

[Ser97] E. Serra, A. Perujo and G. Benamati, Influence of traps on the deuterium behaviour in the low activation martensitic steels F82H and BATMAN, *Journal of Nuclear Materials*, 245(2-3) (1997) 108–114.

[Ser98] E. Serra, G. Benamati and O. V. Ogorodnikova, Hydrogen isotopes transport parameters in fusion reactor materials, *Journal of Nuclear Materials*, 255(2-3) (1998) 105–115.

[Ses05] K. L. Sessions, Processing tritiated water at the Savannah River Site: A production-scale demonstration of a palladium membrane reactor, *Fusion Science and Technology*, 48 (2005) 91–96.

[Sha03a] K. L. Shanahan, J. S. Hoelder, D. R. Bell and J. R. Wermer, Tritium aging effects in $LaNi_{4.25}Al_{0.75}$, *Journal of Alloys and Compounds*, 356-357 (2003) 382–385.

[Sha03b] F. Sharipov, Numerical Calculation of Tritium Flow through the KATRIN Beam Line, technical report, Departamento de Física, Universidad Federal do Paraná, Brazil (2003).

[Sha07] K. L. Shanahan, Tritium Issues in the HAPL IFE Reactor (U), technical report WSRC-2007-00041, Rev. 0, Savannah River National Laboratory, Aiken, SC, USA (2007).

[Sha16] M. Sharpe, W. T. Shmayda and W. U. Schraeder, Tritium migration to the surfaces of type 316 stainless steel; aluminium 6061; and oxygen-free, high-conductivity copper, *Fusion Science and Technology*, 70(1) (2016) 97–111.

[Sha91] C. Shan, A. Wu and Q. Chen, The behavior of diffusion and permeation of tritium through 316L stainless steel, *Journal of Nuclear Materials*, 179-181 (1991) 322–324.

[Sha99] K. L. Shanahan, J. S. Holder and J. R. Wermer, Tritium aging effects in palladium on kieselguhr, *Journal of Alloys and Compounds*, 293-295 (1999) 62–66.

[She02] V. Shestakov, A. Pisarev, V. Sobolev, S. Kulsartov and I. Tazhibaeva, Gas driven deuterium permeation through F82H martensitic steel, *Journal of Nuclear Materials*, 307-311 (2002) 1494–1497.

[She75] R. Sherman, Hardware selection, Tritium operating safety seminar July 30, 1975, LASL Group H-3, Report Task LA-6307-C, Los Alamos Scientific Laboratory, Los Alamos, NM, USA (1975).

[She77a] J. E. Shelby, Molecular diffusion and solubility of hydrogen isotopes in vitreous silica, *Journal of Applied Physics*, 48(8) (1977) 3387–3394.

[She77b] A. E. Sherwood, Tritium removal from air streams by catalytic oxidation and water adsorption, *Proceedings of the 24th Conference on Remote Systems Technology*, Nov. 14–19, 1976, Washington, D.C., USA, (1977) 1–28.

[She79] A. E. Sherwood, B. G. Monahan, R. A. McWilliams, F. S. Uribe and C. M. Griffith, Catalytic Oxidation of Tritium in Air at Ambient Temperature, technical report UCRL-52811, Lawrence Livermore Laboratory, Livermore, CA, USA (1979).

[She80] A. E. Sherwood, Kinetics of catalyzed tritium oxidation in air at ambient temperature, *The International Journal of Applied Radiation and Isotopes*, 31(8) (1980) 478.

[She92] R. H. Sherman, D. J. Taylor, J. R. Bartlit, J. L. Anderson, S. O'hira, H. Nakamura, S. Konishi, K. Okuno and Y. Naruse, Radiochemical reaction studies of tritium mixed gases by laser Raman spectroscopy at TSTA, *Fusion Technology*, 21(2P2) (1992) 457–461.

[She98] R. H. Sherman, D. J. Taylor, K. G. Honnell, S. O'hira, Y. Kawamura, M. Nishi and K. Okuno, Radiochemical reactions between tritium and humid air, *Proceedings of the 17th Symposium on Fusion Engineering (SOFE)*, Oct. 6–10, 1997, San Diego, CA, USA, (1998) 313–316.

[Shi01] K. Shiba, Y. Kohno and A. Kohyama, Progress of research on F82H and JLF-1, *IEA Workshop on Reduced Activation Ferritic/Martensitic Steels*, Nov. 2–3, 2000, Tokyo, Japan, (2001).

[Shi03] T. Shimada, Y. Ueda and M. Nishikawa, Mechanism of blister formation on tungsten surface, *Fusion Engineering and Design*, 66-68 (2003) 247–251.

[Shi08a] M. Shim, H. Chung, S. Cho and H. Yoshida, Disproportionation characteristics of a zirconium-cobalt hydride bed under ITER operating conditions, *Fusion Science and Technology*, 53(3) (2008) 830–840.

[Shi08b] R. Shimizu, K. Hayashida, K. Sawada, Y. Enokida and I. Yamamoto, Preparation of hydrophobic platinum catalyst in supercritical carbon dioxide and its application for isotopic exchange reaction of hydrogen atoms, *Proceedings of the International Symposium on EcoTopia Science 2007*, Nov. 23–25, 2007, Nagoya, Japan, (2008) 1089–1092.

[Shi11a] M. Shimada, R. D. Kolasinski, J. P. Sharpe and R. A. Causey, Tritium Plasma Experiment: Parameters and potentials for fusion plasma-wall interaction studies, *Review of Scientific Instruments*, 82(8) (2011) 083503.

[Shi11b] M. Shimada, T. Otsuka, R. J. Pawelko, P. Calderoni and J. P. Sharpe, Overview of recent tritium experiments in TPE, *Fusion Science and Technology*, 60(4) (2011) 1495–1498.

[Shi83] Y. Shimizu, S. Nagai and M. Hatada, Radiation effects on methane in the presence of molecular sieves, *Journal of the Chemical Society, Faraday Transactions 1: Physical Chemistry in Condensed Phases*, 79(9) (1983) 1973–1986.

[Shi88] A. L. Shilov, M. E. Kost and N. T. Kuznetsov, The system $LaNi_5$–H_2, *Journal of the Less-Common Metals*, 144(1) (1988) 23–30.

[Shi91] M. Shimizu, S. Kiyota and R. Ninimiya, Hydrogen isotope enrichment by hydrophobic Pt-catalyst in Japan and western countries, *Proceedings of the International Symposium on Isotope Separation and Chemical Exchange Uranium Enrichment*, Oct. 29–Nov. 1, 1990, Tokyo, Japan, (1991) 56–73.

[Shi97] T. Shiraishi, S. Odoi and M. Nishikawa, Adsorption and desorption behavior of tritiated water on the piping materials, *Journal of Nuclear Science and Technology*, 34(7) (1997) 687–694.

[Shi98] T. Shiraishi, M. Nishikawa and T. Fukumatsu, Permeation of multi-component hydrogen isotopes through nickel, *Journal of Nuclear Materials*, 254(2-3) (1998) 205–214.

[Shi99] T. Shiraishi, M. Nishikawa, T. Yamaguchi and K. Kenmotsu, Permeation of multi-component hydrogen isotopes through austenitic stainless steels, *Journal of Nuclear Materials*, 273(1) (1999) 60–65.

[Shm02a] W. T. Shmayda, A. Bruggeman, J. Braet and S. Vanderbiesen, Treatment of tritiated solvents, *Fusion Science and Technology*, 41(3P2) (2002) 721–725.

[Shm02b] W. T. Shmayda and R. D. Gallagher, Recovery of tritium from pharmaceutical mixed waste liquids, *Fusion Science and Technology*, 41(3P2) (2002) 726–730.

[Shm15] W. T. Shmayda, M. Sharpe, A. M. Boyce, R. Shea, B. Petroski and W. U. Schroeder, Dependence of tritium release from stainless steel on temperature and water vapor, *Fusion Science and Technology*, 68(4) (2015) 766–771.

[Shm84] W. T. Shmayda and P. Mayer, Uranium beds for temporary tritium storage, *Journal of the Less-Common Metals*, 104(2) (1984) 239–250.

[Shm85] W. T. Shmayda, F. Waelbroeck, J. Winter, P. Wienhold, T. Banno and N. P. Kherani, Tritium pumping based on asymmetric permeation, *Fusion Technology*, 8(2P2) (1985) 2285–2289.

[Shm87] W. T. Shmayda, Tritium Storage and Delivery System for Ontario Hydro Research Division Tritium Laboratory, technical report OH Report 86-164-K, Ontario Hydro Research Division, Toronto, Canada (1987).

[Shm88a] W. T. Shmayda and N. P. Kherani, Application of hydrogen permeation through bilayer metal membranes, *Proceedings of the 12th Symposium on Fusion Engineering (SOFE)*, Oct. 12–16, 1987, Monterey, CA, USA, (1988) 1247–1250.

[Shm88b] W. T. Shmayda, N. P. Kherani and A. G. Heics, Tritium removal from noble gas streams, *Vacuum Science Technology*, A6 (1988) 1259–1262.

[Shm90a] W. T. Shmayda and A. G. Heics, Advanced Tritium Safe Handling Course, course material, Ontario Hydro Research Division, Tritium Laboratory, Canadian Fusion Fuels Technology Program (CFFTP), (1990).

[Shm90b] W. T. Shmayda, A. G. Heics and N. P. Kherani, Comparison of uranium and zirconium cobalt for tritium storage, *Journal of the Less-Common Metals*, 162(1) (1990) 117–127.

[Shm92] W. T. Shmayda, N. P. Kherani, B. Wallace and F. Mazza, Inert gas secondary enclosure clean-up system, *Fusion Technology*, 21(2P2) (1992) 616–621.

[Shm93] W. T. Shmayda, Tritium processing using scavenger beds: Theory and operation, *Eurocourses: Nuclear Science and Technology*, F. Mannone, editor, Springer Netherlands, (1993), 23–52.

[Shu05] W. M. Shu, S. O'hira, T. Suzuki and M. F. Nishi, Radiochemical reactions between tritium molecule and carbon dioxide, *Fusion Science and Technology*, 48(1) (2005) 684–687.

[Shu07] W. M. Shu, G.-N. Luo and T. Yamanishi, Mechanisms of retention and blistering in near-surface region of tungsten exposed to high flux deuterium plasmas of tens of eV, *Journal of Nuclear Materials*, 367-370 (2007) 1463–1467.

[Shu15] W. M. Shu, I. Cristescu, R. Michling, D. Demange, R. S. Willms and M. Glugla, Highly tritiated water processing by isotopic exchange, *Fusion Science and Technology*, 67(3) (2015) 563–566.

[Shu93a] W. M. Shu, K. Okuno and Y. Hayashi, General model for ion-driven permeation at steady state: new transport parameters, *The Journal of Physical Chemistry*, 97(17) (1993) 4497–4499.

[Shu93b] W. M. Shu, K. Okuno, Y. Hayashi and Y. Naruse, Permeation of deuterium implanted into pure iron, *Journal of Nuclear Materials*, 203(1) (1993) 50–55.

[Shu94] J. Shu, B. P. A. Grandjean and S. Kaliaguine, Methane steam reforming in asymmetric Pd- and Pd – Ag/porous SS membrane reactors, *Applied Catalysis A: General*, 119(2) (1994) 305–325.

[Sic71] G. Sicking and H. Buchold, Untersuchungen zur Diffusion von Tritium in Uebergangsmetallen, *Zeitschrift fuer Naturforschung A*, 26(12) (1971) 1973–1980.

[Sie85] C. J. Sienkiewicz, Tritium surface contamination, *The International Journal of Applied Radiation and Isotopes*, 36(7) (1985) 2444–2454.

[Sie88] C. J. Sienkiewicz and J. E. Lentz, Recovery of tritium from water, *Fusion Technology*, 14(2P2A) (1988) 444–449.

[Sil68] R. H. Siller, W. A. Oates and R. B. McLellan, The solubility of carbon in palladium and platinum, *Journal of the Less-Common Metals*, 16(1) (1968) 71–73.

[Sim04] S. P. Simakov, U. Fischer and U. von Moellendorff, Assessment of the ^{3}H and ^{7}Be generation in the IFMIF lithium loop, *Journal of Nuclear Materials*, 329-333 (2004) 213–217.

[Sin84] V. P. Singh, Microwave regeneration of molecular sieves, technical report F–84023, Canadian Fusion Fuels Technology Project (CFFTP), Toronto, Canada (1984).

[Sip02] A. C. C. Sips, R. Arslanbekov, C. Atanasiu, W. Becker, G. Becker, K. Behler, K. Behringer, A. Bergmann, R. Bilato, D. Bolshukhin, K. Borrass, B. Braams, M. Brambilla, F. Braun, A. Buhler, G. Conway, D. Coster, R. Drube, R. Dux, S. Egorov, T. Eich, K. Engelhardt, H.-U. Fahrbach, U. Fantz, H. Faugel, M. Foley, K. B. Fournier, P. Franzen, J. C. Fuchs, J. Gafert, G. Gantenbein, O. Gehre, A. Geier, J. Gernhardt, O. Gruber, A. Gude, S. Guenter, G. Haas, D. Hartmann, B. Heger, B. Heinemann, A. Herrmann, J. Hobirk, F. Hofmeister, H. H. Hohenoecker, L. Horton, V. Igochine, D. Jacobi, M. Jakobi, F. Jenko, A. Kallenbach, O. Kardaun, M. Kaufmann, A. Keller, A. Kendl, J.-W. Kim, K. Kirov, R. Kochergov, H. Kollotzek, W. Kraus, K. Krieger, B. Kurzan, P. T. Lang, P. Lauber, M. Laux, F. Leuterer, A. Lohs, A. Lorenz, C. Maggi, H. Maier, K. Mank, M.-E. Manso, M. Maraschek, K. F. Mast, P. McCarthy, D. Meisel, H. Meister, F. Meo, R. Merkel, D. Merkl, V. Mertens, F. Monaco, A. Mueck, H. W. Mueller, M. Muench, H. Murmann, Y.-S. Na, G. Neu, R. Neu, J. Neuhauser, J.-M. Noterdaeme, I. Nunes, G. Pautasso, A. G. Peeters, G. Pereverzev, S. Pinches, E. Poli, M. Proschek, R. Pugno, E. Quigley, G. Raupp, T. Ribeiro, R. Riedl, S. Riondato, V. Rohde, J. Roth, F. Ryter, S. Saarelma, W. Sandmann, S. Schade, H.-B. Schilling, W. Schneider, G. Schramm, S. Schweizer, B. Scott, U. Seidel, F. Serra, S. Sesnic, C. Sihler, A. Silva, E. Speth, A. Staebler, K.-H. Steuer, J. Stober, B. Streibl, E. Strumberger, W. Suttrop, A. Tabasso, A. Tanga, G. Tardini, C. Tichmann, W. Treutterer, M. Troppmann, P. Varela, O. Vollmer, D. Wagner, U. Wenzel, F. Wesner, R. Wolf, E. Wolfrum, E. Wuersching, Q. Yu, D. Zasche, T. Zehetbauer, H.-P. Zehrfeld and H. Zohm, Steady state advanced scenarios at ASDEX Upgrade, *Plasma Physics and Controlled Fusion*, 44(12B) (2002) B69–B83.

[Sis90] R. A. P. Sissingh and R. L. Rossmassler, Tritium facility at TFTR, *Fusion Engineering and Design*, 12(3) (1990) 383–391.

[Sis94] R. A. P. Sissingh and S. C. Gordon, TFTR, Tritium Systems Course Vol. 1 and 2, Office of Certification and Training, Plasma Physics Laboratory, University of Princeton, Princeton, NJ, USA (1994).

[Ski00] C. H. Skinner, C. A. Gentile, J. P. Coad, R.-D. Penzhorn and J. T. Hogan, Comparison of tritium retention in TFTR and JET, *Proceedings of the Annual Meeting of the Division of Plasma Physics of the American Physics Socciety*, Oct. 23–27, 2000, Quebec, Canada, (2000).

[Ski01] C. Skinner, C. Gentile, K. Young, J. Coad, J. Hogan, R.-D. Penzhorn, N. Bekris and JET EFDA Contributors, Long term tritium trapping in TFTR and JET, report efda-jet-cp(01)02-91, *Proceedings of EPS Conference*, June 18–22, 2001, Madeira, Portugal, (2001).

[Ski02] C. H. Skinner, C. A. Gentile, G. Guttadora, A. Carpe, S. Langish, K. M. Young, M. Nishi and W. Shu, Tritium removal by laser heating and its application to tokamaks, *Fusion Science Technology*, 41 (2002) 716–720.

[Ski03a] C. H. Skinner, N. Bekris, J. P. Coad, C. A. Gentile and M. Glugla, Tritium removal from JET and TFTR tiles by a scanning laser, *Nuclear Materials*, 313-316 (2003) 496–500.

[Ski03b] C. H. Skinner, J. P. Coad and G. Federici, Tritium removal from carbon plasma facing components, *Physica Scripta*, 2004(T111) (2003) 92–97.

[Ski08] C. H. Skinner, A. A. Haasz, V. K. H. Alimov, N. Bekris, R. A. Causey, R. E. H. Clark, J. P. Coad, J. W. Davis, R. P. Doerner, M. Mayer, A. Pisarev, J. Roth and T. Tanabe, Recent advances on hydrogen retention in ITER's plasma-facing materials: Beryllium, carbon, and tungsten, *Fusion Science and Technology*, 54 (2008) 891–945.

[Smi15] R. Smith, D. A. J. Whittaker, B. Butler, A. Hollingsworth, R. E. Lawless, X. Lefebvre, S. A. Medley, A. I. Parracho and B. Wakeling, Hydrogen isotope separation for fusion power applications, *Journal of Alloys and Compounds*, 645 (2015) S51–S55.

[Smi98] I. Smid, M. Akiba, G. Vieider and L. Ploechl, Development of tungsten armour and bonding to copper for plasma-interactive components, *Journal of Nuclear Materials*, 258-263 (1998) 160–172.

[Smo92] G. R. Smolik, B. J. Merrill and R. S. Wallace, Reaction of Porous Beryllium in Steam, INEL report EGG-FSP 10346, Idaho National Engineering Laboratory, Idaho Falls, ID, USA (1992).

[Sne57] A. H. Snell, F. Pleasonton and H. E. Leming, Molecular dissociation following radioactive decay: Tritium hydride, *Journal of Inorganic and Nuclear Chemistry*, 5(2) (1957) 112–117.

[Son10] K. M. Song, B. W. Ko, K. W. Lee and S. H. Sohn, Test of a large volume calorimeter in KEPRI Tritium Laboratory, *IEEE Transactions on Plasma Science*, 38(3) (2010) 295–299.

[Soo92] S. K. Sood, C. Fong, K. M. Kalyanam, O. K. Kveton, A. Busigin and D. M. Ruthven, A new pressure swing adsorption (PSA) process for recovery of tritium from the ITER solid ceramic breeder helium purge gas, *Fusion Technology*, 21(2P2) (1992) 299–304.

[Sou81] P. C. Souers, Heavy ion equilibrium in T_2 gas, *Journal of Physics B: Atomic and Molecular Physics*, 14(11) (1981) L387–L390.

[Sou82] P. C. Souers, E. R. Bissell, G. D. Honoré, L. C. Kang, R. T. Tsugawa and H. H. Miller, Organic getter for tritium, *Journal of Vacuum Science and Technology*, 20(4) (1982) 1132–1134.

[Sou86] P. C. Souers, Hydrogen properties for fusion energy, University of California Press, Berkeley, CA, USA (1986).

[Sta01] C. Stan-Sion, R. Behrisch, J. P. Coad, U. Kreissig, F. Kubo, V. Lazarev, S. Lindig, M. Mayer, E. Nolte, A. Peacock, L. Rohrer and J. Roth, Hydrogen isotope depth profiling in carbon samples from the erosion dominated inner vessel walls of JET, *Journal of Nuclear Materials*, 290-293 (2001) 491–495.

[Sta15] G. C. Staack, M. L. Crowder and J. E. Klein, Thermal release of ^{3}He from tritium aged $LaNi_{4.25}Al_{0.75}$ hydride, *Fusion Science and Technology*, 67(3) (2015) 580–583.

[Sta56] P. A. Staats, H. W. Morgan and J. H. Goldstein, Infrared spectra of T_2O, THO, and TDO, *The Journal of Chemical Physics*, 24(4) (1956) 916–917.

[Sta79] J. L. Stakebake, Kinetics for the reaction of hydrogen with uranium powder, *Journal of The Electrochemical Society*, 126(9) (1979) 1596–1601.

[Sta85] J. Stachurski and A. Frackiewicz, A new phase in the Pd – C system formed during the catalytic hydrogenation of acetylene, *Journal of the Less-Common Metals*, 108(2) (1985) 249–256.

[Ste61] W. H. Stevens, J. G. Bayly, V. B. Thurston and V. Kartha, Heavy Water Analysis in the 1 % to 99 % D_2O Range by Infrared Spectroscopy, AECL report AECL-1391, Atomic Energy of Canada Ltd, Chalk River, Canada (1961).

[Ste67] S. A. Stern and F. S. DiPaolo, The adsorption of atmospheric gases on molecular sieves at low pressures and temperatures. The effect of preadsorbed water, *Journal of Vacuum Science and Technology*, 4(6) (1967) 347–355.

[Ste75] R. H. Steinmeyer and J. D. Braun, Hydrogen isotope permeation in elastomeric materials, *International Conference on Radiation Effects and Tritium Technology for Fusion Reactors*, Oct. 1–3, 1975, Gatlinburg, TN, USA, (1975).

[Ste83] S. A. Steward, Review of Hydrogen Permeabilities through Materials, technical report UCRL-53441, DE84 007362, Lawrence Livermore Laboratory, Livermore, CA, USA (1983).

[Sti72] R. E. Stickney, Diffusion and permeation of hydrogen isotopes in fusion reactors: A survey, *The Chemistry of Fusion Technology*, D. M. Gruen, editor, Springer, Boston, MA US, New York-London, (1972), 241–319.

[Sto00] D. O. Stodilka, N. P. Kherani, W. T. Shmayda and S. J. Thorpe, A tritium tracer technique for the measurement of hydrogen permeation in polymeric materials, *International Journal of Hydrogen Energy*, 25(11) (2000) 1129–1136.

[Sto66] J. J. Stobbs and A. J. Woodward, The oxidation of pure U in CO_2 between 700 - 1000 °C, *Corrosion Science*, 6(11-12) (1966) 499–507.

[Sto84] D. Stoever, H. P. Buchkremer, R. Hecker and H. J. Levers, Status of tritium permeation barrier development on austenitic structural alloys, *Journal of Nuclear Materials*, 123(1-3) (1984) 1541–1546.

[Sto91] R. Stockmeyer, In-situ observation of the ortho-para-hydrogen conversion in chabazite by neutron scattering, *Berichte der Bunsengesellschaft fuer physikalische Chemie*, 95(4) (1991) 458–461.

[Sto92] L. Stobinski and R. Duś, Atomic hydrogen solubility in thin gold films and its influence on hydrogen thermal desorption spectra from the surface, *Applied Surface Science*, 62(1-2) (1992) 77–82.

[Sto99] D. Stork, P. Ageladarakis, A. C. Bell, P. D. Brennan, A. Browne, M. L. Browne, P. R. Butcher, C. Caldwell-Nichols, P. Chuilon, S. J. Cox, N. Davies, J. A. Dobbing, N. Dolgetta, C. G. Elsmore, J. A. How, J. Howie, T. T. C. Jones, A. S. Kaye, Q. King, V. Marchese, W. Obert, J. Orchard, S. Papastergiou, R. J. H. Pearce, L. Svensson, J. van Veen, M. Wright and D. Young, Systems for the safe operation of the JET tokamak with tritium, *Fusion Engineering and Design*, 47(2-3) (1999) 131–172.

[Str13] F. Strauss, N. Gaiser, B. Wirth, A. Gernoth and S. Schlechtriem, Untersuchungen zur Durchstroembarkeit von poroesen Medien mit partikelhaltigen Gasen, *Tagungsband: 62. Deutscher Luft- und Raumfahrtkongress 2013*, Sept. 10–12, 2013, Stuttgart, Federal Republic of Germany, (2013) 1–9.

[Str74] R. A. Strehlow and H. C. Savage, The permeation of hydrogen isotopes through structural metals at low pressures and through metals with oxide film barriers, *Nuclear Technology*, 22(1) (1974) 127–137.

[Stu10] M. Sturm, M. Schlösser, R. J. Lewis, B. Bornschein, G. Drexlin and H. H. Telle, Monitoring of all hydrogen isotopologues at Tritium Laboratory Karlsruhe using Raman spectroscopy, *Laser Physics*, 20 (2010) 493–507.

[Stu21] M. Sturm, F. Priester, M. Roellig, C. Roettele, A. Marsteller, D. Hillesheimer, L. Bornschein, B. Bornschein, R. Groessle and S. Welte, Kilogram scale throughput performance of the KATRIN Tritium Handling System, *Fusion Engineering and Design*, 170 (2021) 112507.

[Stu64] W. I. Stuart and G. H. Price, The high temperature reaction between beryllia and water vapour, *Journal of Nuclear Materials*, 14 (1964) 417–424.

[Sug03] K. Sugiyama, K. Miyasaka, T. Tanabe, M. Glugla, N. Bekris and P. Coad, Tritium distribution on the surface of plasma facing carbon tiles used in JET, *Journal of Nuclear Materials*, 313-316 (2003) 507–513.

[Sug04] K. Sugiyama, T. Tanabe, K. Miyasaka, K. Masaki, K. Tobita, N. Miya, V. Philipps, M. Rubel, C. H. Skinner, C. A. Gentile, T. Saze and K. Nishizawa, Tritium profile in plasma-facing components following D – D operation, *Journal of Nuclear Materials*, 329-333 (2004) 874–879.

[Sug05] T. Sugiyama, Y. Asakura, T. Uda, Y. Abe, T. Shiozaki, Y. Enokida and I. Yamamoto, Hydrogen isotope separation by Combined Electrolysis Catalytic Exchange under reduced pressure, *Fusion Science and Technology*, 48(1) (2005) 132–135.

[Sug84] M. Sugisaki, H. Furuya, K. Ono and K. Idemitsu, Tritium solubility in SUS-316 stainless steel, *Journal of Nuclear Materials*, 120(1) (1984) 36–40.

[Sug85] M. Sugisaki, H. Furuya, H. Ueki and S. Ejima, Surface reaction and bulk diffusion of tritium in SUS-316 stainless steel, *Journal of Nuclear Materials*, 133-134 (1985) 280–283.

[Sun97] G. Y. Sun, M. Friedrich, R. Groetzschel, W. Buerger, R. Behrisch and C. García-Rosales, Quantitative AMS depth profiling of the hydrogen isotopes collected in graphite divertor and wall tiles of the tokamak ASDEX-Upgrade, *Journal of Nuclear Materials*, 246(1) (1997) 9–16.

[Sur88a] R. A. Surette, R. J. Booth, S. R. Bokwa and R. G. C. McElroy, Process tritium monitors in use at Chalk River Nuclear Laboratories, *Fusion Technology*, 14(2P2B) (1988) 1066–1070.

[Sur88b] R. A. Surette and R. G. C. McElroy, Regrowth, retention and evolution of tritium from stainless steel, *Fusion Science and Technology*, 14(2P2B) (1988) 1141–1146.

[Sur95] R. A. Surette and M. J. Wood, An evaluation of instruments and techniques for monitoring of tritium-contaminated surfaces, *Fusion Technology*, 28(3P1) (1995) 957–963.

[Sve61] L. M. Sverdlov, Calculation of the integrated intensities of the infrared bands of isotopically substituted methanes VIII, *Optics and Electronics*, 10 (1961) 17.

[Swa16] Swagelock, Swagelok® Tubing and Tube Accessories, https://products.swagelok.com/en/tubing-tube-accessories/c/800, (2016), (visited on Apr. 13, 2022).

[Swa58] C. G. Swain and A. J. Kresge, Exchange reactions between hydrogen gas and hydroxyl groups. a convenient preparation of tritium-labelled water, *Journal of the American Chemical Society*, 80(19) (1958) 5281–5283.

[Swa79] W. A. Swansiger and R. Bastasz, Tritium and deuterium permeation in stainless steels: Influence of thin oxide films, *Journal of Nuclear Materials*, 85-86 (1979) 335–339.

[Swa84] W. A. Swansiger, V. K. Gabrielson and R. W. Bradshaw, Summary abstract: Recovery of tritium from tritiated water by reaction with uranium, *Journal of Vacuum Science & Technology A: Vacuum, Surfaces, and Films*, 2(2) (1984) 721–722.

[Swa86] W. A. Swansiger, Summary abstract: Tritium solubility in high purity beryllium, *Journal of Vacuum Science & Technology A: Vacuum, Surfaces, and Films*, 4(3) (1986) 1216–1217.

[Swa88] W. A. Swansiger, Measurement of the solubility of tritium in copper and gold at high pressures, *Fusion Technology*, 14(2P2A) (1988) 631–636.

[Swe61] D. E. Swets, R. W. Lee and R. C. Frank, Diffusion coefficients of helium in fused quartz, *The Journal of Chemical Physics*, 34(1) (1961) 17–22.

[Swi66] D. L. Swift, The thermal conductivity of spherical metal powders including the effect of an oxide coating, *International Journal of Heat and Mass Transfer*, 9(10) (1966) 1061–1074.

[Syk15] A. Sykes, A. E. Costley, M. P. Gryaznevich, D. Kingham, J. Hugill, C. Windsor, P. Buxton, J. G. Morgan, B. Huang, G. Hammond, J. Fanthome, G. Smith, S. Ball, S. Chappell and Z. Melhem, Opportunities and challenges for Compact Fusion Energy, *Fusion Science and Technology*, 68(2) (2015) 237–244.

[Tad80] W. E. Tadlock, G. C. Abell and R. H. Steinmeyer, Gas generation by self-radiolysis of tritiated waste materials, *Nuclear Technology*, 47(2) (1980) 358–362.

[Tah85] A. Tahara and Y. Hayashi, Measurements of permeation of hydrogen isotopes through α-iron by pressure modulation and ion bombarding, *Transactions of the Japan Institute of Metals*, 26(12) (1985) 869–875.

[Tai00] J. Tait, R. Brade, P. Carman, P. Edwards, C. Hume, A. Loving, G. Lundqvist, I. Merrigan, S. Mills, S. Sanders, R. Stokes and D. W. Wilson, Further development at JET of remote digital photogrammetry techniques and remote welding under conditions of restricted access, *Proceedings of the 5th International Symposium on Fusion Nuclear Technology*, Sept. 19–24, 1999, Rome, Italy, (2000).

[Tak05] H. Takata, T. Motoshima, S. Satake and M. Nishikawa, Study of tritium behaviour in cement paste, *Fusion Science and Technology*, 48(1) (2005) 589–592.

[Tak07] I. Takagi, M. Akiyoshi, N. Matsubara, T. Nishiuchi, K. Moritani, T. Sasaki and H. Moriyama, Characteristics of traps for hydrogen in helium-irradiated copper, *Journal of Nuclear Materials*, 367-370 (2007) 489–493.

[Tak08a] K. Takai, H. Shoda, H. Suzuki and M. Nagumo, Lattice defects dominating hydrogen-related failure of metals, *Acta Materialia*, 56(18) (2008) 5158–5167.

[Tak08b] H. Takata, K. Furuichi, M. Nishikawa, S. Fukada, K. Katayama, T. Takeishi, K. Kobayashi, T. Hayashi and H. Namba, Concentration profiles of tritium penetrated into concrete, *Fusion Science and Technology*, 54 (2008) 223–226.

[Tak11] I. Takagi, K. Yamamichi, R. Imade, T. Sasaki, H. Tsuchida, K. Moritani and H. Moriyama, Thermal growth of hydrogen trap in ion-irradiated W, *Fusion Science and Technology*, 60(4) (2011) 1451–1454.

[Tak75] T. Takeuchi, O. Takayasu, S. Uchida and Y. Nakano, Autoradiographical studies of the behavior of the tritium produced by $^{6}\mathrm{Li}(\mathrm{n},\alpha)\,^{3}\mathrm{H}$ reaction on nickel, *The International Journal of Applied Radiation and Isotopes*, 26(12) (1975) 736–740.

[Tak81] O. Takayasu, I. Makino and T. Takeuchi, Enrichment of tritium by thermal diffusion column I. TH$-$H$_2$ and TD$-$D$_2$ systems, *The International Journal of Applied Radiation and Isotopes*, 32(11) (1981) 839–842.

[Tak91] I. Takagi, M. Matsuoka, H. Fujita, K. Shin and K. Higashi, In-situ depth-profiling of deuterium in nickel exposed to RF plasma, *Journal of Nuclear Materials*, 179-181 (1991) 319–321.

[Tak92] I. Takagi, H. Fujita, K. Shin and K. Higashi, Observations of deuterium trapping in nickel irradiated by ^{3}He, *Journal of Nuclear Materials*, 191-194 (1992) 1313–1317.

[Tal93] C. L. Talcott, J. L. Anderson, R. V. Carlson, D. O. Coffin, C. R. Walthers, D. Hamerdinger, K. Binning, R. D. Trujillo, J. S. Moya, T. Hayashi, K. Okuno and T. Yamanishi, Three Tritium Systems Test Assembly (TSTA) off-loop experiments, *Proceedings of the 15th Symposium on Fusion Engineering (SOFE)*, Oct. 11–15, 1993, Hyannis, MA, USA, (1993) 198–203.

[Tam08] H. Tamura, The role of rusts in corrosion and corrosion protection of iron and steel, *Corrosion Science*, 50(7) (2008) 1872–1883.

[Tam91a] U. Tamm, E. Hutter and G. Neffe, Experiments on the development of the tritium cleanup system by the getter method for use in the Tritium Laboratory Karlsruhe,

Proceedings of the 16th Symposium on Fusion Technology (SOFT), Sept. 3–7, 1990, London, UK, (1991) 641–645.

[Tam91b] U. Tamm, E. Hutter, G. Neffe and P. Schira, Experiments on the oxidation and air ingress into uranium beds, *Proceedings of the 16th Symposium on Fusion Technology (SOFT)*, Sept. 3–7, 1990, London, UK, (1991) 1235–1239.

[Tam92] U. Tamm, E. Hutter, G. Neffe and P. Schira, Uranium getters for tritium cleanup at the Tritium Laboratory Karlsruhe (TLK), *Fusion Technology*, 21(2P2) (1992) 983–987.

[Tam93] U. Tamm, E. Hutter, G. Neffe and P. Schira, Experiments on the oxidation and air ingress into uranium beds, *Proceeings of Symposium on Fusion Technology (SOFT)*, Sept. 14–18, 1992, Rome, Italy, (1993) 1235–1239.

[Tan00a] T. Tanabe, T. Ohgo, M. Wada, M. Rubel, V. Philipps, J. von Seggern, K. Ohya, A. Huber, A. Pospieszczyk and B. Schweer, Material mixing on W/C twin limiter in TEXTOR-94, *Fusion Engineering and Design*, 49-50 (2000) 355–362.

[Tan00b] T. Tanabe, M. Wada, T. Ohgo, V. Philipps, M. Rubel, A. Huber, J. von Seggern, K. Ohya, A. Pospieszczyk and B. Schweer, Application of tungsten for plasma limiters in TEXTOR, *Journal of Nuclear Materials*, 283-287 (2000) 1128–1133.

[Tan01a] T. Tanabe and V. Philipps, Tritium detection in plasma facing component by imaging plate technique, *Fusion Engineering and Design*, 54(1) (2001) 147–149.

[Tan01b] T. Tanaka, K. Miyasaka, N. Miya, K. Masaki, V. Philipps and M. Rubel, Tritium deposition on plasma facing materials, *IAEA Advisory Group Meeting "Assessment of New Data for Tritium Retention in Fusion Reactor Materials"*, July 2–3, 2001, Vienna, Austria, (2001).

[Tan02] T. Tanabe, K. Miyasaka, T. Saze, K. Nishizawa, T. Kobayashi, T. Hayashi and M. Nishi, Surface tritium detection by imaging plate technique, *Fusion Science and Technology*, 41(3P2) (2002) 528–531.

[Tan03] T. Tanabe, K. Sugiyama, K. Masaki, Y. Gotoh, K. K. Tobita and N. Miya, Tritium distribution on plasma facing graphite tiles of JT-60U, *19^{th} IAEA Fusion Energy Conference*, Oct. 14–19, 2002, Lyon, France, (2003).

[Tan08] Y. Tanaka, H. Saito, Y. Tsutsumi, H. Doi, H. Imai and T. Hanawa, Active hydroxyl groups on surface oxide film of titanium, 316L stainless steel, and cobalt-chromium-molybdenum alloy and its effect on the immobilization of poly(ethylene glycol), *Material Transactions*, 49(4) (2008) 805–811.

[Tan09] M. Tanaka, K. Higashida, T. Shimokawa and T. Morikawa, Brittle-ductile transition in low carbon steel deformed by the accumulative roll bonding process, *Materials Transactions*, 50(1) (2009) 56–63.

[Tan11] T. Tanabe, Tritium handling issues in fusion reactor materials, *Journal of Nuclear Materials*, 417(1-3) (2011) 545–550.

[Tan65] Y.-N. Tang and F. S. Rowland, Recoil tritium reaction: Ring opening and alkyl replacement in substituted cyclopropanes, *The Journal of Physical Chemistry*, 69(12) (1965) 4297–4304.

[Tan79a] T. Tanabe, S. Miura and S. Imoto, Isotope effect in dissociation of uranium hydride, *Journal of Nuclear Science and Technology*, 16(9) (1979) 690–696.

[Tan79b] S. Tanaka and R. Kiyose, Isotope separation of hydrogen and deuterium by permeation through palladium membrane, *Journal of Nuclear Science and Technology*, 16(12) (1979) 923–925.

[Tan83] T. Tanabe, T. Yamamoto and S. Imoto, Recovery of hydrogen isotopes using a uranium bed, *Journal of the Less-Common Metals*, 89(2) (1983) 393–398.

[Tan84] T. Tanabe, Y. Yamanishi, K. Sawada and S. Imoto, Hydrogen transport in stainless steels, *Journal of Nuclear Materials*, 123(1-3) (1984) 1568–1572.

[Tan87] M. Tanase, M. Kato, K. Kurosawa, S. Motoishi, S. Okano, H. Sugai, M. Fijie, K. Onoma and H. Yamabashi, Test production of tritium in 1000 Ci level from ^{6}Li – Al alloy target, *Japan-US Workshop on Tritium Technology*, Oct. 22–23, 1986, Tokyo, Japan, (1987).

[Tan88] M. Tanase, K. Kurosawa, M. Fujie, H. Sugai, S. Okane and M. Kato, Radiogas-chromatographic determination of chemical and isotopic purity of tritium gas in tritium production, *Fusion Technology*, 14(2P2B) (1988) 1090–1095.

[Tan96] K.-I. Tanaka, M. Uetake and M. Nishikawa, Calculation of breakthrough curve of multicomponent hydrogen isotopes using cryosorption column, *Journal of Nuclear Science and Technology*, 33(6) (1996) 492–503.

[Tay00a] N. P. Taylor, I. Cook, C. B. A. Forty, W. E. Han and P. Taylor, SEAFP-2 bounding accident analyses, *Fusion Engineering and Design*, 48(3-4) (2000) 419–433.

[Tay00b] N. P. Taylor, C. B. A. Forty, D. A. Petti and K. A. McCarthy, The impact of materials selection on long-term activation in fusion power plants, *Journal of Nuclear Materials*, 283-287 (2000) 28–34.

[Tay01] D. J. Taylor, M. Glugla and R.-D. Penzhorn, Enhanced Raman sensitivity using an actively stabilized external resonator, *Review of Scientific Instruments*, 72(4) (2001) 1970–1976.

[Tay12] N. Taylor, S. Ciattaglia, P. Cortes, M. Iseli, S. Rosanvallon and L. Topilski, ITER safety and licensing update, *Fusion Engineering and Design*, 87(5-6) (2012) 476–481.

[Tay95] D. Taylor, Tritium Plasma Experiment, technical report TTA-SDD-100-01, RO, Tritium Systems Test Assembly, Los Alamos National Laboratory (LANL), Los Alamos, NM, USA (1995).

[Taz94] I. L. Tazhibaeva, V. P. Shestakov, E. V. Chikhray, O. G. Romanenko, A. K. Klepikov, G. L. Saksaganskiy, Y. G. Prokofiev and S. N. Mazaev, Deuterium permeation through beryllium with surface element composition control, *Proceedings of the 18th Symposium on Fusion Technology (SOFT)*, Aug. 22–26, 1994, Karlsruhe, Federal Republic of Germany, (1994) 427–430.

[Teb99] V. Tebus, L. Rivkis, G. Arutunova, E. Dmitrievsky, V. Filin, Y. Golikov, V. Krivova and V. Kapychev, Investigation of palladium alloy properties degradation during long-time tritium exposure, *Journal of Nuclear Materials*, 271-272 (1999) 345–348.

[Tel13] Teledyne API, Inc, Model T802 Paramagnetic Oxygen Analyzer, 07275B DCN6418, operating manual, San Diego, CA, USA, (2013).

[Ter76] Y. Terashima and T. Kumaki, Effective diffusion coefficients of water molecule in several porous materials, *Proceedings of the Japan Society of Civil Engineers*, 256 (1976) 91–94.

[Tes05] C. Tesch, R. Carlson, R. Michelotti, M. Rogers and S. Willms, Tritium Systems Test Assembly (TSTA) stabilization, *Fusion Science and Technology*, 48(1) (2005) 258–261.

[Tet01] D. F. Teter, R. J. Hanrahan and C. J. Wetteland, Uranium Hydride Nucleation Kinetics: Effects of Oxide Thickness and Vacuum Outgassing, technical report LA-13772-MS, Los Alamos, NM, USA (2001).

[The80] Thermacore, Inc., Investigation of Non-Magnetic Alloys for the Suppression of Tritium Permeation, literature survey DOE/ER10087-T1, Lancaster, PA, USA (1980).

[Thi87] P. A. Thiel and T. E. Madey, The interaction of water with solid surfaces: Fundamental aspects, *Surface Science Reports*, 7(6-8) (1987) 211–385.

[Tho12] C. Thomser, V. Bailescu, S. Brezinsek, J. W. Coenen, H. Greuner, T. Hirai, J. Linke, C. P. Lungu, H. Maier, G. Matthews, P. Mertens, R. Neu, V. Philipps, V. Riccardo, M. Rubel, C. Ruset, A. Schmidt and I. Uytdenhouwen, Plasma facing materials for the JET ITER-like wall, *Fusion Science & Technology*, 62 (2012) 1–8.

[Tho67] C. L. Thomas, Solubility of hydrogen in solid copper, silver, and gold obtained by a rapid quench and extraction technique, *Transactions of the Metallurgical Society of AIME*, 239 (1967) 485–496.

[Tho73] A. W. Thompson, Ductility losses in austenitic stainless steels caused by hydrogen, *Hydrogen in Metals*, AMS (1973) 91–102.

[Tho83] G. J. Thomas and J. M. Mintz, Helium bubbles in palladium tritide, *Journal of Nuclear Materials*, 116(2-3) (1983) 336–338.

[Tho94] M. I. Thornton, G. Grassi and G. Vasallo, Tritium calorimetry in ETHEL, *Proceedings of the 3rd ETHEL-TLK Workshop on Tritium Technology and Safety in Thermonuclear Fusion*, May 24–25, 1993, Karlsruhe, Federal Republic of Germany, (1994).

[Tin66] T. L. Tingey, The Radiolysis of a Mixture of Carbon Dioxide and Hydrogen, technical report BNWL-SA 591, Battelle Northwest Laboratory, Richland, WA, USA (1966).

[Tob06] K. Tobita, S. Nishio, M. Enoeda, M. Sato, T. Isono, S. Sakurai, H. Nakamura, S. Sato, S. Suzuki, M. Ando, K. Ezato, T. Hayashi, T. Hirose, T. Inoue, Y. Kawamura, N.

Koizumi, Y. Kudo, R. Kurihara, T. Kuroda, M. Matsukawa, K. Mouri, Y. Nakamura, M. Nishi, Y. Nomoto, J. Ohmori, N. Oyama, K. Sakamoto, T. Suzuki, M. Takechi, H. Tanigawa, K. Tsuchiya and D. Tsuru, Design study of fusion DEMO plant at JAERI, *Fusion Engineering and Design*, 81(8-14) (2006) 1151–1158.

[Tod58] G. Toda, Rate of permeation and diffusion coefficient of hydrogen through palladium, *Journal of the Research Institute for Catalysis, Hokkaido University*, 6 (1958) 13–19.

[Tog11] Y. Togashi and M. Hara, Water vapor permeability of polypropylene, *Fusion Science and Technology*, 60(4) (2011) 1471–1474.

[Tok05] K. Tokunaga, M. J. Baldwin, R. P. Doerner, N. Noda, Y. Kubota, N. Yoshida, T. Sogabe, T. Kato and B. Schedler, Blister formation and deuterium retention on tungsten exposed to low energy and high flux deuterium plasma, *Journal of Nuclear Materials*, 337-339 (2005) 887–891.

[Tor02] Y. Torikai, A. N. Perevezentsev, M. M. Matsuyama and K. Watanabe, Effect of water on tritium decontamination of stainless steel, *Fusion Science and Technology*, 41 (2002) 736–740.

[Tor04] Y. Torikai, R.-D. Penzhorn, M. Matsuyama and K. Watanabe, Tritium uptake by SS316 and its decontamination, *Journal of Nuclear Materials*, 329-333 (2004) 1624–1628.

[Tor05a] Y. Torikai, M. Matsuyama, N. Bekris, M. Glugla, P. Coad, W. Naegele, A. Erbe, N. Noda, V. Philipps and K. Watanabe, Tritium distribution in JET mark IIA type divertor tiles analysed by BIXS, *Journal of Nuclear Materials*, 337-339 (2005) 575–579.

[Tor05b] Y. Torikai, R.-D. Penzhorn, M. Matsuyama and K. Watanabe, Chronic release of tritium from SS316 at ambient temperature: Correlation between depth profile and tritium liberation, *Fusion Science and Technology*, 48(1) (2005) 177–181.

[Tor07] Y. Torikai, D. Murata, R.-D. Penzhorn, K. Akaishi, K. Watanabe and M. Matsuyama, Migration and release behavior of tritium in SS316 at ambient temperature, *Journal of Nuclear Materials*, 363-365 (2007) 462–466.

[Tor13] Y. Torikai, A. Taguchi, M. Saito, R.-D. Penzhorn, Y. Ueda, H. Kurishita, K. Sugiyama, V. Philipps, A. Kreter and M. Zlobinski, Tritium loading study of tungsten pre-exposed to TEXTOR plasmas, *Journal of Nuclear Materials*, 438 (2013) S1121–S1124.

[Tor15a] Y. Torikai, V. K. Alimov, K. Isobe, M. Oyaidzu, T. Yamanishi, R.-D. Penzhorn, Y. Ueda, H. Kurishita, V. Philipps, A. Kreter and M. Zlobinski, Tritium trapping on the plasma irradiated tungsten surface, *Fusion Science and Technology*, 67(3) (2015) 619–622.

[Tor15b] Y. Torikai and R.-D. Penzhorn, Tritium release from SS316 under vacuum condition, *Fusion Science and Technology*, 67(3) (2015) 615–618.

[Tos01] R. Toschi, P. Barabaschi, D. Campbell, F. Elio, D. Maisonnier and D. Ward, How far is a fusion power reactor from an experimental reactor, *Fusion Engineering and Design*, 56-57 (2001) 163–172.

[Tos97] R. Toschi, Nuclear fusion, an energy source, *Fusion Engineering and Design*, 36(1) (1997) 1–8.

[Tot00] T. C. Totemeier, Characterization of uranium corrosion products involved in a uranium hydride pyrophoric event, *Journal of Nuclear Materials*, 278(2-3) (2000) 301–311.

[Tri77] D. L. Trimm, The formation and removal of coke from nickel catalyst, *Catalysis Reviews*, 16(1) (1977) 155–189.

[Tri91] Tritium Laboratory Karlsruhe, TLK Sicherheitsbetrachtung, Technical Report TLK-S-91/001, (1991).

[Tri96] Tritium Laboratory Karlsruhe, Sicherheitstechnische Beschreibung, Tritium Lager Grundstufe (TLG), Technical Report TLK-5.10/16-1, (1996).

[Tru70] J.-L. Truffier and P. Corpechot, Dosage du Tritium dans Metaux par Combustion sous Oxygéne, technical report CEA-R-4020, Service Central de Documentation du C.E.A., Gif-sur-Yvette, France (1970).

[Tsu11] K. Tsukatani, Y. Ueda, K. Tanimoto, H. T. Lee, Y. Ohtsuka, M. Taniguchi, T. Inoue, K. Sakamoto, I. Takagi and N. Yoshida, Deuterium retention in damaged tungsten, *Fusion Science and Technology*, 60(4) (2011) 1543–1547.

[Tuo88] J. M. Tuohy, R. Cherdack and N. H. Lacy, System design for disposal of tritium at TFTR, *Fusion Technology*, 14(2P2B) (1988) 995–999.

[Tur80] J. Turnbull, S. Kessler and E. G.Y., Investigation of non-magnetic alloys for the suppression of tritium permeation, DOE/ER/10087-T1, Thermacore, Inc, Lancaster, PA, USA (1980).

[Tyb09] B. Tyburska, V. K. Alimov, O. V. Ogorodnikova, K. Schmid and K. Ertl, Deuterium retention in self-damaged tungsten, *Journal of Nuclear Materials*, 395(1-3) (2009) 150–155.

[Tyb11] B. Tyburska, V. K. Alimov, O. V. Ogorodnikova, K. Ertl, K. Schmid and J. Roth, Trapping of permeating deuterium in defect induced at the rear side of tungsten samples, *Journal of Nuclear Materials*, 415(1) (2011) S680–S683.

[Uch02] M. Uchida, E. Ishitsuka and H. Kawamura, Tritium release properties of neutron-irradiated $Be_{12}Ti$, *Journal of Nuclear Materials*, 307-311 (2002) 653–656.

[Uch08] Y. Uchida, K. Katayama, T. Okamura, R. Imaoka, M. Nishikawa and S. Fukada, Hydrogen retention in deposition layers formed from type 316 stainless steel, *Fusion Science and Technology*, 54(2) (2008) 545–548.

[Uch84] H. Uchida, H. Uchida and Y. C. Huang, Effect of the pulverization of $LaNi_5$ on the hydrogen absorption rate and the X-ray diffraction patterns, *Journal of the Less Common Metals*, 101 (1984) 459–468.

[Uda91] T. Uda, K. Okuno, S. O´hira and Y. Naruse, Application study of laser Raman spectroscopy to in situ gas analysis for fusion fuel processing systems, *Fusion Technology*, 19(3P2B) (1991) 1651–1656.

[Uda92a] T. Uda, K. Okuno and Y. Naruse, Application of laser Raman spectroscopy to analysis of isotopie C_2 hydrocarbons in fusion fuel gas processing, *Journal of Nuclear Science and Technology*, 29 (1992) 288–295.

[Uda92b] T. Uda, K. Okuno and Y. Naruse, Application of laser Raman spectroscopy to isotopic methanes analysis in fusion fuel gas processing systems, *Fusion Technology*, 21(2P2) (1992) 436–441.

[Uda92c] T. Uda, K. Okuno and Y. Naruse, Hydrogen isotope exchange reaction rate in tritium and methane mixed gas, *Journal of Radioanalytical and Nuclear Chemistry*, 159(1) (1992) 145–154.

[UK 12] UK Government, Scottish Government, Welsh Government and Department of the Environment, Northern Ireland, Strategy for the Management of Solid Low Level Radioactive Waste from the Non-Nuclear Industry in the United Kingdom: part

1 – anthropogenic radionuclides, policy paper, Department of Energy and Climate Change, (2012).

[Ulm90] D. G. Ulmer and C. J. Alstetter, Mechanism for hydrogen embrittlement of austenitic stainless steels, hydrogen effects on material behavior, Sept. 12–16, 1989, Jackson Hole, WY , USA, (1990) 421–432.

[US 02] US Department of Energy, Radiological Training for Tritium Facilities, DOE Handbook DOE-HDBK-1105-2002, Washington, DC, USA (2002).

[US 08] US Department of Energy, Radiological Worker (RW) Training, DOE Handbook DOE-HDBK-1130-2008, Washington, DC, USA (2008).

[US 15] US Department of Energy, Tritium Handling and Safe Storage, DOE Handbook DOE-STD-1129-2015, Washington, DC, USA (2015).

[US 73] US Department of Energy, DOE Handbook, Tritium Handling and Safe Storage, Tech. report DOE-HDBK-1129-2008, (1973).

[US 94] US Department of Energy, Primer on Tritium Safe Handling Practices, DOE Handbook DOE-HDBK-1079-94, FSC-6910, Washington, DC, USA (1994).

[USN03] USNRC Technical Training Center, Dose Standards and Methods for Protection against Radiation and Contamination, Reactor Concepts Manual Rev 0603, Chattanooga, TN, USA (2003).

[Van79] D. E. Vance, M. E. Smith and G. R. Waterbury, Quantitative Determination of Tritium in Metals and Oxides, technical report LA-7716UC, Los Alamos, NM, USA (1979).

[Van82] E. V. Vansant, A. Thijs, G. Peeters, P. de Bievre P. and I. Verhaert, Occlusion and storage of krypton in solids, *European Applied Research Reports, A Journal of Science and Technology, Nuclear Science and Technology Section*, 4(4) (1982) 893–944.

[Vee88] A. V. Veen, H. A. Filius, J. D. Vries, K. R. Bijkerk, G. J. Rozing and D. Segers, Hydrogen exchange with voids in tungsten observed with TDS and PA, *Journal of Nuclear Materials*, 155-157 (1988) 1113–1117.

[Vei85] K. Veirs, A Raman Spectroscopic Investigation of Molecular Hydrogen, technical report LBNL-20565, Lawrence Berkeley National Laboratory, Berkley, CA, USA (1985).

[Ven02] T. Venhaus, R.-D. Penzhorn and N. Causey R.A.and Bekris, The effect of UV light irradiation on the removal of tritium from co-deposited carbon-tritium layer in fusion reactors, *Journal of Nuclear Materials*, 302 (2002) 224–226.

[Ver05] Y. Verzilov, K. Ochiai and T. Nishitani, Methods for tritium production rate measurement in design-oriented blanket experiments, *Fusion Science and Technology*, 48(1) (2005) 650–653.

[Vit11] A. Vitins, V. Zubkovs, G. Kizane, E. Pajuste and V. Kinerte, Tritium release characteristics of neutron-irradiated reference beryllium pebbles for the Helium Cooled Pebble Bed (HCPB) blanket, *Fusion Science and Technology*, 60(3) (2011) 1143–1146.

[Voe71] J. Voelkl, G. Wollenweber, K.-H. Klatt and G. Alefeld, Notizen: Reversed isotope dependence for hydrogen diffusion in palladium, *Zeitschrift fuer Naturforschung A*, 26(5) (1971) 922–923.

[Vog88] R. Vogd, H. Ringel, H. Hackfort, T. Schober and C. Dieker, Gas chromatographic separation of hydrogen isotopes on molecular sieves, *Fusion Technology*, 14(2P2A) (1988) 574–578.

[Vol95] T. Vollmer, U. Besserer, K. Borcherding, J. Dehne, H. Dilger, L. Doerr, M. Glugla, W. Hellriegel, E. Hutter, R. Kraemer, R.-D. Penzhorn, B. Reinhardt, D. Roehrig and K. Schubert, Safety concept for the Tritium Laboratory Karlsruhe (TLK), *Fusion Technology*, 28(3P1) (1995) 988–994.

[Voo70] M. Voorde, Effects of Radiation on Materials and Components, technical report CERN-70-5, European Organization for Nuclear Research, Geneva, Switzerland (1970).

[Voo95] D. R. Voorhees, R. L. Rossmassler and G. Zimmer, Tritium analysis at TFTR, *Fusion Technology*, 28(3P2) (1995) 1083–1089.

[Wag09] R. Wagner, Design and manufacturing of an ion chamber for activity measurements of tritiated gases, Master's thesis, Faculty of Mechanical Engineering, KIT, (2009).

[Wag15] R. Wagner, D. Demange, E. Fanghaenel, T. L. Le, M. Schwarz and K.-H. Simon, Dismantling of the PETRA glove box: Tritium contamination and inventory assessment, *Fusion Science and Technology*, 67(3) (2015) 631–634.

[Wag83] J. E. Wagner, A Calorimetric Study of the Palladium Hydride and Deuteride Systems, technical report MLM-3283, UC4, Mound Laboratory, Miamisburg, OH, USA (1983).

[Wak98] E. Wakai, N. Hashimoto, K. Shiba, T. Sawai, J. P. Robertson and R. L. Klueh, Microstructural Evolution of HFIR-Irradiated Low Activation F82H and F82H-sup10B Steels, Semi-Annual Report DOE/ER-0313/23, Fusion Materials, Oak Ridge National Laboratory, Oak Ridge, TN, USA (1998).

[Wal02] R. T. Walters, K. Sessions, C. Gentile and L. Ciebiera, Tritiated water on molecular sieve without hydrogen production, *Fusion Science and Technology*, 41(3P2) (2002) 685–689.

[Wal39] L. Waldmann, Zur Theorie des Isotopentrennverfahrens von Clusius und Diekel. I, *Zeitschrift fuer Physik*, 114(1-2) (1939) 53–81.

[Wal90] C. Walthers, D. Sedgley, T. Batzer, D. Lang, D. Hathaway, H. Fukai, K. Okuno, N. Enoeda, T. Ide and Y. Naruse, Co-pumping of deuterium-helium and tritium-helium mixtures at TSTA, *Proceedings of the 13th Symposium on Fusion Engineering (SOFE)*, Oct. 2–6, 1989, Knoxville, TN, USA, (1990) 959–962.

[Wal91a] R. T. Walters, Kinetics and mechanism for the radiolytic formation of NT_3, technical report WSRC-TR-91-390, Tritium Systems Test Assembly, Los Alamos National Laboratory (LANL), Los Alamos, NM, USA (1991).

[Wal91b] C. R. Walthers, E. M. Jenkins, D. W. Sedgley, T. H. Batzer, S. Konishi, S. O´hira and Y. Naruse, Continued studies of co-pumping of deuterium and helium on a single, 4 K activated charcoal panel, *Fusion Technology*, 19(3P2B) (1991) 1811–1813.

[Wal94] C. R. Walthers and E. M. Jenkins, The Tritium Systems Test Assembly self-assaying portable uranium bed, *Proceedings of the 15th Symposium on Fusion Engineering (SOFE)*, Oct. 11–15, 1993, Hyannis, MA, USA, (1994) 56–60.

[Wal97] R. T. Walters, The mechanism of self-radiolysis of tritiated water on molecular sieve: gas phase hydrogen isotopic distribution, *Proceedings of the 19th Symposium on Fusion Technology (SOFT)*, Sept. 16–20, 1996, Lisbon, Portugal, (1997) 1241–1244.

[Wam84] W. R. Wampler, Retention and thermal release of deuterium implanted in beryllium, *Journal of Nuclear Materials*, 123(1-3) (1984) 1598–1602.

[Wam92] W. R. Wampler, Trapping of deuterium in beryllium, *Journal of Nuclear Materials*, 196-198 (1992) 981–985.

[Wam94] W. R. Wampler and B. L. Doyle, Low-energy beta spectroscopy using pin diodes to monitor tritium surface contamination, *Nucl. Instruments and Methods in Physics Research A*, 349 (1994) 473–480.

[Wan01] W. Wang, J. Roth, S. Lindig and C. H. Wu, Blister formation of tungsten due to ion bombardment, *Journal of Nuclear Materials*, 299(2) (2001) 124–131.

[Wan04] D. Wang, T. B. Flanagan and K. L. Shanahan, Permeation of hydrogen through pre-oxidized Pd membranes in the presence and absence of CO, *Journal of Alloys and Compounds*, 372(1-2) (2004) 158–164.

[Wan13] M. N. Y. Wang, B. Yuan, J. Jiang and Y. Wu, Tritium supply assessment for ITER and DEMOnstration power plant, *Fusion Engineering and Design*, 88(9-10) (2013) 2422–2426.

[War05] D. J. Ward, I. Cook, Y. Lechon and R. Saez, The economic viability of fusion power, *Fusion Engineering and Design*, 75-79 (2005) 1221–1227.

[War76] D. K. Warner, R. E. Sprague and D. R. Bohl, Potential Application of Gas Chromatography to the Analysis of Hydrogen Isotopes, technical report MLM-2356, Mound Laboratory, Miamisburg, OH, USA (1976).

[Wat05] K. Watanabe, M. Matsuyama, Y. Hatano, Y. Torikai and M. Hara, Development of methods and techniques for decontamination of metals and alloys contaminated with tritium, research report C012502, University of Toyama, Hydrogen Isotope Research Centre, Toyama, Japan (2005).

[Wat07] D. Watanabe, Y. Sakawa, T. Shibahara, K. Sugiyama, T. Shoji, K. Yamazaki and T. Tanabe, Properties of hydrogen desorption from co-deposits on JT-60 graphite tile by pulsed-laser ablation, *Journal of Nuclear Materials*, 363-365 (2007) 972–976.

[Wat10] K. Watanabe, W. Shu and M. Matsuyama, Kinetics of Methane Decomposition over Zr – Ni alloys, Toyama University Annual Report, Hydrogen Isotope Research Center, Toyama, Japan (2010).

[Wat87] K. Watanabe, H. Miyake and M. Matsuyama, Relative sensitivities of Bayard-Alpert gauges and a quadrupole mass spectrometer for hydrogen isotope molecules, *Journal of Vacuum Science & Technology A: Vacuum, Surfaces, and Films*, 5(2) (1987) 237–241.

[Wat88] K. Watanabe, K. Ichimura, K. Ashida, M. Matsuyama and T. Takeuchi, Gettering of hydrogen isotopes by Zr – Ni alloys, *Fusion Technology*, 14(2P2A) (1988) 729–734.

[Wat89] K. Watanabe, M. Matsuyama, K. Ashida and H. Miyake, Alloying effect on a property of hydrogen gettering materials: an empirical formula to estimate heat of hydride formation for metals and alloys, *Journal of Vacuum Science & Technology A: Vacuum, Surfaces, and Films*, 7(4) (1989) 2725–2729.

[Wat91] K. Watanabe, K. Tanaka, M. Matsuyama and K. Hasegawa, Zr – Ni alloys as candidate getter materials for tritium processing, *Fusion Engineering and Design*, 18 (1991) 27–32.

[Wat95] K. Watanabe, M. Hara, M. Matsuyama, I. Kanesaka and T. Kabutomori, Stability of ZrCo and ZrNi to heat cycles in hydrogen atmosphere, *Fusion Technology*, 28(3P2) (1995) 1437–1442.

[Wea70] R. C. Weast, CRC Handbook of chemistry and physics, 50th edition, The Chemical Rubber Co., Cleveland, OH, USA (1970).

[Wea94] W. W. Weaver, Guidelines for valves in tritium service, *Fusion Technology*, 25(4) (1994) 428–433.

[Weg09] L. Wegener, Status of Wendelstein 7-X construction, *Fusion Engineering and Design*, 84(2-6) (2009) 106–112.

[Wei05] C. Weinheimer, Measuring neutrino properties with tritium, *Fusion Science and Technology*, 48(1) (2005) 723–730.

[Wei99] C. Weinheimer, B. Degenddag, A. Bleile, J. Bonn, L. Bornschein, O. Kazachenko, A. Kovalik and E. W. Otten, High precision measurement of the tritium β spectrum near its endpoint and upper limit on the neutrino mass, *Physics Letters B*, 460(1-2) (1999) 219–226.

[Wel09] S. Welte, G. Ana, I. Cristescu, L. Doerr, B. Kuntz, J. Konrad and R. Michling, Construction and commissioning of an ITER sized Pd/Ag permeator for a water detritiation experiment, *Fusion Engineering and Design*, 84(7-11) (2009) 1969–1972.

[Wel10] S. Welte, D. Demange and R. Wagner, Mechanical design and first experimental results of an upgraded technical PERMCAT reactor for tritium recovery in the fuel cycle of a fusion machine, *Fusion Engineering and Design*, 85(7-9) (2010) 1320–1325.

[Wel11] S. Welte, D. Demange and R. Wagner, Characterisation of a multitube PERMCAT reactor in view of a technical facility for highly tritiated water processing at the Tritium Laboratory Karlsruhe, *Fusion Engineering and Design*, 86(9-11) (2011) 2237–2240.

[Wel12] S. Welte, D. Demange, R. Wagner and N. Gramlich, Development of a technical scale PERMCAT reactor for processing of highly tritiated water, *Fusion Engineering and Design*, 87(7-8) (2012) 1045–1049.

[Wel13] S. Welte, I. Cristescu, H. Dittrich, N. Lohr, C. Melzer, R. Michling, C. Plusczyk and P. Schaefer, Setup and commissioning of a combined water detritiation and isotope

separation experiment at the Tritium Laboratory Karlsruhe, *Fusion Engineering and Design*, 88(9-10) (2013) 2251–2254.

[Wel15] S. Welte, U. Besserer, D. Osenberg and J. Wendel, Tritium Laboratory Karlsruhe: Administrative and technical framework for isotope laboratory operation, *Fusion Science and Technology*, 67(3) (2015) 635–638.

[Wen17a] S. Wen, K. H. He, H. N. Cui, M. Pan, Z. Huang and Y. Zhao, Migration properties of mono-vacancy in W-$4d/5d$ transition metal alloys, *Journal of Alloys and Compounds*, 728 (2017) 363–367.

[Wen17b] S. Wen, H. Zhang, K. H. He, X. S. Yang, H. N. Cui, M. Pan, Z. Huang and Y. Zhao, The study of defect structure in tungsten: Rotation and migration property for the self-interstitial atoms, *Fusion Engineering and Design*, 124 (2017) 1122–1126.

[Wen77] R. G. Wensel, Resistance of O-Ring Seal Compounds to Heat and Ionizing Radiation in Air and in Water, technical report AECL-5697, Atomic Energy of Canada Ltd, Chalk River, Canada (1977).

[Wen82] H. Wenzl, Properties and applications of metal hydrides in energy conversion systems, *International Metals Reviews*, 27(1) (1982) 140–168.

[Wer02] G. Wermann, D. Alber, W. Pritzkow, G. Riebe, J. Vogl and W. Goerner, Determination of the β- branching ratio of ^{64}Cu by mass spectrometric investigations of the decay products in neutron transmuted copper, *Applied Radiation and Isotopes*, 56(1-2) (2002) 145–151.

[Wer92] J. R. Wermer, Quantification of Tritium"Heels"and Isotope Exchange Mechanisms in La-Ni-Al tritides, technical report WSRC-TR-92-368, Westinghouse Savannah River Company, Savannah River Site, Aiken, SC, USA (1992).

[Wer93] J. R. Wermer, Analysis of $LaNi_{4.25}Al_{0.75}$ (LANA75) Tritide after Five Years of Tritium Exposure (U), technical report WSRC-TR-93-453, Westinghouse Savannah River Company, Savannah River Site, Aiken, SC, USA (1993).

[Wer94] J. R. Wermer, Characterization of $LaNi_{4.25}Al_{0.75}$ Tritide for Use as Long Term Tritium Storage Medium (U), technical report WSRC-TR-93-453, Westinghouse Savannah River Company, Savannah River Site, Aiken, SC, USA (1994).

[Wer96] J. R. Wermer, Analysis of Residual Tritium in an LP50 Product Container, technical report WSRC-TR-96-0107, Rev. 1, Westinghouse Savannah River Company, Savannah River Site, Aiken, SC, USA (1996).

[Wes80a] A. J. West and D. C. Rawl, Hydrogen in stainless steels: Isotopic effects on mechanical properties, *The International Journal of Applied Radiation and Isotopes*, 31(8) (1980) 466.

[Wes80b] D. G. Westlake, Stoichiometries and interstitial site occupation in the hydrides of ZrNi and other isostructural intermetallic compounds, *Journal of the Less-Common Metals*, 75(2) (1980) 177–185.

[Wex59] S. Wexler, Dissociation of TH and T_2 by β-decay, *Journal of Inorganic and Nuclear Chemistry*, 10(1-2) (1959) 8–16.

[Whi92] G. D. Whitlock, Tritium surface contamination measurements with international credibility, *Fusion Technology*, 21(2P2) (1992) 523–528.

[Wic62] E. Wicke and K. Otto, Über das system uran — Wasserstoff und die kinetik der uranhydridbildung, *Zeitschrift fuer Physikalische Chemie*, 31(3/4) (1962) 222–248.

[Wic64] E. Wicke and G. H. Nernst, Zustandsdiagramm und thermodynamisches Verhalten der Systeme Pd/H_2 und Pd/D_2 bei normalen Temperaturen; H/D-Trenneffekte, *Berichte der Bunsengesellschaft fuer physikalische Chemie*, 68(3) (1964) 224–235.

[Wie79] R. E. Wieneke, J. J. Dauby, G. C. Abell, W. E. Tadlok, P. H. Lamberger and G. E. G.E. Gibbs, Polymer Impregnated Tritiated Concrete, final report MLM-2644, Mound Laboratories, Miamisburg, Ohio, USA (1979).

[Wie90] P. Wienhold, Wall conditioning techniques for fusion devices, *Vacuum*, 41(4-6) (1990) 1483–1485.

[Wie92] R. E. Wieneke, Catalytic reactor system for the Tritium Emissions Reduction Facility, *Fusion Technology*, 21(2P2) (1992) 577–582.

[Wie97] M. Wielunski, M. Mayer, R. Behrisch, J. Roth and B. M. U. Scherzer, Simultaneous profiling of hydrogen and deuterium by 2.6 MeV ^{4}He ERDA using a ΔE-E telescope detector, *Nuclear Instruments and Methods in Physics Research Section B*, 122 (1997) 113–120.

[Wil02] R. S. Willms and R. Rabun, US tritium activities, *Fusion Science and Technology*, 41(3P2) (2002) 339–345.

[Wil03] R. S. Willms, Tritium supply considerations, *Proceedings of the Fusion Developments Paths Considerations Workshop*, Jan. 14, 2003, (2003).

[Wil05] R. S. Willms, Simplified estimation of tritium inventory in stainless steel, *Fusion Science and Technology*, 48(1) (2005) 204–207.

[Wil66] R. E. Wilson, C. Barnes, R. Koonz and L. Baker, Isothermal reaction of uranium with steam between 400 and 1600 °C, *Nuclear Science and Engineering*, 25(2) (1966) 109–115.

[Wil88] E. Willin, M. Sirch, R.-D. Penzhorn and M. Devillers, Metal getters for tritium storage, *Fusion Technology*, 14(2P2A) (1988) 756–763.

[Wil93] R. S. Willms, M. Glugla and R.-D. Penzhorn, Simplified analysis of a "plug flow" palladium permeator, *Proceedings of the 17th symposium on Fusion Technology (SOFT)*, Sept. 14–18, 1992, Rome, Italy, (1993) 1244–1248.

[Wil94a] R. S. Willms, Cryogenic adsorption of low-concentration hydrogen on charcoal, 5A molecular sieve, UOP S-115, ZSM-5 and Wessalith DAY, *Proceedings of the 15th Symposium on Fusion Engineering (SOFE)*, Oct. 11–15, 1993, Hyannis, MA, USA, (1994) 61–64.

[Wil94b] R. S. Willms and K. Okuno, Recovery of hydrogen from impurities using a palladium membrane reactor, *Proceedings of the 15th Symposium on Fusion Engineering (SOFE)*, Oct. 11–15, 1993, Hyannis, MA, USA, (1994) 85–90.

[Wil95a] R. S. Willms, S. A. Birdsell and R. C. Wilhelm, Recent palladium membrane reactor development at the Tritium Systems Test Assembly, *Fusion Technology*, 28(3P1) (1995) 772–777.

[Wil95b] R. S. Willms, D. Taylor, M. Enoeda and K. Okuno, Practical-scale tests of cryogenic molecular sieve for separating low-concentration hydrogen isotopes from helium, *Fusion Engineering and Design*, 28(1-2) (1995) 386–391.

[Wil95c] R. S. Willms, R. Wilhelm and S. Konishi, Performance of a palladium membrane reactor using an Ni catalyst for fusion fuel impurities processing, *Fusion Engineering and Design*, 28 (1995) 397–405.

[Wil97] M. D. Williams, D-T operation on TFTR, *Fusion Engineering and Design*, 36(1) (1997) 135–142.

[Wim08] E. Wimmer, W. Wolf, J. Sticht, P. Saxe, C. B. Geller, R. Najafabadi and G. A. Young, Temperature-dependent diffusion coefficients from ab initio computations: Hydrogen, deuterium, and tritium in nickel, *Physical Review B*, 77(13) (2008) 134505.

[Win01] J. Winter, Is dust formation a concern for fusion devices?, *Journal of Plasma Fusion Research*, 4 (2001) 153–160.

[Win92] J. Winter, H. G. Esser, V. Philipps, T. Rose, J. von Seggern, E. Vietzke and P. Wienhold, Surface treatment of the first wall in fusion devices (carbonization, boronization and related surface chemistry), *Vacuum*, 43(5-7) (1992) 413–417.

[Wir11a] M. Wirtz, J. Linke, G. Pintsuk, J. Rapp and G. Wright, Influence of high flux hydrogen-plasma exposure on the thermal shock induced crack formation in tungsten, *Journal of Nuclear Materials*, 420 (2011) 124–131.

[Wir11b] M. Wirtz, J. Linke, G. Pintsuk, L. Singheiser and I. Uytdenhouwen, Comparison of the thermal shock performance of different tungsten grades and the influence of microstructure on the damage behaviour, *Physica Scripta*, T145 (2011) 014058.

[Wis72] R. H. Wiswall and J. J. Reilly, Inverse hydrogen isotope effects in some metal hydride systems, *Inorganic Chemistry*, 11(7) (1972) 1691–1696.

[Wit75] L. Wittenberg, J. Bixel, J. Braun, D. Hobrock, C. Kershner, J. Miles, T. Rhinehammer, R. Watkins and W. Wilkes, Evaluation Study of the Tritium-Handling Requirements of a Tokamak Experimental Power Reactor, technical report MLM-2259, TID-4500, Mound Laboratories, Miamisburg, Ohio, USA (1975).

[Wob97] H. Wobig, Der Stellarator als Fusionskraftwerk, *ATW Internationale Zeitschrift fuer Kernenergie*, 42 (1997) 449.

[Wol65] L. Wolniewicz, Variational treatment of the HeH^+ ion and the β-decay in HT, *The Journal of Chemical Physics*, 43(4) (1965) 1087–1091.

[Won84] K. Y. Wong, D. P. Dautovich, P. Mayer and F. Guglielmi, Permeation of tritium through steam generator tubes at CANDU stations, *Proceedings of the 10th Symposium on Fusion Engineering (SOFE)*, Dec. 5–9, 1983, Philadelphia, PA, USA, (1984) 142–146.

[Won91] K. Y. Wong, B. Hircq, R. A. Jalbert and W. T. Shmayda, Tritium decontamination of machine components and walls, *Fusion Engineering and Design*, 16 (1991) 159–172.

[Won92] D. P. Wong, J. L. Hemmerich and J. J. Monahan, The exhaust detritiation system for the JET Active Gas Handling Plant - engineering, construction, installation and first commissioning results, *Fusion Technology*, 21(2P2) (1992) 572–576.

[Woo16] S. Woods and J. A. Lee, Hydrogen Embrittlement, technical report TM-2016-218602, National Aeronautics and Space Agency (NASA), Huntsville, AL, USA (2016).

[Wor13] World Nuclear Transport Institute WNTS, Packages types used for transporting radioactive materials, https://www.wnti.co.uk/wp-content/uploads/2021/01/FS2_EN_MAR13_V2.pdf, (2013), (visited on Apr. 13, 2022).

[Wu90] C. H. Wu, E. Hechtl, H. R. Yang and W. Eckstein, Erosion of beryllium by oxygen, *Journal of Nuclear Materials*, 176-177 (1990) 845–847.

[Wul86] H. G. Wulv and E. Fromm, Hydrogen absorption by FeTi-, $LaNi_5$-, TiNi-, TiPd- and $TiMn_2$-film samples at low pressures and 300 K, *Journal of the Less-Common Metals*, 118(2) (1986) 315–326.

[Wyk05] M. Wykes, Minimisation of the hydrogenic inventory of the ITER neutral beamline and torus cryo-sorption pumps, *Fusion Science and Technology*, 48(1) (2005) 39–42.

[Wyl63] K. F. Wylie, W. A. Bigler and G. R. Grove, Biological half-life of tritium, *Health Physics*, 9(9) (1963) 901–942.

[Xia11] X. Xiao and L. K. Heung, Cryogenic adsorption of hydrogen isotopes over nano-structured materials, *Fusion Science and Technology*, 60(4) (2011) 1415–1418.

[Yam02] M. Yamada, T. Yamanishi, W. Shu, T. Suzuki, H. Nakamura, Y. Kawamura, Y. Iwai, K. Kobayashi, K. Isobe and M. Nishi, Operation results on safety systems of Tritium Process Laboratory in Japan Atomic Energy Research Institute, *Fusion Science and Technology*, 41(3P2) (2002) 593–597.

[Yam08] T. Yamanishi, M. Yamada, T. Suzuki, W. Shu, Y. Kawamura, H. Nakamura, Y. Iwai, K. Kobayashi, K. Isobe, S. Hoshi and T. Hayashi, Operational results of the safety systems of the Tritium Process Laboratory of the Japan Atomic Energy Agency, *Fusion Science and Technology*, 54(1) (2008) 315–318.

[Yam11a] T. Yamanishi, M. Yamada, T. Suzuki, Y. Kawamura, H. Nakamura, Y. Iwai, K. Kobayashi, K. Isobe, H. Inomiya and T. Hayashi, Past 25 years results for large amount of tritium handling technology in JAEA, *Fusion Science and Technology*, 60(3) (2011) 1083–1087.

[Yam11b] H. Yamasaki, K. Kashimura, T. Kanazawa, K. Katayama, N. Yamashita, S. Fukada and M. Nishikawa, Effect of water formation reaction on tritium release behavior from Li_4SiO_4, *Fusion Science and Technology*, 60(3) (2011) 1151–1154.

[Yam77] K. Yamakawa and F. E. Fujita, Diffusion of hydrogen in hydrogen-quenched nickel, *Japanese Journal of Applied Physics*, 16(10) (1977) 1747–1752.

[Yam79] K. Yamakawa, Diffusion of deuterium and isotope effect in nickel, *Journal of the Physical Society of Japan*, 47(1) (1979) 114–121.

[Yam83] Y. Yamanishi, T. Tanabe and S. Imoto, Hydrogen permeation and diffusion through pure Fe, pure Ni and Fe–Ni alloys, *Transactions of the Japan Institute of Metals*, 24(1) (1983) 49–58.

[Yam85] T. Yamanishi, M. Kinoshita, K. Okuno and H. Yoshida, Brief Review on Tritium Recovery from Inert Gases by Uranium Getter Beds, technical report 85-174, Japan Atomic Energy Research Institute, Tokai-mura, Japan (1985).

[Yam88] T. Yamamoto, S. Supardjo, T. Terai, F. Ono, S. Tanaka and M. Yamawaki, Storage of hydrogen isotopes in uranium alloys, *Fusion Technology*, 14(2P2A) (1988) 764–768.

[Yam89] S. Yamanaka, T. Tanaka, S. Tsuboi and M. Miyake, Effect of oxygen on solubility of hydrogen isotopes in titanium, *Fusion Engineering and Design*, 10 (1989) 303–308.

[Yam90] T. Yamamoto, S. Tanaka and M. Yamawaki, Hydrogen absorption-desorption properties of U_2Ti, *Journal of Nuclear Materials*, 170(2) (1990) 140–146.

[Yam91] T. Yamamoto, H. Kayano, S. Sinaga, F. Ono, S. Tanaka and M. Yamawaki, Hydrogen absorption-desorption properties of UCo, *Journal of the Less-Common Metals*, 172-174 (1991) 71–78.

[Yam94] T. Yamanishi and K. Okuno, Mass transfer in cryogenic distillation column separating hydrogen isotopes, *Journal of Nuclear Science and Technology*, 31(6) (1994) 562–571.

[Yam95a] M. Yamada, M. Enoeda, T. Honma, T. Hayashi, Y. Matsuda and K. Okuno, Operation experience on safety system of Tritium Process Laboratory in Japan Atomic Energy Research Institute, *Fusion Technology*, 28(3P2) (1995) 1376–1381.

[Yam95b] H. Yamai, S. Konishi, M. Hara, K. Okuno and I. Yamamoto, Tritiated water processing using liquid phase catalytic exchange and solid oxide electrolyte cell, *Fusion Technology*, 28(3P2) (1995) 1591–1596.

[Yam96] T. Yamanishi, M. Enoeda, K. Okuno and R. H. Sherman, A control method for the cryogenic distillation column with a feedback stream, *Fusion Technology*, 29(2) (1996) 232–243.

[Yam98] T. Yamanishi, S. Konishi, T. Hayashi, Y. Kawamura, Y. Iwai, T. Maruyama, T. Kakuta, S. O'hira, H. Nakamura, K. Kobayashi, M. Nishi, T. Nagashima and M. Ohta, Demonstration of the integrated fusion fuel loop at the Tritium Process Laboratory of the Japan Atomic Energy Research Institute, *Fusion Technology*, 34(3P2) (1998) 536–540.

[Yan16] Y. Yang, S. Peng, H. Wang, Y. Du and J. Li, Preparation of alveolate hydrophobic catalyst for tritium waste gas treatment, *Fusion Engineering and Design*, 113 (2016) 184–189.

[Yan64] J. Y. Yang and L. H. Gevantman, Tritium β-radiation-induced isotopic exchange with water vapor, *The Journal of Physical Chemistry*, 68(11) (1964) 3115–3119.

[Yas75] H. Yasuda and V. Stannett, Permeability coefficients, *Polymer Handbook*, 2nd edition, Wiley, New York, NY, USA, (1975), 229–241.

[Yos01] H. Yoshida, D. Murdoch, M. Nishi, V. Tebus and S. Willms, ITER R&D: Auxiliary Systems: Tritium Systems, *Fusion Engineering and Design*, 55(2-3) (2001) 313–323.

[Yos02] H. Yoshida, M. Glugla, T. Hayashi, R. Laesser, D. Murdoch, M. Nishi and R. Haange, Design of the ITER Tritium Plant, confinement and detritiation facilities, *Fusion Engineering and Design*, 61-62 (2002) 513–523.

[Yos83a] H. Yoshida, S. Konishi and Y. Naruse, Effects of impurities on hydrogen permeability through palladium alloy membranes at comparatively high pressures and temperatures, *Journal of the Less-Common Metals*, 89(2) (1983) 429–436.

[Yos83b] H. Yoshida, S. Konishi and Y. Naruse, Preliminary design of a fusion reactor fuel cleanup system by the palladium-alloy membrane method, *Fusion Science and Technology*, 3(3) (1983) 471–484.

[Yos85] H. Yoshida, K. Okuno, T. Nagasaki, K. Noda, Y. Ishii and H. Takeshita, Study on a Multi-Component Palladium Alloy Membrane for Fusion Fuel Cycle, technical report JAERI-M 85-113 and JAERI 85-165, Japan Atomic Energy Research Institute, Tokai-mura, Japan (1985).

[Yos89] H. Yoshida, Tritium recovery system for ITER driver blanket, *ITER Fuel Cycle Specialist Meeting*, Aug. 1–11, 1989, Garching, Federal Republic of Germany, (1989).

[Yos92] H. Yoshida, A. Ohara, A. Nakamura, T. Kurasawa, K. Ono, K. Ashibe and S. Kobayashi, Beryllium compatibility in the solid breeder-blanket concept, *Ceramic Transactions*, 27 (1992) 157–174.

[You63] J. R. Young, Palladium-diaphragm hydrogen pump, *Review of Scientific Instruments*, 34(4) (1963) 374–377.

[Yun15] S.-H. Yun, M. H. Chang, H.-G. Kang, D. Y. Chung, Y. H. Oh, K. J. Jung, H. Chung, D. Koo, S. H. Sohn and K.-M. Song, Key technologies for tritium storage bed development, *Fusion Science and Technology*, 67(3) (2015) 671–676.

[Zaj01] B. Zajec and V. Nemanič, Hydrogen bulk states in stainless-steel related to hydrogen release kinetics and associated redistribution phenomena, *Vacuum*, 61(2-4) (2001) 447–452.

[Zaj13] B. Zajec, V. Nemanič, M. Žumer, C. Porosnicu and C. P. Lungu, Hydrogen permeability through beryllium films and the impact of surface oxides, *Journal of Nuclear Materials*, 443(1-3) (2013) 185–194.

[Zak75] A. P. Zakharov, V. M. Sharapov and E. I. Evko, Hydrogen permeability of polycrystalline and monocrystalline molybdenum and tungsten, *Soviet Materials Science*, 9(2) (1975) 149–153.

[Zal94] R. K. Zalavutdinov, A. E. Gorodetsky and A. P. Zakharov, Study of chemical bonds in a-B/C:H films by electron probe microanalysis, *Microchimica Acta*, 114(1) (1994) 533–537.

[Zap82] P. E. Zapp, Effects of tritium in elastomers, *Proceedings of the 10^{th} Annual DOE Compatibility Conference*, Oct. 26–29, 1982, Albuquerque, NM, USA, (1982) 10.

[Zar79] A. S. Zarchy and R. C. Axtmann, Tritium permeation through 304 stainless steel at ultra-low pressures, *Journal of Nuclear Materials*, 79(1) (1979) 110–117.

[Zel66] A. H. Zeltmann and A. E. Florin, Autoradiolysis of tritiated ammonia, *Proceedings of the American Chemical Society Southwest Regional Meeting*, Dec. 1966, Albuquerque, NM, USA, (1966).

[Zha04] D. Zhang, A. Kodama, M. Goto and T. Hirose, Kinetics in hydrogen isotopes cryogenic adsorption, *Separation and Purification Technology*, 37(1) (2004) 1–8.

[Zha06] D. Zhang, L. Zhou, W. Su and Y. Sun, Equilibrium modeling for hydrogen isotope separation by cryogenic adsorption, *Chinese Journal of Chemical Engineering*, 14(4) (2006) 526–531.

[Zha10a] K. Zhang and Y. Hatano, Preparation of Mg and Al phosphate coatings on ferritic steel by wet-chemical method as tritium permeation barrier, *Fusion Engineering and Design*, 85(7-9) (2010) 1090–1093.

[Zha10b] L. Zhang, T. Luo and K. Feng, Conceptual design on interface between ITER and tritium extraction system of Chinese helium-cooled solid breeder test blanket module, *Fusion Engineering and Design*, 85(10-12) (2010) 2213–2216.

[Zha11a] K. Zhang and Y. Hatano, Sealing of pores in sol-gel-derived tritium permeation barrier coating by electrochemical technique, *Journal of Nuclear Materials*, 417(1-3) (2011) 1229–1232.

[Zha11b] K. Zhang, C. Ren, Y. D. He and W. Gao, Preparation of YSZ coatings by thermal pressure and filtration of sol-gel paint (TPFSP) for thermal barrier application, *Surface and Coatings Technology*, 205(19) (2011) 4343–4348.

[Zha12] Z. Zhang, W.-C. Yang, Y.-J. Su, H.-Z. Zhu, C. Qin, J.-S. Yang, M. Liu and J. Du, Helium release from aged palladium tritide, *Journal of Nuclear Materials*, 424 (2012) 216–219.

[Zha17] H. Zhang, A. Ying, M. Abdou, M. Shimada, B. Pawelko and S. Cho, Characterization of tritium isotopic permeation through ARAA in diffusion limited and surface limited regimes, *Fusion Science and Technology*, 72 (2017) 416–425.

[Zie85a] S. B. Ziemecki and G. A. Jones, Interstitial carbon in palladium, *Journal of Catalysis*, 95(2) (1985) 621–622.

[Zie85b] S. B. Ziemecki, G. A. Jones, D. G. Swartzfager, R. L. Harlow and J. Faber, Formation of interstitial palladium-carbon phase by interaction of ethylene, acetylene, and carbon monoxide with palladium, *Journal of the American Chemical Society*, 107(15) (1985) 4547–4548.

[Zie87] S. B. Ziemecki, G. A. Jones and D. G. Swartzfager, Coexistence of hydrogen and carbon solutes in the palladium lattice, *Journal of the Less-Common Metals*, 131(1-2) (1987) 157–162.

[Zin00] S. J. Zinkle and N. M. Ghoniem, Operating temperature windows for fusion reactor structural materials, *Fusion Engineering and Design*, 51-52 (2000) 55–71.

Index

Air sampling
  airborne beryllium, 941, 943, 953
  airborne tritium-contaminated particles, 158, 571, 697, 739, 786, 789, 813, 853, 887, 950
  risky activities, 942
  tritium species, 823, 853, 950
ALCATOR C-Mod, 868–870
  dust and flakes, 868, 870
  effect of boronization on plasma, 917
  molybdenum first wall, 917
Alumina
  applications in tritium technology
    gas chromatography, 551, 553, 556, 558
    high temperature gettering beds, 494
    high temperature oxidation reactor, 898
    humidity sensors, 504
    isotope separation, 660
    isotope separation columns, 659, 660
    support of catalyst, 617, 660, 751, 755, 758, 762, 766, 775
    support of molecular sieve membrane for tritium extraction from helium, 497
  permeability, solubility, diffusivity of hydrogen isotopologues, 314
Aluminium
  applications in tritium technology, 329, 345
  diffusivity, solubility, permeability of hydrogen isotopologues, 330
  solubility of tritium in surface, 186
  welding, 329
Analysis of tritium in liquids or solids, 561, 923
  accelerator mass spectrometer, 574
  autoradiography and imaging plate, 595
  beta scintillator, 573
  beta-induced X-ray spectroscopy (BIXS), 591
  bremsstrahlung counting, 590
  calorimetry (see also calorimeters in tritium service), 579

continuous aqueous tritium monitoring, 571
elastic recoil detection analysis(ERDA), 576
etching, chemical or electrochemical, 599
full combustion, 604
indirectly, via decay helium, 607, 925
infrared analysis of
$T_2{}^{16}O$ and $T_2{}^{18}O$, 28
liquified H_2 or D_2, 521
solid H_2 or solid D_2, 29
T_2O, HDO, DTO and D_2O, 28
liquid scintillation counting, 568
composition of LSC cocktail, 568
interferences, 569
nuclear reaction analysis, 577
outgassing from incinerable waste, 923
PIN diode, 598
smear technique, 570, 923
temperature-programmed desorption, 604
thermal de-sorption, 602
ultra low level at Rossendorf, 569
Analysis of tritium-contaminated gases
determination of volumes, 508
gas chromatography, 548
calibration, 559
capillary, deuterium breakthrough along a, 199, 547
capillary, sampling by long, 517, 555
capillary, sampling by pressurized gas, 553
complex gas mixtures at JET, 552
complex gas mixtures at TLK, 555
conventional, 548
hydrogen isotopes, 549–552
micro gas chromatography, 557
gas sampling, 546
grab sampling, 516
in-line analysis, 516
infrared analysis, 27, 518
Fourier Transform, 521
MEKOS, SPECTRAN spectrometers, 518
ionisation chamber, 561
Jesse effect, 562
Kanne configuration, 146, 788, 789
modelling, 565
open mesh, 563, 566
small volume, 562–565
laser Raman spectroscopy, 522
calibration, 531
cells, 523
determination of helium in presence of tritium, 528
hollow optical glass fibre device, 528
multi-detection system, 527
mass spectrometry, 537
calibration, 545
omegatron, 543
quadrupole mass spectrometer, 542

sampling, 546
sector field mass spectrometer, 538
special mass spectrometer, 545
ortho/para equilibration, 16, 549
preparation of gas mixtures for calibration, 512
proportional counter, 567
tritiated water vapour, determination in a gaseous stream, 571
ASDEX, 1–3
deuterium inventory, 309
glow discharge cleaning, 909
silicon first wall, 918
tritium/deuterium depth profiles in CFC, 574, 577
tungsten first wall, 281

Bellows and membranes, 349
Beryllium, 253
air sampling, 943
airborne limit concentration, 943
analysis, 262
application in fusion machines
as first wall material, 264, 325
formation of blisters and codeposits, 268
neutron multiplier in blankets, 270
Beryllium Management Committee, ITER, 943
chemical properties, 258
compatibility with stainless-steel, 261
modelling of Be/steam oxidation, 259
reaction with oxygen, 258
reaction with steam, 258
synthesis of hydride, 258
Code of Practice for the Safe Use of Beryllium, JET, 943
dedicated tritium-compatible facility Beryllium Controlled Area, JET, 942
diffusivity, solubility, permeation of hydrogen isotopologues, 253
influence on tritium breeding ratio, 170, 313, 648
monitoring, 942, 943, 954
optional neutron multiplier: Be-Ti, 271
smear technique, 942
transmutation and activation reactions of plasma facing material, 266, 883
working with and handling of, 263
Beta particles
energy loss in collisions with molecules, 32
generation of bremsstrahlung, 39
linear energy absorption coefficient of gases, 37
range in dense matter, 36
range in hydrogen, 32
Blankets
Helium Cooled Ceramic Breeders, 477
materials for manufacture of structural components, 220, 325
Test Blanket Modules for ITER, 3, 270

tritium extraction from purge gas of
Dual Cooled Lead Lithium Blanket, 653
Helium Cooled Ceramic Breeder, 647
Helium-Cooled Lithium Lead TBM, 652
tritium permeation into cooling water, 214
tritium supply to ITER by the blanket, 49
Broader Approach, activities in Japan, 4

Calibration
accountancy, 688
determination of volumes, 509
gauges
Bayard-Alpert, 500
Viscovac, 500
general remarks, 497, 607, 688
ionisation chamber, 548
laser Raman, 531
mass spectrometry, 545
moisture meters, 505
preparation of gas mixtures, 512
routine calibrations, 607
tritium breakthrough along a SS304 capillary, 188, 199, 518, 547
Calorimeters in tritium service
comparison of calorimeters, 581
inertial guidance large volume, TLK, 585
inertial guidance temperature control, JET, 583
inertial guidance, TLK, 584
isothermal, TLK, Valduc, 581
Joule effect device, 587, 588
large volume twin cup, CEA, 587
measurement methods for storage beds
adiabatic/isothermal with vacuum insulation, 445
flowing gas, 446–452
static gas, 445, 448
measurement methodsfor storage beds
isothermal procedure, 452
portable uranium bed/calorimeter, 444
power compensation isothermal, TLK, 582
Round Robin measurements, 588
thermoelectric vacuum, TLK, 585
twelve twin cup, Mound, 581
twin cell inertial temperature control, 583
twin cell thermal conduction, HRC, Toyama, Japan, 587
twin cup large volume symmetric heat flow, KEPTL, Korea, 587
Catalysts used in tritium systems, 466
active metal on alumina, 751–758
advanced catalyst recombiner, 724
alveolate hydrophobic platinum, 469
comparison of hydrophylic/hydrophobic noble metal catalysts, 468

Hopcalite, 48, 57, 750, 762–764, 853
hydrophobic, 468, 670, 679, 859
hydrophobic Pt catalyst supported on a SS or ceramic Honeycomb matrix, 468
micro channel catalytic reactor, 470
Ni on SiO_2 or ceramic
decomposition of ethylene, 616
decomposition of methane, 616
plasma fuel recycling process, 616
regeneration, 618
noble metal on molecular sieve, 467
ortho/para hydrogen equilibration, 549, 552
turn over rate for methanation of CO, 471
Ceramics
applications in tritium work
calorimetry, 583
capacitance sensor, 499
catalyst support, 468, 631, 752
ceramic supported palladium-silver thimble, 476
cladding of concrete, 166
electrolysis cells, 637, 642
feed through, 347
induction heating in glove box, 797
isotope separation, 659
lithium ceramic pebble bed, 270
oxygen-permeable high temperature electrode, 476, 636
permeation inhibition, 327
pumps, 379, 384, 412
tritium recycling process, 48
ultra hot metal getter beds, 493, 494
diffusivity, permeability and solubility of hydrogen isotopologues, 314, 330
Chronic release of tritium from metals
determination procedures, 600–603, 889
mitigation, 933
Concrete
cladding with impermeable barrier (tile), 166
composition, 158
decontamination by ablation of wall/floor surfaces, 919
interaction with moisture
penetration rate, 153
sorption, 163
reinforced walls, 949
tritium depth profiles, 158, 162, 918
model, 159
Confinement glove box
air lock, 795
alarms, 367, 715, 740, 774, 785, 799, 810, 812, 815, 825, 828, 953
assembly, 794
blower, 799
cleaning and protection of surfaces, 794
decontamination of surfaces and equipment, 906
detection of non-respirable air, 774

drainage, 795
electrical cables inside of glove boxes, 793
fabrics and insulation materials, 801
feedthrough
decontamination, 889
electrical, 795
service, 796
special, 797
tritium conducting pipe, 797
fire and explosion hazards, 805
fire and explosion prevention, 814
gas supply to, 746
pneumatic valves, 746
primary systems, 747
glove box atmosphere cooling, 804
glove material
Butyl rubber, 150, 800
Hypalon, 151, 801
Neoprene, 800
handling liquid cryo-coolants, 806
instrumentation for alarm release, 716
integral leak rates, 793
interlocks, 810, 812, 825, 830, 832
ionisation chambers, 786
materials to be avoided, 803
moisture control, 805
pressure control, 799
pressure relief bubbler, 799
repair glove box, 382, 465
safety cabinet for pressurized gases, 747
solvents and detergents, 802
vacuum pump installation in a glove box, 420
welding´s, 794
window materials, 792
Confinement glove box, decontamination from tritium of
air atmosphere
catalytic exchange, 774
oxidation/adsorption, 749–761
oxygen-doped chemically inert atmosphere
oxidation/adsorption, 761–770
pure inert gas
gettering, 770
Confinement options, 736
caisson, 743
dedicated stainless-steel vessel, 744
glove box, 740
hood, 739
oversize confinement: ITER cryostat, 699
tent, 738
Containment
alarms, 364–368, 394, 501, 519, 812
design principles, 317–321
evacuation, 376, 413, 610
fetch principle, 613
gas recirculation, 394–396, 611
pumps, 713
gas transfer

procedures, 611
within primary system, 701
integral leak rate, 701
interlocks, 716–719
Active Gas Handling System, JET, 718
heated vessel, 334
pneumatic valves, 342
pumps, 378, 395, 611
storage bed, 686
key small components, 331–347
materials and conditions to be avoided, 802
materials for manufacture of tritium-compatible components, 322
aluminium, 329
copper, 329
glass, ceramics, etc., 330
stainless-steel, 322
over-pressure protective measures
design guidelines, 719
design requirements, 721
over-temperature protective measures, 722
passivation of stainless-steel, 325
aluminizing, 326
bulk alloy modification, 327
ceramic permeation barrier, 327
chemical sealing of porosity, 328
controlled surface oxidation, 327
gold layer, 326
ion implantation, 327
planning including maintenance, 733
supply of gases
inert and reagent, 702
tritium, 704
Controlled area: operation safety
air breathing system, independent, 811
automated control systems, 824
IMMS, CATIA, ENOVIA, DELMIA, 832
ITER, 831
JET, 830
Mound Facility, 828
Safety Integrity Levels, 834
TFTR, 829
TLK, 826
TPL, 825
building for tritium handling, 945
design guidelines, 949
design requirements, 947
ventilation system, 950
Central Decontamination and Storage Facility, 934
component failure analysis (see also Failure), 728
Emergency plan, TSTA, HRC, 823
fire and explosion protection, 802, 813
hand washing, 818, 819
Inspection Handbook, 822
licenses, 821
liquid nitrogen supply, 806

Manufacturing Codes, 824
Office of Certification and Training at TFTR, 822
pressure zoning, 699, 810
protective measures against tritium release, 723
safety cabinet for pressurized gases, 622, 747
Safety Description, 822
Safety Instrumental Functions, 834
Service Instructions, 821
Special Working Instructions, 821
Standards Laboratory at Mound, 812
Technical Delivery and Acceptance Terms, 823
Technical Editing Process, 823
way of conduct in controlled areas, 818
Working Permits, 821
Copper and copper-based alloys
application in
fusion machines, 239
tritium handling facilities, 329
chronic release of tritium, 234, 241
diffusivity, solubility, permeability of hydrogen isotopologues, 233
Lennard-Jones potential model, 238
permeation barrier, 241
solubility of tritium in surface, 186
steam enbrittlement, 329
transmutation products, 240
trapping of hydrogen, 235, 238
Corrosion of iron/stainless-steel
basic aspects, 203
induced by
halides and halogens, 136, 140, 144–145
heavy water moderator, 46
highly tritiated water, 60, 230, 861
nitric and hydrochloric acids, 231
tritium and helium, 169, 208
influence of annealing, 180
Pourbaix diagram, 204, 231
prevention, 180, 231, 369–371
Round Robin tests, 220
Cryo-adsorption of hydrogen isotopologues
adsorption capacity of diverse adsorbers, 481, 484
basic aspects, 480–487
isotheres of helium and hydrogen on charcoal, 400
Langmuir coefficients on 4A, 5A and active charcoal, 484
modelling, 483–487
separation factors, 483, 489
separation of hydrogen isotopologues on 3A zeolite at tailored cryo-temperatures, 489
sizable adsorption beds
TLK, 492
TPL, 491
TSTA, 491
Cryogenic retention of water from a

CO_2 stream, 487

N_2/H_2 stream, 489

Cryogenic traps for retention of water, 476

FONTENAY-AUX-ROSES, 477

ISPRA, 477

TLK, 478

TPL, 477

DEMO

availability of tritium, 50

blankets, 647, 649

comparison with ITER, 50

low activation materials, 220–225

objectives of the project, 4

Tritium Retention System (concept), 759

Electrolyzers for (highly) tritiated water, 474

palladium/silver thimble cathode

VALDUC, 475, 642

potassium hydroxide electrolyte

CHALK RIVER, 670

EVIO, 672

JET, 679

solid polymer electrolyte

ITER, 474

JET/ITER, 681

Large Helical Device, 475

MOUND, 670

TLK, 674

TPL/ITER, 676

stabilized zirconia tube

TPL/TSTA, 476, 636

sulfuric acid electrolyte, SCK/CEN, 642

Failure data analysis of components, 728

Event Data Form, 730

JET and TLK, 732

TPL, 731

TSTA, 728

Ferritic and austenitic heat-resistant construction materials

cleaning, 372

coating, 328, 372

embrittlement by hydrogen, 221, 802

material properties, 222

permeation of hydrogen isotopes, 216

Ferritic steel (see also low activation materials)

incompatibilities, precautions, 333

Filters

applications, 350

sinter, 346

pressure drop study, 101, 425, 442

First wall of fusion devices

coating

boronization, 917

molybdenumisation, 917

siliconisation, 918

decontamination ex situ, 914

oxygen/methane open flame, 916

ruby laser, 914

thermal release, 915
decontamination in situ, 908
flash lights, 909, 912
glow discharge with He/O_2, 909
liquid wash and flush procedure, 909, 912
magnetically vibrated conveyor, 912
pellet blasting, 913
pulsed laser ablation, 909, 911
thermal release, 915
thermo-oxidation, 909
water hammer, 913
radioactivity in potential first wall materials, 884
Fittings
Cajon, 344
Swagelok, 344
Flakes
chemical composition, 869
chronic release of tritium, 915
detritiation in situ of machine, 910
generated in JET vacuum vessel
calorimetry, 580
international transport, 938–941
vacuum cleaner, 939
need for recurrent withdrawal from fusion machine, 912
radiotoxicity, 874
Flame arresters, 347, 816
Flanges
Conflat, 345
KF, 345
welding to pipe, 348
Fusion, advanced concepts
cryogenic inertial confinement fusion, 959
aerogel target, 492
high beta fusion reactor, 959
merging plasmoids, 959
protium/boron fuel, 961
spheromac, 959, 961
Fusion, worldwide efforts, 1

Gaskets
Helicoflex, 346
materials, 345
Getter bed applications other than for tritium storage, 442
evacuation of hydrocarbons, 443
hydrogen compression, 439, 443, 714
incessant evacuation of insulation vacuum, 443
noble gas/nitrogen cover gas purification, 442
purification of hydrogen isotopologues, 442
Glass, quartz
diffusivity and solubility of helium, 168
diffusivity of tritium in borosilicate glass, 169
He interaction with glass or fused quartz, 168

HT ingrowth from a tritium pre-exposed vessel, 202
interaction with tritium, 167
solubility of deuterium in vitreous silica, 167
tritium generation by exposure of borosilicate glass to neutrons, 169

Gold
applications in tritium technology, 242
diffusivity, solubility and permeability of hydrogen isotopologues, 243–245
interaction of hydrogen isotopologues with copper alloys or copper-gold brazing alloys, 241
tritium trapping, 244

HD
synthesis, 514

Heated components, 352
active cooling
with chilled water, 353
with gas, 355
coating for permeation reduction, 327
design, 351
in sizeable tritium-handling facility, 953
thermal insulation, 352

IFMIF, 1, 4, 48–52, 221
Engineering Lithium Test Loop (ELTL), 52
objectives, 51, 883
tritium needs, 49

Inconel-625
as fabrication material of tritium facility, 849
chemical composition, 300
degradation by hydrogen, 323

Isotope effects: hydrogen isotopologues
erosion of carbon from the First Wall, 89
saturation vapour pressures of molecular hydrogen isotopologues, 21
thermodynamic properties and dissociation pressures
palladium hydride isotopologues, 109
titanium hydride isotopologues, 114
uranium hydride isotopologues, 98
zirconium cobalt hydride isotopologues, 117
triple points, boiling points, and critical points, 20

Isotope effects: water isotopologues
ionisation constants of
H_2O and D_2O as function of temperature, 31
H_2O, D_2O, and T_2O at 298 K, 31
physical constants, 29
refraction index, 43
relative vapour pressures, 30
solubility of inorganic and organic species in H_2O and D_2O, 43

ITER: some basic tritium-relevant systems
Automated Control System, 832

Cooling Water System, 215
^{16}N in cooling water, 842, 857
safety tasks at ITER, 355
tritium permeation into blanket cooling water, 214
cryostat, 699
divertor, 3, 240, 278–279, 282, 290, 291, 312, 325, 402, 405, 875, 876, 881–882, 885, 913, 914
evacuation by cryo-pumping, 399–406
first wall, 265
Fuel Cycle System, 831
hydrogen isotope separation, 657
Integrated Model Management System, 832
Kalpurex pumping process for inner fuel cycle, 418
limiter, 881, 882, 885, 914
mercury pumps, 418
pumps, 378, 405, 410, 413
Storage and Delivery System, 125, 132, 442, 685
Tritium Confinement and Detritiation System, 955
tritium inventory estimation, 881
tritium needs, 48
Water Detritiation System, 673, 676

JET
Access Facility, 886
beryllium first wall, 263
calorimetry, 452
Code of Practice for the Safe Use of Beryllium, 943
Controller Dresser Units, 942
decontamination of vacuum vessel, 265
divertor, 264, 270, 289, 306–311, 578, 596, 605, 837, 908–916
first wall materials, 300, 306
limiter, 264, 881, 882, 915, 938
pumping, 384, 409, 711
tritium inventory, 310, 311, 397
tungsten inventory, 292

JT60-U
first wall materials, 300
in situ decontamination, 909
tritium inventory, 850
turbo molecular pumps, 378
VAT valves, 342

KATRIN
advanced BIXS system, 592–594
argon frost cryo-pumping experiment TRAP, 406
determination of neutrino mass at TLK, 5, 532, 533, 592, 612
laser Raman callibration
preparation of accurate gas mixtures: HYDE, TRIHYDE, 531–536

Korea Superconducting Tokamak Advanced Research Reactor (KSTAR)
boronization, 917

Leak rate
detection via
bubble test, 374
dye penetration test, 375
helium/halogen by mass spectrometry, 375
pressure rise, 373
sniff test, 374
total leak rate, 375
virtual leak, 373
of diverse valves, 335–343
standard/non standard tests of Swagelock bellows valves, 338
Low activation materials and iron
Advanced Reduced Activation Alloys (ARAA), 229
applications, 220
diffusivity, solubility and permeability of hydrogen isotopologues in iron, MANET, F82H and BATMAN, 221–225
effect of irradiation or interaction with tritium, 220–229
effect of pre-treatment on diffusivity, 227
optimized plasma-exposed materials, 220–229
8Cr2W(Japan), 220–222
9Cr-2WVT (USA), 220
EUROFER (Europe), 220–222
F82H (Japan), 220–225, 227
MANET, 220
Round Robin tests, 220
tritium trapping in MANET, F82H, BATMAN and EUROFER, 222

Measurement of process parameters
Fourier transform infrared spectroscopy, 521
gas flow meters, 506
hygrometers, 502
infrared spectroscopy, MEKOS, SPECTRAN, 518
laser Raman, 522
oxygen monitor, 470, 506, 774
pressure gauges, 498
pyrometers, 501
thermocouples, 501
vacuum gauges, 500
Metal and oxide surfaces
basics on interaction with H, H_2, H_2O, 316
Metals, alloys of less-common application in fusion technology
heat-resistant alloys, ferritic/austenitic construction materials, stainless-steel base metals
permeation of tritium, 216
pure metals and alloys
solubility and diffusivity of tritium, 300

Model on permeation of a hydrogen isotopologue mixture, 227
Modelling of fuel cycle subsystems and their interdependence
EVIO-4, 683
FLOSHEET, 683
Ovcharov, 683
TRIMO, 683
Molecular sieve bed, 473
advanced adsorber bed design, 724
basic design requirements, 473
in line regeneration, 775
Regeneration System (TSTA), 776
Combined System (TPL), 777
Replacement Tritium Facility (SRS), 775
off-line regeneration, 779
AMOR facility (TLK), 780
Two stage PMR (TFTR), 782
resistance towards radiation, 66
Molybdenum
ALCATOR C-Mod, 917
benefit of a high Z divertor, 918
dust and flakes, 870
diffusivity, solubility of tritium, 300
plasma facing material, 286, 302, 917
thermal insulation, 352
tritium analysis by imaging plate, 596

Nickel
applications, 245
chronic release of tritium, 249
diffusivity, solubility and permeability of hydrogen isotopologues, 250
embrittlement of nickel-based alloys, 252
permeation of deuterium
gas-driven, 248, 251
plasma-driven, 250
trapping of hydrogen isotopologues, 249–252

Occupational hygiene, 839
Oil
decontamination, 900
pump oil, 350
storage of contaminated, 932
Ortho/para hydrogen equilibration by
actvated carbon, 549
ferric oxide, 549
magnesium chloride, 551
Oxygen
monitor, 506
monitoring, 470, 646
Ozone
safety, 70, 699

Paints
coating shredded, tritiated waste with paint, 932
coating stainless-steel or concrete, 165
impact of painted concrete on room detritiation, 154–158

solubility, diffusivity, permeability of tritiated water, 155
sorption of tritiated water on organic construction materials, cement and paints, 152–155
sorption/desorption of tritiated water by paint-coated stainless-steel or concrete, 155, 166
Palladium, 292
ageing of tritide, 110
applications in fusion fuel cycle, 299
carbide, 112
diffusivity and solubility of hydrogen isotopologues, 111, 293–295
H, D, T desorption isotherms from respective hydride, 108, 295
helium release from tritide, 110, 300
Permeator
of nickel or nickel-based alloys
diffusivity, solubility and permeability of hydrogen isotopologues, 245–252
influence of helium-3 on mechanical properties, 253
of palladium-silver alloys, 456
catalytic activity, 456
cause of failures, 464
design concepts, 458, 622, 627, 674
effect of annealing, 296
effect of impurities on performance, 297, 456, 462
H, D, T plateau pressures, 296
modelling, 459
post mortem examination, 465
purification of hydrogen, 456
resistance towards tritium, 297–299, 464–466
thermal insulation, 353
Pipes
cleaning from oil, 370
materials, 331
precautions during installation, 332
specifications, 332
Polymers of potential application in tritium systems, 135–145
Buna N, 146–147, 152
Butyl rubber, 140, 146, 149–152, 800
effect of fillers on radiation resistance, 148
ethylene propylene diene monomer (EPDM), 140, 146–148, 335, 793
ethylene propylene rubber (EPR)
conductor insulation material, 793
jacketing materials, 793
tip seal of automatic valve, 337
exposure of O-rings to tritium during pressure cycling, 147
fluorinated ethylene propylene co-polymer (FEP), 142, 145
fluoro elastomer (KALREZ), 147, 346
high density polyethylene (HDPE), 140, 338, 933

per fluoro alkoxy ethylene co-polymer (PFA), 142, 145, 231
permeability, diffusivity, solubility of HT and HTO through rubbers, 149–150
poly carbonate, 740, 792
poly chloro trifluoro ethylene (KelF), 145, 231, 343, 346
poly tetra fluoro ethylene (Teflon), 140, 231, 343, 563, 672, 711, 804
radiation-induced degradation, 140
resistance to ^{60}Co exposure, 983
polyethylene, 568, 793, 838, 904, 931–932
polyethylene tera phtalate (Mylar), 576, 597
polyimide (Vespel), 138, 139, 142, 145, 335, 337, 342, 344, 346, 415, 661, 760
polypropylene, 140, 152, 793
radiation-induced degradation, 139–148
sulfonated tetra fluoro ethylene co-polymer (Nafion), 141–144, 231, 676, 790
tetra fluoro ethylene-propylene co-polymer (AFLAS), 141
ultra-high molecular weight polyethylene (UHMWPE), 138, 337, 344
Viton A, 145, 147, 338
Process options for fusion exhaust clean-up with full recovery of unburned fuel and waste gas decontamination, 614
hot ceramic getter beds/permeator, TLK, 493
permeator/ceramic electrolyzer, JAERI, 476, 636
CAPER (CAPRICE upgrade) TLK, 622
CAPRICE, TLK, 615
PERMCAT (isotopic swamping) TLK , 620
PMR, TSTA , 627
Tritium Purification System, TFTR , 635
Pumps, 376
based on bellows
Interatom, 394
Metal Bellows, 394
cryo-adsorption, 397
isotheres, 400
screening tests, 397
cryo-compound, 397
cryo-condensation, 397
cryo-pump for ITER, 405
inventory evolution, 402
poisoning by water, 400
prototype, 405
regeneration, 402
cryo-trapping in frost layers at
ITER, Cadarache, 406
KATRIN, TLK, 407

installation of pumps in glove boxes, 420
mercury linear diffusion, ITER, 418
mercury liquid ring, ITER, 418
moving spiral (scroll), 385
influence of water vapour on pump performance, 391
surrogate pumps, 393
oil diffusion, 350
permeation pump
bilayer metal membrane, 417
palladium alloy membrane, 417
reciprocating compressor, oil-free, 415
Roots pump, 409
with ferro fluidic seal, 410
rotary, multistage, 385
sputter ion pumps, 413
SRTI pumps, 412
titanium sublimation pumps, 414
turbo molecular drag pumps, 383
turbo molecular magnetically suspended, 377
effect of prolonged exposure to tritium, 379
vane pump, 396

Radiation protection
Access Facility at JET, 886
air supplied plastic suits, 736
bioassay, 786, 819
decontamination of wall and floor, 918
flexible ventilation duct (elephant trunk), 318, 364, 738, 795, 806, 821, 956
handling of contaminated equipment, 368
inhalation of tritium, 35
personal air sampling, 942
portable clean up system, 739
Radiation Protection Service, 367, 717, 819, 887
room air monitors, 716
detection limit, 716
failure rates, 728
tent for work at open glove box, 738
workers protection, 367
Remote handling, 837
In-vessel Training Facility at JET, 837
of contaminated items, 837, 874
tritium contamination of remote handling equipment, 838
Richardson permeation law, 192
Rupture discs, 320, 350, 395, 444, 659, 686, 721, 733, 807

Separation of hydrogen isotopologues
catalyst/packing screening tests, 672
cryogenic distillation
Darlington (TRF), 50, 654, 824, 847, 853
FUGEN Nuclear Power, Tsuruga, 678
Grenoble, 654, 669

ITER, 656
JET, 655
NIFS, 475
TFTR, 635
TLK, 675
TPL, 681
TSTA, 654
Displacement gas chromatography (DGC)
JET, 658
TLK, 660
Efficient Palladium Isotope Chromatographic System (EPIC), Mound, 661
molecular sieving at cryogenic temperatures using zeolite 3A, 489
Thermal cycling absorption process (TCAP)
Savannah River, 666
Valduc, 666
Thermal diffusion column
effect of column diameter, 664
effect of cooling, 664
effect of pressure, 665
effect of temperature, 663
separation factors, 665
Sievert´s law, 114, 118, 186, 199, 295
Silver
applications in tritium technology, 242, 293–297, 337, 345, 349
diffusivity, solubility of hydrogen isotopologues, 242
Soldering, 356
Stainless-steel
chronic release of tritium
at 298 K, 179, 194, 214, 886
mitigation, 933
cleaning of austenitic steel surfaces, 370
cleaning of ferritic steel, 372
cleanliness verification, 372
coating with palladium, 194
corrosion
compatibility with beryllium, 261
rudiments, 203
heterogeneous oxidation of tritium permeated to the backside of SS, 202
homogeneous/non-homogeneous depth profiles of tritium, 176, 195–198
hydrogen content of as-received, 171
importance of pretreatment, 198, 227
influence of hydrogen isotopologues or ^{3}He on mechanical/surface properties, 204
mechanism of hydrogen conversion into water on stainless-steel surface, 180
neutron activation, 213
permeation barriers (passivation), 325
solubility of tritium in sub-surface, 186

solubility, diffusivity, permeability of hydrogen isotopologues, 186–194, 207
trapping of tritium by
gas-driven permeation, 172
plasma/ion-driven permeation, 172
tritium in-growth into stainless-steel containments, 200, 334, 369
tritium leaching into water, 175
tritium uptake at ambient temperature, 175

TEXTOR, 1
diborane flushing, 917
dust formation, 868, 870
retrieval of tritium from first wall, 909
silicon first wall, 918
tungsten limiter
ejection of spray and droplets, 290
exposure to plasmas, 279
exposure to plasmas and tritium, 287
imaging plate analysis, 596
macro brush configuration, 280

TFTR
Automated Control, 829
dust and flakes, 868
first wall
conditioning, 909
materials, 300, 306, 312
molecular sieve regeneration, 785
Office of Certification and Training, 822
plasma exhaust cleanup, 635
pumps, 394, 711
shipment of tritium, 634, 708
tritium inventory, 311
work in Control Area, 821

Titanium, 112
PCT data of hydrogen/titanium system, 112
application in pumps, 413, 414, 417
conditioning for waste disposal, 901
effect of oxygen/helium on hydrogen uptake, 114–115
gettering impurities from inert gas, 770
hydride formation, 112, 169
hydrogen-assisted embrittlement, 209
matrix for tritium storage, 49, 112, 114, 422
transmutation products of plasma facing, 883
trapping of decay helium, 116

Tritium accountancy, 688
bake-off profile, 692
calorimetry, 579, 585, 588, 685–686, 688, 694, 920, 924, 1015
controlled regeneration, 692
direct sampling, 691
empirical estimation in stainless-steel, 695
from $^{3}He/^{4}He$ ratio, 691
isotopic exchange, 690
material balance area, 688

of gaseous tritium, 689
of tritium in solids, 690
Tritium handling processes
basic support operations, 608
evacuation, 610
gas re-circulation, 611
tritium transfer: fetch principle, 613
Tritium, decontamination of ambient air
Air Clean up System at TPL, Japan, 757
during spill and fire, TPL, Japan, 759
effect of catalyst poisons (Freon, Halon), 758
effect of ITER NBI insulator gas SF6 in air, 754
Emergency System: single path vs closed loop
Mound Laboratory, USA, 750
Emergency Tritium Clean up System, TSTA, USA, 758
polyimide separation membrane, 760
wet scrubbing, JET, UK, 684
Tritium, miscellaneous
Annual Limit for Intake (ALI), 13
applications other than for fusion, 52
boiling points, triple points and critical points of hydrogen isotopologues, 20
Derived Air Concentration (DAC), 13
Derived Release Limit for Darlington
airborne elemental, 853
tritiated liquid waste, 858
dissociation energy, zero-point energy, ionization energy of hydrogen isotopologues, 14
environmental tritium in water, 607
heat capacity of hydrogen, 29
molar volume of hydrogen and deuterium, 13
pressurization procedures, 714
properties, chemical, 8
properties, physical and nuclear, 8
radioactive decay heat, 12
rotational states of hydrogen, 15
self-radiolysis of T_2, 53
Tritium Plasma Experiment
ion-induced permeation, TPL, 173
ion-induced permeation, TSTA, 173, 730
vapour pressures of tritiated hydrogens, 21
vicosity, 23
volumetric calculations at elevated pressure, 25
Tritium, reactions of molecular
exchange with H_2 or D_2, 78
exchange with methane, 81
exchange with water, 79
isotopic scrambling of hydrogen isotopologues, 26
with carbon dioxide, 87
with carbon monoxide, 85
with nitrogen, 76

formation rate of NH_3 in a glove box of nitrogen atmosphere, 77
with oxygen
inflammability, explosion, detonation, 67
Tritium, reactions of tritiated water
with carbon dioxide, 89
Tritium, recoil chemistry
generation of hot atoms, 90
reaction with H_2/D_2 mixtures, 91
reaction with ammonia, 91
reactions with organic compounds, 90
Tritium, removal from glove boxes, 748
air atmosphere, catalytic exchange, 774
air atmosphere, catalytic oxidation, 749, 762
inert atmosphere doped with oxygen, 761
issues, 748
kinetics of tritium removal from glove box air, 750–757
oxygen-doped inert gas, 762–765
pure inert gas atmosphere, 770
Replacement Tritium Facility (RTF), SRS, USA, 765–769
risk assessment of JET removal system, 764
STAR concept, 769
TLK concept, 725–728, 755–757, 764
TPL concept, 698, 710, 728, 757, 777, 792, 848
Tritium, sources
man-made, using, 45
boron carbide, 48
fusion machine blankets containing lithium ceramics, 48, 270
lithium aluminum alloy, 47
lithium meta aluminate ceramic, 47, 48
tritium-contaminated heavy water moderator, 45, 49, 654
natural, 44
Tritium, storage of contaminated oil
Vermiculite, 932
Tritium, storage of elemental
by encapsulation in molecular sieves, 134
gas transport vessels
Product Vessel (PV) gas container, WSRC, USA, 707
stainless-steel vessel, 421
type LP-12/LP-50 containers (incoming/exhaust gas), TFTR, USA, 708, 937
getter bed design peculiarities and safety issues, 423
air ingress, 429
bed design dependency from getter type, 433
effect of gas pressure, 423
effect of impurities in hydrogen, 428
formation of eutectics, 432

getter swelling, 425
heat dynamics, 426
hysteresis, 96, 101, 117, 127, 131, 424
in-bed calorimetry, 444–453
measures against rapid pressure evolution, 431
measures against rapid temperature evolution, 431
metallic filters, 425
permeation into insulation vacuum, 431
replacement of heaters or thermocouples, 433
stress/strain analysis, 432
getter tritides used for storage
hydride bed decontamination, 902
lanthanum/nickel/aluminum and alloys, 127
most prospective getters for ITER, 132
palladium, 108
titanium, 112
uranium, 95
zirconium, 116
zirconium cobalt, 116
zirconium nickel, 131
in-bed calorimetry, methods
adiabatic/isothermal, 445
flowing gas, 446
isothermal, 452
static gas, 445
kinetic model of hydride storage bed operation, 441
shipping packages
BU type packages, JAERI, Japan/KAERI, Korea, 432, 441, 687, 707, 934
type A, B or C, IAEA, 708, 937
storage and/or transport of solid specimens/waste
AL-M1-S or DOT 17C/17H containers, 937
specimens for *post mortem* examination, JET/TLK, 938
storage and/or transport using hydride beds
$LaNi_{4.25}Al_{0.75}$ WSRS, USA, 129, 439, 448, 901
axially heated/cooled hydride bed, JET, UK, 437
design criteria, 440
Fast Delivery Hydride bed, TLK, Germany, 434–436
GE Healthcare (Amersham), Canada, 704–707
Replacement Tritium Facility, SRS, USA, 46, 130, 448–452, 765–769, 775
titanium, Chalk River/Darlington, Canada, 46, 434
titanium, KAERI, Korea, 49
titanium, WSRS, USA, 439, 901

Tritium Storage and Transfer System, TLK, Germany, 533, 612, 707, 709, 826
Tritium Storage and Transfer System, TPL, Japan, 710
Tritium Storage and Transfer System, Bruyères-le-Châtel, France, 612
uranium, Hydride Transport Vessel (HTV), WSRC, USA, 439, 708
uranium, KAERI, Korea, 442, 934
uranium, water cooled bed, FZJ, Germany, 434
zirconium/cobalt, JAERI, Japan, 441
storage and/ortransport hydride beds
uranium, KAERI, Korea, 936
Tritium, storage of highly tritiated water
adsorbed on solid matrix: precautions, 931
as liquid, 859, 931
as solid, 860
Tritium, storage of moderate-tritiated water
adsorbed on
diatomaceous earth, 929
molecular sieve, 861, 929, 931
silica gel, 862, 931
solid material upgraded by additives, polymer impregnation or coatings, 930
Vermiculite, 862, 929
as constituent of cement or inorganic hydrates, 862, 930
Tungsten, as plasma facing material, 271
application in fusion machines, 278
bonding with CuCrZr heat sink, 291
brittle to ductile transition, 278
bubble, blister formation, 284–286
chemical properties, 277
crack and fuzz formation, 279, 281, 283, 290
diffusion, solubility and permeation of hydrogen isotopologues, 271
nitrogen, 277
ejection of droplets/spray from melt, 290
influence of tungsten armour material on breeding ratio, 313
interaction wih plasma species, 279
irradiation damage by first principles, 276, 289
retrieval of tritium from first wall, 289
transmutation products, 291, 883
trap formation, 276
trapping of tritium, 282, 309

Valves
design guidelines, 335
design requirements, 335
experience worldwide in tritium service, 339
manual and automatic, 340
non-return valves, 470, 646, 687, 704
quality assurance, 338

stem and gasket materials, 337
variable leak and modulating, 343
Vermiculite, 65, 929–932
Vessels
design requirements, 334
interlock, 334

Waste contaminated by tritium, 846
decontamination of
adsorber beds, 901
getter beds, 901
glove box, equipment, 906
liquid scintillation cocktail, 898
oil, 900
pharmaceuticals, 865, 898
service waste, 904
solvents, 898
stainless-steel, 888
decontamination procedures, 888
disposal sites in France
ANDRA, 843, 872
CIRES, 844, 871
CSA, 872
environmental waste, 887
gaseous inorganic (HT, HTO, particles) released at
JET, 850
JT60-U, 850
Laue-Langevin, 846
Mound, 849
Ontario Hydro, 847
TLK, 846
TPL, 847
TSTA, 847
gaseous inorganic: HT, HTO, particulates, 846
Darlington, 853
gaseous organic, 853
IRAS-index, 871
ITER, operational waste, 874
classification of solid waste in France, 874–876
ex-vessel, solid, 885
in vessel, solid, 875
plasma exposed non-steel metals, 879
plasma-facing carbon waste, 885
transmutation products in structural steel, 877
liquid burnable, 864
liquid non-burnable, 855
mitigation of chronic release from drums, 933
packaging
liquids, 929
solids, 932
sentencing, 585, 843, 867, 868, 882, 888, 914, 919–929
shredding and coating with paint, 932
Water detritiation, low level tritium
catalytic exchange cryo distillation, Grenoble, 654, 669, 846
CECE, MOUND, 670

ISS, FUGEN Nuclear Power Station, Tsuruga, 667, 678
ITER, Cadarache, 682
laser Raman, analytical tool for ISS, 656, 681
LPCE conceptual design, JET, 679
LPCE, Chalk River, 670
LPCE, cryogenic distillation, Korea, 682
LPCE, electrolyzer, cryogenic distillation, TRENTA, TLK, 674
options for Hanford, 785
poly phosphazene membrane, PNNL, 681
Tritium Replacement Facility, Darlington (see also separation of hydrogen isotopologues), 46
Water, highly or pertritiated
corrosion of stainless-steel, 60, 230
density, 30
infrared and Raman absorption, 27
ionization constants of water isotopologues, 31
luminescence, 31
physical constants of water isotopologues, 29
recovery of tritium
electrolysis, 474, 642
hollow Pd/Ag cathode thimble, 476
isotopic exchange, 645
PERMCAT and two stage PERMCAT, 642
stabilized zirconia tube cell, 476
reduction on hot metals, 638
alloys, 641
iron, 640
magnesium, 639
uranium, 639
relative vapour pressures, 30
self-radiolysis
at low temperature, 64
at moderate temperature, 57
immobilized in a solid absorber, 64
under frozen conditions, 63
Welding, 334, 347, 356, 732
acceptance criteria, 361
Delivery and Acceptance Codes, Manufacturing Codes, 823
effect of tritium and helium, 208, 230
glove box penetrations, 794–797
impact on corrosion and leak rates, 210, 373
inspection, 359
interaction with tritium, 362
procedures, 357
remote, 364
requirements, 358
Round Robin tests, 220
Welding of
aluminium, 329
copper, 329
Inconel-625, 849
SS316, 322

tritium-contaminated stainless-steel, 362
tungsten with CuCrZr, 290